May 12, 2008

UNITED STATES OF AMERICA
NUCLEAR REGULATORY COMMISSION

Before the Atomic Safety and Licensing Board

In the Matter of	)	
	)	
Entergy Nuclear Vermont Yankee, LLC	)	Docket No. 50-271-LR
and Entergy Nuclear Operations, Inc.	)	ASLBP No. 06-849-03-LR
	)	
(Vermont Yankee Nuclear Power Station)	)	

EXHIBITS TO ENTERGY'S DIRECT TESTIMONY ON NEC CONTENTION 2 – ENVIRONMENTALLY ASSISTED FATIGUE

INCLUDES EXHIBITS E2-02 THROUGH E2-20

Volume 1

INDEX OF EXHIBITS TO ENTERGY'S DIRECT TESTIMONY ON NEC CONTENTION 2 (ENVIRONMENTALLY ASSISTED FATIGUE)

Volume 1

Exhibit E2-01 - Joint Declaration of James C. Fitzpatrick and Gary L. Stevens [Submitted separately]

Exhibit E2-02 - James C. Fitzpatrick Resume

Exhibit E2-03 - Thadani December 26, 1999 Memo

Exhibit E2-04 - NUREG CR-6260 (excerpt)

Exhibit E2-05 - Section X.M1 of GALL Vol 2

Exhibit E2-06 - NUREG CR-6583

Exhibit E2-07 - NUREG CR-5704

Exhibit E2-08 - Gary L. Stevens Resume

Exhibit E2-09 - VY LRA Amendment 35

Exhibit E2-10 - VY-16Q-301R0

Exhibit E2-11 - VY-16Q-302R0

Exhibit E2-12 - VY-16Q-303r0 REDACTED

Exhibit E2-13 - VY-16Q-304R0

Exhibit E2-14 - VY-16Q-305r0

Exhibit E2-15 - VY-16Q-306R0

Exhibit E2-16 - VY-16Q-307r0

Exhibit E2-17 - VY-16Q-308R0

Exhibit E2-18 - VY-16Q-309R1

Exhibit E2-19 - VY-16Q-310R1

Exhibit E2-20 - VY-16Q-311R0

RESUME
JAMES C. FITZPATRICK

SUMMARY QUALIFICATIONS:

Thirty years experience in design, construction, and modifications of nuclear power plant structures, piping systems, pressure vessels, and anchorage of mechanical and electrical equipment. Twenty-two years of operating plant engineering support in both the mechanical and structural areas. Responsible for development and implementation of plant design changes, inspection programs, equipment specifications, installation support, outage support, and operability evaluations of degraded components.

EDUCATION AND LICENSES:

Northeastern University, Boston Ma. - M.S. Civil Engineering (1984).
Northeastern University, Boston Ma. - B.S. Civil Engineering (1977).
Registered Professional Engineer - Massachusetts, Vermont.

PROFESSIONAL EXPERIENCE:

AREVA NP, Marlborough, MA (March 2008 – present)
Engineering Supervisor – Plants Sector: BOP Structural and Engineering Mechanics

Providing structural and mechanical engineering services to clients. Responsible for supervision and technical support for team of engineers and support staff.

Entergy Nuclear Northeast - Vermont Yankee (2002 – March 2008.) Sr. Lead Engineer, Design Engineering.

Provided support for License Renewal Project for aging management issues related to FAC and metal fatigue. Responsible for review and acceptance of calculations and reports developed to evaluate environmentally assisted fatigue of ASME Class 1 components. Responsible engineer for development of design change for a pre-emptive structural repair of in-vessel Core Spray piping welds using BWRVIP criteria. Responsible Engineer for implementation and maintenance of the Piping FAC Inspection Program until June 2007. Performed piping component inspection selections, evaluations of inspection results, trending of refueling outage inspection data, updating the CHECWORKs predictive models as required. Developed engineering changes for repair or replacement of piping components. Responsible Engineer for mechanical/structural analyses and modifications associated with extended power uprate. Projects include: Alternate Source Term, Seismic Boundary, Cooling Tower Modifications, and a Revised Stress Analysis of Reactor Feedwater Nozzles. Provided engineering support for ASME Section XI and Reactor Vessel Inspection Programs.

Vermont Yankee Nuclear Power Corp. (1997 - 2002) Senior Engineer, Design Engineering.
Yankee Atomic Electric Company (1991 - 1997) Senior Mechanical Engineer, Vermont Yankee Project.

Cognizant engineer with overall responsibility for development and implementation of a number of Engineering Design Changes including replacement of check valves on the Reactor Feedwater System, seismic supports for control room panels and electrical equipment, new station air compressors with associated piping, and GE Mark 1 Torus piping support modifications. Responsible for structural engineering support for ASME Section XI IWE inspections. Developed acceptance criteria for localized thinning of a GE Mark I containment.

Cognizant engineer for Piping Flow Accelerated Corrosion (FAC) Inspection Program. Responsible for program implementation, establishing and maintaining criteria for selection of systems and components susceptible to FAC. Tasks include CHECWORKS modeling of plant piping systems, development of refueling outage inspection scope, providing on-site engineering support, screening and evaluation of piping components, inspection sample expansion, coordination of repairs and replacements, and maintenance of Program Manual and documentation.

Seismic Capability Engineer for Seismic Qualification Utility Group (SQUG) program. Performed equipment walkdowns, screening evaluations, anchorage calculations, and preparation of licensing submittal for resolution of USI-A46 and the seismic portion of the IPEEE. Developed and implemented design changes to resolve SQUG GIP Criteria Outliers and to resolve Design Basis concerns. Provided mechanical/structural engineering support for procurement of new and replacement equipment. Responsible for development of design specifications and review of seismic qualification test reports. Also provided engineering support and evaluations for ASME Section

XI and Service Water inspection programs. Performed evaluations of degraded Service Water piping components for Generic Letter 90-05 submittals.

Yankee Atomic Electric Company (1988 - 1990) Senior Engineer, Vermont Yankee Project.

Responsible for development of a long term Piping Erosion-Corrosion (FAC) Inspection Program, evaluations of plant piping systems for erosion-corrosion using the EPRI CHEC and CHECMATE codes, and for E/C inspection scope and on-site engineering support for both the 1989 and 1990 refueling outages. Designed seismic modifications and developed finite element models for the control room panels. Provided mechanical/structural support for a number of plant design changes. Developed ASME Code Case N-411 Seismic Response Spectra for the Turbine Building.

Yankee Atomic Electric Company (1986 - 1987) Mechanical Engineer, Vermont Yankee Project.

Provided engineering support for a number of plant design changes to both structures and mechanical systems. Projects included: Modifications to the Torus RHR and Core Spray suction strainers, Seismic Re-analysis Program for safety class piping, Revised LOCA pressure loads in the Steam Tunnel, and the design and installation of New Spent Fuel Racks. Performed evaluation for corrosion of the bottom plates in the Condensate Storage Tank and assisted in preparation of the response to NRC Bulletin 87-01 - Pipe Wall Thinning.

Stone and Webster Engineering Corporation (1984 - 1986)

Mechanical Engineer, Engineering Mechanics Division - Beaver Valley Unit No.2 Project, Responsible for qualification of safety related equipment for deadweight, thermal, seismic, and attached piping loads. Duties included the supervision of an engineering group developing allowable piping reactions for Safety Class equipment and performing ASME III stress analyses of tanks and vessels. Responsible for resolution of piping nozzle overloads between the pipe stress analysis and equipment qualification groups.

CYGNA Energy Services (1980 - 1984)

Senior Engineer (1983-84) - Performed engineering studies, analyses, and developed new designs for a number of modifications at both the Maine Yankee and Vermont Yankee plants. Typical projects included; MY 79-02 Base Plate Reanalysis, MY Auxiliary Feedwater Modifications, VY RCIC Room HVAC and Structural Modifications, and VY Torus Attached Piping Modifications.

Lead Engineer - Group Leader (1882-83) - Group Leader for the Diablo Canyon pipe Support Design Review. Responsible for review and approval of design calculations, supervision of pipe support analysts, conceptual pipe support modifications, and providing technical direction to engineers.

Lead Engineer - Group Leader (1981-82) - Supervised on-site engineering group responsible for the analysis and design of over 100 new pipe rupture restraints for Midland units 1 and 2. Responsible for development and implementation of design criteria and work instructions, providing technical direction to engineers, review and approval of calculations and drawings, resolution of interference's with other groups, and the preparation of status reports and schedules.

Staff Engineer (1980-81) - Responsible for development of computer models and amplified response spectra curves for six structures and the NSSS at Maine Yankee . Developed artificial acceleration time histories to envelope NRC R.G.1.60 Ground Response Spectra. Performed analyses and designed seismic modifications for masonry block walls as required by NRC Bulletin 80-11 for Millstone Unit 1.

Stone and Webster Engineering Corporation (1977 - 1980)

Support Engineer, Engineering Mechanics Division - Assigned to the Structural Mechanics Section on the Beaver Valley Unit 2 Project. Developed computer models for generation of seismic floor response spectra curves used for design of plant structures and equipment. Performed design review of the concrete containment internals structure for increased seismic and pipe rupture loads. Reviewed ASME III Stress Reports for design of containment liner, overlay and insert pads, and containment hatches. Developed finite element models for analysis of ASME III Code Class MC containment piping penetrations. Assisted in the development of TVB, an in-house computer code to determine tornado wind and pressure drop effects on structures. Developed models to perform tornado venting studies for BV-2 plant structures.

December 26, 1999

MEMORANDUM TO: William D. Travers
Executive Director for Operations

FROM: Ashok C. Thadani, Director [Original /s/ by A. Thadani]
Office of Nuclear Regulatory Research

SUBJECT: CLOSEOUT OF GENERIC SAFETY ISSUE 190, "FATIGUE EVALUATION OF METAL COMPONENTS FOR 60-YEAR PLANT LIFE"

The staff has completed all actions planned for the resolution of Generic Safety Issue (GSI) 190, and will close out the issue without imposition of new or additional generic action for licensed plants up to 60-year plant life. This GSI was identified in 1996 by a memorandum from T. Speis to A. Thadani, dated 08-26-1996, to supplement the ongoing work on GSI-78, "Monitoring of Fatigue Transient Limits for Reactor Coolant system," and residual work on GSI-166, "Adequacy of Fatigue Life of Metal Components," by addressing fatigue of metal components for 60-year plant life.

The conclusion to close out this issue is based upon the low core damage frequencies from fatigue failures of metal components estimated by technical studies making use of recent fatigue data developed on test specimens. The results of these probabilistic analyses and associated sensitivity studies led the staff to conclude that no generic regulatory action is required. However, calculations including environmental effects, that were performed to support resolution of this issue, and the nature of age-related degradation indicate the potential for an increase in the frequency of pipe leaks as plants continue to operate. Thus, the staff concludes that, consistent with existing requirements in 10 CFR 54.21, licensees should address the effects of the coolant environment on component fatigue life as aging management programs are formulated in support of license renewal. The background information and the basis for the closeout conclusion are presented in Attachment 1.

The advanced light water reactors (ALWRs) that have been certified under 10 CFR Part 52 were designed for a 60-year life expectancy. The associated fatigue analyses accounted for the design cycles based on a 60-year plant life but did not account for the environmental effects as addressed in GSI-190. However, the staff has concluded that there is sufficient conservatism in the fatigue analyses performed for the generic 60-year ALWR plant life to account for environmental effects. The staff therefore concludes for ALWRs that there is not a need for imposing a revision of these fatigue analyses on a generic basis or to impose additional monitoring requirements.

On December 3, 1999, the staff met with the ACRS, and presented the proposed resolution of this issue. The ACRS reviewed and accepted the proposed resolution (Attachment 2).

Interaction with the industry is an important aspect of the resolution of this issue. Therefore, the staff has had several meetings with the Nuclear Energy Institute (NEI) and the Electric Power

Research Institute (EPRI) regarding this issue. Most recently, on November 17, 1999, the staff held a workshop with the industry to discuss the resolution of GSI-190 and plans for addressing the broader range of fatigue issues affecting nuclear plants. In addition, the staff has reviewed several EPRI reports on subject of fatigue. Appendix C to Attachment 1 briefly summarizes the contents and staff review of these reports. The staff is aware that the industry continues to be concerned about what will constitute an acceptable aging management program for fatigue. The industry and NRC are maintaining an ongoing dialogue on this subject.

Attachments:
1. Background Information
2. Letter to W. Travers from D. Powers, dated December 10, 1999

cc: S. Collins
C. Paperiello
F. Miraglia

CONTACT: Khalid Shaukat, MEB/DET/RES
301-415-6592

Distribution:

Reading File DET Branch Reading File
M. Federline
R. Zimmerman
B. Sheron
J. Strosnider
G.Holahan
C. Grimes
E. Rossi
J. Rosenthal
E. Imbro
W. Bateman
K. Manoly
J. Fair
D.Kalinousky
J. Muscara
Public Document Room

*See previous concurrence
DOCUMENT NAME: a:\gi190closeout.wpd **To receive a copy of this document, indicate in the box: "C" = Copy without attachment/enclosure "E" = Copy with attachment/enclosure "N" = No copy**

OFFICE	DET/MEB		DET/MEB		DET/ActingDD		NRR/ADPT		RES/D	
NAME	K. Shaukat *		E. Hackett *		M. Mayfield*		B. Sheron*		A. Thadani	
DATE	12/ 14 /99		12/ 14 /99		12/ 21 /99		12/ 23 /99		12/ 26 /99	

OFFICIAL RECORD COPY RES File Code:: 2D-3

Attachment 1

Resolution of GSI-190, "Fatigue Evaluation of Metal Components for 60-year Plant Life"

Background:

The ASME Boiler and Pressure Vessel Code (B&PV) Section III, Subsection NB contains design requirements for cyclic loading conditions. Appendix I to Section III specifies the code design fatigue curves that are based on strain-controlled tests of small polished specimens at room temperature in air. To obtain these design fatigue curves, best-fit curves to the experimental test data were lowered by a factor of 2 on stress or 20 on cycles, whichever was more conservative, at each point on the best-fit curve. This was intended to account for uncertainties in relating fatigue life of laboratory test specimens to those of actual reactor components. More recent fatigue strain-vs-life (S-N) data from the United States and Japan show that light water reactor (LWR) environments can have potentially significant effects on the fatigue life of carbon steel, low-alloy steel and austenitic stainless steel. Test specimen fatigue life in simulated LWR environments was found to be shorter than that determined by corresponding tests in air (Appendix A). This implies that the factor of 2 or 20 applied to the original best-fit- data curve may not be adequate. Under an NRC/RES-sponsored project, Argonne National Laboratory (ANL) developed interim design fatigue curves which addressed the environmental effects on fatigue life of the materials (NUREG/CR-5999).

GSI-190 Prioritization and Related GSIs:

The effects of the interim design curves, developed by ANL, on fatigue life of selected components were studied under two generic issues; GSI-78, "Monitoring of Fatigue Transient Limits for Reactor Coolant system," and GSI-166, "Adequacy of Fatigue Life of Metal Components."

GSI-78 was developed to determine whether fatigue monitoring was necessary at operating plants, and later included the calculation of risk due to through-wall cracking of metal components due to fatigue. GSI-166 was developed to assess the significance of more recent fatigue test data on the fatigue life of a sample of components in plants where a code fatigue design analysis had been performed. A Fatigue Action Plan (FAP) was developed to coordinate the efforts on fatigue life estimation and addressed the ongoing issues under GSI-78 and GSI-166 for 40-year plant life.

In resolving GSI-166, the staff completed the following studies regarding the concerns related to design basis fatigue transients for the operating plant life of 40-years.

- Under the FAP, a study was made (NUREG/CR-6260) by Idaho National Engineering Laboratory (INEL) to evaluate the design code fatigue cumulative usage factor (CUF) for selected components in primary system environments using the interim fatigue curves of NUREG/CR-5999.

- Existing fatigue data were compiled on specimens cycled to failure in simulated LWR conditions, and statistical models were developed (NUREG/CR-6335) by ANL for estimating the effects of service conditions on fatigue life of selected components.

In SECY 95-245 (Completion of Fatigue Action Plan), dated 09/25/95, the staff concluded that no immediate actions were required to deal with the fatigue issue for the current plant design life of 40 years. This conclusion was based on work indicating that the calculated fatigue usage factors for operating plants were conservative and that a cost/benefit analysis per the GSI process would not support imposing any new requirements for the 40-year operating license period. However, it was recognized that environmental effects could result in fatigue still being an issue for plants operating an additional 20-years under a renewed license . On completion of the FAP, the ACRS letter to the EDO (03/14/96) agreed with the staff's conclusion that the risk from fatigue failure of components in the reactor coolant pressure boundary is very small for a 40-year plant life.

Since the procedures for the resolution of GSIs require consideration of a license renewal period of 20 years, the environmental effects of fatigue on pressure boundary components for 60 years of plant operation were examined. By a memorandum to A. Thadani, from T. Speis, dated 08/26/96, RES documented that this further study for the 20-year life extension of the concerns of GSI-78, and GSI-166, would now be carried on under a new GSI-190, "Fatigue Evaluation of Metal Components for 60-year Plant Life." Therefore, GSI-78 and GSI-166 were considered resolved by a closeout memorandum to H. Thompson, from D. Morrison, dated 02/05/97.

GSI-190 addressed the environmental effects on design basis fatigue transients, studying the probability of fatigue failure, either leakage or pipe failure, and associated core damage frequency (CDF) for 60-year plant life. It did not address all aspects of fatigue-related degradation, including those that are outside the design basis.

Other fatigue-related degradation such as recent cracking problems at Oconee, and in France, which were related to unanticipated operating conditions involving thermal/mechanical stresses, are outside the scope of GSI-190. Several of these more recent fatigue events are discussed in Appendix B. These events are the results of unanticipated cyclic loads and thus are clearly outside the scope of the design basis transients used for fatigue design governed by the Section III of the ASME, B&PV Code. Situations like this may continue to occur.

Interaction with the industry is an important aspect of the resolution of this issue. Therefore, the staff has had several meetings with the Nuclear Energy Institute (NEI) and the Electric Power Research Institute (EPRI) regarding this issue. Most recently, on November 17, 1999, the staff held a workshop with the industry to discuss the resolution of GSI-190 and plans for addressing the broader range of fatigue issues affecting nuclear plants. In addition, the staff has reviewed several EPRI reports on the subject of fatigue. Appendix C to this Attachment briefly summarizes the contents and staff review of these reports.

Technical Analysis:

The approach to resolving GSI-190 built upon the approaches used in resolving GSI-166 for 40-year plant life and in the Fatigue Action Plan studies. The Pacific Northwest National Laboratory (PNNL) performed calculations of the probability of component failure and the Core Damage Frequency (CDF) associated with these failures. PNNL made use of the previous and most recent testing performed to develop fatigue design curves for stainless steel in simulated LWR environmental conditions.

PNNL then performed probabilistic fatigue calculations on 47 sample components from 6 locations in five PWR- and two BWR-plants using the pc-PRAISE code. During this work the staff identified that the pc-PRAISE code could not model the large aspect ratios of the initial cracks (ratio of crack length to crack depth), nor could it model the joining of several small cracks to make a large crack which would subsequently propagate through the wall thickness of the component. The staff concluded that the effect of large aspect ratios was an important factor in fatigue analyses and there was a need to modify the pc-PRAISE code to model these things.

PNNL modified the pc-PRAISE code with the help of a subcontractor who had originally written the code, and performed the fatigue calculations for several small cracks to grow and link together. Testing of the modified code demonstrated that, under strong thermal gradient loading, there was a high likelihood of long cracks being produced which is consistent with service experience. This was viewed as a major improvement in the performance of the pc-PRAISE code and was used in performing the subsequent through-wall cracking frequency calculations.

Using the modified pc-PRAISE code, PNNL performed a probabilistic analysis for the crack initiation and through wall crack growth in the components mentioned above for 40- and 60-year plant life considering both air and LWR environments. Calculations for the air environment and the 40-year life were done to confirm that the effect of the revised fatigue curves, coupled with the modified pc-PRAISE code, provided results that were consistent with the previous studies. An evaluation was performed to estimate the conditional CDF from the fatigue failure of these components. Given a through wall crack, the objective was to estimate the conditional probabilities of a small leak, of a large leak, and of a pipe break. Data on pipe failure events indicate that only a small fraction of through-wall flaws result in large leaks or breaks, and the types of failures are dependent on the particular failure mechanism involved. Probabilistic fracture mechanic models, like the one contained in the pc-PRAISE code, predict that fatigue failures will usually be in the mode of small leaks rather then large leaks or breaks. From the conditional probabilities of small leak, large leak, and pipe break, the conditional CDF was estimated for the seven example plants based on results extracted from probabilistic risk assessment (PRA). The major findings from the calculations include the following points:

- Many of the components have cumulative probabilities of crack initiation and cumulative probabilities of through-wall cracks that approach unity within the 40 to 60-year time period. However, some components, often with similar values of fatigue usage factors, show much lower failure probabilities. This is a result of the ANL statistical fit to the test data which indicates that the probability of crack initiation for a constant CUF value is a function of the strain amplitude of the applied loading.

- The maximum failure rate (through-wall cracks per reactor year) is in the range of 10^{-2}, and those failures were associated with high CUF locations.

- Failure rates for other components having much lower failure probabilities are changed by as much as an order of magnitude from 40 to 60-years, but these components make relatively small overall contributions to the cumulative CDF estimates.

- The maximum CDF based on these calculated failure rates is about 10^{-6} per year. These maximum values correspond to components with very high cumulative failure probabilities, and the failure rates do not change much from 40 to 60 years. The range of CDF was between 10^{-6} to 10^{-15}.

Based upon these low CDFs, the staff concludes that they would not be used as a basis for a cost/benefit backfit analysis to justify imposition of a new regulatory requirement on operating reactors. However, the calculations supporting resolution of this issue, which included consideration of environmental effects, indicates the potential for an increase in the frequency of pipe leaks as plants continue to operate. Thus, with the consideration of risk informed perspective, the staff concludes that, consistent with existing requirements in 10 CFR 54.21, licensees should address the effects of the coolant environment on component fatigue life as aging management programs are formulated in support of license renewal.

Sensitivity Study:

Sensitivity studies were performed by varying important input parameters to the pc-PRAISE code that could significantly alter the results. The parameters chosen for the sensitivity studies were wall thickness, stress gradient, initial flaw (crack) depth, flaw length, multiple crack initiation, correlation between crack initiation and crack growth, start of fatigue crack growth, oxygen content of reactor water, sulfur content of metal, and strain rate.

These studies were primarily aimed at increasing confidence in the results of the above studies, and to better understand the limitations of the assumptions made in the analyses using the revised pc-PRAISE code, which incorporated capabilities for crack linking. The staff concluded that the results from the code were consistent with physical expectations for fatigue crack growth and consistent with observations from actual fatigue failures. Therefore, the results of PNNL report were considered to provide a reasonable basis for our conclusions.

Conclusions:

The estimated contribution to CDF from fatigue failures of the evaluated components is on the order of 10^{-6}, or lower, per year. Recognizing the uncertainties in the calculations, the contribution to CDF from fatigue failures could be of the same order of magnitude as the contribution to CDF from a small LOCA (10^{-5} per year), but still below the threshold normally used to justify additional regulatory requirements for operating reactors.

It should be noted that based on analyses performed for GSI-190, it was expected that the cumulative usage factor (CUF) for certain components would exceed the ASME Code design limit of CUF $\leq$ 1 when evaluated for design basis transients for 60 years. The calculated CDFs

for the components with the highest failure frequencies show essentially no increase in CDF from 40 to 60 years.

The results of the probabilistic analyses, along with the sensitivity studies performed, the interactions with the industry (NEI and EPRI), and the different approaches available to the licensees to manage the effects of aging, lead to the conclusion that no generic regulatory action is required, and that GSI-190 is resolved. This conclusion is based primarily on the negligible calculated increases in CDF in going from 40 years to 60 year lives. However, the calculations supporting resolution of this issue, which included consideration of environmental effects, and the nature of age-related degradation indicate the potential for an increase in the frequency of pipe leaks as plants continue to operate. Thus, the staff concludes that, consistent with existing requirements in 10 CFR 54.21, licensees should address the effects of the coolant environment on component fatigue life as aging management programs are formulated in support of license renewal.

APPENDIX A

Recent Technical Information on Fatigue in the U.S. and Japan

Under an NRC/RES-sponsored project, fatigue tests have been conducted by ANL on Type 304 and 316NG stainless steel to evaluate the effects of various loading variables under water environments. The results confirm decreases in fatigue life in low dissolved oxygen water. The formation and growth of fatigue cracks in air and water environments are discussed in two letter reports by ANL; 1) "Effects of LWR Coolant Environment on Fatigue Lives of Austenitic Stainless Steels," dated November 1997, and 2) "Updated Fatigue Design Curves for Austenitic Stainless Steels in LWR Environments," dated January 19, 1998. The latter report contains the revised fatigue S-N curves developed by ANL and a comparative ASME Mean curve for stainless steel in air and water environments. The report also gives equations and explains a methodology for calculating fatigue life of components based on tests and other databases.

An independent evaluation of fatigue life of metal components has been ongoing in Japan. Dr. Higuchi of the industry and Prof. Iida of the University of Tokyo initiated a research project on this issue in 1991 which is expected to be completed in 2006. Their work involves the study of a fatigue database (254 data points for carbon steels and 319 data points for low alloy steels) and further fatigue tests of specimens under simulated LWR environments. They studied the fatigue behavior of carbon and low alloy steels in high temperature water environments for different dissolved oxygen contents and varying strain rates. Their study thus far shows results similar to those observed by ANL and they have reported their findings to the appropriate ASME Code Committees.

Results from the work described above and other studies have, for a significant time, indicated that the ASME Code design curves for fatigue life need to be modified to account for the effects of light water reactor environments. Since the cognizant Code Committee has not taken actions in this regard, RES/DET has sent a letter to request expeditious ASME Code action on this issue (Letter to J. Ferguson from J. Craig, dated December 1, 1999).

APPENDIX B

Recent Fatigue-related Events

Oconee: This event is discussed in IN 97-46. On April 22, 1997, at 12:50 p.m., Oconee Unit 2 was shut down because of unidentified reactor coolant system (RCS) leakage exceeding the technical specification limit of 1 gpm. Until reactor pressure was sufficiently reduced, the leakage rate rose to approximately 12 gpm. A subsequent containment entry identified a non-isolable leak from a through-wall crack in the weld connecting the MU/HPI pipe and the safe-end of the 2A1 reactor coolant loop (RCL) nozzle.

Preliminary analysis indicates that crack initiation and propagation in the weld was caused by high-cycle fatigue due to a combination of thermal cycling and flow induced vibration. Although the root cause of the cracking is not well understood, the licensee has identified a number of thermal/mechanical conditions that may have contributed to the crack propagation of the 2A1 pipe to safe-end weld. The licensee has hypothesized that, in addition to the thermal cycling experienced at the nozzle during heat up/cool down and other plant transients, a likely contributor to the fatigue may have been the alternate heating and cooling of the weld by intermittent mixing of the hot reactor coolant leaking through the gap in the contact area between the loose thermal sleeve and the safe-end, and the cooler normal makeup water flowing through the associated MU/HPI line. Although the precise contribution of the gap is unknown, it is believed that a gap may be a prerequisite for cracking in the piping since the cracked pipes also had gaps between the thermal sleeve and the safe end.

This phenomenon was identified as the probable cause for similar safe-end cracking observed at Crystal River and other B&W plants (including Oconee) in the early 1980's. This issue was previously addressed in Information Notice 82-09 and Generic Letter 85-20.

Dampierre-1, France: A similar event occurred on December 14, 1996, when a non-isolable leak on piping connecting the safety injection system to the reactor coolant system was found in Dampierre Unit 1 in France. The damaged pipe length was examined and a through wall crack located on an uninterrupted portion of straight piping (not on a stressed area such as a weld or a bend). The licensee has not identified the root cause of the cracking, but concluded that the most probable cause was temperature variations produced by cold water coming from leaking valves located upstream in the safety injection system. The licensee also concluded that the presence of a through-wall defect on a straight portion of a pipe is likely to raise questions about previous assumptions made regarding the root cause of the cracking.

Civaux-1, France: On May 12, 1998, a 30 cubic meter/hour leak from an RHR train occurred in Civaux-1 operating at 50% power less than five months into the reactor's operation. It took several hours to detect the source of the leak: a crack 180 millimeters long on a 250-millimeter-diameter section of pipe that allows bypass of the heat exchanger on the RHR train A. About 300 cubic meters of spilled primary coolant was recovered in the sump.

The probable cause was considered to be a pipe defect in a longitudinal weld between two sections of the elbow and possible related defects elsewhere. In-depth investigations are underway to pinpoint the cause.

APPENDIX C

Interaction with the Industry

During the course of resolving GSI-190, the NRC has had extensive interactions with the Nuclear Energy Institute (NEI) and the Electric Power Research Institute (EPRI). EPRI also submitted five Topical Reports on the subject of environmental effects of fatigue on components from PWRs and BWRs. The staff reviewed these reports and the assessment is briefly discussed below. The staff believes that Aging Management Programs for fatigue must be consistent with the spirit of GDC-14, in that components affected by fatigue should maintain "an extremely low probability of abnormal leakage." Discussion is continuing with industry as to how aging management programs will demonstrate that this current licensing basis requirement will continue to be satisfied during the renewal phase

- EPRI TR-105759, "An Environmental Factor Approach to Account for Reactor Water Effects in Light Water Reactor Pressure Vessel and Piping Fatigue Evaluation," December 1995.

The objective of this report was to develop simplified but not overly conservative procedures for estimating reactor water environmental effects on the reactor vessel and piping in light of new test data. The background is that pressure retaining components in LWRs are designed to meet ASME Code Section III which requires a fatigue evaluation for transient stresses. The laboratory data from various test programs indicate that fatigue lives shorter than the Code design values are possible under water environments. This report proposes use of an environmental correction factor to the current Code fatigue evaluation procedures. The report cites a need for simplified, but not overly conservative, procedures for ASME Section III, NB-3600- and NB-3200-type analyses to account for reactor water environment effects. EPRI suggested introduction of an environmental correction factor F_{en} to obtain fatigue usage reflecting the environmental effects. EPRI also suggested proposed changes to ASME Section III fatigue evaluation procedures for possible consideration by ASME Code Committee to include environmental effects in fatigue evaluations conducted according to NB-3600 and NB-3200. The evaluation procedures could be added as a non-mandatory appendix to the Code.

The staff agrees with the concept of using an environmental correction factor (F_{en}) to obtain fatigue usage reflecting environmental effects. This information and other recommendations mentioned above have been forwarded to the appropriate ASME Code committee (Letter to J. Ferguson from J. Craig, dated December 1, 1999).

- EPRI TR-107515, "Evaluation of Thermal Fatigue Effects on Systems Requiring Aging Management Review for License Renewal for the Calvert Cliffs Nuclear Power Plant," December 1997.

The objective of this report was to demonstrate the current industry technical position on fatigue evaluation for license renewal, through the application of existing methodology, and criteria on selected systems/components in a pilot plant. The report develops a technical evaluation methodology for determining the fatigue life adequacy of these selected locations to be used as a guide for managing fatigue effects for the license renewal period. EPRI's conclusion is that the effects of reactor water environments are already compensated by two existing conservatisms in Class 1 ASME Code fatigue analysis procedures - (1) the low cycle portion of

the design fatigue curve margin factor of 20 on cycles or a factor of 2 on stress, and 2) the design basis definitions of thermal transients. Therefore, the explicit treatment of reactor water environmental effects in fatigue analysis is not considered necessary for license renewal.

The staff assessment of this report was that the latest ANL fatigue data reported in "Updated Fatigue Design Curves for Austenitic Stainless Steels in LWR Environment (March 1998)," were not considered.

- EPRI TR-110043, "Evaluation of Environmental Fatigue Effects for a Westinghouse Nuclear Power Plant," April 1998.

In addition to the main objective of this report evident in its title, another objective was to supplement similar conclusions made by BG&E for license renewal work on Calvert Cliffs.

Fatigue reactor water environmental effects were evaluated at 14 specific components in a Westinghouse PWR plant. The components addressed were: (1) the pressurizer shell, (2) the pressurizer spray nozzle, (3) the pressurizer surge nozzle, (4) the pressurizer water temperature instrument nozzle, (5) RCS hot leg surge nozzle, (6) charging nozzle, and (7 through 14) steam generator feedwater nozzles (4 locations per steam generator for 2 steam generators). They include components fabricated from carbon steel and austenitic stainless steels. They encompass specific component locations for which actual plant transient data were available for at least three years of plant operation from fatigue monitoring.

A selective environmental fatigue methodology was implemented which uses effective environmental fatigue multipliers, F_{en} lower than those produced by applying environmentally adjusted fatigue curves (NUREG/CR-5999) in NUREG/CR-6260. The conclusion was that environmental effects are already compensated by two existing conservatisms in ASME Code Class 1 fatigue analysis procedures: 1) the low cycle portion of the design fatigue curve margin of 20, and 2) the design basis definitions of thermal transients. The combination of these two conservatisms is such that explicit treatment of reactor water environmental effects in fatigue design analysis is not considered necessary for a 60-year plant life.

The staff assessment of this report was that the latest ANL fatigue data reported in "Updated Fatigue Design Curves for Austenitic Stainless Steels in LWR Environment (March 1998)," were not considered.

- EPRI TR-110356, "Evaluation of Environmental Thermal Fatigue Effects on Selected Components in a Boiling Water Reactor Plant," April 1998.

This report evaluated environmental effects at three specific locations in a newer vintage BWR plant; 1) the feedwater nozzle safe ends, 2) the feedwater nozzle forgings, and 3) the control rod drive penetrations. The evaluations included components fabricated from carbon steels and austenitic stainless steels.

A selective environmental fatigue methodology was implemented which used effective environmental fatigue multipliers, F_{en} lower than those produced by applying environmentally adjusted fatigue curves (NUREG/CR-5999) in NUREG/CR-6260.

The conclusion was that environmental effects are already compensated by two existing conservatisms in ASME Code Class 1 fatigue analysis procedures: 1) the low cycle portion of the design fatigue curve margin of 20, and 2) the design basis definitions of thermal transients. The combination of these two conservatisms is such that explicit treatment of reactor water environmental effects in fatigue design analysis is not considered necessary for a 60-year plant life.

The staff assessment of this report was that the latest ANL fatigue data reported in "Updated Fatigue Design Curves for Austenitic Stainless Steels in LWR Environment (March 1998)," were not considered.

- EPRI TR-107943, "Environmental Fatigue Evaluation of Representative BWR Components," May 1998.

This topical report by EPRI considers the latest environmental fatigue data from ANL. In this report, EPRI presented a comparative study done by INEL and by EPRI for calculating cumulative usage factors (CUFs) at six components of a newer vintage BWR, presenting results of the evaluation of environmental fatigue CUFs at the same six components using EPRI/GE methodology. The components are: (1) reactor vessel shell and lower head, (2) reactor vessel feedwater nozzle, (3) reactor recirculating piping, (4) core spray line reactor vessel nozzle and associated Class 1 piping, (5) residual heat removal (RHR) nozzles and associated piping, and (6) feedwater line Class 1 piping. Additionally, a review of available Argonne statistical models and their impact on evaluations is also provided.

The report concludes that even after accounting for environmental effects, the CUFs for analyzed components in a sample BWR plant are predicted to be less than 1.0 for both 40-year and 60-year operating periods. Therefore, a plant specific analysis for environmental fatigue effects is not considered necessary.

The staff assessment of this report was that, although the latest ANL fatigue data for environmental effects were considered, the staff still has some technical concerns with the application of the data. It appears from the results of this report that further plant-specific evaluation will be required.

Attachment 2

December 10, 1999

Dr. William D. Travers
Executive Director for Operations
U.S. Nuclear Regulatory Commission
Washington, D.C. 20555-0001

Dear Dr. Travers:

SUBJECT: PROPOSED RESOLUTION OF GENERIC SAFETY ISSUE-190, "FATIGUE EVALUATION OF METAL COMPONENTS FOR 60-YEAR PLANT LIFE"

During the 468th meeting of the Advisory Committee on Reactor Safeguards, December 2-4, 1999, we reviewed the proposed resolution of Generic Safety Issue (GSI)-190, "Fatigue Evaluation of Metal Components for 60-Year Plant Life." During our review, we had the benefit of discussions with representatives of the NRC staff and of the documents referenced.

RECOMMENDATIONS

- We agree with the staff's proposal that GSI-190 be resolved without any additional regulatory requirements.
- The staff should ensure that utilities requesting license renewal consider the management of environmentally assisted fatigue in their aging management programs.

BACKGROUND

The effects of fatigue for the 40-year initial reactor license period were studied and resolved under GSI-78, "Monitoring of Fatigue Transient Limits for Reactor Coolant System," and GSI-166, "Adequacy of Fatigue Life of Metal Components."

The staff concluded that risk from fatigue failure of components in the reactor coolant pressure boundary was very small for 40-year plant life. In our March 14, 1996 letter, we agreed with the staff's conclusion.

GSI-190 was established to address the residual concerns of GSI-78 and GSI-166 regarding the environmental effects of fatigue on pressure boundary components for 60-years of plant operation. The scope of GSI-190 included design-basis fatigue transients, studying the probability of fatigue failure and its effects on core damage frequency (CDF) of selected metal components for 60-year plant life.

DISCUSSION

Resolution of GSI-190 was based on the results of an NRC-sponsored study performed by the Pacific Northwest National Laboratory (PNNL). In that study, PNNL examined design-basis fatigue transients and the probability of fatigue failure of selected metal components for 60-year plant life and the resulting effects on CDF.

The PNNL study showed that some components have cumulative probabilities of crack initiation and through-wall growth that approach unity within the 40- to 60-year period. The maximum failure rate (through-wall cracks per year) was in the range of 10^{-2} per year, and those failures were associated with high cumulative usage factor locations and components with thinner walls, i.e., pipes more vulnerable to through-wall cracks. There was only a modest increase in the frequency of through-wall cracks in major reactor coolant system components having thicker walls. In most cases, the leakage from these through-wall cracks is small and not likely to lead to core damage. Therefore, the projected increased frequency in through-wall cracks between 40- and 60-years of plant life does not significantly increase CDF. Based on the low contributions to CDF, we agree with the proposed resolution of GSI-190.

Environmentally assisted fatigue degradation should be addressed in aging management programs developed for license renewal. Minimization of leakage is important for operational safety, occupational doses, and for continued economic viability of the plants.

Dr. William J. Shack did not participate in the Committee's deliberations regarding this matter.

Sincerely,

Signed

Dana A. Powers
Chairman

References:

- Memorandum dated November 12, 1999, from Ashok C. Thadani, Director, Office of Nuclear Regulatory Research, NRC, to John T. Larkins, Executive Director, Advisory Committee on Reactor Safeguards, Subject: Generic Safety Issue-190, "Fatigue Evaluation of Metal Components for 60-Year Plant Life."
- Letter dated March 14, 1996, from T. S. Kress, Chairman, Advisory Committee on Reactor Safeguards, to James M. Taylor, Executive Director for Operations, NRC, Subject: Resolution of Generic Safety Issue-78, "Monitoring of Fatigue Transient Limits for the Reactor Coolant System."
- Letter dated October 16, 1995, from T. S. Kress, Chairman, Advisory Committee on Reactor Safeguards, to Shirley Ann Jackson, Chairman, NRC, Subject: Fatigue Action Plan.

IDAHO NATIONAL ENGINEERING LABORATORY

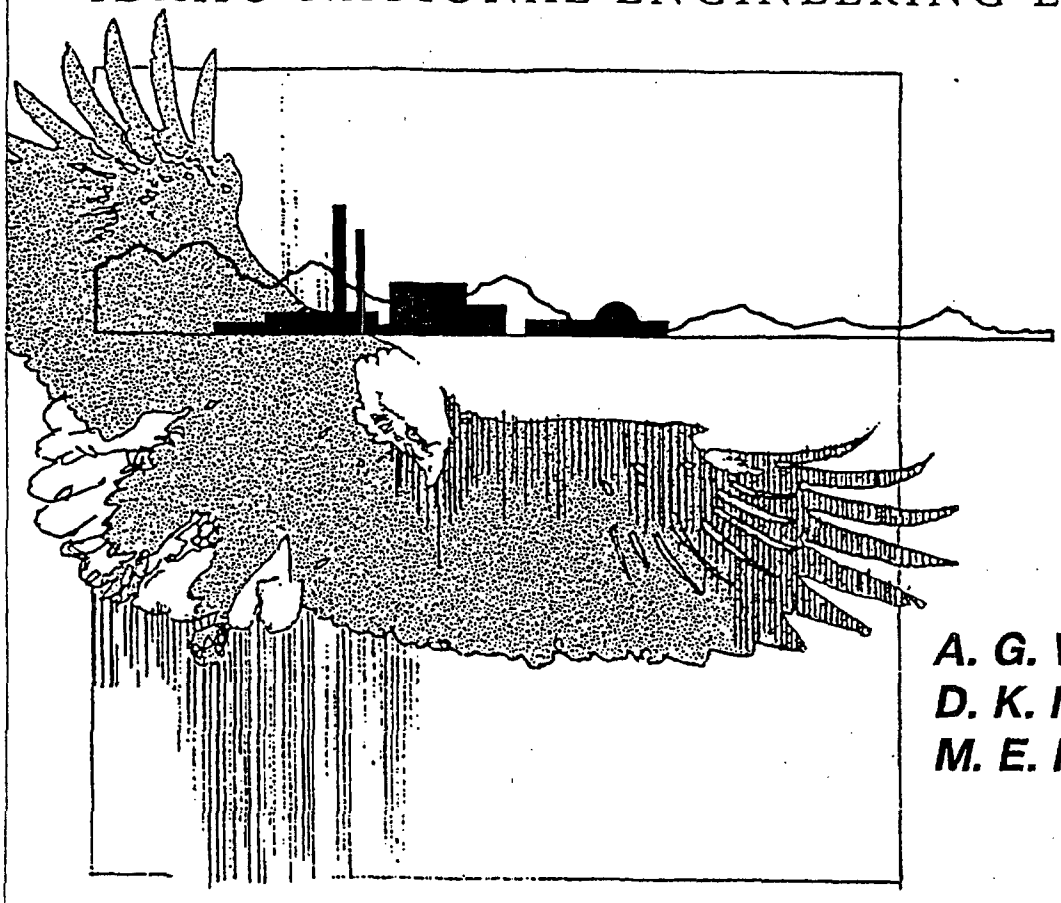

NUREG/CR-6260
INEL-95/0045

February 1995

A. G. Ware
D. K. Morton
M. E. Nitzel

Application of NUREG/CR-5999 Interim Fatigue Curves to Selected Nuclear Power Plant Components

Idaho National Engineering Laboratory

Lockheed Idaho Technologies Company

Work performed under
DOE Contract
No. DE-AC07-94ID13223

NUREG/CR-6260
INEL-95/0045
Distribution Category: R5

Application of NUREG/CR-5999 Interim Fatigue Curves to Selected Nuclear Power Plant Components

A. G. Ware
D. K. Morton
M. E. Nitzel

Manuscript Completed February 1995

Idaho National Engineering Laboratory
Lockheed Idaho Technologies Company
Idaho Falls, Idaho 83415

Prepared for the
Division of Engineering
Office of Nuclear Reactor Regulation
U.S. Nuclear Regulatory Commission
Washington, D.C. 20555
Under DOE Idaho Operations Office
Contract DE-AC07-94ID13223
FIN J2081

ABSTRACT

Recent test data indicate that the effects of the light water reactor (LWR) environment could significantly reduce the fatigue resistance of materials used in the reactor coolant pressure boundary components of operating nuclear power plants. Argonne National Laboratory has developed interim fatigue curves based on test data simulating LWR conditions, and published them in NUREG/CR-5999. In order to assess the significance of these interim fatigue curves, fatigue evaluations of a sample of the components in the reactor coolant pressure boundary of LWRs were performed. The sample consists of components from facilities designed by each of the four U.S. nuclear steam supply system vendors. For each facility, six locations were studied, including two locations on the reactor pressure vessel. In addition, there are older vintage plants where components of the reactor coolant pressure boundary were designed to codes that did not require an explicit fatigue analysis of the components. In order to assess the fatigue resistance of the older vintage plants, an evaluation was also conducted on selected components of three of these plants. This report discusses the insights gained from the application of the interim fatigue curves to components of seven operating nuclear power plants.

CONTENTS

ABSTRACT iii

LIST OF FIGURES viii

LIST OF TABLES ix

EXECUTIVE SUMMARY xix

ACKNOWLEDGEMENTS xxvii

ACRONYMS AND ABBREVIATIONS xxix

1. INTRODUCTION 1-1

2. ASME CODE SECTION III FATIGUE METHODOLOGY 2-1

2.1 Background of ASME Code Fatigue Requirements 2-1

2.1.1 USAS B31.1 and B31.7 2-1
2.1.2 ASME Code 2-2

2.2 Present ASME Code Requirements 2-6

2.2.1 ASME Code NB-3200 Fatigue Analysis Method 2-7
2.2.2 ASME Code NB-3600 Fatigue Analysis Method 2-9
2.2.3 Simplified Elastic-Plastic Multiplier (Ke) 2-10
2.2.4 Thermal Stress Ratchet Check 2-11

3. NUREG/CR-5999 INTERIM FATIGUE CURVES 3-1

3.1 Curve Descriptions 3-1

3.2 Increase in CUF using Interim Curves 3-4

3.3 Interpolation of NUREG/CR-5999 Curves 3-7

3.4 Revised Interim Fatigue Curves 3-12

4. APPROACH 4-1

4.1 Selection of Components for Analysis 4-1

4.2 Application of NUREG/CR-5999 Fatigue Curves 4-1

4.2.1 Interior and Exterior Surfaces 4-1
4.2.2 Cladding 4-2
4.2.3 Life Extension 4-2
4.2.4 Extent of Licensee Calculation Review 4-3
4.2.5 Reporting of Stress Results 4-3
4.2.6 Significant Digits 4-3

4.2.7 High-Cycle Fatigue 4-3
4.2.8 Applicable Temperature and Strain Rate Values 4-3
4.2.9 Fatigue Monitoring 4-4

4.3 Potential Adjustments to Licensees' Calculations that Might Reduce the CUF 4-5

4.4 Examples of Code Changes and Adjustments to Cycles/Transients that Might Increase the CUF in Licensees' Calculations 4-7

5. COMPONENT EVALUATIONS 5-1

5.1 Newer Vintage Combustion Engineering Plant 5-1

5.1.1 Reactor Vessel Shell and Lower Head 5-1
5.1.2 Reactor Vessel Inlet and Outlet Nozzles 5-2
5.1.3 Surge Line 5-4
5.1.4 Charging System Nozzle 5-8
5.1.5 Safety Injection System Nozzle 5-13
5.1.6 Shutdown Cooling Line 5-16
5.1.7 Results and Conclusions 5-18

5.2 Older Vintage Combustion Engineering Plant 5-20

5.2.1 Reactor Vessel Shell and Lower Head 5-20
5.2.2 Reactor Vessel Inlet and Outlet Nozzles 5-21
5.2.3 Surge Line 5-22
5.2.4 Charging Nozzle 5-24
5.2.5 Safety Injection Nozzle 5-27
5.2.6 Shutdown Cooling System Class 1 Piping 5-27
5.2.7 Results and Conclusions 5-30

5.3 B&W Plant 5-31

5.3.1 Reactor Vessel Shell and Lower Head 5-33
5.3.2 Reactor Vessel Inlet and Outlet Nozzles 5-35
5.3.3 Surge Line 5-37
5.3.4 Makeup/High Pressure Injection Nozzle 5-38
5.3.5 Core Flood Nozzle 5-41
5.3.6 Decay Heat Removal System Class 1 Piping 5-42
5.3.7 Results and Conclusions 5-43

5.4 Newer Vintage Westinghouse Plant 5-45

5.4.1 Reactor Vessel Shell and Lower Head 5-47
5.4.2 Reactor Vessel Inlet and Outlet Nozzles 5-47
5.4.3 Surge Line 5-49
5.4.4 Charging Nozzle 5-50
5.4.5 Safety Injection Nozzle 5-54
5.4.6 Residual Heat Removal System Class 1 Piping 5-56
5.4.7 Results and Conclusions 5-58

5.5 Older Vintage Westinghouse Plant 5-62

5.5.1 Reactor Vessel Shell and Lower Head 5-62
5.5.2 Reactor Vessel Inlet and Outlet Nozzles 5-63
5.5.3 Surge Line 5-65
5.5.4 Charging Nozzle 5-66
5.5.5 Safety Injection Nozzle 5-71
5.5.6 Residual Heat Removal System Class 1 Piping 5-76
5.5.7 Results and Conclusions 5-77

5.6 Newer Vintage General Electric Plant 5-79

5.6.1 Reactor Vessel Shell and Lower Head 5-81
5.6.2 Reactor Vessel Feedwater Nozzle 5-84
5.6.3 Reactor Recirculation Piping 5-88
5.6.4 Core Spray Line Reactor Vessel Nozzle and Associated Class 1 Piping 5-92
5.6.5 Feedwater Line Class 1 Piping 5-94
5.6.6 Residual Heat Removal (RHR) Nozzles and Associated Class 1 Piping 5-98
5.6.7 Results and Conclusions 5-99

5.7 Older Vintage General Electric Plant 5-102

5.7.1 Reactor Vessel Shell and Lower Head 5-102
5.7.2 Feedwater Nozzle 5-103
5.7.3 Reactor Recirculation Piping 5-105
5.7.4 Core Spray Line 5-110
5.7.5 RHR Return Line Piping 5-115
5.7.6 Feedwater Piping 5-116
5.7.7 Results and Conclusions 5-118

6. CONCLUSIONS 6-1

6.1 Applications to PWR Plants 6-1

6.2 Applications to BWR Plants 6-3

6.3 CUF Evaluations for Piping Components Designed to the B31.1 Piping Code 6-4

6.4 Overall Conclusion 6-4

7. REFERENCES 7-1

LIST OF FIGURES

2-1. ASME Code carbon and low-alloy steel fatigue curves (ASME, 1992) 2-3

2-2. ASME Code stainless steel and Alloy 600 fatigue curve (ASME, 1992) 2-4

2-3. ASME Code stainless steel and Alloy 600 high-cycle fatigue curves (ASME, 1992) ... 2-5

3-1. Interim fatigue curve for stainless and Alloy 600 steels 3-2

3-2. Interim fatigue curve for carbon and low-alloy steels in low-oxygen water 3-2

3-3. Interim fatigue curve for carbon and low-alloy steels in high-oxygen water at 200°C 3-3

3-4. Interim fatigue curve for carbon and low-alloy steels in high-oxygen water at 250°C 3-3

3-5. Interim fatigue curve for carbon and low-alloy steels in high-oxygen water at 288°C 3-4

3-6. Increase in CUF using NUREG/CR-5999 interim fatigue curve for stainless and Alloy 600 steel 3-5

3-7. Increase in CUF using NUREG/CR-5999 interim fatigue curve for carbon and low-alloy steel in low-oxygen environment 3-5

3-8. Increase in CUF using NUREG/CR-5999 interim fatigue curve for carbon and low-alloy steel in high-oxygen environment at 200°C 3-6

3-9. Increase in CUF using NUREG/CR-5999 interim fatigue curve for carbon and low-alloy steel in high-oxygen environment at 250°C 3-6

3-10. Increase in CUF using NUREG/CR-5999 interim fatigue curve for carbon and low-alloy steel in high-oxygen environment at 288°C 3-7

3-11. Ratio of strain rate cycles at 200°C 3-8

3-12. Ratio of strain rate cycles at 250°C 3-8

3-13. Ratio of strain rate cycles at 288°C 3-9

3-14. Ratio of cycles on 200°C curve to cycles on 250°C curve 3-9

3-15. Ratio of cycles on 200°C curve to cycles on 288°C curve 3-10

3-16. Relationship of strain rate and numbers of cycles 3-10

3-17. Relationship of temperature and numbers of cycles 3-11

3-18. Revised stainless steel interim fatigue design curve (computed from Chopra, 1994) 3-13

3-19. Ratio of revised interim fatigue curve cycles to corresponding ASME Code fatigue curve cycles 3-13

5-1. Shutdown cooling system model isometric view 5-29

5-2. Charging system nozzle finite element model 5-68

5-3. Charging nozzle axisymmetric finite element model 5-69

5-4. Safety injection nozzle finite element model 5-73

5-5. Safety injection nozzle axisymmetric finite element model 5-74

5-6. Residual heat removal system model isometric view 5-78

5-7. BWR/4 recirculation piping system isometric view 5-107

5-8. Comparison of RHR shutdown cooling transients 5-108

5-9. BWR/4 feedwater line with RCIC connection 5-117

LIST OF TABLES

2-1. Values for S (ksi) and N (cycles) [ASME, 1992, Table I-9.0] 2-8

2-2. Values for m and n [ASME, 1992, Table NB-3228.5(b)-1] 2-11

3-1. Applicable figures from NUREG/CR-5999 3-1

5-1. Number of selected design basis transients compared to anticipated number of transients over 40-year license life 5-1

5-2. CUF results for reactor vessel shell/lower head region using NUREG/CR-5999 interim fatigue curve 5-2

5-3. CUF results for reactor vessel inlet nozzle using NUREG/CR-5999 interim fatigue curve 5-3

5-4. CUF results for reactor vessel outlet nozzle using NUREG/CR-5999 interim fatigue curve 5-4

5-5. CUF results for reactor vessel outlet nozzle using NUREG/CR-5999 interim fatigue curve and anticipated cycles 5-5

5-6. CUF results for the surge line using NUREG/CR-5999 interim fatigue curve 5-6

5-7. CUF results for the surge line using NUREG/CR-5999 interim fatigue curve and anticipated cycles 5-7

5-8. Potential for elimination of conservative assumptions to reduce CUF for surge line elbow using NUREG/CR-5999 interim fatigue curve 5-8

5-9. CUF results for the surge line using revised interim fatigue curves and anticipated cycles 5-9

5-10. CUF results for the charging system nozzle forging using NUREG/CR-5999 interim fatigue curve 5-10

5-11. CUF results for the charging system nozzle safe end using NUREG/CR-5999 interim fatigue curve 5-11

5-12. CUF results for the charging system nozzle safe end using NUREG/CR-5999 interim fatigue curve with conservative assumptions removed 5-11

5-13. CUF results for the charging system nozzle safe end using NUREG/CR-5999 interim fatigue curve with conservative assumptions removed and anticipated cycles 5-11

5-14. Potential for elimination of conservative assumptions to reduce CUF for charging nozzle safe end using NUREG/CR-5999 interim fatigue curve 5-12

5-15. CUF results for the charging system nozzle safe end using revised interim fatigue curves with conservative assumptions removed and anticipated cycles 5-13

5-16. CUF results for the safety injection nozzle forging using NUREG/CR-5999 interim fatigue curve 5-14

5-17. CUF results for the safety injection nozzle safe end using NUREG/CR-5999 interim fatigue curve 5-14

5-18. CUF results for the safety injection nozzle forging using NUREG/CR-5999 interim fatigue curve and anticipated cycles 5-15

5-19. CUF results for the safety injection nozzle safe end using NUREG/CR-5999 interim fatigue curve with conservative assumptions removed 5-15

5-20. CUF results for the safety injection nozzle safe end using NUREG/CR-5999 interim fatigue curves with conservative assumptions removed and anticipated cycles 5-15

5-21. CUF results for the safety injection nozzle safe end using revised NUREG/CR-5999 interim fatigue curves with conservative assumptions removed and anticipated cycles 5-16

5-22. CUF results for the shutdown cooling line using NUREG/CR-5999 interim fatigue curve and licensee's design basis stresses 5-17

5-23. CUF results for the shutdown cooling line using NUREG/CR-5999 interim fatigue curve with conservative assumptions removed 5-17

5-24. CUF results for the shutdown cooling line using NUREG/CR-5999 interim fatigue curve with conservative assumptions removed and anticipated cycles 5-17

5-25. CUF results for the shutdown cooling line using revised interim fatigue curves with conservative assumptions removed and anticipated cycles (0.001%/s strain rate) 5-18

5-26. Summary of newer vintage Combustion Engineering plant CUFs 5-19

5-27. Number of selected design basis cycles compared to anticipated number of cycles over 40-year license life 5-21

5-28. CUF results for reactor vessel lower head using NUREG/CR-5999 interim fatigue curve 5-21

5-29. CUF results for reactor vessel inlet nozzle using NUREG/CR-5999 interim fatigue curve 5-22

5-30. CUF results for reactor vessel outlet nozzle using NUREG/CR-5999 interim fatigue curve 5-23

5-31. CUF results for surge line elbow using NUREG/CR-5999 interim fatigue curve 5-23

5-32. CUF results for surge line elbow using NUREG/CR-5999 interim fatigue curve and anticipated cycles 5-24

5-33. Potential for elimination of conservative assumptions to reduce CUF for surge line elbow using NUREG/CR-5999 interim fatigue curve 5-25

5-34. CUF results for surge line elbow using revised interim fatigue curves with conservative assumptions removed and anticipated cycles 5-25

5-35. CUF results for charging nozzle using NUREG/CR-5999 interim fatigue curve 5-26

5-36. CUF results for charging nozzle using NUREG/CR-5999 interim fatigue curve and anticipated cycles 5-26

5-37. CUF results for the charging system nozzle safe end using revised interim fatigue curves with conservative assumptions removed and anticipated cycles 5-27

5-38. CUF results for safety injection nozzle using NUREG/CR-5999 interim fatigue curve 5-28

5-39. CUF results for safety injection nozzle using NUREG/CR-5999 interim fatigue curve and anticipated cycles 5-28

5-40. CUF results for the safety injection nozzle safe end using revised interim fatigue curves with conservative assumptions removed and anticipated cycles 5-28

5-41. CUF results for the shutdown cooling system piping using NUREG/CR-5999 interim fatigue curve 5-30

5-42. CUF results for the shutdown cooling system piping using revised interim fatigue curves 5-31

5-43. Summary of older vintage Combustion Engineering plant CUFs 5-32

5-44. Number of selected design basis cycles compared to anticipated number of cycles over 40-year license life 5-33

5-45. CUF results for reactor vessel lower head using NUREG/CR-5999 interim fatigue curve 5-34

5-46. CUF results for instrumentation penetration weld using NUREG/CR-5999 interim fatigue curve 5-35

5-47. CUF results for instrumentation penetration weld using NUREG/CR-5999 interim fatigue curve and anticipated cycles 5-36

5-48. Potential for elimination of conservative assumptions to reduce CUF for instrumentation penetration weld using NUREG/CR-5999 interim fatigue curve 5-36

5-49. CUF results for instrumentation penetration weld using revised interim fatigue curves with conservative assumptions removed and anticipated cycles 5-36

5-50. CUF results for reactor vessel outlet nozzle using NUREG/CR-5999 interim fatigue curve 5-37

5-51. CUF results for reactor vessel outlet nozzle using NUREG/CR-5999 interim fatigue curve with conservative assumptions removed 5-37

5-52. Potential for elimination of conservative assumptions to reduce CUF for surge line using NUREG/CR-5999 interim fatigue curve 5-39

5-53. CUF results for makeup/HPI nozzle using NUREG/CR-5999 interim fatigue curve 5-39

5-54. CUF results for makeup/HPI nozzle using NUREG/CR-5999 interim fatigue curve and anticipated cycles 5-40

5-55. CUF results for makeup/HPI nozzle using NUREG/CR-5999 interim fatigue curve based on anticipated numbers of cycles and 1992 Code edition Ke 5-40

5-56. Potential for elimination of conservative assumptions to reduce CUF for makeup/high pressure injection nozzle using NUREG/CR-5999 interim fatigue curve 5-41

5-57. CUF results for makeup/HPI nozzle using NUREG/CR-5999 interim fatigue curve based on anticipated numbers of cycles and 1992 Code edition Ke 5-42

5-58. CUF results for core flood nozzle using NUREG/CR-5999 interim fatigue curve 5-43

5-59. CUF results for the decay heat removal system piping using NUREG/CR-5999 interim fatigue curve 5-43

5-60. CUF results for the decay heat removal system piping using NUREG/CR-5999 interim fatigue curve with conservative assumptions removed 5-44

5-61. CUF results for the decay heat removal system piping using NUREG/CR-5999 interim fatigue curve with conservative assumptions removed and anticipated cycles 5-44

5-62. CUF results for the decay heat removal system piping using revised interim fatigue curve with conservative assumptions removed and anticipated cycles 5-45

5-63. Summary of B&W 177 fuel assembly plant CUFs 5-46

5-64. Number of selected design basis cycles compared to anticipated number of cycles over the 40-year license life 5-47

5-65. CUF results for reactor vessel lower head using NUREG/CR-5999 interim fatigue curve 5-48

5-66. CUF results for reactor vessel inlet nozzle using NUREG/CR-5999 interim fatigue curve 5-48

5-67. CUF results for reactor vessel outlet nozzle using NUREG/CR-5999 interim fatigue curve 5-49

5-68. Potential for elimination of conservative assumptions to reduce CUF for surge line hot leg nozzle using NUREG/CR-5999 interim fatigue curve 5-51

5-69. CUF results for charging nozzle using NUREG/CR-5999 interim fatigue curve 5-51

5-70. CUF results for charging nozzle using NUREG/CR-5999 interim fatigue curve with conservative assumptions removed 5-52

5-71. Potential for elimination of conservative assumptions to reduce CUF for charging nozzle using NUREG/CR-5999 interim fatigue curve 5-53

5-72. CUF results for charging nozzle using revised interim fatigue curves with conservative assumptions removed 5-53

5-73. CUF results for safety injection (BIT) nozzle using NUREG/CR-5999 interim fatigue curve 5-54

5-74. CUF results for safety injection (BIT) nozzle using NUREG/CR-5999 interim fatigue curve with conservative assumptions removed 5-55

5-75. CUF results for safety injection (BIT) nozzle using NUREG/CR-5999 interim fatigue curve with conservative assumptions removed and anticipated cycles 5-56

5-76. Potential for elimination of conservative assumptions to reduce CUF for safety injection (BIT) nozzle using NUREG/CR-5999 interim fatigue curve 5-57

5-77. CUF results for safety injection (BIT) nozzle using revised interim fatigue curves with conservative assumptions removed and anticipated cycles 5-57

5-78. CUF results for the residual heat removal system piping using NUREG/CR-5999 interim fatigue curve 5-58

5-79. CUF results for the residual heat removal system piping using NUREG/CR-5999 interim fatigue curve and anticipated cycles 5-59

5-80. Potential for elimination of conservative assumptions to reduce CUF for residual heat removal system using NUREG/CR-5999 interim fatigue curve 5-59

5-81. CUF results for the residual heat removal system piping using revised interim fatigue curve and anticipated cycles 5-60

5-82. Summary of newer vintage Westinghouse plant CUFs 5-61

5-83. Number of selected design basis cycles compared to anticipated number of cycles over 40-year license life 5-62

5-84. CUF results for reactor vessel lower head and shell using NUREG/CR-5999 interim fatigue curve 5-63

5-85. Potential for elimination of conservative assumptions to reduce CUF for reactor vessel lower head/shell using NUREG/CR-5999 interim fatigue curve 5-64

5-86. CUF results for reactor vessel inlet nozzle using NUREG/CR-5999 interim fatigue curve 5-64

5-87. CUF results for reactor vessel outlet nozzle using NUREG/CR-5999 interim fatigue curve 5-65

5-88. Potential for elimination of conservative assumptions to reduce CUF for surge line elbow using NUREG/CR-5999 interim fatigue curve 5-66

5-89. Major charging system transients assumed in the analysis 5-67

5-90. Results for charging nozzle using NB-3200 and NB-3600 methods and ASME Code fatigue curve 5-70

5-91. CUF results for charging nozzle using NUREG/CR-5999 interim fatigue curve 5-72

5-92. CUF results for charging nozzle using revised interim fatigue curve 5-72

5-93. Results for safety injection nozzle using NB-3200 and NB-3600 methods and ASME Code fatigue curve (safety injection/reactor trip) 5-76

5-94. CUF results for safety injection nozzle using NUREG/CR-5999 interim fatigue curve .. 5-77

5-95. CUF results for safety injection nozzle using revised interim fatigue curves 5-77

5-96. CUF results for the residual heat removal system piping using NUREG/CR-5999 interim fatigue curve 5-78

5-97. CUF results for the residual heat removal system piping using revised interim fatigue curve 5-79

5-98. Summary of older vintage Westinghouse plant CUFs 5-80

5-99. Number of selected design basis cycles compared to anticipated number of cycles over 40-year license life 5-81

5-100. CUF results for reactor vessel lower head near CRDM penetration weld using NUREG/CR-5999 interim fatigue curve 5-81

5-101. CUF results for CRDM penetration weld using NUREG/CR-5999 interim fatigue curve 5-82

5-102. CUF results for reactor vessel lower head near CRDM penetration weld using NUREG/CR-5999 interim fatigue curve with conservative assumptions removed 5-82

5-103. CUF results for CRDM penetration weld using NUREG/CR-5999 interim fatigue curve with conservative assumptions removed 5-83

5-104. CUF results for CRDM penetration weld using revised interim fatigue curve with conservative assumptions removed 5-84

5-105. CUF results for reactor vessel feedwater nozzle thermal sleeve using NUREG/CR-5999 interim fatigue curve 5-84

5-106. CUF results for reactor vessel feedwater nozzle safe end using NUREG/CR-5999 interim fatigue curve 5-85

5-107. CUF results for reactor vessel feedwater nozzle thermal sleeve using NUREG/CR-5999 interim fatigue curve and anticipated numbers of cycles 5-86

5-108. Potential for elimination of conservative assumptions to reduce CUF for feedwater nozzle thermal sleeve using NUREG/CR-5999 interim fatigue curve 5-87

5-109. CUF results for reactor vessel feedwater nozzle safe end using NUREG/CR-5999 interim fatigue curve with conservative assumptions removed 5-87

5-110. CUF results for reactor vessel feedwater nozzle safe end using NUREG/CR-5999 interim fatigue curves with conservative assumptions removed and anticipated cycles 5-88

5-111. Potential for elimination of conservative assumptions to reduce CUF for feedwater nozzle safe end using NUREG/CR-5999 interim fatigue curve 5-89

5-112. CUF results for reactor vessel feedwater nozzle thermal sleeve using revised interim fatigue curves 5-89

5-113. CUF results for the recirculation system piping using NUREG/CR-5999 interim fatigue curve 5-90

5-114. CUF results for the recirculation system piping using NUREG/CR-5999 interim fatigue curves 5-91

5-115. Potential for elimination of conservative assumptions to reduce CUF for recirculation system using NUREG/CR-5999 interim fatigue curve 5-92

5-116. CUF results for the recirculation system piping using revised interim fatigue curves ... 5-93

5-117. CUF results for core spray nozzle thermal sleeve using NUREG/CR-5999 interim fatigue curve 5-94

5-118. CUF results for core spray nozzle safe-end extension using NUREG/CR-5999 interim fatigue curve 5-95

5-119. CUF results for core spray nozzle thermal sleeve using NUREG/CR-5999 interim fatigue curve 5-95

5-120. CUF results for core spray nozzle safe-end extension using NUREG/CR-5999 interim fatigue curve with conservative assumptions removed 5-95

5-121. CUF results for core spray nozzle thermal sleeve using revised interim fatigue curves and anticipated cycles 5-95

5-122. CUF results for feedwater line piping using NUREG/CR-5999 interim fatigue curve 5-96

5-123. CUF results for feedwater line piping using NUREG/CR-5999 interim fatigue curve and removing conservative assumptions 5-97

5-124. Potential for elimination of conservative assumptions to reduce CUF for feedwater line piping using NUREG/CR-5999 interim fatigue curve 5-98

5-125. CUF results for the residual heat removal suction line piping using NUREG/CR-5999 interim fatigue curve 5-100

5-126. Potential for elimination of conservative assumptions to reduce CUF for RHR piping using NUREG/CR-5999 interim fatigue curve 5-100

5-127. Summary of newer vintage GE plant CUFs 5-101

5-128. Number of selected design basis cycles compared to anticipated number of cycles over 40-year license life 5-103

5-129. CUF results for reactor vessel shell and lower head using NUREG/CR-5999 interim fatigue curve 5-104

5-130. CUF results for reactor vessel shell and lower head using NUREG/CR-5999 interim fatigue curve with conservative assumptions removed and based on anticipated cycles 5-104

5-131. CUF results for reactor vessel feedwater nozzle using NUREG/CR-5999 interim fatigue curves 5-105

5-132. CUF results for reactor vessel feedwater nozzle using NUREG/CR-5999 interim fatigue curves and anticipated cycles 5-105

5-133. Potential for elimination of conservative assumptions to reduce CUF for feedwater nozzle using NUREG/CR-5999 interim fatigue curve 5-106

5-134. CUF results for recirculation piping system using NUREG/CR-5999 interim fatigue curve 5-110

5-135. CUF results for recirculation piping system using NUREG/CR-5999 interim fatigue curve and anticipated cycles 5-111

5-136. Potential for elimination of conservative assumptions to reduce design CUF for recirculation piping system 5-112

5-137. CUF results for recirculation piping system using revised interim fatigue curves 5-113

5-138. CUF results for core spray nozzle using NUREG/CR-5999 interim fatigue curve 5-113

5-139. CUF results for core spray nozzle safe end using NUREG/CR-5999 interim fatigue curve 5-113

5-140. CUF results for core spray nozzle safe end using NUREG/CR-5999 interim fatigue curve and anticipated cycles 5-114

5-141. Potential for elimination of conservative assumptions to reduce CUF for core spray nozzle safe end using NUREG/CR-5999 interim fatigue curve 5-114

5-142.. CUF results for core spray nozzle safe end using revised interim fatigue curve and anticipated cycles 5-115

5-143. CUF results for RHR piping system using NUREG/CR-5999 interim fatigue curve 5-116

5-144. CUF results for RHR piping system using revised interim fatigue curves 5-116

5-145. CUF results for feedwater piping using NUREG/CR-5999 interim fatigue curves 5-119

5-146. CUF results for feedwater piping using NUREG/CR-5999 interim fatigue curves based on anticipated cycles 5-120

5-147. Potential for elimination of conservative assumptions to reduce design CUF for feedwater piping 5-121

5-148. Summary of older vintage General Electric plant CUFs 5-122

6-1. Summary of component CUFs for 40-year life using NUREG/CR-5999 interim fatigue curves 6-2

EXECUTIVE SUMMARY

ES-1. Introduction

Recent test data indicate that the effects of the light water reactor (LWR) environment could significantly reduce the fatigue resistance of materials used in the reactor coolant pressure boundary components of operating nuclear power plants. The American Society of Mechanical Engineers (ASME) Boiler & Pressure Vessel Code fatigue curves used for the design of these components were based primarily on strain-controlled fatigue tests of small, polished specimens at room temperature in air. Although adjustment factors were applied to the best-fit curves to account for effects such as size, surface finish, environment, and data scatter, some of the recent test data indicate that these factors may not have been sufficiently conservative to account for environmental effects.

In a separate project funded by the United States Nuclear Regulatory Commission (USNRC), the Argonne National Laboratory (ANL) has developed interim fatigue curves based on test data of small, polished specimens cycled to failure in water simulating LWR conditions, and published them in NUREG/CR-5999. In order to assess the significance of the interim fatigue curves in NUREG/CR-5999, fatigue evaluations of a sample of the components in the reactor coolant pressure boundary were performed. The sample consists of components from facilities designed by each of the four U.S. nuclear steam supply system (NSSS) vendors. For each facility, six locations were studied, including two locations on the reactor pressure vessel.

In addition, there are older vintage plants where components of the reactor coolant pressure boundary were designed to codes, such as United States of America Standard (USAS) B31.1, that did not require an explicit fatigue analysis of the components. Since the Code of Federal Regulations currently references the ASME Boiler and Pressure Vessel Code which includes a fatigue evaluation of the components of the reactor coolant pressure boundary (unless certain exemption requirements are met), this has led to a concern regarding the adequacy of the fatigue resistance of these older vintage plants. In order to assess the fatigue resistance of the older vintage plants, an evaluation was also conducted on selected components of these plants. The components selected were the same as in the newer vintage plants. A comparison of the magnitudes of the cumulative usage factors (CUFs) between older and newer vintage plants, and the results of the application of the NUREG/CR-5999 interim fatigue curves to six components in each of the three older vintage plants are presented in this report.

ES-2. ASME Code Section III Fatigue Methodology

In the 1960s Codes and Standards specific to nuclear power plants were developed. Section III, *Nuclear Vessels*, was first issued in 1963 as a separate code. All of the vessel analyses reviewed in this NUREG/CR were performed using the 1965 or later editions of Section III. Prior to 1969, nuclear piping was designed using United States of America Standard (USAS) B31.1; from 1969 to 1971, plants were designed with USAS B31.7-1969 as the standard; and the ASME Code has been used thereafter. The rules of B31.7 were incorporated in NB-3600 of the 1971 edition of Section III.

The ASME Code, Section III, NB-3200 elastic fatigue analysis is applicable to any component, but is generally used exclusively for vessels, fairly frequently for nozzles, but rarely for piping. If neither the elastic or simplified elastic-plastic methods can demonstrate that the ASME Code limits are satisfied, NB-3200 allows a fully plastic analysis. (However, the time and expense needed to perform such an analysis makes this option a last resort.) For Class 1 piping, the ASME Code (Article NB-3600 of Section III) provides for protection against fatigue failures caused by elastic and plastic cycling similar to NB-3200; however, more detailed equations are given leading to a simpler, but generally more conservative, analysis approach.

ES-3. NUREG/CR-5999 Interim Fatigue Curves

The NUREG/CR-5999 figures are very small, use a log-log scale, and contain no background grid. This makes the values very difficult to read from the graphs. Dr. W. J. Shack of ANL supplied us with a spreadsheet with the data points used to construct the interim fatigue curves for use in this project. The spreadsheet values were used to perform the CUF calculations in Section 5 of this report.

In order to assess the increase in the CUF using the interim fatigue curves, values for the numbers of cycles on the ASME Code fatigue curve were divided by the numbers of cycles at corresponding stresses on the interim fatigue curves (using the ANL spreadsheet values). The ASME Code method of interpolating between values was used. The factor of increase depends on the alternating stress intensity. The factor of increase for stainless steel is as high as a factor of 17. For carbon and low-alloy steels in low-oxygen environments, the maximum factor of increase is only about 2.75. For carbon and low-alloy steels in high-oxygen environments at saturated (0.001%/s) strain rates, the maximum factors of increase are about 13, 30, and 55 at temperatures of 200, 250, and 288°C, respectively. The lowest maximum increase of about 3.5 occurs at high strain rates (0.1%/s) at 200°C.

In order to be able to accurately interpolate between the temperature and strain rate values on the interim fatigue curves, studies were carried out to determine appropriate interpolation formulas. The ratios of the numbers of cycles for the three strain rates at the three temperatures on the high-oxygen curves were plotted. In addition, the ratio of the values for the three temperatures at the three strain rates were plotted. From these curves we deduced that interpolation relations can be determined irrespective of alternating stress intensity.

Since the ratios were not dependent on the alternating stress intensity, a value of 55 ksi was chosen to determine the relations between strain rate, temperature, and number of cycles. The logarithms of strain rate and numbers of cycles have a linear relationship, and the temperature and the logarithm of the numbers of cycles are linearly related.

Subsequent to the issue of NUREG/CR-5999, ANL transmitted revised best-estimate fatigue curves for stainless steel (in equation form) to the NRC. The revised curves are strain rate-, temperature-, and material-dependent and differ for Type 316NG and other types of stainless steel. However, none of the stainless steel components investigated as part of this project are Type 316NG stainless steel.

The ANL best-estimate curves were converted to design curves comparable to ASME Code fatigue design curves by reductions of a factor of 1.5 on stress or 20 on cycles, whichever is less. The revised curves increase the CUF by a factor of about 5 (1%/s strain rate) to 11 (0.001 %/s strain rate) over CUFs computed using the ASME Code fatigue design curves. The NUREG/CR-5999 interim fatigue curves increase the CUF by as much as a factor of 17 over the ASME Code design fatigue curves. However, for low strain rates, the revised curves would result in a higher CUF for alternating stress intensities above 90 ksi. The 1%/s strain rate was achieved during tests in which the specimens were loaded by mechanical cycling. It is highly unlikely that such a high strain rate could be achieved during thermal cycling. No strain rates approaching 1%/s were calculated in this study. A 1%/s strain rate corresponds to an equivalent elastic stress rate of 283,000 psi/s.

ES-4. Approach

The components chosen for the evaluation of the five PWR plants [B&W, Combustion Engineering (one older and one newer vintage), and Westinghouse (one older and one newer vintage)] are as follows:

1. Reactor vessel shell and lower head
2. Reactor vessel inlet and outlet nozzles

3. Pressurizer surge line (including hot leg and pressurizer nozzles)

4. Reactor coolant piping charging system nozzle

5. Reactor coolant piping safety injection nozzle

6. Residual heat removal (RHR) system Class 1 piping.

The components chosen for the evaluation of the two BWR plants [General Electric (one older and one newer vintage)] are as follows:

1. Reactor vessel shell and lower head

2. Reactor vessel feedwater nozzle

3. Reactor recirculation piping (including inlet and outlet nozzles)

4. Core spray line reactor vessel nozzle and associated Class 1 piping

5. RHR Class 1 piping

6. Feedwater line Class 1 piping.

For both PWR and BWR plants, these components are not necessarily the locations with the highest design CUFs in the plant, but were chosen to give a representative overview of components that had higher CUFs and/or were important from a risk perspective. For example, the reactor vessel shell (and lower head) was chosen for its risk importance.

NUREG/CR-5999 includes one fatigue curve for stainless steel, but several curves for carbon/low-alloy steels which are based on the sulfur content of the steel and the oxygen level in the coolant. For the five PWR plants, the curves for high-sulfur steel and a low-oxygen environment (typical for PWRs) were used. For the two BWR plants, the curves for high-sulfur steel and a high-oxygen environment were used. The high-oxygen (greater than 100 ppm) environment considered in the selected curves is consistent with the water chemistry in BWRs without hydrogen water chemistry. Neither of the two BWR plants evaluated have used hydrogen water chemistry.

If the CUF for a component exceeded 1.0 using the NUREG/CR-5999 interim fatigue curves, potential changes that could be used to reduce the CUF were sought. In reviewing the licensees' calculations, we found 17 potential changes that could be used to reduce the CUF. Several changes were found from review of the licensees' calculations that might increase the CUF. These mainly consisted of changes to the ASME Code since the edition of record for the plants' licensing bases, and the anticipated numbers of cycles for some transients exceeding the number of design basis cycles.

ES-5. Component Evaluations

The stress results from existing analyses were used to determine revised CUFs based on the NUREG/CR-5999 curves. Since the licensees' design basis analyses were based on the ASME Code of record, it was uneconomical for the licensee to attempt to reduce the CUF to lower and lower values by removing conservative assumptions once the Code requirements were met. Given more funding and time, further calculations could have been performed to reduce the existing stress values by using more realistic loadings or more detailed analysis models. These reduced stresses would result in lower CUFs. Therefore, high CUF values obtained using the NUREG/CR-5999 interim fatigue curves do not reflect the lowest CUF, since in every case where the CUF was greater than 1.0, we have listed one, and in most cases several, steps that could be taken to reduce the CUF by additional analyses and monitoring.

The details of the evaluations for six components for each of the seven plants surveyed are described in Sections 5.1 through 5.7 in the body of the report. It appears that the two most difficult areas to reduce the CUF to lower values are PWR surge lines, which are subject to thermal stratification, and BWR tees joining RHR, recirculation, RCIC, RWCU, feedwater, etc. lines where hot and cold coolant mixing occurs. The results and

conclusions of these evaluations are summarized in ES-6. below.

ES-6. Conclusions

The conclusions from applying the NUREG/CR-5999 interim fatigue curves to the fatigue analyses of seven LWRs (five PWRs and two BWRs) are divided into three parts. Conclusions relating to PWR and BWR plants, and conclusions from comparing plants designed to B31.1 versus plants designed to the ASME Code.

ES-6.1 Applications to PWR plants

1. The anticipated number of cycles are less than the design basis number of cycles for all key transients, notably heatup and cooldown transients and power changes. (For example, the design analyses accounted for load following whereas the plants are being operated as base-loaded.)

2. After removing conservative assumptions and using anticipated numbers of cycles, the CUFs for all the reactor vessel components (shell and lower head, inlet and outlet nozzles) were less than 1.0 for a 40-year life. In two cases, an Alloy 600 instrumentation nozzle and a lower head core support block, the CUFs (1.113 and 1.337, respectively) were slightly above 1.0 for 60 years.

3. The CUFs for the stainless steel surge lines of all five plants exceeded 1.0 for 40 years. The most significant transient for surge lines is thermal stratification which was not accounted for in the original design basis. The surge lines were reanalyzed for fatigue in response to NRC Bulletin 88-11. Fatigue monitoring was used to determine temperature differences and numbers of cycles during times of thermal stratification. More refined analyses to later (circa 1986) editions of the ASME Code, including removal of conservative assumptions, were used by the licensees to reduce the CUF below 1.0 using ASME Code fatigue curves. However, there remain conservative assumptions that could be used to further reduce the CUF. Four of the five analyses used NB-3600 piping methods. A detailed finite analysis of the regions with high CUFs, and, if needed, plastic analyses, could be used to reduce the CUF. The B&W plant's analysis already has incorporated an NB-3200 plastic analysis. Probably the best way to reduce the CUF is more precise monitoring of the individual surge lines. The stratification transients used in the analyses are mainly based on owners group submittals that conservatively define a set of enveloping stratification transients that will apply to several plants.

4. After removing conservative assumptions and using anticipated numbers of cycles, the 40-year CUFs for the stainless steel charging and safety injection nozzles were below 1.0 for 7 of the 10 cases. The other three (two charging and one safety injection nozzle) had CUFs ranging from 1.3 to 4.9 for a 40 year life. The numbers of key transients for these two components (for example, loss of letdown and loss of charging) are not counted on a regular basis as are transient cycles important to overall plant operation (for example, heatups and reactor trips); consequently, it was difficult to estimate anticipated numbers of cycles. It appears that the number and severity of these key cycles are conservative and further studies based on plant operation could be used to reduce the CUF. Based on our results of the CUFs for charging and safety injection nozzles of an older vintage plant using the 1992 ASME Code edition NB-3600 and NB-3200 methods, it appears that by using NB-3200 methods contained in the 1992 ASME Code, the CUFs for all nozzles could be reduced than 1.0.

5. The 40-year CUFs for RHR lines were less than 1.0 for four of the five plants. The fifth plant included cycles for thermal stratification in the RHR line, which were not considered for the other four plants. Excluding thermal stratification, the CUF for the fifth plant would have been compa-

rable to the other four plants. The analysis of the fifth plant used NB-3600 piping methods. A detailed finite analysis using NB-3200 methods, and, if needed, a plastic analysis, could be used to reduce the CUF. Probably the best way to reduce the CUF is fatigue monitoring of the RHR line. The stratification transients may conservatively define a set of enveloping stratification transients or valve leakage.

6. For carbon and low-alloy steel components, the NUREG/CR-5999 interim fatigue curves increased the CUF by an average factor of 2.2 times the design basis CUF. This was before any adjustments based on conservative assumptions removal and anticipated cycles were made. For stainless steel and Alloy 600, the average multiplication factor is 9.2.

ES-6.2 Applications to BWR plants

1. The anticipated number of cycles exceed the design basis numbers of cycles for some transients, notably startup and shutdowns. However, the anticipated number of cycles is less than the design basis number of cycles for other transients such as power changes (the design analyses accounted for load following whereas the plants are being operated as base-loaded.)

2. After removing conservative assumptions and using anticipated numbers of cycles, the CUFs for the reactor vessel shell and lower head were less than 1.0 for 40- and 60-year lives. The core spray nozzle CUF was less than 1.0 for the 40- and 60-year lives of the newer vintage BWR plant, but was greater than 1.0 (2.305) for the older vintage BWR plant for 40 years. Although CUFs for the recirculation nozzles were not calculated using NUREG/CR-5999, the design basis CUFs were 0.002 for the newer vintage plant and 0.300 for the older vintage plant (using very conservative lumped transients). No problem would be expected in reducing the CUFs below 1.0.

3. The 40-year CUF for the feedwater nozzle exceeded 1.0 for both plants. The CUF range was from about 1.9 to 3.2. (The CUF for the thermal sleeve on the BWR/6 plant was about 5). Although we incorporated transient definitions, anticipated cycles, strain rates, and temperatures according to the information available, there remains a great deal of uncertainty concerning these values. There also remain conservative assumptions that could be used to reduce the CUFs. Two studies based on fatigue monitoring of BWR feedwater nozzles in other plants showed that the monitored CUF was a factor of 30 to 50 less than the design basis CUF.

4. The 40-year CUF for the recirculation system is less than 1.0 for the newer vintage BWR, and slightly exceeds 1.0 for 60 years (1.245). The CUF for the older vintage BWR is 3.898. Both CUFs were calculated using NB-3600 methods, and were for tees. Based on our experience with comparing NB-3200 and NB-3600 methods for nozzles, we believe that an NB-3200 analysis and fatigue monitoring would reduce the CUF below 1.0.

5. The CUF for the feedwater lines are 3.688 and 6.980 (at tee locations). The CUF for the tee was calculated using NB-3600 methods. Based on our experience with comparing NB-3200 and NB-3600 methods for nozzles, we believe that an NB-3200 analysis and fatigue monitoring would reduce the CUFs below 1.0.

6. The CUF for the BWR/6 RHR line is 11.26 in a straight run of piping. All transients that contributed to the CUF involved thermal stratification. The analysis used NB-3600 piping methods. A detailed finite analysis using NB-3200 methods, and, if needed, a plastic analysis, could be used to reduce the CUF. Probably the best way to reduce the CUF is more precise monitoring of the RHR line. The stratification transients may con-

servatively define a set of enveloping stratification transients.

ES-6.3 CUF Evaluations for Piping Components Designed to the B31.1 Piping Code

1. The design of PWR components and the transients to which they are subjected to are similar for older and newer vintage plants. An exception is the Westinghouse 3- and 4-loop plants that we studied, which had different safety injection piping configurations. Consequently, we reviewed transients from both the newer vintage Westinghouse and the Combustion Engineering plants to ensure that the transients we used were representative for the older vintage Westinghouse plant.

   The design of some of the BWR systems were not similar for the older vintage (BWR/4) and newer vintage (BWR/6) plants that we reviewed. Several key locations of hot and cold coolant mixing, which on the BWR/4 plant are on piping that would be considered Class 1 today, are included in the Class 2 portions of the BWR/6 piping. We reviewed transients from both a BWR/6 and another BWR/4 plant to ensure that the transients we used were representative for the older vintage BWR plant.

2. While we did not perform additional fatigue evaluations of PWR surge lines because the licensees had already analyzed these lines for fatigue in response to NRC Bulletin 88-11, the results of the fatigue evaluations and CUFs for older and newer vintage plants appear comparable.

3. The charging and safety injection nozzles for one older vintage PWR were analyzed using detailed finite element models (both contained thermal sleeves). The CUF using both the ASME Code and NUREG/CR-5999 curves were less than 1.0.

4. The design basis CUFs for two older vintage PWR RHR lines that we analyzed, including representative transients from other PWRs, were low and comparable to the other PWRs (not including thermal stratification effects).

5. The design basis CUFs for the older vintage BWR plant recirculation, RHR, and feedwater lines that we analyzed, including representative transients from other BWRs, were less than 1.0. The 40-year CUFs using the NUREG/CR-5999 curves were above 1.0 for the recirculation and feedwater lines. The comparable CUFs were above 1.0 for the newer vintage BWR, also, but only about half those computed for the older vintage BWR.

6. The older vintage plants piping typically have thicker walls and larger diameters than do newer vintage plans. This causes higher thermal stresses in the older vintage plants' piping. Thermal stresses were found to be the major type of stress contributor to the CUF. Some stress indices are a function of the pipe diameter and thickness, but this is expected to have only a minor effect on the CUF.

ES-6.4 Overall Conclusion

We were able to show that by removing conservative assumptions and using anticipated numbers of cycles, the CUF could be reduced to below 1.0 for most components, both for older and newer vintage plants. For components which we were not able to reduce the CUF below 1.0, several additional steps that could be taken to further reduce the CUF were listed. The two major remaining steps mentioned were (1) more detailed finite element analyses or (2) fatigue monitoring of the transients. Whereas using ASME Code NB-3200 versus NB-3600 analysis methods will assist with regions of axial thermal gradients, we did not find that the CUF could be reduced when the majority of the stress was caused by radial thermal gradients. A major problem with NB-3200 analyses is that minimal guidance is provided by the ASME Code regarding fatigue strength reduction factors for welds. Analysts typically do not apply fatigue strength reduction factors for welds on nozzles made in

the shop. For field welds, the NB-3600 stress indices can be used, but they may be too conservative. A plastic analysis in which the strains are computed, rather than using the K_e factor to adjust the elastic stresses, will lower the CUF.

The best method to lower the CUF for the few worst locations appears to be fatigue monitoring. For most of the cases where the CUF exceeded 1.0, neither actual numbers of cycles that the plant is experiencing nor the magnitude of temperature differences or thermal shocks were known. Therefore, worst-case design assumptions were used. By using realistic numbers of cycles and severity of transients, we believe that the CUF could be reduced sufficiently without resorting to more detailed analysis methods. However, in some cases, for example where thermal stratification exists, a combination of fatigue monitoring and more refined analyses may be needed.

X.M1 METAL FATIGUE OF REACTOR COOLANT PRESSURE BOUNDARY

Program Description

In order not to exceed the design limit on fatigue usage, the aging management program (AMP) monitors and tracks the number of critical thermal and pressure transients for the selected reactor coolant system components.

The AMP addresses the effects of the coolant environment on component fatigue life by assessing the impact of the reactor coolant environment on a sample of critical components for the plant. Examples of critical components are identified in NUREG/CR-6260. The sample of critical components can be evaluated by applying environmental life correction factors to the existing ASME Code fatigue analyses. Formulae for calculating the environmental life correction factors are contained in NUREG/CR-6583 for carbon and low-alloy steels and in NUREG/CR-5704 for austenitic stainless steels.

As evaluated below, this is an acceptable option for managing metal fatigue for the reactor coolant pressure boundary, considering environmental effects. Thus, no further evaluation is recommended for license renewal if the applicant selects this option under 10 CFR 54.21(c)(1)(iii) to evaluate metal fatigue for the reactor coolant pressure boundary.

Evaluation and Technical Basis

1. ***Scope of Program:*** The program includes preventive measures to mitigate fatigue cracking of metal components of the reactor coolant pressure boundary caused by anticipated cyclic strains in the material.

2. ***Preventive Actions:*** Maintaining the fatigue usage factor below the design code limit and considering the effect of the reactor water environment, as described under the program description, will provide adequate margin against fatigue cracking of reactor coolant system components due to anticipated cyclic strains.

3. ***Parameters Monitored/Inspected:*** The program monitors all plant transients that cause cyclic strains, which are significant contributors to the fatigue usage factor. The number of plant transients that cause significant fatigue usage for each critical reactor coolant pressure boundary component is to be monitored. Alternatively, more detailed local monitoring of the plant transient may be used to compute the actual fatigue usage for each transient.

4. ***Detection of Aging Effects:*** The program provides for periodic update of the fatigue usage calculations.

5. ***Monitoring and Trending:*** The program monitors a sample of high fatigue usage locations. This sample is to include the locations identified in NUREG/CR-6260, as minimum, or propose alternatives based on plant configuration.

6. ***Acceptance Criteria:*** The acceptance criteria involves maintaining the fatigue usage below the design code limit considering environmental fatigue effects as described under the program description.

7. ***Corrective Actions:*** The program provides for corrective actions to prevent the usage factor from exceeding the design code limit during the period of extended operation.

Acceptable corrective actions include repair of the component, replacement of the component, and a more rigorous analysis of the component to demonstrate that the design code limit will not be exceeded during the extended period of operation. For programs that monitor a sample of high fatigue usage locations, corrective actions include a review of additional affected reactor coolant pressure boundary locations. As discussed in the appendix to this report, the staff finds the requirements of 10 CFR Part 50, Appendix B, acceptable to address the corrective actions.

8. ***Confirmation Process:*** Site quality assurance procedures, review and approval processes, and administrative controls are implemented in accordance with the requirements of Appendix B to 10 CFR Part 50. As discussed in the appendix to this report, the staff finds the requirements of 10 CFR Part 50, Appendix B, acceptable to address the confirmation process and administrative controls.

9. ***Administrative Controls:*** See Item 8, above.

10. ***Operating Experience:*** The program reviews industry experience regarding fatigue cracking. Applicable experience with fatigue cracking is to be considered in selecting the monitored locations.

References

NUREG/CR-5704, *Effects of LWR Coolant Environments on Fatigue Design Curves of Austenitic Stainless Steels,* U.S. Nuclear Regulatory Commission, April 1999.

NUREG/CR-6260, *Application of NUREG/CR-5999 Interim Fatigue Curves to Selected Nuclear Power Plant Components,* U.S. Nuclear Regulatory Commission, March 1995.

NUREG/CR-6583, *Effects of LWR Coolant Environments on Fatigue Design Curves of Carbon and Low-Alloy Steels,* U.S. Nuclear Regulatory Commission, March 1998.

NUREG/CR-6583
ANL-97/18

Effects of LWR Coolant Environments on Fatigue Design Curves of Carbon and Low-Alloy Steels

Argonne National Laboratory

U.S. Nuclear Regulatory Commission
Office of Nuclear Regulatory Research
Washington, DC 20555-0001

NUREG/CR-6583
ANL-97/18

Effects of LWR Coolant Environments on Fatigue Design Curves of Carbon and Low-Alloy Steels

Prepared by
O. K. Chopra, W. J. Shack

Argonne National Laboratory

Prepared for
U.S. Nuclear Regulatory Commission

EFFECTS OF LWR COOLANT ENVIRONMENTS ON FATIGUE DESIGN CURVES OF CARBON AND LOW–ALLOY STEELS

by

O. K. Chopra and W. J. Shack

Abstract

The ASME Boiler and Pressure Vessel Code provides rules for the construction of nuclear power plant components. Figures I-9.1 through I-9.6 of Appendix I to Section III of the Code specify fatigue design curves for structural materials. While effects of reactor coolant environments are not explicitly addressed by the design curves, test data indicate that the Code fatigue curves may not always be adequate in coolant environments. This report summarizes work performed by Argonne National Laboratory on fatigue of carbon and low-alloy steels in light water reactor (LWR) environments. The existing fatigue S-N data have been evaluated to establish the effects of various material and loading variables such as steel type, dissolved oxygen level, strain range, strain rate, temperature, orientation, and sulfur content on the fatigue life of these steels. Statistical models have been developed for estimating the fatigue S-N curves as a function of material, loading, and environmental variables. The results have been used to estimate the probability of fatigue cracking of reactor components. The different methods for incorporating the effects of LWR coolant environments on the ASME Code fatigue design curves are presented.

Contents

Executive Summary xiii

Acknowledgments xvii

1 Introduction 1

2 Experimental 5

3 Mechanism of Fatigue Crack Initiation 12

3.1 Formation of Engineering Crack 12

3.2 Environmental Effects 17

4 Overview of Fatigue S-N Data 33

4.1 Air Environment 36

4.1.1 Steel Type 36

4.1.2 Temperature 36

4.1.3 Orientation 36

4.1.4 Strain Rate 37

4.1.5 Cyclic Stress-versus-Strain Behavior 38

4.2 LWR Environments 42

4.2.1 Strain Amplitude 42

4.2.2 Strain Rate 42

4.2.3 Temperature 47

4.2.4 Dissolved Oxygen 50

4.2.5 Sulfur Content in Steel 51

4.2.6 Tensile Hold Period 53

4.2.7 Low Dissolved Oxygen 54

4.2.8 Orientation 55

4.2.9 Temperatures below 150°C 56

5 Statistical Model 58

5.1 Modeling Choices 58

5.2 Least-Squares Modeling within a Fixed Structure 58

5.3 The Model 60

5.4 Distribution of Fatigue Life 61

6 Fatigue Life Correction Factor 65

7 Fatigue S-N Curves for Components 69

7.1 Factors of 2 and 20 70

7.2 Design Fatigue Curves 72

7.3 Significance of Design Curves 76

8 Fatigue Evaluations in LWR Environments 78

9 Summary 82

Nomenclature 86

References 88

Appendix A: Fatigue Test Results A-1

Appendix B: Design Fatigue Curves for LWR Environments B-1

Figures

1. Fatigue S-N data for carbon steels in water 2
2. Fatigue data for carbon and low-alloy steel vessels tested in room-temperature water 4
3. Microstructures of A106-Gr B carbon steel and A533-Gr B low-alloy steel 6
4. Microstructures along fracture planes of A302-Gr B steel specimens with orientations in rolling, transverse, and radial direction 6
5. Configuration of fatigue test specimen 7
6. Schematic diagram of electron-beam-welded bar for machining A302-Gr B fatigue test specimens 7
7. Autoclave system for fatigue tests in water 8
8. Schematic diagram of autoclave system for fatigue tests in water environment 9
9. Loading waveform for variable strain rate tests 10
10. Loading strain applied to specimen gauge section during stroke-controlled tests with a sawtooth waveform 10
11. ECP of platinum during fatigue tests at 288°C as a function of dissolved oxygen in effluent 11
12. ECP of carbon and low-alloy ferritic steels during fatigue tests at 288°C as a function of dissolved oxygen in effluent 12
13. ECP vs. dissolved-oxygen data for carbon and low-alloy steels at 250-290°C 12
14. Two stages of fatigue crack growth in smooth test specimens 13
15. Schematic illustration of plastic blunting process of fatigue crack growth in Stage II 14
16. Growth of cracks in smooth fatigue specimens 15
17. Crack depth plotted as a function of fractional life for carbon and low-alloy steels tested in room-temperature air 15
18. Schematic illustration of short crack behavior 16
19. Photomicrograph of surface crack along longitudinal section of A106-Gr B steel 16

20. SEM photomicrographs of gauge surface of A106-Gr B and A533-Gr B steels tested in different environments at 288°C 18

21. X-ray diffraction results of A533-Gr B steel as a function of dissolved oxygen 19

22. Pitting behavior of A106-Gr B carbon steel and A508-Cl 2 low-alloy steel tested in high-purity water 19

23. Micropits on surface of A106-Gr B carbon steel and A533-Gr B low-alloy steel tested in oxygenated water at 288°C 19

24. Relationship between density of micropits and strain rate 20

25. Environmental effects on formation of fatigue cracks in carbon and low-alloy steels 20

26. Number of cracks along longitudinal section of fatigue specimens tested in different environments 21

27. Nucleation of cracks along slip bands, carbide particles, and ferrite/pearlite phase boundaries of carbon steel fatigue specimen 21

28. Schematic illustration of film rupture/slip dissolution process 23

29. Schematic illustration of hydrogen-induced cracking of low-alloy steels 25

30. Fracture morphology of A106-Gr B carbon steel tested in high-dissolved oxygen water at 288°C and ≈0.4% strain range 27

31. Fracture morphology of A106-Gr B carbon steel tested in simulated PWR water at 288°C and ≈0.75% strain range 28

32. Fracture morphology of A533-Gr B low-alloy steel tested in high-dissolved oxygen water at 288°C and ≈0.4% strain range 29

33. Fracture morphology of A533-Gr B low-alloy steel tested in simulated PWR water at 288°C and ≈0.75% strain range 30

34. Examples of cleavage fracture in A106-Gr B Specimen pulled apart at room temperature after the fatigue test 31

35. Sulfide inclusions on fracture surface of A106-Gr B carbon steel tested in high-dissolved oxygen water at 288°C and ≈0.4% strain range 31

36. Depth of largest crack plotted as a function of fatigue cycles for A533-Gr B low-alloy steel and A106-Gr B carbon steel in air and water environments 32

37. Crack growth rates plotted as a function of crack depth for A533-Gr B low-alloy steel tested in air and water environments 32

38. Photomicrographs of surface cracks along longitudinal sections of A533-Gr B low-alloy steel and A106-Gr B carbon steel in air, simulated PWR environment, and high-dissolved-oxygen water 34

39. Photomicrographs of cracks on gauge surfaces of A533-Gr B low-alloy steel and A106-Gr B carbon steel specimens tested in air, simulated PWR environment, and high-dissolved-oxygen water 35

40. Strain amplitude vs. fatigue life data for carbon and low-alloy steels in air at 288°C 36

41. Strain amplitude vs. fatigue life data for carbon and low-alloy steels in air at room temperature and 288°C 37

42. Effect of material orientation on fatigue life of A302-Gr B low-alloy steel in air at 288°C 37

43. Effect of strain rate and temperature on cyclic stress of carbon and low-alloy steels 39

44. Typical microstructure in A106-Gr B specimen tested at 0.4 %/s strain rate showing immature dislocation walls in three pearlite grains consisting of Fe_3C plates in the ferrite matrix 39

45. Ferrite grain between two pearlite grains in A106-Gr B specimen tested at 0.4 %/s strain rate 40

46. Typical microstructure in A106-Gr B specimen tested at 0.04 %/s strain rate showing a cell structure in ferrite and two pearlite grains 40

47. Formation of dislocation walls in two pearlite grains in A106-Gr B specimen tested at 0.004 %/s strain rate 41

48. Cyclic stress-strain curve for carbon and low-alloy steels at 288°C in air 41

49. Strain amplitude vs. fatigue life data for A533-Gr B and A106-Gr B steels in high-dissolved-oxygen water at 288°C 43

50. Dependence of fatigue life of carbon and low-alloy steels on strain rate 44

51. Fatigue life of A106-Gr B carbon steel at 288°C and 0.75% strain range in air and water environments under different loading waveforms 45

52. Fatigue life of carbon and low-alloy steels tested with loading waveforms where slow strain rate is applied during a fraction of tensile loading cycle 46

53. Change in fatigue life of A333-Gr 6 carbon steel with temperature and DO 47

54. Dependence of fatigue life on temperature for carbon and low-alloy steels in water at two strain rates 49

55. Waveforms for change in temperature during exploratory fatigue tests 49

56. Fatigue life of A333-Gr 6 carbon steel tube specimens under varying temperature, indicated by horizontal bars 50

57. Dependence on DO of fatigue life of carbon steel 51

58. Effect of sulfur content on fatigue life of low-alloy steels in high-dissolved-oxygen water at 288°C 52

59. Effect of strain rate on fatigue life of low-alloy steels with different sulfur contents 52

60. Effect of sulfur content on fatigue life of carbon steels in high-dissolved-oxygen water at 288°C 52

61. Effect of strain rate on fatigue life of A333-Gr 6 carbon steels with different sulfur contents 53

62. Fatigue life of A106-Gr B steel in air and water environments at 288°C, 0.75% strain range, and hold period at peak tensile strain 53

63. Strain amplitude vs. fatigue life data for A106-Gr B and A533-Gr B steels in simulated PWR water at 288°C 54

64. Effect of material orientation on fatigue life of A302-Gr B low-alloy steel in high-dissolved-oxygen water and simulated PWR environments 55

65. Relative fatigue lives of different orientations of A302-Gr B low-alloy steel in high-dissolved-oxygen water and simulated PWR environments 56

66. SEM photomicrograph of fracture surface and longitudinal section of A302-Gr B steel specimen in T2 orientation tested in PWR water at 288°C, ≈0.75% strain range, and slow/fast waveform 57

67. Experimental and predicted fatigue lives of A106-Gr B and A533-Gr B steels in water at temperatures below 150°C 57

68. Fatigue life of A333-Gr 6 carbon steel as a function of dissolved oxygen in water at 100 and 150°C 58

69. Schematic of least-squares curve-fitting of data by minimizing sum of squared Cartesian distances from data points to predicted curve 59

70. Fatigue S-N behavior for carbon and low-alloy steels estimated from model and determined experimentally in air at room temperature 61

71. Experimental data and probability of fatigue cracking in carbon and low-alloy steel test specimens in air 63

72. Experimental data and probability of fatigue cracking in carbon and low-alloy steel test specimens in simulated PWR environments 64

73. Experimental data and probability of fatigue cracking in carbon and low-alloy steel test specimens in high-dissolved-oxygen water 64

74. Experimental fatigue lives and those estimated from statistical and EFD models for carbon and low-alloy steels in simulated PWR water 66

75. Experimental fatigue lives and those estimated from statistical and EFD models for carbon and low-alloy steels in water at temperatures below 150°C 66

76. Experimental fatigue lives and those estimated from statistical and EFD models for carbon and low-alloy steels in high-dissolved-oxygen water 67

77. Dependence on strain rate of fatigue life of carbon steels observed experimentally and that estimated from statistical and EFD models 68

78. Dependence on dissolved oxygen of fatigue life of carbon steels observed experimentally and that estimated from statistical and EFD models 68

79. Adjustment for mean stress effects and factors of 2 and 20 applied to best-fit S-N curves for carbon and low-alloy steels to obtain the ASME Code design fatigue curve 70

80. Fatigue design curves developed from statistical model for carbon and low-alloy steels in air at room temperature and 288°C 73

81. Fatigue design curves developed from statistical model for carbon and low-alloy steels under service conditions where one or more critical threshold values are not satisfied 74

82. Fatigue design curves developed from statistical model for carbon and low-alloy steels under service conditions where all critical threshold values are satisfied 75

83. Probability distribution on fatigue life of carbon and low-alloy steels in air 76

84. Probability of fatigue cracking in low-alloy steel in low-dissolved-oxygen water plotted as a function of cumulative usage factor at different stress levels 77

85. Probability of fatigue cracking in carbon steel in high-dissolved-oxygen water plotted as a function of cumulative usage factor at different stress levels 77

B1. Fatigue design curves developed from statistical model for carbon and low-alloy steels under service conditions in which any one of the critical threshold values is not satisfied B-2

B2. Fatigue design curves developed from statistical model for carbon and low-alloy steels at 200°C in water with ≈0.2 ppm dissolved oxygen B-3

B3. Fatigue design curves developed from statistical model for carbon and low-alloy steels at 250°C in water with ≈0.2 ppm dissolved oxygen B-4

B4. Fatigue design curves developed from statistical model for carbon and low-alloy steels at 288°C in water with ≈0.2 ppm dissolved oxygen B-5

Tables

1. Chemical composition (wt.%) of ferritic steels for fatigue tests..... 5

2. Average room-temperature tensile properties of steels 6

3. Inverse of standard cumulative distribution function 63

4. Factors on cycles and on strain to be applied to mean S-N curve..... 72

5. Fatigue evaluation for SA-508 Cl 1 carbon steel feedwater nozzle safe end for a BWR 80

6. Fatigue evaluation for SA-333 Gr 6 carbon steel feedwater line piping for a BWR..... 80

7. Fatigue evaluation for SA-508 Cl 2 low-alloy steel outlet nozzle for a PWR..... 81

A1. Fatigue test results for A106-Gr B carbon steel at 288°C A-2

A2. Fatigue test results for A533-Gr B low-alloy steel at 288°C A-3

A3. Fatigue test results for A302-Gr B low-alloy steel at 288°C A-4

A4. Results of exploratory fatigue tests in which slow strain rate was applied during only part of tensile-loading cycle A-5

Executive Summary

The ASME Boiler and Pressure Vessel Code Section III, Subsection NB, contains rules for the design of Class 1 components. Figures I-9.1 through I-9.6 of Appendix I to Section III specify the Code design fatigue curves for the applicable structural materials. However, Section III, Subsection NB-3121, of the Code states that effects of the coolant environment on fatigue resistance of a material were not intended to be addressed in these design curves. Therefore, there is uncertainty about the effects of environment on fatigue resistance of materials for operating pressurized water reactor (PWR) and boiling water reactor (BWR) plants, whose primary-coolant-pressure-boundary components were designed in accordance with the Code.

The current ASME Code Section III design fatigue curves were based primarily on strain-controlled fatigue tests of small polished specimens at room temperature in air. Best-fit curves to the experimental test data were lowered by a factor of 2 on stress or a factor of 20 on cycles, whichever was more conservative, to obtain the design fatigue curves. These factors are not safety margins but rather adjustment factors that must be applied to experimental data on specimens to obtain estimates of the lives of components. They were not intended to address the effects of the coolant environment on fatigue life.

Recent fatigue strain vs. life (S-N) data obtained in the U.S. and Japan demonstrate that light water reactor (LWR) environments can have potentially significant effects on the fatigue resistance of materials. Specimen lives in simulated LWR environments can be much shorter than those for corresponding tests in air. Under certain conditions of loading and environment, fatigue lives in water can be up to a factor of 70 shorter than those for the tests in air.

This report summarizes work performed by Argonne National Laboratory on fatigue of carbon and low-alloy ferritic steels in simulated LWR environments. The existing fatigue S-N data, foreign and domestic, for these steels have been evaluated to establish the effects of various material and loading variables on the fatigue life. The influence of reactor environments on the formation and growth of short fatigue cracks is discussed. Statistical methods have been used to develop fatigue S-N curves that include the effects of material, loading, and environmental variables. The results have also been used to estimate the probability of fatigue cracking of reactor components associated with a particular choice of design curve. Several methods for incorporating the effects of LWR coolant environments on the ASME Code fatigue design curves are presented.

Mechanism of Fatigue Crack Initiation

Fatigue life of a material is defined as the number of cycles to form an "engineering" crack, e.g., a 3-mm-deep crack. During cyclic loading, surface cracks, 10 μm or more in length, form quite early in life, i.e., <10% of life even at low strain amplitudes. The fatigue life may be considered to be composed entirely of the growth of these short cracks. Fatigue damage in a material is the current size of the fatigue crack, and damage accumulation is the rate of crack growth. Growth of short fatigue cracks may be divided into three regimes: (a) an initial period that involves growth of microstructurally small cracks that is very sensitive to microstructure and is characterized by a decelerating growth rate, (b) a final period of growth that can be predicted from fracture mechanics methodology and is characterized by

accelerating crack growth rate, and (c) a transition period controlled by a combination of the two regimes.

Tests have been conducted to characterize the formation and growth of short cracks in carbon and low-alloy steels in LWR environments. The results indicate that the decrease in fatigue life of these steels in high-dissolved-oxygen (DO) water is primarily caused by the effects of environment on the growth of short cracks < 100 μm deep. The growth rates of cracks < 100 μm in size in high-DO water are nearly two orders of magnitude higher than those in air. In high-DO water, surface cracks grow entirely as tensile cracks normal to the stress. In air and low-DO water, surface cracks grow initially as shear cracks ≈45° to the stress axis, and then as tensile cracks normal to the stress axis when slip is no longer confined to planes at 45° to the stress axis. The results also suggest that in LWR environments, the growth of short fatigue cracks occurs by anodic dissolution; the growth rates depend on DO level in water and possibly on sulfur content in steel.

Overview of Fatigue S–N Data

In air, the fatigue life of carbon and low-alloy steels depends on steel type, temperature, orientation (rolling or transverse), and strain rate. The fatigue life of carbon steels is a factor of ≈1.5 lower than that of low-alloy steels. For both steels, fatigue life decreases with increase in temperature. Some heats of carbon and low-alloy steels exhibit effects of strain rate and orientation. For these heats, fatigue life decreases with decreasing strain rate. Also, based on the distribution and morphology of sulfides, the fatigue properties in transverse orientation may be inferior to those in the rolling orientation. The data indicate significant heat-to-heat variation; at 288°C, fatigue life may vary by up to a factor of 5 above or below the mean value. The results also indicate that the ASME mean curve for low-alloy steels is in good agreement with the experimental data and that for carbon steels is somewhat conservative.

Environmental effects on fatigue life are significant only when five conditions are satisfied simultaneously, viz., applied strain range, temperature, DO level in water, and sulfur content in steel are above a minimum threshold level, and strain rate is below a critical value. There is little or no difference in susceptibility to environmental degradation of fatigue life of carbon and low-alloy steels. The fatigue life of these steels in air and LWR environments can be estimated from the statistical models presented in this report.

For both steels, the fatigue data indicate threshold values of 150°C for temperature and 0.05 ppm for DO, above which fatigue life may be decreased in LWR environments. The effect of DO content on life saturates at 0.5 ppm. The data also indicate a threshold strain rate of 1%/s, below which fatigue life is decreased in LWR environments; the effect saturates at ≈0.001%/s. Limited data suggest that the threshold strain is either equal to or slightly greater than the fatigue limit of the material. When the threshold conditions for all five parameters are satisfied, fatigue life decreases logarithmically with decreasing strain rate and DO level. Only a moderate decrease in fatigue life is observed in LWR environments when any one of the threshold condition is not satisfied, e.g., at temperatures ≤150°C or in low-DO PWR environments (≤0.05 ppm DO). Under these conditions, life in water is 30–50% lower than that in air.

Statistical Model

The fatigue S-N curves are generally expressed in terms of the Langer equation, which may be used to represent either strain amplitude in terms of life or life in terms of strain amplitude. The parameters of the equation are commonly established through least-squares curve-fitting of the data to minimize the sum of the square of the residual errors for either strain amplitude or fatigue life. A predictive model based on least-squares fit on life is biased for low strain amplitude. The model leads to probability curves that converge to a single value of strain, but the model fails to address the fact that at low strain values, most of the error in life is due to uncertainty associated with either measurement of strain or variation in fatigue limit caused by material variability. On the other hand, a least-squares fit on strain does not work well for higher strain amplitudes. In the present study, statistical models have been developed by combining the two approaches and minimizing the sum of the squared Cartesian distances from the data point to the predicted curve.

The statistical models predict fatigue life of small smooth specimens of carbon and low-alloy steels as a function of various material, loading, and environmental parameters. The functional form and bounding values of these parameters were based upon experimental observations and data trends. The models are recommended for predicted fatigue lives of $\leq 10^6$ cycles. The results indicate that the ASME mean curve for carbon steels is not consistent with the experimental data at strain amplitudes of <0.2%; the mean curve predicts significantly lower fatigue lives than those observed experimentally. The estimated curve for low-alloy steels is comparable with the ASME mean curve. An alternative model, proposed by the Environmental Fatigue Data (EFD) Committee of Japan, for incorporating the effects of LWR environments on fatigue life of carbon and low-alloy steels is also discussed.

The results of a rigorous statistical analysis have been used to estimate the probability of fatigue cracking in smooth fatigue specimens. The results indicate that relative to the mean or 50% probability curve, the 5% probability curve is a factor of ≈2.5 lower in life at strain amplitudes >0.3% and a factor of 1.4–1.7 lower in strain at <0.2% strain amplitudes. Similarly, the 1% probability curve is a factor of ≈3.7 lower in life and a factor of 1.7–2.2 lower in strain.

Fatigue S–N Curves for Components

The design fatigue curves for components have been determined by adjusting the best-fit experimental curve for the effect of mean stress and setting margins of 20 on cycles and 2 on strain. The factor of 20 on cycles is intended to account for the uncertainties in fatigue life associated with material and loading conditions, and the factor of 2 on strain to account for uncertainties in threshold strain caused by material variability. Data available in the literature were reviewed to evaluate the effects of various material, loading, and environmental variables on fatigue life. The results indicate that a factor of at least 10 on cycles and 1.5 on strain is needed to account for the differences and uncertainties in relating the fatigue lives of laboratory test specimens to those of actual components. Design fatigue curves are presented for various LWR service conditions.

The statistical models have been used to interpret the significance of the ASME Code design curves in terms of the implicit probability of initiation associated with the curve. The estimated S-N curves representing 5 and 1% probabilities of fatigue cracking in carbon and

low-alloy steel components in room-temperature air are compared with the ASME Code design fatigue curve. The results indicate that the current design fatigue curve results in a <5% probability of fatigue cracking in LAS components and <1% probability in CS components. The probabilities of fatigue cracking in carbon and low-alloy steel components have also been estimated as a function of cumulative usage factor (CUF) for various service conditions. As expected, the probability of fatigue cracking increases with increasing CUF. For a specific CUF, the probability also depends on the applied stress amplitude. The dependence on stress is relatively weak for high stress levels, but at low stresses the probability is quite sensitive to the stress amplitude. At low stresses, the probability of fatigue cracking is not well characterized by cycle counting, i.e., CUF. Rather, it is controlled by the uncertainty in defining fatigue limit for the material.

Fatigue Evaluations in LWR Environments

Fatigue evaluations are presented for a carbon steel feedwater nozzle safe end and feedwater line piping for a BWR, and for a low-alloy steel outlet nozzle for a PWR vessel. The values of CUF were determined either from the design fatigue curves developed from the statistical model or by applying a fatigue life correction factor that was obtained from the statistical model or the EFD correlations.

The correction factor approach yields higher values of CUF than those obtained from the design fatigue curves. The difference arises because the design curves not only account for the effect of environment but also for the difference between the ASME mean air curve and the statistical model air curve, which better represents the data. For carbon steels, this difference can be significant at stress amplitudes of <180 MPa (<26 ksi). The results also show that for the feedwater nozzle safe end and the feedwater line piping, the BWR environment increases the fatigue usage by a factor of ≈2. For the low-alloy steel outlet nozzle for a PWR, the effect of environment on fatigue usage is insignificant.

Acknowledgments

The authors thank W. F. Burke, T. M. Galvin, D. J. Gavenda, J. L. Smith, J. E. Franklin, and J. Tezak for their contributions to the experimental effort. The authors also thank T. F. Kassner for helpful discussions. This work is sponsored by the Office of Nuclear Regulatory Research, U.S. Nuclear Regulatory Commission, under Job Code W6610-6; Program Manager: Dr. M. B. McNeil.

1 Introduction

The ASME Boiler and Pressure Vessel Code Section III, Subsection NB,[1] which contains rules for the construction of Class 1 components for nuclear power plant, recognizes fatigue as a possible mode of failure in pressure vessel steels and piping materials. Cyclic loadings on a structural component occur because of changes in the mechanical and thermal loadings as the system goes from one load set (e.g., pressure, temperature, moment, and force loading) to any other load set. For each pair of load sets, an individual fatigue usage factor is determined by the ratio of the number of cycles anticipated during the lifetime of the component to the allowable cycles. Figures I-9.1 through I-9.6 of Appendix I to Section III of the Code specify fatigue design curves which define the allowable number of cycles as a function of applied stress amplitude. The cumulative usage factor (CUF) is sum of the individual usage factors. The ASME Code Section III requires that the CUF at each location must not exceed 1.

The Code design fatigue curves were based on strain-controlled tests of small polished specimens at room temperature (RT) in air. In most studies, the fatigue life of a test specimen is defined as the number of cycles for the tensile stress to drop 25% from its peak value, which corresponds to a ≈3-mm-deep crack. Consequently, fatigue life N represents the number of cycles required to initiate a crack ≈3 mm deep. The best-fit curves to the experimental data were expressed in terms of the Langer equation[2] of the form

$$\varepsilon_a = B(N)^{-b} + A, \tag{1.1}$$

where A, B, and b are parameters of the model (Eq. 1.1 may be written in terms of stress amplitude S_a instead of strain amplitude ε_a, where stress amplitude is the product of strain amplitude and elastic modulus, i.e., $S_a = E\,\varepsilon_a$). The design fatigue curves were obtained by decreasing the best-fit curves by a factor of 2 on stress or 20 on cycles, whichever was more conservative, at each point on the best-fit curve. As described in the Section III criteria document, these factors were intended to account for the differences and uncertainties in relating the fatigue lives of laboratory test specimens to those of actual reactor components. The factor of 20 on cycles is the product of three separate subfactors: 2 for scatter of data (minimum to mean), 2.5 for size effects, and 4 for surface finish, atmosphere, etc.[3] "Atmosphere" was intended to reflect the effects of an industrial environment rather than the controlled environment of a laboratory. The factors of 2 and 20 are not safety margins but rather conversion factors that must be applied to the experimental data to obtain reasonable estimates of the lives of actual reactor components. They were not intended to address the effects of the coolant environment on fatigue life.

Subsection NB-3121, of Section III of the Code states that the data on which the fatigue design curves (Figs. I-9.1 through I-9.6) are based did not include tests in the presence of corrosive environments that might accelerate fatigue failure. Article B-2131 in Appendix B to Section III states that the owner's design specifications should provide information regarding any reduction to fatigue design curves necessitated by environmental conditions. Recent fatigue strain-vs.-life (S-N) data illustrate potentially significant effects of light water reactor (LWR) coolant environments on the fatigue resistance of carbon steels (CSs) and low-alloy steels (LASs),[4-14] as well as of austenitic stainless steels (SSs).[15,16] Under certain conditions of loading and environment, fatigue lives of carbon steels can be a factor of 70 lower in the

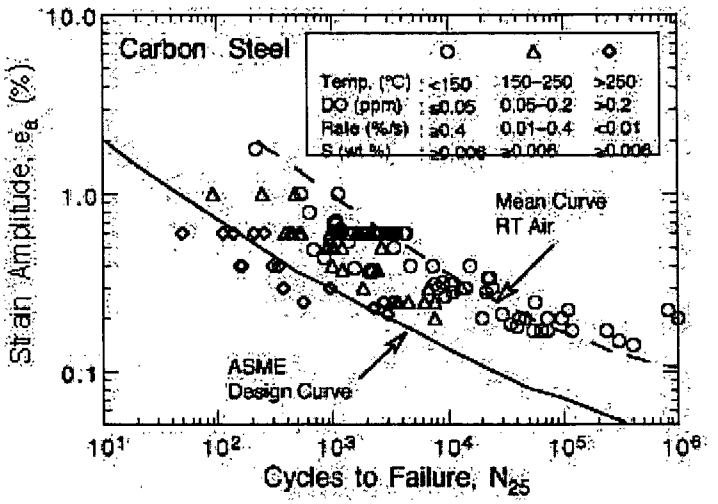

Figure 1. Fatigue S-N data for carbon steels in water

environment than those in air (Fig. 1). Therefore, the margins in the ASME Code may be less conservative than originally intended.

Experience with operating nuclear plants worldwide reveals that many failures may be attributed to fatigue. Examples of such failures include emergency core cooling system (ECCS) or residual heat removal (RHR) system (USNRC Bulletin No. 88-08), pressurizer surge lines (USNRC Bulletin No. 88-11), pressurized water reactor (PWR) feedwater lines (USNRC Information Notice No. 79-13), boiling water reactor (BWR) pressure vessels (USNRC Information Notice No. 90-29), PWR steam generator vessels (USNRC Information Notice No. 90-04), and steam generator feedwater distribution piping (USNRC Information Notice No. 91-19 and No. 93-20). These failures may be classified into three categories: thermal fatigue caused by thermal stratification, cycling, and striping loadings; mechanical fatigue due to vibratory loading; and corrosion fatigue resulting from the exposure to corrosive environment. Significant thermal loadings due to stratification were not included in the original design basis analysis. Some fatigue sensitive locations are routinely monitored in nuclear power plants worldwide to better define the transients and assess CUF more accurately. Occurrences of mechanical-vibration- and thermal-fluctuation-induced fatigue failures in LWR plants in Japan have also been documented.[17]

In 1991, the U. S. Nuclear Regulatory Commission (NRC) issued a draft Branch Technical Position (BTP) for fatigue evaluation of nuclear plant components for license renewal. The BTP raised the concern regarding adequacy of the ASME Code in addressing environmental effects on fatigue resistance of materials for operating PWRs and BWRs, whose primary-coolant-pressure-boundary components are constructed as specified in Section III of the Code. A program was initiated at Argonne National Laboratory (ANL) to provide data and models for predicting environmental effects on fatigue design curves and an assessment of the validity of fatigue damage summation in piping and vessel steels under load histories typical of LWR components. The results have been presented in several progress reports.[18-25] Based on the S-N data available at that time, interim fatigue design curves that address environmental effects on fatigue life of carbon and low-alloy steels and austenitic stainless steels (SSs) have been proposed.[26] More rigorous statistical models have been developed[27,28]

based on a larger data base than that which was available when the interim design curves were developed. Results of the statistical analysis have been used to interpret S-N curves in terms of the probability of fatigue cracking. The Pressure Vessel Research Council (PVRC) has also been compiling and evaluating fatigue S-N data related to the effects of LWR coolant environments on the fatigue life of pressure boundary materials; these results have been summarized by Van Der Sluys and Yukawa.[29]

In 1993, the Commission directed the NRC staff to treat fatigue as potential safety issue within the existing regulatory process for operating reactors. The staff developed a Fatigue Action Plan (FAP) to resolve three principal issues: (a) adequacy of fatigue resistance of older vintage plants designed to the United States of America Standard (USAS) B31.1 Code that did not require an explicit fatigue analysis of components, (b) the effect of LWR environments on the fatigue resistance of primary pressure boundary materials, and (c) the appropriate corrective action required when the Code fatigue allowable limits have been exceeded, i.e., CUF is >1. The Idaho National Engineering Laboratory (INEL) assessed the significance of the interim fatigue design curves by performing fatigue evaluations of a sample of components in the reactor coolant pressure boundary.[30] In all, six locations were evaluated from facilities designed by each of the four U.S. nuclear steam supply system (NSSS) vendors. Selected components from older vintage plants designed using the B31.1 Code were also included in the evaluation. An assessment of risk to reactor coolant pressure boundary components from failure due to fatigue was performed under Generic Safety Issue (GSI) 78, "Monitoring of Fatigue Transient Limits for the Reactor Coolant System." On the basis of these studies, it was concluded* that no immediate action is necessary to deal with fatigue issues addressed in the FAP. The risk study indicated that a fatigue failure of piping is not a significant contributor to the core-melt frequency. While fatigue cracks may occur, they may not propagate to failure and, even if failure did occur, safety systems, such as emergency core cooling system (ECCS), mitigate the consequences. On the basis of the risk assessment, a backfit to incorporate environmental effects in the analysis of fatigue in operating plants could not be justified.

The types and extent of conservatisms present in the ASME Section III fatigue evaluations and the effects of LWR environments on fatigue margins were assessed in a study by the Structural Integrity Associates, Inc., under contract to Sandia National Laboratories for the U.S. Department of Energy and in cooperation with the Electric Power Research Institute (EPRI).[31] A review of numerous stress reports indicated a substantial amount of conservatism in many existing component fatigue evaluations. The sources of conservatism include design transients considerably more severe than those experienced in service, grouping of transients, bounding heat transfer and stress analysis, and simplified elastic-plastic analysis. Environmental effects on two components, the BWR feedwater nozzle/safe end and PWR steam generator feedwater nozzle/safe end, known to be affected by severe thermal transients, were also investigated in the study. It was concluded that the reductions in fatigue life due to environmental effects (factors of up to 40 and 22 for PWR and BWR nozzles, respectively) are more than offset by the margins in fatigue life (≈60 and 90, respectively, for PWR and BWR nozzles) associated with typical ASME Code fatigue evaluations. These margins were defined as the ratio of CUFs based on the mean experimental S-N curve and the Code design fatigue curve, i.e., no allowance was made for any difference between the fatigue life of laboratory specimens and components due to the effects of mean stress, loading history, or component

* Policy Issue, SECY-95-245, Completion of the Fatigue Action Plan, Sept. 25, 1995.

size and geometry. As discussed earlier, the factors of 2 on stress and 20 on cycles should not be considered as safety margins but rather conversion factors that are required to obtain reasonable estimates of the lives of actual reactor components.

The overall conservatism in ASME Code fatigue evaluation procedures have also been demonstrated in fatigue tests on piping welds and components.[32] In air, the margins on the number of cycles to failure for elbows and tees were 118–2500 and 123–1700, respectively, for carbon steels, and 47–170 and 25–322, respectively, for stainless steels. The margins for girth butt welds were significantly lower, e.g., 14–128 and 6–76, respectively, for carbon steels and stainless steels. In these tests on welds and components, the fatigue life was expressed as the number of cycles for the crack to penetrate through the wall, which ranged from 6–18 mm (0.237–0.719 in.). The fatigue design curves represent number of cycles to form a 3-mm-deep crack. Consequently, depending on the wall thickness, the actual margins to failure may be lower by more than a factor of 2.

In addition, fatigue tests conducted on vessels at Southwest Research Institute for the PVRC[33] show that ≈5-mm-deep cracks can form in carbon and low-alloy steels very close to the values predicted by the ASME Code design curve, Fig. 2. The tests were performed on 0.914 m (36 in.)-diameter vessels with a 19 mm (0.75 in.) wall in room-temperature water. These results demonstrate clearly that the current Code design curves do not necessarily guarantee any margin of safety. However, a new nonmandatory Appendix to Section XI has been developed to account for environmental effects.

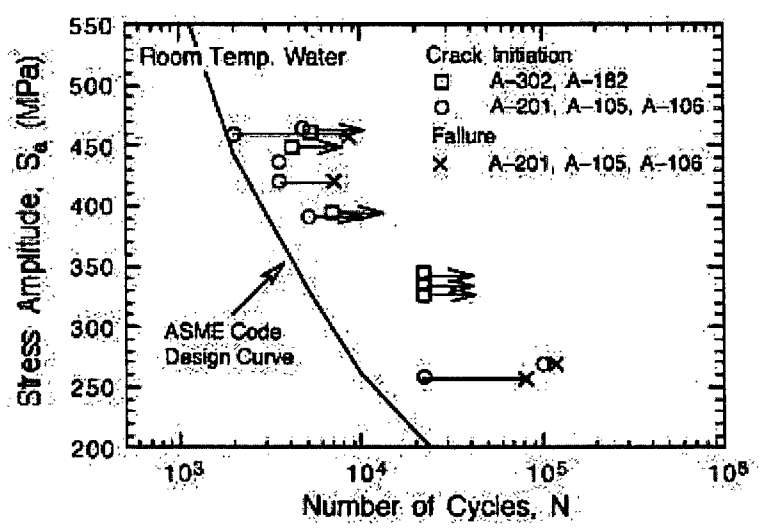

Figure 2. Fatigue data for carbon and low-alloy steel vessels tested in room-temperature water

This report summarizes work performed by ANL on fatigue of carbon and low-alloy ferritic steels in simulated LWR environments. The existing fatigue S-N data, foreign and domestic, for these steels have been evaluated to establish the effects of various material and loading variables on the fatigue life. The influence of reactor environments on the formation and growth of short fatigue cracks is discussed. Correlations have been developed for estimating the fatigue S-N curves as a function of material, loading, and environmental variables. Several

methods for incorporating the effects of LWR coolant environments in fatigue design and analysis are presented.

2 Experimental

Low-cycle fatigue tests have been conducted on A106-Gr B and A333-Gr 6 carbon steels and A533-Gr B and A302-Gr B low-alloy steels with MTS closed-loop electrohydraulic machines. The A106-Gr B material was obtained from a 508-mm-diameter, schedule 140 pipe fabricated by the Cameron Iron Works of Houston, TX. The A333-Gr 6 material was supplied by the Ishikawajima-Harima Heavy Industries Co. (IHI) of Japan and was obtained from a 436-mm-diameter x 36-mm-wall pipe fabricated by Sumitomo Metal Industries, Ltd. The A533-Gr B material was obtained from the lower head of the Midland reactor vessel, which was scrapped before the plant was completed. The A302-Gr B low-alloy steel had been used in a previous study of the effect of temperature and cyclic frequency on fatigue crack growth behavior in a high-temperature aqueous environment at the Bettis Atomic Power Laboratory.[34] The material showed increased crack growth rates (CGRs) in simulated PWR water at 243°C. The chemical compositions and heat treatments of the materials are given in Table 1, and the average room-temperature tensile properties are given in Table 2.

Microstructures of the A106-Gr B carbon steel and A533-Gr B low-alloy steel are shown in Fig. 3. The A106-Gr B carbon steel consists of pearlite and ferrite, and A533-Gr B low-alloy steel contains tempered bainite plus ferrite. Figure 4 shows microstructures of the A302-Gr B steel along three orientations, e.g., rolling (R), transverse (T), and radial (T2) directions.* The structure consists primarily of tempered bainite and ferrite. However, the morphology of sulfides in the three orientations is significantly different.

Table 1. Chemical composition (wt.%) of ferritic steels for fatigue tests

Material	Source	C	P	S	Si	Cr	Ni	Mn	Mo
Carbon Steel									
A106-Gr B[a]	ANL	0.29	0.013	0.015	0.25	0.19	0.09	0.88	0.05
	Supplier	0.29	0.016	0.015	0.24	-	-	0.93	-
A333-Gr 6[b]	IHI (Ref. 8)	0.21	0.016	0.012	0.31	-	-	1.14	-
Low-Alloy Steel									
A533-Gr B[c]	ANL	0.22	0.010	0.012	0.19	0.18	0.51	1.30	0.48
	Supplier	0.20	0.014	0.016	0.17	0.19	0.50	1.28	0.47
A302-Gr B[d]	Bettis (Ref. 34)	0.21	0.021	0.027	0.22	0.14	0.23	1.34	0.51
	Supplier	0.19	0.015	0.027	0.21	-	-	1.17	0.48

[a] 508-mm O.D. schedule 140 pipe fabricated by Cameron Iron Works, Heat J-7201. Actual heat treatment not known.
[b] 436-mm O.D. 36-mm wall pipe fabricated by Sumitomo Metal Industries, Ltd. Austenitized at 900°C for 1/2 h and air cooled.
[c] 162-mm thick hot-pressed plate from Midland reactor lower head. Austenitized at 871-899°C for 5.5 h and brine quenched; then tempered at 649-663°C for 5.5 h and brine quenched. The plate was machined to a final thickness of 127 mm. The inside surface was inlaid with 4.8-mm weld cladding and stress relieved at 607°C for 23.8 h.
[d] 102-mm thick plate. Austenitized at 899-927°C for 4 h, water quenched to 538°C, and air cooled; tempered at 649-677°C; then stress relieved 621-649°C for 6 h (6 cycles).

*The three orientations are represented by the direction that is perpendicular to the fracture plane. Both transverse and radial directions are perpendicular to the rolling direction but the fracture plane is across the thickness of the plate in transverse orientation, and parallel to the plate surface in radial orientation.

Table 2. Average room-temperature tensile properties of steels

Material	Reference[a]	Yield Stress (MPa)	Ultimate Stress (MPa)	Elongation %)	Reduction in Area (%)
Carbon Steel					
A106-Gr B	ANL	301	572	23.5	44.0
A333-Gr 6	IHI (8)	383	549	35.0	-
Low-Alloy Steel					
A533-Gr B	ANL	431	602	27.8	66.6
A302-Gr B	Bettis (34)	389	552	-	-

[a] Reference number given within parentheses.

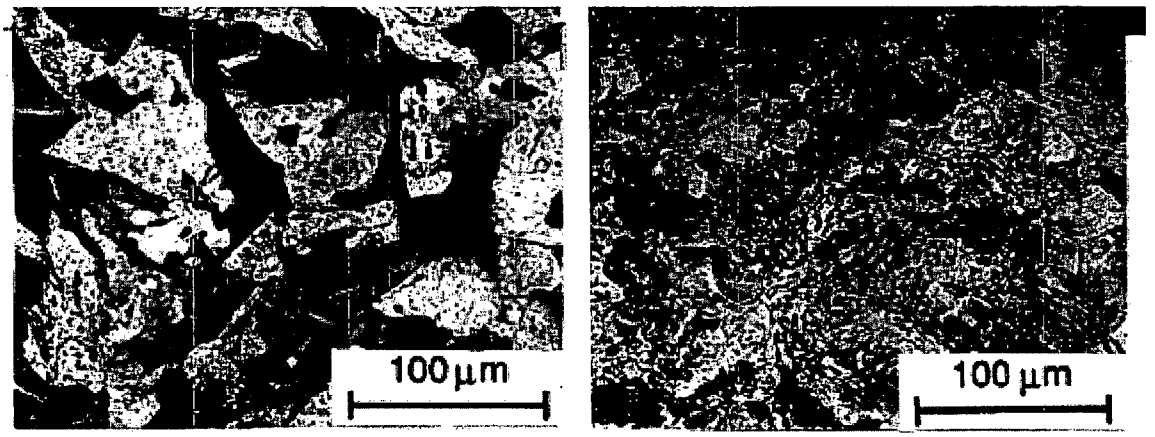

(a) (b)

Figure 3. Microstructures of (a) A106-Gr B carbon steel and (b) A533-Gr B low-alloy steel

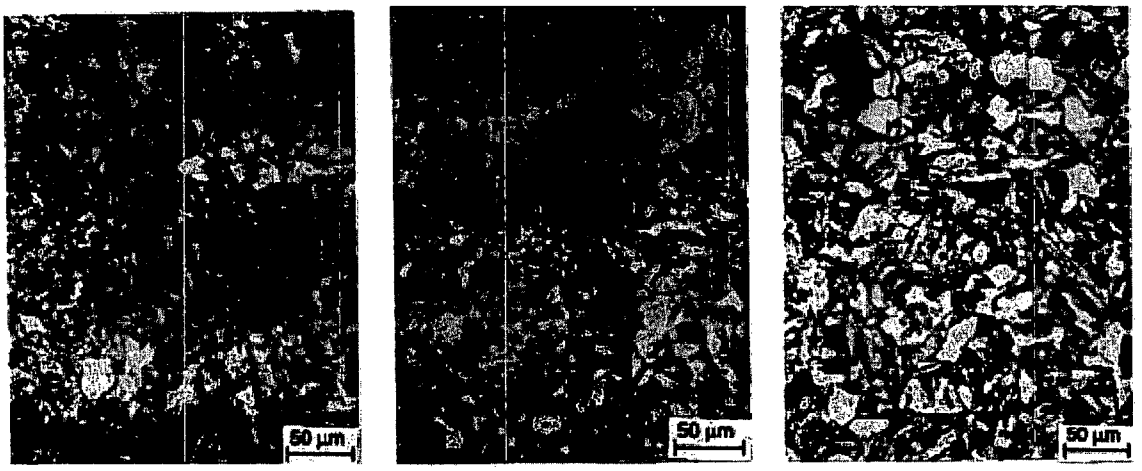

(a) (b) (c)

Figure 4. Microstructures along fracture planes of A302-Gr B steel specimens with orientations in (a) rolling, (b) transverse, and (c) radial direction

Smooth cylindrical specimens with 9.5-mm diameter and 19-mm gauge length were used for the fatigue tests (Fig. 5). Unless otherwise specified, the gauge section of the specimens was oriented along the axial directions of the carbon steel pipes and along the rolling direction for low-alloy steel plates. The test specimens for A302-Gr B steel were machined from a composite bar fabricated by electron-beam welding two 19.8-mm-diameter, 137-mm-long bars of A533-Gr B steel on each side of an 18.8-mm-diameter, 56-mm-long section of A302-Gr B steel (Fig. 6). Thus, the gauge length and shoulders of the specimen were A302-Gr B and the grip region was A533-Gr B steel. After welding, the composite bar was stress relieved at 650°C for 6 h. Specimens of A302-Gr B steel were also fabricated in the transverse and radial orientations. The gauge length of all specimens was given a 1-μm surface finish in the axial direction to prevent circumferential scratches that might act as sites for crack initiation.

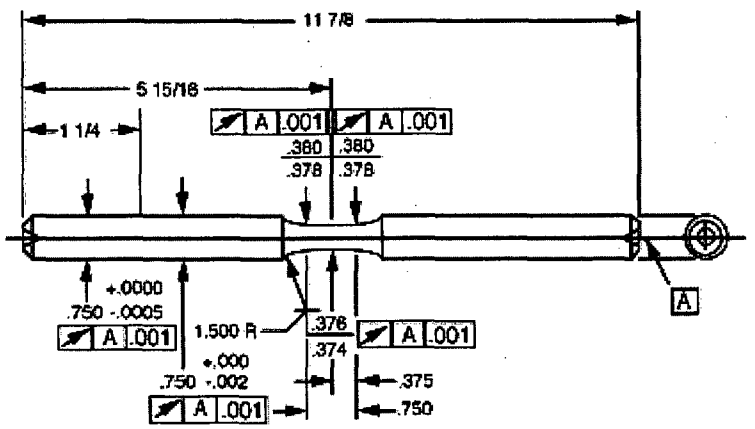

Figure 5. Configuration of fatigue test specimen (all dimensions in inches)

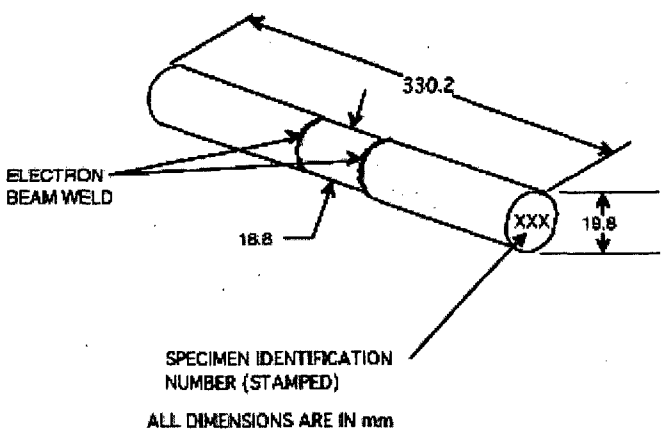

Figure 6. Schematic diagram of electron-beam-welded bar for machining A302-Gr B fatigue test specimens

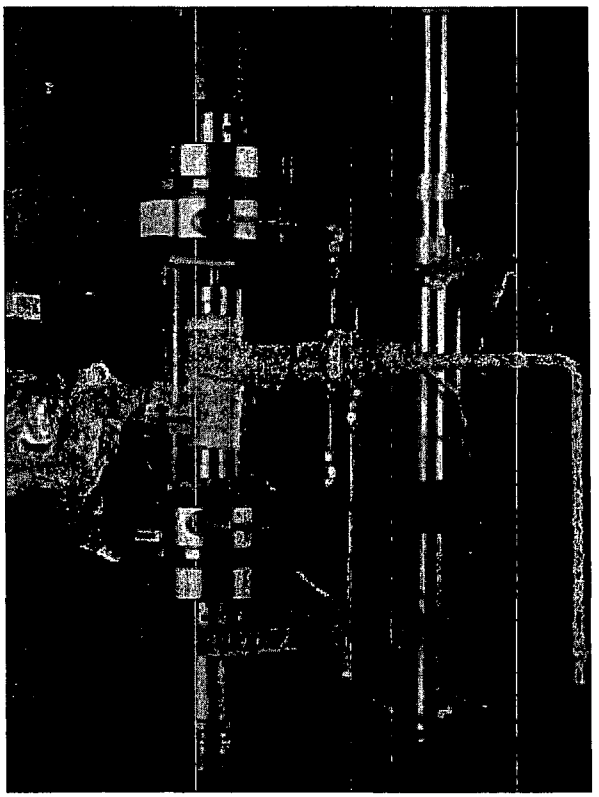

Figure 7.
Autoclave system for fatigue tests in water

Tests in water were conducted in a small autoclave (shown schematically in Fig. 8) with an annular volume of 12 mL (Fig. 7). The once-through system consists of a 132-L supply tank, Pulsafeeder™ pump, heat exchanger, preheater, and autoclave. Water is circulated at a rate of ≈10 mL/min and a system pressure of 9 MPa. The autoclave is constructed of Type 316 SS and contains a titanium liner. The supply tank and most of the low-temperature piping are Type 304 SS; titanium tubing is used in the heat exchanger and for connections to the autoclave and electrochemical potential (ECP) cell. An Orbisphere meter and CHEMetrics™ ampules were used to measure the DO concentrations in the supply and effluent water. The redox and open-circuit corrosion potentials were monitored at the autoclave outlet by measuring ECPs of platinum and an electrode of the test material, respectively, against a 0.1 M KCl/AgCl/Ag external (cold) reference electrode. The measured ECPs, $E_{(meas)}$ (mV), were converted to the standard hydrogen electrode (SHE) scale, $E_{(SHE)}$ (mV), by the polynomial expression[35]

$$E_{(SHE)} = E_{(meas)} + 286.637 - 1.0032(\Delta T) + 1.7447\times10^{-4}(\Delta T)^2 - 3.03004\times10^{-6}(\Delta T)^3, \quad (2.1)$$

where ΔT(°C) is the temperature difference of the salt bridge in a 0.1 M KCl/AgCl/Ag external reference electrode (i.e., the test temperature minus ambient temperature).

The DO level in water was established by bubbling nitrogen that contains 1-2% oxygen through deionized water in the supply tank. The deionized water was prepared by passing purified water through a set of filters that comprise a carbon filter, an Organex-Q filter, two ion exchangers, and a 0.2-mm capsule filter. Water samples were taken periodically to

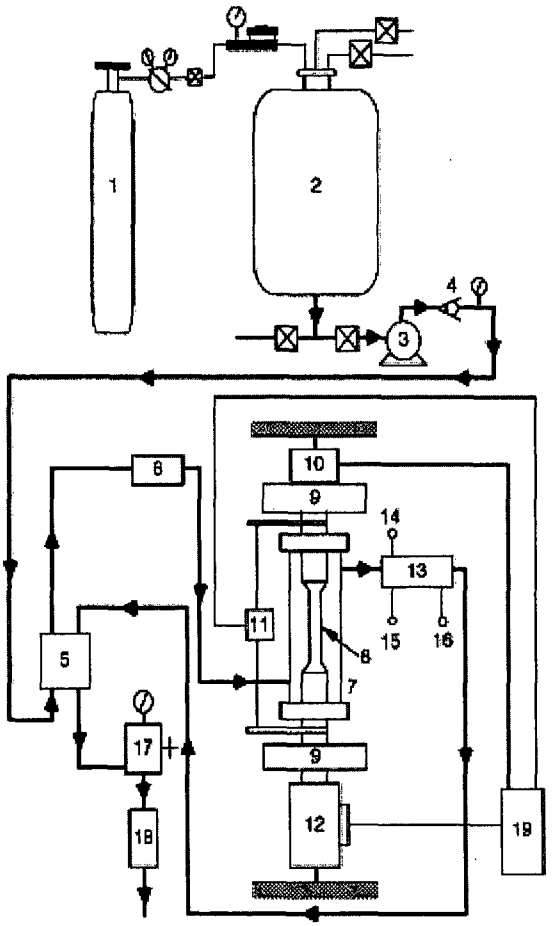

1. Cover-gas supply tank
2. Water supply tank
3. Pulsafeeder high-pressure pump
4. Check valve
5. Heat exchanger
6. Preheat exchanger
7. Pipe autoclave
8. Fatigue test specimen
9. MTS hydraulic collet grips
10. MTS load cell
11. Displacement LVDT
12. MTS hydraulic actuator
13. ECP cell
14. Platinum electrode
15. Specimen electrode
16. Reference electrode
17. Mity Mite™ back-pressure regulator
18. Orbisphere dissolved-oxygen meter
19. MTS electrohydraulic controls

Figure 8. Schematic diagram of autoclave system for fatigue tests in water environment

measure pH, resistivity, and DO concentration. After the desired concentration of DO was achieved, the nitrogen/oxygen gas mixture in the supply tank was maintained at a 20-kPa overpressure. After an initial transition period during which an oxide film develops on the fatigue specimen, both the DO level and the ECP in the effluent water remained constant during the test. Although the difference in the DO levels between the feedwater and the effluent water was 0.10-0.35 ppm, most of the decrease in DO occurred across the preheater, i.e., item 6 in Fig. 8. The difference between the inlet and outlet of the autoclave was ≈0.02 ppm. Test conditions were described in terms of the DO in effluent water.

Simulated PWR water was obtained by dissolving boric acid and lithium hydroxide in 20 L of deionized water before adding the solution to the supply tank. The DO in the deionized water was reduced to <10 ppb by bubbling nitrogen through the water. A vacuum was drawn on the tank cover gas to speed deoxygenation. After the DO was reduced to the desired level, a 34-kPa overpressure of hydrogen was maintained to provide ≈2 ppm dissolved hydrogen (or ≈23 cc/kg) in the feedwater.

The tests were conducted with fully reversed axial loading (i.e., strain ratio R = -1) and a triangular or sawtooth waveform. The strain rate for the triangular wave and fast-loading half

of the sawtooth wave was 0.4%/s. Tests were also conducted with a hold period at peak tensile strain and with variable strain rate. The loading waveform for the variable strain rate tests is shown in Fig. 9. Tests were conducted with up to three different strain rates during the tensile-loading cycle. The strain ranges at which the strain rates were changed are designated as ε_{T1} and ε_{T2} (measured from peak compressive strain). The strain rates for the three segments are designated $\dot{\varepsilon}_{T1}$, $\dot{\varepsilon}_{T2}$, and $\dot{\varepsilon}_{T3}$, respectively.

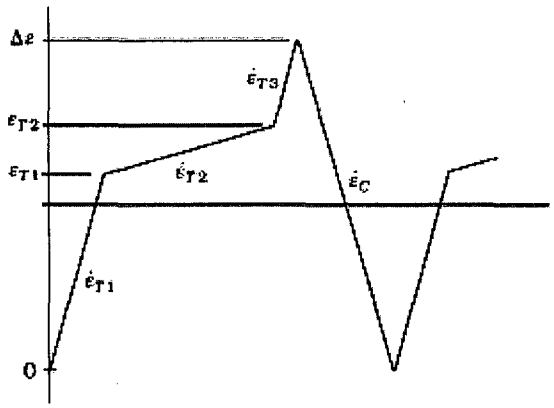

Figure 9.
Loading waveform for variable strain rate tests

The tests in water were performed under stroke control, where the specimen strain was controlled between two locations outside the autoclave. Tests in air were performed under strain control with an axial extensometer; the stroke at the location used for control in the water tests was also recorded. Information from the air tests was used to determine the stroke required to maintain constant strain in the specimen gauge length. To account for cyclic hardening of the material, the stroke needed to maintain constant strain was gradually increased during the test. The accuracy of the procedure was checked by conducting stroke-controlled tests in air and monitoring the strain in the gauge section of the specimen. The relative errors between the estimated and measured values of the strain range were typically ±2%.

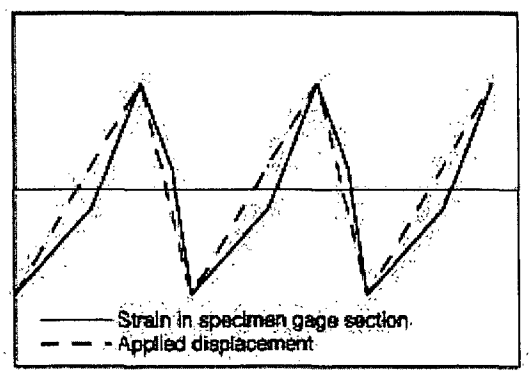

Figure 10.
Loading strain applied to specimen gauge section (solid line) during stroke-controlled tests with a sawtooth waveform (dashed line)

The actual strain in the specimen gauge section during a stroke-controlled tests with a sawtooth waveform is shown in Fig. 10. The fraction of applied displacement that goes to the specimen gauge section is not constant but varies with the loading strain. Consequently, the loading rate also varies during the fatigue cycle; it is lower than the applied strain rate at strain levels below the elastic limit and higher at larger strains.

The fatigue results obtained for A106-Gr B, A333-Gr 6, A533-Gr B, and A302-Gr B steels are summarized in Appendix A. The fatigue life is defined as the number of cycles N_{25} for tensile stress to drop 25% from its peak value; this corresponds to an ≈3-mm-deep crack in the test specimen. Fatigue lives defined by other criteria, e.g., a 50% decrease in peak tensile stress or complete failure, may be converted to N_{25} value according to

$$N_{25} = N_X / (0.947 + 0.00212\,X), \tag{2.2}$$

where X is the failure criteria, i.e., 25, 50, or 100% decrease in peak tensile stress. For stroke controlled tests, the reported strain rates represent target values, the actual values are within ±5% of the reported rates. Because the strain rate varies during the loading cycle (Fig. 10), the reported strain rates for tests in water are average values over the tensile or compressive portion of the cycle. Similarly, the strain rates for the tests conducted with a sine waveform are also average values.

For the tests in water, the DO levels in feedwater and the effluent, and the ECPs of platinum and steel electrodes are included in the fatigue data tabulated in Appendix A. The DO levels for the tests were represented by the values in effluent water. The ECPs of platinum and carbon or low-alloy steel measured during the various tests are plotted as a function of DO levels in the effluent in Figs. 11 and 12, respectively. For both electrodes, the ECP values varied from approximately -700 mV at low DO levels (<10 ppb DO) to ≈200 mV at high DO levels (>200 ppb DO); the ECPs of platinum at low- and high-DO levels were ≈16 mV higher than those of carbon or low-alloy steel. In the transition region between ≈10 and 200 ppb DO, the ECPs of platinum follow the typical sigmoidal curve. For the few tests conducted at 10-200 ppb DO levels, the ECPs of the steel were either above 100 mV or below -600 mV. The results from the present study are compared in Fig. 13 with the ECP vs. DO data from other studies.[36-40]

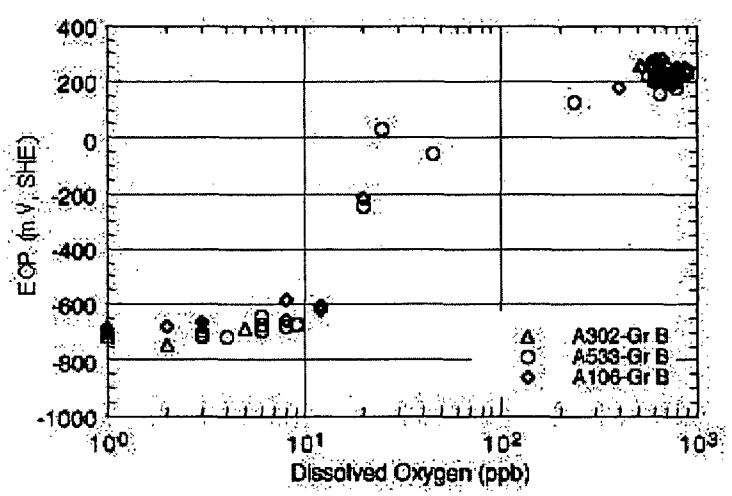

Figure 11. ECP of platinum during fatigue tests at 288°C as a function of dissolved oxygen in effluent

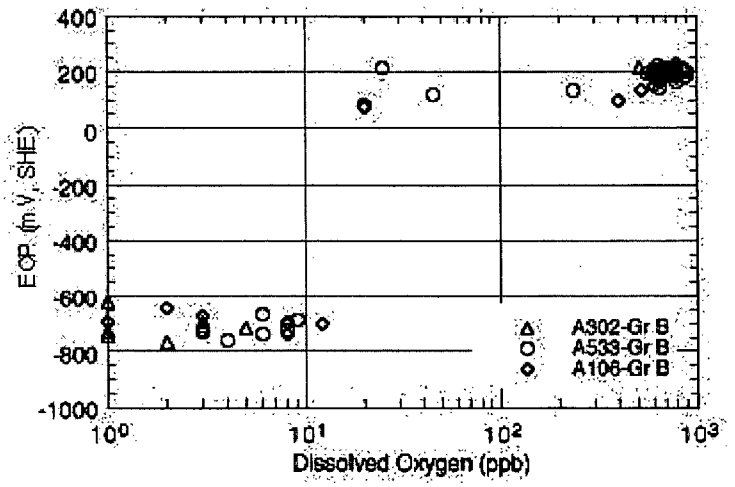

Figure 12. ECP of carbon and low-alloy ferritic steels during fatigue tests at 288°C as a function of dissolved oxygen in effluent

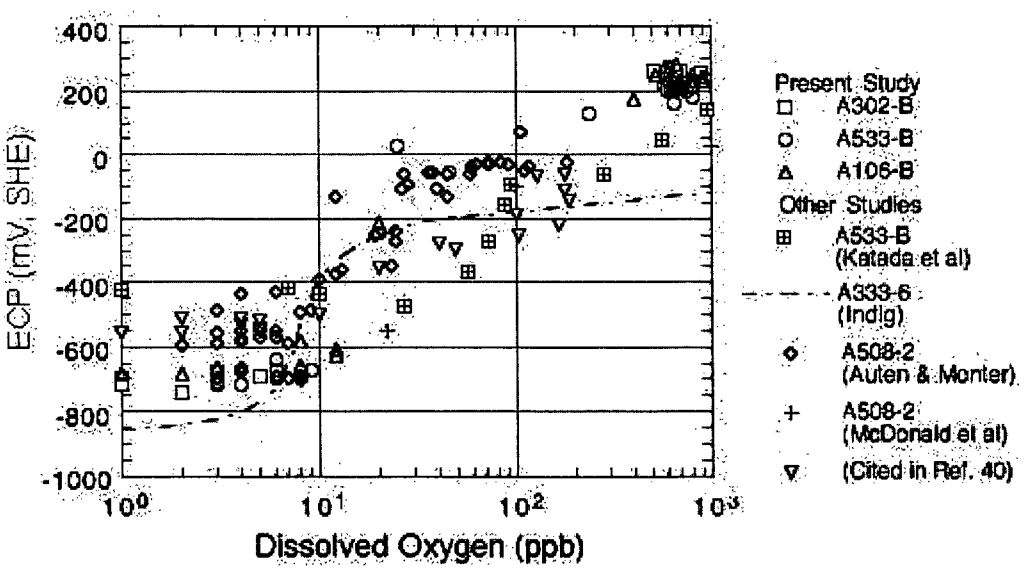

Figure 13. ECP vs. dissolved-oxygen data for carbon and low-alloy steels at 250-290°C

3 Mechanism of Fatigue Crack Initiation

3.1 Formation of Engineering Crack

Deformation and microstructural changes in the surface grains are responsible for fatigue cracking. During cyclic straining, the irreversibility of dislocation glide leads to the development of surface roughness. Strain localization in persistent slip bands (PSBs) results in the formation of extrusions and intrusions. With continued cycling, microcracks ultimately form in PSBs or at the edges of slip-band extrusions. At high strain amplitudes, microcracks

form in notches that develop at grain, twin, or phase boundaries (e.g., ferrite/pearlite) or by cracking of second-phase particles (e.g., sulfide or oxide inclusions).

Once a microcrack forms, it continues to grow along its slip plane or a PSB as a Mode II (shear) crack in Stage I growth (orientation of the crack is usually at 45° to the stress axis). At low strain amplitudes, a Stage I crack may extend across several grain diameters before the increasing stress intensity of the crack promotes slip on systems other than the primary slip. A dislocation cell structure normally forms at the crack tip. Because slip is no longer confined to planes at 45° to the stress axis, the crack begins to propagate as a Mode I (tensile) crack, normal to the stress axis in Stage II growth. At high strain amplitudes, the stress intensity is quite large and the crack propagates entirely by the Stage II process. Stage II crack propagation continues until the crack reaches an engineering size (≈3 mm deep). The two stages of fatigue crack growth in smooth specimens are shown in Fig. 14.

In air or mildly corrosive environments, Stage II cracking is characterized by fatigue striations. The process of Stage II fatigue crack growth and formation of fatigue striations[41] is illustrated in Fig. 15. As tensile load is applied, slip bands form at the double notch or "ears" of the crack tip (Fig. 15b). The slip bands widen with further straining, causing blunting of the crack tip (Fig. 15c). Crack surfaces close during compressive loading and slip is reversed, producing ears at the edges of the blunt crack tip (Figs. 15d and 15e). The ears are observed as fatigue striations on the fracture surface. However, there is not necessarily a 1:1 correlation between striation spacing and fatigue cycles. At high strain amplitudes, several striations may be created during one cycle, whereas at low strain amplitudes one striation may represent several cycles.

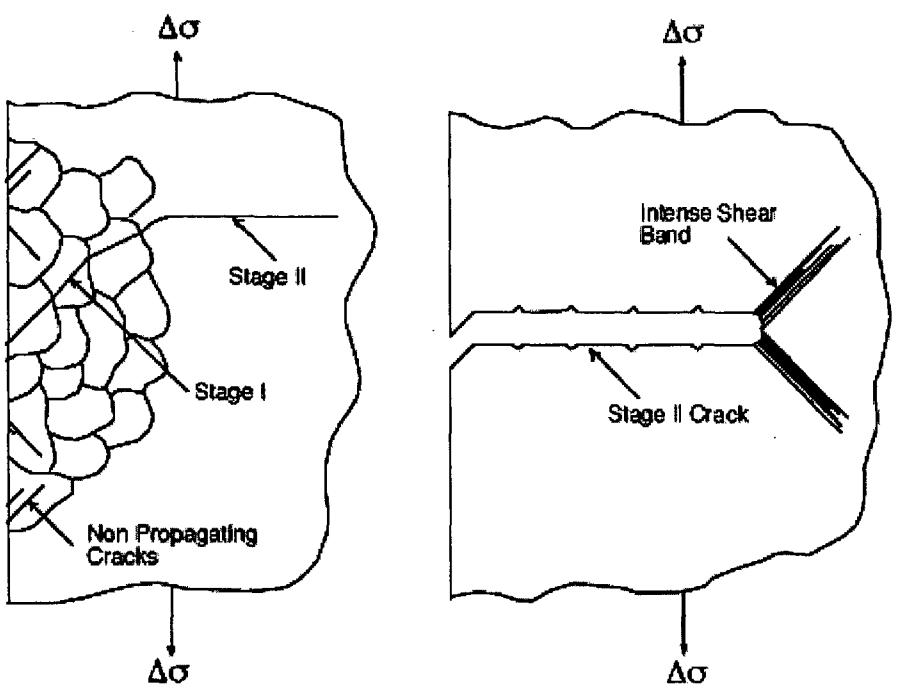

Figure 14. Two stages of fatigue crack growth in smooth test specimens

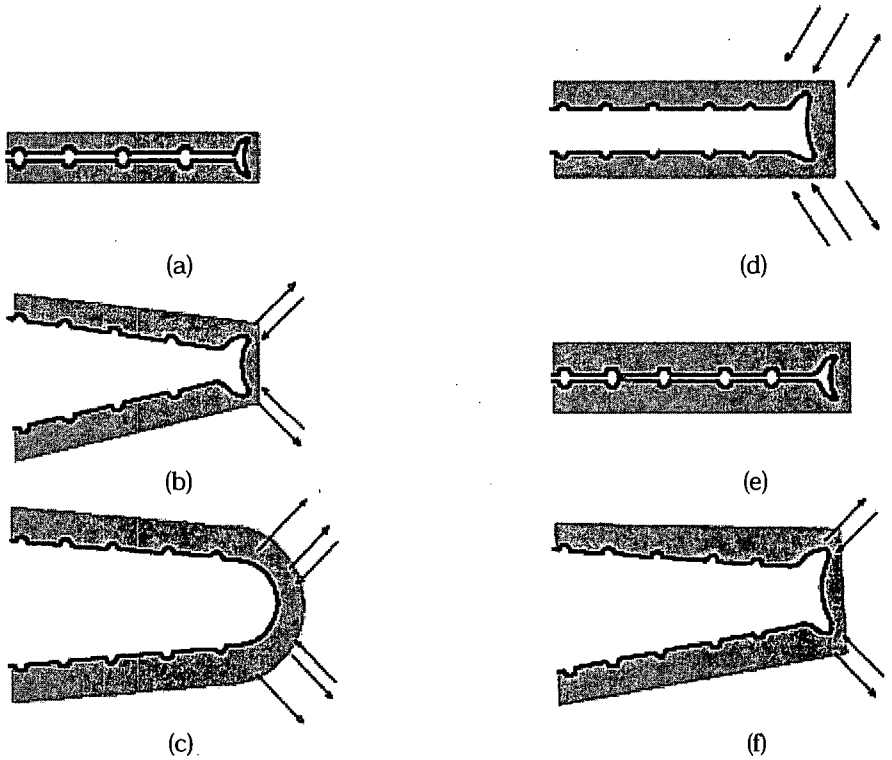

Figure 15. Schematic illustration of plastic blunting process of fatigue crack growth in Stage II: (a) zero load; (b) small tensile load; (c) maximum tensile load, widening of slip bands; (d) crack closure, and formation of "ears" at crack tip; (e) maximum compressive load; (f) small tensile load in next cycle

The formation of surface cracks and their growth as shear and tensile cracks (Stage I and II growth) to an "engineering" size (e.g., a 3-mm-deep crack) constitute the fatigue life of a material, which is represented by the fatigue S-N curves. The curves specify, for a given stress or strain amplitude, the number of cycles needed to form an engineering crack. Fatigue life has conventionally been represented by two stages: (a) initiation, which represents the cycles N_i for formation of microcracks on the surface; and (b) propagation, which represents cycles N_p for propagation of the surface cracks to an engineering size. Thus, fatigue life N is the sum of the two stages, $N = N_i + N_p$. The increase in length of cracks greater than "engineering" size is usually described in terms of fracture mechanics models rather than in terms of S-N behavior. N_i is considered to be sensitive to the stress or strain amplitude, e.g., at low strain amplitudes, most of the life may be spent in initiating a crack whereas, at high strain amplitudes, cracks initiate easily.

An alternative approach considers fatigue life of engineering structures and components to be entirely composed of the growth of short fatigue cracks, i.e., cracks less than "engineering " size.[42,43] For polycrystalline materials, the period for the formation of surface cracks is negligible (Fig. 16). Fatigue damage in a material is the current size of the fatigue crack, and damage accumulation is the rate of crack growth.[43] However, the growth rates of short cracks can not be predicted accurately from fracture mechanics methodology on the basis of range of stress intensity factor (ΔK). Under cyclic loading and the same ΔK, short

fatigue cracks (i.e., having lengths comparable to the unit size of the microstructure) grow at a faster rate than long fatigue cracks.[44] Also, short cracks can grow at ΔK values below those predicted from linear elastic fracture mechanics (LEFM). The differences between the growth rates of short and long cracks have been attributed to interactions with microstructural features, contributions of crack closure with increasing crack length, effects of mixed mode crack propagation, and an inadequate characterization of the crack tip stress/strain fields associated with short cracks.

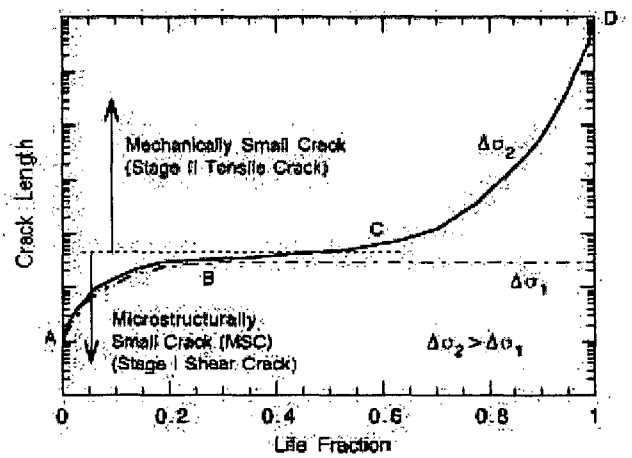

Figure 16.
Growth of cracks in smooth fatigue specimens

Recent studies indicate that during fatigue loading of smooth test specimens, surface cracks 10 μm or longer form quite early in life, i.e., <10% of life even at low strain amplitudes (Fig. 17).[45-47] These cracks form at surface irregularities/discontinuities either already in existence or produced by slip bands, grain boundaries, second-phase particles, etc. Growth of these surface cracks may be divided into three regimes: (a) initial period that involves growth of microstructurally small cracks (MSCs) below a critical length, characterized by decelerating crack growth rate, seen in region AB of Fig. 16; (b) final period of growth, characterized by accelerating crack growth rate, region CD; and (c) a transition period controlled, by a combination of the two regimes, region BC. The crack growth rates as a function of crack length during the three regimes of fatigue life are shown in Fig. 18.

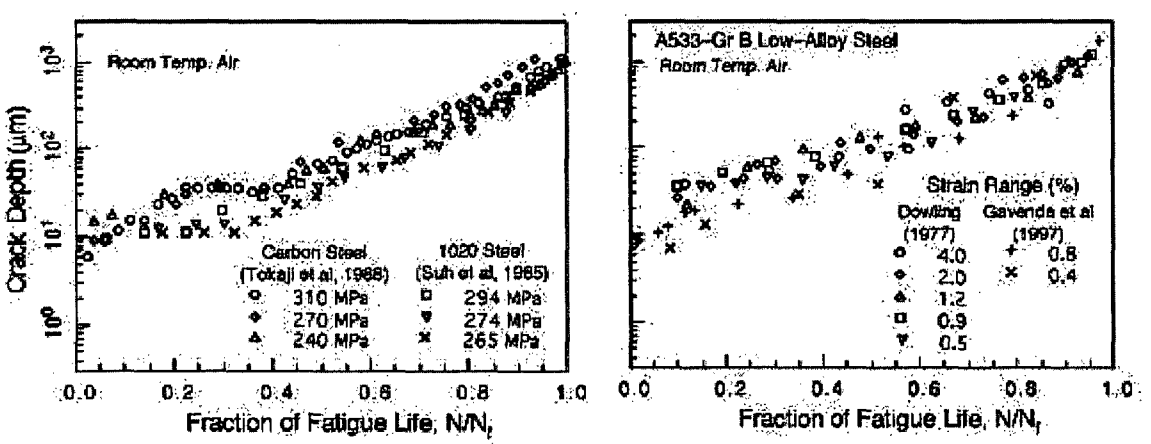

Figure 17. Crack depth plotted as a function of fractional life for carbon and low-alloy steels tested in room-temperature air

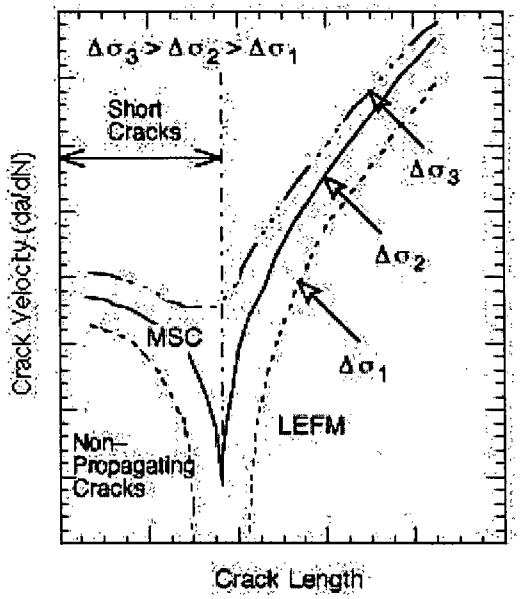

Figure 18.
Schematic illustration of short crack behavior

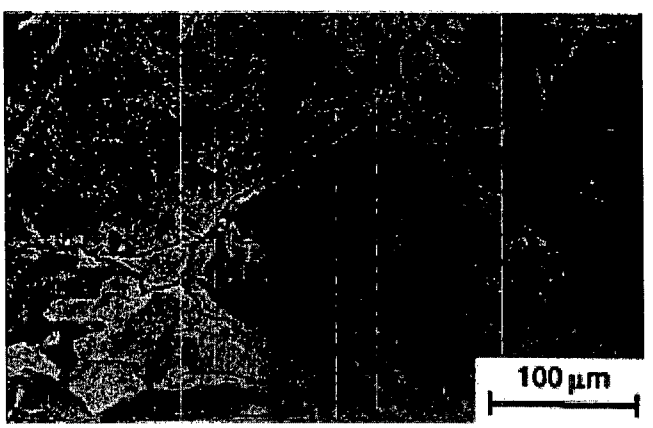

Figure 19.
Photomicrograph of surface crack along longitudinal section of A106-Gr B steel tested in air

The growth of MSCs is very sensitive to microstructure.[47-53] The MSCs correspond to Stage I cracks and grow along slip planes as shear cracks in the early stage of growth. For MSCs, microstructural effects are strong because of Stage I growth, i.e., crystallographic growth. The growth rates are markedly decreased by grain boundaries, triple points, and phase boundaries. In ferritic-pearlitic steels, fatigue cracks initiate and propagate preferentially in the ferrite phase that forms as long allotriomorphs at prior austenite phase boundaries.[47,52,53] An example of surface cracking in an A106-Gr B specimen tested in air is shown in Fig. 19. The ferrite/pearlite phase boundaries act as strong barriers to crack propagation, and growth rates decrease significantly when small cracks grow into the pearlite from the ferrite.[47] Limited data suggest that microstructural effects are more pronounced at negative stress ratios; the compressive component of the applied load plays an important role in the formation of Stage I facets and as a driving force during the formation of cracks.[50]

Fatigue cracks greater than the critical length of MSCs show little or no influence of microstructure and are termed mechanically small cracks.[49,50] For a stress ratio of -1, the transition from MSC to a mechanically small crack for several materials has been estimated to be ≈8 times the unit size of the microstructure.[50] Mechanically small cracks correspond to Stage II, or tensile, cracks characterized by striated crack growth, with a fracture surface normal to the maximum principal stress. Their growth rates tend to decrease as the cracks grow because crack closure becomes more significant for larger cracks. For ferritic-pearlitic steels, Stage II crack propagation occurs when stress intensity and mode of growth attain a critical level and break through the pearlite and join other ferrite cracks.[52]

At low stress levels, e.g., $\Delta\sigma_1$ in Figs. 16 and 18, the transition from MSC growth to accelerating crack growth does not occur and the cracks are nonpropagating. This circumstance represents the fatigue limit for the smooth specimen. Although cracks can form below the fatigue limit, they can grow to engineering size only at stresses greater than the fatigue limit. Note that possible preexisting large cracks in the material, e.g., defects in welded samples, or those created by growth of microcracks at high stresses, can grow at stress levels below the fatigue limit, and their growth can be estimated from ΔK-based LEFM.

3.2 Environmental Effects

The available fatigue S-N data indicate a significant decrease in fatigue life of CSs and LASs in LWR environments when five conditions are satisfied simultaneously, viz., the applied strain range, temperature, DO in water, and sulfur content in steel are above a minimum threshold level, and strain rate is below a critical value. Although the structure and cyclic hardening behavior of carbon and low-alloy steels are distinctly different, there is little or no difference in susceptibility to environmental degradation of fatigue life of these steels. Reduction in life in LWR coolant environments may arise from easy formation of surface microcracks and/or an increase in growth rates of cracks, during either the initial stage of MSC and shear crack growth or the transition and final stage of tensile crack growth. Carbon and low-alloy steel specimens tested in water show surface micropitting and cavities that form either by corrosion of the material in oxygenated water or by selective dissolution of MnS or other inclusions. These micropits can act as sites for the formation of fatigue cracks.

Photomicrographs of the gauge surfaces[20] of A106-Gr B CS and A533-Gr B LAS specimens tested at 288°C in air, simulated PWR, and high-DO water (≈0.7 ppm DO) are shown in Fig. 20. The specimens tested in air show slight discoloration, while those tested in water develop a gray/black corrosion scale and are covered with magnetite (Fe_3O_4) at all DO levels and hematite (α-Fe_2O_3) forms at DO levels >200 ppb.[10,20,36] The amount of hematite increases with increasing DO levels in water[36] (Fig. 21). The pitting behavior of CSs[54] and LASs[39] in high-purity water at different temperatures and DO levels is shown in Fig. 22. The results indicate that pitting corrosion does not occur in these steels at all temperatures in low-DO PWR environments (typically <0.01 ppm DO), and at temperatures >200°C in water that contains 0.1-0.2 ppm DO, which represents normal BWR water chemistry. However, even under these conditions, micropits form in both carbon and low-alloy steels due to dissolution of MnS inclusions[6] or by anodic reaction in the S contaminated matrix[55] close to sulfide inclusions. However, micropits formed by these processes stop growing when either the MnS inclusion dissolves completely or falls off. Typical examples of micropits on A106-Gr B and A533-Gr B steel specimens are shown in Fig. 23.

The reduction in fatigue life in high-temperature water has been attributed to the presence of micropits[6] that act as stress raisers and provide preferred sites for the formation of fatigue cracks. The strain rate effects in water, i.e., fatigue life decreases with decreasing strain rate, have been explained on the basis of higher density of micropits at lower strain rates (Fig. 24). It has been argued that the longer test durations for slow strain rate tests result in higher density of micropits and hence shorter periods for formation of surface

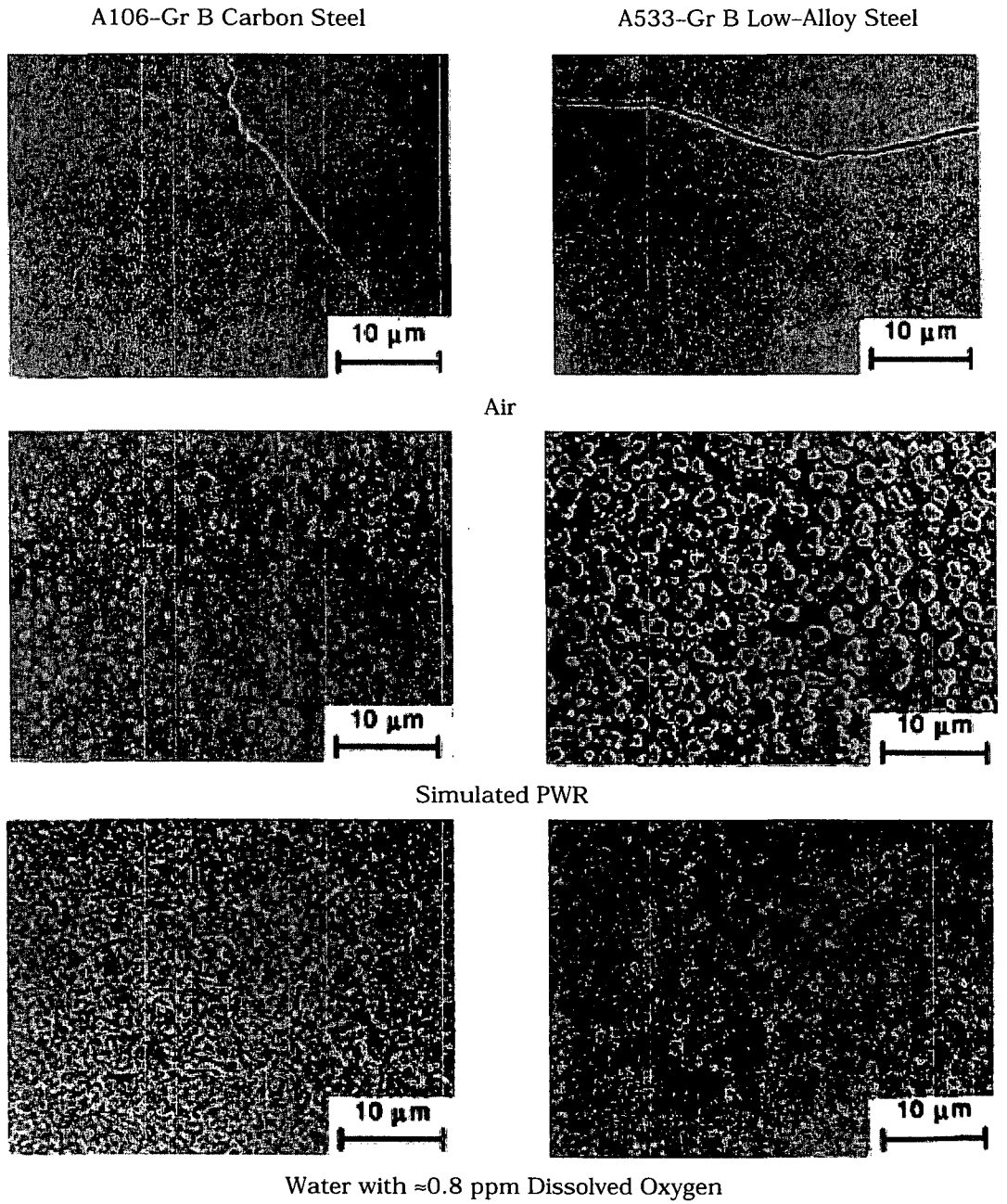

Figure 20. SEM photomicrographs of gauge surface of A106-Gr B and A533-Gr B steels tested in different environments at 288°C

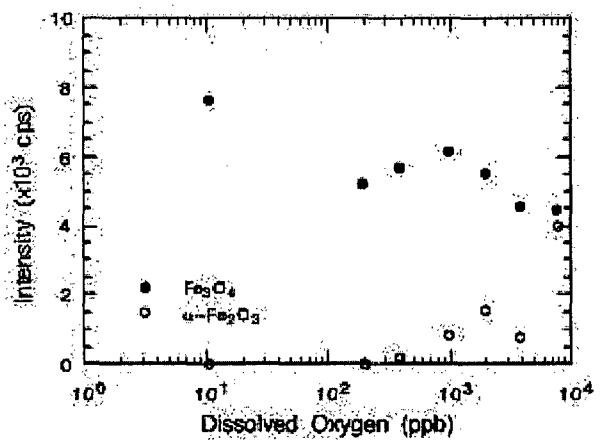

Figure 21.
X-ray diffraction results of A533-Gr B steel as a function of dissolved oxygen

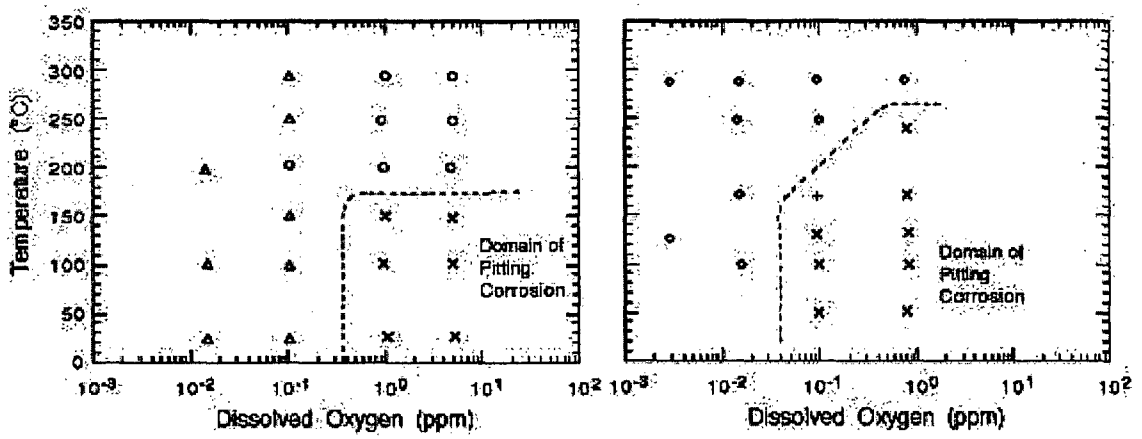

(a) (b)

Figure 22. Pitting behavior of (a) A106-Gr B carbon steel (0.025 wt.% S) and (b) A508-Cl 2 low-alloy steel (0.015 wt.% S) tested in high-purity water. Δ: no pits ductile fracture, o: no pits stress corrosion cracking, x: pitting corrosion, ◊: no pits, +: slight pitting.

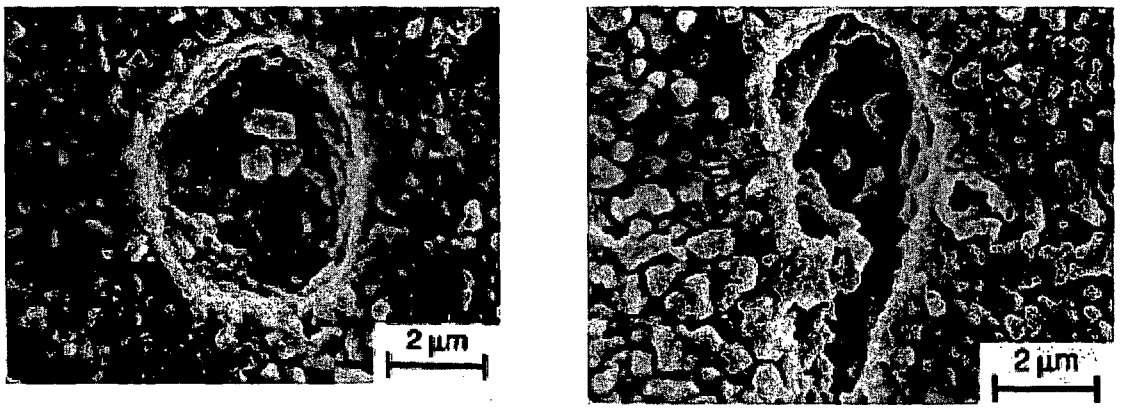

(a) (b)

Figure 23. Micropits on surface of (a) A106-Gr B carbon steel and (b) A533-Gr B low-alloy steel tested in oxygenated water at 288°C

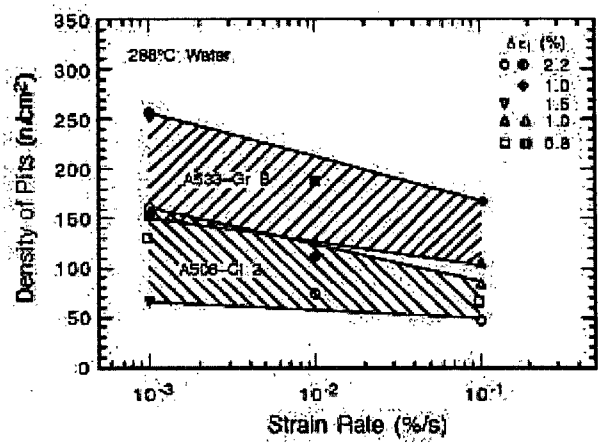

Figure 24.
Relationship between density of micropits and strain rate

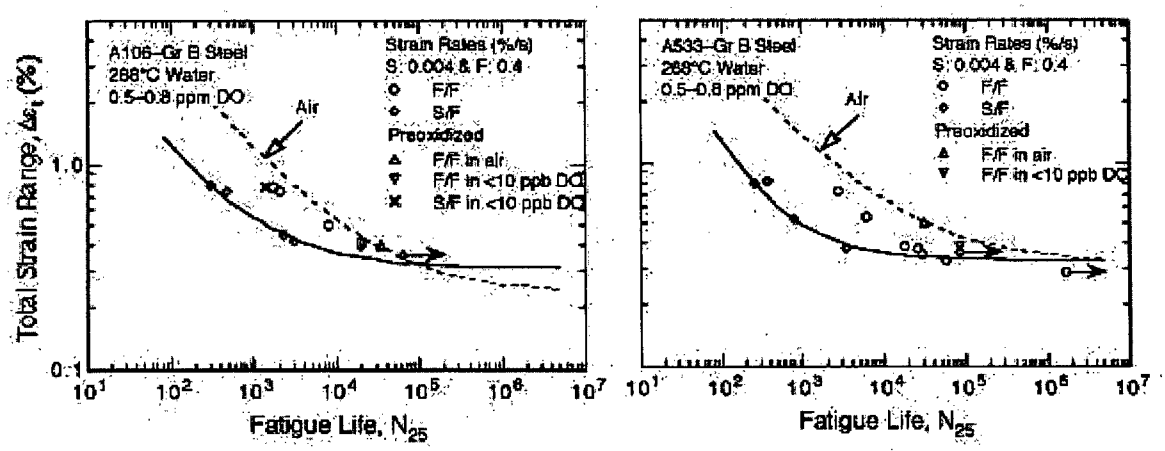

Figure 25. Environmental effects on formation of fatigue cracks in carbon and low-alloy steels. Preoxidized specimens were exposed at 288°C for 30-100 h in water with 06-0.8 ppm dissolved oxygen.

microcracks.[6] If the presence of micropits was responsible for reduction in fatigue lives of carbon and low-alloy steels in LWR environments, then specimens preexposed to high-DO water and then tested in air should also show a decrease in fatigue life.

The fatigue lives of A106-Gr B CS and A533-Gr B LAS specimens preexposed at 288°C for 30-100 h in water with 0.6-0.8 ppm DO and then tested in air or low-DO water (<0.01 ppm DO), are shown in Fig. 25.[11-14,21] Fatigue lives of the preoxidized specimens are identical to those of unoxidized specimens; life would be expected to decrease if surface micropits facilitate the formation of fatigue cracks. Only a moderate decrease in life is observed for both preoxidized and unoxidized specimens tested in low-DO water. Furthermore, if micropits were responsible for the decrease in fatigue life in LWR environments, then fatigue limit of these steels should be lower in water than in air. Fatigue data in high-DO water[11-14,21] indicate that the fatigue limit in water is either the same or ≈20% higher than in air (Fig. 25).

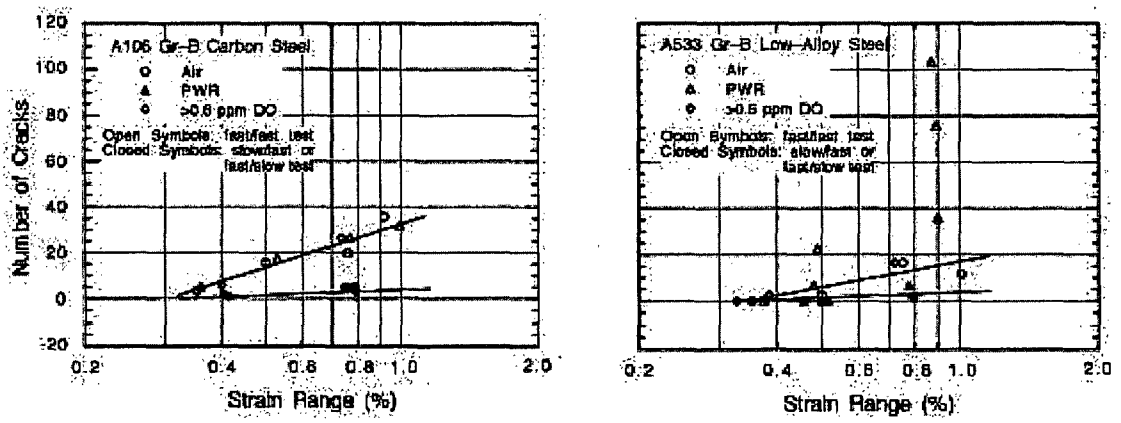

Figure 26. Number of cracks along longitudinal section of fatigue specimens tested in different environments

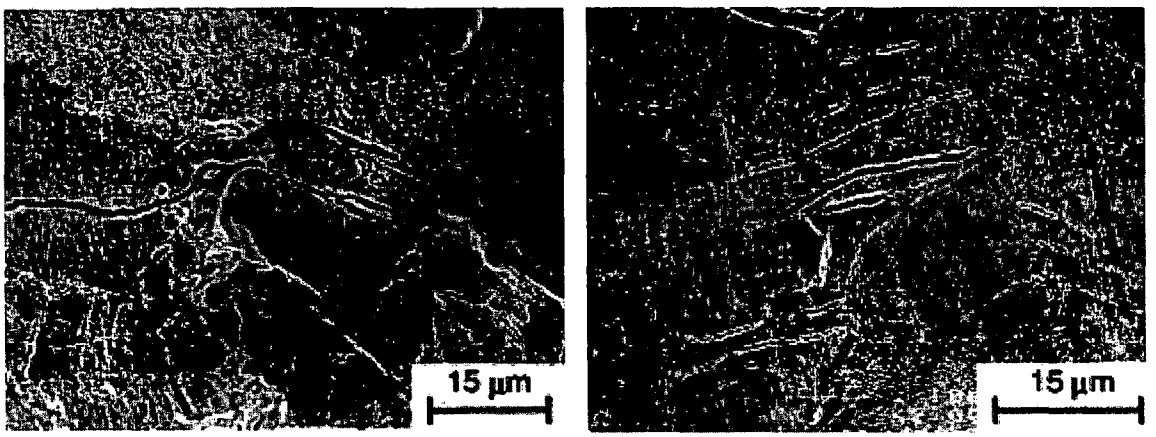

Figure 27. Nucleation of cracks along slip bands, carbide particles, and ferrite/pearlite phase boundaries of carbon steel fatigue specimen

Figure 26 shows plots of the number of cracks, greater than 10 µm, along longitudinal sections of the gauge length of A106-Gr B and A533-Gr B specimens as a function of strain range in air, simulated PWR, and high-DO water at two different strain rates.[21] In all cases, the number of cracks represents the average value along a 7 mm gauge length. The results show that with the exception of the LAS tested in simulated PWR water, environment has no effect on the frequency (number per unit gauge length) of cracks. For similar loading conditions, the number of cracks in the specimens tested in air and high-DO water are identical, although fatigue life is lower by a factor of ≈8 in water. If the reduction in life is caused by enhanced crack nucleation, the specimens tested in high-DO water should show more cracks. Detailed metallographic evaluations of the fatigue test specimens[21] also indicate that water environment has little or no effect on the formation of surface microcracks. Irrespective of environment, cracks in carbon and low-alloy steels nucleate along slip bands, carbide particles, or at the ferrite/pearlite phase boundaries (Fig. 27).[21,45]

The environmental enhancement of fatigue crack growth in pressure vessel steels in high-temperature oxygenated water and the effects of sulfur content, loading rate, and flow

velocities are well known.[34,56-72] The enhanced growth rates in LWR environments have been attributed to either slip oxidation/dissolution[73-76] or hydrogen-induced cracking[77-79] mechanisms. A critical concentration of sulfide (S^{2-}) or hydrosulfide (HS^-) ions, which are produced by the dissolution of sulfide inclusions in the steel, is required at the crack tip for environmental effects to occur. The crack tip is supplied with S^{2-} and HS^- ions as the advancing crack intersects the sulfide inclusions, and the inclusions dissolve in the high-temperature water environment. Sulfide ions are removed from the crack tip by one or more of the following processes: (a) diffusion due to concentration gradient, (b) ion transport due to ECP gradient, (c) pumping action due to cyclic loading on the crack, and (d) fluid flow induced within the crack due to the flow of coolant outside the crack. The morphology, size, and distribution of sulfide inclusions and the probability of advancing crack to intercept sulfide inclusions are important parameters affecting growth rates of CSs and LASs in LWR environments.[57,60,67-70] The main electrochemical and chemical reactions in the crack cavity are given below.

Dissolution of sulfide:

$$MnS + 2H^+ = H_2S + Mn^{2+} \tag{3.1}$$

Anodic reactions:

$$Fe = Fe^{2+} + 2e^- \tag{3.2}$$

$$S^{2-} + 4H_2O = 8H^+ + 8e^- + SO_4^{2-} \tag{3.3}$$

Hydrolysis reactions:

$$Fe^{2+} + 2H_2O = Fe(OH)_2^+ + 2H^+ + e^- \tag{3.4}$$

$$Mn^{2+} + 2H_2O = Mn(OH)_2^+ + 2H^+ + e^- \tag{3.5}$$

$$3Fe^{2+} + 4H_2O = Fe_3O_4 + 8H^+ + 2e^- \tag{3.6}$$

Cathodic reactions:

$$2H^+ + 2e^- = H_2 \tag{3.7}$$

$$2H_2O + 2e^- = 2OH^- + H_2 \tag{3.8}$$

$$SO_4^{2-} + H_2O + 2e^- = SO_3^{2-} + 2OH^- \tag{3.9}$$

$$O_2 + 4H^+ + 4e^- = 2H_2O \tag{3.10}$$

$$2H_2O + O_2 + 4e^- = 4OH^- \tag{3.11}$$

Reactions 3.10 and 3.11 occur in high-DO water.

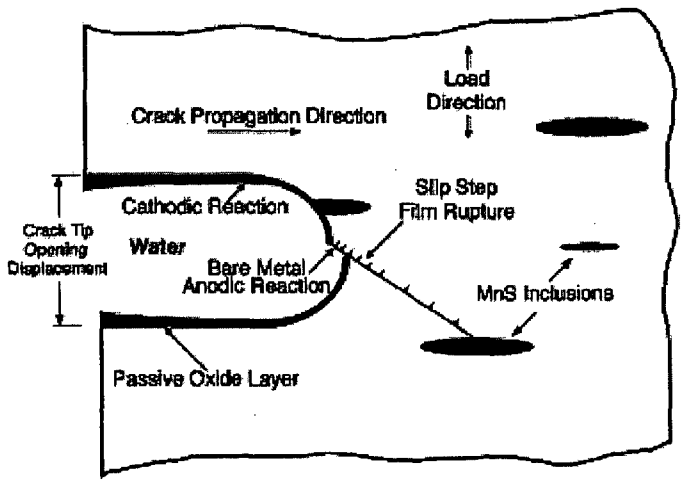

Figure 28.
Schematic illustration of film rupture/slip dissolution process

The requirements for a slip dissolution model are that a protective oxide film is thermodynamically stable to ensure that a crack will propagate with a high aspect ratio without degrading into a blunt pit, and that a strain increment occurs to rupture that film and thereby expose the underlying matrix to the environment, Fig. 28. Once the passive oxide film is ruptured, crack extension is controlled by dissolution of freshly exposed surfaces and by the oxidation characteristics. Ford and Andresen[40,74] have proposed that the average environmentally assisted crack growth rate $\overline{V}_t$ (cm s^{-1}) for slip dissolution is related to the crack tip strain rate $\dot{\varepsilon}_{ct}$ (s^{-1}) by the relationship

$$\overline{V}_t = A(\dot{\varepsilon}_{ct})^n, \tag{3.12}$$

where the constants A and n depend on the material and environmental conditions at the crack tip. There is a lower limit of crack propagation rate associated either with blunting when the crack tip cannot keep up with general corrosion rate of the crack sides, or with the fact that a critical level of sulfide ions cannot be maintained at the crack tip. For example, the latter condition may occur when crack growth rate falls below a critical value so that a high concentration of sulfide ions can not be maintained at the crack tip. The critical crack growth rate at which this transition occurs will depend on DO level, flow rate, and S content in steel. Based on these factors, the maximum and minimum environmentally controlled growth rates have been estimated.[40,74] For crack-tip sulfide ion concentrations above the critical level,

$$\overline{V}_t = 2.25x10^{-4}\,\dot{\varepsilon}_{ct}^{\,0.35} \tag{3.13a}$$

and for crack-tip sulfide ion concentrations below the critical level,

$$\overline{V}_t = 10^{-2}\,\dot{\varepsilon}_{ct}^{\,1.0}. \tag{3.13b}$$

In Eqs. 3.13a and 3.13b, the crack tip strain rate $\dot{\varepsilon}_{ct}$ is a function of applied stress, stress intensity, applied strain rate, as well as the crack growth rate $\overline{V}_t$. Empirical correlations have been developed to estimate the crack tip strain rate under various loading conditions.[40,74,76] For LASs, the crack tip strain rate $\dot{\varepsilon}_{ct}$ (s^{-1}) under constant slow strain rates is given by

$$\dot{\varepsilon}_{ct} = 10\dot{\varepsilon}_{app} \tag{3.14a}$$

and under cyclic loading (for stress ratio R <0.42) by

$$\dot{\varepsilon}_{ct} = 1.335x10^{-11}\,\dot{v}\Delta K^4, \tag{3.14b}$$

where ΔK is the stress intensity range (MPa√ m) and $\dot{v}$ is the frequency of cyclic loading (s^{-1}). For cyclic loads, the crack tip strain rate estimated from Eq. 3.14b is typically 10–100 times the growth rate in an inert environment.[40,73] The latter has been expressed in terms of R ratio and ΔK in Eq. 3.14b; it can also be obtained from experimental data.

It is assumed that there is no environmental enhancement of crack propagation during the compressive load cycle, because during that period the water does not have access to the crack tip. The total crack advance per cycle Δa_{total} is given by the summation of crack advance in air Δa_{air} due to mechanical factors, and crack advance from a slip-dissolution mechanism Δa_r, once the tensile strain increment exceeds the fracture strain of the oxide ε_f. If the fatigue life is considered to represent the number of cycles required to form a 0.3 cm crack, the crack advance per loading cycle in air is given by $0.3/N_{air}$. Thus, assuming that environmental conditions are such as to maintain a high sulfide ion concentrations at the crack tip (Eq. 3.13a) and that for short cracks, the crack-tip strain rate $\dot{\varepsilon}_{ct}$ is the same as the applied strain rate $\dot{\varepsilon}_{app}$ (s^{-1}), the environmental increment in crack growth is given by integrating Eq. 3.13a

$$\Delta a_r = \int_0^{a_r} da = \int_{\varepsilon_f/\dot{\varepsilon}}^{t_r} 2.25x10^{-4}\left(\dot{\varepsilon}_{app}\right)^{0.35} dt \tag{3.15}$$

or

$$\Delta a_r = 2.25x10^{-4}\left(\dot{\varepsilon}_{app}\right)^{0.35}\left(\frac{\Delta\varepsilon}{\dot{\varepsilon}_{app}} - \frac{\varepsilon_f}{\dot{\varepsilon}_{app}}\right), \tag{3.16}$$

where the relevant time for integration is the rise time t_r (s) minus the time taken for the strain increment to exceed the fracture strain of the oxide $\left(\varepsilon_f/\dot{\varepsilon}_{app}\right)$, and Δε is the applied strain range. Similarly, increment in crack growth when the concentration of sulfide ions at the crack tip is low, can be obtained by integrating Eq. 3.13b

$$\Delta a_r = 10^{-2}\left(\Delta\varepsilon - \varepsilon_f\right). \tag{3.17}$$

Crack growth under low crack-tip sulfide ion concentration is independent of $\dot{\varepsilon}_{app}$.

In the case of a high sulfide ion concentration, from Eq. 3.16, the total crack advance per cycle Δa_{total} (cm) is given by

$$\Delta a_{total} = \Delta a_{air} + \Delta a_r = \frac{0.3}{N_{air}} + 2.25x10^{-4}\left(\Delta\varepsilon - \varepsilon_f\right)\left(\dot{\varepsilon}_{app}\right)^{-0.65}. \tag{3.18}$$

The fatigue life in water N_{water} is given by the initiation crack depth (0.3 cm) divided by the total crack advance per cycle Δa_{total} Hence, Ford et al. estimate the fatigue life in water as

$$N_{water} = 0.3\Big/\left[\frac{0.3}{N_{air}} + 2.25x10^{-4}\left(\Delta\varepsilon - \varepsilon_f\right)\left(\dot{\varepsilon}_{app}\right)^{-0.65}\right]. \tag{3.19}$$

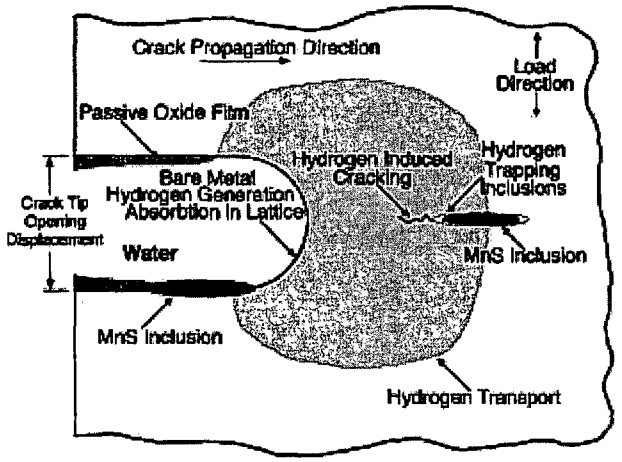

Figure 29. Schematic illustration of hydrogen-induced cracking of low-alloy steels

The fatigue lives estimated from Eq. 3.19 show fair agreement with those observed experimentally for high-sulfur steels tested in high-DO water.[74,75,80]

Hydrogen-induced cracking of LASs is explained as follows (Fig. 29): hydrogen produced by the oxidation reaction at or near the crack tip is partly absorbed into the metal; the absorbed hydrogen diffuses ahead of the crack tip and interacts with MnS inclusions and leads to the formation of cleavage cracks at the inclusion matrix interface; and linkage of the cleavage cracks results in discontinuous crack extension in addition to extension caused by mechanical fatigue. For hydrogen-induced cracking, the average environmentally assisted growth rate $\overline{V}_t$ (cm s^{-1}) may be expressed as

$$\overline{V}_t = \frac{X}{t_c} \tag{3.20}$$

where X is the distance from the crack tip to the region of cleavage cracks and t_c is the time for the concentration of absorbed hydrogen to reach a critical level to cause cleavage cracks.

Other hydrogen-induced fracture processes may also enhance crack growth rates in LWR environments. According to the decohesion mechanism, significant accumulation of hydrogen at or near the crack tip decreases the cohesive interatomic strength of the lattice.[81] Hydrogen-induced bond rupture ahead of the crack tip link up with the main crack resulting in discontinuous but enhanced crack growth. The hydrogen adsorption mechanism states that adsorbed hydrogen lowers the surface energy of the metal, thus facilitating crack growth at a lower fracture stress level. Also, hydrogen can cause localized crack tip plasticity by reducing the stress required for dislocation motion.[82]

Both slip-oxidation/dissolution and hydrogen-induced cracking mechanisms are dependent on oxide rupture rates, passivation rates, and liquid diffusion rates. Therefore, it is often difficult to differentiate between the two mechanism or to establish their relative contribution to crack growth rates in LWR environments. Dissolution of MnS inclusions changes the water chemistry near the crack tip, making it more aggressive. This results in enhanced crack growth rates because either (a) the dissolved sulfides decrease the repassivation rate, which increases the amount of metal dissolution for a given oxide rupture rate;[72] or (b) the dissolved sulfide poisons the recombination of H atoms liberated by

corrosion, which enhances H uptake by the steel at the crack tip.[83] A change in fracture appearance from ductile striations in air to brittle facets or cleavage-like fracture in LWR environments lend the greatest support for hydrogen-induced cracking.[67,70,78,79]

In crack growth studies in long cracks, brittle fracture is generally associated with MnS inclusions and spreads like a fan from these inclusions,[78,79] which is reminiscent of the quasi-cleavage facets produced in hydrogen-charged specimens. In LWR environments, fracture surface often has a terraced appearance produced by linkage of main crack with the hydrogen-induced cracks ahead of the crack tip at inclusion matrix interface. However, such fracture morphologies are not observed for short cracks produced in cylindrical fatigue test specimens used for obtaining fatigue S-N data. Fracture morphologies of A106-Gr B CS and A533-Gr B LAS specimens tested at 288°C in high-DO water and simulated PWR environment are shown in Figs. 30-33. High-magnification photomicrographs of select regions of the specimens before and after they were descaled (with an electroyte of 2 g hexamethylene tetramine in 1000 cm^3 of 1 N HCl) are also shown in the figures. The specimens tested in water show the following salient features.

(a) All specimen exhibit a ductile fatigue fracture; quasi-cleavage facets or fan-like features extending from MnS inclusions are not observed. Examples of cleavage fracture in A106-Gr B CS fatigue specimen pulled apart at room temperature after the fatigue test at 288°C in water, are shown in Fig. 34. Note that in CSs, cleavage fracture occurs entirely along the ferrite matrix, with ductile tearing of the pearlite regions. In LWR environments, although some regions of the fracture surface resemble a fan-like fracture morphology before chemical cleaning (e.g., Fig. 30), examination of the specimens after chemical cleaning indicates that cracks propagate across phase boundaries through both ferrite and pearlite regions.

(b) A terraced morphology which is generally produced by linkage of hydrogen-induced cracks at the sulfide/matrix interface ahead of the main crack, was not observed in any of the specimens. The number of sulfide inclusions observed on the fracture surface of specimens tested in water is similar to that observed for tests in air. Also, as seen in Fig. 35, the sulfide inclusions that are observed on the surface do not appear to change the fracture morphology. As discussed later in Section 4.2.5, the existing fatigue S-N data indicate that in high-DO water (>0.05 ppm DO), environmental effects on fatigue life of carbon steels seem to be independent of sulfur content in the range of 0.002-0.015 wt.%.

(c) Faint fatigue striations are observed for crack depths greater than ≈0.8 mm. Further examination of the specimens after chemical cleaning suggests that these striations are most likely produced by rupture of the surface oxide film rather than the formation of double notches or "ears" at the crack tip. Also, note that in CS specimens, the striations extend across both ferrite and pearlite regions.

Studies on the formation and growth characteristics of short cracks in carbon and low-alloy steels in LWR environments indicate that environmentally assisted reduction in fatigue life of these steels is caused primarily by slip dissolution/oxidation mechanism and is discussed later in this section.

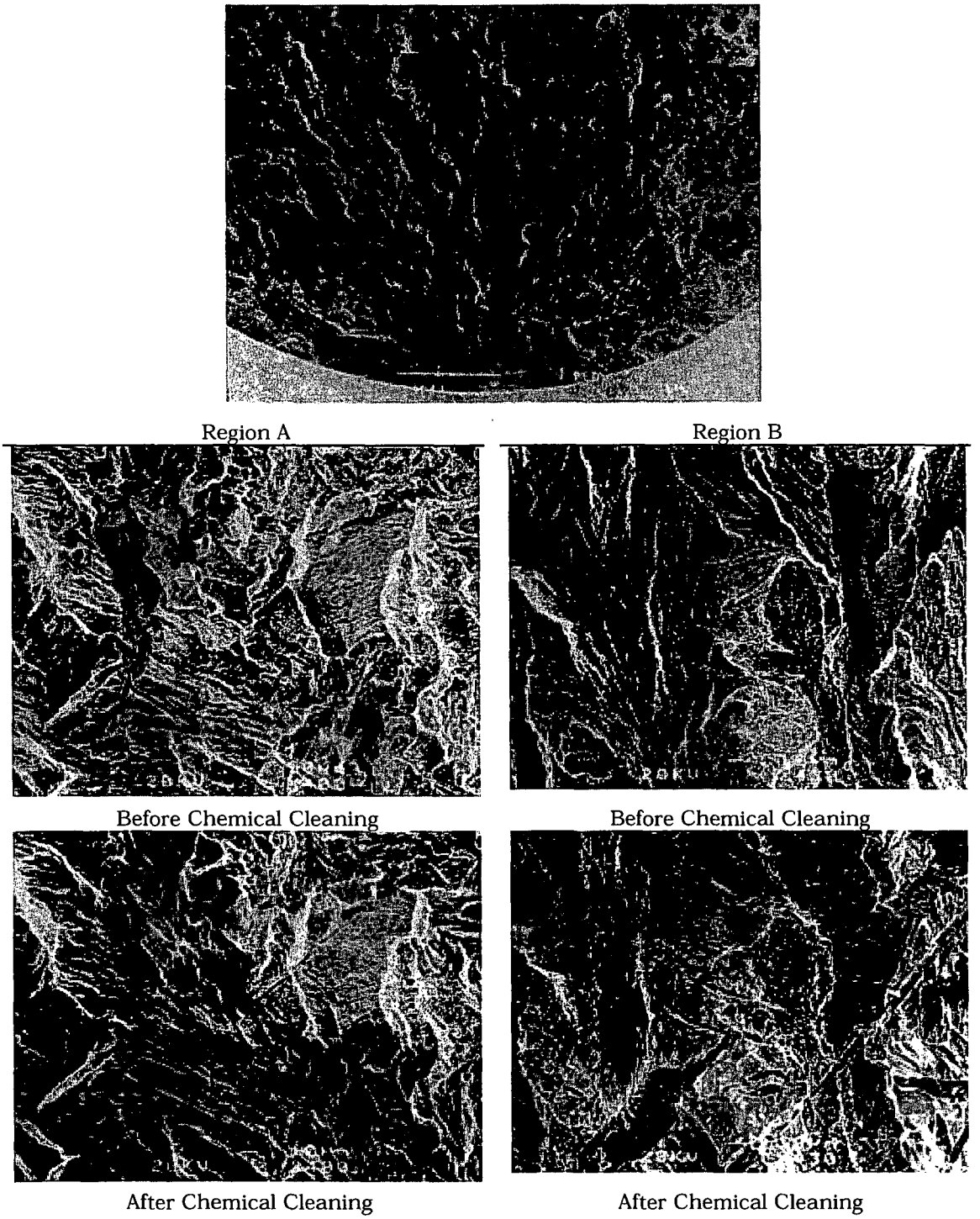

Figure 30. Fracture morphology of A106-Gr B carbon steel tested in high-dissolved oxygen water at 288°C and ≈0.4% strain range

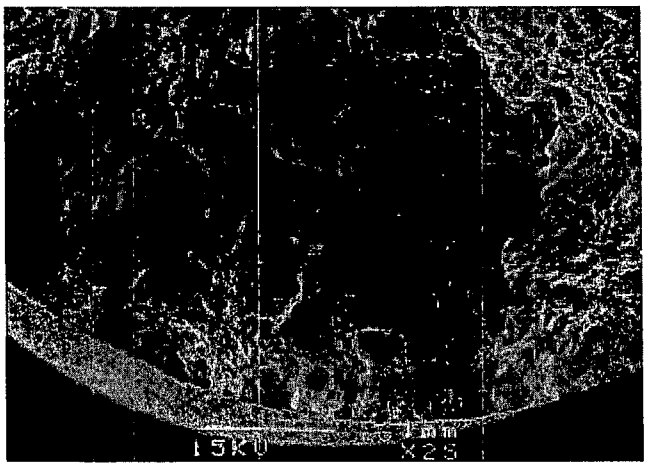

Region A

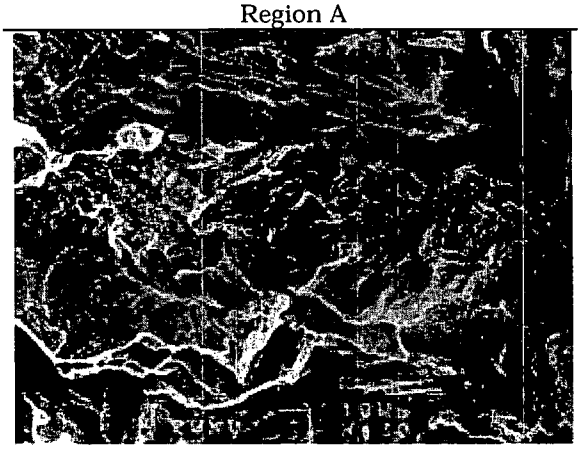

Before Chemical Cleaning

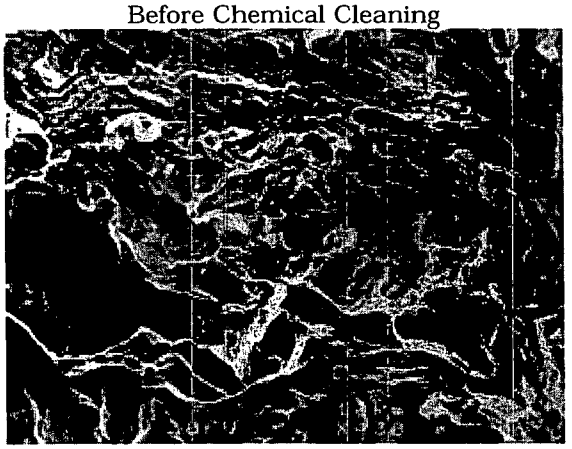

After Chemical Cleaning

Region B

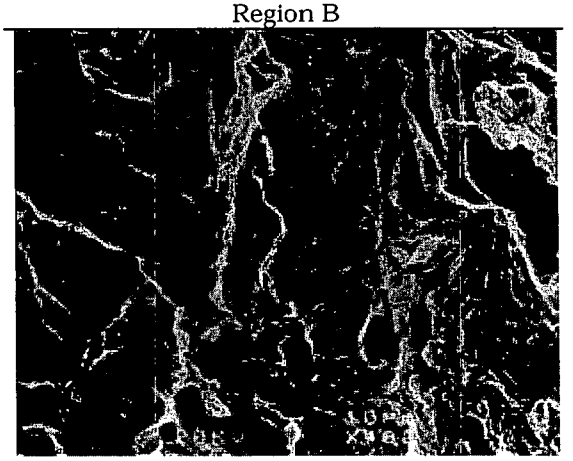

Before Chemical Cleaning

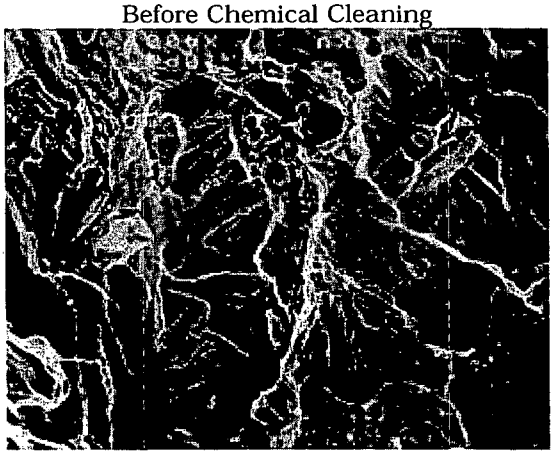

After Chemical Cleaning

Figure 31. Fracture morphology of A106-Gr B carbon steel tested in simulated PWR water at 288°C and ≈0.75% strain range

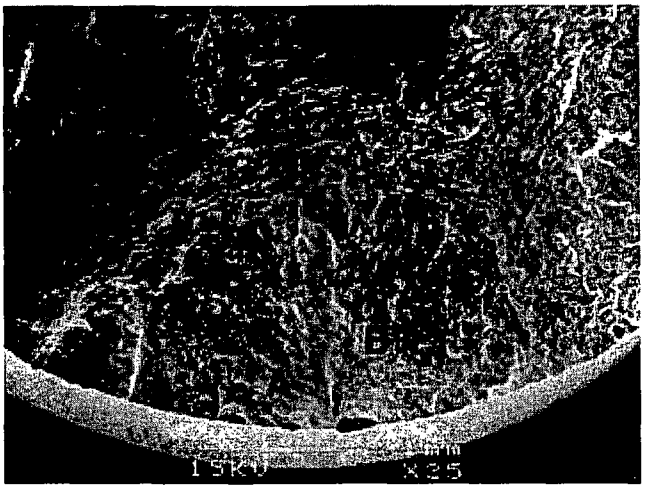

Region A

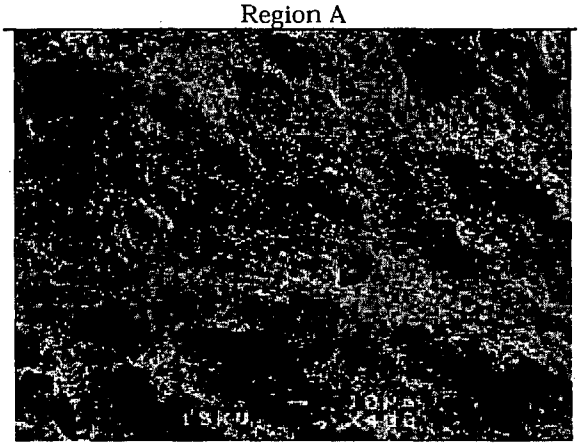

Before Chemical Cleaning

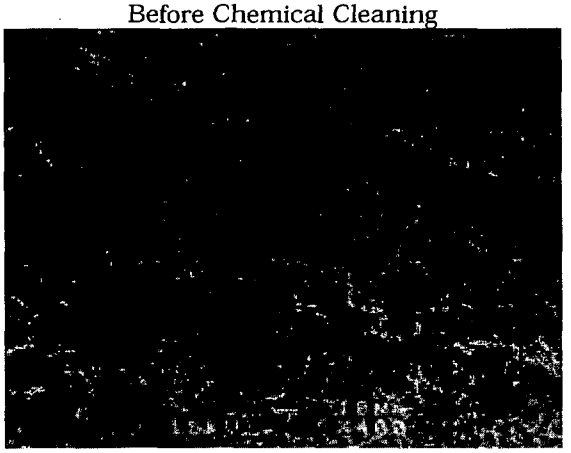

After Chemical Cleaning

Region B

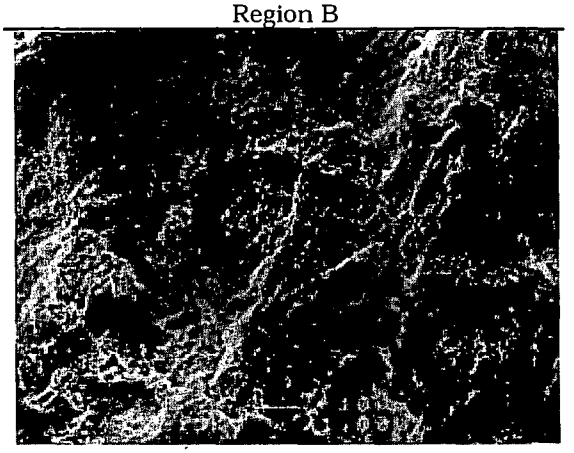

Before Chemical Cleaning

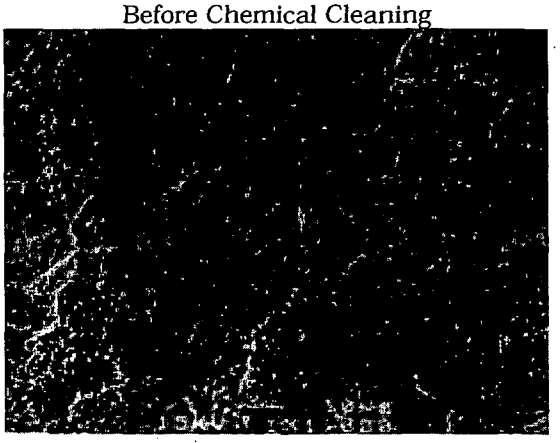

After Chemical Cleaning

Figure 32. Fracture morphology of A533-Gr B low-alloy steel tested in high-dissolved oxygen water at 288°C and ≈0.75% strain range

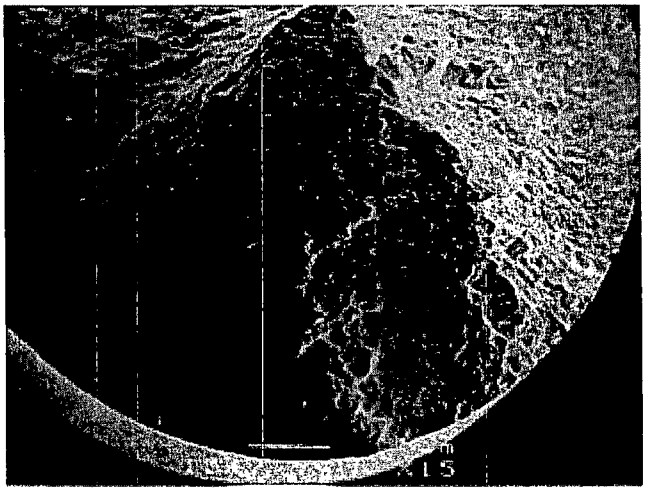

Region A

Region B

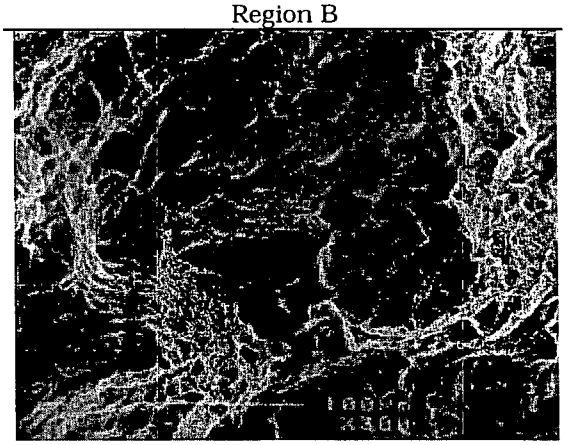

Before Chemical Cleaning

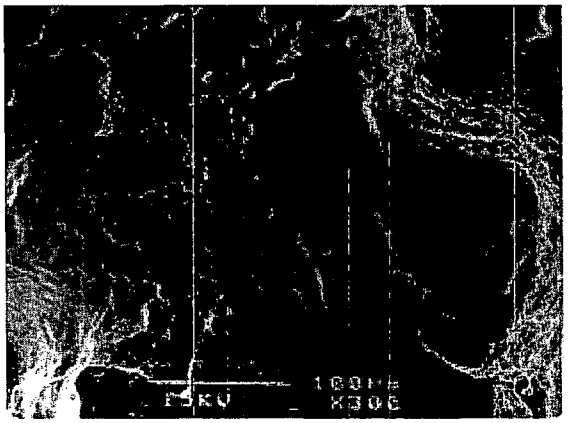

After Chemical Cleaning

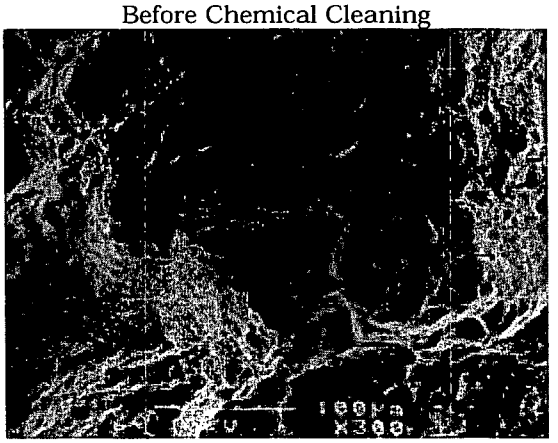

After Chemical Cleaning

Figure 33. Fracture morphology of A533-Gr B low-alloy steel tested in simulated PWR water at 288°C and ≈0.75% strain range

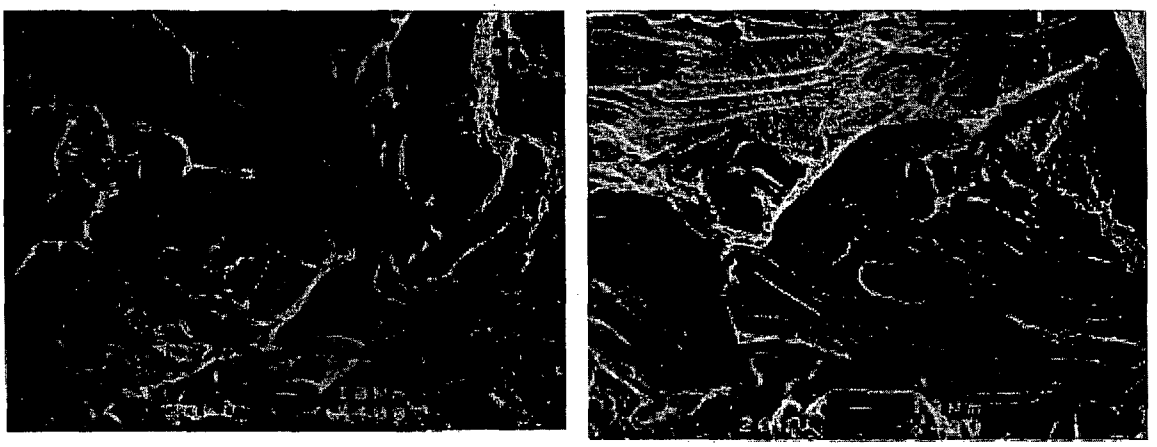

Figure 34. Examples of cleavage fracture in A106-Gr B specimen pulled apart at room temperature after the fatigue test

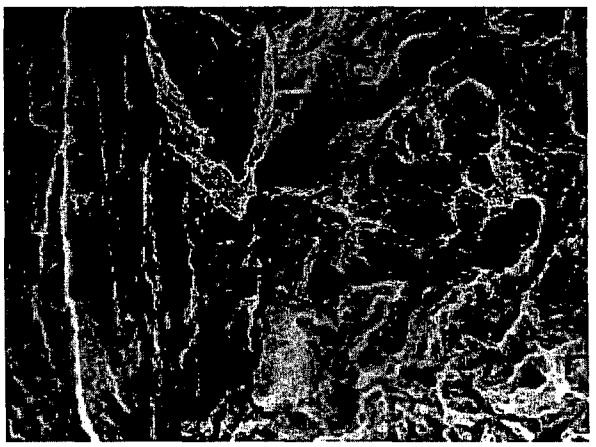

Figure 35. Sulfide inclusions on fracture surface of A106-Gr B carbon steel tested in high-dissolved oxygen water at 288°C and ≈0.4% strain range

Estimates of the average critical velocity $\overline{V}_{in}$ (mm/s) for initiation of environmentally assisted enhancement of crack growth based on a balance between sulfide supply rate and mass transport away from the crack tip[62,63] give

$$\overline{V}_{in} = \frac{1.27 x 10^{-6}}{a} \tag{3.21}$$

where a is the crack depth (mm). However, nearly all of the studies that support Eq. 3.21 have been conducted in low-DO environments, i.e., <0.05 ppm DO. For a 2.54 mm crack depth, a minimum average crack velocity of 5 x 10^{-7} mm/s is required to produce the sulfide ion concentration for environmental effects on crack growth.[62] In addition, the critical velocity must be maintained for a minimum crack extension of 0.33 mm before environmental effects can occur.[63] Equation 3.21 indicates that the minimum crack velocity to initiate environmental effects on crack growth increases with decreasing crack depth. For crack depths of 0.01-3 mm, crack velocities in the range of 1.27 x 10^{-4} to 4.23 x 10^{-7} mm/s are required for environmentally assisted reduction in fatigue life of CSs and LASs in low-DO water. For smooth cylindrical fatigue specimens, these growth rates are not achieved under

the loading conditions typically used for fatigue S-N data, which suggests that environmental effects on fatigue life in low-DO environments will not be significant. This result is consistent with the existing fatigue S-N data; for most compositions of CSs and LASs, only moderate reductions in fatigue life (less than a factor of 2) are observed in 288°C water containing <0.01 ppm DO.

Recent studies that characterize the influence of reactor environment on the formation and growth of fatigue cracks in polished smooth specimens of CSs and LASs indicate that the decrease in fatigue life of these steels in high-DO water is primarily caused by the effects of environment on the growth of short crack.[45] Measured crack lengths as a function of fatigue cycles for smooth cylindrical specimens of A533-Gr B LAS and A106-Gr B CS tested in air, simulated PWR, and high-DO water are shown in Fig. 36. The corresponding crack growth rates for A533-Gr B steel are plotted as a function of crack length in Fig. 37. The results indicate that at ≈0.8% strain range, only 30-50 cycles are needed to form a 100-μm crack in high-DO water, whereas ≈450 cycles are required to form a 100-μm crack in low-DO PWR environment and more than 3000 cycles in air. These values correspond to average growth rates of ≈2.5, 0.22, and 0.033 μm/cycle in high-DO water, low-DO PWR environment, and air,

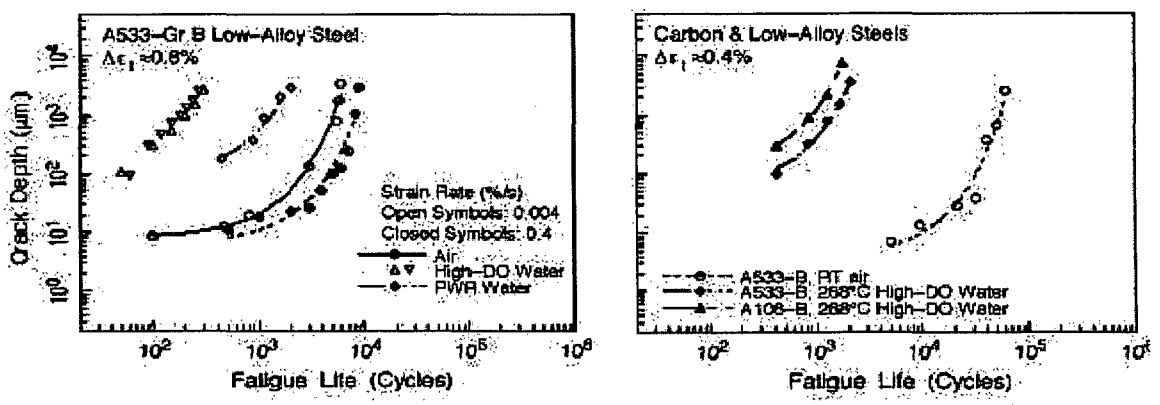

Figure 36. Depth of largest crack plotted as a function of fatigue cycles for A533-Gr B low-alloy steel and A106-Gr B carbon steel in air and water environments

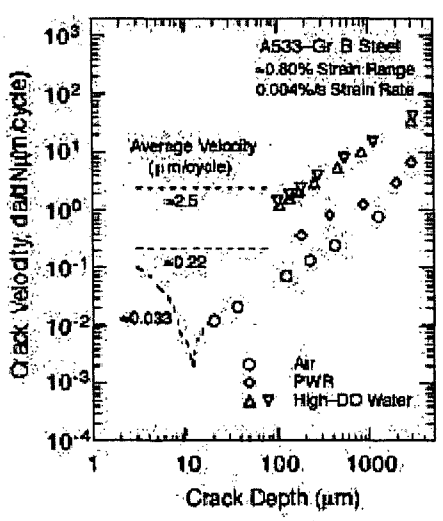

Figure 37.
Crack growth rates plotted as a function of crack depth for A533-Gr B low-alloy steel tested in air and water environments

respectively. The results also indicate that relative to air, crack growth rates in high-DO water are nearly two orders of magnitude higher during the initial stages of fatigue life (i.e., for crack sizes <100 μm), and are one order of magnitude higher for crack sizes >100 μm.

Metallographic examination of the test specimens indicates that in high-DO water, the surface cracks appear to grow entirely in Stage II growth as Mode I tensile cracks normal to the stress axis (Fig. 38).[45] In air as well as in low-DO PWR environments, both Stage I and Stage II growth is observed, i.e., surface cracks grow initially as Mode II (shear) crack along planes 45° to the stress axis and, when the stress intensities are large enough to promote slip on systems other than the primary slip, they grow as Mode I (tensile) crack normal to the stress axis. Also, for CSs, Stage I crack growth in air and low-DO water occurs entirely along the soft ferrite grains, whereas in high-DO water, cracks propagate across both ferrite and pearlite regions. A similar crack morphology is also observed on gauge surfaces (Fig. 39); surface cracks in high-DO water are always straight and normal to stress axis, whereas in air or simulated PWR environments, they are 45° to the stress axis. The different crack morphology, absence of Stage I crack growth, and propagation of cracks across pearlite regions suggest that factors other than mechanical fatigue are important for growth of surface cracks in high-DO water.

These results are consistent with the slip oxidation/dissolution mechanism of crack growth, i.e., in LWR environments, the growth of MSCs probably occurs by anodic dissolution. The growth rates depend on DO level in water and S content in the steel. In LWR environments, the formation of engineering cracks may be explained as follows: (a) surface microcracks form quite early in fatigue life at PSBs, edges of slip-band extrusions, notches that develop at grain or phase boundaries, or second-phase particles, (b) during cyclic loading, the protective oxide film is ruptured at strains greater than the fracture strain of surface oxides, and the microcracks or MSCs grow by anodic dissolution of the freshly exposed surface to sizes larger than the critical length of MSCs, and (c) growth of these large cracks characterized by accelerating growth rates. The growth rates during the final stage are controlled by both environmental and mechanical factors, and may be represented by the proposed ASME Section XI reference curves for CSs and LASs in water environments.[84] Growth rates during the initial stage are controlled primarily by the environment but mechanical fatigue is required for film rupture. For A533-Gr B steel tested in water at 288°C, 0.8% strain range, and 0.004% strain rate, the initial growth rates, from Eqs. 3.18 and 3.17, are ≈7 and 0.4 μm/cycle, respectively, for high- and low-DO levels in water. These values are a factor of ≈2 higher than the measured growth rates (Fig. 37).

4 Overview of Fatigue S–N Data

The primary sources of relevant S-N data for CSs and LASs are the tests performed by General Electric Co. (GE) in a test loop at the Dresden 1 reactor;[85,86] work sponsored by EPRI at GE;[4,87] the work of Terrell at Mechanical Engineering Associates (MEA);[88-90] the present work at ANL on fatigue of pressure vessel and piping steels;[11-14,20-25] the large JNUFAD* data base for "Fatigue Strength of Nuclear Plant Component" and recent studies at IHI, Hitachi, and Mitsubishi Heavy Industries in Japan.[6-10] The data base is composed of ≈1200 tests,

*Private communication from M. Higuchi, Ishikawajima-Harima Heavy Industries Co., Japan, to M. Prager of the Pressure Vessel Research Council, 1992. The old data base "FADAL" has been revised and renamed "JNUFAD."

A106-Gr B Carbon Steel | A533-Gr B Low-Alloy Steel

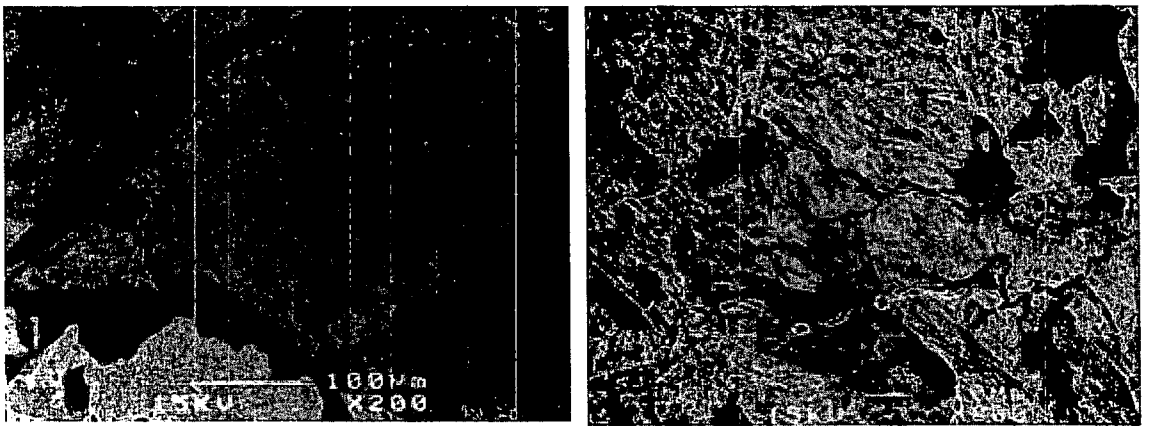

Air

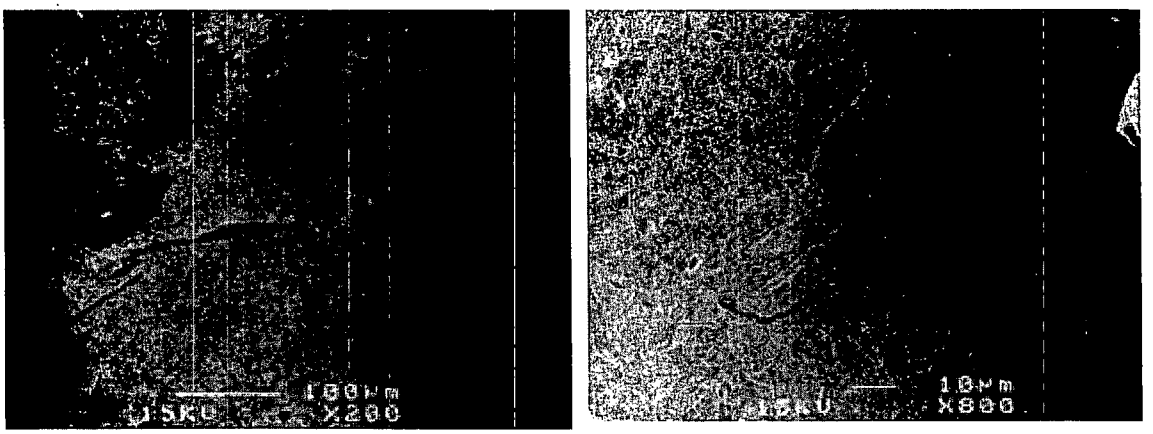

Simulated PWR Environment

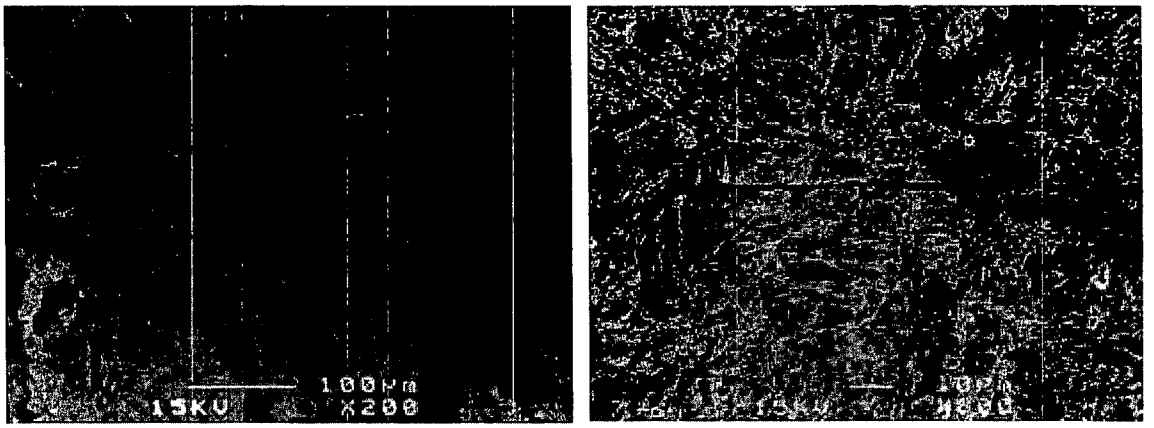

Water with ≈0.7 ppm Dissolved Oxygen

Figure 38. Photomicrographs of surface cracks along longitudinal sections of A533-Gr B low-alloy steel and A106-Gr B carbon steel in air, simulated PWR environment, and high-dissolved-oxygen water.

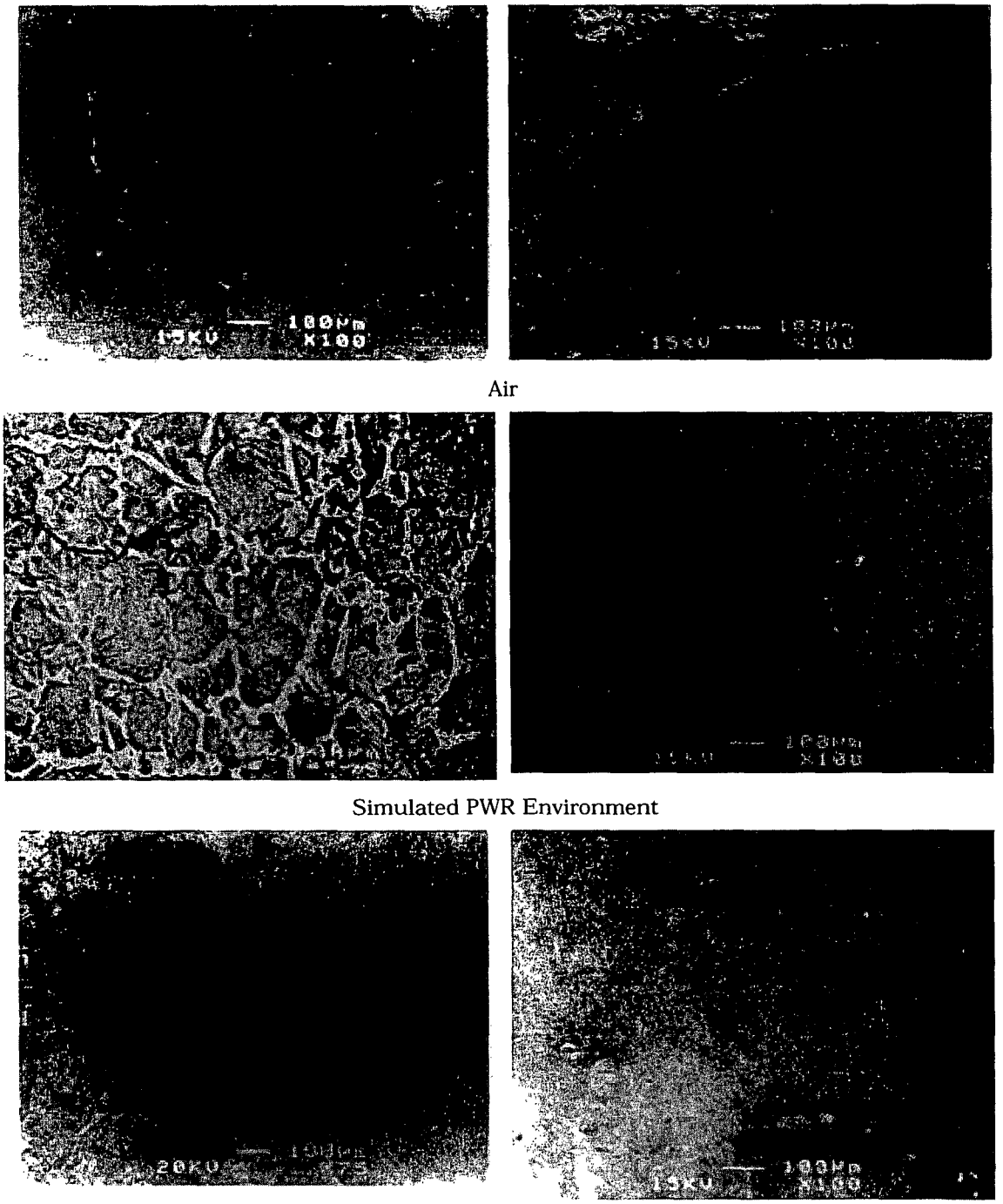

Figure 39. Photomicrographs of cracks on gauge surfaces of A533-Gr B low-alloy steel and A106-Gr B carbon steel specimens tested in air, simulated PWR environment, and high-dissolved-oxygen water.

≈600 each in air and water environments. Carbon steels include ≈10 heats of A533-Grade 6, A106-Grade B, A516-Grade 70, and A508-Class 1 steel, while LASs include ≈15 heats of A533-Grade B, A302-Grade B, and A508-Class 2 and 3 steels.

4.1 Air Environment

4.1.1 Steel Type

In air, the fatigue life of carbon and low-alloy steels depends on steel type, temperature, orientation (i.e., rolling or transverse) and for some comparisons on applied strain rate. Fatigue S-N data from various investigations[4,6,7,11-14,88] on CSs and LASs are shown in Fig. 40. The ASME Section III mean-data curves (at room temperature) are also included in the figures. The results indicate that although there is significant scatter due to material variability, the fatigue lives of LASs are a factor of ≈1.5 greater than those of CSs. Also, the fatigue limit of LASs is slightly higher than that of CSs. The data for CSs are inconsistent with the ASME mean data curve; the data are above the mean curve at strain amplitudes >0.2% and below the curve at <0.2% strain. The data for LASs show good agreement with the ASME mean data curve.

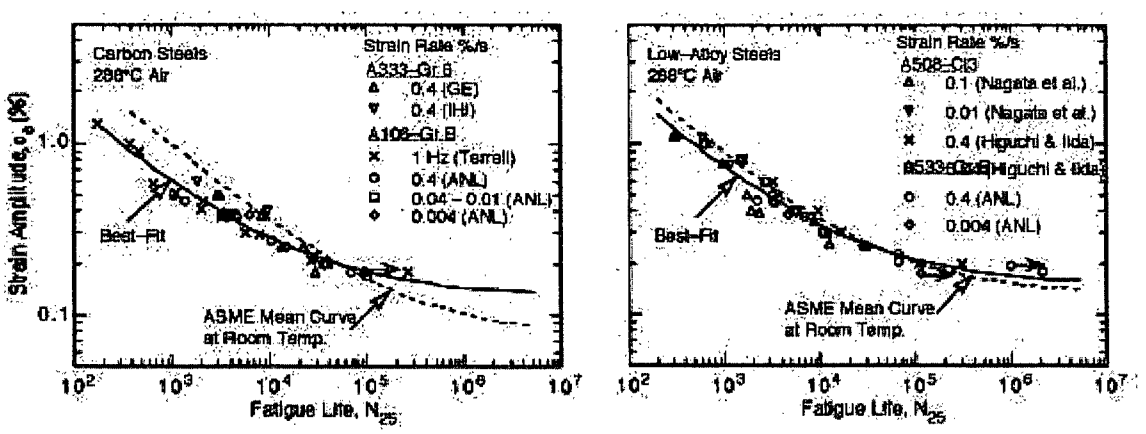

Figure 40. Strain amplitude vs. fatigue life data for carbon and low-alloy steels in air at 288°C

4.1.2 Temperature

For both carbon and low-alloy steels, fatigue life decreases as temperature increases from room temperature to 320°C. Fatigue S-N data from the JNUFAD data base and other investigations[4,11-14,88] in air at room temperature and ≈288°C are shown in Fig. 41. For each grade of steel, the data represent several heats of material. The results indicate a factor of ≈1.5 decrease in fatigue life of both CSs and LASs with increasing temperature.

4.1.3 Orientation

Some steels show very poor fatigue properties in the transverse orientation, e.g., the fatigue life as well as the fatigue limit may be lower in the transverse orientation than in the

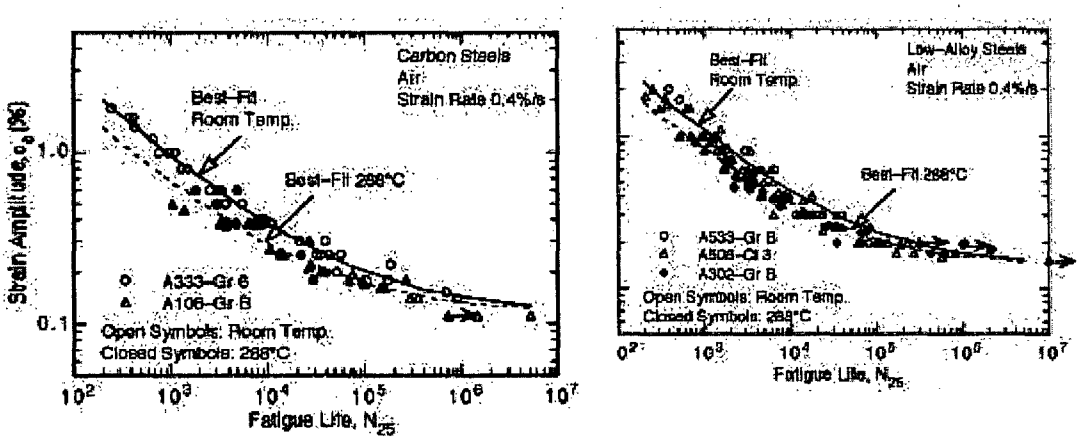

Figure 41. Strain amplitude vs. fatigue life data for carbon and low-alloy steels in air at room temperature and 288°C

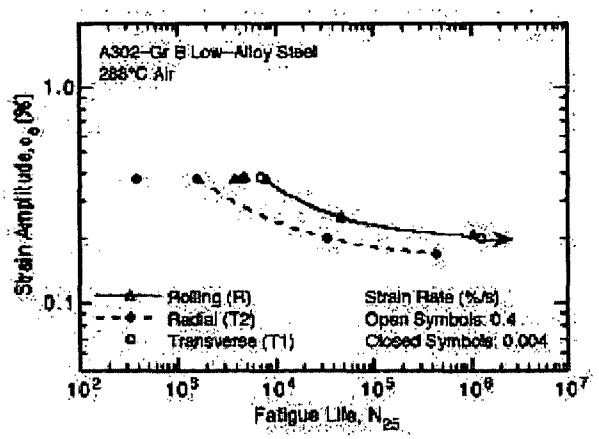

Figure 42. Effect of material orientation on fatigue life of A302-Gr B low-alloy steel in air at 288°C

rolling orientation.[13,14] The fatigue lives of A302-Gr B steel in three orientations* in air at 288°C are shown in Fig. 42. The results indicate that fatigue lives for the R and T1 orientations are approximately the same, but for T2 orientation both fatigue life and fatigue limit are lower than those in the other orientations. At slow strain rates, fatigue life in the T2 orientation is nearly one order of magnitude lower than in the R orientation. Metallographic examination indicates that structural factors, such as distribution and morphology of sulfides, are responsible for the poor fatigue resistance in transverse orientations, in which a fatigue crack propagates preferentially along the sulfide stringers.

4.1.4 Strain Rate

The existing fatigue S-N data indicate that in the temperature range of dynamic strain aging (200-370°C), some heats of CS and LAS are sensitive to strain rate even in an inert environment; with decreasing strain rate, the fatigue life may be either unaffected,[11-14] decrease for some heats,[91] or increase for others.[92] At 288°C, a decrease in strain rate by 2

*Both transverse and radial directions are perpendicular to the rolling direction but the fracture plane is across the thickness of the plate in transverse orientation and parallel to the plate surface in radial orientation.

orders of magnitude has little or no effect on fatigue lives of the ANL heats of A106-Gr B and A533-Gr B steel (Fig. 40), whereas fatigue lives of A302-Gr B steel in radial orientation (Fig. 42) decreased by a factor of ≈5. A decrease in life with decreasing strain rate is observed for the A333-Gr 6 CS, see Table A2 of the Appendix. Inhomogeneous plastic deformation can result in localized plastic strains, this localization retards blunting of propagating cracks that is usually expected when plastic deformation occurs and can result in higher crack growth rates.[90] The increases in fatigue life have been attributed to retardation of crack growth rates due to crack branching and suppression of plastic zone. Formation of cracks is easy in the presence of dynamic strain aging.[92]

4.1.5 Cyclic Stress–versus–Strain Behavior

The cyclic stress-strain response of carbon and low-alloy steels varies with steel type, temperature, and strain rate. In general, these steels show initial cyclic hardening, followed by cyclic softening or a saturation stage at all strain rates. The CSs, with a pearlite and ferrite structure and low yield stress, exhibit significant initial hardening. The LASs, which consist of tempered ferrite and a bainitic structure, have a relatively high yield stress, and show little or no initial hardening, may exhibit cyclic softening during testing. For both steels, maximum stress increases as applied strain increases and generally decreases as temperature increases. However, at 200-370°C, these steels exhibit dynamic strain aging, which results in enhanced cyclic hardening, a secondary hardening stage, and negative strain rate sensitivity.[91,92] The temperature range and extent of dynamic strain aging vary with composition and structure. Under conditions of dynamic strain aging, cyclic stress increases with decreases in strain rate.

The effect of strain rate and temperature on the cyclic stress response of A106-Gr B, A333-Gr 6, A533-Gr B, and A302-Gr B steels is shown in Fig. 43. For both carbon and low-alloy steels, cyclic stresses are higher at 288°C than at room temperature. At 288°C, all steels exhibit greater cyclic and secondary hardening because of dynamic strain aging. The extent of hardening increases as applied strain rate decreases.

During cyclic loading, the stress response is essentially controlled by microstructural changes that occur in the material during the test. In the temperature regime of dynamic strain aging, the microstructural changes are significantly altered because of the interactions between mobile dislocations and interstitial carbon or nitrogen atoms. Such interactions are strongly dependent on temperature and strain rate. The microstructures that developed in A106-Gr B carbon steel specimens tested at 288°C, ≈0.75% strain range, and three different strain rates are shown in Figs. 44-47.* The results indicate that the dislocation structure varies significantly with strain rate; the lower the strain rate the more mature the dislocation structure. At 0.4 %/s strain rate, there is no well-established dislocation structure, although immature dislocation walls can be observed (Figs. 44 and 45). A mature microstructure consisting of dislocation cells, walls, and/or veins with high dislocation density is observed in both the ferrite and pearlite grains at 0.04 and 0.004 %/s strain rates (Figs. 46 and 47). The dislocation walls may cross individual cementite plates or particles within a pearlite grain to keep a consistent crystallographic structure.

---

* Work performed by Ms. Gordana Avramovic-Cingara and Prof. Zhirui Wang, Department of Metallurgy and Materials Science, University of Toronto, November 1994.

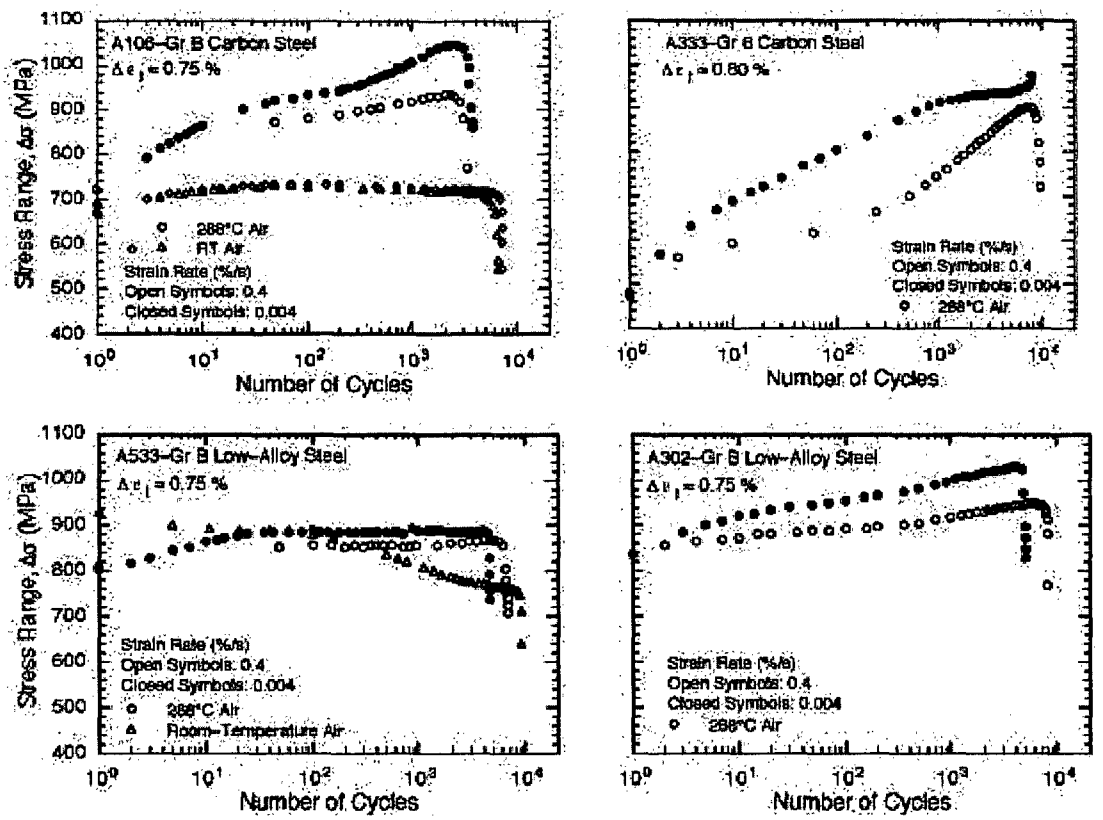

Figure 43. Effect of strain rate and temperature on cyclic stress of carbon and low-alloy steels

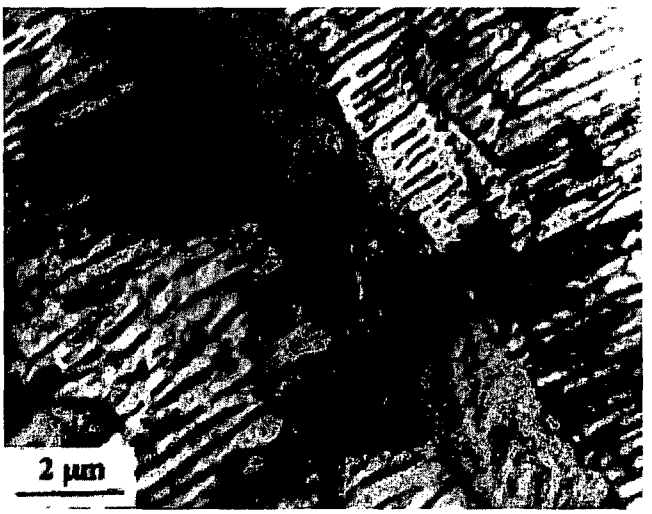

Figure 44. Typical microstructure in A106-Gr B specimen tested at 0.4 %/s strain rate showing immature dislocation walls in three pearlite grains consisting of Fe_3C plates in the ferrite matrix

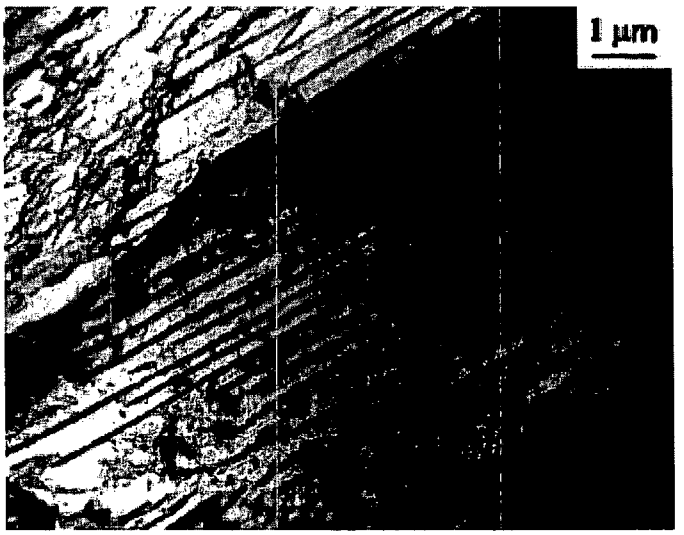

Figure 45. Ferrite grain between two pearlite grains in A106-Gr B specimen tested at 0.4 %/s strain rate

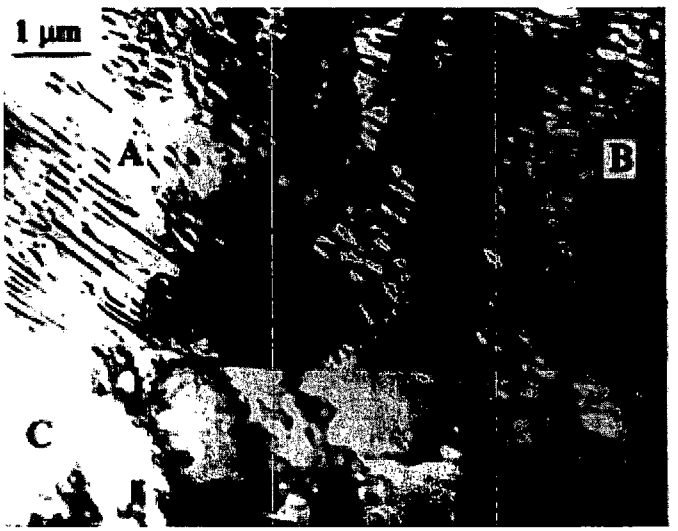

Figure 46. Typical microstructure in A106-Gr B specimen tested at 0.04 %/s strain rate showing a cell structure in ferrite (C) and two pearlite grains (A and B)

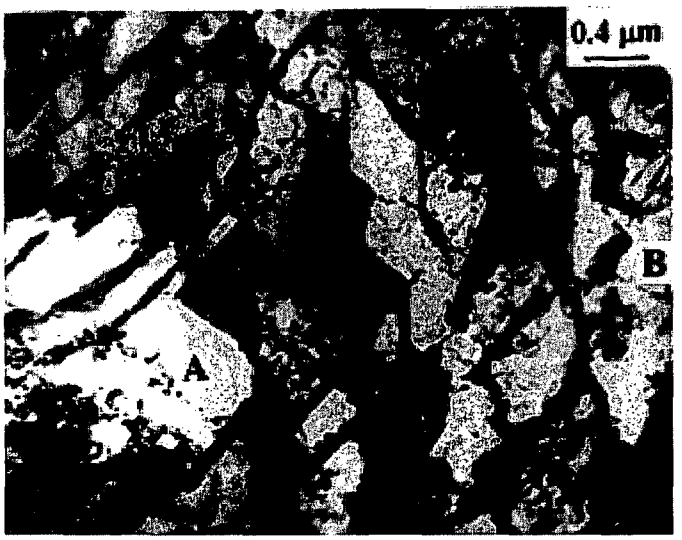

Figure 47. Formation of dislocation walls in two pearlite grains (A and B) in A106-Gr B specimen tested at 0.004 %/s strain rate

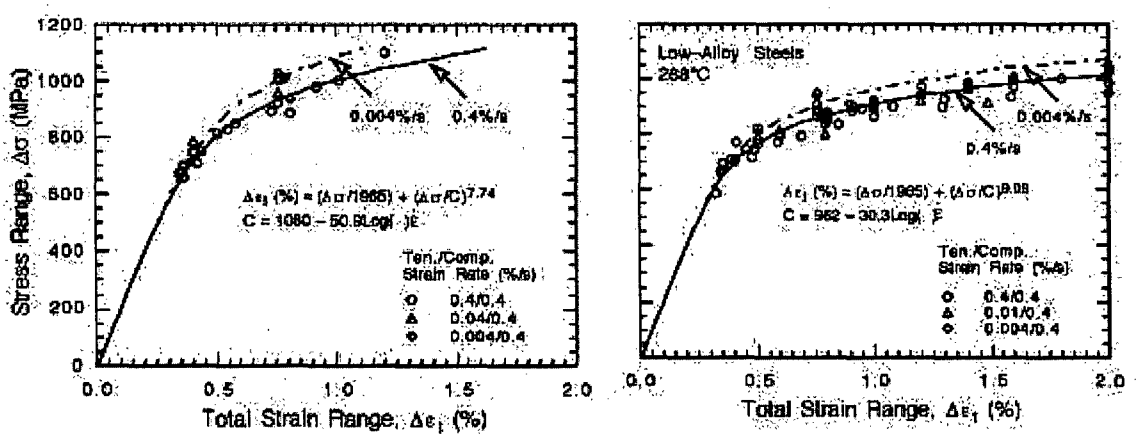

Figure 48. Cyclic stress-strain curve for carbon and low-alloy steels at 288°C in air

The cyclic-stress-vs.-strain curves for carbon and low-alloy steels at 288°C are shown in Fig. 48; cyclic stress corresponds to the value at half life. The stress-strain curve for carbon steels can be represented with the equation

$$\Delta\varepsilon_t = \frac{\Delta\sigma}{1965} + \left(\frac{\Delta\sigma}{C}\right)^{7.74}, \tag{4.1a}$$

where the constant C is expressed as

$$C = 1080 - 50.9\,Log(\dot{\varepsilon}); \tag{4.1b}$$

and for low-alloy steels, with the equation

$$\Delta\varepsilon_t = \frac{\Delta\sigma}{1965} + \left(\frac{\Delta\sigma}{D}\right)^{9.09}, \tag{4.2a}$$

where the constant D is expressed as

$$D = 962 - 30.3Log(\dot{\varepsilon}), \tag{4.2b}$$

where $\Delta\sigma$ is the cyclic stress range (MPa), and $\dot{\varepsilon}$ is applied total strain rate (%/s). The cyclic stress response is lower at room temperature than at 288°C.

4.2 LWR Environments

The fatigue data in LWR environments indicate a significant decrease in fatigue life of CSs and LASs when five conditions are satisfied simultaneously, viz., applied strain range, service temperature, DO in the water, and sulfur content of the steel are above a minimum threshold level, and the loading strain rate is below a threshold value. Although the microstructures and cyclic-hardening behavior of CSs and LASs are significantly different, environmental degradation of fatigue life of these steels is identical. Also, studies on fatigue crack growth behavior of CSs and LASs indicate that flow rate is an important parameter for environmental effects on crack growth rate in water.[39,58,59,64] However, experimental data to establish either the dependence of fatigue life on flow rate or the threshold flow rate for environmental effects to occur are not available. For both steels, environmental effects on fatigue life are minimal if any one of these conditions is not satisfied. The effects of these parameters on fatigue life are discussed below in greater detail to define the threshold values.

4.2.1 Strain Amplitude

A minimum threshold strain is required for environmentally assisted decrease in fatigue life. This behavior is consistent with the slip-dissolution model for crack propagation;[74,76] the applied strain must exceed a threshold value to rupture the passive surface film in order for environmental effects to occur. This threshold value most likely depends both on material parameters such as amount and distribution of sulfides, and on parameters such as temperature, strain rate, and DO level in water. The fatigue lives of A533-Gr B and A106-Gr B steels in high-DO water at 288°C and various strain rates[13,14] are shown in Fig. 49. For these heats of carbon and low-alloy steels, the threshold strain amplitude appears to be at ≈0.18%, i.e., a value ≈20% higher than the fatigue limit of these specific heats of steel.

4.2.2 Strain Rate

The effects of strain rate on fatigue life of CSs and LASs in LWR environments depend on whether or not all threshold conditions are satisfied. When any one of the threshold conditions is not satisfied, e.g., low-DO PWR environment, the effects of strain rate are similar to those in air; heats of steel that are sensitive to strain rate in air also show a decrease in fatigue life in water with decreasing strain rate (discussed further in Section 4.2.7). Effects of strain rate are much greater when all threshold conditions are satisfied. The existing data

indicate that a slow strain rate applied during the tensile-loading cycle is primarily responsible for environmentally assisted reduction in fatigue life. A slow strain rate applied during both tensile- and compressive-load cycles does not cause further decrease in fatigue life, e.g., solid diamonds and square in Fig. 49 for A106-Gr B steel. These results are consistent with a slip oxidation/dissolution mechanism[74-76] discussed in Section 3.2. During tensile load cycle, the protective oxide film is ruptured at strains greater than the fracture strain of surface oxides, and growth rates are enhanced because of anodic dissolution of the freshly exposed surface. The effect of environment increases with decreasing strain rate. The mechanism assumes that environmental effects do not occur during the compressive load cycle, because during that period water does not have access to the crack tip.

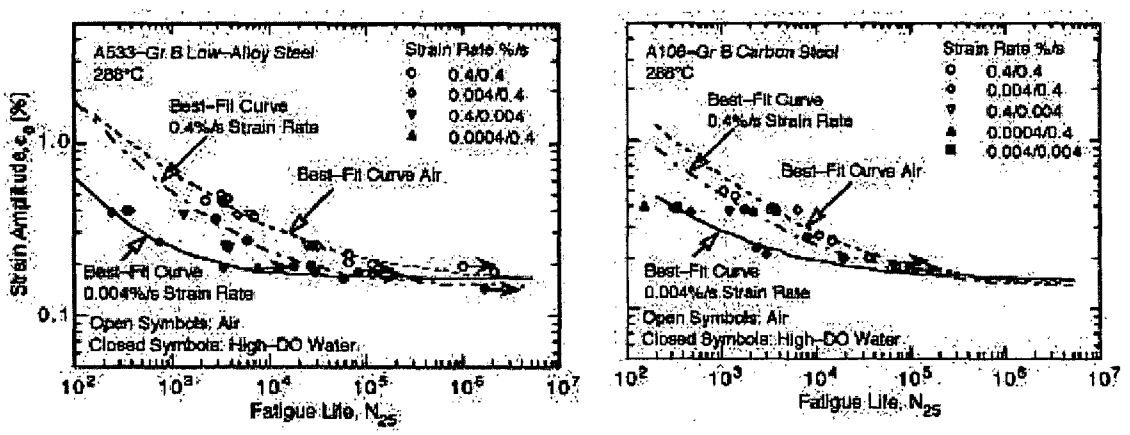

Figure 49. Strain amplitude vs. fatigue life data for A533-Gr B and A106-Gr B steels in high-dissolved-oxygen water at 288°C

However, limited data indicate that a slow strain rate during the compressive load cycle also decreases fatigue life, although the decrease in life is small. For example, the fatigue life of A533-Gr B steel at 288°C, 0.7 ppm DO, and ≈0.5% strain range decreased by factors of 5, 8, and 35 for the fast/fast, fast/slow, and slow/fast tests, respectively, i.e., solid circles, diamonds, and inverted triangles in Fig. 49. Similar results have been observed for A333-Gr 6 carbon steel;[8] relative to the fast/fast test, fatigue life for slow/fast and fast/slow tests at 288°C, 8 ppm DO, and 1.2% strain range decreased by factors of 7.4 and 3.4, respectively. For fast/slow tests, reduction in life is most likely caused by enhanced growth rates due to anodic dissolution of freshly exposed surface during the period starting from film rupture during the fast tensile load cycle, to repassivation of the surface during the slow compressive load cycle. The major contribution of environment occurs during slow compressive loading near peak tensile load.

The S-N data indicate that strain rates above 1 %/s have little or no effect on fatigue life of CSs and LASs in LWR environments. For strain rates <1 %/s, fatigue life decreases rapidly with decreasing strain rate. The fatigue lives of several heats of CSs and LASs[6-14] are plotted as a function of strain rate in Fig. 50. The results indicate that when the five threshold conditions are satisfied, fatigue life decreases with decreasing strain rate and increasing levels of DO in water. Only a moderate decrease in fatigue life is observed in low-DO water, e.g., at DO levels of ≤0.05 ppm. For two heats of steel, e.g., A106-Gr B CS and A533-Gr B LAS, the effect of strain rate on fatigue life appears to saturate at ≈0.001%/s strain rate. This is

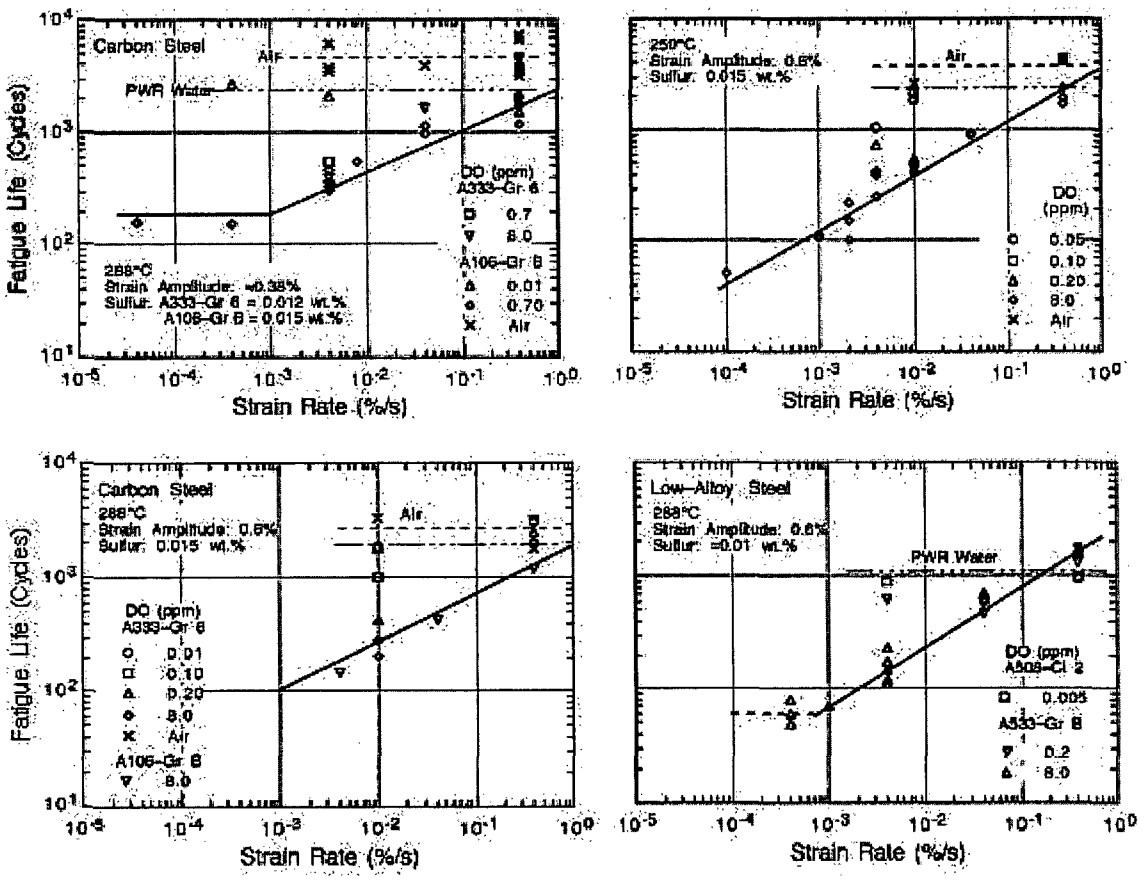

Figure 50. Dependence of fatigue life of carbon and low-alloy steels on strain rate

consistent with the predictions of a crack growth model.[26] However, a heat of A333-Gr 6 carbon steel did not show saturation at this strain rate at 250°C and 8 ppm DO. Saturation strain rates are likely to depend both on material and environmental variables.

Nearly all of the existing fatigue S-N data have been obtained under loading histories with constant strain rate, temperature, and strain amplitude. Actual loading histories encountered during service of nuclear power plants are far more complex. Exploratory fatigue tests have been conducted with waveforms in which the slow strain rate is applied during only a fraction of the tensile loading cycle.[8,11-14] The results of such tests provide guidance for developing procedures and rules for fatigue evaluation of components under complex loading histories.

Results for A106-Gr B steel tested in air and low- and high-DO environments at 288°C and ≈0.75% strain range are summarized in Fig. 51. The waveforms consist of segments of loading and unloading at fast and slow strain rates. The variation in fatigue life of A106-Gr B and A333-Gr 6 carbon steels and A533-Gr B low-alloy steel[8,13,14] is plotted as a function of the fraction of loading strain at slow strain rate in Fig. 52. Open symbols indicate tests where the slow portions occurred near the maximum tensile strain. Closed symbols indicate tests where the slow portions occurred near the maximum compressive strain. In Fig. 52, if the relative damage were independent of strain amplitude, fatigue life should decrease linearly

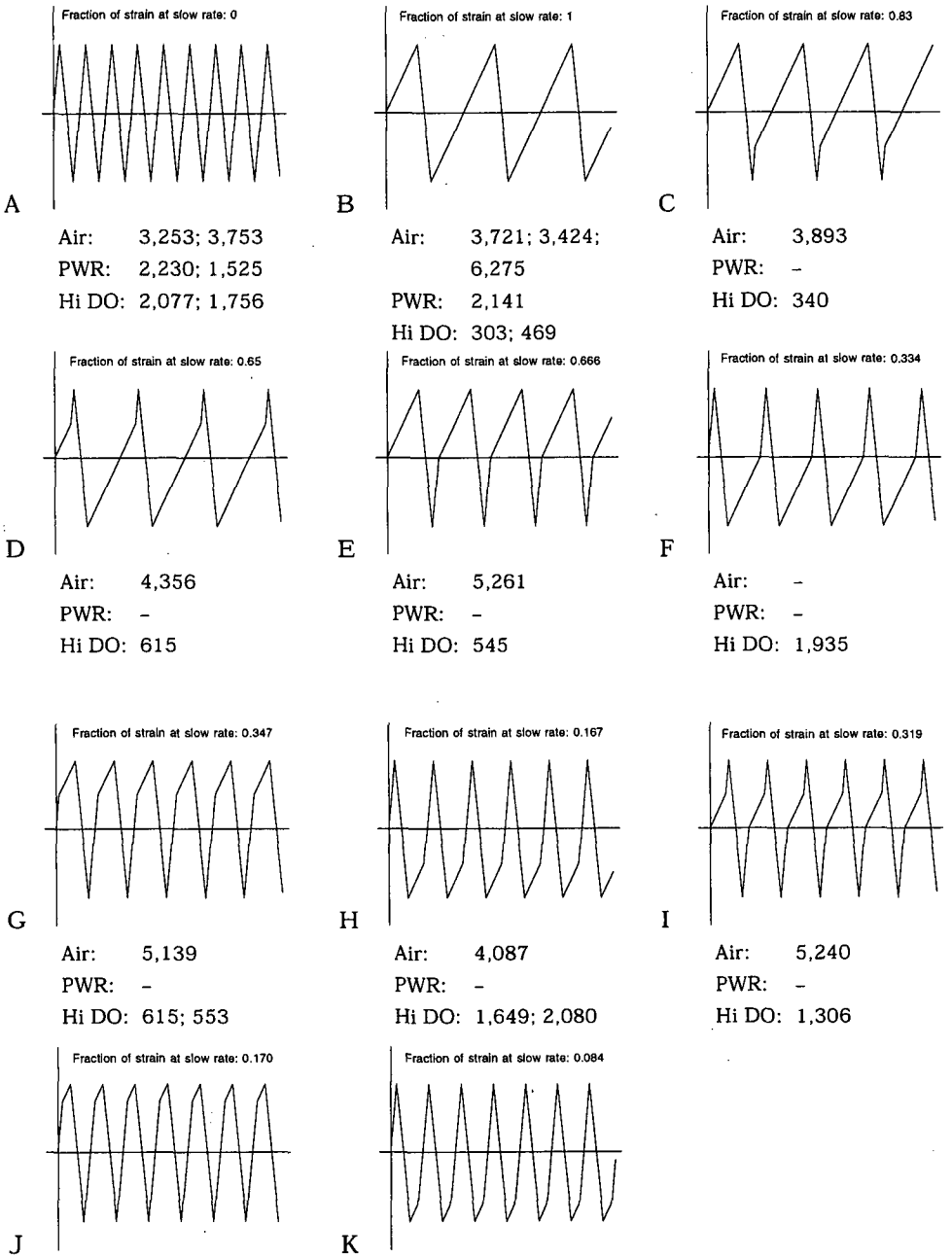

Figure 51. Fatigue life of A106-Gr B carbon steel at 288°C and 0.75% strain range in air and water environments under different loading waveforms

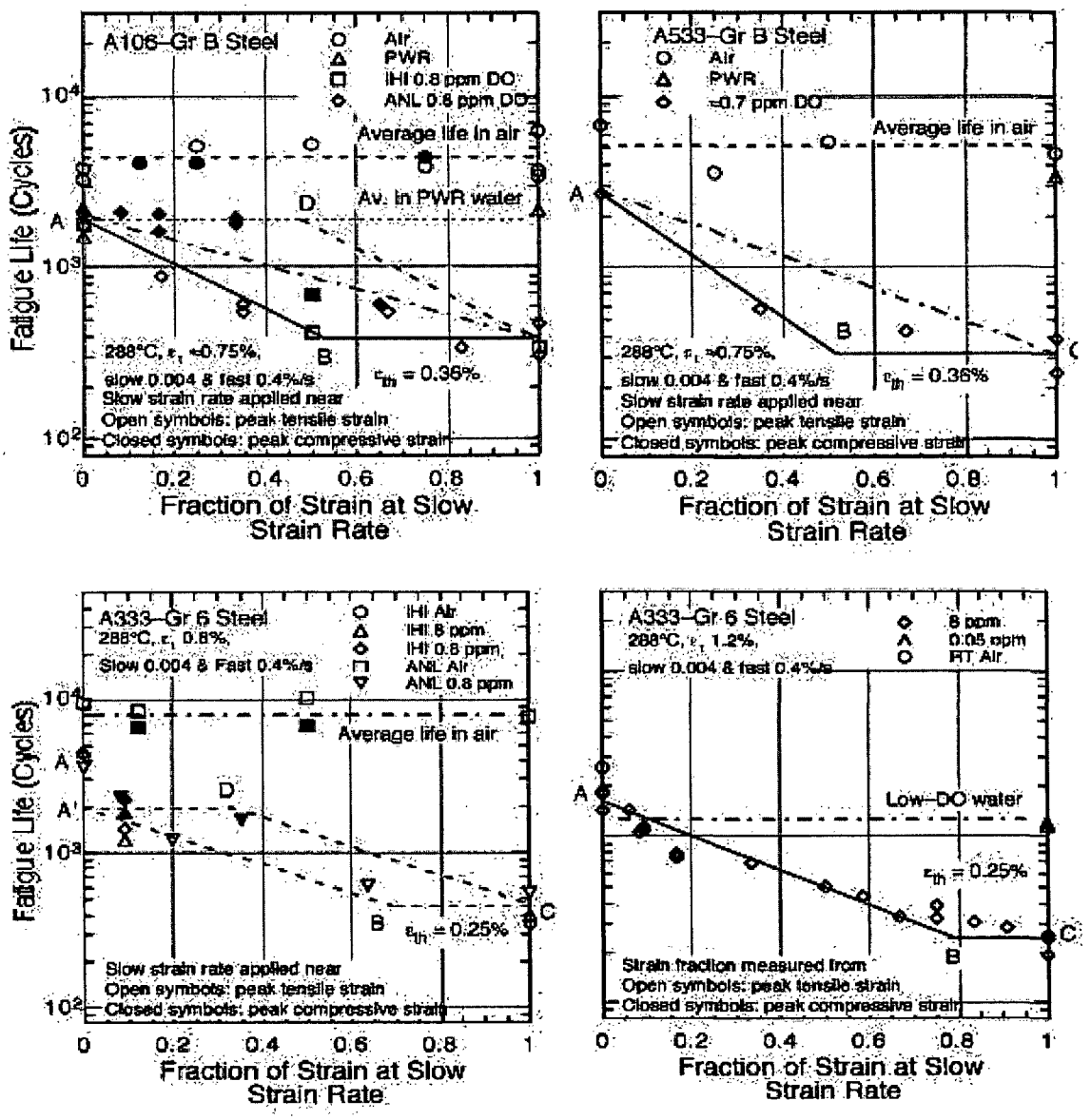

Figure 52. Fatigue life of carbon and low-alloy steels tested with loading waveforms where slow strain rate is applied during a fraction of tensile loading cycle

from A to C along the chain-dot line. Instead, the results indicate that the relative damage due to slow strain rate is independent of strain amplitude once the amplitude exceeds a threshold value to rupture the passive surface film. The threshold strain range is 0.36 % for A106-Gr B steel; a value of 0.25% was assumed for A333-Gr 6 steel.

Loading histories with slow strain rate applied near maximum compressive strain (i.e., waveforms D, F, H, or K) produce no damage (line AD) until the fraction of the strain is sufficiently large that slow strain rates are occurring for strain amplitudes greater than the threshold. In contrast, loading histories with slow strain rate applied near the maximum

tensile strain (i.e., waveforms C, E, G, or J) show continuous decreases in life (line AB) and then saturation when a portion of the slow strain rate occurs at amplitudes below the threshold value (line BC). For A106-Gr B steel, the decrease in fatigue life follows line ABC when a slow rate occurs near the maximum tensile strain and line ADC when it occurs near maximum compressive strain. The results for A106-Gr B and A533-Gr B carbon steels follow this trend.

The A333-Gr 6 steel exhibits a somewhat different trend. A slow strain rate near peak compressive strain appears to cause a significant reduction in fatigue life, while as discussed previously, slow strain rate had a significant effect on fatigue life of A106-Gr B steel only when it occurred at strains greater than the threshold strain. For this heat of A333-Gr 6 CS, a threshold strain for environmental effects has not been observed for tests in high-DO water at 288°C and 0.6% strain amplitude, i.e., fatigue damage was independent of strain amplitude.[8] The apparent disagreement may be attributed to the effect of strain rate on fatigue life. This heat exhibits a strain rate effect in air, e.g., fatigue life in air decreased ≈20% when the strain rate decreases from 0.4 to 0.004 %/s (Table A4 of Appendix A). The cyclic hardening behavior of the steel is also quite different than that of the A106-Gr B steel, Fig. 41. The A333-Gr 6 steel has a very low yield stress and shows significant cyclic hardening during the entire test. The A106-Gr B steel has a higher yield stress and exhibits cyclic hardening only during the initial 100 cycles. In Fig. 52, the decrease in fatigue life from A to A' is most likely caused by a strain rate effect that is independent of the environment. If the hypothesis that each portion of the loading cycle above the threshold strain is equally damaging is valid, the decrease in fatigue life due to environmental effects should follow line A'BC when a slow rate is applied near peak tensile strain, and line A'DC when it is applied near peak compressive strain. This behavior is consistent with the slip-oxidation/dissolution mechanism.[74,76]

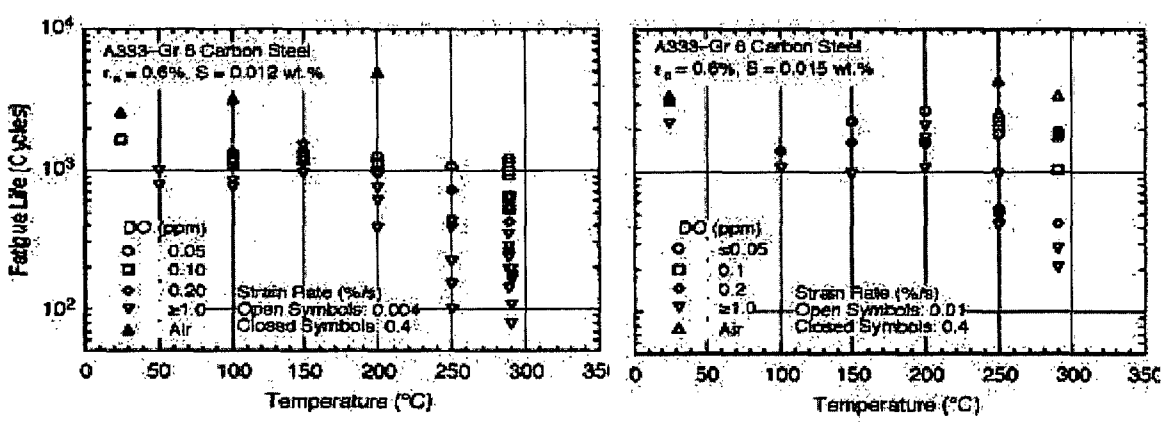

Figure 53. Change in fatigue life of A333-Gr 6 carbon steel with temperature and DO

4.2.3 Temperature

The change in fatigue life of two heats of A333-Gr 6 carbon steel[6,7,10] with test temperature at different levels of DO is shown in Fig. 53. Other parameters, e.g., strain amplitude and strain rate, were kept constant; the applied strain amplitude was above and strain rate was below the critical threshold value. In air, the two heats have a fatigue life of ≈3300 cycles. The results indicate a threshold temperature of 150°C, above which

environment decreases fatigue life if DO in water is also above the critical level. In the temperature range of 150-320°C, fatigue life decreases linearly with temperature; the decrease in life is greater at high temperatures and DO levels. Only a moderate decrease in fatigue life is observed in water at temperatures below the threshold value of 150°C or at DO levels ≤0.05 ppm. Under these conditions, fatigue life in water is 30-50% lower than in air; Fig. 53 shows an average life of ≈2100 cycles for the heat with 0.015 wt.% sulfur and ≈1200 cycles for the 0.012 wt.% sulfur steel. For the latter, the larger decrease in fatigue life in low-DO water relative to room temperature air, is most likely due to strain rate effects. As discussed in the preceding section, the A333-Gr 6 steel with 0.012 wt.% sulfur is sensitive to strain rate even in air; life decreases with a decrease in strain rate.[13,24] The strain rate effects are similar in air and in water when any one of the threshold conditions is not satisfied.

Fatigue S-N data on high-sulfur LASs are inadequate to determine the temperature dependence of fatigue life in water. Establishing the threshold conditions and the functional forms for the dependence of fatigue life on various loading and environmental conditions requires complete data sets where one parameter is varied while others are kept constant. Although the existing fatigue S-N data for LASs cover an adequate range of material, loading, and environmental parameters, they provide incomplete data sets for temperature. An artificial neural network (ANN) has been used to find patterns and identify the threshold in fatigue S-N data for CSs and LASs in LWR environments.[93] The main benefits of the ANN approach are that estimates of life are based purely on the data and not on preconceptions, and that the network can interpolate effects where data are not present by learning trends. The factors which effect fatigue life can have synergistic effects on one another. A neural network can detect and utilize these effects in its predictions.

A neural network, consisting of two hidden layers with the first containing ten nodes and the second containing six nodes, was trained six times; each training was based on the same data set, but the order in which the data were presented to the ANN for training was varied and the initial ANN weights were randomized to guard against overtraining and to ensure that the network did not arrive at a solution that was a local minimum. The effect of temperature on the fatigue life of CSs and LASs estimated from ANN is shown in Fig. 54. The solid line represents estimates based on the statistical model[27,28] and open circles represent the experimental data. The results indicate that at high strain rate (0.4%/s), fatigue life is relatively insensitive to change in temperature. At low strain rate (0.004%/s), fatigue life decreases with increase in temperature beyond a threshold value of ≈150°C. The precision of the data indicates that this trend is present in the data used to train the ANN.

As discussed in the previous section, actual loading histories encountered during service of nuclear power plants involve variable loading and environmental conditions, whereas the existing fatigue S-N data have been obtained under loading histories with constant strain rate, temperature, and strain amplitude. Fatigue tests have been conducted in Japan on tube specimens (1 or 3 mm wall thickness) of A333-Gr 6 carbon steel in oxygenated water under combined mechanical and thermal cycling.[9] Triangular waveforms were used for both strain and temperature cycling. Two sequences were selected for temperature cycling (Fig. 55): an in-phase sequence in which temperature cycling was synchronized with mechanical strain cycling, and another sequence in which temperature and strain were out of phase, i.e., maximum temperature occurred at minimum strain level and vice-versa. Three temperature ranges, 50-290°C, 50-200°C, and 200-290°C, were selected for the tests. The results are

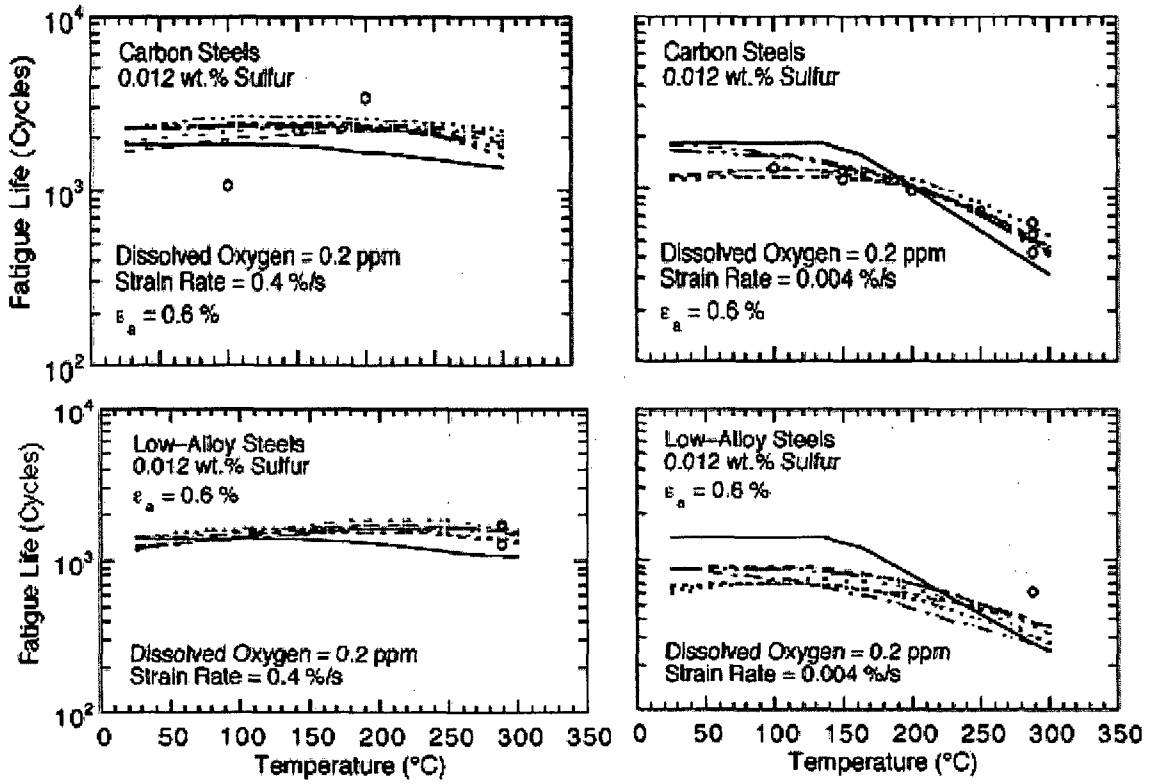

Figure 54. Dependence of fatigue life on temperature for carbon and low-alloy steels in water at two strain rates: Open circles = experimental data; solid line = statistical model; other lines = ANN estimates for the six trained data sets.

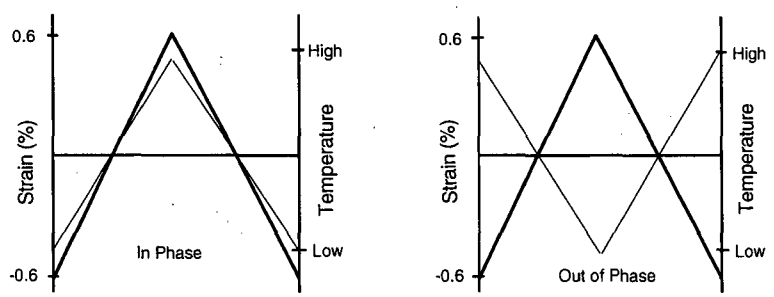

Figure 55. Waveforms for change in temperature during exploratory fatigue tests

shown in Fig. 56. An average temperature is used for the thermal cycling tests. Because environmental effects on fatigue life are moderate and independent of temperature below 150°C, the temperature for tests cycled in the range of 50–290°C or 50–200°C was determined from the average of 150°C and the maximum temperature.

The results of constant temperature tests are consistent with the results in Fig. 53 and confirm that environmental effects on fatigue life are minimal at temperatures below 150°C. The results also indicate that the fatigue life for in-phase temperature cycling is comparable to that for out-of-phase cycling. At first glance, these results are somewhat surprising. If we consider that the tensile-load cycle is primarily responsible for environmentally assisted

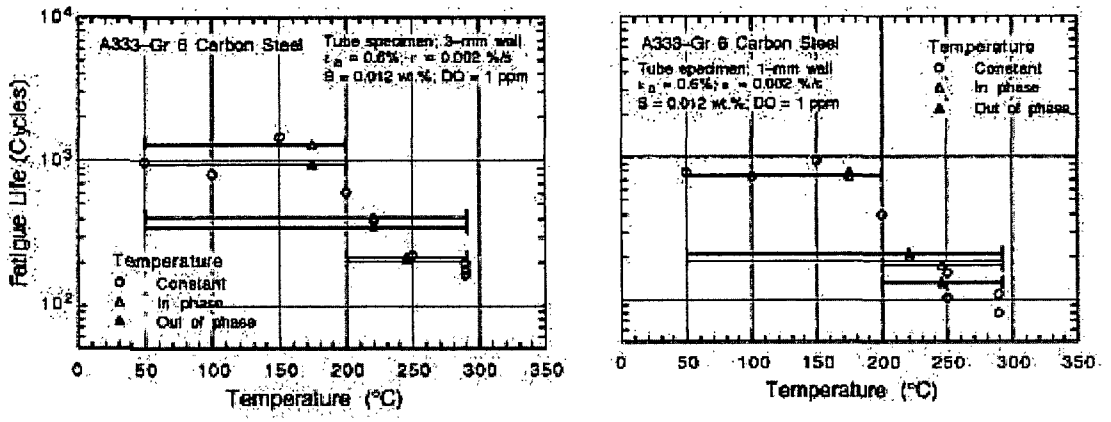

Figure 56. Fatigue life of A333-Gr 6 carbon steel tube specimens under varying temperature, indicated by horizontal bars

reduction in fatigue life and that the applied strain and temperature must be above a minimum threshold value for environmental effects to occur, then life for the out-of-phase tests should be longer than for the in-phase tests, because applied strains above the threshold strain occur at temperatures above 150°C for in-phase tests, whereas they occur at temperatures below 150°C for the out-of-phase tests. If environmental effects on fatigue life are considered to be minimal below the threshold values of 150°C for temperatures and <0.25 % for strain range, the average temperatures for the out-of-phase tests at 50-290°C, 50-200°C, and 200-290°C temperature ranges should be 195, 160, and 236°C, respectively, instead of 220, 175, and 245°C, as plotted in Fig. 56. The fatigue lives of out-of-phase tests should be at least 50% higher than those of the in-phase tests.

The nearly identical fatigue lives for the two sequences suggest that environmental effects can occur at strain levels below the threshold strain. These results are difficult to reconcile in terms of the slip oxidation/dissolution mechanism; the surface oxide film must be ruptured for environmental effects to occur. However, the results may be explained by considering the effect of compressive-load cycle on fatigue life. As was discussed in the previous section, the fatigue data suggest that a slow strain rate during the compressive-load cycle could also decrease fatigue life. The thermal cycling test results shown in Fig. 56 were obtained with a triangular waveform. For out-of-phase tests, although maximum temperatures occur at strain levels that are below the threshold value for the tensile-loading cycle, they occur at maximum strain levels for the compressive-loading cycle. The contribution of compressive loading cycle on fatigue life may result in nearly the same fatigue life for in-phase and out-of-phase tests. For in-phase tests, maximum temperatures occur at strain levels that are below the threshold value for the compressive-loading cycle; the contribution of the compressive cycle on fatigue life would be negligible.

4.2.4 Dissolved Oxygen

The dependence of fatigue life of carbon steel on DO content in water[6,10] is shown in Fig. 57. The test temperature, applied strain amplitude, and sulfur content in steel were above, and strain rate was below, the critical threshold values. The results indicate a

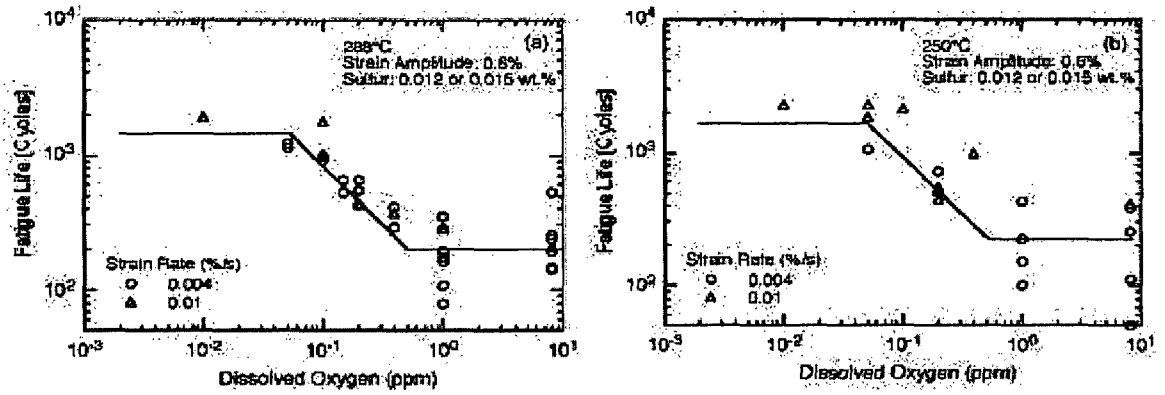

Figure 57. Dependence on DO of fatigue life of carbon steel

minimum DO level of 0.05 ppm, above which environment decreases the fatigue life of the steel. The effect of DO content on fatigue life saturates at 0.5 ppm, i.e., increases in DO levels above 0.5 ppm do not cause further decreases in life. In Fig. 57, for DO levels between 0.05 and 0.5 ppm, fatigue life appears to decrease logarithmically with DO. Estimates of fatigue life from a trained ANN also show a similar effect of DO on the fatigue life of CSs and LASs.[93]

4.2.5 Sulfur Content in Steel

It is well known that sulfur content and morphology are the most important material-related parameters that determine susceptibility of LASs to environmentally enhanced fatigue crack growth rates.[64,65,69-71] A critical concentration of S^{2-} or HS^- ions is required at the crack tip for environmental effects to occur. Corrosion fatigue crack growth rates are controlled by the synergistic effect of sulfur content, environmental conditions, and flow rate. Both the corrosion fatigue growth rates and threshold stress intensity factor ΔK_{th} are a function of the sulfur content in the range 0.003–0.019 wt.%.[70] The probability of environmental enhancement of fatigue crack growth rates in precracked specimens of LASs appears to diminish markedly for sulfur contents <0.005 wt.%. The fatigue S-N data for LASs also indicate a dependence of fatigue life on sulfur content. When all the threshold conditions are satisfied, environmental effects on the fatigue life increase with increased sulfur content (Fig. 58). The fatigue lives of A508-Cl 3 steel with 0.003 wt.% sulfur and A533-Gr B steel with 0.010 wt.% sulfur are plotted as a function of strain rate in Fig. 59. However, the available data sets are too sparse to establish a functional form for dependence of fatigue life on sulfur content and to define either a lower threshold for sulfur content below which environmental effects are unimportant or an upper limit above which the effect of sulfur on fatigue life may saturate. A linear dependence of fatigue life on sulfur content has been assumed in correlations for estimating fatigue life of CSs and LASs in LWR environments.[27,28] Limited data suggest that environmental effects on fatigue life may saturate at sulfur contents above 0.012 wt.%, e.g., in Fig. 58, A302-Gr B steel with 0.027 wt.% sulfur and A533-Gr B steel with 0.012 wt.% sulfur yield identical fatigue lives in water at 288°C and ≈0.7 ppm DO.[24]

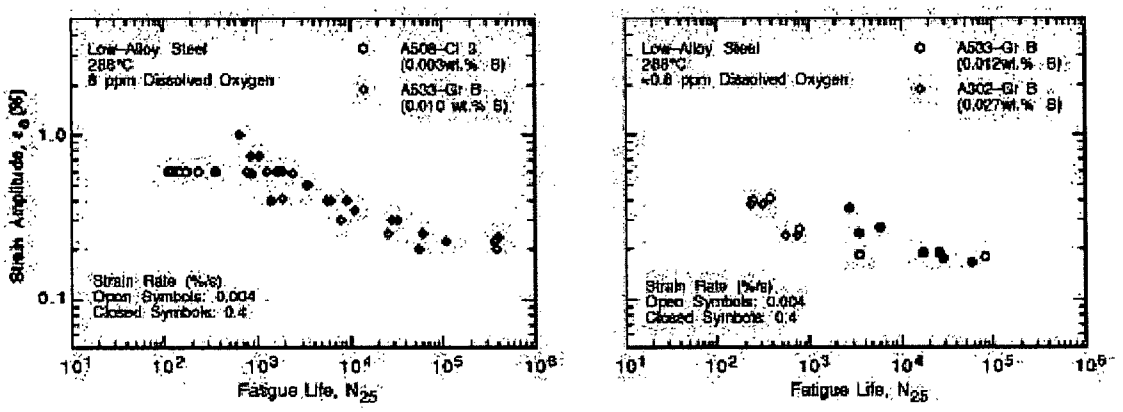

Figure 58. Effect of sulfur content on fatigue life of low-alloy steels in high-dissolved-oxygen water at 288°C

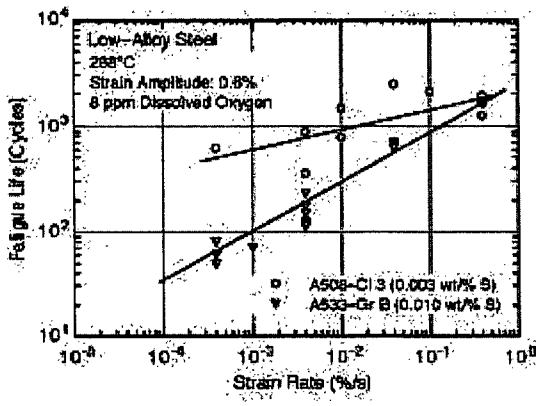

Figure 59.
Effect of strain rate on fatigue life of low-alloy steels with different sulfur contents

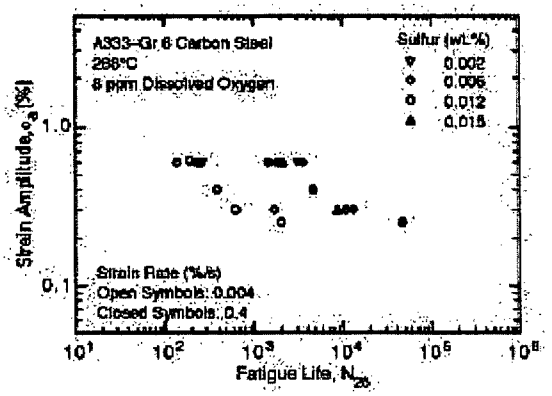

Figure 60.
Effect of sulfur content on fatigue life of carbon steels in high-dissolved-oxygen water at 288°C

In contrast to LASs, the existing fatigue S-N data for CSs indicate significant reductions in fatigue life* of some heats of steel with sulfur levels as low as 0.002 wt.%. The fatigue lives of A333-Gr 6 CSs with sulfur contents in the range of 0.002-0.015 wt.% in high-DO water at 288°C are plotted in Fig. 60; the lives of these steels at 0.6% strain amplitude are plotted as a function of strain rate in Fig. 61. Environmental effects on the fatigue life of these steels seem to be independent of sulfur content in the range of 0.002-0.015 wt.%.

* M. Higuchi, presented at the Pressure Vessel Research Council Meeting, June 1995, Milwaukee.

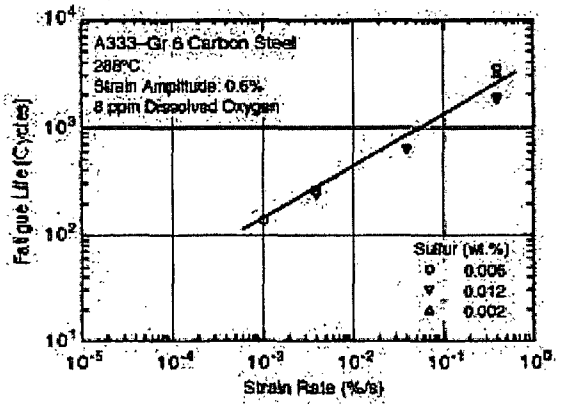

Figure 61.
Effect of strain rate on fatigue life of A333-Gr 6 carbon steels with different sulfur contents

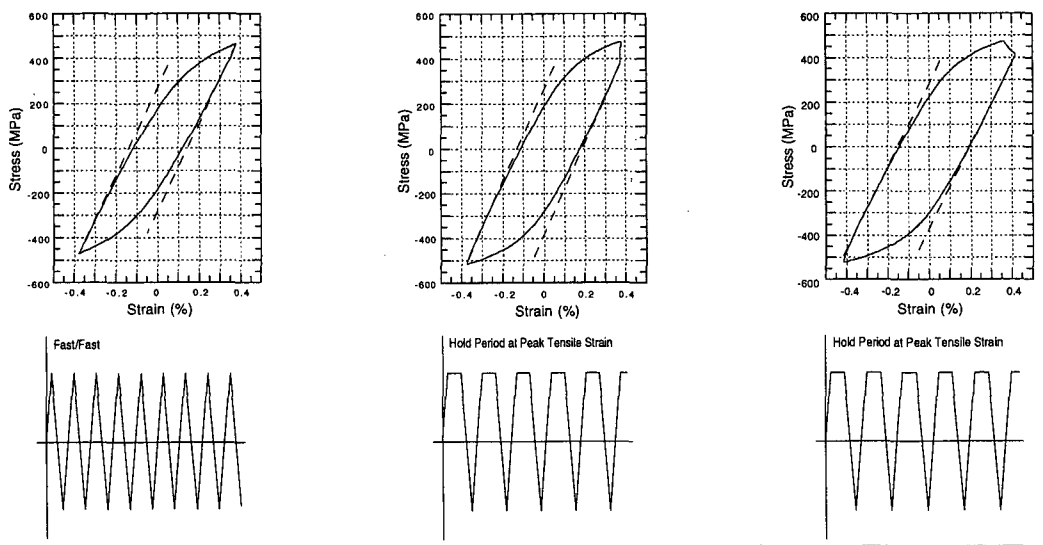

Strain or Stroke Control		Strain Control		Stroke Control (5-min hold)	
Air:	4740±1250 cycles	Air:	6,275 cycles	Air:	2592 cycles
PWR:	1965±385 cycles			High DO:	1007, 1092 cycles
High DO:	2077 cycles			Stroke Control (30-min hold)	
				High DO:	840 cycles

Figure 62. Fatigue life of A106-Gr B steel in air and water environments at 288°C, 0.75% strain range, and hold period at peak tensile strain. Hysteresis loops are for tests in air.

4.2.6 Tensile Hold Period

Fatigue data indicate that a hold period at peak tensile strain decreases fatigue life in high-DO water but not in air. Loading waveforms, hysteresis loops, and fatigue lives for the tests are shown in Fig. 62. A 300-s hold period is sufficient to reduce fatigue life; a longer hold period results in life only slightly decreased from that with a 300-s-hold period. Two 300-s-hold tests at 288°C and ≈0.8% strain range in oxygenated water with 0.7 ppm DO gave fatigue lives of 1,007 and 1,092 cycles. Fatigue life in a 1800-s-hold test was 840 cycles. These tests were conducted in stroke-control mode and are somewhat different than the conventional hold-time test in strain-control mode. In the strain-control test, the total strain in the sample is held constant during the hold period. However, a portion of the elastic strain

is converted to plastic strain because of stress relaxation. In a stroke-control test, there is an additional plastic strain in the sample due to relaxation of elastic strain from the load train (Fig. 62). Consequently, these are not true constant-strain-hold periods and significant strain changes occur during the hold period; the measured plastic strains during the hold period were ≈0.028% from relaxation of the gauge and 0.05-0.06% from relaxation of the load train. These conditions resulted in strain rates of 0.005-0.02%/s during the hold period. The reduction in life may be attributed to the slow strain rates during the hold period.

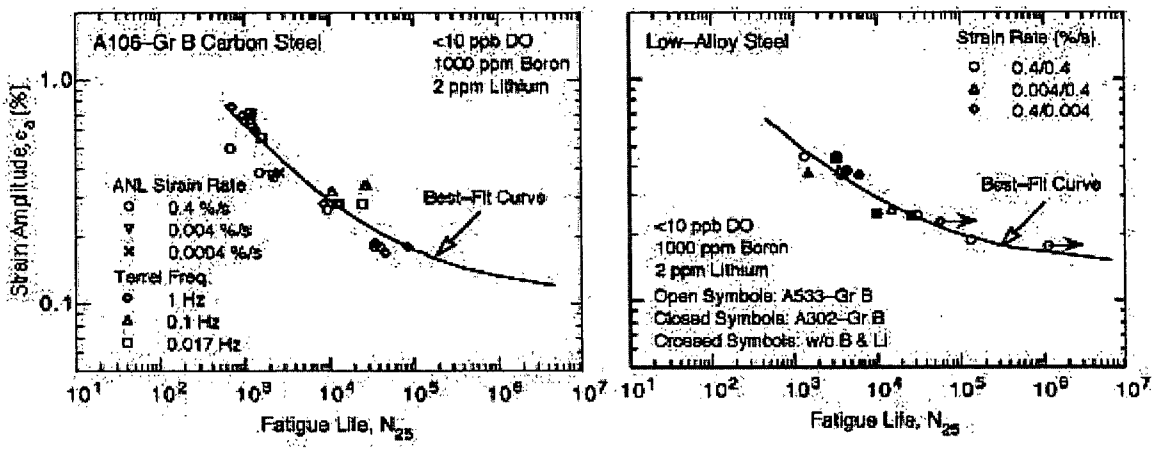

Figure 63. Strain amplitude vs. fatigue life data for A106-Gr B and A533-Gr B steels in simulated PWR water at 288°C

4.2.7 Low Dissolved Oxygen

With a few exceptions, only a moderate decrease in fatigue life of carbon and low-alloy steels has been observed in water when any one of the threshold conditions is not satisfied, e.g., low-DO PWR environments.[7,10-14,89,90] The fatigue life of CSs and LASs in simulated PWR water is shown in Fig. 56. For both steels, fatigue lives in a PWR environment are lower than those in air by a factor of less than 2. The exception to this behavior are the high-S steels, which exhibit enhanced crack growth rates in PWR water.[34] Limited data indicate that heats of high-S steels that have unfavorable sulfide distribution and morphology, fatigue life may decrease by more than a factor of 2 in low-DO PWR water (see next section).

In low-DO water, the effects of strain rate are similar to those in air; heats of CS and LAS that are sensitive to strain rate in air, also show a decrease in fatigue life in PWR water with decreasing strain rate. In air, the fatigue life of some heats decreased by a factor of ≈4 when strain rate decreased from 0.4 to 0.004%/s, e.g. the A302-Gr B steel tested in the radial orientation (Fig. 42), whereas for other heats, a decrease in the strain rate by three orders of magnitude did not cause any additional decrease in fatigue life, e.g., ANL heats of A106-Gr B and A533-Gr B steel in Fig. 40. However, certain orientations of high-S steels that have an unfavorable sulfide distribution and morphology may exhibit strain rate effects larger than those in air because of the contribution of the environment.

4.2.8 Orientation

In air, some steels exhibit very poor fatigue properties in the transverse orientation because of structural factors such as the distribution and morphology of sulfides. In air, the effect of strain rate on fatigue life can also be larger for these orientations than for other orientations. Limited data indicate that orientation may also influence growth rates of CSs and LASs in LWR environments. As discussed in Section 3.2, a critical concentration of S^{2-} or HS^- ions, which are produced by the dissolution of sulfide inclusions in the steel, is required at the crack tip for environmental effects to occur. Therefore, the distribution, morphology, and size of sulfide inclusions and the probability of advancing crack to intercept these inclusions are important parameters that influence growth rates of CSs and LASs in LWR environments.

The fatigue lives of A302-Gr B steel in the rolling (R), transverse (T1), and radial (T2) orientations in air and low- and high-DO water at 288°C are shown in Fig. 64. The relative life (ratio of life in water and air) is plotted as a function of strain rate in Fig. 65. The size and distribution of sulfide inclusions for the three orientations are significantly different, Fig. 4. The results indicate that in high-DO water (0.6-0.8 ppm DO), the fatigue life of A302-Gr B steel is insensitive to the differences in sulfide distribution and size; life for both the R and T1

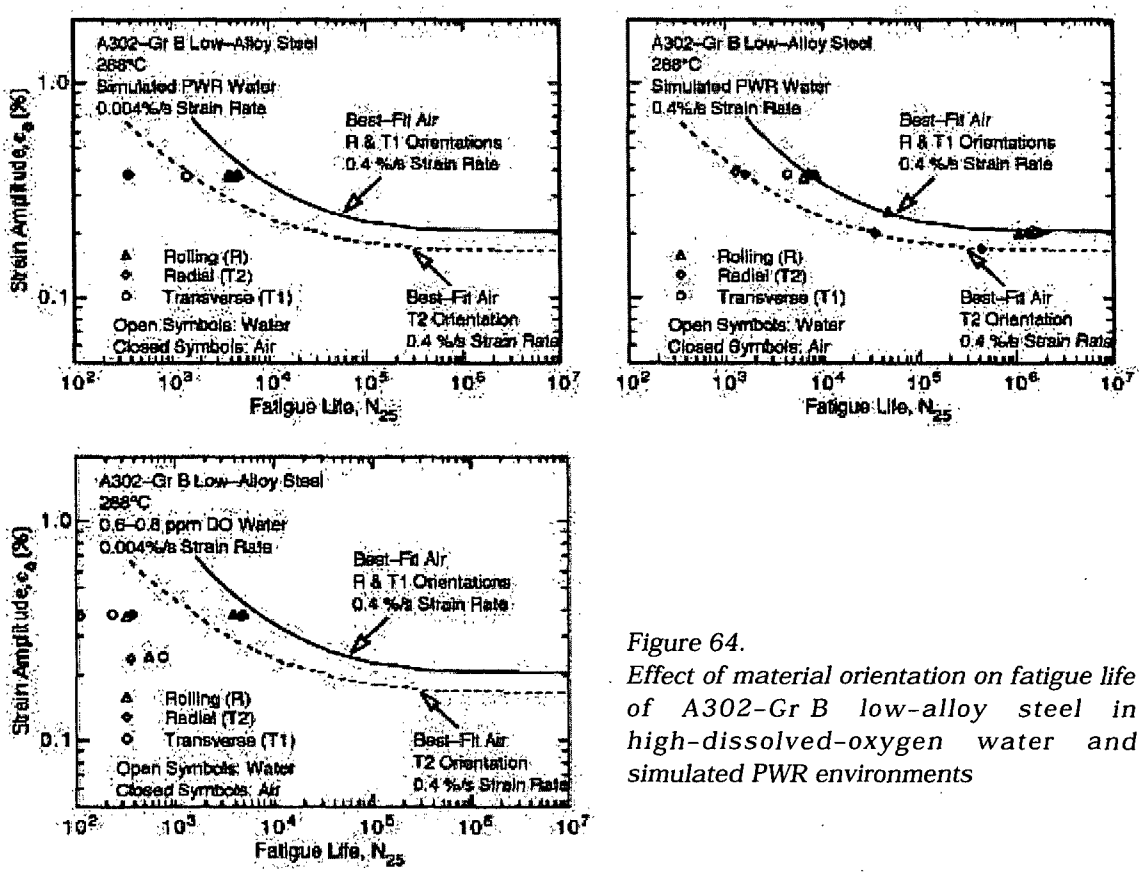

Figure 64.
Effect of material orientation on fatigue life of A302-Gr B low-alloy steel in high-dissolved-oxygen water and simulated PWR environments

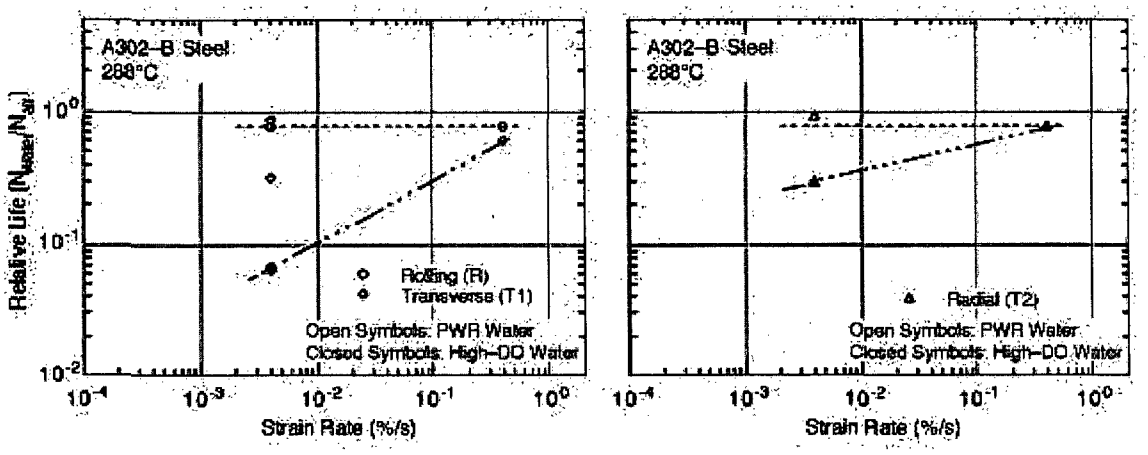

Figure 65. Relative fatigue lives of different orientations of A302-Gr B low-alloy steel in high-dissolved-oxygen water and simulated PWR environments

orientations is a factor of ≈14 lower than in air. However, in PWR water, larger sulfide inclusions may result in a larger decrease in life, e.g., life in T1 orientation shown as diamonds in Fig. 65.

Metallographic examination of the specimens indicates that structural factors are responsible for poor fatigue resistance of the radial orientation. The fracture surface and longitudinal section of A302-Gr B steel in the T2 orientation tested in PWR water at 288°C, ≈0.75% strain range, and slow/fast waveform are shown in Fig. 66. The longitudinal section of the specimen shows an abundance of cracks that connect the sulfide stringers. These cracks are present throughout the specimen away from the fracture surface. A fatigue crack propagates preferentially along these sulfide stringers; the fracture surface contains several fractured sulfide stringers. These results suggest that environmental effects on fatigue life are not necessarily cumulative; the reduction in life due to environment alone may be small for those steels that have inherently low fatigue life in air because of microstructural or other factors.

4.2.9 Temperatures below 150°C

As discussed in Section 4.2.7, only a moderate decrease in fatigue life of carbon and low-alloy steels is observed in water when any one of the threshold conditions is not satisfied, e.g., temperatures below 150°C or low-DO PWR environments.[7,10-14,89,90] The fatigue lives of CSs and LASs in water at <150°C are shown in Fig. 67. The results show only a moderate decrease in fatigue life in water at temperatures below the threshold value of 150°C. At these temperatures, life in water is 30-50% lower than in room-temperature air. The fatigue life of A333-Gr 6 carbon steel in water at 100 and 150°C, 0.6% strain amplitude, and 0.004%/s strain rate is plotted as a function of DO in Fig. 68. At these temperatures, the fatigue life of the steel does not change even when the DO level is increased from 0.005 to 1 ppm.

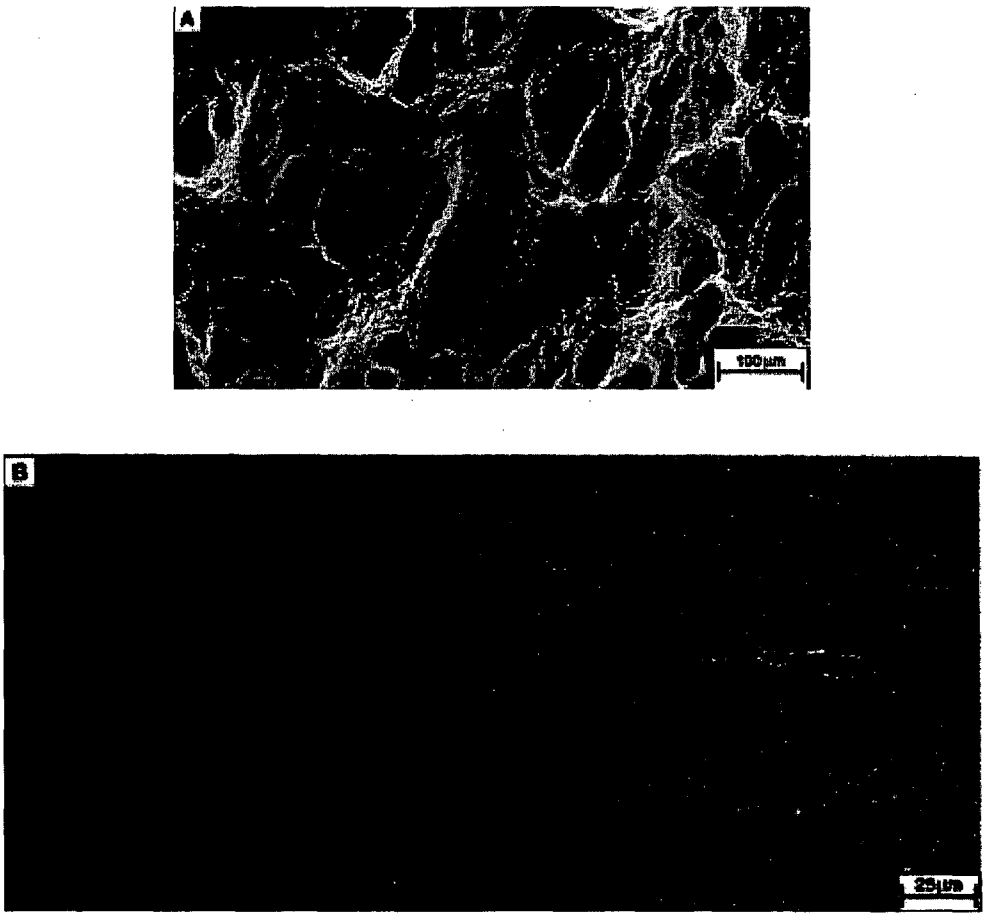

Figure 66. SEM photomicrograph of fracture surface (A) and longitudinal section (B) of A302-Gr B steel specimen in T2 orientation tested in PWR water at 288°C, ≈0.75% strain range, and slow/fast waveform

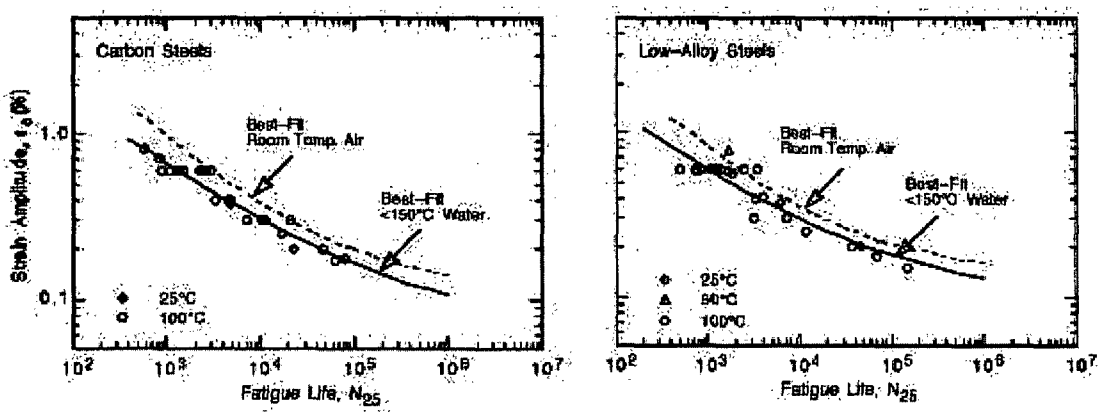

Figure 67. Experimental and predicted fatigue lives of A106-Gr B and A533-Gr B steels in water at temperatures below 150°C

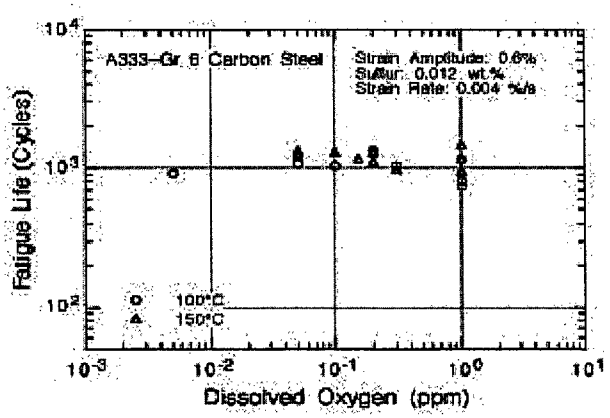

Figure 68.
Fatigue life of A333-Gr 6 carbon steel as a function of dissolved oxygen in water at 100 and 150°C

5 Statistical Model

5.1 Modeling Choices

In attempting to develop a statistical model from incomplete data and where physical processes are only partially understood, care must be taken to avoid overfitting the data. Different functional forms of the predictive equations (e.g., different procedures for transforming the measured variables into data used for fitting equations) were tried for several aspects of the model. Fatigue S-N data are generally expressed by Eq. 1.1, which may be rearranged to express fatigue life N in terms of strain amplitude ε_a as

$$\ln(N) = [\ln B - \ln(\varepsilon_a - A)]/b. \tag{5.1}$$

Additional terms may be added to the model that would improve agreement with the current data set. However, such changes may not hold true in other data sets, and the model would typically be less robust, i.e., it would not predict new data well. In general, complexity in a statistical model is undesirable unless it is consistent with accepted physical processes. Although there are statistical tools that can help manage the tradeoff between robustness and detail in the model, engineering judgment is required. Model features that would be counter to known effects are excluded. Features that are consistent with previous studies use such results as guidance, e.g., defining the threshold or saturation values for an effect, but where there are differences from previous findings, the reasons for the differences are evaluated and an appropriate set of assumptions is incorporated into the model.

5.2 Least-Squares Modeling within a Fixed Structure

The parameters of the model are commonly established through least-squares curve-fitting of the data to either Eq. 1.1 or 5.1. An optimization program sets the parameters so as to minimize the sum of the square of the residual errors, which are the differences between the predicted and actual values of ε_a or ln(N). A predictive model based on least-squares fit on ln(N) is biased for low ε_a; in particular, runoff data cannot be included. The model also leads to probability curves that converge to a single value of threshold strain.

However, the model fails to address the fact that at low ε_a, most of the error in life is due to uncertainty associated with either measurement of stress or strain or variation in threshold strain caused by material variability. On the other hand, a least-squares fit on ε_a does not work well for higher strain amplitudes. The two kinds of models are merely transformations of each other, although the precise values of the coefficients differ.

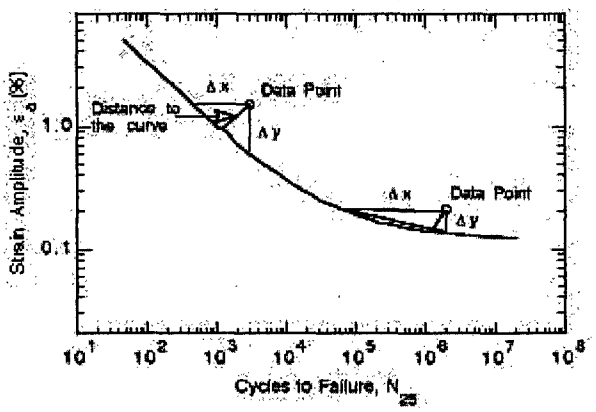

Figure 69.
Schematic of least-squares curve-fitting of data by minimizing sum of squared Cartesian distances from data points to predicted curve

The statistical models[27,28] were developed by combining the two approaches and minimizing the sum of squared Cartesian distances from the data points to the predicted curve (Fig. 69). For low ε_a, this is very close to optimizing the sum of squared errors in predicted ε_a; at high ε_a, it is very close to optimizing the sum of squared errors in predicted life; and at medium ε_a, this model combines both factors. However, because the model includes many nonlinear transformations of variables and because different variables affect different parts of the data, the actual functional form and transformations are partly responsible for minimizing the squares of the errors. The functional forms and transformation are chosen a priori, and no direct computational means exist for establishing them.

To perform the optimization, it was necessary to normalize the x and y axes by assigning relative weights to be used in combining the error in life and strain amplitude because x and y axes are not in comparable units. In this analysis, errors in strain amplitude (%) are weighted 20 times as heavily as errors in ln(N). A value of 20 was selected for two related reasons. First, this factor leads to approximately equal weighting of low- and high-strain-amplitude data in the least-squared error computation of model coefficients. Second, when applied to the model to generate probability curves, it yielded a standard deviation on strain amplitude comparable to that obtained from the best-fit of the high cycle fatigue data to Eq. 1.1. Because there is necessarily judgment applied in the selection of this value, a sensitivity analysis was performed, and it showed that the coefficients of the model do not change much for weight factors between 10 and 25. Distance from the curve was estimated as

$$D = \left\{(x - \hat{x})^2 + \left[k(y - \hat{y})\right]^2\right\}^{1/2}, \tag{5.2}$$

where $\hat{x}$ and $\hat{y}$ represent predicted values, and k = 20.

5.3 The Model

Based on the existing fatigue S-N data base, statistical models have been developed for estimating the effects of material and loading conditions on the fatigue lives of CSs and LASs.[27,28] The dependence of fatigue life on DO level has been modified because it was determined that in the range of 0.05-0.5 ppm, the effect of DO was more logarithmic than linear.[45,93] In this report, the models have been further optimized with a larger fatigue S-N data base. Because of the conflicting possibilities that with decreasing strain rate, fatigue life may either be unaffected, decrease for some heats, or increase for others, effects of strain rate in air were not explicitly considered in the model. The effects of orientation, i.e., size and distribution of sulfide inclusions, on fatigue life were also excluded because the existing data base does not include information on sulfide distribution and morphology. In air, the fatigue data for CSs are best represented by

$$\ln(N_{25}) = 6.595 - 1.975 \ln(\varepsilon_a - 0.113) - 0.00124\ T \tag{5.3a}$$

and for LASs by

$$\ln(N_{25}) = 6.658 - 1.808 \ln(\varepsilon_a - 0.151) - 0.00124\ T. \tag{5.3b}$$

In LWR environments, the fatigue data for CSs are best represented by

$$\ln(N_{25}) = 6.010 - 1.975 \ln(\varepsilon_a - 0.113) + 0.101\ S^*\ T^*\ O^*\ \dot{\varepsilon}^* \tag{5.4a}$$

and for LASs by

$$\ln(N_{25}) = 5.729 - 1.808 \ln(\varepsilon_a - 0.151) + 0.101\ S^*\ T^*\ O^*\ \dot{\varepsilon}^*, \tag{5.4b}$$

where S^*, T^*, O^*, and $\dot{\varepsilon}^*$ = transformed sulfur content, temperature, DO, and strain rate, respectively, defined as follows:

$$\begin{aligned} S^* &= S && (0 < S \le 0.015 \text{ wt.\%}) \\ S^* &= 0.015 && (S > 0.015 \text{ wt.\%}) \end{aligned} \tag{5.5a}$$

$$\begin{aligned} T^* &= 0 && (T < 150°C) \\ T^* &= T - 150 && (T = 150\text{-}350°C) \end{aligned} \tag{5.5b}$$

$$\begin{aligned} O^* &= 0 && (DO < 0.05 \text{ ppm}) \\ O^* &= \ln(DO/0.04) && (0.05 \text{ ppm} \le DO \le 0.5 \text{ ppm}) \\ O^* &= \ln(12.5) && (DO > 0.5 \text{ ppm}) \end{aligned} \tag{5.5c}$$

$$\begin{aligned} \dot{\varepsilon}^* &= 0 && (\dot{\varepsilon} > 1 \text{ \%/s}) \\ \dot{\varepsilon}^* &= \ln(\dot{\varepsilon}) && (0.001 \le \dot{\varepsilon} \le 1 \text{ \%/s}) \\ \dot{\varepsilon}^* &= \ln(0.001) && (\dot{\varepsilon} < 0.001 \text{ \%/s}) \end{aligned} \tag{5.5d}$$

The functional form and bounding values of the transformed parameters S^*, T^*, O^*, and $\dot{\varepsilon}^*$ were based upon experimental observations and data trends discussed in Section 4.2. Significant features of the model for estimating fatigue life in LWR environments are as follows:

(a) The model assumes that environmental effects on fatigue life occur primarily during the tensile-loading cycle; minor effects during the compressive loading cycle have been excluded. Consequently, the loading and environmental conditions, e.g., temperature, strain rate, and DO, during the tensile-loading cycle are used for estimating fatigue lives.

(b) When any one of the threshold condition is not satisfied, e.g., <0.05 ppm DO in water, the effect of strain rate is not considered in the model, although limited data indicate that heats of steel that are sensitive to strain rate in air also show a decrease in life in water with decreasing strain rate.

(c) The model assumes a linear dependence of S^* on S content in steel and saturation at 0.015 wt.% S.

The model is recommended for predicted fatigue lives of $\leq 10^6$ cycles. For fatigue lives of 10^6 to 10^8 cycles, the results should be used with caution because, in this range, the model is based on very limited data obtained from relatively few heats of material.

The estimated and experimental S-N curves for CS and LAS in air at room temperature and 288°C are shown in Fig. 70. The mean curves used in developing the ASME Code design curve and the average curves of Higuchi and Iida[7] are also included in the figure. The results indicate that the ASME mean curve for carbon steels is not consistent with the experimental data; at strain amplitudes <0.2%, the mean curve predicts significantly lower fatigue lives than those observed experimentally. The estimated curve for low-alloy steels is comparable with the ASME mean curve. For both steels, Eq. 5.3 shows good agreement with the average curves of Higuchi and Iida.

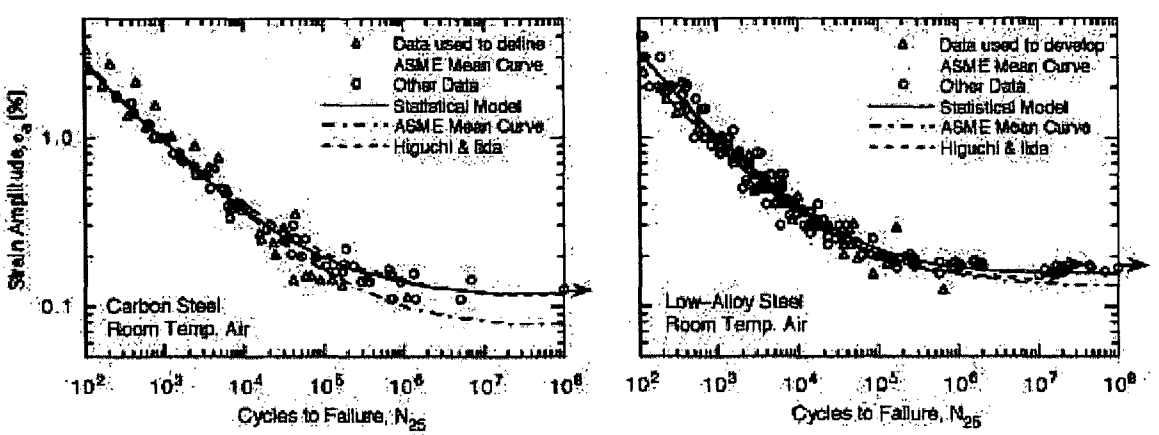

Figure 70. Fatigue S-N behavior for carbon and low-alloy steels estimated from model and determined experimentally in air at room temperature

5.4 Distribution of Fatigue Life

For a given steel type, the average distance of data points from the mean curve does not vary much for different environmental conditions. To develop a distribution on life, we start with the assumption that there are three sources of prediction error: (a) measurement errors

for the applied strain amplitude, (b) variations in the threshold strain amplitude due to material variability, and (c) errors due to uncertainty in test and material conditions or other unexplained variation. Because measurement errors are small at high strain amplitudes, the standard deviation of distance from the mean curve at high strain amplitudes is a good measure of the scatter in fatigue life due to unexplained variations. At low amplitudes where the S-N curve is almost horizontal, the errors (as measured by the distance from the mean curve) are dominated by the variation in strain amplitude. The standard deviation of the error in strain amplitude was taken to be equal to the standard deviation in the predicted fatigue life divided by a factor of 20 consistent with the weighting factor used for optimization. The standard deviation on life was 0.52 for CSs and LASs. These results can be combined with Eq. 5.3 to estimate the distribution in life for smooth test specimens. In air, the xth percentile of the distribution on life $N_{25}[x]$ for CSs is

$$\ln(N_{25}) = 6.595 + 0.52\, F^{-1}[x] - 1.975 \ln(\varepsilon_a - 0.113 + 0.026\, F^{-1}[1-x]) - 0.00124\, T \qquad (5.6a)$$

and for LASs it is

$$\ln(N_{25}) = 6.658 + 0.52\, F^{-1}[x] - 1.808 \ln(\varepsilon_a - 0.151 + 0.026\, F^{-1}[1-x]) - 0.00124\, T\,. \qquad (5.6b)$$

In LWR environments, the xth percentile of the distribution on life $N_{25}[x]$ for CSs is

$$\ln(N_{25}) = 6.010 + 0.52\, F^{-1}[x] - 1.975 \ln(\varepsilon_a - 0.113 + 0.026\, F^{-1}[1-x]) + 0.101\, S^*\, T^*\, O^*\, \dot{\varepsilon}^* \qquad (5.7a)$$

and for LASs it is

$$\ln(N_{25}) = 5.729 + 0.52\, F^{-1}[x] - 1.808 \ln(\varepsilon_a - 0.151 + 0.026\, F^{-1}[1-x]) + 0.101\, S^*\, T^*\, O^*\, \dot{\varepsilon}^*. \qquad (5.7b)$$

The parameters S^*, T^*, O^*, and $\dot{\varepsilon}^*$ are defined in Eqs. 5.5, and $F^{-1}[\cdot]$ denotes the inverse of the standard normal cumulative distribution function. The coefficients of distribution functions $F^{-1}[x]$ and $F^{-1}[1-x]$ represent the standard deviation on life and strain amplitude, respectively. For convenience, values of the inverse of standard normal cumulative distribution function in Eqs. 5.6 and 5.7 are given in Table 3. The standard deviation of 0.026 on strain amplitude obtained from the analysis may be an overly conservative value. A more realistic value for the standard deviation on strain could be obtained by analysis of the fatigue limits of different heats of material. The existing data are inadequate for such an analysis because (a) not enough heats of materials are included in the data base, and (b) there are very few high-cycle fatigue data for accurate estimations of the fatigue limit for specific heats.

The estimated probability curves for the fatigue life of CSs and LASs in an air and LWR environments in Figs. 71-73 show good agreement with experimental data; nearly all of the data are bounded by the 5% probability curve. Relative to the 50% probability curve, the 5% probability curve is a factor of ≈2.5 lower in life at strain amplitudes >0.3% and a factor of 1.4-1.7 lower in strain at <0.2% strain amplitudes. Similarly, the 1% probability curve is a factor of ≈3.7 lower in life and a factor of 1.7-2.2 lower in strain.

Table 3. Inverse of standard cumulative distribution function

Probability	$F^{-1}[x]$	$F^{-1}[1-x]$	Probability	$F^{-1}[x]$	$F^{-1}[1-x]$
0.01	-3.7195	3.7195	3.00	-1.8808	1.8808
0.02	-3.5402	3.5402	5.00	-1.6449	1.6449
0.03	-3.4319	3.4319	7.00	-1.4758	1.4758
0.05	-3.2905	3.2905	10.00	-1.2816	1.2816
0.07	-3.1947	3.1947	20.00	-0.8416	0.8416
0.10	-3.0902	3.0902	30.00	-0.5244	0.5244
0.20	-2.8782	2.8782	50.00	0.0000	0.0000
0.30	-2.7478	2.7478	65.00	0.3853	-0.3853
0.50	-2.5758	2.5758	80.00	0.8416	-0.8416
0.70	-2.4573	2.4573	90.00	1.2816	-1.2816
1.00	-2.3263	2.3263	95.00	1.6449	-1.6449
2.00	-2.0537	2.0537	98.00	2.0537	-2.0537

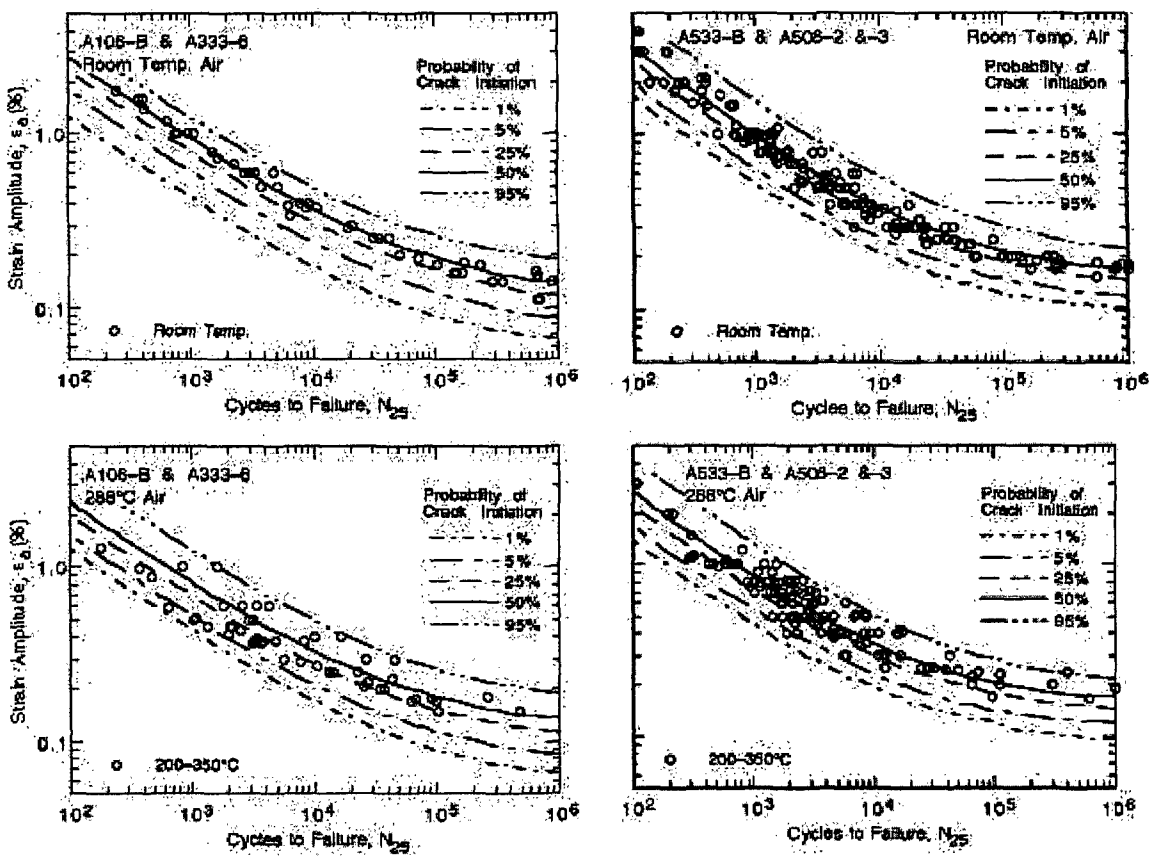

Figure 71. Experimental data and probability of fatigue cracking in carbon and low-alloy steel test specimens in air

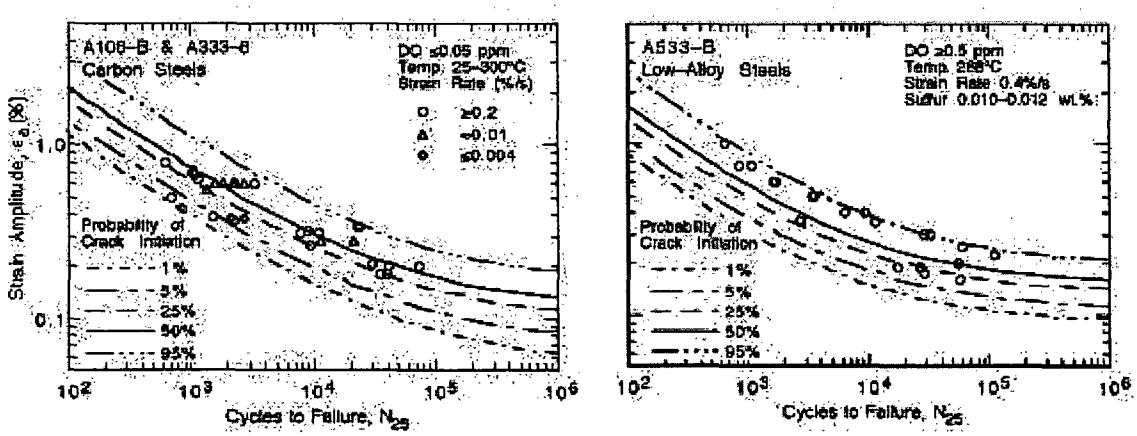

Figure 72. Experimental data and probability of fatigue cracking in carbon and low-alloy steel test specimens in simulated PWR environments

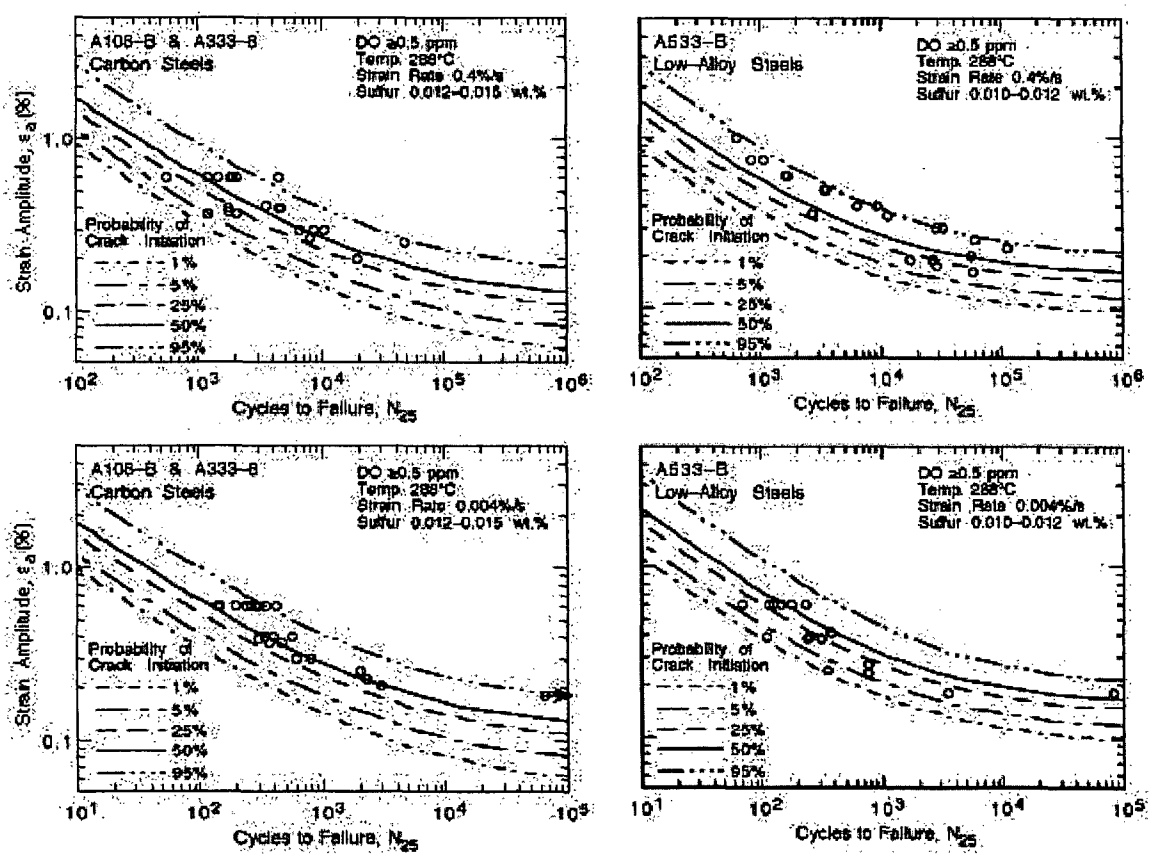

Figure 73. Experimental data and probability of fatigue cracking in carbon and low-alloy steel test specimens in high-dissolved-oxygen water

As with other aspects of this model, the estimates of the probability of cracking should not be extrapolated much beyond the data. The probabilities assume a normal distribution, which is consistent with the data for most of the range. The existing data are not sufficient to determine precise distributions because more data are required to estimate distributions than to estimate the mean curve. However, the assumption of normality is reasonable (and conservative) down to 0.1-1% probability of cracking and it is empirically verified by the number of data points that fall below the respective curves. The probability is not expected to deviate significantly from the normal curve for another order of magnitude (one more standard deviation) even if the probability distribution is not the same. Because estimates of extremely low or high probabilities are sensitive to the choice of distribution, the probability distribution curves should not be extrapolated beyond 0.02% probability.

6 Fatigue Life Correction Factor

An alternative approach for incorporating the effects of reactor coolant environments on fatigue S-N curves has been proposed by the Environmental Fatigue Data (EFD) Committee of the Thermal and Nuclear Power Engineering Society (TENPES) of Japan.* A fatigue life correction factor F_{en} is defined as the ratio of the life in air at room temperature to that in water at the service temperature. The fatigue usage for a specific load pair based on the current Code fatigue design curve is multiplied by the correction factor to account for the environmental effects. Note that the fatigue life correction factor does not account for any differences that might exist between the current ASME mean air curves and the present mean air curves developed from a larger data base. The specific expression for F_{en}, proposed initially by Higuchi and Iida,[7] assumes that life in the environment N_{water} is related to life in air N_{air} at room temperature through a power-law dependence on the strain rate

$$F_{en} = \frac{N_{air}}{N_{water}} = (\dot{\varepsilon})^{-P}, \tag{6.1a}$$

or

$$\ln(F_{en}) = \ln(N_{air}) - \ln(N_{water}) = -P\ln(\dot{\varepsilon}). \tag{6.1b}$$

In air at room temperature, the fatigue life N_{air} of CSs is expressed as

$$\ln(N_{air}) = 6.653 - 2.119\ \ln(\varepsilon_a - 0.108) \tag{6.2a}$$

and for LASs by

$$\ln(N_{air}) = 6.578 - 1.761\ \ln(\varepsilon_a - 0.140), \tag{6.2b}$$

where ε_a is the applied strain amplitude (%). Only the tensile loading cycle is considered to be important for environmental effects on fatigue life. The exponent P is a product of a environmental factor R_p, which depends on temperature T (°C) and DO level (ppm), and a material factor P_c, which depends on the ultimate tensile strength σ_u (MPa) and sulfur content S (wt/.%) of the steel. Thus

$$P = R_p\ P_c, \tag{6.3a}$$

* Presented at the Pressure Vessel Research Council Meeting, April 1996, Orlando, FL.

$$P_c = 0.864 - 0.00092\,\sigma_u + 14.6\,S, \tag{6.3b}$$

$$R_p = \frac{R_{pT} - 0.2}{2.64}\ln(DO) + 1.75R_{pT} - 0.035, \qquad 0.2 \le R_p \le R_{pT} \tag{6.3c}$$

and $R_{pT} = 0.198\exp(0.00557T)$. (6.3d)

The fatigue lives of carbon and low-alloy steels measured experimentally and those estimated from the statistical and EFD models are shown in Figs. 74-78. Although the EFD correlations for exponent P were based entirely on data for carbon steels, Eqs. 6.3a-6.3d were also used for estimating the fatigue lives of LASs. Also, σ_u in Eq. 6.3b was assumed to be 520 and 650 MPa, respectively, for CSs and LASs. The significant differences between the two models are as follows:

(a) The EFD correlations have been developed from data for CSs alone.

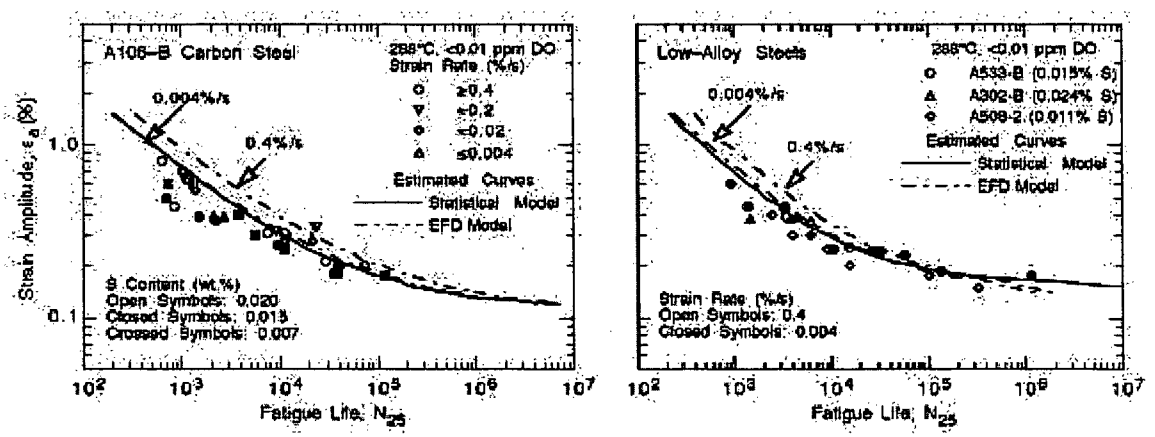

Figure 74. Experimental fatigue lives and those estimated from statistical and EFD models for carbon and low-alloy steels in simulated PWR water

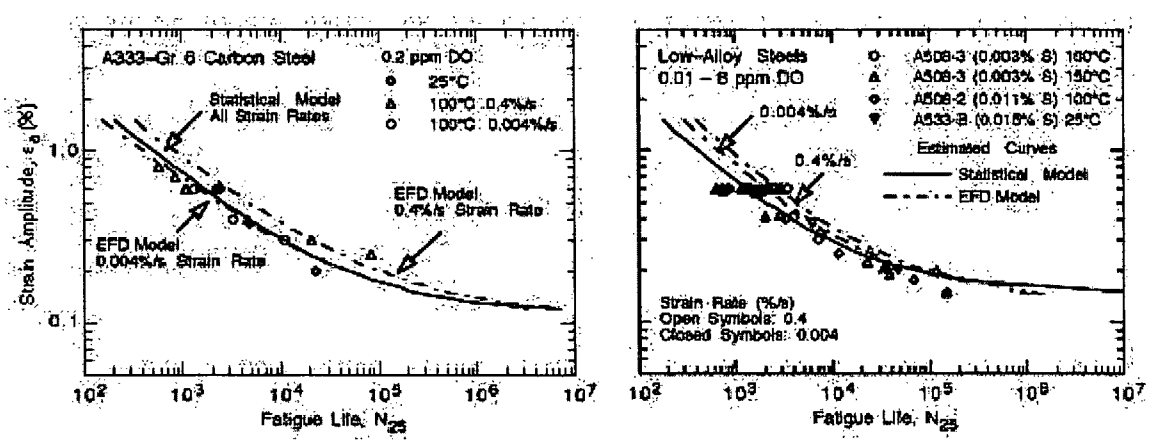

Figure 75. Experimental fatigue lives and those estimated from statistical and EFD models for carbon and low-alloy steels in water at temperatures below 150°C

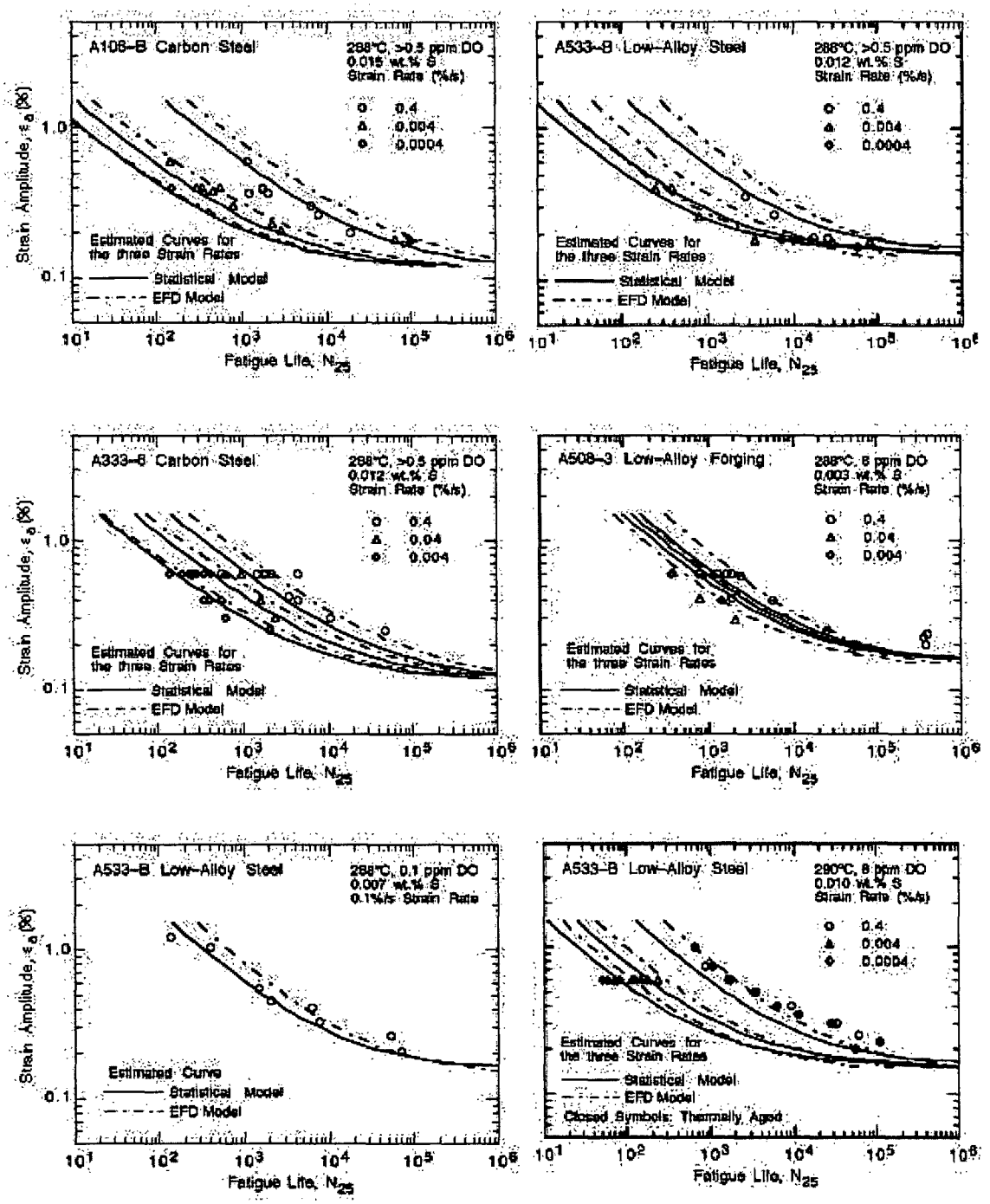

Figure 76. Experimental fatigue lives and those estimated from statistical and EFD models for carbon and low-alloy steels in high-dissolved-oxygen water

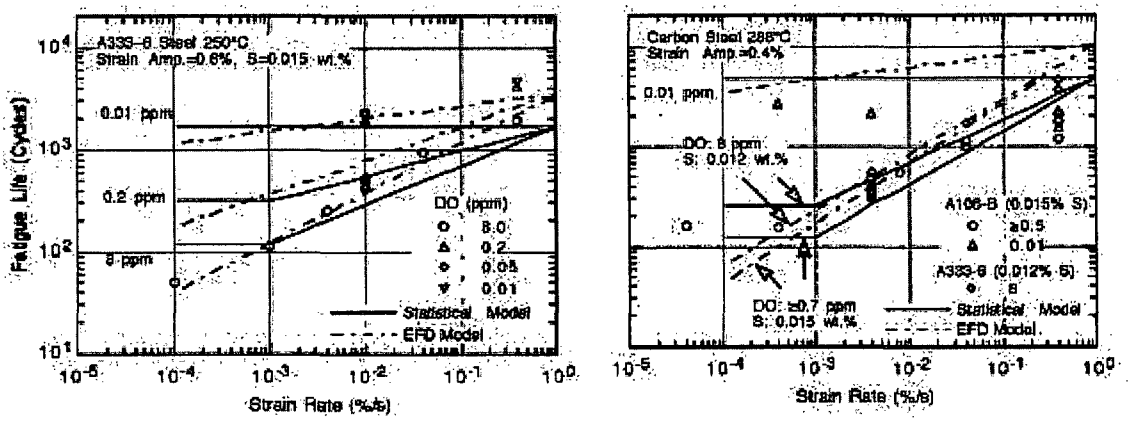

Figure 77. Dependence on strain rate of fatigue life of carbon steels observed experimentally and that estimated from statistical and EFD models

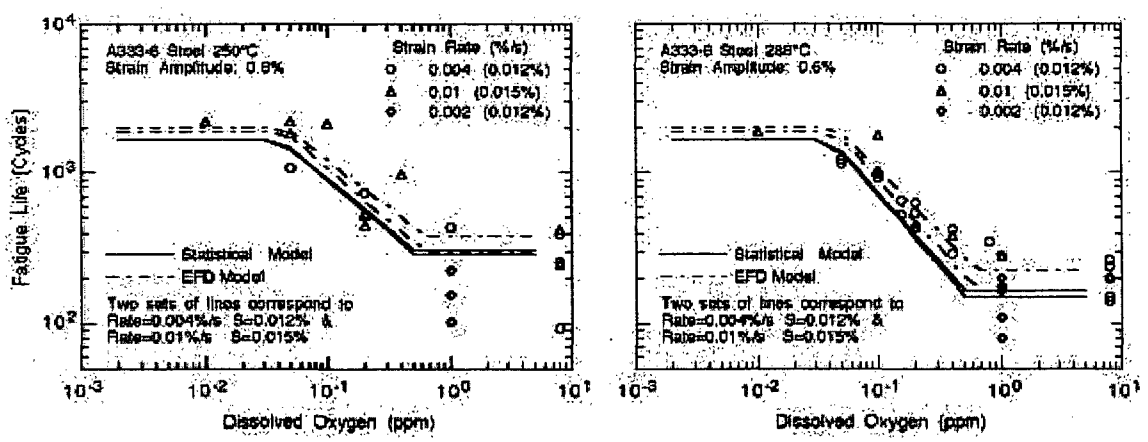

Figure 78. Dependence on dissolved oxygen of fatigue life of carbon steels observed experimentally and that estimated from statistical and EFD models

(b) The statistical model assumes that the effects of strain rate on fatigue life saturate below 0.001%/s, Fig. 77. Such a saturation is not considered in the EFD model.

(c) A threshold temperature of 150°C below which environmental effects on fatigue life are modest is incorporated in the statistical model but not in the EFD model.

(d) The EFD model includes the effect of tensile strength on fatigue life of CSs in LWR environments.

Another estimate of the fatigue life correction factor F_{en} can also be obtained from the statistical model. Since

$$\ln(F_{en}) = \ln(N_{air}) - \ln(N_{water}), \tag{6.4}$$

from Eqs. 5.3a and 5.4a, the fatigue life correction factor for CSs is given by

$$\ln(F_{en}) = 0.585 - 0.00124T - 0.101S^*T^*O^*\dot{\varepsilon}^* \tag{6.5a}$$

and from Eqs. 5.3b and 5.4b, the fatigue life correction factor for LASs is given by

$$\ln(F_{en}) = 0.929 - 0.00124T - 0.101S^*T^*O^*\dot{\varepsilon}^*, \tag{6.5b}$$

where the threshold and saturation values for S^*, T^*, O^*, and $\dot{\varepsilon}^*$ are defined in Eqs. 5.5. A value of 25°C is used for T in Eqs. 6.5a and 6.5b if the fatigue life correction factor is defined relative to RT air. Otherwise, both T and T^* represent the service temperature. A fatigue life correction factor F_{en} based on the statistical model has been proposed as part of a nonmandatory Appendix to ASME Section IX fatigue evaluations.[94,95]

7 Fatigue S–N Curves for Components

The current ASME Section III Code design fatigue curves were based on experimental data on small polished test specimens. The best-fit or mean curve to the experimental data used to develop the Code design curve, expressed in terms of stress amplitude S_a (MPa) and fatigue cycles N, for carbon steels is given by

$$S_a = 59{,}736/\sqrt{N} + 149.24 \tag{7.1a}$$

and for low-alloy steels by

$$S_a = 49{,}222/\sqrt{N} + 265.45. \tag{7.1b}$$

The stress amplitude S_a is the product of strain amplitude ε_a and elastic modulus E; the room temperature value of 206.8 GPa (30,000 ksi) for the elastic modulus for carbon and low-alloy steels was used in converting the experimental strain-versus-life data to stress-versus-life curves. To obtain design fatigue curves the best-fit curves (Eqs. 7.1a and 7.1b) were first adjusted for the effect of mean stress based on the modified Goodman relation

$$S'_a = S_a\left(\frac{\sigma_u - \sigma_y}{\sigma_u - S_a}\right) \qquad \text{for } S_a < \sigma_y, \tag{7.2a}$$

and

$$S'_a = S_a \qquad \text{for } S_a > \sigma_y, \tag{7.2b}$$

where S'_a is the adjusted value of stress amplitude, and σ_y and σ_u are yield and ultimate strengths of the material, respectively. The Goodman relation assumes the maximum possible mean stress and typically gives a conservative adjustment for mean stress at least when environmental effects are not significant. The design fatigue curves were then obtained by lowering the adjusted best-fit curve by a factor of 2 on stress or 20 on cycles, whichever was more conservative, at each point on the curve. The factor of 20 on cycles was intended to account for the uncertainties in fatigue life associated with material and loading conditions, and the factor of 2 on strain was intended to account for uncertainties in threshold strain caused by material variability. This procedure is illustrated for CSs and LASs in Fig. 79.

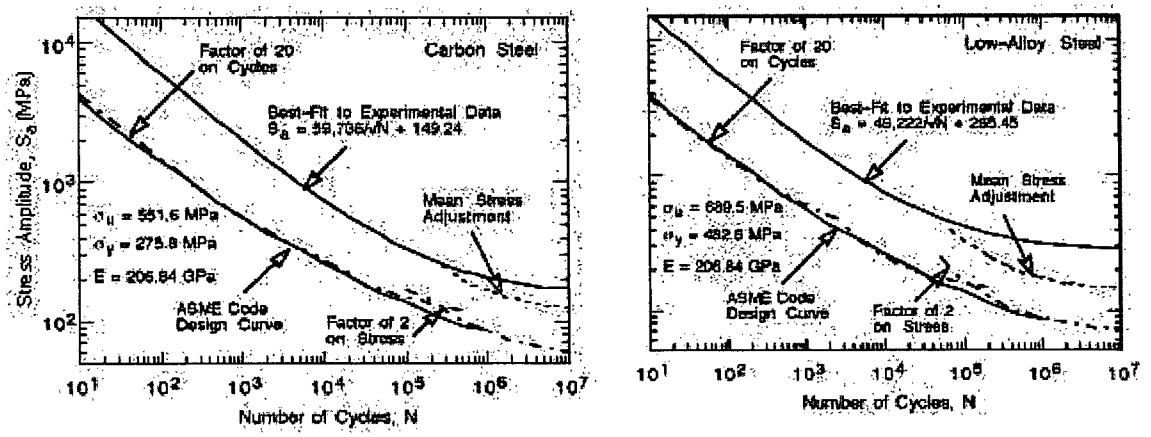

Figure 79. Adjustment for mean stress effects and factors of 2 and 20 applied to best-fit S-N curves for carbon and low-alloy steels to obtain the ASME Code design fatigue curve

7.1 Factors of 2 and 20

The ASME Code design fatigue curves were obtained by lowering the best-fit S-N curve by a factor of 2 on strain and 20 on cycles to account for the differences and uncertainties in relating the fatigue lives of laboratory test specimens to those of actual reactor components. These factors were intended to cover several variables that can influence fatigue life.[3] The actual contribution of these variables is not well documented. Although the factors of 2 and 20 were intended to be somewhat conservative, they should not be considered as safety margins. The variables that can effect fatigue life in air and LWR environments can be broadly classified into three groups:

(a) Material
- (i) Composition: sulfur content
- (ii) Metallurgy: grain size, inclusions, orientation within a forging or plate
- (iii) Processing: cold work, heat treatment
- (iv) Size and geometry
- (v) Surface finish: fabrication surface condition
- (vi) Surface preparation: surface work hardening

(b) Loading
- (i) Strain rate: rise time
- (ii) History: linear damage summation or Miner's rule
- (iii) Mean stress
- (iv) Biaxial effects: constraints

(c) Environment
- (i) Water chemistry: DO, lithium hydroxide, boric acid concentrations
- (ii) Temperature
- (iii) Flow rate

The existing fatigue S-N data base covers an adequate range of material parameters (i)-(iii), loading parameter (i), and environment parameters (i) and (ii); therefore, the variability and uncertainty in fatigue life due to these parameters have been incorporated into the model.

The results indicate that relative to the mean curve, the curve representing a 5% probability of fatigue cracking is a factor of ≈2.5 lower in life and a factor of 1.4-1.7 lower in strain. Therefore, factors of 2.5 on life and 1.7 on strain provide a 90% confidence for the variations in fatigue life associated with compositional and metallurgical differences, material processing, and experimental scatter. As discussed in Section 5.4, the factor of 1.7 on strain has been estimated from the standard deviation on cycles and, therefore may be a conservative value.

Biaxial effects are covered by design procedures and need not be considered in the design fatigue curves. The existing data are conservative with respect to the effects of surface preparation because the fatigue S-N data are obtained for specimens that are free of surface cold work; specimens with surface cold work typically give longer fatigue lives. Fabrication procedures for fatigue test specimens generally follow ASTM guidelines, which require that the final polishing of the specimens avoid surface work hardening. Insufficient data are available to evaluate the contributions of flow rate on fatigue life; most of the tests in water have been conducted at relatively low flow rates. Based on the results for environmentally assisted cracking,[58,59,64] it appears that the available fatigue S-N data on environmental effects should be conservative compared with the results expected at the higher flow velocities expected in most reactor applications. However, it is difficult to assess the degree of conservatism introduced by the low flow rates.

Because the effects of the environment can be included in mean S-N curves for test specimens, only the contributions of size, geometry, surface finish, and loading history (Miner's rule) need to be considered in development of the design fatigue curves that are applicable to components. The effect of specimen size on the fatigue life of CSs and LASs has been investigated for smooth specimens of various diameters in the range of 2-60 mm.[96-99] No intrinsic size effect has been observed for smooth specimens tested in axial loading or plain bending. However, a size effect does occur in specimens tested in rotating bending; the fatigue endurance limit decreases by ≈25% by increasing the specimen size from 2 to 16 mm but does not decrease further with larger sizes.[99] In addition, some effect of size and geometry has been observed on small-scale vessel tests conducted at the Ecole Polytechnique in conjunction with the large-size pressure vessel tests carried out by the Southwest Research Institute.[33] The tests at the Ecole Polytechnique were conducted in room temperature water on ≈305-mm-inner-diameter, 19-mm-thick shells with nozzles made of machined bar stock. The results indicate that the number of cycles to form a 3-mm-deep crack in an 19-mm-thick shell may be 30-50% lower than those in a small test specimen.[27] Thus, a factor of ≈1.4 on cycles and a factor of ≈1.25 on strain can be used to account for size and geometry.

Fatigue life is sensitive to surface finish; cracks can initiate at surface irregularities that are normal to the stress axis. The height, spacing, shape, and distribution of surface irregularities are important for crack initiation. The most common measure of roughness is average surface roughness R_a, which is a measure of the height of the irregularities. Investigations of the effects of surface roughness on the low-cycle fatigue of Type 304 SS in air at 593°C indicate that fatigue life decreases as surface roughness increases.[100,101] The effect of roughness on crack initiation $N_i(R)$ is given by

$$N_i(R_q) = 1012\ R_q^{-0.21}, \tag{7.3}$$

where the RMS value of surface roughness R_q is in micrometers. Typical values of R_a for surfaces finished by different metalworking processes in the automotive industry[102] indicate

that an R_a of 3 μm (or an R_q of 4 μm) represents the maximum surface roughness for drawing/extrusion, grinding, honing, and polishing processes and a mean value for the roughness range for milling or turning processes. For carbon steel or low-alloy steel, an R_q of 4 μm in Eq. 7.3 (R_q of a smooth polished specimen is ≈0.0075 μm) would decrease fatigue life by a factor of ≈3.[100] No information on the effect of surface finish on fatigue limit of carbon steels and low-alloy steels is available. It may be approximated as a factor of ≈1.3 on strain.* A study of the effect of surface finish on fatigue life of carbon steel in room temperature air showed a factor of 2 decrease in life when R_a is increased from 0.3 to 5.3 μm.[103] These results are consistent with Eq. 7.3. Thus, a factor of 2-3 on cycles and ≈1.3 on strain may be used to account for the effects of surface finish.

The effects of load history during variable amplitude fatigue of smooth specimens is well known.[104-107] The presence of a few cycles at high strain amplitude in a load history causes the fatigue life at a smaller strain amplitude to be significantly lower than that at constant amplitude loading. Furthermore, fatigue damage and crack growth in smooth specimens occur at strain levels below the fatigue limit of the material. The results also indicate that the fatigue limit of medium carbon steels is lowered even after low-stress high-cycle fatigue; the higher the stress, the greater the decrease in fatigue threshold.[108] In general, the mean fatigue S-N curves are lowered to account for damaging cycles that occur below the constant-amplitude fatigue limit of the material.[109,110] A factor of 1.5-2.5 on cycles and ≈1.5 on strain may be used to incorporate the effects of load histories on fatigue life.

The subfactors that may be used to account for the effects of various material, loading, and environmental variables on fatigue life are summarized in Table 4. The factors on strain primarily account for the variation in threshold strain (i.e., fatigue limit of the material) caused by material variability, component size and surface finish, and load history. The effects of these parameters on threshold strain are judged not to be cumulative but rather are controlled by the parameter that has the largest effect. Thus, a factor of at least 1.5 on strain and 10 on cycles is needed to account for the differences and uncertainties in relating the fatigue lives of laboratory test specimens to those of actual reactor components.

Table 4. Factors on cycles and on strain to be applied to mean S-N curve

Parameter	Factor on Life	Factor on Strain
Material variability & experimental scatter	2.5	1.4-1.7
Size effect	1.4	1.25
Surface finish	2.0-3.0	1.3
Loading history	1.5-2.5	1.5
Total adjustment:	10.0-26.0	1.5-1.7

7.2 Design Fatigue Curves

The design fatigue curves for LWR environments are obtained by the same procedure that has been used for developing the current ASME Code design fatigue curves. For a specific set

*The factor applied on strain (K_S) is obtained from the factor applied on cycles (K_N) by using the relationship $K_S = (K_N)^{0.2326}$.

of environmental conditions, the best-fit curve obtained from Eqs. 5.3-5.5 is first adjusting for the effect of mean stress using the Goodman relation (Eq. 7.2) and then the curve lowered by factors of 2 on stress and 20 on cycles to account for the differences and uncertainties in fatigue life associated with material and loading conditions. The stress-versus-life design curves were obtained from the strain-versus-life curves by using the room-temperature values of elastic modulus. The design fatigue curves based on the statistical model for CSs and LASs in air at room temperature and 288°C are shown in Fig. 80. The results indicate that for both steels the current ASME Code curve is conservative relative to the curves obtained from the statistical model. For LASs, the difference between the two curves is insignificant, whereas for CSs, the fatigue lives predicted by the current Code curve at stress levels of 100-200 MPa (14.5-29 ksi) are more than a factor of 3 lower than those predicted by the curve from the statistical model.

Figure 81 shows the design curves for LWR environments under service conditions where any one of the following critical threshold conditions is true.

Temperature:	<150°C
Dissolved-oxygen:	<0.05 ppm
Strain Rate:	≥1%/s

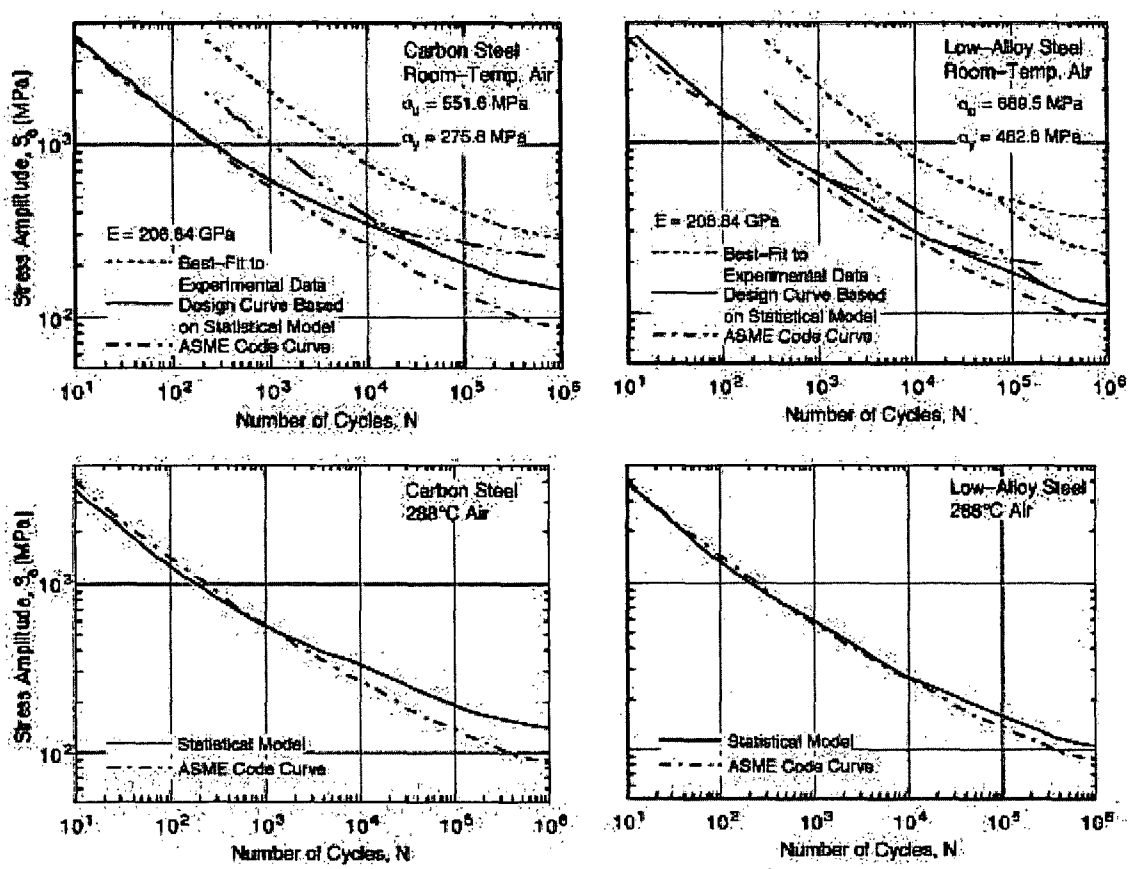

Figure 80. Fatigue design curves developed from statistical model for carbon and low-alloy steels in air at room temperature and 288°C

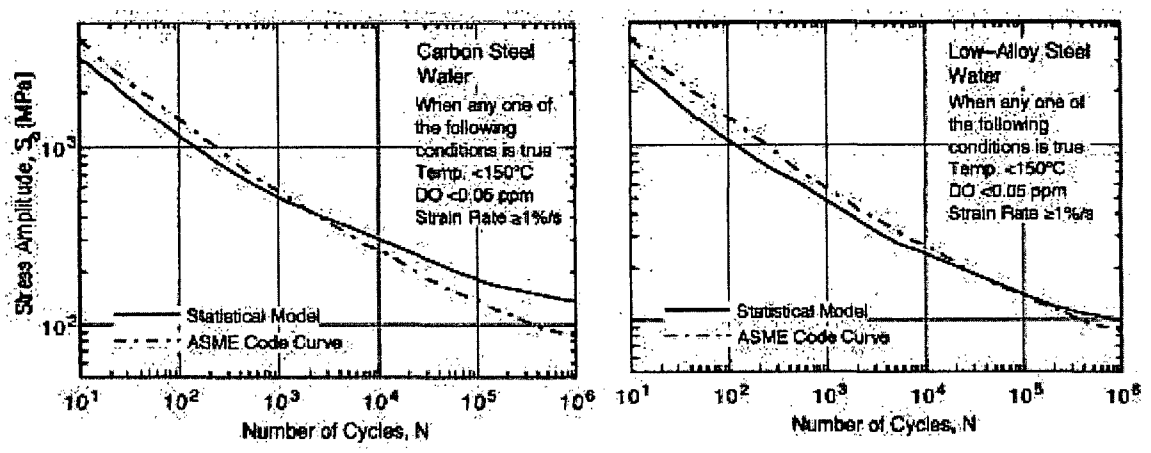

Figure 81. Fatigue design curves developed from statistical model for carbon and low-alloy steels under service conditions where one or more critical threshold values are not satisfied

A threshold value of sulfur content in the steel is not defined because, as discussed in Section 4.2.5, limited data suggest that in high-DO water the fatigue life of CSs may be independent of sulfur content in the range of 0.002-0.015 wt.%.

Figure 82 shows the design curves under service conditions where temperature and DO level are above the threshold value and strain rate is <1%/s. The design fatigue curves in water at 200, 250, and 288°C, corresponding to strain rates of 0.1, 0.01, and a saturation value of 0.001%/s, are shown in the figure. A DO level of 0.2 ppm in water and high sulfur content (0.015 wt.% or higher) is assumed in the steels. Also, a minimum threshold strain amplitude is defined below which environmental effects are modest and are represented by the curves shown in Fig. 81. In Section 4.2.1 it was shown that the threshold strain appears to be ≈20% higher than the fatigue limit of the steel. This translates to strain amplitudes of 0.140 and 0.185%, respectively, for CSs and LASs. These values have to be adjusted for mean stress effects and variability due to material and experimental scatter. To account for the effects of mean stress, the threshold strain amplitudes are decreased by ≈15% for CSs and by ≈40% for LASs; which results in a threshold strain amplitude of ≈0.12% for both steels. A factor of 1.7 on strain provides a 90% confidence for the variations in fatigue life associated with material variability and experimental scatter. Thus, a threshold strain amplitude of 0.07% (or a stress amplitude of 145 MPa) was selected for both steels.

The design fatigue curves in Figs. 81 and 82 can be used for fatigue evaluations in LWR applications. For convenience, the design fatigue curves for LWR environments are reproduced in Appendix B. Note that these curves not only account for environmental effects but also include minor differences between the current ASME mean air curves and the present mean air curves that have been developed from a more extensive data base. Figure 80 shows that the differences are insignificant for LASs and may result in lower values of fatigue usage for CSs.

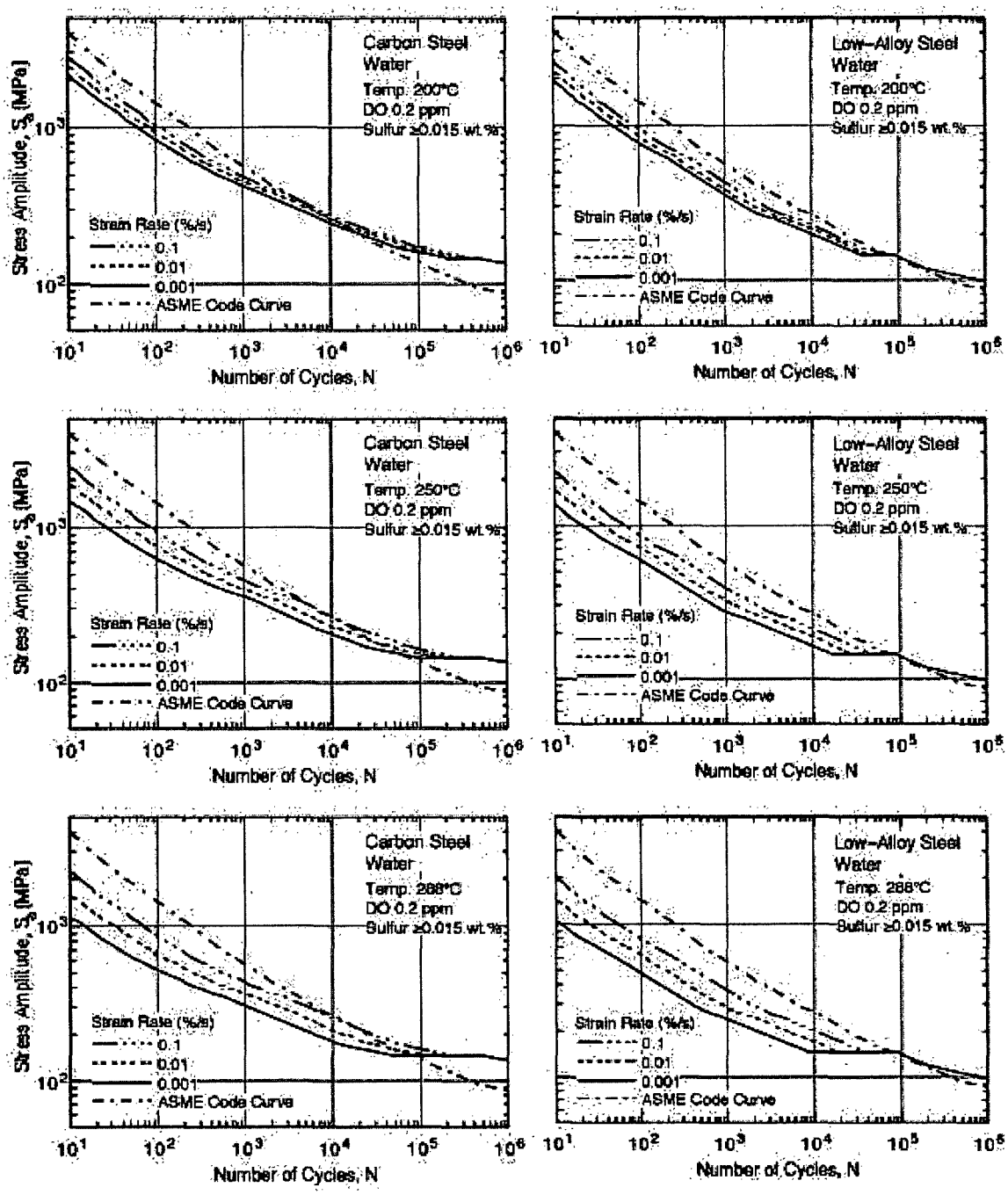

Figure 82. Fatigue design curves developed from statistical model for carbon and low-alloy steels under service conditions where all critical threshold values are satisfied

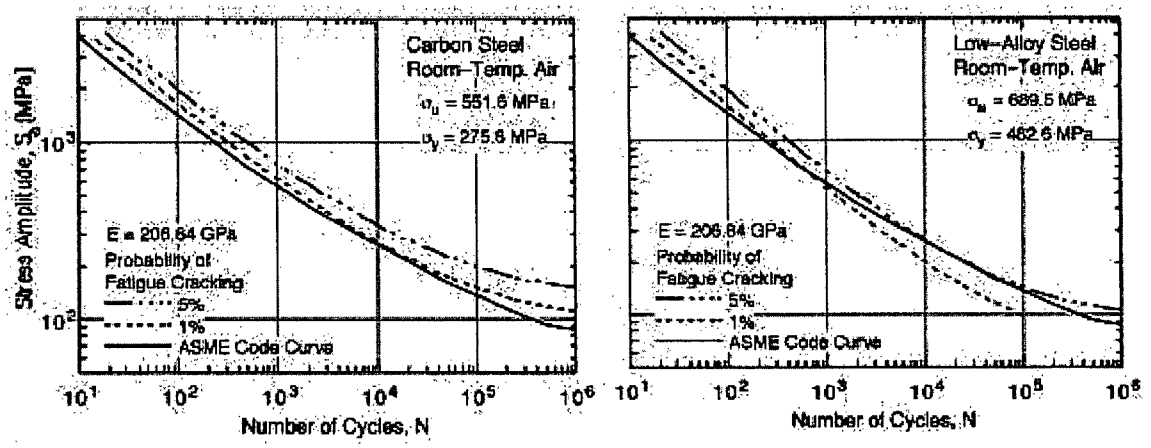

Figure 83. Probability distribution on fatigue life of carbon and low-alloy steels in air

7.3 Significance of Design Curves

The fatigue life of a material is defined as the number of cycles to form an engineering crack, i.e., ≈3 mm deep crack. The best-fit S-N curves to the experimental data represent a 50% probability of forming a fatigue crack in a small polished test specimen under constant loading conditions. It is not clear whether the design fatigue curves represent greater than, equal to, or less than 50% probability of forming a fatigue crack in power plant components.

Statistical models have been used to evaluate the significance of ASME Code design curves in terms of the probability of fatigue cracking associated with the curves.[27,28] Equations 5.6 and 5.7 for the probability distribution of life indicate that relative to the mean curve (50% probability), the 5% probability for fatigue cracking in smooth specimens is lower by a factor of 2.5 on cycles and 1.7 on strain. The factors on strain primarily account for the uncertainties in the fatigue limit. The effects of these factors are judged not to be cumulative but rather are controlled by the parameter that has the largest effect. Therefore, a factor of 1.7 on strain, i.e., a fatigue curve corresponding to probabilities of 5% or less, is adequate to account for the differences and uncertainties in fatigue life associated with material and loading conditions. The probability distribution curves for components can be obtained by lowering the mean-stress-adjusted curves for smooth specimens (Eqs. 5.6 and 5.7) by a factor of 4 (i.e., product of 1.4 and 3) on cycles to include the effects of size/geometry and surface finish in the low cycle regime. Because the Goodman relation assumes maximum possible mean stress, the mean-stress-adjusted curves typically yield conservative estimates of life.

The estimated S-N curves representing 5 and 1% probabilities of fatigue cracking in CS and LAS components in RT air are compared with the ASME Code design fatigue curve in Fig. 83. The results indicate that the current design fatigue curve represents <5% probability of fatigue cracking in LAS components and <1% probability in CS components. A typical fatigue analysis has additional conservatisms due to the stress analysis and loading history assumptions that are unaccounted for in these estimates.

The significance of the proposed interim fatigue design curves in fatigue evaluation of reactor components has also been evaluated with the statistical models.[27,28] The probabilities of fatigue cracking in carbon and low-alloy ferritic steel components have been estimated as a

function of CUF for various service conditions. The CUFs were calculated using the interim fatigue design curves corresponding to low DO water typical of PWRs or high-DO water, which represent a conservative estimate of environmental effects on fatigue life in BWRs. The probability of fatigue cracking was estimated from the statistical models.

The probabilities of fatigue cracking in LASs in low-DO water and in CSs in high-DO water are plotted as a function of CUF in Figs. 84 and 85, respectively. As expected, the probability of fatigue cracking increases with increasing CUF. However, because the curves of constant probability are not parallel, for a given CUF, the probability also depends on the applied stress amplitude. This dependence on stress amplitude is relatively weak for high stress levels, but at low stresses the probability is quite sensitive to the stress amplitude. At stress amplitudes below the fatigue limit for the material, the probability of cracking is relatively insensitive to CUF values above 0.2.

Although these results seem somewhat surprising upon first examination, they do seem heuristically plausible upon further reflection. Because the scatter in life is so large at low

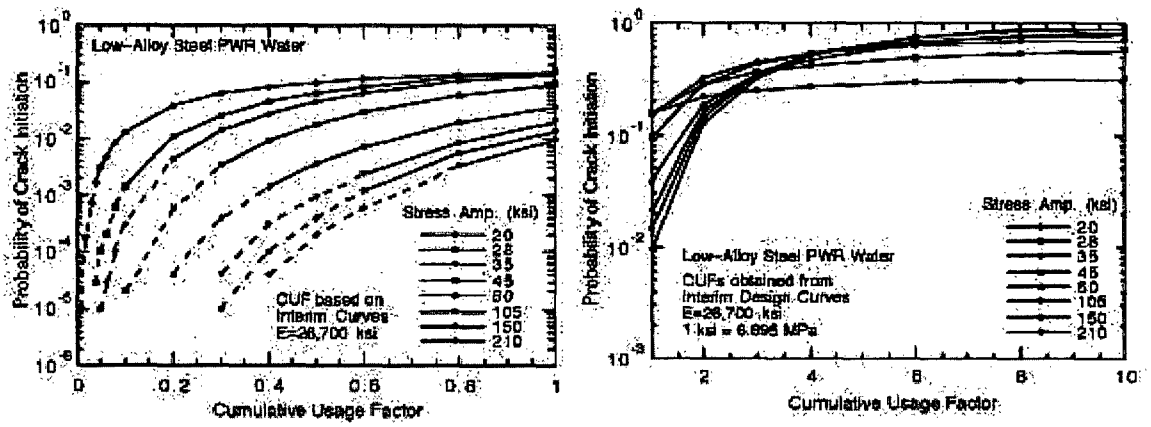

Figure 84. Probability of fatigue cracking in low-alloy steel in low-dissolved-oxygen water (<0.05 ppm) plotted as a function of cumulative usage factor at different stress levels

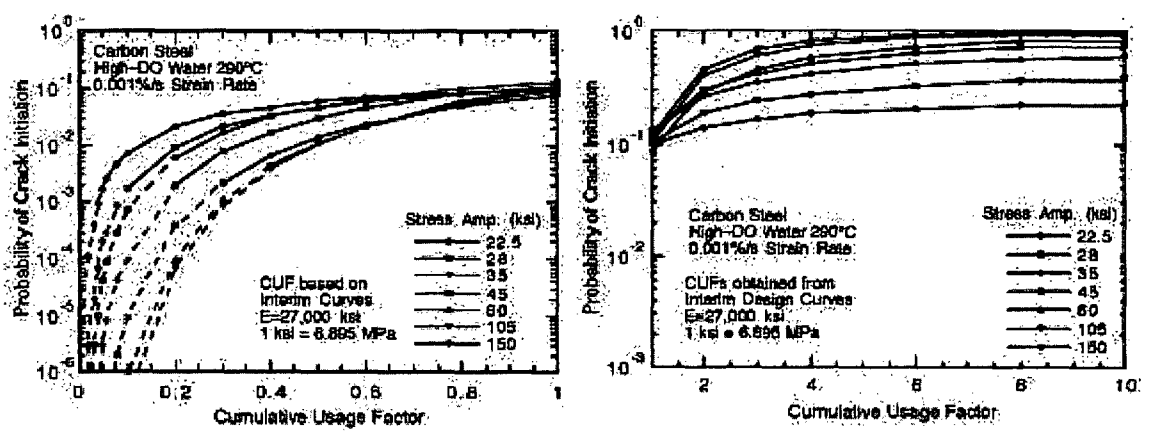

Figure 85. Probability of fatigue cracking in carbon steel in high-dissolved-oxygen water (≥0.5 ppm) plotted as a function of cumulative usage factor at different stress levels

strain amplitudes, the probability of fatigue cracking in this region is not very well characterized by cycle counting, i.e., CUF. Rather, the probability of fatigue cracking is controlled primarily by the uncertainty in defining fatigue limit for the material. This is reflected in the relative insensitivity to CUF value. Because we have relatively little data in the high-cycle regime, the uncertainty in the probability estimates at low strain amplitudes is rather large.

8 Fatigue Evaluations in LWR Environments

The ASME Boiler and Pressure Vessel Code Section III[1] contains rules for the construction of nuclear power plant Class 1 components. It provides the requirements for design against cyclic loadings that occur on a structural component because of changes in the mechanical and thermal loadings as the system goes from one load set (pressure, temperature, moment, and force) to any other load set. The ASME Section III, NB-3600 (piping design) methodology is used exclusively for piping and sometimes for branch nozzles. The ASME Section III, NB-3200 (design by analysis) methodology is generally used for vessels and frequently for nozzles. In both analyses, first the various sets of load states are defined at the most highly stressed locations in the component. The load states are defined in terms of the three principal stresses in NB-3200 analysis, and in terms of internal pressure, moments, average temperature, and temperature gradients in NB-3600 analysis. A peak stress-intensity range and an alternating stress-intensity amplitude S_a is then calculated for each load state. The value of S_a is used to first obtain the allowable number of cycles from the design fatigue curve and then to calculate the fatigue usage associated with that load state. The CUF is sum of the partial usage factors. The Section III, NB-3200- or NB-3600-type analyses for components for service in LWR environments can be performed with the design fatigue curves presented in Figs. B1-B4. Note that fatigue evaluations performed with these updated curves not only account for the environmental effects but they also include minor differences that exist between the current ASME mean air curves and the statistical model air curves.

An alternative approach for fatigue evaluations in LWR environments has been proposed by EPRI[94,95] and by the EFD committee of TENPES.* As was discussed in Section 6, the effects of LWR coolant environments on the fatigue S-N curves are expressed in terms of fatigue life correction factor F_{en}. In the EPRI approach, F_{en} is expressed as the ratio of the life in air to that in water, both at service temperature, whereas in the EFD approach, F_{en} is expressed as the ratio of the life in air at room temperature to that in water at service temperature. The effects of environment are incorporated into the ASME fatigue evaluation by obtaining a fatigue usage for a specific load pair based on the current Code design curves and multiplying it by the correction factor. Fatigue evaluations performed using F_{en} incorporate the effect of environment alone in the EPRI approach, and effects of environment as well as temperature that might exist in air in the EFD approach.

Both these approaches require additional information regarding the service conditions, e.g., temperature, strain rate, and DO level. The procedure for obtaining these parameters depends on the details of the available information, i.e., whether the elapsed time versus temperature information for the transient is available. The values of temperature and DO may be conservatively taken as the maximum values for the transient. As discussed in

* Presented at the Pressure Vessel Research Council Meeting, April 1996, Orlando, FL.

Section 4.2.3, an average temperature may be used if the time versus temperature information is available. Because environmental effects on fatigue life are modest below 150°C and the threshold strain, the average temperature should be determined by the average of the maximum temperature and either 150°C or the temperature at threshold strain, whichever is higher. An average strain rate is generally used for each load state; it is obtained from the peak strain and elapsed time for the transient. However, fatigue monitoring data indicate that actual strain rates may vary significantly during the transient. The slowest strain rate can be used for a conservative estimate of life.

An "improved rate approach" has been proposed in Japan for obtaining the fatigue life correction factor F_{en} under conditions of varying temperature, strain rate, and DO level.[9] During each loading cycle, F_{en} is assumed to vary linearly with strain increments. The effective correction factor F'_{en} for varying conditions is expressed as

$$F'_{en} = 1 + \int_{\varepsilon_{th}}^{\varepsilon_{max}} \frac{F_{en} - 1}{\varepsilon_{max} - \varepsilon_{th}} d\varepsilon, \tag{8.1}$$

where ε_{max} and ε_{th} are the maximum and threshold values of strain, respectively. For varying service conditions, Eq. 8.1 may be written in terms of the effective fatigue life in water N'_{water} expressed as

$$\frac{1}{N'_{water}} = \int_{\varepsilon_{th}}^{\varepsilon_{max}} \frac{1}{N_{water}} \frac{d\varepsilon}{(\varepsilon_{max} - \varepsilon_{th})} \tag{8.2}$$

or

$$\frac{1}{N'_{water}} = \int_{T_{th}}^{T_{max}} \frac{1}{N_{water}} \frac{dT}{(T_{max} - T_{th})}, \tag{8.3}$$

where N_{water} is the life under constant temperature and strain rate, and T_{max} and T_{th} are the maximum and threshold values of temperature, respectively.

Sample fatigue evaluations have been performed for a SA-508 Cl 1 CS feedwater nozzle safe end and SA-333 Gr 6 CS feedwater line piping for a BWR and a SA-508 Cl 2 LAS outlet nozzle for a PWR vessel; the results are given in Tables 5-7. The stress records and the associated service conditions were obtained from Ref. 30. The following three methods were used to calculate the CUF.

(a) For each set of load pair, a partial usage factor was obtained from the appropriate design fatigue curve shown in Figs. B1-B4.

(b) For each set of load pair, first a partial usage factor was obtained from the current ASME Code design curve. This value was adjusted for environmental effects by multiplying by F_{en}, which is calculated from Eqs. 6.5a and 6.5b. F_{en} values were calculated for only those load pairs that satisfy the following three threshold conditions: temperature ≥150°C, strain rate ≤1%/s, and stress amplitude ≥145 MPa (≥21 ksi). The DO level was assumed to be 0.2 ppm. Also, because the sulfur content in the steel is not always available, a conservative value of 0.015 wt.% was assumed.

Table 5. Fatigue evaluation for SA-508 Cl 1 carbon steel feedwater nozzle safe end for a BWR

S_{alt}	Temp.	Strain Rate	Design Cycles	ASME Code Curve		Curves Based on Statistical Model		orrection Based on Statistical Model		Correction Based on EFD Model	
(MPa)	(°C)	(%/s)	n	N	U_{air}	N	U_{env}	F_{en}	U_{env}	F_{en}	U_{env}
567.2	200	0.028	120	1024	0.1172	417	0.2878	2.18	0.2552	2.52	0.2956
500.6	200	0.026	90	1429	0.0630	617	0.1459	2.20	0.1384	2.57	0.1619
444.1	200	0.026	142	1967	0.0722	1000	0.1420	2.20	0.1586	2.57	0.1856
268.8	200	0.002	555	9272	0.0599	6457	0.0860	3.01	0.1804	4.99	0.2989
201.9	200	0.001	10	23830	0.0004	21878	0.0005	3.28	0.0014	5.97	0.0025
143.8	200	0.001	120	81350	0.0015	229087	0.0005	1.00	0.0015	1.00	0.0015
132.4	200	0.001	98	115630	0.0008	1288250	0.0001	1.00	0.0008	1.00	0.0008
121.1	200	0.001	10	159810	0.0001	2000000	-	1.00	0.0001	1.00	0.0001
120.2	288	0.001	10	163810	0.0001	2000000	-	1.00	0.0001	1.00	0.0001
95.5	288	0.001	222	444850	0.0005	2000000	0.0001	1.00	0.0005	1.00	0.0005
92.6	200	0.001	666	523970	0.0013	2000000	0.0003	1.00	0.0013	1.00	0.0013
91.9	288	0.001	120	560450	0.0002	2000000	-	1.00	0.0002	1.00	0.0002
					0.3171		0.6632		0.7384		0.9489

Table 6. Fatigue evaluation for SA-333 Gr 6 carbon steel feedwater line piping for a BWR

S_{alt}	Temp.	Strain Rate	Design Cycles	ASME Code Curve		Curves Based on Statistical Model		orrection Based on Statistical Model		Correction Based on EFD Model	
(MPa)	(°C)	(%/s)	n	N	U_{air}	N	U_{env}	F_{en}	U_{env}	F_{en}	U_{env}
758.9	200	0.117	5	447	0.0112	229	0.0218	1.82	0.0204	1.74	0.0195
744.4	200	0.114	5	468	0.0107	245	0.0204	1.83	0.0195	1.75	0.0187
734.4	200	0.113	5	490	0.0102	251	0.0199	1.83	0.0186	1.76	0.0179
654.2	200	0.001	8	692	0.0116	363	0.0396	3.25	0.0376	5.97	0.0691
616.4	200	0.095	10	776	0.0129	407	0.0246	1.87	0.0241	1.84	0.0237
608.6	200	0.094	5	832	0.0060	437	0.0114	1.87	0.0112	1.84	0.0111
598.3	200	0.041	126	871	0.1447	479	0.2630	2.07	0.2991	2.29	0.3306
561.4	215	0.086	10	1096	0.0091	603	0.0166	2.03	0.0185	1.97	0.0180
468.4	200	0.001	97	1698	0.0571	603	0.1609	3.25	0.1858	5.97	0.3412
459.9	200	0.001	14	1820	0.0077	676	0.0207	3.25	0.0250	5.97	0.0460
422.6	200	0.001	6	2344	0.0026	955	0.0063	3.25	0.0083	5.97	0.0153
421.7	212	0.001	64	2239	0.0286	955	0.0670	3.92	0.1121	6.59	0.1884
382.7	200	0.001	92	3090	0.0298	1445	0.0637	3.25	0.0968	5.97	0.1779
321.5	215	0.001	88	5623	0.0157	3090	0.0285	4.11	0.0643	6.76	0.1058
295.6	212	0.001	15	7413	0.0020	4467	0.0034	3.92	0.0079	6.59	0.0133
271.9	215	0.001	212	8710	0.0243	6310	0.0336	4.11	0.1000	6.76	0.1646
262.9	224	0.001	69	9772	0.0071	7244	0.0095	4.73	0.0334	7.32	0.0517
253.7	224	0.001	11	11220	0.0010	8511	0.0013	4.73	0.0046	7.32	0.0072
236.6	215	0.001	60	13804	0.0043	11220	0.0053	4.11	0.0179	6.76	0.0294
227.2	200	0.001	203	15849	0.0128	13490	0.0150	3.25	0.0416	5.97	0.0765
224.3	200	0.001	360	16218	0.0222	14125	0.0255	3.25	0.0722	5.97	0.1326
205.3	200	0.025	222	21878	0.0101	26687	0.0083	2.20	0.0223	2.60	0.0264
179.9	212	0.028	30	33884	0.0009	50720	0.0006	2.37	0.0021	2.65	0.0023
179.5	200	0.028	81	33113	0.0024	50720	0.0016	2.17	0.0053	2.52	0.0062
149.2	212	0.001	96	63096	0.0015	141254	0.0007	3.92	0.0060	6.59	0.0100
141.8	200	0.001	40	83176	0.0005	602560	0.0001	1.00	0.0005	1.00	0.0005
97.8	200	0.001	30	389045	0.0001	2137962	0.0000	1.00	0.0001	1.00	0.0001
77.4	200	0.001	11545	2238721	0.0052			1.00	0.0052	1.00	0.0052
					0.4522		0.8693		1.2603		1.9091

Table 7. Fatigue evaluation for SA-508 Cl 2 low-alloy steel outlet nozzle for a PWR

S_{alt}	Temp.	Strain Rate	Design Cycles	ASME Code Curve		Curves Based on Statistical Model		orrection Based on Statistical Model		Correction Based on EFD Model[a]	
(MPa)	(°C)	(%/s)	n	N	U_{air}	N	U_{env}	F_{en}	U_{env}	F_{en}	U_{env}
335.6	-	-	80	4670	0.0171	2573	0.0311	1.77	0.0303	-	-
313.0	-	-	10	5741	0.0017	3091	0.0032	1.77	0.0031	-	-
305.7	-	-	20	6010	0.0033	3388	0.0059	1.77	0.0059	-	-
275.4	-	-	20	8098	0.0025	4670	0.0043	1.77	0.0044	-	-
237.1	-	-	70	13723	0.0051	9508	0.0074	1.77	0.0090	-	-
202.1	-	-	130	23795	0.0055	24912	0.0052	1.77	0.0097	-	-
195.1	-	-	150	26082	0.0058	27939	0.0054	1.77	0.0102	-	-
186.8	-	-	50	29251	0.0017	32061	0.0016	1.77	0.0030	-	-
186.1	-	-	30	28587	0.0010	33566	0.0009	1.77	0.0019	-	-
147.3	-	-	40	68338	0.0006	76641	0.0005	1.77	0.0010	-	-
139.3	-	-	1930	94211	0.0205	94211	0.0205	1.00	0.0205	-	-
139.3	-	-	2000	94211	0.0212	94211	0.0212	1.00	0.0212	-	-
138.8	-	-	9270	94211	0.0984	94211	0.0984	1.00	0.0984	-	-
130.0	-	-	60	115810	0.0005	115810	0.0005	1.00	0.0005	-	-
127.1	-	-	230	132894	0.0017	129881	0.0018	1.00	0.0017	-	-
126.5	-	-	10	135977	0.0001	135977	0.0001	1.00	0.0001	-	-
124.5	-	-	80	142360	0.0006	149041	0.0005	1.00	0.0006	-	-
121.6	-	-	160	149041	0.0011	183210	0.0009	1.00	0.0011	-	-
121.6	-	-	26400	152499	0.1731	167150	0.1579	1.00	0.1731	-	-
117.6	-	-	2000	167150	0.0120	205470	0.0097	1.00	0.0120	-	-
113.0	-	-	400	191809	0.0021	252575	0.0016	1.00	0.0021	-	-
110.2	-	-	13200	215114	0.0614	310479	0.0425	1.00	0.0614	-	-
106.0	-	-	13200	241252	0.0547	364547	0.0362	1.00	0.0547	-	-
102.7	-	-	80	289835	0.0003	617784	0.0001	1.00	0.0003	-	-
102.3	-	-	80	289835	0.0003	603777	0.0001	1.00	0.0003	-	-
101.4	-	-	70	317682	0.0002	777031	0.0001	1.00	0.0002	-	-
					0.4924		0.4576		0.5266		

[a] Not calculated because strain rates were not available in the stress records.

(c) Same procedure as item (b), except that F_{en} was calculated from the EFD correlations of Eqs. 6.1-6.3 for the load pairs with stress amplitude ≥145 MPa (≥21 ksi). The DO level was assumed to be 0.2 ppm and sulfur content of 0.015 wt.%. Also, σ_u in Eq. 6.3b was assumed to be 520 MPa for CSs and 650 MPa for LASs.

The results indicate that the approach using F_{en} yields higher values of CUF than those obtained from the design fatigue curves that have been adjusted for environmental effects. The difference arises because the environmentally adjusted design curves account not only for the environment but also for the differences between the ASME mean air curve and statistical model air curve. Figure 80 show that for CSs, this difference can be significant at stress amplitudes <180 MPa (<26 ksi). The results also show that for the feedwater nozzle safe end and the feedwater line piping, the BWR environment increases the fatigue usage by a factor of ≈2. For the LAS outlet nozzle of a PWR, the effect environment on fatigue usage is insignificant. The CUF values from the EFD model were not calculated because information regarding the strain rate was not available in the stress records. For stress levels above ≈145 MPa (21 ksi), the EFD approach would yield F_{en} values of 1.25 and 1.95 for strain rates of 0.1 and 0.001%/s, respectively.

9 Summary

The work performed at ANL on fatigue of carbon and low-alloy steels in LWR environments is summarized. The existing fatigue S-N data have been evaluated to establish the effects of various material and loading variables such as steel type, strain range, strain rate, temperature, sulfur content in steel, orientation, and DO level in water on the fatigue life of these steels. Current understanding of the fatigue S-N behavior of carbon and low-alloy steels may be summarized as follows.

Air Environment

(a) *Steel Type*: The fatigue life of carbon steels is a factor of ≈1.5 lower than that of low-alloy steels.

(b) *Temperature*: For both steels, life is decreased by a factor of ≈1.5 when temperature is increased from room temperature to 288°C.

(c) *Orientation*: Transverse orientations may have poor fatigue resistance than the rolling orientations because of the distribution and morphology of sulfide inclusions.

(d) *Strain Rate*: In the temperature range of dynamic strain aging (200-370°C), some heats of carbon and low-alloy steels are sensitive to strain rate. The effect strain rate on fatigue life is not clear; life may either be unaffected, decrease for some heats, or increase for others. In this temperature range, however, cyclic stresses increase with decreasing strain rate.

(e) *Heat-to-heat Variation*: At 288°C, both steels show significant heat-to-heat variation; fatigue life may vary up to a factor of 5 above or below the mean value.

(f) *ASME Code Mean Curve*: The ASME mean curve for low-alloy steels is in good agreement with the existing fatigue S-N data and that for carbon steels is somewhat conservative.

LWR Environments

(a) *Environmental Effects*: The fatigue life of both carbon and low-alloy steels is decreased significantly when five conditions are satisfied simultaneously, viz., strain amplitude, temperature, DO level in water, and sulfur content in steel are above a minimum level, and strain rate is below a threshold value. Only moderate decrease in life (by a factor of less than 2) is observed when any one of these conditions is not satisfied.

(b) *Steel Type*: The effect of LWR environments on fatigue life of both carbon and low-alloy steels is comparable.

(c) *Strain Amplitude*: A minimum threshold strain is required for environmentally assisted decrease in fatigue life of these steels. The threshold value most likely corresponds to the rupture strain of the surface oxide film. Limited data suggest that the threshold value is ≈20% higher than the fatigue limit for the steel.

(d) *Loading Cycle*: Environmental effects on fatigue life occur primarily during the tensile-loading cycle, and at strain levels greater than the threshold value required to rupture the surface oxide film. Compressive-loading cycle has little or no effect on life. Consequently, loading and environmental conditions, e.g., strain rate, temperature, and DO level, during the tensile-loading cycle in excess of the oxide rupture strain, are important parameters for environmentally assisted reduction in fatigue life of these steels.

(e) *Strain Rate*: When any one of the threshold conditions is not satisfied, e.g., DO <0.05 ppm or temperature <150°C, the effects of strain rate are consistent with those in air, i.e., heats that are sensitive to strain rate in air, also show a decrease in life in water. When all other threshold conditions are satisfied, fatigue life decreases logarithmically with decreasing strain rate below 1%/s; the effect of environment on life saturates at ≈0.001%/s.

(f) *Temperature*: When other threshold conditions are satisfied, fatigue life decreases linearly with temperature above 150°C and up to 320°C. Fatigue life is insensitive to temperatures below 150°C or when any other threshold condition is not satisfied.

(g) *Dissolved Oxygen in Water*: When other threshold conditions are satisfied, fatigue life decreases logarithmically with DO above 0.05 ppm; the effect saturates at ≈0.5 ppm DO.

(h) *Sulfur Content in Steel*: Although sulfur content and morphology are the most important parameters that determine susceptibility of carbon and low-alloy steels to environmentally enhanced fatigue crack growth rates, the existing fatigue S-N data are inadequate to establish unequivocally the effect of sulfur content on the fatigue life of these steels. When any one of the threshold conditions is not satisfied, environmental effects on life are minimal and relatively insensitive to changes in sulfur content. When the threshold conditions are satisfied, i.e., high-temperature high-DO water, the fatigue life of low-alloy steels decreases with increasing sulfur content. Limited data suggest that the effects of environment on life saturate at sulfur contents above 0.012 wt.%. However, in high-temperature high-DO water, the fatigue life of carbon steels seems to be insensitive to sulfur content in the range of 0.002-0.015 wt.%. The effect of sulfur on the growth of short cracks (during crack initiation) may be different than that of long cracks and need to be further investigated.

(i) *Orientation*: The effect of orientation on fatigue life is expected because of differences in the distribution and morphology of sulfide inclusions, and is well known in crack growth studies with precracked specimens. Existing fatigue S-N data indicate that in high-DO water (≤0.1 ppm DO), the fatigue life of low-alloy steels is insensitive to the differences in sulfide distribution and size. In low-DO PWR environments, larger sulfide inclusions may result in a larger decrease in life; however, environmental effects on fatigue life in low-DO water are minimal.

(j) *Flow Rate*: Studies on fatigue crack growth behavior of carbon and low-alloy steels indicate that flow rate is an important parameter for environmental effects on crack growth rates. However, experimental data to establish either the dependence of fatigue life on flow rate or the threshold flow rate for environmental effects to occur are not available and should be developed.

Mechanism of Fatigue Crack Initiation

Fatigue life of a material is defined as the number of cycles to form an "engineering" crack, e.g., a 3-mm-deep crack. During cyclic loading, surface cracks of 10 μm or longer form quite early in life, i.e., <10% of life even at low strain amplitudes. The fatigue life may be considered to be composed entirely of the growth of these short cracks.

Fatigue tests have been conducted to determine the formation and growth characteristics of short cracks in carbon and low-alloy steels in LWR environments. The results indicate that the decrease in fatigue life of these steels in high-DO water is primarily caused by the effects of environment on the growth of short cracks <100 μm deep. In LWR environments, the formation of engineering cracks or fatigue crack initiation may be explained as follows: (a) surface microcracks form quite early in fatigue life at persistent slip bands, edges of slip-band extrusions, notches that develop at grain or phase boundaries, or second-phase particles; (b) during cyclic loading, the protective oxide film is ruptured at strains greater than the rupture strain of surface oxides, and the microcracks grow by anodic dissolution/oxidation of the freshly exposed surface to sizes >100 μm; and (c) growth of these large cracks characterized by accelerating growth rates that may be represented by the proposed ASME Section XI reference curves for these steels in water environments.

Statistical Model

Statistical models have been developed to predict fatigue life of small smooth specimens of carbon and low-alloy steels as a function of various material, loading, and environmental parameters. The functional form and bounding values of these parameters were based upon experimental observations and data trends. The statistical models were obtained by minimizing the squared Cartesian distances from the data point to the predicted curve instead of minimizing the sum of the square of the residual errors for either strain amplitude or fatigue life. The models are recommended for predicted fatigue lives of $\leq 10^6$ cycles. The results indicate that the ASME mean curve for carbon steels is not consistent with the experimental data at strain amplitudes <0.2% or stress amplitudes <410 MPa (<60 ksi); the ASME mean curve is conservative. The statistical model for low-alloy steels is comparable with the ASME mean curve.

The results of statistical analysis have been used to estimate the probability of fatigue cracking in smooth fatigue specimens. The results indicate that relative to the mean or 50% probability curve, the 5% probability curve is a factor of ≈2.5 lower in life in the low-cycle fatigue regime and a factor of 1.4-1.7 lower in strain in the high-cycle regime.

Fatigue Design Curves in LWR Environments

The design fatigue curves for carbon and low-alloy steels in LWR environments were obtained by the procedure that has been used to develop the current ASME Code design fatigue curves. The design fatigue curve for a specific service condition is obtained by adjusting the best-fit experimental curve for the effect of mean stress and setting margins of 20 on cycles and 2 on strain to account for the uncertainties in life associated with material and loading conditions. Data available in the literature were reviewed to evaluate the effects of various material, loading, and environmental variables on fatigue life. The results indicate that the current ASME design fatigue curve represents <5% probability of fatigue cracking in

low-alloy steel components and <1% probability in carbon steel components. The margins of 20 on cycles and 2 on strain may be decreased and still maintain a 5% probability of fatigue cracking in reactor components.

Sample fatigue evaluations have been performed for carbon and low-alloy steel components. The values of cumulative usage factor were determined either from the design fatigue curves based on the statistical model or by applying a fatigue life correction factor that was obtained from the statistical model or the correlations developed by EFD committee of Japan. For carbon steels, the approach using a correction factor yields higher values of usage than those determined from the proposed design fatigue curves. The difference arises because the environmentally adjusted design curves not only account for the environment but also for the difference between the ASME mean air curve and statistical model air curve. For carbon steels, this difference can be significant at low stress amplitudes; the current Code design curve yields higher values of fatigue usage.

Nomenclature

Δa_r	Crack advance from a slip-dissolution mechanism (cm)
$\Delta \varepsilon_t$	Total strain range (%)
ΔK	Stress intensity range (MPa√m)
$\Delta \sigma$	Total stress range (MPa)
ΔT	Temperature difference in salt bridge in external reference electrode
ε_a	Applied strain amplitude (%)
ε_f	Fracture strain of surface oxide
ε_{max}	Maximum strain for loading cycle
ε_{th}	Threshold strain below which environmental effects on fatigue life are insignificant
$\dot{\varepsilon}$	Applied total strain rate (s^{-1})
$\dot{\varepsilon}^*$	Transformed total strain rate
$\dot{\varepsilon}_{app}$	Applied strain rate (s^{-1})
$\dot{\varepsilon}_{ct}$	Crack tip strain rate (s^{-1})
σ_a	Cyclic stress amplitude (MPa)
σ_u	Ultimate strength (MPa)
σ_y	Yield strength (MPa)
$\dot{\nu}$	Frequency of cyclic loading (s^{-1})
a	crack depth (mm)
DO	Dissolved oxygen in water (ppm, ppb)
E	Young's modulus
$E_{(meas)}$	Measured electrochemical potential (ECP)
$E_{(SHE)}$	ECP converted to standard hydrogen electrode (SHE)
$F^{-1}[\cdot]$	Inverse of standard normal cumulative distribution function
F_{en}	Fatigue life correction factor under constant loading and environmental conditions
F'_{en}	Fatigue life correction factor under varying loading and environmental conditions
K_N	Factor applied on life to account for uncertainties in relating fatigue lives of smooth test specimens to those of reactor components
K_S	Factor applied on strain to account for uncertainties in relating fatigue lives of smooth test specimens to those of reactor components
N	Fatigue life defined as number of cycles to initiate fatigue crack
N_{25}	Fatigue life of smooth test specimen defined as number of cycles for tensile stress to drop 25% from its peak value
$N_{25}(x)$	xth percentile of probability distribution on life for smooth test specimens
N_{air}	Fatigue life in air
N_i	Number of cycles to initiate a crack
N_{water}	Fatigue life in water under constant loading and environmental conditions
N'_{water}	Fatigue life in water under varying loading and environmental conditions
N_x	Fatigue life of smooth test specimen defined as number of cycles for tensile stress to drop x% from its peak value
N(x)	Number of cycles corresponding to xth percentile of probability for fatigue crack initiation in a component
O^*	Transformed dissolved oxygen (ppm)
P	Exponent of power-law dependence of fatigue life on strain rate defined as the product of P_c and R_p
P_c	Material parameter that depends on tensile strength and sulfur content of steel

R_a	Average surface roughness, defined as arithmetic mean deviation of surface height from mean line through profile
R_p	Environmental parameter that depends on temperature and dissolved oxygen
R_{pT}	Parameter that defines temperature dependence of environmental factor R_p
R_q	RMS surface roughness, defined as root-mean-square deviation of surface profile from mean line
S	Sulfur content of steel (wt.%)
S^*	Transformed sulfur content (wt.%)
S_a	Applied stress amplitude (MPa)
S'_a	Value of stress amplitude adjusted for mean stress (MPa)
t_c	Time for concentration of absorbed hydrogen to reach a critical level to cause cleavage fracture
T_r	Rise time of loading cycle (s)
T	Test temperature (°C)
T^*	Transformed temperature (°C)
$\overline{V}_{in}$	Average critical velocity for initiation of environmentally assisted enhancement of crack growth ($mm \cdot s^{-1}$)
$\overline{V}_t$	Average environmentally assisted crack growth rate ($cm \cdot s^{-1}$)
x	Percentile of probability distribution
X	Failure criteria defined as 25, 50, or 100% decrease in peak tensile stress

References

1. *ASME Boiler and Pressure Vessel Code Section III - Rules for Construction of Nuclear Power Plant Components*, The American Society of Mechanical Engineers, New York, 1992 Ed.

2. B. F. Langer, *Design of Pressure Vessels for Low-Cycle Fatigue*, ASME J. of Basic Engineering 84 (1962) 389-402.

3. *Tentative Structural Design Basis for Reactor Pressure Vessels and Directly Associated Components (Pressurized, Water Cooled Systems)*, PB 151987, U.S. Dept. of Commerce, Office of Technical Service, 1 Dec. 1958 Revision.

4. S. Ranganath, J. N. Kass, and J. D. Heald, *Fatigue Behavior of Carbon steel Components in High-Temperature Water Environments*, in BWR Environmental Cracking Margins for Carbon Steel Piping, EPRI NP-2406, Electric Power Research Institute, Palo Alto, CA, Appendix 3 (May 1982).

5. W. A. Van Der Sluys, *Evaluation of the Available Data on the Effect of the Environment on the Low Cycle Fatigue Properties in Light Water Reactor Environments*, in Proc. 6th Intl. Symp. on Environmental Degradation of Materials in Nuclear Power Systems - Water Reactors, R. E. Gold and E. P. Simonen, eds., The Metallurgical Society, Warrendale, PA, pp. 1-4 (1993).

6. N. Nagata, S. Sato, and Y. Katada, *Low-Cycle Fatigue Behavior of Pressure Vessel Steels in High-Temperature Pressurized Water*, ISIJ Intl. **31** (1), 106-114 (1991).

7. M. Higuchi and K. Iida, *Fatigue Strength Correction Factors for Carbon and Low-Alloy Steels in Oxygen-Containing High-Temperature Water*, Nucl. Eng. Des. **129**, 293-306 (1991).

8. M. Higuchi, K. Iida, and Y. Asada, *Effects of Strain Rate Change on Fatigue Life of Carbon steel in High-Temperature Water*, in Fatigue and Crack Growth: Environmental Effects, Modeling Studies, and Design Considerations, PVP Vol. 306, S. Yukawa, ed., American Society of Mechanical Engineers, New York, pp. 111-116 (1995); also in *Proc. of Symp. on Effects of the Environment on the Initiation of Crack Growth*, ASTM STP 1298, American Society for Testing and Materials, Philadelphia (1997).

9. H. Kanasaki, M. Hayashi, K. Iida, and Y. Asada, *Effects of Temperature Change on Fatigue Life of Carbon steel in High Temperature Water*, in Fatigue and Crack Growth: Environmental Effects, Modeling Studies, and Design Considerations, PVP Vol. 306, S. Yukawa, ed., American Society of Mechanical Engineers, New York, pp. 117-122 (1995).

10. G. Nakao, H. Kanasaki, M. Higuchi, K. Iida, and Y. Asada, *Effects of Temperature and Dissolved Oxygen Content on Fatigue Life of Carbon and Low-Alloy Steels in LWR Water Environment*, in Fatigue and Crack Growth: Environmental Effects, Modeling Studies, and Design Considerations, PVP Vol. 306, S. Yukawa, ed., American Society of Mechanical Engineers, New York, pp. 123-128 (1995).

11. O. K. Chopra and W. J. Shack, *Effects of LWR Environments on Fatigue Life of Carbon and Low-Alloy Steels*, in Fatigue and Crack Growth: Environmental Effects, Modeling Studies, and Design Considerations, PVP Vol. 306, S. Yukawa, ed., American Society of Mechanical Engineers, New York, pp. 95-109 (1995).

12. O. K. Chopra and W. J. Shack, *Effects of Material and Loading Variables on Fatigue Life of Carbon and Low-Alloy Steels in LWR Environments*, in Transactions of 13th Int. Conf. on Structural Mechanics in Reactor Technology (SMiRT 13), Vol. II, M. M. Rocha and J. D. Riera, eds., Escola de Engenharia - Universidade Federal do Rio Grande do Sul, Porto Alegre, Brazil, pp. 551-562 (1995).

13. O. K. Chopra and W. J. Shack, *Evaluation of Effects of LWR Coolant Environments on Fatigue Life of Carbon and Low-Alloy Steels*, in Effects of the Environment on the Initiation of Crack Growth, ASTM STP 1298, W. A. Van Der Sluys, R. S. Piascik, and R. Zawierucha, eds., American Society for Testing and Materials, Philadelphia, pp. 247-266 (1997).

14. O. K. Chopra and W. J. Shack, *Low-Cycle Fatigue of Piping and Pressure Vessel Steels in LWR Environments*, Nucl. Eng. Des. (1998).

15. H. Mimaki, H. Kanasaki, I. Suzuki, M. Koyama, M. Akiyama, T. Okubo, and Y. Mishima, *Material Aging Research Program for PWR Plants*, in Aging Management Through Maintenance Management, PVP Vol. 332, I. T. Kisisel, ed., American Society of Mechanical Engineers, New York, pp. 97-105 (1996).

16. W. J. Shack and W. F. Burke, *Fatigue of Type 316NG SS*, in Environmentally Assisted Cracking in Light Water Reactors, Semiannual Report, October 1989-March 1990, NUREG/CR-4667 Vol. 10, ANL-91/5, pp. 3-19 (March 1991).

17. K. Iida, *A Review of Fatigue Failures in LWR Plants in Japan*, Nucl. Eng. Des. **138**, 297-312 (1992).

18. P. D. Hicks, in *Environmentally Assisted Cracking in Light Water Reactors: Semiannual Report October 1990--March 1991*, NUREG/CR-4667 Vol. 12, ANL-91/24, pp. 3-18 (Aug. 1991).

19. P. D. Hicks and W. J. Shack, in *Environmentally Assisted Cracking in Light Water Reactors, Semiannual Report, April-September 1991*, NUREG/CR-4667 Vol. 13, ANL-92/6, pp. 3-8 (March 1992).

20. O. K. Chopra, W. F. Michaud, and W. J. Shack, in *Environmentally Assisted Cracking in Light Water Reactors, Semiannual Report, October 1992-March 1993*, NUREG/CR-4667 Vol. 16, ANL-93/27, pp. 3-19 (Sept. 1993).

21. O. K. Chopra, W. F. Michaud, W. J. Shack, and W. K. Soppet, in *Environmentally Assisted Cracking in Light Water Reactors, Semiannual Report, April-September 1993*, NUREG/CR-4667 Vol. 17, ANL-94/16, pp. 1-22 (June 1994).

22. O. K. Chopra, W. F. Michaud, and W. J. Shack, in *Environmentally Assisted Cracking in Light Water Reactors, Semiannual Report, October 1993—March 1994*, NUREG/CR-4667 Vol. 18, ANL-95/2, pp. 1-10 (March 1995).

23. O. K. Chopra, D. J. Gavenda, and W. J. Shack, in *Environmentally Assisted Cracking in Light Water Reactors, Semiannual Report, April-September 1994*, NUREG/CR-4667 Vol. 19, ANL-95/25, pp. 1-17 (Sept. 1995).

24. O. K. Chopra, D. J. Gavenda, and W. J. Shack, in *Environmentally Assisted Cracking in Light Water Reactors, Semiannual Report, October 1994-March 1995*, NUREG/CR-4667 Vol. 20, ANL-95/41, pp. 1-19 (Jan. 1996).

25. O. K. Chopra and W. J. Shack, in *Environmentally Assisted Cracking in Light Water Reactors, Semiannual Report, April 1995-December 1995*, NUREG/CR-4667 Vol. 21, ANL-96/1, pp. 1-27 (July 1996).

26. S. Majumdar, O. K. Chopra, and W. J. Shack, *Interim Fatigue Design Curves for Carbon, Low-Alloy, and Austenitic Stainless Steels in LWR Environments*, NUREG/CR-5999, ANL-93/3 (April 1993).

27. J. Keisler, O. K. Chopra, and W. J. Shack, *Fatigue Strain-Life Behavior of Carbon and Low-Alloy Steels, Austenitic Stainless Steels, and Alloy 600 in LWR Environments*, NUREG/CR-6335, ANL-95/15 (Aug. 1995).

28. J. Keisler, O. K. Chopra, and W. J. Shack, *Statistical Models for Estimating Fatigue Strain-Life Behavior of Pressure Boundary Materials in Light Water Reactor Environments*, Nucl. Eng. Des. **167**, 129-154 (1996).

29. W. A. Van Der Sluys and S. Yukawa, *Status of PVRC Evaluation of LWR Coolant Environmental Effects on the S-N Fatigue Properties of Pressure Boundary Materials*, in Fatigue and Crack Growth: Environmental Effects, Modeling Studies, and Design Considerations, PVP Vol. 306, S. Yukawa, ed., American Society of Mechanical Engineers, New York, pp. 47-58 (1995).

30. A. G. Ware, D. K. Morton, and M. E. Nitzel, *Application of NUREG/CR-5999 Interim Design Curves to Selected Nuclear Power Plant Components*, NUREG/CR-6260, INEL-95/0045 (March 1995).

31. A. F. Deardorff and J. K. Smith, *Evaluation of Conservatisms and Environmental Effects in ASME Code, Section III, Class 1 Fatigue Analysis*, SAND94-0187, prepared by Structural Integrity Associates, San Jose, CA, under contract to Sandia National Laboratories (Aug. 1994).

32. M. E. Mayfield, E. C. Rodabaugh, and R. J. Eiber, *A Comparison of Fatigue Test Data on Piping with the ASME Code Fatigue Evaluation Procedure*, ASME paper 79-PVP-92, American Society of Mechanical Engineers, New York (1979).

33. L. F. Kooistra, E. A. Lange, and A. G. Pickett, *Full-Size Pressure Vessel Testing and Its Application to Design*, J. Eng. Power **86**, 419-428 (1964).

34. L. A. James, *The Effect of Temperature and Cyclic Frequency Upon Fatigue Crack Growth Behavior of Several Steels in an Elevated Temperature Aqueous Environment,* J. Pressure Vessel Technol. **116**, 122-127 (1994).

35. D. D. Macdonald, A. C. Scott, and P. Wentrcek, *External Reference Electrodes for Use in High Temperature Aqueous Systems,* J. Electrochem. Soc. **126**, 908-911 (1979).

36. Y. Katada, N. Nagata, and S. Sato, *Effect of Dissolved Oxygen Concentration on Fatigue Crack Growth Behavior of A533 B Steel in High Temperature Water,* ISIJ Intl. **33** (8), 877-883 (1993).

37. M. E. Indig, *Environmental Aspects of Carbon Steel Stress Corrosion in High Purity Water,* in BWR Environmental Cracking Margins for Carbon steel Piping, EPRI NP-2406, Electric Power Research Institute, Palo Alto, CA, Appendix 1 (May 1982).

38. T. A. Auten and J. V. Monter, *Temperature and Environmentally Assisted Cracking in Low Alloy Steel,* in Proc. Seventh Intl. Symp. on Environmental Degradation of Materials in Nuclear Power Systems - Water Reactors, G. Airey et al., eds., The Metallurgical Society, Warrendale, PA, pp. 1145-1156 (1995).

39. H. Choi, S. Smialowska, and D. D. Macdonald, *Stress Corrosion Cracking of ASME SA508-Cl2 Pressure Vessel Steel,* EPRI-2853, Electric Power Research Institute, Palo Alto, CA, Section 4 (Feb. 1983).

40. F. P. Ford, D. F. Taylor, and P. L. Andresen, *Corrosion-Assisted Cracking of Stainless and Low-Alloy Steels in LWR Environments,* EPRI NP-5064S, Electric Power Research Institute, Palo Alto, CA (Feb. 1987) .

41. C. Laird, *The Influence of Metallurgical Structure on the Mechanism of Fatigue Crack Propagation,* in Fatigue Crack Propagation, ASTM STP 415, American Society for Testing and Materials, Philadelphia, pp. 131-180 (1967).

42. K. J. Miller, *Initiation and Growth Rates of Short Cracks,* in Fundamentals of Deformation and Fracture, B. A. Bilby, K. J. Miller, and J. R. Willis, eds., Cambridge United Press, pp. 476-500 (1984).

43. K. J. Miller, *Damage in Fatigue: A New Outlook,* in Pressure Vessels and Piping Codes and Standard: Volume 1 - Current Applications, PVP Vol. 313-1, K. R. Rao and Y. Asada, eds., American Society of Mechanical Engineers, New York, pp. 191-192 (1995).

44. S. Suresh and R. O. Ritchie, *Propagation of Short Fatigue Cracks,* Int. Metals Reviews **29**, 445-476 (1984).

45. D. J. Gavenda, P. R. Luebbers, and O. K. Choprea, *Crack Initiation and Crack Growth Behavior of Carbon and Low-Alloy Steelss,* in Fatigue and Fracture 1, PVP Vol. 350, S. Rahman, K. K. Yoon, S. Bhandari, R. Warke, and J. M. Bloom, eds., American Society of Mechanical Engineers, New York, pp. 243-255 (1997).

46. C. M. Suh, R. Yuuki, and H. Kitagawa, *Fatigue Microcracks in a Low Carbon Steel*, Fatigue Fract. Engng. Mater. Struct. **8**, 193-203 (1985).

47. K. Tokaji, T. Ogawa, and S. Osako, *The Growth of Microstructurally Small Fatigue Cracks in a Ferritic-Pearlitic Steel*, Fatigue Fract. Engng. Mater. Struct. **11**, 331-342 (1988).

48. K. Tokaji, T. Ogawa, and Y. Harada, *The Growth of Small Fatigue Cracks in a Low Carbon Steel; The Effect of Microstructure and Limitations of Linear Elastic Fracture Mechanics*, Fatigue Fract. Engng. Mater. Struct. **9**, 205-217 (1986).

49. M. W. Brown, *Interface Between Short, Long, and Non-Propagating Cracks*, in The Behavior of Short Cracks, EGF Pub. 1, M. J. Miller and E. R. de los Rios, eds., Mechanical Engineering Publication, London, pp. 423-439 (1986).

50. K. Tokaji and T. Ogawa, *The Growth of Microstructurally Small Fatigue Cracks in Metals*, in Short Fatigue Cracks, ESIS 13, M. J. Miller and E. R. de los Rios, eds., Mechanical Engineering Publication, London, pp. 85-99 (1992).

51. K. Tokaji, T. Ogawa, Y. Harada, and Z. Ando, *Limitations of Linear Elastic Fracture Mechanics in Respect of Small Fatgue Cracks and Microstructure*, Fatigue Fract. Engng. Mater. Struct. **9**, 1-14 (1986).

52. E. R. de los Rios, Z. Tang, and K. J. Miller, *Short Crack Fatigue Behavior in a Medium Carbon Steel*, Fatigue of Engineering Materials and Structures **7**, 97-108 (1984).

53. E. R. de los Rios, A. Navarro, and K. Hussain, *Microstructural Variations in Short Fatigue Crack Propagation of a C-Mn Steel*, in Short Fatigue Cracks, ESIS 13, M. J. Miller and E. R. de los Rios, eds., Mechanical Engineering Publication, London, pp. 115-132 (1992).

54. T. Mizuno, S. Pednekar, S. Smialowska, and D. D. Macdonald, *Corrosion Behavior of Carbon Steel in Oxygenated Water Environments*, EPRI-2853, Electric Power Research Institute, Palo Alto, CA, Section 2 (Feb. 1983).

55. G. Wranglen, *Pitting and Sulphide Inclusions in Steel*, Corr. Sci. **14**, 331-349 (1974).

56. J. H. Bulloch, *A Review of the Fatigue Crack Extension Behaviour of Ferritic Reactor Pressure Vessels Materials in Pressurized Water Reactor Environments*, Res. Mech. **26**, 95-172 (1989).

57. W. A. Van Der Sluys and R. H. Emanuelson, *Environmental Acceleration of Fatigue Crack Growth in Reactor Pressure Vessel Materials*, EPRI Report TR-102796 (Aug. 1993).

58. E. Lenz, N. Wieling, and H. Munster, *Influence of Variation of Flow Rates and Temperature on the Cyclic Crack Growth Rate under BWR Conditions*, in Proc. 3rd Int. Symp. on Environmental Degradation of Materials in Nuclear Power Systems - Water Reactors, G. J. Theus and J. R. Weeks, eds., The Metallurgical Society, Warrendale, PA, pp. 283-288 (1988).

59. L. A. James, G. L. Wire, and W. H. Cullen, *The Effect of Water Flow Rate Upon the Environmentally-Assisted Cracking Response of a Low-Alloy Steel*, J. Pressure Vessel Technol. **117** (3), 238-244 (1995).

60. L. A. James and T. J. Poskie, *Correlation Between MnS Area Fraction and EAC Behavior*, WAPD-T-3012, USDOE Office of Scientific Technical Information, Oak Ridge, TN (1993).

61. L. A. James, H. B. Lee, G. L. Wire, S. R. Novak, and W. H. Cullen, *Corrosion Fatigue Crack Growth in Clad Low-Alloy Steels - Part II: Water Flow Rate Effects in High-Sulfur Plate Steel*, J. Pressure Vessel Technol. **119** (3), pp. 255-263 (1997).

62. G. L. Wire, and Y. Y. Li, *Initiation of Environmentally-Assisted Cracking in Low-Alloy Steels*, in Fatigue and Fracture Volume 1, PVP Vol. 323, H. S. Mehta, ed., American Society of Mechanical Engineers, New York, pp. 269-289 (1996).

63. L. A. James, *The Initiation of Environmentally-Assisted Cracking in Semi-Elliptical Surface Cracks*, in Pressure Vessel and Piping Codes and Standards, PVP Vol. 353, T. C. Esselman, ed., American Society of Mechanical Engineers, New York, pp. 125-139 (1997).

64. W. H. Cullen, M. Kemppainen, H. Hänninen, and K. Törrönen, *The Effects of Sulfur Chemistry and Flow Rate on Fatigue Crack Growth Rates in LWR Environments*, NUREG/CR-4121 (1985).

65. J. H. Bulloch, *Environmental Assisted Cracking Phenomena in Reactor Pressure Vessel Steel - The Role of Manganese Sulphide Segregation*, in Proc. 3rd Int. Symp. on Environmental Degradation of Materials in Nuclear Power Systems - Water Reactors, G. J. Theus and J. R. Weeks, eds., The Metallurgical Society, Warrendale, PA, pp. 261-267 (1988).

66. H. Hänninen, M. Vulli, and W. H. Cullen, *Study of Corrosion Products on Fatigue Fracture Surfaces of Pressure Vessel Steels Tested in PWR Environments by Using X-Ray Photoelectron and Auger Electron Spectroscopy*, in Proc. 3rd Int. Symp. on Environmental Degradation of Materials in Nuclear Power Systems - Water Reactors, G. J. Theus and J. R. Weeks, eds., The Metallurgical Society, Warrendale, PA, pp. 289-298 (1988).

67. J. D. Atkinson, J. H. Bulloch, and J. E. Forrest, *A Fractographic Study of Fatigue Cracks Produced in A533B Pressure Vessel Steel Exposed to Simulated PWR Primary Water Environments*, in Proc. 2nd Int. Atomic Energy Agency Specialists' Meeting on Subcritical Crack Growth, NUREG/CP-0067, MEA-2090, Vol. 2, pp. 269-290 (April 1986).

68. J. D. Atkinson and J. E. Forrest, *The Role of MnS Inclusions in the Development of Environmentally Assisted Cracking of Nuclear Reactor Pressure Vessel Steels*, in Proc. 2nd Int. Atomic Energy Agency Specialists' Meeting on Subcritical Crack Growth, NUREG/CP-0067, MEA-2090, Vol. 2, pp. 153-178 (April 1986).

69. W. A. Van Der Sluys and R. H. Emanuelson, *Environmental Acceleration of Fatigue Crack Growth in Reactor Pressure Vessel Materials and Environments, in Environmentally Assisted Cracking: Science and Engineering*, ASTM STP 1049, W. B. Lisagor, T. W. Crooker, and B. N. Leis, eds., American Society for Testing and Materials, Philadelphia, PA, pp. 117-135 (1990).

70. J. D. Atkinson, J. Yu, and Z.-Y. Chen, *An Analysis of the Effects of Sulfur Content and Potential on Corrosion Fatigue Crack Growth in Reactor Pressure Vessel Steels*, Corros. Sci. **38** (5), 755-765 (1996).

71. T. A. Auten, S. Z. Hayden, and R. H. Emanuelson, *Fatigue Crack Growth Rate Studies of Medium Sulfur Low Alloy Steels Tested in High Temperature Water*, in Proc. 6th Int. Symp. on Environmental Degradation of Materials in Nuclear Power Systems - Water Reactors, R. E. Gold and E. P. Simonen, eds., The Metallurgical Society, Warrendale, PA, pp. 35-40 (1993).

72. F. P. Ford and P. L. Andresen, *Stress Corrosion Cracking of Low-Alloy Pressure Vessel Steel in 288°C Water*, in Proc. 3rd Int. Atomic Energy Agency Specialists' Meeting on Subcritical Crack Growth, NUREG/CP-0112, Vol. 1, pp. 37-56 (Aug. 1990).

73. F. P. Ford, *Overview of Collaborative Research into the Mechanisms of Environmentally Controlled Cracking in the Low Alloy Pressure Vessel Steel/Water System*, in Proc. 2nd Int. Atomic Energy Agency Specialists' Meeting on Subcritical Crack Growth, NUREG/CP-0067, MEA-2090, Vol. 2, pp. 3-71 (April 1986).

74. F. P. Ford, S. Ranganath, and D. Weinstein, *Environmentally Assisted Fatigue Crack Initiation in Low-Alloy Steels - A Review of the Literature and the ASME Code Design Requirements*, EPRI Report TR-102765 (Aug. 1993).

75. F. P. Ford, *Prediction of Corrosion Fatigue Initiation in Low-Alloy and Carbon Steel/Water Systems at 288°C*, in Proc. 6th Int. Symp. on Environmental Degradation of Materials in Nuclear Power Systems - Water Reactors, R. E. Gold and E. P. Simonen, eds., The Metallurgical Society, Warrendale, PA, pp. 9-17 (1993).

76. F. P. Ford, *Quantitative Prediction of Environmentally Assisted Cracking*, Corros. **52** (5), 375-395 (1996).

77. H. Hänninen, K. Törrönen, and W. H. Cullen, *Comparison of Proposed Cyclic Crack Growth Mechanisms of Low Alloy Steels in LWR Environments*, in Proc. 2nd Int. Atomic Energy Agency Specialists' Meeting on Subcritical Crack Growth, NUREG/CP-0067, MEA-2090, Vol. 2, pp. 73-97 (April 1986).

78. H. Hänninen, K. Törrönen, M. Kempainen, and S. Salonen, *On the Mechanisms of Environment Sensitive Cyclic Crack Growth of Nuclear Reactor Pressure Vessel Steels*, Corros. Sci. **23**, 663-679 (1983).

79. K. Törrönen, M. Kempainen, and H. Hänninen, *Fractographic Evaluation of Specimens of A533B Pressure Vessel Steel*, EPRI Report NP-3483, Project 1325-7 (May 1984).

80. O. K. Chopra and W. J. Shack, *Effects of LWR Coolant Environments on Fatigue S-N Curves for Carbon and Low-Alloy Steels*, in Pressure Vessel and Piping Codes and Standards, PVP Vol. 339, T. C. Esselman, ed., American Society of Mechanical Engineers, New York, pp. 185-198 (1996).

81. R. A. Oriani, *A Mechanistic Theory of Hydrogen Embrittlement of Steels*, Ber. Bunsenges. Phys. Chem. **76**, 848-857 (1972).

82. C. D. Beachem, *A New Model for Hydrogen Assisted Cracking*, Met. Trans. **3A** (2), 437-451 (1972).

83. T. F. Kassner, W. J. Shack, W. E. Ruther, and J. H. Park, *Environmentally Assisted Cracking of Ferritic Steels*, in Environmentally Assisted Cracking in Light Water Reactors, Semiannual Report, April-September 1990, NUREG/CR-4667 Vol. 11, ANL-91/9, pp. 2-9 (May 1991).

84. E. D. Eason, E. E. Nelson, and J. D. Gilman, *Modeling of Fatigue Crack Growth Rate for Ferritic Steels in Light Water Reactor Environments*, PVP-Vol. 286, Changing Priorities of Code and Standards, ASME, pp. 131-142 (1994).

85. D. A. Hale, S. A. Wilson, E. Kiss, and A. J. Gianuzzi, *Low Cycle Fatigue Evaluation of Primary Piping Materials in a BWR Environment*, GEAP-20244, U.S. Nuclear Regulatory Commission (Sept. 1977).

86. D. A. Hale, S. A. Wilson, J. N. Kass, and E. Kiss, *Low Cycle Fatigue Behavior of Commercial Piping Materials in a BWR Environment*, J. Eng. Mater. Technol. **103**, 15-25 (1981).

87. S. Ranganath, J. N. Kass, and J. D. Heald, *Fatigue Behavior of Carbon steel Components in High-Temperature Water Environments*, in Low-Cycle Fatigue and Life Prediction, ASTM STP 770, C. Amzallag, B. N. Leis, and P. Rabbe, eds., American Society for Testing and Materials, Philadelphia, pp. 436-459 (1982).

88. J. B. Terrell, *Fatigue Life Characterization of Smooth and Notched Piping Steel Specimens in 288°C Air Environments*, NUREG/CR-5013, EM-2232 Materials Engineering Associates, Inc., Lanham, MD (May 1988).

89. J. B. Terrell, *Fatigue Strength of Smooth and Notched Specimens of ASME SA 106-B Steel in PWR Environments*, NUREG/CR-5136, MEA-2289, Materials Engineering Associates, Inc., Lanham, MD (Sept. 1988).

90. J. B. Terrell, *Effect of Cyclic Frequency on the Fatigue Life of ASME SA-106-B Piping Steel in PWR Environments*, J. Mater. Eng. **10**, 193-203 (1988).

91. H. Abdel-Raouf, A. Plumtree, and T. H. Topper, *Effects of Temperature and Deformation Rate on Cyclic Strength and Fracture of Low-Carbon steel*, in Cyclic Stress-Strain Behavior - Analysis, Experimentation, and Failure Prediction, ASTM STP 519, American Society for Testing and Materials, Philadelphia, pp. 28-57 (1973).

92. B. H. Lee, and I. S. Kim, *Dynamic Strain Aging in the High-Temperature Low-Cycle Fatigue of SA 508 Cl. 3 Forging Steel*, J. Nucl. Mater. **226**, 216-225 (1995).

93. T. T. Pleune and O. K. Chopra, *Artificial Neural Networks and Effects of Loading Cinditions on Fatigue Life of Carbon and Low-Alloy Steels*, in Fatigue and Fracture 1, PVP Vol. 350, S. Rahman, K. K. Yoon, S. Bhandari, R. Warke, and J. M. Bloom, eds., American Society of Mechanical Engineers, New York, pp. 413-423 (1997).

94. H. S. Mehta and S. R. Gosselin, *An Environmental Factor Approach to Account for Reactor Water Effects in Light Water Reactor Pressure Vessel and Piping Fatigue Evaluations*, EPRI Report TR-105759 (Dec. 1995).

95. H. S. Mehta and S. R. Gosselin, *An Environmental Factor Approach to Account for Reactor Water Effects in Light Water Reactor Pressure Vessel and Piping Fatigue Evaluations*, in Fatigue and Fracture Volume 1, PVP Vol. 323, H. S. Mehta, ed., American Society of Mechanical Engineers, New York, pp. 171-185 (1996).

96. R. E. Peterson, *Fatigue Tests of Small Specimens with Particular Reference to Size Effect*, Trans. Amer. Soc. Steel Testing **18**, 1041-1053 (1930).

97. D. Morkovin and H. F. Moore, *Third Progress Report on the Effect of Size of Specimen on Fatigue Strength of Three Types of Steel*, Proc. Amer. Soc. Test. Mater. **44**, 137-158 (1944).

98. C. E. Philips and R. B. Heywood, *The Size Effect in Fatigue of Plain and Notched Steel Specimens Loaded Under Reversed Direct Stress*, Proc. Inst. Mech. Engr. **165**, 113-124 (1951).

99. C. Massonnet, *The Effect of Size, Shape, and Grain Size on the Fatigue Strength of Medium Carbon steel*, Proc. Amer. Soc. Test. Mater. **56**, 954-978 (1956).

100. P. S. Maiya and D. E. Busch, *Effect of Surface Roughness on Low-Cycle Fatigue Behavior of Type 304 Stainless Steel*, Met. Trans. **6A**, 1761-1766 (1975).

101. P. S. Maiya, *Effect of Surface Roughness and Strain Range on Low-Cycle Fatigue Behavior of Type 304 Stainless Steel*, Scripta Metall. **9**, 1277-1282 (1975).

102. K. J. Stout, *Surface Roughness - Measurement, Interpretation, and Significance of Data*, Mater. Eng. **2**, 287-295 (1981).

103. K. Iida, *A Study of Surface Finish Effect Factor in ASME B & PV Code Section III, in Pressure Vessel Technology*, Vol. 2, L. Cengdian and R. W. Nichols, eds., Pergamon Press, New York, pp. 727-734 (1989).

104. M. A. Pompetzki, T. H. Topper, and D. L. DuQuesnay, *The Effect of Compressive Underloads and Tensile Overloads on Fatigue Damage Accumulation in SAE 1045 Steel*, Int. J. Fat. **12** (3), 207-213 (1990).

105. A. Conle and T. H. Topper, *Evaluation of Small Cycle Omission Criteria for Shortening of Fatigue Service Histories*, Int. J. Fat. **1**, 23-28 (1979).

106. A. Conle and T. H. Topper, *Overstrain Effects During Variable Amplitude Service History Testing*, Int. J. Fat. **2**, 130-136 (1980).

107. Li Nian and Du Bai-Ping, *Effect of Monotonic and Cyclic Prestrain on the Fatigue Threshold in Medium-Carbon steels*, Int. J. Fat. **14** (1), 41-44 (1992).

108. Li Nian and Du Bai-Ping, *The Effect of Low-Stress High-Cycle Fatigue on the Microstructure and Fatigue Threshold of a 40Cr Steel*, Int. J. Fat. **17** (1), 43-48 (1995).

109. E. Haibach and D. Schutz, *Fatigue Life Evaluation with Particular Attention to Local Strain and Stress Time Histories*, Proc. Inst. Mech. Engr., 1974.

110. D. J. Dowdell, H. H. E. Leipholz, and T. H. Topper, *The Modified Life Law Applied to SAE-1045 Steel*, Int. J. Fract. **31**, 29-36 (1986).

Appendix A: Fatigue Test Results

Table A1. Fatigue test results for A106-Gr B carbon steel at 288°C

Test Number	Environ -ment[a]	Dissolved Oxygen[b] (ppb)	pH at RT	Conducti-v ity (µS/cm)	Tensile Rate (%/s)	Compres-sive Rate (%/s)	Stress Range (MPa)	Strain Range (%)	Life N_{25} (Cycles)
1508	Air	–	–	–	0.4	0.4	910.9	1.002	3,305
1524	Air	–	–	–	0.4	0.4	892.3	0.950	3,714
1523	Air	–	–	–	0.4	0.4	898.6	0.917	2,206
1521	Air	–	–	–	0.4	0.4	889.4	0.910	3,219
1522	Air	–	–	–	0.4	0.4	905.4	0.899	3,398
1515	Air	–	–	–	0.4	0.4	866.1	0.752	6,792
1749[c]	Air	–	–	–	0.4	0.4	–	–	6,372
1717	Air	–	–	–	0.4	0.004	884.6	0.758	6,217
1625	Air	–	–	–	0.004	0.4	887.7	0.757	4,592
1629[d]	Air	–	–	–	0.4	0.4	782.9	0.503	31,243
1590	Air	–	–	–	0.4	0.004	821.1	0.503	24,471
1576	Air	–	–	–	0.004	0.4	805.8	0.503	28,129
1505	Air	–	–	–	0.4	0.4	767.6	0.501	31,200
1525	Air	–	–	–	0.4	0.4	743.6	0.452	65,758
1640	Air	–	–	–	0.4	0.4	710.9	0.402	65,880
1538	Air	–	–	–	0.4	0.4	708.0	0.387	>1,000,000
1517	Air	–	–	–	0.4	0.4	692.5	0.353	2,053,295
1659	Air	–	–	–	0.004	0.4	656.2	0.343	>114,294
1526	DI	–	–	–	0.4	0.4	876.4	0.873	3,332
1527	DI	–	6.0	–	0.4	0.4	752.8	0.493	10,292
1528	DI	5	5.8	–	0.4	0.4	744.1	0.488	25,815
1743[e]	DI	<1	6.5	0.08	0.4	0.4	712.6	0.386	84,700
1530	PWR	3	6.9	41.67	0.4	0.4	885.5	0.894	1,355
1545	PWR	8	6.9	22.73	0.4	0.4	889.7	0.886	3,273
1533	PWR	4	6.9	45.45	0.004	0.4	916.0	0.774	3,416
1529	PWR	3	6.9	45.45	0.4	0.4	743.4	0.484	31,676
1605	PWR	9	6.5	23.81	0.4	0.004	785.2	0.460	>57,443
1588	PWR	6	6.5	23.26	0.004	0.4	828.7	0.514	15,321
1539	PWR	6	6.8	38.46	0.4	0.4	690.9	0.373	136,570
1542	PWR	6	6.6	27.03	0.4	0.4	631.8	0.354	>1,154,892
1645	Hi DO	800	6.1	0.07	0.4	0.4	831.1	0.721	2,736
1768	Hi DO	600	6.0	0.07	0.4	0.004	907.3	0.755	1,350
1626	Hi DO	900	5.9	0.13	0.004	0.4	910.1	0.788	247
1715	Hi DO	600	5.9	0.08	0.004	0.4	904.1	0.813	381
1711	Hi DO	630	5.8	0.31	0.4	0.4	772.1	0.542	5,850
1707	Hi DO	650	5.9	0.08	0.4	0.004	803.0	0.488	3,942
1709	Hi DO	650	5.9	0.11	0.4	0.004	805.1	0.501	3,510
1627	Hi DO	800	5.9	0.10	0.004	0.4	826.8	0.534	769
1641	Hi DO	800	5.9	0.09	0.4	0.4	693.0	0.385	17,367
1665	Hi DO	800	6.1	0.08	0.004	0.4	717.0	0.376	3,455
1666	Hi DO	750	6.1	0.09	0.0004	0.4	729.6	0.376	>7,380
1647	Hi DO	800	6.1	0.09	0.4	0.4	688.0	0.380	26,165
1660	Hi DO	750	6.1	0.11	0.004	0.4	689.6	0.360	>83,024
1649	Hi DO	700	6.3	0.08	0.4	0.4	673.4	0.352	28,710
1652	Hi DO	700	6.1	0.09	0.4	0.4	638.1	0.328	56,923
1655	Hi DO	750	6.1	0.10	0.4	0.4	567.6	0.289	>1,673,954

[a] DI = Deionized water and PWR = simulated PWR water with 2 ppm lithium and 1000 ppm boron.
[b] Represent DO levels in effluent water.
[c] Tested with 5-min hold period at peak tensile strain.
[d] Specimen preoxidized in water with 600 ppb DO for 100 h at 288°C.
[e] Specimen preoxidized in water with 600 ppb DO for 30 h at 288°C.

Table A2. Fatigue test results for A533-Gr B low-alloy steel at 288°C

Test Number	Environ -ment[a]	Dissolved Oxygen[b] (ppb)	pH at RT	Conducti-v ity (µS/cm)	Tensile Rate (%/s)	Compres-sive Rate (%/s)	Stress Range (MPa)	Strain Range (%)	Life N_{25} (Cycles)
1508	Air	-	-	-	0.4	0.4	910.9	1.002	3,305
1524	Air	-	-	-	0.4	0.4	892.3	0.950	3,714
1523	Air	-	-	-	0.4	0.4	898.6	0.917	2,206
1521	Air	-	-	-	0.4	0.4	889.4	0.910	3,219
1522	Air	-	-	-	0.4	0.4	905.4	0.899	3,398
1515	Air	-	-	-	0.4	0.4	866.1	0.752	6,792
1749[c]	Air	-	-	-	0.4	0.4	-	-	6,372
1717	Air	-	-	-	0.4	0.004	884.6	0.758	6,217
1625	Air	-	-	-	0.004	0.4	887.7	0.757	4,592
1629[d]	Air	-	-	-	0.4	0.4	782.9	0.503	31,243
1590	Air	-	-	-	0.4	0.004	821.1	0.503	24,471
1576	Air	-	-	-	0.004	0.4	805.8	0.503	28,129
1505	Air	-	-	-	0.4	0.4	767.6	0.501	31,200
1525	Air	-	-	-	0.4	0.4	743.6	0.452	65,758
1640	Air	-	-	-	0.4	0.4	710.9	0.402	65,880
1538	Air	-	-	-	0.4	0.4	708.0	0.387	>1,000,000
1517	Air	-	-	-	0.4	0.4	692.5	0.353	2,053,295
1659	Air	-	-	-	0.004	0.4	656.2	0.343	>114,294
1526	DI	-	-	-	0.4	0.4	876.4	0.873	3,332
1527	DI	-	6.0	-	0.4	0.4	752.8	0.493	10,292
1528	DI	5	5.8	-	0.4	0.4	744.1	0.488	25,815
1743[e]	DI	<1	6.5	0.08	0.4	0.4	712.6	0.386	84,700
1530	PWR	3	6.9	41.67	0.4	0.4	885.5	0.894	1,355
1545	PWR	8	6.9	22.73	0.4	0.4	889.7	0.886	3,273
1533	PWR	4	6.9	45.45	0.004	0.4	916.0	0.774	3,416
1529	PWR	3	6.9	45.45	0.4	0.4	743.4	0.484	31,676
1605	PWR	9	6.5	23.81	0.4	0.004	785.2	0.460	>57,443
1588	PWR	6	6.5	23.26	0.004	0.4	828.7	0.514	15,321
1539	PWR	6	6.8	38.46	0.4	0.4	690.9	0.373	136,570
1542	PWR	6	6.6	27.03	0.4	0.4	631.8	0.354	>1,154,892
1645	Hi DO	800	6.1	0.07	0.4	0.4	831.1	0.721	2,736
1768	Hi DO	600	6.0	0.07	0.4	0.004	907.3	0.755	1,350
1626	Hi DO	900	5.9	0.13	0.004	0.4	910.1	0.788	247
1715	Hi DO	600	5.9	0.08	0.004	0.4	904.1	0.813	381
1711	Hi DO	630	5.8	0.31	0.4	0.4	772.1	0.542	5,850
1707	Hi DO	650	5.9	0.08	0.4	0.004	803.0	0.488	3,942
1709	Hi DO	650	5.9	0.11	0.4	0.004	805.1	0.501	3,510
1627	Hi DO	800	5.9	0.10	0.004	0.4	826.8	0.534	769
1641	Hi DO	800	5.9	0.09	0.4	0.4	693.0	0.385	17,367
1665	Hi DO	800	6.1	0.08	0.004	0.4	717.0	0.376	3,455
1666	Hi DO	750	6.1	0.09	0.0004	0.4	729.6	0.376	>7,380
1647	Hi DO	800	6.1	0.09	0.4	0.4	688.0	0.380	26,165
1660	Hi DO	750	6.1	0.11	0.004	0.4	689.6	0.360	>83,024
1649	Hi DO	700	6.3	0.08	0.4	0.4	673.4	0.352	28,710
1652	Hi DO	700	6.1	0.09	0.4	0.4	638.1	0.328	56,923
1655	Hi DO	750	6.1	0.10	0.4	0.4	567.6	0.289	>1,673,954

[a] DI = Deionized water and PWR = simulated PWR water with 2 ppm lithium and 1000 ppm boron.
[b] Represent DO levels in effluent water.
[c] Tested with 5-min hold period at peak tensile strain.
[d] Specimen preoxidized in water with 600 ppb DO for 100 h at 288°C.
[e] Specimen preoxidized in water with 600 ppb DO for 30 h at 288°C.

Table A3. Fatigue test results for A302-Gr B low-alloy steel at 288°C

Test Number	Environ -ment[a]	Dissolved Oxygen[b] (ppb)	pH at RT	Conducti -vity (µS/cm)	Tensile Rate (%/s)	Compres- sive Rate (%/s)	Stress Range (MPa)	Strain Range (%)	Life N_{25} (Cycles)
1697 (R)	Air	–	–	–	0.4	0.4	944.5	0.756	8,070
1701 (R)	Air	–	–	–	0.004	0.4	1021.4	0.757	4,936
1712 (R)	Air	–	–	–	0.0004[c]	0.4	1041.9	0.759	5,350
1789 (R)	Air	–	–	–	0.4	0.4	859.5	0.505	46,405
1783 (R)	Air	–	–	–	0.4	0.4	796.1	0.408	>1,050,000
1780 (T2)	Air	–	–	–	0.4	0.4	908.6	0.756	1,598
1781 (T2)	Air	–	–	–	0.004	0.4	952.4	0.755	375
1782 (T2)	Air	–	–	–	0.4	0.4	752.8	0.404	33,650
1787 (T2)	Air	–	–	–	0.4	0.4	667.5	0.342	431,150
1702 (R)	PWR	3	6.5	20.00	0.4	0.4	921.2	0.735	6,212
1704 (R)	PWR	3	6.5	19.23	0.004	0.4	1022.6	0.745	3,860
1716 (R)	PWR	5	6.5	19.23	0.0004[c]	0.4	1042.3	0.739	3,718
1777 (T)	PWR	1	6.4	19.23	0.4	0.4	913.8	0.765	4,366
1775 (T)	PWR	1	6.5	19.42	0.004	0.4	995.6	0.750	1,458
1776 (T2)	PWR	1	6.4	18.40	0.4	0.4	887.1	0.765	1,244
1774 (T2)	PWR	2	6.4	19.42	0.004	0.4	949.7	0.758	348
1788 (R)	Hi DO	650	5.9	0.10	0.004	0.4	957.0	0.754	317
1784 (T2)	Hi DO	510	6.0	0.07	0.004	0.4	937.6	0.783	111

[a] Simulated PWR water with 2 ppm lithium and 1000 ppm boron.
[b] Represent DO levels in effluent water.
[c] Slow strain rate applied only during 1/8 cycle near peak tensile strain.

Table A4. Results of exploratory fatigue tests in which slow strain rate was applied during only part of tensile-loading cycle

Test Number	DO[a] (ppb)	pH at RT	Conduct -ivity (μS/cm)	Wave-form[b]	Strain at Rate Change (%) ε_{T1}	ε_{T2}	Tensile Strain Rate[c] (%/s) $\dot{\varepsilon}_{T1}$	$\dot{\varepsilon}_{T2}$	$\dot{\varepsilon}_{T3}$	Stress Range (MPa)	Strain Range (%)	Life N_{25} (Cycles)
A106-Gr B Steel												
1760	-	-	-	C	0.189	-	0.4	0.004	-	1042.8	0.756	3,893
1762	-	-	-	D	0.568	-	0.004	0.4	-	1027.5	0.758	4,356
1667	-	-	-	E	0.379	-	0.4	0.004	-	999.2	0.758	5,261
1668	-	-	-	G	0.569	-	0.4	0.004	-	998.5	0.758	5,139
1695	-	-	-	I	0.378	0.567	0.4	0.004	0.4	993.4	0.756	5,240
1722	-	-	-	H	0.569	-	0.004	0.4	-	955.8	0.758	4,087
1734	-	-	-	J	0.662	-	0.4	0.004	-	970.0	0.757	4,122
1737	-	-	-	K	0.095	-	0.004	0.4	-	963.7	0.757	4,105
1763	620	5.9	0.07	C	0.144	-	0.4	0.004	-	974.9	0.848	340
1765	590	6.0	0.07	D	0.524	-	0.004	0.4	-	977.3	0.806	615
1677	800	6.0	0.11	E	0.255	-	0.4	0.004	-	926.5	0.762	545
1684	700	6.0	0.09	F	0.255	-	0.004	0.4	-	964.0	0.762	1,935
1753	670	5.9	0.07	F	0.260	-	0.004	0.4	-	982.6	0.777	1,831
1678	700	5.9	0.14	G	0.509	-	0.4	0.004	-	944.4	0.780	615
1703	650	5.9	0.13	G	0.496	-	0.4	0.004	-	942.4	0.760	553
1692[c]	700	6.0	0.10	G	0.499	-	0.4	0.004	-	936.4	0.764	261
1728	700	5.9	0.07	H	0.124	-	0.004	0.4	-	969.3	0.740	1,649
1732	600	5.9	0.08	H	0.123	-	0.004	0.4	-	954.5	0.734	2,080
1698	600	6.1	0.08	I	0.253	0.494	0.4	0.004	0.4	909.1	0.756	1,306
1741	600	6.0	0.09	J	0.652	-	0.4	0.004	-	896.8	0.785	888
1742	520	6.0	0.09	K	0.066	-	0.004	0.4	-	948.0	0.783	2,093
A533-Gr B Steel												
1708	-	-	-	E	0.377	-	0.4	0.004	-	898.2	0.754	5,355
1710	-	-	-	G	0.565	-	0.4	0.004	-	885.6	0.753	3,630
1767	-	-	-	I	0.376	0.564	0.4	0.004	0.4	886.3	0.752	7,502
1713	670	5.9	0.07	E	0.254	-	0.4	0.004	-	890.8	0.761	426
1714	570	5.9	0.08	G	0.488	-	0.4	0.004	-	886.1	0.748	578
1769	630	6.0	0.07	I	0.243	0.476	0.4	0.004	0.4	877.2	0.729	976
A333-Gr 6 Steel												
1739	-	-	-	A	-	-	0.4	-	-	882.9	0.809	9,483
1740	-	-	-	B	-	-	0.004	-	-	936.8	0.808	7,665
1756	-	-	-	E	0.404	-	0.4	0.004	-	967.4	0.808	10,156
1754	-	-	-	F	0.403	-	0.004	0.4	-	963.2	0.806	6,696
1745	-	-	-	J	0.707	-	0.4	0.004	-	961.3	0.808	8,519
1747	-	-	-	K	0.101	-	0.004	0.4	-	964.6	0.810	6,537
1746	715	6.1	0.09	A	-	-	0.4	-	-	788.3	0.829	3,550
1748	645	6.0	0.10	B	-	-	0.004	-	-	881.3	0.794	555
1758	560	5.8	0.07	E	0.267	-	0.4	0.004	-	892.3	0.799	620
1755	660	5.9	0.07	F	0.268	-	0.004	0.4	-	933.5	0.803	1,670
1750	680	5.9	0.10	J	0.673	-	0.4	0.004	-	886.7	0.811	1,235
1751	590	5.9	0.07	K	0.068	-	0.004	0.4	-	913.1	0.808	2,325

[a] Represent DO levels in effluent water.
[b] The waveforms A-K are defined in Fig. 51
[c] Compressive strain rate was 0.4%/s for all tests.
[d] A slow strain rate of 0.0004%/s was used for this test.

Appendix B: Design Fatigue Curves for LWR Environments

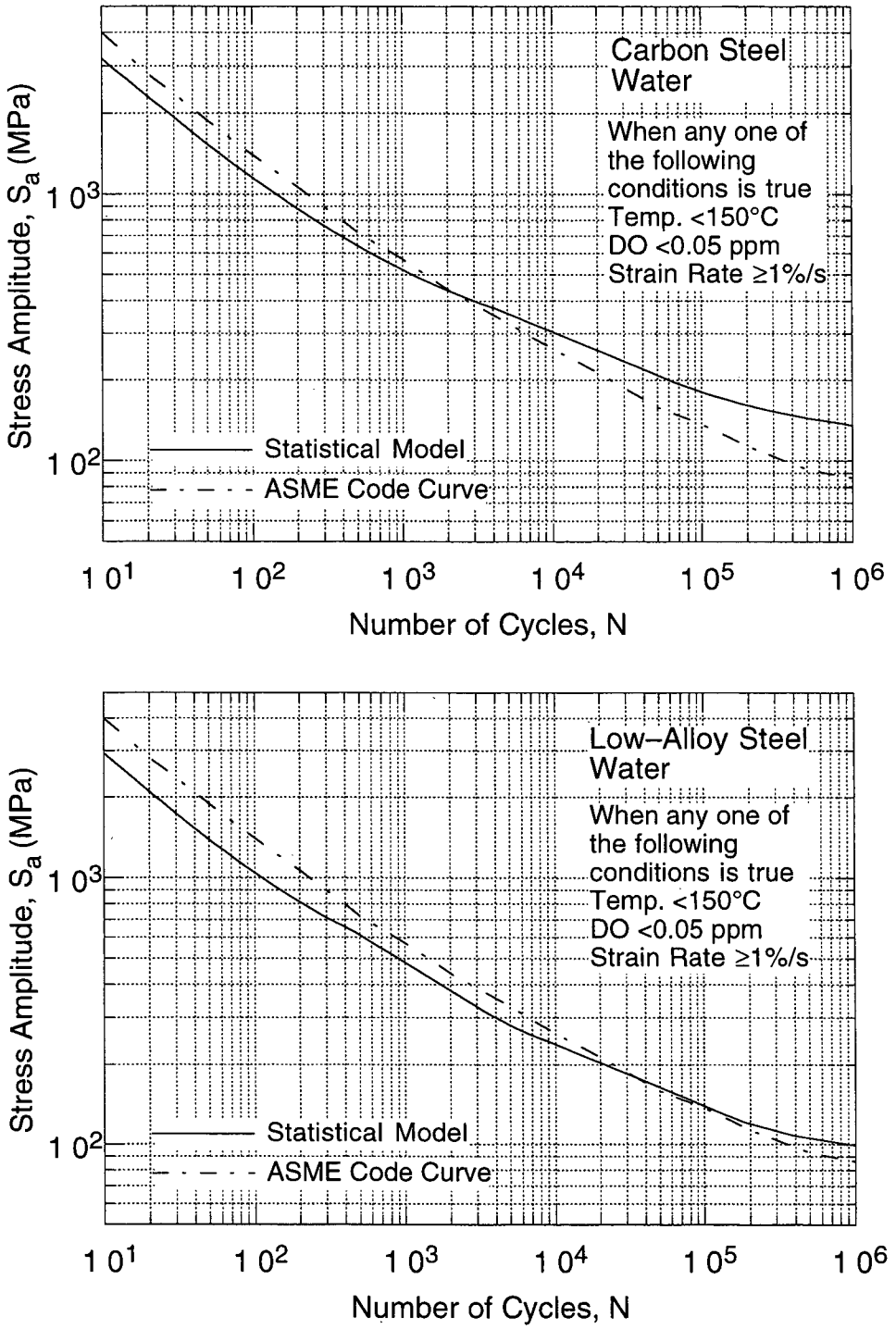

Figure B1. Fatigue design curves developed from statistical model for carbon and low-alloy steels under service conditions in which any one of the critical threshold values is not satisfied

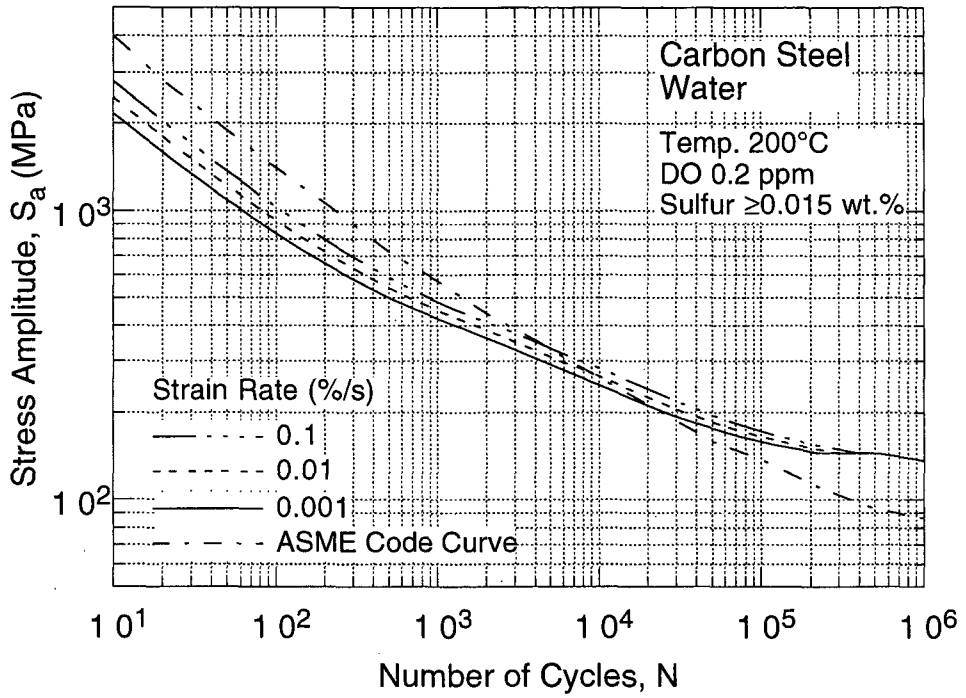

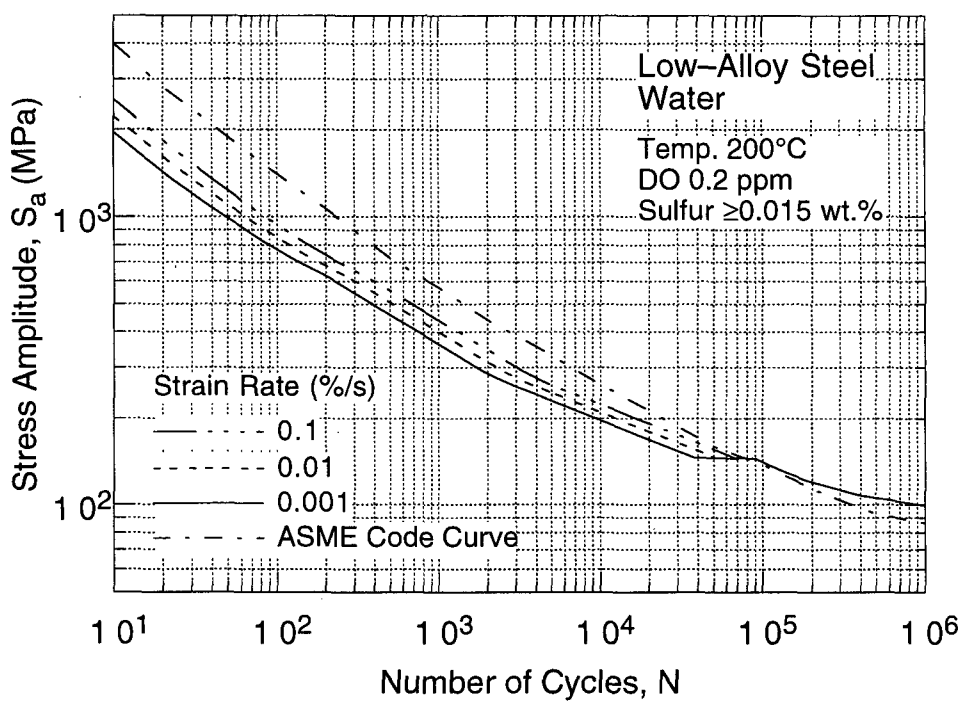

Figure B2. Fatigue design curves developed from statistical model for carbon and low-alloy steels at 200°C in water with ≈0.2 ppm dissolved oxygen

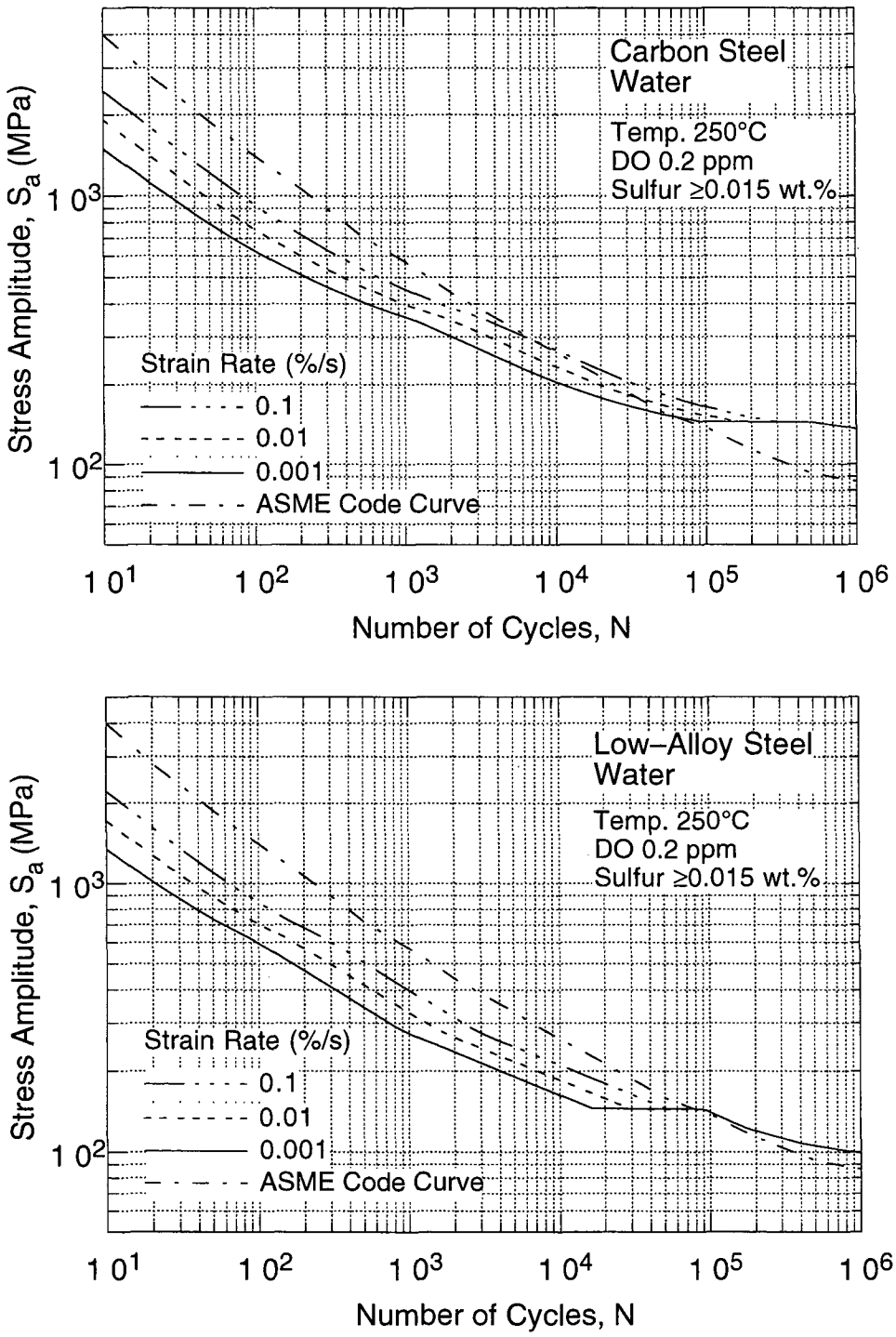

Figure B3. Fatigue design curves developed from statistical model for carbon and low-alloy steels at 250°C in water with ≈0.2 ppm dissolved oxygen

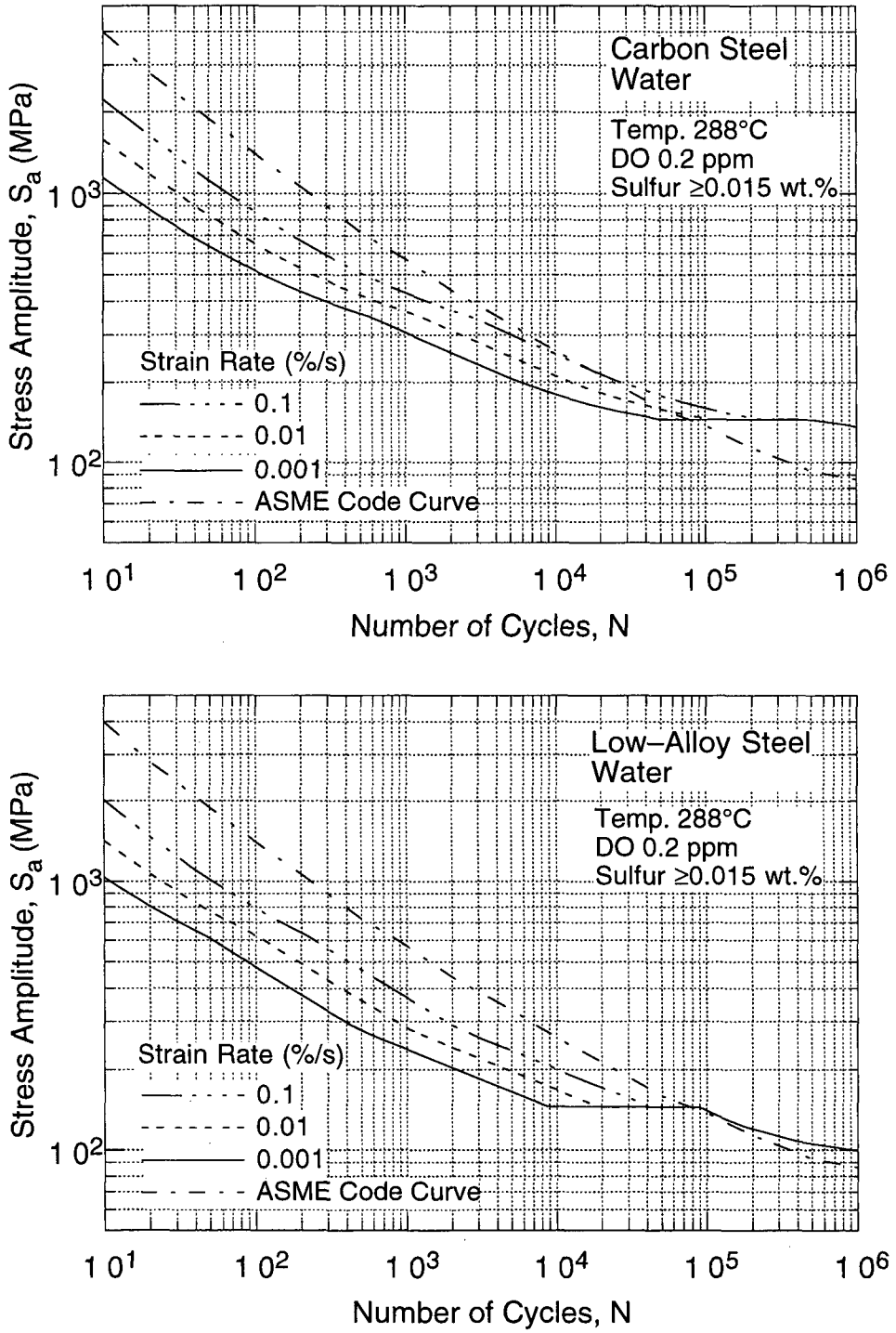

Figure B4. Fatigue design curves developed from statistical model for carbon and low-alloy steels at 288°C in water with ≈0.2 ppm dissolved oxygen

NRC FORM 335
(2-89)
NRCM 1102,
3201, 3202

U. S. NUCLEAR REGULATORY COMMISSION

BIBLIOGRAPHIC DATA SHEET

(See instructions on the reverse)

1. REPORT NUMBER
(Assigned by NRC. Add Vol., Supp., Rev., and Addendum Numbers, if any.)
NUREG/CR-6583
ANL-97/18

2. TITLE AND SUBTITLE
Effects of LWR Coolant Environments on Fatigue Design Curves of Carbon and Low-Alloy Steels

3. DATE REPORT PUBLISHED

MONTH	YEAR
February	1998

4. FIN OR GRANT NUMBER
W6610

5. AUTHOR(S)
O. K. Chopra and W. J. Shack

6. TYPE OF REPORT
Technical

7. PERIOD COVERED *(Inclusive Dates)*

8. PERFORMING ORGANIZATION – NAME AND ADDRESS *(If NRC, provide Division, Office or Region, U.S. Nuclear Regulatory Commission, and mailing address; if contractor, provide name and mailing address.)*
Argonne National Laboratory
9700 South Cass Avenue
Argonne, IL 60439

9. SPONSORING ORGANIZATION – NAME AND ADDRESS *(If NRC, type "Same as above": if contractor, provide NRC Division, Office or Region, U.S. Nuclear Regulatory Commission, and mailing address.)*
Engineering Issues Branch
Office of Nuclear Regulatory Research
U. S. Nuclear Regulatory Commission
Washington, DC 20555

10. SUPPLEMENTARY NOTES
M. McNeil, NRC Project Manager

11. ABSTRACT (200 words or less)
The ASME Boiler and Pressure Vessel Code provides rules for the construction of nuclear power plant components. Figures I-9.1 through I-9.6 of Appendix I to Section III of the Code specify fatigue design curves for structural materials. While effects of reactor coolant environments are not explicitly addressed by the design curves, test data indicate that the Code fatigue curves may not always be adequate in coolant environments. This report summarizes work performed by Argonne National Laboratory on fatigue of carbon and low-alloy steels in light water reactor (LWR) environments. The existing fatigue S-N data have been evaluated to establish the effects of various material and loading variables such as steel type, dissolved oxygen level, strain range, strain rate, temperature, orientation, and sulfur content on the fatigue life of these steels. Statistical models have been developed for estimating the fatigue S-N curves as a function of material, loading, and environmental variables. The results have been used to estimate the probability of fatigue cracking of reactor components. The different methods for incorporating the effects of LWR coolant environments on the ASME Code fatigue design curves are presented.

12. KEY WORDS/DESCRIPTORS *(List words or phrases that will assist researchers in locating this report.)*
Fatigue Strain-Life Curves
Fatigue Design Curves
LWR Environments
Carbon Steels
Low-Alloy Steels
Fatigue Crack Initiation
Probability of Crack Initiation

13. AVAILABILITY STATEMENT
Unlimited

14. SECURITY CLASSIFICATION
(This Page)
Unclassified
(This Report)
Unclassified

15. NUMBER OF PAGES

16. PRICE

NUREG/CR-5704
ANL-98/31

Effects of LWR Coolant Environments on Fatigue Design Curves of Austenitic Stainless Steels

Argonne National Laboratory

U.S. Nuclear Regulatory Commission
Office of Nuclear Regulatory Research
Washington, DC 20555-0001

NUREG/CR-5704
ANL-98/31

Effects of LWR Coolant Environments on Fatigue Design Curves of Austenitic Stainless Steels

Manuscript Completed: November 1998
Date Published: April 1999

Prepared by
O. K. Chopra

Argonne National Laboratory
9700 South Cass Avenue
Argonne, IL 60439

M. McNeil, NRC Project Manager

Prepared for
Division of Engineering Technology
Office of Nuclear Regulatory Research
U.S. Nuclear Regulatory Commission
Washington, DC 20555-0001
NRC Job Code W6610

EFFECTS OF LWR COOLANT ENVIRONMENTS ON FATIGUE DESIGN CURVES OF AUSTENITIC STAINLESS STEELS

by

O. K. Chopra

Abstract

The ASME Boiler and Pressure Vessel Code provides rules for the construction of nuclear power plant components. Figures I-9.1 through I-9.6 of Appendix I to Section III of the Code specify fatigue design curves for structural materials. While effects of reactor coolant environments are not explicitly addressed by the design curves, test data indicate that the Code fatigue curves may not always be adequate in coolant environments. This report summarizes work performed by Argonne National Laboratory on fatigue of austenitic stainless steels in light water reactor (LWR) environments. The existing fatigue S-N data have been evaluated to establish the effects of various material and loading variables such as steel type, dissolved oxygen level, strain range, strain rate, and temperature on the fatigue lives of these steels. Statistical models are presented for estimating the fatigue S-N curves as a function of material, loading, and environmental variables. Design fatigue curves have been developed for austenitic stainless steel components in LWR environments. The extent of conservatism in the design fatigue curves and an alternative method for incorporating the effects of LWR coolant environments into the ASME Code fatigue evaluations are discussed.

Contents

Executive Summary ix

Acknowledgments xi

1 Introduction 1

2 Experimental 3

3 Overview of Fatigue S-N Data 9

3.1 Air Environment 9

3.2 LWR Environments 12

3.2.1 Strain Rate 13

3.2.2 Strain Amplitude 13

3.2.3 Dissolved Oxygen 14

3.2.4 Temperature 15

3.3 Cast Stainless Steels 16

4 Mechanism of Fatigue Crack Initiation 18

4.1 Formation of Engineering Cracks 18

4.2 Environmental Effects 20

5 Statistical Model 24

6 Design Fatigue Curves 28

7 Fatigue Life Correction Factor 31

8 Conservatism in Design Fatigue Curves 31

9 Fatigue Evaluations in LWR Environments 33

10 Summary 33

10.1 Air Environment 34

10.2 LWR Environments 34

10.3 Fatigue Design Curves in LWR Environments 35

References 35

Figures

1. Fatigue S-N data for CSs and austenitic SSs in water 2

2. Configuration of fatigue test specimen 4

3. Schematic diagram of autoclave system for fatigue tests in water environment 4

4. Total applied displacement and strain in specimen gauge section during stroke-controlled tests with a sawtooth waveform 6

5. Fatigue S-N behavior for Types 304, 316, and 316NG austenitic SSs in air at various temperatures 10

6. Effect of strain rate on fatigue lives of austenitic SSs in air for various strain ranges . 10

7. Effect of strain range on cyclic strain-hardening behavior of Type 316NG SS in air at room temperature and 288°C 11

8. Cyclic stress-strain curves for Types 316NG, 304, and 316 SSs in air at room temperature and 288°C 11

9. Fatigue strain amplitude-vs.-life data for Types 316NG and 304 SS in water at 288°C 12

10. Dependence of fatigue life of austenitic SSs on strain rate in low- and high-DO water 13

11. Results of strain rate change tests on Type 316 SS in low-DO water at 325°C 14

12. Change in fatigue lives of austenitic SSs in low-DO water with temperature 15

13. Waveforms for change in temperature during exploratory fatigue tests 15

14. Fatigue life of Type 316 SS under varying temperature indicated by horizontal bars... 16

15. Fatigue strain amplitude-vs.-life data for CF-8M cast SSs in air 17

16. Effect of strain rate on cyclic-hardening behavior of wrought and cast SSs in air at 288°C 17

17. Fatigue strain amplitude-vs.-life data for CF-8M cast SSs in water 18

18. Dependence of fatigue lives of CF-8M cast SSs on strain rate in low-DO water at various strain amplitudes 18

19. Growth of cracks in smooth fatigue specimens 19

20. Schematic illustration of short-crack behavior 20

21. Photomicrographs of gauge surface of Type 316NG SS specimens tested in air, simulated PWR water, and high-DO water 21

22. Schematic illustration of film rupture/slip dissolution process 22

23. Photomicrographs of fracture surfaces of Types 304 and 316NG SS specimens tested in air, high-DO water, and low-DO, simulated PWR water 23

24. Experimental and predicted values of fatigue lives of austenitic SSs in air and water environments 26

25. Experimental fatigue lives and those estimated from statistical models for austenitic SSs in water environments 26

26. Residual error for austenitic SSs as a function of test temperature 27

27. Residual error for austenitic SSs as a function of material heat 27

28. Residual error for austenitic SSs as a function of loading strain rate 27

29. Residual error for austenitic SSs as a function of applied strain amplitude 28

30. Residual error for austenitic SSs as a function of dissolved oxygen in water 28

31. ASME and statistical-model design fatigue curves for Types 304 and 316 SS in air .. 30

32. ASME and statistical-model design fatigue curves for Types 304 and 316 SS in water with <0.05 ppm DO 30

33. ASME and statistical-model design fatigue curves for Types 304 and 316 SS in water with ≥0.05 ppm DO 30

Tables

1. Composition (in wt.%) of wrought and cast SSs used for fatigue tests 3

2. Fatigue test results for Type 316NG austenitic SS 7

3. Fatigue test results for Type 304 austenitic SS at 288°C 8

4. Fatigue test results for CF-8M cast SSs at 288°C 8

5. Subfactors that may be used to account for effects of various variables on fatigue life 32

Executive Summary

Section III, Subsection NB of the ASME Boiler and Pressure Vessel Code contains rules for the design of Class 1 components. Figures I-9.1 through I-9.6 of Appendix I to Section III specify the Code design fatigue curves for applicable structural materials. However, Section III, Subsection NB-3121 of the Code states that effects of the coolant environment on fatigue resistance of a material were not intended to be addressed in these design curves. Therefore, there is uncertainty about the effects of environment on fatigue resistance of materials used in operating pressurized water reactor (PWR) and boiling water reactor (BWR) plants, whose primary-coolant-pressure-boundary components were designed in accordance with the Code.

The current Section-III design fatigue curves of the ASME Code were based primarily on strain-controlled fatigue tests of small polished specimens at room temperature in air. Best-fit curves to the experimental test data on stress or on cycles, were lowered by a factor of 2 on stress or 20 on cycles, whichever was more conservative, to obtain the design fatigue curves. These factors are not safety margins but rather adjustment factors that must be applied to experimental data to obtain estimates of the lives of components. They were not intended to address the effects of the coolant environment on fatigue life. Recent fatigue strain vs. life (S-N) data obtained in the U.S. and Japan demonstrate that light water reactor (LWR) environments can have potentially significant effects on the fatigue resistance of materials. Specimen lives obtained from tests in simulated LWR environments can be much shorter than those obtained from corresponding tests in air.

This report summarizes work performed by Argonne National Laboratory on fatigue of austenitic stainless steels (SSs) in simulated LWR environments. The existing fatigue S-N data, foreign and domestic, for wrought and cast stainless steels have been evaluated to establish the effects of various material and loading variables on fatigue life. Statistical methods have been used to develop fatigue S-N curves that include the effects of material, loading, and environmental variables. An alternative method for incorporating the effects of LWR coolant environments into the ASME Code fatigue design curves is presented.

Overview of Fatigue S-N Data

In air, the fatigue lives of Types 304 and 316 SS are comparable; those of Type 316NG are superior. The fatigue S-N behavior of cast CF-8 and CF-8M SSs is similar to that of wrought austenitic SSs. The fatigue life of all steels is independent of temperature in the range from room temperature to 427°C; at temperatures above 260°C, it may decrease with decreasing strain rate. The ASME mean curve for austenitic SSs is nonconservative with respect to the existing fatigue S-N data; at strain amplitudes <0.5%, the mean curve predicts significantly longer fatigue lives than those observed experimentally.

The fatigue lives of cast and wrought austenitic SSs is decreased in LWR environments. The reduction in life depends on strain rate, dissolved oxygen (DO) level in water, and temperature. The effect of LWR environments on fatigue life is comparable for all steels. The results indicate that a minimum threshold strain is required to produce an environmentally assisted decrease in the fatigue life of these steels. The threshold value most likely corresponds to the rupture strain of the surface oxide film; limited data suggest that the threshold strain is between 0.32 and 0.36%.

The effects of environment on fatigue life occur primarily during the tensile-loading cycle, and at strain levels greater than the threshold value required to rupture the surface oxide film. Consequently, loading and environmental conditions, e.g., strain rate, temperature, and DO level, in excess of the oxide rupture strain during the tensile-loading cycle, are important parameters for environmentally assisted reduction of fatigue life of these steels. Unlike ferritic steels, where environmental effects are greater in high-DO environments, environmental effects on fatigue life of austenitic stainless steels are more pronounced in low- than in high-DO water. The reduction in life is greater by a factor of ≈2 in simulated PWR environment, i.e., <0.01 ppm DO, than in high-DO water, i.e., ≥0.1 ppm DO. Existing data are inadequate to establish the functional form for the dependence of fatigue life on DO content. Recent data indicate that conductivity of water is important for environmental effects on fatigue life in high-DO water. The fatigue lives of cast SSs are approximately the same in both high- and low-DO water and are comparable to those observed for wrought SSs in low-DO water.

The fatigue lives of austenitic SSs decrease with decreasing strain rate; the effect is greater in a low-DO PWR environment than in high-DO water. The results indicate that the rate below which the effects of strain rate on fatigue life saturate may depend on both steel type and DO level. In low-DO PWR environments, saturation strain rate appears to be at ≈0.0004%/s for Type 304 SS and somewhat higher for Type 316 SS. The existing data are inadequate to establish the functional form for the dependence of life on temperature. Limited data indicate that environmental effects on fatigue life are significant at 250°C and minimal below 200°C.

Fatigue Design Curves in LWR Environments

Statistical models have been developed to predict fatigue lives of small smooth specimens of austenitic SSs as a function of material, loading, and environmental parameters. The functional form and bounding values of these parameters were based on experimental observations and data trends. The statistical models were obtained by minimizing the squared Cartesian distances from the data point to the predicted curve instead of minimizing the sum of the square of the residual errors for either strain amplitude or fatigue life. The models are recommended for predicted fatigue lives $\leq 10^6$ cycles. The results indicate that the ASME mean curve for SSs is not consistent with the experimental data at strain amplitudes <0.5% or stress amplitudes <975 MPa (<141 ksi); the ASME mean curve is non conservative.

The design fatigue curves for austenitic SSs in LWR environments were obtained by the procedure that has been used to develop the current ASME Code design fatigue curves, i.e., by adjusting the best-fit experimental curve for the effect of mean stress and setting margins of 20 on cycles and 2 on strain to account for the uncertainties in life that are associated with material and loading conditions. However, because the margin on strain for the current ASME Code design fatigue curve is closer to 1.5 than 2, a factor of 1.5 was used in developing the design fatigue curves for LWR environments. Data available in the literature were reviewed to evaluate the conservatism in the existing Code fatigue design curves. The use of a fatigue life correction factor to incorporate the effects of environment into the ASME Code fatigue evaluations is also discussed.

Acknowledgments

The author thanks J. L. Smith, W. F. Burke, T. M. Galvin, and J. Tezak for their contributions to the experimental effort and W. J. Shack and T. F. Kassner for helpful discussions. This work is sponsored by the Office of Nuclear Regulatory Research, U.S. Nuclear Regulatory Commission, under Job Code W6610-6; Program Manager: Dr. M. B. McNeil.

1 Introduction

Experience with operating nuclear power plants worldwide reveals that many failures, e.g., in piping components, nozzles, valves, and pumps, may be attributed to fatigue.[1-3] In most cases, these failures have been associated with thermal loading due to thermal stratification or thermal striping, or with mechanical loading due to vibration. Significant thermal loadings due to flow stratification were not included in the original design basis analysis. The effect of these loadings may also have been aggravated by corrosion effects due to exposure to high-temperature aqueous environments. Fatigue cracks have been observed in pressurizer surge lines in pressurized water reactors (PWRs) (NRC Bulletin No. 88-11), and in feedwater lines connected to nozzles of pressure vessels in boiling water reactors (BWRs) and steam generators in PWRs (NRC IE Bulletin, 79-13; NRC Information Notice 93-20). These cracks have been attributed to corrosion fatigue (NRC IE Bulletin, 79-13) or strain-induced corrosion cracking[4] caused by cyclic loading due to thermal stratification during startup (hot standby) and shutdown periods.

Cyclic loadings on a structural component occur because of changes in the mechanical and thermal loadings as the system goes from one set of pressure, temperature, moment, and force loading to any other load set. For each pair of load sets, an individual fatigue usage factor is determined by the ratio of the number of cycles anticipated during the lifetime of the component to the allowable cycles. Figures I-9.1 through I-9.6 of Appendix I to Section III of the ASME Boiler and Pressure Vessel Code[5] specifies fatigue design curves that define the allowable number of cycles as a function of applied stress amplitude. The cumulative usage factor (CUF) is the sum of the individual usage factors, and Section III of the ASME Code requires that the CUF at each location must not exceed 1.

The Code design fatigue curves were based on strain-controlled tests of small polished specimens at room temperature in air. In most studies, the fatigue life of a test specimen is defined as the number of cycles required for the tensile stress to drop 25% from its peak value. Such a drop corresponds to an ≈3-mm-deep crack. Consequently, fatigue life N represents the number of cycles required to initiate a crack ≈3 mm deep. The best-fit curves to the experimental data were expressed in terms of the Langer equation[6] of the form

$$\varepsilon_a = B(N)^{-b} + A, \qquad (1)$$

where A, B, and b are parameters of the model. Equation 1 may be written in terms of stress amplitude S_a instead of strain amplitude ε_a, in which case stress amplitude is the product of strain amplitude and elastic modulus, i.e., $S_a = E_a \varepsilon$ The design fatigue curves were obtained by decreasing the best-fit curves by a factor of 2 on stress or 20 on cycles, whichever was more conservative, at each point on the best-fit curve. As described in the ASME Section-III criteria document, these factors were intended to account for the differences and uncertainties in relating the fatigue lives of laboratory test specimens to those of actual reactor components. The factor of 20 on cycles is the product of three separate subfactors: 2 for scatter of data (minimum to mean), 2.5 for size effects, and 4 for surface finish, atmosphere, etc. "Atmosphere" was intended to reflect the effects of an industrial environment rather than the controlled environment of a laboratory. The factors of 2 and 20 are not safety margins but rather conversion factors that must be applied to the experimental data to obtain reasonable

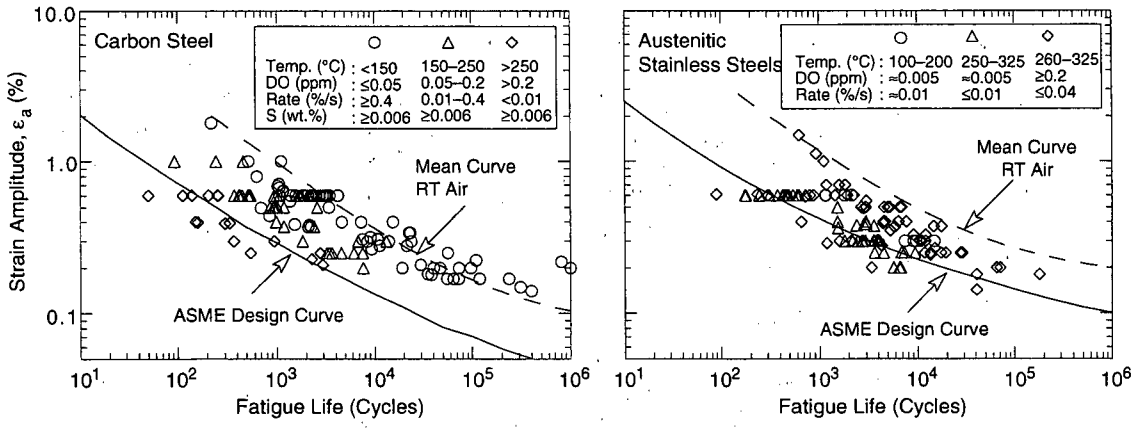

Figure 1. Fatigue S-N data for CSs and austenitic SSs in water (RT = room temperature)

estimates of the lives of actual reactor components. In a benign environment, some fraction of the factors actually represents a safety margin.

Subsection NB-3121 of Section III of the Code states that the data on which the fatigue design curves (Figs. I-9.1 through I-9.6) are based did not include tests in the presence of corrosive environments that might accelerate fatigue failure. Article B-2131 in Appendix B to Section III states that the owner's design specifications should provide information about any reduction to fatigue design curves that is required because of environmental conditions. Recent fatigue strain-vs.-life (S-N) data illustrate potentially significant effects of light water reactor (LWR) coolant environments on the fatigue resistance of carbon steels (CSs) and low-alloy steels (LASs),[7-20] as well as of austenitic stainless steels (SSs),[21-31] (Fig. 1). Under certain conditions of loading and environment, fatigue lives of CSs can be a factor of 70 lower in the environment than in air.[10,17-20] Therefore, the margins in the ASME Code may be less conservative than originally intended.

A program is being conducted at Argonne National Laboratory (ANL) to develop data and models for predicting the effects of environment on fatigue design curves of pressure vessel and piping steels and to assess the additivity of fatigue damage under load histories typical of LWR components. Fatigue tests are being conducted to establish the effects of various loading and environmental variables on the fatigue S-N behavior of pressure boundary steels. Interim design fatigue curves that address environmental effects on fatigue life of carbon and low-alloy steels and austenitic SSs have been proposed; they are based on existing fatigue S-N data.[32] Statistical models have also been developed at ANL for estimating the effects of various material and loading conditions on the fatigue life of these materials.[33,34] Results of the statistical analysis have been used to estimate the probability of fatigue cracking in reactor components. The statistical models for carbon and low-alloy steels have recently been updated with a larger fatigue S-N data base.[18-20]

The interim design curve and statistical model for austenitic SSs were based on limited data. For example, nearly all of the data in water were obtained at high temperatures (280-320°C) and high levels of dissolved oxygen (DO) (0.2-8 ppm). The data were inadequate to define the loading and environmental conditions that can decrease fatigue life of austenitic SSs. The threshold for strain amplitude above which environment can decrease fatigue life, and the value of strain rate below which environmental effects saturate, were based on the data for carbon and low-alloy steels. Fatigue lives in LWR environments were assumed to be independent of temperature. Furthermore, although the proposed interim fatigue design curve[33,34] for austenitic SSs was based on data

obtained in high-DO water, the curve was recommended for use at all oxygen levels until additional data became available, on the assumption that this was a conservative estimate of the likely effect of DO. Recent experimental results indicate that this assumption is not true.[29-31] Also, the effects of LWR environments on the fatigue lives of cast SSs have not been addressed. Recent test results and a larger fatigue S-N data base have led to the update of statistical models that were developed earlier for estimating the fatigue lives of austenitic SSs in LWR environments.[31]

This report summarizes available data on the effects of various material and loading variables, such as steel type, DO level, strain range, and strain rate, on the fatigue lives of wrought and cast austenitic SSs. The data have been analyzed to identify key parameters that influence fatigue life and define the threshold and saturation values of these parameters. The updated statistical models for estimating the fatigue lives of austenitic SSs in LWR environments are presented. The significance of the effect of environment on the current Code design curve is evaluated.

2 Experimental

Fatigue tests have been conducted on Types 316NG and 304 SS and two heats of CF-8M cast SS to establish the effects of LWR coolant environments on fatigue lives of these steels. The chemical composition of the steels is given in Table 1. For the CF-8M steels, fatigue specimens were obtained from material that was thermally aged for 10,000 h at 400°C; Heat 74 was tested both in the unaged and aged condition. Smooth cylindrical specimens with 9.5-mm diameter and 19-mm gauge length were used for the fatigue tests (Fig. 2). A 1-μm surface finish in the axial direction on the specimen gauge length to prevent circumferential scratches that might act as sites for crack initiation.

Table 1. Composition (in wt.%) of wrought and cast SSs used for fatigue tests

Material	Heat	Source	C	P	S	Si	Cr	Ni	Mn	Mo	Cu	N
Type 316NG[a]	D432804	Vendor	0.011	0.020	0.001	0.52	17.55	13.00	1.76	2.49	0.10	0.108
		ANL	0.013	0.020	0.002	0.49	17.54	13.69	1.69	2.45	0.10	0.105
Type 304[b]	30956	Vendor	0.060	0.019	0.007	0.48	18.99	8.00	1.54	0.44	-	0.100
CF-8M [c]	74	ANL	0.064	-	-	0.73	19.11	9.03	0.54	2.51	-	0.048
CF-8M [d]	75	ANL	0.065	-	-	0.67	20.86	9.12	0.53	2.58	-	0.052

[a]ASME SA312 seamless stainless steel pipe (hot-finished), 610-mm O.D. and 30.9-mm wall, fabricated by Sumitomo Metal Industries, Ltd. Solution-annealed at 1038-1093°C for 0.5 h and water-quenched.
[b]Solution-annealed at 1050°C for 0.5 h.
[c]Solutionannealed 1065-1120°C and waterquenched, measured ferrite content 18%.
[d]Solutionannealed 1065-1120°C and waterquenched, measured ferrite content 28%.

Tests in water were conducted in a small autoclave with an annular volume of 12 mL; see Fig. 3. The once-through system consists of a 132-L supply tank, Pulsafeeder™ pump, heat exchanger, preheater, and autoclave. Water is circulated at a rate of ≈10 mL/min and a system pressure of 9 MPa. The autoclave is constructed of Type 316 SS and contains a titanium liner. The supply tank and most of the low-temperature piping are Type 304 SS;

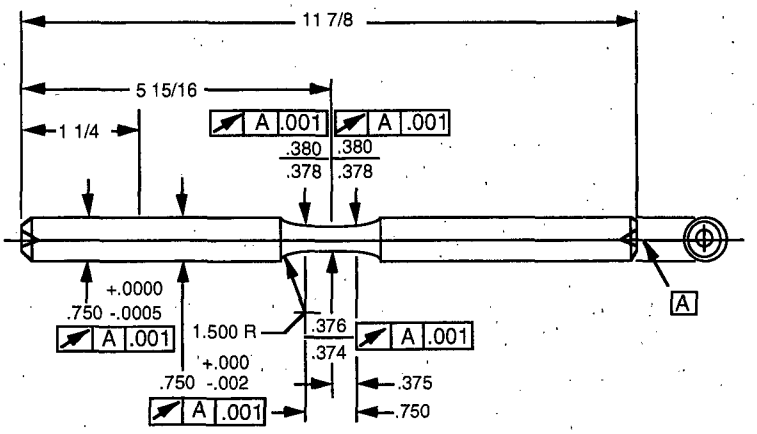

Figure 2. Configuration of fatigue test specimen (all dimensions in inches)

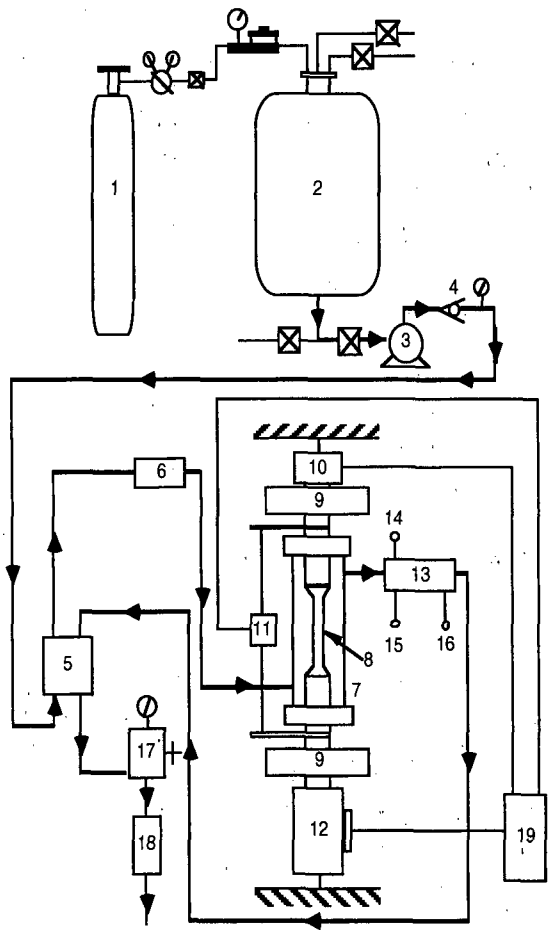

1. Cover-gas supply tank
2. Water supply tank
3. Pulsafeeder high-pressure pump
4. Check valve
5. Heat exchanger
6. Preheat exchanger
7. Pipe autoclave
8. Fatigue test specimen
9. MTS hydraulic collet grips
10. MTS load cell
11. Displacement LVDT
12. MTS hydraulic actuator
13. ECP cell
14. Platinum electrode
15. Specimen electrode
16. Reference electrode
17. Mity Mite™ back-pressure regulator
18. Orbisphere dissolved-oxygen meter
19. MTS electrohydraulic controls

Figure 3. Schematic diagram of autoclave system for fatigue tests in water environment

titanium tubing is used in the heat exchanger and for connections to the autoclave and electrochemical potential (ECP) cell. An Orbisphere meter and CHEMetrics™ ampules were used to measure the DO concentrations in the supply and effluent water. The redox and open-circuit

corrosion potentials were monitored at the autoclave outlet by measuring the ECPs of platinum and an electrode of the test material, respectively, against a 0.1-M KCl/AgCl/Ag external (cold) reference electrode. The measured ECPs, $E_{(meas)}$ (mV), were converted to the standard hydrogen electrode (SHE) scale, $E_{(SHE)}$ (mV), by the polynomial expression[35]

$$E_{(SHE)} = E_{(meas)} + 286.637 - 1.0032(\Delta T) + 1.7447\times10^{-4}(\Delta T)^2 - 3.03004\times10^{-6}(\Delta T)^3, \quad (2)$$

where ΔT (°C) is the test temperature of the salt bridge in the reference electrode minus the ambient temperature. The test facility was later modified from a once-through system to a recirculating system. For fatigue tests in high-DO environments, an ion-exchange filter was added to the return line to maintain the high resistivity of the water. Also, a filter was installed in the cover-gas line to eliminate possible contamination. A similar recirculating system was used for fatigue tests in simulated low-DO PWR environments, except that the ECP cell was bypassed during recirculation and the ion-exchange filter in the return line from the autoclave to the feedwater supply tank was excluded.

After an initial transition period, when an oxide film develops on the fatigue sample, the DO level and ECP remain constant during the fatigue tests in either the once-through or recirculating water system. Although the difference between the DO levels in the feedwater and effluent water is >0.1 ppm, the difference between the DO levels at the inlet and outlet of the autoclave is ≈0.02 ppm.

The DO level in the water was established by bubbling nitrogen that contains 1-2% oxygen through deionized water in the supply tank. The deionized water was prepared by passing purified water through a set of filters that comprise a carbon filter, an Organex-Q filter, two ion exchangers, and a 0.2-mm capsule filter. Water samples were taken periodically to measure pH, resistivity, and DO concentration. When the desired concentration of DO was attained, the nitrogen/oxygen gas mixture in the supply tank was maintained at a 20-kPa overpressure. After an initial transition period during which an oxide film develops on the fatigue specimen, the DO level and the ECP in the effluent water remained constant during the test. Test conditions are described in terms of the DO in effluent water.

Simulated PWR water was obtained by dissolving boric acid and lithium hydroxide in 20 L of deionized water before adding the solution to the supply tank. The DO in the deionized water was reduced to <10 ppb by bubbling nitrogen through the water. A vacuum was drawn on the tank cover gas to speed deoxygenation. After the DO was reduced to the desired level, a 34-kPa overpressure of hydrogen was maintained to provide ≈2 ppm dissolved hydrogen (or ≈23 cm^3/kg) in the feedwater.

All tests were conducted at 288°C, with fully reversed axial loading (i.e., R = -1) and a triangular or sawtooth waveform. The tests in water were performed under stroke control, wherein the specimen strain was controlled between two locations outside the autoclave. Tests in air were performed under strain control with an axial extensometer; the stroke at the location used to control the water tests was also recorded. Information from the air tests was

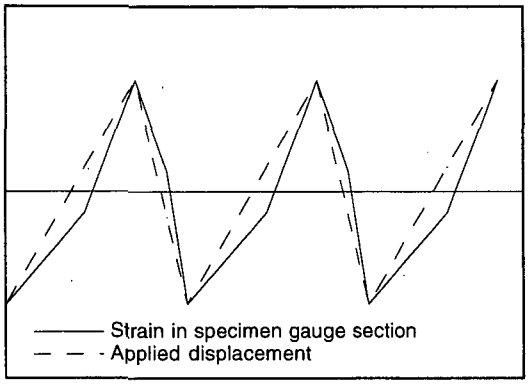

Figure 4.
Total applied displacement (dashed line) and strain in specimen gauge section (solid line) during stroke-controlled tests with a sawtooth waveform

used to determine the stroke required to maintain constant strain in the specimen gauge. To account for cyclic hardening of the material, the stroke that was needed to maintain constant strain was gradually increased during the test. Figure 4 shows the actual strain in the specimen gauge section during a stroke-controlled test with a sawtooth waveform. The fraction of applied displacement that goes to the specimen gauge section is not constant but varies with loading strain. Consequently, the loading rate also varies during the fatigue cycle; it is lower than the applied strain rate at strain levels below the elastic limit and higher at larger strains.

The strain-controlled fatigue tests in air on cast SS specimens showed strain ratcheting in compression. Although strain in the gauge section of the specimens remained constant, overall length of the specimens decreased during the test. The results indicated that strain ratcheting was caused by differences in the strain hardening behavior of these steels in tension and compression. For both heats of CF-8M steel, strain hardening was greater in compression than in tension. The result of this difference was a mean compressive stress, which caused strain ratcheting of the shoulder region of the specimens. To prevent strain racheting, tests in water were conducted under stroke control with a small tensile strain.

To date, the fatigue results obtained on Types 316NG and 304 SS and two heats of CF-8M cast SS in air and LWR environments are summarized in Tables 2-4. The fatigue life N_{25} is defined as the number of cycles for tensile stress to drop 25% from its peak value. Fatigue lives defined by other criteria, e.g., a 50% decrease in peak tensile stress or complete failure, may be converted to an N_{25} value by solving the equation

$$N_{25} = N_X / (0.947 + 0.00212\,X), \qquad (3)$$

where X is the failure criteria, i.e., 25, 50, or 100% decrease in peak tensile stress. For tests in water, the DO level and ECPs of platinum and SS electrodes represent the values in the effluent, and the pH and conductivity of water were both measured in the supply tank.

Table 2. Fatigue test results for Type 316NG austenitic SS

Test No.	Env.[a]	DO[b] (ppb)	pH at RT	Conductivity[c] (µS/cm)	ECP Pt mV (SHE)	ECP Steel mV (SHE)	Ten. Rate (%/s)	Comp. Rate (%/s)	Stress Range (MPa)	Strain Range (%)	Life N_{25} (Cycles)
Room Temp.											
1394	Air	–	–	–	–	–	5.0E-1	5.0E-1	694.7	1.51	4,649
1391	Air	–	–	–	–	–	5.0E-1	5.0E-1	554.8	1.00	13,561
1390	Air	–	–	–	–	–	5.0E-1	5.0E-1	518.1	0.75	25,736
1396	Air	–	–	–	–	–	5.0E-1	5.0E-1	506.7	0.76	30,000
1420	Air	–	–	–	–	–	4.9E-1	4.9E-1	495.3	0.49	54,249
1392	Air	–	–	–	–	–	5.0E-1	5.0E-1	475.9	0.51	60,741
1393	Air	–	–	–	–	–	5.0E-1	5.0E-1	464.7	0.41	127,386
1395	Air	–	–	–	–	–	5.0E-1	5.0E-1	456.7	0.35	183,979
1397	Air	–	–	–	–	–	5.0E-1	5.0E-1	446.0	0.30	347,991
1398	Air	–	–	–	–	–	5.0E-1	5.0E-1	436.7	0.27	666,000
1399	Air	–	–	–	–	–	5.0E-1	5.0E-1	431.8	0.25	>1,900,000
1400	Air	–	–	–	–	–	5.0E-1	5.0E-1	427.4	0.25	1,775,000
288°C											
1408	Air	–	–	–	–	–	5.0E-1	5.0E-1	416.6	0.76	21,548
1790	Air	–	–	–	–	–	5.0E-3	5.0E-1	452.8	0.75	16,765
1409	Air	–	–	–	–	–	5.0E-1	5.0E-1	377.2	0.50	53,144
1410	Air	–	–	–	–	–	5.0E-1	5.0E-1	377.6	0.50	51,194
1792	Air						5.0E-3	5.0E-1	413.4	0.51	35,710
1407	Air	–	–	–	–	–	5.0E-1	5.0E-1	364.4	0.40	82,691
1430	Air	–	–	–	–	–	5.0E-1	5.0E-1	348.3	0.30	168,852
1435	Air	–	–	–	–	–	5.0E-1	5.0E-1	342.0	0.25	314,352
1480	Air	–	–	–	–	–	4.9E-1	4.9E-1	340.1	0.25	319,308
1485	Air	–	–	–	–	–	5.1E-1	5.1E-1	340.4	0.25	369,206
320°C											
1405	Air	–	–	–	–	–	5.0E-1	5.0E-1	426.0	0.75	20,425
1404	Air	–	–	–	–	–	5.0E-1	5.0E-1	387.4	0.50	47,011
1406	Air	–	–	–	–	–	5.0E-1	5.0E-1	371.6	0.40	82,691
288°C											
1796	PWR	5	6.4	20.20	-677	-673	5.0E-1	5.0E-1	403.6	0.80	12,500
1812	PWR	2	6.5	20.00	-689	-686	5.0E-2	5.0E-1	413.9	0.80	6,375
1791	PWR	4	6.5	19.23	-697	-697	5.0E-3	5.0E-1	441.9	0.77	3,040
1793	PWR	4	6.4	19.23	-699	-700	5.0E-3	5.0E-1	434.3	0.80	3,020
1794	PWR	4	6.4	20.00	-690	-689	5.0E-3	5.0E-1	390.9	0.50	7,370
1814	PWR	1	6.5	20.00	-694	-691	5.0E-2	5.0E-1	348.7	0.29	33,200
1426	Hi DO	>200	–	–	–	–	8.0E-1	8.0E-1	405.1	0.80	12,069
1427	Hi DO	>200	–	–	–	–	8.2E-2	8.2E-2	421.7	0.82	6,679
1428	Hi DO	>200	–	–	–	–	7.4E-3	7.4E-3	441.4	0.74	5,897
1797	Hi DO	750	5.9	0.076	199	64	5.0E-3	5.0E-1	437.3	0.78	4,520
1414	Hi DO	>200	–	–	–	–	5.0E-1	5.0E-1	375.3	0.50	26,230
1418	Hi DO	>200	–	–	–	–	5.0E-1	5.0E-1	375.5	0.50	25,714
1423	Hi DO	>200	–	–	–	–	5.0E-2	5.0E-2	378.8	0.50	17,812
1425	Hi DO	>200	–	–	–	–	4.9E-3	4.9E-3	393.2	0.49	13,684
1431	Hi DO	>200	–	–	–	–	2.9E-1	2.9E-1	356.5	0.29	116,754
1434	Hi DO	>200	–	–	–	–	2.9E-2	2.9E-2	350.0	0.29	40,643
1436	Hi DO	>200	–	–	–	–	2.5E-2	2.5E-2	354.0	0.25	>1,719,851
1512	Hi DO	>200	–	–	–	–	2.4E-1	2.4E-1	361.2	0.24	2,633,954

[a]PWR = simulated PWR water containing 2 ppm lithium and 1000 ppm boron.
[b]DO and ECPs measured in effluent.
[c]Conductivity of water measured in feedwater supply tank.

Table 3. Fatigue test results for Type 304 austenitic SS at 288°C

Test No.	Env.[a]	DO[b] (ppb)	pH at RT	Conductivity[c] (μS/cm)	ECP Pt mV (SHE)	ECP Steel mV (SHE)	Ten. Rate (%/s)	Comp. Rate (%/s)	Stress Range (MPa)	Strain Range (%)	Life N_{25} (Cycles)
1801	Air	–	–	–	–	–	4.0E-1	4.0E-1	419.2	0.76	24,500
1805	Air	–	–	–	–	–	4.0E-3	4.0E-1	467.9	0.76	14,410
1804	Air	–	–	–	–	–	4.0E-1	4.0E-1	382.8	0.51	61,680
1817	Air	–	–	–	–	–	4.0E-3	4.0E-1	421.7	0.51	42,180
1825	Air	–	–	–	–	–	4.0E-2	4.0E-1	394.4	0.30	>625,860
1846	Air	–	–	–	–	–	4.0E-2	4.0E-1	396.4	0.32	>316,000
1806	PWR	4	6.0	18.87	-678	-675	4.0E-1	4.0E-1	428.9	0.73	11,500
1810	PWR	5	6.4	18.89	-684	-681	4.0E-2	4.0E-1	447.6	0.77	5,800
1808	PWR	4	6.4	18.87	-689	-686	4.0E-3	4.0E-1	468.3	0.77	2,850
1821	PWR	2	6.5	22.22	-696	-693	4.0E-3	4.0E-1	474.3	0.76	2,420
1829	PWR	2	6.5	18.18	-701	-701	4.0E-4	4.0E-1	493.6	0.73	1,560
1834	PWR	2	6.5	18.18	-707	-708	9.0E-5	4.0E-1	535.9	0.69	1,415
1807	PWR	4	6.5	18.87	-681	-678	4.0E-1	4.0E-1	374.6	0.51	25,900
1823	PWR	3	6.6	23.06	-697	-695	4.0E-3	4.0E-1	408.2	0.51	6,900
1826	PWR	2	6.5	18.76	-707	-706	1.0E-2	4.0E-1	375.8	0.29	>89,860
1847	PWR	5	6.5	18.87	-696	-692	1.0E-2	4.0E-1	388.9	0.32	>165,300
1852	Hi DO	790	6.1	0.061	239	153	4.0E-1	4.0E-1	429.1	0.74	10,800
1827	Hi DO	850	6.0	0.086	258	80	4.0E-3	4.0E-1	475.8	0.75	3,650
1845	Hi DO	870	6.0	0.063	274	185	4.0E-4	4.0E-1	488.7	0.71	>7,310

[a]PWR = simulated PWR water containing 2 ppm lithium and 1000 ppm boron.
[b]DO and ECPs measured in effluent.
[c]Conductivity of water measured in feedwater supply tank.

Table 4. Fatigue test results for CF-8M cast SSs at 288°C

Test No.	Env.[a]	DO[b] (ppb)	pH at RT	Conductivity[c] (μS/cm)	ECP Pt mV (SHE)	ECP Steel mV (SHE)	Ten. Rate (%/s)	Comp. Rate (%/s)	Stress Range (MPa)	Strain Range (%)	Life N_{25} (Cycles)
1831	Air	–	–	–	–	–	4.0E-1	4.0E-1	429.7	0.76	26,500
1832	Air	–	–	–	–	–	4.0E-3	4.0E-1	534.0	0.76	9,050
1848	Air	–	–	–	–	–	4.0E-1	4.0E-1	440.7	0.76	17,900
1850	PWR	5	6.5	17.241	-691	-689	4.0E-3	4.0E-1	419.5	0.76	10,700
1854	PWR	2	6.5	18.692	-695	-691	4.0E-2	4.0E-1	448.4	0.75	4,720
1839	Air	–	–	–	–	–	4.0E-1	4.0E-1	474.2	0.76	15,290
1840	Air	–	–	–	–	–	4.0E-3	4.0E-1	534.8	0.75	19,800
1851	PWR	4	6.5	18.182	-696	-695	4.0E-1	4.0E-1	482.1	0.75	6,420
1844	PWR	2	6.5	18.182	-667	-680	4.0E-3	4.0E-1	527.7	0.72	2,180
1842	Hi DO	820	6.1	0.063	271	145	4.0E-3	4.0E-1	508.5	0.75	1,375
1835	Air	–	–	–	–	–	4.0E-3	4.0E-1	631.2	0.76	7,200
1843	PWR	2	6.5	18.182	-568	-576	4.0E-3	4.0E-1	625.3	0.80	1,464
1838	Hi DO	870	6.5	0.061	261	113	4.0E-3	4.0E-1	636.1	0.78	1,320

[a]PWR = simulated PWR water that contained 2 ppm lithium and 1000 ppm boron.
[b]DO and ECPs measured in effluent.
[c]Conductivity of water measured in feedwater supply tank.

3 Overview of Fatigue S–N Data

The relevant fatigue S–N data for austenitic SSs in air include the data compiled by Jaske and O'Donnell[36] for developing fatigue design criteria for pressure vessel alloys, the JNUFAD* data base from Japan, and the results of Conway et al.[37] and Keller.[38] In water, the existing fatigue S–N data include the tests performed by General Electric Co. (GE) in a test loop at the Dresden 1 reactor,[39] the JNUFAD data base, studies at Mitshubishi Heavy Industries, Ltd., (MHI),[21–24] Ishikawajima-Harima Heavy Industries Co., (IHI),[25] and Hitachi[26,27] in Japan, and the present work at ANL.[28–31] The data base for austenitic SSs is composed of 500 tests in air (240 tests on 26 heats of Type 304 SS, 170 tests on 15 heats of Type 316 SS, and 90 tests on 4 heats of Type 316 NG) and 290 tests in water (135 tests on 9 heats of Type 304 SS, 55 tests on 3 heats of Type 316 SS, and 100 tests on 4 heats of Type 316NG). Nearly 60% of the tests in air were conducted at room temperature, 20% at 250–325°C, and 20% at 350–450°C. Nearly 90% of the tests in water were conducted at temperatures between 260 and 325°C; the remainder were at lower temperatures. The data on Type 316NG in water have been obtained primarily at DO levels ≥0.2 ppm and those on Type 316 SS, at ≤0.005 ppm DO; half of the tests on Type 304 SS are at low-DO and the remaining at high-DO levels.

3.1 Air Environment

The existing fatigue S–N data, both domestic and from abroad, indicate that the fatigue lives of Types 304 and 316 SS are comparable; those of Type 316NG are superior. Fatigue life in air is independent of temperature in the range from room temperature to 427°C (Fig. 5). The three curves in Fig. 5 are based on the current ASME mean curve, the best-fit curve developed by Jaske and O'Donnell,[36] and the updated statistical model that is discussed later in this report. The results indicate that the ASME mean curve is not consistent with the existing fatigue S–N data for austenitic SSs. At strain amplitudes <0.5%, the mean curve predicts significantly longer fatigue lives than those observed experimentally. The results also indicate that at temperatures above 260°C, the fatigue life of austenitic SSs may decrease with decreasing strain rate (Fig. 6). The effect of strain rate on fatigue life seems to be significant at 400–430°C. However, other studies[40] have shown no effect of strain rate on the fatigue life of Type 316 SS at 0.4–0.008%/s strain rates and temperatures up to 450°C.

During cyclic loading, austenitic SSs exhibit rapid hardening during the first 50–100 cycles; the extent of hardening increases with increasing strain amplitude and decreasing temperature and strain rate.[27,28,41] The cyclic strain hardening of Type 316NG SS tested in air at room temperature and 288°C is shown in Fig. 7. The initial hardening is followed by softening and a saturation stage at 288°C, and by continuous softening at room temperature.

The cyclic stress-vs.-strain curves for Types 304, 316, and 316NG SS at room temperature and 288°C are shown in Fig. 8; cyclic stress corresponds to the value at half life and at a strain rate of 0.4%/s. For the various steels, cyclic stresses increase in magnitude in the following order: Types 316NG, 304, and 316. At room temperature, the strain amplitude ε_a(%) for Type 316 SS can be expressed in terms of the cyclic stress amplitude σ_a(MPa) by the equation

---

* M. Higuchi, Ishikawajima-Harima Heavy Industries Co., Japan, private communication to M. Prager of the Pressure Vessel Research Council, 1992.

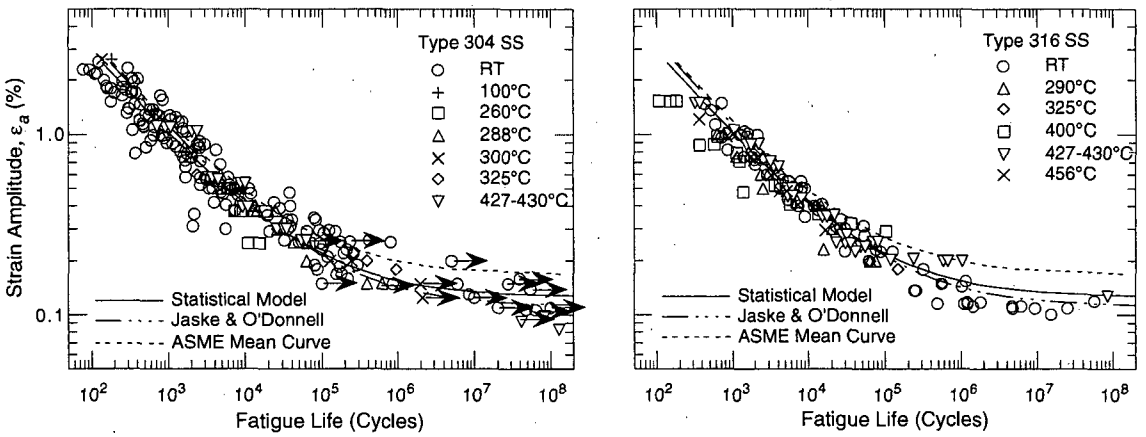

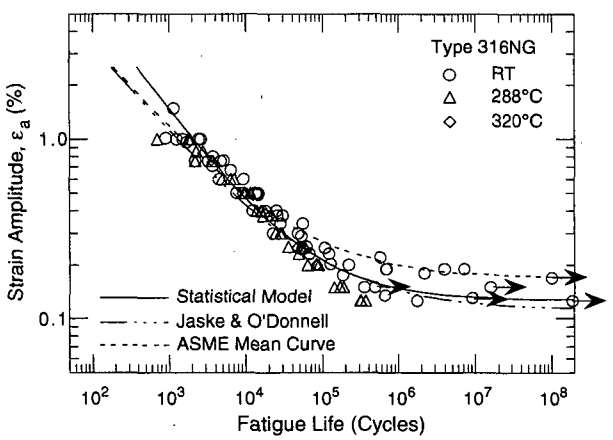

Figure 5.
Fatigue S-N behavior for Types 304, 316, and 316NG austenitic SSs in air at various temperatures

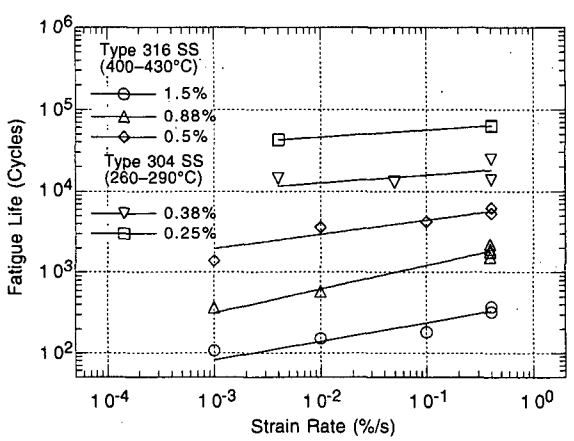

Figure 6.
Effect of strain rate on fatigue lives of austenitic SSs in air for various strain ranges

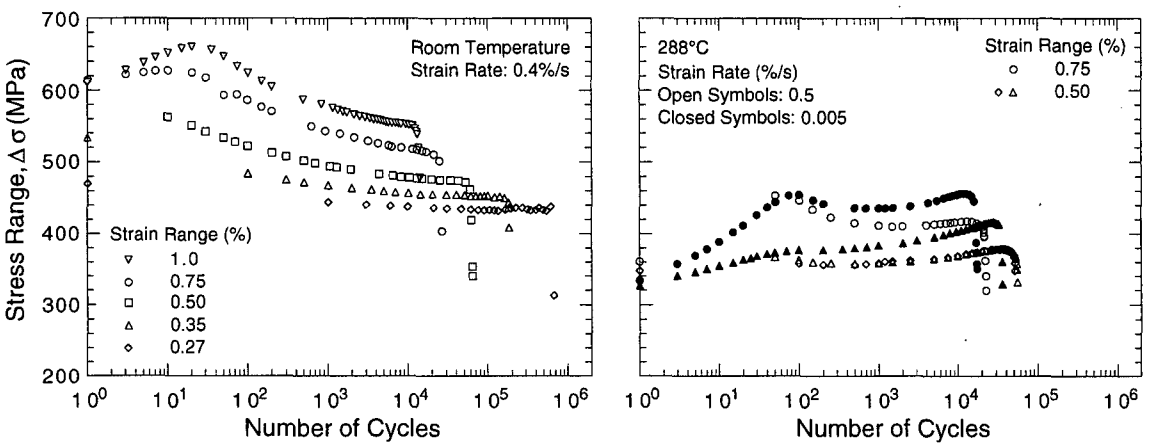

Figure 7. Effect of strain range on cyclic strain-hardening behavior of Type 316NG SS in air at room temperature and 288°C

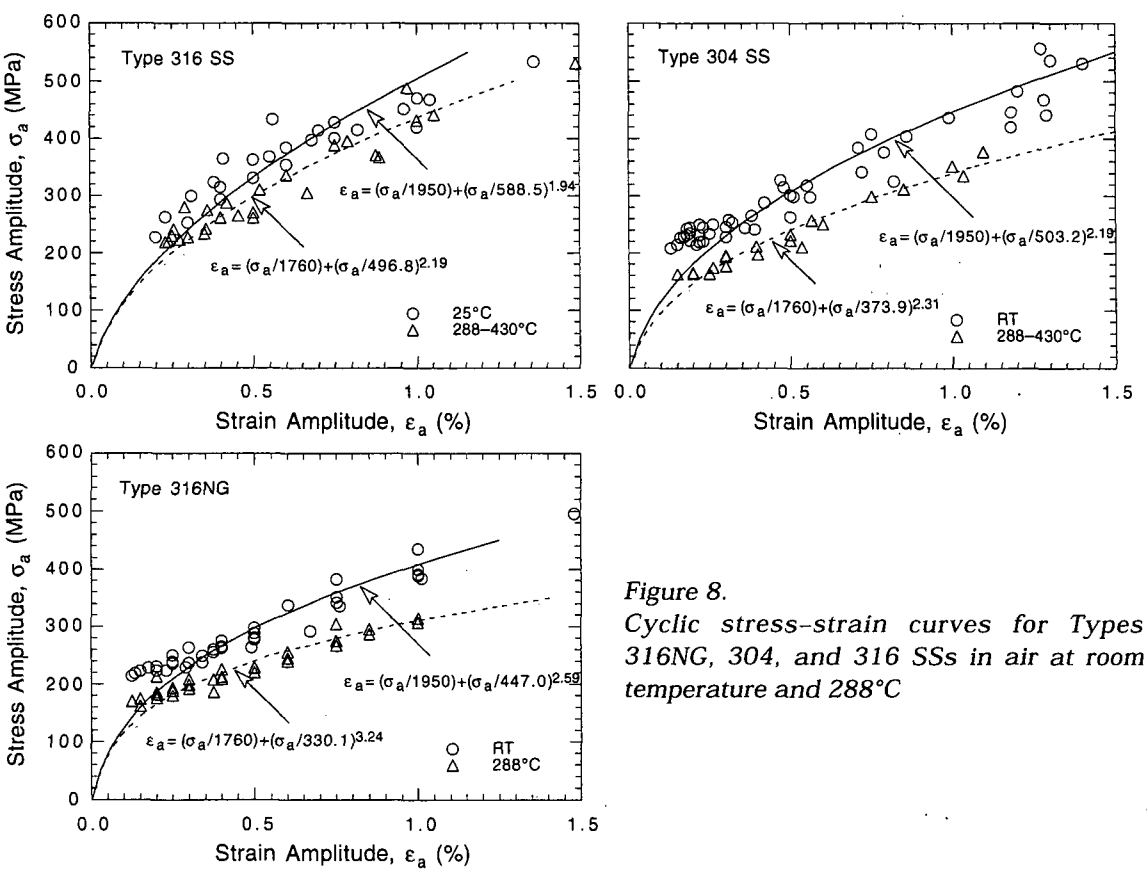

Figure 8.
Cyclic stress-strain curves for Types 316NG, 304, and 316 SSs in air at room temperature and 288°C

$$\varepsilon_a = \frac{\sigma_a}{1950} + \left(\frac{\sigma_a}{588.5}\right)^{1.94}, \tag{4a}$$

for Type 304 SS, by

$$\varepsilon_a = \frac{\sigma_a}{1950} + \left(\frac{\sigma_a}{503.2}\right)^{2.19}, \tag{4b}$$

and for Type 316NG, by

$$\varepsilon_a = \frac{\sigma_a}{1950} + \left(\frac{\sigma_a}{447.0}\right)^{2.59}. \tag{4c}$$

At 288–430°C, the cyclic stress-vs.-strain curve for Type 316 SS can be expressed by

$$\varepsilon_a = \frac{\sigma_a}{1760} + \left(\frac{\sigma_a}{496.8}\right)^{2.19}, \tag{4d}$$

for Type 304 SS, by

$$\varepsilon_a = \frac{\sigma_a}{1760} + \left(\frac{\sigma_a}{373.9}\right)^{2.31}, \tag{4e}$$

and for Type 316NG, by

$$\varepsilon_a = \frac{\sigma_a}{1760} + \left(\frac{\sigma_a}{330.1}\right)^{3.24}. \tag{4f}$$

3.2 LWR Environments

The fatigue S-N data indicate a significant decrease in fatigue life in LWR environments (Fig. 9). The reduction in life depends on strain rate, DO level in water, and temperature.[21-31] Also, environmental effects on fatigue life are comparable for all steels. To define the threshold values, the effects of various parameters on fatigue life are discussed below in greater detail.

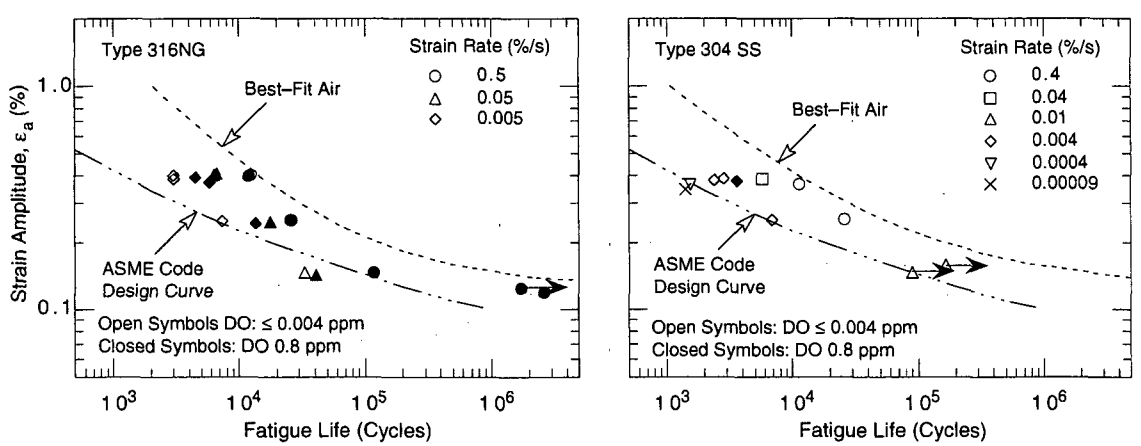

Figure 9. Fatigue strain amplitude-vs.-life data for Types 316NG and 304 SS in water at 288°C

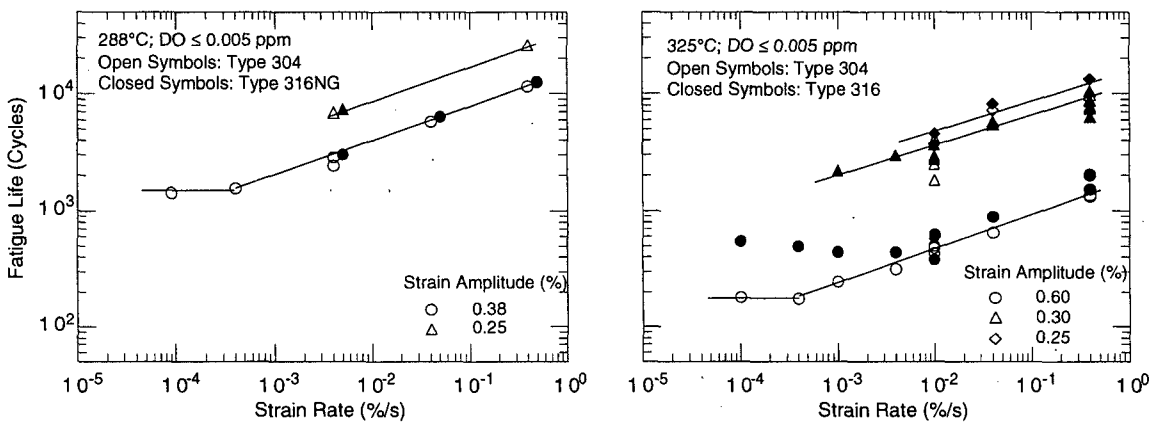

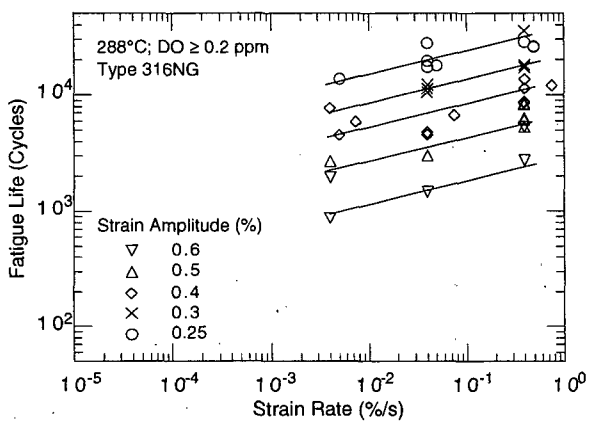

Figure 10.
Dependence of fatigue life of austenitic SSs on strain rate in low- and high-DO water

3.2.1 Strain Rate

A slow strain rate applied during the tensile-loading cycle (i.e., up-ramp with increasing strain) is primarily responsible for environmentally assisted reduction in fatigue life. Slow rates applied during both tensile- and compressive-loading cycles (i.e., up- and down-ramps) do not cause further decrease in fatigue life.[29-31] The fatigue lives of austenitic SSs in low- and high-DO water are plotted as a function of tensile strain rate in Fig. 10. At both low- and high-DO levels, fatigue lives decrease with decreasing strain rate. The effect of strain rate is greater in a low-DO PWR environment than in high-DO water. In a simulated PWR environment, a decrease in strain rate from 0.4 to 0.0004%/s decreases fatigue life by a factor of ≈10. The results indicate that the strain rate below which effects of strain rate on fatigue life saturate may depend on both steel type and DO level. In low-DO PWR environments, saturation strain rate appears to be at ≈0.0004%/s for Type 304 SS and somewhat higher for Type 316 SS (best estimate of ≈0.004%/s). Limited data suggest that the saturation strain rate is also higher in high- than in low-DO water.

3.2.2 Strain Amplitude

Nearly all of the existing fatigue S-N data have been obtained under loading histories with constant strain rate, temperature, and strain amplitude. Actual loading histories encountered

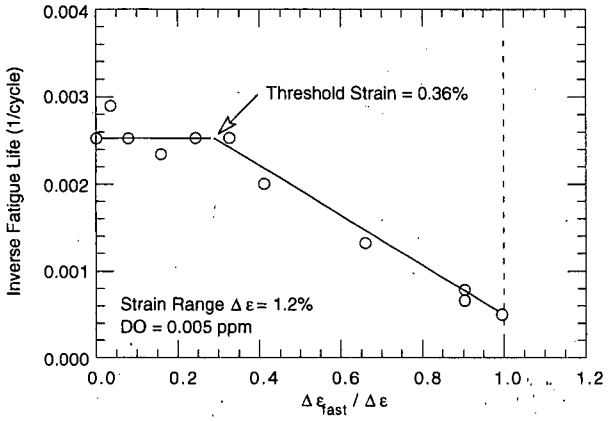

Figure 11.
Results of strain rate change tests on Type 316 SS in low-DO water at 325°C

during service of nuclear power plants are far more complex. Exploratory fatigue tests have been conducted with waveforms in which the slow strain rate is applied during only a fraction of the tensile loading cycle.[24] The results indicate that a minimum threshold strain is required to produce an environmentally assisted decrease in fatigue life of these steels. Figure 11 shows that, for a heat of Type 316 SS, the threshold strain in low-DO water at 325°C is ≈0.36%. During each cycle, relative damage due to slow strain rate is the same once the strain amplitude exceeds the threshold value.

Fatigue data from the present study indicate a threshold strain range of ≈0.32% for the ANL heat of Type 304 SS. For example, the test at 0.15% strain amplitude and 0.01%/s strain rate (as shown by a runoff triangle symbol in Fig. 9), failed after an additional 41,240 cycles when the strain amplitude was increased to 0.16%. Another test at 0.16% strain amplitude failed after an additional 50,700 cycles at 0.17% strain amplitude. The threshold strain most likely corresponds to rupture strain of the passive oxide film. These results are similar to those observed for carbon and low-alloy steels.[16-20]

3.2.3 Dissolved Oxygen

The results also indicate that environmental effects on the fatigue life of austenitic SSs differ from those on carbon and low-alloy steels; they are more pronounced in low-DO than in high-DO water.[18,19] At a strain rate of 0.004%/s, the reduction in fatigue life of Type 316NG (Fig. 10) is greater by a factor of ≈2 in a simulated PWR environment (<0.01 ppm DO) than in high-DO water (≥0.2 ppm DO). For carbon and low-alloy steels, environmental effects on fatigue life increase with increasing DO content above a minimum threshold value of 0.05 ppm; only a modest decrease in life is observed at DO levels <0.05 ppm.[11-13,16-20]

Existing data are inadequate to establish the functional form for the dependence of fatigue life of austenitic SSs on DO level. Recent test results indicate that the fatigue lives of austenitic SSs may depend on the conductivity of the water rather than on the DO content, e.g., fatigue life is longer at lower conductivity (<0.1 μS/cm). In the existing fatigue S-N data base, most of the tests in high-DO water have been performed at conductivities up to 0.2 μS/cm. Recent tests in high-DO water with conductivities <0.08 μS/cm show only a modest effect of environment on the fatigue lives of these steels. Tests are in progress to establish the effects of water chemistry on the fatigue lives of austenitic SSs.

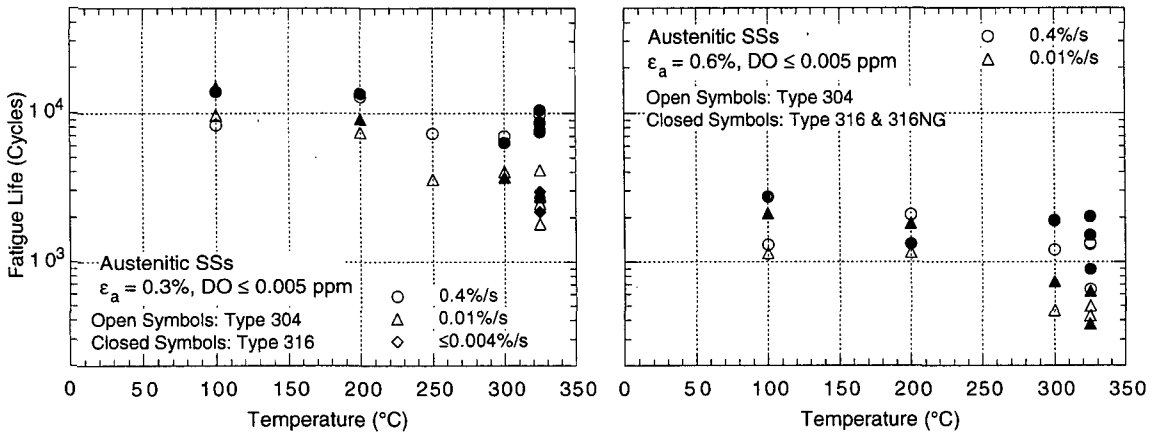

Figure 12. Change in fatigue lives of austenitic SSs in low-DO water with temperature

3.2.4 Temperature

The existing fatigue S-N data are inadequate to establish the functional form for the dependence of life on temperature. Limited data indicate that environmental effects on the fatigue lives of austenitic SSs are significant at temperatures above 250°C and are minimal at temperatures ≤200°C (Fig. 12). At 250-330°C, fatigue life appears to be relatively insensitive to changes in temperature.

As discussed in the previous section, actual loading histories encountered during service in nuclear power plants involve variable loading and environmental conditions, whereas the existing fatigue S-N data have been obtained under loading histories with constant strain rate, temperature, and strain amplitude. Fatigue tests have been conducted at MHI Japan on Type 316 SS under combined mechanical and thermal cycling.[24] Triangular waveforms were used for both strain and temperature cycling. Two sequences were selected for temperature cycling (Fig. 13): an in-phase sequence, in which temperature cycling was synchronized with mechanical strain cycling; and a sequence in which temperature and strain were out of phase, i.e., maximum temperature occurred at minimum strain level and vice-versa. Two temperature ranges, 100-325°C and 200-325°C, were selected for the tests.

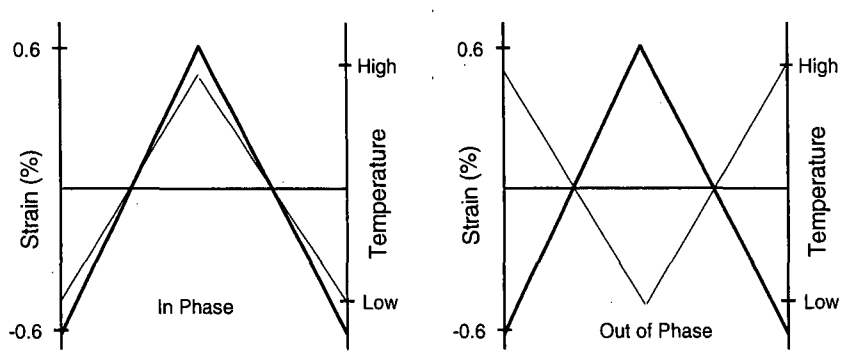

Figure 13. Waveforms for change in temperature during exploratory fatigue tests

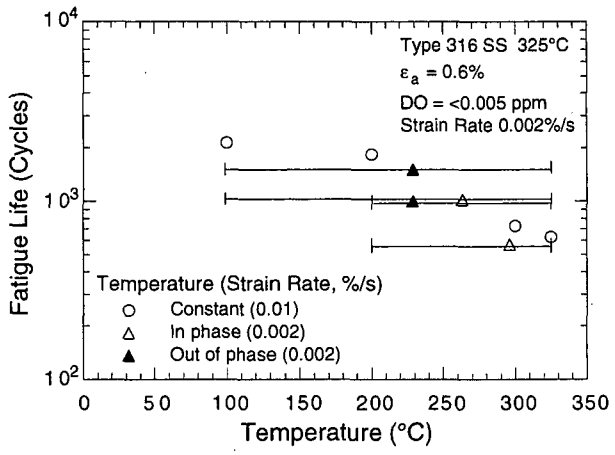

Figure 14.
Fatigue life of Type 316 SS under varying temperature, indicated by horizontal bars

The results are shown in Fig. 14, with the data obtained from tests at constant temperature. If we consider that the tensile-load cycle is primarily responsible for environmentally assisted reduction in fatigue life and that the applied strain and temperature must be above a minimum threshold value for environmental effects to occur, then, life should be longer for out-of-phase tests than for in-phase tests, because applied strains above the threshold strain occur at temperatures above 200°C for in-phase tests, whereas they occur at temperatures below 200°C for out-of-phase tests. An average temperature is used in Fig. 14 for the thermal cycling tests, i.e., the average of the temperature at peak strain and the temperature at threshold strain or 200°C (whichever is higher). The results from thermal cycling tests agree well with those from constant-temperature tests. The data suggest a linear decrease in life at temperatures above 200°C. Fatigue tests are in progress at 200-320°C to establish the temperature dependence of fatigue life in LWR environments.

3.3 Cast Stainless Steels

Available fatigue S-N data[23,31] indicate that in air, the fatigue lives of cast CF-8 and CF-8M SSs are similar to that of wrought austenitic SSs (Fig. 15). It is well known that the Charpy impact and fracture toughness properties of cast SSs are decreased significantly after thermal aging at temperatures between 300 and 450°C.[42,43] The cyclic-hardening behavior of cast SSs is also influenced by thermal aging (Fig. 16). At 288°C, cyclic stresses of steels aged for 10,000 h at 400°C are higher than those for unaged material or wrought SSs. Also, strain rate effects on cyclic stress are greater for aged than for unaged steel, i.e., cyclic stresses increase significantly with decreasing strain rate. However, existing data are inadequate to establish unequivocally the effect of thermal aging on the fatigue life of these steels. For example, thermal aging for 25,200 h at 465°C exerted no effect on the fatigue life of a CF-8M steel in air at 325°C,[24] whereas, in the present study, aging for 10,000 h at 400°C decreased the fatigue life of Heat 74 at 288°C, particularly in water (discussed later in this section). These differences are most likely caused by microstructural differences that arise from thermal aging temperature. Aging at 400°C results in spinodal decomposition of the ferrite to form Cr-rich regions that very effectively increase tensile strength, whereas, aging at 465°C for extended periods results in the formation of Cr-rich α' particles and over-aging.

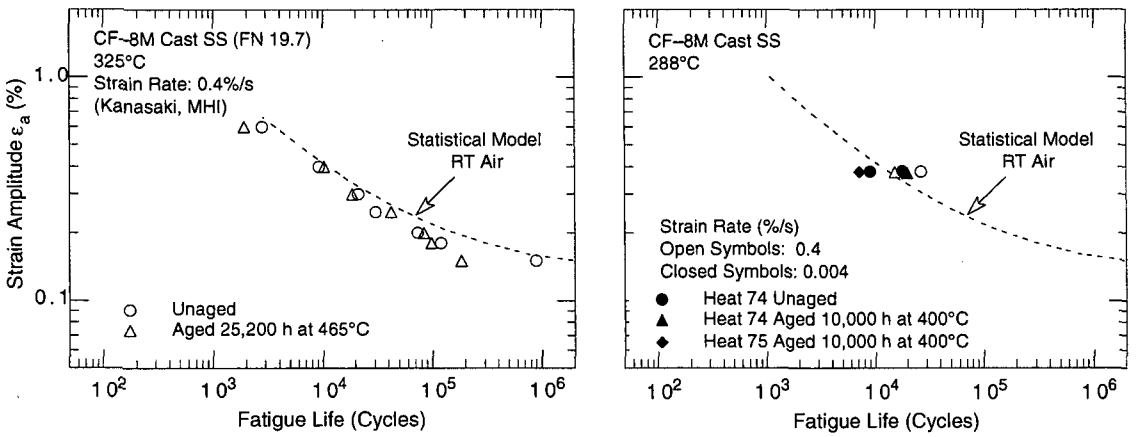

Figure 15. Fatigue strain amplitude-vs.-life data for CF-8M cast SSs in air

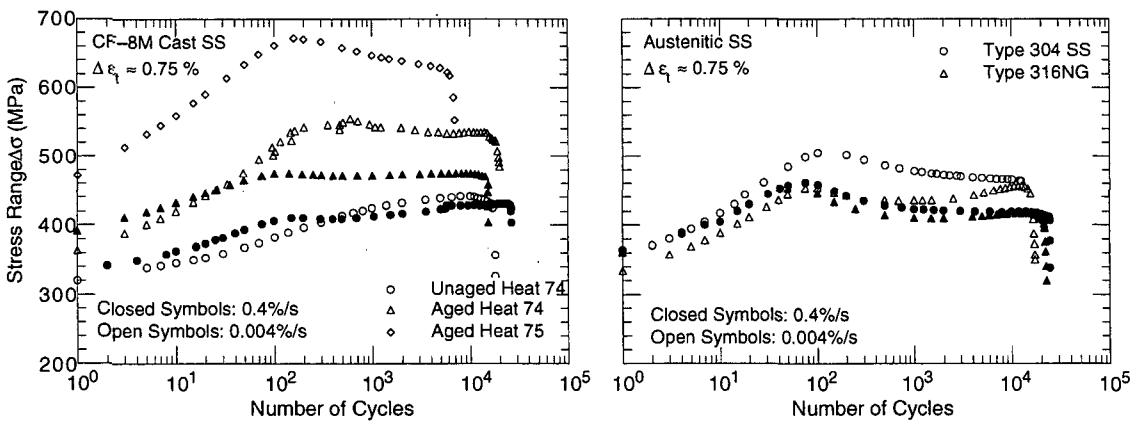

Figure 16. Effect of strain rate on cyclic-hardening behavior of wrought and cast SSs in air at 288°C

The existing fatigue S-N data[23,31] for cast SSs in LWR environments indicate that the fatigue lives of cast SSs are approximately the same in both high- or low-DO water and are comparable to those observed for wrought SSs in low-DO water (Fig. 17). The results also indicate that thermal aging decreases the fatigue lives of these steels. The reduction in life in LWR environments depends on strain rate (Fig. 18). The effects of strain rate are the same in low- and high-DO water. Existing data are inadequate to establish the saturation strain rate for cast SSs. For unaged material, environmental effects on life do not appear to saturate at strain rates as low as 0.00001%/s.[23] Also, the fatigue lives of these steels are relatively insensitive to changes in ferrite content in the range of 12-28%.[23]

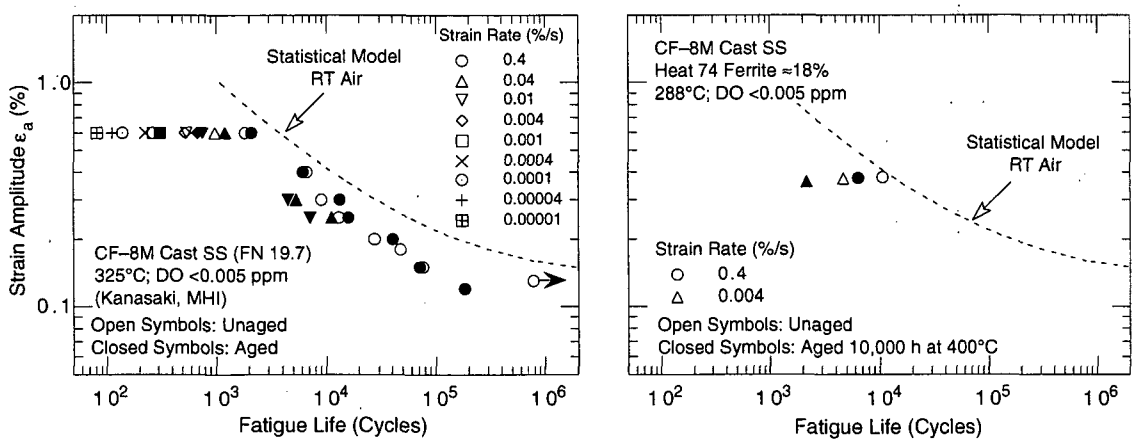

Figure 17. Fatigue strain amplitude-vs.-life data for CF-8M cast SSs in water

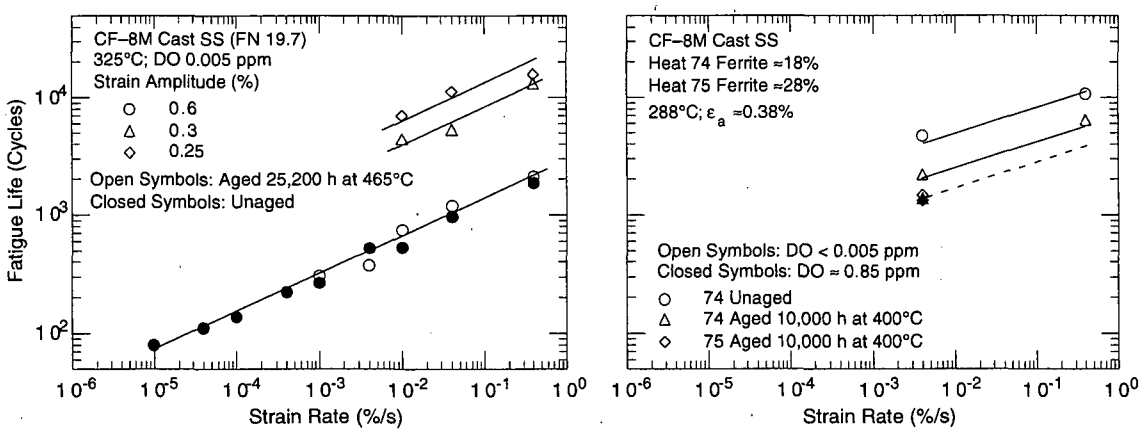

Figure 18. Dependence of fatigue lives of CF-8M cast SSs on strain rate in low-DO water at various strain amplitudes

4 Mechanism of Fatigue Crack Initiation

4.1 Formation of Engineering Cracks

The formation of surface cracks and their growth to an "engineering" size (3 mm deep) constitute the fatigue life of a material, which is represented by the fatigue S-N curves. Fatigue life has conventionally been divided into two stages: initiation, expressed as the cycles required to form microcracks on the surface; and propagation, expressed as cycles required to propagate the surface cracks to engineering size. During cyclic straining, microcracks form at surface irregularities/discontinuities either already in existence or produced by slip bands, grain boundaries, second-phase particles, etc. Once a microcrack forms, it continues to grow along its slip plane as a Mode II (shear) crack in Stage I growth (orientation of the crack is usually at 45° to the stress axis). At low strain amplitudes, a Stage I crack may extend across several grain diameters before the increasing stress intensity of the crack promotes slip on systems other than the primary slip. A dislocation cell structure normally forms at the crack

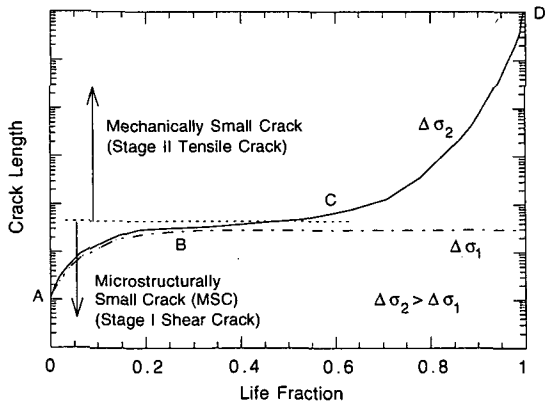

Figure 19.
Growth of cracks in smooth fatigue specimens

tip. Because slip is no longer confined to planes at 45° to the stress axis, the crack begins to propagate as a Mode I (tensile) crack, normal to the stress axis in Stage II growth. At high strain amplitudes, the stress intensity is quite large and the crack propagates entirely by the Stage II process. Stage II crack propagation continues until the crack reaches engineering size (≈3 mm deep). In air or mildly corrosive environments, Stage II cracking is characterized by fatigue striations.

An alternative approach considers fatigue life to be entirely composed of the growth of short surface cracks.[44] In polycrystalline materials, the period for the formation of surface cracks is negligible, Fig. 19. However, the growth rates of short cracks cannot be predicted accurately from fracture mechanics methodology on the basis of the range of the stress intensity factor (ΔK). Under cyclic loading and the same ΔK, short fatigue cracks (i.e., with lengths comparable to the unit size of the microstructure) grow at a faster rate than long fatigue cracks.[45] Also, short cracks can grow at ΔK values below those predicted from linear elastic fracture mechanics (LEFM). The differences between the growth rates of short and long cracks have been attributed to interactions among microstructural features, contributions of crack closure with increasing crack length, effects of mixed-mode crack propagation, and an inadequate characterization of the crack tip stress/strain fields associated with short cracks.

Recent studies indicate that during fatigue loading of smooth test specimens, surface cracks 10 μm or longer form quite early, i.e., <10% of life, even at low strain amplitudes.[46,47] Growth of these surface cracks may be divided into three regimes: (a) initial period that involves growth of microstructurally small cracks (MSCs) below a critical length, characterized by decelerating crack growth rate, seen in region AB of Fig. 19; (b) final period of growth, characterized by accelerating crack growth rate, region CD; and (c) a transition period controlled by a combination of the two regimes, region BC. The crack growth rates as a function of crack length during the three regimes of fatigue life are shown in Fig. 20.

The growth of MSCs is very sensitive to microstructure.[46,48] The MSCs correspond to Stage I cracks and grow along slip planes as shear cracks in the early stage of growth. Microstructural effects on MSCs are strong because of Stage I growth, i.e., crystallographic growth. Fatigue cracks greater than the critical length of MSCs show little or no influence of microstructure and are termed mechanically small cracks. For a stress ratio of -1, the transition from an MSC to a mechanically small crack for several materials has been estimated

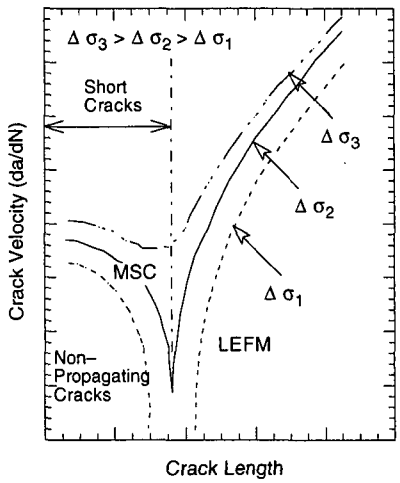

Figure 20.
Schematic illustration of short-crack behavior

to be ≈8 times the unit size of the microstructure.[48] Mechanically small cracks correspond to Stage II (tensile) cracks, which are characterized by striated crack growth, with a fracture surface normal to the maximum principal stress.

At low stress levels, e.g., $\Delta\sigma_1$ in Figs. 19 and 20, the transition from MSC growth to accelerating crack growth does not occur and the cracks are nonpropagating. This circumstance represents the fatigue limit for the smooth specimen. Although cracks can form below the fatigue limit, they can grow to engineering size only at stresses greater than the fatigue limit. Possible preexisting large cracks in the material, e.g., defects in welded samples, or those created by growth of microcracks at high stresses, can grow at stress levels below the fatigue limit, and their growth can be estimated from ΔK-based LEFM.

4.2 Environmental Effects

The reduction in fatigue life in LWR coolant environments may arise from easy formation of surface microcracks and/or an increase in growth rates of cracks during either the initial stage of MSC and shear crack growth or during the transition and final stage of tensile crack growth. Photomicrographs of the gauge surface of Type 316NG specimens tested in air, simulated PWR water, and high-DO water are shown in Fig. 21. Specimens tested in water contain crystalline oxides and a thin gray corrosion scale. X-ray diffraction analyses of specimens tested in water indicate that the corrosion scale consists primarily of magnetite (Fe_3O_4) or ferroferric oxide ($FeFe_2O_4$), chromium oxide (CrO), and maghemite (γ-Fe_2O_3). In addition to these phases, specimens tested in high-DO water also contained hematite (ferric oxide or α-Fe_2O_3). The specimens tested in water also show some surface micropitting.

The reduction in fatigue life in high-temperature water has often been attributed to the presence of micropits[10] that act as stress raisers and provide preferred sites for the formation of fatigue cracks. However, the fatigue data for carbon and low-alloy steel indicate that the large reductions in the fatigue lives of these steels in LWR environments cannot be explained on the basis of micropits alone.[18-20] If the presence of micropits was responsible for reducing the fatigue lives of carbon and low-alloy steels in LWR environments, specimens preexposed to high-DO water and then tested in air should also show a decrease in fatigue life. Fatigue lives

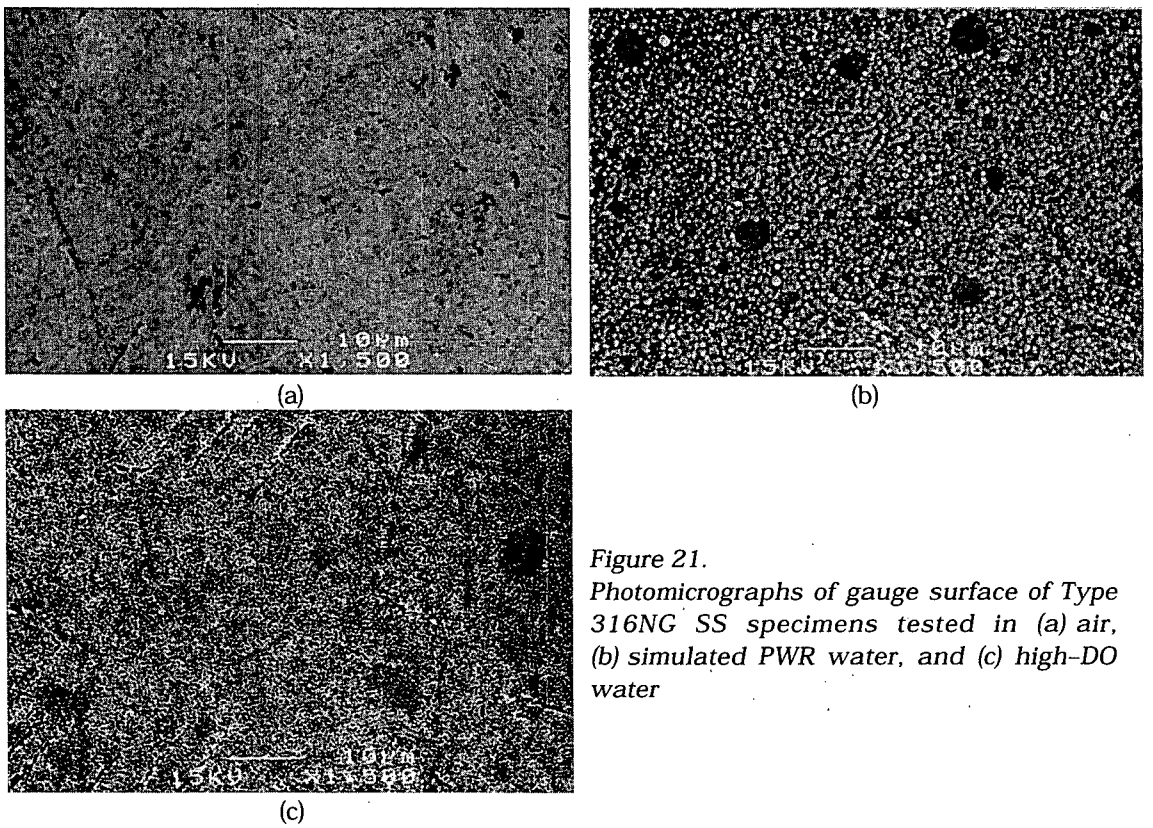

Figure 21.
Photomicrographs of gauge surface of Type 316NG SS specimens tested in (a) air, (b) simulated PWR water, and (c) high-DO water

of the preoxidized and unoxidized specimens are identical; life would be expected to decrease if surface micropits facilitate the formation of fatigue cracks.[18-20] Only a moderate decrease in life is observed for both preoxidized and unoxidized specimens that were tested in low-DO water. The significant reduction in fatigue life in LWR coolant environments may be attributed to enhanced growth rates of cracks either during the initial growth stage of microstructurally small and shear cracks or the transition and final stage of tensile crack growth.

The enhanced growth rates of long cracks in pressure vessel and piping steels in LWR environments have been attributed to either slip oxidation/dissolution[49] or hydrogen-induced cracking[50] mechanisms. The requirements for a slip dissolution model are that a protective oxide film is thermodynamically stable to ensure that a crack will propagate with a high aspect ratio without degrading into a blunt pit, and that a strain increment occurs to rupture that film and thereby expose the underlying matrix to the environment; see Fig. 22. Once the passive oxide film is ruptured, crack extension is controlled by dissolution of freshly exposed surfaces and by the oxidation characteristics.

Hydrogen-induced cracking is explained as follows: hydrogen produced by the oxidation reaction at or near the crack tip is partly absorbed into the metal; the absorbed hydrogen diffuses ahead of the crack tip, interacts with inclusions, and leads to the formation of cleavage cracks at the inclusion/matrix interface; and linkage of the cleavage cracks leads to discontinuous crack extension in addition to extension caused by mechanical fatigue. Other hydrogen-induced fracture processes may also enhance growth rates in LWR environments.

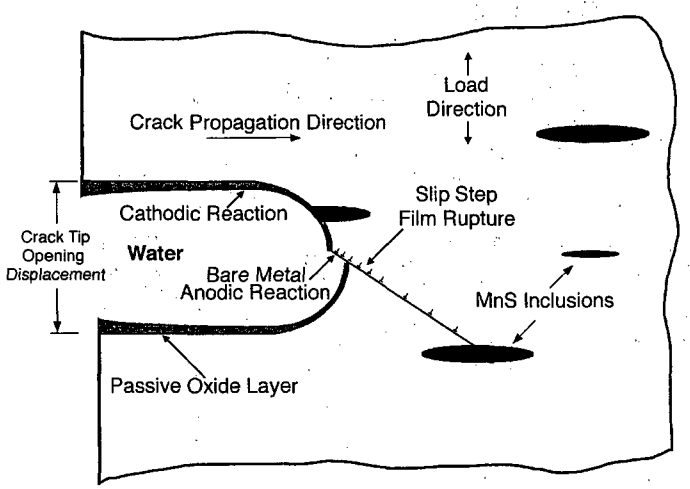

Figure 22.
Schematic illustration of film rupture/slip dissolution process

For example, significant accumulation of hydrogen at or near the crack tip decreases the cohesive interatomic strength of the lattice. Thus, hydrogen-induced bond rupture ahead of the crack tip links up with the main crack, producing discontinuous but enhanced crack growth. The hydrogen adsorption mechanism states that adsorbed hydrogen lowers the surface energy of the metal and thus facilitates crack growth at a lower fracture stress level. Also, hydrogen can cause localized crack tip plasticity by reducing the stress required for dislocation motion.

Both mechanisms depend on the rates of oxide rupture, passivation, and liquid diffusion. Therefore, it is often difficult to differentiate between the two processes or to establish their relative contribution to crack growth in LWR environments. Studies on crack initiation in smooth fatigue specimens indicate that the decrease in fatigue lives of carbon and low-alloy steels in LWR environments is caused primarily by the effects of environment on the growth of cracks that are <100 μm deep.[18-20,47] For cracks <100 μm deep, the growth rates are nearly two orders of magnitude higher in high-DO water than in air. For cracks >100 μm deep. the growth rates are one order of magnitude higher in high-DO water than in air. In LWR environments, crack initiation in carbon and low-alloy steels may be explained as follows: (a) surface microcracks form quite early in fatigue life; (b) during cyclic loading, the protective oxide film is ruptured at strains greater than the fracture strain of surface oxides, and the microcracks grow by anodic dissolution of the freshly exposed surface to crack depths greater than the critical length of MSCs; and (c) a final period of growth that can be predicted from fracture mechanics methodology and is characterized by accelerating growth rates.

For austenitic SSs, lower fatigue lives in low-DO water than in high-DO water are difficult to reconcile in terms of the slip oxidation/dissolution mechanism. In general, crack growth rates increase with increasing DO in the water. It may be argued that the lower lives in low-DO water are due to a lower rupture strain for surface oxides in low-DO than in high-DO water. As discussed above, oxide rupture strain in low-DO water may be in the range of 0.32-0.36%. The rupture strain in high-DO water must be significantly higher than this value to produce the observed difference of a factor of ≈2 in fatigue life. Metallographic examinations of the test specimens indicate that environmentally assisted reduction in fatigue lives of austenitic SSs is most likely caused by hydrogen-induced cracking.[29-31] Figure 23 shows photomicrographs of fracture surfaces of Type 304 and 316NG, after chemical cleaning and at

Type 304 SS Type 316NG SS

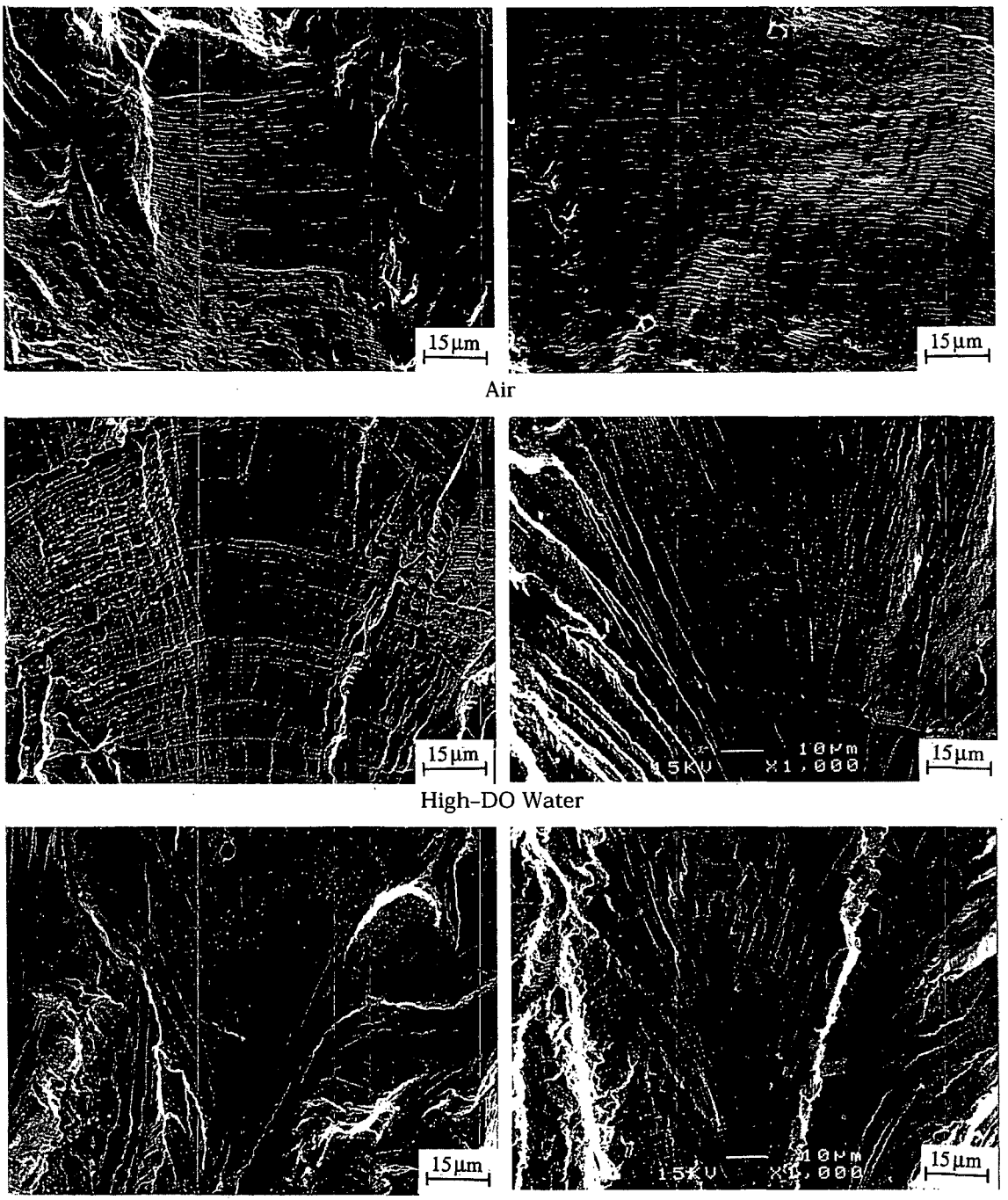

Figure 23. Photomicrographs of fracture surfaces of Types 304 and 316NG SS specimens tested in air, high-DO water, and low-DO, simulated PWR water

approximately the same crack length; specimens were tested at 288°C and ≈0.75% strain range in air, high-DO water, and a low-DO simulated PWR water. All of the specimens show fatigue striations; the spacing between striations indicates that crack growth increases in the following sequence: air, high-DO water, and low-DO PWR water. The presence of well defined striations suggests that the enhanced crack growth rates in austenitic SSs are most likely due to

hydrogen-induced cracking. Fatigue striations should not be observed if enhancement of crack growth is caused by the slip oxidation/dissolution process.

5 Statistical Model

The fatigue S-N curves are generally expressed in terms of the Langer equation,[6] which may be used to represent either strain amplitude in terms of life or life in terms of strain amplitude. The parameters of the equation are commonly established through least-squares curve-fitting of the data to minimize the sum of the square of the residual errors for either fatigue life or strain amplitude. A predictive model based on least-squares fit on life is biased for low strain amplitude. The model leads to probability curves that converge to a single value of strain, and fails to address the fact that at low strain values, most of the error in life is due to uncertainty associated with either measurement of strain or variation in fatigue limit caused by material variability. On the other hand, a least-squares fit on strain does not work well for higher strain amplitudes. Statistical models have been developed at ANL[33,34] by combining the two approaches and minimizing the sum of the squared Cartesian distances from the data point to the predicted curve; the models were later updated with a larger fatigue S-N data base.[31] The functional forms and transformation for the different variables were based on experimental observations and data trends.

In air, the model assumes that fatigue life is independent of temperature and that strain rate effects occur at temperatures >250°C. It is also assumed that the effect of strain rate on life depends on temperature. One data set, obtained on Type 316 SS in room-temperature air, was excluded from the analysis. The tests in this data set were conducted in load-control mode at stress levels in the range of 190-230 MPa. The strain amplitudes were calculated only as elastic strains, i.e., strain amplitudes of 0.1-0.12% (the data are shown as circles in Fig. 5, with fatigue lives of 4×10^5 to 3×10^7). Based on cyclic stress vs. strain correlations for Type 316 SS (Eqs. 4a-4f), actual strain amplitudes for these tests should be 0.23-0.32%. In air, the fatigue life N of Types 304 and 316 SS is expressed as

$$\ln(N) = 6.703 - 2.030 \ln(\varepsilon_a - 0.126) + T^* \dot{\varepsilon}^* \tag{5a}$$

and that of Type 316NG, as

$$\ln(N) = 7.422 - 1.671 \ln(\varepsilon_a - 0.126) + T^* \dot{\varepsilon}^*, \tag{5b}$$

where ε_a is the strain amplitude (%) and T^* and $\dot{\varepsilon}^*$ are transformed temperature and strain rate, respectively, defined as follows:

$$\begin{aligned} T^* &= 0 && (T < 250°C) \\ T^* &= [(T - 250)/525]^{0.84} && (250 \le T < 400°C) \end{aligned} \tag{6a}$$

$$\begin{aligned} \dot{\varepsilon}^* &= 0 && (\dot{\varepsilon} > 0.4\%/s) \\ \dot{\varepsilon}^* &= \ln(\dot{\varepsilon}/0.4) && (0.0004 \le \dot{\varepsilon} \le 0.4\%/s) \\ \dot{\varepsilon}^* &= \ln(0.0004/0.4) && (\dot{\varepsilon} < 0.0004\%/s). \end{aligned} \tag{6b}$$

In LWR environments, the fatigue lives of austenitic SSs depends on strain rate, DO level, and temperature; the decrease in life is greater at low-DO levels and high temperatures. However, existing data are inadequate to establish the functional form for the dependence of fatigue life on DO level or temperature. Separate correlations have been developed for low- and high-DO levels (< or ≥ 0.05 ppm), and low and high temperatures (< or ≥ 200°C). Also, a threshold strain rate of

0.4%/s and saturation rate of 0.0004%/s is assumed in the model. Furthermore, for convenience in incorporating environmental effects into fatigue evaluations, the slope of the S-N curve in LWR environments was assumed to be the same as that in air although the best-fit of the experimental data in water yielded a slope for the S-N curve that differed from the slope of the curve that was obtained in air. In LWR environments, the fatigue life N of Types 304 and 316 SS is expressed as

$$\ln(N) = 5.768 - 2.030 \ln(\varepsilon_a - 0.126) + T^* \dot{\varepsilon}^* O^* \tag{7a}$$

and that of Type 316NG, as

$$\ln(N) = 6.913 - 1.671 \ln(\varepsilon_a - 0.126) + T^* \dot{\varepsilon}^* O^*, \tag{7b}$$

where the constants for transformed temperature, strain rate, and DO are defined as follows:

$$\begin{aligned} T^* &= 0 && (T < 200°C) \\ T^* &= 1 && (T \geq 200°C) \end{aligned} \tag{8a}$$

$$\begin{aligned} \dot{\varepsilon}^* &= 0 && (\dot{\varepsilon} > 0.4\%/s) \\ \dot{\varepsilon}^* &= \ln(\dot{\varepsilon}/0.4) && (0.0004 \leq \dot{\varepsilon} \leq 0.4\%/s) \\ \dot{\varepsilon}^* &= \ln(0.0004/0.4) && (\dot{\varepsilon} < 0.0004\%/s) \end{aligned} \tag{8b}$$

$$\begin{aligned} O^* &= 0.260 && (DO < 0.05 \text{ ppm}) \\ O^* &= 0.172 && (DO \geq 0.05 \text{ ppm}). \end{aligned} \tag{8c}$$

The model is recommended for predicted fatigue lives $\leq 10^6$ cycles. Recent test results indicate that for high-DO environments, conductivity of water is important for environmental effects on fatigue life of austenitic SSs. Therefore, the above correlations may be conservative for high-DO, i.e., ≥0.05 ppm DO, environments. The experimental values of fatigue life in air and water and those predicted from Eqs. 5-8 are plotted in Fig. 24. The estimated fatigue S-N curves for Types 304, 316, and 316NG SSs in air and LWR environments are shown in Figs. 5 and 25, respectively. The predicted fatigue lives show good agreement with the experimental data. Note that the ASME mean curve is not consistent with the existing fatigue S-N data (Fig. 5). Also, although the best-fit of the S-N data in LWR environments (Fig. 25) yields a steeper slope, the slope of the S-N curve in water was assumed to be the same as in air.

Upon completion of the modeling phase, the residual errors (i.e., the Cartesian distance from the prediction curve) should not show significant patterns, such as heteroskedasticity (changing variance), or a nonzero slope. The residual errors for each variable, grouped by steel type and environment (air or water), are plotted in Figs. 26-30. Most data subsets and plots

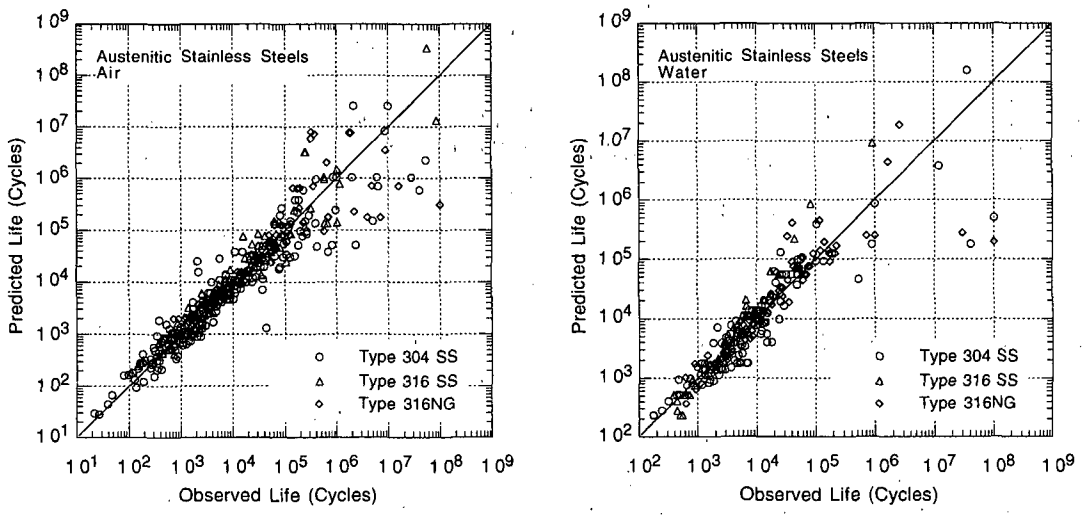

Figure 24. Experimental and predicted values of fatigue lives of austenitic SSs in air and water environments

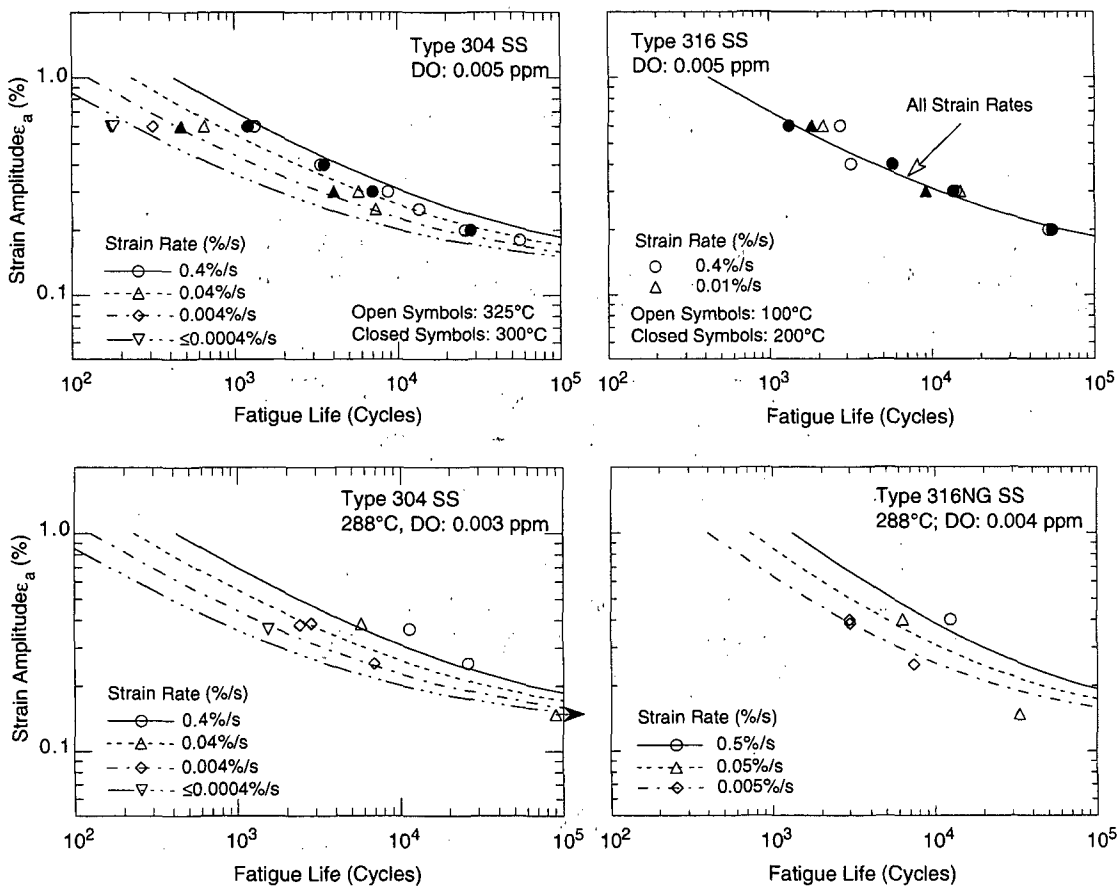

Figure 25. Experimental fatigue lives and those estimated from statistical models for austenitic SSs in water environments

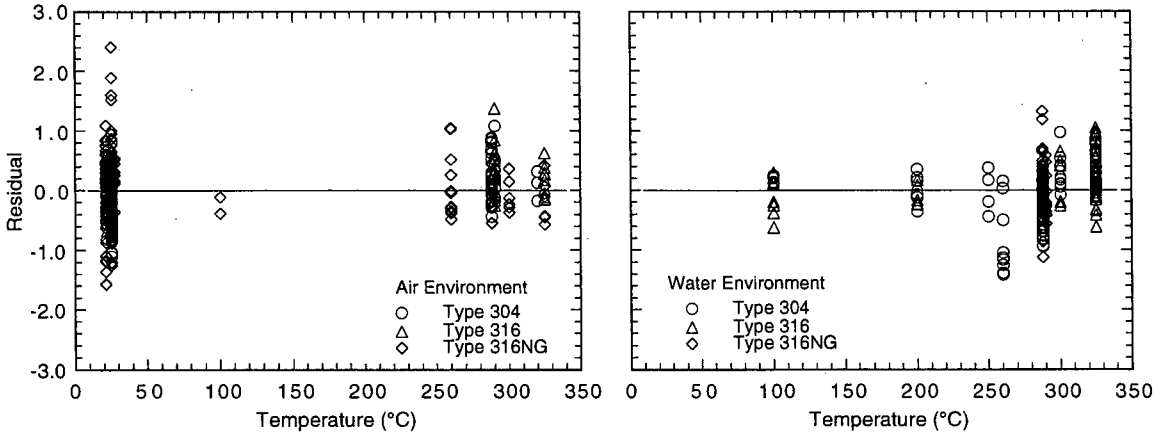

Figure 26. Residual error for austenitic SSs as a function of test temperature

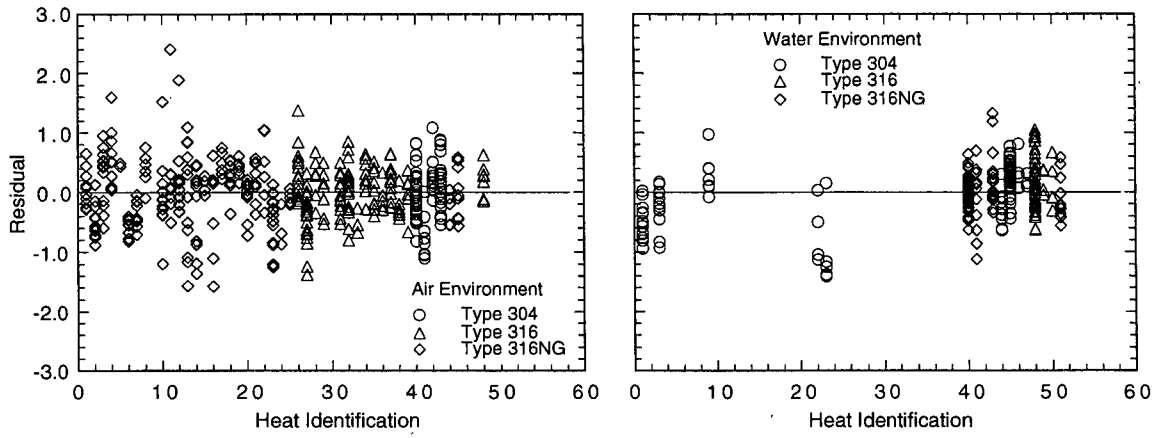

Figure 27. Residual error for austenitic SSs as a function of material heat

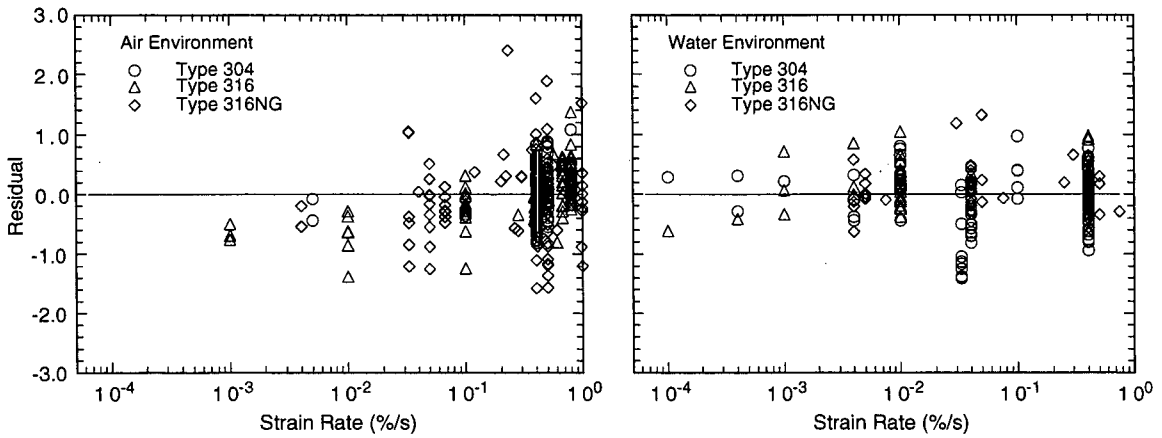

Figure 28. Residual error for austenitic SSs as a function of loading strain rate

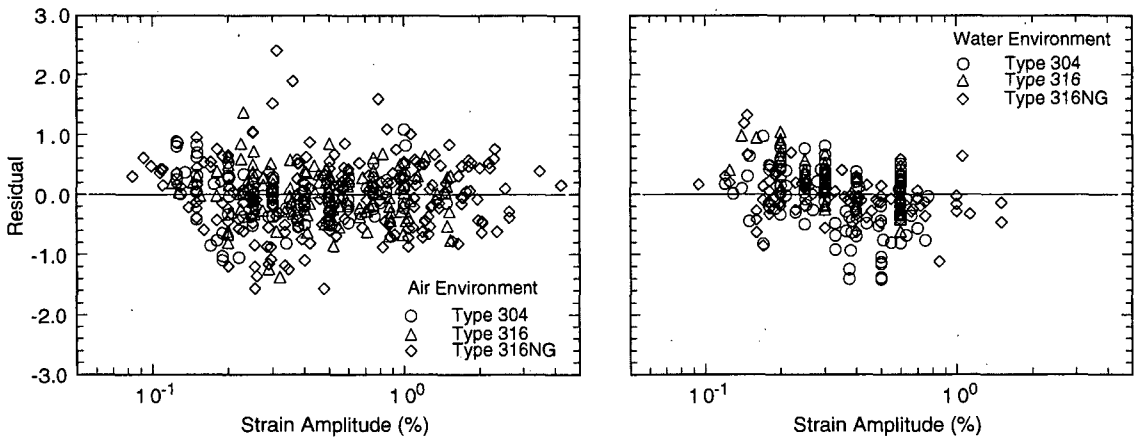

Figure 29. Residual error for austenitic SSs as a function of applied strain amplitude

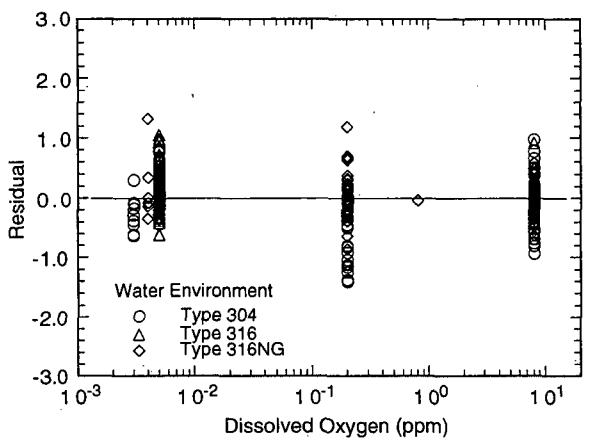

Figure 30.
Residual error for austenitic SSs as a function of dissolved oxygen in water

do not show patterns. In general, high variance tends to be associated with longer lives and lower strain amplitudes. Furthermore, biases seem to be traceable to heat-to-heat variation.

6 Design Fatigue Curves

The design fatigue curves in the current ASME Section III Code were based on experimental data on small polished test specimens. The curves were obtained by adjusting the best-fit curve for the effect of mean stress and then lowering the adjusted curve by a factor of 2 on stress or 20 on life, whichever was more conservative, at each point of the curve. The best-fit curve to the experimental data,[51] expressed in terms of strain amplitude ε_a (%) and fatigue cycles N, for austenitic SSs is given by

$$\ln[N] = 6.954 - 2.0 \ln(\varepsilon_a - 0.167). \tag{9}$$

The mean curve, expressed in terms of stress amplitude S_a (MPa), which is the product of ε_a and elastic modulus E, is given by

$$S_a = 58020/(N)^{1/2} + 299.92. \tag{10}$$

Gary L. Stevens, P. E.

Senior Associate

Education

MS, Mechanical Engineering, San Jose State University (1991)
BS, Mechanical Engineering, California Polytechnic State University (1981)

Professional Associations

Registered Professional Mechanical Engineer, State of California
Registered Professional Mechanical Engineer, State of Colorado

Professional Experience

1999 to present	Structural Integrity Associates, Inc., Centennial, CO Senior Associate
1996 to 1999	Structural Integrity Associates, Inc., San Jose, CA Associate
1995 to 1996	Structural Integrity Associates, Inc., San Jose, CA Senior Consultant
1981 to 1995	GE Nuclear Energy San Jose, CA

Summary

Mr. Stevens has 25 years of technical and supervisory experience in the nuclear energy field. His experience includes ASME Code stress and fatigue analysis, fracture mechanics analysis, analytical computer applications, and on-line fatigue monitoring of critical plant components. Mr. Stevens has achieved a significant amount of business management experience and skill, which includes technical project management, extensive technical proposal preparation and related customer interface, hardware design interface, and computer application development and management. He is currently SI's Product Lead for BWR License Renewal Services, BWR Fatigue Monitoring, and BWR Pressure-Temperature Curves.

At Structural Integrity Associates, Mr. Stevens has been responsible for a variety of projects for both PWR and BWR systems. These include the development of Class 1 fatigue management programs for plant license renewal applications (including environmental fatigue-related issues), the management, development, and installation of on-line fatigue and fatigue crack growth

monitoring systems, finite element model stress and fatigue analyses, and a variety of fracture mechanics applications including limit load and linear elastic fracture mechanics methodologies. Mr. Stevens has authored several technical papers enveloping all of these areas, has been an active member and participant in ASME Code Section XI Task Groups, Working Groups, Subgroups and Subcommittee, and has provided selected technical training to customers in the areas of fatigue and fracture mechanics. Mr. Stevens has developed an extensive working knowledge of the stress, fatigue and fracture mechanics areas through this experience.

Mr. Stevens is actively involved with the SI team developing nuclear plant Class 1 fatigue management programs. In particular, he has supported the development and deployment of the **FatiguePro** system, which is an on-line fatigue-damage monitoring system for power plants and other thermo-mechanical systems, at many plants world-wide. He has also been involved with various feedwater nozzle analyses throughout his career, and he continues to be a key contributor to the fracture mechanics work related to BWR internals, which is being studied by the BWR Vessel and Internals Project (BWRVIP).

At GE, Mr. Stevens began his career as a participant in the Edison Engineering Training Program, which provided three rotating work assignments before participants accepted a permanent position. This rotational work experience included nuclear fuel channel design, computer program design and development, spare parts, document database development, and structural analysis and design. After selecting a permanent position in March 1983, Mr. Stevens spent over 12 years performing ASME Code stress and fatigue analyses and various fracture mechanics evaluations for BWR vessel, piping, and vessel internals components. He was a key participant on most BWR vessel internals structural issues from the first significant incidences of detected cracking in 1993. During his tenure at GE, Mr. Stevens became recognized as a structural analysis expert for BWR services.

While at GE, Mr. Stevens received the prestigious "Young Engineer Award" for his contributions in the structural analysis area, as well as the "Product Application - Service Engineering Award" for his successful implementation of thermal cycle monitoring in Japan.

Over the years, Mr. Stevens has gained related computer experience in several computer environments (C, FORTRAN, BASIC, UNIX, and HP BASIC). In addition, he has extensive past experience in the use and application of the ANSYS finite element computer code.

The strain-vs.-life data were converted to stress-vs.-life curves by using the room-temperature value of 195.1 GPa (28300 ksi) for the elastic modulus. The best-fit curves were adjusted for the effect of mean stress by using the modified Goodman relationship[46]

$$S'_a = S_a\left(\frac{\sigma_u - \sigma_y}{\sigma_u - S_a}\right) \qquad \text{for } S_a < \sigma_y, \tag{10a}$$

and $$S'_a = S_a \qquad \text{for } S_a > \sigma_y, \tag{10b}$$

where S'_a is the adjusted value of stress amplitude, and σ_y and σ_u are yield and ultimate strengths of the material, respectively. The Goodman relationship assumes the maximum possible mean stress and typically gives a conservative adjustment for mean stress, at least when environmental effects are not significant. The design fatigue curves were then obtained by lowering the adjusted best-fit curve by a factor of 2 on stress or 20 on cycles, whichever was more conservative, to account for differences and uncertainties in fatigue life associated with material and loading conditions.

The same procedure has been used to develop design fatigue curves for LWR environments. However, because of the differences between the ASME mean curve and the best-fit curve to existing fatigue data (Fig. 5), the margin on strain for the current ASME Code design fatigue curve is closer to 1.5 than 2. Therefore, to be consistent with the current Code design curve, a factor of 1.5 rather than 2 was used in developing the design fatigue curves from the updated statistical models in air and LWR environments.

The design fatigue curves based on the statistical model for Types 304 and 316 SS in air and low- and high-DO water are shown in Figs. 31-33. A similar set of curves can be obtained for Type 316NG SS. Because the fatigue life of Type 316NG is superior to that of Types 304 or 316 SS, Figs. 31-33 may be used conservatively for Type 316NG SS. Also, as mentioned earlier, recent test results indicate that the conductivity of water is important for environmental effects on fatigue life of austenitic SSs in high-DO environments. Therefore, the design fatigue curves for Type 304 and 316 SS in water with ≥0.05 ppm DO (Fig. 33) may be conservative.

Although, in air at low stress levels, the differences between the current ASME Code design curve and the design curve obtained from the updated statistical model at temperatures <250°C have been reduced or eliminated by reducing the margin on stress from 2 to 1.5, significant differences still exist between the two curves. For example, at stress amplitudes >300 MPa, estimates of life from the updated design curve are a factor of ≈2 lower than those from the ASME Code curve. Therefore, the actual margins on stress and life for the current ASME Code design fatigue curve are 1.5 and 10, respectively, instead of 2 and 20.

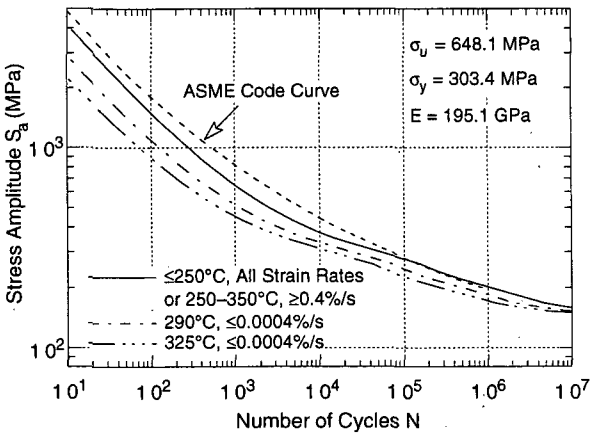

Figure 31.
ASME and statistical-model design fatigue curves for Types 304 and 316 SS in air

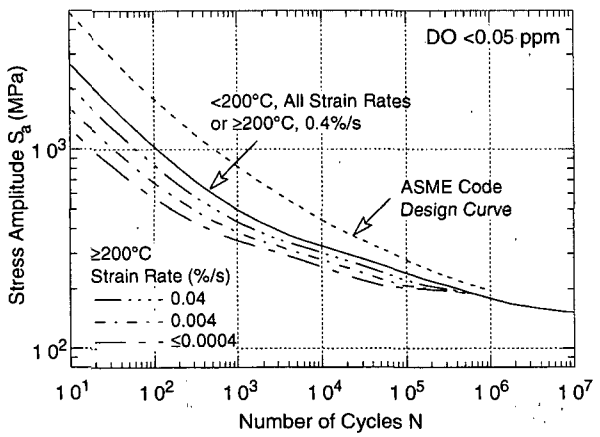

Figure 32.
ASME and statistical-model design fatigue curves for Types 304 and 316 SS in water with <0.05 ppm DO

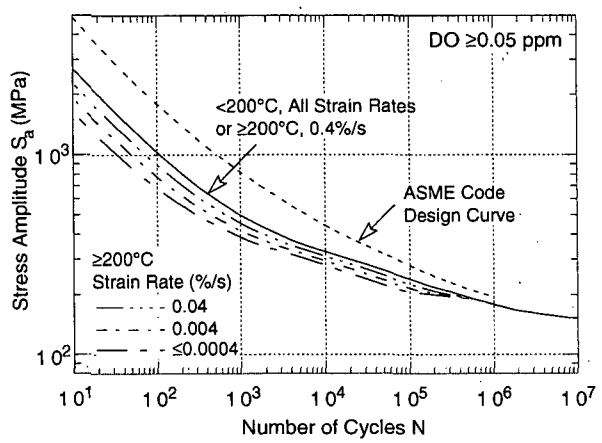

Figure 33.
ASME and statistical-model design fatigue curves for Types 304 and 316 SS in water with ≥0.05 ppm DO

As discussed above, the existing fatigue data indicate a threshold strain range of ≈0.32%, below which environmental effects on the fatigue life of austenitic SSs either do not occur or are insignificant. This value must be adjusted for the effects of mean stress and uncertainties due to material and loading variability. Threshold strain amplitudes are decreased by ≈10% to account for mean stress effects and by a factor of 1.5 to account for uncertainties in fatigue life associated with material and loading variability. Thus, a threshold strain amplitude of 0.097% (stress amplitude of 189 MPa) was selected, below which environmental effects on life are modest and are represented by the design curve for temperatures <200°C (shown by the solid line in Figs. 31 and 32).

These curves can be used to perform ASME Code fatigue evaluations of components that are in service in LWR environments. For each set of load pairs, a partial usage factor is obtained from the appropriate design fatigue curve. Information about the service conditions, such as temperature, strain rate, and DO level, are required for the evaluations. The procedure for obtaining these parameters depends on whether the elapsed-time-vs.-temperature information for the transient is available. The maximum values of temperature and DO level and the slowest strain rate during the transient may be used for a conservative estimate of life. Note that the design curves in LWR environments not only account for environmental effects on life but also include the difference between the current Code design curve and the updated design curve in air, i.e., the difference between the solid and dashed curves in Fig. 31.

7 Fatigue Life Correction Factor

The effects of reactor coolant environments on fatigue life have also been expressed in terms of a fatigue life correction factor F_{en}, which is the ratio of the life in air at room temperature to that in water at the service temperature.[11,52,53] To incorporate environmental effects into the ASME Code fatigue evaluation, a fatigue usage for a specific load pair, based on the current Code fatigue design curve, is multiplied by the correction factor. A fatigue life correction factor F_{en} can also be obtained from the statistical model, where

$$\ln(F_{en}) = \ln(N_{air}) - \ln(N_{water}). \tag{12}$$

From Eqs. 5a and 7a, the fatigue life correction factor relative to room-temperature air for Types 304 and 316 SSs is given by

$$F_{en} = \exp(0.935 - T^* \dot{\varepsilon}^* O^*), \tag{13}$$

where the threshold and saturation values for T^*, $\dot{\varepsilon}^*$, and O^* are defined in Eqs. 8a-8c. At temperatures ≥200°C and strain rates ≤0.0004%/s, Eq. 13 yields an F_{en} of ≈15 in low-DO PWR water (<0.05 ppm DO) and ≈8 in high-DO water (≥0.05 ppm DO). At temperatures <200°C, F_{en} is ≈2.5 in both low- and high-DO water at all strain rates.

8 Conservatism in Design Fatigue Curves

The overall conservatism in ASME Code fatigue evaluations has also been demonstrated in fatigue tests on piping welds and components.[54] In air, the margins on the number of cycles to failure for austenitic SS elbows and tees were 40-310 and 104-510, respectively. The margins for girth butt welds were significantly lower at 6-77. In these tests, fatigue life was expressed as the number of cycles for the crack to penetrate through the wall, which ranged in thickness from 6 to 18 mm (0.237 to 0.719 in). The fatigue design curves represent the number of cycles that are necessary to form a 3-mm-deep crack. Consequently, depending on wall thickness, the actual margins to failure may be lower by a factor of >2.

Deardorff and Smith[55] have discussed the types and extent of conservatisms present in the ASME Section III fatigue evaluations and the effects of LWR environments on fatigue margins. The sources of conservatism include design transients considerably more severe than those experienced in service, grouping of transients, and simplified elastic-plastic analysis. Environmental effects on two components, the BWR feedwater nozzle/safe end and PWR steam generator feedwater nozzle/safe end, both constructed from LAS and known to be affected by severe thermal transients,

were also investigated in the study. When environmental effects on fatigue life were not considered, Deardorff and Smith[55] estimated that the ratio of the CUFs for the PWR and BWR nozzles (both constructed from LAS), computed with the mean experimental curve for test specimen data, to CUFs computed with the Code fatigue design curve were ≈60 and 90, respectively. To maintain the factor of 20 on life that was used in the present Code fatigue design curves to account for the uncertainties due to material and loading variability, the margins for the PWR and BWR nozzles are reduced to 3 and 4.5, respectively. These results suggest that, for carbon and low-alloy steels, the Code Design procedures provide some margin in life that can be used to account for environmental effects on life. However, as noted previously in Section 6, the Code fatigue design curve for austenitic SSs is not consistent with the existing fatigue S-N data; the actual margins on stress and life are 1.5 and 10, respectively, instead of 2 and 20. Consequently, the Code fatigue design curve for austenitic SSs provides little or no margin in life to account for environmental effects.

Data available in the literature have been reviewed to evaluate the effects of various material, loading, and environmental variables on the fatigue life of structural materials in air and LWR environments.[33] The subfactors that may be used to account for the effects of these variables on fatigue life are summarized in Table 5. The factors on strain primarily account for variation in the fatigue limit of a material caused by material variability, component size and surface finish, and loading history. Because the reduction in fatigue life is associated with the growth of short cracks (<100 μm), the effects of these variables on threshold strain are typically not cumulative but rather are controlled by the variable that has the largest effect. The values in Table 5 suggest that a factor of at least 1.5 on strain and 10 on cycles is needed to account for the differences and uncertainties of relating the fatigue lives of laboratory test specimens to those of large components. Beacuse SSs develop a corrosion scale in LWR environments, the effect of surface finish may not be significant; the subfactor on life to account for surface finish effects may be as low as 1.5 or may be eliminated completely. Therefore, a factor of 1.5 or 2 on life may be able to account for the effects of environment on the fatigue lives of austenitic SSs.

Table 5. Subfactors that may be used to account for effects of various variables on fatigue life

Variable	Factor on Life	Factor on Strain
Material variability and experimental scatter	2.5	1.4–1.7
Size	1.4	1.25
Surface finish	2.0–3.0	1.3
Loading history	1.5–2.5	1.5
Total adjustment	10.0–26.0	1.5–1.7

9 Fatigue Evaluations in LWR Environments

Section III of the ASME Boiler and Pressure Vessel Code contains rules for the construction of nuclear power plant Class 1 components.[5] It provides requirements for designs that will withstand cyclic loadings on a structural component that occur because of changes in mechanical and thermal loadings as the system goes from one load set (pressure, temperature, moment, and force) to any other load set. ASME Section III, NB-3600 (piping design) methodology is used exclusively for piping and sometimes for branch nozzles. ASME Section III, NB-3200 (design by analysis) methodology is generally used for vessels and frequently for nozzles. In both cases, the various sets of load states at the most highly stressed locations in the component are defined first. The load states are defined in terms of the three principal stresses in NB-3200 methodology, and in terms of

internal pressure, moments, average temperature, and temperature gradients in NB-3600 methodology. A peak stress-intensity range and an alternating stress-intensity amplitude S_a is then calculated for each load state. The value of S_a is used to first obtain the allowable number of cycles from the design fatigue curve and then to calculate the fatigue usage associated with that load state. The CUF is the sum of the partial usage factors. The Section III, NB-3200- or NB-3600-type analyses of components for service in LWR environments can be performed with the design fatigue curves presented in Figs. 32 and 33. Note that fatigue evaluations performed with these updated curves not only account for the environmental effects but they also include the difference between the current ASME mean air curve and the statistical-model air curve.

An alternative approach to fatigue evaluations in LWR environments has been proposed by Electric Power Research Institute (EPRI)[52,53] and by the Environmental Fatigue Data (EFD) committee of Thermal and Nuclear Power Engineering Society (TENPES) of Japan.* As discussed in Section 7, the effects of LWR coolant environments on the fatigue S-N curves are expressed in terms of fatigue life correction factor F_{en}, defined as the ratio of the life in air at room temperature to that in water at service temperature. The effects of environment are incorporated into the ASME fatigue evaluation by obtaining a fatigue usage for a specific load pair based on the current Code design curves and multiplying it by the correction factor. Fatigue evaluations performed with the F_{en} incorporate only the effect of environment.

Both of these approaches require additional information about the service conditions, e.g., temperature, strain rate, and DO level. The procedure for obtaining these parameters depends on whether the elapsed-time-vs.-temperature information for the transient is available. The values of temperature and DO may be conservatively taken as the maximum values for the transient. An average strain rate is generally used for each load state; it is obtained from the peak strain and elapsed time for the transient. However, fatigue-monitoring data indicate that actual strain rates may vary significantly during the transient. The slowest strain rate can be used for a conservative estimate of life.

10 Summary

The work performed at ANL on fatigue of wrought and cast austenitic SSs in LWR environments is summarized. The existing fatigue S-N data have been evaluated to establish the effects of various material and loading variables, such as steel type, strain range, strain rate, temperature,and DO level in water on the fatigue lives of these steels. Current understanding of the fatigue S-N behavior of austenitc SSs may be summarized as follows.

10.1 Air Environment

- *Steel Type*: The fatigue lives of Types 304 and 316 SS are comparable; those of Type 316NG are superior. The fatigue S-N behavior of cast CF-8 and CF-8M SSs is similar to that of wrought austenitic SSs.
- *Temperature*: For all steels, life is independent of temperature in the range from room temperature to 427°C.
- *Strain Rate*: At temperatures above 260°C, the fatigue lives of austenitic SSs may decrease with decreasing strain rate.

*Presented at the Pressure Vessel Research Council Meeting, April 1996, Orlando, FL.

- *ASME Code Mean Curve*: The ASME mean curve for austenitic SSs is nonconservative with respect to existing fatigue S-N data; at strain amplitudes <0.5%, it predicts fatigue lives that are significantly longer than those observed experimentally.

10.2 LWR Environments

- *Environmental Effects*: The fatigue lives of cast and wrought austenitc SSs are decreased in LWR environments; the decrease depends on strain rate, DO level in water, and temperature.
- *Steel Type*: The effects of LWR environments on fatigue life are comparable for all steels.
- *Strain Amplitude*: A minimum threshold strain is required for environmentally assisted decrease in fatigue lives of the tested steels. The threshold value most likely corresponds to the rupture strain of the surface oxide film. Limited data suggest that the threshold strain is between 0.32 and 0.36%.
- *Loading Cycle*: Environmental effects on fatigue life occur primarily during the tensile-loading cycle, and at strain levels greater than the threshold value required to rupture the surface oxide film. Consequently, loading and environmental conditions, e.g., strain rate, temperature, and DO level, during the tensile-loading cycle in excess of the oxide rupture strain, are important parameters for environmentally assisted reduction in fatigue lives of the tested steels.
- *Dissolved Oxygen in Water*: Environmental effects on fatigue life are more pronounced in low-DO, i.e., <0.01 ppm DO, than in high-DO water, i.e., ≥0.1 ppm DO. The reduction in life is greater by a factor of ≈2 in a simulated PWR environment than in high-DO water. The fatigue lives of cast SSs are approximately the same in both high- or low-DO water and are comparable to those observed for wrought SSs in low-DO water. Recent data suggest that the fatigue lives of austenitic SSs may depend on parameters other than DO level in water, e.g., conductivity of water may be important.
- *Strain Rate*: Fatigue lives decrease with decreasing strain rate; the effect is greater in a low-DO PWR environment than in high-DO water. The results indicate that the strain rate below which effects of strain rate on fatigue life saturate may depend both on steel type and DO level. In low-DO PWR environments, saturation strain rate appears to be ≈0.0004%/s for Type 304 SS and somewhat higher for Type 316 SS.
- *Temperature*: Existing data are inadequate to establish the functional form for the dependence of life on temperature. Limited data indicate that environmental effects on fatigue life are significant at 250°C and minimal below 200°C. At 250-330°C, fatigue life appears to be relatively insensitive to changes in temperature.

10.3 Fatigue Design Curves in LWR Environments

Statistical models have been developed to predict fatigue life of small smooth specimens of austenitic SSs as a function of material, loading, and environmental parameters. Functional form and bounding values of these parameters were based on experimental observations and data trends. Statistical models were obtained by minimizing the squared Cartesian distances from the data point to the predicted curve instead of minimizing the sum of the square of the residual errors for either strain amplitude or fatigue life. The models are recommended for predicted fatigue lives of $\leq 10^6$ cycles. The results indicate that the ASME mean curve for SSs is not consistent with the

experimental data at strain amplitudes <0.5% or stress amplitudes <975 MPa (<141 ksi); the ASME mean curve is nonconservative.

The design fatigue curves for austenitic SSs in LWR environments were obtained by the procedure that was used to develop the current ASME Code design fatigue curves, i.e., by adjusting the best-fit experimental curve for the effect of mean stress and by setting margins of 20 on cycles and 2 on strain to account for the uncertainties in life associated with material and loading conditions. However, because the margin on strain for the current ASME Code design fatigue curve is closer to 1.5 than 2, a factor of 1.5 was used when the design fatigue curves in LWR environments were developed. Data available in the literature were reviewed to evaluate the conservatism in the existing Code fatigue design curves. The use of a fatigue life correction factor to incorporate the effects of environment into the ASME Code fatigue evaluations is also discussed.

References

1. K. Iida, *A Review of Fatigue Failures in LWR Plants in Japan*, Nucl. Eng. Des. **138**, 297-312 (1992).

2. K. Kussmaul, R. Rintamaa, J. Jansky, M. Kemppainen, and K. Törrönen, *On the Mechanism of Environmental Cracking Introduced by Cyclic Thermal Loading*, in IAEA Specialists Meeting Corrosion and Stress Corrosion of Steel Pressure Boundary Components and Steam Turbines, VTT Symp. 43, Espoo, Finland, pp. 195-243 (1983).

3. K. Kussmaul, D. Blind, and J. Jansky, *Formation and Growth of Cracking in Feed Water Pipes and RPV Nozzles*, Nucl. Eng. Des. **81**, 105-119 (1984).

4. E. Lenz, B. Stellwag, and N. Wieling, *The Influence of Strain Induced Corrosion Cracking on the Crack Initiation in Low Alloy Steels in HT-Water - A Relation Between Monotonic and Cyclic Crack Initiation Behavior*, in IAEA Specialists Meeting Corrosion and Stress Corrosion of Steel Pressure Boundary Components and Steam Turbines, VTT Symp. 43, Espoo, Finland, pp. 243-267 (1983).

5. *ASME Boiler and Pressure Vessel Code Section III - Rules for Construction of Nuclear Power Plant Components*, The American Society of Mechanical Engineers, New York (1992).

6. B. F. Langer, *Design of Pressure Vessels for Low-Cycle Fatigue*, ASME J. Basic Eng. **84**, 389-402 (1962) .

7. *Tentative Structural Design Basis for Reactor Pressure Vessels and Directly Associated Components (Pressurized, Water Cooled Systems)*, PB 151987, U.S. Dept. of Commerce, Office of Technical Service, 1 Dec. 1958 Revision.

8. S. Ranganath, J. N. Kass, and J. D. Heald, *Fatigue Behavior of Carbon Steel Components in High-Temperature Water Environments*, in BWR Environmental Cracking Margins for Carbon Steel Piping, EPRI NP-2406, Electric Power Research Institute, Palo Alto, CA, Appendix 3 (May 1982).

9. W. A. Van Der Sluys, *Evaluation of the Available Data on the Effect of the Environment on the Low Cycle Fatigue Properties in Light Water Reactor Environments*, in Proc. 6th Int. Symp. on Environmental Degradation of Materials in Nuclear Power Systems - Water Reactors, R. E. Gold and E. P. Simonen, eds., The Metallurgical Society, Warrendale, PA, pp. 1-4 (1993).

10. N. Nagata, S. Sato, and Y. Katada, *Low-Cycle Fatigue Behavior of Pressure Vessel Steels in High-Temperature Pressurized Water*, ISIJ Int. **31** (1), 106-114 (1991).

11. M. Higuchi and K. Iida, *Fatigue Strength Correction Factors for Carbon and Low-Alloy Steels in Oxygen-Containing High-Temperature Water*, Nucl. Eng. Des. **129**, 293-306 (1991).

12. M. Higuchi, K. Iida, and Y. Asada, *Effects of Strain Rate Change on Fatigue Life of Carbon Steel in High-Temperature Water*, in Fatigue and Crack Growth: Environmental Effects, Modeling Studies, and Design Considerations, PVP Vol. 306, S. Yukawa, ed., American Society of Mechanical Engineers, New York, pp. 111-116 (1995); also in Proc. of Symp. on Effects of the Environment on the Initiation of Crack Growth, ASTM STP 1298, American Society for Testing and Materials, Philadelphia (1997).

13. H. Kanasaki, M. Hayashi, K. Iida, and Y. Asada, *Effects of Temperature Change on Fatigue Life of Carbon Steel in High Temperature Water*, in Fatigue and Crack Growth: Environmental Effects, Modeling Studies, and Design Considerations, PVP Vol. 306, S. Yukawa, ed., American Society of Mechanical Engineers, New York, pp. 117-122 (1995).

14. G. Nakao, H. Kanasaki, M. Higuchi, K. Iida, and Y. Asada, *Effects of Temperature and Dissolved Oxygen Content on Fatigue Life of Carbon and Low-Alloy Steels in LWR Water Environment*, in Fatigue and Crack Growth: Environmental Effects, Modeling Studies, and Design Considerations, PVP Vol. 306, S. Yukawa, ed., American Society of Mechanical Engineers, New York, pp. 123-128 (1995).

15. O. K. Chopra and W. J. Shack, *Effects of LWR Environments on Fatigue Life of Carbon and Low-Alloy Steels*, in Fatigue and Crack Growth: Environmental Effects, Modeling Studies, and Design Considerations, PVP Vol. 306, S. Yukawa, ed., American Society of Mechanical Engineers, New York, pp. 95-109 (1995).

16. O. K. Chopra and W. J. Shack, *Evaluation of Effects of LWR Coolant Environments on Fatigue Life of Carbon and Low-Alloy Steels*, in Effects of the Environment on the Initiation of Crack Growth, ASTM STP 1298, W. A. Van Der Sluys, R. S. Piascik, and R. Zawierucha, eds., American Society for Testing and Materials, Philadelphia, pp. 247-266 (1997).

17. O. K. Chopra and W. J. Shack, *Low-Cycle Fatigue of Piping and Pressure Vessel Steels in LWR Environments*, Nucl. Eng. Des. **184**, 49-76 (1998).

18. O. K. Chopra and W. J. Shack, *Effects of LWR Coolant Environments on Fatigue Design Curves of Carbon and Low-Alloy Steels*, NUREG/CR-6583, ANL-97/18 (March 1998).

19. O. K. Chopra and W. J. Shack, *Fatigue Crack Initiation in Carbon and Low-Alloy Steels in Light Water Reactor Environments - Mechanism and Prediction*, in Fatigue, Environmental Factors, and New Materials, PVP Vol. 374, H. S. Mehta, R. W. Swindeman, J. A. Todd, S. Yukawa, M. Zako, W. H. Bamford, M. Higuchi, E. Jones, H. Nickel, and S. Rahman, eds., American Society of Mechanical Engineers, New York, pp. 155-168 (1998).

20. O. K. Chopra and W. J. Shack, *Overview of Fatigue Crack Initiation in Carbon and Low-Alloy Steels in Light Water Reactor Environments*, J. Pressure Vessel Technol. **121**, 49-60 (1999).

21. M. Fujiwara, T. Endo, and H. Kanasaki, *Strain Rate Effects on the Low Cycle Fatigue Strength of 304 Stainless Steel in High Temperature Water Environment, Fatigue Life: Analysis and Prediction*, in Proc. of the Int. Conf. and Exposition on Fatigue, Corrosion Cracking, Fracture Mechanics, and Failure Analysis, ASM, Metals Park, OH, pp. 309-313 (1986).

22. H. Mimaki, H. Kanasaki, I. Suzuki, M. Koyama, M. Akiyama, T. Okubo, and Y. Mishima, *Material Aging Research Program for PWR Plants*, in Aging Management Through Maintenance Management, PVP Vol. 332, I. T. Kisisel, ed., American Society of Mechanical Engineers, New York, pp. 97-105 (1996).

23. H. Kanasaki, R. Umehara, H. Mizuta, and T. Suyama, *Fatigue Lives of Stainless Steels in PWR Primary Water*, Trans. 14th Int. Conf. on Structural Mechanics in Reactor Technology (SMiRT 14), Lyon, France, pp. 473-483 (1997).

24. H. Kanasaki, R. Umehara, H. Mizuta, and T. Suyama, *Effects of Strain Rate and Temperature Change on the Fatigue Life of Stainless Steel in PWR Primary Water*, Trans. 14th Intl. Conf. on Structural Mechanics in Reactor Technology (SMiRT 14), Lyon, France, pp. 485-493 (1997).

25. M. Higuchi and K. Iida, *Reduction in Low-Cycle Fatigue Life of Austenitic Stainless Steels in High-Temperature Water*, in Pressure Vessel and Piping Codes and Standards, PVP Vol. 353, D. P. Jones, B. R. Newton, W. J. O'Donnell, R. Vecchio, G. A. Antaki, D. Bhavani, N. G. Cofie, and G. L. Hollinger, eds., American Society of Mechanical Engineers, New York, pp. 79-86 (1997).

26. M. Hayashi, *Thermal Fatigue Strength of Type 304 Stainless Steel in Simulated BWR Environment*, Nucl. Eng. Des. **184**, 135-144 (1998).

27. M. Hayashi, K. Enomoto, T. Saito, and T. Miyagawa, *Development of Thermal Fatigue Testing with BWR Water Environment and Thermal Fatigue Strength of Austenitic Stainless Steels*, Nucl. Eng. Des. **184**, 113-122 (1998).

28. W. J. Shack and W. F. Burke, *Fatigue of Type 316NG SS*, in Environmentally Assisted Cracking in Light Water Reactors, Semiannual Report, October 1989-March 1990, NUREG/CR-4667 Vol. 10, ANL-91/5, pp. 3-19 (March 1991).

29. O. K. Chopra and D. J. Gavenda, *Effects of LWR Coolant Environments on Fatigue Lives of Austenitic Stainless Steels*, in Pressure Vessel and Piping Codes and Standards, PVP Vol. 353, D. P. Jones, B. R. Newton, W. J. O'Donnell, R. Vecchio, G. A. Antaki, D. Bhavani, N. G. Cofie, and G. L. Hollinger, eds., American Society of Mechanical Engineers, New York, pp. 87-97 (1997).

30. O. K. Chopra and D. J. Gavenda, *Effects of LWR Coolant Environments on Fatigue Lives of Austenitic Stainless Steels*, J. Pressure Vessel Technol. **120**, 116-121 (1998).

31. O. K. Chopra and J. L. Smith, *Estimation of Fatigue Strain-Life Curves for Austenitic Stainless Steels in Light Water Reactor Environments*, in Fatigue, Environmental Factors, and New Materials, PVP Vol. 374, H. S. Mehta, R. W. Swindeman, J. A. Todd, S. Yukawa, M. Zako, W. H. Bamford, M. Higuchi, E. Jones, H. Nickel, and S. Rahman, eds., American Society of Mechanical Engineers, New York, pp. 249-259 (1998).

32. S. Majumdar, O. K. Chopra, and W. J. Shack, *Interim Fatigue Design Curves for Carbon, Low-Alloy, and Austenitic Stainless Steels in LWR Environments*, NUREG/CR-5999, ANL-93/3 (April 1993).

33. J. Keisler, O. K. Chopra, and W. J. Shack, *Fatigue Strain-Life Behavior of Carbon and Low-Alloy Steels, Austenitic Stainless Steels, and Alloy 600 in LWR Environments*, NUREG/CR-6335, ANL-95/15 (Aug. 1995).

34. J. Keisler, O. K. Chopra, and W. J. *Shack, Statistical Models for Estimating Fatigue Strain-Life Behavior of Pressure Boundary Materials in Light Water Reactor Environments*, Nucl. Eng. Des. **167**, 129-154 (1996).

35. D. D. Macdonald, A. C. Scott, and P. Wentrcek, *External Reference Electrodes for Use in High Temperature Aqueous Systems*, J. Electrochem. Soc. **126**, 908-911 (1979).

36. C. E. Jaske, and W. J. O'Donnell, *Fatigue Design Criteria for Pressure Vessel Alloys*, Trans. ASME J. Pressure Vessel Technol. **99**, 584-592 (1977).

37. J. B. Conway, R. H. Stentz, and J. T. Berling, *Fatigue, Tensile, and Relaxation Behavior of Stainless Steels*, TID-26135, U.S. Atomic Energy Commission, Washington, DC (1975).

38. D. L. Keller, *Progress on LMFBR Cladding, Structural, and Component Materials Studies During July, 1971 through June, 1972, Final Report*, Task 32, Battelle-Columbus Laboratories, BMI-1928 (1977).

39. D. A. Hale, S. A. Wilson, E. Kiss, and A. J. Gianuzzi, *Low Cycle Fatigue Evaluation of Primary Piping Materials in a BWR Environment*, GEAP-20244, U.S. Nuclear Regulatory Commission (Sept. 1977).

40. C. Amzallag, P. Rabbe, G. Gallet, H. -P. Lieurade, *Influence des Conditions de Sollicitation Sur le Comportement en Fatigue Oligocyclique D'aciers Inoxydables Austénitiques*, Memoires Scientifiques Revue Metallurgie Mars 1978, pp. 161-173

41. A. Pellissier-Tanon, J. L. Bernard, C. Amzallag, and P. Rabbe, *Evaluation of the Resistance of Type 316 Stainless Steel Against Progressive Deformation*, in Low-Cycle Fatigue and Life Prediction, ASTM STP 770, C. Amzallag, B. N. Leis, and P. Rabbe, eds., American Society for Testing and Materials, Philadelphia, pp. 69-80 (1982).

42. Slama, G., Petrequin, P., and Mager, T., *Effect of Aging on Mechanical Properties of Austenitic Stainless Steel Castings and Welds*, in Assuring Structural Integrity of Steel Reactor Pressure Boundary Components, SMiRT Post Conference Seminar 6, Monterey, CA, 1983.

43. O. K. Chopra, *Effect of Thermal Aging on Mechanical Properties of Cast Stainless Steels*, in Proc. of the 2nd Int. Conf. on Heat-Resistant Materials, K. Natesan, P. Ganesan, and G. Lai, eds., ASM International, Materials Park, OH, pp. 479-485 (1995).

44. K. J. Miller, *Damage in Fatigue: A New Outlook*, in Pressure Vessels and Piping Codes and Standard: Volume 1 - Current Applications, PVP Vol. 313-1, K. R. Rao and Y. Asada, eds., American Society of Mechanical Engineers, New York, pp. 191-192 (1995).

45. S. Suresh and R. O. Ritchie, *Propagation of Short Fatigue Cracks*, Int. Metals Reviews **29**, 445-476 (1984).

46. K. Tokaji, T. Ogawa, and S. Osako, *The Growth of Microstructurally Small Fatigue Cracks in a Ferritic-Pearlitic Steel*, Fatigue Fract. Eng. Mater. Struct. **11**, 331-342 (1988).

47. D. J. Gavenda, P. R. Luebbers, and O. K. Chopra, *Crack Initiation and Crack Growth Behavior of Carbon and Low-Alloy Steels*, in Fatigue and Fracture 1, PVP Vol. 350, S. Rahman, K. K. Yoon, S. Bhandari, R. Warke, and J. M. Bloom, eds., American Society of Mechanical Engineers, New York, pp. 243-255 (1997).

48. K. Tokaji and T. Ogawa, *The Growth of Microstructurally Small Fatigue Cracks in Metals*, in Short Fatigue Cracks, ESIS 13, M. J. Miller and E. R. de los Rios, eds., Mechanical Engineering Publication, London, pp. 85-99 (1992).

49. F. P. Ford, *Overview of Collaborative Research into the Mechanisms of Environmentally Controlled Cracking in the Low Alloy Pressure Vessel Steel/Water System*, in Proc. 2nd Int. Atomic Energy Agency Specialists' Meeting on Subcritical Crack Growth, NUREG/CP-0067, MEA-2090, Vol. 2, pp. 3-71 (1986).

50. H. Hänninen, K. Törrönen, and W. H. Cullen, *Comparison of Proposed Cyclic Crack Growth Mechanisms of Low Alloy Steels in LWR Environments*, in Proc. 2nd Int. Atomic Energy Agency Specialists' Meeting on Subcritical Crack Growth, NUREG/CP-0067, MEA-2090, Vol. 2, pp. 73-97 (1986).

51. American Society of Mechanical Engineers, *Criteria of the ASME Boiler and Pressure Vessel Code for Design by Analysis in Sections III and VIII, Division 2*, ASME, New York (1969).

52. H. S. Mehta and S. R. Gosselin, *An Environmental Factor Approach to Account for Reactor Water Effects in Light Water Reactor Pressure Vessel and Piping Fatigue Evaluations*, EPRI Report TR-105759 (Dec. 1995).

53. H. S. Mehta and S. R. Gosselin, *An Environmental Factor Approach to Account for Reactor Water Effects in Light Water Reactor Pressure Vessel and Piping Fatigue Evaluations*, in Fatigue and Fracture Vol. 1, PVP 323, H. S. Mehta, ed., American Society of Mechanical Engineers, New York, pp. 171-185 (1996).

54. M. E. Mayfield, E. C. Rodabaugh, and R. J. Eiber, *A Comparison of Fatigue Test Data on Piping with the ASME Code Fatigue Evaluation Procedure*, ASME paper 79-PVP-92, American Society of Mechanical Engineers, New York (1979).

55. A. F. Deardorff and J. K. Smith, *Evaluation of Conservatisms and Environmental Effects in ASME Code, Section III, Class 1 Fatigue Analysis*, SAND94-0187, prepared by Structural Integrity Associates, San Jose, CA, under contract to Sandia National Laboratories (Aug. 1994).

NRC FORM 335 (2-89) NRCM 1102, 3201, 3202

U. S. NUCLEAR REGULATORY COMMISSION

BIBLIOGRAPHIC DATA SHEET

(See instructions on the reverse)

1. REPORT NUMBER *(Assigned by NRC. Add Vol., Supp., Rev., and Addendum Numbers, if any.)*
NUREG/CR-5704
ANL-98/31

2. TITLE AND SUBTITLE
Effects of LWR Coolant Environments on Fatigue Design Curves of Austenitic Stainless Steels

3. DATE REPORT PUBLISHED

MONTH	YEAR
March	1999

4. FIN OR GRANT NUMBER
W6610

5. AUTHOR(S)
O. K. Chopra

6. TYPE OF REPORT
Technical

7. PERIOD COVERED *(Inclusive Dates)*

8. PERFORMING ORGANIZATION – NAME AND ADDRESS *(If NRC, provide Division, Office or Region, U.S. Nuclear Regulatory Commission, and mailing address; if contractor, provide name and mailing address.)*

Argonne National Laboratory
9700 South Cass Avenue
Argonne, IL 60439

9. SPONSORING ORGANIZATION – NAME AND ADDRESS *(If NRC, type "Same as above": if contractor, provide NRC Division, Office or Region, U.S. Nuclear Regulatory Commission, and mailing address.)*

Engineering Issues Branch
Office of Nuclear Regulatory Research
U. S. Nuclear Regulatory Commission
Washington, DC 20555

10. SUPPLEMENTARY NOTES
M. McNeil, NRC Project Manager

11. ABSTRACT (200 words or less)

The ASME Boiler and Pressure Vessel Code provides rules for the construction of nuclear power plant components. Figures I-9.1 through I-9.6 of Appendix I to Section III of the Code specify fatigue design curves for structural materials. Although effects of reactor coolant environments are not explicitly addressed by the design curves, test data indicate that the Code fatigue curves may not always be adequate for coolant environments. This report summarizes work performed by Argonne National Laboratory on the fatigue of austenitic stainless steels in light water reactor (LWR) environments. Existing fatigue S-N data have been evaluated to establish the effects of various material and loading variables, such as steel type, dissolved oxygen level, strain range, strain rate, and temperature, on the fatigue lives of these steels. Statistical models are presented for estimating the fatigue S-N curves as a function of material, loading, and environmental variables. Design fatigue curves have been developed for austenitic stainless steel components in LWR environments. The extent of conservatism in the design fatigue curves and alternative methods for incorporating the effects of LWR coolant environments into the ASME Code fatigue evaluations are discussed.

12. KEY WORDS/DESCRIPTORS *(List words or phrases that will assist researchers in locating this report.)*
Fatigue Strain-Life Curves
Fatigue Design Curves
LWR Environments
Austenitic Stainless Steels
Cast Austenitic Stainless Steels
Fatigue Crack Initiation

13. AVAILABILITY STATEMENT
Unlimited

14. SECURITY CLASSIFICATION
(This Page)
Unclassified
(This Report)
Unclassified

15. NUMBER OF PAGES

16. PRICE

NRC FORM 335 (2-89)

Entergy

Entergy Nuclear Operations, Inc.
Vermont Yankee
P.O. Box 0250
320 Governor Hunt Road
Vernon, VT 05354
Tel 802 257 7711

February 5, 2008
BVY 08-008

ATTN: Document Control Desk
U.S. Nuclear Regulatory Commission
Washington, DC 20555-0001

References:
1) Letter, Entergy to USNRC, "Vermont Yankee Nuclear Power Station, License No. DPR-28, License Renewal Application," BVY 06-009, dated January 25, 2006
2) Letter, Entergy to USNRC, "Update of Aging Management Program Audit Q&A Database," BVY 07-079, dated November 14, 2007
3) Letter, USNRC to Entergy, "Update on Extension of Schedule for the Conduct of Review of the Vermont Yankee Nuclear Power Station License Renewal Application," NVY 07-157, dated November 27, 2007
4) Letter, Entergy to USNRC, "License Renewal Application, Amendment 33," BVY 07-082, dated December 11, 2007
5) Letter, Entergy to USNRC, "License Renewal Application, Amendment 34," BVY 08-002, dated January 30, 2008

Subject: **Vermont Yankee Nuclear Power Station**
License No. DPR-28 (Docket No. 50-271)
License Renewal Application, Amendment 35

On January 25, 2006, Entergy Nuclear Operations, Inc. and Entergy Nuclear Vermont Yankee, LLC (Entergy) submitted Reference (1), the License Renewal Application (LRA) for the Vermont Yankee Nuclear Power Station (VYNPS).

VYNPS submitted Reference (2) following an NRC audit of the VYNPS Aging Management Program and subsequently received Reference (3), which included an NRC Request for Additional Information. References (4) and (5), respectively, provided the initial response to Reference (3) and later clarifications to that response. Additional clarification and details regarding recirculation nozzle Cumulative Usage Factor (CUF) and water chemistry effects are provided in Attachments 1 and 2 to this letter. VYNPS information meeting the NRC's position on Extended Power Uprate (EPU) operating experience evaluation for Aging Management Programs is also discussed below.

VYNPS had not yet entered operation at EPU levels at the time Reference (1) was submitted. EPU power ascension began in March of 2006. To ensure that operating experience at EPU levels is properly addressed by aging management programs, Entergy will perform an evaluation of operating experience at EPU levels prior to the period of extended operation. In addition to VYNPS operating experience, the evaluation will include operating experience from other BWR plants operating at EPU levels.

A117
NRR

This is a new commitment, and has been entered as Commitment #51 on the VYNPS License Renewal Commitment List, Revision 9 (Attachment 3).

Should you have any questions concerning this submittal, please contact Mr. David Mannai at (802) 451-3304.

I declare under penalty of perjury that the foregoing is true and correct.

Executed on February 5, 2008.

Sincerely,

Ted A. Sullivan
Site Vice President
Vermont Yankee Nuclear Power Station

Attachment 1: Additional Information Regarding Recirculation Nozzle CUF
Attachment 2: Additional Information Regarding Water Chemistry Effects
Attachment 3: License Renewal Commitment List, Revision 9

cc: Mr. James Dyer, Director
U.S. Nuclear Regulatory Commission
Office O5E7
Washington, DC 20555-00001

Mr. Samuel J. Collins, Regional Administrator, Region 1
U.S. Nuclear Regulatory Commission
475 Allendale
Road King of Prussia, PA 19406-1415

Mr. Jack Strosnider, Director
U.S. Nuclear Regulatory Commission
Office T8A23
Washington, DC 20555-00001

Mr. Jonathan Rowley, Senior Project Manager
U.S. Nuclear Regulatory Commission
11555 Rockville Pike
MS-O-11F1
Rockville, MD 20853

Mr. Mike Modes
USNRC RI
475 Allendale Road
King of Prussia, PA 19406

Mr. James S. Kim, Project Manager
U.S. Nuclear Regulatory Commission
Mail Stop O-8-C2A
Washington, DC 20555

USNRC Resident Inspector
Entergy Nuclear Vermont Yankee, LLC
P.O. Box 157
Vernon, Vermont 05354

Mr. David O'Brien, Commissioner
VT Department of Public Service
112 State Street – Drawer 20
Montpelier, Vermont 05620-2601

Diane Curran, Esq.
Harmon, Curran, Spielberg & Eisenberg, LLP
1726 M Street, N.W., Suite 600
Washington, DC 20036

Attachment 1

Vermont Yankee Nuclear Power Station
License No. DPR-28 (Docket No. 50-271)

License Renewal Application

Amendment 35

Additional Information Regarding Recirculation Nozzle CUF

Additional Information Regarding Recirculation Nozzle CUF

NRC Request:

Demonstrate why the confirmatory analysis for the feedwater nozzle bounds the geometry of the recirculation outlet nozzle.

Response:

The feedwater nozzle was chosen for the confirmatory analysis since it has the largest number of, and most severe, transients and the highest calculated fatigue usage of the three nozzles which used the VY fatigue analysis approach. The analysis of the feedwater nozzle is bounding for the recirculation outlet nozzle since the calculated usage factors and thermal transient stresses are significantly less than those for the feedwater nozzle.

As pointed out during the January 8, 2008 presentation to the NRC Staff, the recirculation outlet nozzle has a different geometry (i.e., "skewed") as compared to the other nozzles. However, the feedwater nozzle configuration remains conservative and bounding when compared to the recirculation outlet nozzle configuration for the following reasons:

- The previous comparisons of nozzle corner stress factors from BWRVIP-108, which included evaluation of a recirculation outlet nozzle, demonstrate that the recirculation outlet nozzle configuration does not provide results that are significantly different from the other nozzle configurations.
- The transients experienced by the recirculation outlet nozzle are significantly less severe and less numerous than the transients that affect the feedwater nozzle.
- The most significant thermal transient (improper start causing reverse flow) was modeled directly in the Finite Element Model due to its unique characteristics.
- In the nozzle corner, the thermal stresses are small compared to the pressure stresses.
- The previous analyses for all three nozzles for VY yielded significantly lower fatigue usage for the recirculation outlet nozzle compared to the feedwater nozzle.
- Industry experience for the BWR fleet has repeatedly demonstrated that the recirculation outlet nozzle fatigue usage is significantly lower than feedwater nozzle fatigue usage.

Attachment 2

Vermont Yankee Nuclear Power Station
License No. DPR-28 (Docket No. 50-271)

License Renewal Application

Amendment 35

Additional Information Regarding Water Chemistry Effects

Additional Information Regarding Water Chemistry Effects

NRC Request:

Describe how water chemistry effects were accounted for in the evaluation of environmentally assisted fatigue.

Response:

Per Section X.M1 of NUREG 1801 (GALL Report) the environmentally assisted fatigue (EAF) evaluations used appropriate Fatigue Life Correction Factors (F_{en}) calculated using the methodology in NUREG/CR-6583 for carbon and low alloy steels and NUREG/CR-5704 for stainless steels.

For carbon and low alloy steels the F_{en} factor relationships are shown on page 69 of NUREG/CR-6583. As shown on page 60 of NUREG/CR-6583, the input values used to develop the F_{en} factors are sulfur content, strain rate, temperature, and dissolved oxygen content in the fluid. Input values for these parameters were chosen to maximize the F_{en} factors calculated for all components.

The F_{en} factor relationship for stainless steels is shown on page 31 of NUREG/CR-5704. As shown on page 25 of NUREG/CR-5704, the input values used to develop the F_{en} factors are strain rate, temperature, and dissolved oxygen content in the fluid. Similar to the carbon and low alloy steel calculations, the input values were chosen to maximize the F_{en} factors.

The inputs were selected as follows:

- For the carbon and low alloy steel expressions, the transformed sulfur content parameter was set equal to the maximum value of 0.015 to maximize the effects of this parameter.
- For all expressions, the transformed strain rate parameter was set equal to the minimum strain rate (i.e., less than 0.001%/sec) for all transients to maximize the effects of this parameter.
- For all expressions, the transformed temperature parameter was computed using 550°F for all locations. This temperature envelopes normal operating temperatures to maximize the effects of this parameter, and is very conservative for feedwater temperature.
- For the transformed dissolved oxygen parameter, dissolved oxygen (DO) data was taken from recorded plant data for the feedwater line. For all other locations evaluated in the reactor coolant system, the EPRI BWRVIA code was used to determine DO levels. The EPRI BWRVIA model was used to determine DO at component locations at original licensed power (OLP) for both BWR normal water chemistry (NWC) and noble metal water chemistry (NMCA+HWC). Also, current licensed power with NMCA+HWC was evaluated.

For the purposes of ensuring that the DO effects on F_{en} are conservative and bounding with respect to water chemistry, the F_{en} values used accounted for variations in plant recorded feedwater DO data. It is noted that excursions observed in the plant data used are small in number and are of short duration. Approximately 13 years of recorded feedwater DO measurements, including excursions, were evaluated for input to the EAF analysis. A DO value (50 ppb) was used to calculate bounding F_{en} value for the feedwater piping. This represents the mean of the measured data plus one standard deviation.

For locations in the reactor coolant system, the BWRVIA model was run varying the DO content for the power/water chemistry conditions discussed above. The results of these sensitivity studies showed that the resulting variations in DO at component locations are significantly less than the changes input to the feedwater DO. The variation of feedwater DO (mean plus one standard deviation) was evaluated. This resulted in less than a 2% change in the bounding F_{en} used in the EAF analysis for the low alloy steel components in the beltline and lower sections of the reactor vessel. There is no effect on the bounding F_{en} values from the input feedwater DO variations for the stainless steel components.

The F_{en} factors are determined using several parameters and, collectively, these parameters were chosen to conservatively maximize their contribution. The F_{en} factors are bounding for each location based on all of the input values. The bounding F_{en} factors for each location and material were used for all stress range pairs in the cumulative usage factor calculations.

Attachment 3

Vermont Yankee Nuclear Power Station
License No. DPR-28 (Docket No. 50-271)

License Renewal Application

Amendment 35

License Renewal Commitment List
Revision 9

VERMONT YANKEE NUCLEAR POWER STATION
LICENSE RENEWAL COMMITMENT LIST
REVISION 9

During the development and review of the Vermont Yankee Nuclear Power Station License Renewal Application, Entergy made commitments to provide aging management programs to manage the effects of aging on structures and components during the extended period of operation. The following table lists these license renewal commitments, along with the implementation schedule and the source of the commitment.

ITEM	COMMITMENT	IMPLEMENTATION SCHEDULE	SOURCE	Related LRA Section No./ Comments
1	Guidance for performing examinations of buried piping will be enhanced to specify that coating degradation and corrosion are attributes to be evaluated.	March 21, 2012	BVY 06-009	B.1.1 Audit Items 5 & 130
2	Fifteen (15) percent of the top guide locations will be inspected using enhanced visual inspection technique, EVT-1, within the first 18 years of the period of extended operation, with at least one-third of the inspections to be completed within the first 6 years and at least two-thirds within the first 12 years of the period of extended operation. Locations selected for examination will be areas that have exceeded the neutron fluence threshold.	As stated in the commitment	BVY 06-009	B.1.7 Audit Item 14
3	The Diesel Fuel Monitoring Program will be enhanced to ensure ultrasonic thickness measurement of the fuel oil storage and fire pump diesel storage (day) tank bottom surfaces will be performed every 10 years during tank cleaning and inspection.	March 21, 2012	BVY 06-009 BVY 07-018	B.1.9 and regional inspection
4	The Diesel Fuel Monitoring Program will be enhanced to specify UT measurements of the fuel oil storage and fire pump diesel storage (day) tank bottom surfaces will have acceptance criterion ≥ 60% Tnom.	March 21, 2012	BVY 06-009 BVY 07-018	B.1.9 and regional inspection

ITEM	COMMITMENT	IMPLEMENTATION SCHEDULE	SOURCE	Related LRA Section No./ Comments
5	The Fatigue Monitoring Program will be modified to require periodic update of cumulative fatigue usage factors (CUFs), or to require update of CUFs if the number of accumulated cycles approaches the number assumed in the design calculation.	March 21, 2012	BVY 06-009	B.1.11
6	A computerized monitoring program (e.g., FatiguePro) will be used to directly determine cumulative fatigue usage factors (CUFs) for locations of interest.	March 21, 2012	BVY 06-009	B.1.11
7	The allowable number of effective transients will be established for monitored transients. This will allow quantitative projection of future margin.	March 21, 2012	BVY 06-009	B.1.11
8	Procedures will be enhanced to specify that fire damper frames in fire barriers will be inspected for corrosion. Acceptance criteria will be enhanced to verify no significant corrosion.	March 21, 2012	BVY 06-009	B.1.12.1 Audit Items 35, 151, 152, 153 and 159
9	Procedures will be enhanced to state that the diesel engine sub-systems (including the fuel supply line) will be observed while the pump is running. Acceptance criteria will be enhanced to verify that the diesel engine did not exhibit signs of degradation while it was running; such as fuel oil, lube oil, coolant, or exhaust gas leakage.	March 21, 2012	BVY 06-009	B.1.12.1 Audit Items 33, 150 & 155

ITEM	COMMITMENT	IMPLEMENTATION SCHEDULE	SOURCE	Related LRA Section No./ Comments
10	Fire Water System Program procedures will be enhanced to specify that in accordance with NFPA 25 (2002 edition), Section 5.3.1.1.1, when sprinklers have been in place for 50 years a representative sample of sprinkler heads will be submitted to a recognized testing laboratory for field service testing. This sampling will be repeated every 10 years.	March 21, 2012	BVY 06-009	B.1.12.2
11	The Fire Water System Program will be enhanced to specify that wall thickness evaluations of fire protection piping will be performed on system components using non-intrusive techniques (e.g., volumetric testing) to identify evidence of loss of material due to corrosion. These inspections will be performed before the end of the current operating term and during the period of extended operation. Results of the initial evaluations will be used to determine the appropriate inspection interval to ensure aging effects are identified prior to loss of intended function.	March 21, 2012	BVY 06-009	B.1.12.2 Audit Items 37 & 41
12	Implement the Heat Exchanger Monitoring Program as described in LRA Section B.1.14.	March 21, 2012	BVY 06-009	B.1.14
13	Implement the Non-EQ Inaccessible Medium-Voltage Cable Program as described in LRA Section B.1.17.	March 21, 2012	BVY 06-009	B.1.17
14	Implement the Non-EQ Instrumentation Circuits Test Review Program as described in LRA Section B.1.18.	March 21, 2012	BVY 06-009	B.1.18
15	Implement the Non-EQ Insulated Cables and Connections Program as described in LRA Section B.1.19.	March 21, 2012	BVY 06-009	B.1.19

ITEM	COMMITMENT	IMPLEMENTATION SCHEDULE	SOURCE	Related LRA Section No./ Comments
16	Implement the One-Time Inspection Program as described in LRA Section B.1.21.	March 21, 2012	BVY 06-009 BVY 07-009	B.1.21 Audit Items 239, 240, 330, 331
17	Enhance the Periodic Surveillance and Preventive Maintenance Program to assure that the effects of aging will be managed as described in LRA Section B.1.22.	March 21, 2012	BVY 06-009	B.1.22 Audit Item 377
18	Enhance the Reactor Vessel Surveillance Program to proceduralize the data analysis, acceptance criteria, and corrective actions described in the program description in LRA Section B.1.24.	March 21, 2012	BVY 06-009	B.1.24
19	Implement the Selective Leaching Program as described in LRA Section B.1.25.	March 21, 2012	BVY 06-009	B.1.25
20	Enhance the Structures Monitoring Program to specify that process facility crane rails and girders, condensate storage tank (CST) enclosure, CO_2 tank enclosure, N_2 tank enclosure and restraining wall, CST pipe trench, diesel generator cable trench, fuel oil pump house, service water pipe trench, man-way seals and gaskets, and hatch seals and gaskets are included in the program.	March 21, 2012	BVY 06-009	B.1.27.2 Audit Item 377
21	Guidance for performing structural examinations of wood to identify loss of material, cracking, and change in material properties will be added to the Structures Monitoring Program.	March 21, 2012	BVY 06-009	B.1.27.2

ITEM	COMMITMENT	IMPLEMENTATION SCHEDULE	SOURCE	Related LRA Section No./ Comments
22	Guidance for performing structural examinations of elastomers (seals and gaskets) to identify cracking and change in material properties (cracking when manually flexed) will be enhanced in the Structures Monitoring Program procedure.	March 21, 2012	BVY 06-009	B.1.27.2
23	Guidance for performing structural examinations of PVC cooling tower fill to identify cracking and change in material properties will be added to the Structures Monitoring Program procedure.	March 21, 2012	BVY 06-009	B.1.27.2
24	System walkdown guidance documents will be enhanced to perform periodic system engineer inspections of systems in scope and subject to aging management review for license renewal in accordance with 10 CFR 54.4 (a)(1) and (a)(3). Inspections shall include areas surrounding the subject systems to identify hazards to those systems. Inspections of nearby systems that could impact the subject system will include SSCs that are in scope and subject to aging management review for license renewal in accordance with 10 CFR 54.4 (a)(2).	March 21, 2012	BVY 06-009	B.1.28 Audit Items 187, 188 & 190
25	Implement the Thermal Aging and Neutron Irradiation Embrittlement of Cast Austenitic Stainless Steel (CASS) Program as described in LRA Section B.1.29.	March 21, 2012	BVY 06-009	B.1.29
26	Procedures will be enhanced to flush the John Deere Diesel Generator cooling water system and replace the coolant and coolant conditioner every three years.	March 21, 2012	BVY 06-009	B.1.30.1 Audit Items 84 & 164

ITEM	COMMITMENT	IMPLEMENTATION SCHEDULE	SOURCE	Related LRA Section No./ Comments
27	At least 2 years prior to entering the period of extended operation, for the locations identified in NUREG/CR-6260 for BWRs of the VY vintage, VY will refine our current fatigue analyses to include the effects of reactor water environment and verify that the cumulative usage factors (CUFs) are less than 1. This includes applying the appropriate Fen factors to valid CUFs determined in accordance with one of the following: 1. For locations, including NUREG/CR-6260 locations, with existing fatigue analysis valid for the period of extended operation, use the existing CUF to determine the environmentally adjusted CUF. 2. More limiting VY-specific locations with a valid CUF may be added in addition to the NUREG/CR-6260 locations. 3. Representative CUF values from other plants, adjusted to or enveloping the VY plant specific external loads may be used if demonstrated applicable to VY. 4. An analysis using an NRC-approved version of the ASME code or NRC-approved alternative (e.g., NRC-approved code case) may be performed to determine a valid CUF. During the period of extended operation, VY may also use one of the following options for fatigue management if ongoing monitoring indicates a potential for a condition outside the analysis bounds noted above: 1) Update and/or refine the affected analyses described above. 2) Implement an inspection program that has been reviewed and approved by the NRC (e.g., periodic nondestructive examination of the affected locations at inspection intervals to be determined by a method acceptable to the NRC). 3) Repair or replace the affected locations before exceeding a CUF of 1.0.	March 21, 2012 March 21, 2010 for performing a fatigue analysis that addresses the effects of reactor coolant environment on fatigue (in accordance with an NRC approved version of the ASME Code)	BVY-06-058	4.3.3 Audit Items 29, 107 & 318

ITEM	COMMITMENT	IMPLEMENTATION SCHEDULE	SOURCE	Related LRA Section No./ Comments
28	Revise program procedures to indicate that the Instrument Air Program will maintain instrument air quality in accordance with ISA S7.3	March 21, 2012	BVY 06-009	B.1.16 Audit Item 47
29	VYNPS will perform one of the following: 1. Install core plate wedges, or, 2. Complete a plant-specific analysis to determine acceptance criteria for continued inspection of core plate hold down bolting in accordance with BWRVIP-25 and submit the inspection plan and analysis to the NRC two years prior to the period of extended operation for NRC review and approval.	March 21, 2012	BVY 06-009	B.1.7 Audit Item 9
30	Revise System Walkdown Program to specify CO2 system inspections every 6 months.	March 21, 2012	BVY 06-009	B.1.28 Audit Items 30, 141, 146 & 298
31	Revise Fire Water System Program to specify annual fire hydrant gasket inspections and flow tests.	March 21, 2012	BVY 06-009	B.1.12.2 Audit Items 39 & 40
32	Implement the Metal Enclosed Bus Program. Details are provided in a LRA Amendment 16, Attachment 3 and LRA Amendment 23, 7.	March 21, 2012	BVY 06-058 BVY 07-003 BVY 06-091	Audit Item 97

ITEM	COMMITMENT	IMPLEMENTATION SCHEDULE	SOURCE	Related LRA Section No./ Comments
33	Include within the Structures Monitoring Program provisions that will ensure an engineering evaluation is made on a periodic basis (at least once every five years) of groundwater samples to assess aggressiveness of groundwater to concrete. Samples will be monitored for sulfates, pH and chlorides.	March 21, 2012	BVY 06-009	B.1.27 Audit Item 77 RAI 3.5-7
34	Implement the Bolting Integrity Program. Details are provided in a LRA Amendment 16, Attachment 2 and LRA Amendment 23, Attachment 5.	March 21, 2012	BVY 06-058 BVY 07-003 BVY 06-091	Audit Items 198, 216, 218, 237, 331 & 333
35	Provide within the System Walkdown Training Program a process to document biennial refresher training of Engineers to demonstrate inclusion of the methodology for aging management of plant equipment as described in EPRI Aging Assessment Field Guide or comparable instructional guide.	March 21, 2012	BVY 06-058	Audit Item 384
36	If technology to inspect the hidden jet pump thermal sleeve and core spray thermal sleeve welds has not been developed and approved by the NRC at least two years prior to the period of extended operation, VYNPS will initiate plant-specific action to resolve this issue. That plant specific action may be justification that the welds do not require inspection.	March 21, 2010	BVY06-058	Audit Item 12
37	Continue inspections in accordance with the Steam Dryer Monitoring Program, Revision 3 in the event that the BWRVIP-139 is not approved prior to the period of extended operation.	March 21, 2010	BVY 06-079	Audit Item 204

ITEM	COMMITMENT	IMPLEMENTATION SCHEDULE	SOURCE	Related LRA Section No./ Comments
38	The BWRVIP-116 report which was approved by the Staff will be implemented at VYNPS with the conditions documented in Sections 3 and 4 of the Staff's final SE dated March 1, 2006, for the BWRVIP-116 report.	March 21, 2012	BVY 06-088	Response to RAI B.1.24-1
39	If the VYNPS standby capsule is removed form the reactor vessel without the intent to test it, the capsule will be stored in a manner which maintains it in a condition which would permit its future use, including during the period of extended operation, if necessary.	March 21, 2012	BVY 06-088	Response to RAI B.1.24-2
40	This Commitment has been deleted and replaced with Commitment 43.	N/A	BVY 07-018	N/A
41	This Commitment has been deleted and replaced with Commitment 43.	N/A	BVY 07-018	N/A
42	Implement the Bolted Cable Connections Program. Details are provided in LRA Amendment 23, attachment 7.	March 21, 2012	BVY 07-003 BVY 07-018	Response to: RAI 3.6.2.2-N-01 LRA Sections: 3.6.2.1 A.2.1.39 B.1.33 Table 3.6.1 Table 3.6.2-1
43	Establish and implement a program that will require testing of the two 13.8 kV cables from the two Vernon Hydro Station 13.8 kV switchgear buses to the 13.8 kV / 69 kV step up transformers before the period of extended operation and at least once every 10 years after the initial test.	March 21, 2012	BVY 07-009 BVY 07-018	Am. 24 Response to: RAIs 3.6.2.2-N-08-2 3.6.2.2-N-08-4

ITEM	COMMITMENT	IMPLEMENTATION SCHEDULE	SOURCE	Related LRA Section No./ Comments
44	Guidance for performing examinations of buried piping will be revised to include the following. "A focused inspection will be performed within the first 10 years of the period of extended operation, unless an opportunistic inspection (or an inspection via a method that allows an assessment of pipe condition without excavation) occurs within this ten-year period."	March 21, 2012	BVY 07-018	Regional inspection
45	Enhance the Service Water Integrity Program to require a periodic visual inspection of the RHRSW pump motor cooling coil internal surface for loss of material.	March 21, 2012	BVY 07-018	Regional inspection
46	Enhance the Diesel Fuel Monitoring Program to specify that fuel oil in the fire pump diesel storage (day) tank will be analyzed according to ASTM D975-02 and for particulates per ASTM D2276. Also, fuel oil in the John Deere diesel storage tank will be analyzed for particulates per ASTM D2276.	March 21, 2012	BVY 07-018	Regional inspection
47	Enhance the Diesel Fuel Monitoring Program to specify that fuel oil in the common portable fuel oil storage tank will be analyzed according to ASTM D975-02, per ASTM D2276 for particulates, and ASTM D1796 for water and sediment.	March 21, 2012	BVY 07-018	Regional inspection
48	Perform an internal inspection of the underground Service Water piping before entering the period of extended operation.	March 21, 2012	BVY 07-018	Regional inspection
49	Revise station procedures to specify fire hydrant hose testing, inspection, and replacement, if necessary, in accordance with NFPA code specifications for fire hydrant hoses.	March 21, 2012	BVY 07-009	Audit Item 38

ITEM	COMMITMENT	IMPLEMENTATION SCHEDULE	SOURCE	Related LRA Section No./ Comments
50	During the period of extended operation, review the Vernon Dam owner FERC required report(s) at a minimum of every five years to confirm that the Vernon Dam owner is performing the required FERC inspections. Document deficiencies in the Entergy Corrective Actions Program and evaluate operability as described in BVY 96-043 and BVY 97-043 if it is determined that the required inspections are not being performed.	March 21, 2012	BVY 06-009 BVY 07-047	RAI 3.6.2.2.N-08-1
51	Entergy will perform an evaluation of operating experience at extended power uprate (EPU) levels prior to the period of extended operation to ensure that operating experience at EPU levels is properly addressed by the aging management programs. The evaluation will include Vermont Yankee (VY) and other BWR plants operating at EPU levels.	March 21, 2012	BVY-08-008	N/A

Structural Integrity Associates, Inc.	File No.: VY-16Q-301
CALCULATION PACKAGE	Project No.: VY-16Q

PROJECT NAME:

Environmental Fatigue Analysis of VYNPS

CONTRACT NO.:

10150394

CLIENT:	**PLANT:**
Entergy Nuclear Operations, Inc	Vermont Yankee Nuclear Power Station

CALCULATION TITLE:

Feedwater Nozzle Stress History Development for Green Functions

Document Revision	Affected Pages	Revision Description	Project Manager Approval Signature & Date	Preparer(s) & Checker(s) Signatures & Date
0	1-27, Appendix: A1-A2	Initial Issue	Terry J. Herrmann 07/12/2007	Minghao Qin 07/11/07 John F. Staples 07/11/07

Table of Contents

1.0 OBJECTIVE 4
2.0 FEEDWATER NOZZLE MODEL 4
3.0 APPLIED LOADS 4
4.0 THERMAL AND PRESSURE LOAD RESULTS 7
5.0 REFERENCES 9
APPENDIX A FINITE ELEMENT ANALYSIS FILES A1

List of Tables

Table 1: Material Properties @ 300°F 10
Table 2: Nodal Force Calculation for End Cap Load 10
Table 3: Pressure Results 11
Table 4: Heat Transfer Coefficients for Region 1 (40% Flow) 11

List of Figures

Figure 1: ANSYS Finite Element Model 12
Figure 2: Feedwater Nozzle Internal Pressure Distribution 13
Figure 3: Feedwater Nozzle Pressure Cap Load 14
Figure 4: Feedwater Nozzle Vessel Boundary Conditions 15
Figure 5: Nozzle and Vessel Wall Thermal and Heat Transfer Boundaries [1] 16
Figure 6: Safe End Critical Thermal Stress Location 17
Figure 7: Safe End Limiting Linearized Stress Paths 18
Figure 8: Blend Radius Limiting Pressure Stress Location 19
Figure 9: Blend Radius Linearized Stress Path 20
Figure 10: Safe End 100% Flow Total Stress Intensity 21
Figure 11: Blend Radius 100% Flow Total Stress Intensity 21
Figure 12: Safe End Total Stress History for 100% Flow 22
Figure 13: Safe End Membrane Plus Bending Stress History for 100% Flow 22
Figure 14: Safe End Total Stress History for 40% Flow 23
Figure 15: Safe End Membrane Plus Bending Stress History for 40% Flow 23
Figure 16: Safe End Total Stress History for 25% Flow 24
Figure 17: Safe End Membrane Plus Bending Stress History for 25% Flow 24
Figure 18: Blend Radius Total Stress History for 100% Flow 25
Figure 19: Blend Radius Membrane Plus Bending Stress History for 100% Flow 25
Figure 20: Blend Radius Total Stress History for 40% Flow 26
Figure 21: Blend Radius Membrane Plus Bending Stress History for 40% Flow 26
Figure 22: Blend Radius Total Stress History for 25% Flow 27
Figure 23: Blend Radius Membrane Plus Bending Stress History for 25% Flow 27

1.0 OBJECTIVE

The objective of this calculation is to compute the pressure stresses, thermal stresses, and the Green's Functions for high (100%), mid (40%), and low (25%) flow thermal loading of the Vermont Yankee Nuclear Power Station feedwater nozzle.

2.0 FEEDWATER NOZZLE MODEL

An axisymmetric finite element model of the feedwater nozzle was developed in Reference [1] using ANSYS [2]. The geometry used in Reference [1] was utilized in this calculation. The material properties are taken at an average temperature of 300°F. This average temperature is based on a thermal shock of 500°F to 100°F which will be applied to the FE model for Green's Function development. Table 1 listed the material properties at 300°F. The meshed model is shown in Figure 1.

3.0 APPLIED LOADS

Both pressure and thermal loads will be applied to the finite element model.

3.1 Pressure Load

A uniform pressure of 1000 psi was applied along the inside surface of the feedwater nozzle and the vessel wall. A pressure load of 1000 psi was used because it is easily scaled up or down to account for different pressures that occur during transients. In addition, a cap load was applied to the piping at the end of the nozzle. Since only nodes were modeled, the nodal forces shown in Table 2 are defined by the following equation:

$$F_{element} = \pi (IR)^2 P \cdot \frac{\pi\left(R_o^{\,2} - R_i^{\,2}\right)}{\pi\left(OR^2 - IR^2\right)}$$

where:

P = Pressure = 1,000 psi
IR = Inner Radius = 4.8345 in
OR = Outer Radius = 5.42 in
R_i = Inside Radius of element that node is attached to
R_o = Outside Radius of element that node is attached to
F_{node} = The average of the element forces on either side of the node.
Note: The force on the innermost and outermost nodes is calculated as one half of the force on the element that they are attached to.

The calculated nodal forces were applied as positive values so they would exert tension on the end of the model. The ANSYS input file FWP_VY.INP, in the computer files, contains the feedwater

nozzle geometry as well as the pressure loading. Figures 2, 3, and 4 show the internal pressure distribution, cap load, and symmetry condition applied to the vessel end of the model, respectively.

3.2 Thermal Load

Thermal loads are applied to the feedwater nozzle model. The heat transfer coefficients after power uprate were determined from Reference [1]. These values were determined for various regions of the finite element model for 100% (4,590 GPM), and 25% (1,148 GPM) [1]. The annulus leakage flow rate is assumed to be 25 GPM for non-EPU conditions and 31 GPM for EPU conditions. The 25 GPM value is calculated by scaling the 23 GPM [Page 6, 4] value up by approximately 9%. The 23 GPM value is scaled up to provide some conservatism and allow for inaccuracies in the determination of leakage flow. The 31 GPM value is calculated by multiplying the 25 GPM value by 1.25 [Page 6, 4]. Based on this, the annulus leakage flow rate is assumed to be 8 GPM for EPU conditions with 25% flow rate. The temperatures used are based upon a thermal shock from 500°F to 100°F. An additional 40% flow rate (1836 GPM and 13 GPM) was added in this calculation.

3.2.1 *Heat Transfer Coefficients*

Referring to Figure 5, heat transfer coefficients were applied as following:

Region 1

The heat transfer coefficient, h, for 100% flow is 3705 BTU/hr-ft^2-°F at 300°F. [1, Table 5]

The heat transfer coefficient, h, for 40% flow is 1780 BTU/hr-ft^2-°F at 300°F. [Table 4]

The heat transfer coefficient, h, for 25% flow is 1222.2 BTU/hr-ft^2-°F at 300°F. [1, Table 4]

Region 2

Per Reference [1], the heat transfer coefficient for Region 2 (safe end-to-thermal sleeve contact region) should be linearly transitioned from the value of the heat transfer coefficient used in Region 1 to the value used in Region 3.

Region 3

The heat transfer coefficient, h, for 100% flow is 1489 BTU/hr-ft^2-°F at 300°F. [1, Table 9]

The heat transfer coefficient, h, for 40% flow is 743 BTU/hr-ft^2-°F at 300°F. [1, Table 9]

The heat transfer coefficient, h, for 25% flow is 504 BTU/hr-ft^2-°F at 300°F. [1, Table 9]

Region 4

Per Reference [1], the he heat transfer coefficient for Region 4 (thermal sleeve transition in diameter) should be linearly transitioned from the value of the heat transfer coefficient used in Region 3 to the value used in Region 5.

Region 5

The heat transfer coefficient, h, for 100% flow is 177.4 BTU/hr-ft^2-°F at 300°F. [1, Table 16]

The heat transfer coefficient, h, for 40% flow is 88.5 BTU/hr-ft^2-°F at 300°F. [1, Table 16]

The heat transfer coefficient, h, for 25% flow is 60 BTU/hr-ft^2-°F at 300°F. [1, Table 16]

Region 6

Per Reference [1], the heat transfer coefficient for Region 6 (nozzle inner blend radius) should be linearly transitioned from the value of the heat transfer coefficient used in Region 5 to the value used in Region 7.

Region 7

Per Reference [1], the heat transfer coefficient for Region 7 (reactor vessel inside wall) is a constant of 864 BTU/hr-ft^2-°F. This value is consistent with the feedwater nozzle work performed in the past for VY and should be used for all reactor conditions.

Region 8

The heat transfer coefficient, h, is 0.2 BTU/hr-ft^2-°F [1].

3.2.2 *Boundary Fluid Temperatures*

For the Green's Functions, a 500°F – 100°F thermal shock is run to determine the stress response to a one-degree change in temperature. The following temperatures are valid when there is water flow. Values between defined points are linearly interpolated. For the 100%, 40%, and 25% flow cases, the thermal shock is run as follows:

Regions 1 to 5
T = 500°F – 100°F
Region 6
Linearly transitioned from the value of the temperature used in Region 5 to the value used in Region 7
Region 7
T = 500°F
Region 8
T = 120°F

4.0 THERMAL AND PRESSURE LOAD RESULTS

The three flow dependent thermal load cases outlined in Section 3.0 were run on the finite element model. Appendix A contains the thermal transient input files FWT_VY_100.INP, FWT_VY_40.INP, and FWT_VY_25.INP for 100%, 40%, and 25% full flow rate, respectively. The three flow dependent input files for the stress runs are also included in Appendix A. The stress filenames are FWS_VY_100.INP, FWS_VY_40.INP, and FWS_VY_25.INP for 100%, 40%, and 25% full flow rate, respectively.

The critical safe end location was chosen as node 192, which has the highest stress intensity due to thermal loading under high flow conditions. As shown in Figures 6 and 7, Node 192 is located on the inside diameter of the nozzle safe end of the model and the maximum stress occurs at 1.4 seconds.

The critical blend radius location was chosen, based upon the highest pressure stress. Conservatively assuming the cladding has cracked, the critical location is selected as node 657 at base metal of the nozzle, as shown in Figures 8 and 9.

The stress intensity for use in the Green's functions are calculated from the component stresses (X, Y, and Z) and compared to the stress intensity reported by ANSYS. As seen in Figure 10, the Z-X calculated total stress intensity best matches the ANSYS reported stress intensity for 100% flow at the safe end. Therefore, the Z-X stress will be used for the total and membrane plus bending Green's functions for all flow rates for the safe end. As seen in Figure 11, the Z-X calculated total stress intensity best matches the ANSYS reported stress intensity for 100% flow at the blend radius in very beginning. Therefore, the Z-X stress will be used for the total and membrane plus bending Green's functions for all flow rates for the blend radius.

The stress time history for the critical paths was extracted during the stress run for 100% flow rate. This produced two files, HFSE.OUT and HFBLEND.OUT, which contain the thermal stress history. The membrane plus bending stresses and total stresses for the Green's Functions were extracted from these files to produce the files HFSE_Inside.RED and HFBLEND_Inside.RED, where SE and BLEND corresponded to the safe end and blend radius locations, respectively.

The stress time history for the critical paths was extracted during the stress run for 40% flow rate. This produced two files, MFSE.OUT and MFBLEND.OUT, which contain the thermal stress history. The membrane plus bending stresses and total stresses for the Green's Functions were extracted from these files to produce the files MFSE_Inside.RED and MFBLEND_Inside.RED, where SE and BLEND corresponded to the safe end and blend radius locations, respectively.

The stress time history for the critical paths was extracted during the stress run for 25% flow rate. This produced two files, LFSE.OUT and LFBLEND.OUT, which contain the thermal stress history. The membrane plus bending stresses and total stresses for the Green's Functions were extracted from these files to produce the files LFSE_Inside.RED and LFBLEND_Inside.RED, where SE and BLEND corresponded to the safe end and blend radius locations, respectively.

As the models were run with a 400°F step change in temperature, and the Green's Functions are for a 1°F step change in temperature, all data values were divided by 400. The governing Green's Functions for the feedwater nozzle during 100% flow, 40% flow, and 25% flow are shown in Figures 12 to 23. The data for the Green's Functions is included in the files HFBR_M+B-Green.xls, HFBR_T-Green.xls, HFSE_M+B-Green.xls, HFSE_T-Green.xls, MFBR_M+B-Green.xls, MFBR_T-Green.xls, MFSE_M+B-Green.xls, MFSE_T-Green.xls, LFBR_M+B-Green.xls, LFBR_T-Green.xls,LFSE_M+B-Green.xls, and LFSE_T-Green.xls in the project Files. Where HF, MF, and LF corresponded to 100% flow, 40% flow, and 25% flow rate, respectively. M+B and T corresponded to membrane plus bending stress and total stress, respectively.

The pressure stress intensities for the path were extracted during the pressure run. The pressure stresses were extracted along the nodal paths as shown in Figures 7 and 9. This produced two files, PSE.OUT and PBLEND.OUT for the safe end and blend radius locations, respectively.

For the pressure loading specified (1,000 psig), the total stress intensity at Node 192 and Node 657 were determined to be 8,891 psi and 28,300 psi, respectively. The membrane plus bending stress intensity at Node 192 and Node 657 were determined to be 8,693 and 27,490 psi, respectively. Table 3 shows the pressure results.

Results were also extracted from the vessel portion of the model to verify the accuracy of the pressure results obtained from the ANSYS model, and to check the results due to the use of the 1.5 multiplier on the vessel radius. These results are contained in the file, PVESS.OUT. Based on earlier work [1], the radius of the finite element model (FEM) was multiplied by a factor of 1.5 to account for the fact that the vessel portion of the two-dimensional (2D) axisymmetric model is a sphere, but the true geometry is the intersection of two cylinders.

The equation for the membrane hoop stress for a sphere is:

$$\sigma = \frac{(pressure) \times (radius)}{2 \times thickness}$$

Considering a vessel base metal radius, R, of 105.90625 inches increased by a factor of 1.5, a vessel base metal thickness, t, of 5.4375 inches, and an applied pressure, P, of 1,000 psi, the calculated stress for a sphere is PR/(2t) = 14,608 psi. This compares very well with the remote vessel wall membrane hoop stress from the ANSYS result file, PVESS.OUT, of 13,410 psi. Thus, considering the peak total pressure stress of 28,300 psi reported above, the stress concentrating effect of the nozzle corner is 28,300/14,608 = 1.94. In other words, the peak nozzle corner stress is 1.94 times higher than nominal vessel wall stress for the 2D axisymmetric model.

The equation for the membrane hoop stress in a cylinder is:

$$\sigma = \frac{(pressure) \times (radius)}{thickness}$$

Based on the previous dimensions, the calculated stress for a cylinder without the 1.5 factor is 19,477 psi. Increasing this by a factor of 1.94 yields an expected peak nozzle corner stress of 37,785 psi, which would be expected from a cylindrical geometry that is representative of the nozzle configuration. Therefore, the result from the ANSYS file for the peak nozzle corner stress (28,300 psi) is lower than the peak nozzle corner stress for a cylindrical geometry because of the use of the 1.5 multiplier. This is consistent with SI's experience where a factor of two increase in radius is typical for representing the three-dimensional (3D) effect in a 2D axisymmetric model.

Based on the foregoing, the ANSYS pressure stresses for the vessel blend radius are increased for use in the subsequent fatigue analysis by 1.33 (2.0/1.5). Thus, the blend radius results presented in Table 3 were obtained by multiplying the ANSYS stresses for the pressure loading by a 1.33X multiplication factor.

5.0 REFERENCES

1. SI Calculation No. VY-10Q-301, Revision 0, "Feedwater Nozzle Finite Element Model and Heat Transfer Coefficients."
2. ANSYS, Release 8.1 (w/Service Pack 1), ANSYS, Inc., June 2004.
3. American Society of Mechanical Engineers, Boiler and Pressure Vessel Code, Section II, Part D, 1998 Edition, 2000 Addenda.
4. VY Calculation Change Notice (CCN), CCN Number 1 for Calculation VYC1005 Revision 2, "This CCN Provides a Basis for the Power Uprate Safety Analysis Report being submitted as part of the power uprate project. The 50.59 assessment will be handled by the EPU design change and NRC SER for this submittal." SI File Number VY-05Q-208.
5. J. P. Holman, "Heat Transfer," 4th Edition, McGraw-Hill, 1976.
6. J. P. Holman, "Heat Transfer," 5th Edition, 1981.
7. GE Nuclear Energy Certified Design Specification, "Reactor Vessel – Extended Power Uprate," Revision 1, SI File No. VY-05Q-236.
8. N. P. Cheremisinoff, "Heat Transfer Pocket Handbook," Gulf Publishing Co, 1984.

Table 1: Material Properties @ 300°F (1)

Material Ident.	Young's Modulus, E x 10^6 (psi)	Instantaneous Coefficient of Thermal Expansion, α x 10^{-6} (in/in-°F)	Density, ρ (lb/in^3) (assumed)	Conductivity, k (BTU/hr-ft-°F)	Diffusivity, d (ft^2/hr)	Specific Heat, c_p (BTU/lbm-°F) (see Note 5)	Poisson's Ratio (assumed)
SA533 Grade B, A508 Class II (see Note 2)	26.7	7.3	0.283	23.4	0.401	0.119	0.3
SS Clad (see Note 3)	27.0	9.8	0.283	9.8	0.160	0.125	0.3
A508 Class I (see Note 4)	28.1	7.3	0.283	32.3	0.561	0.118	0.3
A106 Grade B (see Note 4)	28.3	7.3	0.283	32.3	0.561	0.118	0.3

Notes

1. The material properties applied in the analyses are taken from ASME Section II Part D 1998 Edition with 2000 Addenda. This is consistent with information provided in the Design Input Record (page 13 of VY EC No. 1773, SI File No. VY-16Q-209). The use of a later code edition than that used for the original design code is acceptable since later editions typically reflect more accurate material properties than was published in prior Code editions. Material Properties are evaluated at 300°F from the 1998 ASME Code, 2000 Addenda, Section II, Part D, except for density and Poisson's ratio, which are assumed typical values [3].
2. Properties of A508 Class II are used (3/4Ni-1/2Mo-1/3Cr-V).
3. Properties of 18Cr - 8Ni austenitic stainless steel are used.
4. Composition = C-Si.
5. Calculated as $[k/(\rho d)]/12^3$.

Table 2: Nodal Force Calculation for End Cap Load

Node Number	Element Number	Radius (in)	Δ Radius (in)	R_o^2-Ri^2 (in^2)	$F_{element}$ (lb)	F_{node} (lb)
1		5.42				7678.0
	1022		0.1171	1.25565	15356.1	
2		5.3029				15188.4
	1021		0.1171	1.22823	15020.7	
3		5.1858				14853.0
	1020		0.1171	1.20080	14685.3	
4		5.0687				14517.6
	1019		0.1171	1.17338	14349.9	
5		4.9516				14182.2
	1018		0.1171	1.14595	14014.5	
6		4.8345				7007.3

Table 3: Pressure Results

Location	Membrane Plus Bending Stress Intensity (psi)	Total Stress Intensity (psi)
Safe End	8693	8891
Blend Radius	36653	37733

Note: The results for the Blend Radius have been increased by a factor of 1.33 (2.0/1.5) as discussed in Section 4.0.

Table 4: Heat Transfer Coefficients for Region 1 (40% Flow)

Calculation of Heat Transfer Coefficients for Feedwater Nozzle Flow Path

Pipe Inside Diameter, D = 9.669 inches = 0.806 ft = 0.246 m

Flow, % of rated = 40%

Fluid Velocity, V = 8.022 ft/sec = 1,836.0 gpm = 0.793742524 Mlb/hr

Characteristic Length, L = D = 0.806 ft = 0.246 m

100% rated flow = 4,590 gpm; @ T = 391.9 °F; Density, ρ = 53.8997 lbm/ft³

$T_{fluid} - T_{surface}$, ΔT = assumed to be 12% of fluid temperature = 8.40 12.00 24.00 36.00 48.00 60.00 72.00 °F

= 4.67 6.67 13.33 20.00 26.67 33.33 40.00 °C

Note: The above assumption is based on experience with past RPV heat transfer analyses.

		Value at Fluid Temperature, T [8]							Units
Water Property	**Conversion Factor [5]**	**70**	**100**	**200**	**300**	**400**	**500**	**600**	°F
		21.11	**37.78**	**93.33**	**148.89**	**204.44**	**260.00**	**315.56**	°C
k	1.7307	0.5997	0.6300	0.6784	0.6836	0.6611	0.6040	0.5071	W/m-°C
(Thermal Conductivity)		0.3465	0.3640	0.3920	0.3950	0.3820	0.3490	0.2930	Btu/hr-ft-°F
c_p	4.1869	4.185	4.179	4.229	4.313	4.522	4.982	6.322	kJ/kg-°C
(Specific Heat)		1.000	0.998	1.010	1.030	1.080	1.190	1.510	Btu/lbm-°F
ρ	16.018	997.1	994.7	962.7	917.8	858.6	784.9	679.2	kg/m³
(Density)		62.3	62.1	60.1	57.3	53.6	49.0	42.4	lbm/ft³
β	1.8	1.89E-04	3.24E-04	6.66E-04	1.01E-03	1.40E-03	1.98E-03	3.15E-03	m³/m³-°C
(Volumetric Rate of Expansion)		1.05E-04	1.80E-04	3.70E-04	5.60E-04	7.80E-04	1.10E-03	1.75E-03	ft³/ft³-°F
g	0.3048	9.806	9.806	9.806	9.806	9.806	9.806	9.806	m/s²
(Gravitational Constant)		32.17	32.17	32.17	32.17	32.17	32.17	32.17	ft/s²
μ	1.4881	9.96E-04	6.82E-04	3.07E-04	1.93E-04	1.38E-04	1.04E-04	8.62E-05	kg/m-s
(Dynamic Viscosity)		6.69E-04	4.58E-04	2.06E-04	1.30E-04	9.30E-05	7.00E-05	5.79E-05	lbm/ft-s
Pr		6.980	4.510	1.910	1.220	0.950	0.859	1.070	---
(Prandtl Number)									
Calculated Parameter	**Formula**	**70**	**100**	**200**	**300**	**400**	**500**	**600**	°F
Reynold's Number, Re	$\rho VD/\mu$	6.0147E+05	8.7645E+05	1.8859E+06	2.8491E+06	3.7255E+06	4.5248E+06	4.7336E+06	---
Grashof Number, Gr	$g\beta\Delta TL^3/(\mu/\rho)^2$	1.2852E+08	6.6834E+08	1.2721E+10	6.5918E+10	2.0931E+11	5.4429E+11	1.1372E+12	---
Rayleigh Number, Ra	GrPr	8.9710E+08	3.0142E+09	2.4297E+10	8.0420E+10	1.9885E+11	4.6755E+11	1.2168E+12	---
From [5]:									
Inside Surface Forced Convection Heat Transfer Coefficient:									
H_{forced} =	$0.023Re^{0.8}Pr^{0.4}k/D$	5,132.76	6,119.10	8,626.61	10,107.53	10,960.57	11,236.63	10,678.39	W/m²-°C
		903.95	**1,077.66**	**1,519.26**	**1,780.07**	**1,930.31**	**1,978.92**	**1,880.61**	Btu/hr-ft²-°F
		1.744E-03	**2.079E-03**	**2.931E-03**	**3.434E-03**	**3.724E-03**	**3.817E-03**	**3.628E-03**	Btu/sec-in²-°F
From [5]:									
Inside Surface Natural Convection Heat Transfer Coefficient:									
Case:	Enclosed cylinder		C =	0.55	n =	0.25	(see page 289 of [6])		
H_{free} =	$C(GrPr)^n k/L$	232.43	330.57	599.85	815.28	988.69	1,118.54	1,192.73	W/m²-°C
		40.93	**58.22**	**105.64**	**143.58**	**174.12**	**196.99**	**210.06**	Btu/hr-ft²-°F
		7.896E-05	**1.123E-04**	**2.038E-04**	**2.770E-04**	**3.359E-04**	**3.800E-04**	**4.052E-04**	Btu/sec-in²-°F

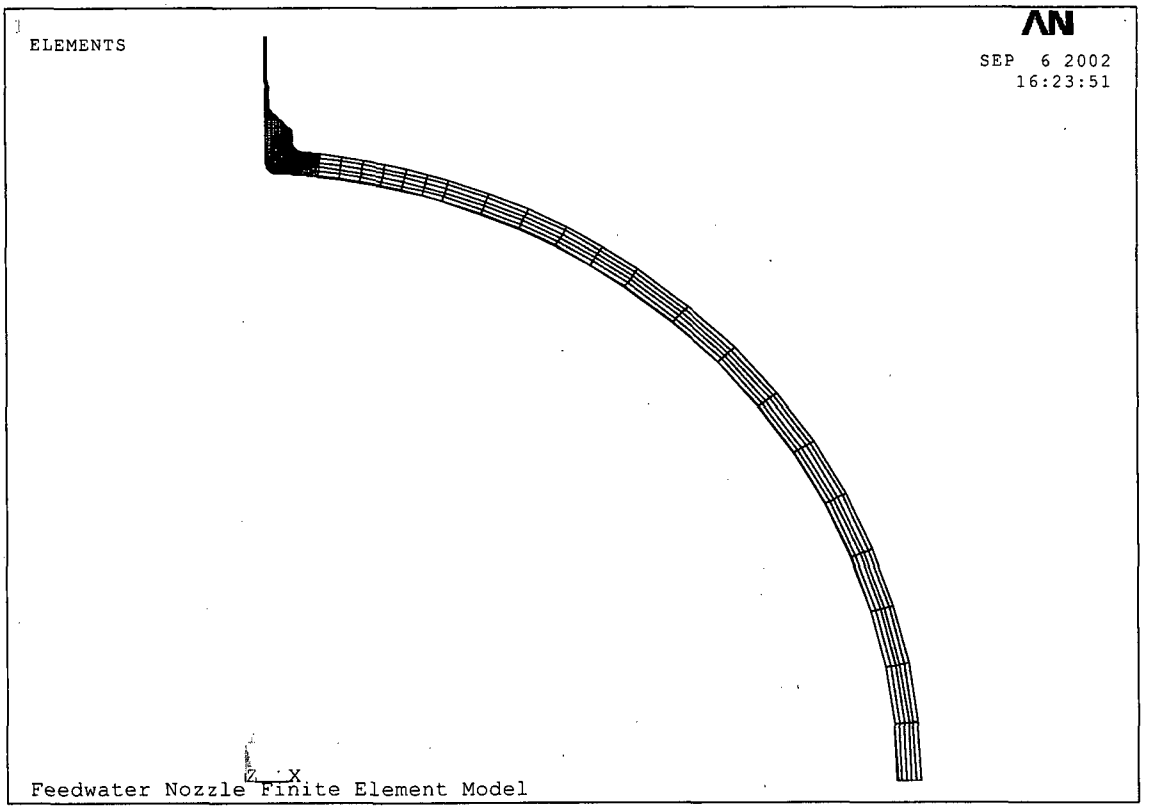

Figure 1: ANSYS Finite Element Model

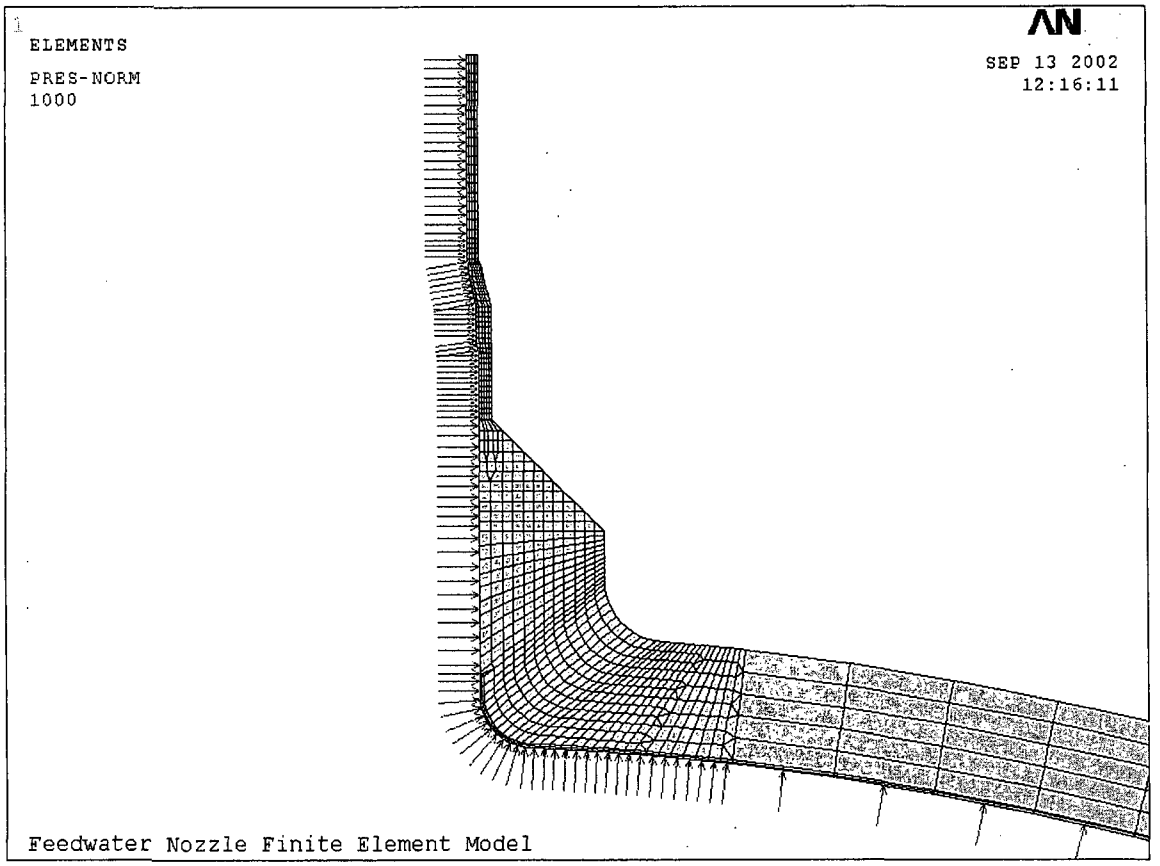

Figure 2: Feedwater Nozzle Internal Pressure Distribution

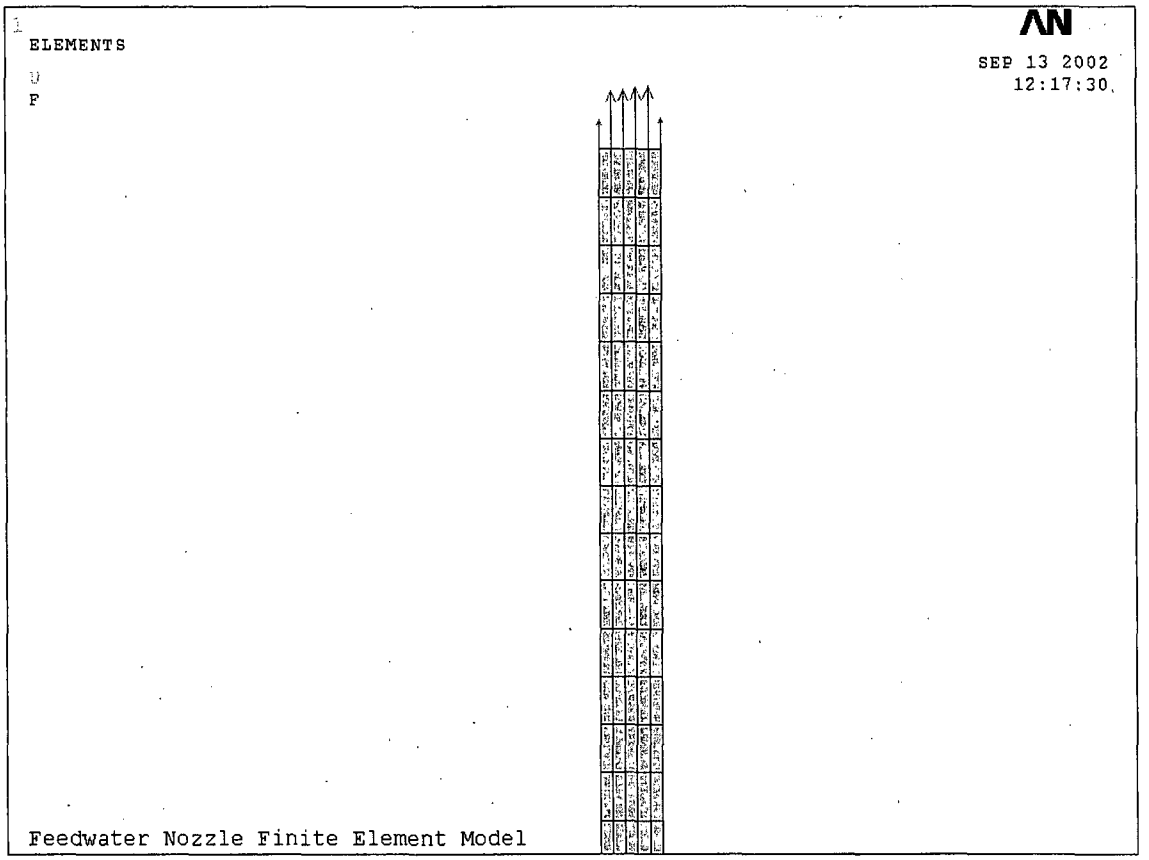

Figure 3: Feedwater Nozzle Pressure Cap Load

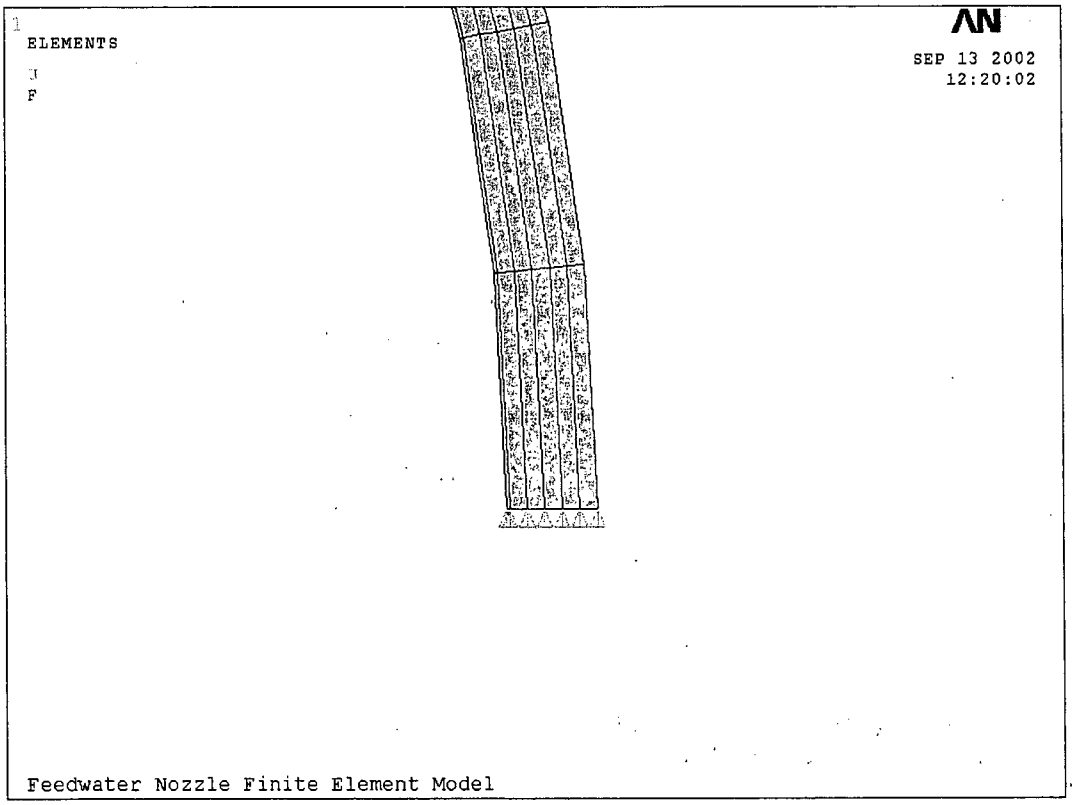

Figure 4: Feedwater Nozzle Vessel Boundary Conditions

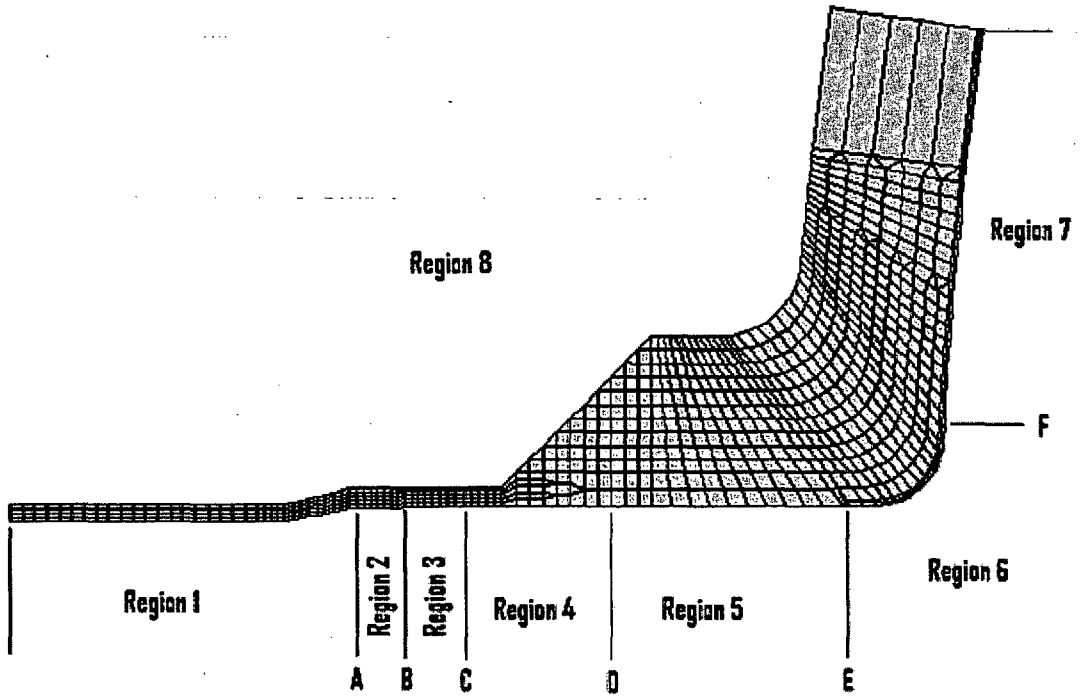

Notes: Point A: End of thermal sleeve = Node 204 = 0.25" from feedwater inlet side of thermal sleeve flat.
Point B: Beginning of annulus = Node 252.
Point C: Beginning of thermal sleeve transition = approximately 4.0" from Point A = Node 294.
Point D: End of thermal sleeve transition = approximately 9.5" from Point A = Node 387.
Point E: End of inner blend radius (nozzle side) = Node 553.
Point F: End of inner blend radius (vessel wall side) = Node 779.

Figure 5: Nozzle and Vessel Wall Thermal and Heat Transfer Boundaries [1]

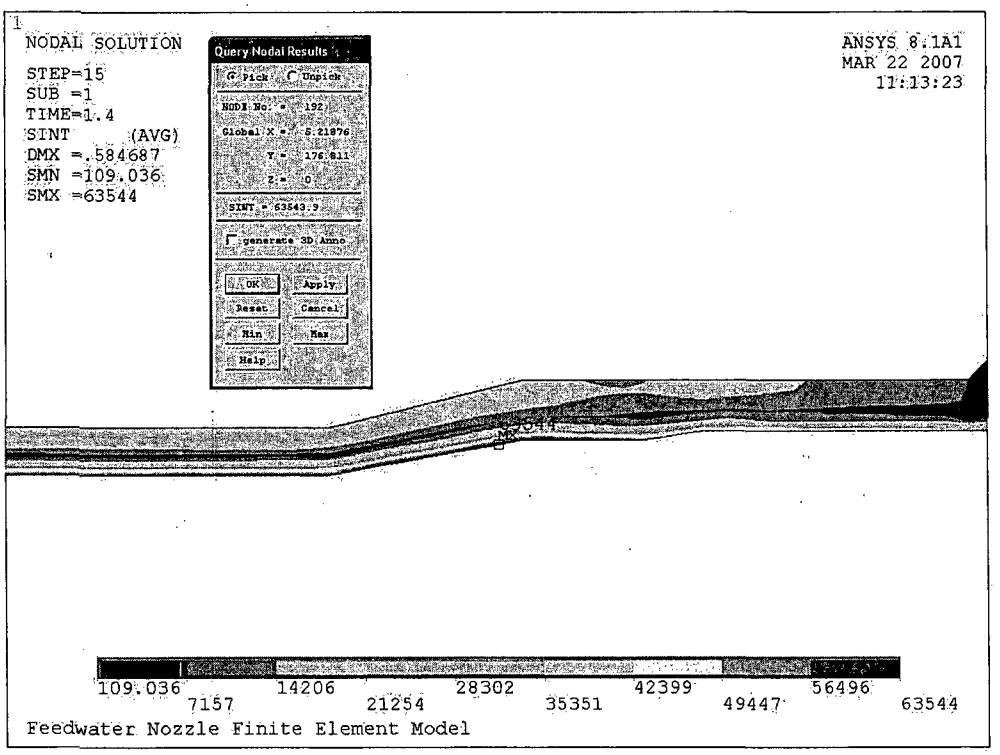

Figure 6: Safe End Critical Thermal Stress Location

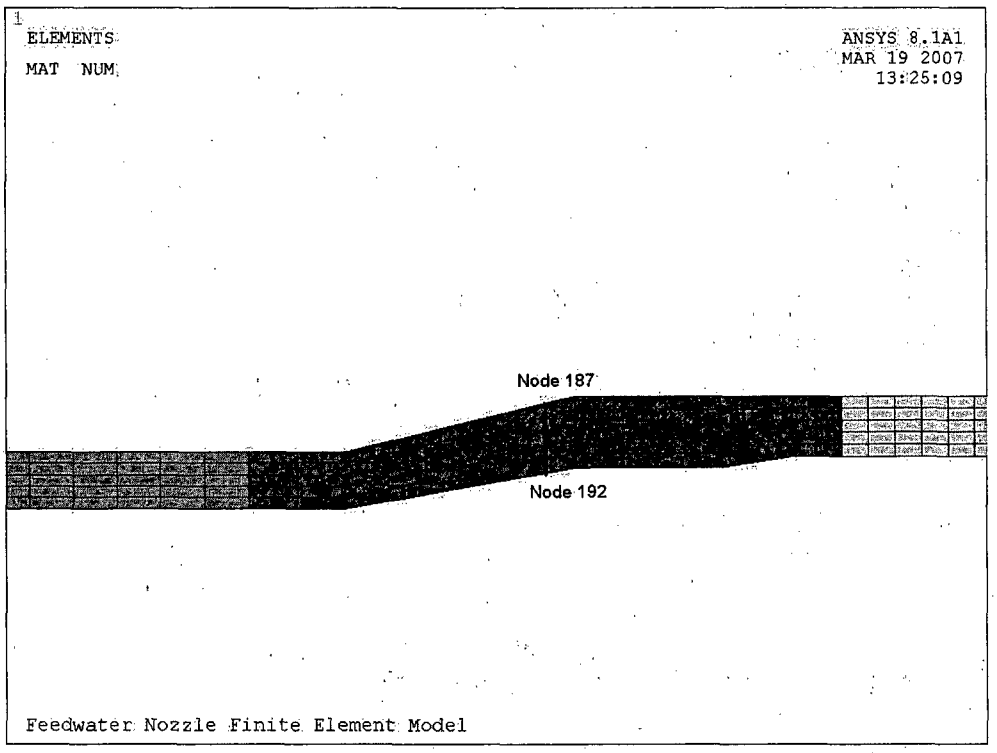

Figure 7: Safe End Limiting Linearized Stress Paths

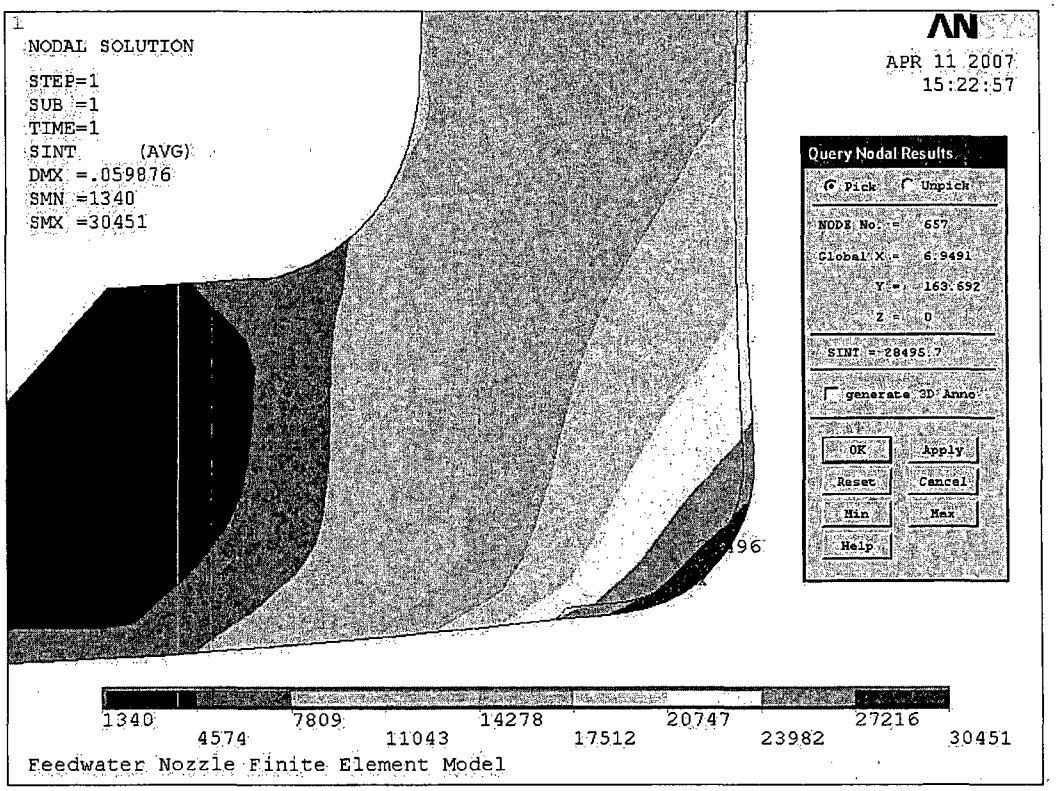

Figure 8: Blend Radius Limiting Pressure Stress Location

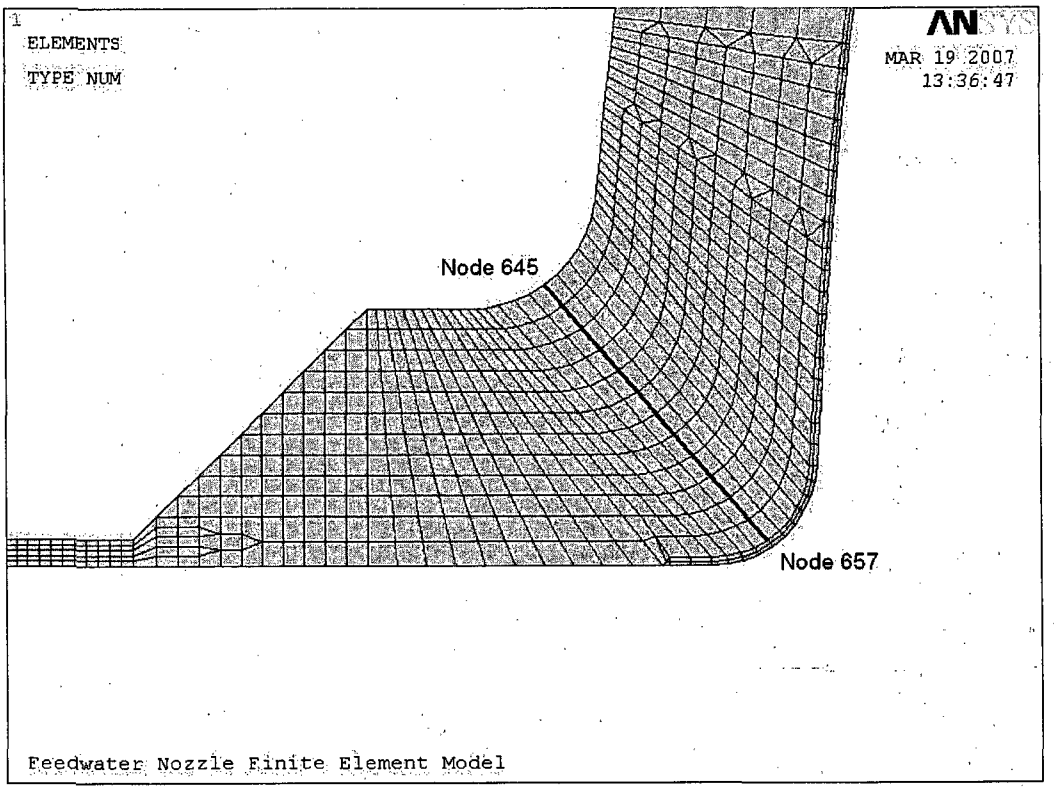

Figure 9: Blend Radius Linearized Stress Path

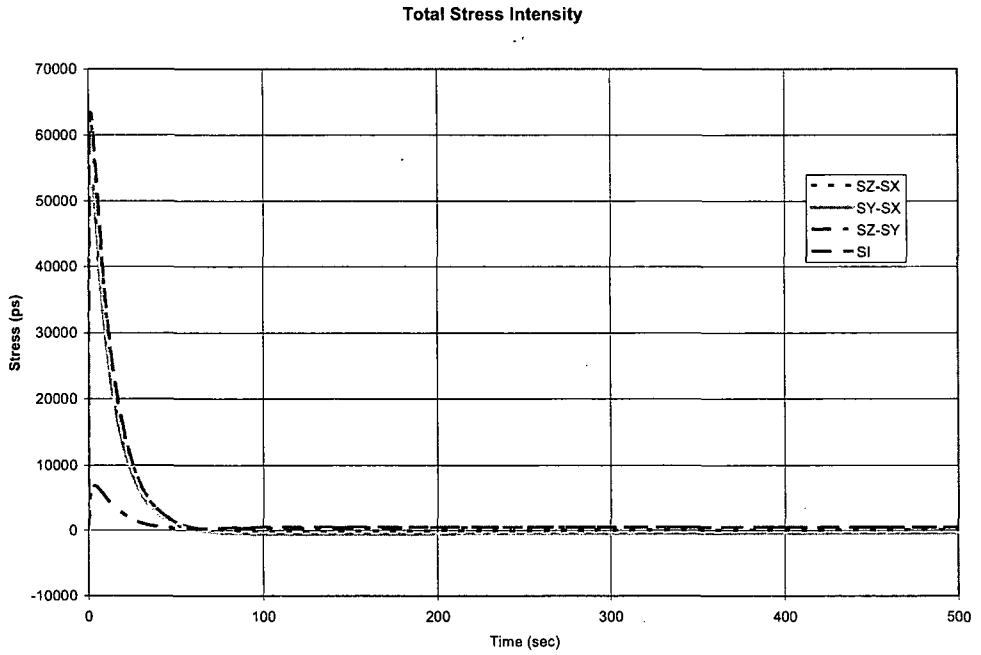

Figure 10: Safe End 100% Flow Total Stress Intensity

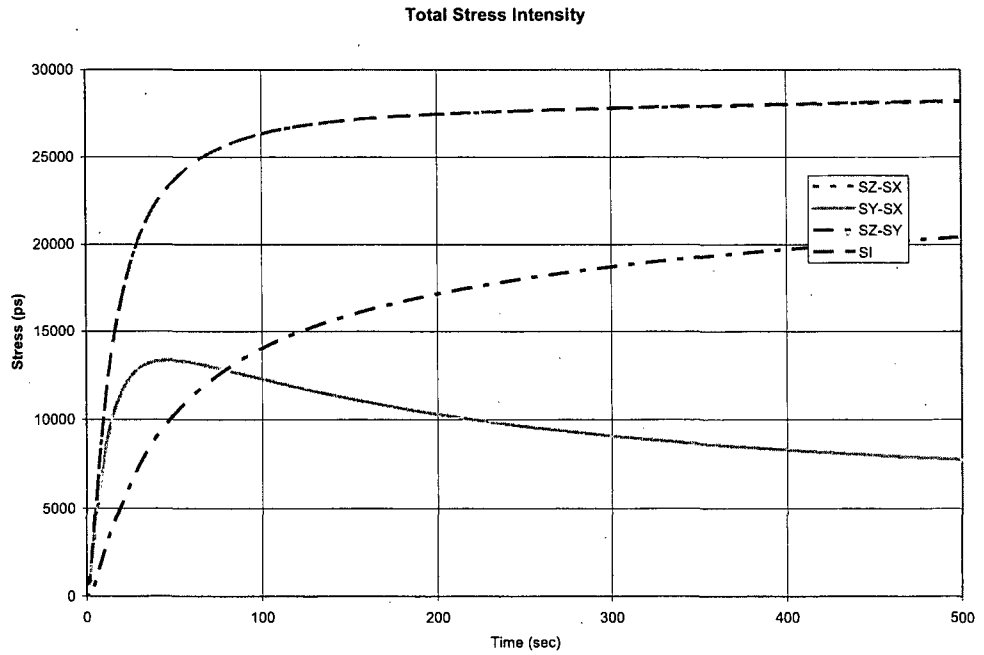

Figure 11: Blend Radius 100% Flow Total Stress Intensity

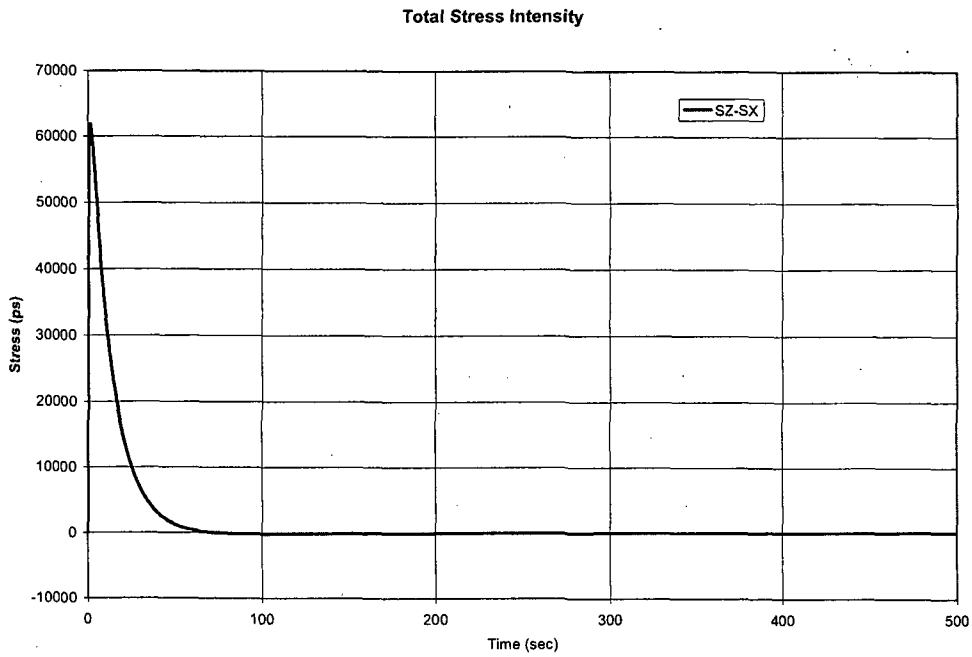

Figure 12: Safe End Total Stress History for 100% Flow

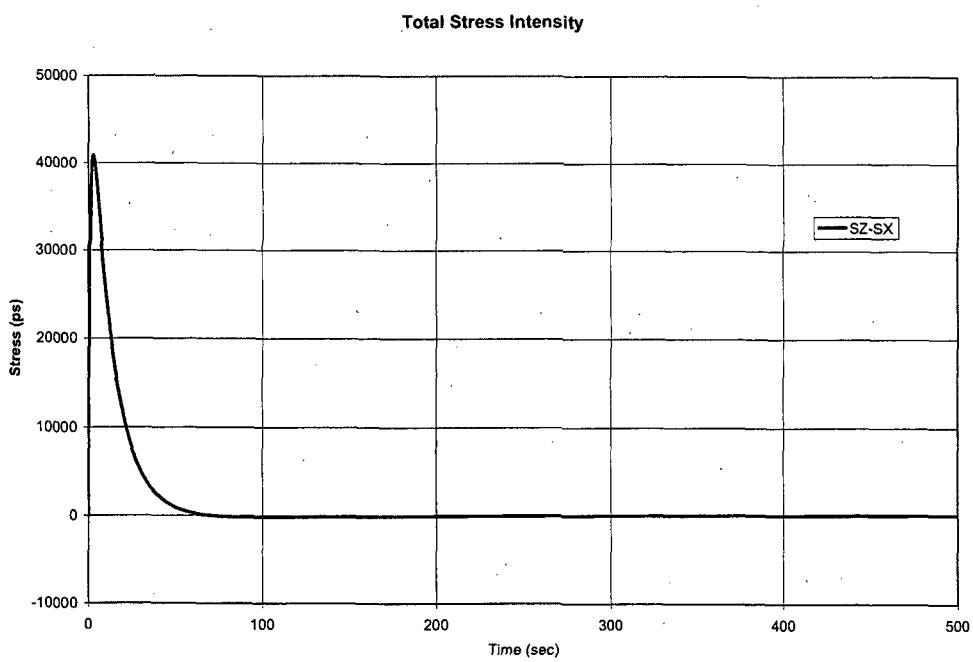

Figure 13: Safe End Membrane Plus Bending Stress History for 100% Flow

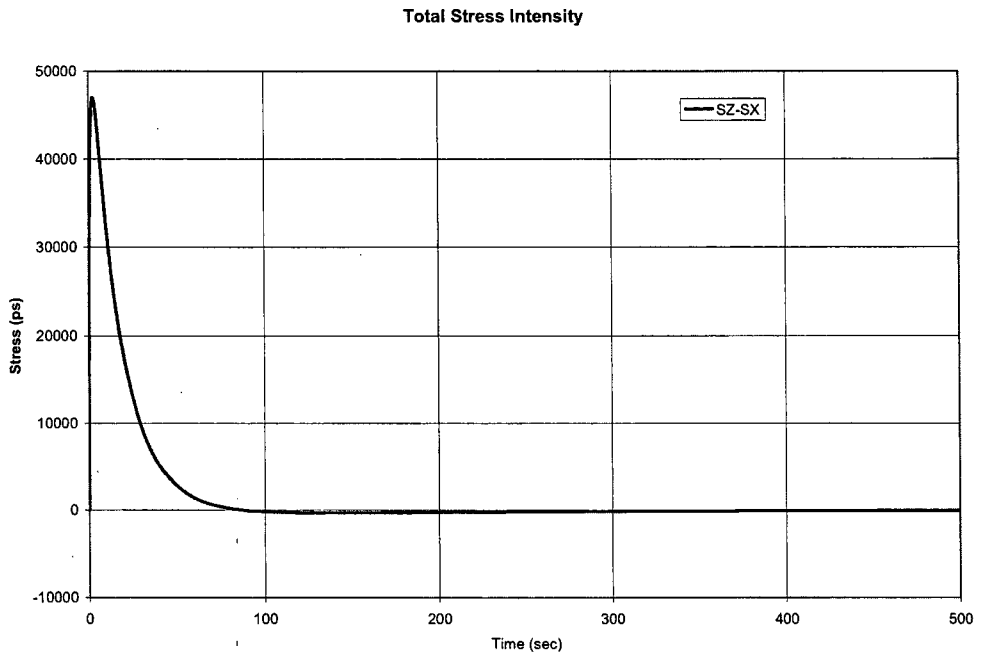

Figure 14: Safe End Total Stress History for 40% Flow

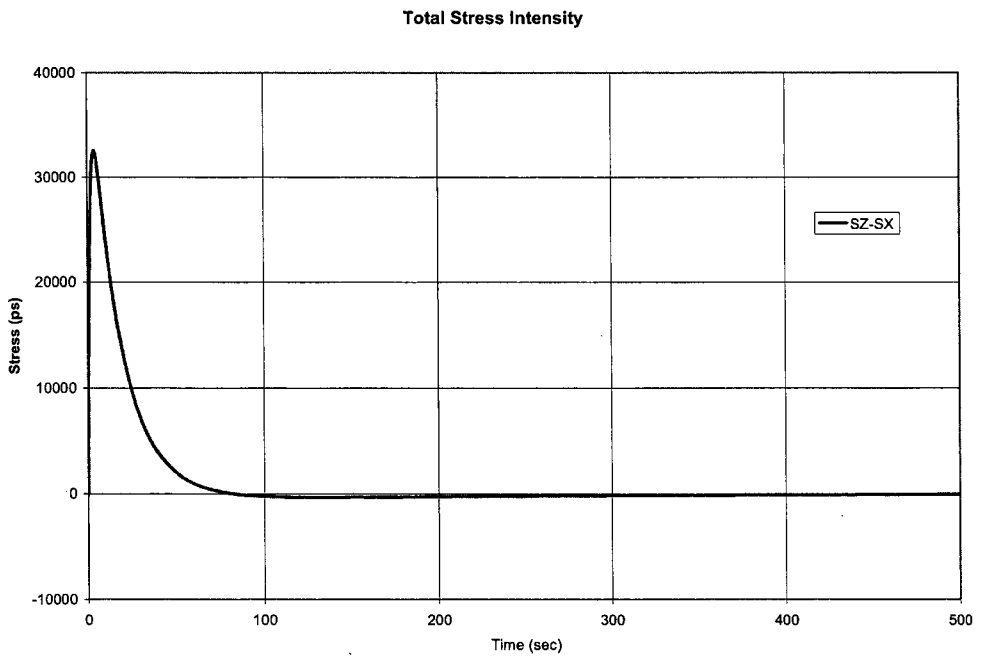

Figure 15: Safe End Membrane Plus Bending Stress History for 40% Flow

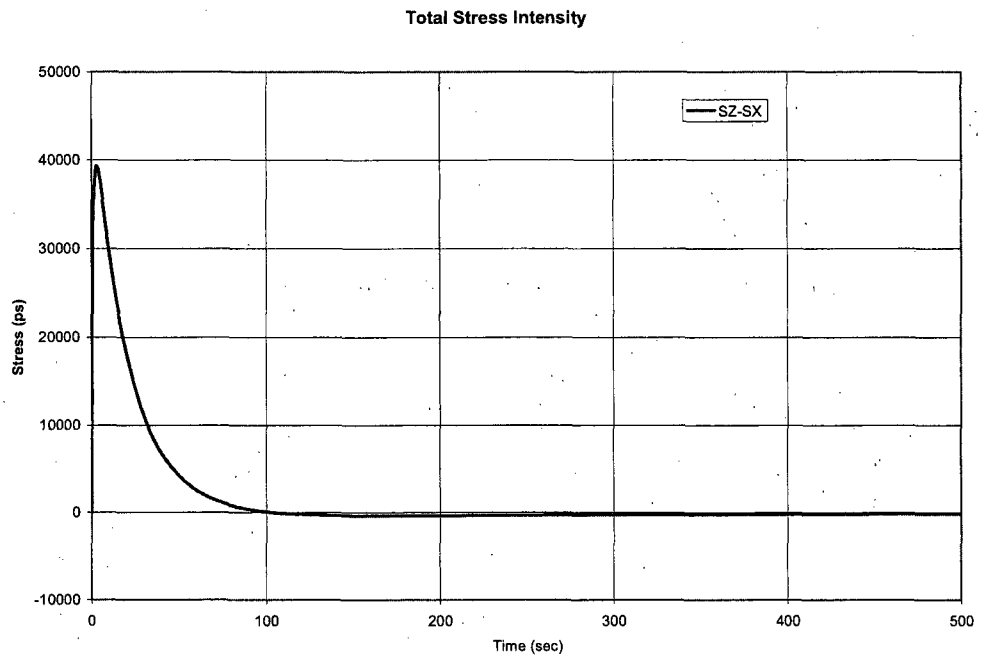

Figure 16: Safe End Total Stress History for 25% Flow

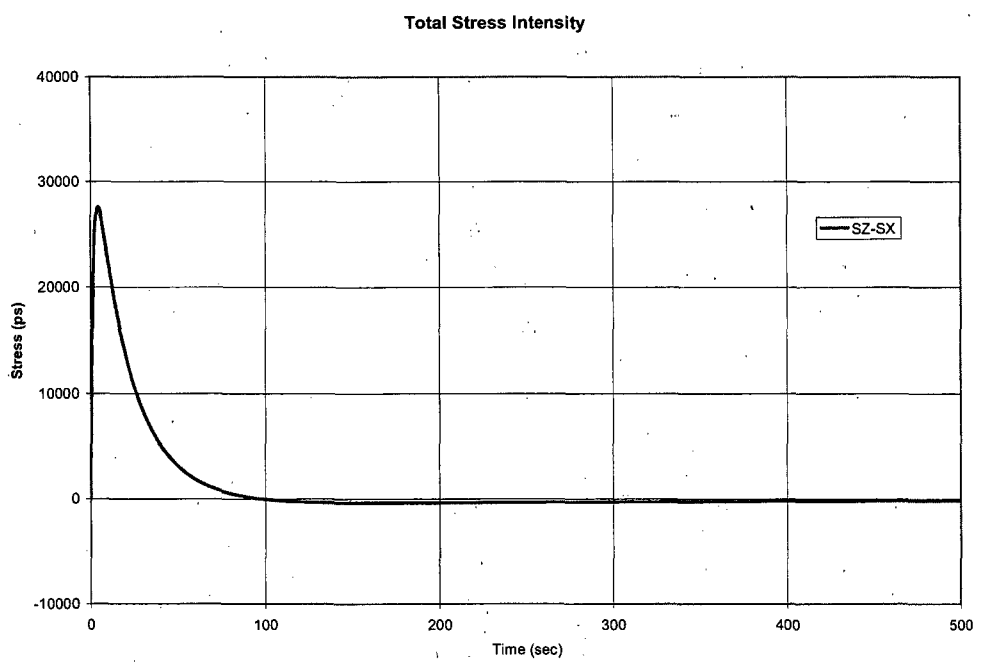

Figure 17: Safe End Membrane Plus Bending Stress History for 25% Flow

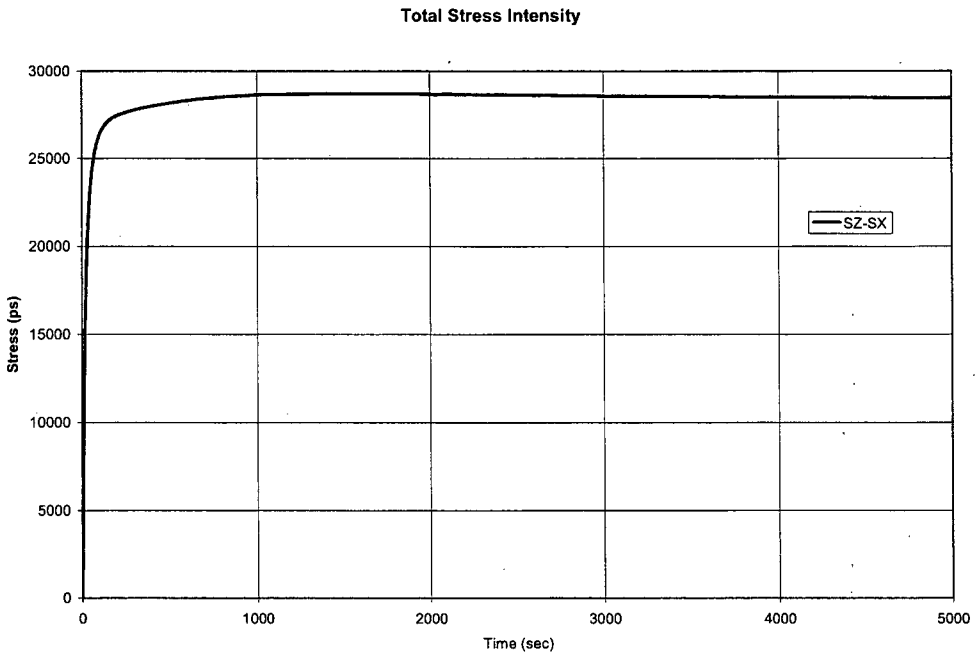

Figure 18: Blend Radius Total Stress History for 100% Flow

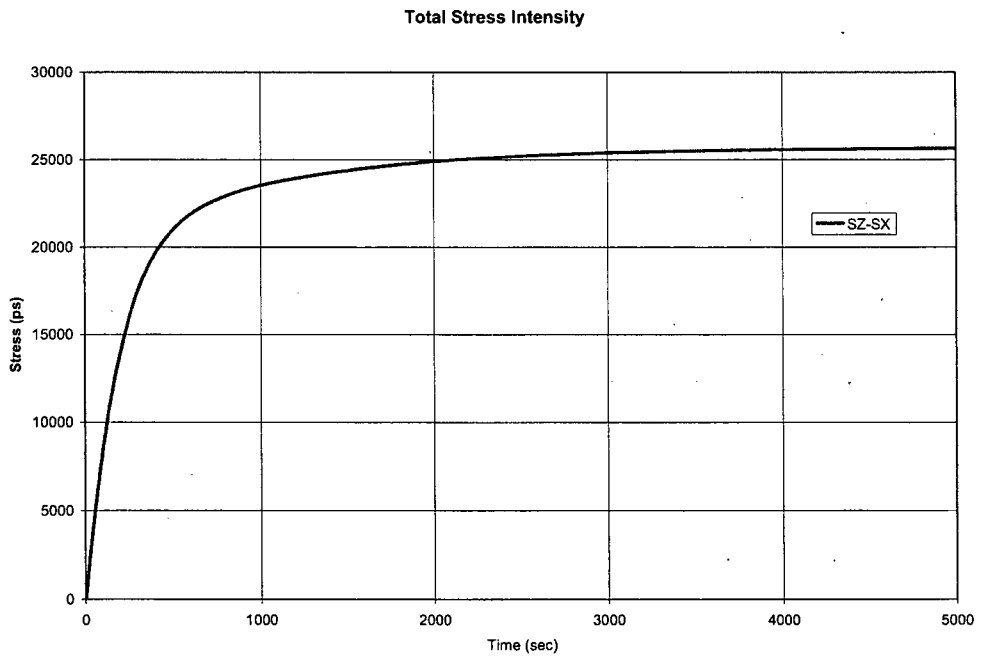

Figure 19: Blend Radius Membrane Plus Bending Stress History for 100% Flow

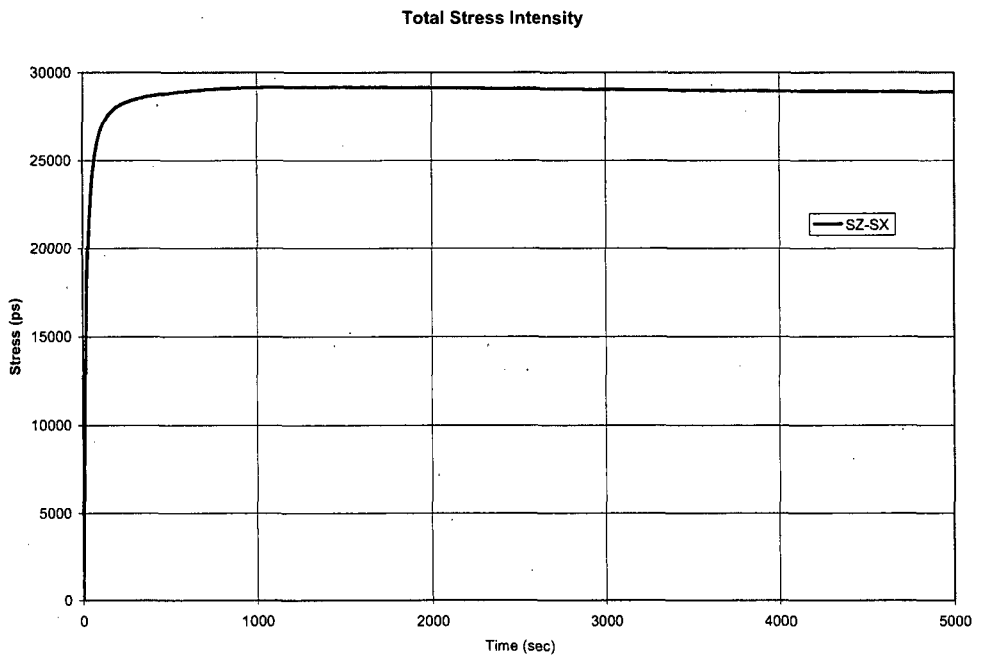

Figure 20: Blend Radius Total Stress History for 40% Flow

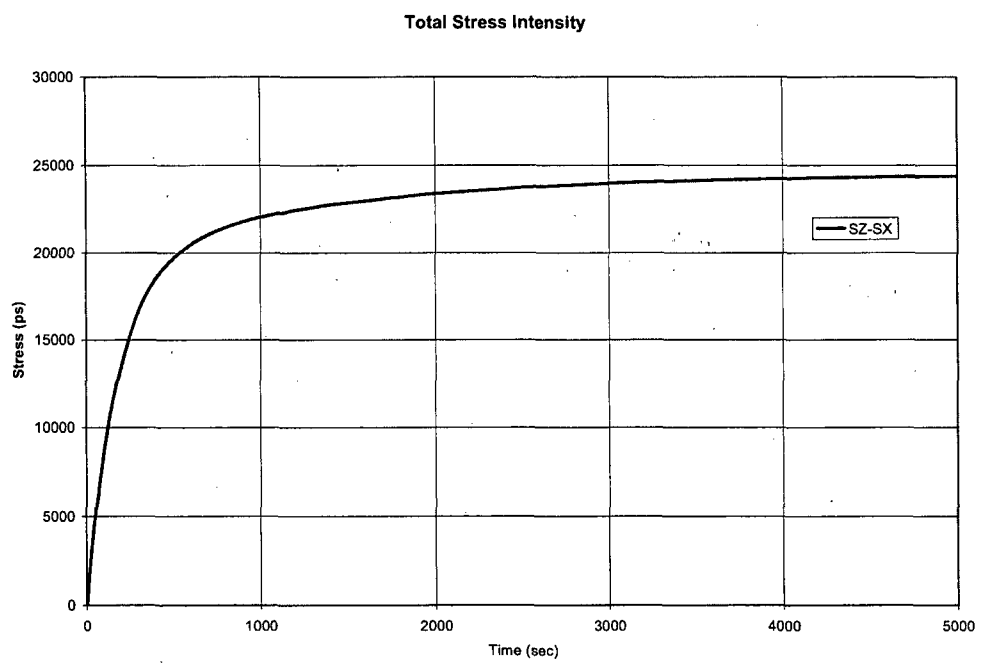

Figure 21: Blend Radius Membrane Plus Bending Stress History for 40% Flow

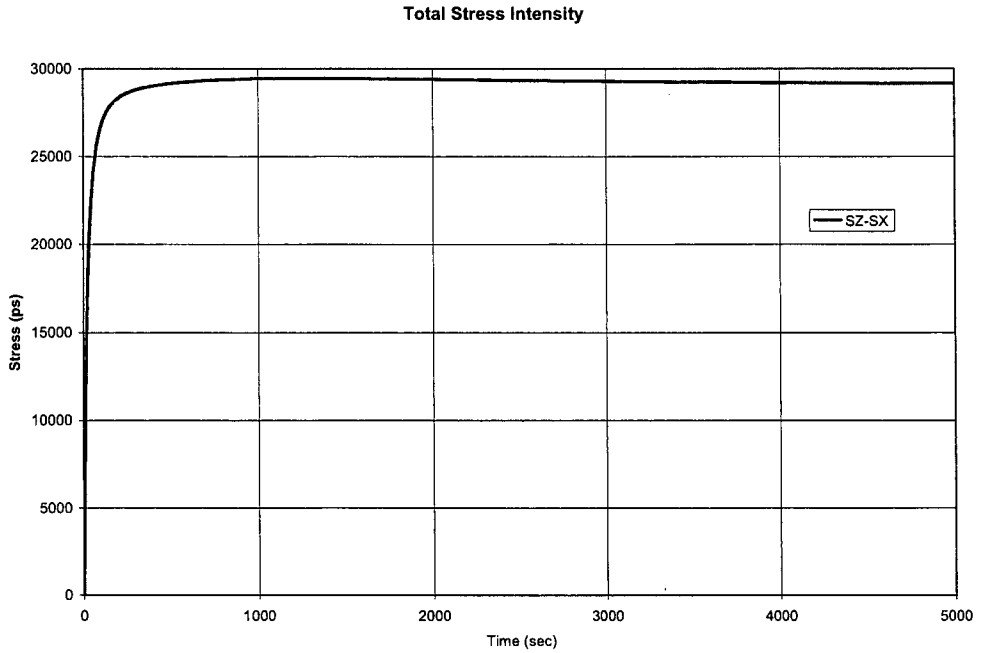

Figure 22: Blend Radius Total Stress History for 25% Flow

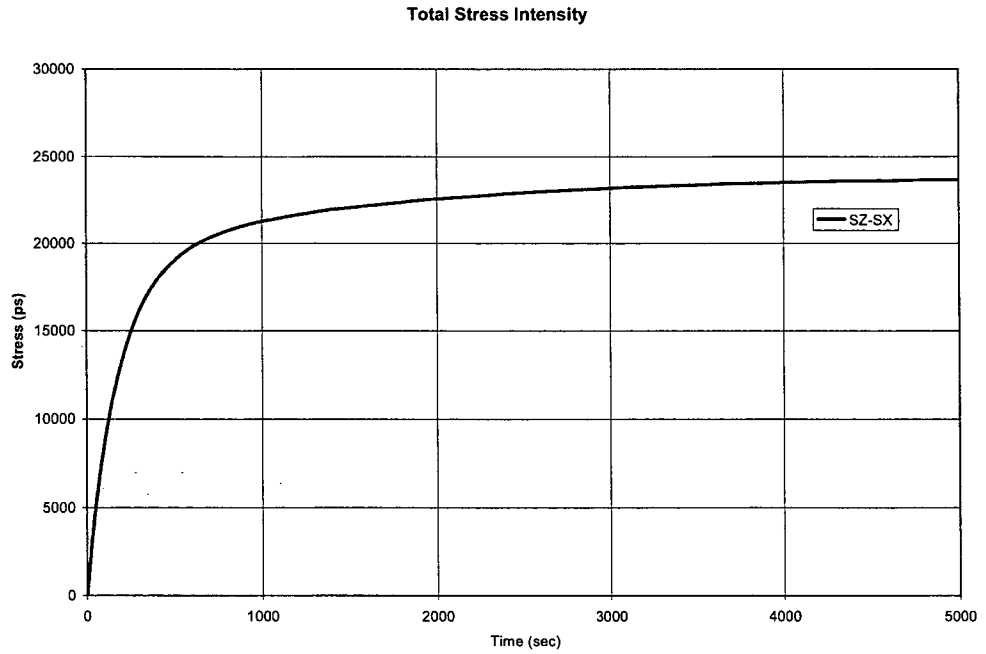

Figure 23: Blend Radius Membrane Plus Bending Stress History for 25% Flow

APPENDIX A

FINITE ELEMENT ANALYSIS FILES

FWP_VY.INP	Input File for Pressure Load	In Computer files
FWT_VY_100.INP	Input File for 100% Flow Thermal Analysis	In Computer files
FWS_VY_100.INP	Input File for 100% Flow Stress Analysis	In Computer files
FWT_VY_40.INP	Input File for 40% Flow Thermal Analysis	In Computer files
FWS_VY_40.INP	Input File for 40% Flow Stress Analysis	In Computer files
FWT_VY_25.INP	Input File for 25% Flow Thermal Analysis	In Computer files
FWS_VY_25.INP	Input File for 25% Flow Stress Analysis	In Computer files
PSE.OUT	Stress Output at Safe End with Pressure Load	In Computer files
PBLEND.OUT	Stress Output at Blend Radius with Pressure Load	In Computer files
PVESS.OUT	Stress Output at Vessel with Pressure Load	In Computer files
#FSE.OUT	Stress Output at Safe End	In Computer files
#FBLEND.OUT	Stress Output at Blend Radius	In Computer files
#FSE_INSIDE.RED	Stress Extracted at Safe End	In Computer files
#FBLEND_INSIDE.RED	Stress Extracted at Blend Radius	In Computer files
#FSE_T-Green.XLS	Green Function with Total Stress at Safe End	In Computer files
#FSE_M+B-Green.XLS	Green Function with Membrane plus Bending Stress at Safe End	In Computer files
#FBR_T-Green.XLS	Green Function with Total Stress at Blend Radius	In Computer files
#FBR_M+B-Green.XLS	Green Function with Membrane plus Bending Stress at Blend Radius	In Computer files

Where # is H, M, L meaning 100%, 40%, and 25% flow rate, respectively.

Structural Integrity Associates, Inc.	File No.: VY-16Q-302
CALCULATION PACKAGE	**Project No.:** VY-16Q

PROJECT NAME:

Environmental Fatigue Analysis of VYNPS

CONTRACT NO.:

10150394

CLIENT:	**PLANT:**
Entergy Nuclear Operations, Inc.	Vermont Yankee Nuclear Power Station

CALCULATION TITLE:

Fatigue Analysis of Feedwater Nozzle

Document Revision	Affected Pages	Revision Description	Project Manager Approval Signature & Date	Preparer(s) & Checker(s) Signatures & Date
0	1-34, Appendix: A1-A2	Initial Issue	Terry J. Herrmann 7/18/2007	Minghao Qin 7/12/2007 John F. Staples 7/12/2007

Table of Contents

1.0 OBJECTIVE 4
2.0 METHODOLOGY 4
3.0 ANALYSIS 7
4.0 FATIGUE USAGE RESULTS 11
5.0 ENVIRONMENTAL FATIGUE ANALYSIS 11
6.0 REFERENCES 12
APPENDIX A SUMMARY OF OUTPUT FILES A1

List of Tables

Table 1: Blend Radius Transients 14
Table 2: Safe End Transient 14
Table 3: Maximum Piping Stress Intensity Calculations 15
Table 4: Blend Radius Stress Summary 16
Table 5: Safe End Stress Summary 18
Table 6: Fatigue Results for Blend Radius (60 Years) 20
Table 7: Fatigue Results for Safe End (60 Years) 22

List of Figures

Figure 1: Typical Green's Functions for Thermal Transient Stress 24
Figure 2: Typical Stress Response Using Green's Functions 25
Figure 3: External Forces and Moments on the Feedwater Nozzle 26
Figure 4: Transient 1, Bolt-up 26
Figure 5: Transient 2, Design HYD Test 27
Figure 6: Transient 3, Startup 27
Figure 7: Transient 4, Turbine Roll and Increased to Rated Power 28
Figure 8: Transient 5, Daily Reduction 75% Power 28
Figure 9: Transient 6, Weekly Reduction 50% Power 29
Figure 10: Transient 9, Turbine Trip at 25% Power 29
Figure 11: Transient 10, Feedwater Bypass 30
Figure 12: Transient 11, Loss of Feedwater Pumps 30
Figure 13: Transient 12, Turbine Generator Trip 31
Figure 14: Transient 14, SRV Blowdown 31
Figure 15: Transient 19, Reduction to 0% Power 32
Figure 16: Transient 20, Hot Standby (Heatup Portion) 32
Figure 17: Transient 20A, Hot Standby (Feedwater Injection Portion) 33
Figure 18: Transient 21-23, Shutdown 33
Figure 19: Transient 24, Hydrostatic Test 34
Figure 20: Transient 25, Unbolt 34

1.0 OBJECTIVE

The purpose of this calculation is to perform a revised fatigue analysis for the feedwater nozzle. Two locations will be analyzed for fatigue acceptance: the safe end (SA508 Class 1) and the blend radius (SA508 Class 2). Both locations are chosen based on the highest overall stress of the analysis performed in Reference [1]. A revised cumulative fatigue factor (CUF) will be determined for both locations, the nozzle forging and safe end, respectively. In the end, the environmental fatigue usage factors will be determined for both locations.

2.0 METHODOLOGY

In order to provide an overall approach and strategy for evaluating the feedwater nozzle, the Green's Function methodology and associated ASME Code stress and fatigue analyses are described in this section.

Revised stress and fatigue analyses are being performed for the feedwater nozzle using ASME Code, Section III methodology. These analyses are being performed to address license renewal requirements to evaluate environmental fatigue for this component in response to Generic Aging Lessons Learned (GALL) Report [11] requirements. The revised analysis is being performed to refine the fatigue usage so that an environmental fatigue factor can be determined for subsequent license renewal efforts.

Two sets of rules are available under ASME Code, Section III, Class 1 [10]. Subparagraph NB-3600 of Section III provides simplified rules for analysis of piping components, and NB-3200 allows for more detailed analysis of vessel components. The NB-3600 piping equations combine by absolute sum the stresses due to pressure, moments and through wall thermal gradient effects, regardless of where within the pipe cross-section the maximum value of the components of stress are located. By considering stress signs, affected surface (inside or outside) and azimuthal position, the stress ranges may be significantly reduced. In addition, NB-3600 assigns stress indices by which the stresses are multiplied to conservatively incorporate the effects of geometric discontinuities. In NB-3200, stress indices are not required, as the stresses are calculated by finite element analysis and consider applicable stress concentration factors. In addition, NB-3200 methodology accounts for the different locations within a component where stresses due to thermal, pressure or other mechanical loading are a maximum. This generally results in a net reduction of the stress ranges and consequently, in the calculated fatigue usage. Article 4 [12] methodology was originally used to evaluate the feedwater nozzle. NB-3200 methodology, which is the modern day equivalent to Article 4, is used in this analysis to be consistent with the Section III design bases for this component, as well as to allow a more detailed analysis of this component. In addition, several of the conservatisms originally used in the original feedwater nozzle evaluation (such as grouping of transients) are removed in the current evaluation so as to achieve a more accurate CUF.

For the feedwater nozzle evaluated as a part of this work, stress histories will be computed by a time integration of the product of a pre-determined Green's Function and the transient data. This Green's

Function integration scheme is similar in concept to the well-known Duhamel theory used in structural dynamics. A detailed derivation of this approach and examples of its application to specific plant locations is contained in Reference [2]. A general outline is provided in this section.

The steps involved in the evaluation are as follows:

- Develop finite element model
- Develop heat transfer coefficients and boundary conditions for the finite element model
- Develop Green's Functions
- Develop thermal transient definitions
- Perform stress analysis to determine stresses for thermal transients
- Perform fatigue analysis

A Green's Function is derived by using finite-element methods to determine the transient stress response of the component to a step change in loading (usually a thermal shock). The critical location in the component is identified based on the maximum stress, and the thermal stress response over time is extracted for this location. This response to the input thermal step is the "Green's Function." Figure 1 shows a typical set of two Green's Functions, each for a different set of heat transfer coefficients (representing different flow rate conditions).

To compute the thermal stress response for an arbitrary transient, the loading parameter (usually local fluid temperature) is deconstructed into a series of step-loadings. By using the Green's Function, the response to each step can be quickly determined. By the principle of superposition, these can be added (algebraically) to determine the response to the original load history. The result is demonstrated in Figure 2. The input transient temperature history contains five step-changes of varying size, as shown in the upper plot in Figure 2. These five step changes produce the five successive stress responses in the second plot shown in Figure 2. By adding all five response curves, the real-time stress response for the input thermal transient is computed.

The Green's Function methodology produces identical results compared to running the input transient through the finite element model. The advantage of using Green's Functions is that many individual transients can be run with a significant reduction of effort compared to running all transients through the finite element model. The trade-off in this process is that the Green's Functions are based on constant material properties and heat transfer coefficients. Therefore, these parameters are chosen to bound all transients that constitute the majority of fatigue usage, i.e., the heat transfer coefficients at 300°F bound the cold water injection transient. In addition, the instantaneous value for the coefficient of thermal expansion is used instead of the mean value for the coefficient of thermal expansion. This conservatism is more than offset by the benefit of not having to analyze every transient, which was done in the VY reactor feedwater nozzle evaluation.

Once the stress history is obtained for all transients using the Green's Function approach, the remainder of the fatigue analysis is carried out using traditional methodologies in accordance with ASME Code, Section III requirements.

Fatigue calculations are performed in accordance with ASME Code, Section III, Subsection NB-3200 methodology. Fatigue analysis is performed for the two limiting locations (one in the safe end and one in the nozzle forging, representing the two materials of the nozzle assembly) using the Green's Functions developed for thee three feedwater flow conditions and 60-year projected cycle counts.

Three Structural Integrity utility programs will be used to perform the fatigue analysis. The first two calculate stresses in response to transients. The transients analyzed are those described in the thermal cycle diagrams [3] for the feedwater nozzle. These transients are shown in Figures 4 – 20. The temperatures and pressures for these transients have been modified to account for power uprate [4]. The power uprate pressures and temperatures were used for this analysis. The last program calculates fatigue based on the stress output. The three programs are STRESS.EXE, P-V.EXE, and FATIGUE.EXE. The first program, STRESS.EXE, calculates a stress history in response to a thermal transient using a Green's Function. The second program, P-V.EXE, reduces the stress history to peaks and valleys, as required by ASME Code fatigue evaluation methods. The third program, FATIGUE.EXE, calculates fatigue from the reduced peak and valley history using ASME Code, Section III range-pair methodology. All three programs are explained in detail and have been independently verified for generic use in the Reference [5] calculation.

In order to perform the fatigue analysis, Green's Functions are developed using the finite element model. Then, input files with the necessary data are prepared and the three utility computer programs are run. The first program (STRESS.EXE) requires the following three input files:

- Input file "GREEN.DAT": This file contains the Green's Function for the location being evaluated. For each flow condition, two Green's Functions are determined: a membrane plus bending stress intensity Green's Function and a total stress intensity Green's Function. This allows computation of total stress, as well as membrane plus bending stress, which is necessary to compute K_e per ASME Code, Section III requirements.
- Input file "GREEN.CFG": This file is a configuration file containing parameters that define the Green's Function (i.e., number of points, temperature drop analyzed, etc.).
- Input file "TRANSNT.INP": This file contains the input transient history for all thermal transients to be analyzed for the location being evaluated.

Pressure and piping stress intensities are also included for each transient case, based on pressure stress results from finite element analysis and attached piping load calculations.
The second program (P-V.EXE) simply extracts only the maxima and minima stress (i.e., the peaks and valleys) from the stress histories generated by program STRESS.EXE.

The third program (FATIGUE.EXE) performs the ASME Code peak event-pairing required to calculate a fatigue usage value. The input data consists of the output peak and valley history from program P-V.EXE and a configuration input file that provides ASME Code configuration data relevant to the fatigue analysis (i.e., K_e parameters, S_m, Young's modulus, etc.). The output is the final fatigue calculation for the location being evaluated.

The Green's Function methodology described above uses standard industry stress and fatigue analysis practices, and is the same as the methodology used in typical stress reports. Special approval for the use of this methodology is therefore not required.

3.0 ANALYSIS

The fatigue analysis involves the preparing of input files for, and running of three programs verified and described in Reference [5]. The programs STRESS.EXE and P-V.EXE are run together through the use of a batch file. The program FATIGUE.EXE is run after processing the output from P_V.EXE. The steps associated with this process are described in the following sub-sections.

3.1 Transient Definitions (for program STRESS.EXE)

The program STRESS.EXE requires the following three input files for analyzing an individual transient:

- Green.dat. There are 12 stress history functions obtained from Reference [1]. They represent the membrane plus bending and total stress intensities at the blend radius and safe end locations. Both of the blend radius and the safe end have two stress history functions for each of the following flow conditions; 100%, 40%, and 25% flow.
- Green.cfg is configured as described in Reference [5].
- Transnt.inp. These files are created to represent the transients shown on the thermal cycle diagrams and redefined by power uprate. Note that transients 12, 13, and 15 are nearly identical on the thermal cycle diagram [3] and the results from running transient 12 will be used for all three transients. Transient 16, 17 and 18 will not be considered since there is no temperature change. Tables 1 and 2 show the thermal history used to represent each transient. Based upon the thermal cycle diagram for the feedwater nozzle [3], the transients are split into the following groups based upon flow rate:
    - Transients 3, 20, 20A, and 21-23 are run at 25% flow. Although Reference [3] shows 15% flow rate, it is conservative to use 25% flow rate for these transients. Transient 20, Hot Standby, is split up into two parts. The first portion is "Heatup portion" and the second portion is "Feedwater Injection portion" that are defined from Reference [3].
    - Transient 11 is run at 40% flow. Transient 11 starts off and ends at 100% flow.
    - Transients 5, 6, 9, 10, and 19 are run at 100% flow.
    - Transient 4 is run at 100% flow only to obtain the last stress point. The remainder of the stress points for transient 4 is obtained from the 25% flow stress results. The results are pulled from the two flow case results based upon the flow rates defined in the thermal cycle diagram [3].
    - Transients 12, 13, 14 and 15 were run at 100% flow. Heat transfer coefficients were not re-calculated for the 1 minute intervals each of these transients is at 110% flow. The effect of this small flow rate increase for such a relatively short duration should be minor.
    - Transients 1, 2, 24, and 25 are set as no thermal stress due to very small temperature changes (70°F to 100°F) at these transients.

3.2 Peak and Valley Points of the Stress History (for program P-V.EXE)

The program P-V.exe is then run to extract the peaks and valleys from the STRESS.OUT file produced by the STRESS.EXE program. The only input required for this program is STRESS.OUT and it outputs all the peaks and valleys to P-V.OUT. Columns 2 through 5 of Tables 4 (for the blend radius) and 5 (for the safe end) show the final peak and valley output. The pressure for column 6 is then filled in using the thermal cycle diagrams. Pressure and piping loads have to be added to the peak and valley points to calculate the final stress values used for fatigue analysis.

3.3 Pressure Load

The pressure stress associated with a 1000 psi internal pressure was determined in Reference [1]. These values are as follows:

Pressure stress for the safe end:

- 8693 psi membrane plus bending stress intensity.
- 8891 psi total linearized stress intensity.

Pressure stress for the blend radius:

- 36653 psi membrane plus bending stress intensity.
- 37733 psi total linearized stress intensity.

These pressure stress values for each location were linearly scaled with pressure. The actual pressure for column 6 of Tables 4 and 5 is obtained from Tables 1 and 2. The scaled pressure stress values are shown in columns 7 and 8 of Tables 4 and 5.

The pressure stress is combined with the thermal and piping loads to calculate the final stress values used for fatigue analysis.

3.4 Attached Piping Loads

Additionally, the piping stress intensity (stress caused by the attached piping) was determined. These piping forces and moments are determined as shown in Figure 3.

The following formulas are used to determine the maximum stress intensity in the nozzle at the two locations of interest. From engineering statics, the piping loads at the end of the model can be translated to the first and second cut locations using the following equations:

For Cut I:

$$(M_x)_1 = M_x - F_y L_1$$
$$(M_y)_1 = M_y + F_x L_1$$

For Cut II:

$$(M_x)_2 = M_x - F_y L_2$$
$$(M_y)_2 = M_y + F_x L_2$$

The total bending moment and shear loads are obtained using the equations below:

For Cut I:

$$M_{xy} = \sqrt{(M_x)_1^{\,2} + (M_y)_1^{\,2}}$$
$$F_{xy} = \sqrt{(F_x)_1^{\,2} + (F_y)_1^{\,2}}$$

For Cut II:

$$M_{xy} = \sqrt{(M_x)_2^{\,2} + (M_y)_2^{\,2}}$$
$$F_{xy} = \sqrt{(F_x)_2^{\,2} + (F_y)_2^{\,2}}$$

The distributed loads for a thin-walled cylinder are obtained using the equations below:

$$N_z = \frac{1}{\pi R_N}\left[\frac{1}{2}F_z + \frac{M_{xy}}{R_N}\right]$$
$$q_N = \frac{1}{\pi R_N}\left[F_{xy} - \frac{M_z}{2R_N}\right]$$

To determine the primary stresses, P_M, due to internal pressure and piping loads, the following equations are used.

For Cut I, using thin-walled equations:

$$(P_M)_z = \frac{Pa_N}{2t_N} + \frac{Nz}{t_N}$$
$$(P_M)_\theta = \frac{Pa_N}{t_N}$$
$$(P_M)_R = -P$$
$$\tau_M = \frac{q_N}{t_N}$$
$$SI_{MAX} = 2\sqrt{\left(\frac{(P_M)_\theta - (P_M)_R}{2}\right)^2 + (\tau_M)_{z\theta}^{\,2}}$$

or

$$SI_{MAX} = 2\sqrt{\left(\frac{(P_M)_z - (P_M)_R}{2}\right)^2 + (\tau_M)_{z\theta}^{\,2}}$$

Because pressure was considered separately in this analysis, the equations used for Cut I are valid for Cut II.

where: L_1 = The length from the end of the nozzle where the piping loads are applied to the location of interest in the safe end.
L_2 = The length from the end of the nozzle where the piping loads are applied to the location of interest in the blend radius.
M_{xy} = The maximum bending moment in the xy plane.
F_{yx} = The maximum shear force in the xy plane.
N_z = The normal force per inch of circumference applied to the end of the nozzle in the z direction.
q_N = The shear force per inch of circumference applied to the nozzle.
R_N = The mid-wall nozzle radius.

Since the pressure was considered separately in this analysis, the equations can be simplified as follows:

$$(P_M)_z = \frac{Nz}{t_N}$$
$$(P_M)_\theta = 0$$
$$(P_M)_R = 0$$
$$\tau_M = \frac{q_N}{t_N}$$
$$SI_{MAX} = 2(\tau_M)_{z\theta}$$
$$or$$
$$SI_{MAX} = 2\sqrt{\left(\frac{Nz}{2t_N}\right)^2 + (\tau_M)_{z\theta}^{\ 2}}$$

Per Reference [6], the feedwater nozzle piping loads are as follows:

F_x = 3,000 lbs	M_x = 28,000 ft-lb = 336,000 in-lb
F_y = 15,000 lbs	M_y = 13,000 ft-lb = 156,000 in-lb
F_z = 3,200 lbs	M_z = 40,000 ft-lb = 480,000 in-lb

The loads are applied at the connection of the piping and safe end. Therefore, the L_1 is equal to 12.0871 inches and the L_2 is equal to 27.572 inches. The calculations for the safe end and blend radius are shown in Table 3. The first cut location is the same as the Green's Function cross section per [1] at the safe end, and the second cut is from Node 645 (outside) to Node 501 (inside). The maximum stress intensities due to piping loads are 5707.97 psi at the safe end and 265.47 psi at the blend radius, respectively. The piping load sign is set as the same as the thermal stress sign.

These piping stress values are scaled assuming no stress occurs at an ambient temperature of 70°F and the full values are reached at reactor design temperature, 575°F. The scaled piping stress values

are shown in columns 9 and 10 of Tables 4 and 5. Columns 11 and 12 of Tables 4 and 5 show the summation of all stresses for each thermal peak and valley stress point.

3.5 Fatigue Analysis (for program FATIGUE.EXE)

The number of cycles projected for the 60-year operating life is used for each transient [3]:

Column 13 in Tables 4 and 5 shows the number of cycles associated with each transient. The number of cycles for 60 years was obtained from Reference [3].

The program FATIGUE.EXE performs the "ASME Code style" peak event pairing required to calculate a fatigue usage value. The input data for FATIGUE.CFG is as follows:

	Blend Radius	Safe End
Parameters *m* and *n* for Computing K_e	2.0 & 0.2 (low alloy steel) [10]	3.0 & 0.2 (carbon steel) [10]
Design Stress Intensity Values, S_m	26700 psi [8] @ 600°F	17800 psi [8] @ 600°F
Elastic Modulus from Applicable Fatigue Curve	30.0×10^6 psi [10]	30.0×10^6 psi [10]
Elastic Modulus Used in Finite Element Model	26.7×10^6 psi	28.1×10^6 psi
The Geometric Stress Concentration Factor K_t	1.0	1.34 [7, page 35 of S4]

The results of the fatigue analyses are presented in Tables 6 and 7 for the blend radius and safe end for 60 years, respectively.

The results described are contained in EXCEL files *BRresults.xls* and *SEresults.xls*, which are contained in the computer files.

4.0 FATIGUE USAGE RESULTS

The blend radius cumulative usage factor (CUF) from system cycling is 0.0636 for 60 years. The safe end CUF is 0.1471 for 60 years.

5.0 ENVIRONMENTAL FATIGUE ANALYSIS

In the response to NRC request for additional information (RAI) 4.3-H-02, VYNPS states that they have conservatively assumed that fatigue cracks may be present in the clad. VYNPS manages this cracking by performing periodic inspections that were implemented in response to Generic Letters 80-095 and

81-11, and NUREG-0619. The inspection frequency is based on the calculated fatigue crack growth of a postulated flaw in the nozzle inner blend radius. The VYNPS fatigue crack growth calculation uses methods in compliance with GE BWR Owners Group Topical Report "Alternate BWR Feedwater Nozzle Inspection Requirements", GE-NE-523-A71-0594, Revision 1, August 1999 and the associated NRC Final Safety Evaluation (TAC No. MA6787) dated March 10, 2000. The NRC has reviewed and approved this approach to handling FW nozzle inner blend radius cracking (Letter D.H. Dorman (USNRC) to D.A. Reid (VYNPC), Subject: Evaluation of Request for Relief from NUREG-0619 for VYNPS dated 2/6/95, (TAC No. M88803)).

The analysis performed for the feedwater nozzle calculated fatigue in the blend radius base metal, not the clad. This is consistent with the VYNPS position stated in the response to RAI 4.3-H-02, and is also consistent with ASME Code methodology since cladding is structurally neglected in fatigue analyses, per ASME Code, Section III, NB-3122.3.

Per Reference [9], the dissolved Oxygen (DO) calculation shows the overall HWC availability is 47%. This means the time ratio under NWC (pre-HWC) is 53%.

For the safe end location, the environmental fatigue factors for post-HWC and pre-HWC are all 1.74 from Table 3 of Reference [9]. It results in an EAF adjusted CUF of 1.74 x 0.1471 = 0.2560 for 60 years, which is acceptable (i.e., less than the allowable value of 1.0). The overall environmental multiplier is 1.74.

For the blend radius location, the environmental fatigue factors for post-HWC and pre-HWC are 11.14 and 8.82 from Table 4 of Reference [9]. These results in an EAF adjusted CUF of (11.14 x 53% + 8.82 x 47%) x 0.0636 = 0.6392 for 60 years, which is acceptable (i.e., less than the allowable value of 1.0). The overall environmental multiplier is 10.0496.

6.0 REFERENCES

1. SI Calculation No. VY-16Q-301, Revision 0, "Feedwater Nozzle Stress History Development for Green Functions."
2. Kuo, A. Y., Tang, S. S., and Riccardella, P. C., "An On-Line Fatigue Monitoring System for Power Plants, Part I - Direct Calculation of Transient Peak Stress Through Transfer Matrices and Green's Functions," ASME PVP Conference, Chicago, 1986.
3. Entergy Design Input Record (DIR) EC No. 1773, Revision 0, "Environmental Fatigue Analysis for Vermont Yankee Nuclear Power Station," 7/3/07, SI File No. VY-16Q-209.
4. GE Certified Design Specification No. 26A6019, Revision 1, "Reactor Vessel – Extended Power Uprate," SI File No. VY-05Q-236.
5. Structural Integrity Associates Calculation (Generic) No. SW-SPVF-01Q-301, Revision 0, "STRESS.EXE, P-V.EXE, and FATIGUE.EXE Software Verification."
6. GE Drawing No. 919D294, Revision 11, Sht. No. 7, "Reactor Vessel," SI File No. VY-05Q-241.
7. Chicago Bridge & Iron Company Contractor 9-6201, Revision 2, "Section S4, Stress Analysis Feedwater Nozzle Vermont Yankee Reactor Vessel," SI File No. VY-05Q-238.

8. American Society of Mechanical Engineers, Boiler and Pressure Vessel Code, Section II, Part D, 1998 Edition, 2000 Addenda.
9. SI Calculation No. VY-16Q-303, Revision 0, "Environmental Fatigue Evaluation of Reactor Recirculation Inlet Nozzle and Vessel Shell Bottom Head."
10. American Society of Mechanical Engineers, Boiler and Pressure Vessel Code, Section III Subsection NB, 1998 Edition, 2000 Addenda.
11. NUREG-1801, Revision 1, "Generic Aging Lessons Learned (GALL) Report," U. S. Nuclear Regulatory Commission, September 2005.
12. American Society of Mechanical Engineers, Boiler and Pressure Vessel Code, Section III, Subsection A, Article 4, 1965 Edition with Winter 1966 Addenda.

Table 1: Blend Radius Transients

Transient Number	Time (s)	Temp (°F)	Time Step (s)	Pressure (psig)
1. Bolt-up	0	70		0
123 Cycles	10	70	10	0
2. Design	0	70		0
HYD Test	1080	100	1080	0
120 Cycles	1680	100	600	1100
	5280	100	3600	1100
	5880	100	600	50
	10880	100	5000	50
3. Startup	0	100		50
300 Cycles	16164	549	16164	1010
LF_25	21164	549	5000	1010
4. Turbine Roll	0	549		1010
and Increased to	1	100	1	1010
Rated	*1801*	*100*	*1800*	*1010*
Power	1802	260	1	1010
300 cycles	3602	392	1800	1010
LF_25, HF_100	8602	392	5000	1010
5. Daily	0	392		1010
Reduction	900	310	900	1010
75% Power	2700	310	1800	1010
10,000 Cycles	3600	392	900	1010
HF_100	8600	392	5000	1010
6. Weekly Reduct	0	392		1010
50% Power	1800	280	1800	1010
2,000 Cycles	3600	280	1800	1010
HF_100	5400	392	1800	1010
	10400	392	5000	1010
9. Turbine	0	392		1010
Trip at 25%	1800	265	1800	1010
Power	1980	265	180	1010
10 Cycles	2340	90	360	1010
HF_100	2520	90	180	1010
	3420	265	900	1010
	3600	265	180	1010
	5400	392	1800	1010
	10400	392	5000	1010

Transient Number	Time (s)	Temp (°F)	Time Step (s)	Pressure (psig)
10. FW Heater	0	392		1010
Bypass	90	265	90	1010
70 Cycles	1890	265	1800	1010
HF_100	2070	392	180	1010
	7070	392	5000	1010
11. Loss of	0	392		1010
FW Pumps	1	565	1	1010
10 Cycles	3.5	565	2.5	1190
MF_40, HF_100	4.5	50	1	1185
	13.5	50	9	1135
	184.5	50	171	1135
	1564.5	440	1380	1135
	1565.5	565	1	1135
	2165.5	*565*	*600*	*1135*
	2166.5	50	1	1135
	2346.5	50	180	885
	5406.5	440	3060	1055
	5407.5	565	1	1055
	6727.5	565	1320	1135
	6728.5	50	1	1135
	7148.5	50	420	675
	7448.5	300	300	675
	11048.5	400	3600	232
	16411.5	549	5363	885
	16412.5	549	1	1010
	18212.5	549	1800	1010
	18213.5	100	1	1010
	20013.5	100	1800	1010
	20014.5	260	1	1010
	21814.5	392	1800	1010
	26814.5	392	5000	1010
12. Turbine	0	392		1010
Generator Trip	10	392	*10*	1135/1375[2]
60 Cycles	15	392	*5*	1135/1375[2]
13. Reactor	30	392	15	940
Overpressure	*90*	*275*	*60*	*940*
1 Cycles	990	100	900	940
15. Other	2790	100	1800	940
SCRAMs	2791	260	1	940
228 cycles	3210	291	419	1010
HF_100	4591	392	1381	1010
	9591	392	5000	1010

Transient Number	Time (s)	Temp (°F)	Time Step (s)	Pressure (psig)
14. SRV	0	392		1010
Blowdown	60	275	60	885
1 Cycles	960	100	900	50
HF_100	5960	100	5000	50
19. Reduction to 0%	0	392		1010
Power 300 Cycles	1800	265	1800	1010
HF_100	6800	265	5000	1010
20. Hot Standby	0	265		1010
(Heatup Portion)	1	440	1	1010
300 Cycles	3925	549	3924	1010
LF_25	8925	549	5000	1010
20A. Hot Standby	0	549		1010
(FW Injection Portion)	1	100	1	1010
300 Cycles	*181*	*100*	*180*	*1010*
LF_25	241	290	60	1010
	451	549	210	1010
	5451	549	5000	1010
21-23. Shutdown	0	549		1010
300 Cycles	6264	375	6264	50
LF_25	6864	330	600	50
	15144	100	8280	50
	20144	100	5000	50
24. Hydrostatic	0	100		50
Test	600	100	600	1563
1 Cycles	1200	100	600	1563
	1800	100	600	50
	2400	100	600	50
25. Unbolt	0	100		0
123 Cycles	1080	70	1080	0
	6080	70	5000	0

Note: 1. The indicated time or pressure was assumed.
2. 1375 psi is for Transient 13 only.

Table 2: Safe End Transient

Transient Number	Time (s)	Temp (°F)	Time Step (s)	Pressure (psig)
1. Bolt-up	0	70		0
123 Cycles	10	70	10	0
2. Design	0	70		0
HYD Test	1080	100	1080	0
120 Cycles	1680	100	600	1100
	5280	100	3600	1100
	5880	100	600	50
	6380	100	500	50
3. Startup	0	100		50
300 Cycles	16164	549	16164	1010
LF_25	16664	549	500	1010
4. Turbine Roll	0	549		1010
and Increased to	1	100	1	1010
Rated	1801	100	1800	1010
Power	1802	260	1	1010
300 cycles	3602	392	1800	1010
LF_25, HF_100	4102	392	500	1010
5. Daily	0	392		1010
Reduction	900	310	900	1010
75% Power	2700	310	1800	1010
10,000 Cycles	3600	392	900	1010
HF_100	4100	392	500	1010
6. Weekly Reduct	0	392		1010
50% Power	1800	280	1800	1010
2,000 Cycles	3600	280	1800	1010
HF_100	5400	392	1800	1010
	5900	*392*	*500*	*1010*
9. Turbine	0	392		1010
Trip at 25%	1800	265	1800	1010
Power	1980	265	180	1010
10 Cycles	2340	90	360	1010
HF_100	2520	90	180	1010
	3420	265	900	1010
	3600	265	180	1010
	5400	392	1800	1010
	5900	392	500	1010

Transient Number	Time (s)	Temp (°F)	Time Step (s)	Pressure (psig)
10. FW Heater	0	392		1010
Bypass	90	265	90	1010
70 Cycles	1690	265	1800	1010
HF_100	2070	392	180	1010
	2570	392	500	1010
11. Loss of	0	392		1010
FW Pumps	1	565	1	1010
10 Cycles	3.5	565	2.5	1190
MF_40, HF_100	4.5	50	1	1185
	13.5	50	9	1135
	184.5	50	171	1135
	1564.5	440	1380	1135
	1565.5	565	1	1135
	2165.5	565	600	1135
	2166.5	50	1	1135
	2346.5	50	180	885
	5406.5	440	3060	1055
	5407.5	565	1	1055
	6727.5	565	1320	1135
	6728.5	50	1	1135
	7148.5	50	420	675
	7448.5	300	300	675
	11048.5	400	3600	232
	16411.5	549	5363	885
	16412.5	549	1	1010
	18212.5	549	1800	1010
	18213.5	100	1	1010
	20013.5	*100*	*1800*	*1010*
	20014.5	260	1	1010
	21814.5	392	1800	1010
	22314.5	392	500	1010
12. Turbine	0	392		1010
Generator Trip	10	392	*10*	1135/1375[2]
60 Cycles	15	392	*5*	1135/1375[2]
13. Reactor	30	392	15	940
Overpressure	90	275	60	940
1 Cycles	990	100	900	940
15. Other	2790	100	1800	940
SCRAMs	2791	260	1	940
228 cycles	3210	291	419	1010
HF_100	4591	392	1381	1010
	5091	392	500	1010

Transient Number	Time (s)	Temp (°F)	Time Step (s)	Pressure (psig)
14. SRV	0	392		1010
Blowdown	60	275	60	885
1 Cycles	960	100	900	50
HF_100	1460	100	500	50
19. Reduction to 0%	0	392		1010
Power 300 Cycles	1800	265	1800	1010
HF_100	2300	265	500	1010
20. Hot Standby	0	265		1010
(Heatup Portion)	1	440	1	1010
300 Cycles	3925	549	3924	1010
LF_25	4425	549	500	1010
20A. Hot Standby	0	549		1010
(FW Injection Portion)	1	100	1	1010
300 Cycles	181	100	180	1010
LF_25	241	290	60	1010
	451	549	210	1010
	951	549	500	1010
21-23. Shutdown	0	549		1010
300 Cycles	6264	375	6264	50
LF_25	6864	330	600	50
	15144	100	8280	50
	15644	100	500	50
24. Hydrostatic	0	100		50
Test	600	100	600	1563
1 Cycles	1200	100	600	1563
	1800	100	600	50
	2400	100	600	50
25. Unbolt	*0*	*100*		*0*
123 Cycles	1080	70	1080	0
	1580	70	500	0

Note: 1. These transients are the same as in Table 1 with the exception of the 500 second steady state time increment that is used. The transients in Table 1 are plotted using a 5000 second steady state increment. The difference is due to the length of the Green's Function for the safe end which is shorter compared to the blend Radius.
2. The indicated time or pressure was assumed.
3. 1375 psi is for Transient 13 only.

Table 3: Maximum Piping Stress Intensity Calculations

Safe End External Piping Loads		
Parameters		
F_x =	3.00	kips
F_y =	15.00	kips
F_Z =	3.20	kips
M_x =	336.00	in-kips
M_y =	156.00	in-kips
M_Z =	480.00	in-kips
OD=	11.86	in
ID=	10.409	in
R_N =	5.57	in
L =	12.09	in
t_N =	0.72	in
$(M_x)_1$ =	154.69	in-kips
$(M_y)_1$ =	192.26	in-kips
M_{xy} =	246.77	in-kips
F_{xy} =	15.30	kips
N_Z =	2.63	kips/in
q_N =	-1.59	kips/in
Primary Membrane Stress Intensity		
PM_Z =	3.63	ksi
τ =	-2.20	ksi
SI_{max} =	5.71	ksi
SI_{max} =	5707.97	psi

Blend Radius External Piping Loads		
Parameters		
F_x =	3.00	kips
F_y =	15.00	kips
F_Z =	3.20	kips
M_x =	336.00	in-kips
M_y =	156.00	in-kips
M_Z =	480.00	in-kips
OD=	22.67	in
ID=	10.750	in
R_N =	8.35	in
L =	27.57	in
t_N =	5.96	in
$(M_x)_2$ =	-77.58	in-kips
$(M_y)_2$ =	238.72	in-kips
M_{xy} =	251.01	in-kips
F_{xy} =	15.30	kips
N_Z =	1.21	kips/in
q_N =	-0.51	kips/in
Primary Membrane Stress Intensity		
PM_Z =	0.20	ksi
τ =	-0.09	ksi
SI_{max} =	0.27	ksi
SI_{max} =	265.47	psi

Note: The locations for Cut I and Cut II were defined in Reference [1] for safe end and blend radius paths, respectively.

Table 4: Blend Radius Stress Summary

1	2	3	4	5	6	7	8	9	10	11	12	13
Transient Number	Time (s)	Total Stress (psi)	M+B Stress (psi)	Temperature F	Pressure (psig)	Total Pressure Stress (psi)	M+B Pressure Stress (psi)	Total Piping Stress (psi)	M+B Piping Stress (psi)	Total Total Stress (psi)	Total M+B Stress (psi)	Number of Cycles (60 years)
1	0	0	0	70	0	0	0	0	0	0.00	0.00	123
2	0	0	0	70	0	0	0	0	0	0.00	0.00	120
	1680	0	0	100	1100	41506.3	40318.3	15.77042	15.77042	41522.07	40334.07	120
	10880	0	0	100	50	1886.65	1832.65	15.77042	15.77042	1902.42	1848.42	120
3	0	29166	23676	100	50	1886.65	1832.65	15.77042	15.77042	31068.42	25524.42	300
	16782.8	-3577	-3138	549	1010	38110.33	37019.53	-251.801	-251.801	34281.53	33629.73	300
	21164	-3532	-3138	549	1010	38110.33	37019.53	-251.801	-251.801	34326.53	33629.73	300
4	0	-3530	-3158	549	1010	38110.33	37019.53	-251.801	-251.801	34328.53	33609.73	300
	1801.9	29465	22266	244.004	1010	38110.33	37019.53	91.47053	91.47053	67666.80	59377.00	300
	8602	7720	6749	392	1010	38110.33	37019.53	169.2692	169.2692	45999.60	43937.80	300
5	0	7720	6752	392	1010	38110.33	37019.53	169.2692	169.2692	45999.60	43940.80	10000
	2229.8	13598	11941	311.002	1010	38110.33	37019.53	126.6901	126.6901	51835.02	49087.22	10000
	8600	7720	6752	392	1010	38110.33	37019.53	169.2692	169.2692	45999.60	43940.80	10000
6	0	7720	6752	392	1010	38110.33	37019.53	169.2692	169.2692	45999.60	43940.80	2000
	2820.3	15742	13892	280.691	1010	38110.33	37019.53	110.7562	110.7562	53963.09	51022.29	2000
	10400	7720	6752	392	1010	38110.33	37019.53	169.2692	169.2692	45999.60	43940.80	2000
9	0	7720	6752	392	1010	38110.33	37019.53	169.2692	169.2692	45999.60	43940.80	10
	2524	29006	23417	118.311	1010	38110.33	37019.53	25.39616	25.39616	67141.73	60461.93	10
	10400	7720	6752	392	1010	38110.33	37019.53	169.2692	169.2692	45999.60	43940.80	10
10	0	7720	6752	392	1010	38110.33	37019.53	169.2692	169.2692	45999.60	43940.80	70
	1632.4	16828	14701	267.399	1010	38110.33	37019.53	103.7688	103.7688	55042.10	51824.30	70
	7070	7720	6752	392	1010	38110.33	37019.53	169.2692	169.2692	45999.60	43940.80	70
11	0	7720	6752	392	1010	38110.33	37019.53	169.2692	169.2692	45999.60	43940.80	10
	3.5	6620	6632	565	1190	44902.27	43617.07	260.2119	260.2119	51782.48	50509.28	10
	4.5	6190	6608	50	1185	44713.61	43433.81	10.51361	10.51361	50914.12	50052.32	10
	194.5	31720	21067	109.348	1135	42826.96	41601.16	20.68448	20.68448	74567.64	62688.84	10
	2166.3	-4761	-1859	513.483	972	36676.48	35626.72	-233.1304	-233.1304	31682.35	33534.59	10
	2362.5	31268	22070	102.255	1010	38110.33	37019.53	16.95583	16.95583	69395.29	59106.49	10
	6728.3	-4913	-3149	513.448	1010	38110.33	37019.53	-233.112	-233.112	32964.22	33637.42	10
	7149.9	32114	21472	83.333	1010	38110.33	37019.53	7.0089	7.0089	70231.34	58498.54	10
	18213.3	-3565	-3162	503.978	1010	38110.33	37019.53	-228.1338	-228.1338	34317.20	33629.40	10
	19122.6	29156	23083	100.048	1010	38110.33	37019.53	15.79565	15.79565	67282.13	60118.33	10
	26814.5	7720	6410	392	1010	38110.33	37019.53	169.2692	169.2692	45999.60	43598.80	10
12	0	7720	6752	392	1010	38110.33	37019.53	169.2692	169.2692	45999.60	43940.80	60
	10	7720	6752	392	1135	42826.96	41601.16	169.2692	169.2692	50716.22	48522.42	60
	30	7720	6752	392	940	35469.02	34453.82	169.2692	169.2692	43358.29	41375.09	60
	2033.7	28648	25301	132.007	940	35469.02	34453.82	32.59588	32.59588	64149.62	59787.42	60
	9591	7720	6752	392	1010	38110.33	37019.53	169.2692	169.2692	45999.60	43940.80	60
13	0	7720	6752	392	1010	38110.33	37019.53	169.2692	169.2692	45999.60	43940.80	1
	10	7720	6752	392	1375	51882.88	50397.88	169.2692	169.2692	59772.14	57319.14	1
	30	7720	6752	392	940	35469.02	34453.82	169.2692	169.2692	43358.29	41375.09	1
	2033.7	28648	25301	132.007	1010	38110.33	37019.53	32.59588	32.59588	66790.93	62353.13	1
	9591	7720	6752	392	1010	38110.33	37019.53	169.2692	169.2692	45999.60	43940.80	1
14	0	7720	6752	392	1010	38110.33	37019.53	169.2692	169.2692	45999.60	43940.80	1
	5960	28487	25650	100	50	1886.65	1832.65	15.77042	15.77042	30389.42	27498.42	1
15	0	7720	6752	392	1010	38110.33	37019.53	169.2692	169.2692	45999.60	43940.80	228
	10	7720	6752	392	1135	42826.96	41601.16	169.2692	169.2692	50716.22	48522.42	228
	30	7720	6752	392	940	35469.02	34453.82	169.2692	169.2692	43358.29	41375.09	228
	2033.7	28648	25301	132.007	1010	38110.33	37019.53	32.59588	32.59588	66790.93	62353.13	228
	9591	7720	6752	392	1010	38110.33	37019.53	169.2692	169.2692	45999.60	43940.80	228
19	0	7720	6752	392	1010	38110.33	37019.53	169.2692	169.2692	45999.60	43940.80	300
	6800	16752	14971	265	1010	38110.33	37019.53	102.5077	102.5077	54964.84	52093.04	300
20	0	17151	13815	265	1010	38110.33	37019.53	102.5077	102.5077	55363.84	50937.04	300
	8925	-3531	-3146	549	1010	38110.33	37019.53	-251.801	-251.801	34327.53	33621.73	300
20A	0	-3530	-3158	549	1010	38110.33	37019.53	-251.801	-251.801	34328.53	33609.73	300
	183	28102	12153	233	1010	38110.33	37019.53	85.68595	85.68595	66298.02	49258.22	300
	5451	-3530	-3158	549	1010	38110.33	37019.53	-251.801	-251.801	34328.53	33609.73	300
21-23	0	-3530	-3158	549	1010	38110.33	37019.53	-251.801	-251.801	34328.53	33609.73	300
	20144	29168	23656	100	50	1886.65	1832.65	15.77042	15.77042	31070.42	25504.42	300
24	0	0	0	100	50	1886.65	1832.65	15.77042	15.77042	1902.42	1848.42	1
	600	0	0	100	1563	58976.68	57288.64	15.77042	15.77042	58992.45	57304.41	1
	2400	0	0	100	50	1886.65	1832.65	15.77042	15.77042	1902.42	1848.42	1
25	0	0	0	100	0	0	0	15.77042	15.77042	15.77	15.77	123
	1580	0	0	70	0	0	0	0	0	0.00	0.00	123

Table 4: Blend Radius Stress Summary (Continue)

NOTES:
- Column 1: Transient number identification.
- Column 2: Time during transient where a maxima or minima stress intensity occurs from P-V.OUT output file.
- Column 3: Maxima or minima total stress intensity from P-V.OUT output file.
- Column 4: Maxima or minima membrane plus bending stress intensity from P-V.OUT output file.
- Column 5: Temperature per total stress intensity.
- Column 6: Pressure per Table 1.
- Column 7: Total pressure stress intensity from the quantity (Column 6 x 37733)/1000 [Table3, 1].
- Column 8: Membrane plus bending pressure stress intensity from the quantity (Column 6 x 36653)/1000 [Table 3, 1].
- Column 9: Total external stress from calculation in Table 3, 265.47 psi*(Column 5-70°F)/(575°F -70°F).
- Column 10: Same as Column 9, but for M+B stress.
- Column 11: Sum of total stresses (Columns 3, 7, and 9).
- Column 12: Sum of membrane plus bending stresses (Columns 4, 8, and 10).
- Column 13: Number of cycles for the transient (60 years).

Table 5: Safe End Stress Summary

1	2	3	4	5	6	7	8	9	10	11	12	13
Transient Number	Time (s)	Total Stress (psi)	M+B Stress (psi)	Temperature F	Pressure (psig)	Total Pressure Stress (psi)	M+B Pressure Stress (psi)	Total Piping Stress (psi)	M+B Piping Stress (psi)	Total Total Stress (psi)	Total M+B Stress (psi)	Number of Cycles (60 years)
1	0	0	0	70	0	0	0	0	0	0.00	0.00	123
2	0	0	0	70	0	0	0	0	0	0.00	0.00	120
	1680	0	0	100	1100	9780.1	9562.3	339.0875	339.0875	10119.19	9901.39	120
	6960	0	0	100	50	444.55	434.65	339.0875	339.0875	783.64	773.74	120
3	0	-170	-165	100	50	444.55	434.65	-339.0875	-339.0875	-64.54	-69.44	300
	153.2	-235	-212	104.256	50	444.55	434.65	-387.1927	-387.1927	-177.64	-164.54	300
	16328.2	2	3	549	1010	8979.91	8779.93	5414.097	5414.097	14396.01	14197.03	300
	16664	-1	0	549	1010	8979.91	8779.93	-5414.097	5414.097	3564.81	14194.03	300
4	0	-3	-2	549	1010	8979.91	8779.93	-5414.097	-5414.097	3562.81	3363.83	300
	3.6	44060	30988	100	1010	8979.91	8779.93	339.0875	339.0875	53379.00	40107.02	300
	1804.6	-15889	-11224	260.286	1010	8979.91	8779.93	-2150.787	-2150.787	-9059.88	-4594.86	300
	4102	21	23	392	1010	8979.91	8779.93	3639.539	3639.539	12640.45	12442.47	300
5	0	22	23	392	1010	8979.91	8779.93	3639.539	3639.539	12641.45	12442.47	10000
	900.1	244	189	310	1010	8979.91	8779.93	2712.7	2712.7	11936.61	11681.63	10000
	3600	-169	-110	392	1010	8979.91	8779.93	-3639.539	-3639.539	5171.37	5030.39	10000
	3684.4	33	35	392	1010	8979.91	8779.93	3639.539	3639.539	12652.45	12454.47	10000
	4100	22	23	392	1010	8979.91	8779.93	3639.539	3639.539	12641.45	12442.47	10000
6	0	22	23	392	1010	8979.91	8779.93	3639.539	3639.539	12641.45	12442.47	2000
	1800.1	196	159	280	1010	8979.91	8779.93	2373.612	2373.612	11549.52	11312.54	2000
	5400.2	-108	-68	392	1010	8979.91	8779.93	-3639.539	-3639.539	5232.37	5072.39	2000
	5496.6	29	31	392	1010	8979.91	8779.93	3639.539	3639.539	12648.45	12450.47	2000
	5900	22	23	392	1010	8979.91	8779.93	3639.539	3639.539	12641.45	12442.47	2000
9	0	22	23	392	1010	8979.91	8779.93	3639.539	3639.539	12641.45	12442.47	10
	97.3	180	137	385.135	1010	8979.91	8779.93	3561.945	3561.945	12721.85	12478.87	10
	1884.1	63	65	265	1010	8979.91	8779.93	2204.069	2204.069	11246.98	11049.00	10
	2059.2	1161	859	226.597	1010	8979.91	8779.93	1770.003	1770.003	11910.91	11408.93	10
	3420.1	-334	-211	265	1010	8979.91	8779.93	-2204.069	-2204.069	6441.84	6364.86	10
	3490.2	97	98	265	1010	8979.91	8779.93	2204.069	2204.069	11280.98	11082.00	10
	5400.1	-126	-80	392	1010	8979.91	8779.93	-3639.539	-3639.539	5214.37	5060.39	10
	5470.6	31	32	392	1010	8979.91	8779.93	3639.539	3639.539	12650.45	12451.47	10
	5900	22	23	392	1010	8979.91	8779.93	3639.539	3639.539	12641.45	12442.47	10
10	0	23	22	392	1010	8979.91	8779.93	3639.539	3639.539	12642.45	12441.47	70
	77.1	2308	3188	285.461	1010	8979.91	8779.93	2435.338	2435.338	13723.25	14403.27	70
	169.4	-12	-13	265	1010	8979.91	8779.93	-2204.069	-2204.069	6763.84	6562.86	70
	1890	74	72	265	1010	8979.91	8779.93	2204.069	2204.069	11257.98	11056.00	70
	1968.2	-1069	-1511	322.362	1010	8979.91	8779.93	-2852.427	-2852.427	5058.48	4416.50	70
	2147.2	91	90	392	1010	8979.91	8779.93	3639.539	3639.539	12710.45	12509.47	70
	2570	23	22	392	1010	8979.91	8779.93	3639.539	3639.539	12642.45	12441.47	70
11	0	-29	-27	392	1010	8979.91	8779.93	-3639.539	-3639.539	5311.37	5113.39	10
	2.9	-20317	-13859	565	1147	10197.98	9970.871	-5594.944	-5594.944	-15713.97	-9483.07	10
	6.8	42852	29563	565	1172	10420.25	10188.2	5594.944	5594.944	58867.20	45346.14	10
	1567.4	-15216	-10526	565	1135	10091.29	9866.555	-5594.944	-5594.944	-10719.66	-6254.39	10
	2168.4	60377	41773	50	1134	10082.39	9857.862	-226.0583	-226.0583	70233.34	51404.80	10
	5409.4	-14924	-10329	565	1054	9371.114	9162.422	-5594.944	-5594.944	-11147.83	-6761.52	10
	6730.4	60377	41773	50	1133	10073.5	9849.169	-226.0583	-226.0583	70224.44	51396.11	10
	7243.2	-1965	-1434	128.917	675	6001.425	5867.775	-665.9339	-665.9339	3370.49	3767.84	10
	18215.4	52636	36417	100	1010	8979.91	8779.93	339.0875	339.0875	61955.00	45536.02	10
	20015.5	-24511	-16189	260.183	1010	8979.91	8779.93	-2149.623	-2149.623	-17680.71	-9558.69	10
	22314.5	22	23	392	937	8330.867	8145.341	3639.539	3639.539	11992.41	11807.88	10
12	0	23	22	392	1010	8979.91	8779.93	3639.539	3639.539	12642.45	12441.47	60
	10	23	22	392	1135	10091.29	9866.555	3639.539	3639.539	13753.82	13528.09	60
	30	23	22	392	940	8357.54	8171.42	3639.539	3639.539	12020.08	11832.96	60
	90	3174	4383	275	940	8357.54	8171.42	2317.098	2317.098	13848.64	14871.52	60
	2793.5	-16189	-24511	260.183	941	8366.431	8180.113	-2149.623	-2149.623	-9972.19	-18480.51	60
	5091	23	22	392	1010	8979.91	8779.93	3639.539	3639.539	12642.45	12441.47	60
13	0	23	22	392	1010	8979.91	8779.93	3639.539	3639.539	12642.45	12441.47	1
	10	23	22	392	1375	12225.13	11952.88	3639.539	3639.539	15887.66	15614.41	1
	30	23	22	392	940	8357.54	8171.42	3639.539	3639.539	12020.08	11832.96	1
	90	3174	4383	275	940	8357.54	8171.42	2317.098	2317.098	13848.64	14871.52	1
	2793.5	-16189	-24511	260.183	941	8366.431	8180.113	-2149.623	-2149.623	-9972.19	-18480.51	1
	5091	23	22	392	1010	8979.91	8779.93	3639.539	3639.539	12642.45	12441.47	1

Table 5: Safe End Stress Summary (continue)

1	2	3	4	5	6	7	8	9	10	11	12	13
Transient Number	Time (s)	Total Stress (psi)	M+B Stress (psi)	Temperature F	Pressure (psig)	Total Pressure Stress (psi)	M+B Pressure Stress (psi)	Total Piping Stress (psi)	M+B Piping Stress (psi)	Total Total Stress (psi)	Total M+B Stress (psi)	Number of Cycles (60 years)
14	0	22	23	392	1010	8979.91	8779.93	3639.539	3639.539	12641.45	12442.47	1
	60	4383	3174	275	885	7868.535	7693.305	2317.098	2317.098	14568.63	13184.40	1
	148	420	300	258.492	803	7139.473	6980.479	2130.509	2130.509	9689.98	9410.99	1
	960	544	424	100	50	444.55	434.65	339.0875	339.0875	1327.64	1197.74	1
	1460	137	139	100	50	444.55	434.65	339.0875	339.0875	920.64	912.74	1
15	0	23	22	392	1010	8979.91	8779.93	3639.539	3639.539	12642.45	12441.47	228
	10	23	22	392	1135	10091.29	9866.555	3639.539	3639.539	13753.82	13528.09	228
	30	23	22	392	940	8357.54	8171.42	3639.539	3639.539	12020.08	11832.96	228
	90	3174	4383	275	940	8357.54	8171.42	2317.098	2317.098	13848.64	14871.52	228
	2793.5	-16189	-24511	260.183	941	8366.431	8180.113	-2149.623	-2149.623	-9972.19	-18480.51	228
	5091	23	22	392	1010	8979.91	8779.93	3639.539	3639.539	12642.45	12441.47	228
19	0	22	23	392	1010	8979.91	8779.93	3639.539	3639.539	12641.45	12442.47	300
	1800	219	177	265	1010	8979.91	8779.93	2204.069	2204.069	11402.98	11161.00	300
	2300	72	74	265	1010	8979.91	8779.93	2204.069	2204.069	11255.98	11058.00	300
20	0	-109	-105	265	1010	8979.91	8779.93	-2204.069	-2204.069	6666.84	6470.86	300
	4	-17288	-12189	440.106	1010	8979.91	8779.93	-4183.277	-4183.277	-12491.37	-7592.35	300
	4425	-2	-1	549	1010	8979.91	8779.93	-5414.097	-5414.097	3563.81	3364.83	300
20A	0	-3	-2	549	1010	8979.91	8779.93	-5414.097	-5414.097	3562.81	3363.83	300
	4	44060	30988	100	1010	8979.91	8779.93	339.0875	339.0875	53379.00	40107.02	300
	241	-7461	-5525	290.247	1010	8979.91	8779.93	-2489.433	-2489.433	-970.52	765.50	300
	572	128	132	549	1010	8979.91	8779.93	5414.097	5414.097	14522.01	14326.03	300
	951	-3	-2	549	1010	8979.91	8779.93	-5414.097	-5414.097	3562.81	3363.83	300
21-23	0	-3	-2	549	1010	8979.91	8779.93	-5414.097	-5414.097	3562.81	3363.83	300
	138	62	45	545.167	989	8793.199	8597.377	5370.773	5370.773	14225.97	14013.15	300
	6264	-5	-20	374.97	50	444.55	434.65	-3447.05	-3447.05	-3007.50	-3032.40	300
	6390	104	59	366.172	50	444.55	434.65	3347.607	3347.607	3896.16	3841.26	300
	15644	-173	-167	100	50	444.55	434.65	-339.0875	-339.0875	-67.54	-71.44	300
24	0	0	0	100	50	444.55	434.65	339.0875	339.0875	783.64	773.74	1
	600	0	0	100	1563	13896.63	13587.16	339.0875	339.0875	14235.72	13926.25	1
	2400	0	0	100	50	444.55	434.65	339.0875	339.0875	783.64	773.74	1
25	0	0	0	100	0	0	0	339.0875	339.0875	339.09	339.09	123
	1580	0	0	70	0	0	0	0	0	0.00	0.00	123

NOTES: Column 1: Transient number identification.
Column 2: Time during transient where a maxima or minima stress intensity occurs from P-V.OUT output file.
Column 3: Maxima or minima total stress intensity from P-V.OUT output file.
Column 4: Maxima or minima membrane plus bending stress intensity from P-V.OUT output file.
Column 5: Temperature per total stress intensity.
Column 6: Pressure per Table 2.
Column 7: Total pressure stress intensity from the quantity (Column 6 x 8891)/1000 [Table 3, 1].
Column 8: Membrane plus bending pressure stress intensity from the quantity (Column 6 x 8693)/1000 [Table3, 1].
Column 9: Total external stress from calculation in Table 3, 5707.97 psi*(Column 5-70°F)/(575°F -70°F).
Column 10: Same as Column 9, but for M+B stress.
Column 11: Sum of total stresses (Columns 3, 7, and 9).
Column 12: Sum of membrane plus bending stresses (Columns 4, 8, and 10).
Column 13: Number of cycles for the transient (60 years).

Table 6: Fatigue Results for Blend Radius (60 Years)

LOCATION = LOCATION NO. 2 -- BLEND RADIUS
FATIGUE CURVE = 1 (1 = CARBON/LOW ALLOY, 2 = STAINLESS STEEL)
m = 2.0
n = .2
Sm = 26700. psi
Ecurve = 3.000E+07 psi
Eanalysis = 2.670E+07 psi
Kt = 1.00

MAX	MIN	RANGE	MEM+BEND	Ke	Salt	Napplied	Nallowed	U
74568.	0.	74568.	62689.	1.000	41892.	1.000E+01	7.488E+03	.0013
70231.	0.	70231.	58499.	1.000	39456.	1.000E+01	8.944E+03	.0011
69395.	0.	69395.	59106.	1.000	38986.	1.000E+01	9.268E+03	.0011
67667.	0.	67667.	59377.	1.000	38015.	9.300E+01	9.988E+03	.0093
67667.	0.	67667.	59377.	1.000	38015.	1.200E+02	9.988E+03	.0120
67667.	0.	67667.	59377.	1.000	38015.	8.700E+01	9.988E+03	.0087
67282.	0.	67282.	60118.	1.000	37799.	1.000E+01	1.018E+04	.0010
67142.	0.	67142.	60462.	1.000	37720.	1.000E+01	1.025E+04	.0010
66791.	0.	66791.	62353.	1.000	37523.	1.000E+00	1.044E+04	.0001
66791.	0.	66791.	62353.	1.000	37523.	1.500E+01	1.044E+04	.0014
66791.	16.	66775.	62337.	1.000	37514.	1.230E+02	1.045E+04	.0118
66791.	1902.	64889.	60505.	1.000	36454.	9.000E+01	1.152E+04	.0078
66298.	1902.	64396.	47410.	1.000	36177.	3.000E+01	1.182E+04	.0025
66298.	1902.	64396.	47410.	1.000	36177.	1.000E+00	1.182E+04	.0001
66298.	1902.	64396.	47410.	1.000	36177.	1.000E+00	1.182E+04	.0001
66298.	30389.	35909.	21760.	1.000	20173.	1.000E+00	9.581E+04	.0000
66298.	31068.	35230.	23734.	1.000	19792.	2.670E+02	1.038E+05	.0026
64150.	31068.	33081.	34263.	1.000	18585.	3.300E+01	1.303E+05	.0003
64150.	31070.	33079.	34283.	1.000	18584.	2.700E+01	1.303E+05	.0002
59772.	31070.	28702.	31815.	1.000	16125.	1.000E+00	2.222E+05	.0000
58992.	31070.	27922.	31800.	1.000	15687.	1.000E+00	2.519E+05	.0000
55364.	31070.	24293.	25433.	1.000	13648.	2.710E+02	4.757E+05	.0006
55364.	31682.	23681.	17402.	1.000	13304.	1.000E+01	5.703E+05	.0000
55364.	32964.	22400.	17300.	1.000	12584.	1.000E+01	9.414E+05	.0000
55364.	34282.	21082.	17307.	1.000	11844.	9.000E+00	1.912E+06	.0000
55042.	34282.	20761.	18195.	1.000	11663.	7.000E+01	2.231E+06	.0000
54965.	34282.	20683.	18463.	1.000	11620.	2.210E+02	2.310E+06	.0001
54965.	34317.	20648.	18464.	1.000	11600.	1.000E+01	2.348E+06	.0000
54965.	34327.	20638.	18463.	1.000	11595.	6.900E+01	2.358E+06	.0000
53963.	34327.	19637.	17393.	1.000	11032.	2.310E+02	3.757E+06	.0001
53963.	34328.	19636.	17401.	1.000	11031.	3.000E+02	3.758E+06	.0001
53963.	34329.	19635.	17413.	1.000	11031.	3.000E+02	3.760E+06	.0001
53963.	34329.	19635.	17413.	1.000	11031.	3.000E+02	3.760E+06	.0001
53963.	34329.	19635.	17413.	1.000	11031.	3.000E+02	3.760E+06	.0001
53963.	34329.	19635.	17413.	1.000	11031.	3.000E+02	3.760E+06	.0001
53963.	41522.	12441.	10688.	1.000	6989.	1.200E+02	1.000E+20	.0000
53963.	43358.	10605.	9647.	1.000	5958.	6.000E+01	1.000E+20	.0000
53963.	43358.	10605.	9647.	1.000	5958.	1.000E+00	1.000E+20	.0000
53963.	43358.	10605.	9647.	1.000	5958.	8.800E+01	1.000E+20	.0000
51835.	43358.	8477.	7712.	1.000	4762.	1.400E+02	1.000E+20	.0000
51835.	46000.	5835.	5149.	1.000	3278.	3.000E+02	1.000E+20	.0000
51835.	46000.	5835.	5146.	1.000	3278.	9.560E+03	1.000E+20	.0000
51782.	46000.	5783.	6568.	1.000	3249.	1.000E+01	1.000E+20	.0000

50914.	46000.	4915.	6112.	1.000	2761.	1.000E+01	1.000E+20	.0000
50716.	46000.	4717.	4582.	1.000	2650.	6.000E+01	1.000E+20	.0000
50716.	46000.	4717.	4582.	1.000	2650.	2.280E+02	1.000E+20	.0000
46000.	46000.	0.	0.	1.000	0.	1.320E+02	1.000E+20	.0000
46000.	46000.	0.	0.	1.000	0.	1.000E+04	1.000E+20	.0000
46000.	46000.	0.	0.	1.000	0.	2.000E+03	1.000E+20	.0000
46000.	46000.	0.	0.	1.000	0.	2.000E+03	1.000E+20	.0000
46000.	46000.	0.	0.	1.000	0.	1.000E+01	1.000E+20	.0000
46000.	46000.	0.	0.	1.000	0.	1.000E+01	1.000E+20	.0000
46000.	46000.	0.	0.	1.000	0.	7.000E+01	1.000E+20	.0000
46000.	46000.	0.	0.	1.000	0.	7.000E+01	1.000E+20	.0000
46000.	46000.	0.	0.	1.000	0.	1.000E+01	1.000E+20	.0000
46000.	46000.	0.	0.	1.000	0.	1.000E+01	1.000E+20	.0000
46000.	46000.	0.	0.	1.000	0.	6.000E+01	1.000E+20	.0000
46000.	46000.	0.	0.	1.000	0.	6.000E+01	1.000E+20	.0000
46000.	46000.	0.	0.	1.000	0.	1.000E+00	1.000E+20	.0000
46000.	46000.	0.	0.	1.000	0.	1.000E+00	1.000E+20	.0000
46000.	46000.	0.	0.	1.000	0.	1.000E+00	1.000E+20	.0000
46000.	46000.	0.	0.	1.000	0.	2.280E+02	1.000E+20	.0000
46000.	46000.	0.	0.	1.000	0.	2.280E+02	1.000E+20	.0000
								=======
							TOTAL USAGE FACTOR =	.0636

Table 7: Fatigue Results for Safe End (60 Years)

```
      LOCATION = LOCATION NO. 1 -- SAFE END
 FATIGUE CURVE = 1 (1 = CARBON/LOW ALLOY, 2 = STAINLESS STEEL)
             m = 3.0
             n =  .2
            Sm = 17800. psi
        Ecurve = 3.000E+07 psi
     Eanalysis = 2.810E+07 psi
            Kt = 1.34
```

MAX	MIN	RANGE	MEM+BEND	Ke	Salt	Napplied	Nallowed	U
70233.	-17681.	87914.	60963.	1.283	74422.	1.000E+01	1.338E+03	.0075
70224.	-15714.	85938.	60879.	1.280	72869.	1.000E+01	1.415E+03	.0071
61955.	-12491.	74446.	53128.	1.000	49383.	1.000E+01	4.568E+03	.0022
58867.	-12491.	71359.	52938.	1.000	47700.	1.000E+01	5.094E+03	.0020
53379.	-12491.	65870.	47699.	1.000	43819.	2.800E+02	6.552E+03	.0427
53379.	-11148.	64527.	46869.	1.000	42951.	1.000E+01	6.953E+03	.0014
53379.	-10720.	64099.	46361.	1.000	42631.	1.000E+01	7.109E+03	.0014
53379.	-9972.	63351.	58588.	1.194	53087.	6.000E+01	3.628E+03	.0165
53379.	-9972.	63351.	58588.	1.194	53087.	1.000E+00	3.628E+03	.0003
53379.	-9972.	63351.	58588.	1.194	53087.	2.280E+02	3.628E+03	.0628
53379.	-9060.	62439.	44702.	1.000	41444.	1.100E+01	7.731E+03	.0014
15888.	-9060.	24948.	20209.	1.000	16985.	1.000E+00	1.802E+05	.0000
14569.	-9060.	23629.	17779.	1.000	15840.	1.000E+00	2.410E+05	.0000
14522.	-9060.	23582.	18921.	1.000	16022.	2.870E+02	2.287E+05	.0013
14522.	-3008.	17530.	17358.	1.000	12508.	1.300E+01	9.944E+05	.0000
14396.	-3008.	17404.	17229.	1.000	12417.	2.870E+02	1.083E+06	.0003
14396.	-971.	15367.	13432.	1.000	10641.	1.300E+01	5.165E+06	.0000
14236.	-971.	15206.	13161.	1.000	10506.	1.000E+00	5.563E+06	.0000
14226.	-971.	15196.	13248.	1.000	10516.	2.860E+02	5.531E+06	.0001
14226.	-178.	14404.	14178.	1.000	10262.	1.400E+01	6.379E+06	.0000
13849.	-178.	14026.	15036.	1.000	10216.	6.000E+01	6.547E+06	.0000
13849.	-178.	14026.	15036.	1.000	10216.	1.000E+00	6.547E+06	.0000
13849.	-178.	14026.	15036.	1.000	10216.	2.250E+02	6.547E+06	.0000
13849.	-68.	13916.	14943.	1.000	10141.	3.000E+00	6.837E+06	.0000
13754.	-68.	13821.	13600.	1.000	9846.	6.000E+01	8.117E+06	.0000
13754.	-68.	13821.	13600.	1.000	9846.	2.280E+02	8.117E+06	.0000
13723.	-68.	13791.	14475.	1.000	9989.	9.000E+00	7.465E+06	.0000
13723.	-65.	13788.	14473.	1.000	9987.	6.100E+01	7.474E+06	.0000
12722.	-65.	12786.	12548.	1.000	9103.	1.000E+01	1.729E+07	.0000
12710.	-65.	12775.	12579.	1.000	9102.	7.000E+01	1.730E+07	.0000
12652.	-65.	12717.	12524.	1.000	9061.	1.590E+02	1.833E+07	.0000
12652.	0.	12652.	12454.	1.000	9014.	1.230E+02	1.959E+07	.0000
12652.	0.	12652.	12454.	1.000	9014.	1.200E+02	1.959E+07	.0000
12652.	0.	12652.	12454.	1.000	9014.	1.230E+02	1.959E+07	.0000
12652.	339.	12313.	12115.	1.000	8772.	1.230E+02	2.905E+07	.0000
12652.	784.	11869.	11681.	1.000	8456.	1.200E+02	4.952E+07	.0000
12652.	784.	11869.	11681.	1.000	8456.	1.000E+00	4.952E+07	.0000
12652.	784.	11869.	11681.	1.000	8456.	1.000E+00	4.952E+07	.0000
12652.	921.	11732.	11542.	1.000	8357.	1.000E+00	5.462E+07	.0000
12652.	1328.	11325.	11257.	1.000	8088.	1.000E+00	7.100E+07	.0000
12652.	3370.	9282.	8687.	1.000	6531.	1.000E+01	1.000E+20	.0000
12652.	3563.	9090.	9091.	1.000	6502.	3.000E+02	1.000E+20	.0000
12652.	3563.	9090.	9091.	1.000	6502.	3.000E+02	1.000E+20	.0000

12652.	3563.	9090.	9091.	1.000	6502.	3.000E+02	1.000E+20	.0000
12652.	3563.	9090.	9091.	1.000	6502.	3.000E+02	1.000E+20	.0000
12652.	3564.	9089.	9090.	1.000	6501.	3.000E+02	1.000E+20	.0000
12652.	3565.	9088.	-1740.	1.000	4535.	3.000E+02	1.000E+20	.0000
12652.	3896.	8756.	8613.	1.000	6237.	3.000E+02	1.000E+20	.0000
12652.	5058.	7594.	8038.	1.000	5513.	7.000E+01	1.000E+20	.0000
12652.	5171.	7481.	7424.	1.000	5341.	7.048E+03	1.000E+20	.0000
12650.	5171.	7479.	7421.	1.000	5339.	1.000E+01	1.000E+20	.0000
12648.	5171.	7477.	7420.	1.000	5338.	2.000E+03	1.000E+20	.0000
12642.	5171.	7471.	7411.	1.000	5333.	7.000E+01	1.000E+20	.0000
12642.	5171.	7471.	7411.	1.000	5333.	7.000E+01	1.000E+20	.0000
12642.	5171.	7471.	7411.	1.000	5333.	6.000E+01	1.000E+20	.0000
12642.	5171.	7471.	7411.	1.000	5333.	6.000E+01	1.000E+20	.0000
12642.	5171.	7471.	7411.	1.000	5333.	1.000E+00	1.000E+20	.0000
12642.	5171.	7471.	7411.	1.000	5333.	1.000E+00	1.000E+20	.0000
12642.	5171.	7471.	7411.	1.000	5333.	2.280E+02	1.000E+20	.0000
12642.	5171.	7471.	7411.	1.000	5333.	2.280E+02	1.000E+20	.0000
12641.	5171.	7470.	7412.	1.000	5333.	2.240E+02	1.000E+20	.0000
12641.	5214.	7427.	7382.	1.000	5304.	1.000E+01	1.000E+20	.0000
12641.	5232.	7409.	7370.	1.000	5293.	2.000E+03	1.000E+20	.0000
12641.	5311.	7330.	7329.	1.000	5243.	1.000E+01	1.000E+20	.0000
12641.	6442.	6200.	6078.	1.000	4412.	1.000E+01	1.000E+20	.0000
12641.	6667.	5975.	5972.	1.000	4273.	3.000E+02	1.000E+20	.0000
12641.	6764.	5878.	5880.	1.000	4205.	7.000E+01	1.000E+20	.0000
12641.	9690.	2951.	3031.	1.000	2126.	1.000E+00	1.000E+20	.0000
12641.	10119.	2522.	2541.	1.000	1808.	1.200E+02	1.000E+20	.0000
12641.	11247.	1394.	1393.	1.000	997.	1.000E+01	1.000E+20	.0000
12641.	11256.	1385.	1384.	1.000	991.	3.000E+02	1.000E+20	.0000
12641.	11258.	1383.	1386.	1.000	990.	7.000E+01	1.000E+20	.0000
12641.	11281.	1360.	1360.	1.000	973.	1.000E+01	1.000E+20	.0000
12641.	11403.	1238.	1281.	1.000	894.	3.000E+02	1.000E+20	.0000
12641.	11550.	1092.	1130.	1.000	788.	2.000E+03	1.000E+20	.0000
12641.	11911.	731.	1034.	1.000	578.	1.000E+01	1.000E+20	.0000
12641.	11937.	705.	761.	1.000	514.	4.555E+03	1.000E+20	.0000
12641.	11937.	705.	761.	1.000	514.	5.445E+03	1.000E+20	.0000
12641.	11992.	649.	635.	1.000	462.	1.000E+01	1.000E+20	.0000
12641.	12020.	621.	610.	1.000	442.	6.000E+01	1.000E+20	.0000
12641.	12020.	621.	610.	1.000	442.	1.000E+00	1.000E+20	.0000
12641.	12020.	621.	610.	1.000	442.	2.280E+02	1.000E+20	.0000
12641.	12640.	1.	0.	1.000	1.	3.000E+02	1.000E+20	.0000
12641.	12641.	0.	0.	1.000	0.	3.956E+03	1.000E+20	.0000
12641.	12641.	0.	0.	1.000	0.	2.000E+03	1.000E+20	.0000
12641.	12641.	0.	0.	1.000	0.	2.000E+03	1.000E+20	.0000
12641.	12641.	0.	0.	1.000	0.	1.000E+01	1.000E+20	.0000
12641.	12641.	0.	0.	1.000	0.	1.000E+01	1.000E+20	.0000
12641.	12641.	0.	0.	1.000	0.	1.000E+00	1.000E+20	.0000
								=======
							TOTAL USAGE FACTOR =	.1471

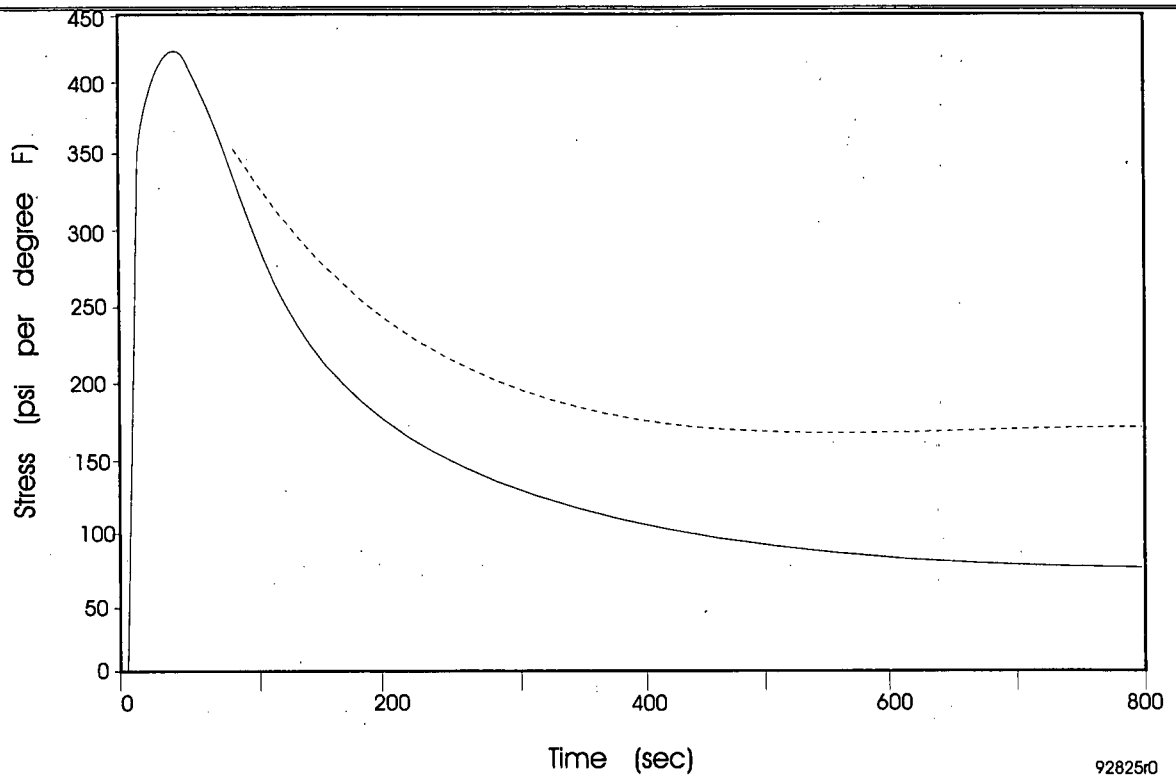

Note: A typical set of two Green's Functions is shown, each for a different set of heat transfer coefficients (representing different flow rate conditions).

Figure 1: Typical Green's Functions for Thermal Transient Stress

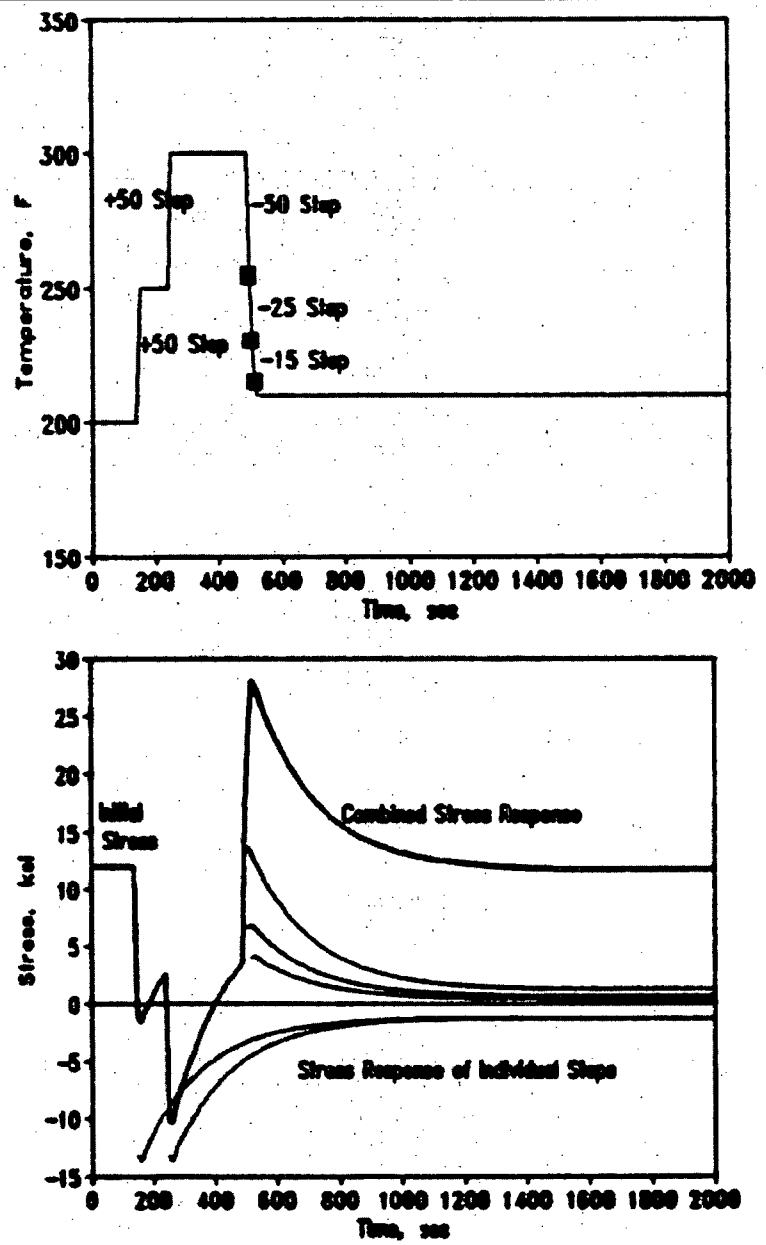

Figure 2: Typical Stress Response Using Green's Functions

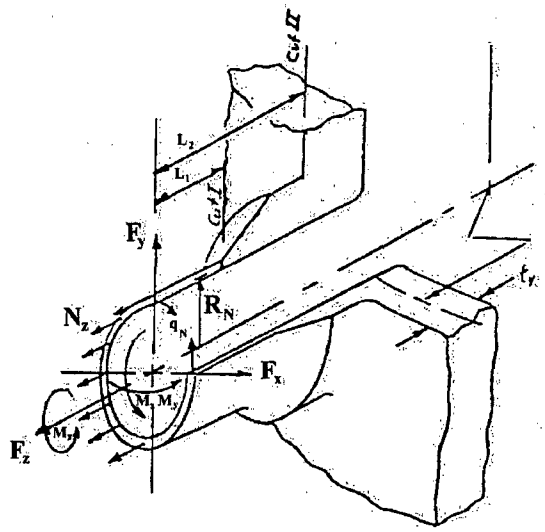

Figure 3: External Forces and Moments on the Feedwater Nozzle

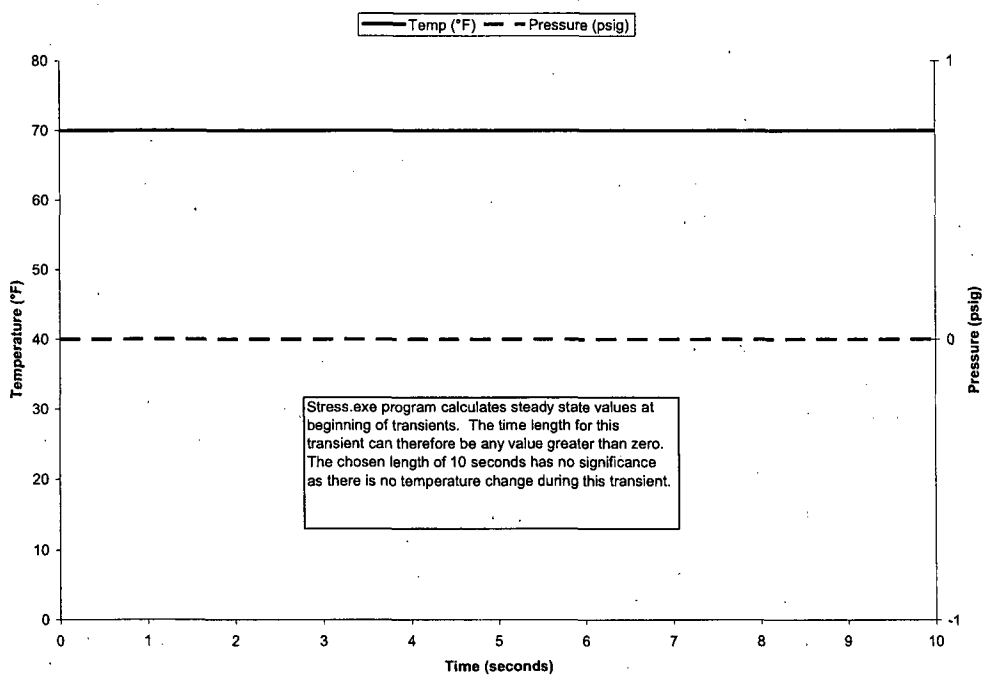

Figure 4: Transient 1, Bolt-up

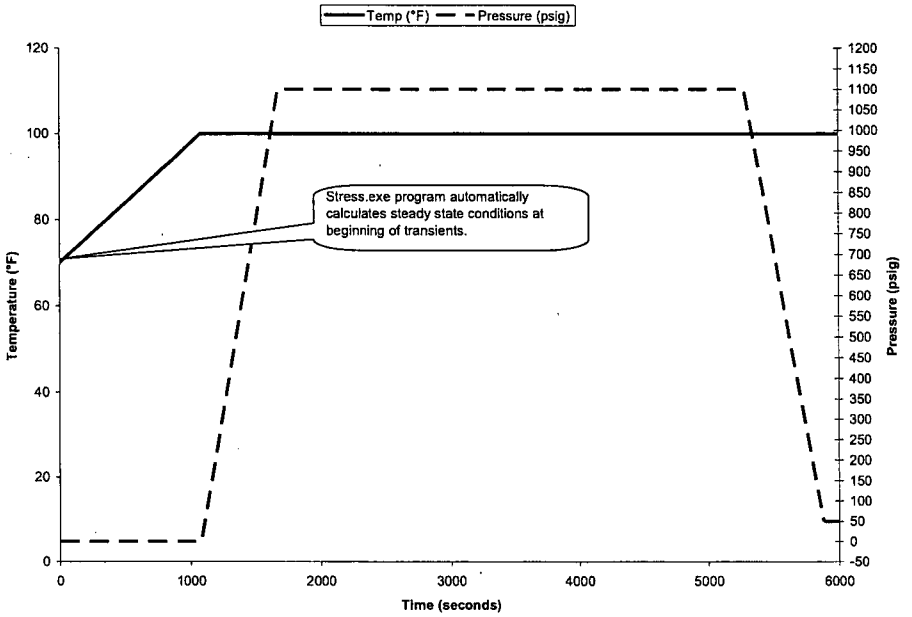

Figure 5: Transient 2, Design HYD Test

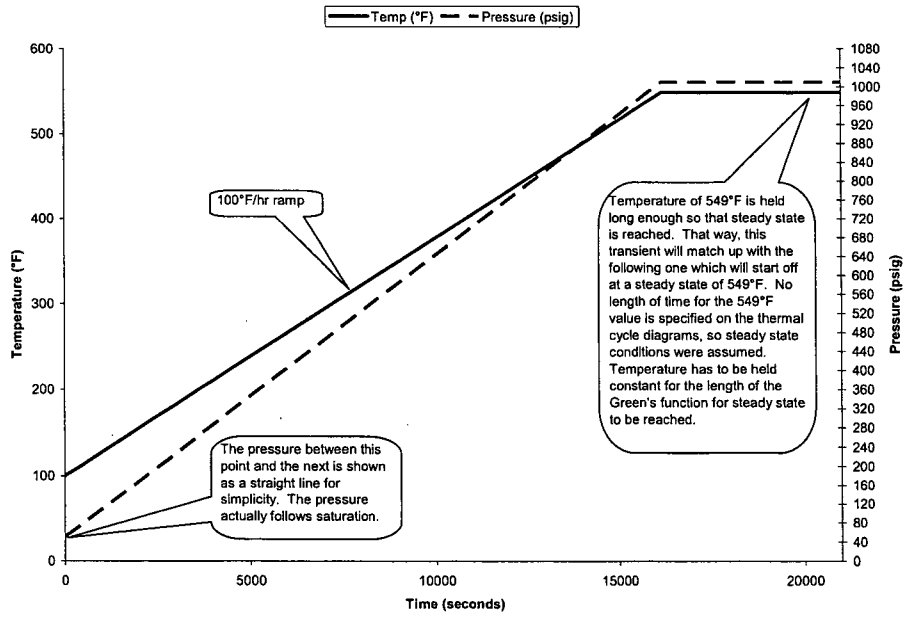

Figure 6: Transient 3, Startup

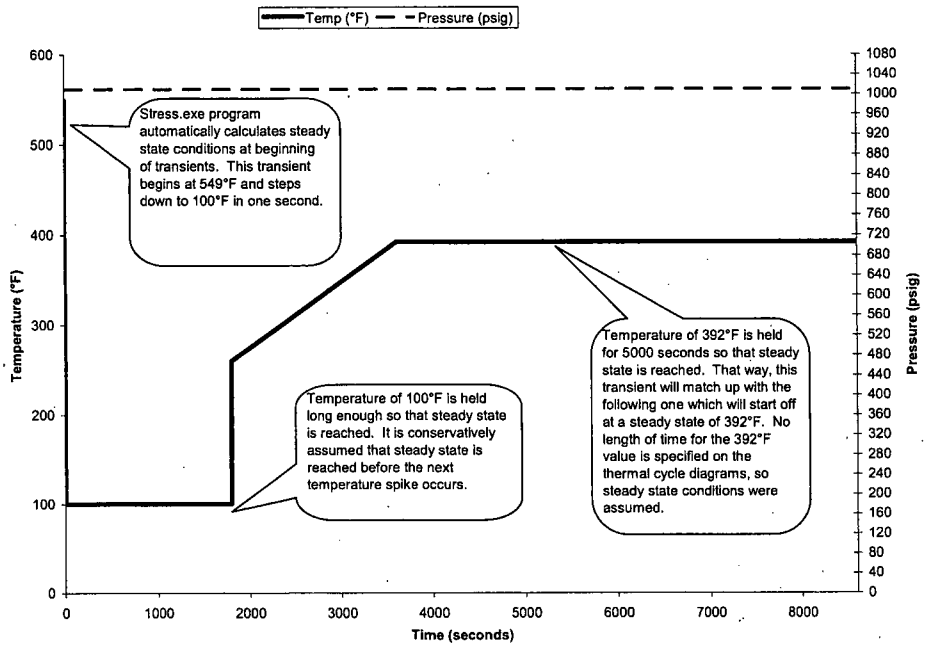

Figure 7: Transient 4, Turbine Roll and Increased to Rated Power

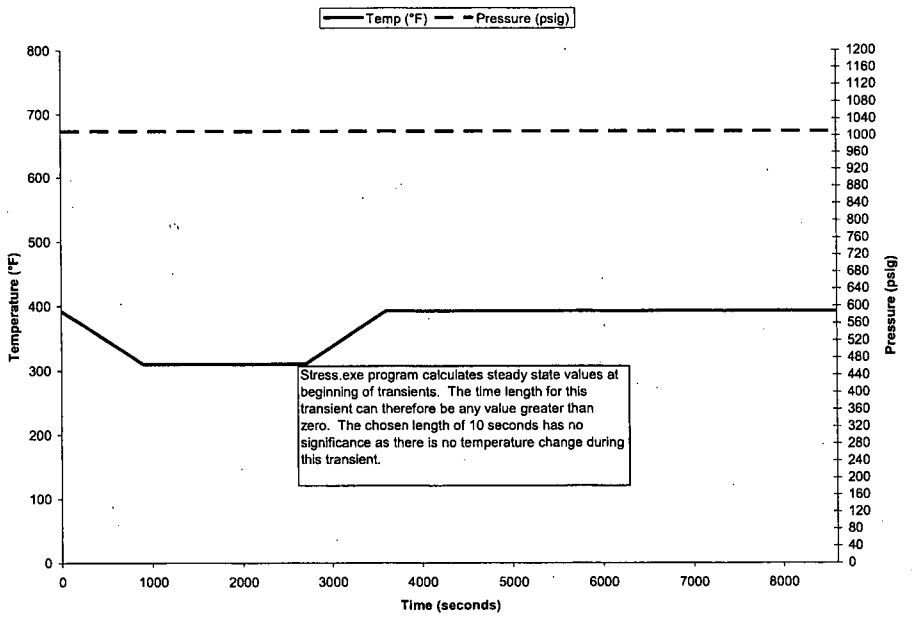

Figure 8: Transient 5, Daily Reduction 75% Power

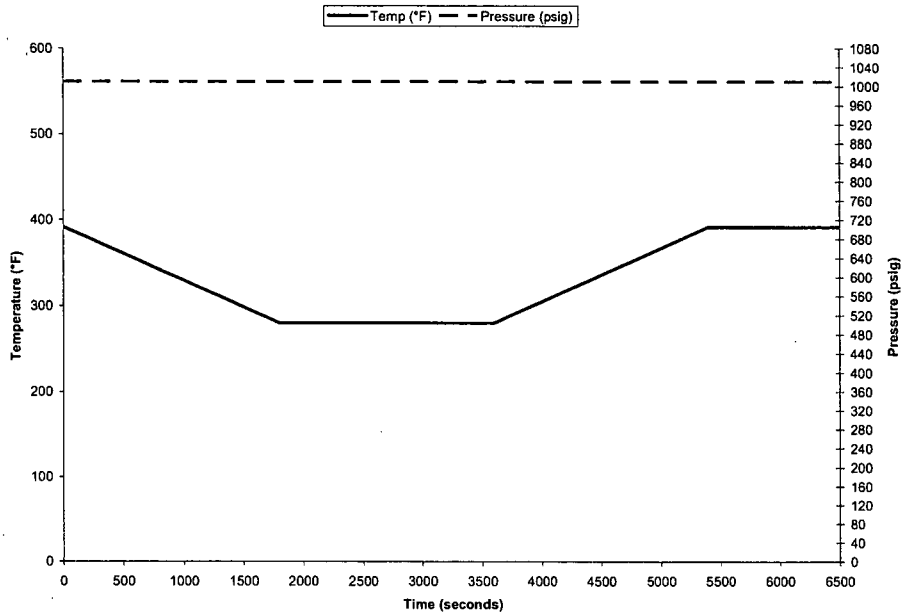

Figure 9: Transient 6, Weekly Reduction 50% Power

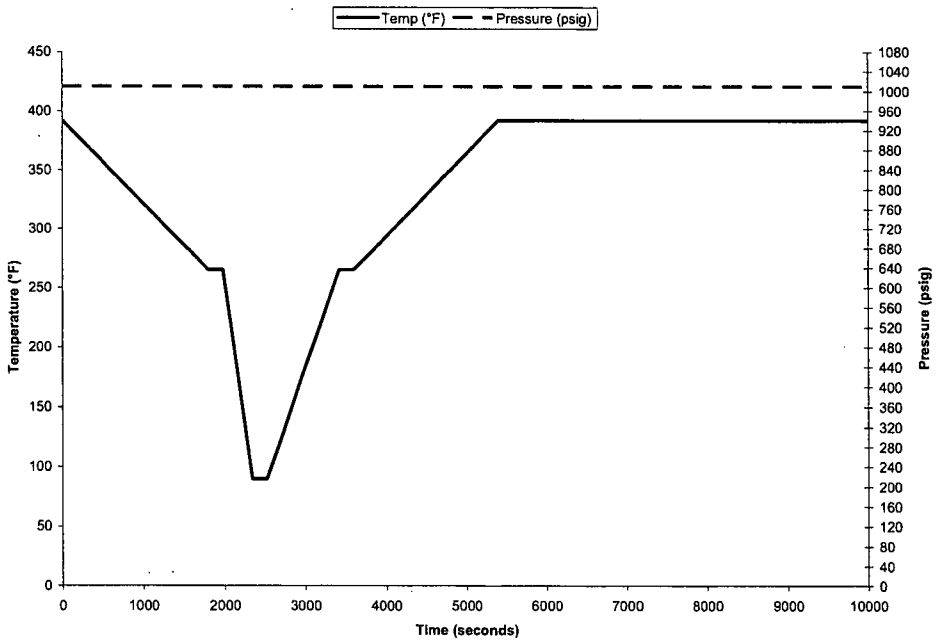

Figure 10: Transient 9, Turbine Trip at 25% Power

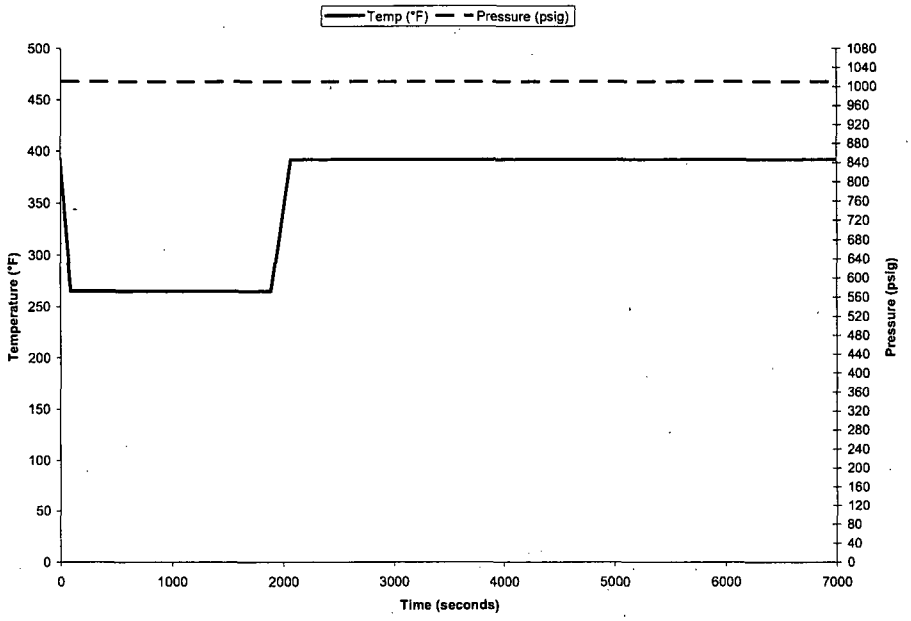

Figure 11: Transient 10, Feedwater Bypass

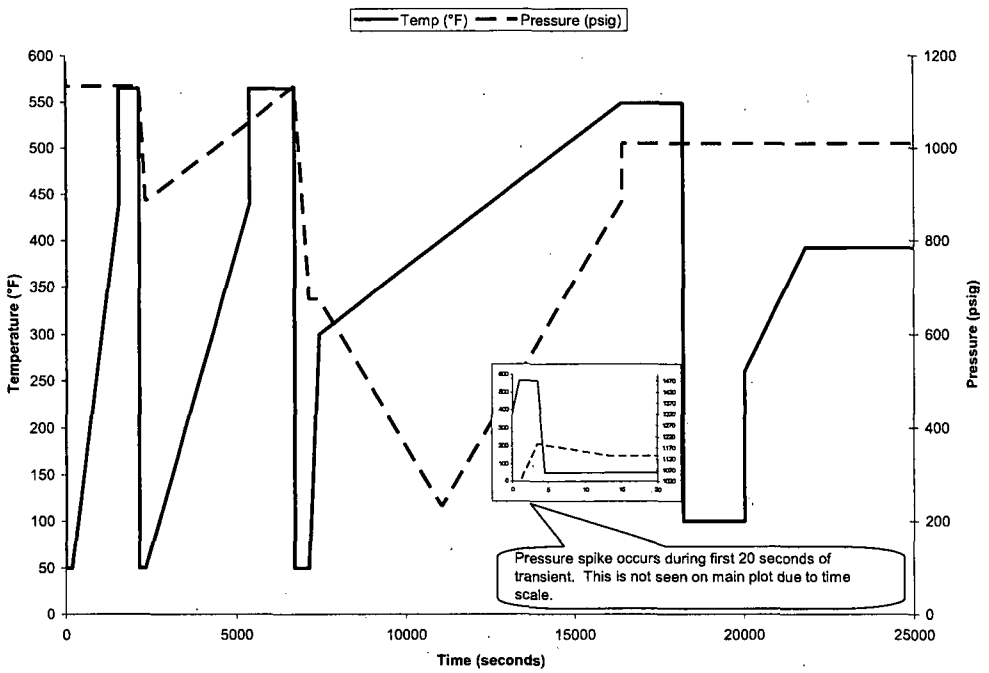

Figure 12: Transient 11, Loss of Feedwater Pumps

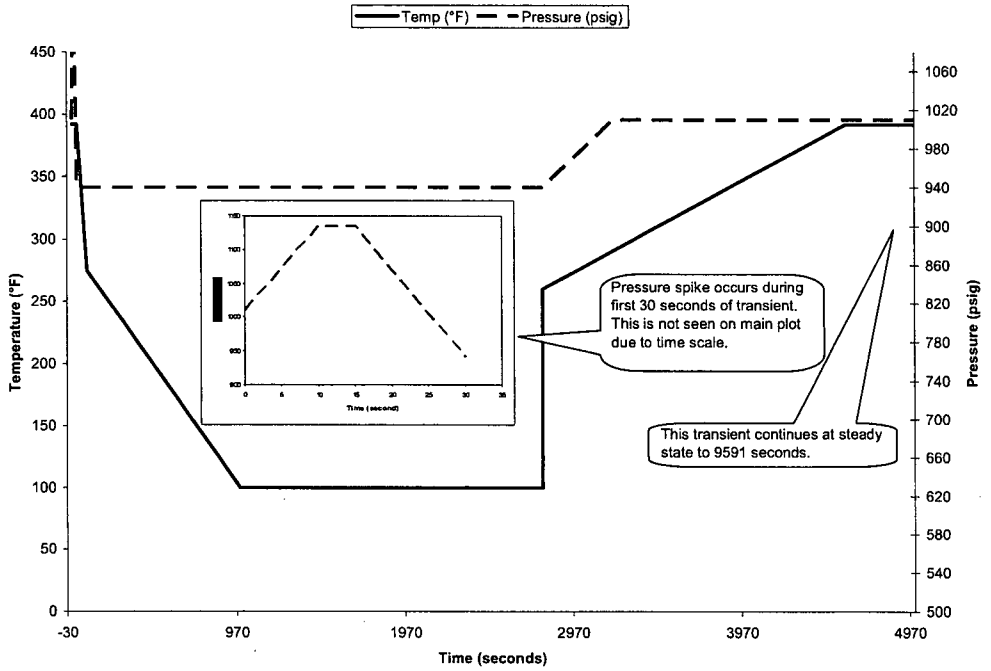

Figure 13: Transient 12, Turbine Generator Trip

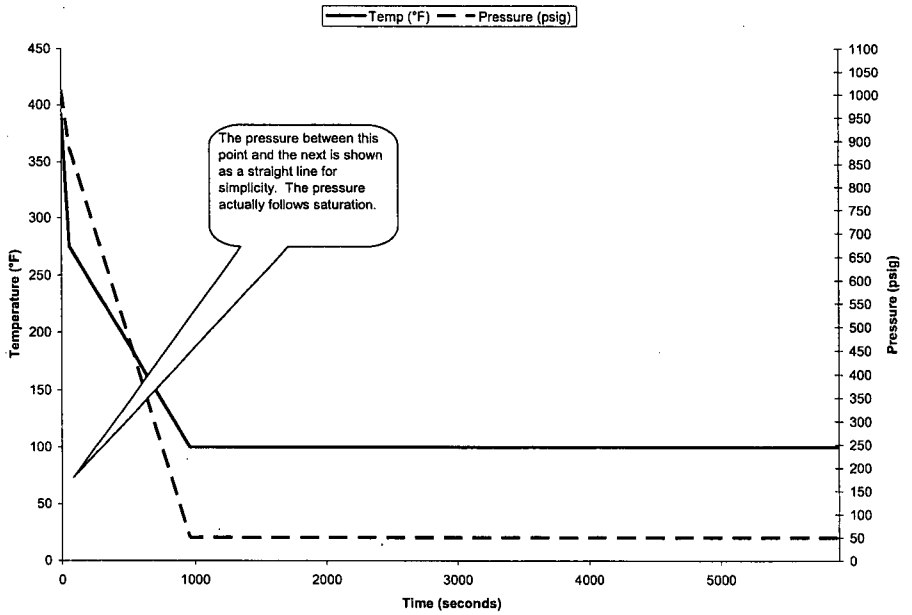

Figure 14: Transient 14, SRV Blowdown

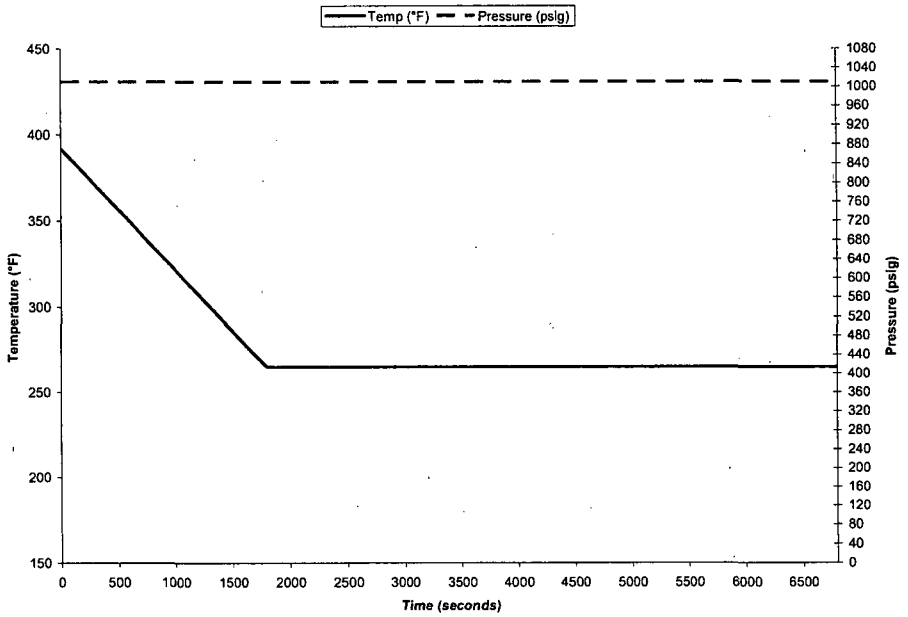

Figure 15: Transient 19, Reduction to 0% Power

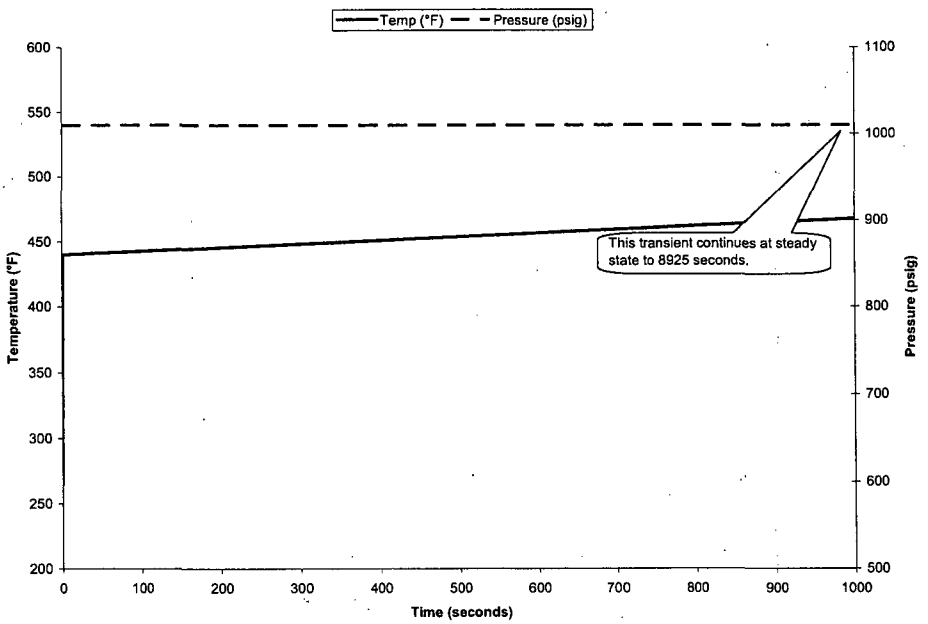

Figure 16: Transient 20, Hot Standby (Heatup Portion)

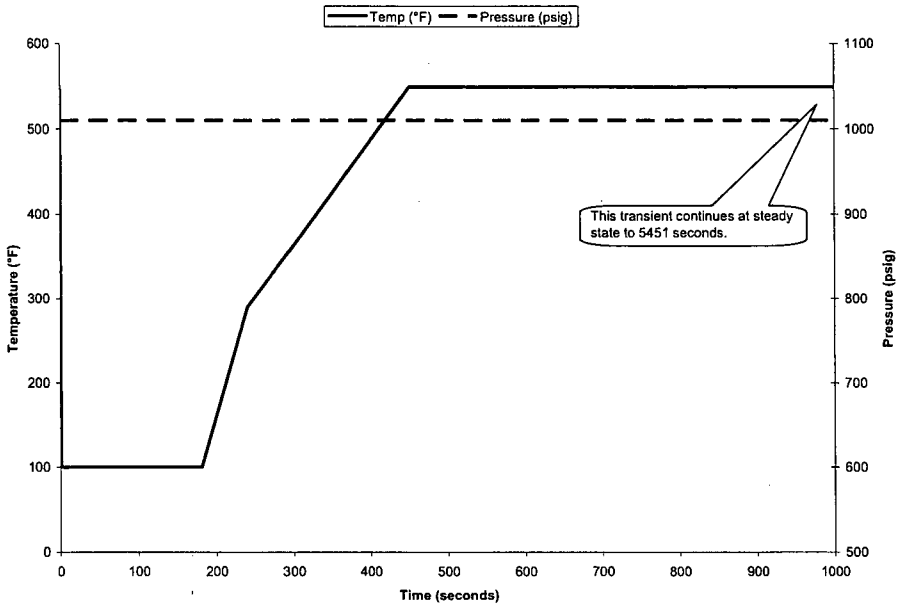

Figure 17: Transient 20A, Hot Standby (Feedwater Injection Portion)

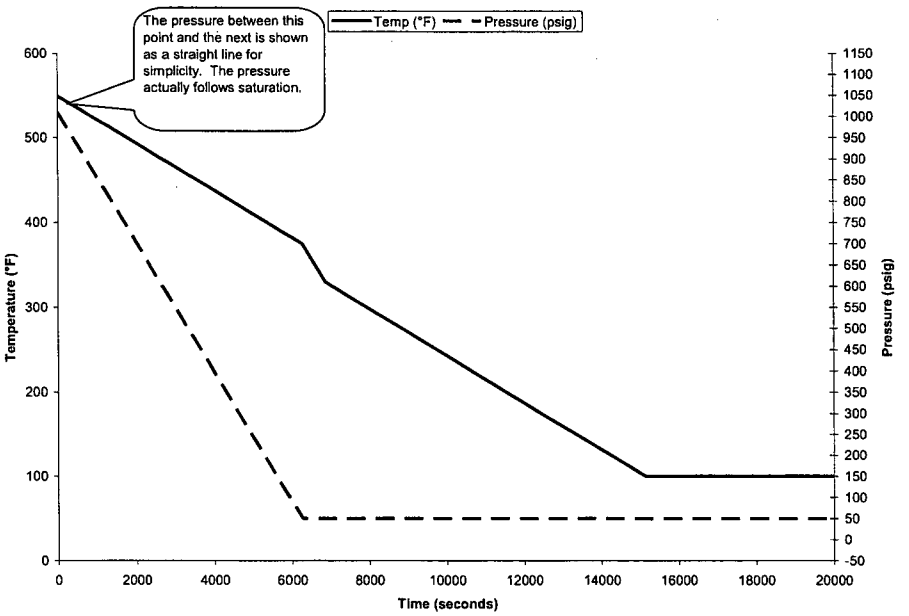

Figure 18: Transient 21-23, Shutdown

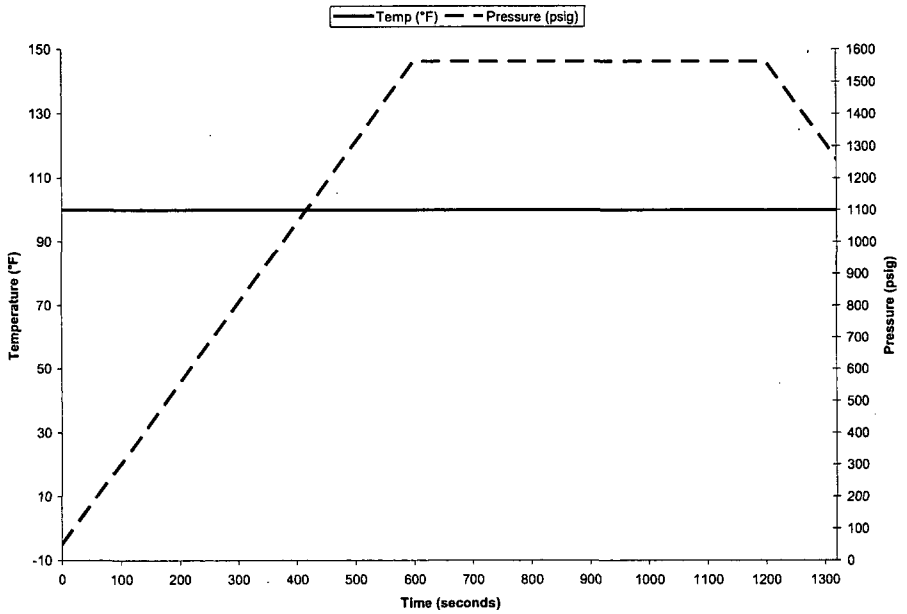

Figure 19: Transient 24, Hydrostatic Test

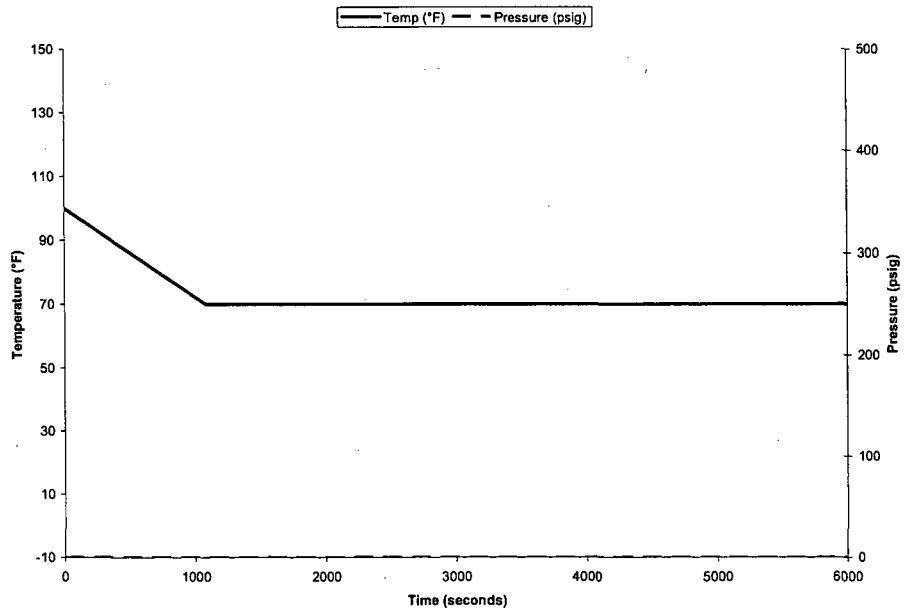

Figure 20: Transient 25, Unbolt

APPENDIX A

SUMMARY OF OUTPUT FILES

Transient Table.xls	Definition of Transients	In Computer files
BRresults.xls	Blend Radius Stress Summary	In Computer files
SEresults.xls	Safe End Stress Summary	In Computer files
TRANSNT_XX.INP	Input File for Each Transient	In Computer files
Green.dat	Input File for Green Functions	In Computer files
P-V_XX.OUT	Output File for Stress Analysis	In Computer files
GREEN.CFG	Input File for Defining Green Function	In Computer files
FATIGUE.CFG	Input File for Defining Fatigue Analysis	In Computer files
FATIGUE.DAT	Input File for Fatigue Curves	In Computer files
FATIGUE.inp	Input file for Fatigue Analysis from BRresults.xls or SEresults.xls	In Computer files
FATIGUE.OUT	Fatigue Output File	In Computer files

Where XX is defined for each transient.

REDACTED COPY

REDACTED COPY

Structural Integrity Associates, Inc.	File No.: VY-16Q-303
CALCULATION PACKAGE	**Project No.:** VY-16Q

PROJECT NAME:

Environmental Fatigue Analysis of VYNPS

CONTRACT NO.:

10150394

CLIENT:	**PLANT:**
Entergy Nuclear Operations, Inc.	Vermont Yankee

CALCULATION TITLE:

Environmental Fatigue Evaluation of Reactor Recirculation Inlet Nozzle and Vessel Shell/Bottom Head

Document Revision	Affected Pages	Revision Description	Project Manager Approval Signature & Date	Preparer(s) & Checker(s) Signatures & Date
0	1 - 24, Appendices: A1 – A2, B1 – B2 In computer files	Initial issue.	Terry J. Herrmann 07/05/07	Gary L. Stevens 07/05/07 Terry J. Herrmann 07/05/07

F0306-01R0

Table of Contents

1.0 INTRODUCTION/STATEMENT OF PROBLEM/ OBJECTIVE 3
2.0 TECHNICAL APPROACH OR METHODOLOGY 3
3.0 ASSUMPTIONS / DESIGN INPUTS 4
4.0 CALCULATIONS 6
4.1 RPV Lower Head 7
4.2 RR Inlet Nozzle 9
5.0 RESULTS OF ANALYSIS 11
6.0 CONCLUSIONS AND DISCUSSION 11
7.0 REFERENCES 12
APPENDIX A VY WATER CHEMISTRY INFORMATION [8] A1
APPENDIX B VY LICENSE DATE [10] B1

List of Tables

Table 1: Water Chemistry Calculations 14
Table 2: Bounding F_{en} Multipliers for Recirculation Line 15
Table 3: Bounding F_{en} Multipliers for Feedwater Line 16
Table 4: Bounding F_{en} Multipliers for RPV Upper Region 17
Table 5: Bounding F_{en} Multipliers for RPV Beltline Region 18
Table 6: Bounding F_{en} Multipliers for RPV Bottom Head Region 19
Table 7: EAF Evaluation for RPV Shell/Bottom Head Location 20
Table 8: EAF Evaluation for Limiting RPV Shell/Shroud Support Location 21
Table 9: EAF Evaluation for RR Inlet Nozzle Forging Location 22
Table 10: EAF Evaluation for RR Inlet Nozzle Safe End Location 23
Table 11: Summary of EAF Evaluation Results for VY 24

1.0 INTRODUCTION/STATEMENT OF PROBLEM/ OBJECTIVE

The purpose of this calculation is to perform a plant-specific evaluation of reactor water environmental effects for the reactor recirculation (RR) inlet nozzle and the reactor pressure vessel (RPV) shell/bottom head locations identified within NUREG/CR-6260 [1] for the older vintage General Electric (GE) plant for the Vermont Yankee Nuclear Power Plant (VY).

The water chemistry input used in this calculation covers several portions of the RPV, as well as the feedwater and recirculation lines. Although these regions encompass more areas than needed to address the two components of interest in this calculation, environmental fatigue multipliers are developed for all of these regions in this calculation for potential use in other evaluations associated with this project.

2.0 TECHNICAL APPROACH OR METHODOLOGY

Per Chapter X, "Time-Limited Aging Analyses Evaluation of Aging Management Programs Under 10 CFR 54.21(c)(1)(iii)," Section X.M1, "Metal Fatigue of Reactor Coolant Pressure Boundary," of the Generic Aging Lessons Learned (GALL) Report [2], detailed, vintage-specific, fatigue calculations are required for plants applying for license renewal for the locations identified for the appropriate vintage plant in NUREG/CR-6260.

In this calculation, detailed environmentally assisted fatigue (EAF) calculations are performed for VY for two of the locations associated with the older vintage GE plant in NUREG/CR-6260. The older-vintage GE plant is the appropriate comparison to VY since the original piping design at VY was in accordance with USAS B31.1 [3], as well as the fact that the older-vintage boiling water reactor (BWR) in NUREG/CR-6260 was a BWR-4 plant, which is the same as VY.

Entergy performed an initial assessment of EAF effects for VY in their License Renewal Application (LRA) that was submitted to the NRC in January 2006. Table 4.3-3 of the VY LRA provides the results of those evaluations. All but two of the VY locations evaluated for EAF in the LRA did not yield acceptable results for 60 years of operation. Further refined analyses are currently underway in other calculations associated with this project to address those components. This calculation documents the EAF evaluation for the RR inlet nozzle and RPV shell/bottom head locations, where it is expected that acceptable EAF results can be achieved based on the existing analyses without the need for additional refined evaluations.

3.0 ASSUMPTIONS / DESIGN INPUTS

Per Section X.M1 of the GALL Report [2], the EAF evaluation must use the appropriate F_{en} relationships from NUREG/CR-6583 [4] (for carbon/low alloy steels) and NUREG/CR-5704 [5] (for stainless steels), as appropriate for the material for each location. These expressions are:

For Carbon Steel [4, p. 69]: $F_{en} = \exp(0.585 - 0.00124T' - 0.101S^*T^*O^*\dot{\varepsilon}^*)$

Substituting T' = 25°C in the above expression, as required by NUREG/CR-6583 to relate room temperature air data to service temperature data in water [6], the following is obtained:

$$F_{en} = \exp(0.585 - 0.00124(25°C) - 0.101\ S^*\ T^*\ O^*\ \dot{\varepsilon}^*)$$
$$= \exp(0.554 - 0.101\ S^*\ T^*\ O^*\ \dot{\varepsilon}^*)$$

For Low Alloy Steel [4, p. 69]: $F_{en} = \exp(0.929 - 0.00124T' - 0.101S^*T^*O^*\dot{\varepsilon}^*)$

Substituting T' = 25°C in the above expression, as required by NUREG/CR-6583 to relate room temperature air data to service temperature data in water [6], the following is obtained:

$$F_{en} = \exp(0.929 - 0.00124(25°C) - 0.101\ S^*\ T^*\ O^*\ \dot{\varepsilon}^*)$$
$$= \exp(0.898 - 0.101\ S^*\ T^*\ O^*\ \dot{\varepsilon}^*)$$

where [4, pp. 60 and 65]:

F_{en}	=	fatigue life correction factor
S^*	=	S for 0 < sulfur content, S ≤ 0.015 wt. %
	=	0.015 for S > 0.015 wt. %
T^*	=	0 for T < 150°C
	=	(T - 150) for 150 ≤ T ≤ 350°C
T	=	fluid service temperature (°C)
O^*	=	0 for dissolved oxygen, DO < 0.05 parts per million (ppm)
	=	ln(DO/0.04) for 0.05 ppm ≤ DO ≤ 0.5 ppm
	=	ln(12.5) for DO > 0.5 ppm
$\dot{\varepsilon}^*$	=	0 for strain rate, $\dot{\varepsilon}$ > 1%/sec
	=	$\ln(\dot{\varepsilon}^*)$ for 0.001 ≤ $\dot{\varepsilon}$ ≤ 1%/sec
	=	ln(0.001) for $\dot{\varepsilon}$ < 0.001%/sec

For Types 304 and 316 Stainless Steel [5, p. 31]: $F_{en} = \exp(0.935 - T^* \dot{\varepsilon}^* O^*)$

where [5, pp. 25 and 31]:

F_{en}	=	fatigue life correction factor
T^*	=	0 for $T < 200°C$
	=	1 for $T \geq 200°C$
T	=	fluid service temperature (°C)
$\dot{\varepsilon}^*$	=	0 for strain rate, $\dot{\varepsilon} > 0.4\%/sec$
	=	$\ln(\dot{\varepsilon}/0.4)$ for $0.0004 \leq \dot{\varepsilon} \leq 0.4\%/sec$
	=	$\ln(0.0004/0.4)$ for $\dot{\varepsilon} < 0.0004\%/sec$
O^*	=	0.260 for dissolved oxygen, DO < 0.05 parts per million (ppm)
	=	0.172 for DO ≥ 0.05 ppm

Bounding F_{en} values are determined or, where necessary, computed for each load pair in the detailed fatigue calculation for each component. The environmental fatigue is then determined as $U_{env} = (U)(F_{en})$, where U is the original fatigue usage and U_{env} is the environmentally assisted fatigue (EAF) usage factor. All calculations can be found in Excel spreadsheet "*VY-16Q-303 (Env. Fat. Calcs).xls*" associated with this calculation.

From Reference [7], for the BWR, typical DO levels range from just over 200 ppb for normal water chemistry (NWC) conditions to less than 10 ppb for hydrogen water chemistry (HWC) conditions. Typical HWC system availabilities are greater than 90%. Based on VY-specific water chemistry input for Entergy [8], which is also contained in Appendix A of this calculation, the input shown in Table 1 is defined for use in this calculation.

The water chemistry input covers several portions of the RPV, as well as the feedwater and recirculation lines. Although these regions encompass more areas than needed to address the two components of interest in this calculation, environmental fatigue multipliers are developed for all of these regions in this calculation for potential use in other evaluations associated with this project.

Therefore, based on Table 1 and for the purposes of this calculation, the following is assumed:

- Over the 60-year operating life of the plant, HWC conditions exist for 47% of the time, and NWC conditions exist for 53% of the time.
- All operation through 11/1/2003 was assumed as NWC using the dissolved oxygen values from the "Pre-NMCA" column in Appendix A, and all operation after 11/1/2003 was assumed as HWC using the maximum oxygen values from the "Post-NMCA + HWC (OLP)", "Post-NMCA + HWC (EPU)", and "Future Operation" columns in Appendix A.
- Recirculation line DO is 122 ppb pre-HWC and 48 ppb post-HWC.
- Feedwater line DO is 40 ppb for pre-HWC and 40 ppb for post-HWC conditions.
- RPV Upper Region DO is 114 ppb pre-HWC and 97 ppb post-HWC.
- RPV Beltline DO is 123 ppb pre-HWC and 46 ppb post-HWC.
- RPV Bottom Head Region DO is 128 ppb pre-HWC and 69 ppb post-HWC.

Based on the above typical DO levels, bounding F_{en} multipliers for each of the three applicable materials (carbon, low alloy, and stainless steels) are shown in Tables 2 through 6 for the various RPV and piping regions.

The projected number of cycles used in this calculation is based on the number of cycles actually experienced by the plant in the past and forward-projected with some additional margin for 60 years of operation, as documented in Reference [9]. In addition, the latest governing stress analysis for each location was utilized, and any relevant effects of Extended Power Uprate (EPU) operation were incorporated as necessary. With these assumptions, the cumulative usage factor (CUF) values documented in this calculation are considered applicable for sixty years of operation including all relevant EAF and EPU effects.

4.0 CALCULATIONS

The analyses for the NUREG/CR-6260 locations identified in Section 2.0 are provided in this section. As previously noted, the fatigue calculations for 60 years for all locations make use of the 60-year projected cycles for VY from Reference [9], and incorporate EPU effects.

Since the F_{en} methodology documented in References [4] and [5] is relatively "new" technology, it is intended to apply to "modern-day" fatigue analyses, i.e., applied to fatigue analyses that use current ASME Code fatigue curves, etc. Therefore, to be consistent with this approach, the evaluation for the all locations will also utilize modern-day fatigue calculation methodology using the 1998 Edition, 2000 Addenda of the ASME Code [11]. This involves applying a Young's Modulus correction factor (i.e., $E_{fatigue\ curve}/E_{analysis}$) to the calculated stresses, applying K_e where appropriate, and utilizing the 2000 Addenda fatigue curve.

NOTE: It is recognized that some of the references used in this calculation are not the latest revision; for example, Reference [12] (VYC-378, Revision 0) has been revised. However, the details necessary to perform the evaluations in this calculation are not necessarily contained in the latest revision of all documents. Therefore, wherever necessary, the appropriate revision of the governing document is referenced in order to obtain all appropriate inputs necessary to perform the EAF calculations. So, it should be recognized that, despite using what appear to be outdated revisions of some references, use of these references is for input data use only. All calculations represent the latest available analyses for all locations.

NOTE: Hand calculations may yield results slightly different than the values shown in the tables of this calculation due to round-off based on the significant figures utilized by the spreadsheet used for these calculations.

4.1 RPV Lower Head

The 60-year CUF value (without EAF effects) for the RPV shell/bottom head location was reported in Table 4.3-3 of the VY LRA submittal to be 0.400. The EAF CUF estimated by Entergy for this location was 0.98, based on an overall F_{en} of 2.45. Based on this result, further refined analysis would not normally be necessary to show acceptable EAF CUF results for this component. However, the calculation for this location is updated in this section to reflect the updated water chemistry information supplied for this project.

The CUF value reported in the VY LRA for the RPV shell/bottom head location is 0.400. This value is the original design basis CUF from the RPV Stress Report, as noted on page B8 of Reference [12]. However, as noted on page A61 of Reference [12], this CUF corresponds to Point 8, which is located on the outside surface of the RPV bottom head at the junction with the support skirt. Therefore, this location is not exposed to the reactor coolant, and EAF effects do not apply. Based on this, evaluation of the limiting location along the inside surface of the RPV bottom head was performed.

Based on a review of the primary plus secondary stresses tabulated for all locations along the bottom head on page A52 of Reference [12], Point 14 was selected for EAF evaluation. Per Section 3.2.1.2 of Reference [13], none of the CUF values for the RPV bottom head region were evaluated for the effects of EPU, as the CUF values are below the EPU screening criteria value of 0.5. Therefore, as a part of the evaluation for this location, EPU effects were included. Per References [14] and [19], the RPV shell material is low alloy steel (A-533, Grade B).

The new CUF calculation for Point 14 for 40 years, which includes the use of updated methodology and incorporates EPU effects [14], is shown at the top portion of Table 7. The CUF for 40 years (without EAF effects) is 0.0057.

The fatigue calculation for 60 years for the RPV shell/bottom head location is also shown in Table 7. The results show a CUF (without EAF effects) of 0.0085 for 60 years. The fatigue calculation for 60 years makes use of the 60-year projected cycles for VY from Reference [9].

The resulting environmental fatigue calculation for the RPV shell/bottom head location is shown in Table 7. Bounding F_{en} multipliers were applied in the calculations. RPV bottom head water chemistry conditions from Tables 1 and 6 are used for this location. The results show an EAF adjusted CUF of 0.0809 for 60 years, which is acceptable (i.e., less than the allowable value of 1.0).

The CUF determined for Point 14 is very low. Comparison to other locations of the RPV shell/bottom head region indicates it is not the limiting location from a fatigue perspective. Review of the CUF values in Table 3-1 of Reference [15] reveals that the shroud support (at vessel wall junction) location is potentially more limiting, so EAF evaluation of that location is also performed.

Per page S3-99f of Reference [16], the design basis CUF of 0.06 is for Point 9. Page S3-85 of Reference [16] reveals that this point is on the RPV shell at the junction of the shroud support plate. Per References [14] and [19], the RPV shell material is low alloy steel (A-533, Grade B).

The revised and updated CUF calculation for Point 9 for 40 years, which includes the use of updated methodology and incorporates EPU effects, is shown at the top portion of Table 8. The CUF for 40 years (without EAF effects) is 0.0549. This CUF value is more limiting than the RPV shell/bottom head location evaluated in Table 7, so it is considered to be the governing location for VY with respect to the equivalent NUREG/CR-6260 RPV shell/bottom head location.

The fatigue calculation for 60 years for the RPV shell/shroud support location is also shown in Table 8. The results show a CUF (without EAF effects) of 0.0774 for 60 years. The fatigue calculation for 60 years makes use of the 60-year projected cycles for VY from Reference [9].

The resulting environmental fatigue calculation for the RPV shell/shroud support location is shown in Table 8. Bounding F_{en} multipliers were applied in the calculations. RPV bottom head water chemistry conditions from Table 6 are used for this location. The results show an EAF adjusted CUF of 0.7364 for 60 years, which is acceptable (i.e., less than the allowable value of 1.0).

4.2 RR Inlet Nozzle

For conservatism due to the different materials involved, two locations are evaluated for the RR inlet nozzle: (1) the limiting location in the nozzle forging, and (2) the limiting location in the safe end.

The 60-year CUF value (without EAF effects) for the RR inlet nozzle in the VY LRA submittal is 0.610. However, that analysis used conservative transient definitions and cyclic projections for 60 years of operation that have since been updated. The applicable CUF values are those shown in Table 3-1 of Reference [15] (0.1058 for the safe end, and 0.03 for the nozzle for 40-years), except that these values are pre-EPU.

For the RR inlet nozzle forging, the governing CUF calculation is shown on page B28 of Reference [12], where a value of 0.03 was obtained. From pages A269 and A270 of Reference [12], the CUF calculation corresponds to Point 12 in the nozzle forging, which is on the outside surface of the nozzle on the outboard end of the nozzle transition. Although this location is not exposed to the reactor coolant, it will be conservatively evaluated for EAF effects as it is the bounding fatigue location in the nozzle forging. As a part of the evaluation for this location, EPU effects were included. Per page I-S8-4 of Reference [17], the RR inlet nozzle material is low alloy steel (A-508 Class II).

The new CUF calculation for Point 12 for 40 years, which includes the use of updated methodology and incorporates EPU effects [14], is shown at the top portion of Table 9. The CUF for 40 years (without EAF effects) is 0.0433.

The fatigue calculation for 60 years for the RR inlet nozzle forging location is also shown in Table 9. The results show a CUF (without EAF effects) of 0.0650 for 60 years. The fatigue calculation for 60 years makes use of the 60-year projected cycles for VY from Reference [9].

The resulting environmental fatigue calculation for the RR inlet nozzle forging location is shown in Table 9. Bounding F_{en} multipliers were applied in the calculations. RPV beltline water chemistry conditions from Table 5 are used for this location. The results show an EAF adjusted CUF of 0.5034 for 60 years, which is acceptable (i.e., less than the allowable value of 1.0)

For the RR inlet nozzle safe end, the governing CUF calculation is shown on page B27 of Reference [12], where a value of 0.1058 was obtained. From pages A257 and A259 of Reference [12], the CUF calculation corresponds to Line 6 at the inside surface of the safe end. Page A238 of Reference [12] reveals that this location is location at the nozzle-to-safe end weld. Per Section 3.2.1.2 of Reference [13], the CUF value for the RR inlet nozzle safe end was evaluated for the effects of EPU, since the original CUF calculated in Reference [18] was 0.551 (which was adjusted downward to 0.1058 by Entergy in Reference [12] based on further refined evaluation). Therefore, as a part of the evaluation for this location, EPU effects were included. Per page 8 of Reference [18], the RR inlet nozzle safe end material is 316L stainless steel.

The new CUF calculation for the RR inlet nozzle safe end for 40 years, which includes the use of updated methodology and incorporates EPU effects [14], is shown at the top portion of Table 10. The CUF for 40 years (without EAF effects) is 0.0017.

The fatigue calculation for 60 years for the RR inlet nozzle safe end location is also shown in Table 10. The results show a CUF (without EAF effects) of 0.0017 for 60 years. The fatigue calculation for 60 years makes use of the 60-year projected cycles for VY from Reference [9].

The resulting environmental fatigue calculation for the RR inlet nozzle safe end location is shown in Table 10. Bounding F_{en} multipliers were applied in the calculations. Recirculation line water chemistry conditions from Table 2 are used for this location. The results show an EAF adjusted CUF of 0.0199 for 60 years, which is acceptable (i.e., less than the allowable value of 1.0)

5.0 RESULTS OF ANALYSIS

The final environmental fatigue results contained in Sections 4.1 and 4.2 (and associated Tables 7 through 10) for the RPV shell/bottom head and RR inlet nozzle locations are summarized in Table 11.

6.0 CONCLUSIONS AND DISCUSSION

In this calculation, EAF calculations were performed in accordance with the GALL Report [2] for the following VY locations:

- RR inlet nozzle, consisting of the following bounding locations:
  - Nozzle forging (low alloy steel)
  - Safe end (stainless steel)
- RPV shell/bottom head, consisting of the following bounding locations:
  - Limiting bottom head shell inside surface location (low alloy steel)
  - Limiting RPV shell/shroud support location (low alloy steel)

The above locations were selected based on the locations identified in NUREG/CR-6260 for the older vintage GE plant and plant-specific fatigue calculations that determined the limiting locations for VY. Calculations for the remaining NUREG/CR-6260 locations will be documented in other analyses performed under this project.

The EAF results for the locations identified above are shown in Table 11. These results indicate that the fatigue usage factors, including environmental effects, are within the allowable value for 60 years of operation for all locations evaluated. The calculations for all locations make use of the 60-year projected cycles for VY and incorporate EPU effects. Therefore, no additional evaluation is required for these components, and the GALL requirements are satisfied.

7.0 REFERENCES

1. NUREG/CR-6260 (INEL-95/0045), "Application of NUREG/CR-5999 Interim Fatigue Curves to Selected Nuclear Power Plant Components," March 1995.

2. NUREG-1801, Revision 1, "Generic Aging Lessons Learned (GALL) Report," U. S. Nuclear Regulatory Commission, September 2005.

3. USAS B31.1.0 – 1967, USA Standard Code for Pressure Piping, "Power Piping," American Society of Mechanical Engineers, New York.

4. NUREG/CR-6583 (ANL-97/18), "Effects of LWR Coolant Environments on Fatigue Design Curves of Carbon and Low-Alloy Steels," March 1998.

5. NUREG/CR-5704 (ANL-98/31), "Effects of LWR Coolant Environments on Fatigue Design Curves of Austenitic Stainless Steels," April 1999.

6. EPRI/BWRVIP Memo No. 2005-271, "Potential Error in Existing Fatigue Reactor Water Environmental Effects Analyses," July 1, 2005.

REDACTED

8. "Vermont Yankee Dissolved Oxygen (DO) Levels for Use in EAF Evaluations," page 11 of Entergy Design Input Record (DIR) EC No. 1773, Revision 0, "Environmental Fatigue Analysis for Vermont Yankee Nuclear Power Station," 7/3/07, SI File No. VY-16Q-209.

9. "Reactor Thermal Cycles for 60 Years of Operation," Attachment 1 of Entergy Design Input Record (DIR) EC No. 1773, Revision 0, "Environmental Fatigue Analysis for Vermont Yankee Nuclear Power Station," 7/3/07, SI File No. VY-16Q-209.

10. VY LRA, page 1-4 (*included as Appendix B to this calculation*).

11. American Society of Mechanical Engineers Boiler & Pressure Vessel Code, Section III, Rules for Construction of Nuclear Facility Components, and Section II, Materials, Part D, "Properties (Customary)," 1998 Edition including the 2000 Addenda.

12. Yankee Atomic Electric Company Calculation No. VYC-378, Revision 0, "Vermont Yankee Reactor Cyclic Limits for Transient Events," 10/16/85, SI File No. VY-05Q-211.

REDACTED

14. GE Nuclear Energy Certified Design Specification No. 26A6019, Revision 1, "Reactor Vessel – Extended Power Uprate," June 2, 2003, SI File No. VY-05Q-236.

15. Structural Integrity Associates Report No. SIR-01-130, Rev. 0, "System Review and Recommendations for a Transient and Fatigue Monitoring System at the Vermont Yankee Nuclear Power Station," February 2002, SI File No. W-VY-05Q-401.

16. CB&I RPV Stress Report, Section S3, Revision 4, "Stress Analysis, Shroud Support, Vermont Yankee Reactor Vessel, CB&I Contract 9-6201," 2-3-70, SI File No. VY-16Q-203.

17. CB&I RPV Stress Report, Section S8, Revision 4, "Stress Analysis, Recirculation Inlet Nozzle, Vermont Yankee Reactor Vessel, CB&I Contract 9-6201," 2-3-70, SI File No. VY-16Q-203.

18. GE Nuclear Energy Certified Stress Report No. 23A4292, Revision 4, "Reactor Vessel – Recirculation Inlet Safe End Nozzle," March 12, 1986, SI File No. VY-16Q-203.

19. Entergy Drawing No. 5920-5752, Revision 3 (CB&I Drawing No. R15, Revision 1), "Vessel & Attachments Mat'l. Identifications," 1/20/88, SI File No. VY-16Q-209.

Table 1: Water Chemistry Calculations

Date of HWC Implementation:	11/01/2003	*(see Appendix A)*
Availability of HWC System Since HWC Implementation:	98.54%	*(see Appendix A)*
Projected Future HWC System Availability:	98.5%	*(see Appendix A, assume same as recent experience)*
Recirculation Line DO		
pre-HWC:	122	ppb *(see Appendix A)*
post-HWC:	48	ppb *(see Appendix A)*
Feedwater Line DO		
pre-HWC:	40	ppb *(see Appendix A)*
post-HWC:	40	ppb *(see Appendix A)*
RPV Upper Region DO		
pre-HWC:	114	ppb *(see Appendix A)*
post-HWC:	97	ppb *(see Appendix A)*
RPV Beltline Region DO		
pre-HWC:	123	ppb *(see Appendix A)*
post-HWC:	46	ppb *(see Appendix A)*
RPV Bottom Head Region DO		
pre-HWC:	128	ppb *(see Appendix A)*
post-HWC:	69	ppb *(see Appendix A)*
Plant Startup Date:	03/22/1972	*(see Appendix B)*
Time at pre-HWC Conditions:	31.61	years *(calculated, includes leap years.)*
Date of Calculations:	04/30/2007	
Time Since HWC Implementation:	3.49	years *(calculated, includes leap years.)*
Projected Future Time for HWC Operation:	24.90	years *(calculated, includes leap years.)*
Overall HWC Availability:	47%	

Note: All operation through 11/1/2003 was assumed as NWC using the dissolved oxygen values from the "Pre-NMCA" column in Appendix A, and all operation after 11/1/2003 was assumed as HWC using the maximum oxygen values from the "Post-NMCA + HWC (OLP)", "Post-NMCA + HWC (EPU)", and "Future Operation" columns in Appendix A.

Table 2: Bounding F_{en} Multipliers for Recirculation Line

Low Alloy Steel:

$F_{en} = \exp(0.898 - 0.101S^*T^*O^*\varepsilon^*)$

Assume $S^* = 0.015$ (maximum)
Assume $\varepsilon^* = \ln(0.001) = -6.908$ (minimum)

For a BWR with HWC environment (post-HWC implementation):
DO = 48 ppb = 0.048 ppm
DO < 0.050 ppm, so $O^* = 0$
Thus:

T (°C)	T (°F)	F_{en}
0	32	2.45
50	122	2.45
100	212	2.45
150	302	2.45
200	392	2.45
250	482	2.45
288	550	2.45

Thus, maximum F_{en} = 2.45

For a BWR with NWC environment (pre-HWC implementation):
DO = 122 ppb = 0.122 ppm, so $O^* = \ln(0.122/0.04) = 1.115$

Thus:

T (°C)	T (°F)	F_{en}
0	32	2.45
50	122	2.45
100	212	2.45
150	302	2.45
200	392	4.40
250	482	7.89
288	550	12.29

Thus, maximum F_{en} = 12.29

[$T^* = (T-150)$ for $T > 150°C$]

Carbon Steel:

$F_{en} = \exp(0.554 - 0.101S^*T^*O^*\varepsilon^*)$

Assume $S^* = 0.015$ (maximum)
Assume $\varepsilon^* = \ln(0.001) = -6.908$ (minimum)

For a BWR with HWC environment (post-HWC implementation):
DO = 48 ppb = 0.048 ppm
DO < 0.050 ppm, so $O^* = 0$
Thus:

T (°C)	T (°F)	F_{en}
0	32	1.74
50	122	1.74
100	212	1.74
150	302	1.74
200	392	1.74
250	482	1.74
288	550	1.74

Thus, maximum F_{en} = 1.74

For a BWR with NWC environment (pre-HWC implementation):
DO = 122 ppb = 0.122 ppm, so $O^* = \ln(0.122/0.04) = 1.115$

Thus:

T (°C)	T (°F)	F_{en}
0	32	1.74
50	122	1.74
100	212	1.74
150	302	1.74
200	392	3.12
250	482	5.59
288	550	8.71

Thus, maximum F_{en} = 8.71

[$T^* = (T-150)$ for $T > 150°C$]

Stainless Steel:

$F_{en} = \exp(0.935 - T^*\varepsilon^*O^*)$

For a BWR with HWC environment (post-HWC implementation):
DO = 48 ppb = 0.048 ppm < 0.050 ppm, so $O^* = 0.260$
Conservatively use $T^* = 1$ for $T > 200°C$
Thus:

$\varepsilon^* = 0$ for $\varepsilon > 0.4$%/sec	so F_{en} =	2.55
$\varepsilon^* = \ln(\varepsilon/0.4)$ for $0.0004 <= \varepsilon <= 0.4$%/sec	so F_{en} ranges from	2.55
	to	15.35
$\varepsilon^* = \ln(0.0004/0.4)$ for $\varepsilon < 0.0004$%/sec	so F_{en} =	15.35
	Thus, maximum F_{en} =	15.35

For a BWR with NWC environment (pre-HWC implementation):
DO = 122 ppb = 0.122 ppm > 0.05 ppm, so $O^* = 0.172$
Conservatively use $T^* = 1$ for $T > 200°C$
Thus:

$\varepsilon^* = 0$ for $\varepsilon > 0.4$%/sec	so F_{en} =	2.55
$\varepsilon^* = \ln(\varepsilon/0.4)$ for $0.0004 <= \varepsilon <= 0.4$%/sec	so F_{en} ranges from	2.55
	to	8.36
$\varepsilon^* = \ln(0.0004/0.4)$ for $\varepsilon < 0.0004$%/sec	so F_{en} =	8.36
	Thus, maximum F_{en} =	8.36

Table 3: Bounding F_{en} Multipliers for Feedwater Line

Low Alloy Steel:

$F_{en} = \exp(0.898 - 0.101S^*T^*O^*\varepsilon^*)$

Assume $S^* = 0.015$ (maximum)
Assume $\varepsilon^* = \ln(0.001) = -6.908$ (minimum)

For a BWR with HWC environment (post-HWC implementation):
DO = 40 ppb = 0.040 ppm < 0.050 ppm so O* = 0
Thus:

T (°C)	T (°F)	F_{en}
0	32	2.45
50	122	2.45
100	212	2.45
150	302	2.45
200	392	2.45
250	482	2.45
288	550	2.45

Thus, maximum F_{en} = 2.45

For a BWR with NWC environment (pre-HWC implementation):
DO = 40 ppb = 0.040 ppm < 0.050 ppm so O* = 0
Thus:

T (°C)	T (°F)	F_{en}
0	32	2.45
50	122	2.45
100	212	2.45
150	302	2.45
200	392	2.45
250	482	2.45
288	550	2.45

Thus, maximum F_{en} = 2.45

[T* = (T-150) for T > 150°C]

Carbon Steel:

$F_{en} = \exp(0.554 - 0.101S^*T^*O^*\varepsilon^*)$

Assume $S^* = 0.015$ (maximum)
Assume $\varepsilon^* = \ln(0.001) = -6.908$ (minimum)

For a BWR with HWC environment (post-HWC implementation):
DO = 40 ppb = 0.040 ppm < 0.050 ppm so O* = 0
Thus:

T (°C)	T (°F)	F_{en}
0	32	1.74
50	122	1.74
100	212	1.74
150	302	1.74
200	392	1.74
250	482	1.74
288	550	1.74

Thus, maximum F_{en} = 1.74

For a BWR with NWC environment (pre-HWC implementation):
DO = 40 ppb = 0.040 ppm < 0.050 ppm so O* = 0
Thus:

T (°C)	T (°F)	F_{en}
0	32	1.74
50	122	1.74
100	212	1.74
150	302	1.74
200	392	1.74
250	482	1.74
288	550	1.74

Thus, maximum F_{en} = 1.74

[T* = (T-150) for T > 150°C]

There is no stainless steel in the Class 1 feedwater line.

Table 4: Bounding F_{en} Multipliers for RPV Upper Region

Low Alloy Steel:

$F_{en} = \exp(0.898 - 0.101S^*T^*O^*\varepsilon^*)$

Assume $S^* = 0.015$ (maximum)
Assume $\varepsilon^* = \ln(0.001) = -6.908$ (minimum)

For a BWR with HWC environment (post-HWC implementation):
DO = 97 ppb = 0.097 ppm, so $O^* = \ln(0.097/0.04) = 0.886$

Thus:

T (°C)	T (°F)	F_{en}
0	32	2.45
50	122	2.45
100	212	2.45
150	302	2.45
200	392	3.90
250	482	6.20
288	550	8.82

Thus, maximum F_{en} = 8.82

For a BWR with NWC environment (pre-HWC implementation):
DO = 114 ppb = 0.114 ppm, so $O^* = \ln(0.114/0.04) = 1.047$

Thus:

T (°C)	T (°F)	F_{en}
0	32	2.45
50	122	2.45
100	212	2.45
150	302	2.45
200	392	4.25
250	482	7.35
288	550	11.14

Thus, maximum F_{en} = 11.14

[$T^* = (T-150)$ for $T > 150°C$]

Carbon Steel:

$F_{en} = \exp(0.554 - 0.101S^*T^*O^*\varepsilon^*)$

Assume $S^* = 0.015$ (maximum)
Assume $\varepsilon^* = \ln(0.001) = -6.908$ (minimum)

For a BWR with HWC environment (post-HWC implementation):
DO = 97 ppb = 0.097 ppm, so $O^* = \ln(0.097/0.04) = 0.886$

Thus:

T (°C)	T (°F)	F_{en}
0	32	1.74
50	122	1.74
100	212	1.74
150	302	1.74
200	392	2.77
250	482	4.40
288	550	6.25

Thus, maximum F_{en} = 6.25

For a BWR with NWC environment (pre-HWC implementation):
DO = 114 ppb = 0.114 ppm, so $O^* = \ln(0.114/0.04) = 1.047$

Thus:

T (°C)	T (°F)	F_{en}
0	32	1.74
50	122	1.74
100	212	1.74
150	302	1.74
200	392	3.01
250	482	5.21
288	550	7.90

Thus, maximum F_{en} = 7.90

[$T^* = (T-150)$ for $T > 150°C$]

Stainless Steel:

$F_{en} = \exp(0.935 - T^*\varepsilon^*O^*)$

For a BWR with HWC environment (post-HWC implementation):
DO = 97 ppb = 0.097 ppm > 0.050 ppm, so $O^* = 0.172$
Conservatively use $T^* = 1$ for $T > 200°C$

Thus:

$\varepsilon^* = 0$ for $\varepsilon > 0.4$%/sec	so F_{en} =	2.55
$\varepsilon^* = \ln(\varepsilon/0.4)$ for $0.0004 <= \varepsilon <= 0.4$%/sec	so F_{en} ranges from	2.55
	to	8.36
$\varepsilon^* = \ln(0.0004/0.4)$ for $\varepsilon < 0.0004$%/sec	so F_{en} =	8.36
	Thus, maximum F_{en} =	8.36

For a BWR with NWC environment (pre-HWC implementation):
DO = 114 ppb = 0.114 ppm > 0.05 ppm, so $O^* = 0.172$
Conservatively use $T^* = 1$ for $T > 200°C$

Thus:

$\varepsilon^* = 0$ for $\varepsilon > 0.4$%/sec	so F_{en} =	2.55
$\varepsilon^* = \ln(\varepsilon/0.4)$ for $0.0004 <= \varepsilon <= 0.4$%/sec	so F_{en} ranges from	2.55
	to	8.36
$\varepsilon^* = \ln(0.0004/0.4)$ for $\varepsilon < 0.0004$%/sec	so F_{en} =	8.36
	Thus, maximum F_{en} =	8.36

Table 5: Bounding F_{en} Multipliers for RPV Beltline Region

Low Alloy Steel:

$F_{en} = \exp(0.898 - 0.101S^*T^*O^*\varepsilon^*)$

Assume $S^* = 0.015$ (maximum)
Assume $\varepsilon^* = \ln(0.001) = -6.908$ (minimum)

For a BWR with HWC environment (post-HWC implementation):
DO = 46 ppb = 0.046 ppm
DO < 0.050 ppm, so $O^* = 0$
Thus:

T (°C)	T (°F)	F_{en}
0	32	2.45
50	122	2.45
100	212	2.45
150	302	2.45
200	392	2.45
269.45	517.01	2.45
288	550	2.45

Thus, maximum F_{en} = 2.45

For a BWR with NWC environment (pre-HWC implementation):
DO = 123 ppb = 0.123 ppm, so $O^* = \ln(0.123/0.04) = 1.123$

Thus:

T (°C)	T (°F)	F_{en}
0	32	2.45
50	122	2.45
100	212	2.45
150	302	2.45
200	392	4.42
269.45	517.01	10.00
288	550	12.43

Thus, maximum F_{en} = 12.43

[$T^* = (T-150)$ for $T > 150°C$]

Carbon Steel:

$F_{en} = \exp(0.554 - 0.101S^*T^*O^*\varepsilon^*)$

Assume $S^* = 0.015$ (maximum)
Assume $\varepsilon^* = \ln(0.001) = -6.908$ (minimum)

For a BWR with HWC environment (post-HWC implementation):
DO = 46 ppb = 0.046 ppm
DO < 0.050 ppm, so $O^* = 0$
Thus:

T (°C)	T (°F)	F_{en}
0	32	1.74
50	122	1.74
100	212	1.74
150	302	1.74
200	392	1.74
250	482	1.74
288	550	1.74

Thus, maximum F_{en} = 1.74

For a BWR with NWC environment (pre-HWC implementation):
DO = 123 ppb = 0.123 ppm, so $O^* = \ln(0.123/0.04) = 1.123$

Thus:

T (°C)	T (°F)	F_{en}
0	32	1.74
50	122	1.74
100	212	1.74
150	302	1.74
200	392	3.13
250	482	5.64
288	550	8.81

Thus, maximum F_{en} = 8.81

[$T^* = (T-150)$ for $T > 150°C$]

Stainless Steel:

$F_{en} = \exp(0.935 - T^*\varepsilon^*O^*)$

For a BWR with HWC environment (post-HWC implementation):
DO = 46 ppb = 0.046 ppm < 0.050 ppm, so $O^* = 0.260$
Conservatively use $T^* = 1$ for $T > 200°C$
Thus:

$\varepsilon^* = 0$ for $\varepsilon > 0.4$%/sec	so F_{en} =	2.55
$\varepsilon^* = \ln(\varepsilon/0.4)$ for $0.0004 <= \varepsilon <= 0.4$%/sec	so F_{en} ranges from	2.55
	to	15.35
$\varepsilon^* = \ln(0.0004/0.4)$ for $\varepsilon < 0.0004$%/sec	so F_{en} =	15.35
	Thus, maximum F_{en} =	15.35

For a BWR with NWC environment (pre-HWC implementation):
DO = 123 ppb = 0.123 ppm > 0.05 ppm, so $O^* = 0.172$
Conservatively use $T^* = 1$ for $T > 200°C$
Thus:

$\varepsilon^* = 0$ for $\varepsilon > 0.4$%/sec	so F_{en} =	2.55
$\varepsilon^* = \ln(\varepsilon/0.4)$ for $0.0004 <= \varepsilon <= 0.4$%/sec	so F_{en} ranges from	2.55
	to	8.36
$\varepsilon^* = \ln(0.0004/0.4)$ for $\varepsilon < 0.0004$%/sec	so F_{en} =	8.36
	Thus, maximum F_{en} =	8.36

Table 6: Bounding F_{en} Multipliers for RPV Bottom Head Region

Low Alloy Steel:

$F_{en} = \exp(0.898 - 0.101S^*T^*O^*\varepsilon^*)$

Assume $S^* = 0.015$ (maximum)
Assume $\varepsilon^* = \ln(0.001) = -6.908$ (minimum)

For a BWR with HWC environment (post-HWC implementation):
DO = 69 ppb = 0.069 ppm, so $O^* = \ln(0.069/0.04) = 0.545$
Thus:

T (°C)	T (°F)	F_{en}
0	32	2.45
50	122	2.45
100	212	2.45
150	302	2.45
200	392	3.27
250	482	4.34
288	550	5.39

Thus, maximum F_{en} = 5.39

For a BWR with NWC environment (pre-HWC implementation):
DO = 128 ppb = 0.128 ppm, so $O^* = \ln(0.128/0.04) = 1.163$
Thus:

T (°C)	T (°F)	F_{en}
0	32	2.45
50	122	2.45
100	212	2.45
150	302	2.45
200	392	4.51
250	482	8.29
288	550	13.17

Thus, maximum F_{en} = 13.17

[T*= (T-150) for T > 150°C]

Carbon Steel:

$F_{en} = \exp(0.554 - 0.101S^*T^*O^*\varepsilon^*)$

Assume $S^* = 0.015$ (maximum)
Assume $\varepsilon^* = \ln(0.001) = -6.908$ (minimum)

For a BWR with HWC environment (post-HWC implementation):
DO = 69 ppb = 0.069 ppm, so $O^* = \ln(0.069/0.04) = 0.545$
Thus:

T (°C)	T (°F)	F_{en}
0	32	1.74
50	122	1.74
100	212	1.74
150	302	1.74
200	392	2.31
250	482	3.08
288	550	3.82

Thus, maximum F_{en} = 3.82

For a BWR with NWC environment (pre-HWC implementation):
DO = 128 ppb = 0.128 ppm, so $O^* = \ln(0.128/0.04) = 1.163$
Thus:

T (°C)	T (°F)	F_{en}
0	32	1.74
50	122	1.74
100	212	1.74
150	302	1.74
200	392	3.20
250	482	5.88
288	550	9.34

Thus, maximum F_{en} = 9.34

[T*= (T-150) for T > 150°C]

Stainless Steel:

$F_{en} = \exp(0.935 - T^*\varepsilon^*O^*)$

For a BWR with HWC environment (post-HWC implementation):
DO = 69 ppb = 0.069 ppm > 0.050 ppm, so $O^* = 0.172$
Conservatively use $T^* = 1$ for T > 200°C
Thus:

$\varepsilon^* = 0$ for $\varepsilon > 0.4$%/sec	so F_{en} =	2.55
$\varepsilon^* = \ln(\varepsilon/0.4)$ for $0.0004 <= \varepsilon <= 0.4$%/sec	so F_{en} ranges from	2.55
	to	8.36
$\varepsilon^* = \ln(0.0004/0.4)$ for $\varepsilon < 0.0004$%/sec	so F_{en} =	8.36
	Thus, maximum F_{en} =	8.36

For a BWR with NWC environment (pre-HWC implementation):
DO = 128 ppb = 0.128 ppm > 0.05 ppm, so $O^* = 0.172$
Conservatively use $T^* = 1$ for T > 200°C
Thus:

	so F_{en} =	2.55
	so F_{en} ranges from	2.55
	to	8.36
	so F_{en} =	8.36
	Thus, maximum F_{en} =	8.36

Table 7: EAF Evaluation for RPV Shell/Bottom Head Location

Component: RPV Shell/Bottom Head
NUREG/CR-6260 CUF: 0.032 *(for reference only)*
Reference: NUREG/CR-6260, p. 5-102
Stress Report CUF: 0.0057 *(for Point 14, see below)*
Material: Low Alloy Steel *(Material = A-533 Gr. B per References [14] and [19])*

Design Basis CUF Calculation for 40 years:

$E_{fatigue\ curve}/E_{analysis}$ =	1.149	*Conservatively used minimum E of 26.1 from Section S2 Appendix of RPV Stress Report.*
Power Uprate =	1.0067	*=(549 - 100) / (546 - 100) per 4.4.1.b of 26A6019, Rev. 1 [14]*
K_t =	1.000	*stress concentration factor*
m =	2.0	*NB-3228.5 of ASME Code, Section III [11]*
n =	0.2	*NB-3228.5 of ASME Code, Section III [11]*
S_m =	26,700	psi *(ASME Code, Section II, Part D [11])*

P_L+P_B+Q *(see Note 1)*	K_e *(see Note 2)*	S_{alt} *(see Note 3)*	n *(see Note 4)*	N *(see Note 5)*	U
44,526	1.00	25,762	200	35,300	0.0057
				Total, U_{40} =	**0.0057**

Notes:
1. *P_L+P_B+Q is obtained for Point 14 from p. A52 of VYC-378, Rev. 0.*
2. *K_e computed in accordance with NB-3228.5 of ASME Code, Section III.*
3. *$S_{alt} = 0.5 * K_e * K_t * E_{fatigue\ curve}/E_{analysis} *$ Power Uprate $* (P_L+P_B+Q)$.*
4. *n for 40 years is the number of Heatup-Cooldown cycles, per p. B8 of VYC-378, Rev. 0.*
5. *N obtained from Figure I-9.1 of Appendix I of ASME Code, Section III.*
6. *n for 60 years is the projected number of Heatup-Cooldown cycles.*

Revised CUF Calculation for 60 Years:

P_L+P_B+Q *(see Note 1)*	K_e *(see Note 2)*	S_{alt} *(see Note 3)*	n *(see Note 6)*	N *(see Note 4)*	U
44,526	1.00	25,762	300	35,300	0.0085
				Total, U_{60} =	**0.0085**

Environmental CUF Calculation for 60 Years:

Maximum $F_{en\text{-}HWC}$ Multiplier for HWC Conditions =	5.39	*(from Table 6)*
Maximum $F_{en\text{-}NWC}$ Multiplier for NWC Conditions =	13.17	*(from Table 6)*

$U_{env\text{-}60} = U_{60} \times F_{en\text{-}NWC} \times 0.53 + U_{60} \times F_{en\text{-}HWC} \times 0.47$ = 0.0809
Overall Multiplier = $U_{env\text{-}60}/U_{60}$ = 9.51

Table 8: EAF Evaluation for Limiting RPV Shell/Shroud Support Location

Component: RPV Shell at Shroud Support
NUREG/CR-6260 CUF: 0.032 *(for reference only)*
Reference: NUREG/CR-6260, p. 5-102
Stress Report CUF: 0.0549 *(for Point 9, see below)*
Material: Low Alloy Steel *(Material = A-533 Gr. B per References [14] and [19])*

Design Basis CUF Calculation for 40 years:

Hydrotest σ_ϕ =	26,240	psi	*(p. S3-97 of RPV Stress Report)*
Hydrotest σ_r =	-1,250	psi	*(p. S3-97 of RPV Stress Report)*
Stress Concentration Factor, K_t =	2.40		*(p. S3-99d of RPV Stress Report)*
Hydrotest $K_t\sigma_\phi$ =	62,976	psi	*(p. S3-97 of RPV Stress Report)*
Improper Startup σ_ϕ =	28,060	psi	*(p. S3-98 of RPV Stress Report)*
Improper Startup σ_r =	-1,025	psi	*(p. S3-98 of RPV Stress Report)*
Improper Startup Skin Stress =	156,099	psi	*(p. S3-98 of RPV Stress Report)*
Improper Startup $K_t\sigma_\phi$ + Skin Stress =	223,443	psi	*(p. S3-98 of RPV Stress Report)*
Warmup σ_ϕ =	-5,707	psi	*(p. S3-99a of RPV Stress Report)*
Warmup σ_r =	-102	psi	*(p. S3-99a of RPV Stress Report)*
Warmup $K_t\sigma_\phi$ =	-13,696	psi	*(p. S3-99a of RPV Stress Report)*
$E_{fatigue\ curve}/E_{analysis}$ =	1.0417		*30.0 / 28.8 per S3-99f of RPV Stress Report and ASME Code fatigue curve*
Power Uprate =	1.0067		*=(549 - 100) / (546 - 100) per 4.4.1.b of 26A6019, Rev. 1 [14]*
m =	2.0		*NB-3228.5 of ASME Code, Section III [11]*
n =	0.2		*NB-3228.5 of ASME Code, Section III [11]*
S_m =	26,700	psi	*(ASME Code, Section II, Part D [11])*

P_L+P_B+Q *(see Note 1)*	Events	K_e *(see Note 2)*	S_{alt} *(see Note 3)*	n *(see Note 4)*	N *(see Note 5)*	U
34,690	Improper Startup - Warmup	1.00	124,825	5	332	0.0151
33,095	Hydrotest - Warmup	1.00	40,804	322	8,095	0.0398
					Total, U_{40} =	**0.0549**

Notes:
1. *P_L+P_B+Q is computed for Point 9 based on the $[(\sigma_\phi - \sigma_r)_{Event\ 1} - (\sigma_\phi - \sigma_r)_{Event\ 2}]$ stress intensity.*
2. *K_e computed in accordance with NB-3228.5 of ASME Code, Section III.*
3. *$S_{alt} = 0.5 * K_e * E_{fatigue\ curve}/E_{analysis} *$ Power Uprate $* [(K_t\sigma_\phi - \sigma_r)_{Event\ 1} - (K_t\sigma_\phi - \sigma_r)_{Event\ 2}]$.*
4. *n for 40 years is the number of cycles as follows per p. S3-99e and S3-99f of the RPV Stress Report:*

Improper Startup =	*5*	*cycles*
Hydrotest =	*2*	*cycles*
Isothermal at 70°F and 1,000 psi =	*120*	*cycles (same as number of Startup events)*
Warmup-Cooldown =	*199*	*cycles*
Warmup-Blowdown =	*1*	*cycle*
TOTAL =	*327*	*cycles*

5. *N obtained from Figure I-9.1 of Appendix I of ASME Code, Section III.*
6. *n for 60 years is the projected number of cycles as follows:*

Improper Startup =	*1*	*cycles*
Hydrotest =	*1*	*cycles*
Isothermal at 70°F and 1,000 psi =	*300*	*cycles (same as number of Startup events)*
Warmup-Cooldown =	*300*	*cycles*
Warmup-Blowdown =	*1*	*cycle*
TOTAL =	*603*	*cycles*

Revised CUF Calculation for 60 Years:

P_L+P_B+Q *(see Note 1)*		K_e *(see Note 2)*	S_{alt} *(see Note 3)*	n *(see Note 6)*	N *(see Note 4)*	U
34,690	Improper Startup - Warmup	1.00	124,825	1	332	0.0030
33,095	Hydrotest - Warmup	1.00	40,804	602	8,095	0.0744
					Total, U_{60} =	**0.0774**

Environmental CUF Calculation for 60 Years:

Maximum $F_{en\text{-}HWC}$ Multiplier for HWC Conditions =	5.39	*(from Table 6)*
Maximum $F_{en\text{-}NWC}$ Multiplier for NWC Conditions =	13.17	*(from Table 6)*

$U_{env\text{-}60} = U_{60} \times F_{en\text{-}NWC} \times 0.53 + U_{60} \times F_{en\text{-}HWC} \times 0.47 =$ 0.7364
Overall Multiplier = $U_{env\text{-}60}/U_{60} =$ 9.51

Table 9: EAF Evaluation for RR Inlet Nozzle Forging Location

Component: Recirculation Inlet Nozzle Forging
NUREG/CR-6260 CUF: 0.310 *(for reference only)*
Reference: NUREG/CR-6260, p. 5-105
Stress Report CUF: 0.0433 *(updated for Point 12, see below)*
Material: Low Alloy Steel *(Material = A-508 Cl. II per p. I-S8-4 of CBIN Stress Report Section S8)*

Design Basis CUF Calculation for 40 years:

$E_{fatigue\ curve}/E_{analysis}$ =	1.1278	*= 30.0 / 26.6 (per p. I-S8-24 of CBIN Stress Report Section S8 and ASME Code fatigue curve)*
Power Uprate =	1.0067	*=(549 - 100) / (546 - 100) per 4.4.1.b of 26A6019, Rev. 1 [14]*
K_t =	1.660	*stress concentration factor (p. A270 of VYC-378, Rev. 0 [12])*
m =	2.0	*NB-3228.5 of ASME Code, Section III [11]*
n =	0.2	*NB-3228.5 of ASME Code, Section III [11]*
S_m =	26,700	psi *(ASME Code, Section II, Part D [11])*

P_L+P_B+Q *(see Note 1)*	Skin Stress *(see Note 2)*	K_e *(see Note 3)*	S_{alt} *(see Note 4)*	n *(see Note 5)*	N *(see Note 6)*	U
43,110	15,145	1.00	49,224	200	4,614	0.0433
					Total, U_{40} =	**0.0433**

Notes:
1. *P_L+P_B+Q is obtained for Point 12 from p. A270 of VYC-378, Rev. 0.*
2. *Skin Stress is obtained for Point 12 from p. A270 of VYC-378, Rev. 0.*
3. *K_e computed in accordance with NB-3228.5 of ASME Code, Section III.*
4. *$S_{alt} = 0.5 * K_e * E_{fatigue\ curve}/E_{analysis} *$ Power Uprate $*[(P_L+P_B+Q)\ K_t$ + Skin Stress].*
5. *n for 40 years is the number of Heatup-Cooldown cycles, per p. B28 of VYC-378, Rev. 0.*
6. *N obtained from Figure I-9.1 of Appendix I of ASME Code, Section III.*
7. *n for 60 years is the projected number of Heatup-Cooldown cycles.*

Revised CUF Calculation for 60 Years:

P_L+P_B+Q *(see Note 1)*	Skin Stress *(see Note 2)*	K_e *(see Note 3)*	S_{alt} *(see Note 4)*	n *(see Note 7)*	N *(see Note 6)*	U
43,110	15,145	1.00	49,224	300	4,614	0.0650
					Total, U_{60} =	**0.0650**

Environmental CUF Calculation for 60 Years:

Maximum $F_{en\text{-}HWC}$ Multiplier for HWC Conditions = 2.45 *(from Table 5)*
Maximum $F_{en\text{-}NWC}$ Multiplier for NWC Conditions = 12.43 *(from Table 5)*

$U_{env\text{-}60} = U_{60} \times F_{en\text{-}NWC} \times 0.53 + U_{60} \times F_{en\text{-}HWC} \times 0.47$ = 0.5034
Overall Multiplier = $U_{env\text{-}60}/U_{60}$ = 7.74

Table 10: EAF Evaluation for RR Inlet Nozzle Safe End Location

Component: Recirculation Inlet Nozzle Safe End
NUREG/CR-6260 CUF: 0.310 *(for reference only)*
Reference: NUREG/CR-6260, p. 5-105
Stress Report CUF: 0.0017 *(updated for Location 6-I, see below)*
Material: Stainless Steel *(316L per p. 8 of 23A4292, Rev. 4)*

Design Basis CUF Calculation for 40 years:

$E_{fatigue\ curve}/E_{analysis}$ =	1.1076	*= 28.3 / 25.55 (per p. 62 of Reference [18] and ASME Code fatigue curve)*
Power Uprate =	1.0067	*=(549 - 100) / (546 - 100) per 4.4.1.b of 26A6019, Rev. 1 [14]*
K_t =	1.280	*stress concentration factor (p. B27 of VYC-378, Rev. 0 [12])*
m =	1.7	*NB-3228.5 of ASME Code, Section III [11]*
n =	0.3	*NB-3228.5 of ASME Code, Section III [11]*
S_m =	16,600 psi	*(ASME Code, Section II, Part D [11])*

P_L+P_B+Q *(see Note 1)*	P+Q+F *(see Note 2)*	K_e *(see Note 3)*	S_{alt} *(see Note 4)*	n *(see Note 5)*	N *(see Note 6)*	U
47,183	36,972	1.00	26,385	2,076	1,242,266	0.0017
					Total, U_{40} =	**0.0017**

Notes:
1. *P_L+P_B+Q is obtained for Surface I (after weld overlay) from p. 117 of Reference [18].*
2. *P+Q+F is obtained for Point 6-I from p. 118 of Reference [18] (BEFORE weld overlay).*
3. *K_e computed in accordance with NB-3228.5 of ASME Code, Section III.*
4. *$S_{alt} = 0.5 * K_e * E_{fatigue\ curve}/E_{analysis} *$ Power Uprate $* [(P+Q+F) K_t]$.*
5. *n for 40 years is the number of cycles as follows per p. B26 of VYC-378, Rev. 0:*

Design Hydrotest =	*130*	
Loss of Feedpumps Composite:		
Startup/Shutdown =	*290*	
SRV Blowdown =	*8*	
Loss of Feedwater Pumps	*30*	*10 events x 3 up/down cycles per event*
SCRAM =	*270*	
Normal +/- Seismic =	*11*	*10 cycles of upset seismic, plus 1 Level C seismic event*
Normal =	*739*	*= Sum of all of above events*
Zeroload =	*598*	*= Startup/Shutdown + SRV Blowdown + Scram + LOFP*
Total number of cycles =	*2,076*	

6. *N obtained from Figure I-9.2 of Appendix I of ASME Code, Section III.*
7. *n for 60 years is the projected number of cycles as follows:*

Design Hydrotest =	*120*	
Loss of Feedpumps Composite:		
Startup/Shutdown =	*300*	
SRV Blowdown =	*1*	
Loss of Feedwater Pumps	*30*	*10 events x 3 up/down cycles per event*
SCRAM =	*289*	*All remaining scrams*
Normal +/- Seismic =	*11*	*Assume the same*
Normal =	*751*	*= Sum of all of above events*
Zeroload =	*620*	*= Startup/Shutdown + SRV Blowdown + Scram + LOFP*
Total number of cycles =	*2,122*	

Revised CUF Calculation for 60 Years:

P_L+P_B+Q *(see Note 1)*	P+Q+F *(see Note 2)*	K_e *(see Note 3)*	S_{alt} *(see Note 4)*	n *(see Note 5)*	N *(see Note 7)*	U
47,183	36,972	1.00	26,385	2,122	1,242,266	0.0017
					Total, U_{60} =	**0.0017**

Environmental CUF Calculation for 60 Years:

Maximum $F_{en\text{-}HWC}$ Multiplier for HWC Conditions =	15.35	*(from Table 2)*
Maximum $F_{en\text{-}NWC}$ Multiplier for NWC Conditions =	8.36	*(from Table 2)*
$U_{env\text{-}60} = U_{60} \times F_{en\text{-}NWC} \times 0.53 + U_{60} \times F_{en\text{-}HWC} \times 0.47$ =	**0.0199**	
Overall Multiplier = $U_{env\text{-}60}/U_{60}$ =	**11.64**	

Table 11: Summary of EAF Evaluation Results for VY

No.	Component	Material	40-Year Design CUF (1)	60-Year CUF (2)	Overall Environmental Multiplier	60-Year Environmental CUF (2,3)
1	RPV Shell/Bottom Head	Low Alloy Steel	0.0057	0.0085	9.51	0.0809
2	RPV Shell at Shroud Support	Low Alloy Steel	0.0549	0.0774	9.51	0.7364
3	Recirculation Inlet Nozzle Safe End	Stainless Steel	0.0017	0.0017	11.64	0.0199
4	Recirculation Inlet Nozzle Forging	Low Alloy Steel	0.0433	0.0650	7.74	0.5034

Notes:
1. Updated 40-year CUF calculation based on recent ASME Code methodology and design basis cycles.
2. CUF results using updated ASME Code methodology and actual cycles accumulated to-date and projected to 60 years.
3. An F_{en} multiplier was used for each respective component with the following conditions:
   + 47% HWC conditions and 53% NWC conditions

APPENDIX A

VY WATER CHEMISTRY INFORMATION [8]

Location	Pre-NMCA 1593 MWth (OLP)	Post-NMCA + HWC 1593 MWth (OLP)	Post-NMCA + HWC 1912 MWth (EPU)	Future Operation Post-NMCA + HWC 1912 MWth (EPU)
	---	Average Availability 98.5%	Average Availability 98.5%	Average Availability 99%
	Implementation Date = 11/1972	NMCA Application Date = 04/27/2001 HWC Implementation Date = 11/01/2003	EPU Implementation Date = 5/2006	---
FW Line	40 ppb	40 ppb	40 ppb	40 ppb
Recirc. Line	122 ppb	48 ppb	34 ppb	34 ppb
RPV Bottom Head **	128 ppb	69 ppb	55 ppb	55 ppb
RPV Upper Region	114 ppb	97 ppb	90 ppb	90 ppb
RPV Beltline Region	123 ppb	46 ppb	31 ppb	31 ppb

** RPV Bottom head at "Lower Plenum, Downflow" (i.e. outside core support columns)

APPENDIX B

VY LICENSE DATE [10]

Michael A. Balduzzi Vice President - Pilgrim Nuclear Power Station	Pilgrim Nuclear Power Station 600 Rocky Hill Road Plymouth, Massachusetts 02360
Fred R. Dacimo Vice President - Indian Point Energy Center	Indian Point Energy Center Bleakley Avenue & Broadway Buchanon, New York 10511
Randall K. Edington Vice President - Operations Support	Cooper Nuclear Power Station 1200 Prospect Road P.O. Box 98 Brownsville, Nebraska 68321
Christopher J. Schwarz Vice President - Operations Support	Entergy Nuclear Operations, Inc 440 Hamilton Avenue White Plains, New York 10601
Theodore A. Sullivan Vice President - Fitzpatrick Nuclear Power Station	Fitzpatrick Nuclear Power Station 268 Lake Road East Lycoming, New York 13093
Jay K. Thayer Vice President - Vermont Yankee Nuclear Power Station	Entergy Nuclear Vermont Yankee Corporate Office P.O. Box 0500 185 Old Ferry Road Brattleboro, VT 05302-0500

1.1.5 Class and Period of License Sought

ENO requests renewal of the facility operating license for VYNPS (facility operating license DPR-28) for a period of 20 years. The license was issued under Section 104b of the Atomic Energy Act of 1954 as amended. License renewal would extend the facility operating license from midnight March 21, 2012, to midnight March 21, 2032.

This application also applies to renewal of those NRC source materials, special nuclear material, and by-product material licenses that are subsumed or combined with the facility operating license.

1.1.6 Alteration Schedule

ENO does not propose to construct or alter any production or utilization facility in connection with this renewal application.

Structural Integrity Associates, Inc.	File No.: VY-16Q-304
CALCULATION PACKAGE	**Project No.:** VY-16Q

PROJECT NAME:

Environmental Fatigue Analysis of VYNPS

CONTRACT NO.:

10150394

CLIENT:	**PLANT:**
Entergy Nuclear Operations, Inc	Vermont Yankee Nuclear Power Station

CALCULATION TITLE:

Recirculation Outlet Nozzle Finite Element Model

Document Revision	Affected Pages	Revision Description	Project Manager Approval Signature & Date	Preparer(s) & Checker(s) Signatures & Date
0	1-6, Appendix: A1-A20	Initial Issue	Terry J. Herrmann 7/12/2007	Minghao Qin 7/12/2007 Jennifer E. Smith 7/12/2007

Table of Contents

1.0 OBJECTIVE 3
2.0 GEOMETRY / MATERIAL PROPERTIES 3
3.0 PROGRAM INPUT 3
4.0 REFERENCES 4
APPENDIX A RON_VY.INP A1

List of Tables

Table 1: Material Properties @ 300°F 5

List of Figures

Figure 1: ANSYS Finite Element Model 6

1.0 OBJECTIVE

The objective of this calculation is to create a finite element model of the Vermont Yankee Nuclear Power Station recirculation outlet nozzle. This model will be used to develop a Green's Function to be used in a subsequent fatigue analysis.

2.0 GEOMETRY / MATERIAL PROPERTIES

A 2-D axisymmetric finite element model (FEM) of the nozzle was developed with element type PLANE182. The developed model includes the safe end, the nozzle forging, a portion of the vessel shell, and cladding. The model used the vessel radius multiplied by a factor 2.0 due to the model being axisymmetric.

The 2-D axisymmetric FEM was constructed using the dimensions and information from References [4 and 5] based on ANSYS [2] finite element software. Figure 1 shows the resulting finite element model.

The materials of the various components of the model are listed below:

- Safe End – SA182 F316 [4] (16Cr-12Ni-2Mo)
- Piping – SA376 TP316 [7] (16Cr-12Ni-2Mo)
- Nozzle Forging – SA508 Class 2 [5] (3/4Ni-1/2Mo-1/3Cr-V)
- Vessel – SA533 Grade B [6] (Mn-1/2Mo-1.2Ni)
- Cladding – SA240 Type 304 [1, Sheet 7] (18Cr-8Ni)

Material properties for these materials are based upon the 1998 ASME Code, Section II, Part D, with 2000 Addenda [3] and are shown in Table 1. The properties are taken at an average temperature of 300°F. This average temperature is based on a thermal shock of 500°F to 100°F which will be applied to the FEM model for Green's Function development.

3.0 PROGRAM INPUT

The input file, RON_VY.INP (included in Appendix A), creates the finite element model for the recirculation outlet nozzle.

4.0 REFERENCES

1. GE. Stress Report No. 23A4316, Revision 0, "Reactor Vessel Recirculation Outlet Safe End," SI File No. VY-16Q-204.
2. ANSYS, Release 8.1 (w/Service Pack 1), ANSYS, Inc., June 2004.
3. American Society of Mechanical Engineers, Boiler and Pressure Vessel Code, Section II, Part D, 1998 Edition, 2000 Addenda.
4. Vermont Yankee Drawing 5920-06623, Rev. 0, (Hitachi, Ltd. Drawing No IOR290-127), "Recirc. Outlet Safe End," SI File No. VY-16Q-204.
5. Vermont Yankee Drawing 5920-00238, Rev. 4, (Chicago Bridge & Iron Company, Contract No. 9-6201, Drawing No. 21), "36"x28" Nozzles Mk N1A/B," SI File No. VY-16Q-204.
6. Vermont Yankee Drawing 5920-05752, Rev. 3, "Vessel & Attachments Material Identifications," SI File No. VY-16Q-209.
7. SI File No. VY-16Q-103, "Vermont Yankee Comments on VY-16Q-304."

Table 1: Material Properties @ 300°F (1)

Material	SA533 Grade B (Mn-1/2Mo-1/2Ni)	SA508 Class 2 (3/4Ni-1/2Mo-1/3Cr-V)	SA240 Type 304 (18Cr-8Ni)	SA182 F316/ SA376 TP316 (16Cr-12Ni-2Mo)
Modulus of Elasticity, e-6 psi	28.0	26.7	27.0	27.0
Coefficient of Thermal Expansion, e-6, in/in/°F	7.7	7.3	9.8	9.8
Thermal Conductivity, Btu/hr-ft-°F	23.4	23.4	9.8	9.3
Thermal Diffusivity, ft^2/hr	0.401	0.401	0.160	0.150
Specific Heat, Btu/lb-°F (2)	0.119	0.119	0.125	0.127
Density, lb/in^3	0.283	0.283	0.283	0.283
Poisson's Ratio	0.3	0.3	0.3	0.3

Notes:

1. The material properties applied in the analyses are taken from ASME Section II Part D 1998 Edition with 2000 Addenda. This is consistent with information provided in the Design Input Record (page 13 of VY EC No. 1773, SI File No. VY-16Q-209). The use of a later code edition than that used for the original design code is acceptable since later editions typically reflect more accurate material properties than was published in prior Code editions. Material Properties are evaluated at 300°F from the 1998 ASME Code, Section II, Part D, with 2000 Addenda, except for density and Poisson's ratio, which are assumed typical values.
2. Calculated as $[k/(\rho d)]/12^3$.

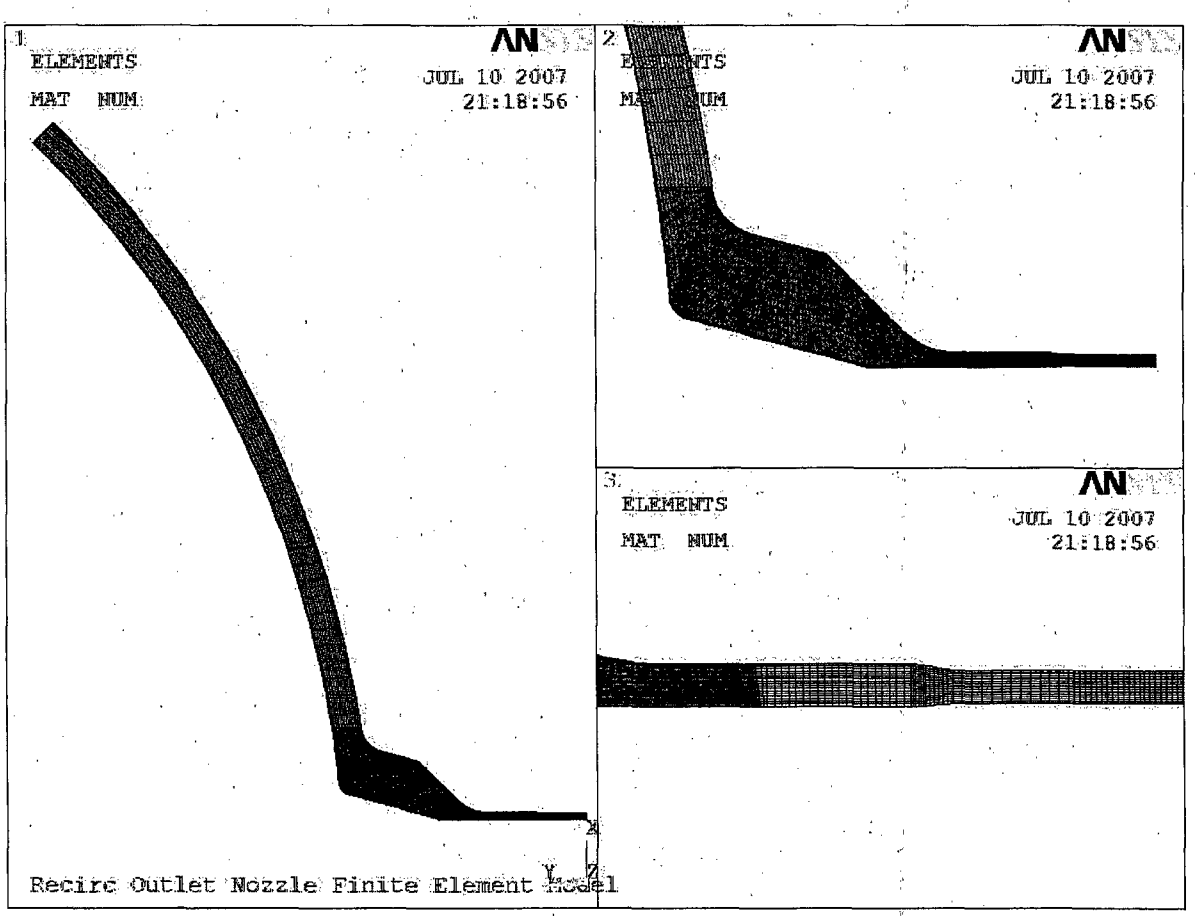

Figure 1: ANSYS Finite Element Model

APPENDIX A

RON_VY.inp

```
finish
/clear,start
/prep7
/title, Recirc Outlet Nozzle Finite Element Model

/com, PLANE182, 2-D Solid
et,1,PLANE182,,,1    !Axisymmetric

/com, ****************************
/com, Material Properties @T=300F
/com, ****************************

/COM, Material #1 (Safe-End and Piping)  SA-182 F316  (16Cr-12Ni-2Mo)
mp,ex,1,27E+06
mp,alpx,1,9.8E-06
mp,kxx,1,9.3/3600/12
mp,c,1,0.127
mp,nuxy,1,0.3
mp,dens,1,0.283

/COM, Material #2 (Nozzle Forging) SA-508 Class 2 (3/4Ni-1/2Mo-1/3Cr-V)
mp,ex,2,26.7E+06
mp,alpx,2,7.3E-06
mp,kxx,2,23.4/3600/12
mp,c,2,0.119
mp,nuxy,2,0.3
mp,dens,2,0.283

/COM, Material #3 (Cladding) SA-240 Type 304 (18Cr-8Ni)
mp,ex,3,27E+06
mp,alpx,3,9.8E-06
mp,kxx,3,9.8/3600/12
mp,c,3,0.125
mp,nuxy,3,0.3
mp,dens,3,0.283

/COM, Material #4 (Vessel) SA-533, GR. B (Mn-1/2Mo-1/2Ni)
mp,ex,4,28.0E+06
mp,alpx,4,7.7E-06
mp,kxx,4,23.4/3600/12
mp,c,4,0.119
mp,nuxy,4,0.3
mp,dens,4,0.283

*AFUN,DEG
/com, *** Geometric Parameters ***
*set,vira,(103+3/16)      !Actual Vessel Inner Radius to base metal used for model
*set,vir,2.0*vira          !2.0 time of  Vessel Inner Radius to base metal used for model
*set,tvw,5+5/8-3/16       !Vessel Wall Thickness
*set,ri1,25.75/2
*set,ro1,28.375/2
*set,L1,5
*set,ro2,28.375/2
```

```
*set,L2,4.25
*set,ro3,28.875/2
*set,ro4,48.75/2
*set,L3,1.5
*set,L4,5.25
*set,L5,7+1/16
*set,L6,12+13/16
*set,L7,9+7/8
*set,L8,9+3/8
*set,L9,31+15/16
*set,L10,L9-12-13/16-tvw
*set,ra,7
*set,rb,1
*set,rc,5.25
*set,rd,2.5
*set,tv,3/16
*set,dimA,vir-(tv*2.0)+L9+11+L1  !Vessel Centerline to End of Safe End used for model
*set,L21,1
*set,L22,4.25
*set,ri21,(25+15/16)/2

/com,*****************************************************************
/com, Geometry
/com,*****************************************************************
local,13,0,,dimA,,,,

csys,13

/com, Begin at end of Safe-End - Carbon Section

k, 1, ri1, -1*(dimA)
k, 2, ri1+tv, -1*(dimA)
k, 3, ro1, -1*(dimA)
k, 4, ri1, -1*(dimA-L1)
k, 5, ri1+tv, -1*(dimA-L1)
k, 6, ro1, -1*(dimA-L1)
k, 7, ri1, -1*(dimA-L1-L2)
k, 8, ri1+tv, -1*(dimA-L1-L2)
k, 9, ro2, -1*(dimA-L1-L2)
k, 10, ri1, -1*(dimA-L1-L2-L3)
k, 11, ri1+tv, -1*(dimA-L1-L2-L3)
k, 12, ro3, -1*(dimA-L1-L2-L3)
k, 13, ri1, -1*(dimA-L1-L2-L3-L4)
k, 14, ri1+tv, -1*(dimA-L1-L2-L3-L4)
k, 15, ro3, -1*(dimA-L1-L2-L3-L4)
k, 16, ri1, -1*(dimA-L1-L2-L3-L4-L5)
k, 17, ri1+tv, -1*(dimA-L1-L2-L3-L4-L5)
k, 18, ro3, -1*(dimA-L1-L2-L3-L4-L5)

k,19,    ro4, -1*(dimA-L1-L2-L3-L4-L5-L7)! Temporary Point
l,19,18
l,18,15
lfillt,1,2,ra
k,22,    ro4+(L8+6)*tan(15), -1*(dimA-L1-L2-L3-L4-L5-L7-(L8+6))
l,19,22
```

```
LFILLT,1,4,rb

k, 25, ri1, -1*(dimA-L1-L2-L3-L4-L6)
k, 26, ri1+tv, -1*(dimA-L1-L2-L3-L4-L6)

k, 27, ri1+(L10+tvw+tv+4)*tan(15), -1*(vir-tv-4)
k, 28, ri1+tv+(L10+tvw+tv+4)*tan(15), -1*(vir-tv-4)

k,29,    (vir+tvw+tv)*sin(45), -1*(vir+tvw+tv)*cos(45)
k,30,    0, -1*(vir+tvw+tv)   ! Temporary Point
k,31,    0, 0 ! Temporary Point

larc,29,30,31,vir+tvw+tv

k,32,    (vir+tv)*sin(45), -1*(vir+tv)*cos(45)
k,33,    0, -1*(vir+tv)   ! Temporary Point
larc,32,33,31,vir+tv

k,34,    vir*sin(45), -1*vir*cos(45)
k,35,    0, -1*vir   ! Temporary Point
larc,34,35,31,vir

LSTR,    4,    5
LSTR,    5,    6
LSTR,    6,    9
LSTR,    9,   12
LSTR,   12,   15
LSTR,    5,    8
LSTR,    4,    7
LSTR,    7,   10
LSTR,    8,   11
LSTR,   11,   14
LSTR,   10,   13
LSTR,   13,   16
LSTR,   14,   17
LSTR,   16,   25
LSTR,   17,   26
LSTR,   26,   28
LSTR,   25,   27
LSTR,    4,    1
LSTR,    1,    2
LSTR,    2,    3
LSTR,    3,    6
LSTR,    5,    2
LSTR,    7,    8
LSTR,    8,    9
LSTR,   12,   11
LSTR,   11,   10
LSTR,   13,   14
LSTR,   14,   15

FLST,2,2,4,ORDE,2
FITEM,2,4
FITEM,2,6
LPTN,P51X
```

```
FLST,2,2,4,ORDE,2
FITEM,2,8
FITEM,2,25
LPTN,P51X

FLST,2,2,4,ORDE,2
FITEM,2,7
FITEM,2,24
LPTN,P51X

FLST,2,6,4,ORDE,6
FITEM,2,6
FITEM,2,25
FITEM,2,37
FITEM,2,40
FITEM,2,42
FITEM,2,44
LDELE,P51X, , ,1

!*
LFILLT,4,41,rd, ,
!*
LFILLT,43,8,rd, ,
!*
LFILLT,39,38,rc, ,

FLST,2,3,4,ORDE,3
FITEM,2,1
FITEM,2,3
FITEM,2,5
LCOMB,P51X, ,0
LSTR,    16,    17
LSTR,    17,    21
LSTR,    25,    26
LSTR,    26,    24
LSTR,    22,    30
LSTR,    30,    35
LSTR,    27,    28
LSTR,    28,    33
LSTR,    29,    32
LSTR,    32,    34

k,39,    0, -1*(vir+tvw+tv)

!Create Areas
FLST,2,4,4
FITEM,2,27
FITEM,2,30
FITEM,2,26
FITEM,2,9
AL,P51X
FLST,2,4,4
FITEM,2,28
FITEM,2,29
```

```
FITEM,2,10
FITEM,2,30
AL,P51X
FLST,2,4,4
FITEM,2,11
FITEM,2,32
FITEM,2,10
FITEM,2,14
AL,P51X
FLST,2,4,4
FITEM,2,15
FITEM,2,14
FITEM,2,9
FITEM,2,31
AL,P51X
FLST,2,4,4
FITEM,2,32
FITEM,2,33
FITEM,2,12
FITEM,2,17
AL,P51X
FLST,2,4,4
FITEM,2,16
FITEM,2,17
FITEM,2,31
FITEM,2,34
AL,P51X
FLST,2,4,4
FITEM,2,36
FITEM,2,13
FITEM,2,33
FITEM,2,18
AL,P51X
FLST,2,4,4
FITEM,2,19
FITEM,2,18
FITEM,2,35
FITEM,2,34
AL,P51X
FLST,2,4,4
FITEM,2,2
FITEM,2,5
FITEM,2,36
FITEM,2,21
AL,P51X
FLST,2,4,4
FITEM,2,20
FITEM,2,21
FITEM,2,3
FITEM,2,35
AL,P51X
FLST,2,4,4
FITEM,2,1
FITEM,2,37
FITEM,2,23
```

```
FITEM,2,5
AL,P51X
FLST,2,4,4
FITEM,2,22
FITEM,2,23
FITEM,2,25
FITEM,2,3
AL,P51X
FLST,2,4,4
FITEM,2,38
FITEM,2,42
FITEM,2,37
FITEM,2,8
AL,P51X
FLST,2,4,4
FITEM,2,4
FITEM,2,8
FITEM,2,25
FITEM,2,40
AL,P51X
FLST,2,4,4
FITEM,2,24
FITEM,2,45
FITEM,2,7
FITEM,2,42
AL,P51X
FLST,2,4,4
FITEM,2,6
FITEM,2,7
FITEM,2,44
FITEM,2,40
AL,P51X
FLST,2,4,4
FITEM,2,41
FITEM,2,43
FITEM,2,47
FITEM,2,44
AL,P51X
FLST,2,4,4
FITEM,2,39
FITEM,2,46
FITEM,2,45
FITEM,2,43
AL,P51X

! define materials
FLST,5,8,5,ORDE,2
FITEM,5,1
FITEM,5,-8
CM,_Y,AREA
ASEL, , , ,P51X
CM,_Y1,AREA
CMSEL,S,_Y
!*
CMSEL,S,_Y1
```

```
AATT,     1, ,  1,     0,
CMSEL,S,_Y
CMDELE,_Y
CMDELE,_Y1
!*
FLST,5,5,5,ORDE,5
FITEM,5,9
FITEM,5,11
FITEM,5,13
FITEM,5,15
FITEM,5,18
CM,_Y,AREA
ASEL, , , ,P51X
CM,_Y1,AREA
CMSEL,S,_Y
!*
CMSEL,S,_Y1
AATT,     2, ,  1,     0,
CMSEL,S,_Y
CMDELE,_Y
CMDELE,_Y1
!*
FLST,5,5,5,ORDE,5
FITEM,5,10
FITEM,5,12
FITEM,5,14
FITEM,5,16
FITEM,5,-17
CM,_Y,AREA
ASEL, , , ,P51X
CM,_Y1,AREA
CMSEL,S,_Y
!*
CMSEL,S,_Y1
AATT,     3, ,  1,     0,
CMSEL,S,_Y
CMDELE,_Y
CMDELE,_Y1
!*

!/com, Map mesh areas
FLST,5,10,4,ORDE,10
FITEM,5,5
FITEM,5,10
FITEM,5,28
FITEM,5,32
FITEM,5,-33
FITEM,5,36
FITEM,5,-37
FITEM,5,42
FITEM,5,45
FITEM,5,-46
CM,_Y,LINE
LSEL, , , ,P51X
CM,_Y1,LINE
```

```
CMSEL,,_Y
!*
LESIZE,_Y1, , ,15, , , , ,1
!*
FLST,5,10,4,ORDE,10
FITEM,5,3
FITEM,5,9
FITEM,5,25
FITEM,5,27
FITEM,5,31
FITEM,5,34
FITEM,5,-35
FITEM,5,40
FITEM,5,44
FITEM,5,47
CM,_Y,LINE
LSEL, , , ,P51X
CM,_Y1,LINE
CMSEL,,_Y
!*
LESIZE,_Y1, , ,2, , , , ,1
!*
FLST,5,3,4,ORDE,3
FITEM,5,39
FITEM,5,41
FITEM,5,43
CM,_Y,LINE
LSEL, , , ,P51X
CM,_Y1,LINE
CMSEL,,_Y
!*
LESIZE,_Y1, , ,80, , , , ,1
!*
FLST,5,3,4,ORDE,3
FITEM,5,6
FITEM,5,-7
FITEM,5,24
CM,_Y,LINE
LSEL, , , ,P51X
CM,_Y1,LINE
CMSEL,,_Y
!*
LESIZE,_Y1, , ,20, , , , ,1
!*
FLST,5,3,4,ORDE,3
FITEM,5,4
FITEM,5,8
FITEM,5,38
CM,_Y,LINE
LSEL, , , ,P51X
CM,_Y1,LINE
CMSEL,,_Y
!*
LESIZE,_Y1, , ,40, , , , ,1
!*
```

```
FLST,5,3,4,ORDE,3
FITEM,5,1
FITEM,5,22
FITEM,5,-23
CM,_Y,LINE
LSEL, , , ,P51X
CM,_Y1,LINE
CMSEL,,_Y
!*
LESIZE,_Y1, , ,30, , , , ,1
!*
FLST,5,6,4,ORDE,6
FITEM,5,2
FITEM,5,20
FITEM,5,-21
FITEM,5,26
FITEM,5,29
FITEM,5,-30
CM,_Y,LINE
LSEL, , , ,P51X
CM,_Y1,LINE
CMSEL,,_Y
!*
LESIZE,_Y1, , ,40, , , , ,1
!*
FLST,5,9,4,ORDE,2
FITEM,5,11
FITEM,5,-19
CM,_Y,LINE
LSEL, , , ,P51X
CM,_Y1,LINE
CMSEL,,_Y
!*
LESIZE,_Y1, , ,20, , , , ,1
!*

! Meshing
FLST,5,18,5,ORDE,2
FITEM,5,1
FITEM,5,-18
CM,_Y,AREA
ASEL, , , ,P51X
CM,_Y1,AREA
CHKMSH,'AREA'
CMSEL,S,_Y
!*
MSHKEY,1
AMESH,_Y1
MSHKEY,0
!*
CMDELE,_Y
CMDELE,_Y1
CMDELE,_Y2
!*
```

```
!Modify the safe end ID
FLST,2,6,5,ORDE,2
FITEM,2,1
FITEM,2,-6
ACLEAR,P51X
FLST,2,6,5,ORDE,2
FITEM,2,1
FITEM,2,-6
ADELE,P51X
FLST,2,9,4,ORDE,7
FITEM,2,9
FITEM,2,14
FITEM,2,-17
FITEM,2,26
FITEM,2,-27
FITEM,2,30
FITEM,2,-31
LDELE,P51X, , ,1

FLST,2,3,4,ORDE,3
FITEM,2,10
FITEM,2,28
FITEM,2,32
LDELE,P51X, , ,1
FLST,3,2,3,ORDE,2
FITEM,3,3
FITEM,3,6
KGEN,2,P51X, , ,-ro2+ri21, , , ,0
FLST,3,1,3,ORDE,1
FITEM,3,2
KGEN,2,P51X, , , ,L22, , ,0
FLST,3,3,3,ORDE,3
FITEM,3,1
FITEM,3,-2
FITEM,3,4
KGEN,2,P51X, , ,tv, , , ,0
FLST,3,2,3,ORDE,2
FITEM,3,10
FITEM,3,-11
KGEN,2,P51X, , , ,-(L3-L21), , ,0
FLST,3,1,3,ORDE,1
FITEM,3,23
KGEN,2,P51X, , ,5, , , ,0
LSTR,     23,     40
FLST,2,2,4,ORDE,2
FITEM,2,9
FITEM,2,12
LPTN,P51X
LDELE,     16, , ,1
FLST,2,4,3
FITEM,2,11
FITEM,2,23
FITEM,2,41
FITEM,2,12
A,P51X
```

```
FLST,2,4,3
FITEM,2,23
FITEM,2,8
FITEM,2,9
FITEM,2,41
A,P51X
FLST,2,4,3
FITEM,2,8
FITEM,2,7
FITEM,2,6
FITEM,2,9
A,P51X
FLST,2,4,3
FITEM,2,7
FITEM,2,5
FITEM,2,3
FITEM,2,6
A,P51X
FLST,2,4,3
FITEM,2,10
FITEM,2,20
FITEM,2,23
FITEM,2,11
A,P51X
FLST,2,4,3
FITEM,2,20
FITEM,2,4
FITEM,2,8
FITEM,2,23
A,P51X
FLST,2,4,3
FITEM,2,4
FITEM,2,2
FITEM,2,7
FITEM,2,8
A,P51X
FLST,2,4,3
FITEM,2,2
FITEM,2,1
FITEM,2,5
FITEM,2,7
A,P51X
FLST,5,8,5,ORDE,4
FITEM,5,1
FITEM,5,-6
FITEM,5,19
FITEM,5,-20
CM,_Y,AREA
ASEL, , , ,P51X
CM,_Y1,AREA
CMSEL,S,_Y
!*
CMSEL,S,_Y1
AATT,     1, ,  1,     0,
CMSEL,S,_Y
```

```
CMDELE,_Y
CMDELE,_Y1
!*
FLST,5,4,4,ORDE,4
FITEM,5,15
FITEM,5,-16
FITEM,5,26
FITEM,5,28
CM,_Y,LINE
LSEL, , , ,P51X
CM,_Y1,LINE
CMSEL,,_Y
!*
LESIZE,_Y1, , ,15, , , , ,1
!*
FLST,5,4,4,ORDE,4
FITEM,5,31
FITEM,5,48
FITEM,5,50
FITEM,5,52
CM,_Y,LINE
LSEL, , , ,P51X
CM,_Y1,LINE
CMSEL,,_Y
!*
LESIZE,_Y1, , ,2, , , , ,1
!*
FLST,5,6,4,ORDE,6
FITEM,5,9
FITEM,5,-10
FITEM,5,12
FITEM,5,14
FITEM,5,30
FITEM,5,32
CM,_Y,LINE
LSEL, , , ,P51X
CM,_Y1,LINE
CMSEL,,_Y
!*
LESIZE,_Y1, , ,6, , , , ,1
!*
FLST,5,3,4,ORDE,3
FITEM,5,11
FITEM,5,17
FITEM,5,49
CM,_Y,LINE
LSEL, , , ,P51X
CM,_Y1,LINE
CMSEL,,_Y
!*
LESIZE,_Y1, , ,12, , , , ,1
!*
FLST,5,3,4,ORDE,3
FITEM,5,27
FITEM,5,29
```

```
FITEM,5,51
CM,_Y,LINE
LSEL, , , ,P51X
CM,_Y1,LINE
CMSEL,,_Y
!*
LESIZE,_Y1, , ,25, , , , ,1
!*
FLST,5,8,5,ORDE,4
FITEM,5,1
FITEM,5,-6
FITEM,5,19
FITEM,5,-20
CM,_Y,AREA
ASEL, , , ,P51X
CM,_Y1,AREA
CHKMSH,'AREA'
CMSEL,S,_Y
!*
MSHKEY,1
AMESH,_Y1
MSHKEY,0
!*
CMDELE,_Y
CMDELE,_Y1
CMDELE,_Y2
!*

FLST,2,2,5,ORDE,2
FITEM,2,17
FITEM,2,-18
ACLEAR,P51X

csys,0
k, 51,62/2,0,0
k, 52,62/2,60,0
LSTR,    51,    52
FLST,2,2,5,ORDE,2
FITEM,2,17
FITEM,2,-18
ADELE,P51X
lplo
FLST,2,4,4,ORDE,4
FITEM,2,39
FITEM,2,41
FITEM,2,43
FITEM,2,53
LPTN,P51X
FLST,2,2,4,ORDE,2
FITEM,2,60
FITEM,2,-61
LDELE,P51X, , ,1
FLST,2,4,4
FITEM,2,54
FITEM,2,62
```

```
FITEM,2,55
FITEM,2,44
AL,P51X
FLST,2,4,4
FITEM,2,55
FITEM,2,63
FITEM,2,58
FITEM,2,45
AL,P51X
FLST,2,4,4
FITEM,2,63
FITEM,2,56
FITEM,2,57
FITEM,2,46
AL,P51X
FLST,2,4,4
FITEM,2,47
FITEM,2,59
FITEM,2,57
FITEM,2,62
AL,P51X

CM,_Y,AREA
ASEL, , , ,    18
CM,_Y1,AREA
CMSEL,S,_Y
!*
CMSEL,S,_Y1
AATT,    2, ,  1,    0,
CMSEL,S,_Y
CMDELE,_Y
CMDELE,_Y1
!*
FLST,5,2,5,ORDE,2
FITEM,5,17
FITEM,5,22
CM,_Y,AREA
ASEL, , , ,P51X
CM,_Y1,AREA
CMSEL,S,_Y
!*
CMSEL,S,_Y1
AATT,    3, ,  1,    0,
CMSEL,S,_Y
CMDELE,_Y
CMDELE,_Y1
!*
CM,_Y,AREA
ASEL, , , ,    21
CM,_Y1,AREA
CMSEL,S,_Y
!*
CMSEL,S,_Y1
AATT,    4, ,  1,    0,
CMSEL,S,_Y
```

```
CMDELE,_Y
CMDELE,_Y1
!*
FLST,5,3,4,ORDE,3
FITEM,5,54
FITEM,5,-55
FITEM,5,58
CM,_Y,LINE
LSEL, , , ,P51X
CM,_Y1,LINE
CMSEL,,_Y
!*
LESIZE,_Y1, , ,8, , , , ,1
!*
FLST,5,3,4,ORDE,3
FITEM,5,56
FITEM,5,-57
FITEM,5,59
CM,_Y,LINE
LSEL, , , ,P51X
CM,_Y1,LINE
CMSEL,,_Y
!*
LESIZE,_Y1, , ,40, , , , ,1
!*
FLST,5,2,5,ORDE,2
FITEM,5,17
FITEM,5,-18
CM,_Y,AREA
ASEL, , , ,P51X
CM,_Y1,AREA
CHKMSH,'AREA'
CMSEL,S,_Y
!*
MSHKEY,1
AMESH,_Y1
MSHKEY,0
!*
CMDELE,_Y
CMDELE,_Y1
CMDELE,_Y2
!*
FLST,5,2,5,ORDE,2
FITEM,5,21
FITEM,5,-22
CM,_Y,AREA
ASEL, , , ,P51X
CM,_Y1,AREA
CHKMSH,'AREA'
CMSEL,S,_Y
!*
MSHKEY,1
AMESH,_Y1
MSHKEY,0
!*
```

```
CMDELE,_Y
CMDELE,_Y1
CMDELE,_Y2
!*

!Simulating Butter
FLST,2,2,5,ORDE,2
FITEM,2,9
FITEM,2,-10
ACLEAR,P51X
FLST,2,2,5,ORDE,2
FITEM,2,9
FITEM,2,-10
ADELE,P51X

KGEN,2,15, , , ,11/16, , ,0
KGEN,2,44, , , ,-0.25, , ,0
KGEN,2,14, , , ,11/16-1.375*tan(7.5), , ,0
KGEN,2,46, , , ,-0.25, , ,0

FLST,2,3,4,ORDE,3
FITEM,2,2
FITEM,2,20
FITEM,2,-21
LDELE,P51X
LSTR,    21,    44
LSTR,    44,    45
LSTR,    45,    15
LSTR,    17,    46
LSTR,    46,    47
LSTR,    47,    14
LSTR,    46,    44
LSTR,    45,    47
LSTR,    13,    16
FLST,3,2,3,ORDE,2
FITEM,3,46
FITEM,3,-47
KGEN,2,P51X, , ,-0.25, , , ,0
LSTR,    48,    46
LSTR,    49,    47
FLST,2,3,4,ORDE,3
FITEM,2,61
FITEM,2,64
FITEM,2,-65
LPTN,P51X
FLST,2,2,4,ORDE,2
FITEM,2,70
FITEM,2,-71
LDELE,P51X, , ,1
FLST,2,4,4
FITEM,2,67
FITEM,2,39
FITEM,2,68
FITEM,2,3
AL,P51X
```

```
FLST,2,4,4
FITEM,2,39
FITEM,2,5
FITEM,2,2
FITEM,2,53
AL,P51X
FLST,2,4,4
FITEM,2,20
FITEM,2,60
FITEM,2,53
FITEM,2,41
AL,P51X
FLST,2,4,4
FITEM,2,72
FITEM,2,68
FITEM,2,69
FITEM,2,41
AL,P51X
FLST,2,4,4
FITEM,2,21
FITEM,2,60
FITEM,2,36
FITEM,2,43
AL,P51X
FLST,2,4,4
FITEM,2,66
FITEM,2,69
FITEM,2,35
FITEM,2,43
AL,P51X

CM,_Y,AREA
ASEL, , , ,    10
CM,_Y1,AREA
CMSEL,S,_Y
!*
CMSEL,S,_Y1
AATT,    2, ,  1,    0,
CMSEL,S,_Y
CMDELE,_Y
CMDELE,_Y1
!*
FLST,5,3,5,ORDE,3
FITEM,5,9
FITEM,5,23
FITEM,5,-24
CM,_Y,AREA
ASEL, , , ,P51X
CM,_Y1,AREA
CMSEL,S,_Y
!*
CMSEL,S,_Y1
AATT,    3, ,  1,    0,
CMSEL,S,_Y
CMDELE,_Y
```

```
CMDELE,_Y1
!*
FLST,5,2,5,ORDE,2
FITEM,5,25
FITEM,5,-26
CM,_Y,AREA
ASEL, , , ,P51X
CM,_Y1,AREA
CMSEL,S,_Y
!*
CMSEL,S,_Y1
AATT,     1, ,  1,     0,
CMSEL,S,_Y
CMDELE,_Y
CMDELE,_Y1
!*
FLST,5,3,4,ORDE,3
FITEM,5,2
FITEM,5,39
FITEM,5,67
CM,_Y,LINE
LSEL, , , ,P51X
CM,_Y1,LINE
CMSEL,,_Y
!*
LESIZE,_Y1, , ,10, , , , ,1
!*
FLST,5,6,4,ORDE,6
FITEM,5,20
FITEM,5,-21
FITEM,5,41
FITEM,5,43
FITEM,5,66
FITEM,5,72
CM,_Y,LINE
LSEL, , , ,P51X
CM,_Y1,LINE
CMSEL,,_Y
!*
LESIZE,_Y1, , ,2, , , , ,1
!*
FLST,5,2,5,ORDE,2
FITEM,5,9
FITEM,5,-10
CM,_Y,AREA
ASEL, , , ,P51X
CM,_Y1,AREA
CHKMSH,'AREA'
CMSEL,S,_Y
!*
MSHKEY,1
AMESH,_Y1
MSHKEY,0
!*
CMDELE,_Y
```

```
CMDELE,_Y1
CMDELE,_Y2
!*
FLST,5,4,5,ORDE,2
FITEM,5,23
FITEM,5,-26
CM,_Y,AREA
ASEL, , , ,P51X
CM,_Y1,AREA
CHKMSH,'AREA'
CMSEL,S,_Y
!*
MSHKEY,1
AMESH,_Y1
MSHKEY,0
!*
CMDELE,_Y
CMDELE,_Y1
CMDELE,_Y2
!*

save
finish
```

Structural Integrity Associates, Inc.	File No.: VY-16Q-305
CALCULATION PACKAGE	**Project No.:** VY-16Q

PROJECT NAME:

Environmental Fatigue Analysis of VYNPS

CONTRACT NO.:

10150394

CLIENT:	**PLANT:**
Entergy Nuclear Operations, Inc.	Vermont Yankee Nuclear Power Station

CALCULATION TITLE:

Recirculation Outlet Stress History Development for Nozzle Green Function

Document Revision	Affected Pages	Revision Description	Project Manager Approval Signature & Date	Preparer(s) & Checker(s) Signatures & Date
0	1-29, Appendix: A1-A2	Initial Issue	Terry J. Herrmann 07/18/2007	Jennifer E. Smith 07/18/2007 Minghao Qin 07/18/2007

Table of Contents

1.0 OBJECTIVE 4
2.0 RECIRCULATION OUTLET NOZZLE MODEL 4
3.0 APPLIED LOADS 4
4.0 THERMAL AND PRESSURE LOAD RESULTS 7
5.0 REFERENCES 10
APPENDIX A FINITE ELEMENT ANALYSIS FILES A1

List of Tables

Table 1: Material Properties @ 300°F 11
Table 2: Pressure Results 11
Table 3: 0% Flow Regions 1 and 3 Heat Transfer Coefficients 12
Table 4: 0% Flow Region 5 Heat Transfer Coefficient 13

List of Figures

Figure 1: ANSYS Finite Element Model 14
Figure 2: Recirculation Outlet Nozzle Internal Pressure Distribution 15
Figure 3: Recirculation Outlet Nozzle Pressure Cap Load 16
Figure 4: Recirculation Outlet Nozzle Vessel Boundary Conditions 17
Figure 5: Nozzle and Vessel Wall Thermal and Heat Transfer Boundaries 18
Figure 6: Safe End Critical Thermal Stress Location 19
Figure 7: Safe End Limiting Linearized Stress Paths 20
Figure 8: Blend Radius Limiting Pressure Stress Location 21
Figure 9: Blend Radius Linearized Stress Path 22
Figure 10: Safe End 100% Flow Total Stress Intensity 23
Figure 11: Blend Radius 100% Flow Total Stress Intensity 23
Figure 12: Safe End Total Stress History for 100% Flow 24
Figure 13: Safe End Membrane Plus Bending Stress History for 100% Flow 24
Figure 14: Safe End Total Stress History for 50% Flow 25
Figure 15: Safe End Membrane Plus Bending Stress History for 50% Flow 25
Figure 16: Safe End Total Stress History for 0% Flow 26
Figure 17: Safe End Membrane Plus Bending Stress History for 0% Flow 26
Figure 18: Blend Radius Total Stress History for 100% Flow 27
Figure 19: Blend Radius Membrane Plus Bending Stress History for 100% Flow 27
Figure 20: Blend Radius Total Stress History for 50% Flow 28
Figure 21: Blend Radius Membrane Plus Bending Stress History for 50% Flow 28
Figure 22: Blend Radius Total Stress History for 0% Flow 29
Figure 23: Blend Radius Membrane Plus Bending Stress History for 0% Flow 29

1.0 OBJECTIVE

The objective of this calculation is to compute the pressure stresses, thermal stresses, and the Green's Functions for high (100%), mid (50%), and no (0%) flow thermal loading of the Vermont Yankee Nuclear Power Station recirculation outlet nozzle.

2.0 RECIRCULATION OUTLET NOZZLE MODEL

An axisymmetric finite element model of the recirculation outlet nozzle was developed in Reference [1] using ANSYS [2]. The geometry and model in Reference [1] is used in this calculation. The material properties are taken at an average temperature of 300°F. This average temperature is based on a thermal shock of 500°F to 100°F which will be applied to the FE model for Green's Function development. Table 1 listed the material properties at 300°F. The meshed model is shown in Figure 1.

3.0 APPLIED LOADS

Both pressure and thermal loads will be applied to the finite element model.

3.1 Pressure Load

A uniform pressure of 1000 psi was applied along the inside surface of the recirculation outlet nozzle and the vessel wall. A pressure load of 1000 psi was used because it is easily scaled up or down to account for different pressures that occur during transients. In addition, a cap load was applied to the piping at the end of the nozzle. This cap load was calculated as follows:

$$P_{cap} = P \cdot \frac{\left(D_i^{\,2}\right)}{\left(D_o^{\,2} - D_i^{\,2}\right)}$$

where:

P = Pressure = 1,000 psi
D_i = Inner Radius = 12.96875 in
D_o = Outer Radius = 14.18750 in
P_{cap} = Tension stress on the end of the nozzle. (psi)

Therefore, the cap load is 5081.7 psi. The calculated value was given a negative sign in order for it to exert tension on the end of the model. The ANSYS input file VY_RON_P.INP, in the computer files, applies the pressure loading to the geometry in file RON_VY.INP. Figures 2, 3, and 4 show the internal pressure distribution, cap load, and symmetry condition applied to the vessel end of the model, respectively.

3.2 Thermal Load

Thermal loads are applied to the recirculation outlet nozzle model. The heat transfer coefficients after power uprate were determined by scaling the values from Reference [4]. These values were determined for various regions of the finite element model and for 100% (28;294 GPM, converted from 12.3 Mlbm/hr [7]), 50% (14,147 GPM), and 0% (0 GPM) flow rates. The temperatures used are based upon a thermal shock from 500°F to 100°F. The calculated heat transfer coefficients for each region are shown below. The GPM values are calculated from the Mlbm/hr values at an average temperature of 300°F.

3.2.1 *Heat Transfer Coefficients*

The heat transfer coefficients for the 100% flow and 50% flow cases were calculated from Reference [4] as follows:

$$h_{Df} = h_{300}\left(\frac{f_{Df}}{25}\right)^{0.8}\left(\frac{26}{D_{Df}}\right)^{0.2}$$

Where:
h_{Df} = the heat transfer coefficient at a Diameter and flow rate
h_{300} = the heat transfer coefficient from Reference [4] at 300°F
f_{Df} = the flow rate corresponding to h_{Df} (ft/sec)
D_{Df} = the diameter corresponding to h_{Df} (in)

The heat transfer coefficients for 0% flow were calculated in spreadsheet Ht_coeffs.xls for natural convection and are shown in Tables 3 and 4.

As shown in Figure 5, the following heat transfer coefficients were applied:

<u>Region 1</u>

The heat transfer coefficient, h, for 100% flow is $4789\left(\frac{17.364}{25}\right)^{0.8} = 3577.8$ BTU/hr-ft^2-°F at 300°F. [4]

where 17.364 ft/sec is converted from 28,294 GPM and 25.8 in ID.

The heat transfer coefficient, h, for 50% flow is $4789\left(\frac{8.682}{25}\right)^{0.8} = 2054.9$ BTU/hr-ft^2-°F at 300°F. [4]

where 8.682 ft/sec is converted from 14,147 GPM and 25.8 in ID.

The heat transfer coefficient, h, for 0% flow is 112.34 BTU/hr-ft^2-°F at 300°F. [Table 3, for natural convection]

Region 2

The heat transfer coefficient for Region 2 is linearly transitioned from the value of the heat transfer coefficient used in Region 1 to the value used for Region 3.

Region 3 (the point between Region 2 and Region 4)

The heat transfer coefficient, h, for 100% flow is 4789 $\left(\frac{17.364}{25}\right)^{0.8} \cdot \left(\frac{26}{35.49}\right)^{0.2} = 3361$ BTU/hr-ft^2-°F at 300°F. [4]

where the flow rate is the same as that for Region 1, and the ID is 35.49 in.

The heat transfer coefficient, h, for 50% flow is 4789 $\left(\frac{8.682}{25}\right)^{0.8} \cdot \left(\frac{26}{35.49}\right)^{0.2} = 1930.9$ BTU/hr-ft^2-°F at 300°F. [4]

where the flow rate is the same as that for Region 1, and the ID is 35.49 in.

The heat transfer coefficient, h, for 0% flow is 112.34 BTU/hr-ft^2-°F at 300°F. using the same HTC as Region 1 [Table 3, for natural convection]

Region 4

Per Reference [1], the heat transfer coefficient for Region 4 (Nozzle Blend Radius) is linearly transitioned from the value of the heat transfer coefficient used in Region 3 to the value used in Region 5.

Region 5

The heat transfer coefficient, h, for 100% flow is 0.5 x 3577.8 = 1788.9 BTU/hr-ft^2-°F at 300°F. [4]

The heat transfer coefficient, h, for 50% flow is 0.5 x 2054.9 = 1027.4 BTU/hr-ft^2-°F at 300°F. [4]

The heat transfer coefficient, h, for 0% flow is 101 BTU/hr-ft^2-°F at 300°F. [Table 4, for natural convection] by using 40 in. hydraulic diameter [4].

Region 6

The heat transfer coefficient, h, is 0.4 BTU/hr-ft^2-°F [4].

3.2.2 *Boundary Fluid Temperatures*

For the Green's Functions, a 500°F to 100°F thermal shock is run to determine the stress response to a one-degree change in temperature. The following temperatures are valid when there is water flow. Values between defined points are linearly interpolated. For the 100%, 50%, and 0% flow cases, the thermal shock is run as follows:

Regions 1 to 5
T = 500°F – 100°F
Region 6
T = 120°F

4.0 THERMAL AND PRESSURE LOAD RESULTS

The three flow dependent thermal load cases outlined in Section 3.0 were run on the finite element model. Appendix A contains the thermal transient input files VY_RON_T_100.INP, VY_RON_T_50.INP, and VY_RON_T_0.INP for 100%, 50%, and 0% flow rates, respectively. The three flow dependent input files for the stress runs are also included in Appendix A. The stress filenames are VY_RON_S_100.INP, VY_RON_S_50.INP, and VY_RON_S_0.INP for 100%, 50%, and 0% flow rates, respectively.

The critical safe end location was chosen as node 6395, which has the highest stress intensity due to thermal loading under high flow conditions. As shown in Figures 6 and 7, Node 6395 is located on the inside diameter of the nozzle safe end of the model and the maximum stress occurs at 5.1 seconds.

The critical blend radius location was chosen, based upon the highest pressure stress. Assumed the cladding has cracked, therefore, as shown in Figures 8 and 9, the critical location is selected as node 3829 at base metal of the nozzle.

The stress intensity for use in the Green's functions are calculated from the component stresses (X, Y, and Z) and compared to the stress intensity reported by ANSYS. As seen in Figure 10, the Y-X calculated total stress intensity best matches the ANSYS reported stress intensity for 100% flow at the safe end. Therefore, the Y-X stress will be used for the total and membrane plus bending Green's functions for all flow rates for the safe end. As seen in Figure 11, the Z-X calculated total stress intensity best matches the ANSYS reported stress intensity for 100% flow at the blend radius in very beginning. Therefore, the Z-X stress will be used for the total and membrane plus bending Green's functions for all flow rates for the blend radius.

The stress time history for the critical paths was extracted during the stress run for 100% flow rate. This produced two files, HFSE.OUT and HFBR.OUT, which contain the thermal stress history. The membrane plus bending stresses and total stresses for the Green's Functions were extracted from these files to produce the files HFSE_Inside.RED and HFBR_Inside.RED, where SE and BR corresponded to the safe end and blend radius locations, respectively. The total stress intensity (SI) was extracted from these files to produce the files HFSE.CLD and HFBR.CLD, where SE and BR corresponded to the safe end and the blend radius, respectively.

The stress time history for the critical paths was extracted during the stress run for 50% flow rate. This produced two files, MFSE.OUT and MFBR.OUT which contains the thermal stress history. The membrane plus bending stresses and total stresses for the Green's Functions were extracted from the file to produce the file MFSE_Inside.RED, where SE corresponds to the safe end location.

The stress time history for the critical paths was extracted during the stress run for 0% flow rate. This produced two files, LFSE.OUT and LFBR.OUT which contain the thermal stress history. The membrane plus bending stresses and total stresses for the Green's Functions were extracted from the file to produce the file LFSE_Inside.RED, where SE corresponds to the safe end location.

The stress time history for the recirculation outlet nozzle during 100% flow, 50% flow, and 0% flow are shown in Figures 12 to 23. The data for the Green's Functions is included in the files HFBR_M+B-Green.xls, HFBR_T-Green.xls, HFSE_M+B-Green.xls, HFSE_T-Green.xls, MFBR_M+B-Green.xls, MFBR_T_Green.xls, MFSE_M+B-Green.xls, MFSE_T-Green.xls, LFBR_M+B-Green.xls, LFBR_T-Green.xls, LFSE_M+B-Green.xls, and LFSE_T-Green.xls in the project Files. Where HF, MF, and LF corresponded to 100% flow, 50% flow, and 0% flow rate, respectively. M+B and T corresponded to membrane plus bending stress and total stress, respectively.

The pressure stress intensities for the path were extracted during the pressure run. The pressure stresses were extracted along the nodal path as shown in Figures 7 and 9. This produced two files, PSE.OUT and PBR.OUT for the safe end and blend radius locations, respectively.

For the pressure loading specified (1000 psig), the total stress intensities at Node 6395 and Node 3829 were determined to be 11490 psi and 31300 psi, respectively. The membrane plus bending stress intensities at Node 6395 and Node 3829 were determined to be 11350 psi and 33640 psi, respectively. Table 2 shows the final pressure results.

Results were also extracted from the vessel portion of the model to verify the accuracy of the results obtained from the ANSYS model, and to check the results due to the use of the 2.0 multiplier on the vessel radius. These results are contained in the file PVESS.OUT. The radius of the finite element model (FEM) was multiplied by a factor of 2.0 [1] to account for the fact that the vessel portion of the 2D axisymmetric model is a sphere but the true geometry is the intersection of two cylinders.

The equation for the membrane hoop stress for a sphere is:

$$\sigma = \left(\frac{(pressure) \times (radius)}{2 \times thickness} \right)$$

Considering a vessel base metal radius, R, of 105.906 inches increased by a factor of 2.0, a vessel base metal thickness, t, of 5.4375 inches, and an applied pressure, P, of 1,000 psi, the calculated stress for a sphere is PR/(2t) = 19,477 psi. This compares very well with the remote vessel wall membrane hoop stress from the ANSYS result file, PVESS.OUT, of 19,540 psi. Thus, considering the peak total pressure stress of 31,300 psi reported above, the stress concentrating effect of the nozzle corner is 31,300/19,477 = 1.61. In other words, the peak nozzle corner stress is 1.61 times higher than nominal vessel wall stress for the 2D axisymmetric model.

The equation for the membrane hoop stress in a cylinder is:

$$\sigma = \left(\frac{(pressure) \times (radius)}{thickness} \right).$$

Based on the previous dimensions, the calculated stress for a cylinder without the 2.0 factor is 19,477 psi. Increasing this by a factor of 1.61 yields an expected peak nozzle corner stress of 31,358 psi, which would be expected from a cylindrical geometry that is representative of the nozzle configuration. Therefore, the result from the ANSYS file for the peak nozzle corner stress (31,300 psi) is close to the peak nozzle corner stress for a cylindrical geometry because of the use of the 2.0 multiplier. This is consistent with SI's experience where a factor of two increase in radius is typical for representing the three-dimensional (3D) effect in a 2D axisymmetric model.

5.0 REFERENCES

1. SI Calculation No. VY-16Q-304, Revision 0, "Recirculation Outlet Nozzle Finite Element Model"
2. ANSYS, Release 8.1 (w/Service Pack 1), ANSYS, Inc., June 2004.
3. American Society of Mechanical Engineers, Boiler and Pressure Vessel Code, Section II, Part D, 1998 Edition, 2000 Addenda.
4. CB&I, RPV Stress Report Section: T9 "Thermal Analysis Recirculation Outlet Nozzle Vermont Yankee Reactor Vessel." 9-6201, SI document, VY-16Q-204.
5. J. P. Holman, "Heat Transfer," 4th Edition, McGraw-Hill, 1976.
6. J. P. Holman, "Heat Transfer," 5th Edition, 1981.
7. Entergy Nuclear Northeast Engineering Report, Report No. VY-RPT-05-00022, "Task T0100 Reactor Heat Balance EPU Task Report for ER-04-1409," SI File No. VY-16Q-205.

Table 1: Material Properties @ 300°F[1]

Material	SA-533 Gr B (Mn-1/2Mo-1/2Ni)	SA-508 Cl 2 (3/4Ni-1/2Mo-1/3Cr-V)	SA-240 Type 304 (18Cr-8Ni)	SA-182 F316/ SA 376 TP316 (16Cr-12Ni-2Mo)
Modulus of Elasticity, e^{-6} psi	28.0	26.7	27.0	27.0
Coefficient of Thermal Expansion, e^{-6}, in/in/°F	7.7	7.3	9.8	9.8
Thermal Conductivity, Btu/hr-ft-°F	23.4	23.4	9.8	9.3
Thermal Diffusivity, ft^2/hr	0.401	0.401	0.160	0.150
Calculated Specific Heat, Btu/lb-°F [2]	0.119	0.119	0.125	0.127
Density, lb/in³	0.283	0.283	0.283	0.283
Poisson's Ratio	0.3	0.3	0.3	0.3

Notes: [1]The material properties applied in the analyses are taken from ASME Section II Part D 1998 Edition with 2000 Addenda. This is consistent with information provided in the Design Input Record (page 13 of VY EC No. 1773, SI File No. VY-16Q-209). The use of a later code edition than that used for the original design code is acceptable since later editions typically reflect more accurate material properties than was published in prior Code editions. Material Properties are evaluated at 300°F from the 1998 ASME Code, Section II, Part D, with 2000 Addenda, except for density and Poisson's ratio, which are assumed typical values.
[2] Calculated as $[k/(\rho d)]/12^3$.

Table 2: Pressure Results

Location	Membrane Plus Bending Stress Intensity (psi)	Total Stress Intensity (psi)
Safe End	11350	11490
Blend Radius	33640	31300

Table 3: 0% Flow Regions 1 and 3 Heat Transfer Coefficients

Pipe Inside Diameter, D =	25.800	inches =	2.150	ft				
		=	0.655	m				
Outer Pipe, Inside radius, r_o =	12.9	inches =	1.075	ft				
			0.328	m				
Inner Pipe Outside Diameter, D =	n/a	inches =	0.000	ft				
		=	0.000	m			0.000	
Inner Pipe, Outside radius, r_i =	0	inches =	0.000	ft				
			0.000	m				
Fluid Velocity, V =	17.364	ft/sec =	28293.595	gpm=		12.3 Mlb/hr		
Characteristic Length, L = D =	2.150	ft =	0.655	m				
(Outside) T_{fluid} - $T_{surface}$, ΔT =	8.40	12.00	24.00	36.00	48.00	60.00	72.00	°F
=	4.67	6.67	13.33	20.00	26.67	33.33	40.00	°C

		Value at Fluid Temperature, T [3]							Units
	Conversion	70	100	200	300	400	500	600	°F
Water Property	Factor [1]	21.11	37.78	93.33	148.89	204.44	260.00	315.56	°C
k	1.7307	0.5997	0.6300	0.6784	0.6836	0.6611	0.6040	0.5071	W/m-°C
(Thermal Conductivity)		0.3465	0.3640	0.3920	0.3950	0.3820	0.3490	0.2930	Btu/hr-ft-°F
c_p	4.1869	4.185	4.179	4.229	4.313	4.522	4.982	6.322	kJ/kg-°C
(Specific Heat)		1.000	0.998	1.010	1.030	1.080	1.190	1.510	Btu/lbm-°F
ρ	16.018	997.1	994.7	962.7	917.8	858.6	784.9	679.2	kg/m^3
(Density)		62.3	62.1	60.1	57.3	53.6	49.0	42.4	lbm/ft^3
β	1.8	1.89E-04	3.24E-04	6.66E-04	1.01E-03	1.40E-03	1.98E-03	3.15E-03	m^3/m^3-°C
(Volumetric Rate of Expansion)		1.05E-04	1.80E-04	3.70E-04	5.60E-04	7.80E-04	1.10E-03	1.75E-03	ft^3/ft^3-°F
g	0.3048	9.806	9.806	9.806	9.806	9.806	9.806	9.806	m/s^2
(Gravitational Constant)		32.17	32.17	32.17	32.17	32.17	32.17	32.17	ft/s^2
μ	1.4881	9.96E-04	6.82E-04	3.07E-04	1.93E-04	1.38E-04	1.04E-04	8.62E-05	kg/m-s
(Dynamic Viscosity)		6.69E-04	4.58E-04	2.06E-04	1.30E-04	9.30E-05	7.00E-05	5.79E-05	lbm/ft-s
Pr		6.980	4.510	1.910	1.220	0.950	0.859	1.070	---
(Prandtl Number)									
Calculated Parameter	**Formula**	**70**	**100**	**200**	**300**	**400**	**500**	**600**	**°F**
Reynold's Number, Re	$\rho VD/\mu$	3473691	5061789	10891437	16454670	21515912	26132199	27337904	---
Grashof Number, Gr	$g\beta\Delta TL^3/(\mu/\rho)^2$	2441754517	1.2697E+10	2.417E+11	1.252E+12	3.977E+12	1.034E+13	2.16049E+13	---
Grashof Number, Gr_δ	$g\beta\Delta T(r_o-r_i)^3/(\mu/\rho)^3$	3.05E+08	1.59E+09	3.02E+10	1.57E+11	4.97E+11	1.29E+12	2.70E+12	---
Rayleigh Number, Ra	GrPr	17043446531	5.7265E+10	4.616E+11	1.528E+12	3.778E+12	8.883E+12	2.31172E+13	---
Rayleigh Number, Ra	$Gr_\delta Pr$	2.13E+09	7.16E+09	5.77E+10	1.91E+11	4.72E+11	1.11E+12	2.89E+12	---
From [1]:									
Inside Surface Forced Convection Heat Transfer Coefficient:									
H_{forced}	$0.023Re^{0.8}Pr^{0.4}k/D$	7,823.02	9,326.34	13,148.12	15,405.24	16,705.40	17,126.15	16,275.32	W/m^2-°C
		1,377.74	1,642.50	2,315.56	2,713.07	2,942.05	3,016.15	2,866.31	$Btu/hr\text{-}ft^2$-°F
From [1]:									
Inside Surface Natural Convection Heat Transfer Coefficient:									
Case:	Enclosed cylinder		C =	0.55	n =	0.25			
H_{free}	$C(GrPr)^n k/L$	181.85	258.65	469.34	637.89	773.57	875.17	933.22	W/m^2-°C
		32.03	45.55	82.66	112.34	136.24	154.13	164.35	$Btu/hr\text{-}ft^2$-°F

Table 4: 0% Flow Region 5 Heat Transfer Coefficient

Heat Transfer Coefficients

References: 1. J. P. Holman, "Heat Transfer," 4th Edition, McGraw-Hill, 1976.
2. J. P. Holman, "Heat Transfer," 5th Edition, 1981.
3. N. P. Cheremisinoff, "Heat Transfer Pocket Handbook," Gulf Publishing Co., 1984.

(Required Inputs are Shaded!)

Title =	Piping							
Pipe Inside Diameter, D =	40.000	inches =	3.333	ft				
		=	1.016	m				
Outer Pipe, Inside radius, r_o =	20	inches =	1.667	ft				
			0.508	m				
Inner Pipe Outside Diameter, D =	n/a	inches =	0.000	ft				
		=	0.000	m			0.000	
Inner Pipe, Outside radius, r_i =	0	inches =	0.000	ft				
			0.000	m				
Fluid Velocity, V =	7.224	ft/sec =	28293.595	gpm=	12.3 Mlb/hr			
Characteristic Length, L = D =	3.333	ft =	1.016	m				
(Outside) T_{fluid} - $T_{surface}$, ΔT =	8.40	12.00	24.00	36.00	48.00	60.00	72.00	°F
=	4.67	6.67	13.33	20.00	26.67	33.33	40.00	°C

		Value at Fluid Temperature, T [3]							Units
	Conversion	70	100	200	300	400	500	600	°F
Water Property	Factor [1]	21.11	37.78	93.33	148.89	204.44	260.00	315.56	°C
k	1.7307	0.5997	0.6300	0.6784	0.6836	0.6611	0.6040	0.5071	W/m-°C
(Thermal Conductivity)		0.3465	0.3640	0.3920	0.3950	0.3820	0.3490	0.2930	Btu/hr-ft-°F
c_p	4.1869	4.185	4.179	4.229	4.313	4.522	4.982	6.322	kJ/kg-°C
(Specific Heat)		1.000	0.998	1.010	1.030	1.080	1.190	1.510	Btu/lbm-°F
ρ	16.018	997.1	994.7	962.7	917.8	858.6	784.9	679.2	kg/m^3
(Density)		62.3	62.1	60.1	57.3	53.6	49.0	42.4	lbm/ft^3
β	1.8	1.89E-04	3.24E-04	6.66E-04	1.01E-03	1.40E-03	1.98E-03	3.15E-03	m^3/m^3-°C
(Volumetric Rate of Expansion)		1.05E-04	1.80E-04	3.70E-04	5.60E-04	7.80E-04	1.10E-03	1.75E-03	ft^3/ft^3-°F
g	0.3048	9.806	9.806	9.806	9.806	9.806	9.806	9.806	m/s^2
(Gravitational Constant)		32.17	32.17	32.17	32.17	32.17	32.17	32.17	ft/s^2
μ	1.4881	9.96E-04	6.82E-04	3.07E-04	1.93E-04	1.38E-04	1.04E-04	8.62E-05	kg/m-s
(Dynamic Viscosity)		6.69E-04	4.58E-04	2.06E-04	1.30E-04	9.30E-05	7.00E-05	5.79E-05	lbm/ft-s
Pr		6.980	4.510	1.910	1.220	0.950	0.859	1.070	---
(Prandtl Number)									
Calculated Parameter	**Formula**	**70**	**100**	**200**	**300**	**400**	**500**	**600**	**°F**
Reynold's Number, Re	$\rho VD/\mu$	2240531	3264854	7024977	10613262	13877763	16855268	17632948	---
Grashof Number, Gr	$g\beta\Delta TL^3/(\mu/\rho)^2$	9099611606	4.732E+10	9.01E+11	4.667E+12	1.48E+13	3.85E+13	8.05143E+13	---
Grashof Number, Gr_δ	$g\beta\Delta T(r_o-r_i)^3/(\mu/\rho)^3$	1.14E+09	5.91E+09	1.13E+11	5.83E+11	1.85E+12	4.82E+12	1.01E+13	---
Rayleigh Number, Ra	GrPr	6.3515E+10	2.134E+11	1.72E+12	5.694E+12	1.41E+13	3.31E+13	8.61503E+13	---
Rayleigh Number, Ra	$Gr_\delta Pr$	7.94E+09	2.67E+10	2.15E+11	7.12E+11	1.76E+12	4.14E+12	1.08E+13	---
From [1]:									
Inside Surface Forced Convection Heat Transfer Coefficient:									
H_{forced}	$0.023Re^{0.8}Pr^{0.4}k/D$	3,552.89	4,235.64	5,971.33	6,996.42	7,586.90	7,777.99	7,391.58	W/m^2-°C
		625.71	745.95	1,051.63	1,232.17	1,336.16	1,369.81	1,301.76	$Btu/hr\text{-}ft^2$-°F
From [1]:									
Inside Surface Natural Convection Heat Transfer Coefficient:									
Case:	Enclosed cylinder		C =	0.55	n =	0.25			
H_{free}	$C(GrPr)^nk/L$	162.97	231.79	420.60	571.66	693.25	784.30	836.32	W/m^2-°C
		28.70	40.82	74.07	100.68	122.09	138.13	147.29	$Btu/hr\text{-}ft^2$-°F

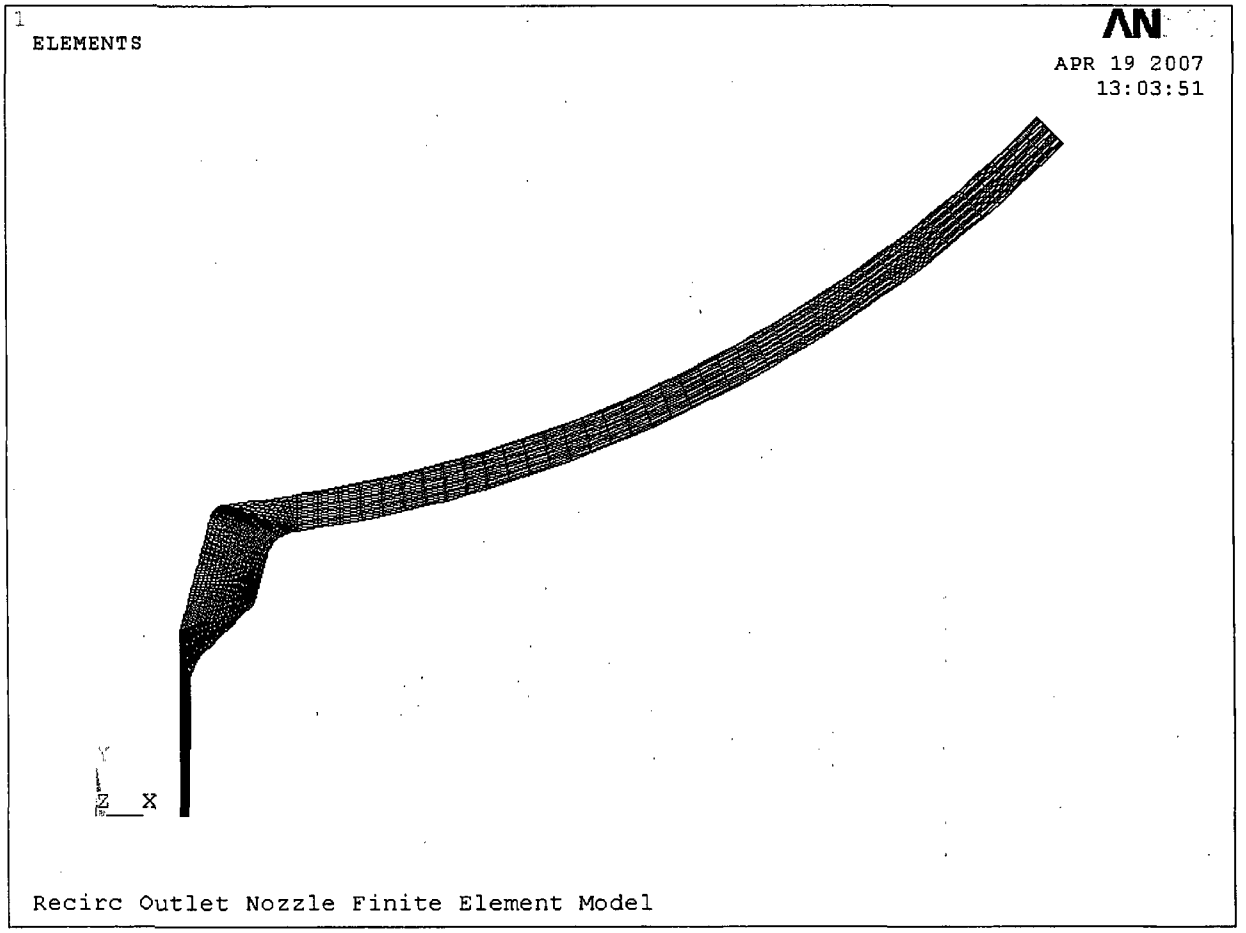

Figure 1: ANSYS Finite Element Model

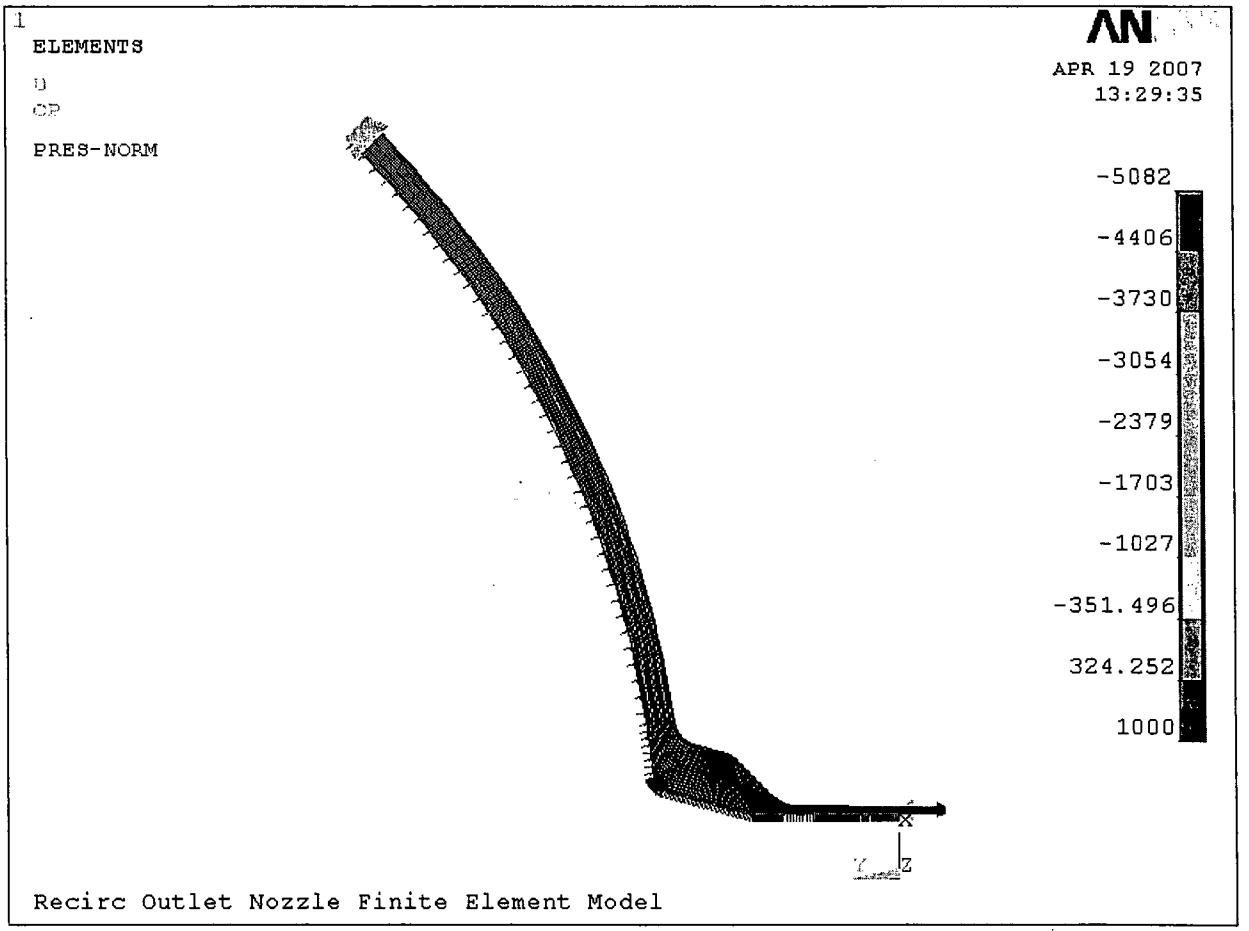

Figure 2: Recirculation Outlet Nozzle Internal Pressure Distribution

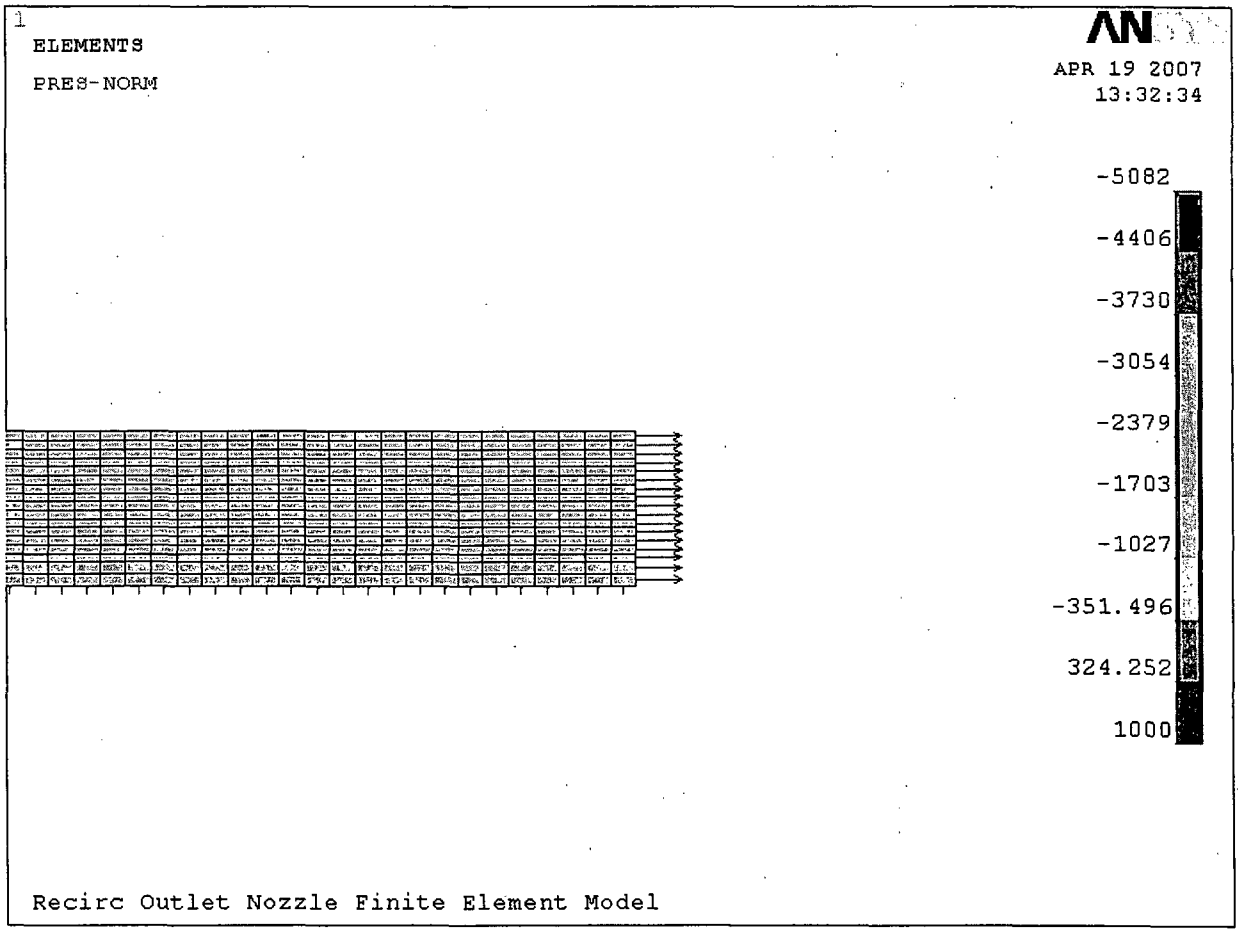

Figure 3: Recirculation Outlet Nozzle Pressure Cap Load

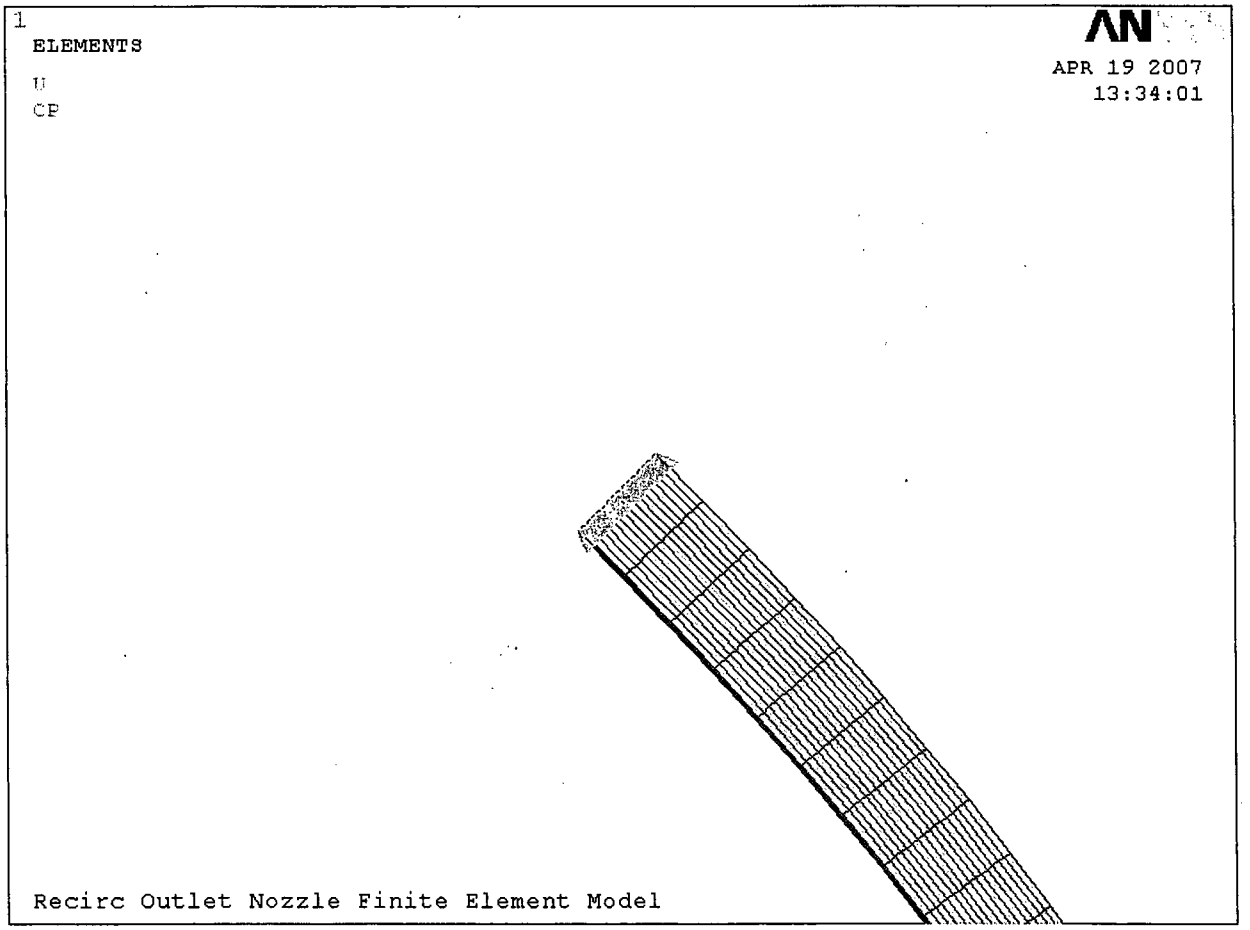

Figure 4: Recirculation Outlet Nozzle Vessel Boundary Conditions

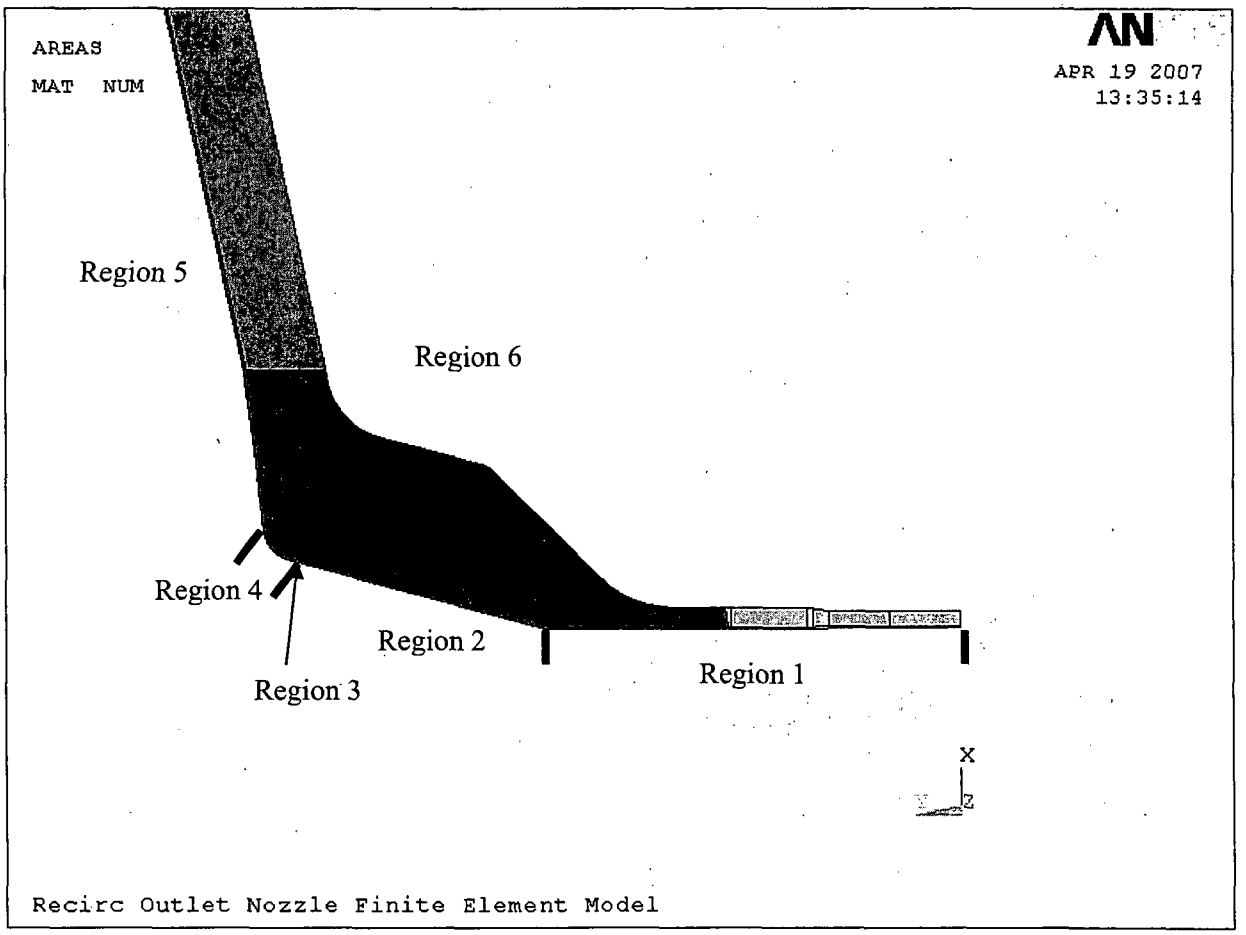

Figure 5: Nozzle and Vessel Wall Thermal and Heat Transfer Boundaries

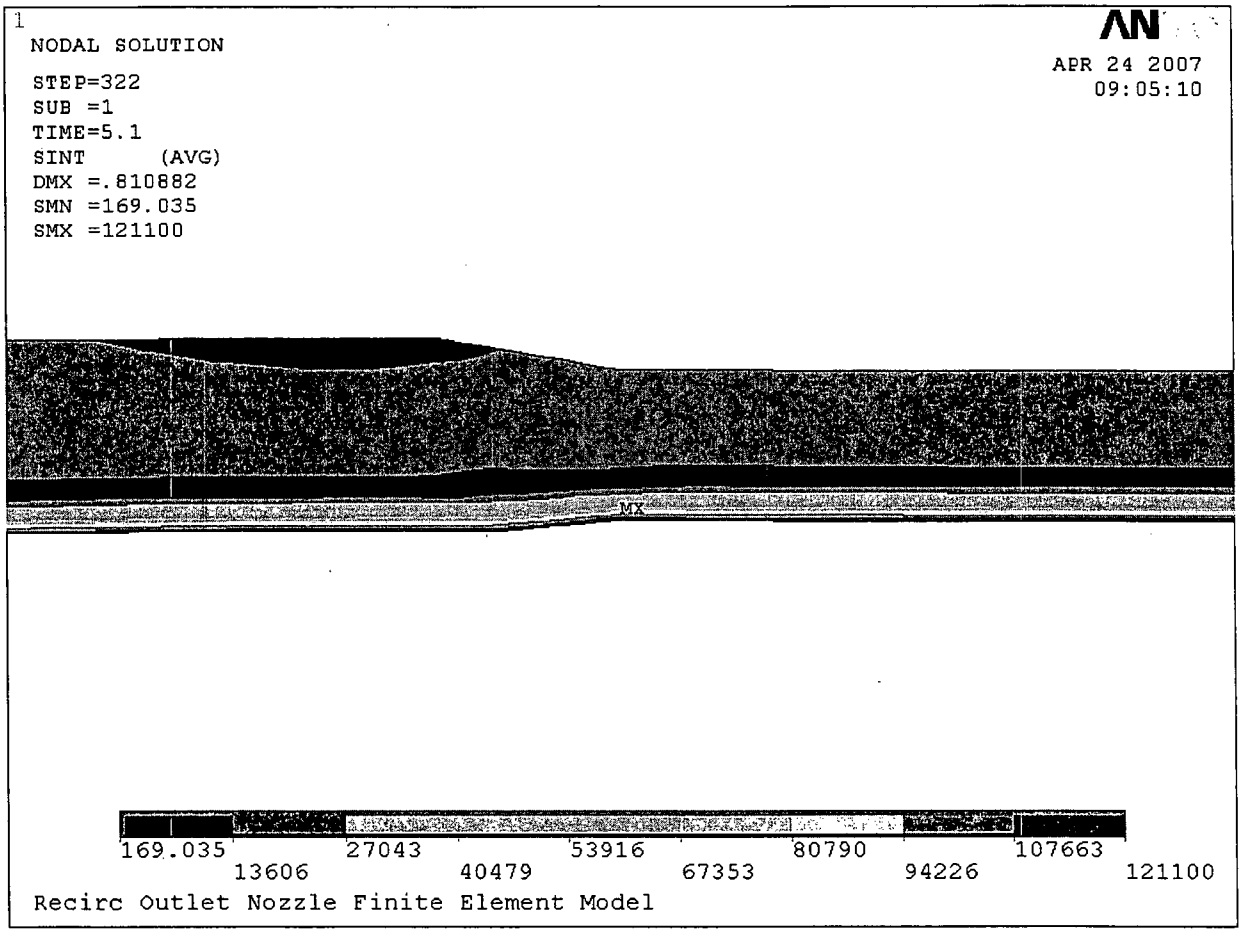

Figure 6: Safe End Critical Thermal Stress Location

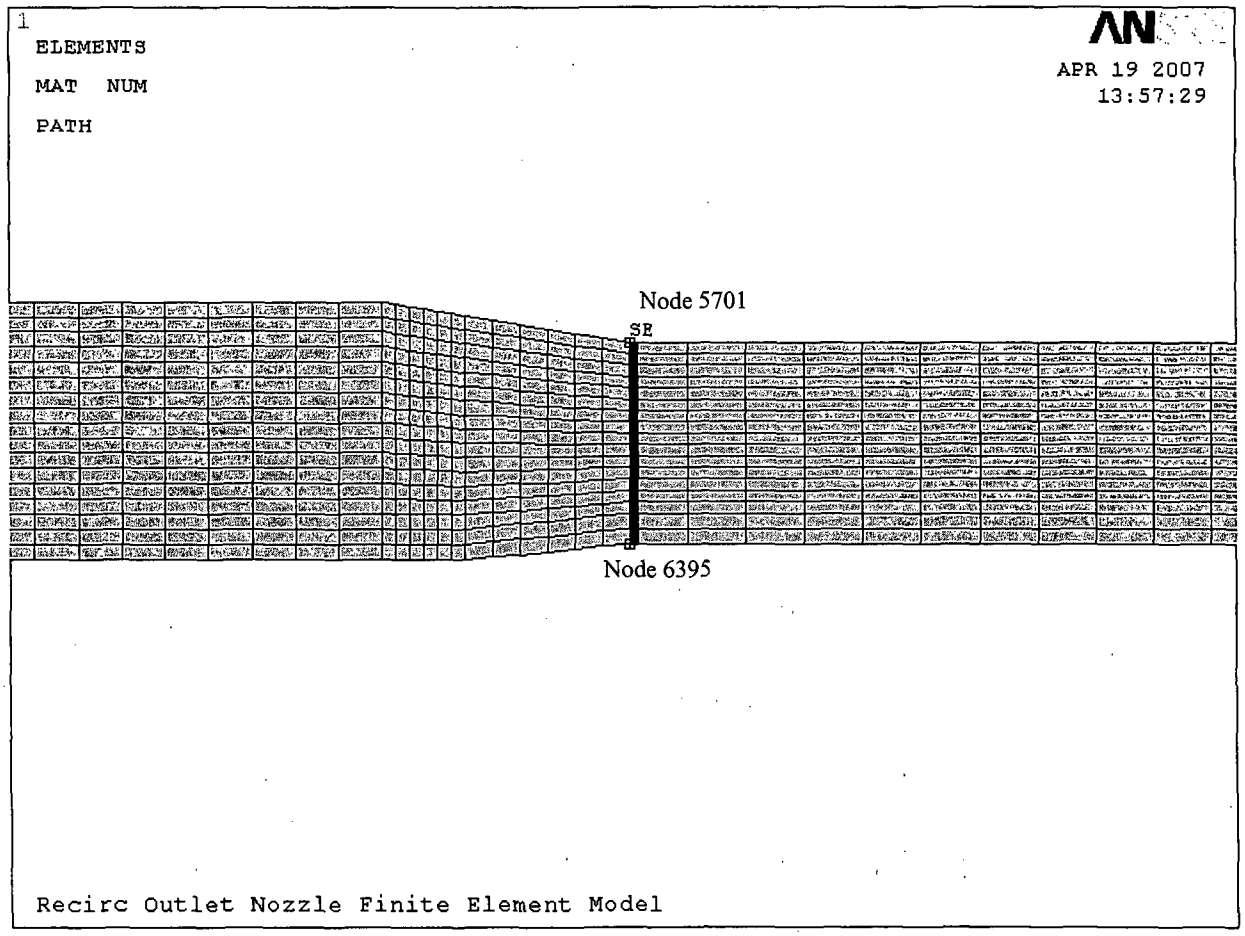

Figure 7: Safe End Limiting Linearized Stress Paths

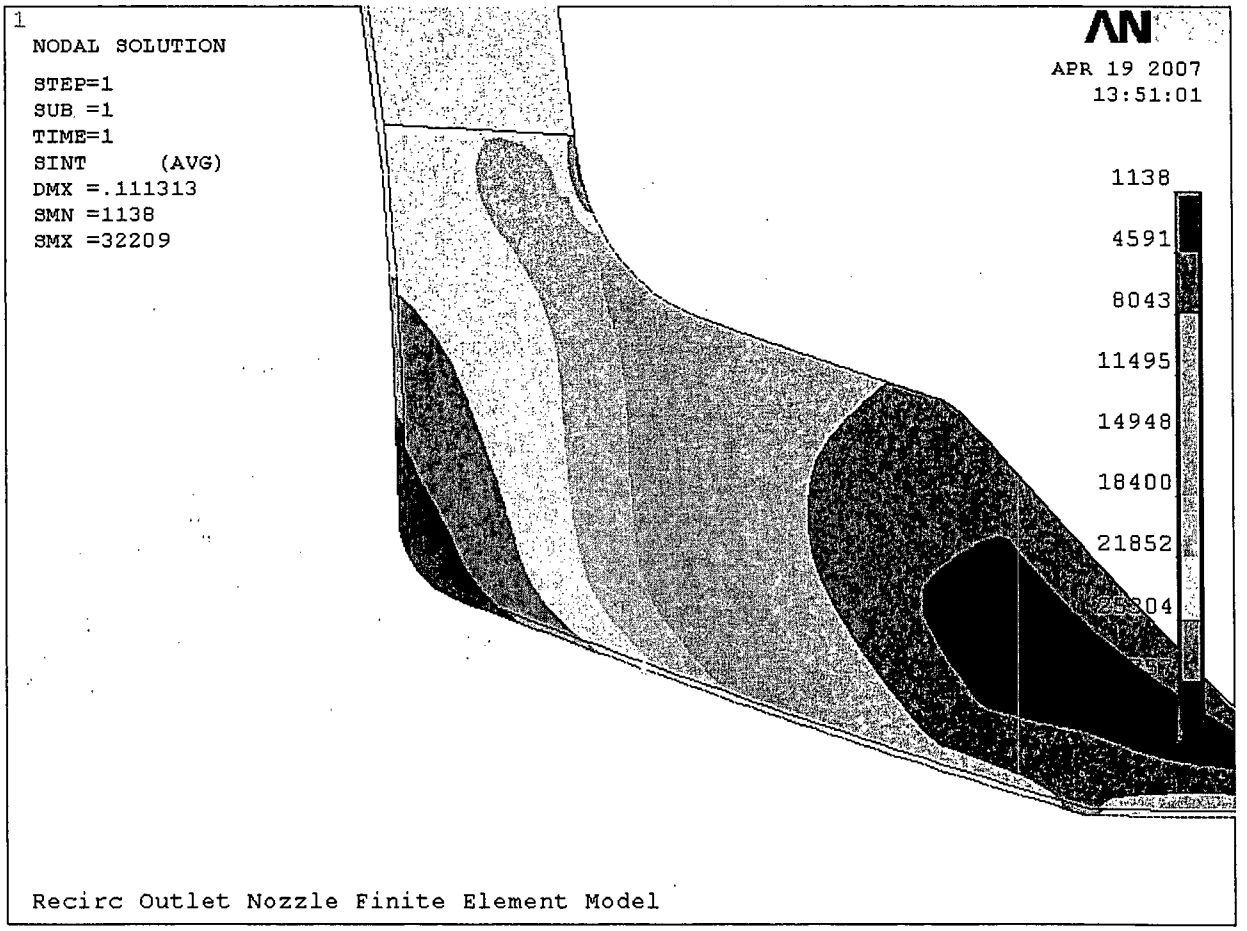

Figure 8: Blend Radius Limiting Pressure Stress Location

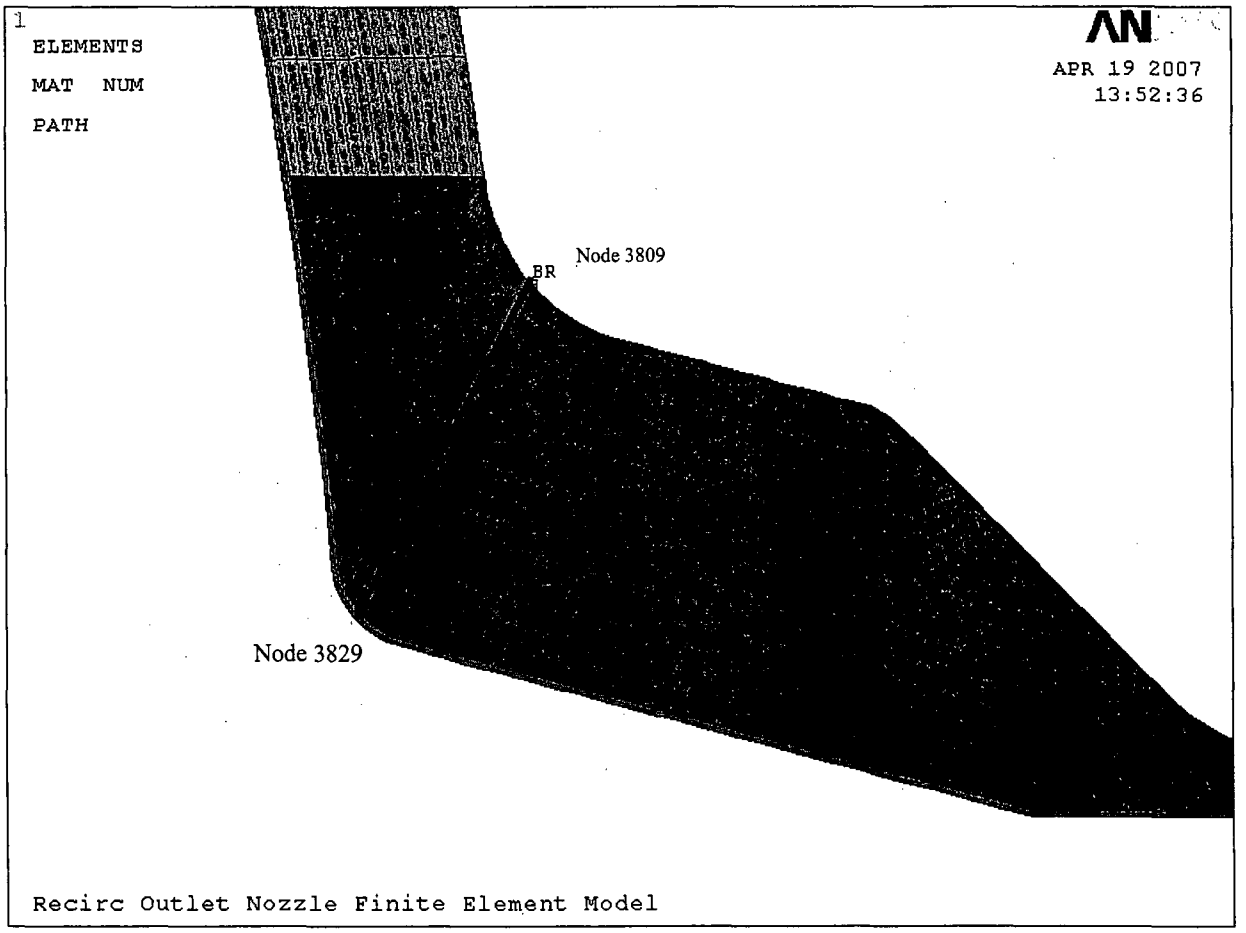

Figure 9: Blend Radius Linearized Stress Path

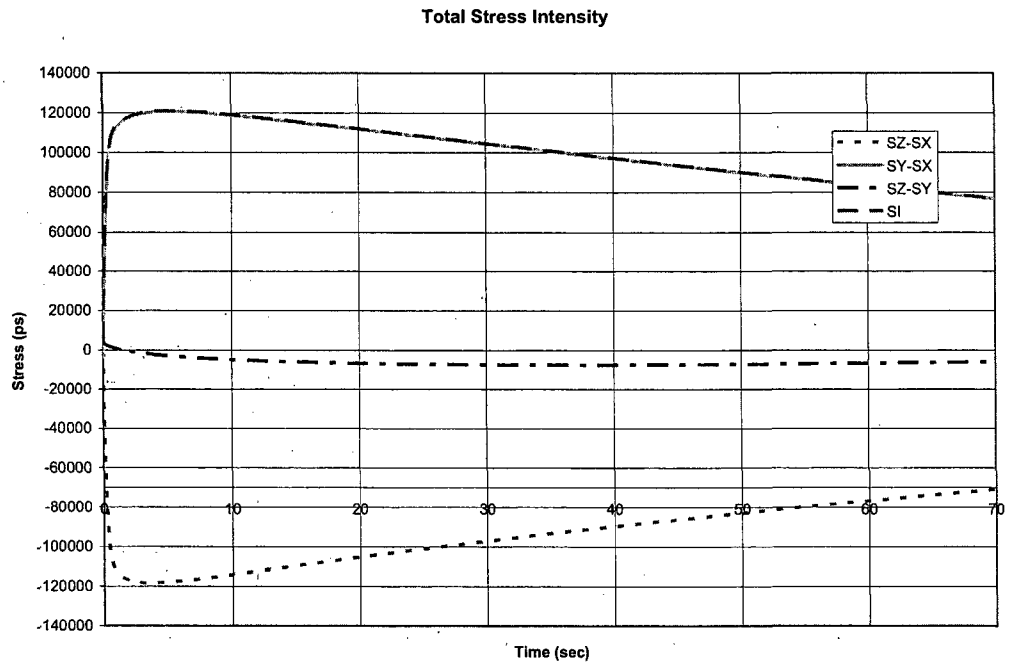

Figure 10: Safe End 100% Flow Total Stress Intensity

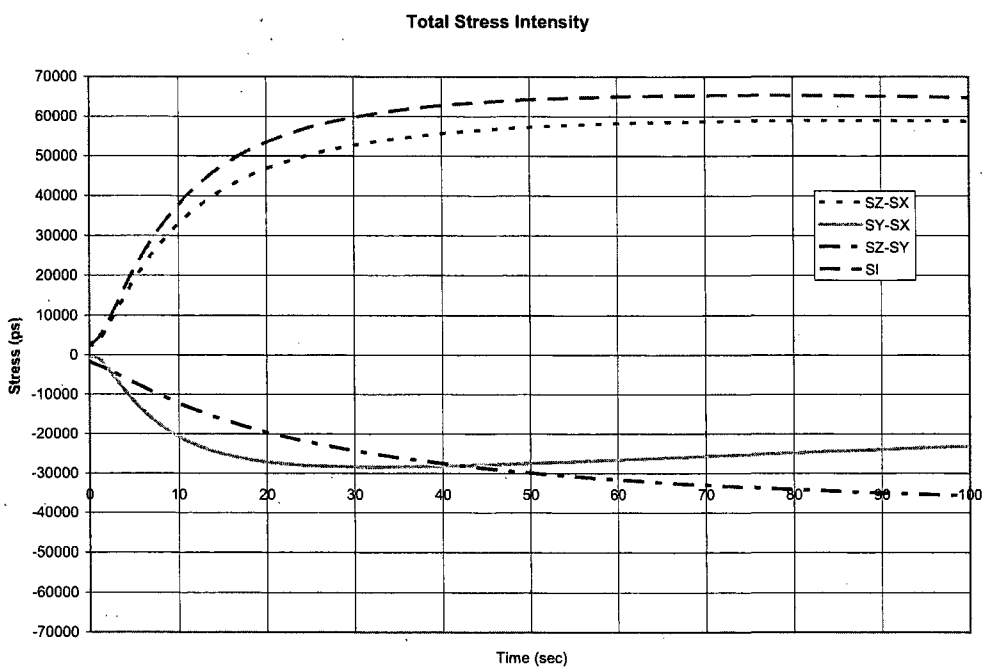

Figure 11: Blend Radius 100% Flow Total Stress Intensity

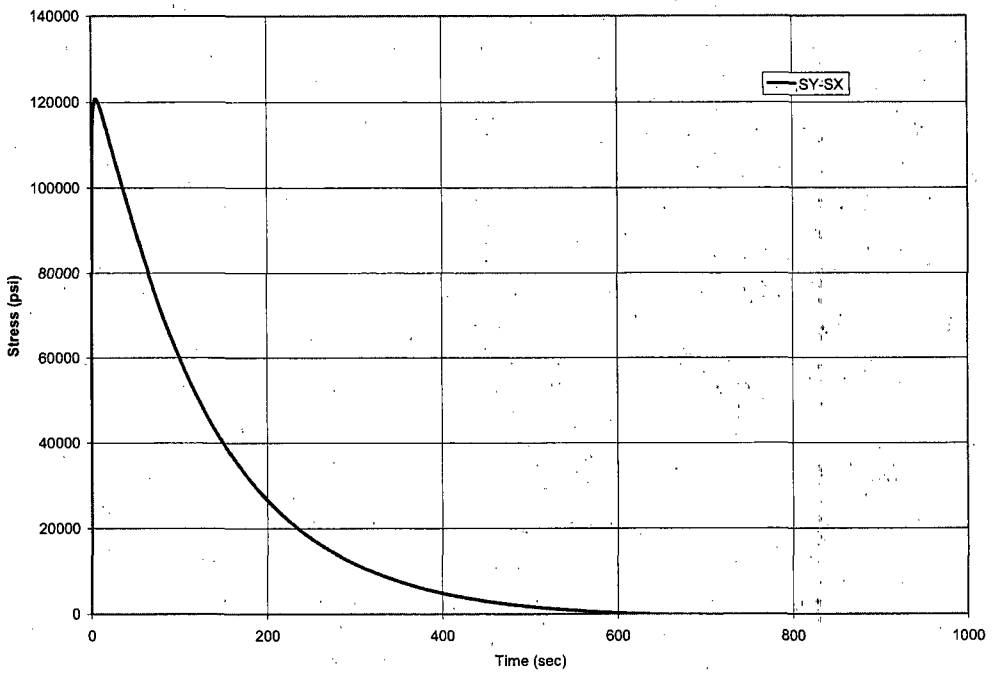

Figure 12: Safe End Total Stress History for 100% Flow

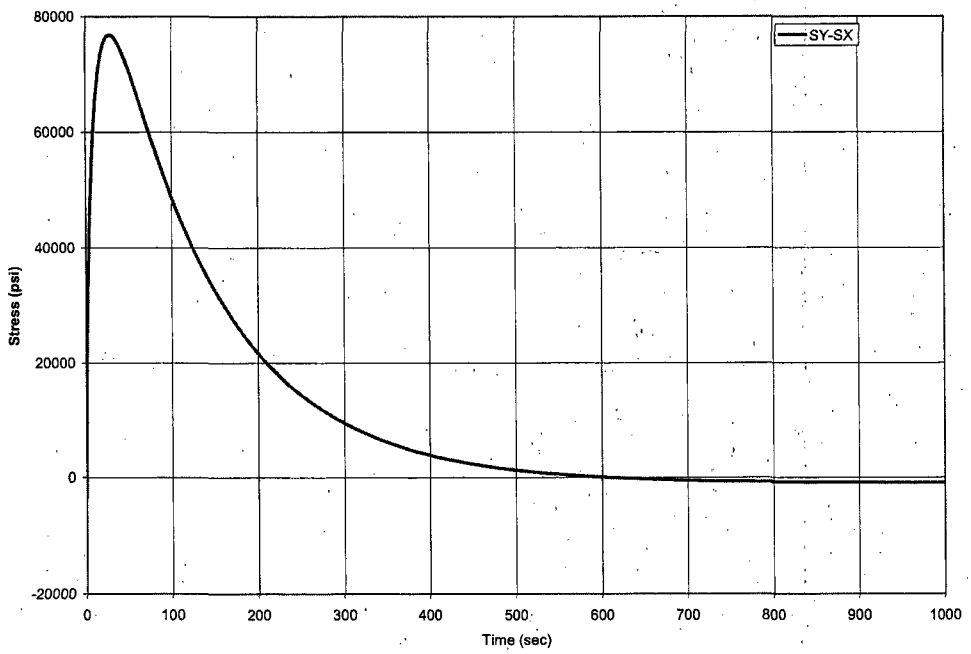

Figure 13: Safe End Membrane Plus Bending Stress History for 100% Flow

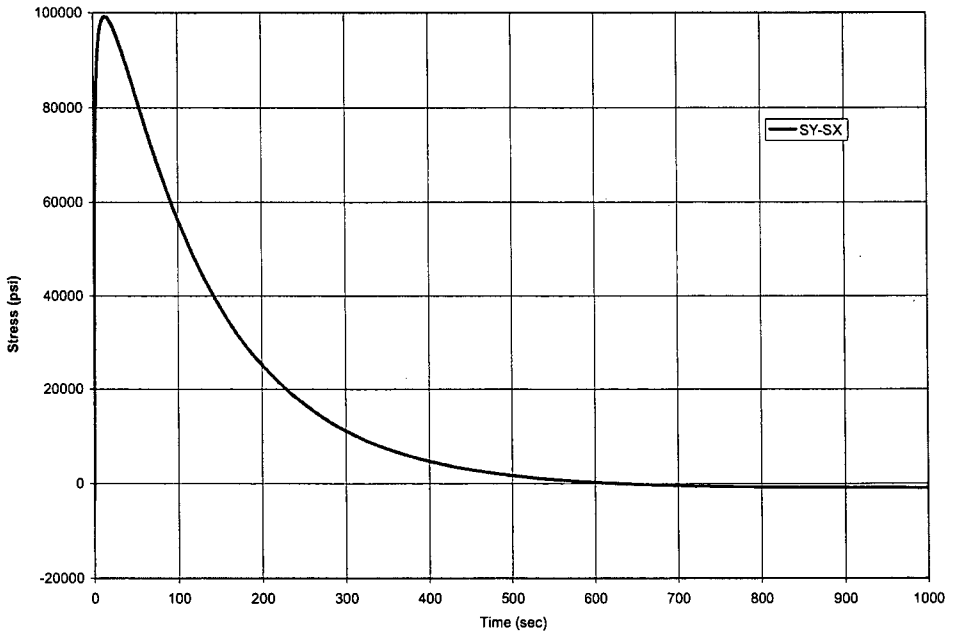

Figure 14: Safe End Total Stress History for 50% Flow

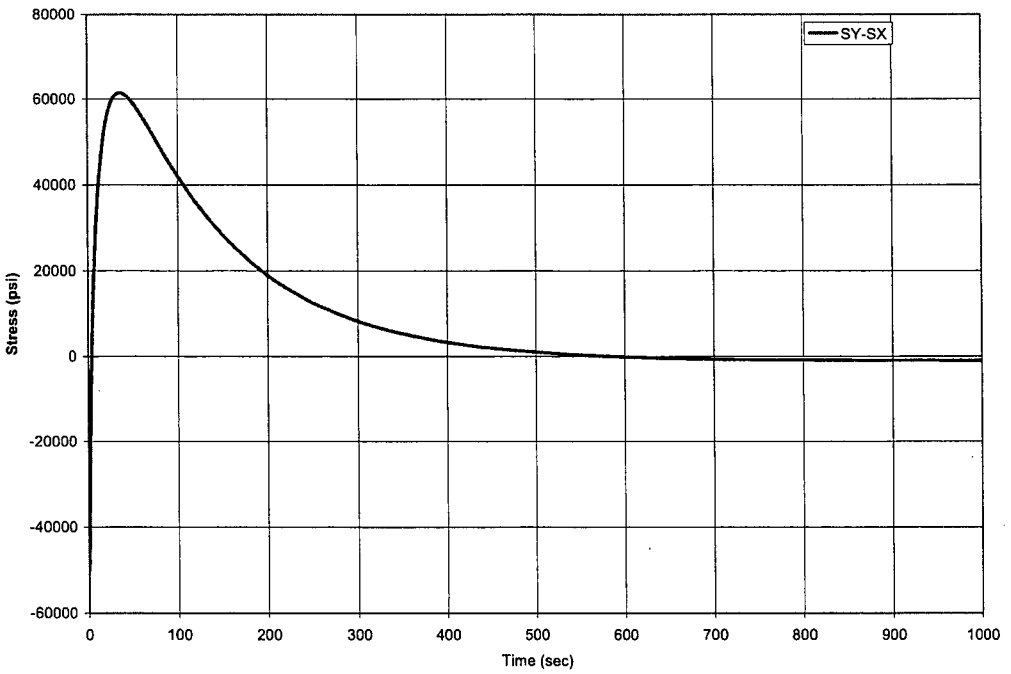

Figure 15: Safe End Membrane Plus Bending Stress History for 50% Flow

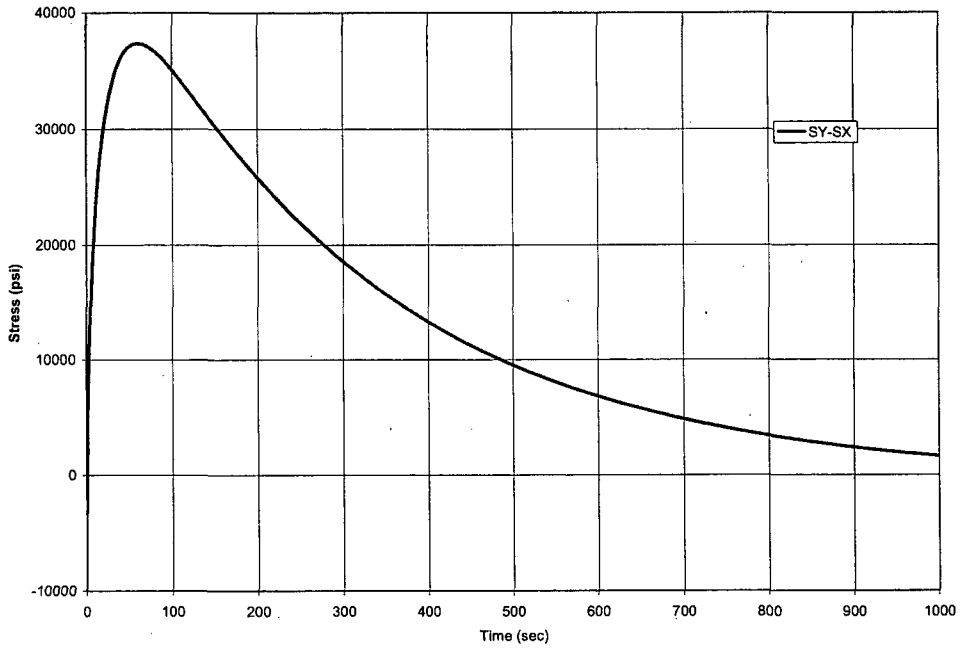

Figure 16: Safe End Total Stress History for 0% Flow

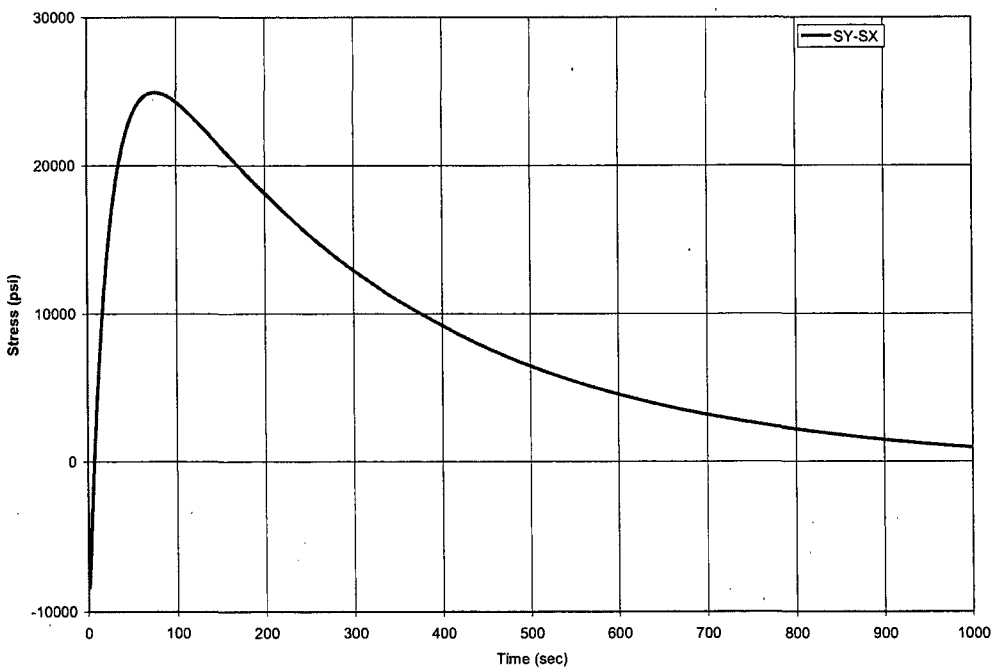

Figure 17: Safe End Membrane Plus Bending Stress History for 0% Flow

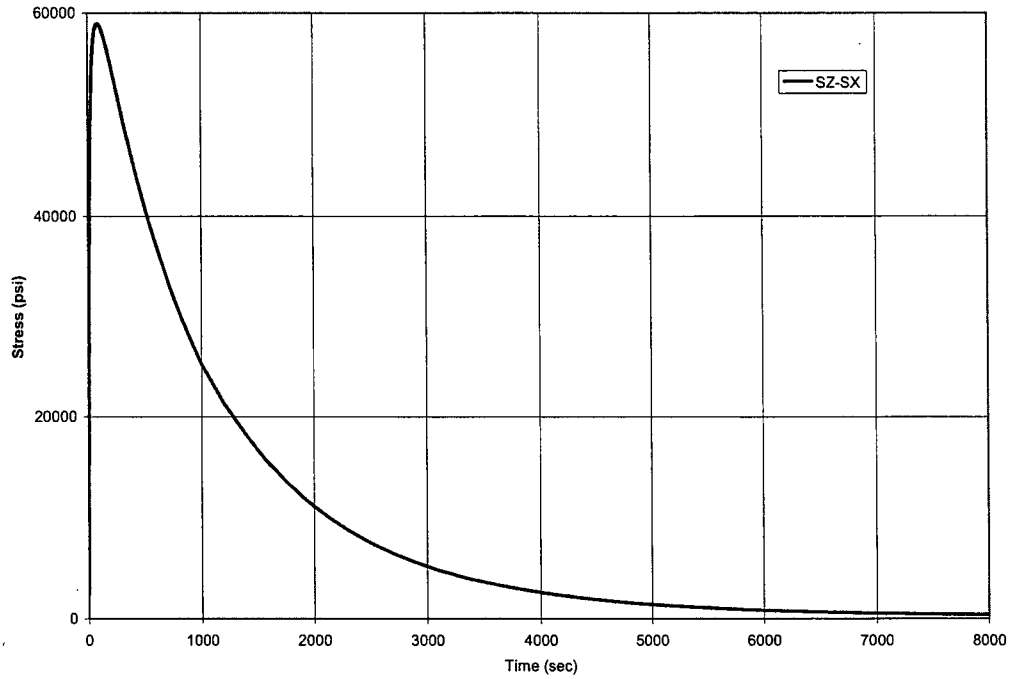

Figure 18: Blend Radius Total Stress History for 100% Flow

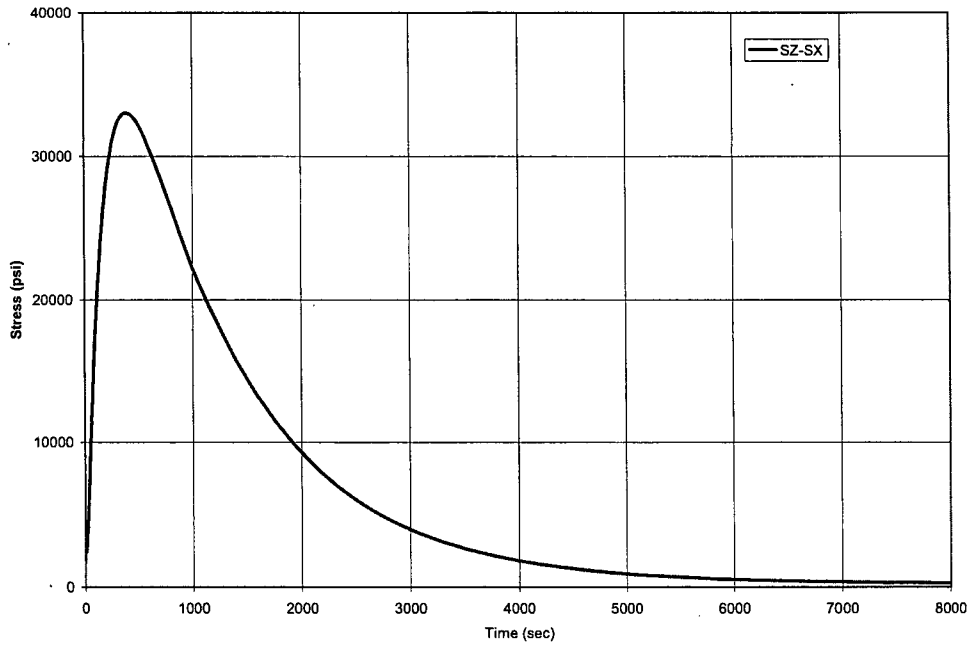

Figure 19: Blend Radius Membrane Plus Bending Stress History for 100% Flow

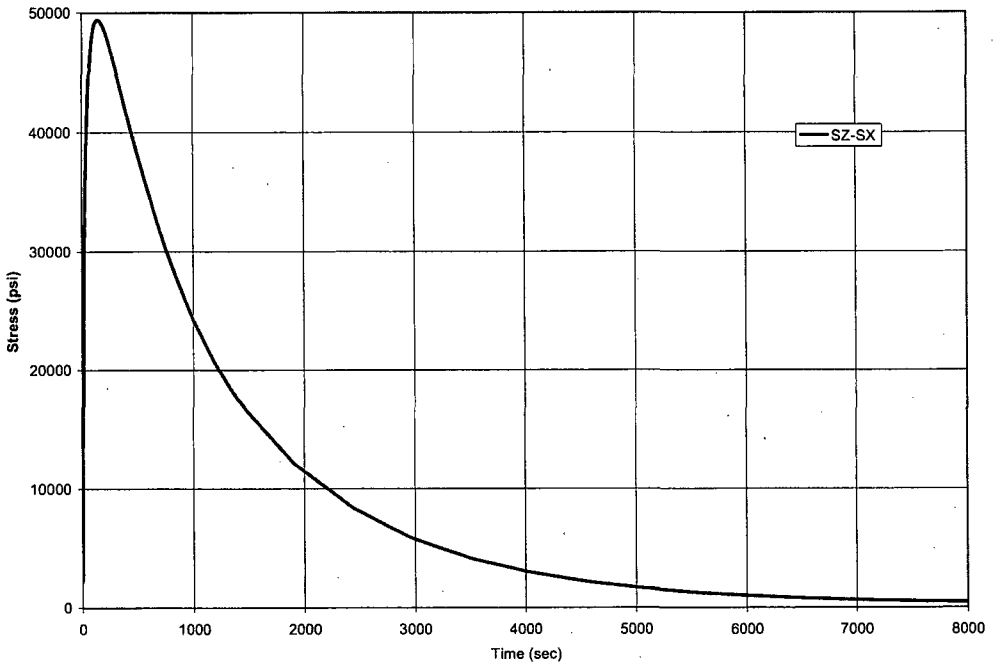

Figure 20: Blend Radius Total Stress History for 50% Flow

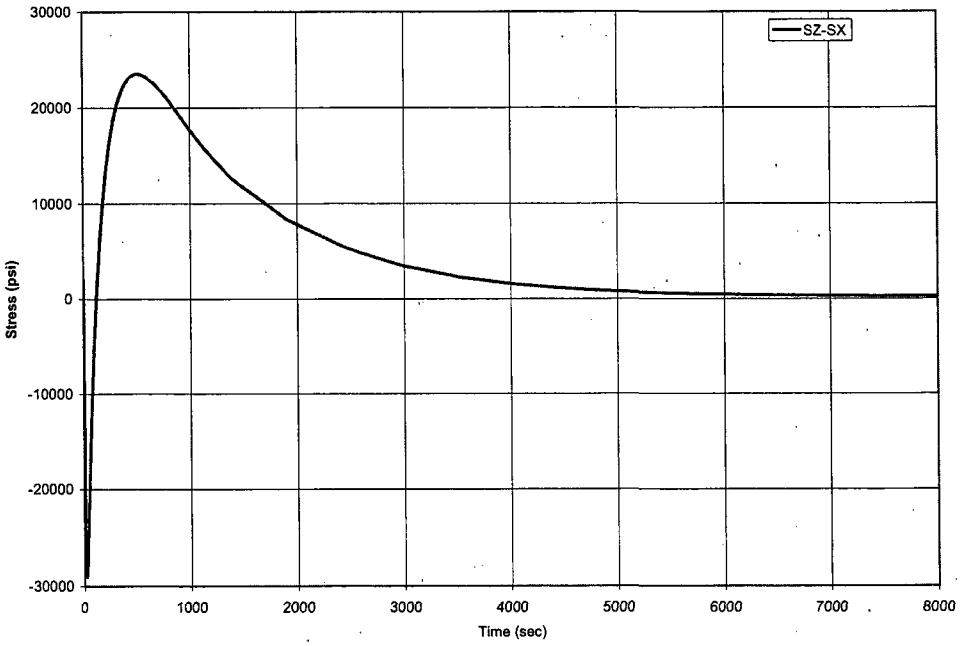

Figure 21: Blend Radius Membrane Plus Bending Stress History for 50% Flow

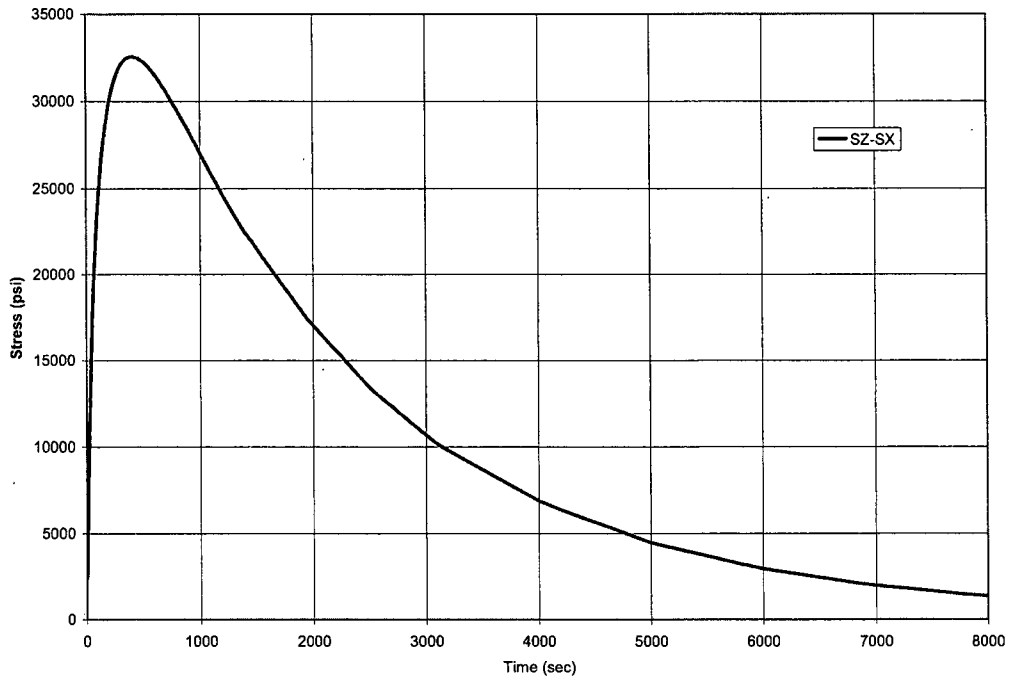

Figure 22: Blend Radius Total Stress History for 0% Flow

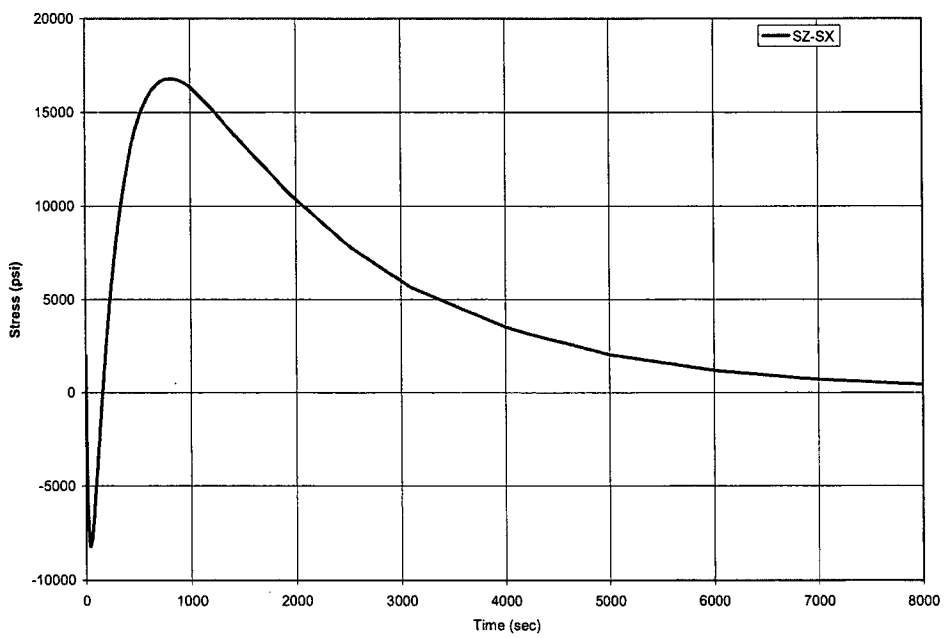

Figure 23: Blend Radius Membrane Plus Bending Stress History for 0% Flow

APPENDIX A

FINITE ELEMENT ANALYSIS FILES

RON_VY.INP	Input File for Pressure Load	In Computer files
VY_RON_T_100.INP	Input File for 100% Flow Thermal Analysis	In Computer files
VY_RON_S_100.INP	Input File for 100% Flow Stress Analysis	In Computer files
VY_RON_T_50.INP	Input File for 50% Flow Thermal Analysis	In Computer files
VY_RON_T_50.INP	Input File for 50% Flow Stress Analysis	In Computer files
VY_RON_0.INP	Input File for 0% Flow Thermal Analysis	In Computer files
VY_RON_0.INP	Input File for 0% Flow Stress Analysis	In Computer files
PVESS.OUT	Stress Output across the shell with Pressure Load	In Computer files
PSE.OUT	Stress Output at Safe End with Pressure Load	In Computer files
PBLEND.OUT	Stress Output at Blend Radius with Pressure Load	In Computer files
#FSE.OUT	Stress Output at Safe End	In Computer files
#FBR.OUT	Stress Output at Blend Radius	In Computer files
#FSE_INSIDE.RED	Stress Extracted at Safe End	In Computer files
#FBR_INSIDE.RED	Stress Extracted at Blend Radius	In Computer files
#FSE_T-Green.XLS	Green Function with Total Stress at Safe End	In Computer files
#FSE_M+B-Green.XLS	Green Function with Membrane plus Bending Stress at Safe End	In Computer files
HFBR_T-Green.XLS	Green Function with Total Stress at Blend Radius at 100% flow	In Computer files
HFBR_M+B-Green.XLS	Green Function with Membrane plus Bending Stress at Blend Radius at 100% flow	In Computer files

Where # is H, M, L meaning 100%, 50%, and 0% flow rate, respectively.

Structural Integrity Associates, Inc.	File No.: VY-16Q-306
CALCULATION PACKAGE	Project No.: VY-16Q

PROJECT NAME:

Environmental Fatigue Analysis of VYNPS

CONTRACT NO.:

10150394

CLIENT:	**PLANT:**
Entergy Nuclear Operations, Inc.	Vermont Yankee Nuclear Power Station

CALCULATION TITLE:

Fatigue Analysis of Recirculation Outlet Nozzle

Document Revision	Affected Pages	Revision Description	Project Manager Approval Signature & Date	Preparer(s) & Checker(s) Signatures & Date
0	1-34, Appendix: A1-A1	Initial Issue	Terry J. Herrmann 7/27/2007	J. E. Smith 7/27/2007 Minghao Qin 7/27/2007

Table of Contents

1.0 OBJECTIVE 4
2.0 METHODOLOGY 4
3.0 ANALYSIS 7
4.0 CALCULATION OF THERMAL STRESSES FOR TRANSIENT 9 11
5.0 FATIGUE USAGE RESULTS 14
6.0 ENVIRONMENTAL FATIGUE ANALYSIS 14
7.0 REFERENCES 15
APPENDIX A SUMMARY OF OUTPUT FILES A1

List of Tables

Table 1: Maximum Piping Stress Intensity Calculations 16
Table 2: Blend Radius Transients 17
Table 3: Safe End Transients 18
Table 4: Blend Radius Stress Summary 19
Table 5: Safe End Stress Summary 20
Table 6: Fatigue Results for Blend Radius (60 Years) 21
Table 7: Fatigue Results for Safe End (60 Years) 23
Table 8: Material Properties (For Transient 9) 25

List of Figures

Figure 1: External Forces and Moments on the Recirculation Outlet Nozzle 26
Figure 2: Nozzle and Vessel Wall Thermal and Heat Transfer Boundaries for Transient 9 27
Figure 3: Transient 1 – Normal Startup at 100°F/hr 28
Figure 4: Transient 2 – Turbine Roll and Increase to Rated Power 28
Figure 5: Transient 3 – Loss of Feedwater Heaters and Turbine Trip 25% Power 29
Figure 6: Transient 4 – Loss of Feedwater Pumps 29
Figure 7: Transient 5 – Turbine Generator Trip 30
Figure 8: Transient 6 – Reactor Overpressure 30
Figure 9: Transient 7 – SRV Blowdown 31
Figure 10: Transient 8 – SCRAM Other 31
Figure 11: Transient 9 – Improper Startup 32
Figure 12: Transient 10 – Shutdown 32
Figure 13: Typical Green's Functions for Thermal Transient Stress 33
Figure 14: Typical Stress Response Using Green's Functions 34

1.0 OBJECTIVE

The purpose of this calculation is to perform a revised fatigue analysis for the Entergy Vermont Yankee (VY) reactor pressure vessel (RPV) recirculation outlet nozzle. Two locations will be analyzed for fatigue acceptance: the safe end (SA182 F316) and the nozzle inner corner blend radius (SA508 Class 2). Both locations are chosen based on the highest overall stress of the analysis performed in Reference [1]. Fatigue usage will be determined for each location, the nozzle forging and safe end, respectively. An environmental fatigue usage factor will also be determined for each of these locations.

2.0 METHODOLOGY

In order to provide an overall approach and strategy for evaluating the recirculation outlet nozzle, the Green's Function methodology and associated ASME Code stress and fatigue analyses are described in this section.

Revised stress and fatigue analyses are being performed for the recirculation outlet nozzle using ASME Code, Section III methodology. These analyses are being performed to address license renewal requirements to evaluate environmental fatigue for this component in response to Generic Aging Lessons Learned (GALL) Report [14] requirements. The revised analysis is being performed to refine the fatigue usage so that an environmental fatigue factor can be determined for subsequent license renewal efforts.

Two sets of rules are available under ASME Code, Section III, Class 1 [13]. Subparagraph NB-3600 of Section III provides simplified rules for analysis of piping components, and NB-3200 allows for more detailed analysis of vessel components. The NB-3600 piping equations combine by absolute sum the stresses due to pressure, moments and through wall thermal gradient effects, regardless of where within the pipe cross-section the maximum value of the components of stress are located. By considering stress signs, affected surface (inside or outside) and azimuthal position, the stress ranges may be significantly reduced. In addition, NB-3600 assigns stress indices by which the stresses are multiplied to conservatively incorporate the effects of geometric discontinuities. In NB-3200, stress indices are not required, as the stresses are calculated by finite element analysis and consider applicable stress concentration factors. In addition, NB-3200 methodology accounts for the different locations within a component where stresses due to thermal, pressure or other mechanical loading are a maximum. This generally results in a net reduction of the stress ranges and consequently, in the calculated fatigue usage. Article 4 [17] methodology was originally used to evaluate the recirculation outlet nozzle. NB-3200 methodology, which is the modern day equivalent to Article 4, is used in this analysis to be consistent with the Section III design bases for this component, as well as to allow a more detailed analysis of this component. In addition, several of the conservatisms originally used in the original recirculation outlet nozzle evaluation (such as grouping of transients) are removed in the current evaluation so as to achieve a more accurate CUF.

For the recirculation outlet nozzle evaluated as a part of this work, stress histories will be computed by a time integration of the product of a pre-determined Green's Function and the transient data.

This Green's Function integration scheme is similar in concept to the Duhamel theory used in structural dynamics. A detailed derivation of this approach and examples of its application to specific plant locations is contained in Reference [15]. A general outline is provided in this section.

The steps involved in the evaluation are as follows:

- Develop finite element model
- Develop heat transfer coefficients and boundary conditions for the finite element model
- Develop Green's Functions
- Develop thermal transient definitions
- Perform stress analysis to determine stresses for thermal transients
- Perform fatigue analysis

A Green's Function is derived by using finite-element methods to determine the transient stress response of the component to a step change in loading (usually a thermal shock). The critical location in the component is identified based on the maximum stress, and the thermal stress response over time is extracted for this location. This response to the input thermal step is the "Green's Function." Figure 13 shows a typical set of two Green's Functions, each for a different set of heat transfer coefficients (representing different flow rate conditions).

To compute the thermal stress response for an arbitrary transient, the loading parameter (usually local fluid temperature) is deconstructed into a series of step-loadings. By using the Green's Function, the response to each step can be quickly determined. By the principle of superposition, these can be added (algebraically) to determine the response to the original load history. The result is demonstrated in Figure 14. The input transient temperature history contains five step-changes of varying size, as shown in Figure 14. These five step changes produce the five successive stress responses in the second plot shown in Figure 14. By adding all five response curves, the real-time stress response for the input thermal transient is computed.

The Green's Function methodology produces identical results compared to running the input transient through the finite element model. The advantage of using Green's Functions is that many individual transients can be run with a significant reduction of effort compared to running all transients through the finite element model. The trade-off in this process is that the Green's Functions are based on constant material properties and heat transfer coefficients. Therefore, these parameters are chosen to bound all transients that constitute the majority of fatigue usage, i.e., the heat transfer coefficients at 300°F bound the cold water injection transient. In addition, the instantaneous value for the coefficient of thermal expansion is used instead of the mean value for the coefficient of thermal expansion. This conservatism is more than offset by the benefit of not having to analyze every transient, which was done in the VY reactor recirculation outlet nozzle evaluation.

Once the stress history is obtained for all transients using the Green's Function approach, the remainder of the fatigue analysis is carried out using traditional methodologies in accordance with ASME Code, Section III requirements.

Fatigue calculations are performed in accordance with ASME Code, Section III, Subsection NB-3200 methodology. Fatigue analysis is performed for the two limiting locations (one in the safe end and one in the nozzle forging, representing the two materials of the nozzle assembly) using the Green's Functions developed for these three Recirculation flow conditions and 60-year projected cycle counts.

Three Structural Integrity utility computer programs are used to facilitate the fatigue analysis process: STRESS.EXE, P V.EXE, and FATIGUE.EXE. The first program, STRESS.EXE, calculates a stress history in response to a thermal transient using a Green's Function. The second program, P-V.EXE, reduces the stress history to peaks and valleys, as required by ASME Code fatigue evaluation methods. The third program, FATIGUE.EXE, calculates fatigue from the reduced peak and valley history using ASME Code, Section III range-pair methodology. All three programs are explained in detail and have been independently verified for generic use in the Reference [5] calculation.

In order to perform the fatigue analysis, Green's Functions are developed using the finite element model. Then, input files with the necessary data are prepared and the three utility computer programs are run. The first program (STRESS.EXE) requires the following three input files:

- Input file "GREEN.DAT": This file contains the Green's Function for the location being evaluated. For each flow condition, two Green's Functions are determined: a membrane plus bending stress intensity Green's Function and a total stress intensity Green's Function. This allows computation of total stress, as well as membrane plus bending stress, which is necessary to compute K_e per ASME Code, Section III requirements.
- Input file "GREEN.CFG": This file is a configuration file containing parameters that define the Green's Function (i.e., number of points, temperature drop analyzed, etc.).
- Input file "TRANSNT.INP": This file contains the input transient history for all thermal transients to be analyzed for the location being evaluated.

Pressure and piping stress intensities are also included for each transient case, based on pressure stress results from finite element analysis and attached piping load calculations.
The second program (P-V.EXE) simply extracts only the maxima and minima stress (i.e., the peaks and valleys) from the stress histories generated by program STRESS.EXE.

The third program (FATIGUE.EXE) performs the ASME Code peak event-pairing required to calculate a fatigue usage value. The input data consists of the output peak and valley history from program P-V.EXE and a configuration input file that provides ASME Code configuration data relevant to the fatigue analysis (i.e., K_e parameters, S_m, Young's modulus, etc.). The output is the final fatigue calculation for the location being evaluated.

The Green's Function methodology described above uses standard industry stress and fatigue analysis practices, and is the same as the methodology used in typical stress reports. Special approval for the use of this methodology is therefore not required.

The 10 transients to be analyzed are described in Reference [2], for the recirculation outlet nozzle. Transients 11 and 12 are hydrostatic tests that have only a small temperature change and are not

modeled. Transients 1 to 10 are shown in Figures 3 – 12. The analysis of transient 9 is an exception to this process because there are two different thermal shocks at the nozzle and vessel regions. Transient 9 is analyzed separately using ANSYS instead of STRESS.EXE and P-V.EXE. The results from ANSYS are input directly into FATIGUE.EXE with the other transient stress results.

3.0 ANALYSIS

The fatigue analysis involves preparing the input files and running the three programs. The programs STRESS.EXE and P-V.EXE are run together through the use of a batch file. The program FATIGUE.EXE is run after processing the output from P-V.EXE. The ANSYS results from transient 9 are added to the P-V.EXE results for the other transients and input into FATIGUE.EXE.

The steps associated with this process are described in the following sub-sections.

3.1 Transient Definitions (for program STRESS.EXE)

The program STRESS.EXE requires the following three input files for analyzing an individual transient:

- GREEN.DAT. There are 12 stress history functions (Green's Functions) obtained from Reference [1]. They represent the membrane plus bending and total stress intensities at the blend radius and safe end locations. The blend radius and the safe end have three stress history functions for the 100% flow, 50%, and no-flow conditions.
- GREEN.CFG is configured as described in Reference [5].
- Several TRANSNT.INP files are created to simulate the transients shown on Reference [2]. Tables 2 and 3 show the thermal history used to simulate each transient for the blend radius and safe end locations, respectively. The aforementioned transient information for each location is contained in EXCEL files *Blend_Radius_Transients.xls* and *Safe_End_Transients.xls,* which are contained in the computer files. Transients are split into the following groups based upon flow rate:
    - Transients 2, 3, 5, 6, 7, and 8 are run at 100% flow Green's Function
    - Transients 1 and 10 are run at 50% flow Green's Function
    - Transient 4 is run at no flow, 50% flow, and 100% flow Green's Functions, as shown in Tables 2 and 3.
    - Transient 9 is simulated by ANSYS [11] model and the thermal results are taken from ANSYS directly. See Section 4 for details.
    - Transients 11 and 12 have only small temperature change (70°F to 100°F). Therefore, the thermal stresses for these two transient are ignored. Only the piping load and the pressure load are considered in these two transients.
    - The loss of feedwater heaters (Feedwater Heater Bypass) event has a negligible temperature change (526 °F to 516 °F) associated with it. Therefore this transient is ignored.

3.2 Peak and Valley Points of the Stress History (for program P-V.EXE)

After STRESS.EXE runs are completed, the program P-V.EXE is run to extract only the peaks and valleys from the STRESS.OUT stress history file produced by the STRESS.EXE program. The only input required for this program is the stress history file (STRESS.OUT), and the program outputs all of the resulting peaks and valleys to output file P-V.OUT. The resulting peak and valley stress summaries for all transients are summarized in Tables 4 and 5 for both locations. Columns 2 through 5 of Tables 4 (for the blend radius) and 5 (for the safe end) show the final peak and valley output. These final peaks and valleys were selected from the total stress and membrane plus bending stress intensities that were calculated by STRESS.EXE and screened with P-V.EXE.

3.3 Pressure Load

The pressure stress associated with a 1,000 psi internal pressure was determined in Reference [1]. These values are as follows:

Pressure stress for the safe end:

- 11,350 psi membrane plus bending linearized stress intensity.
- 11,490 psi total stress intensity.

Pressure stress for the blend radius:

- 33,640 psi membrane plus bending linearized stress intensity.
- 31,300 psi total stress intensity.

The pressure stress intensity values for each transient were linearly scaled based on the pressure. The actual pressure for column 6 of Tables 4 and 5 is obtained from Tables 2 and 3, respectively. The scaled pressure stress values are shown in columns 7 and 8 of Tables 4 and 5.

The pressure stress is combined with the peak and valley points to calculate the final stress values used for fatigue analysis.

3.4 Attached Piping Loads

Additionally, the piping stress intensity (stress caused by the attached piping) was determined. These piping forces and moments are determined as shown in Figure 1.

The following formulas are used to determine the maximum stress intensity in the nozzle at the two locations of interest. From engineering statics, the piping loads at the end of the model can be translated to the first and second cut locations using the following equations:

For Cut I:

$$(M_x)_1 = M_x - F_y L_1$$
$$(M_y)_1 = M_y + F_x L_1$$

For Cut II:
$$(M_x)_2 = M_x - F_y L_2$$
$$(M_y)_2 = M_y + F_x L_2$$

The total bending moment and shear loads are obtained using the equations below:

For Cut I:
$$M_{xy} = \sqrt{(M_x)_1^2 + (M_y)_1^2}$$
$$F_{xy} = \sqrt{(F_x)_1^2 + (F_y)_1^2}$$

For Cut II:
$$M_{xy} = \sqrt{(M_x)_2^2 + (M_y)_2^2}$$
$$F_{xy} = \sqrt{(F_x)_2^2 + (F_y)_2^2}$$

The distributed loads for a thin-walled cylinder are obtained using the equations below:

$$N_z = \frac{1}{\pi R_N}\left[\frac{1}{2}F_z + \frac{M_{xy}}{R_N}\right]$$
$$q_N = \frac{1}{\pi R_N}\left[F_{xy} - \frac{M_z}{2R_N}\right]$$

To determine the primary stresses, P_M, due to internal pressure and piping loads, the following equations are used.

For Cut I, using thin-walled equations:

$$(P_M)_z = \frac{Pa_N}{2t_N} + \frac{Nz}{t_N}$$
$$(P_M)_\theta = \frac{Pa_N}{t_N}$$
$$(P_M)_R = -P$$
$$\tau_M = \frac{q_N}{t_N}$$
$$SI_{MAX} = 2\sqrt{\left(\frac{(P_M)_\theta - (P_M)_R}{2}\right)^2 + (\tau_M)_{z\theta}^2}$$

or

$$SI_{MAX} = 2\sqrt{\left(\frac{(P_M)_z - (P_M)_R}{2}\right)^2 + (\tau_M)_{z\theta}^2}$$

Because pressure was considered separately in this analysis, the equations used for Cut I are valid for Cut II.

where:
- L_1 = The length from the end of the nozzle where the piping loads are applied to the location of interest in the safe end.
- L_2 = The length from the end of the nozzle where the piping loads are applied to the location of interest in the blend radius.
- M_{xy} = The maximum bending moment in the xy plane.
- F_{yx} = The maximum shear force in the xy plane.
- N_z = The normal force per inch of circumference applied to the end of the nozzle in the z direction.
- q_N = The shear force per inch of circumference applied to the nozzle.
- R_N = The mid-wall nozzle radius.

Since the pressure was considered separately in this analysis, the equations can be simplified as follows:

$$(P_M)_z = \frac{Nz}{t_N}$$

$$(P_M)_\theta = 0$$

$$(P_M)_R = 0$$

$$\tau_M = \frac{q_N}{t_N}$$

$$SI_{MAX} = 2(\tau_M)_{z\theta}$$

or

$$SI_{MAX} = 2\sqrt{\left(\frac{Nz}{2t_N}\right)^2 + (\tau_M)_{z\theta}^{\ 2}}$$

Per Reference [7], the recirculation outlet nozzle piping loads (Total thermal, weight and seismic loads) are as follows:

F_x = 20,000 lbs	M_x = 2,004,000 in-lb
F_y = 20,000 lbs	M_y = 3,000,000 in-lb
F_z = 30,000 lbs	M_z = 2,004,000 in-lb

L_1 is equal to 4.25 inches and the L_2 is equal to 42.77 inches. The calculations for the safe end and blend radius are shown in Table 1. The first cut location is the same as the Green's Function cross section per [1] at the safe end, and the second cut is from Node 3829 (inside) to Node 3809 (outside). This gives the maximum ID and minimum OD for the cross section calculation. The maximum stress intensities due to the piping loads are 5708.89 psi at the safe end and 280.16 psi at the blend radius. The piping load sign is set as the same as the thermal stress sign.

These piping stress values are scaled assuming no stress occurs at an ambient temperature of 70°F, and the full values are reached at reactor design temperature, 575°F [6]. The scaled piping stress values are shown in columns 9 and 10 of Tables 4 and 5. Columns 11 and 12 of Tables 4 and 5 show the summation of all stresses for each thermal peak and valley stress point.

3.5 Fatigue Analysis (for program FATIGUE.EXE)

The number of cycles projected for the 60-year operating life is used for each transient [2]:

Column 13 in Tables 4 and 5 shows the number of cycles associated with each transient. The number of cycles for 60 years was obtained from Reference [2] unless otherwise noted.

The program FATIGUE.EXE performs the "ASME Code style" peak event pairing required to calculate a fatigue usage value. The input data for FATIGUE.CFG is as follows:

	Blend Radius	Safe End
Parameters *m* and *n* for Computing K_e	2.0 & 0.2 (low alloy steel) [13]	1.7 & 0.3 (stainless steel) [13]
Design Stress Intensity Values, S_m	26700 psi [9] @ 600°F	17000 psi [9] @ 600°F
Elastic Modulus from Applicable Fatigue Curve	30.0×10^6 psi [13]	28.3×10^6 psi [13]
Elastic Modulus Used in Finite Element Model	26.7×10^6 psi [1]	27.0×10^6 psi [1]
The Geometric Stress Concentration Factor K_t	1.0	1.53 [3]

The results of the fatigue analyses are presented in Tables 6 and 7 for the blend radius and safe end for 60 years, respectively.

The fatigue run inputs described are contained in EXCEL files *BRresults.xls* and *SEresults.xls*, which are contained in the computer files.

4.0 CALCULATION OF THERMAL STRESSES FOR TRANSIENT 9

Per Tables 2 and 3, the thermal shocks are from 526°F to 268°F and from 526°F to 130°F at the blend radius and the safe end, respectively. Therefore, the average temperatures for these two locations are about 400°F and 330°F. Since there are two different temperature shocks in the same model, ANSYS [10] will be used to calculate stresses directly. In this section, ANSYS [10] is used to simulate this transient and the results will then be used as input to FATIGUE.EXE, as shown in Tables 4 and 5. This case corresponds to the downhill (RPV) side of the blend radius.

An additional case was also run to simulate the uphill (RPV) side of the blend radius, where the thermal shocks are from 526°F to 130°F at the safe end, and no temperature change at the blend

radius. This case at the uphill side of the blend radius was found to produce lower stresses than the previously mentioned downhill case. Due to this, the downhill case was used for the rest of the analysis in this calculation.

4.1 Thermal Load

Since the average temperatures in the blend radius and safe end respectively are 400°F and 330°F, the material properties for 400°F are used for the blend radius, cladding and vessel. Table 8 shows the material properties at 400°F. The flow rate at this transient is 3395.2 GPM (calculated from 12% of max flow rate [2]) and is shown in Tables 2 and 3.

Heat transfer coefficients listed on Reference [4] are for pre power uprate. The heat transfer coefficients can be scaled by power uprate flow rate and diameter to values corresponding to the flow and location conditions. Referring to Figure 2, heat transfer coefficients were applied as follows:

Region 1

Per [4], the heat transfer coefficient at 500°F, h, for 3395.2 GPM (2.084 ft/s) flow is

$$4911 \cdot \left(\frac{2.084}{25}\right)^{0.8} = 672.8 \text{ BTU/hr-ft}^2\text{-°F.}$$

Per [4], the heat transfer coefficient at 100°F, h, for 3395.2 GPM (2.084 ft/s) flow is

$$2250 \cdot \left(\frac{2.084}{25}\right)^{0.8} = 308.24 \text{ BTU/hr-ft}^2\text{-°F.}$$

The fluid temperature shock is:

T = 526°F - 130°F - 526°F

Region 2

Per [4], the heat transfer coefficient at 500°F, h, for 3395.2 GPM (2.084 ft/s) flow is

$$4911 \cdot \left(\frac{2.084}{25}\right)^{0.8} \left(\frac{26}{35.49}\right)^{0..2} = 632.21 \text{ BTU/hr-ft}^2\text{-°F.}$$

Per [4], the heat transfer coefficient at 300°F, h, for 3395.2 GPM (2.084 ft/s) flow is

$$4789 \cdot \left(\frac{2.084}{25}\right)^{0.8} \left(\frac{26}{35.49}\right)^{0..2} = 616.57 \text{ BTU/hr-ft}^2\text{-°F.}$$

The fluid temperature shock is:

T = 526°F - 268°F - 526°F

Region 3

Per [4], the heat transfer coefficient at 500°F, h, for 3395.2 GPM flow is

$672.8(0.5) = 336.4$ BTU/hr-ft^2-°F.

Per [4], the heat transfer coefficient at 300°F, h, for 3395.2 GPM flow is

$$336.4\left(\frac{4789}{4911}\right) = 328.04 \text{ BTU/hr-ft}^2\text{-°F}.$$

The fluid temperature shock is:

Case 1: T = 526°F - 268°F - 526°F
Case 2: T = 526°F

Region 4

The heat transfer coefficient, h, is 0.4 BTU/hr-ft^2-°F [4].

The temperature is:

T = 120°F

4.2 Thermal Results

The flow dependent thermal load case outlined in Section 4.1 was run on the finite element model. Appendix A contains the thermal transient input file VY_RON_T_T9.INP for 3395.2 GPM flow rate. The flow dependent input files for the stress run is also included in Appendix A. The stress filename is VY_RON_S_T9.INP for 3395.2 GPM flow rate.

The critical safe end and blend radius locations are defined in Reference [1] at nodes 6395 and 3829, respectively.

The stress time history for the critical paths was extracted during the stress run. This produced two files, T9SE.OUT and T9BR.OUT, which contain the thermal stress history. The membrane plus bending stresses and total stresses were extracted from these files to produce the files T9SE_Inside.RED and T9BR_Inside.RED, where SE and BR corresponded to the safe end and blend radius locations, respectively.

The data for the stress results is included in the files T9BR_M+B.xls, T9BR_T.xls, T9SE_M+B.xls, and T9SE_T.xls in the project Files. Where SE and BR corresponded to the safe end and blend radius locations, respectively. M+B and T corresponded to membrane plus bending stress and total stress, respectively.

5.0 FATIGUE USAGE RESULTS

The blend radius cumulative usage factor (CUF) from system cycling is 0.0108 for 60 years (Table 6). The safe end CUF is 0.0015 for 60 years (Table 7).

6.0 ENVIRONMENTAL FATIGUE ANALYSIS

The Recirculation Outlet nozzle has three materials: a Ni-Cr-Fe dissimilar metal weld (DMW), a low alloy steel forging, and a stainless steel safe end. To ensure the maximum CUF considering environmental effects was identified, locations in the safe end and nozzle forging were selected. This selection produces bounding environmental fatigue results for the entire nozzle assembly for the following reasons:

- The highest thermal stresses from the FEM analysis occur in the stainless steel safe end. Stainless steel Fen multipliers are significantly higher than Ni-Cr-Fe multipliers (Fen values are 2.55 or higher for stainless steel [12] vs. a constant value of 1.49 for Ni-Cr-Fe [16]). Therefore, evaluation of the safe end bounds the Ni-Cr-Fe weld material.
- The highest pressure stresses from the FEM analysis occur in the low alloy steel nozzle forging. Low alloy steel Fen multipliers are higher than Ni-Cr-Fe multipliers (Fen values are 2.45 or higher for low alloy steel [12] vs. a constant value of 1.49 for Ni-Cr-Fe [16]). Therefore, evaluation of the nozzle forging bounds the Ni-Cr-Fe weld material.

Per Reference [12], the dissolved oxygen (DO) calculation shows the overall hydrogen water chemistry (HWC) availability is 47%. This means the time ratio under normal water chemistry (NWC, or pre-HWC) is 53%.

For the safe end location, the environmental fatigue factors for post-HWC and pre-HWC are 15.35 and 8.36 from Table 5 of Reference [12]. These result in an EAF adjusted CUF of (15.35 x 47% + 8.36 x 53%) x 0.0015 = 0.0175 for 60 years, which is acceptable (i.e., less than the allowable value of 1.0). The overall environmental multiplier is 11.6453.

For the blend radius location, the environmental fatigue factors for post-HWC and pre-HWC are 2.45 and 12.43 from Table 5 of Reference [12]. These result in an EAF adjusted CUF of (2.45 x 47% + 12.43 x 53%) x 0.0108 = 0.08358 for 60 years, which is acceptable (i.e., less than the allowable value of 1.0). The overall environmental multiplier is 7.739.

7.0 REFERENCES

1. Structural Integrity Associates Calculation No. VY-16Q-305, Revision 0, "Recirculation Outlet Nozzle Green's Functions."
2. Entergy Design Input Record (DIR), Rev. 1, EC No. 1773, Rev. 0, "Environmental Fatigue Analysis for Vermont Yankee Nuclear Power Station," 7/26/07, SI File No. VY-16Q-209.
3. CB&I, RPV Stress Report Section: S9 "Stress Analysis Recirculation Outlet Nozzle Vermont Yankee Reactor Vessel." 9-6201, SI document, VY-16Q-204.
4. CB&I, RPV Stress Report Section: T9 "Thermal Analysis Recirculation Outlet Nozzle Vermont Yankee Reactor Vessel." 9-6201, SI document, VY-16Q-204.
5. Structural Integrity Associates Calculation (Generic) No. SW-SPVF-01Q-301, Revision 0, "STRESS.EXE, P-V.EXE, and FATIGUE.EXE Software Verification."
6. VY Drawing, 5920-06623 Rev. 0, (Hitachi, Ltd. Drawing No IOR290-127, Revision 0), "Recirc. Outlet Safe End," SI File No. VY-16Q-204.
7. GE. Stress Report No. 23A4316, Revision 0, "Reactor Vessel Recirculation Outlet Safe End," SI File No. VY-16Q-204.
8. VY Drawing 5920-00238 Rev. 4, (Chicago Bridge & Iron Company, Contract No. 9-6201, Drawing No. 21, Revision 4), "36"x28" Nozzles Mk N1A/B," SI File No. VY-16QQ-204.
9. ASME Boiler and Pressure Vessel Code, Section II, Materials, Part D, Properties, 1998 Edition with 2000 Addenda.
10. ANSYS, Release 8.1 (w/Service Pack 1), ANSYS, Inc., June 2004.
11. Structural Integrity Associates Calculation No. VY-16Q-304, Revision 0, "Recirculation Outlet Nozzle Finite Element Model."
12. Structural Integrity Associates Calculation No. VY-16Q-303, Revision 0, "Environmental Fatigue Evaluation of Reactor Recirculation Inlet Nozzle and Vessel Shell/Bottom Head."
13. American Society of Mechanical Engineers, Boiler and Pressure Vessel Code, Section III, Subsection NB, 1998 Edition, 2000 Addenda.
14. NUREG-1801, Revision 1, "Generic Aging Lessons Learned (GALL) Report," U. S. Nuclear Regulatory Commission, September 2005.
15. Kuo, A. Y., Tang, S. S., and Riccardella, P. C., "An On-Line Fatigue Monitoring System for Power Plants, Part I - Direct Calculation of Transient Peak Stress Through Transfer Matrices and Green's Functions," ASME PVP Conference, Chicago, 1986.
16. EPRI Report No. TR-105759, "An Environmental Factor Approach to Account for Reactor Water Effects in Light Water Reactor Pressure Vessel and Piping Fatigue Evaluations," December 1995.
17. American Society of Mechanical Engineers, Boiler and Pressure Vessel Code, Section III, Subsection A, 1965 Edition with Winter 1966 Addenda.

Table 1: Maximum Piping Stress Intensity Calculations

Blend Radius External Piping Loads		
Parameters		
F_x =	20.00	kips
F_y =	20.00	kips
F_Z =	30.00	kips
M_x =	2004.00	in-kips
M_y =	3000.00	in-kips
M_Z =	2004.00	in-kips
OD=	55.88	in
ID=	37.368	in
R_N =	23.31	in
L =	42.77	in
t_N =	9.25	in
$(M_x)_2$ =	1148.54	in-kips
$(M_y)_2$ =	3855.46	in-kips
M_{xy} =	4022.90	in-kips
F_{xy} =	28.28	kips
N_Z =	2.56	kips/in
q_N =	-0.20	kips/in
Primary Membrane Stress Intensity		
PM_Z =	0.28	ksi
τ =	-0.02	ksi
SI_{max} =	0.28	ksi
SI_{max} =	280.16	psi

Safe End External Piping Loads		
Parameters		
F_x =	20.00	kips
F_y =	20.00	kips
F_Z =	30.00	kips
M_x =	2004.00	in-kips
M_y =	3000.00	in-kips
M_Z =	2004.00	in-kips
OD=	28.38	in
ID=	25.938	in
R_N =	13.58	in
L =	4.25	in
t_N =	1.22	in
$(M_x)_1$ =	1919.00	in-kips
$(M_y)_1$ =	3085.00	in-kips
M_{xy} =	3633.15	in-kips
F_{xy} =	28.28	kips
N_Z =	6.62	kips/in
q_N =	-1.07	kips/in
Primary Membrane Stress Intensity		
PM_Z =	5.43	ksi
τ =	-0.88	ksi
SI_{max} =	5.71	ksi
SI_{max} =	5708.89	psi

Note: The locations for Cut I and Cut II were defined in Reference [1] for safe end and blend radius paths, respectively.

Table 2: Blend Radius Transients

Transient Number	Time (s)	Temp (°F)	Time Step (s)	Pressure (psig)	Flow Rate (GPM)
1. Normal Startup with Heatup at 100°F/hr 300 Cycles	0	100		0	14147.0 (50%)'
	16164	549	16164	1010	
	22164	549	6000	1010	
2. Turbine Roll and Increase to Rated Power 300 Cycles	0	549		1010	28294 (100%)'
	1	542	1	1010	
	601	542	600	1010	
	602	526	1	1010	
	6602	526	6000	1010	
3. Loss of Feedwater Heaters Turbine Trip 25% Power 10 Cycles	0	526		1010	28294 (100%)'
	1800	542	1800	1010	
	2100	542	300	1010	
	2460	526	360	1010	
	3060	526	600	1010	
	3960	542	900	1010	
	4260	542	300	1010	
	6060	526	1800	1010	
	12060	526	6000	1010	
4. Loss of Feedwater Pumps 10 Cycles	0	526		1010	0 (0%)'
	3	526	3	1190	
	13	526	10	1135	
	233	300	220	1135	
	2213	500	1980	1136	
	2393	300	180	885	
	6773	500	4380	1135	
	7193	300	420	675	14147 (50%)
	7493	300	300	675	
	11093	400	3600	240	
	16457	549	5364	1010	
	16517	549	60	1010	
	16518	542	1	1010	28294 (100%)
	17118	542	600	1010	
	17119	526	1	1010	
	23119	526	6000	1010	
5. Turbine Generator Trip 60 Cycles	0	526		1010	28294 (100%)'
	10	526	10	1135	
	15	526	5	1135	
	30	526	15	940	
	1830	526	1800	940	
	2250	549	420	1010	
	2310	549	60	1010	
	2311	542	1	1010	
	2911	542	600	1010	
	2912	526	1	1010	
	8912	526	6000	1010	

Transient Number	Time (s)	Temp (°F)	Time Step (s)	Pressure (psig)	Flow Rate (GPM)
6. Reactor Overpressure 1 Cycle	0	526		1010	28294 (100%)'
	2	526	2	1375	
	32	526	30	940	
	1832	526	1800	940	
	2252	549	420	1010	
	2312	549	60	1010	
	2313	542	1	1010	
	2913	542	600	1010	
	2914	526	1	1010	
	8914	526	6000	1010	
7. SRV Blowdown 1 Cycle	0	526		1010	28294 (100%)'
	600	375	600	170	
	11580	70	10980	50	
	17580	70	6000	50	
8. SCRAM Other 228 Cycles	0	526		1010	28294 (100%)'
	15	526	15	940	
	1815	526	1800	940	
	2235	549	420	1010	
	2295	549	60	1010	
	2296	542	1	1010	
	2356	542	60	1010	
	2357	526	1	1010	
	8357	526	6000	1010	
9. Improper Startup 1 Cycle	0	526		1010	3395 (12%)'
	1	268 (3)	1	1010	
	27	268 (3)	26	1010	
	28	526	1	1010	
	6028	526	6000	1010	
10. Shutdown 300 Cycles	0	549		1010	14147 (50%)'
	6264	375	6264	170	
	6864	330	600	88	
	16224	70	9360	50	
	22224	70	6000	50	
11. Design Hydrostatic Test 120 cycles	—	100	—	50	1981 (7%)
				1563	
				50	
12. Hydrostatic Test 1 Cycle	—	100	—	0	1981 (7%)
				1100	
				50	

Notes:

1. The instant temperature change is assumed as 1 second time step.
2. The number of cycles is for 60 years [2].
3. 268°F is the blend radius temperature for this transient. The safe end has a different temperature for Transient 9. [2]

Table 3: Safe End Transients

Transient Number	Time (s)	Temp (°F)	Time Step (s)	Pressure (psig)	Flow Rate (GPM)
1. Normal Startup with Heatup at 100°F/hr 300 Cycles	0	100		0	14147.0 (50%)'
	16164	549	16164	1010	
	16864	549	700	1010	
2. Turbine Roll and Increase to Rated Power 300 Cycles	0	549		1010	28294 (100%)'
	1	542	1	1010	
	601	542	600	1010	
	602	526	1	1010	
	1302	526	700	1010	
3. Loss of Feedwater Heaters Turbine Trip 25% Power 10 Cycles	0	526		1010	28294 (100%)'
	1800	542	1800	1010	
	2100	542	300	1010	
	2460	526	360	1010	
	3060	526	600	1010	
	3960	542	900	1010	
	4260	542	300	1010	
	6060	526	1800	1010	
	6760	526	700	1010	
4. Loss of Feedwater Pumps 10 Cycles	0	526		1010	0 (0%)'
	3	526	3	1190	
	13	526	10	1135	
	233	300	220	1135	
	2213	500	1980	1135	
	2393	300	180	885	
	6773	500	4380	1135	
	7193	300	420	675	14147 (50%)'
	7493	300	300	675	
	11093	400	3600	240	
	16457	549	5364	1010	
	16517	549	60	1010	
	16518	542	1	1010	28294 (100%)'
	17118	542	600	1010	
	17119	526	1	1010	
	17819	526	700	1010	
5. Turbine Generator Trip 60 Cycles	0	526		1010	28294 (100%)'
	10	526	10	1135	
	15	526	5	1135	
	30	526	15	940	
	1830	526	1800	940	
	2250	549	420	1010	
	2310	549	60	1010	
	2311	542	1	1010	
	2911	542	600	1010	
	2912	526	1	1010	
	3612	526	700	1010	
6. Reactor Overpressure 1 Cycle	0	526		1010	28294 (100%)'
	2	526	2	1375	
	32	526	30	940	
	1832	526	1800	940	
	2252	549	420	1010	
	2312	549	60	1010	
	2313	542	1	1010	
	2913	542	600	1010	
	2914	526	1	1010	
	3614	526	700	1010	
7. SRV Blowdown 1 Cycle	0	526		1010	28294 (100%)'
	600	375	600	170	
	11580	70	10980	50	
	12280	70	700	50	
8. SCRAM Other 228 Cycles	0	526		1010	28294 (100%)'
	15	526	15	940	
	1815	526	1800	940	
	2235	549	420	1010	
	2295	549	60	1010	
	2296	542	1	1010	
	2356	542	60	1010	
	2357	526	1	1010	
	3057	526	700	1010	
9. Improper Startup 1 Cycle	0	526		1010	3395 (12%)'
	1	130 (3)	1	1010	
	27	130 (3)	26	1010	
	28	526	1	1010	
	728	526	700	1010	
10. Shutdown 300 Cycles	0	549		1010	14147 (50%)'
	6264	375	6264	170	
	6864	330	600	88	
	16224	70	9360	50	
	16924	70	700	50	
11. Design Hydrostatic Test 120 Cycles	—	100	—	0	1981 (7%)'
				1100	
				50	
12. Hydrostatic Test 1 Cycle	—	100	—	50	1981 (7%)'
				1563	
				50	

Notes:
1. The instant temperature change is assumed as 1 second time step.
2. The number of cycles is for 60 years [2].
3. 130°F is the safe end temperature for this transient. The blend radius has a different temperature for Transient 9. [2]

Note: These transients are the same as in Table 2 with the exception of the 700 second steady state time increment that is used. The transients in Table 2 are plotted using a 6000 second steady state increment. The difference is due to the length of the Green's Function for the safe end which is shorter compared to the blend Radius.

Table 4: Blend Radius Stress Summary

1	2	3	4	5	6	7	8	9	10	11	12	13
Transient Number	Time (s)	Total Stress (psi)	M+B Stress (psi)	Temperature F	Pressure (psig)	Total Pressure Stress (psi)	M+B Pressure Stress (psi)	Total Piping Stress (psi)	M+B Piping Stress (psi)	Total Total Stress (psi)	Total M+B Stress (psi)	Number of Cycles (60 years)
1	0	459	388	100.00	0	0	0	16.64312	16.64312	475.64	404.64	300
	4303	-3417	-1594	219.53	1010	31613	33976.4	-82.95209	-82.95209	28113.05	32299.45	300
	22164	2713	2306	549.00	1010	31613	33976.4	265.7352	265.7352	34591.74	36548.14	300
2	0.00	3094	1934	549	1010	31613	33976.4	265.7352	265.7352	34972.74	36176.14	300
	94.30	4079	2481	542	1010	31613	33976.4	261.8518	261.8518	35953.85	36719.25	300
	601.70	3683	2435	538.8	1010	31613	33976.4	260.0765	260.0765	35556.08	36671.48	300
	680.10	5891	3489	526	1010	31613	33976.4	252.9754	252.9754	37756.98	37718.38	300
	6602.00	2977	1859	526	1010	31613	33976.4	252.9754	252.9754	34842.98	36088.38	300
3	0.00	2959	1849	526	1010	31613	33976.4	252.9754	252.9754	34824.98	36078.38	10
	1807.20	1834	1043	542	1010	31613	33976.4	261.8518	261.8518	33708.85	35281.25	10
	2491.50	4425	2667	526	1010	31613	33976.4	252.9754	252.9754	36290.98	36896.38	10
	3974.40	1706	1060	542	1010	31613	33976.4	261.8518	261.8518	33580.85	35298.25	10
	6070.80	3971	2551	526	1010	31613	33976.4	252.9754	252.9754	35836.98	36780.38	10
	12060.00	2965	1852	526	1010	31613	33976.4	252.9754	252.9754	34830.98	36081.38	10
4	0	2465	-703	526.00	1010	31613	33976.4	252.9754	-252.9754	34330.98	33020.42	10
	3	2465	-703	526.00	1190	37247	40031.6	252.9754	-252.9754	39964.98	39075.62	10
	13	2465	-703	526.00	1135	35525.5	38181.4	252.9754	-252.9754	38243.48	37225.42	10
	435.6	18138	9690	356.38	1135	35525.5	38181.4	158.8774	158.8774	53822.38	48030.28	10
	2222.5	-1169	-2598	489.44	1135	35525.5	38181.4	-232.6952	-232.6952	34123.80	35350.70	10
	2665.5	12763	6695	328.40	885	27700.5	29771.4	143.3539	143.3539	40606.85	36609.75	10
	6779.2	-4008	-2829	497.05	1010	31613	33976.4	-236.9137	-236.9137	27368.09	30910.49	10
	7243.8	19275	9965	302.91	1010	31613	33976.4	129.2122	129.2122	51017.21	44070.61	10
	13996	-2135	34	542.00	1010	31613	33976.4	-261.8518	261.8518	29216.15	34272.25	10
	17247	3413	2074	526.00	1010	31613	33976.4	252.9754	252.9754	35278.98	36303.38	10
	23119	2971	1855	526.00	1010	31613	33976.4	252.9754	252.9754	34836.98	36084.38	10
5	0.00	2959	1849	526	1010	31613	33976.4	252.9754	252.9754	34824.98	36078.38	60
	10.00	2959	1849	526	1135	35525.5	38181.4	252.9754	252.9754	38737.48	40283.38	60
	15.00	2959	1849	526	940	29422	31621.6	252.9754	252.9754	32633.98	33723.58	60
	2269.50	111	295	549	1010	31613	33976.4	265.7352	265.7352	31989.74	34537.14	60
	3010.10	4407	2579	526	1010	31613	33976.4	252.9754	252.9754	36272.98	36808.38	60
	8912.00	2968	1854	526	1010	31613	33976.4	252.9754	252.9754	34833.98	36083.38	60
6	0.00	2959	1849	526.00	1010	31613	33976.4	252.9754	252.9754	34824.98	36078.38	1
	2.00	2959	1849	526.00	1375	43037.5	46255	252.9754	252.9754	46249.48	48356.98	1
	32.00	2959	1849	526.00	940	29422	31621.6	252.9754	252.9754	32633.98	33723.58	1
	2271.50	111	295	549.00	1010	31613	33976.4	265.7352	265.7352	31989.74	34537.14	1
	3022.00	4407	2579	526.00	1010	31613	33976.4	252.9754	252.9754	36272.98	36808.38	1
	8914.00	2968	1854	526.00	1010	31613	33976.4	252.9754	252.9754	34833.98	36083.38	1
7	0.00	2959	1849	526	1010	31613	33976.4	252.9754	252.9754	34824.98	36078.38	1
	615.10	20260	12980	374.581	170	5321	5718.8	168.9726	168.9726	25749.97	18867.77	1
	17580.00	279	179	70	50	1565	1682	0	0	1844.00	1861.00	1
8	0.00	2959	1849	526	1010	31613	33976.4	252.9754	252.9754	34824.98	36078.38	228
	15.00	2959	1849	526	940	29422	31621.6	252.9754	252.9754	32633.98	33723.58	228
	2254.50	111	295	549	1010	31613	33976.4	265.7352	265.7352	31989.74	34537.14	228
	2491.20	3792	2234	526	1010	31613	33976.4	252.9754	252.9754	35657.98	36463.38	228
	8357.00	2963	1851	526	1010	31613	33976.4	252.9754	252.9754	34828.98	36080.38	228
9	0	2058	961	525.8	1010	31613	33976.4	252.8645	252.8645	33923.86	35190.26	1
	0.52	1956	734	525.6	1010	31613	33976.4	252.7535	252.7535	33821.75	34963.15	1
	28	23747	3188	504.5	1010	31613	33976.4	241.0479	241.0479	55601.05	37405.45	1
	425	1520	611	525.5	1010	31613	33976.4	252.698	252.698	33385.70	34840.10	1
	12400	2058	879	525.8	1010	31613	33976.4	252.8645	252.8645	33923.86	35108.26	1
10	0	2767	2176	549	1010	31613	33976.4	265.7352	265.7352	34645.74	36418.14	300
	4240.8	6643	4158	445.775	441	13803.3	14835.24	208.469	208.469	20654.77	19201.71	300
	6268	6498	3675	374.7	170	5321	5718.8	169.0386	169.0386	11988.04	9562.84	300
	6891.8	9282	5241	329.228	88	2754.4	2960.32	143.8121	143.8121	12180.21	8345.13	300
	22224	361	120	70	50	1565	1682	0	0	1926.00	1802.00	300
11		0	0	100	0	0	0	16.64312	16.64312	16.64	16.64	120
		0	0	100	1100	34430	37004	16.64312	16.64312	34446.64	37020.64	120
		0	0	100	50	1565	1682	16.64312	16.64312	1581.64	1698.64	120
12		0	0	100	50	1565	1682	16.64312	16.64312	1581.64	1698.64	1
		0	0	100	1563	48921.9	52579.32	16.64312	16.64312	48938.54	52595.96	1
		0	0	100	50	1565	1682	16.64312	16.64312	1581.64	1698.64	1

NOTES: Column 1: Transient number identification.
Column 2: Time during transient where a maxima or minima stress intensity occurs from P-V.OUT output file.
Column 3: Maxima or minima total stress intensity from P-V.OUT output file.
Column 4: Maxima or minima membrane plus bending stress intensity from P-V.OUT output file.
Column 5: Temperature per total stress intensity.
Column 6: Pressure per Table 2.
Column 7: Total pressure stress intensity from the quantity (Column 6 x 31300)/1000.
Column 8: Membrane plus bending pressure stress intensity from the quantity (Column 6 x 33640)/1000.
Column 9: Total external stress from calculation in Table 1, 280.16 psi*(Column 5-70°F)/(575°F -70°F).
Column 10: Same as Column 9, but for M+B stress.
Column 11: Sum of total stresses (Columns 3, 7, and 9).
Column 12: Sum of membrane plus bending stresses (Columns 4, 8, and 10).
Column 13: Number of cycles for the transient (60 years).

Table 5: Safe End Stress Summary

1	2	3	4	5	6	7	8	9	10	11	12	13
Transient Number	Time (s)	Total Stress (psi)	M+B Stress (psi)	Temperature F	Pressure (psig)	Total Pressure Stress (psi)	M+B Pressure Stress (psi)	Total Piping Stress (psi)	M+B Piping Stress (psi)	Total Total Stress (psi)	Total M+B Stress (psi)	Number of Cycles (60 years)
1	0	-925	-949	100.00	0	0	0	-339.1419	-339.1419	-1264.14	-1288.14	300
	16164	-4814	-4433	549.00	1010	11604.9	11463.5	-5414.966	-5414.966	1375.93	1615.53	300
	16864	-3749	-3705	549.00	1010	11604.9	11463.5	-5414.966	-5414.966	2440.93	2343.53	300
2	0	-3838	-3665	549	1010	11604.9	11463.5	-5414.966	-5414.966	2351.93	2383.53	300
	6	-1664	-2263	542	1010	11604.9	11463.5	-5335.833	-5335.833	4605.07	3864.67	300
	601	-3773	-3607	542	1010	11604.9	11463.5	-5335.833	-5335.833	2496.07	2520.67	300
	606.6	1196	-403	526	1010	11604.9	11463.5	5154.958	-5154.958	17955.86	5905.54	300
	1302	-3670	-3509	526	1010	11604.9	11463.5	-5154.958	-5154.958	2779.94	2799.54	300
3	0	-3688	-3522	526	1010	11604.9	11463.5	-5154.958	-5154.958	2761.94	2786.54	10
	1800.1	-4165	-3904	542	1010	11604.9	11463.5	-5335.833	-5335.833	2104.07	2223.67	10
	2460.2	-1932	-2200	526	1010	11604.9	11463.5	-5154.958	-5154.958	4517.94	4108.54	10
	3960.2	-4537	-4185	542	1010	11604.9	11463.5	-5335.833	-5335.833	1732.07	1942.67	10
	6060.2	-3315	-3241	526	1010	11604.9	11463.5	-5154.958	-5154.958	3134.94	3067.54	10
	6760	-3687	-3522	526	1010	11604.9	11463.5	-5154.958	-5154.958	2762.94	2786.54	10
4	0.00	-3756	-3716	526	1020	11719.8	11577	-5154.958	-5154.958	2808.84	2706.04	10
	3.00	-3756	-3716	526	1190	13673.1	13506.5	-5154.958	-5154.958	4762.14	4635.54	10
	13.00	-3756	-3716	526	1135	13041.15	12882.25	-5154.958	-5154.958	4130.19	4011.29	10
	242.30	15878	10049	302.374	1135	13041.15	12882.25	2626.926	2626.926	31546.08	25558.18	10
	2213.10	-6388	-5428	499.889	1135	13041.15	12882.25	-4859.78	-4859.78	1793.37	2594.47	10
	2408.60	13203	8265	301.443	885	10168.65	10044.75	2616.401	2616.401	25988.05	20926.15	10
	6773.40	-4763	-4312	499.809	1135	13041.15	12882.25	-4858.875	-4858.875	3419.27	3711.37	10
	7193.10	15374	9801	300	675	7755.75	7661.25	2600.088	2600.088	25729.84	20062.34	10
	16457.50	-4812	-5032	549	240	2757.6	2724	-5414.966	-5414.966	-7469.37	-7722.97	10
	16524.70	-2358	-2725	542	1010	11604.9	11463.5	-5335.833	-5335.833	3911.07	3402.67	10
	17118.00	-3778	-3610	541.996	1010	11604.9	11463.5	-5335.788	-5335.788	2491.11	2517.71	10
	17123.60	1192	-406	526	1010	11604.9	11463.5	5154.958	-5154.958	17951.86	5902.54	10
	17819.00	-3670	-3509	526	1010	11604.9	11463.5	-5154.958	-5154.958	2779.94	2799.54	10
5	0.00	-3688	-3522	526	1010	11604.9	11463.5	-5154.958	-5154.958	2761.94	2786.54	60
	10.00	-3688	-3522	526	1135	13041.15	12882.25	-5154.958	-5154.958	4198.19	4205.29	60
	30.00	-3688	-3522	526	940	10800.6	10669	-5154.958	-5154.958	1957.64	1992.04	60
	2250.10	-6054	-5337	549	1010	11604.9	11463.5	-5414.966	-5414.966	135.93	711.53	60
	2319.90	-2977	-3123	542	1010	11604.9	11463.5	-5335.833	-5335.833	3292.07	3004.67	60
	2911.00	-3782	-3613	541.999	1010	11604.9	11463.5	-5335.822	-5335.822	2487.08	2514.68	60
	2916.70	1188	-408	526	1010	11604.9	11463.5	5154.958	-5154.958	17947.86	5900.54	60
	3612.00	-3670	-3509	526	1010	11604.9	11463.5	-5154.958	-5154.958	2779.94	2799.54	60
6	0.00	-3688	-3522	5.26E+02	1010	11604.9	11463.5	-5154.958	-5154.958	2761.94	2786.54	1
	2.00	-3688	-3522	5.26E+02	1375	15798.75	15606.25	-5154.958	-5154.958	6955.79	6929.29	1
	32.00	-3688	-3522	5.26E+02	940	10800.6	10669	-5154.958	-5154.958	1957.64	1992.04	1
	2252.10	-6054	-5337	5.49E+02	1010	11604.9	11463.5	-5414.966	-5414.966	135.93	711.53	1
	2322.20	-2977	-3123	5.42E+02	1010	11604.9	11463.5	-5335.833	-5335.833	3292.07	3004.67	1
	2913.00	-3782	-3613	5.42E+02	1010	11604.9	11463.5	-5335.822	-5335.822	2487.08	2514.68	1
	2918.70	1188	-408	5.26E+02	1010	11604.9	11463.5	5154.958	-5154.958	17947.86	5900.54	1
	3614.00	-3670	-3509	5.26E+02	1010	11604.9	11463.5	-5154.958	-5154.958	2779.94	2799.54	1
7	0	-3688	-3522	526	1010	11604.9	11463.5	-5154.958	-5154.958	2761.94	2786.54	1
	600	7773	5336	375	170	1953.3	1929.5	3447.943	3447.943	13174.24	10713.44	1
	1367.9	-1390	-1567	354.172	162	1861.38	1838.7	-3212.488	-3212.488	-2741.11	-2940.79	1
	11580.1	454	190	70	50	574.5	567.5	0	0	1028.50	757.50	1
	12280	-707	-689	70	50	574.5	567.5	0	0	-132.50	-121.50	1
8	0.00	-3688	-3522	526	1010	11604.9	11463.5	-5154.958	-5154.958	2761.94	2786.54	228
	15.00	-3688	-3522	526	940	10800.6	10669	-5154.958	-5154.958	1957.64	1992.04	228
	2235.10	-6054	-5337	549	1010	11604.9	11463.5	-5414.966	-5414.966	135.93	711.53	228
	2305.20	-2977	-3123	542	1010	11604.9	11463.5	-5335.833	-5335.833	3292.07	3004.67	228
	2356.00	-3183	-3151	541.999	1010	11604.9	11463.5	-5335.822	-5335.822	3086.08	2976.68	228
	2361.50	1761	-28	526	1010	11604.9	11463.5	5154.958	-5154.958	18520.86	6280.54	228
	3057.00	-3667	-3506	526	1010	11604.9	11463.5	-5154.958	-5154.958	2782.94	2802.54	228
9	0	-2968	-2837	525.7	1010	11604.9	11463.5	-5151.566	-5151.566	3485.22	3474.82	1
	27	68473	45303	291.3	1010	11604.9	11463.5	2501.737	2501.737	82579.74	59268.34	1
	80.7	-11546	-8877	518.4	1010	11604.9	11463.5	-5069.042	-5069.042	-5010.04	-2482.14	1
	5200	-2967	-2832	525.7	1010	11604.9	11463.5	-5151.566	-5151.566	3486.21	3479.78	1
10	0	-3745	-3709	549	1010	11604.9	11463.5	-5414.966	-5414.966	2444.93	2339.53	300
	6864.2	501	-405	329.994	170	1953.3	1929.5	2939.162	-2939.162	5393.46	-1414.66	300
	7455.5	-1183	-1528	314.325	88	1011.12	998.8	-2762.029	-2762.029	-2933.91	-3291.23	300
	16224.1	334	-35	70	50	574.5	567.5	0	0	908.50	532.50	300
	16924	-731	-763	70	50	574.5	567.5	0	0	-156.50	-195.50	300
11		0	0	100	0	0	0	339.1419	339.1419	339.14	339.14	120
		0	0	100	1100	12639	12485	339.1419	339.1419	12978.14	12824.14	120
		0	0	100	50	574.5	567.5	339.1419	339.1419	913.64	906.64	120
12		0	0	100	50	574.5	567.5	339.1419	339.1419	913.64	906.64	1
		0	0	100	1563	17958.87	17740.05	339.1419	339.1419	18298.01	18079.19	1
		0	0	100	50	574.5	567.5	339.1419	339.1419	913.64	906.64	1

NOTES: Column 1: Transient number identification.

Column 2: Time during transient where a maxima or minima stress intensity occurs from P-V.OUT output file.

Column 3: Maxima or minima total stress intensity from P-V.OUT output file.

Column 4: Maxima or minima membrane plus bending stress intensity from P-V.OUT output file.

Column 5: Temperature per total stress intensity.

Column 6: Pressure per Table 3.

Column 7: Total pressure stress intensity from the quantity (Column 6 x 11490)/1000.

Column 8: Membrane plus bending pressure stress intensity from the quantity (Column 6 x 11350)/1000.

Column 9: Total external stress from calculation in Table 1, 5708.89 psi*(Column 5-70°F)/(575°F -70°F).

Column 10: Same as Column 9, but for M+B stress.

Column 11: Sum of total stresses (Columns 3, 7, and 9).

Column 12: Sum of membrane plus bending stresses (Columns 4, 8, and 10).

Column 13: Number of cycles for the transient (60 years).

Table 6: Fatigue Results for Blend Radius (60 Years)

```
       LOCATION = LOCATION NO. 2 -- BLEND RADIUS
  FATIGUE CURVE = 1 (1 = CARBON/LOW ALLOY, 2 = STAINLESS STEEL)
              m = 2.0
              n =  .2
             Sm = 26700. psi
         Ecurve = 3.000E+07 psi
      Eanalysis = 2.670E+07 psi
             Kt = 1.00
```

MAX	MIN	RANGE	MEM+BEND	Ke	Salt	Napplied	Nallowed	U
55601.	17.	55584.	37389.	1.000	31227.	1.000E+00	1.951E+04	.0001
53822.	17.	53806.	48014.	1.000	30228.	1.000E+01	2.161E+04	.0005
51017.	17.	51001.	44054.	1.000	28652.	1.000E+01	2.547E+04	.0004
48939.	17.	48922.	52579.	1.000	27484.	1.000E+00	2.894E+04	.0000
46249.	17.	46233.	48340.	1.000	25974.	1.000E+00	3.443E+04	.0000
40607.	17.	40590.	36593.	1.000	22803.	1.000E+01	5.217E+04	.0002
39965.	17.	39948.	39059.	1.000	22443.	1.000E+01	5.647E+04	.0002
38737.	17.	38721.	40267.	1.000	21753.	6.000E+01	6.592E+04	.0009
38243.	17.	38227.	37209.	1.000	21476.	1.000E+01	7.025E+04	.0001
37757.	17.	37740.	37702.	1.000	21202.	7.000E+00	7.486E+04	.0001
37757.	476.	37281.	37314.	1.000	20945.	2.930E+02	7.954E+04	.0037
36291.	476.	35815.	36492.	1.000	20121.	7.000E+00	9.705E+04	.0001
36291.	1582.	34709.	35198.	1.000	19500.	3.000E+00	1.096E+05	.0000
36273.	1582.	34691.	35110.	1.000	19490.	6.000E+01	1.098E+05	.0005
36273.	1582.	34691.	35110.	1.000	19490.	1.000E+00	1.098E+05	.0000
35954.	1582.	34372.	35021.	1.000	19310.	5.600E+01	1.135E+05	.0005
35954.	1582.	34372.	35021.	1.000	19310.	1.000E+00	1.135E+05	.0000
35954.	1582.	34372.	35021.	1.000	19310.	1.000E+00	1.135E+05	.0000
35954.	1844.	34110.	34858.	1.000	19163.	1.000E+00	1.167E+05	.0000
35954.	1926.	34028.	34917.	1.000	19117.	2.410E+02	1.177E+05	.0020
35837.	1926.	33911.	34978.	1.000	19051.	1.000E+01	1.191E+05	.0001
35658.	1926.	33732.	34661.	1.000	18951.	4.900E+01	1.214E+05	.0004
35658.	11988.	23670.	26901.	1.000	13298.	1.790E+02	5.728E+05	.0003
35556.	11988.	23568.	27109.	1.000	13240.	1.210E+02	5.955E+05	.0002
35556.	12180.	23376.	28326.	1.000	13133.	1.790E+02	6.411E+05	.0003
35279.	12180.	23099.	27958.	1.000	12977.	1.000E+01	7.138E+05	.0000
34973.	12180.	22793.	27831.	1.000	12805.	1.110E+02	8.050E+05	.0001
34973.	20655.	14318.	16974.	1.000	8044.	1.890E+02	7.421E+07	.0000
34843.	20655.	14188.	16887.	1.000	7971.	1.110E+02	7.983E+07	.0000
34843.	25750.	9093.	17221.	1.000	5108.	1.000E+00	1.000E+20	.0000
34843.	27368.	7475.	5178.	1.000	4199.	1.000E+01	1.000E+20	.0000
34843.	28113.	6730.	3789.	1.000	3781.	1.780E+02	1.000E+20	.0000
34837.	28113.	6724.	3785.	1.000	3777.	1.000E+01	1.000E+20	.0000
34834.	28113.	6721.	3784.	1.000	3776.	6.000E+01	1.000E+20	.0000
34834.	28113.	6721.	3784.	1.000	3776.	1.000E+00	1.000E+20	.0000
34831.	28113.	6718.	3782.	1.000	3774.	1.000E+01	1.000E+20	.0000
34829.	28113.	6716.	3781.	1.000	3773.	4.100E+01	1.000E+20	.0000
34829.	29216.	5613.	1808.	1.000	3153.	1.000E+01	1.000E+20	.0000
34829.	31990.	2839.	1543.	1.000	1595.	6.000E+01	1.000E+20	.0000
34829.	31990.	2839.	1543.	1.000	1595.	1.000E+00	1.000E+20	.0000
34829.	31990.	2839.	1543.	1.000	1595.	1.160E+02	1.000E+20	.0000
34825.	31990.	2835.	1541.	1.000	1593.	1.000E+01	1.000E+20	.0000
34825.	31990.	2835.	1541.	1.000	1593.	6.000E+01	1.000E+20	.0000

34825.	31990.	2835.	1541.	1.000	1593.	1.000E+00	1.000E+20	.0000
34825.	31990.	2835.	1541.	1.000	1593.	1.000E+00	1.000E+20	.0000
34825.	31990.	2835.	1541.	1.000	1593.	4.000E+01	1.000E+20	.0000
34825.	32634.	2191.	2355.	1.000	1231.	6.000E+01	1.000E+20	.0000
34825.	32634.	2191.	2355.	1.000	1231.	1.000E+00	1.000E+20	.0000
34825.	32634.	2191.	2355.	1.000	1231.	1.270E+02	1.000E+20	.0000
34646.	32634.	2012.	2695.	1.000	1130.	1.010E+02	1.000E+20	.0000
34646.	33386.	1260.	1578.	1.000	708.	1.000E+00	1.000E+20	.0000
34646.	33581.	1065.	1120.	1.000	598.	1.000E+01	1.000E+20	.0000
34646.	33709.	937.	1137.	1.000	526.	1.000E+01	1.000E+20	.0000
34646.	33822.	824.	1455.	1.000	463.	1.000E+00	1.000E+20	.0000
34646.	33924.	722.	1228.	1.000	406.	1.000E+00	1.000E+20	.0000
34646.	33924.	722.	1310.	1.000	406.	1.000E+00	1.000E+20	.0000
34646.	34124.	522.	1067.	1.000	293.	1.000E+01	1.000E+20	.0000
34646.	34331.	315.	3398.	1.000	177.	1.000E+01	1.000E+20	.0000
34646.	34447.	199.	-603.	1.000	112.	1.200E+02	1.000E+20	.0000
34646.	34592.	54.	-130.	1.000	30.	3.500E+01	1.000E+20	.0000
								=======
							TOTAL USAGE FACTOR =	.0108

Table 7: Fatigue Results for Safe End (60 Years)

```
      LOCATION = LOCATION NO. 1 -- SAFE END
 FATIGUE CURVE = 2 (1 = CARBON/LOW ALLOY, 2 = STAINLESS STEEL)
             m = 1.7
             n =  .3
            Sm = 17000. psi
        Ecurve = 2.830E+07 psi
     Eanalysis = 2.700E+07 psi
            Kt = 1.53
```

MAX	MIN	RANGE	MEM+BEND	Ke	Salt	Napplied	Nallowed	U
82580.	-7469.	90049.	66991.	2.045	134573.	1.000E+00	6.765E+02	.0015
31546.	-7469.	39015.	33281.	1.000	29691.	9.000E+00	6.857E+05	.0000
31546.	-5010.	36556.	28040.	1.000	26947.	1.000E+00	1.160E+06	.0000
25988.	-2934.	28922.	24217.	1.000	21884.	1.000E+01	2.383E+06	.0000
25730.	-2934.	28664.	23354.	1.000	21509.	1.000E+01	2.566E+06	.0000
18521.	-2934.	21455.	9572.	1.000	13903.	2.280E+02	9.710E+08	.0000
18298.	-2934.	21232.	21370.	1.000	17063.	1.000E+00	7.876E+06	.0000
17956.	-2934.	20890.	9197.	1.000	13502.	5.100E+01	1.000E+20	.0000
17956.	-2741.	20697.	8846.	1.000	13304.	1.000E+00	1.000E+20	.0000
17956.	-1264.	19220.	7194.	1.000	12071.	2.480E+02	1.000E+20	.0000
17952.	-1264.	19216.	7191.	1.000	12068.	1.000E+01	1.000E+20	.0000
17948.	-1264.	19212.	7189.	1.000	12065.	4.200E+01	1.000E+20	.0000
17948.	-157.	18104.	6096.	1.000	11181.	1.800E+01	1.000E+20	.0000
17948.	-157.	18104.	6096.	1.000	11181.	1.000E+00	1.000E+20	.0000
13174.	-157.	13331.	10909.	1.000	10016.	1.000E+00	1.000E+20	.0000
12978.	-157.	13135.	13020.	1.000	10500.	1.200E+02	1.000E+20	.0000
6956.	-157.	7112.	7125.	1.000	5706.	1.000E+00	1.000E+20	.0000
5393.	-157.	5550.	-1219.	1.000	2570.	1.590E+02	1.000E+20	.0000
5393.	-133.	5526.	-1293.	1.000	2537.	1.000E+00	1.000E+20	.0000
5393.	136.	5258.	-2126.	1.000	2165.	6.000E+01	1.000E+20	.0000
5393.	136.	5258.	-2126.	1.000	2165.	1.000E+00	1.000E+20	.0000
5393.	136.	5258.	-2126.	1.000	2165.	7.900E+01	1.000E+20	.0000
4762.	136.	4626.	3924.	1.000	3514.	1.000E+01	1.000E+20	.0000
4605.	136.	4469.	3153.	1.000	3218.	1.390E+02	1.000E+20	.0000
4605.	339.	4266.	3526.	1.000	3215.	1.200E+02	1.000E+20	.0000
4605.	909.	3697.	3332.	1.000	2863.	4.100E+01	1.000E+20	.0000
4518.	909.	3609.	3576.	1.000	2885.	1.000E+01	1.000E+20	.0000
4198.	909.	3290.	3673.	1.000	2744.	6.000E+01	1.000E+20	.0000
4130.	909.	3222.	3479.	1.000	2655.	1.000E+01	1.000E+20	.0000
3911.	909.	3003.	2870.	1.000	2371.	1.000E+01	1.000E+20	.0000
3486.	909.	2578.	2947.	1.000	2170.	1.000E+00	1.000E+20	.0000
3485.	909.	2577.	2942.	1.000	2168.	1.000E+00	1.000E+20	.0000
3419.	909.	2511.	3179.	1.000	2199.	1.000E+01	1.000E+20	.0000
3292.	909.	2384.	2472.	1.000	1936.	6.000E+01	1.000E+20	.0000
3292.	909.	2384.	2472.	1.000	1936.	1.000E+00	1.000E+20	.0000
3292.	909.	2384.	2472.	1.000	1936.	9.600E+01	1.000E+20	.0000
3292.	914.	2378.	2098.	1.000	1829.	1.200E+02	1.000E+20	.0000
3292.	914.	2378.	2098.	1.000	1829.	1.000E+00	1.000E+20	.0000
3292.	914.	2378.	2098.	1.000	1829.	1.000E+00	1.000E+20	.0000
3292.	1029.	2264.	2247.	1.000	1810.	1.000E+00	1.000E+20	.0000
3292.	1376.	1916.	1389.	1.000	1390.	9.000E+00	1.000E+20	.0000
3135.	1376.	1759.	1452.	1.000	1325.	1.000E+01	1.000E+20	.0000
3086.	1376.	1710.	1361.	1.000	1274.	2.280E+02	1.000E+20	.0000

2809.	1376.	1433.	1091.	1.000	1054.	1.000E+01	1.000E+20	.0000
2783.	1376.	1407.	1187.	1.000	1067.	4.300E+01	1.000E+20	.0000
2783.	1732.	1051.	860.	1.000	790.	1.000E+01	1.000E+20	.0000
2783.	1793.	990.	208.	1.000	576.	1.000E+01	1.000E+20	.0000
2783.	1958.	825.	811.	1.000	658.	6.000E+01	1.000E+20	.0000
2783.	1958.	825.	811.	1.000	658.	1.000E+00	1.000E+20	.0000
2783.	1958.	825.	811.	1.000	658.	1.040E+02	1.000E+20	.0000
2780.	1958.	822.	808.	1.000	655.	1.240E+02	1.000E+20	.0000
2780.	2104.	676.	576.	1.000	514.	1.000E+01	1.000E+20	.0000
2780.	2352.	428.	416.	1.000	340.	1.660E+02	1.000E+20	.0000
2780.	2352.	428.	416.	1.000	340.	1.000E+01	1.000E+20	.0000
2780.	2352.	428.	416.	1.000	340.	6.000E+01	1.000E+20	.0000
2780.	2352.	428.	416.	1.000	340.	1.000E+00	1.000E+20	.0000
2763.	2352.	411.	403.	1.000	327.	1.000E+01	1.000E+20	.0000
2762.	2352.	410.	403.	1.000	327.	1.000E+01	1.000E+20	.0000
2762.	2352.	410.	403.	1.000	327.	4.300E+01	1.000E+20	.0000
2762.	2441.	321.	443.	1.000	291.	1.700E+01	1.000E+20	.0000
2762.	2441.	321.	443.	1.000	291.	1.000E+00	1.000E+20	.0000
2762.	2441.	321.	443.	1.000	291.	1.000E+00	1.000E+20	.0000
2762.	2441.	321.	443.	1.000	291.	2.280E+02	1.000E+20	.0000
2496.	2441.	55.	177.	1.000	78.	5.300E+01	1.000E+20	.0000
2496.	2445.	51.	181.	1.000	77.	2.470E+02	1.000E+20	.0000
2491.	2445.	46.	178.	1.000	74.	1.000E+01	1.000E+20	.0000
2487.	2445.	42.	175.	1.000	71.	4.300E+01	1.000E+20	.0000
2487.	2487.	0.	0.	1.000	0.	1.700E+01	1.000E+20	.0000
								=======
							TOTAL USAGE FACTOR =	.0015

Table 8: Material Properties (For Transient 9)[1]

Material	SA-533 Gr B @400 °F (Mn-1/2Mo-1/2Ni)	SA-508 Cl 2 @400 °F (3/4Ni-1/2Mo-1/3Cr-V)	SA-240 Type 304 @400 °F (18Cr-8Ni)	SA-182 F316 @300 °F (16Cr-12Ni-2Mo)
Modulus of Elasticity, e^{-6} psi	27.4	26.1	26.5	27.0
Coefficient of Thermal Expansion, e^{-6}, in/in/°F	8.0	7.7	10.2	9.8
Thermal Conductivity, Btu/hr-ft-°F	23.1	23.1	10.4	9.3
Thermal Diffusivity, ft^2/hr	0.378	0.378	0.165	0.150
Specific Heat, Btu/lb-°F[2]	0.125	0.125	0.129	0.127
Density, lb/in^3	0.283	0.283	0.283	0.283
Poisson's Ratio	0.3	0.3	0.3	0.3

Notes: [1] Material Properties are evaluated at 400°F from the 1998 ASME Code, Section II, Part D, with 2000 Addenda, except for density and Poisson's ratio, which are assumed typical values. This is consistent with information provided in the Design Input Record (page 13 of VY EC No. 1773, SI File No. VY-16Q-209). The use of a later code edition than that used for the original design code is acceptable since later editions typically reflect more accurate material properties than was published in prior Code editions. The safe end material properties were used for 300°F, the Code table values closest to the average temperature for the safe end for transient 9.

[2] Calculated as $[k/(\rho d)]/12^3$.

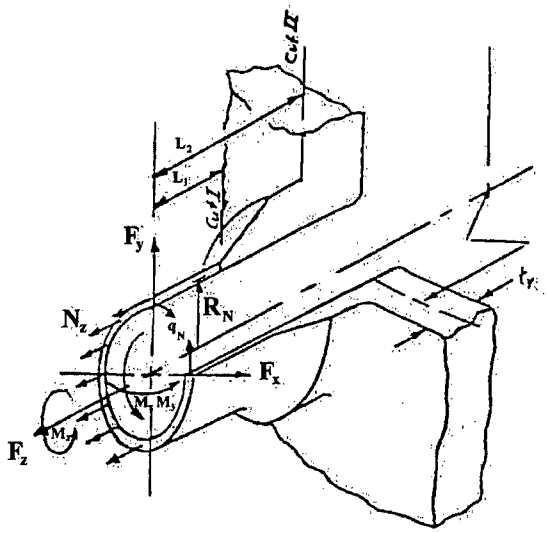

Figure 1: External Forces and Moments on the Recirculation Outlet Nozzle

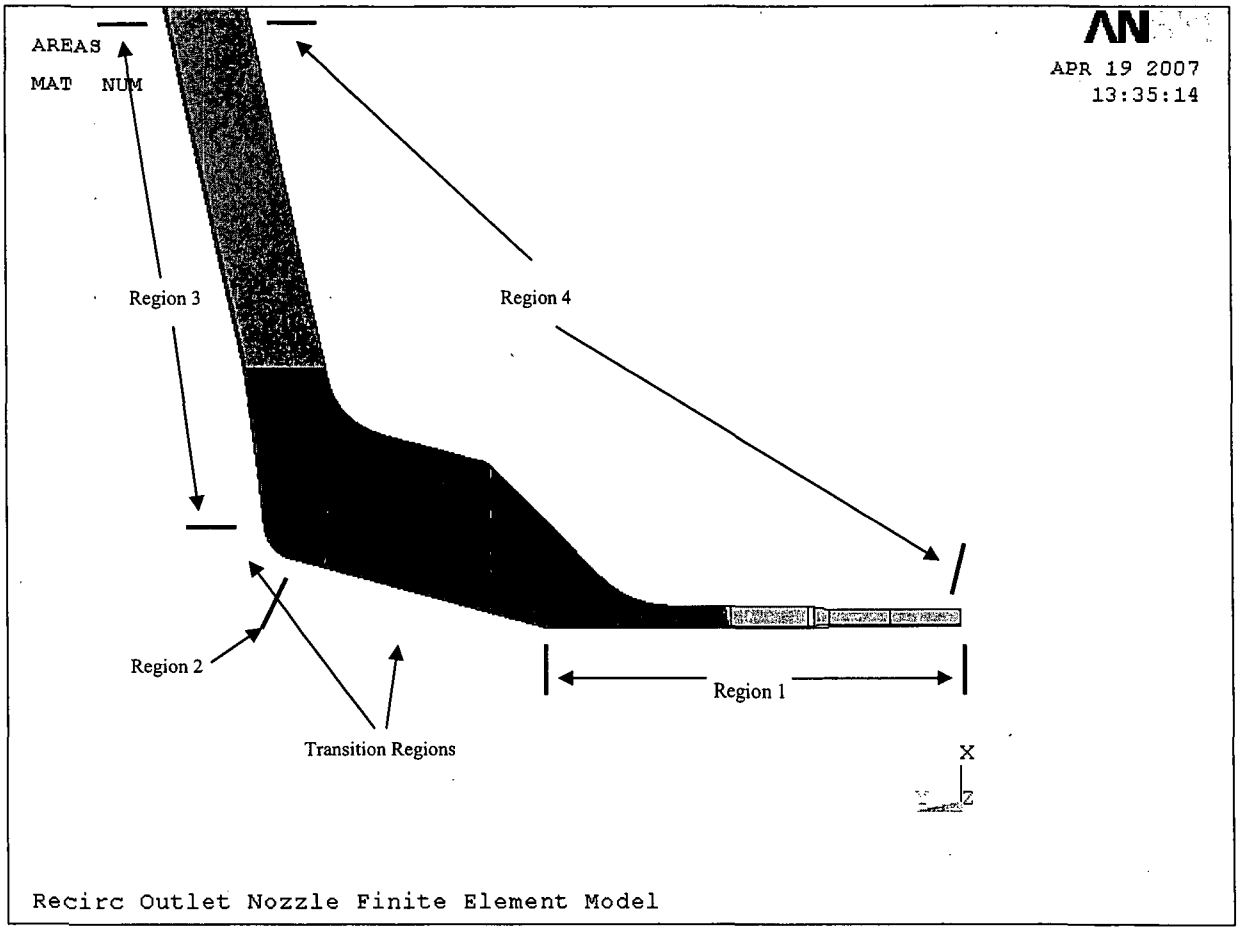

Figure 2: Nozzle and Vessel Wall Thermal and Heat Transfer Boundaries for Transient 9

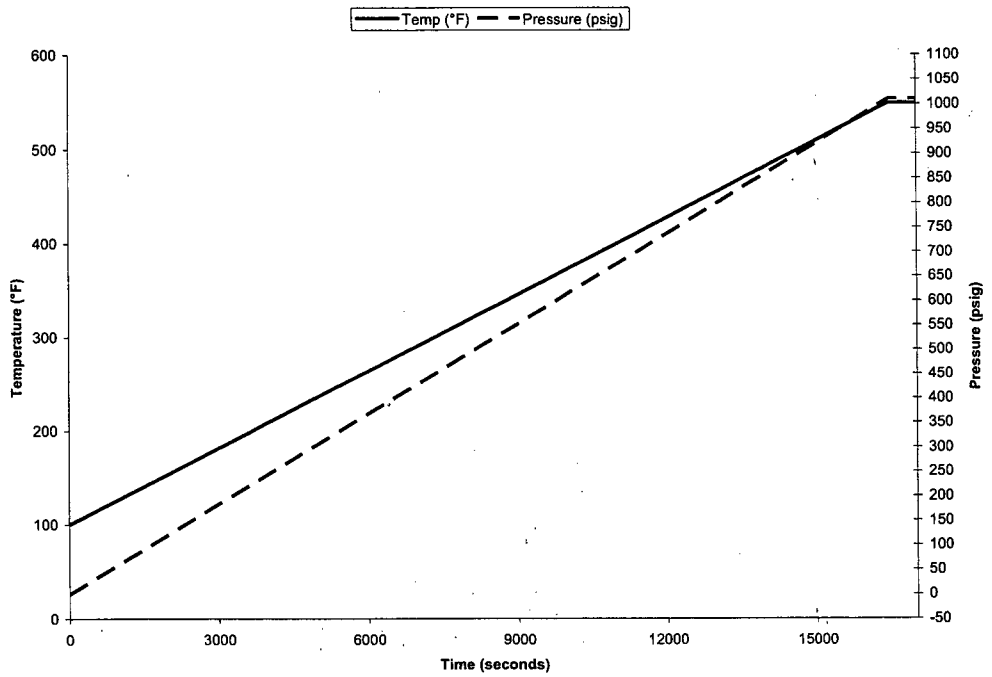

Figure 3: Transient 1 – Normal Startup at 100°F/hr

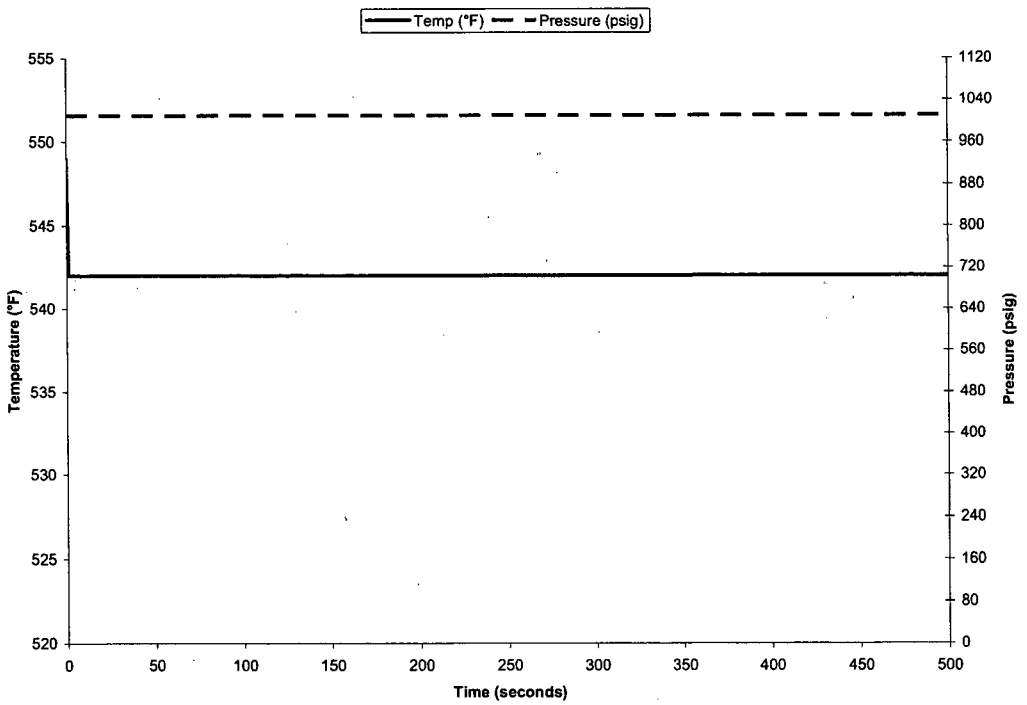

Figure 4: Transient 2 – Turbine Roll and Increase to Rated Power

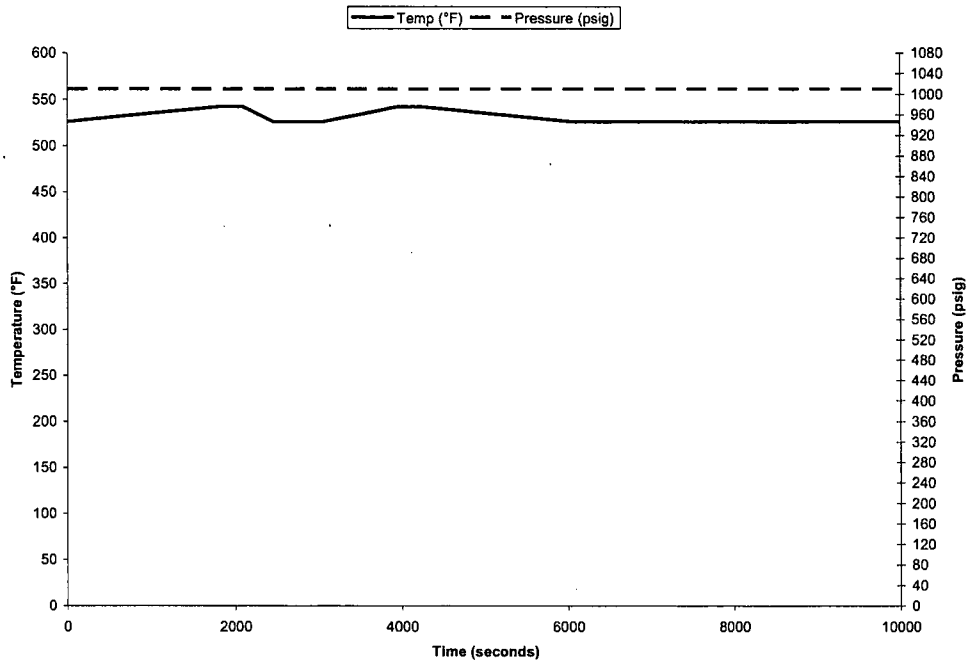

Figure 5: Transient 3 – Loss of Feedwater Heaters and Turbine Trip 25% Power

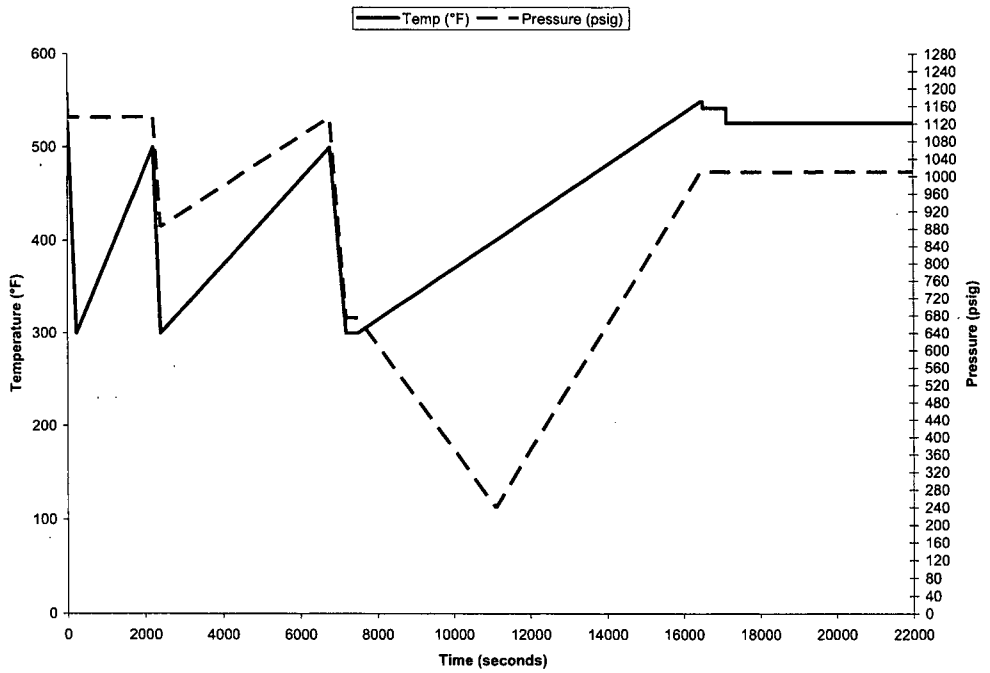

Figure 6: Transient 4 – Loss of Feedwater Pumps

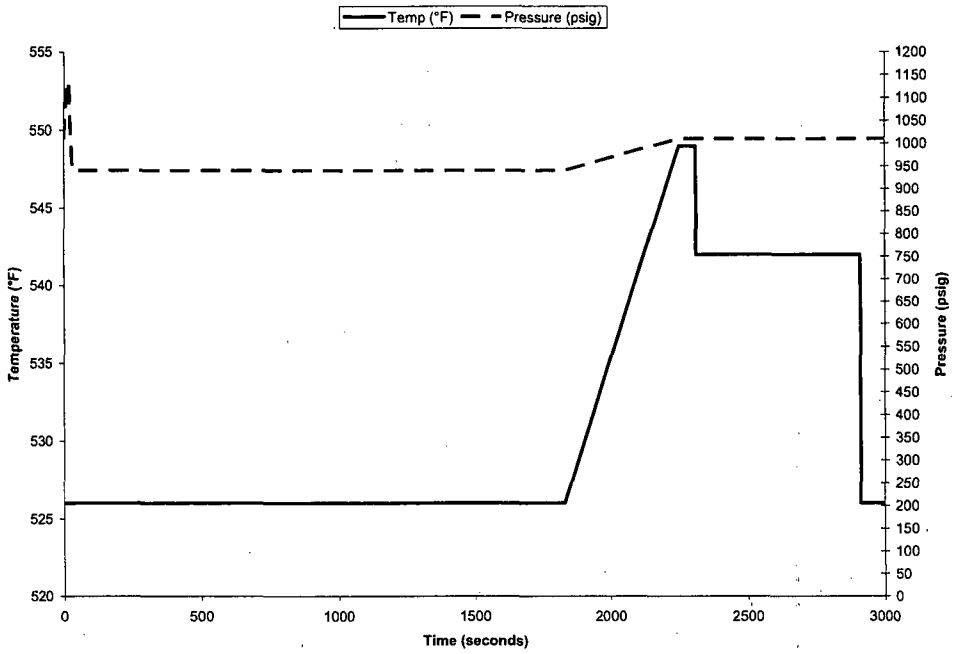

Figure 7: Transient 5 – Turbine Generator Trip

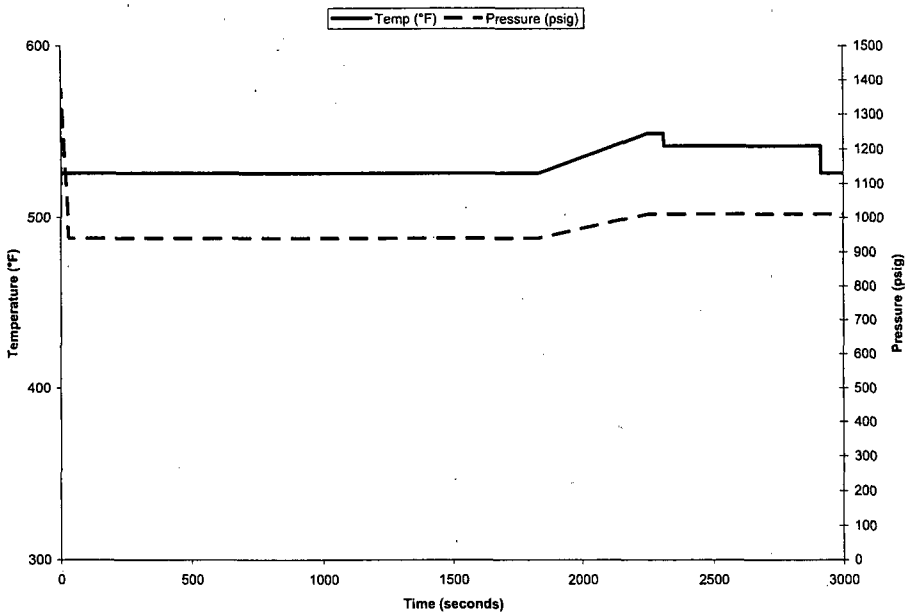

Figure 8: Transient 6 – Reactor Overpressure

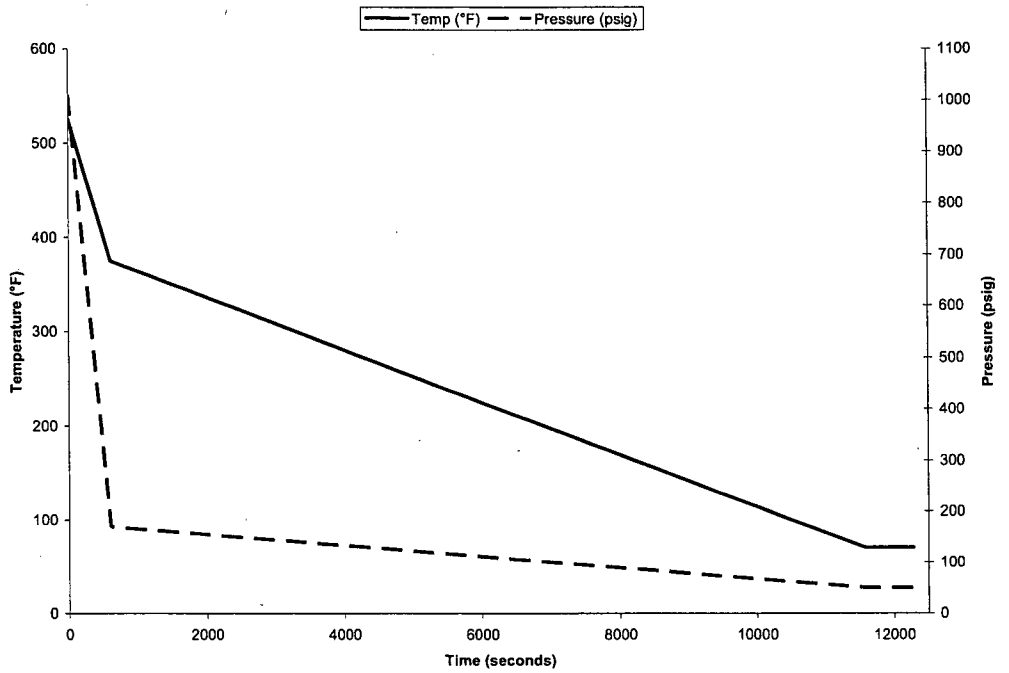

Figure 9: Transient 7 – SRV Blowdown

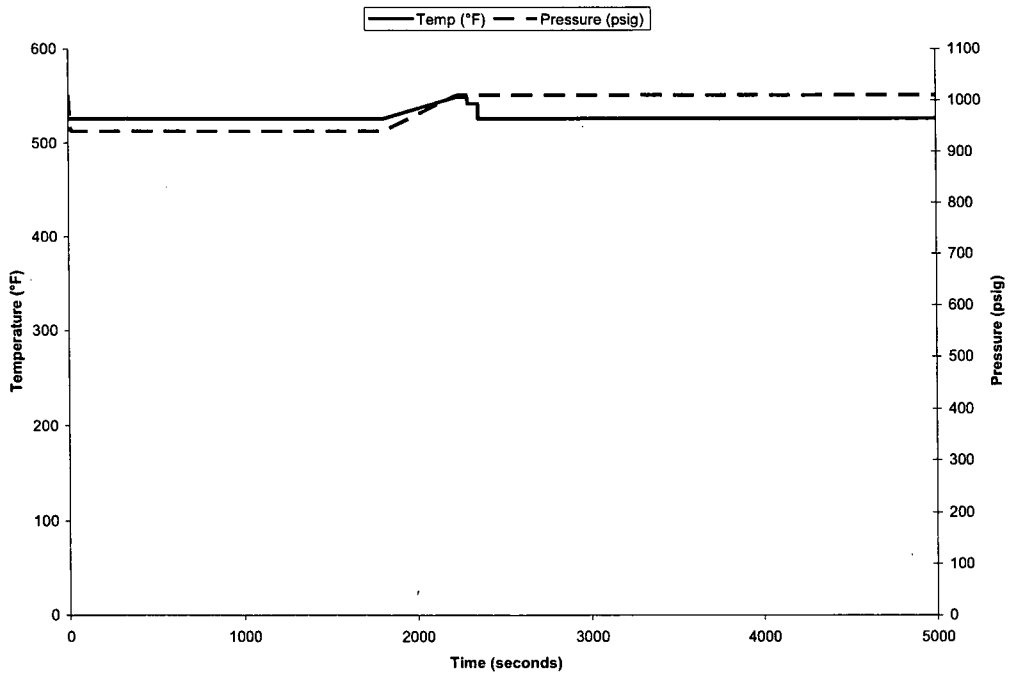

Figure 10: Transient 8 – SCRAM Other

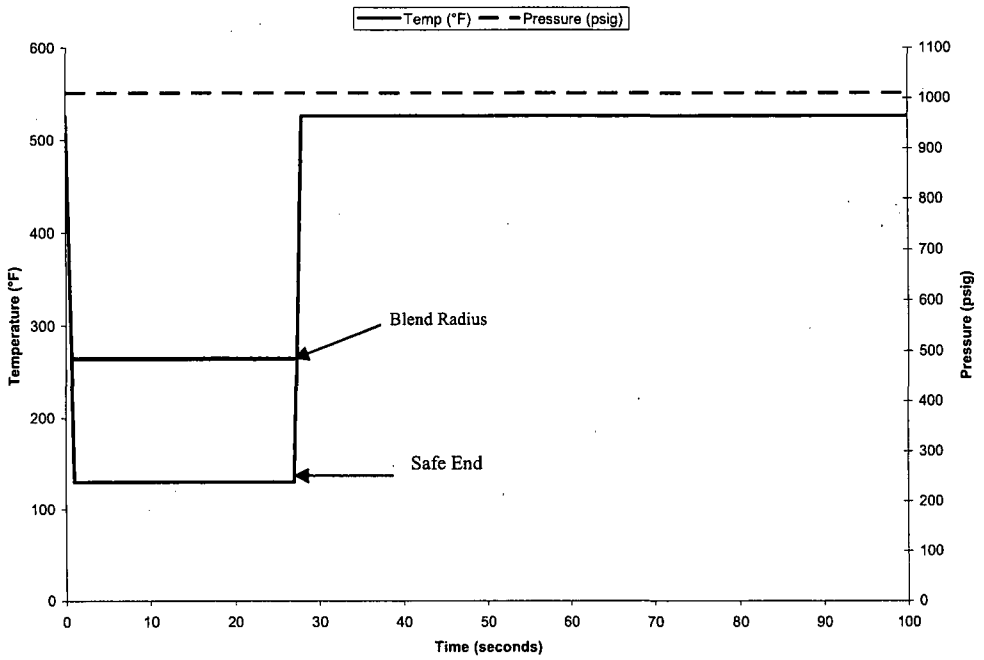

Figure 11: Transient 9 – Improper Startup

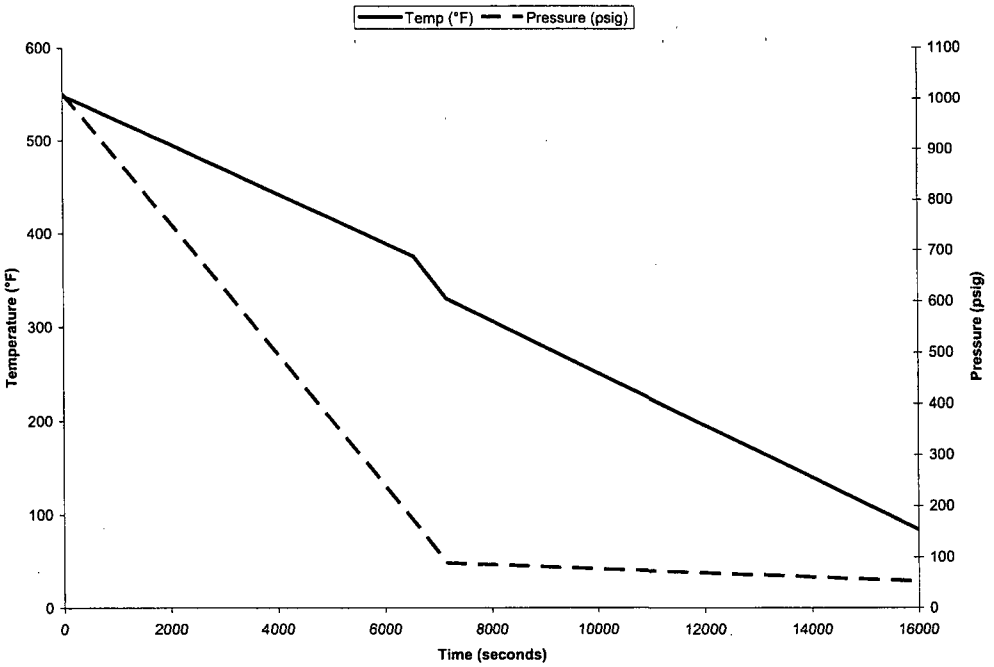

Figure 12: Transient 10 – Shutdown

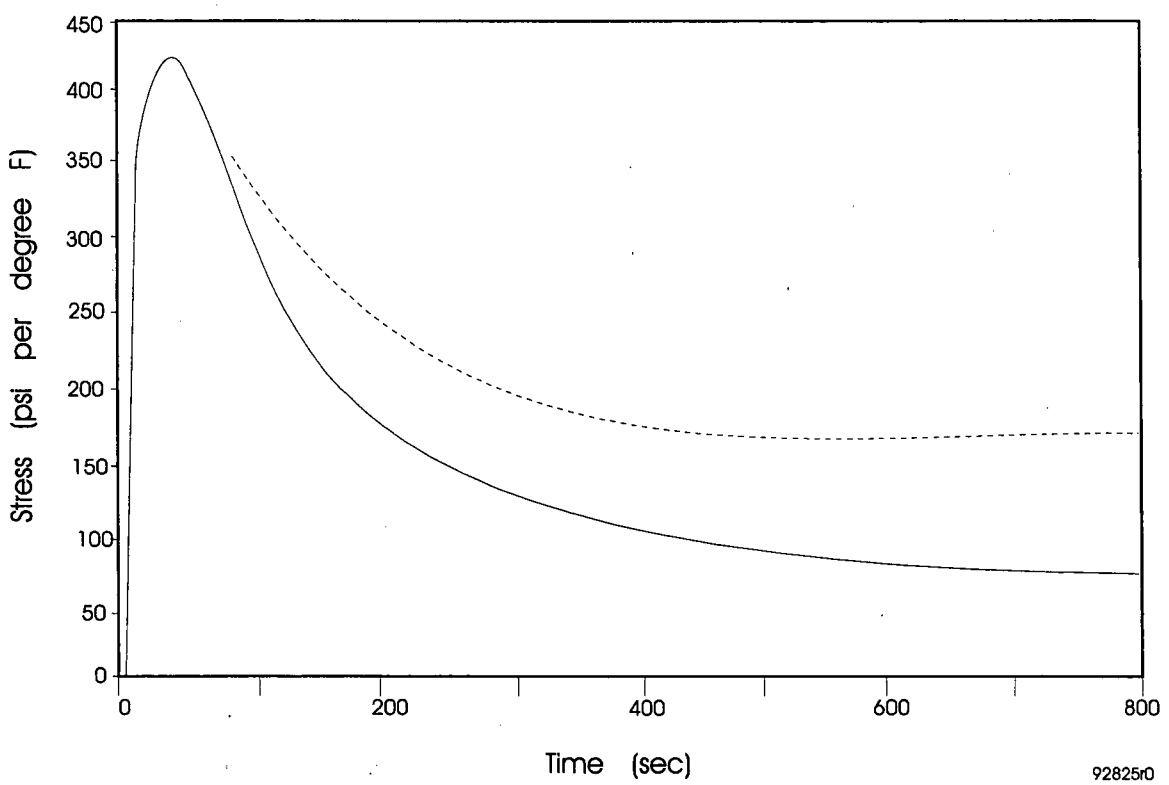

Note: A typical set of two Green's Functions is shown, each for a different set of heat transfer coefficients (representing different flow rate conditions).

Figure 13: Typical Green's Functions for Thermal Transient Stress

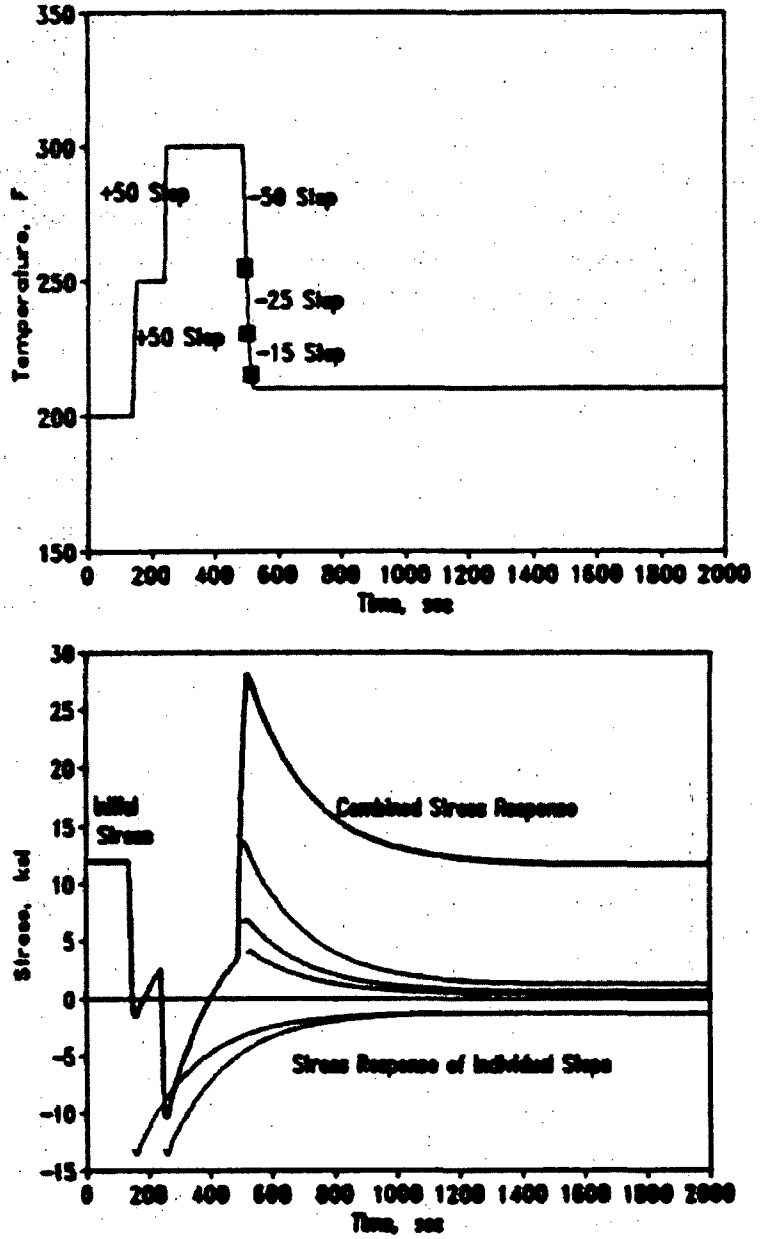

Figure 14: Typical Stress Response Using Green's Functions

APPENDIX A

SUMMARY OF OUTPUT FILES

VY_RON_T_T9.INP	Input File for Transient 9 Thermal Analysis	In Computer files
VY_RON_S_T9.INP	Input File for Transient 9 Stress Analysis	In Computer files
LFSE.OUT	Stress Output at Safe End	In Computer files
LFBR.OUT	Stress Output at Blend Radius	In Computer files
LFSE_INSIDE.RED	Stress Extracted at Safe End	In Computer files
LFBR_INSIDE.RED	Stress Extracted at Blend Radius	In Computer files
LFSE_T.XLS	Stress Results with Total Stress at Safe End	In Computer files
LFSE_M+B.XLS	Stress Results with Membrane plus Bending Stress at Safe End	In Computer files
LFBR_T.XLS	Stress Results with Total Stress at Blend Radius	In Computer files
LFBR_M+B.XLS	Stress Results with Membrane plus Bending Stress at Blend Radius	In Computer files
T9SE.OUT	Transient 9 Safe End stress output	In Computer files
T9BR.OUT	Transient 9 Blend Radius stress output	In Computer files
T9SE_Inside.RED	Transient 9 Stress Extracted at Safe End	In Computer files
T9BR_Inside.RED	Transient 9 Stress Extracted at Blend Radius	In Computer files
T9BR_M+B.xls	Transient 9 Stress Results with Membrane plus Bending Stress at Blend Radius	In Computer files
T9BR_T.xls	Transient 9 Stress Results with Total Stress at Blend Radius	In Computer files
T9SE_M+B.xls	Transient 9 Stress Results with Membrane plus Bending Stress at Safe End	In Computer files
T9SE_T.xls	Transient 9 Stress Results with Total Stress at Safe End	In Computer files
FATIGUE.OUT	Output file from FATIGUE.EXE	In Computer files
FATIGUE.inp	Input file for FATIGUE.EXE	In Computer files
TRANSNT_XX.inp	Input files for STRESS.EXE	In Computer files
P-V_XX.OUT	Output file from P-V.EXE	In Computer files

Structural Integrity Associates, Inc.	File No.: VY-16Q-307
CALCULATION PACKAGE	**Project No.:** VY-16Q

PROJECT NAME:

Environmental Fatigue Analysis of VYNPS

CONTRACT NO.:

10150394

CLIENT:	**PLANT:**
Entergy Nuclear Operations, Inc.	Vermont Yankee Nuclear Power Station

CALCULATION TITLE:

Recirculation Class 1 Piping Fatigue and EAF Analysis

Document Revision	Affected Pages	Revision Description	Project Manager Approval Signature & Date	Preparer(s) & Checker(s) Signatures & Date
0	1-16 A1-A51 B1-B5 Computer Files	Initial Issue	T. J. Herrmann 07/27/2007	R.V. Perry 07/27/2007 K.R. Evon 07/27/2007 P. Hirschberg 07/27/2007 C.J. Fourcade 07/27/2007

Table of Contents

1.0 OBJECTIVE 3
2.0 METHODOLOGY 3
2.1 Background 3
2.2 Design Transients and Fatigue Analysis 4
3.0 ASSUMPTIONS/DESIGN INPUTS 4
4.0 ANALYSIS 12
5.0 RESULTS OF ANALYSIS 14
6.0 REFERENCES 15
APPENDIX A PIPESTRESS INPUT FILES A1
APPENDIX B PIPESTRESS OUTPUT B1

List of Tables

Table 1: Material Properties [1] [3] 6
Table 2: Recirculation and RHR Piping Segment Numbers 7
Table 3: VY Thermal Transients 9
Table 4: Recirc/RHR Piping Size Information [3] 12
Table 5: Thermal Cycle Load Sets 13

List of Figures

Figure 1. Recirculation and RHR Piping Diagram 8

1.0 OBJECTIVE

The purpose of this calculation is to perform an ASME Section III, NB-3600 fatigue usage calculation (including environmental fatigue) for the Loop A NUREG/CR-6260 locations in the Reactor Recirculation (RR) and Residual Heat Removal (RHR) piping.

The fatigue calculation performed herein is not a certified ASME Code NB-3600 stress and fatigue analysis. Rather, it is an evaluation for the purposes of establishing fatigue usage to accommodate fatigue monitoring of the subject B31.1 piping. Although the PIPESTRESS program implements all ASME Code NB-3600 equations, only the fatigue usage results are utilized. All stress limit checks, although calculated by the program, are ignored since satisfactory stress limit checks were performed as a part of the already existing governing B31.1 stress analyses for all piping systems.

2.0 METHODOLOGY

2.1 Background

Since ASME Section III Design Specifications do not exist for the subject piping systems, SI developed transient definitions and expected number of cycles for the subject piping in a previous evaluation. These definitions are based on SI's experience in piping analysis at other BWR plants, as well as review of VY-specific operating procedures, and are appropriate for BWR-4 plants and tailored specifically to VY. Those transient definitions will reflect current plant operating conditions as shown in references [7 through 10]. Using the PIPESTRESS computer code [5], heat transfer analysis will be performed for the transients defined to establish the necessary parameters for use in an NB-3600 fatigue evaluation. This will result in a detailed usage factor calculation for the RR and RHR NUREG/CR-6260 locations from which to base the environmental fatigue evaluation.

2.2 Design Transients and Fatigue Analysis

The temperature time histories are obtained from the reactor thermal cycle diagrams [7] [8]. These diagrams also provide the changes in flow rate and system pressures. These temperatures and pressures were updated to account for EPU [9].

The computer program PIPESTRESS [5] was used, which is a full function, verified piping analysis package. The ASME Code methodology for fatigue analysis of Class 1 piping systems requires determination of the through-wall thermal gradient terms ΔT_1 (linear gradient), ΔT_2 (nonlinear gradient), and T_a-T_b (transition gradient) for each transient containing a non-trivial ramp rate. PIPESTRESS calculates these terms for each thermal transient. Load sets were then developed for the critical time points of the transients, that include loads due to pressure, thermal expansion, OBE seismic, and thermal gradient stresses. PIPESTRESS was then used to determine the range of primary plus secondary plus peak stresses for each load set pair, and calculate the cumulative fatigue usage for the design numbers of cycles.

3.0 ASSUMPTIONS/DESIGN INPUTS

The Code of construction for VY is ANSI B31.1, 1967 Edition [3, 10]. In order to take advantage of improvements in the ASME Code that result in a lower calculated fatigue usage, this evaluation is done to the ASME Boiler and Pressure Vessel Code, Section III, 1998 Edition with 2000 Addenda [1]. The 1998 Edition of Section III (with 2000 Addenda) has been accepted by the US NRC for use in design analyses. Although there are a few restrictions on the application of this Edition, they involve the use of optional increased allowables that are not being used in this calculation.

The piping analysis input information was based on references provided by VY. The ADLPIPE input file [6] was the source for the piping geometry, and pipe support locations and types. Additional piping support information was obtained from plant drawings [15]. The pipe size, schedule, insulation, and weight per foot, were obtained from [3] (page 10). The flow element located between the pump and RHR return tee was not included in the model. The weight of the element would have no significant impact on the analysis and the element is remote from any areas of severe thermal transients such as the RHR return tee. The weight of the contents was automatically added by the PIPESTRESS program. The design temperature and piping material was obtained from reference [3] (page 9). Table 1 summarizes the material properties used in this analysis.

Reference [6] contains an SSE response spectrum. This spectrum was conservatively used as the OBE spectrum in this analysis. Code case N-411 damping is utilized and directional loading is combined by SRSS [3] (page 20).

Per Reference [9] (Item 14, section 3.2.1), the normal recirculation flow per loop, post EPU, is 12.3Mlbm/hr (at 526°F). Flow is converted to gpm as follows:

$$Q = 12{,}300{,}000\frac{lbm}{hr}\left(\frac{1ft^3}{47.45lbm}\right)\left(\frac{7.48gal}{ft^3}\right)\left(\frac{1hr}{60\min}\right) = 32{,}316gpm$$

Where flow is stopped, a flow rate that gives an equivalent natural convection heat transfer coefficient is calculated.

The applicable transients to consider for the RR and RHR systems are shown in the thermal cycle diagrams [7] and [8]. Level C transients are not required to be included in the fatigue analysis per NB-3224.4. Reference [3] describes which transients are considered level C. Note that a transient for RHR initiation is not accounted for on these diagrams. In order to account for this transient, RHR temperature data from RFO 25 [11] was used to conservatively determine an appropriate temperature change while reference [12] was used to determine flow rates and pressures. Table 2 describes each section and Figure 1 shows the piping model with node numbers. Table 3 contains a list of applicable transients. (Note that the transient RHR initiation contains a section 3B. This section accounts for the portion of the recirculation pump discharge piping that is affected by this transient.) OBE cycles are not listed in Table 3 but are included as Load Set 26 for +OBE and Load Set 27 for –OBE. A review of shutdown cooling mode operation since the recirculation piping was replaced in 1986 was performed by the station and the number of cycles per loop was conservatively estimated to be 150 through year 60 [10]. Based on this, the cycle counts for the Recirculation piping were reduced by a factor of 150/300 (50%) for all transients with the exception of transients that have fewer than 10 transient cycles.

To ensure this cycle reduction adequately considered the potential impact on carbon steel RHR piping, the full number of transient cycles [7] was initially applied to the PIPESTRESS model and the highest CUF for the carbon steel portion of the RHR piping, which has not been replaced, was lower than the value obtained for the recirculation piping with reduced cycles. The Recirculation and RHR line sizes are specified in reference [3] and are shown in Table 4.

Table 1: Material Properties [1] [3]

ASTM A-106 Grade B (C-Si)							
Temperature (°F)	Young's Modulus ($x10^6$ psi)	Thermal Conductivity (Btu/hr-ft-°F)	Thermal Diffusivity (ft^2/hr)	Coefficient of Linear Thermal Expansion (in/100 ft)	Mean Coefficient of Thermal Expansion (10-6 /in/in/°F)	Design Stress Intensity (ksi)	Yield Strength (ksi)
70	29.5	27.5	0.529	0.00	6.40	20.0	35.0
100	29.3	27.6	0.512	0.20		20.0	35.0
200	28.8	27.6	0.486	1.00		20.0	32.1
300	28.3	27.2	0.453	1.90		20.0	31.0
400	27.7	26.7	0.428	2.80		20.0	29.9
500	27.3	25.9	0.398	3.70		18.9	28.5
600	26.7	25.0	0.374	4.70		17.3	26.8

ASME SA-376 TP 316 (16Cr-12Ni-2Mo)							
Temperature (°F)	Young's Modulus ($x10^6$ psi)	Thermal Conductivity (Btu/hr-ft-°F)	Thermal Diffusivity (ft^2/hr)	Coefficient of Linear Thermal Expansion (in/100 ft)	Mean Coefficient of Thermal Expansion (10-6 /in/in/°F)	Design Stress Intensity (ksi)	Yield Strength (ksi)
70	28.3	8.2	0.139	0.00	8.50	20.0	30.0
100	28.1	8.3	0.140	0.30		20.0	30.0
200	27.6	8.8	0.145	1.40		20.0	25.9
300	27.0	9.3	0.150	2.50		20.0	23.4
400	26.5	9.8	0.155	3.70		19.3	21.4
500	25.8	10.2	0.160	5.00		18.0	20.0
600	25.3	10.7	0.165	6.30		17.0	18.9

ASME SA-403 WP 316 (16Cr-12Ni-2Mo)							
Temperature (°F)	Young's Modulus ($x10^6$ psi)	Thermal Conductivity (Btu/hr-ft-°F)	Thermal Diffusivity (ft^2/hr)	Coefficient of Linear Thermal Expansion (in/100 ft)	Mean Coefficient of Thermal Expansion (10-6 /in/in/°F)	Design Stress Intensity (ksi)	Yield Strength (ksi)
70	28.3	8.2	0.139	0.00	8.50	20.0	30.0
100	28.1	8.3	0.140	0.30		20.0	30.0
200	27.6	8.8	0.145	1.40		20.0	25.9
300	27	9.3	0.150	2.50		20.0	23.4
400	26.5	9.8	0.155	3.70		18.7	21.4
500	25.8	10.2	0.160	5.00		17.5	20.0
600	25.3	10.7	0.165	6.30		16.4	18.9

The material properties applied in the analyses are taken from ASME Section II Part D 1998 Edition with 2000 Addenda. This is consistent with information provided in the Design Input Record (page 13 of VY EC No. 1773, SI File No. VY-16Q-209). The use of a later code edition than that used for the original design code is acceptable since later editions typically reflect more accurate material properties than was published in prior Code editions.

Table 2: Recirculation and RHR Piping Segment Numbers

Piping Region	Node Points		Description
	Start	End	
1	3	500	Outlet
2	500	50	Pump suction
3	150	210	Pump discharge
3B*	188	210	Down Stream of RHR Return
4	210	340	Inlet Header
	210	320	Inlet Header
5A	340	365	Riser
5B	340	345	Riser
5C	210	334	Riser
5D	320	325	Riser
5E	320	315	Riser
6A	365	366	Inlet Nozzle
6B	345	346	Inlet Nozzle
6C	334	336	Inlet Nozzle
6D	325	326	Inlet Nozzle
6E	315	316	Inlet Nozzle
7A	500	550	RHR Supply; tee to valve
7B	550	565	RHR Supply; valve to penetration
8	152	176	4" Bypass
9A	600	660	RHR Return; valve to tee
9B	660	675	RHR Return; penetration to valve

*Only applicable for RHR initiation

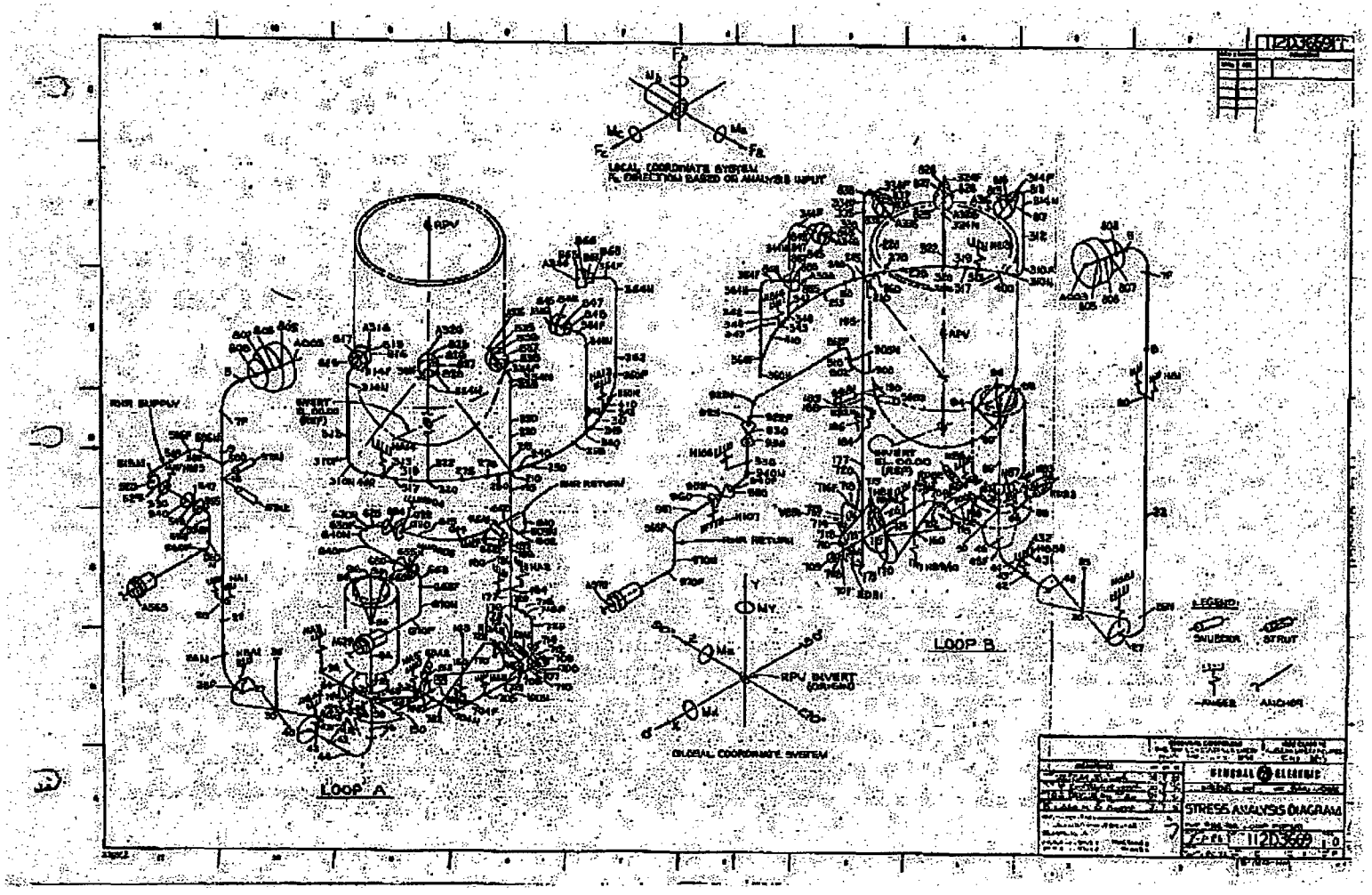

Figure 1. Recirculation and RHR Piping Diagram

Table 3: VY Thermal Transients

Transient Case	Description	Piping Region	Thermal Conditions [4] [7] [8] [10] Oper. Temp. (°F)	T_{init} (°F)	T_{final} (°F)	Time (sec.)	Rate (°F/hr)	Flow [9] (gpm)	Pressure Initial (psig)	Final (psig)	No. of Cycles [10]
1	Design Hydrotest (Leak Test) +	1	100	70	100	1800	60	2,262	0	1,100	60
		2	100	70	100	1800	60	2,262	0	1,100	
		3	100	70	100	1800	60	2,262	0	1,100	
		4	100	70	100	1800	60	905	0	1,100	
		5	100	70	100	1800	60	452	0	1,100	
		6	100	70	100	1800	60	452	0	1,100	
		7A	100	70	100	1800	60	0	0	1,100	
		7B	100	70	100	1800	60	0	0	120	
		8	100	70	100	1800	60	0	0	1,100	
		9A	100	70	100	1800	60	0	0	1,100	
		9B	100	70	100	1800	60	0	0	1,100	
2	Design Hydrotest (Leak Test) -	1	100	100	100	1800	0	2,262	1,100	50	60
		2	100	100	100	1800	0	2,262	1,100	50	
		3	100	100	100	1800	0	2,262	1,100	50	
		4	100	100	100	1800	0	905	1,100	50	
		5	100	100	100	1800	0	452	1,100	50	
		6	100	100	100	1800	0	452	1,100	50	
		7A	100	100	100	1800	0	0	1,100	50	
		7B	100	100	100	1800	0	0	120	50	
		8	100	100	100	1800	0	0	1,100	50	
		9A	100	100	100	1800	0	0	1,100	50	
		9B	100	100	100	1800	0	0	1,100	50	
3	Startup	1	549	100	549	16164	100	16,158	50	1,010	150
		2	549	100	549	16164	100	16,158	50	1,010	
		3	549	100	549	16164	100	16,158	50	1,035	
		4	549	100	549	16164	100	6,463	50	1,035	
		5	549	100	549	16164	100	3,232	50	1,035	
		6	549	100	549	16164	100	3,232	50	1,035	
		7A	549	100	549	16164	100	300	50	1,010	
		7B	150	100	150	16164	0	0	50	120	
		8	549	100	549	16164	100	168	50	1,035	
		9A	549	100	549	16164	100	0	50	1,035	
		9B	150	100	150	16164	11	0	50	1,035	
4	Turbine Roll & Increase to Rated Power + SCRAM - 1	1	542	549	542	0	STEP	32,316	1,010	1,010	290
		2	542	549	542	0	STEP	32,316	1,010	1,010	
		3	542	549	542	0	STEP	32,316	1,035	1,035	
		4	542	549	542	0	STEP	12,926	1,035	1,035	
		5	542	549	542	0	STEP	6,463	1,035	1,035	
		6	542	549	542	0	STEP	6,463	1,035	1,035	
		7A	542	549	542	0	STEP	364	1,010	1,010	
		7B	150	150	150	0	STEP	0	120	120	
		8	542	549	542	0	STEP	335	1,035	1,035	
		9A	542	549	542	0	STEP	520	1,035	1,035	
		9B	150	150	150	0	STEP	0	1,035	1,035	
5	Turbine Roll & Increase to Rated Power + SCRAM - 2	1	526	542	526	0	STEP	32,316	1,010	1,010	290
		2	526	542	526	0	STEP	32,316	1,010	1,010	
		3	526	542	526	0	STEP	32,316	1,035	1,035	
		4	526	542	526	0	STEP	12,926	1,035	1,035	
		5	526	542	526	0	STEP	6,463	1,035	1,035	
		6	526	542	526	0	STEP	6,463	1,035	1,035	
		7A	526	542	526	0	STEP	358	1,010	1,010	
		7B	150	150	150	0	STEP	0	120	120	
		8	526	542	526	0	STEP	335	1,035	1,035	
		9A	526	542	526	0	STEP	511	1,035	1,035	
		9B	150	150	150	0	STEP	0	1,035	1,035	
6	Loss of Feedwater Heater, Turbine Trip (+)	1	542	526	542	900	64	32,316	1,010	1,010	5 x 2
		2	542	526	542	900	64	32,316	1,010	1,010	
		3	542	526	542	900	64	32,316	1,035	1,035	
		4	542	526	542	900	64	12,926	1,035	1,035	
		5	542	526	542	900	64	6,463	1,035	1,035	
		6	542	526	542	900	64	6,463	1,035	1,035	
		7A	542	526	542	900	64	358	1,010	1,010	
		7B	150	150	150	900	0	0	120	120	
		8	542	526	542	900	64	335	1,035	1,035	
		9A	542	526	542	900	64	511	1,035	1,035	
		9B	150	150	150	900	0	0	1,035	1,035	
7	Loss of Feedwater Heater, Turbine Trip (-)	1	526	542	526	360	160	32,316	1,010	1,010	5 x 2
		2	526	542	526	360	160	32,316	1,010	1,010	
		3	526	542	526	360	160	32,316	1,035	1,035	
		4	526	542	526	360	160	12,926	1,035	1,035	
		5	526	542	526	360	160	6,463	1,035	1,035	
		6	526	542	526	360	160	6,463	1,035	1,035	
		7A	526	542	526	360	160	358	1,010	1,010	
		7B	150	150	150	360	0	0	120	120	
		8	526	542	526	360	160	335	1,035	1,035	
		9A	526	542	526	360	160	511	1,035	1,035	
		9B	150	150	150	360	0	0	1,035	1,035	

Table 3: VY Thermal Transients (continued)

Transient Case	Description	Piping Region	Thermal Conditions [4] [7] [8] [10] Oper. Temp. (°F)	T_{init} (°F)	T_{final} (°F)	Time (sec.)	Rate (°F/hr)	Flow [9] (gpm)	Pressure Initial (psig)	Pressure Final (psig)	No. of Cycles [10]
8	Loss of Feedwater Heater, Partial FW Heater Bypass (-)	1	516	526	516	0	STEP	32,316	1,010	1,010	35
		2	516	526	516	0	STEP	32,316	1,010	1,010	
		3	516	526	516	0	STEP	32,316	1,035	1,035	
		4	516	526	516	0	STEP	12,926	1,035	1,035	
		5	516	526	516	0	STEP	6,463	1,035	1,035	
		6	516	526	516	0	STEP	6,463	1,035	1,035	
		7A	516	526	516	0	STEP	351	1,010	1,010	
		7B	150	150	150	0	STEP	0	120	120	
		8	516	526	516	0	STEP	335	1,035	1,035	
		9A	516	526	516	0	STEP	502	1,035	1,035	
		9B	150	150	150	0	STEP	0	1,035	1,035	
9	Loss of Feedwater Heater, Partial FW Heater Bypass (+)	1	526	516	526	0	STEP	32,316	1,010	1,010	35
		2	526	516	526	0	STEP	32,316	1,010	1,010	
		3	526	516	526	0	STEP	32,316	1,035	1,035	
		4	526	516	526	0	STEP	12,926	1,035	1,035	
		5	526	516	526	0	STEP	6,463	1,035	1,035	
		6	526	516	526	0	STEP	6,463	1,035	1,035	
		7A	526	516	526	0	STEP	351	1,010	1,010	
		7B	150	150	150	0	STEP	0	120	120	
		8	526	516	526	0	STEP	335	1,035	1,035	
		9A	526	516	526	0	STEP	502	1,035	1,035	
		9B	150	150	150	0	STEP	0	1,035	1,035	
10	Loss of Feedwater Pumps (Isolation Valves Close) 1st step down	1	300	526	300	220	3698	600	1,190	1,135	5
		2	300	526	300	220	3698	600	1,190	1,135	
		3	300	526	300	220	3698	600	1,215	1,160	
		4	300	526	300	220	3698	400	1,215	1,160	
		5	300	526	300	220	3698	200	1,215	1,160	
		6	300	526	300	220	3698	200	1,215	1,160	
		7A	300	526	300	220	3698	306	1,190	1,135	
		7B	150	150	150	0.01	0	0	120	120	
		8	300	526	300	220	3698	6	1,215	1,160	
		9A	300	526	300	220	3698	437	1,215	1,160	
		9B	150	150	150	0.01	0	0	1,215	1,160	
11	Loss of Feedwater Pumps (Isolation Valves Close) 1st & 2nd step up	1	500	300	500	1980	364	600	885	1,135	5 X 2
		2	500	300	500	1980	364	600	885	1,135	
		3	500	300	500	1980	364	600	910	1,160	
		4	500	300	500	1980	364	400	910	1,160	
		5	500	300	500	1980	364	200	910	1,160	
		6	500	300	500	1980	364	200	910	1,160	
		7A	500	300	500	1980	364	301	885	1,135	
		7B	150	150	150	0.01	0	0	120	120	
		8	500	300	500	1980	364	6	910	1,160	
		9A	500	300	500	1980	364	429	910	1,160	
		9B	150	150	150	0.01	0	0	910	1,160	
12	Loss of Feedwater Pumps (Isolation Valves Close) 2nd & 3rd step down	1	300	500	300	180	4000	600	1,135	675	5 X 2
		2	300	500	300	180	4000	600	1,135	675	
		3	300	500	300	180	4000	600	1,160	700	
		4	300	500	300	180	4000	400	1,160	700	
		5	300	500	300	180	4000	200	1,160	700	
		6	300	500	300	180	4000	200	1,160	700	
		7A	300	500	300	180	4000	301	1,135	675	
		7B	150	150	150	0.01	0	0	120	121	
		8	300	500	300	180	4000	6	1,160	700	
		9A	300	500	300	180	4000	429	1,160	700	
		9B	150	150	150	0.01	0	0	1,160	700	
13	Loss of Feedwater Pumps (Isolation Valves Close) last step up	1	549	300	549	8964	100	16,158	240	1,010	5
		2	549	300	549	8964	100	16,158	240	1,010	
		3	549	300	549	8964	100	16,158	265	1,035	
		4	549	300	549	8964	100	6,463	265	1,035	
		5	549	300	549	8964	100	3,232	265	1,035	
		6	549	300	549	8964	100	3,232	265	1,035	
		7A	549	300	549	8964	100	310	240	1,010	
		7B	150	150	150	8964	100	0	120	120	
		8	549	300	549	8964	100	168	265	1,035	
		9A	549	300	549	8964	100	443	265	1,035	
		9B	150	150	150	8967	100	0	265	1,035	
14	Reduction to 0% Power	1	549	526	549	0	STEP	32,316	1,010	1,010	150
		2	549	526	549	0	STEP	32,316	1,010	1,010	
		3	549	526	549	0	STEP	32,316	1,035	1,035	
		4	549	526	549	0	STEP	12,926	1,035	1,035	
		5	549	526	549	0	STEP	6,463	1,035	1,035	
		6	549	526	549	0	STEP	6,463	1,035	1,035	
		7A	549	526	549	0	STEP	360	1,010	1,010	
		7B	150	150	150	0	STEP	0	120	120	
		8	549	526	549	0	STEP	335	1,035	1,035	
		9A	549	526	549	0	STEP	514	1,035	1,035	
		9B	150	150	150	0	STEP	0	1,035	1,035	

Table 3: VY Thermal Transients (continued)

Transient Case	Description	Piping Region	Thermal Conditions [4] [7] [8] [10] Oper. Temp. (°F)	T_{init} (°F)	T_{final} (°F)	Time (sec.)	Rate (°F/hr)	Flow [9] (gpm)	Pressure Initial (psig)	Pressure Final (psig)	No. of Cycles [10]
15	Shutdown 1	1	375	549	375	6264	100	16,158	1,010	170	150
		2	375	549	375	6264	100	16,158	1,010	170	
		3	375	549	375	6264	100	16,158	1,035	195	
		4	375	549	375	6264	100	6,463	1,035	195	
		5	375	549	375	6264	100	3,232	1,035	195	
		6	375	549	375	6264	100	3,232	1,035	195	
		7A	375	549	375	6264	100	320	1,035	170	
		7B	150	150	150	0.01	0	0	120	120	
		8	375	549	375	6264	100	168	1,035	195	
		9A	375	549	375	6264	100	458	1,035	195	
		9B	150	150	150	0.01	0	0	1,035	195	
16	Shutdown 2	1	330	375	330	600	270	16,158	170	90	150
		2	330	375	330	600	270	16,158	170	90	
		3	330	375	330	600	270	16,158	195	115	
		4	330	375	330	600	270	6,463	195	115	
		5	330	375	330	600	270	3,232	195	115	
		6	330	375	330	600	270	3,232	195	115	
		7A	330	375	330	600	270	282	170	90	
		7B	150	150	150	600	0	0	120	90	
		8	330	375	330	600	270	168	195	115	
		9A	330	375	330	600	270	403	195	115	
		9B	150	150	150	600	0	0	195	115	
17	Shutdown 3	1	225	330	225	3780	100	16,158	90	0	150
		2	225	330	225	3780	100	16,158	90	0	
		3	225	330	225	3780	100	16,158	115	25	
		4	225	330	225	3780	100	6,463	115	25	
		5	225	330	225	3780	100	3,232	115	25	
		6	225	330	225	3780	100	3,232	115	25	
		7A	225	330	225	3780	100	260	90	0	
		7B	150	150	150	0	0	0	90	0	
		8	225	330	225	3780	100	168	115	25	
		9A	225	330	225	3780	100	260	115	25	
		9B	150	150	150	0	0	0	115	25	
18	Shutdown 4 (RHR SDC Flow is on)	1	100	225	100	4500	100	22,858	0	0	150
		2	100	225	100	4500	100	16,158	0	0	
		3	100	225	100	4500	100	16,158	25	25	
		3B	100	225	100	4500	100	22,858	25	25	
		4	100	225	100	4500	100	9,143	25	25	
		5	100	225	100	4500	100	4,572	25	25	
		6	100	225	100	4500	100	4,572	25	25	
		7A	100	225	100	4500	100	6,700	0	0	
		7B	100	225	100	4500	100	6,700	0	0	
		8	100	225	100	4500	100	168	25	25	
		9A	100	225	100	4500	100	6,700	100	100	
		9B	100	225	100	4500	100	6,700	100	100	
19	Code Hydro	1	100	100	100	0.01	0	2,262	25	1,563	1
		2	100	100	100	0.01	0	2,262	25	1,563	
		3	100	100	100	0.01	0	2,262	25	1,563	
		4	100	100	100	0.01	0	905	25	1,563	
		5	100	100	100	0.01	0	452	25	1,563	
		6	100	100	100	0.01	0	452	25	1,563	
		7A	100	100	100	0.01	0	158	25	1,563	
		7B	100	100	100	0.01	0	0	0	450	
		8	100	100	100	0.01	0	23	25	1,563	
		9A	100	100	100	0.01	0	226	25	1,563	
		9B	100	100	100	0.01	0	0	25	1,563	
20	RHR Initiation (+)	1	225	225	225	0.01	0	22,858	0	0	150
		2	225	225	225	0.01	0	16,158	0	0	
		3	225	225	225	0.01	0	16,158	25	25	
		3B	225	180	225	60	2700	22,858	25	25	
		4	225	180	225	60	2700	9,143	25	25	
		5	225	180	225	60	2700	4,572	25	25	
		6	225	180	225	60	2700	4,572	25	25	
		7A	225	225	225	60	0	6,700	0	0	
		7B	225	150	225	60	4500	6,700	0	0	
		8	225	225	225	0.01	0	237	25	25	
		9A	225	70	225	60	9300	6,700	25	25	
		9B	225	70	225	60	9300	6,700	25	25	
21	RHR Initiation (-)	1	225	225	225	0.01	0	22,858	0	0	150
		2	225	225	225	0.01	0	16,158	0	0	
		3	225	225	225	0.01	0	16,158	25	25	
		3B	180	225	180	60	2700	22,858	25	25	
		4	180	225	180	60	2700	9,143	25	25	
		5	180	225	180	60	2700	4,572	25	25	
		6	180	225	180	60	2700	4,572	25	25	
		7A	225	225	225	60	0	6,700	0	0	
		7B	150	150	150	0.01	0	6,700	0	0	
		8	225	225	225	0.01	0	237	25	25	
		9A	70	225	70	60	9300	6,700	25	25	
		9B	70	150	70	60	9290	6,700	25	25	

Table 4: Recirc/RHR Piping Size Information [3]

Regions	1, 2	3	4	5	6	7A, 7B	8	9A, 9B
Piping Nom. O.D. (in.)	28.169	28.339	21.878	12.748	14.17	20	4.5	24
Piping Nom. Wall (in.)	1.244	1.339	1.043	0.685	1.395	1.031	0.3385	1.217
Pipe Weight[1] (lb/ft)	386.1	415.1	257.2	103.4	207.5	221.9	23.2	316.5

Note:

1. Weight of contents automatically added by the PIPESTRESS Program.

4.0 ANALYSIS

Through-wall thermal gradient terms were calculated by the PIPESTRESS program for all of the transients. Thermal transient cases were modeled for each transient, as shown in Table 3. Some transients were similar in nature and were lumped together and the number of cycles added together. Listings of the PIPESTRESS input files are included as Appendix A.

The forces and moments due to thermal expansion need to be included in the fatigue evaluation. The thermal expansion cases as analyzed by the piping program, PIPESTRESS, correspond to the end temperature and pressure of the transient. Table 5 lists the thermal expansion cases.

The material properties were obtained from the ASME Code Section III, 1998 Edition, Appendix I, with 2000 Addenda [1]. E and α are taken at 70°F, and k, ρ, and c_p are taken at the average temperature over the range of the individual transients.

The internal heat transfer coefficient h for the transients with flow occurring in the pipe is calculated based on the following relation for forced convection [13]:

$$h = 0.023\ Re^{0.8}\ Pr^{0.4}\ k/D$$

Where Re = Reynolds number
Pr = Prandtl number
k = Thermal conductivity
D = Pipe diameter

The heat transfer coefficients were calculated by PIPESTRESS using the above relation. The flow rates described for each transient in Section 3 were used. For the transients where flow is stopped, the natural convection heat transfer coefficient was used. The formula for h is [13]:

$$h = 0.55\,(Gr\,Pr)^{0.25} k/L$$

Where Gr = Grashof Number
L = Pipe diameter

PIPESTRESS only has the forced convection heat transfer formula built in, so an equivalent flow rate was determined that would give the same heat transfer coefficient as the free convection coefficient.

Since the replacement of the Recirculation piping [10], HWC conditions exist for 39% of the time, and NWC conditions exist for 61% of the time. This is based on 17.5 years of operation with NWC between March and July 1986 when the piping was replaced and November 2003 when HWC was implemented and the 46 years from March 1986 to the end of the period of extended operation in March 2032. Using the bounding EAF multipliers (8.36 for HWC and 15.35 for NWC) [14], an overall multiplier may be calculated as follows:

$$(15.35)0.61 + (8.36)0.39 = 12.62$$

Table 5: Thermal Cycle Load Sets

Load Set	Transient Case	Region Temperatures (°F)												Region Pressures (psig)			
		1	2	3	3B	4	5	6	7A	7B	8	9A	9B	1, 2, 7A	3, 4, 5, 6, 8, 9A, 9B	7B	3B
1	1	100	100	100	-	100	100	100	100	100	100	100	100	1,100	1,100	120	-
2	2	100	100	100	-	100	100	100	100	100	100	100	100	50	50	50	-
3	3	549	549	549	-	549	549	549	549	150	549	549	150	1,010	1,035	120	-
4	4	542	542	542	-	542	542	542	542	150	542	542	150	1,010	1,035	120	-
5	5	526	526	526	-	526	526	526	526	150	526	526	150	1,010	1,035	120	-
6	6	542	542	542	-	542	542	542	542	150	542	542	150	1,010	1,035	120	-
7	7	526	526	526	-	526	526	526	526	150	526	526	150	1,010	1,035	120	-
8	8	516	516	516	-	516	516	516	516	150	516	516	150	1,010	1,035	120	-
9	9	526	526	526	-	526	526	526	526	150	526	526	150	1,010	1,035	120	-
10	10	300	300	300	-	300	300	300	300	150	300	300	150	1,135	1,160	120	-
11	11	500	500	500	-	500	500	500	500	150	500	500	150	1,135	1,160	120	-
12	12	300	300	300	-	300	300	300	300	150	300	300	150	675	700	121	-
13	13	549	549	549	-	549	549	549	549	150	549	549	150	1,010	1,035	120	-
14	14	549	549	549	-	549	549	549	549	150	549	549	150	1,010	1,035	120	-
15	15	375	375	375	-	375	375	375	375	150	375	375	150	170	195	120	-
16	16	330	330	330	-	330	330	330	330	150	330	330	150	90	115	90	-
17	17	225	225	225	-	225	225	225	225	150	225	225	150	0	25	0	-
18	18	100	100	100	100	100	100	100	100	100	100	100	100	0	25	0	25
19	19	100	100	100	-	100	100	100	100	100	100	100	100	1,563	1,563	450	-
20	20	225	225	225	225	225	225	225	225	225	225	225	225	0	25	0	25
21	21	225	225	225	180	180	180	180	225	150	225	70	70	0	25	0	25

5.0 RESULTS OF ANALYSIS

To perform the fatigue analysis, program PIPESTRESS [5] was used. PIPESTRESS calculates the thermal expansion and seismic moments, the ASME Code Equation 10, 12, and 13 stresses, performs the thermal stress ratchet check, and performs fatigue analysis per Equation 11 and 14. For each operating state of the recirculation/RHR piping, load sets are created. A load set includes the coincident pressure, thermal expansion moment, through-wall thermal gradient terms, number of cycles, and temperature at which the allowable S_m is taken. In general, the pressures and thermal expansion moments are taken at the end point of the transient, the thermal gradients taken at the point of maximum total thermal gradient stress during the transient, and the S_m allowable is initially conservatively taken at the highest temperature of the transient. Table 5 lists the inputs to the load sets.

In calculating fatigue, the range of stress in going from one load set to another is determined. Since the Code assumes that any transient could follow any other, all pairs of load sets are evaluated to determine the range of stresses for the Code stress equations. The number of allowable cycles for each load set pair is determined. The incremental fatigue usage is obtained by dividing the number of design cycles by the allowable cycles. The incremental fatigue usages for all load set pairs are then summed to obtain the total fatigue usage.

The cumulative fatigue usage for the Loop A recirculation RHR return isolation valve-to-pipe location (Node 641), prior to considering environmental effects, is 0.0128. Taking into account environmental effects, the bounding multiplier for stainless steel is 12.62. This results in a total fatigue usage of 0.1615. (Note that since the RHR carbon steel piping has not been replaced, these results represent the full projected 60 year cycle count.)

The cumulative fatigue usage for the RHR return tee (Node 600), prior to considering environmental effects, is 0.0590. Taking into account environmental effects, the bounding multiplier for stainless steel is 12.62. This results in a total fatigue usage of 0.7446.

Appendix A contains the PIPESTRESS input files. Appendix B contains the fatigue usage summary for both locations.

6.0 REFERENCES

1. ASME Boiler and Pressure Vessel Code, Section III, 1998 Edition with 2000 Addenda.
2. ASME Boiler and Pressure Vessel Code, Section XI, 1998 Edition.
3. Vermont Yankee Calculation 23A5569, "Recirculation System Stress Analysis Loop A", Revision 0, SI File No. VY-05Q-227.
4. Email from Jim Fitzpatrick (Entergy) to Terry Herrmann (SI), "RE: RHR Thermal Transients," dated: June 29, 2007 11:19AM, SI File Number VY-09Q-209.
5. Program PIPESTRESS, Version 3.5.1+26, DST Computer Services, S.A., June 2004.
6. ADLPIPE Model Input Listing, Vermont Yankee Calculation VYC-2030, Rev. 0, "Temporary Shielding Recirculation & RHR Piping Loop A," File c2030n2, SI File No. W-VY-05Q-227.
7. "Reactor Thermal Cycles for 60 Years of Operation," Attachment 1 of Entergy Design Input Record (DIR) Revision 1, EC No. 1773, Revision 0, "Environmental Fatigue Analysis for Vermont Yankee Nuclear Power Station," SI File No. VY-16Q-209.
8. "Nozzle Thermal Cycles (Recirculation Outlet)," Attachment 1, page 4, of Entergy Design Input Record (DIR) Revision 1, EC No. 1773, Revision 0, "Environmental Fatigue Analysis for Vermont Yankee Nuclear Power Station," SI File No. VY-16Q-209.
9. Entergy Nuclear Report VY-RPT-05-00022, "Task T0100 Reactor Heat Balance EPU Task Report for ER-0401409", Revision 0, SI File No. VY-16Q-205.
10. Design Input Record (DIR) Revision 1, EC No. 1773, Revision 0, "Environmental Fatigue Analysis for Vermont Yankee Nuclear Power Station," SI File No. VY-16Q-209.
11. "RHR Shutdown Cooling Temperature Data," page 8, of Entergy Design Input Record (DIR) EC No. 1773, Revision 1, "Environmental Fatigue Analysis for Vermont Yankee Nuclear Power Station," SI File No. VY-16Q-209.
12. "RHR Shutdown Cooling Flow Rate and Pressure Data," page 9, of Entergy Design Input Record (DIR) Revision 1, EC No. 1773, Revision 0, "Environmental Fatigue Analysis for Vermont Yankee Nuclear Power Station," SI File No. VY-16Q-209.
13. Holman, J.P., *Heat Transfer*, Fifth Edition, McGraw-Hill, 1981.

14. SI Calculation, "Environmental Fatigue Evaluation of Reactor Recirculation Inlet Nozzle and Vessel Shell/Bottom Head," Revision 0, SI File Number VY-16Q-303.

15. VY Drawings, SI File No. VY-16Q-205:

    a. 5920-6801, Sheet 1, Revision 1.
    b. 5920-6802, Sheet 1, Revision 2, Sheet2, Revision 2, Sheet 3, Revision 3, Sheet 4, Revision 2, Sheet 5, Revision 2, Sheet 6, Revision 2.
    c. 5920-6808 Sheet 1, Revision 0.

APPENDIX A

PIPESTRESS Input Files

Input File	Description
Recirc_15.fre	Piping model and general input for reduced cycle count
RHR_15.fre	Piping model and general input for 60 year cycle count
Reg1.inp	Region 1 transient definitions
Reg2.inp	Region 2 transient definitions
Reg3.inp	Region 3 transient definitions
Reg4.inp	Region 4 transient definitions
Reg5.inp	Region 5 transient definitions
Reg6.inp	Region 6 transient definitions
Reg7A.inp	Region 7A transient definitions
Reg7B.inp	Region 7B transient definitions
Reg8.inp	Region 8 transient definitions
Reg9A.inp	Region 9A transient definitions
Reg9B.inp	Region 9B transient definitions

Recirc 15.fre

```
IDEN JB=3    *Job number (1 to 9999)
     CD=1    *1=ASME Class 1
     GR=-Y   *Direction of gravity
     VA=0    *0=Calculate            2=Verify
     IU=1    *Input units            1=USA
     OU=1    *Output units           1=USA
     CH=$    *Delimiter character
     AB=T    *FREE errors = abort
     PL=$Vermont Yankee$
     EN=$RVP$
TITL BL=3    *Modeling option:
             *  3 = uniform mass for static analysis
             *      lumped mass for dynamic analysis
             *      rotational inertia ignored
     GL=1    *Report forces/moment         0=Global     1=Local     2=G et L
     SU=1    *Support summary              0=No         1=Yes
     CV=15   *Code version - See Manual
     HS=1    *Highest 20 stress ratios for each case
     MD=1    *Hot modulus
     J6=1    *File generated by program
     TI=$Vermont Yankee Recirculation $
        $Fatigue Analysis$
FREQ RF=1 RP=8 FR=36 MP=20 RC=0 MX=70 TI=$SEISMIC$
*
*************************************
**** THERMAL CYCLE LOAD CASES****
*************************************
LCAS RF=0 CA=1 TY=0 TI=$LC-1$      *TC-1
LCAS RF=0 CA=2 TY=0 TI=$LC-2$      *TC-2
LCAS RF=0 CA=3 TY=0 TI=$LC-3$      *TC-3
LCAS RF=0 CA=4 TY=0 TI=$LC-4$      *TC-4
LCAS RF=0 CA=5 TY=0 TI=$LC-5$      *TC-5
LCAS RF=0 CA=6 TY=0 TI=$LC-6$      *TC-6
LCAS RF=0 CA=7 TY=0 TI=$LC-7$      *TC-7
LCAS RF=0 CA=8 TY=0 TI=$LC-8$      *TC-8
LCAS RF=0 CA=9 TY=0 TI=$LC-9$      *TC-9
LCAS RF=0 CA=10 TY=0 TI=$LC-10$    *TC-10
LCAS RF=0 CA=11 TY=0 TI=$LC-11$    *TC-11
LCAS RF=0 CA=12 TY=0 TI=$LC-12$    *TC-12
LCAS RF=0 CA=13 TY=0 TI=$LC-13$    *TC-13
LCAS RF=0 CA=14 TY=0 TI=$LC-14$    *TC-14
LCAS RF=0 CA=15 TY=0 TI=$LC-15$    *TC-15
LCAS RF=0 CA=16 TY=0 TI=$LC-16$    *TC-16
LCAS RF=0 CA=17 TY=0 TI=$LC-17$    *TC-17
LCAS RF=0 CA=18 TY=0 TI=$LC-18$    *TC-18
LCAS RF=0 CA=19 TY=0 TI=$LC-19$    *TC-19
LCAS RF=0 CA=20 TY=0 TI=$LC-20$    *TC-20
LCAS RF=0 CA=21 TY=0 TI=$LC-21$    *TC-21
LCAS RF=0 CA=22 TY=0 TI=$LC-22$    *TC-22
LCAS RF=0 CA=23 TY=0 TI=$LC-23$    *TC-23
LCAS RF=0 CA=24 TY=0 TI=$LC-24$    *TC-24
LCAS RF=0 CA=25 TY=0 TI=$LC-25$    *TC-25
*
*********************
**** WEIGHT CASES****
*********************
LCAS CA=101  RF=1  TY=3  TI=$OPERATING WEIGHT$
LCAS CA=102  RF=2  TY=4  TI=$HYDROTEST WEIGHT$
*
```

```
********************************
**** THERMAL TRANSIENT CASES****
********************************
TCAS CA=201 TI=$Design Hydrotest (+) $
TCAS CA=202 TI=$Design Hydrotest (-) $
TCAS CA=203 TI=$Startup              $
TCAS CA=204 TI=$TRoll & Inc. PWR1    $
TCAS CA=205 TI=$TRoll & Inc. PWR2    $
TCAS CA=206 TI=$LOFWH+TT PWR1        $
TCAS CA=207 TI=$LOFWH+TT PWR2        $
TCAS CA=208 TI=$LOFWH+PFWHTR Byp1    $
TCAS CA=209 TI=$LOFWH+PFWHTR Byp2    $
TCAS CA=210 TI=$LOFWP, ISO Cl DN 1   $
TCAS CA=211 TI=$LOFWP, ISO Cl UP 1   $
TCAS CA=212 TI=$LOFWP, ISO Cl DN 2   $
TCAS CA=213 TI=$LOFWP, ISO Cl UP 2   $
TCAS CA=214 TI=$Reduction to 0% PWR  $
TCAS CA=215 TI=$Shutdown1            $
TCAS CA=216 TI=$Shutdown2            $
TCAS CA=217 TI=$Shutdown3            $
TCAS CA=218 TI=$Shutdown4            $
TCAS CA=219 TI=$Code Hydrotest       $
TCAS CA=220 TI=$RHR Initiation UP    $
TCAS CA=221 TI=$RHR Initiation DN    $
TCAS CA=222 TI=$Inadvert. Inj. DOWN  $
TCAS CA=223 TI=$Inadvert. Inj. UP    $
TCAS CA=224 TI=$Single Relief BD DN  $
TCAS CA=225 TI=$Single Relief BD UP  $
*
**********************
**** SEISMIC CASES****
**********************
RCAS CA=103 EQ=3 EV=1 TY=1 SU=1 LO=1 FX=1 FY=1 FZ=1 TI=$OBE INERTIA$
*
** *************************
**** LOAD COMBINATION CASES *
** *************************
CCAS RF=1 CA=104      ME=1 FL=1  C1=103 CY=10  TI=$OBE$
CCAS RF=1 CA=401 SS=1 ME=1 EQ=3  C1=101 C2=103 TI=$EQUATION 9 LEVEL B$
CCAS RF=1 CA=402 SS=1 ME=3 F1=1  C1=103 C2=1   TI=$NORMAL+OBE$
CCAS RF=1 CA=403 SS=1 ME=3 F1=-1 C1=103 C2=1   TI=$NORMAL-OBE$
*
******************
**** LOAD SETS****
******************
*
LSET RF=1  FC=0 RP=1 CY=60   PR=1  MO=1  TR=201  TI=$Design Hydrotest (+)LS-1$
LSET RF=2  FC=0 RP=1 CY=60   PR=2  MO=2  TR=-202 TI=$Design Hydrotest (-)LS-2$
LSET RF=3  FC=0 RP=1 CY=150  PR=3  MO=3  TR=203  TI=$Startup             LS-3$
LSET RF=3  FC=0 RP=1 CY=290  PR=4  MO=4  TR=-204 TI=$TRoll & Inc. PWR1   LS-4$
LSET RF=4  FC=0 RP=1 CY=290  PR=5  MO=5  TR=-205 TI=$TRoll & Inc. PWR2   LS-5$
LSET RF=4  FC=0 RP=1 CY=10   PR=6  MO=6  TR=206  TI=$LOFWH+TT PWR1       LS-6$
LSET RF=4  FC=0 RP=1 CY=10   PR=7  MO=7  TR=-207 TI=$LOFWH+TT PWR2       LS-7$
LSET RF=5  FC=0 RP=1 CY=35   PR=8  MO=8  TR=-208 TI=$LOFWH+PFWHTR Byp1   LS-8$
LSET RF=5  FC=0 RP=1 CY=35   PR=9  MO=9  TR=209  TI=$LOFWH+PFWHTR Byp2   LS-9$
LSET RF=5  FC=0 RP=1 CY=5    PR=10 MO=10 TR=-210 TI=$LOFWP, ISO Cl DN 1  LS-10$
LSET RF=11 FC=0 RP=1 CY=10   PR=11 MO=11 TR=211  TI=$LOFWP, ISO Cl UP 1  LS-11$
LSET RF=11 FC=0 RP=1 CY=10   PR=12 MO=12 TR=-212 TI=$LOFWP, ISO Cl DN 2  LS-12$
LSET RF=3  FC=0 RP=1 CY=5    PR=13 MO=13 TR=213  TI=$LOFWP, ISO Cl UP 2  LS-13$
LSET RF=3  FC=0 RP=1 CY=150  PR=14 MO=14 TR=214  TI=$Reduction to 0% PWR LS-14$
```

```
LSET RF=5  FC=0 RP=1 CY=150  PR=15 MO=15 TR=-215 TI=$Shutdown1          LS-15$
LSET RF=15 FC=0 RP=1 CY=150  PR=16 MO=16 TR=-216 TI=$Shutdown2          LS-16$
LSET RF=16 FC=0 RP=1 CY=150  PR=17 MO=17 TR=-217 TI=$Shutdown3          LS-17$
LSET RF=20 FC=0 RP=1 CY=150  PR=18 MO=18 TR=-218 TI=$Shutdown4          LS-18$
LSET RF=19 FC=0 RP=1 CY=1    PR=19 MO=19 TR=219  TI=$Code Hydrotest     LS-19$
LSET RF=20 FC=0 RP=1 CY=150  PR=20 MO=20 TR=220  TI=$RHR Initiation UP  LS-20$
LSET RF=20 FC=0 RP=1 CY=150  PR=21 MO=21 TR=-221 TI=$RHR Initiation DN  LS-21$
LSET RF=5  FC=0 RP=1 CY=0    PR=22 MO=22 TR=-222 TI=$Inadvert. Inj. DOWN LS-22$
LSET RF=5  FC=0 RP=1 CY=0    PR=23 MO=23 TR=223  TI=$Inadvert. Inj. UP  LS-23$
LSET RF=23 FC=0 RP=1 CY=0    PR=24 MO=24 TR=-224 TI=$Single Relief BD DN LS-24$
LSET RF=24 FC=0 RP=1 CY=0    PR=25 MO=25 TR=225  TI=$Single Relief BD UP LS-25$
*
LSET RF=2 FC=0 CY=5 FL=1 PR=2 MO=402 TI=$NORMAL+OBE  LS-26$
LSET RF=2 FC=0 CY=5 FL=1 PR=2 MO=403 TI=$NORMAL-OBE  LS-27$
******
*FATG AT=500 AF=502
*FATG AT=600 AF=602
*
**************************
**** RESPONSE SPECTRA****
*************************
SPEC FS=OBE EV=1 ME=3 FP=0  TI=$RESPONSE$
      LV=1 DX=1 DY=1 DZ=1
      DI=X
        0.30/0.100  0.40/0.100  0.90/0.200  1.25/0.400  2.25/0.450  2.30/0.700
        3.30/0.700  4.40/0.750  4.41/0.900  4.75/1.100  5.20/1.100  5.80/1.600
        8.70/1.600 12.00/0.650 17.00/0.400 20.00/0.350 30.00/0.350 36.00/0.350
      DI=Y
        0.30/0.030  0.40/0.030  0.50/0.050  0.60/0.075  1.00/0.075  1.20/0.100
        2.00/0.220  2.40/0.350  3.50/0.350  3.60/0.300  5.30/0.300  5.75/0.330
        8.25/0.330  8.75/0.250 17.50/0.250 25.00/0.120 30.00/0.120 36.00/0.120
      DI=Z
        0.30/0.100  0.40/0.100  0.50/0.130  0.90/0.150  1.00/0.250  1.60/0.250
        1.90/0.600  3.50/0.600  3.75/0.700  4.40/0.700  4.50/0.800  6.25/1.500
        8.50/1.500 12.50/0.500 20.00/0.350 30.00/0.350 36.00/0.350
*
****************************
**** MATERIAL PROPERTIES ****
****************************
* ASTM A-106 Grade B, PIPE *
MATH CD=106     EX=0       TY=1     *C-Si
MATD TE=70      EH=29.5    EX=0.0   SM=20.0   SY=35
MATD TE=100     EH=29.3    EX=0.20  SM=20.0   SY=35
MATD TE=200     EH=28.8    EX=1.00  SM=20.0   SY=32.1
MATD TE=300     EH=28.3    EX=1.90  SM=20.0   SY=31
MATD TE=400     EH=27.7    EX=2.80  SM=20.0   SY=29.9
MATD TE=500     EH=27.3    EX=3.70  SM=18.9   SY=28.5
MATD TE=600     EH=26.7    EX=4.70  SM=17.3   SY=26.8
* ASME SA-376 Grade TP316, PIPE *
MATH CD=376.316 EX=0       TY=4     *16Cr-12Ni-2Mo
MATD TE=70      EH=28.3    EX=0.0   SM=20.0   SY=30.0
MATD TE=100     EH=28.1    EX=0.30  SM=20.0   SY=30.0
MATD TE=200     EH=27.6    EX=1.40  SM=20.0   SY=25.9
MATD TE=300     EH=27.0    EX=2.50  SM=20.0   SY=23.4
MATD TE=400     EH=26.5    EX=3.70  SM=19.3   SY=21.4
MATD TE=500     EH=25.8    EX=5.00  SM=18.0   SY=20.0
MATD TE=600     EH=25.3    EX=6.30  SM=17.0   SY=18.9
* ASME SA-403 Grade WP316, ELBOWS *
MATH CD=403.316 EX=0       TY=4     *16Cr-12Ni-2Mo
MATD TE=70      EH=28.3    EX=0.0   SM=20.0   SY=30.0
```

```
MATD TE=100     EH=28.1    EX=0.30  SM=20.0   SY=30.0
MATD TE=200     EH=27.6    EX=1.40  SM=20.0   SY=25.9
MATD TE=300     EH=27.0    EX=2.50  SM=20.0   SY=23.4
MATD TE=400     EH=26.5    EX=3.70  SM=18.7   SY=21.4
MATD TE=500     EH=25.8    EX=5.00  SM=17.5   SY=20.0
MATD TE=600     EH=25.3    EX=6.30  SM=16.4   SY=18.9
*** Cross Sectional Properties
CROS CD=1  OD=50.0   WT=8.87   MA=3977.2 *CALC. PER GE SPEC. NO. 23A5569 [3]
           SO=1      ST=1.0              *RECIRCULATION OUTLET NOZZLE
CROS CD=2  OD=37.85  WT=6.1    MA=2122.2 *CALC. PER GE SPEC. NO. 23A5569 [3]
           SO=1      ST=1.0
CROS CD=3  OD=28.875 WT=1.56   MA=484.9  *CALC. PER GE SPEC. NO. 23A5569 [3]
           SO=1      ST=1.0
CROS CD=4  OD=28.638 WT=1.45   MA=450.4  *CALC. PER GE SPEC. NO. 23A5569 [3]
           SO=1      ST=1.0
CROS CD=5  OD=28.169 WT=1.244  MA=386.1  *CALC. PER GE SPEC. NO. 23A5569 [3]
           SO=1      ST=1.0
CROS CD=7  OD=28.166 WT=2.125  MA=0.001  *VALVE
           SO=1      ST=1.0    KL=1
CROS CD=8  OD=42.507 WT=2.486  MA=0.001  *PUMP
           SO=.001   ST=.001   KL=1
CROS CD=11 OD=6.625  WT=0.432  MA=0.001  *PUMP RIGID STRUTS
           SO=0.001  ST=0.001  KL=1
CROS CD=13 OD=28.339 WT=1.339  MA=415.1  *CALC. PER GE SPEC. NO. 23A5569 [3]
           SO=1      ST=1
CROS CD=14 OD=28.339 WT=2.67   MA=0.001  *VALVE
           SO=1      ST=1.0    KL=1
CROS CD=15 OD=12.748 WT=0.685  MA=103.4  *CALC. PER GE SPEC. NO. 23A5569 [3]
           SO=1      ST=1.0
CROS CD=16 OD=14.17  WT=1.395  MA=207.5  *CALC. PER GE SPEC. NO. 23A5569 [3]
           SO=1      ST=1.0
CROS CD=17 OD=15.5   WT=2      MA=307.7  *CALC. PER GE SPEC. NO. 23A5569 [3]
           SO=1      ST=1.0
CROS CD=18 OD=21.88  WT=4.06   MA=803.2  *CALC. PER GE SPEC. NO. 23A5569 [3]
           SO=1      ST=1.0
CROS CD=19 OD=28.25  WT=7.25   MA=1673.1 *CALC. PER GE SPEC. NO. 23A5569 [3]
           SO=1      ST=1.0
CROS CD=20 OD=21.878 WT=1.043  MA=257.2  *CALC. PER GE SPEC. NO. 23A5569 [3]
           SO=1      ST=1.0
CROS CD=25 OD=20     WT=1.031  MA=221.9  *CALC. PER GE SPEC. NO. 23A5569 [3]
           SO=1      ST=1
CROS CD=26 OD=20     WT=1.875  MA=0.001  *VALVE
           SO=1      ST=1      KL=1
CROS CD=27 OD=4.5    WT=0.3385 MA=23.2   *CALC. PER GE SPEC. NO. 23A5569 [3]
           SO=1      ST=1      KL=1      *4 inch bypass line
CROS CD=28 OD=4.5    WT=0.67   MA=0.001  *VALVE V2-54A
           SO=1      ST=1      KL=1
CROS CD=29 OD=24     WT=1.217  MA=316.5  *CALC. PER GE SPEC. NO. 23A5569 [3]
           SO=1      ST=1
CROS CD=30 OD=24     WT=2.43   MA=0.001  *VALVE
           SO=1      ST=1      KL=1
CROS CD=40 OD=4.5    WT=0.3385 MA=0.001  *4 inch bypass STRUTS
           SO=0.001  ST=0.001  KL=1
CROS CD=41 OD=2.875  WT=0.276  MA=0.001  *STRUT RDA1, RDA5, & VBA1
           SO=0.001  ST=0.001  KL=1
CROS CD=42 OD=28.339 WT=1.339  MA=0.001  *RIGID FROM RECIRC ELBOW TO RDA1 STRUT
           SO=0.001  ST=0.001  KL=1
**********************
* STRUCTURE AND LOADS
**********************
```

```
*-----------------------------------------------------------------------------
DESN  TE=575.0  PR=1250.0 *Reference 12 GE Design Requirements Rpt VY-05Q-227
*-----------------------------------------------------------------------------
*-----------------------------------------------------------------------
*BEGIN REGION 1 TRANSIENT CARDS & GEOMETRY FROM RHR SUPPLY TO TEE
*-----------------------------------------------------------------
*
INCL FN=Z:\SISJ-PROJECTS\VY-16Q\Rev0\REG1.INP
*
* RUN   1     FROM ANCHOR TO REACTOR VESSEL N3B
*GROUP 1 FROM ANCHOR TO REACTOR VESSEL N3B
*NOTE
*NOTE NODE 003 - RECIRC SUCTION NOZZLE N1A (EL. 279'5 INCH)
*NOTE NODE 003 IS AT THE SAFE END TO VESSEL NOZZLE CONNECTION
*NOTE
*NOTE SAFE END FROM NODES 003 TO 808
*NOTE CONNECTION TO VESSEL AT NODE 003
*NOTE OD AND WALL THICKNESS FOR SAFE END TAKEN FROM GE CALC
*NOTE WEIGHT FOR SAFE END BASED ON THICKNESS
*NOTE
MATL CD=376.316
CROS CD=1
COOR PT=3    AX=0  AY=0  AZ=0
ANCH PT=3
AMVT    CA=1    PT=3    DX=0.0000  DY=0.0176  DZ=-0.0201
AMVT    CA=2    PT=3    DX=0.0000  DY=0.3141  DZ=-0.3602
AMVT    CA=3    PT=3    DX=0.0000  DY=0.3112  DZ=-0.3568
AMVT    CA=4    PT=3    DX=0.0000  DY=0.2995  DZ=-0.3434
AMVT    CA=5    PT=3    DX=0.0000  DY=0.3112  DZ=-0.3568
AMVT    CA=6    PT=3    DX=0.0000  DY=0.2995  DZ=-0.3434
AMVT    CA=7    PT=3    DX=0.0000  DY=0.2922  DZ=-0.3350
AMVT    CA=8    PT=3    DX=0.0000  DY=0.2995  DZ=-0.3434
AMVT    CA=9    PT=3    DX=0.0000  DY=0.1422  DZ=-0.1630
AMVT    CA=10   PT=3    DX=0.0000  DY=0.2807  DZ=-0.3218
AMVT    CA=11   PT=3    DX=0.0000  DY=0.1422  DZ=-0.1630
AMVT    CA=12   PT=3    DX=0.0000  DY=0.3141  DZ=-0.3602
AMVT    CA=13   PT=3    DX=0.0000  DY=0.3141  DZ=-0.3602
AMVT    CA=14   PT=3    DX=0.0000  DY=0.1928  DZ=-0.2521
AMVT    CA=15   PT=3    DX=0.0000  DY=0.1624  DZ=-0.1986
AMVT    CA=16   PT=3    DX=0.0000  DY=0.0946  DZ=-0.1084
AMVT    CA=17   PT=3    DX=0.0000  DY=0.0176  DZ=-0.0201
AMVT    CA=18   PT=3    DX=0.0000  DY=0.0176  DZ=-0.0201
AMVT    CA=19   PT=3    DX=0.0000  DY=0.0946  DZ=-0.1084
AMVT    CA=20   PT=3    DX=0.0000  DY=0.0946  DZ=-0.1084
AMVT    CA=21   PT=3    DX=0.0000  DY=0.0361  DZ=-0.0413
AMVT    CA=22   PT=3    DX=0.0000  DY=0.2995  DZ=-0.3434
AMVT    CA=23   PT=3    DX=0.0000  DY=0.1928  DZ=-0.2521
AMVT    CA=24   PT=3    DX=0.0000  DY=0.0176  DZ=-0.0201


*
TANG PT=805  DZ=-1.017  EW=1
CROS CD=2
TANG PT=806  DZ=-0.823  EW=1
CROS CD=3
TANG PT=807  DZ=-0.58  EW=1
CROS CD=4
TANG PT=808  DZ=-0.47
CROS CD=5
TANG PT=5    DZ=-5.59 EW=1
```

```
MATL CD=403.316
BRAD PT=7    RA=3.5 EW=1
MATL CD=376.316
TANG PT=9    DY=-6.69  EW=1
TANG PT=500  DY=-2.31
*---------------------------------------------
*END REGION 1 GEOMETRY FROM RHR SUPPLY TO TEE
*---------------------------------------------
*
*-----------------------------------------------------------------------
*BEGIN REGION 2 TRANSIENT CARDS & GEOMETRY FROM RHR SUPPLY TEE TO PUMP
*-----------------------------------------------------------------------
*GROUP 2 RHR SUPPLY TEE TO PUMP
INCL FN=Z:\SISJ-PROJECTS\VY-16Q\Rev0\REG2.INP
*
TANG PT=11   DY=-2.22  EW=1
CROS CD=5
TANG PT=12   DY=-1.78
TANG PT=20   DY=-6.77
TANG PT=22   DY=-3.25
TANG PT=25   DY=-15.49  EW=1
MATL CD=403.316
BRAD PT=26   RA=3.5  EW=1
MATL CD=376.316
TANG PT=27   DX=-3.3 DZ=1.27  EW=1
CROS CD=7
VALV PT=30   DX=-2.28 DZ=0.89 MA=10.368 PL=1
JUNC PT=30
VALV PT=40   DX=-2.31 DZ=0.9 PL=2  EW=1
JUNC PT=30
RIGD PT=35   DY=7
LUMP PT=35   MA=1.132
JUNC PT=40
CROS CD=5
TANG PT=42 DX=-1.18 DZ=0.46
TANG PT=43 DX=-0.55 DZ=0.21
TANG PT=44 DX=-3.31 DZ=1.28  EW=1
MATL CD=403.316
BRAD PT=46 RA=2.33  EW=1
MATL CD=376.316
CROS CD=8
TANG PT=50 DY=4.33  EW=0
LUMP PT=50 MA=28  *NOTE WEIGHT OF PUMP FLOODED 28K (EXCLUDING MOTOR)
TANG PT=75 DY=0.5
TANG PT=83 DY=2.13
TANG PT=86 DY=3.38
LUMP PT=86 MA=32  *NOTE TOTAL WEIGHT OF PUMP MOTOR 32000 LBS
TANG PT=90 DY=4.08 *TOP OF PUMP
*NOTE SNUBBERS ON TOP OF PUMPS WERE DELETED DURING
*NOTE THE RECIRC PIPE REPLACEMENT PROJECT
*NOTE - RIGID LINKS FOR CONSTANT SUPPORTS AT PUMP FOLLOW
*---------------------------
*END REGION 2 GEOMETRY FROM RHR SUPPLY TEE TO PUMP
*---------------------------
*
*----------------------------------------
*BEGIN REGION 3 TRANSIENT CARDS & GEOMETRY FROM PUMP DISCHARGE TO HEADER
*----------------------------------------
*GROUP 3 FROM PUMP DISCHARGE TO HEADER
INCL FN=Z:\SISJ-PROJECTS\VY-16Q\Rev0\REG3.INP
```

```
*
JUNC PT=50
CROS CD=8
RIGD PT=54 DX=1.06 DZ=1.06
RIGD PT=56 DX=1.06 DY=0.75 DZ=1.06  *NOTE CONSTANT SUPPORT HA3 AT NODE 56
JUNC PT=50
RIGD PT=66 DZ=-3.83
RIGD PT=69 DY=1                     *NOTE CONSTANT SUPPORT HA4 AT NODE 69
JUNC PT=50
CROS CD=8
RIGD PT=60 DX=-3.83
RIGD PT=63 DY=1                     *CONSTANT SUPPORT HA5 AT NODE 63
*
* *** CODING FOR PUMP RIGID STRUTS FOLLOW ***
*     CODED FROM PUMP CENTERLINE
CROS CD=11
JUNC PT=66
RIGD PT=15    DY=0.7071 DZ=-0.7071
*
JUNC PT=60
RIGD PT=16    DX=-0.7071 DY=0.7071
* *** END OF CODING FOR PUMP SUPPORTS ***
*PUMP INLET
CROS CD=8
JUNC PT=50
TANG PT=150 DX=-2.17
BRAN PT=151 DZ=2.333  TE=1
*NOTE PUMP DISCHARGE CONNECTION TO PIPE AT NODE 151
CROS CD=13
TANG PT=152 DZ=1.25
TANG PT=155 DZ=1  EW=1
CROS CD=14
VALV PT=160 PL=1 DX=0.0 DY=0.0  DZ=2.52 MA=6.8285
JUNC PT=160
RIGD PT=163 DX=0.0 DY=7.12 DZ=0.0
LUMP PT=163 MA=0.9715
JUNC PT=160
VALV PT=170 PL=2 DX=0.0 DY=0.0 DZ=6.18  EW=1
CROS CD=13
MATL CD=403.316
BRAD PT=175 RA=3.5  EW=1
MATL CD=376.316
TANG PT=176 DY=5.95
TANG PT=177 DY=4.42
*NOTE ***WEIGHT OF FLOW ELEMENT NOT INCLUDED***
*NOTE ***REF. DWG. 5920-6800 FOR DIMENSIONS***
TANG PT=184 DY=4.42
TANG PT=186 DY=3.02
TANG PT=188 DY=1.51
TANG PT=189 DY=0.74
TANG PT=190 DY=1.15  EW=1
TANG PT=600 DY=1.06

***INPUT FILE TO INCLUDE EFFECTS OF RHR INITIATION ON LINE NEAR RHR RETURN TO HEADER
INCL FN=Z:\SISJ-PROJECTS\VY-16Q\Rev0\REG3B.INP

JUNC PT=600
TANG PT=195 DY=2.08  EW=1
TANG PT=210 DX=0.0  DY=1.83 DZ=0.0  KL=1 *CENTER OF CROSS, RECIRC HEADER
*MUST HAVE INDI CARD FOR EACH MEMBER CONNECTED TO CROSS CENTER
```

```
*---------------------------
*END REGION 3 GEOMETRY FROM PUMP DISCHARGE TO HEADER
*---------------------------
*
*----------------------------------------
*BEGIN REGION 5 TRANSIENT CARDS & GEOMETRY RISER TO NOZZLE NODE 336
*----------------------------------------
*GROUP 5 RISER TO NOZZLE NODE 336
INCL FN=Z:\SISJ-PROJECTS\VY-16Q\Rev0\REG5.INP
*
*NOTE CROSS AND REDUCER DIMENSIONS TAKEN FROM 5920-6632 SHT.3
CROS CD=13
MATL CD=376.316
TANG PT=215 DX=0.0 DY=2.59  DZ=0.0  EW=0
CRED PT=220 DY=1.29  AN=30  EW=1  *AL=$CONC. REDUCER$
CROS CD=15
TANG PT=330 DY=4.58
TANG PT=335 DY=3.29  EW=1
MATL CD=403.316
BRAD PT=334 RA=1.5  EW=1
*---------------------------
*END REGION 5 GEOMETRY RISER TO NOZZLE NODE 336
*---------------------------
*
*----------------------------------------
*BEGIN REGION 6 TRANSIENT CARDS & GEOMETRY TO NOZZLE NODE 336
*----------------------------------------
*GROUP 6 TO NOZZLE NODE 336
INCL FN=Z:\SISJ-PROJECTS\VY-16Q\Rev0\REG6.INP
*
MATL CD=376.316
TANG PT=838 DX=3.875
CROS CD=16
TANG PT=837 DX=0.875  EW=1
CROS CD=17
TANG PT=836 DX=0.37  EW=1
CROS CD=18
TANG PT=835 DX=0.53  EW=1
CROS CD=19
TANG PT=336 DX=0.704  EW=1
NOZZ PT=336
AMVT    CA=1    PT=336  DX=-0.0201  DY=0.0246  DZ=0.0000
AMVT    CA=2    PT=336  DX=-0.3602  DY=0.4398  DZ=0.0000
AMVT    CA=3    PT=336  DX=-0.3568  DY=0.4316  DZ=0.0000
AMVT    CA=4    PT=336  DX=-0.3434  DY=0.4152  DZ=0.0000
AMVT    CA=5    PT=336  DX=-0.3568  DY=0.4050  DZ=0.0000
AMVT    CA=6    PT=336  DX=-0.3434  DY=0.2940  DZ=0.0000
AMVT    CA=7    PT=336  DX=-0.3350  DY=0.3229  DZ=0.0000
AMVT    CA=8    PT=336  DX=-0.3434  DY=0.2700  DZ=0.0000
AMVT    CA=9    PT=336  DX=-0.1630  DY=0.1991  DZ=0.0000
AMVT    CA=10   PT=336  DX=-0.3218  DY=0.1626  DZ=0.0000
AMVT    CA=11   PT=336  DX=-0.1630  DY=0.0246  DZ=0.0000
AMVT    CA=12   PT=336  DX=-0.3602  DY=0.4398  DZ=0.0000
AMVT    CA=13   PT=336  DX=-0.3602  DY=0.4316  DZ=0.0000
AMVT    CA=14   PT=336  DX=-0.2193  DY=0.4152  DZ=0.0000
AMVT    CA=15   PT=336  DX=-0.1862  DY=0.4050  DZ=0.0000
AMVT    CA=16   PT=336  DX=-0.1084  DY=0.2940  DZ=0.0000
AMVT    CA=17   PT=336  DX=-0.0201  DY=0.3229  DZ=0.0000
AMVT    CA=18   PT=336  DX=-0.0201  DY=0.2700  DZ=0.0000
AMVT    CA=19   PT=336  DX=-0.1084  DY=0.1991  DZ=0.0000
```

```
AMVT    CA=20   PT=336  DX=-0.0201  DY=0.1626  DZ=0.0000
AMVT    CA=21   PT=336  DX=-0.0413  DY=0.3229  DZ=0.0000
AMVT    CA=22   PT=336  DX=-0.3434  DY=0.2700  DZ=0.0000
AMVT    CA=23   PT=336  DX=-0.2211  DY=0.1991  DZ=0.0000
AMVT    CA=24   PT=336  DX=-0.0201  DY=0.1626  DZ=0.0000


*NOTE SAFE END FROM NODES 838 TO 336
*NOTE CONNECTION TO VESSEL AT NODE 336
*NOTE OD AND WALL THICKNESS FOR SAFE END TAKEN FROM GE CALC
*NOTE WEIGHT BASED ON THICKNESS
*----------------------------
*END REGION 6 GEOMETRY TO NOZZLE NODE 336
*----------------------------
*
*----------------------------------------
*BEGIN REGION 4 TRANSIENT CARDS & GEOMETRY HEADER TO NOZZLE NODE 366
*----------------------------------------
*GROUP 4 HEADER TO NOZZLE NODE 366
INCL FN=Z:\SISJ-PROJECTS\VY-16Q\Rev0\REG4.INP
*
JUNC PT=210
CROS CD=20
BRAN PT=240 DX=0.1786 DY=0.0 DZ=1.7
TANG PT=250 DX=0.3 DZ=2.853  EW=0
BRAD PT=255 RA=4.578  EW=0 *NOTE BEND RADIUS IS 4.578 FEET
TANG PT=340 DX=1.799 DZ=3.108
*----------------------------
*END REGION 4 GEOMETRY HEADER TO NOZZLE NODE 366
*----------------------------
*
*----------------------------------------
*BEGIN REGION 5 TRANSIENT CARDS & GEOMETRY RISER TO NOZZLE NODE 366
*----------------------------------------
*GROUP 5 RISER TO NOZZLE NODE 366
INCL FN=Z:\SISJ-PROJECTS\VY-16Q\Rev0\REG5.INP
*
TANG PT=349 DX=0.71 DZ=1.23  EW=0
CRED PT=347 DX=0.75 DZ=1.3  AN=30
CROS CD=15
TANG PT=343 DX=0.5525 DZ=0.957  EW=1
BRAD PT=410 RA=1.5  EW=1
TANG PT=360 DX=3.483 DZ=2.011  EW=1
MATL CD=403.316
BRAD PT=361 RA=1.5  EW=1
MATL CD=376.316
CROS CD=15
TANG PT=362 DY=3.18
TANG PT=364 DY=8.56  EW=1
MATL CD=403.316
BRAD PT=365 RA=1.5  EW=1
*----------------------------
*END REGION 5 GEOMETRY RISER TO NOZZLE NODE 366
*----------------------------

*----------------------------------------
*BEGIN REGION 6 TRANSIENT CARDS & GEOMETRY TO NOZZLE NODE 366
*----------------------------------------
*GROUP 6 TO NOZZLE NODE 366
INCL FN=Z:\SISJ-PROJECTS\VY-16Q\Rev0\REG6.INP
```

```
*
MATL CD=376.316
TANG PT=868 DX=1.8 DZ=-3.1
CROS CD=16
TANG PT=867 DX=0.4375 DZ=-0.76  EW=1
CROS CD=17
TANG PT=866 DX=0.185 DZ=-0.32  EW=1
CROS CD=18
TANG PT=865 DX=0.265 DZ=-0.46  EW=1
CROS CD=19
TANG PT=366 DX=0.352 DZ=-0.61  EW=1
NOZZ PT=366
AMVT    CA=1    PT=366  DX=-0.0101  DY=0.0246  DZ=0.0174
AMVT    CA=2    PT=366  DX=-0.1800  DY=0.4398  DZ=0.3120
AMVT    CA=3    PT=366  DX=-0.1783  DY=0.4357  DZ=0.3091
AMVT    CA=4    PT=366  DX=-0.1716  DY=0.4193  DZ=0.2974
AMVT    CA=5    PT=366  DX=-0.1783  DY=0.4357  DZ=0.3091
AMVT    CA=6    PT=366  DX=-0.1716  DY=0.4193  DZ=0.2974
AMVT    CA=7    PT=366  DX=-0.1674  DY=0.4091  DZ=0.2902
AMVT    CA=8    PT=366  DX=-0.1716  DY=0.4193  DZ=0.2974
AMVT    CA=9    PT=366  DX=-0.0815  DY=0.1991  DZ=0.1412
AMVT    CA=10   PT=366  DX=-0.1609  DY=0.3930  DZ=0.2788
AMVT    CA=11   PT=366  DX=-0.0815  DY=0.1991  DZ=0.1412
AMVT    CA=12   PT=366  DX=-0.1800  DY=0.4398  DZ=0.3120
AMVT    CA=13   PT=366  DX=-0.1800  DY=0.4398  DZ=0.3120
AMVT    CA=14   PT=366  DX=-0.1097  DY=0.2678  DZ=0.1899
AMVT    CA=15   PT=366  DX=-0.0931  DY=0.2275  DZ=0.1613
AMVT    CA=16   PT=366  DX=-0.0542  DY=0.1324  DZ=0.0939
AMVT    CA=17   PT=366  DX=-0.0101  DY=0.0246  DZ=0.0174
AMVT    CA=18   PT=366  DX=-0.0101  DY=0.0246  DZ=0.0174
AMVT    CA=19   PT=366  DX=-0.0542  DY=0.1324  DZ=0.0939
AMVT    CA=20   PT=366  DX=-0.0101  DY=0.0246  DZ=0.0174
AMVT    CA=21   PT=366  DX=-0.0207  DY=0.0505  DZ=0.0358
AMVT    CA=22   PT=366  DX=-0.1716  DY=0.4193  DZ=0.2974
AMVT    CA=23   PT=366  DX=-0.1105  DY=0.2700  DZ=0.1915
AMVT    CA=24   PT=366  DX=-0.0101  DY=0.0246  DZ=0.0174

*---------------------------
*END REGION 6 GEOMETRY TO NOZZLE NODE 366
*---------------------------

*----------------------------------------
*BEGIN REGION 4 TRANSIENT CARDS & GEOMETRY HEADER TO NOZZLES NODE 326 & 316
*----------------------------------------
*GROUP 4 HEADER TO NOZZLES NODE 326 & 316
INCL FN=Z:\SISJ-PROJECTS\VY-16Q\Rev0\REG4.INP
*
JUNC PT=210
CROS CD=20
BRAN PT=260 DX=0.1786 DY=0.0 DZ=-1.7 TE=2
TANG PT=270 DX=0.3 DZ=-2.853  EW=0
BRAD PT=275 RA=4.578  EW=0
TANG PT=320 DX=1.799 DZ=-3.108
*---------------------------
*END REGION 4 GEOMETRY HEADER TO NOZZLES NODE 326 & 316
*---------------------------

*----------------------------------------
*BEGIN REGION 5 TRANSIENT CARDS & GEOMETRY RISER TO NOZZLE NODE 316
*----------------------------------------
```

```
*GROUP 5 RISER TO NOZZLE NODE 316
INCL FN=Z:\SISJ-PROJECTS\VY-16Q\Rev0\REG5.INP
*
TANG PT=319 DX=0.71 DZ=-1.23  EW=1
CRED PT=317 DX=0.75 DZ=-1.3  AN=30
CROS CD=15
TANG PT=313 DX=0.5525 DZ=-0.957  EW=1
BRAD PT=400 RA=1.5  EW=1
TANG PT=310 DX=3.483 DZ=-2.011  EW=1
MATL CD=403.316
BRAD PT=311 RA=1.5  EW=1
MATL CD=376.316
CROS CD=15
TANG PT=312 DY=4.74
TANG PT=314 DY=6.99  EW=1
MATL CD=403.316
BRAD PT=315 RA=1.5  EW=1
*---------------------------
*END REGION 5 GEOMETRY RISER TO NOZZLE NODE 316
*---------------------------
*
*----------------------------------------
*BEGIN REGION 6 TRANSIENT CARDS & GEOMETRY TO NOZZLE NODE 316
*----------------------------------------
*GROUP 6 TO NOZZLE NODE 316
INCL FN=Z:\SISJ-PROJECTS\VY-16Q\Rev0\REG6.INP
*
MATL CD=376.316
TANG PT=818 DX=1.84 DZ=3.19
CROS CD=16
TANG PT=817 DX=0.4375 DZ=0.76  EW=1
CROS CD=17
TANG PT=816 DX=0.185 DZ=0.32  EW=1
CROS CD=18
TANG PT=815 DX=0.265 DZ=0.46  EW=1
CROS CD=19
TANG PT=316 DX=0.352 DZ=0.61  EW=1
NOZZ PT=316
AMVT    CA=1    PT=316  DX=-0.0101  DY=0.0246  DZ=-0.0174
AMVT    CA=2    PT=316  DX=-0.1800  DY=0.4398  DZ=-0.3120
AMVT    CA=3    PT=316  DX=-0.1783  DY=0.4357  DZ=-0.3091
AMVT    CA=4    PT=316  DX=-0.1716  DY=0.4193  DZ=-0.2974
AMVT    CA=5    PT=316  DX=-0.1783  DY=0.4357  DZ=-0.3091
AMVT    CA=6    PT=316  DX=-0.1716  DY=0.4193  DZ=-0.2974
AMVT    CA=7    PT=316  DX=-0.1674  DY=0.4091  DZ=-0.2902
AMVT    CA=8    PT=316  DX=-0.1716  DY=0.4193  DZ=-0.2974
AMVT    CA=9    PT=316  DX=-0.0815  DY=0.1991  DZ=-0.1412
AMVT    CA=10   PT=316  DX=-0.1609  DY=0.3930  DZ=-0.2788
AMVT    CA=11   PT=316  DX=-0.0815  DY=0.1991  DZ=-0.1412
AMVT    CA=12   PT=316  DX=-0.1800  DY=0.4398  DZ=-0.3120
AMVT    CA=13   PT=316  DX=-0.1800  DY=0.4398  DZ=-0.3120
AMVT    CA=14   PT=316  DX=-0.1097  DY=0.2678  DZ=-0.1899
AMVT    CA=15   PT=316  DX=-0.0931  DY=0.2275  DZ=-0.1613
AMVT    CA=16   PT=316  DX=-0.0542  DY=0.1324  DZ=-0.0939
AMVT    CA=17   PT=316  DX=-0.0101  DY=0.0246  DZ=-0.0174
AMVT    CA=18   PT=316  DX=-0.0101  DY=0.0246  DZ=-0.0174
AMVT    CA=19   PT=316  DX=-0.0542  DY=0.1324  DZ=-0.0939
AMVT    CA=20   PT=316  DX=-0.0101  DY=0.0246  DZ=-0.0174
AMVT    CA=21   PT=316  DX=-0.0207  DY=0.0505  DZ=-0.0358
AMVT    CA=22   PT=316  DX=-0.1716  DY=0.4193  DZ=-0.2974
```

```
AMVT    CA=23   PT=316  DX=-0.1105  DY=0.2700  DZ=-0.1915
AMVT    CA=24   PT=316  DX=-0.0101  DY=0.0246  DZ=-0.0174
*---------------------------
*END REGION 6 GEOMETRY TO NOZZLE NODE 316
*---------------------------
*
*----------------------------------------
*BEGIN REGION 5 TRANSIENT CARDS & GEOMETRY RISER TO NOZZLE NODE 346
*----------------------------------------
*GROUP 5 RISER TO NOZZLE NODE 346
INCL FN=Z:\SISJ-PROJECTS\VY-16Q\Rev0\REG5.INP
*
JUNC PT=340
CROS CD=15
BRAN PT=342 DY=1.36  TE=2
TANG PT=344 DY=10.39  EW=0
MATL CD=403.316
BRAD PT=345 RA=1.5  EW=1
*---------------------------
*END REGION 5 GEOMETRY RISER TO NOZZLE NODE 346
*---------------------------
*
*----------------------------------------
*BEGIN REGION 6 TRANSIENT CARDS & GEOMETRY TO NOZZLE NODE 346
*----------------------------------------
*GROUP 6 TO NOZZLE NODE 346
INCL FN=Z:\SISJ-PROJECTS\VY-16Q\Rev0\REG6.INP
*
MATL CD=376.316
TANG PT=848 DX=3.17 DZ=-1.83
CROS CD=16
TANG PT=847 DX=0.758 DZ=-0.4375  EW=1
CROS CD=17
TANG PT=846 DX=0.32 DZ=-0.185  EW=1
CROS CD=18
TANG PT=845 DX=0.46 DZ=-0.265  EW=1
CROS CD=19
TANG PT=346 DX=0.61 DZ=-0.352  EW=1
NOZZ PT=346
AMVT    CA=1    PT=346  DX=-0.0174  DY=0.0246  DZ=0.0101
AMVT    CA=2    PT=346  DX=-0.3120  DY=0.4398  DZ=0.1800
AMVT    CA=3    PT=346  DX=-0.3091  DY=0.4357  DZ=0.1783
AMVT    CA=4    PT=346  DX=-0.2974  DY=0.4193  DZ=0.1716
AMVT    CA=5    PT=346  DX=-0.3091  DY=0.4357  DZ=0.1783
AMVT    CA=6    PT=346  DX=-0.2974  DY=0.4193  DZ=0.1716
AMVT    CA=7    PT=346  DX=-0.2902  DY=0.4091  DZ=0.1674
AMVT    CA=8    PT=346  DX=-0.2974  DY=0.4193  DZ=0.1716
AMVT    CA=9    PT=346  DX=-0.1412  DY=0.1991  DZ=0.0815
AMVT    CA=10   PT=346  DX=-0.2788  DY=0.3930  DZ=0.1609
AMVT    CA=11   PT=346  DX=-0.1412  DY=0.1991  DZ=0.0815
AMVT    CA=12   PT=346  DX=-0.3120  DY=0.4398  DZ=0.1800
AMVT    CA=13   PT=346  DX=-0.3120  DY=0.4398  DZ=0.1800
AMVT    CA=14   PT=346  DX=-0.1899  DY=0.2678  DZ=0.1097
AMVT    CA=15   PT=346  DX=-0.1613  DY=0.2275  DZ=0.0931
AMVT    CA=16   PT=346  DX=-0.0939  DY=0.1324  DZ=0.0542
AMVT    CA=17   PT=346  DX=-0.0174  DY=0.0246  DZ=0.0101
AMVT    CA=18   PT=346  DX=-0.0174  DY=0.0246  DZ=0.0101
AMVT    CA=19   PT=346  DX=-0.0939  DY=0.1324  DZ=0.0542
AMVT    CA=20   PT=346  DX=-0.0174  DY=0.0246  DZ=0.0101
AMVT    CA=21   PT=346  DX=-0.0358  DY=0.0505  DZ=0.0207
```

```
AMVT    CA=22   PT=346  DX=-0.2974  DY=0.4193  DZ=0.1716
AMVT    CA=23   PT=346  DX=-0.1915  DY=0.2700  DZ=0.1105
AMVT    CA=24   PT=346  DX=-0.0174  DY=0.0246  DZ=0.0101
*---------------------------
*END REGION 6 GEOMETRY TO NOZZLE NODE 346
*---------------------------
*
*----------------------------------------
*BEGIN REGION 5 TRANSIENT CARDS & GEOMETRY RISER TO NOZZLE NODE 326
*----------------------------------------
*GROUP 5 RISER TO NOZZLE NODE 326
INCL FN=Z:\SISJ-PROJECTS\VY-16Q\Rev0\REG5.INP
*
JUNC PT=320
CROS CD=15
BRAN PT=322 DY=1.42  TE=2
TANG PT=324 DY=10.33  EW=1
MATL CD=403.316
BRAD PT=325 RA=1.5  EW=1
*---------------------------
*END REGION 5 GEOMETRY RISER TO NOZZLE NODE 326
*---------------------------
*
*----------------------------------------
*BEGIN REGION 6 TRANSIENT CARDS & GEOMETRY TO NOZZLE NODE 326
*----------------------------------------
*GROUP 6 TO NOZZLE NODE 326
INCL FN=Z:\SISJ-PROJECTS\VY-16Q\Rev0\REG6.INP
*
MATL CD=376.316
TANG PT=828 DX=3.18 DZ=1.84
CROS CD=16
TANG PT=827 DX=0.758 DZ=0.4375  EW=1
CROS CD=17
TANG PT=826 DX=0.32 DZ=0.185  EW=1
CROS CD=18
TANG PT=825 DX=0.46 DZ=0.265  EW=1
CROS CD=19
TANG PT=326 DX=0.61 DZ=0.352  EW=1
NOZZ PT=326
AMVT    CA=1    PT=326  DX=-0.0174  DY=0.0246  DZ=-0.0101
AMVT    CA=2    PT=326  DX=-0.3120  DY=0.4398  DZ=-0.1800
AMVT    CA=3    PT=326  DX=-0.3091  DY=0.4357  DZ=-0.1783
AMVT    CA=4    PT=326  DX=-0.2974  DY=0.4193  DZ=-0.1716
AMVT    CA=5    PT=326  DX=-0.3091  DY=0.4357  DZ=-0.1783
AMVT    CA=6    PT=326  DX=-0.2974  DY=0.4193  DZ=-0.1716
AMVT    CA=7    PT=326  DX=-0.2902  DY=0.4091  DZ=-0.1674
AMVT    CA=8    PT=326  DX=-0.2974  DY=0.4193  DZ=-0.1716
AMVT    CA=9    PT=326  DX=-0.1412  DY=0.1991  DZ=-0.0815
AMVT    CA=10   PT=326  DX=-0.2788  DY=0.3930  DZ=-0.1609
AMVT    CA=11   PT=326  DX=-0.1412  DY=0.1991  DZ=-0.0815
AMVT    CA=12   PT=326  DX=-0.3120  DY=0.4398  DZ=-0.1800
AMVT    CA=13   PT=326  DX=-0.3120  DY=0.4398  DZ=-0.1800
AMVT    CA=14   PT=326  DX=-0.1899  DY=0.2678  DZ=-0.1097
AMVT    CA=15   PT=326  DX=-0.1613  DY=0.2275  DZ=-0.0931
AMVT    CA=16   PT=326  DX=-0.0939  DY=0.1324  DZ=-0.0542
AMVT    CA=17   PT=326  DX=-0.0174  DY=0.0246  DZ=-0.0101
AMVT    CA=18   PT=326  DX=-0.0174  DY=0.0246  DZ=-0.0101
AMVT    CA=19   PT=326  DX=-0.0939  DY=0.1324  DZ=-0.0542
AMVT    CA=20   PT=326  DX=-0.0174  DY=0.0246  DZ=-0.0101
```

```
AMVT    CA=21   PT=326  DX=-0.0358  DY=0.0505  DZ=-0.0207
AMVT    CA=22   PT=326  DX=-0.2974  DY=0.4193  DZ=-0.1716
AMVT    CA=23   PT=326  DX=-0.1915  DY=0.2700  DZ=-0.1105
AMVT    CA=24   PT=326  DX=-0.0174  DY=0.0246  DZ=-0.0101
*---------------------------
*END REGION 6 GEOMETRY TO NOZZLE NODE 326
*---------------------------
*
*----------------------------------------
*BEGIN REGION 7A TRANSIENT CARDS & GEOMETRY TO RHR SUPPLY VALVE NODE 550
*----------------------------------------
*GROUP 7 TO RHR SUPPLY VALVE NODE 550
INCL FN=Z:\SISJ-PROJECTS\VY-16Q\Rev0\REG7A.INP
*
MATL CD=376.316
JUNC PT=500
CROS CD=25
BRAN PT=502 DX=1.67  EW=0  TE=1
TANG PT=506 DX=2.53  EW=0
MATL CD=403.316
BRAD PT=507 RA=1.67  EW=1
MATL CD=376.316
TANG PT=508 DZ=-4.01
TANG PT=515 DZ=-4.53  EW=1
MATL CD=403.316
BRAD PT=520 RA=1.67  EW=1
MATL CD=376.316
CROS CD=26
VALV PT=525 DX=-3.34 PL=1
JUNC PT=525
VALV PT=530 DX=-1.99 PL=2  EW=1
JUNC PT=525
RIGD PT=526 DY=2.5
LUMP PT=526 MA=7.569
JUNC PT=530
CROS CD=25
TANG PT=540 DX=-1.13  EW=1
CROS CD=26
VALV PT=545 DX=-1.97 PL=1
JUNC PT=545
RIGD PT=547 DY=2.5
LUMP PT=547 MA=7.355
JUNC PT=545
VALV PT=550 DX=-1.98 PL=2  EW=1
*---------------------------
*END REGION 7A GEOMETRY TO RHR SUPPLY VALVE NODE 550
*---------------------------
*
*----------------------------------------
*BEGIN REGION 7B TRANSIENT CARDS & GEOMETRY FROM RHR SUPPLY VALVE TO PENET. NODE 565
*----------------------------------------
*GROUP 17 FROM RHR SUPPLY VALVE TO PENET. NODE 565
INCL FN=Z:\SISJ-PROJECTS\VY-16Q\Rev0\REG7B.INP
*
CROS CD=25
MATL CD=106
TANG PT=555 DX=-3.36  EW=1
BRAD PT=556 RA=1.67  EW=1
TANG PT=560 DY=-10.17  EW=1
BRAD PT=561 RA=1.67  EW=1
```

```
TANG PT=563 DZ=-6.92
TANG PT=565 DZ=-6.92
*---------------------------
*END REGION 7B GEOMETRY FROM RHR SUPPLY VALVE TO PENET. NODE 565
*---------------------------
*
*----------------------------------------
*BEGIN REGION 8 TRANSIENT CARDS & GEOMETRY FOR 4 INCH BYPASS
*----------------------------------------
*GROUP 8 4 INCH BYPASS
INCL FN=Z:\SISJ-PROJECTS\VY-16Q\Rev0\REG8.INP
*
*NOTE CODING FOR 4 INCH BYPASS STARTS HERE
JUNC PT=152
CROS CD=27
MATL CD=376.316
BRAN PT=700 DX=-1.19  TE=4
TANG PT=702 DX=-0.61
TANG PT=703 DX=-1.43  EW=0
MATL CD=403.316
BRAD PT=704 RA=0.5  EW=0
MATL CD=376.316
TANG PT=705 DZ=5.08
*NOTE CONSTANT SUPPORT HA11 AT NODE 705
TANG PT=721 DZ=1.12
TANG PT=706 DZ=2.47
TANG PT=707 DZ=1.03
TANG PT=708 DZ=0.34
TANG PT=709 DZ=0.38
JUNC PT=707
BRAN PT=710 DY=0.34 TE=1
CROS CD=28
VALV PT=712 DY=0.71 MA=0.3669 PL=1  *AL=$VALVE V2-54A$
VALV PT=715 DZ=-3.5 MA=0.1831 PL=3
JUNC PT=712
VALV PT=714 DY=0.71          PL=2
CROS CD=27
TANG PT=723 DY=4.19
MATL CD=403.316
BRAD PT=716 RA=0.5
MATL CD=376.316
TANG PT=718 DX=1.48
TANG PT=720 DX=0.56
BRAN PT=176 DX=1.19  TE=4
************CODING FOR STRUTS RDA5 AND VAB1 FOLLOW
JUNC PT=170
CROS CD=40  *OD=4.5 inch
RIGD PT=725 DP=0 DX=-0.583 DY=1.84  *AL=$RDA5$
CROS CD=41  *OD=2.875 inch
RIGD PT=715 DP=0 DX=-2.67 DY=-0.79
RIGD PT=721 DP=0 DY=-1.05  *AL=$VAB1$
*************CODING FOR RDA1 STRUT FOLLOWS
CROS CD=42  *OD=28.339 inch
JUNC PT=175
RIGD PT=173 DP=0 DY=-3.5 DZ=0.34
CROS CD=41  *OD=2.875 inch
RIGD PT=708 DP=0 DX=-3.21  *AL=$RDA1$
*---------------------------
*END REGION 8 GEOMETRY  FOR 4 INCH BYPASS
*---------------------------
```

```
*
*----------------------------------------
*BEGIN REGION 9A TRANSIENT CARDS & GEOMETRY FOR RHR RETURN FROM TEE TO VALVE NODE 660
*----------------------------------------
*GROUP 9 RHR RETURN FROM TEE TO VALVE NODE 660
INCL FN=Z:\SISJ-PROJECTS\VY-16Q\Rev0\REG9A.INP
*
*NOTE CODING FOR RHR RETURN STARTS HERE
CROS CD=29
JUNC PT=600
MATL CD=376.316
BRAN PT=602 DX=-3.8123  TE=1
MATL CD=403.316
BRAD PT=610 RA=2  EW=1
TANP        DY=4
BRAD PT=612 RA=2  EW=1
MATL CD=376.316
TANG PT=614 DZ=-10.38  EW=1
MATL CD=403.316
BRAD PT=615 RA=10  EW=1
MATL CD=376.316
TANG PT=620 DX=5.98 DZ=-3.45  EW=1
*NOTE
*NOTE VARIABLE SPRING H104 AT NODE 620
*NOTE
*NOTE VALVE V10-81A DATA FROM 5920-4590 WEIGHT - 6845.#
*NOTE WEIGHT APPLIED AT ESTIMATED CENTER OF GRAVITY (NODE 623)
CROS CD=30
VALV PT=622 DX=1.98 DZ=-1.15 PL=1  *AL=$VALVE V10-81A$
JUNC PT=622
VALV PT=624 DX=1.98 DZ=-1.15 PL=2  EW=1
JUNC PT=622
RIGD PT=623 DY=2.5
LUMP PT=623 MA=7.32 *VALVE ACTUATOR
CROS CD=29
JUNC PT=624
TANG PT=625 DX=1.867 DZ=-1.078
TANG PT=630 DX=2.598 DZ=-1.5  EW=1
MATL CD=403.316
BRAD PT=631 RA=3  EW=1
MATL CD=376.316
TANG PT=640 DZ=-4.54  EW=1
MATL CD=403.316
BRAD PT=641 RA=2  EW=1
MATL CD=376.316
*NOTE VALVE V10-46A DATA FROM 5920-4718 WEIGHT - 5295.#
CROS CD=30
VALV PT=655 DX=-3.79 PL=1 TA=2 *AL=$VALVE V10-46A$
LUMP PT=655 MA=5.77

*---------------------------
*END REGION 9A GEOMETRY FOR RHR RETURN FROM TEE TO VALVE NODE 660
*---------------------------
*
*----------------------------------------
*BEGIN REGION 9B TRANSIENT CARDS & GEOMETRY FOR RHR RETURN FROM VALVE NODE 660 TO PENET. NODE
675
*----------------------------------------
*GROUP 19 RHR RETURN FROM VALVE NODE 660 TO PENET. NODE 675
INCL FN=Z:\SISJ-PROJECTS\VY-16Q\Rev0\REG9B.INP
```

```
*
*NOTE
*NOTE VARIABLE SPRING H105 AT NODE 655
*NOTE
VALV PT=660 DX=-1.79 PL=2  EW=1
*NOTE SPEC CHANGE TO CARBON STEEL
MATL CD=106
CROS CD=29
TANG PT=661 DX=-1
TANG PT=663 DX=-3.31  EW=1
BRAD PT=665 RA=2  EW=1
TANG PT=670 DY=-10.5 DZ=0.38  EW=1
BRAD PT=671 RA=2  EW=1
TANG PT=673 DZ=-7.74
TANG PT=675 DZ=-7.74
*---------------------------
*END REGION 9B GEOMETRY FOR RHR RETURN FROM VALVE NODE 660 TO PENET. NODE 675
*---------------------------
*
*---------------------------
***STRESS INDICES AT CROSS POINT
*---------------------------
*
INDI AT=210 AF=195 B1=0.5 C1=1 K1=4 B2=2.256 C2=3.024 K2=1 C3=1 K3=1 CP=0.5
INDI AT=210 AF=215 B1=0.5 C1=1 K1=4 B2=2.256 C2=3.024 K2=1 C3=1 K3=1 CP=0.5
INDI AT=210 AF=240 B1=0.5 C1=1 K1=4 B2=1.805 C2=3.024 K2=1 C3=1 K3=1 CP=0.5
INDI AT=210 AF=260 B1=0.5 C1=1 K1=4 B2=1.805 C2=3.024 K2=1 C3=1 K3=1 CP=0.5
*---------------------------
*** SUPPORTS
*---------------------------
RSTN PT=675  DX=1  SP=16000          *RHR SUPPLY PENET.
RSTN PT=675  DY=1  SP=16000          *RHR SUPPLY PENET.
RSTN PT=675  DZ=1  SP=23000          *RHR SUPPLY PENET.
ROTR PT=675  RX=1  SP=300000         *RHR SUPPLY PENET.
ROTR PT=675  RY=1  SP=300000         *RHR SUPPLY PENET.
ROTR PT=675  RZ=1  SP=340000         *RHR SUPPLY PENET.
RSTN PT=565  DX=1  SP=16000          *RHR SUPPLY PENET.
RSTN PT=565  DY=1  SP=16000          *RHR SUPPLY PENET.
RSTN PT=565  DZ=1  SP=23000          *RHR SUPPLY PENET.
ROTR PT=565  RX=1  SP=300000         *RHR SUPPLY PENET.
ROTR PT=565  RY=1  SP=300000         *RHR SUPPLY PENET.
ROTR PT=565  RZ=1  SP=340000         *RHR SUPPLY PENET.
*
SNUB PT=12   DZ=-1 SP=1000    *AL=$SNUBBER SS-7A-1$
SNUB PT=12   DX=1  SP=1000    *AL=$SNUBBER SS-7A-2$
SNUB PT=190  DX=-1 SP=1000    *AL=$SNUBBER SS-6-A1$
SNUB PT=190  DZ=1  SP=1000    *AL=$SNUBBER SS-6-A2$
*
VSUP PT=20   DY=1  FO=24.8  SP=2.664  *AL=$VARI. SUPT. HA-1$
*
CSUP PT=27   DY=1  FO=8.3   KP=0.01   *AL=$CONST. SUPT. H-8-A1$
CSUP PT=42   DY=1  FO=8.3   KP=0.01   *AL=$CONST. SUPT. H-8-A2$
CSUP PT=56   DY=1  FO=18.05 KP=0.01   *AL=$CONST. SUPT. HA3 FOR PUMP$
CSUP PT=69   DY=1  FO=18.0  KP=0.01   *AL=$CONST. SUPT. HA4 FOR PUMP$
CSUP PT=63   DY=1  FO=18.02 KP=0.01   *AL=$CONST. SUPT. HA5 FOR PUMP$
CSUP PT=160  DY=-1 FO=11.8  KP=0.01   *AL=$CONST. SUPT. HA-9 & HA-10$
CSUP PT=705  DY=1  FO=0.960 KP=0.01   *AL=$CONST. SUPT. HA-11 ON 4 INCH BYPASS$
*
VSUP PT=184  DY=1  FO=36.0 SP=3.542   *AL=$VARI. SUPT. HA-2$
VSUP PT=343  DY=1  FO=7.1  SP=3.014   *AL=$VARI. SUPT. HA13$
```

```
VSUP PT=313  DY=1  FO=7.1  SP=3.014   *AL=$VARI. SUPT. HA14$
*
VSUP PT=530  DY=1  SP=9.420 FO=26.0   *AL=$HANGER H109 RHR SUPPLY VALVE$
VSUP PT=620  DY=1  SP=7.084 FO=14.9   *AL=$HANGER H104 RHR RETURN VALVE$
VSUP PT=655  DY=1  SP=4.710 FO=22.0   *AL=$HANGER H105 RHR RETURN VALVE$
*
RSTN PT=15   DY=0.7071 DZ=-0.7071  SP=6000    *RECIRC PUMP
RSTN PT=16   DX=-0.7071 DY=0.7071  SP=6000    *RECIRC PUMP
ENDP
```

RHR_15.inp

```
IDEN JB=3   *Job number (1 to 9999)
     CD=1    *1=ASME Class 1
     GR=-Y   *Direction of gravity
     VA=0    *0=Calculate            2=Verify
     IU=1    *Input units            1=USA
     OU=1    *Output units           1=USA
     CH=$    *Delimiter character
     AB=T    *FREE errors = abort
     PL=$Vermont Yankee$
     EN=$RVP$
TITL BL=3    *Modeling option:
             *  3 = uniform mass for static analysis
             *      lumped mass for dynamic analysis
             *      rotational inertia ignored
     GL=1    *Report forces/moment         0=Global     1=Local     2=G et L
     SU=1    *Support summary              0=No         1=Yes
     CV=15   *Code version - See Manual
     HS=1    *Highest 20 stress ratios for each case
     MD=1    *Hot modulus
     J6=1    *File generated by program
     TI=$Vermont Yankee Recirculation $
        $Fatigue Analysis$
FREQ RF=1 RP=8 FR=36 MP=20 RC=0 MX=70 TI=$SEISMIC$
*
*************************************
**** THERMAL CYCLE LOAD CASES****
*************************************
LCAS RF=0 CA=1 TY=0 TI=$LC-1$     *TC-1
LCAS RF=0 CA=2 TY=0 TI=$LC-2$     *TC-2
LCAS RF=0 CA=3 TY=0 TI=$LC-3$     *TC-3
LCAS RF=0 CA=4 TY=0 TI=$LC-4$     *TC-4
LCAS RF=0 CA=5 TY=0 TI=$LC-5$     *TC-5
LCAS RF=0 CA=6 TY=0 TI=$LC-6$     *TC-6
LCAS RF=0 CA=7 TY=0 TI=$LC-7$     *TC-7
LCAS RF=0 CA=8 TY=0 TI=$LC-8$     *TC-8
LCAS RF=0 CA=9 TY=0 TI=$LC-9$     *TC-9
LCAS RF=0 CA=10 TY=0 TI=$LC-10$   *TC-10
LCAS RF=0 CA=11 TY=0 TI=$LC-11$   *TC-11
LCAS RF=0 CA=12 TY=0 TI=$LC-12$   *TC-12
LCAS RF=0 CA=13 TY=0 TI=$LC-13$   *TC-13
LCAS RF=0 CA=14 TY=0 TI=$LC-14$   *TC-14
LCAS RF=0 CA=15 TY=0 TI=$LC-15$   *TC-15
LCAS RF=0 CA=16 TY=0 TI=$LC-16$   *TC-16
LCAS RF=0 CA=17 TY=0 TI=$LC-17$   *TC-17
LCAS RF=0 CA=18 TY=0 TI=$LC-18$   *TC-18
LCAS RF=0 CA=19 TY=0 TI=$LC-19$   *TC-19
LCAS RF=0 CA=20 TY=0 TI=$LC-20$   *TC-20
LCAS RF=0 CA=21 TY=0 TI=$LC-21$   *TC-21
LCAS RF=0 CA=22 TY=0 TI=$LC-22$   *TC-22
```

```
LCAS RF=0 CA=23 TY=0 TI=$LC-23$   *TC-23
LCAS RF=0 CA=24 TY=0 TI=$LC-24$   *TC-24
LCAS RF=0 CA=25 TY=0 TI=$LC-25$   *TC-25
*
*********************
**** WEIGHT CASES****
*********************
LCAS CA=101  RF=1  TY=3  TI=$OPERATING WEIGHT$
LCAS CA=102  RF=2  TY=4  TI=$HYDROTEST WEIGHT$
*
*******************************
**** THERMAL TRANSIENT CASES****
*******************************
TCAS CA=201 TI=$Design Hydrotest (+) $
TCAS CA=202 TI=$Design Hydrotest (-) $
TCAS CA=203 TI=$Startup              $
TCAS CA=204 TI=$TRoll & Inc. PWR1    $
TCAS CA=205 TI=$TRoll & Inc. PWR2    $
TCAS CA=206 TI=$LOFWH+TT PWR1        $
TCAS CA=207 TI=$LOFWH+TT PWR2        $
TCAS CA=208 TI=$LOFWH+PFWHTR Byp1    $
TCAS CA=209 TI=$LOFWH+PFWHTR Byp2    $
TCAS CA=210 TI=$LOFWP, ISO Cl DN 1   $
TCAS CA=211 TI=$LOFWP, ISO Cl UP 1   $
TCAS CA=212 TI=$LOFWP, ISO Cl DN 2   $
TCAS CA=213 TI=$LOFWP, ISO Cl UP 2   $
TCAS CA=214 TI=$Reduction to 0% PWR  $
TCAS CA=215 TI=$Shutdown1            $
TCAS CA=216 TI=$Shutdown2            $
TCAS CA=217 TI=$Shutdown3            $
TCAS CA=218 TI=$Shutdown4            $
TCAS CA=219 TI=$Code Hydrotest       $
TCAS CA=220 TI=$RHR Initiation UP    $
TCAS CA=221 TI=$RHR Initiation DN    $
TCAS CA=222 TI=$Inadvert. Inj. DOWN  $
TCAS CA=223 TI=$Inadvert. Inj. UP    $
TCAS CA=224 TI=$Single Relief BD DN  $
TCAS CA=225 TI=$Single Relief BD UP  $
*
**********************
**** SEISMIC CASES****
**********************
RCAS CA=103 EQ=3 EV=1 TY=1 SU=1 LO=1 FX=1 FY=1 FZ=1 TI=$OBE INERTIA$
*
** *************************
**** LOAD COMBINATION CASES *
** *************************
CCAS RF=1 CA=104      ME=1 FL=1  C1=103 CY=10  TI=$OBE$
CCAS RF=1 CA=401 SS=1 ME=1 EQ=3  C1=101 C2=103 TI=$EQUATION 9 LEVEL B$
CCAS RF=1 CA=402 SS=1 ME=3 F1=1  C1=103 C2=1   TI=$NORMAL+OBE$
CCAS RF=1 CA=403 SS=1 ME=3 F1=-1 C1=103 C2=1   TI=$NORMAL-OBE$
*
******************
**** LOAD SETS****
******************
*
LSET RF=1  FC=0 RP=1 CY=120  PR=1  MO=1  TR=201  TI=$Design Hydrotest (+)LS-1$
LSET RF=2  FC=0 RP=1 CY=120  PR=2  MO=2  TR=-202 TI=$Design Hydrotest (-)LS-2$
LSET RF=3  FC=0 RP=1 CY=300  PR=3  MO=3  TR=203  TI=$Startup            LS-3$
LSET RF=3  FC=0 RP=1 CY=579  PR=4  MO=4  TR=-204 TI=$TRoll & Inc. PWR1   LS-4$
```

```
LSET RF=4  FC=0 RP=1 CY=579  PR=5  MO=5  TR=-205 TI=$TRoll & Inc. PWR2   LS-5$
LSET RF=4  FC=0 RP=1 CY=20   PR=6  MO=6  TR=206  TI=$LOFWH+TT PWR1       LS-6$
LSET RF=4  FC=0 RP=1 CY=20   PR=7  MO=7  TR=-207 TI=$LOFWH+TT PWR2       LS-7$
LSET RF=5  FC=0 RP=1 CY=70   PR=8  MO=8  TR=-208 TI=$LOFWH+PFWHTR Byp1   LS-8$
LSET RF=5  FC=0 RP=1 CY=70   PR=9  MO=9  TR=209  TI=$LOFWH+PFWHTR Byp2   LS-9$
LSET RF=5  FC=0 RP=1 CY=10   PR=10 MO=10 TR=-210 TI=$LOFWP, ISO Cl DN 1  LS-10$
LSET RF=11 FC=0 RP=1 CY=20   PR=11 MO=11 TR=211  TI=$LOFWP, ISO Cl UP 1  LS-11$
LSET RF=11 FC=0 RP=1 CY=20   PR=12 MO=12 TR=-212 TI=$LOFWP, ISO Cl DN 2  LS-12$
LSET RF=3  FC=0 RP=1 CY=10   PR=13 MO=13 TR=213  TI=$LOFWP, ISO Cl UP 2  LS-13$
LSET RF=3  FC=0 RP=1 CY=300  PR=14 MO=14 TR=214  TI=$Reduction to 0% PWR LS-14$
LSET RF=5  FC=0 RP=1 CY=300  PR=15 MO=15 TR=-215 TI=$Shutdown1           LS-15$
LSET RF=15 FC=0 RP=1 CY=300  PR=16 MO=16 TR=-216 TI=$Shutdown2           LS-16$
LSET RF=16 FC=0 RP=1 CY=300  PR=17 MO=17 TR=-217 TI=$Shutdown3           LS-17$
LSET RF=20 FC=0 RP=1 CY=300  PR=18 MO=18 TR=-218 TI=$Shutdown4           LS-18$
LSET RF=19 FC=0 RP=1 CY=1    PR=19 MO=19 TR=219  TI=$Code Hydrotest      LS-19$
LSET RF=20 FC=0 RP=1 CY=300  PR=20 MO=20 TR=220  TI=$RHR Initiation UP   LS-20$
LSET RF=20 FC=0 RP=1 CY=300  PR=21 MO=21 TR=-221 TI=$RHR Initiation DN   LS-21$
LSET RF=5  FC=0 RP=1 CY=0    PR=22 MO=22 TR=-222 TI=$Inadvert. Inj. DOWN LS-22$
LSET RF=5  FC=0 RP=1 CY=0    PR=23 MO=23 TR=223  TI=$Inadvert. Inj. UP   LS-23$
LSET RF=23 FC=0 RP=1 CY=0    PR=24 MO=24 TR=-224 TI=$Single Relief BD DN LS-24$
LSET RF=24 FC=0 RP=1 CY=0    PR=25 MO=25 TR=225  TI=$Single Relief BD UP LS-25$
*
LSET RF=2 FC=0 CY=5 FL=1 PR=2 MO=402 TI=$NORMAL+OBE  LS-26$
LSET RF=2 FC=0 CY=5 FL=1 PR=2 MO=403 TI=$NORMAL-OBE  LS-27$
******
*FATG AT=500 AF=502
*FATG AT=600 AF=602
*
***************************
**** RESPONSE SPECTRA****
*************************
SPEC FS=OBE EV=1 ME=3 FP=0  TI=$RESPONSE$
      LV=1 DX=1 DY=1 DZ=1
      DI=X
        0.30/0.100  0.40/0.100  0.90/0.200  1.25/0.400  2.25/0.450  2.30/0.700
        3.30/0.700  4.40/0.750  4.41/0.900  4.75/1.100  5.20/1.100  5.80/1.600
        8.70/1.600 12.00/0.650 17.00/0.400 20.00/0.350 30.00/0.350 36.00/0.350
      DI=Y
        0.30/0.030  0.40/0.030  0.50/0.050  0.60/0.075  1.00/0.075  1.20/0.100
        2.00/0.220  2.40/0.350  3.50/0.350  3.60/0.300  5.30/0.300  5.75/0.330
        8.25/0.330  8.75/0.250 17.50/0.250 25.00/0.120 30.00/0.120 36.00/0.120
      DI=Z
        0.30/0.100  0.40/0.100  0.50/0.130  0.90/0.150  1.00/0.250  1.60/0.250
        1.90/0.600  3.50/0.600  3.75/0.700  4.40/0.700  4.50/0.800  6.25/1.500
        8.50/1.500 12.50/0.500 20.00/0.350 30.00/0.350 36.00/0.350
*
****************************
**** MATERIAL PROPERTIES ****
****************************
* ASTM A-106 Grade B, PIPE *
MATH CD=106     EX=0       TY=1     *C-Si
MATD TE=70      EH=29.5    EX=0.0   SM=20.0   SY=35
MATD TE=100     EH=29.3    EX=0.20  SM=20.0   SY=35
MATD TE=200     EH=28.8    EX=1.00  SM=20.0   SY=32.1
MATD TE=300     EH=28.3    EX=1.90  SM=20.0   SY=31
MATD TE=400     EH=27.7    EX=2.80  SM=20.0   SY=29.9
MATD TE=500     EH=27.3    EX=3.70  SM=18.9   SY=28.5
MATD TE=600     EH=26.7    EX=4.70  SM=17.3   SY=26.8
* ASME SA-376 Grade TP316, PIPE *
MATH CD=376.316 EX=0       TY=4     *16Cr-12Ni-2Mo
```

```
MATD TE=70       EH=28.3    EX=0.0    SM=20.0    SY=30.0
MATD TE=100      EH=28.1    EX=0.30   SM=20.0    SY=30.0
MATD TE=200      EH=27.6    EX=1.40   SM=20.0    SY=25.9
MATD TE=300      EH=27.0    EX=2.50   SM=20.0    SY=23.4
MATD TE=400      EH=26.5    EX=3.70   SM=19.3    SY=21.4
MATD TE=500      EH=25.8    EX=5.00   SM=18.0    SY=20.0
MATD TE=600      EH=25.3    EX=6.30   SM=17.0    SY=18.9
* ASME SA-403 Grade WP316, ELBOWS *
MATH CD=403.316 EX=0        TY=4      *16Cr-12Ni-2Mo
MATD TE=70       EH=28.3    EX=0.0    SM=20.0    SY=30.0
MATD TE=100      EH=28.1    EX=0.30   SM=20.0    SY=30.0
MATD TE=200      EH=27.6    EX=1.40   SM=20.0    SY=25.9
MATD TE=300      EH=27.0    EX=2.50   SM=20.0    SY=23.4
MATD TE=400      EH=26.5    EX=3.70   SM=18.7    SY=21.4
MATD TE=500      EH=25.8    EX=5.00   SM=17.5    SY=20.0
MATD TE=600      EH=25.3    EX=6.30   SM=16.4    SY=18.9
*** Cross Sectional Properties
CROS CD=1  OD=50.0    WT=8.87    MA=3977.2 *CALC. PER GE SPEC. NO. 23A5569 [3]
           SO=1       ST=1.0               *RECIRCULATION OUTLET NOZZLE
CROS CD=2  OD=37.85   WT=6.1     MA=2122.2 *CALC. PER GE SPEC. NO. 23A5569 [3]
           SO=1       ST=1.0
CROS CD=3  OD=28.875  WT=1.56    MA=484.9  *CALC. PER GE SPEC. NO. 23A5569 [3]
           SO=1       ST=1.0
CROS CD=4  OD=28.638  WT=1.45    MA=450.4  *CALC. PER GE SPEC. NO. 23A5569 [3]
           SO=1       ST=1.0
CROS CD=5  OD=28.169  WT=1.244   MA=386.1  *CALC. PER GE SPEC. NO. 23A5569 [3]
           SO=1       ST=1.0
CROS CD=7  OD=28.166  WT=2.125   MA=0.001  *VALVE
           SO=1       ST=1.0     KL=1
CROS CD=8  OD=42.507  WT=2.486   MA=0.001  *PUMP
           SO=.001    ST=.001    KL=1
CROS CD=11 OD=6.625   WT=0.432   MA=0.001  *PUMP RIGID STRUTS
           SO=0.001   ST=0.001   KL=1
CROS CD=13 OD=28.339  WT=1.339   MA=415.1  *CALC. PER GE SPEC. NO. 23A5569 [3]
           SO=1       ST=1
CROS CD=14 OD=28.339  WT=2.67    MA=0.001  *VALVE
           SO=1       ST=1.0     KL=1
CROS CD=15 OD=12.748  WT=0.685   MA=103.4  *CALC. PER GE SPEC. NO. 23A5569 [3]
           SO=1       ST=1.0
CROS CD=16 OD=14.17   WT=1.395   MA=207.5  *CALC. PER GE SPEC. NO. 23A5569 [3]
           SO=1       ST=1.0
CROS CD=17 OD=15.5    WT=2       MA=307.7  *CALC. PER GE SPEC. NO. 23A5569 [3]
           SO=1       ST=1.0
CROS CD=18 OD=21.88   WT=4.06    MA=803.2  *CALC. PER GE SPEC. NO. 23A5569 [3]
           SO=1       ST=1.0
CROS CD=19 OD=28.25   WT=7.25    MA=1673.1 *CALC. PER GE SPEC. NO. 23A5569 [3]
           SO=1       ST=1.0
CROS CD=20 OD=21.878  WT=1.043   MA=257.2  *CALC. PER GE SPEC. NO. 23A5569 [3]
           SO=1       ST=1.0
CROS CD=25 OD=20      WT=1.031   MA=221.9  *CALC. PER GE SPEC. NO. 23A5569 [3]
           SO=1       ST=1
CROS CD=26 OD=20      WT=1.875   MA=0.001  *VALVE
           SO=1       ST=1       KL=1
CROS CD=27 OD=4.5     WT=0.3385  MA=23.2   *CALC. PER GE SPEC. NO. 23A5569 [3]
           SO=1       ST=1       KL=1      *4 inch bypass line
CROS CD=28 OD=4.5     WT=0.67    MA=0.001  *VALVE V2-54A
           SO=1       ST=1       KL=1
CROS CD=29 OD=24      WT=1.217   MA=316.5  *CALC. PER GE SPEC. NO. 23A5569 [3]
           SO=1       ST=1
CROS CD=30 OD=24      WT=2.43    MA=0.001  *VALVE
```

```
            SO=1       ST=1       KL=1
CROS CD=40 OD=4.5     WT=0.3385 MA=0.001  *4 inch bypass STRUTS
            SO=0.001  ST=0.001  KL=1
CROS CD=41 OD=2.875  WT=0.276  MA=0.001  *STRUT RDA1, RDA5, & VBA1
            SO=0.001  ST=0.001  KL=1
CROS CD=42 OD=28.339 WT=1.339  MA=0.001  *RIGID FROM RECIRC ELBOW TO RDA1 STRUT
            SO=0.001  ST=0.001  KL=1
**********************
* STRUCTURE AND LOADS
**********************
*-----------------------------------------------------------------------------
DESN  TE=575.0  PR=1250.0 *Reference 12 GE Design Requirements Rpt VY-05Q-227
*-----------------------------------------------------------------------------
*-----------------------------------------------------------------
*BEGIN REGION 1 TRANSIENT CARDS & GEOMETRY FROM RHR SUPPLY TO TEE
*-----------------------------------------------------------------
*
INCL FN=Z:\SISJ-PROJECTS\VY-16Q\Rev0\REG1.INP
*
* RUN   1     FROM ANCHOR TO REACTOR VESSEL N3B
*GROUP 1 FROM ANCHOR TO REACTOR VESSEL N3B
*NOTE
*NOTE NODE 003 - RECIRC SUCTION NOZZLE N1A (EL. 279'5 INCH)
*NOTE NODE 003 IS AT THE SAFE END TO VESSEL NOZZLE CONNECTION
*NOTE
*NOTE SAFE END FROM NODES 003 TO 808
*NOTE CONNECTION TO VESSEL AT NODE 003
*NOTE OD AND WALL THICKNESS FOR SAFE END TAKEN FROM GE CALC
*NOTE WEIGHT FOR SAFE END BASED ON THICKNESS
*NOTE
MATL CD=376.316
CROS CD=1
COOR PT=3    AX=0  AY=0  AZ=0
ANCH PT=3
AMVT    CA=1    PT=3    DX=0.0000  DY=0.0176  DZ=-0.0201
AMVT    CA=2    PT=3    DX=0.0000  DY=0.3141  DZ=-0.3602
AMVT    CA=3    PT=3    DX=0.0000  DY=0.3112  DZ=-0.3568
AMVT    CA=4    PT=3    DX=0.0000  DY=0.2995  DZ=-0.3434
AMVT    CA=5    PT=3    DX=0.0000  DY=0.3112  DZ=-0.3568
AMVT    CA=6    PT=3    DX=0.0000  DY=0.2995  DZ=-0.3434
AMVT    CA=7    PT=3    DX=0.0000  DY=0.2922  DZ=-0.3350
AMVT    CA=8    PT=3    DX=0.0000  DY=0.2995  DZ=-0.3434
AMVT    CA=9    PT=3    DX=0.0000  DY=0.1422  DZ=-0.1630
AMVT    CA=10   PT=3    DX=0.0000  DY=0.2807  DZ=-0.3218
AMVT    CA=11   PT=3    DX=0.0000  DY=0.1422  DZ=-0.1630
AMVT    CA=12   PT=3    DX=0.0000  DY=0.3141  DZ=-0.3602
AMVT    CA=13   PT=3    DX=0.0000  DY=0.3141  DZ=-0.3602
AMVT    CA=14   PT=3    DX=0.0000  DY=0.1928  DZ=-0.2521
AMVT    CA=15   PT=3    DX=0.0000  DY=0.1624  DZ=-0.1986
AMVT    CA=16   PT=3    DX=0.0000  DY=0.0946  DZ=-0.1084
AMVT    CA=17   PT=3    DX=0.0000  DY=0.0176  DZ=-0.0201
AMVT    CA=18   PT=3    DX=0.0000  DY=0.0176  DZ=-0.0201
AMVT    CA=19   PT=3    DX=0.0000  DY=0.0946  DZ=-0.1084
AMVT    CA=20   PT=3    DX=0.0000  DY=0.0946  DZ=-0.1084
AMVT    CA=21   PT=3    DX=0.0000  DY=0.0361  DZ=-0.0413
AMVT    CA=22   PT=3    DX=0.0000  DY=0.2995  DZ=-0.3434
AMVT    CA=23   PT=3    DX=0.0000  DY=0.1928  DZ=-0.2521
AMVT    CA=24   PT=3    DX=0.0000  DY=0.0176  DZ=-0.0201
```

```
*
TANG PT=805  DZ=-1.017  EW=1
CROS CD=2
TANG PT=806  DZ=-0.823  EW=1
CROS CD=3
TANG PT=807  DZ=-0.58  EW=1
CROS CD=4
TANG PT=808  DZ=-0.47
CROS CD=5
TANG PT=5    DZ=-5.59 EW=1
MATL CD=403.316
BRAD PT=7    RA=3.5 EW=1
MATL CD=376.316
TANG PT=9    DY=-6.69  EW=1
TANG PT=500  DY=-2.31
*----------------------------------------------
*END REGION 1 GEOMETRY FROM RHR SUPPLY TO TEE
*----------------------------------------------
*
*-----------------------------------------------------------------------
*BEGIN REGION 2 TRANSIENT CARDS & GEOMETRY FROM RHR SUPPLY TEE TO PUMP
*-----------------------------------------------------------------------
*GROUP 2 RHR SUPPLY TEE TO PUMP
INCL FN=Z:\SISJ-PROJECTS\VY-16Q\Rev0\REG2.INP
*
TANG PT=11   DY=-2.22  EW=1
CROS CD=5
TANG PT=12   DY=-1.78
TANG PT=20   DY=-6.77
TANG PT=22   DY=-3.25
TANG PT=25   DY=-15.49  EW=1
MATL CD=403.316
BRAD PT=26   RA=3.5  EW=1
MATL CD=376.316
TANG PT=27   DX=-3.3 DZ=1.27  EW=1
CROS CD=7
VALV PT=30   DX=-2.28 DZ=0.89 MA=10.368 PL=1
JUNC PT=30
VALV PT=40   DX=-2.31 DZ=0.9 PL=2  EW=1
JUNC PT=30
RIGD PT=35   DY=7
LUMP PT=35   MA=1.132
JUNC PT=40
CROS CD=5
TANG PT=42 DX=-1.18 DZ=0.46
TANG PT=43 DX=-0.55 DZ=0.21
TANG PT=44 DX=-3.31 DZ=1.28  EW=1
MATL CD=403.316
BRAD PT=46 RA=2.33  EW=1
MATL CD=376.316
CROS CD=8
TANG PT=50 DY=4.33  EW=0
LUMP PT=50 MA=28  *NOTE WEIGHT OF PUMP FLOODED 28K (EXCLUDING MOTOR)
TANG PT=75 DY=0.5
TANG PT=83 DY=2.13
TANG PT=86 DY=3.38
LUMP PT=86 MA=32  *NOTE TOTAL WEIGHT OF PUMP MOTOR 32000 LBS
TANG PT=90 DY=4.08 *TOP OF PUMP
*NOTE SNUBBERS ON TOP OF PUMPS WERE DELETED DURING
*NOTE THE RECIRC PIPE REPLACEMENT PROJECT
```

```
*NOTE - RIGID LINKS FOR CONSTANT SUPPORTS AT PUMP FOLLOW
*---------------------------
*END REGION 2 GEOMETRY FROM RHR SUPPLY TEE TO PUMP
*---------------------------
*
*----------------------------------------
*BEGIN REGION 3 TRANSIENT CARDS & GEOMETRY FROM PUMP DISCHARGE TO HEADER
*----------------------------------------
*GROUP 3 FROM PUMP DISCHARGE TO HEADER
INCL FN=Z:\SISJ-PROJECTS\VY-16Q\Rev0\REG3.INP
*
JUNC PT=50
CROS CD=8
RIGD PT=54 DX=1.06 DZ=1.06
RIGD PT=56 DX=1.06 DY=0.75 DZ=1.06  *NOTE CONSTANT SUPPORT HA3 AT NODE 56
JUNC PT=50
RIGD PT=66 DZ=-3.83
RIGD PT=69 DY=1                     *NOTE CONSTANT SUPPORT HA4 AT NODE 69
JUNC PT=50
CROS CD=8
RIGD PT=60 DX=-3.83
RIGD PT=63 DY=1                     *CONSTANT SUPPORT HA5 AT NODE 63
*
* *** CODING FOR PUMP RIGID STRUTS FOLLOW ***
*     CODED FROM PUMP CENTERLINE
CROS CD=11
JUNC PT=66
RIGD PT=15    DY=0.7071 DZ=-0.7071
*
JUNC PT=60
RIGD PT=16    DX=-0.7071 DY=0.7071
* *** END OF CODING FOR PUMP SUPPORTS ***
*PUMP INLET
CROS CD=8
JUNC PT=50
TANG PT=150 DX=-2.17
BRAN PT=151 DZ=2.333  TE=1
*NOTE PUMP DISCHARGE CONNECTION TO PIPE AT NODE 151
CROS CD=13
TANG PT=152 DZ=1.25
TANG PT=155 DZ=1  EW=1
CROS CD=14
VALV PT=160 PL=1 DX=0.0 DY=0.0  DZ=2.52 MA=6.8285
JUNC PT=160
RIGD PT=163 DX=0.0 DY=7.12 DZ=0.0
LUMP PT=163 MA=0.9715
JUNC PT=160
VALV PT=170 PL=2 DX=0.0 DY=0.0 DZ=6.18  EW=1
CROS CD=13
MATL CD=403.316
BRAD PT=175 RA=3.5  EW=1
MATL CD=376.316
TANG PT=176 DY=5.95
TANG PT=177 DY=4.42
*NOTE ***WEIGHT OF FLOW ELEMENT NOT INCLUDED***
*NOTE ***REF. DWG. 5920-6800 FOR DIMENSIONS***
TANG PT=184 DY=4.42
TANG PT=186 DY=3.02
TANG PT=188 DY=1.51
TANG PT=189 DY=0.74
```

```
TANG PT=190 DY=1.15  EW=1
TANG PT=600 DY=1.06

***INPUT FILE TO INCLUDE EFFECTS OF RHR INITIATION ON LINE NEAR RHR RETURN TO HEADER
INCL FN=Z:\SISJ-PROJECTS\VY-16Q\Rev0\REG3B.INP

JUNC PT=600
TANG PT=195 DY=2.08  EW=1
TANG PT=210 DX=0.0  DY=1.83 DZ=0.0  KL=1 *CENTER OF CROSS, RECIRC HEADER
*MUST HAVE INDI CARD FOR EACH MEMBER CONNECTED TO CROSS CENTER
*---------------------------
*END REGION 3 GEOMETRY FROM PUMP DISCHARGE TO HEADER
*---------------------------
*
*----------------------------------------
*BEGIN REGION 5 TRANSIENT CARDS & GEOMETRY RISER TO NOZZLE NODE 336
*----------------------------------------
*GROUP 5 RISER TO NOZZLE NODE 336
INCL FN=Z:\SISJ-PROJECTS\VY-16Q\Rev0\REG5.INP
*
*NOTE CROSS AND REDUCER DIMENSIONS TAKEN FROM 5920-6632 SHT.3
CROS CD=13
MATL CD=376.316
TANG PT=215 DX=0.0 DY=2.59  DZ=0.0  EW=0
CRED PT=220 DY=1.29  AN=30  EW=1  *AL=$CONC. REDUCER$
CROS CD=15
TANG PT=330 DY=4.58
TANG PT=335 DY=3.29  EW=1
MATL CD=403.316
BRAD PT=334 RA=1.5  EW=1
*---------------------------
*END REGION 5 GEOMETRY RISER TO NOZZLE NODE 336
*---------------------------
*
*----------------------------------------
*BEGIN REGION 6 TRANSIENT CARDS & GEOMETRY TO NOZZLE NODE 336
*----------------------------------------
*GROUP 6 TO NOZZLE NODE 336
INCL FN=Z:\SISJ-PROJECTS\VY-16Q\Rev0\REG6.INP
*
MATL CD=376.316
TANG PT=838 DX=3.875
CROS CD=16
TANG PT=837 DX=0.875  EW=1
CROS CD=17
TANG PT=836 DX=0.37  EW=1
CROS CD=18
TANG PT=835 DX=0.53  EW=1
CROS CD=19
TANG PT=336 DX=0.704  EW=1
NOZZ PT=336
AMVT    CA=1    PT=336  DX=-0.0201  DY=0.0246  DZ=0.0000
AMVT    CA=2    PT=336  DX=-0.3602  DY=0.4398  DZ=0.0000
AMVT    CA=3    PT=336  DX=-0.3568  DY=0.4316  DZ=0.0000
AMVT    CA=4    PT=336  DX=-0.3434  DY=0.4152  DZ=0.0000
AMVT    CA=5    PT=336  DX=-0.3568  DY=0.4050  DZ=0.0000
AMVT    CA=6    PT=336  DX=-0.3434  DY=0.2940  DZ=0.0000
AMVT    CA=7    PT=336  DX=-0.3350  DY=0.3229  DZ=0.0000
AMVT    CA=8    PT=336  DX=-0.3434  DY=0.2700  DZ=0.0000
AMVT    CA=9    PT=336  DX=-0.1630  DY=0.1991  DZ=0.0000
```

```
AMVT    CA=10   PT=336  DX=-0.3218  DY=0.1626  DZ=0.0000
AMVT    CA=11   PT=336  DX=-0.1630  DY=0.0246  DZ=0.0000
AMVT    CA=12   PT=336  DX=-0.3602  DY=0.4398  DZ=0.0000
AMVT    CA=13   PT=336  DX=-0.3602  DY=0.4316  DZ=0.0000
AMVT    CA=14   PT=336  DX=-0.2193  DY=0.4152  DZ=0.0000
AMVT    CA=15   PT=336  DX=-0.1862  DY=0.4050  DZ=0.0000
AMVT    CA=16   PT=336  DX=-0.1084  DY=0.2940  DZ=0.0000
AMVT    CA=17   PT=336  DX=-0.0201  DY=0.3229  DZ=0.0000
AMVT    CA=18   PT=336  DX=-0.0201  DY=0.2700  DZ=0.0000
AMVT    CA=19   PT=336  DX=-0.1084  DY=0.1991  DZ=0.0000
AMVT    CA=20   PT=336  DX=-0.0201  DY=0.1626  DZ=0.0000
AMVT    CA=21   PT=336  DX=-0.0413  DY=0.3229  DZ=0.0000
AMVT    CA=22   PT=336  DX=-0.3434  DY=0.2700  DZ=0.0000
AMVT    CA=23   PT=336  DX=-0.2211  DY=0.1991  DZ=0.0000
AMVT    CA=24   PT=336  DX=-0.0201  DY=0.1626  DZ=0.0000


*NOTE SAFE END FROM NODES 838 TO 336
*NOTE CONNECTION TO VESSEL AT NODE 336
*NOTE OD AND WALL THICKNESS FOR SAFE END TAKEN FROM GE CALC
*NOTE WEIGHT BASED ON THICKNESS
*---------------------------
*END REGION 6 GEOMETRY TO NOZZLE NODE 336
*---------------------------
*
*----------------------------------------
*BEGIN REGION 4 TRANSIENT CARDS & GEOMETRY HEADER TO NOZZLE NODE 366
*----------------------------------------
*GROUP 4 HEADER TO NOZZLE NODE 366
INCL FN=Z:\SISJ-PROJECTS\VY-16Q\Rev0\REG4.INP
*
JUNC PT=210
CROS CD=20
BRAN PT=240 DX=0.1786 DY=0.0 DZ=1.7
TANG PT=250 DX=0.3 DZ=2.853  EW=0
BRAD PT=255 RA=4.578  EW=0 *NOTE BEND RADIUS IS 4.578 FEET
TANG PT=340 DX=1.799 DZ=3.108
*---------------------------
*END REGION 4 GEOMETRY HEADER TO NOZZLE NODE 366
*---------------------------
*
*----------------------------------------
*BEGIN REGION 5 TRANSIENT CARDS & GEOMETRY RISER TO NOZZLE NODE 366
*----------------------------------------
*GROUP 5 RISER TO NOZZLE NODE 366
INCL FN=Z:\SISJ-PROJECTS\VY-16Q\Rev0\REG5.INP
*
TANG PT=349 DX=0.71 DZ=1.23  EW=0
CRED PT=347 DX=0.75 DZ=1.3  AN=30
CROS CD=15
TANG PT=343 DX=0.5525 DZ=0.957  EW=1
BRAD PT=410 RA=1.5  EW=1
TANG PT=360 DX=3.483 DZ=2.011  EW=1
MATL CD=403.316
BRAD PT=361 RA=1.5  EW=1
MATL CD=376.316
CROS CD=15
TANG PT=362 DY=3.18
TANG PT=364 DY=8.56  EW=1
MATL CD=403.316
```

```
BRAD PT=365 RA=1.5  EW=1
*---------------------------
*END REGION 5 GEOMETRY RISER TO NOZZLE NODE 366
*---------------------------

*----------------------------------------
*BEGIN REGION 6 TRANSIENT CARDS & GEOMETRY TO NOZZLE NODE 366
*----------------------------------------
*GROUP 6 TO NOZZLE NODE 366
INCL FN=Z:\SISJ-PROJECTS\VY-16Q\Rev0\REG6.INP
*
MATL CD=376.316
TANG PT=868 DX=1.8 DZ=-3.1
CROS CD=16
TANG PT=867 DX=0.4375 DZ=-0.76  EW=1
CROS CD=17
TANG PT=866 DX=0.185 DZ=-0.32  EW=1
CROS CD=18
TANG PT=865 DX=0.265 DZ=-0.46  EW=1
CROS CD=19
TANG PT=366 DX=0.352 DZ=-0.61  EW=1
NOZZ PT=366
AMVT    CA=1    PT=366  DX=-0.0101  DY=0.0246  DZ=0.0174
AMVT    CA=2    PT=366  DX=-0.1800  DY=0.4398  DZ=0.3120
AMVT    CA=3    PT=366  DX=-0.1783  DY=0.4357  DZ=0.3091
AMVT    CA=4    PT=366  DX=-0.1716  DY=0.4193  DZ=0.2974
AMVT    CA=5    PT=366  DX=-0.1783  DY=0.4357  DZ=0.3091
AMVT    CA=6    PT=366  DX=-0.1716  DY=0.4193  DZ=0.2974
AMVT    CA=7    PT=366  DX=-0.1674  DY=0.4091  DZ=0.2902
AMVT    CA=8    PT=366  DX=-0.1716  DY=0.4193  DZ=0.2974
AMVT    CA=9    PT=366  DX=-0.0815  DY=0.1991  DZ=0.1412
AMVT    CA=10   PT=366  DX=-0.1609  DY=0.3930  DZ=0.2788
AMVT    CA=11   PT=366  DX=-0.0815  DY=0.1991  DZ=0.1412
AMVT    CA=12   PT=366  DX=-0.1800  DY=0.4398  DZ=0.3120
AMVT    CA=13   PT=366  DX=-0.1800  DY=0.4398  DZ=0.3120
AMVT    CA=14   PT=366  DX=-0.1097  DY=0.2678  DZ=0.1899
AMVT    CA=15   PT=366  DX=-0.0931  DY=0.2275  DZ=0.1613
AMVT    CA=16   PT=366  DX=-0.0542  DY=0.1324  DZ=0.0939
AMVT    CA=17   PT=366  DX=-0.0101  DY=0.0246  DZ=0.0174
AMVT    CA=18   PT=366  DX=-0.0101  DY=0.0246  DZ=0.0174
AMVT    CA=19   PT=366  DX=-0.0542  DY=0.1324  DZ=0.0939
AMVT    CA=20   PT=366  DX=-0.0101  DY=0.0246  DZ=0.0174
AMVT    CA=21   PT=366  DX=-0.0207  DY=0.0505  DZ=0.0358
AMVT    CA=22   PT=366  DX=-0.1716  DY=0.4193  DZ=0.2974
AMVT    CA=23   PT=366  DX=-0.1105  DY=0.2700  DZ=0.1915
AMVT    CA=24   PT=366  DX=-0.0101  DY=0.0246  DZ=0.0174

*---------------------------
*END REGION 6 GEOMETRY TO NOZZLE NODE 366
*---------------------------

*----------------------------------------
*BEGIN REGION 4 TRANSIENT CARDS & GEOMETRY HEADER TO NOZZLES NODE 326 & 316
*----------------------------------------
*GROUP 4 HEADER TO NOZZLES NODE 326 & 316
INCL FN=Z:\SISJ-PROJECTS\VY-16Q\Rev0\REG4.INP
*
JUNC PT=210
CROS CD=20
BRAN PT=260 DX=0.1786 DY=0.0 DZ=-1.7 TE=2
```

```
TANG PT=270 DX=0.3 DZ=-2.853  EW=0
BRAD PT=275 RA=4.578  EW=0
TANG PT=320 DX=1.799 DZ=-3.108
*---------------------------
*END REGION 4 GEOMETRY HEADER TO NOZZLES NODE 326 & 316
*---------------------------

*----------------------------------------
*BEGIN REGION 5 TRANSIENT CARDS & GEOMETRY RISER TO NOZZLE NODE 316
*----------------------------------------
*GROUP 5 RISER TO NOZZLE NODE 316
INCL FN=Z:\SISJ-PROJECTS\VY-16Q\Rev0\REG5.INP
*
TANG PT=319 DX=0.71 DZ=-1.23  EW=1
CRED PT=317 DX=0.75 DZ=-1.3  AN=30
CROS CD=15
TANG PT=313 DX=0.5525 DZ=-0.957  EW=1
BRAD PT=400 RA=1.5  EW=1
TANG PT=310 DX=3.483 DZ=-2.011  EW=1
MATL CD=403.316
BRAD PT=311 RA=1.5  EW=1
MATL CD=376.316
CROS CD=15
TANG PT=312 DY=4.74
TANG PT=314 DY=6.99  EW=1
MATL CD=403.316
BRAD PT=315 RA=1.5  EW=1
*---------------------------
*END REGION 5 GEOMETRY RISER TO NOZZLE NODE 316
*---------------------------
*
*----------------------------------------
*BEGIN REGION 6 TRANSIENT CARDS & GEOMETRY TO NOZZLE NODE 316
*----------------------------------------
*GROUP 6 TO NOZZLE NODE 316
INCL FN=Z:\SISJ-PROJECTS\VY-16Q\Rev0\REG6.INP
*
MATL CD=376.316
TANG PT=818 DX=1.84 DZ=3.19
CROS CD=16
TANG PT=817 DX=0.4375 DZ=0.76  EW=1
CROS CD=17
TANG PT=816 DX=0.185 DZ=0.32  EW=1
CROS CD=18
TANG PT=815 DX=0.265 DZ=0.46  EW=1
CROS CD=19
TANG PT=316 DX=0.352 DZ=0.61  EW=1
NOZZ PT=316
AMVT    CA=1    PT=316  DX=-0.0101  DY=0.0246  DZ=-0.0174
AMVT    CA=2    PT=316  DX=-0.1800  DY=0.4398  DZ=-0.3120
AMVT    CA=3    PT=316  DX=-0.1783  DY=0.4357  DZ=-0.3091
AMVT    CA=4    PT=316  DX=-0.1716  DY=0.4193  DZ=-0.2974
AMVT    CA=5    PT=316  DX=-0.1783  DY=0.4357  DZ=-0.3091
AMVT    CA=6    PT=316  DX=-0.1716  DY=0.4193  DZ=-0.2974
AMVT    CA=7    PT=316  DX=-0.1674  DY=0.4091  DZ=-0.2902
AMVT    CA=8    PT=316  DX=-0.1716  DY=0.4193  DZ=-0.2974
AMVT    CA=9    PT=316  DX=-0.0815  DY=0.1991  DZ=-0.1412
AMVT    CA=10   PT=316  DX=-0.1609  DY=0.3930  DZ=-0.2788
AMVT    CA=11   PT=316  DX=-0.0815  DY=0.1991  DZ=-0.1412
AMVT    CA=12   PT=316  DX=-0.1800  DY=0.4398  DZ=-0.3120
```

```
AMVT    CA=13   PT=316  DX=-0.1800  DY=0.4398  DZ=-0.3120
AMVT    CA=14   PT=316  DX=-0.1097  DY=0.2678  DZ=-0.1899
AMVT    CA=15   PT=316  DX=-0.0931  DY=0.2275  DZ=-0.1613
AMVT    CA=16   PT=316  DX=-0.0542  DY=0.1324  DZ=-0.0939
AMVT    CA=17   PT=316  DX=-0.0101  DY=0.0246  DZ=-0.0174
AMVT    CA=18   PT=316  DX=-0.0101  DY=0.0246  DZ=-0.0174
AMVT    CA=19   PT=316  DX=-0.0542  DY=0.1324  DZ=-0.0939
AMVT    CA=20   PT=316  DX=-0.0101  DY=0.0246  DZ=-0.0174
AMVT    CA=21   PT=316  DX=-0.0207  DY=0.0505  DZ=-0.0358
AMVT    CA=22   PT=316  DX=-0.1716  DY=0.4193  DZ=-0.2974
AMVT    CA=23   PT=316  DX=-0.1105  DY=0.2700  DZ=-0.1915
AMVT    CA=24   PT=316  DX=-0.0101  DY=0.0246  DZ=-0.0174
*---------------------------
*END REGION 6 GEOMETRY TO NOZZLE NODE 316
*---------------------------
*
*----------------------------------------
*BEGIN REGION 5 TRANSIENT CARDS & GEOMETRY RISER TO NOZZLE NODE 346
*----------------------------------------
*GROUP 5 RISER TO NOZZLE NODE 346
INCL FN=Z:\SISJ-PROJECTS\VY-16Q\Rev0\REG5.INP
*
JUNC PT=340
CROS CD=15
BRAN PT=342 DY=1.36  TE=2
TANG PT=344 DY=10.39  EW=0
MATL CD=403.316
BRAD PT=345 RA=1.5  EW=1
*---------------------------
*END REGION 5 GEOMETRY RISER TO NOZZLE NODE 346
*---------------------------
*
*----------------------------------------
*BEGIN REGION 6 TRANSIENT CARDS & GEOMETRY TO NOZZLE NODE 346
*----------------------------------------
*GROUP 6 TO NOZZLE NODE 346
INCL FN=Z:\SISJ-PROJECTS\VY-16Q\Rev0\REG6.INP
*
MATL CD=376.316
TANG PT=848 DX=3.17 DZ=-1.83
CROS CD=16
TANG PT=847 DX=0.758 DZ=-0.4375  EW=1
CROS CD=17
TANG PT=846 DX=0.32 DZ=-0.185  EW=1
CROS CD=18
TANG PT=845 DX=0.46 DZ=-0.265  EW=1
CROS CD=19
TANG PT=346 DX=0.61 DZ=-0.352  EW=1
NOZZ PT=346
AMVT    CA=1    PT=346  DX=-0.0174  DY=0.0246  DZ=0.0101
AMVT    CA=2    PT=346  DX=-0.3120  DY=0.4398  DZ=0.1800
AMVT    CA=3    PT=346  DX=-0.3091  DY=0.4357  DZ=0.1783
AMVT    CA=4    PT=346  DX=-0.2974  DY=0.4193  DZ=0.1716
AMVT    CA=5    PT=346  DX=-0.3091  DY=0.4357  DZ=0.1783
AMVT    CA=6    PT=346  DX=-0.2974  DY=0.4193  DZ=0.1716
AMVT    CA=7    PT=346  DX=-0.2902  DY=0.4091  DZ=0.1674
AMVT    CA=8    PT=346  DX=-0.2974  DY=0.4193  DZ=0.1716
AMVT    CA=9    PT=346  DX=-0.1412  DY=0.1991  DZ=0.0815
AMVT    CA=10   PT=346  DX=-0.2788  DY=0.3930  DZ=0.1609
AMVT    CA=11   PT=346  DX=-0.1412  DY=0.1991  DZ=0.0815
```

```
AMVT    CA=12   PT=346  DX=-0.3120  DY=0.4398  DZ=0.1800
AMVT    CA=13   PT=346  DX=-0.3120  DY=0.4398  DZ=0.1800
AMVT    CA=14   PT=346  DX=-0.1899  DY=0.2678  DZ=0.1097
AMVT    CA=15   PT=346  DX=-0.1613  DY=0.2275  DZ=0.0931
AMVT    CA=16   PT=346  DX=-0.0939  DY=0.1324  DZ=0.0542
AMVT    CA=17   PT=346  DX=-0.0174  DY=0.0246  DZ=0.0101
AMVT    CA=18   PT=346  DX=-0.0174  DY=0.0246  DZ=0.0101
AMVT    CA=19   PT=346  DX=-0.0939  DY=0.1324  DZ=0.0542
AMVT    CA=20   PT=346  DX=-0.0174  DY=0.0246  DZ=0.0101
AMVT    CA=21   PT=346  DX=-0.0358  DY=0.0505  DZ=0.0207
AMVT    CA=22   PT=346  DX=-0.2974  DY=0.4193  DZ=0.1716
AMVT    CA=23   PT=346  DX=-0.1915  DY=0.2700  DZ=0.1105
AMVT    CA=24   PT=346  DX=-0.0174  DY=0.0246  DZ=0.0101
*---------------------------
*END REGION 6 GEOMETRY TO NOZZLE NODE 346
*---------------------------
*
*----------------------------------------
*BEGIN REGION 5 TRANSIENT CARDS & GEOMETRY RISER TO NOZZLE NODE 326
*----------------------------------------
*GROUP 5 RISER TO NOZZLE NODE 326
INCL FN=Z:\SISJ-PROJECTS\VY-16Q\Rev0\REG5.INP
*
JUNC PT=320
CROS CD=15
BRAN PT=322 DY=1.42  TE=2
TANG PT=324 DY=10.33  EW=1
MATL CD=403.316
BRAD PT=325 RA=1.5  EW=1
*---------------------------
*END REGION 5 GEOMETRY RISER TO NOZZLE NODE 326
*---------------------------
*
*----------------------------------------
*BEGIN REGION 6 TRANSIENT CARDS & GEOMETRY TO NOZZLE NODE 326
*----------------------------------------
*GROUP 6 TO NOZZLE NODE 326
INCL FN=Z:\SISJ-PROJECTS\VY-16Q\Rev0\REG6.INP
*
MATL CD=376.316
TANG PT=828 DX=3.18 DZ=1.84
CROS CD=16
TANG PT=827 DX=0.758 DZ=0.4375  EW=1
CROS CD=17
TANG PT=826 DX=0.32 DZ=0.185  EW=1
CROS CD=18
TANG PT=825 DX=0.46 DZ=0.265  EW=1
CROS CD=19
TANG PT=326 DX=0.61 DZ=0.352  EW=1
NOZZ PT=326
AMVT    CA=1    PT=326  DX=-0.0174  DY=0.0246  DZ=-0.0101
AMVT    CA=2    PT=326  DX=-0.3120  DY=0.4398  DZ=-0.1800
AMVT    CA=3    PT=326  DX=-0.3091  DY=0.4357  DZ=-0.1783
AMVT    CA=4    PT=326  DX=-0.2974  DY=0.4193  DZ=-0.1716
AMVT    CA=5    PT=326  DX=-0.3091  DY=0.4357  DZ=-0.1783
AMVT    CA=6    PT=326  DX=-0.2974  DY=0.4193  DZ=-0.1716
AMVT    CA=7    PT=326  DX=-0.2902  DY=0.4091  DZ=-0.1674
AMVT    CA=8    PT=326  DX=-0.2974  DY=0.4193  DZ=-0.1716
AMVT    CA=9    PT=326  DX=-0.1412  DY=0.1991  DZ=-0.0815
AMVT    CA=10   PT=326  DX=-0.2788  DY=0.3930  DZ=-0.1609
```

```
AMVT    CA=11   PT=326  DX=-0.1412  DY=0.1991  DZ=-0.0815
AMVT    CA=12   PT=326  DX=-0.3120  DY=0.4398  DZ=-0.1800
AMVT    CA=13   PT=326  DX=-0.3120  DY=0.4398  DZ=-0.1800
AMVT    CA=14   PT=326  DX=-0.1899  DY=0.2678  DZ=-0.1097
AMVT    CA=15   PT=326  DX=-0.1613  DY=0.2275  DZ=-0.0931
AMVT    CA=16   PT=326  DX=-0.0939  DY=0.1324  DZ=-0.0542
AMVT    CA=17   PT=326  DX=-0.0174  DY=0.0246  DZ=-0.0101
AMVT    CA=18   PT=326  DX=-0.0174  DY=0.0246  DZ=-0.0101
AMVT    CA=19   PT=326  DX=-0.0939  DY=0.1324  DZ=-0.0542
AMVT    CA=20   PT=326  DX=-0.0174  DY=0.0246  DZ=-0.0101
AMVT    CA=21   PT=326  DX=-0.0358  DY=0.0505  DZ=-0.0207
AMVT    CA=22   PT=326  DX=-0.2974  DY=0.4193  DZ=-0.1716
AMVT    CA=23   PT=326  DX=-0.1915  DY=0.2700  DZ=-0.1105
AMVT    CA=24   PT=326  DX=-0.0174  DY=0.0246  DZ=-0.0101
*---------------------------
*END REGION 6 GEOMETRY TO NOZZLE NODE 326
*---------------------------
*
*----------------------------------------
*BEGIN REGION 7A TRANSIENT CARDS & GEOMETRY TO RHR SUPPLY VALVE NODE 550
*----------------------------------------
*GROUP 7 TO RHR SUPPLY VALVE NODE 550
INCL FN=Z:\SISJ-PROJECTS\VY-16Q\Rev0\REG7A.INP
*
MATL CD=376.316
JUNC PT=500
CROS CD=25
BRAN PT=502 DX=1.67  EW=0  TE=1
TANG PT=506 DX=2.53  EW=0
MATL CD=403.316
BRAD PT=507 RA=1.67  EW=1
MATL CD=376.316
TANG PT=508 DZ=-4.01
TANG PT=515 DZ=-4.53  EW=1
MATL CD=403.316
BRAD PT=520 RA=1.67  EW=1
MATL CD=376.316
CROS CD=26
VALV PT=525 DX=-3.34 PL=1
JUNC PT=525
VALV PT=530 DX=-1.99 PL=2  EW=1
JUNC PT=525
RIGD PT=526 DY=2.5
LUMP PT=526 MA=7.569
JUNC PT=530
CROS CD=25
TANG PT=540 DX=-1.13  EW=1
CROS CD=26
VALV PT=545 DX=-1.97 PL=1
JUNC PT=545
RIGD PT=547 DY=2.5
LUMP PT=547 MA=7.355
JUNC PT=545
VALV PT=550 DX=-1.98 PL=2  EW=1
*---------------------------
*END REGION 7A GEOMETRY TO RHR SUPPLY VALVE NODE 550
*---------------------------
*
*----------------------------------------
*BEGIN REGION 7B TRANSIENT CARDS & GEOMETRY FROM RHR SUPPLY VALVE TO PENET. NODE 565
```

```
*----------------------------------------
*GROUP 17 FROM RHR SUPPLY VALVE TO PENET. NODE 565
INCL FN=Z:\SISJ-PROJECTS\VY-16Q\Rev0\REG7B.INP
*
CROS CD=25
MATL CD=106
TANG PT=555 DX=-3.36  EW=1
BRAD PT=556 RA=1.67  EW=1
TANG PT=560 DY=-10.17  EW=1
BRAD PT=561 RA=1.67  EW=1
TANG PT=563 DZ=-6.92
TANG PT=565 DZ=-6.92
*---------------------------
*END REGION 7B GEOMETRY FROM RHR SUPPLY VALVE TO PENET. NODE 565
*---------------------------
*
*----------------------------------------
*BEGIN REGION 8 TRANSIENT CARDS & GEOMETRY FOR 4 INCH BYPASS
*----------------------------------------
*GROUP 8 4 INCH BYPASS
INCL FN=Z:\SISJ-PROJECTS\VY-16Q\Rev0\REG8.INP
*
*NOTE CODING FOR 4 INCH BYPASS STARTS HERE
JUNC PT=152
CROS CD=27
MATL CD=376.316
BRAN PT=700 DX=-1.19  TE=4
TANG PT=702 DX=-0.61
TANG PT=703 DX=-1.43  EW=0
MATL CD=403.316
BRAD PT=704 RA=0.5  EW=0
MATL CD=376.316
TANG PT=705 DZ=5.08
*NOTE CONSTANT SUPPORT HA11 AT NODE 705
TANG PT=721 DZ=1.12
TANG PT=706 DZ=2.47
TANG PT=707 DZ=1.03
TANG PT=708 DZ=0.34
TANG PT=709 DZ=0.38
JUNC PT=707
BRAN PT=710 DY=0.34 TE=1
CROS CD=28
VALV PT=712 DY=0.71 MA=0.3669 PL=1  *AL=$VALVE V2-54A$
VALV PT=715 DZ=-3.5 MA=0.1831 PL=3
JUNC PT=712
VALV PT=714 DY=0.71          PL=2
CROS CD=27
TANG PT=723 DY=4.19
MATL CD=403.316
BRAD PT=716 RA=0.5
MATL CD=376.316
TANG PT=718 DX=1.48
TANG PT=720 DX=0.56
BRAN PT=176 DX=1.19  TE=4
************CODING FOR STRUTS RDA5 AND VAB1 FOLLOW
JUNC PT=170
CROS CD=40  *OD=4.5 inch
RIGD PT=725 DP=0 DX=-0.583 DY=1.84  *AL=$RDA5$
CROS CD=41  *OD=2.875 inch
RIGD PT=715 DP=0 DX=-2.67 DY=-0.79
```

```
RIGD PT=721 DP=0 DY=-1.05  *AL=$VAB1$
*************CODING FOR RDA1 STRUT FOLLOWS
CROS CD=42  *OD=28.339 inch
JUNC PT=175
RIGD PT=173 DP=0 DY=-3.5 DZ=0.34
CROS CD=41  *OD=2.875 inch
RIGD PT=708 DP=0 DX=-3.21  *AL=$RDA1$
*---------------------------
*END REGION 8 GEOMETRY  FOR 4 INCH BYPASS
*---------------------------
*
*----------------------------------------
*BEGIN REGION 9A TRANSIENT CARDS & GEOMETRY FOR RHR RETURN FROM TEE TO VALVE NODE 660
*----------------------------------------
*GROUP 9 RHR RETURN FROM TEE TO VALVE NODE 660
INCL FN=Z:\SISJ-PROJECTS\VY-16Q\Rev0\REG9A.INP
*
*NOTE CODING FOR RHR RETURN STARTS HERE
CROS CD=29
JUNC PT=600
MATL CD=376.316
BRAN PT=602 DX=-3.8123  TE=1
MATL CD=403.316
BRAD PT=610 RA=2  EW=1
TANP        DY=4
BRAD PT=612 RA=2  EW=1
MATL CD=376.316
TANG PT=614 DZ=-10.38  EW=1
MATL CD=403.316
BRAD PT=615 RA=10  EW=1
MATL CD=376.316
TANG PT=620 DX=5.98 DZ=-3.45  EW=1
*NOTE
*NOTE VARIABLE SPRING H104 AT NODE 620
*NOTE
*NOTE VALVE V10-81A DATA FROM 5920-4590 WEIGHT - 6845.#
*NOTE WEIGHT APPLIED AT ESTIMATED CENTER OF GRAVITY (NODE 623)
CROS CD=30
VALV PT=622 DX=1.98 DZ=-1.15 PL=1  *AL=$VALVE V10-81A$
JUNC PT=622
VALV PT=624 DX=1.98 DZ=-1.15 PL=2  EW=1
JUNC PT=622
RIGD PT=623 DY=2.5
LUMP PT=623 MA=7.32 *VALVE ACTUATOR
CROS CD=29
JUNC PT=624
TANG PT=625 DX=1.867 DZ=-1.078
TANG PT=630 DX=2.598 DZ=-1.5  EW=1
MATL CD=403.316
BRAD PT=631 RA=3  EW=1
MATL CD=376.316
TANG PT=640 DZ=-4.54  EW=1
MATL CD=403.316
BRAD PT=641 RA=2  EW=1
MATL CD=376.316
*NOTE VALVE V10-46A DATA FROM 5920-4718 WEIGHT - 5295.#
CROS CD=30
VALV PT=655 DX=-3.79 PL=1 TA=2 *AL=$VALVE V10-46A$
LUMP PT=655 MA=5.77
```

```
*---------------------------
*END REGION 9A GEOMETRY FOR RHR RETURN FROM TEE TO VALVE NODE 660
*---------------------------
*
*----------------------------------------
*BEGIN REGION 9B TRANSIENT CARDS & GEOMETRY FOR RHR RETURN FROM VALVE NODE 660 TO PENET. NODE
675
*----------------------------------------
*GROUP 19 RHR RETURN FROM VALVE NODE 660 TO PENET. NODE 675
INCL FN=Z:\SISJ-PROJECTS\VY-16Q\Rev0\REG9B.INP
*
*NOTE
*NOTE VARIABLE SPRING H105 AT NODE 655
*NOTE
VALV PT=660 DX=-1.79 PL=2  EW=1
*NOTE SPEC CHANGE TO CARBON STEEL
MATL CD=106
CROS CD=29
TANG PT=661 DX=-1
TANG PT=663 DX=-3.31  EW=1
BRAD PT=665 RA=2  EW=1
TANG PT=670 DY=-10.5 DZ=0.38  EW=1
BRAD PT=671 RA=2  EW=1
TANG PT=673 DZ=-7.74
TANG PT=675 DZ=-7.74
*---------------------------
*END REGION 9B GEOMETRY FOR RHR RETURN FROM VALVE NODE 660 TO PENET. NODE 675
*---------------------------
*
*---------------------------
***STRESS INDICES AT CROSS POINT
*---------------------------
*
INDI AT=210 AF=195 B1=0.5 C1=1 K1=4 B2=2.256 C2=3.024 K2=1 C3=1 K3=1 CP=0.5
INDI AT=210 AF=215 B1=0.5 C1=1 K1=4 B2=2.256 C2=3.024 K2=1 C3=1 K3=1 CP=0.5
INDI AT=210 AF=240 B1=0.5 C1=1 K1=4 B2=1.805 C2=3.024 K2=1 C3=1 K3=1 CP=0.5
INDI AT=210 AF=260 B1=0.5 C1=1 K1=4 B2=1.805 C2=3.024 K2=1 C3=1 K3=1 CP=0.5
*---------------------------
*** SUPPORTS
*---------------------------
RSTN PT=675  DX=1  SP=16000          *RHR SUPPLY PENET.
RSTN PT=675  DY=1  SP=16000          *RHR SUPPLY PENET.
RSTN PT=675  DZ=1  SP=23000          *RHR SUPPLY PENET.
ROTR PT=675  RX=1  SP=300000         *RHR SUPPLY PENET.
ROTR PT=675  RY=1  SP=300000         *RHR SUPPLY PENET.
ROTR PT=675  RZ=1  SP=340000         *RHR SUPPLY PENET.
RSTN PT=565  DX=1  SP=16000          *RHR SUPPLY PENET.
RSTN PT=565  DY=1  SP=16000          *RHR SUPPLY PENET.
RSTN PT=565  DZ=1  SP=23000          *RHR SUPPLY PENET.
ROTR PT=565  RX=1  SP=300000         *RHR SUPPLY PENET.
ROTR PT=565  RY=1  SP=300000         *RHR SUPPLY PENET.
ROTR PT=565  RZ=1  SP=340000         *RHR SUPPLY PENET.
*
SNUB PT=12   DZ=-1 SP=1000    *AL=$SNUBBER SS-7A-1$
SNUB PT=12   DX=1  SP=1000    *AL=$SNUBBER SS-7A-2$
SNUB PT=190  DX=-1 SP=1000    *AL=$SNUBBER SS-6-A1$
SNUB PT=190  DZ=1  SP=1000    *AL=$SNUBBER SS-6-A2$
*
VSUP PT=20   DY=1  FO=24.8  SP=2.664  *AL=$VARI. SUPT. HA-1$
*
```

```
CSUP PT=27   DY=1  FO=8.3   KP=0.01   *AL=$CONST. SUPT. H-8-A1$
CSUP PT=42   DY=1  FO=8.3   KP=0.01   *AL=$CONST. SUPT. H-8-A2$
CSUP PT=56   DY=1  FO=18.05 KP=0.01   *AL=$CONST. SUPT. HA3 FOR PUMP$
CSUP PT=69   DY=1  FO=18.0  KP=0.01   *AL=$CONST. SUPT. HA4 FOR PUMP$
CSUP PT=63   DY=1  FO=18.02 KP=0.01   *AL=$CONST. SUPT. HA5 FOR PUMP$
CSUP PT=160  DY=-1 FO=11.8  KP=0.01   *AL=$CONST. SUPT. HA-9 & HA-10$
CSUP PT=705  DY=1  FO=0.960 KP=0.01   *AL=$CONST. SUPT. HA-11 ON 4 INCH BYPASS$
*
VSUP PT=184  DY=1  FO=36.0 SP=3.542   *AL=$VARI. SUPT. HA-2$
VSUP PT=343  DY=1  FO=7.1  SP=3.014   *AL=$VARI. SUPT. HA13$
VSUP PT=313  DY=1  FO=7.1  SP=3.014   *AL=$VARI. SUPT. HA14$
*
VSUP PT=530  DY=1  SP=9.420 FO=26.0   *AL=$HANGER H109 RHR SUPPLY VALVE$
VSUP PT=620  DY=1  SP=7.084 FO=14.9   *AL=$HANGER H104 RHR RETURN VALVE$
VSUP PT=655  DY=1  SP=4.710 FO=22.0   *AL=$HANGER H105 RHR RETURN VALVE$
*
RSTN PT=15   DY=0.7071 DZ=-0.7071  SP=6000    *RECIRC PUMP
RSTN PT=16   DX=-0.7071 DY=0.7071  SP=6000    *RECIRC PUMP
ENDP
```

Reg1.inp

```
*-----------------------------------------------------------------
*BEGIN REGION 1 TRANSIENT CARDS & GEOMETRY FROM RHR SUPPLY TO TEE
*-----------------------------------------------------------------
*
OPER CA=1   TE=100  PR=1100
OPER CA=2   TE=100  PR=50
OPER CA=3   TE=549  PR=1010
OPER CA=4   TE=542  PR=1010
OPER CA=5   TE=526  PR=1010
OPER CA=6   TE=542  PR=1010
OPER CA=7   TE=526  PR=1010
OPER CA=8   TE=516  PR=1010
OPER CA=9   TE=526  PR=1010
OPER CA=10  TE=300  PR=1135
OPER CA=11  TE=500  PR=1135
OPER CA=12  TE=300  PR=675
OPER CA=13  TE=549  PR=1010
OPER CA=14  TE=549  PR=1010
OPER CA=15  TE=375  PR=170
OPER CA=16  TE=330  PR=90
OPER CA=17  TE=225  PR=0
OPER CA=18  TE=100  PR=0
OPER CA=19  TE=100  PR=1563
OPER CA=20  TE=225  PR=0
OPER CA=21  TE=225  PR=0
OPER CA=22  TE=130  PR=1010
OPER CA=23  TE=526  PR=1010
OPER CA=24  TE=375  PR=200
OPER CA=25  TE=100  PR=0
*
TRAN  CA=201  IS=1 FS=1 IT=70  FT=100  TT=1800  FL=2262  IP=15   FP=1115  TP=0
TRAN  CA=202  IS=1 FS=1 IT=100 FT=100  TT=1800  FL=2262  IP=1115 FP=65  TP=0
TRAN  CA=203  IS=1 FS=1 IT=100 FT=549  TT=16164 FL=16158 IP=65   FP=1025  TP=0
TRAN   CA=204  IS=1 FS=1 IT=549 FT=542  TT=0     FL=32316 IP=1025 FP=1025  TP=0
TRAN   CA=205  IS=1 FS=1 IT=542 FT=526  TT=0     FL=32316 IP=1025 FP=1025  TP=0
TRAN   CA=206  IS=1 FS=1 IT=526 FT=542  TT=900   FL=32316 IP=1025 FP=1025  TP=0
TRAN   CA=207  IS=1 FS=1 IT=542 FT=526  TT=360   FL=32316 IP=1025 FP=1025  TP=0
TRAN   CA=208  IS=1 FS=1 IT=526 FT=516  TT=0     FL=32316 IP=1025 FP=1025  TP=0
TRAN   CA=209  IS=1 FS=1 IT=516 FT=526  TT=0     FL=32316 IP=1025 FP=1025  TP=0
```

```
TRAN   CA=210  IS=1 FS=1 IT=526 FT=300  TT=220   FL=600   IP=1205 FP=1150   TP=0
TRAN  CA=211  IS=1 FS=1 IT=300 FT=500  TT=1980  FL=600   IP=900  FP=1150  TP=0
TRAN   CA=212  IS=1 FS=1 IT=500 FT=300  TT=180   FL=600   IP=1150  FP=690  TP=0
TRAN  CA=213  IS=1 FS=1 IT=300 FT=549  TT=8964  FL=16158 IP=255  FP=1025  TP=0
TRAN   CA=214  IS=1 FS=1 IT=526 FT=549  TT=0     FL=32316 IP=1025 FP=1025  TP=0
TRAN  CA=215  IS=1 FS=1 IT=549 FT=375  TT=6264  FL=16158 IP=1025 FP=185   TP=0
TRAN   CA=216  IS=1 FS=1 IT=375 FT=330  TT=600   FL=16158 IP=185  FP=105   TP=0
TRAN  CA=217  IS=1 FS=1 IT=330 FT=225  TT=3780  FL=16158 IP=105  FP=15    TP=0
TRAN  CA=218  IS=1 FS=1 IT=225 FT=100  TT=4500  FL=22858 IP=15   FP=15    TP=0
TRAN   CA=219  IS=1 FS=1 IT=100 FT=100  TT=0     FL=2262  IP=40   FP=1578  TP=0
TRAN   CA=220
TRAN   CA=221
TRAN   CA=222  IS=1 FS=1 IT=526 FT=130  TT=0     FL=32316 IP=1025  FP=1025 TP=0
TRAN   CA=223  IS=1 FS=1 IT=130 FT=526  TT=0     FL=32316 IP=1025  FP=1025 TP=0
TRAN   CA=224  IS=1 FS=1 IT=526 FT=375  TT=600   FL=32316 IP=1025  FP=215  TP=0
TRAN  CA=225  IS=1 FS=1 IT=375 FT=100  TT=9900  FL=32316 IP=215   FP=15   TP=0
*
PAIR  CA=201 CO=8.3  DI=0.140  EX=8.5 *Tavg=85.0
PAIR  CA=202 CO=8.3  DI=0.140  EX=8.5 *Tavg=100.0
PAIR  CA=203 CO=9.4  DI=0.151  EX=8.5 *Tavg=324.5
PAIR   CA=204 CO=10.5 DI=0.162  EX=8.5 *Tavg=545.5
PAIR   CA=205 CO=10.4 DI=0.161  EX=8.5 *Tavg=534.0
PAIR   CA=206 CO=10.4 DI=0.161  EX=8.5 *Tavg=534.0
PAIR   CA=207 CO=10.4 DI=0.161  EX=8.5 *Tavg=534.0
PAIR   CA=208 CO=10.3 DI=0.161  EX=8.5 *Tavg=521.0
PAIR   CA=209 CO=10.3 DI=0.161  EX=8.5 *Tavg=521.0
PAIR   CA=210 CO=9.9  DI=0.156  EX=8.5 *Tavg=413.0
PAIR  CA=211 CO=9.8  DI=0.155  EX=8.5 *Tavg=400.0
PAIR   CA=212 CO=9.8  DI=0.155  EX=8.5 *Tavg=400.0
PAIR  CA=213 CO=9.9  DI=0.156  EX=8.5 *Tavg=424.5
PAIR   CA=214 CO=10.4 DI=0.162  EX=8.5 *Tavg=537.5
PAIR  CA=215 CO=10.0 DI=0.158  EX=8.5 *Tavg=462.0
PAIR   CA=216 CO=9.5  DI=0.152  EX=8.5 *Tavg=352.5
PAIR  CA=217 CO=9.2  DI=0.149  EX=8.5 *Tavg=277.5
PAIR  CA=218 CO=8.7  DI=0.143  EX=8.5 *Tavg=162.5
PAIR   CA=219 CO=8.3  DI=0.140  EX=8.5 *Tavg=100.0
*PAIR  CA=220 CO=9.0  DI=0.146  EX=8.5 *Tavg=225.0
*PAIR  CA=221 CO=9.0  DI=0.146  EX=8.5 *Tavg=225.0
PAIR   CA=222 CO=9.4  DI=0.151  EX=8.5 *Tavg=328.0
PAIR   CA=223 CO=9.4  DI=0.151  EX=8.5 *Tavg=328.0
PAIR   CA=224 CO=10.0 DI=0.157  EX=8.5 *Tavg=450.5
PAIR  CA=225 CO=9.0  DI=0.147  EX=8.5 *Tavg=237.5
```

Reg2.inp

```
*-----------------------------------------------------------------------
*BEGIN REGION 2 TRANSIENT CARDS & GEOMETRY FROM RHR SUPPLY TEE TO PUMP
*-----------------------------------------------------------------------
*
OPER CA=1   TE=100  PR=1100
OPER CA=2   TE=100  PR=50
OPER CA=3   TE=549  PR=1010
OPER CA=4   TE=542  PR=1010
OPER CA=5   TE=526  PR=1010
OPER CA=6   TE=542  PR=1010
OPER CA=7   TE=526  PR=1010
OPER CA=8   TE=516  PR=1010
OPER CA=9   TE=526  PR=1010
OPER CA=10  TE=300  PR=1135
OPER CA=11  TE=500  PR=1135
OPER CA=12  TE=300  PR=675
```

```
OPER CA=13  TE=549  PR=1010
OPER CA=14  TE=549  PR=1010
OPER CA=15  TE=375  PR=170
OPER CA=16  TE=330  PR=90
OPER CA=17  TE=225  PR=0
OPER CA=18  TE=100  PR=0
OPER CA=19  TE=100  PR=1563
OPER CA=20  TE=225  PR=0
OPER CA=21  TE=225  PR=0
OPER CA=22  TE=130  PR=1010
OPER CA=23  TE=526  PR=1010
OPER CA=24  TE=375  PR=200
OPER CA=25  TE=100  PR=0
*
TRAN  CA=201  IS=1 FS=1 IT=70  FT=100  TT=1800  FL=2262  IP=15   FP=1115  TP=0
TRAN  CA=202  IS=1 FS=1 IT=100 FT=100  TT=1800  FL=2262  IP=1115 FP=65    TP=0
TRAN  CA=203  IS=1 FS=1 IT=100 FT=549  TT=16164 FL=16158 IP=65   FP=1025  TP=0
TRAN   CA=204  IS=1 FS=1 IT=549 FT=542  TT=0     FL=32316 IP=1025 FP=1025  TP=0
TRAN   CA=205  IS=1 FS=1 IT=542 FT=526  TT=0     FL=32316 IP=1025 FP=1025  TP=0
TRAN   CA=206  IS=1 FS=1 IT=526 FT=542  TT=900   FL=32316 IP=1025 FP=1025  TP=0
TRAN   CA=207  IS=1 FS=1 IT=542 FT=526  TT=360   FL=32316 IP=1025 FP=1025  TP=0
TRAN   CA=208  IS=1 FS=1 IT=526 FT=516  TT=0     FL=32316 IP=1025 FP=1025  TP=0
TRAN   CA=209  IS=1 FS=1 IT=516 FT=526  TT=0     FL=32316 IP=1025 FP=1025  TP=0
TRAN   CA=210  IS=1 FS=1 IT=526 FT=300  TT=220   FL=600   IP=1205 FP=1150  TP=0
TRAN  CA=211  IS=1 FS=1 IT=300 FT=500  TT=1980  FL=600   IP=900  FP=1150  TP=0
TRAN   CA=212  IS=1 FS=1 IT=500 FT=300  TT=180   FL=600   IP=1150 FP=690   TP=0
TRAN  CA=213  IS=1 FS=1 IT=300 FT=549  TT=8964  FL=16158 IP=255  FP=1025  TP=0
TRAN   CA=214  IS=1 FS=1 IT=526 FT=549  TT=0     FL=32316 IP=1025 FP=1025  TP=0
TRAN  CA=215  IS=1 FS=1 IT=549 FT=375  TT=6264  FL=16158 IP=1025 FP=185   TP=0
TRAN   CA=216  IS=1 FS=1 IT=375 FT=330  TT=600   FL=16158 IP=185  FP=105   TP=0
TRAN  CA=217  IS=1 FS=1 IT=330 FT=225  TT=3780  FL=16158 IP=105  FP=15    TP=0
TRAN  CA=218  IS=1 FS=1 IT=225 FT=100  TT=4500  FL=16158 IP=15   FP=15    TP=0
TRAN   CA=219  IS=1 FS=1 IT=100 FT=100  TT=0     FL=2262  IP=40   FP=1578  TP=0
TRAN   CA=220
TRAN   CA=221
TRAN   CA=222  *IS=1 FS=1 IT=526 FT=130  TT=0     FL=32316 IP=1025  FP=1025 TP=0
TRAN   CA=223  IS=1 FS=1 IT=130 FT=526  TT=0     FL=32316 IP=1025  FP=1025 TP=0
TRAN   CA=224  IS=1 FS=1 IT=526 FT=375  TT=600   FL=32316 IP=1025  FP=215  TP=0
TRAN  CA=225  IS=1 FS=1 IT=375 FT=100  TT=9900  FL=32316 IP=215   FP=15   TP=0
*
PAIR  CA=201 CO=8.3  DI=0.140  EX=8.5 *Tavg=85.0
PAIR  CA=202 CO=8.3  DI=0.140  EX=8.5 *Tavg=100.0
PAIR  CA=203 CO=9.4  DI=0.151  EX=8.5 *Tavg=324.5
PAIR   CA=204 CO=10.5 DI=0.162  EX=8.5 *Tavg=545.5
PAIR   CA=205 CO=10.4 DI=0.161  EX=8.5 *Tavg=534.0
PAIR   CA=206 CO=10.4 DI=0.161  EX=8.5 *Tavg=534.0
PAIR   CA=207 CO=10.4 DI=0.161  EX=8.5 *Tavg=534.0
PAIR   CA=208 CO=10.3 DI=0.161  EX=8.5 *Tavg=521.0
PAIR   CA=209 CO=10.3 DI=0.161  EX=8.5 *Tavg=521.0
PAIR   CA=210 CO=9.9  DI=0.156  EX=8.5 *Tavg=413.0
PAIR  CA=211 CO=9.8  DI=0.155  EX=8.5 *Tavg=400.0
PAIR   CA=212 CO=9.8  DI=0.155  EX=8.5 *Tavg=400.0
PAIR  CA=213 CO=9.9  DI=0.156  EX=8.5 *Tavg=424.5
PAIR   CA=214 CO=10.4 DI=0.162  EX=8.5 *Tavg=537.5
PAIR  CA=215 CO=10.0 DI=0.158  EX=8.5 *Tavg=462.0
PAIR   CA=216 CO=9.5  DI=0.152  EX=8.5 *Tavg=352.5
PAIR  CA=217 CO=9.2  DI=0.149  EX=8.5 *Tavg=277.5
PAIR  CA=218 CO=8.7  DI=0.143  EX=8.5 *Tavg=162.5
PAIR   CA=219 CO=8.3  DI=0.140  EX=8.5 *Tavg=100.0
*PAIR  CA=220 CO=9.0  DI=0.146  EX=8.5 *Tavg=225.0
```

```
*PAIR  CA=221 CO=9.0  DI=0.146  EX=8.5 *Tavg=225.0
*PAIR   CA=222 CO=9.4  DI=0.151  EX=8.5 *Tavg=328.0
PAIR   CA=223 CO=9.4  DI=0.151  EX=8.5 *Tavg=328.0
PAIR   CA=224 CO=10.0 DI=0.157  EX=8.5 *Tavg=450.5
PAIR  CA=225 CO=9.0  DI=0.147  EX=8.5 *Tavg=237.5
```

Reg3.inp

```
*----------------------------------------
*BEGIN REGION 3 TRANSIENT CARDS & GEOMETRY FROM PUMP DISCHARGE TO HEADER
*----------------------------------------
*
OPER CA=1   TE=100  PR=1100
OPER CA=2   TE=100  PR=50
OPER CA=3   TE=549  PR=1035
OPER CA=4   TE=542  PR=1035
OPER CA=5   TE=526  PR=1035
OPER CA=6   TE=542  PR=1035
OPER CA=7   TE=526  PR=1035
OPER CA=8   TE=516  PR=1035
OPER CA=9   TE=526  PR=1035
OPER CA=10  TE=300  PR=1160
OPER CA=11  TE=500  PR=1160
OPER CA=12  TE=300  PR=700
OPER CA=13  TE=549  PR=1035
OPER CA=14  TE=549  PR=1035
OPER CA=15  TE=375  PR=195
OPER CA=16  TE=330  PR=115
OPER CA=17  TE=225  PR=25
OPER CA=18  TE=100  PR=25
OPER CA=19  TE=100  PR=1563
OPER CA=20  TE=225  PR=25
OPER CA=21  TE=225  PR=25
OPER CA=22  TE=130  PR=1035
OPER CA=23  TE=526  PR=1035
OPER CA=24  TE=375  PR=225
OPER CA=25  TE=100  PR=25
*
TRAN  CA=201  IS=1 FS=1 IT=70  FT=100  TT=1800  FL=2262  IP=15   FP=1115  TP=0
TRAN  CA=202  IS=1 FS=1 IT=70  FT=100  TT=1800  FL=2262  IP=1115 FP=65    TP=0
TRAN  CA=203  IS=1 FS=1 IT=100 FT=549  TT=16164 FL=16158 IP=65   FP=1050  TP=0
TRAN   CA=204  IS=1 FS=1 IT=549 FT=542  TT=0     FL=32316 IP=1050 FP=1050  TP=0
TRAN   CA=205  IS=1 FS=1 IT=542 FT=526  TT=0     FL=32316 IP=1050 FP=1050  TP=0
TRAN   CA=206  IS=1 FS=1 IT=526 FT=542  TT=900   FL=32316 IP=1050 FP=1050  TP=0
TRAN   CA=207  IS=1 FS=1 IT=542 FT=526  TT=360   FL=32316 IP=1050 FP=1050  TP=0
TRAN   CA=208  IS=1 FS=1 IT=526 FT=516  TT=0     FL=32316 IP=1050 FP=1050  TP=0
TRAN   CA=209  IS=1 FS=1 IT=516 FT=526  TT=0     FL=32316 IP=1050 FP=1050  TP=0
TRAN   CA=210  IS=1 FS=1 IT=526 FT=300  TT=220   FL=600   IP=1230 FP=1175  TP=0
TRAN  CA=211  IS=1 FS=1 IT=300 FT=500  TT=1980  FL=600   IP=925  FP=1175  TP=0
TRAN   CA=212  IS=1 FS=1 IT=500 FT=300  TT=180   FL=600   IP=1175 FP=715   TP=0
TRAN  CA=213  IS=1 FS=1 IT=300 FT=549  TT=8964  FL=16158 IP=280  FP=1050  TP=0
TRAN   CA=214  IS=1 FS=1 IT=526 FT=549  TT=0     FL=32316 IP=1050 FP=1050  TP=0
TRAN  CA=215  IS=1 FS=1 IT=549 FT=375  TT=6264  FL=16158 IP=1050 FP=210   TP=0
TRAN   CA=216  IS=1 FS=1 IT=375 FT=330  TT=600   FL=16158 IP=210  FP=130   TP=0
TRAN  CA=217  IS=1 FS=1 IT=330 FT=225  TT=3780  FL=16158 IP=130  FP=40    TP=0
TRAN  CA=218  IS=1 FS=1 IT=225 FT=100  TT=4500  FL=16158 IP=40   FP=40    TP=0
TRAN   CA=219  IS=1 FS=1 IT=100 FT=100  TT=0     FL=2262  IP=40   FP=1578  TP=0
TRAN   CA=220
TRAN   CA=221
TRAN   CA=222  *IS=1 FS=1 IT=526 FT=130  TT=0     FL=32316 IP=1050  FP=1050 TP=0
TRAN   CA=223  IS=1 FS=1 IT=130 FT=526  TT=0     FL=32316 IP=1050  FP=1050 TP=0
```

```
TRAN   CA=224  IS=1 FS=1 IT=526 FT=375  TT=600   FL=32316 IP=1050  FP=240  TP=0
TRAN  CA=225  IS=1 FS=1 IT=375 FT=100  TT=9900  FL=32316 IP=240   FP=40   TP=0
*
PAIR  CA=201 CO=8.3  DI=0.140 EX=8.5 *Tavg=85.0
PAIR  CA=202 CO=8.3  DI=0.140 EX=8.5 *Tavg=100.0
PAIR  CA=203 CO=9.4  DI=0.151 EX=8.5 *Tavg=324.5
PAIR   CA=204 CO=10.5 DI=0.162 EX=8.5 *Tavg=545.5
PAIR   CA=205 CO=10.4 DI=0.161 EX=8.5 *Tavg=534.0
PAIR   CA=206 CO=10.4 DI=0.161 EX=8.5 *Tavg=534.0
PAIR   CA=207 CO=10.4 DI=0.161 EX=8.5 *Tavg=534.0
PAIR   CA=208 CO=10.3 DI=0.161 EX=8.5 *Tavg=521.0
PAIR   CA=209 CO=10.3 DI=0.161 EX=8.5 *Tavg=521.0
PAIR   CA=210 CO=9.9  DI=0.156 EX=8.5 *Tavg=413.0
PAIR  CA=211 CO=9.8  DI=0.155 EX=8.5 *Tavg=400.0
PAIR   CA=212 CO=9.8  DI=0.155 EX=8.5 *Tavg=400.0
PAIR  CA=213 CO=9.9  DI=0.156 EX=8.5 *Tavg=424.5
PAIR   CA=214 CO=10.4 DI=0.162 EX=8.5 *Tavg=537.5
PAIR  CA=215 CO=10.0 DI=0.158 EX=8.5 *Tavg=462.0
PAIR   CA=216 CO=9.5  DI=0.152 EX=8.5 *Tavg=352.5
PAIR  CA=217 CO=9.2  DI=0.149 EX=8.5 *Tavg=277.5
PAIR  CA=218 CO=8.7  DI=0.143 EX=8.5 *Tavg=162.5
PAIR   CA=219 CO=8.3  DI=0.140 EX=8.5 *Tavg=100.0
*PAIR  CA=220 CO=9.0  DI=0.146 EX=8.5 *Tavg=225.0
*PAIR  CA=221 CO=9.0  DI=0.146 EX=8.5 *Tavg=225.0
*PAIR   CA=222 CO=9.4  DI=0.151 EX=8.5 *Tavg=328.0
PAIR   CA=223 CO=9.4  DI=0.151 EX=8.5 *Tavg=328.0
PAIR   CA=224 CO=10.0 DI=0.157 EX=8.5 *Tavg=450.5
PAIR  CA=225 CO=9.0  DI=0.147 EX=8.5 *Tavg=237.5
```

Reg3B.inp

```
*----------------------------------------
*BEGIN REGION 3B TRANSIENT CARDS & GEOMETRY AFFECTED BY RHR INITIATION
*----------------------------------------
*
OPER CA=20  TE=225  PR=25
OPER CA=21  TE=180  PR=25
*
TRAN CA=220 IS=1 FS=1 IT=180  FT=225 TT=60 FL=22858 IP=40 FP=40
TRAN CA=221 IS=1 FS=1 IT=225 FT=180  TT=60 FL=22858 IP=40 FP=40
PAIR  CA=220 CO=8.8 DI=0.145 EX=8.5 *Tavg=202.5
PAIR  CA=221 CO=8.8 DI=0.145 EX=8.5 *Tavg=202.5
```

Reg4.inp

```
*----------------------------------------
*BEGIN REGION 4 TRANSIENT CARDS & GEOMETRY HEADER TO NOZZLE NODE 366
*----------------------------------------
*
OPER CA=1   TE=100  PR=1100
OPER CA=2   TE=100  PR=50
OPER CA=3   TE=549  PR=1035
OPER CA=4   TE=542  PR=1035
OPER CA=5   TE=526  PR=1035
OPER CA=6   TE=542  PR=1035
OPER CA=7   TE=526  PR=1035
OPER CA=8   TE=516  PR=1035
OPER CA=9   TE=526  PR=1035
OPER CA=10  TE=300  PR=1160
OPER CA=11  TE=500  PR=1160
OPER CA=12  TE=300  PR=700
OPER CA=13  TE=549  PR=1035
```

```
OPER CA=14  TE=549  PR=1035
OPER CA=15  TE=375  PR=195
OPER CA=16  TE=330  PR=115
OPER CA=17  TE=225  PR=25
OPER CA=18  TE=100  PR=25
OPER CA=19  TE=100  PR=1563
OPER CA=20  TE=225  PR=25
OPER CA=21  TE=180  PR=25
OPER CA=22  TE=130  PR=1035
OPER CA=23  TE=526  PR=1035
OPER CA=24  TE=375  PR=225
OPER CA=25  TE=100  PR=25
*
TRAN  CA=201 IS=1 FS=1 IT=70  FT=100 TT=1800  FL=905    IP=15   FP=1115 TP=0
TRAN  CA=202 IS=1 FS=1 IT=100 FT=100 TT=1800  FL=905    IP=1115 FP=65   TP=0
TRAN  CA=203 IS=1 FS=1 IT=100 FT=549 TT=16164 FL=6463   IP=65   FP=1050 TP=0
TRAN   CA=204 IS=1 FS=1 IT=549 FT=542 TT=0     FL=12926  IP=1050 FP=1050 TP=0
TRAN   CA=205 IS=1 FS=1 IT=542 FT=526 TT=0     FL=12926  IP=1050 FP=1050 TP=0
TRAN   CA=206 IS=1 FS=1 IT=526 FT=542 TT=900   FL=12926  IP=1050 FP=1050 TP=0
TRAN   CA=207 IS=1 FS=1 IT=542 FT=526 TT=360   FL=12926  IP=1050 FP=1050 TP=0
TRAN   CA=208 IS=1 FS=1 IT=526 FT=516 TT=0     FL=12926  IP=1050 FP=1050 TP=0
TRAN   CA=209 IS=1 FS=1 IT=516 FT=526 TT=0     FL=12926  IP=1050 FP=1050 TP=0
TRAN   CA=210 IS=1 FS=1 IT=526 FT=300 TT=220   FL=400    IP=1230 FP=1175 TP=0
TRAN  CA=211 IS=1 FS=1 IT=300 FT=500 TT=1980  FL=400    IP=925  FP=1175 TP=0
TRAN   CA=212 IS=1 FS=1 IT=500 FT=300 TT=180   FL=400    IP=1175 FP=715  TP=0
TRAN  CA=213 IS=1 FS=1 IT=300 FT=549 TT=8964  FL=6463   IP=280  FP=1050 TP=0
TRAN   CA=214 IS=1 FS=1 IT=526 FT=549 TT=0     FL=12926  IP=1050 FP=1050 TP=0
TRAN  CA=215 IS=1 FS=1 IT=549 FT=375 TT=6264  FL=6463   IP=1050 FP=210  TP=0
TRAN   CA=216 IS=1 FS=1 IT=375 FT=330 TT=600   FL=6463   IP=210  FP=130  TP=0
TRAN  CA=217 IS=1 FS=1 IT=330 FT=225 TT=3780  FL=6463   IP=130  FP=40   TP=0
TRAN  CA=218 IS=1 FS=1 IT=225 FT=100 TT=4500  FL=9143   IP=40   FP=40   TP=0
TRAN   CA=219 IS=1 FS=1 IT=100 FT=100 TT=0     FL=905    IP=40   FP=1578 TP=0
TRAN   CA=220 IS=1 FS=1 IT=180 FT=225 TT=60    FL=9143   IP=40   FP=40   TP=0
TRAN   CA=221 IS=1 FS=1 IT=225 FT=180 TT=60    FL=9143   IP=40   FP=40   TP=0
TRAN   *CA=222 IS=1 FS=1 IT=526 FT=130 TT=0     FL=12926  IP=1050 FP=1050 TP=0
TRAN   CA=223 IS=1 FS=1 IT=130 FT=526 TT=0     FL=12926  IP=1050 FP=1050 TP=0
TRAN   CA=224 IS=1 FS=1 IT=526 FT=375 TT=600   FL=12926  IP=1050 FP=240  TP=0
TRAN  CA=225 IS=1 FS=1 IT=375 FT=100 TT=9900  FL=12926  IP=240  FP=40   TP=0
*
PAIR CA=201 CO=8.3  DI=0.140 EX=8.5 *Tavg=85.0
PAIR CA=202 CO=8.3  DI=0.140 EX=8.5 *Tavg=100.0
PAIR CA=203 CO=9.4  DI=0.151 EX=8.5 *Tavg=324.5
PAIR  CA=204 CO=10.5 DI=0.162 EX=8.5 *Tavg=545.5
PAIR  CA=205 CO=10.4 DI=0.161 EX=8.5 *Tavg=534.0
PAIR  CA=206 CO=10.4 DI=0.161 EX=8.5 *Tavg=534.0
PAIR  CA=207 CO=10.4 DI=0.161 EX=8.5 *Tavg=534.0
PAIR  CA=208 CO=10.3 DI=0.161 EX=8.5 *Tavg=521.0
PAIR  CA=209 CO=10.3 DI=0.161 EX=8.5 *Tavg=521.0
PAIR  CA=210 CO=9.9  DI=0.156 EX=8.5 *Tavg=413.0
PAIR CA=211 CO=9.8  DI=0.155 EX=8.5 *Tavg=400.0
PAIR  CA=212 CO=9.8  DI=0.155 EX=8.5 *Tavg=400.0
PAIR CA=213 CO=9.9  DI=0.156 EX=8.5 *Tavg=424.5
PAIR  CA=214 CO=10.4 DI=0.162 EX=8.5 *Tavg=537.5
PAIR CA=215 CO=10.0 DI=0.158 EX=8.5 *Tavg=462.0
PAIR  CA=216 CO=9.5  DI=0.152 EX=8.5 *Tavg=352.5
PAIR CA=217 CO=9.2  DI=0.149 EX=8.5 *Tavg=277.5
PAIR CA=218 CO=8.7  DI=0.143 EX=8.5 *Tavg=162.5
PAIR  CA=219 CO=8.3  DI=0.140 EX=8.5 *Tavg=100.0
PAIR  CA=220 CO=8.8  DI=0.145 EX=8.5 *Tavg=202.5
PAIR  CA=221 CO=8.8  DI=0.145 EX=8.5 *Tavg=202.5
```

```
*PAIR  CA=222 CO=9.4  DI=0.151 EX=8.5 *Tavg=328.0
PAIR  CA=223 CO=9.4  DI=0.151 EX=8.5 *Tavg=328.0
PAIR  CA=224 CO=10.0 DI=0.157 EX=8.5 *Tavg=450.5
PAIR CA=225 CO=9.0  DI=0.147 EX=8.5 *Tavg=237.5
```

Reg5.inp

```
*----------------------------------------
*BEGIN REGION 5 TRANSIENT CARDS & GEOMETRY RISER TO NOZZLE NODE 336
*----------------------------------------
*
OPER CA=1   TE=100  PR=1100
OPER CA=2   TE=100  PR=50
OPER CA=3   TE=549  PR=1035
OPER CA=4   TE=542  PR=1035
OPER CA=5   TE=526  PR=1035
OPER CA=6   TE=542  PR=1035
OPER CA=7   TE=526  PR=1035
OPER CA=8   TE=516  PR=1035
OPER CA=9   TE=526  PR=1035
OPER CA=10  TE=300  PR=1160
OPER CA=11  TE=500  PR=1160
OPER CA=12  TE=300  PR=700
OPER CA=13  TE=549  PR=1035
OPER CA=14  TE=549  PR=1035
OPER CA=15  TE=375  PR=195
OPER CA=16  TE=330  PR=115
OPER CA=17  TE=225  PR=25
OPER CA=18  TE=100  PR=25
OPER CA=19  TE=100  PR=1563
OPER CA=20  TE=225  PR=25
OPER CA=21  TE=180  PR=25
OPER CA=22  TE=130  PR=1035
OPER CA=23  TE=526  PR=1035
OPER CA=24  TE=375  PR=225
OPER CA=25  TE=100  PR=25
*
TRAN  CA=201 IS=1 FS=1 IT=70  FT=100  TT=1800  FL=452   IP=15   FP=1115 TP=0
TRAN  CA=202 IS=1 FS=1 IT=100 FT=100  TT=1800  FL=452   IP=1115 FP=65   TP=0
TRAN  CA=203 IS=1 FS=1 IT=100 FT=549  TT=16164 FL=3232  IP=65   FP=1050 TP=0
TRAN   CA=204 IS=1 FS=1 IT=549 FT=542  TT=0     FL=6463  IP=1050 FP=1050 TP=0
TRAN   CA=205 IS=1 FS=1 IT=542 FT=526  TT=0     FL=6463  IP=1050 FP=1050 TP=0
TRAN   CA=206 IS=1 FS=1 IT=526 FT=542  TT=900   FL=6463  IP=1050 FP=1050 TP=0
TRAN   CA=207 IS=1 FS=1 IT=542 FT=526  TT=360   FL=6463  IP=1050 FP=1050 TP=0
TRAN   CA=208 IS=1 FS=1 IT=526 FT=516  TT=0     FL=6463  IP=1050 FP=1050 TP=0
TRAN   CA=209 IS=1 FS=1 IT=516 FT=526  TT=0     FL=6463  IP=1050 FP=1050 TP=0
TRAN   CA=210 IS=1 FS=1 IT=526 FT=300  TT=220   FL=200   IP=1230 FP=1175 TP=0
TRAN  CA=211 IS=1 FS=1 IT=300 FT=500  TT=1980  FL=200   IP=925  FP=1175 TP=0
TRAN   CA=212 IS=1 FS=1 IT=500 FT=300  TT=180   FL=200   IP=1175 FP=715  TP=0
TRAN  CA=213 IS=1 FS=1 IT=300 FT=549  TT=8964  FL=3232  IP=280  FP=1050 TP=0
TRAN   CA=214 IS=1 FS=1 IT=526 FT=549  TT=0     FL=6463  IP=1050 FP=1050 TP=0
TRAN  CA=215 IS=1 FS=1 IT=549 FT=375  TT=6264  FL=3232  IP=1050 FP=210  TP=0
TRAN   CA=216 IS=1 FS=1 IT=375 FT=330  TT=600   FL=3232  IP=210  FP=130  TP=0
TRAN  CA=217 IS=1 FS=1 IT=330 FT=225  TT=3780  FL=3232  IP=130  FP=40   TP=0
TRAN  CA=218 IS=1 FS=1 IT=225 FT=100  TT=4500  FL=4571  IP=40   FP=40   TP=0
TRAN   CA=219 IS=1 FS=1 IT=100 FT=100  TT=0     FL=452   IP=40   FP=1578 TP=0
TRAN   CA=220 IS=1 FS=1 IT=180 FT=225  TT=60    FL=4572  IP=40   FP=40   TP=0
TRAN   CA=221 IS=1 FS=1 IT=225 FT=180  TT=60    FL=4572  IP=40   FP=40   TP=0
TRAN   *CA=222 IS=1 FS=1 IT=526 FT=130  TT=0     FL=6463  IP=1050 FP=1050 TP=0
TRAN   CA=223 IS=1 FS=1 IT=130 FT=526  TT=0     FL=6463  IP=1050 FP=1050 TP=0
TRAN   CA=224 IS=1 FS=1 IT=526 FT=375  TT=600   FL=6463  IP=1050 FP=240  TP=0
```

```
TRAN  CA=225 IS=1 FS=1 IT=375 FT=100  TT=9900  FL=6463  IP=240  FP=40   TP=0
*
PAIR  CA=201 CO=8.3  DI=0.140 EX=8.5 *Tavg=85.0
PAIR  CA=202 CO=8.3  DI=0.140 EX=8.5 *Tavg=100.0
PAIR  CA=203 CO=9.4  DI=0.151 EX=8.5 *Tavg=324.5
PAIR   CA=204 CO=10.5 DI=0.162 EX=8.5 *Tavg=545.5
PAIR   CA=205 CO=10.4 DI=0.161 EX=8.5 *Tavg=534.0
PAIR   CA=206 CO=10.4 DI=0.161 EX=8.5 *Tavg=534.0
PAIR   CA=207 CO=10.4 DI=0.161 EX=8.5 *Tavg=534.0
PAIR   CA=208 CO=10.3 DI=0.161 EX=8.5 *Tavg=521.0
PAIR   CA=209 CO=10.3 DI=0.161 EX=8.5 *Tavg=521.0
PAIR   CA=210 CO=9.9  DI=0.156 EX=8.5 *Tavg=413.0
PAIR   CA=211 CO=9.8  DI=0.155 EX=8.5 *Tavg=400.0
PAIR   CA=212 CO=9.8  DI=0.155 EX=8.5 *Tavg=400.0
PAIR  CA=213 CO=9.9  DI=0.156 EX=8.5 *Tavg=424.5
PAIR   CA=214 CO=10.4 DI=0.162 EX=8.5 *Tavg=537.5
PAIR  CA=215 CO=10.0 DI=0.158 EX=8.5 *Tavg=462.0
PAIR   CA=216 CO=9.5  DI=0.152 EX=8.5 *Tavg=352.5
PAIR  CA=217 CO=9.2  DI=0.149 EX=8.5 *Tavg=277.5
PAIR  CA=218 CO=8.7  DI=0.143 EX=8.5 *Tavg=162.5
PAIR   CA=219 CO=8.3  DI=0.140 EX=8.5 *Tavg=100.0
PAIR   CA=220 CO=8.8  DI=0.145 EX=8.5 *Tavg=202.5
PAIR   CA=221 CO=8.8  DI=0.145 EX=8.5 *Tavg=202.5
*PAIR   CA=222 CO=9.4  DI=0.151 EX=8.5 *Tavg=328.0
PAIR   CA=223 CO=9.4  DI=0.151 EX=8.5 *Tavg=328.0
PAIR   CA=224 CO=10.0 DI=0.157 EX=8.5 *Tavg=450.5
PAIR  CA=225 CO=9.0  DI=0.147 EX=8.5 *Tavg=237.5
```

Reg6.inp

```
*----------------------------------------
*BEGIN REGION 6 TRANSIENT CARDS & GEOMETRY TO NOZZLE NODE 336
*----------------------------------------
*
OPER CA=1   TE=100  PR=1100
OPER CA=2   TE=100  PR=50
OPER CA=3   TE=549  PR=1035
OPER CA=4   TE=542  PR=1035
OPER CA=5   TE=526  PR=1035
OPER CA=6   TE=542  PR=1035
OPER CA=7   TE=526  PR=1035
OPER CA=8   TE=516  PR=1035
OPER CA=9   TE=526  PR=1035
OPER CA=10  TE=300  PR=1160
OPER CA=11  TE=500  PR=1160
OPER CA=12  TE=300  PR=700
OPER CA=13  TE=549  PR=1035
OPER CA=14  TE=549  PR=1035
OPER CA=15  TE=375  PR=195
OPER CA=16  TE=330  PR=115
OPER CA=17  TE=225  PR=25
OPER CA=18  TE=100  PR=25
OPER CA=19  TE=100  PR=1563
OPER CA=20  TE=225  PR=25
OPER CA=21  TE=180  PR=25
OPER CA=22  TE=130  PR=1035
OPER CA=23  TE=526  PR=1035
OPER CA=24  TE=375  PR=225
OPER CA=25  TE=100  PR=25
*
TRAN CA=201  IS=1 FS=1 IT=70  FT=100  TT=1800  FL=452  IP=15   FP=1115 TP=0
```

```
TRAN CA=202  IS=1 FS=1 IT=100 FT=100  TT=1800  FL=452  IP=1115 FP=65   TP=0
TRAN CA=203  IS=1 FS=1 IT=100 FT=549  TT=16164 FL=3232 IP=65   FP=1050 TP=0
TRAN  CA=204  IS=1 FS=1 IT=549 FT=542  TT=0     FL=6463 IP=1050 FP=1050 TP=0
TRAN  CA=205  IS=1 FS=1 IT=542 FT=526  TT=0     FL=6463 IP=1050 FP=1050 TP=0
TRAN  CA=206  IS=1 FS=1 IT=526 FT=542  TT=900   FL=6463 IP=1050 FP=1050 TP=0
TRAN  CA=207  IS=1 FS=1 IT=542 FT=526  TT=360   FL=6463 IP=1050 FP=1050 TP=0
TRAN  CA=208  IS=1 FS=1 IT=526 FT=516  TT=0     FL=6463 IP=1050 FP=1050 TP=0
TRAN  CA=209  IS=1 FS=1 IT=516 FT=526  TT=0     FL=6463 IP=1050 FP=1050 TP=0
TRAN  CA=210  IS=1 FS=1 IT=526 FT=300  TT=220   FL=200  IP=1230 FP=1175 TP=0
TRAN CA=211  IS=1 FS=1 IT=300 FT=500  TT=1980  FL=200  IP=925  FP=1175 TP=0
TRAN  CA=212  IS=1 FS=1 IT=500 FT=300  TT=180   FL=200  IP=1175 FP=715  TP=0
TRAN CA=213  IS=1 FS=1 IT=300 FT=549  TT=8964  FL=3232 IP=280  FP=1050 TP=0
TRAN  CA=214  IS=1 FS=1 IT=526 FT=549  TT=0     FL=6463 IP=1050 FP=1050 TP=0
TRAN CA=215  IS=1 FS=1 IT=549 FT=375  TT=6264  FL=3232 IP=1050 FP=210  TP=0
TRAN  CA=216  IS=1 FS=1 IT=375 FT=330  TT=600   FL=3232 IP=210  FP=130  TP=0
TRAN CA=217  IS=1 FS=1 IT=330 FT=225  TT=3780  FL=3232 IP=130  FP=40   TP=0
TRAN CA=218  IS=1 FS=1 IT=225 FT=100  TT=4500  FL=4572 IP=40   FP=40   TP=0
TRAN  CA=219  IS=1 FS=1 IT=100 FT=100  TT=0     FL=452  IP=40   FP=1578 TP=0
TRAN  CA=220  IS=1 FS=1 IT=180 FT=225  TT=60    FL=4572 IP=40   FP=40   TP=0
TRAN  CA=221  IS=1 FS=1 IT=225 FT=180  TT=60    FL=4572 IP=40   FP=40   TP=0
TRAN  CA=222  IS=1 FS=1 IT=526 FT=130  TT=0     FL=6463 IP=1050 FP=1050 TP=0
TRAN  CA=223  IS=1 FS=1 IT=130 FT=526  TT=0     FL=6463 IP=1050 FP=1050 TP=0
TRAN  CA=224  IS=1 FS=1 IT=526 FT=375  TT=600   FL=6463 IP=1050 FP=240  TP=0
TRAN CA=225  IS=1 FS=1 IT=375 FT=100  TT=9900  FL=6463 IP=240  FP=40   TP=0
*
PAIR  CA=201 CO=8.3  DI=0.140 EX=8.5 *Tavg=85.0
PAIR  CA=202 CO=8.3  DI=0.140 EX=8.5 *Tavg=100.0
PAIR  CA=203 CO=9.4  DI=0.151 EX=8.5 *Tavg=324.5
PAIR   CA=204 CO=10.5 DI=0.162 EX=8.5 *Tavg=545.5
PAIR   CA=205 CO=10.4 DI=0.161 EX=8.5 *Tavg=534.0
PAIR   CA=206 CO=10.4 DI=0.161 EX=8.5 *Tavg=534.0
PAIR   CA=207 CO=10.4 DI=0.161 EX=8.5 *Tavg=534.0
PAIR   CA=208 CO=10.3 DI=0.161 EX=8.5 *Tavg=521.0
PAIR   CA=209 CO=10.3 DI=0.161 EX=8.5 *Tavg=521.0
PAIR   CA=210 CO=9.9  DI=0.156 EX=8.5 *Tavg=413.0
PAIR  CA=211 CO=9.8  DI=0.155 EX=8.5 *Tavg=400.0
PAIR   CA=212 CO=9.8  DI=0.155 EX=8.5 *Tavg=400.0
PAIR  CA=213 CO=9.9  DI=0.156 EX=8.5 *Tavg=424.5
PAIR   CA=214 CO=10.4 DI=0.162 EX=8.5 *Tavg=537.5
PAIR  CA=215 CO=10.0 DI=0.158 EX=8.5 *Tavg=462.0
PAIR   CA=216 CO=9.5  DI=0.152 EX=8.5 *Tavg=352.5
PAIR  CA=217 CO=9.2  DI=0.149 EX=8.5 *Tavg=277.5
PAIR  CA=218 CO=8.7  DI=0.143 EX=8.5 *Tavg=162.5
PAIR   CA=219 CO=8.3  DI=0.140 EX=8.5 *Tavg=100.0
PAIR   CA=220 CO=8.8  DI=0.145 EX=8.5 *Tavg=202.5
PAIR   CA=221 CO=8.8  DI=0.145 EX=8.5 *Tavg=202.5
PAIR   CA=222 CO=9.4  DI=0.151 EX=8.5 *Tavg=328.0
PAIR   CA=223 CO=9.4  DI=0.151 EX=8.5 *Tavg=328.0
PAIR   CA=224 CO=10.0 DI=0.157 EX=8.5 *Tavg=450.5
PAIR  CA=225 CO=9.0  DI=0.147 EX=8.5 *Tavg=237.5
```

Reg7A.inp

```
*----------------------------------------
*BEGIN REGION 7A TRANSIENT CARDS & GEOMETRY TO RHR SUPPLY VALVE NODE 550
*----------------------------------------
*
OPER CA=1   TE=100  PR=1100
OPER CA=2   TE=100  PR=50
OPER CA=3   TE=549  PR=1010
OPER CA=4   TE=542  PR=1010
```

```
OPER CA=5   TE=526  PR=1010
OPER CA=6   TE=542  PR=1010
OPER CA=7   TE=526  PR=1010
OPER CA=8   TE=516  PR=1010
OPER CA=9   TE=526  PR=1010
OPER CA=10  TE=300  PR=1135
OPER CA=11  TE=500  PR=1135
OPER CA=12  TE=300  PR=675
OPER CA=13  TE=549  PR=1010
OPER CA=14  TE=549  PR=1010
OPER CA=15  TE=375  PR=170
OPER CA=16  TE=330  PR=90
OPER CA=17  TE=225  PR=0
OPER CA=18  TE=100  PR=0
OPER CA=19  TE=100  PR=1563
OPER CA=20  TE=225  PR=0
OPER CA=21  TE=225  PR=0
OPER CA=22  TE=130  PR=1010
OPER CA=23  TE=526  PR=1010
OPER CA=24  TE=375  PR=200
OPER CA=25  TE=100  PR=0
*
TRAN CA=201  IS=1 FS=1 IT=70  FT=100  TT=1800  FL=143  IP=15   FP=1115 TP=0
TRAN CA=202  IS=1 FS=1 IT=100 FT=100  TT=1800  FL=143  IP=1115 FP=65   TP=0
TRAN CA=203  IS=1 FS=1 IT=100 FT=549  TT=16164 FL=300  IP=65   FP=1025 TP=0
TRAN  CA=204  IS=1 FS=1 IT=549 FT=542  TT=0     FL=364  IP=1025 FP=1025 TP=0
TRAN  CA=205  IS=1 FS=1 IT=542 FT=526  TT=0     FL=358  IP=1025 FP=1025 TP=0
TRAN  CA=206  IS=1 FS=1 IT=526 FT=542  TT=900   FL=358  IP=1025 FP=1025 TP=0
TRAN  CA=207  IS=1 FS=1 IT=542 FT=526  TT=360   FL=358  IP=1025 FP=1025 TP=0
TRAN  CA=208  IS=1 FS=1 IT=526 FT=516  TT=0     FL=351  IP=1025 FP=1025 TP=0
TRAN  CA=209  IS=1 FS=1 IT=516 FT=526  TT=0     FL=351  IP=1025 FP=1025 TP=0
TRAN  CA=210  IS=1 FS=1 IT=526 FT=300  TT=220   FL=306  IP=1205 FP=1150 TP=0
TRAN CA=211  IS=1 FS=1 IT=300 FT=500  TT=1980  FL=301  IP=900  FP=1150 TP=0
TRAN  CA=212  IS=1 FS=1 IT=500 FT=300  TT=180   FL=301  IP=1150 FP=690  TP=0
TRAN CA=213  IS=1 FS=1 IT=300 FT=549  TT=8964  FL=310  IP=255  FP=1025 TP=0
TRAN  CA=214  IS=1 FS=1 IT=526 FT=549  TT=0     FL=360  IP=1025 FP=1025 TP=0
TRAN CA=215  IS=1 FS=1 IT=549 FT=375  TT=6264  FL=320  IP=1050 FP=185  TP=0
TRAN  CA=216  IS=1 FS=1 IT=375 FT=330  TT=600   FL=282  IP=185  FP=105  TP=0
TRAN CA=217  IS=1 FS=1 IT=330 FT=225  TT=3780  FL=260  IP=105  FP=15   TP=0
TRAN CA=218  IS=1 FS=1 IT=225 FT=100  TT=4500  FL=6700 IP=15   FP=15   TP=0
TRAN  CA=219  IS=1 FS=1 IT=100 FT=100  TT=0     FL=158  IP=40   FP=1578 TP=0
TRAN  CA=220 *IS=1 FS=1 IT=225 FT=225  TT=60    FL=6700 IP=15   FP=15   TP=0
TRAN  CA=221 *IS=1 FS=1 IT=225 FT=225  TT=60    FL=6700 IP=15   FP=15   TP=0
TRAN  CA=222 *IS=1 FS=1 IT=526 FT=130  TT=0     FL=272  IP=1025 FP=1025 TP=0
TRAN  CA=223  IS=1 FS=1 IT=130 FT=526  TT=0     FL=272  IP=1025 FP=1025 TP=0
TRAN  CA=224  IS=1 FS=1 IT=526 FT=375  TT=600   FL=320  IP=1025 FP=215  TP=0
TRAN CA=225  IS=1 FS=1 IT=375 FT=100  TT=9900  FL=234  IP=215  FP=15   TP=0
*
PAIR  CA=201 CO=8.3  DI=0.140 EX=8.5 *Tavg=85.0
PAIR  CA=202 CO=8.3  DI=0.140 EX=8.5 *Tavg=100.0
PAIR  CA=203 CO=9.4  DI=0.151 EX=8.5 *Tavg=324.5
PAIR   CA=204 CO=10.5 DI=0.162 EX=8.5 *Tavg=545.5
PAIR   CA=205 CO=10.4 DI=0.161 EX=8.5 *Tavg=534.0
PAIR   CA=206 CO=10.4 DI=0.161 EX=8.5 *Tavg=534.0
PAIR   CA=207 CO=10.4 DI=0.161 EX=8.5 *Tavg=534.0
PAIR   CA=208 CO=10.3 DI=0.161 EX=8.5 *Tavg=521.0
PAIR   CA=209 CO=10.3 DI=0.161 EX=8.5 *Tavg=521.0
PAIR   CA=210 CO=9.9  DI=0.156 EX=8.5 *Tavg=413.0
PAIR  CA=211 CO=9.8  DI=0.155 EX=8.5 *Tavg=400.0
PAIR   CA=212 CO=9.8  DI=0.155 EX=8.5 *Tavg=400.0
```

```
PAIR  CA=213 CO=9.9  DI=0.156 EX=8.5 *Tavg=424.5
PAIR   CA=214 CO=10.4 DI=0.162 EX=8.5 *Tavg=537.5
PAIR  CA=215 CO=10.0 DI=0.158 EX=8.5 *Tavg=462.0
PAIR   CA=216 CO=9.5  DI=0.152 EX=8.5 *Tavg=352.5
PAIR  CA=217 CO=9.2  DI=0.149 EX=8.5 *Tavg=277.5
PAIR  CA=218 CO=8.7  DI=0.143 EX=8.5 *Tavg=162.5
PAIR   CA=219 CO=8.3  DI=0.140 EX=8.5 *Tavg=100.0
*PAIR   CA=220 CO=9.0  DI=0.146 EX=8.5 *Tavg=225.0
*PAIR   CA=221 CO=9.0  DI=0.146 EX=8.5 *Tavg=225.0
*PAIR   CA=222 CO=9.4  DI=0.151 EX=8.5 *Tavg=328.0
PAIR   CA=223 CO=9.4  DI=0.151 EX=8.5 *Tavg=328.0
PAIR   CA=224 CO=10.0 DI=0.157 EX=8.5 *Tavg=450.5
PAIR  CA=225 CO=9.0  DI=0.147 EX=8.5 *Tavg=237.5
```

Reg7B.inp

```
*----------------------------------------
*BEGIN REGION 7B TRANSIENT CARDS & GEOMETRY FROM RHR SUPPLY VALVE TO PENET. NODE 565
*----------------------------------------
*
OPER CA=1   TE=100  PR=120
OPER CA=2   TE=100  PR=50
OPER CA=3   TE=150  PR=120
OPER CA=4   TE=150  PR=120
OPER CA=5   TE=150  PR=120
OPER CA=6   TE=150  PR=120
OPER CA=7   TE=150  PR=120
OPER CA=8   TE=150  PR=120
OPER CA=9   TE=150  PR=120
OPER CA=10  TE=150  PR=120
OPER CA=11  TE=150  PR=120
OPER CA=12  TE=150  PR=120
OPER CA=13  TE=150  PR=120
OPER CA=14  TE=150  PR=120
OPER CA=15  TE=150  PR=120
OPER CA=16  TE=150  PR=120
OPER CA=17  TE=150  PR=100
OPER CA=18  TE=100  PR=0
OPER CA=19  TE=100  PR=450
OPER CA=20  TE=225  PR=25
OPER CA=21  TE=150  PR=25
OPER CA=22  TE=150  PR=100
OPER CA=23  TE=150  PR=1035
OPER CA=24  TE=150  PR=100
OPER CA=25  TE=150  PR=100
*
TRAN CA=201 IS=1 FS=1 IT=70  FT=100 TT=1800  FL=143 IP=15  FP=135 TP=0
TRAN CA=202 IS=1 FS=1 IT=100 FT=100 TT=1800  FL=143 IP=135 FP=65 TP=0
TRAN CA=203 IS=1 FS=1 IT=100 FT=150 TT=16164 FL=300 IP=65  FP=135  TP=0
TRAN  CA=204
TRAN  CA=205
TRAN  CA=206
TRAN  CA=207
TRAN  CA=208
TRAN  CA=209
TRAN  CA=210
TRAN CA=211
TRAN  CA=212
TRAN CA=213
TRAN  CA=214
TRAN CA=215
```

```
TRAN  CA=216
TRAN CA=217
TRAN CA=218 IS=1 FS=1 IT=225 FT=100  TT=4500 FL=6700 IP=15  FP=15 TP=0
TRAN  CA=219  IS=1 FS=1 IT=100 FT=100  TT=0  FL=143  IP=15  FP=465 TP=0
TRAN  CA=220  IS=1 FS=1 IT=150 FT=225  TT=60 FL=6700 IP=40  FP=40 TP=0
TRAN  CA=221 *IS=1 FS=1 IT=150 FT=150   TT=0 FL=6700 IP=40  FP=40 TP=0
TRAN  CA=222
TRAN  CA=223
TRAN  CA=224
TRAN CA=225
*
PAIR  CA=201 CO=27.6 DI=0.529 EX=6.4 *Tavg=85.0
PAIR  CA=202 CO=27.6 DI=0.512 EX=6.4 *Tavg=100.0
PAIR  CA=203 CO=27.6 DI=0.506 EX=6.4 *Tavg=125.0
*PAIR  CA=204 CO=27.6 DI=0.499 EX=6.4 *Tavg=150.0
*PAIR  CA=205 CO=27.6 DI=0.499 EX=6.4 *Tavg=150.0
*PAIR  CA=206 CO=27.6 DI=0.499 EX=6.4 *Tavg=150.0
*PAIR  CA=207 CO=27.6 DI=0.499 EX=6.4 *Tavg=150.0
*PAIR  CA=208 CO=27.6 DI=0.499 EX=6.4 *Tavg=150.0
*PAIR  CA=209 CO=27.6 DI=0.499 EX=6.4 *Tavg=150.0
*PAIR  CA=210 CO=27.6 DI=0.499 EX=6.4 *Tavg=150.0
*PAIR  CA=211 CO=27.6 DI=0.499 EX=6.4 *Tavg=150.0
*PAIR  CA=212 CO=27.6 DI=0.499 EX=6.4 *Tavg=150.0
*PAIR  CA=213 CO=27.6 DI=0.499 EX=6.4 *Tavg=150.0
*PAIR  CA=214 CO=27.6 DI=0.499 EX=6.4 *Tavg=150.0
*PAIR  CA=215 CO=27.6 DI=0.499 EX=6.4 *Tavg=150.0
*PAIR  CA=216 CO=27.6 DI=0.499 EX=6.4 *Tavg=150.0
*PAIR  CA=217 CO=27.6 DI=0.499 EX=6.4 *Tavg=150.0
PAIR  CA=218 CO=27.6 DI=0.496 EX=6.4 *Tavg=162.5
PAIR   CA=219 CO=27.6 DI=0.512 EX=6.4 *Tavg=100.0
PAIR   CA=220 CO=27.6 DI=0.489 EX=6.4 *Tavg=187.5
PAIR   CA=221 CO=27.6 DI=0.499 EX=6.4 *Tavg=150.0
*PAIR  CA=222 CO=27.6 DI=0.499 EX=6.4 *Tavg=150.0
*PAIR  CA=223 CO=27.6 DI=0.499 EX=6.4 *Tavg=150.0
*PAIR  CA=224 CO=27.6 DI=0.499 EX=6.4 *Tavg=150.0
*PAIR  CA=225 CO=27.6 DI=0.499 EX=6.4 *Tavg=150.0
```

Reg8.inp

```
*----------------------------------------
*BEGIN REGION 8 TRANSIENT CARDS & GEOMETRY FOR 4 INCH BYPASS
*----------------------------------------
*
OPER CA=1   TE=100  PR=1100
OPER CA=2   TE=100  PR=50
OPER CA=3   TE=549  PR=1035
OPER CA=4   TE=542  PR=1035
OPER CA=5   TE=526  PR=1035
OPER CA=6   TE=542  PR=1035
OPER CA=7   TE=526  PR=1035
OPER CA=8   TE=516  PR=1035
OPER CA=9   TE=526  PR=1035
OPER CA=10  TE=300  PR=1160
OPER CA=11  TE=500  PR=1160
OPER CA=12  TE=300  PR=700
OPER CA=13  TE=549  PR=1035
OPER CA=14  TE=549  PR=1035
OPER CA=15  TE=375  PR=195
OPER CA=16  TE=330  PR=115
OPER CA=17  TE=225  PR=25
OPER CA=18  TE=100  PR=25
```

```
OPER CA=19  TE=100  PR=1563
OPER CA=20  TE=225  PR=25
OPER CA=21  TE=225  PR=25
OPER CA=22  TE=130  PR=1035
OPER CA=23  TE=526  PR=1035
OPER CA=24  TE=375  PR=225
OPER CA=25  TE=100  PR=25
*
TRAN CA=201 IS=1 FS=1 IT=70  FT=100  TT=1800  FL=23.5  IP=15   FP=1115 TP=0
TRAN CA=202 IS=1 FS=1 IT=100 FT=100  TT=1800  FL=23.5  IP=1115 FP=65   TP=0
TRAN CA=203 IS=1 FS=1 IT=100 FT=549  TT=16164 FL=168   IP=65   FP=1050 TP=0
TRAN  CA=204 IS=1 FS=1 IT=549 FT=542  TT=0     FL=335   IP=1050 FP=1050 TP=0
TRAN  CA=205 IS=1 FS=1 IT=542 FT=526  TT=0     FL=335   IP=1050 FP=1050 TP=0
TRAN  CA=206 IS=1 FS=1 IT=526 FT=542  TT=900   FL=335   IP=1050 FP=1050 TP=0
TRAN  CA=207 IS=1 FS=1 IT=542 FT=526  TT=360   FL=335   IP=1050 FP=1050 TP=0
TRAN  CA=208 IS=1 FS=1 IT=526 FT=516  TT=0     FL=335   IP=1050 FP=1050 TP=0
TRAN  CA=209 IS=1 FS=1 IT=516 FT=526  TT=0     FL=335   IP=1050 FP=1050 TP=0
TRAN  CA=210 IS=1 FS=1 IT=526 FT=300  TT=220   FL=6     IP=1230 FP=1175 TP=0
TRAN CA=211 IS=1 FS=1 IT=300 FT=500  TT=1980  FL=6     IP=925  FP=1175 TP=0
TRAN  CA=212 IS=1 FS=1 IT=500 FT=300  TT=180   FL=6     IP=1175 FP=715  TP=0
TRAN CA=213 IS=1 FS=1 IT=300 FT=549  TT=8964  FL=167.5 IP=280  FP=1050 TP=0
TRAN  CA=214 IS=1 FS=1 IT=526 FT=549  TT=0     FL=335   IP=1050 FP=1050 TP=0
TRAN CA=215 IS=1 FS=1 IT=549 FT=375  TT=6264  FL=167.5 IP=1050 FP=210  TP=0
TRAN  CA=216 IS=1 FS=1 IT=375 FT=330  TT=600   FL=167.5 IP=210  FP=130  TP=0
TRAN CA=217 IS=1 FS=1 IT=330 FT=225  TT=3780  FL=167.5 IP=130  FP=40   TP=0
TRAN CA=218 IS=1 FS=1 IT=225 FT=100  TT=4500  FL=167.5 IP=40   FP=40   TP=0
TRAN  CA=219 IS=1 FS=1 IT=100 FT=100  TT=0     FL=23.5  IP=40   FP=1578 TP=0
TRAN  CA=220
TRAN  CA=221
TRAN  CA=222 *IS=1 FS=1 IT=526 FT=130  TT=0     FL=335 IP=1050  FP=1050 TP=0
TRAN  CA=223 IS=1 FS=1 IT=130 FT=526  TT=0     FL=335 IP=1050  FP=1050 TP=0
TRAN  CA=224 IS=1 FS=1 IT=526 FT=375  TT=600   FL=335 IP=1050  FP=240  TP=0
TRAN CA=225 IS=1 FS=1 IT=375 FT=100  TT=9900  FL=335 IP=240   FP=40   TP=0
*
PAIR CA=201 CO=8.3  DI=0.140 EX=8.5 *Tavg=85.0
PAIR CA=202 CO=8.3  DI=0.140 EX=8.5 *Tavg=100.0
PAIR CA=203 CO=9.4  DI=0.151 EX=8.5 *Tavg=324.5
PAIR  CA=204 CO=10.5 DI=0.162 EX=8.5 *Tavg=545.5
PAIR  CA=205 CO=10.4 DI=0.161 EX=8.5 *Tavg=534.0
PAIR  CA=206 CO=10.4 DI=0.161 EX=8.5 *Tavg=534.0
PAIR  CA=207 CO=10.4 DI=0.161 EX=8.5 *Tavg=534.0
PAIR  CA=208 CO=10.3 DI=0.161 EX=8.5 *Tavg=521.0
PAIR  CA=209 CO=10.3 DI=0.161 EX=8.5 *Tavg=521.0
PAIR  CA=210 CO=9.9  DI=0.156 EX=8.5 *Tavg=413.0
PAIR CA=211 CO=9.8  DI=0.155 EX=8.5 *Tavg=400.0
PAIR  CA=212 CO=9.8  DI=0.155 EX=8.5 *Tavg=400.0
PAIR CA=213 CO=9.9  DI=0.156 EX=8.5 *Tavg=424.5
PAIR  CA=214 CO=10.4 DI=0.162 EX=8.5 *Tavg=537.5
PAIR CA=215 CO=10.0 DI=0.158 EX=8.5 *Tavg=462.0
PAIR  CA=216 CO=9.5  DI=0.152 EX=8.5 *Tavg=352.5
PAIR CA=217 CO=9.2  DI=0.149 EX=8.5 *Tavg=277.5
PAIR CA=218 CO=8.7  DI=0.143 EX=8.5 *Tavg=162.5
PAIR  CA=219 CO=8.3  DI=0.140 EX=8.5 *Tavg=100.0
*PAIR CA=220 CO=9.0  DI=0.146 EX=8.5 *Tavg=225.0
*PAIR CA=221 CO=9.0  DI=0.146 EX=8.5 *Tavg=225.0
*PAIR  CA=222 CO=9.4  DI=0.151 EX=8.5 *Tavg=328.0
PAIR  CA=223 CO=9.4  DI=0.151 EX=8.5 *Tavg=328.0
PAIR  CA=224 CO=10.0 DI=0.157 EX=8.5 *Tavg=450.5
PAIR CA=225 CO=9.0  DI=0.147 EX=8.5 *Tavg=237.5
```

Reg9A.inp

```
*----------------------------------------
*BEGIN REGION 9A TRANSIENT CARDS & GEOMETRY FOR RHR RETURN FROM TEE TO VALVE NODE 660
*----------------------------------------
*
OPER CA=1   TE=100  PR=1100
OPER CA=2   TE=100  PR=50
OPER CA=3   TE=549  PR=1035
OPER CA=4   TE=542  PR=1035
OPER CA=5   TE=526  PR=1035
OPER CA=6   TE=542  PR=1035
OPER CA=7   TE=526  PR=1035
OPER CA=8   TE=516  PR=1035
OPER CA=9   TE=526  PR=1035
OPER CA=10  TE=300  PR=1160
OPER CA=11  TE=500  PR=1160
OPER CA=12  TE=300  PR=700
OPER CA=13  TE=549  PR=1035
OPER CA=14  TE=549  PR=1035
OPER CA=15  TE=375  PR=195
OPER CA=16  TE=330  PR=115
OPER CA=17  TE=225  PR=25
OPER CA=18  TE=100  PR=100
OPER CA=19  TE=100  PR=1563
OPER CA=20  TE=225  PR=25
OPER CA=21  TE=70   PR=25
OPER CA=22  TE=130  PR=1035
OPER CA=23  TE=526  PR=1035
OPER CA=24  TE=375  PR=225
OPER CA=25  TE=100  PR=25
*
TRAN  CA=201  IS=1 FS=1 IT=70  FT=100  TT=1800  FL=204  IP=15   FP=1115 TP=0
TRAN  CA=202  IS=1 FS=1 IT=100 FT=100  TT=1800  FL=204  IP=1115 FP=65   TP=0
TRAN  CA=203  IS=1 FS=1 IT=100 FT=549  TT=16164 FL=247  IP=65   FP=1050 TP=0
TRAN  CA=204  IS=1 FS=1 IT=549 FT=542  TT=0     FL=520  IP=1050 FP=1050 TP=0
TRAN  CA=205  IS=1 FS=1 IT=542 FT=526  TT=0     FL=511  IP=1050 FP=1050 TP=0
TRAN  CA=206  IS=1 FS=1 IT=526 FT=542  TT=900   FL=511  IP=1050 FP=1050 TP=0
TRAN  CA=207  IS=1 FS=1 IT=542 FT=526  TT=360   FL=511  IP=1050 FP=1050 TP=0
TRAN  CA=208  IS=1 FS=1 IT=526 FT=516  TT=0     FL=502  IP=1050 FP=1050 TP=0
TRAN  CA=209  IS=1 FS=1 IT=516 FT=526  TT=0     FL=502  IP=1050 FP=1050 TP=0
TRAN  CA=210  IS=1 FS=1 IT=526 FT=300  TT=220   FL=437  IP=1230 FP=1175 TP=0
TRAN  CA=211  IS=1 FS=1 IT=300 FT=500  TT=1980  FL=429  IP=925  FP=1175 TP=0
TRAN  CA=212  IS=1 FS=1 IT=500 FT=300  TT=180   FL=429  IP=1175 FP=715  TP=0
TRAN  CA=213  IS=1 FS=1 IT=300 FT=549  TT=8964  FL=443  IP=280  FP=1050 TP=0
TRAN  CA=214  IS=1 FS=1 IT=526 FT=549  TT=0     FL=514  IP=1050 FP=1050 TP=0
TRAN  CA=215  IS=1 FS=1 IT=549 FT=375  TT=6264  FL=458  IP=1050 FP=210  TP=0
TRAN  CA=216  IS=1 FS=1 IT=375 FT=330  TT=600   FL=403  IP=210  FP=130  TP=0
TRAN  CA=217  IS=1 FS=1 IT=330 FT=225  TT=3780  FL=260  IP=130  FP=40   TP=0
TRAN  CA=218  IS=1 FS=1 IT=225 FT=100  TT=4500  FL=6700 IP=115  FP=115  TP=0
TRAN  CA=219  IS=1 FS=1 IT=100 FT=100  TT=0     FL=226  IP=40   FP=1578 TP=0
TRAN  CA=220  IS=1 FS=1 IT=70  FT=225  TT=60    FL=6700 IP=40   FP=40   TP=0
TRAN  CA=221  IS=1 FS=1 IT=225 FT=70   TT=60    FL=6700 IP=40   FP=40   TP=0
TRAN  CA=222  *IS=1 FS=1 IT=526 FT=130  TT=0     FL=389  IP=1050 FP=1050 TP=0
TRAN  CA=223  IS=1 FS=1 IT=130 FT=526  TT=0     FL=389  IP=1050 FP=1050 TP=0
TRAN  CA=224  IS=1 FS=1 IT=526 FT=375  TT=600   FL=458  IP=1050 FP=240  TP=0
TRAN  CA=225  IS=1 FS=1 IT=375 FT=100  TT=9900  FL=334  IP=240  FP=40   TP=0
*
PAIR  CA=201 CO=8.3  DI=0.140  EX=8.5 *Tavg=85.0
PAIR  CA=202 CO=8.3  DI=0.140  EX=8.5 *Tavg=100.0
PAIR  CA=203 CO=9.4  DI=0.151  EX=8.5 *Tavg=324.5
```

```
PAIR   CA=204 CO=10.5 DI=0.162  EX=8.5 *Tavg=545.5
PAIR   CA=205 CO=10.4 DI=0.161  EX=8.5 *Tavg=534.0
PAIR   CA=206 CO=10.4 DI=0.161  EX=8.5 *Tavg=534.0
PAIR   CA=207 CO=10.4 DI=0.161  EX=8.5 *Tavg=534.0
PAIR   CA=208 CO=10.3 DI=0.161  EX=8.5 *Tavg=521.0
PAIR   CA=209 CO=10.3 DI=0.161  EX=8.5 *Tavg=521.0
PAIR   CA=210 CO=9.9  DI=0.156  EX=8.5 *Tavg=413.0
PAIR  CA=211 CO=9.8  DI=0.155  EX=8.5 *Tavg=400.0
PAIR   CA=212 CO=9.8  DI=0.155  EX=8.5 *Tavg=400.0
PAIR  CA=213 CO=9.9  DI=0.156  EX=8.5 *Tavg=424.5
PAIR   CA=214 CO=10.4 DI=0.162  EX=8.5 *Tavg=537.5
PAIR  CA=215 CO=10.0 DI=0.158  EX=8.5 *Tavg=462.0
PAIR   CA=216 CO=9.5  DI=0.152  EX=8.5 *Tavg=352.5
PAIR  CA=217 CO=9.2  DI=0.149  EX=8.5 *Tavg=277.5
PAIR  CA=218 CO=8.7  DI=0.143  EX=8.5 *Tavg=162.5
PAIR   CA=219 CO=8.3  DI=0.140  EX=8.5 *Tavg=100.0
PAIR  CA=220 CO=8.6  DI=0.142  EX=8.5 *Tavg=147.5
PAIR  CA=221 CO=8.6  DI=0.142  EX=8.5 *Tavg=147.5
*PAIR   CA=222 CO=9.4  DI=0.151  EX=8.5 *Tavg=328.0
PAIR   CA=223 CO=9.4  DI=0.151  EX=8.5 *Tavg=328.0
PAIR   CA=224 CO=10.0 DI=0.157  EX=8.5 *Tavg=450.5
PAIR  CA=225 CO=9.0  DI=0.147  EX=8.5 *Tavg=237.5
```

Reg9B.inp

```
*----------------------------------------
*BEGIN REGION 9B TRANSIENT CARDS & GEOMETRY FOR RHR RETURN FROM VALVE NODE 660 TO PENET. NODE
675
*----------------------------------------
*
OPER CA=1   TE=100  PR=1100
OPER CA=2   TE=100  PR=50
OPER CA=3   TE=150  PR=1035
OPER CA=4   TE=150  PR=1035
OPER CA=5   TE=150  PR=1035
OPER CA=6   TE=150  PR=1035
OPER CA=7   TE=150  PR=1035
OPER CA=8   TE=150  PR=1035
OPER CA=9   TE=150  PR=1035
OPER CA=10  TE=150  PR=1160
OPER CA=11  TE=150  PR=1160
OPER CA=12  TE=150  PR=700
OPER CA=13  TE=150  PR=1035
OPER CA=14  TE=150  PR=1035
OPER CA=15  TE=150  PR=195
OPER CA=16  TE=150  PR=115
OPER CA=17  TE=150  PR=25
OPER CA=18  TE=100  PR=100
OPER CA=19  TE=100  PR=1563
OPER CA=20  TE=225  PR=25
OPER CA=21  TE=70   PR=25
OPER CA=22  TE=150  PR=1035
OPER CA=23  TE=150  PR=1035
OPER CA=24  TE=150  PR=225
OPER CA=25  TE=150  PR=25
*
TRAN CA=201 IS=1 FS=1 IT=70  FT=100 TT=1800  FL=204  IP=15   FP=1115 TP=0
TRAN CA=202 IS=1 FS=1 IT=100 FT=100 TT=1800  FL=204  IP=1115 FP=65   TP=0
TRAN CA=203 IS=1 FS=1 IT=100 FT=150 TT=16164 FL=247  IP=65   FP=1050 TP=0
TRAN  CA=204
TRAN  CA=205
```

```
TRAN  CA=206
TRAN  CA=207
TRAN  CA=208
TRAN  CA=209
TRAN  CA=210
TRAN CA=211
TRAN  CA=212 IS=1 FS=1 IT=150 FT=150 TT=0     FL=429  IP=1175 FP=715  TP=0
TRAN CA=213
TRAN  CA=214
TRAN CA=215
TRAN  CA=216 IS=1 FS=1 IT=150 FT=150 TT=600   FL=403  IP=210  FP=130  TP=0
TRAN CA=217
TRAN CA=218 IS=1 FS=1 IT=225 FT=100 TT=4500  FL=6700 IP=115  FP=115  TP=0
TRAN  CA=219 IS=1 FS=1 IT=100 FT=100 TT=0     FL=247  IP=40   FP=1578 TP=0
TRAN  CA=220 IS=1 FS=1 IT=70  FT=225 TT=60    FL=6700 IP=40   FP=40   TP=0
TRAN  CA=221 IS=1 FS=1 IT=150 FT=70  TT=60    FL=6700 IP=40   FP=40   TP=0
TRAN  CA=222
TRAN  CA=223
TRAN  CA=224 IS=1 FS=1 IT=150 FT=150 TT=0     FL=458  IP=1040 FP=240  TP=0
TRAN  CA=225 IS=1 FS=1 IT=150 FT=150 TT=0     FL=334  IP=240  FP=40   TP=0
*
PAIR  CA=201 CO=27.6 DI=0.521 EX=6.4 *Tavg=85.0
PAIR  CA=202 CO=27.6 DI=0.512 EX=6.4 *Tavg=100.0
PAIR  CA=203 CO=27.6 DI=0.506 EX=6.4 *Tavg=125.0
*PAIR  CA=204 CO=27.6 DI=0.499 EX=6.4 *Tavg=150.0
*PAIR  CA=205 CO=27.6 DI=0.499 EX=6.4 *Tavg=150.0
*PAIR  CA=206 CO=27.6 DI=0.499 EX=6.4 *Tavg=150.0
*PAIR  CA=207 CO=27.6 DI=0.499 EX=6.4 *Tavg=150.0
*PAIR  CA=208 CO=27.6 DI=0.499 EX=6.4 *Tavg=150.0
*PAIR  CA=209 CO=27.6 DI=0.499 EX=6.4 *Tavg=150.0
*PAIR  CA=210 CO=27.6 DI=0.499 EX=6.4 *Tavg=150.0
*PAIR  CA=211 CO=27.6 DI=0.499 EX=6.4 *Tavg=150.0
PAIR   CA=212 CO=27.6 DI=0.499 EX=6.4 *Tavg=150.0
*PAIR  CA=213 CO=27.6 DI=0.499 EX=6.4 *Tavg=150.0
*PAIR  CA=214 CO=27.6 DI=0.499 EX=6.4 *Tavg=150.0
*PAIR  CA=215 CO=27.6 DI=0.499 EX=6.4 *Tavg=150.0
PAIR   CA=216 CO=27.6 DI=0.499 EX=6.4 *Tavg=150.0
*PAIR  CA=217 CO=27.6 DI=0.499 EX=6.4 *Tavg=150.0
PAIR  CA=218 CO=27.6 DI=0.496 EX=6.4 *Tavg=162.5
PAIR   CA=219 CO=27.6 DI=0.512 EX=6.4 *Tavg=100.0
PAIR   CA=220 CO=27.6 DI=0.500 EX=6.4 *Tavg=147.5
PAIR   CA=221 CO=27.6 DI=0.509 EX=6.4 *Tavg=110.0
*PAIR  CA=222 CO=27.6 DI=0.499 EX=6.4 *Tavg=150.0
*PAIR  CA=223 CO=27.6 DI=0.499 EX=6.4 *Tavg=150.0
PAIR   CA=224 CO=27.6 DI=0.499 EX=6.4 *Tavg=150.0
PAIR   CA=225 CO=27.6 DI=0.499 EX=6.4 *Tavg=150.0
```

APPENDIX B

PIPESTRESS Output

Output File	Description
Recirc_15.prf	Fatigue results for reduced cycle count
RHR_15.prf	Fatigue results for full 60 year cycle count

Recirc 15.prf

D S T C O M P U T E R S E R V I C E S S. A. F-4.2 PAGE NO. 3947

++ DST/PIPESTRESS ++ Vermont Yankee Version 3.5.1+026 PC-EXE Release: Jun 2004

CALCULATION NUMBER 3 CODE SECTION III CLASS 1 ASME-1998 RVP 2007/07/26 08:42:12 [4282]
Vermont Yankee Recirculation Fatigue Analysis

FATIGUE ANALYSIS AT POINT 600, WELDING TEE 600 TO 602

****
INDIVIDUAL STRESS RANGE CHECK
****

DELTA T1 IN DEGREES F
STRESSES IN PSI

LOAD SET I	PAIR J	SALT EQN.14	OCCURENCES NI	OCCURENCES NJ		NUMBER USED	SETS ELIMINATED DYNAM.	NO. CYCLES TO FAILURE	USAGE FACTOR	REMARKS
11	21	88675.	10	150		10	11	2801.	0.0036	
			0	140						
14	21	84491.	150	140		140	21	3359.	0.0417	
			10	0						
19	20	67184.	1	150		1	19	8221.	0.0001	
			0	149						
14	27	65876.	10	5		5	27	8900.	0.0006	
			5	0	45					
10	20	62914.	5	149		5	10	10868.	0.0005	
			0	144						
14	20	55493.	5	144		5	14	20012.	0.0002	
			0	139						
9	20	54186.	35	139		35	9	22574.	0.0016	
			0	104						
5	20	53739.	290	104		104	20	23541.	0.0044	
			186	0						
2	3	46216.	60	150		60	2	50502.	0.0012	
			0	90						
1	26	46169.	60	5		5	26	50782.	0.0001	
			55	0	45					
3	17	42799.	90	150		90	3	76939.	0.0012	
			0	60						
6	17	42219.	10	60		10	6	82911.	0.0001	
			0	50						
5	18	42196.	186	150		150	18	83156.	0.0018	
			36	0						
13	17	42131.	5	50		5	13	83864.	0.0001	
			0	45						
8	17	41392.	35	45		35	8	92408.	0.0004	
			0	10						

D S T C O M P U T E R S E R V I C E S S. A. F-4.2 PAGE NO. 3948

++ DST/PIPESTRESS ++ Vermont Yankee Version 3.5.1+026 PC-EXE Release: Jun 2004

CALCULATION NUMBER 3 CODE SECTION III CLASS 1 ASME-1998 RVP 2007/07/26 08:42:12 [4283]
Vermont Yankee Recirculation Fatigue Analysis

FATIGUE ANALYSIS AT POINT 600, WELDING TEE 600 TO 602

****
INDIVIDUAL STRESS RANGE CHECK
****

DELTA T1 IN DEGREES F
STRESSES IN PSI

LOAD SET I	PAIR J	SALT EQN.14	OCCURENCES NI	OCCURENCES NJ	NUMBER USED	SETS ELIMINATED DYNAM.	NO. CYCLES TO FAILURE	USAGE FACTOR	REMARKS
7	17	41326.	10	10	10	7,17	93222.	0.0001	
			0	0					
1	15	38663.	55	150	55	1	133841.	0.0004	
			0	95					
4	16	35177.	290	150	150	16	227086.	0.0007	
			140	0					
4	15	34727.	140	95	95	15	246096.	0.0004	
			45	0					
4	12	25167.	45	10	10	12	1449206.	0.0000	
			35	0					
26	27	23758.	45	45	45	,27 26	1748766.	0.0000	DYN. RANGE OF EVENT NO. 1
			0	0					
4	5	2773.	35	36	35	4	>100000000000.	0.0000	
			0	1					

TOTAL USAGE FACTOR = 0.0590

Notes a: Fails
f: Weld ISI
j: Rupture Location

RHR_15.prf

D S T   C O M P U T E R   S E R V I C E S   S. A.   F-4.2   PAGE NO. 4019

++ DST/PIPESTRESS ++   Vermont Yankee   Version 3.5.1+026 PC-EXE   Release: Jun 2004

CALCULATION NUMBER   3   CODE SECTION III CLASS 1 ASME-1998   RVP   2007/07/26 08:44:06 [4354]
Vermont Yankee Recirculation Fatigue Analysis

FATIGUE ANALYSIS AT POINT 641, SR ELBOW   640 TO   641

****
INDIVIDUAL STRESS RANGE CHECK
****

DELTA T1 IN DEGREES F
STRESSES IN PSI

LOAD SET PAIR I	J	SALT EQN.14	OCCURENCES NI	NJ	NUMBER USED	SETS ELIMINATED DYNAM.	NO. CYCLES TO FAILURE	USAGE FACTOR	REMARKS
10	20	100252.	10	300	10	10	1788.	0.0056	
			0	290					
11	21	68706.	20	300	20	11	7511.	0.0027	
			0	280					
12	20	64893.	20	290	20	12	9456.	0.0021	
			0	270					
20	21	39947.	270	280	270	20	112120.	0.0024	
			0	10					
3	21	35368.	300	10	10	21	219528.	0.0000	
			290	0					
3	17	20439.	290	300	290	3	3190872.	0.0000	
			0	10					
13	17	19221.	10	10	10	13,17	4148766.	0.0000	
			0	0					
14	18	14925.	300	300	300	14,18	>100000000000.	0.0000	
			0	0					
15	19	14877.	300	1	1	19	>100000000000.	0.0000	
			299	0					
1	15	14434.	120	299	120	1	>100000000000.	0.0000	
			0	179					
6	15	12896.	20	179	20	6	>100000000000.	0.0000	
			0	159					
9	15	12506.	70	159	70	9	>100000000000.	0.0000	
			0	89					
4	15	11542.	579	89	89	15	>100000000000.	0.0000	
			490	0					
7	27	10017.	20	5	5	27	>100000000000.	0.0000	
			15	0 45					
4	16	9993.	490	300	300	16	>100000000000.	0.0000	
			190	0					

D S T C O M P U T E R S E R V I C E S S. A. F-4.2 PAGE NO. 4020

++ DST/PIPESTRESS ++ Vermont Yankee Version 3.5.1+026 PC-EXE Release: Jun 2004

CALCULATION NUMBER 3 CODE SECTION III CLASS 1 ASME-1998 RVP 2007/07/26 08:44:06 [4355]
Vermont Yankee Recirculation Fatigue Analysis

FATIGUE ANALYSIS AT POINT 641, SR ELBOW 640 TO 641

****
INDIVIDUAL STRESS RANGE CHECK
****

DELTA T1 IN DEGREES F
STRESSES IN PSI

LOAD SET PAIR I	J	SALT EQN.14	OCCURENCES NI	NJ	NUMBER USED	SETS ELIMINATED DYNAM.	NO. CYCLES TO FAILURE	USAGE FACTOR	REMARKS
2	7	9353.	120	15	15	7	>100000000000.	0.0000	
			105	0					
2	5	9353.	105	579	105	2	>100000000000.	0.0000	
			0	474					
5	26	8235.	474	5	5	26	>100000000000.	0.0000	
			469	0 45					
26	27	2019.	45	45	45	,27 26	>100000000000.	0.0000	DYN. RANGE OF EVENT NO. 1
			0	0					
4	5	1570.	190	469	190	4	>100000000000.	0.0000	
			0	279					
5	8	1512.	279	70	70	8	>100000000000.	0.0000	
			209	0					

TOTAL USAGE FACTOR = 0.0128

Notes a: Fails
f: Weld ISI
j: Rupture Location

Structural Integrity Associates, Inc.	File No.: VY-16Q-308
CALCULATION PACKAGE	Project No.: VY-16Q

PROJECT NAME:

Environmental Fatigue Analysis of VYNPS

CONTRACT NO.:

10150394

CLIENT:	**PLANT:**
Entergy Nuclear Operations, Inc.	Vermont Yankee Nuclear Power Station

CALCULATION TITLE:

Core Spray Nozzle Finite Element Model

Document Revision	Affected Pages	Revision Description	Project Manager Approval Signature & Date	Preparer(s) & Checker(s) Signatures & Date
0	1-7, Appendix: A1-A17	Initial Issue	Terry J. Herrmann 07/19/2007	Roland Horvath 07/12/2007 John Staples 07/12/2007

Table of Contents

1.0 OBJECTIVE 3
2.0 GEOMETRY / MATERIAL PROPERTIES 3
3.0 PROGRAM INPUT 4
4.0 REFERENCES 5
APPENDIX A VY_CSN_GEOM.INP A1

List of Tables

Table 1: Material Properties @ 300°F [1] 6

List of Figures

Figure 1: ANSYS Finite Element Model 7

1.0 OBJECTIVE

The objective of this calculation is to create a finite element model of the Vermont Yankee Nuclear Power Station Core Spray Nozzle. This model will be used to develop a Green's Function to be used in a subsequent fatigue analysis.

2.0 GEOMETRY / MATERIAL PROPERTIES

A 2-D axisymmetric finite element model (FEM) of the nozzle was developed with element type PLANE82. The developed model includes the part of the pipe, the safe end, the nozzle forging, a portion of the vessel shell, and the cladding. The radius of the vessel in the finite element model was multiplied by a factor of 2 to account for the fact that the vessel portion of the 2D axisymmetric model is a sphere, but the true geometry is a cylinder. The equation for the membrane hoop stress for a sphere is:

$$\sigma = \frac{(pressure) \times (radius)}{2 \times thickness}$$

The equation for the membrane hoop stress in a cylinder is:

$$\sigma = \frac{(pressure) \times (radius)}{thickness}$$

The factor of two was verified in Reference [11] where actual stress results were compared to the results of this analytical form.

The 2-D axisymmetric FEM was constructed using the dimensions and information from References [1 -8] based on ANSYS [9] finite element software. Figure 1 shows the resulting finite element model.

The materials of the various components of the model are listed below:

- Safe End – SB 166 [1] (72Ni-15Cr-8Fe, N06600)
- 8Ø x 10Ø Conc. Reduction – SA312 TP304 [7] (18Cr-8Ni)
- Nozzle Forging – SA508 Class II [1] (¾ Ni-1/2Mo-1/3 Cr-V)
- Vessel – SA533 Grade B [7] (Mn-1/2Mo-1/2Ni)
- Cladding – SA240 TP 304 [7] (18Cr-8Ni)

Note: In the FEM, the 8Ø x 10Ø Conc. Reduction was modeled as a straight pipe with the material properties of the original design [7]. Later, this piping section was replaced by a new material (SA403 T316L) [10]. These two stainless steels have the same modulus of elasticity and thermal coefficient properties.

Material properties for these materials are based upon the 1998 ASME Code, Section II, Part D, with 2000 Addenda [8] and are shown in Table 1. The properties are taken at an average temperature of 300°F. This average temperature is based on a thermal shock of 500°F to 100°F, which will be applied to the FEM model for Green's Function development.

3.0 PROGRAM INPUT

The input file, VY_CSN_GEOM.inp (included in Appendix A), creates the finite element model for the core spray nozzle.

4.0 REFERENCES

1. Reactor 8 In. Dia. Nozzles Mk. N5A & B, 5920-00624 Rev. 8, SI File No. VY-16Q-207.

2. Core Spray Nozzle Weld Overlay Profile N5A & N5B, 5920-06813, Sh. 1 of 2 Rev. 0, SI File No. VY-16Q-206.

3. N5A/B Thermal Sleeve Details, 5920-00898, Rev 1, SI File No. VY-16Q-206.

4. Special Safe End Forging for Nozzles N2A/B & N5A/B, 5920-00655, Rev. 6, SI File No. VY-16Q-206.

5. Special Forgings for Nozzles N5A & N5B, 5920-00069, Rev 1, SI File No. VY-16Q-206.

6. Core Spray Nozzle Weld Overlay Profile N5A & N5B, 5920-06813, Sh. 2 of 2 Rev. 0, SI File No. VY-16Q-204.

7. CB&I RPV Stress Report, Section S7, "Stress Analysis Core Spray and Flooding Nozzle, Vermont Yankee Reactor Vessel, CB&I Contract 9-6201, SI File No. VY-16Q-206.

8. American Society of Mechanical Engineers, Boiler and Pressure Vessel Code, Section II, Part D, 1998 Edition, 2000 Addenda.

9. ANSYS, Release 8.1 (w/Service Pack 1), ANSYS, Inc., June 2004.

10. "10" x 8" SA403 T316L CONC REDUCER", Page 18 of Attachment 2 of Entergy Design Input Record (DIR) EC No. 1773, Revision 0, "Environmental Fatigue Analysis for Vermont Yankee Nuclear Power Station," 7/3/07, SI File No. VY-16Q-209.

11. SI Calculation No. VY-16Q-309, Revision 0, "Core Spray Nozzle Green's Functions".

Table 1: Material Properties @ 300°F (1)

Material ID	Part Description	Material		Modulus of Elasticity, e+6 psi [EX]	Coefficient of Thermal Expansion, e-6, in/in/°F [ALPX]	Thermal Conductivity, Btu/hr-ft-°F [KXX]	Thermal Diffusivity, ft^2/hr	Specific Heat, Btu/lb-°F [C] (3)	Poisson's Ratio [NUXY]	Density, lb/in^3 [DENS]
2	Safe End	SB 166	72Ni-15Cr-8Fe N06600	29.8	7.9	9.6	0.160	0.1157	0.29	0.3
2	Weld Overlay	INCONEL 82	72Ni-15Cr-8Fe N06600	29.8	7.9	9.6	0.160	0.1157	0.29	0.3
1	Nozzle	SA508 Class II	¾ Ni-1/2Mo-1/3 Cr-V	26.7	7.3	23.4	0.401	0.1193	0.3	0.283
3	Vessel	SA533 Grade B	Mn-1/2Mo-1/2Ni	28.0	7.7	23.4	0.401	0.1193	0.3	0.283
4	3/16 Clad	SA240 TP 304	18Cr-8Ni	27.0	9.8	9.8	0.160	0.1252	0.3	0.283
4	8Ø x 10Ø Conc. Reduction(2)	SA312 TP304	18Cr-8Ni	27.0	9.8	9.8	0.160	0.1252	0.3	0.283

Notes:

1. The material properties applied in the analyses are taken from ASME Code, Section II, Part D 1998 Edition, with 2000 Addenda. This is consistent with information provided in the Design Input Record (page 13 of VY EC No. 1773, SI File No. VY-16Q-209). The use of a later code edition than that used for the original design code is acceptable, since later editions typically reflect more accurate material properties than was published in prior Code editions. Material Properties are evaluated at 300°F from the 1998 ASME Code, 2000 Addenda, Section II, Part D, except for density and Poisson's ratio, which are assumed typical values [8].
2. In the FEM, the 8Ø x 10Ø Conc. Reduction was modeled as a straight pipe with the material properties of the original design. Later this piping section was replaced by a new material (SA403 T316L). These two stainless steels have the same modulus of elasticity and thermal coefficient properties [8].
3. Calculated as $[k/(\rho d)]/12^3$.

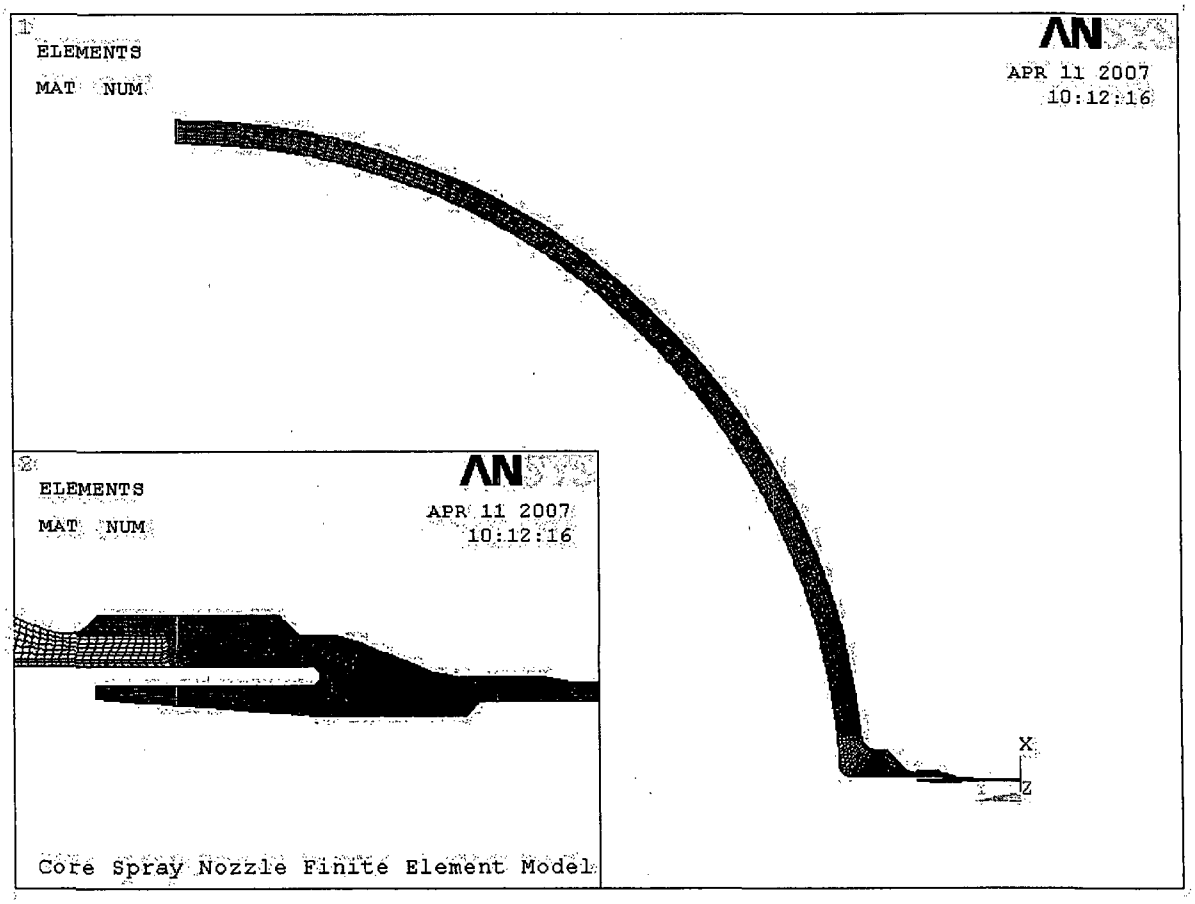

Figure 1: ANSYS Finite Element Model

APPENDIX A

VY_CSN_GEOM.INP

```
!finish
!/clear,start
!/prep7

et,1,PLANE182,,,1    !Axisymmetric
/com, ***************************
/com, Material Properties @T=300F
/com, ***************************
/COM, Material #1 (Nozzle: SA-508 Class II, 3/4Ni-1/2Mo-1/3Cr-V)
mp,ex  ,1,26.7E+06
mp,alpx,1,7.3E-06
mp,kxx ,1,23.4   /3600/12
mp,c   ,1,0.1193277
mp,nuxy,1,0.3
mp,dens,1,0.283

/COM, Material #2 (Safe End: N06600, Inconel 82 Weld Overlay)
mp,ex  ,2,29.8E+06
mp,alpx,2,7.9E-06
mp,kxx ,2,9.6   /3600/12
mp,c   ,2,0.1157407
mp,nuxy,2,0.29
mp,dens,2,0.3

/COM, Material #3 (Vessel: SA-533 Grade B, Mn-1/2Mo-1/2Ni)
mp,ex  ,3,28.00E+06
mp,alpx,3,7.7E-06
mp,kxx ,3,23.4   /3600/12
mp,c   ,3,0.1193277
mp,nuxy,3,0.3
mp,dens,3,0.283

/COM, Material #4 (3/16 Clad: SA-240 TP304, 8-10 Diam. Conc. Red.: SA-312 TP 304, Thermal
Sleeve: SA-312 TP304)
mp,ex  ,4,27.0E+06
mp,alpx,4,9.8E-06
mp,kxx ,4,9.8   /3600/12
mp,c   ,4,0.1252495
mp,nuxy,4,0.3
mp,dens,4,0.283


/com, **********************
/com, Geometric Parameters
/com, **********************
*AFUN,deg
```

```
/com, pipe parameters
*set, pID, 9.834
*set, pOD, 10.815
*set, pL,        8

k, 1, pID/2, 0
k, 2, POD/2, 0
k, 3, POD/2, pL
k, 4, PID/2, pL

l, 1, 2
l, 2, 3
l, 3, 4
l, 4, 1


/com, ******************
/com, Safe End Parameters
/com, ******************
*set, seBX, pL
*set, seID01, 9.834
*set, seID02, 9
*set, seID03, 9 + 31/32
*set, seID04, 11+ 3/4

*set, seOD01, 10.815
*set, seOD02, 11 + 1/6
*set, seOD03, 13 + 27/64
*set, seOD04, 10 + 11/16

*set, seL01,  3 + 1/32
*set, seL02,  7/8
*set, seL03,  1+11/16
*set, seL04,  13/32
*set, seL05,  4
*set, seL06,  3+1/2
*set, seL07,  12+4+1/16
*set, seL08,  seL07-(seL01+seL02+seL03+seL04+seL05+seL06)
*set, seR01,  3
*set, seR02,  3/4
*set, seR03,  1/4
*set, seR04,  1/8


k, 5, seOD01/2, seBX+seL01
k, 6, seOD02/2, seBX+seL01+seL02
```

```
k, 7, seOD02/2, seBX+seL01+seL02+seL03+seL04 +.496
k, 8, (seOD02+seOD03)/4, seBX+seL01+seL02+seL03+seL04+seL05/2
k, 9, seOD03/2, seBX+seL01+seL02+seL03+seL04+seL05
k, 10, seOD03/2, seBX+seL01+seL02+seL03+seL04+seL05+seL06
k, 11, seID04/2, seBX+seL01+seL02+seL03+seL04+seL05+seL06
k, 12, seID04/2, seBX+seL01+seL02+seL03+seL04+seL05
k, 13, seOD04/2, seBX+seL01+seL02+seL03+seL04+seL05
k, 14, seOD04/2, seBX+seL07
k, 15, seID03/2, seBX+seL07
k, 16, seID02/2, seBX+seL01+seL02+seL03+seL04+seL05
k, 17, seID02/2, seBX+seL01+seL02+seL03+seL04
k, 18, seID01/2, seBX+seL01+seL02+seL03

l, 3, 5
l, 5, 6
l, 6, 7
l, 9, 10
l, 10, 11
l, 11, 12
l, 12, 13
l, 13, 14
l, 14, 15
l, 15, 16
l, 16, 17
l, 17, 18
l, 18, 4

k, 19, seOD02/2+seR01, seBX+seL01+seL02+seL03+seL04 +.496
k, 8, seOD02/2+seR01, seBX+seL01+seL02+seL03+seL04+seR01 +.496
larc, 7, 8, 19, seR01

k, 20, seOD03/2-seR01, seBX+seL01+seL02+seL03+seL04+seL05
k, 21, seOD03/2-seR01, seBX+seL01+seL02+seL03+seL04+seL05-seR01
larc, 9, 21, 20, seR01
L2ANG,19,18,0,0,,,
ldele, 20, 21, ,1

lfillt, 5, 6, seR02
lfillt, 6, 7, seR02
lfillt, 10, 11, seR03
lfillt, 11, 12, seR03
lfillt, 15, 16, seR04
lfillt, 16, 17, seR04

/com, weld 1/8 gap
*set, wgap, 1/8
```

```
k, 40, seOD03/2, seBX+seL01+seL02+seL03+seL04+seL05+seL06 + wgap
k, 41, seID04/2, seBX+seL01+seL02+seL03+seL04+seL05+seL06 + wgap

l, 10, 40
l, 40, 41
l, 41, 11

/com, **********************
/com, Nozzle
/com, **********************

*set, nID01, seOD01
*set, nOD01, seOD03
*set, nOD02, 24+1/4
*set, nOD03, 2*12+7.25
*set, nOD04, 2*12+7.25-1-1/8

*set, nL01, 4+5/16
*set, nL02, 5+3/8
*set, nL03, 5+1/8+5+5/8
*set, nW01, 1/16
*set, wClad, 3/16
*set, wReactor, 5+5/8-wClad
*set, nL04, 7/16
*set, nR01, 1/4
*set, nR02, 3/16
*set, nR03, (8*12+7)*2
*set, nR04, 2.5
*set, nR05, nR04-wClad
*set, nR06, 3.5
*set, nR07, 3 +7/8
*set, nR08, 0.5

K, 42, KX(11) + nW01, KY(11)
K, 43, KX(41) + wClad, KY(41)+nL04+nR01
K, 44, KX(43) + nR01, KY(43)
K, 46, KX(44) + nR01*sin(15), KY(44)-nR01*cos(15)
K, 47, KX(46) + 10*nR01*cos(15), KY(46)+10*nR01*sin(15)
K, 48, KX(43), KY(43) + 24
K, 49, KX(41), KY(41) + 24
K, 50, KX(40), KY(40) + nL01
K, 51, KX(44) + (nR01+wClad)*sin(15), KY(44)-(nR01+wClad)*cos(15)
K, 52, KX(51) + 10*nR01*cos(15), KY(51)+10*nR01*sin(15)
K, 53, KX(51) - 10*nR01*cos(15), KY(51)-10*nR01*sin(15)
K, 54, KX(42), KY(42)+wClad*2
larc, 43, 46, 44, nR01
```

```
L, 46, 47
L, 43, 48
L, 41, 49
L, 40, 50
L, 53, 52
L, 42, 54

LOVLAP, 35,36
LDELE, 39, 40,,0

LOVLAP, 31,34,38
LDELE, 40,42,2,0

lfillt, 37, 35, nR02

K, 60, nOD02/2, KY(40) + nL01+nL02
K, 61, nOD02/2, KY(40) + nL01+nL02+nL03
K, 62, 0, KY(40) + nL01+nL02+nL03+nR03
K, 63, 0, KY(62) - nR03
K, 64, nR03, KY(62)
K, 65, 0, KY(63)-wClad
K, 66, nR03+wClad, KY(62)
K, 67, 0, KY(65)-wReactor
K, 68, nR03+wReactor, KY(62)

LARC, 63, 64, 62, nR03
LARC, 65, 66, 62, nR03+wClad
LARC, 67, 68, 62, nR03+wReactor

L, 64, 66
L, 66, 68

LOVLAP, 34, 33
LDELE, 46,47

LOVLAP, 32, 38
LDELE, 34
LDELE, 46

LFILLT,45,48,nR04, ,
LFILLT,33,47,nR05, ,

L, 50, 60
L, 60, 61

LOVLAP, 40, 46
```

```
LDELE, 50, 51
LFILLT,49,52,nR06
LFILLT,38,41,nR07
LFILLT,49,38,nR08

/com, Nozzle and Vessel border
K,      80,     nOD03/2, KY(60)+2*nL03
K,      81, nOD03/2, KY(60)
K,      82,     nOD04/2, KY(60)+2*nL03
K,      83, nOD04/2, KY(60)
L,      80, 81
L,      82, 83

LPTN, 53, 48
LPTN, 51, 52
LDELE, 56, 59,1,0
LSTR,  76, 75
LPTN, 51, 47
KL,40,0.5, ,
KL,34,0.5, ,
KL,32,0.5, ,

LSTR,  78, 79
LSTR,  79, 84

K, 90, KX(73)+wReactor*2*cos(160), KY(73)+wReactor*2*sin(160)
L, 73, 90
LPTN, 59, 33
LPTN, 63, 45
LDELE, 65

K, 91, KX(71)+wReactor*2*cos(170), KY(71)+wReactor*2*sin(170)
L, 71, 91
LPTN, 45, 60
LPTN, 33, 67
LDELE, 69
KCENTER,KP,69,78,70,0
LSTR,    89,    58
LSTR,    89,    57

LPTN, 40, 33, 67
LDELE, 73, 74

L, 58, 56
L, 57, 55
```

```
/com, **********************
/com, Weld Overlay
/com, **********************
*set, woA, 3.100
*set, woB, 0.781
*set, woC, 2.500
*set, woD, 3.734
*set, woE, 3.480
*set, woF, 6.310
*set, woG, 8.313
*set, woH, 0.535
*set, woR01, 7/16

K, 80, KX(40), KY(40)-wgap/2-woA
K, 81, KX(80)+woH, KY(80)+woH
K, 83, KX(40), KY(40)-wgap/2+woB/2+woC
K, 82, KX(83)+woH, KY(83)-woH

L, 80, 81
L, 81, 82
L, 82, 83


LPTN, 74, 46
LDELE, 79
LFILLT,78,76,woR01, ,
LSTR,     94,     96

/com, *************************
/com, Heat transfer coef. points
/com, *************************
*set, tsL01, 2.25
*set, tsL02, 3.5

K, 100, KX(41),      KY(11)+seL08+tsL01
K, 101, KX(41)+wClad, KY(11)+seL08+tsL01

K, 102, KX(41),      KY(11)+seL08+tsL01+tsL02
K, 103, KX(41)+wClad, KY(11)+seL08+tsL01+tsL02
L, 100, 101
L, 102, 103

LDELE, 51
LDELE, 47
```

```
K, 104, KX(103)+wReactor*cos(-20), KY(103)+wReactor*sin(-20)
K, 105, KX(101)+wReactor*cos(-10), KY(101)+wReactor*sin(-10)
L, 103, 104
L, 101, 105
LPTN, 38, 47
LPTN, 76, 51

LDELE, 86
LDELE, 84
LDELE, 65
LDELE, 68

LDELE, 63
LDELE, 45
LDELE, 66
LDELE, 60

LSTR,    43,    101
LSTR,   101,    103
LSTR,   103,     85
LSTR,    86,    102
LSTR,   102,    100
LSTR,   100,     41

LDIV,30,0.5, ,2,0
K, 106, KX(99)+wReactor*cos(200), KY(99)+wReactor*sin(200)
K, 107, KX(38)+wReactor*cos(160), KY(38)+wReactor*sin(160)
L, 99, 106
L, 38, 107
LPTN, 66, 84
LPTN, 88, 76

LDELE, 89,90
LSTR,    99,     38
LDELE, 28
LSTR,    26,      9
LSTR,    29,     16

LCOMB,11,23,0
LCOMB,11,24,0
LDIV,11, , ,3,0

K, 110, KX(22)+wReactor*cos(180), KY(22)+wReactor*sin(180)
L, 110, 22
LPTN, 15, 89
LDELE, 94
```

```
LSTR,    28,   111
LSTR,    27,    22
LSTR,    17,     7
K, 112, KX(33)+wReactor, KY(33)
L, 33, 112
LPTN, 7, 95
LDELE, 99
K, 114, KX(25)+wReactor*cos(180), KY(25)+wReactor*sin(180)
L, 114,25
K, 115, KX(8)+wReactor*cos(180), KY(8)+wReactor*sin(180)
L, 115, 8
LPTN, 95,17
LPTN, 7,101
LDELE, 102,103


/com, *************************
/com, Creating Areas and Meshing
/com, *************************
allsel,all,all

MSHKEY,1    ! MAPPED MESHING
AL,1,2,3,4
MAT,4                        ! Pipe
LESIZE,1,,,8
LESIZE,3,,,8
LESIZE,2,,,20
LESIZE,4,,,20
AMESH, 1

MAT,2                        ! Safe End
AL, 3, 5, 100, 99
LESIZE,3,,,8
LESIZE,100,,,8
LESIZE,5,,,20
LESIZE,99,,,20
AMESH, 2

LCOMB, 20,6,0
LCOMB, 6,21,0
AL, 100, 6, 17, 104
LESIZE,100,,,8
LESIZE,17,,,8
LESIZE,6,,,10
LESIZE,104,,,10
AMESH, 3
```

```
AL, 17, 97, 98, 95
LESIZE,17,,,8
LESIZE,98,,,8
LESIZE,97,,,10
LESIZE,95,,,10
AMESH, 4

LDELE, 94
LSTR,     7,     30
LCOMB, 26,16,0
LCOMB, 16,25,0
AL, 98, 96, 7, 16
LESIZE,98,,,8
LESIZE,7,,,8
LESIZE,96,,,8
LESIZE,16,,,8
AMESH, 5


LCOMB, 18, 22
AL, 7, 18, 92, 93
LESIZE,7,,,8
LESIZE,92,,,8
LESIZE,18,,,10
LESIZE,93,,,10
AMESH, 6

AL, 92, 89, 23, 15
LESIZE,92,,,8
LESIZE,23,,,8
LESIZE,89,,,8
LESIZE,15,,,8
AMESH, 7

AL, 15, 24, 88, 90
LESIZE,15,,,8
LESIZE,24,,,8
LESIZE,88,,,8
LESIZE,90,,,8
AMESH, 8

AL, 89, 19, 28, 11
LESIZE,89,,,8
LESIZE,19,,,8
LESIZE,28,,,8
```

```
LESIZE,11,,,8
AMESH, 9


AL, 88, 12, 13, 14
LESIZE,88,,,8
LESIZE,13,,,8
LESIZE,12, , ,28,5, , , ,1
LESIZE,14, , ,28,0.2, , , ,1
AMESH, 10


K, 118, KX(80)+wReactor*cos(180), KY(80)+wReactor*sin(180)
L, 118, 80
LPTN, 10,20,8
LDELE, 101
AL, 28, 21, 94 , 26
LESIZE,28,,,8
LESIZE,94,,,8
LESIZE,21,,,6
LESIZE,26,,,6
AMESH, 11

LDELE, 9
LSTR,    42,    11
LSTR,    42,    10

LESIZE,8, , ,2, , , , ,1
LESIZE,9, , ,6, , , , ,1
LESIZE,22, , ,20,0.2, , , ,1
LESIZE,25, , ,20,0.2, , , ,1
AL, 94, 22, 9, 8, 25
AMAP,12,11,10,80,21


LCOMB, 37, 31
LCOMB, 27, 36
AL, 9, 27, 35, 31
LESIZE,35,,,6
LESIZE,27,,,4
LESIZE,31,,,4
AMESH, 13

MAT,4                    ! Clad
LCOMB, 68, 39
```

```
LCOMB, 29, 87
AL, 8, 31, 86, 29
LESIZE,8,,,2
LESIZE,86,,,2
LESIZE,31,,,4
LESIZE,29,,,4
AMESH, 14

AL, 35, 43, 39, 76
LESIZE,35,,,6
LESIZE,39,,,6
LESIZE,43,,,4
LESIZE,76,,,4
AMESH, 15


AL, 86, 76, 66, 91
LESIZE,86,,,2
LESIZE,66,,,2
LESIZE,76,,,4
LESIZE,91,,,4
AMESH, 16

MAT,1                    ! Nozzle
LCOMB, 41, 77,
LCOMB, 41, 74,
LCOMB, 41, 47,
LDELE, 41
LDELE, 47

LESIZE,45, , ,19, , , , ,1
LESIZE,30, , ,1, , , , ,1
LESIZE,10,,,20
LESIZE,85,,,6
AL, 39, 10, 85, 45, 30
AMAP,17,101,98,36,99

MAT,4                    ! Clad
LESIZE, 79,,,2
LESIZE,84,,,20
AL, 66, 30, 45, 79, 84
AMAP,18,100,101,99,109

MAT,1                    ! Nozzle
LCOMB, 38, 81
LESIZE, 38,,,14
```

```
LESIZE, 83,,,6
LESIZE, 51,,,14
AL, 85, 38, 83, 51
AMESH, 19

MAT,4                    ! Clad
LESIZE, 80,,,2
LESIZE, 65,,,14
AL, 79, 51, 80, 65
AMESH, 20

MAT,1                    ! Nozzle
LCOMB, 82, 50
LESIZE, 50,,,20
LESIZE, 62,,,6
LESIZE, 60,,,20
AL, 83, 50, 62, 60
AMESH, 21

MAT,4                    ! Clad
LESIZE, 64,,,2
LESIZE, 63,,,20
AL, 80, 60, 64, 63
AMESH, 22

MAT,1                    ! Nozzle
LCOMB, 49, 71
LESIZE, 49,,, 20
LESIZE, 69,,,6
LESIZE, 61,,,20
AL, 62,49,69,61
AMESH, 23

MAT,4                    ! Clad
LESIZE, 40,,,2
LESIZE, 59,,,20
AL, 64, 61, 40, 59
AMESH, 24

MAT,1                    ! Nozzle
LESIZE, 75,,,6
LESIZE, 70,,,6
LESIZE, 34,,,6
AL, 69, 75, 70, 34
AMESH, 25
```

```
MAT,4                    ! Clad
LESIZE, 33,,,2
LESIZE, 32,,,6
AL, 40, 34, 33, 32
AMESH, 26

MAT,1                    ! Nozzle
LCOMB, 53, 72
LESIZE, 53,,,8
LESIZE, 58,,,6
LESIZE, 52,,,8
AL, 70, 53, 58, 52
AMESH, 27

MAT,4                    ! Clad
LESIZE, 57,,,2
LESIZE, 54,,,8
AL, 33, 52, 57, 54
AMESH, 28

MAT,3                    ! Vessel
LESIZE, 57,,,2
LESIZE, 54,,,8
LESIZE, 48,,,100,0.2, , , ,1
LESIZE, 55,,,100,0.2, , , ,1
LESIZE, 56,,,100,0.2, , , ,1
AL, 48, 44, 56, 58
AMESH, 29

MAT,4                    ! Clad
LESIZE, 42,,,2
AL, 57, 56, 42, 55
AMESH, 30


MAT,1                    ! Nozzle
ACLEAR,     17
ADELE,      17
LOVLAP,10, 46
NUMMRG,KP, , , ,LOW
LCOMB,37,41 ,0
AL, 20, 37, 85, 45, 30, 39
AMAP,17,101,98,36,99
```

```
MAT,2                    ! Safe End
LCOMB, 36, 78
LESIZE, 67,,,6
LESIZE, 36,,,6, 0.2,,,1
AL, 67, 73,36,20,43,27,22
AMAP,31,23,82,81,80


/COM,**********************
/COM, HTC point of Region 3
/COM,**********************
ACLEAR, 4
ADELE,  4
LDELE,  95
LDELE,  97
K, 120, KX(18), KY(18) - 3/8
K, 121, KX(25), KY(120)
L, 25, 121
L, 121, 113
L, 117, 120
L, 120, 33
L, 120, 121

MAT,2                    ! Safe End
AL, 17, 10, 68, 46
LESIZE,10,,,12
LESIZE,68,,,8
LESIZE,46,,,12
AMESH, 4

AL, 68, 41, 98, 47
LESIZE,41,,,4
LESIZE,98,,,8
LESIZE,47,,,4
AMESH, 32


/COM,**********************
/COM, HTC point of Region 7
/COM,**********************
MAT,4                    ! Clad
ACLEAR,     18
ADELE,      18
K, 122, KX(14)+wReactor, KY(14)
L, 14,122
LSBL, 84, 71
```

```
LESIZE, 72,,,10
LESIZE, 74,,,10
AL, 66, 30,45,79,72,74
AMAP,18,100,101,99,109


/COM,*************************************
/COM, HTC point of Region 3
/COM,*************************************
MAT,2                          ! Safe End
ACLEAR,  2
ADELE,   2
K, 123, KX(120), KY(120)-3
K, 124, KX(4), KY(4)+1+1/16
LDELE, 99
L, 4, 124
L, 124, 123
L, 123, 116
AL, 3, 5, 100, 78, 77, 71
AMAP,2,116,8,3,4



/COM,*********************************
/COM, Define DOF constraints on lines
/COM,*********************************
DL,42, ,SYMM
DL,44, ,SYMM

FLST,4,9,1,ORDE,2
FITEM,4,1
FITEM,4,-9
CP,1,UY,P51X
```

Structural Integrity Associates, Inc.	File No.: VY-16Q-309
CALCULATION PACKAGE	Project No.: VY-16Q

PROJECT NAME:

Environmental Fatigue Analysis of VYNPS

CONTRACT NO.:

10150394

CLIENT:	PLANT:
Entergy Nuclear Operations, Inc.	Vermont Yankee Nuclear Power Station

CALCULATION TITLE:

Core Spray Nozzle Green's Functions

Document Revision	Affected Pages	Revision Description	Project Manager Approval Signature & Date	Preparer(s) & Checker(s) Signatures & Date
0	1-32, Appendix: A1-A2	Initial Issue	Terry J. Herrmann 7/20/2007	Roland Horvath 07/19/2007 John F. Staples 07/19/2007
1	1-35, Appendix: A1-A2	Correcting error in FEM input file (CAR-07-25 and NCR 07-11), editorial corrections.	Terry J. Herrmann 12/10/2007	Minghao Qin 12/10/2007 Timothy J. Gilman 12/10/2007

Table of Contents

1.0 OBJECTIVE 4
2.0 CORE SPRAY NOZZLE MODEL DESCRIPTION 4
3.0 APPLIED LOADS 7
3.1 Pressure Load 7
3.2 Thermal Load 11
3.2.1 Boundary Fluid Temperatures 11
3.2.2 Heat Transfer Coefficients 11
4.0 THERMAL AND PRESSURE LOAD RESULTS 25
5.0 REFERENCES 35
APPENDIX A FINITE ELEMENT ANALYSIS FILES A1

List of Tables

Table 1: Material Properties @ 300°F 5
Table 2: Heat Transfer Coefficients 13
Table 3: Heat Transfer Coefficients for Region 1 14
Table 4: First Partial Heat Transfer Coefficients for Region 3 15
Table 5: Second Partial Heat Transfer Coefficients for Region 3 16
Table 6: First Partial Heat Transfer Coefficients for Region 5 17
Table 7: Second Partial Heat Transfer Coefficients for Region 5 18
Table 8: First Partial Heat Transfer Coefficients for Region 7 19
Table 9: Second Partial Heat Transfer Coefficients for Region 7 20
Table 10: Third Partial Heat Transfer Coefficients for Region 7 21
Table 11: First Partial Heat Transfer Coefficients for Region 9 22
Table 12: Second Partial Heat Transfer Coefficients for Region 9 23
Table 13: Resultant Heat Transfer Coefficients for the Regions 24
Table 14: Pressure Results (1,000 psi) 33

List of Figures

Figure 1: ANSYS Finite Element Model 6
Figure 2: Core Spray Nozzle Internal Pressure Distribution 8
Figure 3: Core Spray Nozzle Pressure Cap Load 9
Figure 4: Core Spray Nozzle Vessel Wall Boundary Conditions 10
Figure 5: Nozzle and Vessel Wall Thermal and Heat Transfer Boundaries (not to scale) 12
Figure 6: Safe End Critical Thermal Stress Location, Node 3719 25
Figure 7: Blend Radius Limiting Pressure Stress Location, Node 2166 26
Figure 8: Safe End 100% Flow Total Stress Intensity 28
Figure 9: Blend Radius 100% Flow Total Stress Intensity 28
Figure 10: Safe End Total Stress History, 100% Flow, (Sz-Sx) 29
Figure 11: Safe End Membrane + Bending Stress History, 100% Flow, (Sz-Sx) 29
Figure 12: Blend Radius Total Stress History, 100% Flow, (Sz-Sx) 30
Figure 13: Blend Radius Membrane + Bending Stress History, 100% Flow, (Sz-Sx) 30
Figure 14: Safe End Total Stress History, 0% Flow, (Sz-Sx) 31
Figure 15: Safe End Membrane + Bending Stress History, 0% Flow, (Sz-Sx) 31
Figure 16: Blend Radius Total Stress History, 0% Flow, (Sz-Sx) 32
Figure 17: Blend Radius Membrane + Bending Stress History, 0% Flow, (Sz-Sx) 32

1.0 OBJECTIVE

The objective of this calculation is to compute the pressure stresses, thermal stresses, and the Green's Functions for high (100%) and no (0%) flow thermal loading of the Vermont Yankee Nuclear Power Station Core Spray Nozzle.

2.0 CORE SPRAY NOZZLE MODEL DESCRIPTION

An axisymmetric finite element model of the core spray nozzle was developed in Reference [1] using ANSYS [2]. The geometry used in Reference [1] was utilized in this calculation. The material properties are taken at an average temperature of 300°F. This average temperature is based on a thermal shock of 500°F to 100°F, which will be applied to the FE model for Green's Function development. Table 1 lists the material properties at 300°F. The meshed model is shown in Figure 1.

Table 1: Material Properties @ 300°F (1)

Part Description	Material		Modulus of Elasticity, e+6 psi [EX]	Coefficient of Thermal Expansion, e-6, in/in/°F [ALPX]	Thermal Conductivity, Btu/hr-ft-°F [KXX]	Thermal Diffusivity, ft^2/hr	Specific Heat, Btu/lb-°F [C] (3)	Poisson's Ratio [NUXY]	Density, lb/in^3 [DENS]
Safe End	SB 166	72Ni-15Cr-8Fe N06600	29.8	7.9	9.6	0.160	0.1157	0.29	0.3
Weld Overlay	INCONEL 82								
Nozzle	SA508 Class II	¾ Ni-1/2Mo-1/3 Cr-V	26.7	7.3	23.4	0.401	0.1193	0.3	0.283
Vessel	SA533 Grade B	Mn-1/2Mo-1/2Ni	28.0	7.7	23.4	0.401	0.1193	0.3	0.283
3/16 Clad	SA240 TP 304	18Cr-8Ni	27.0	9.8	9.8	0.160	0.1252	0.3	0.283
8Ø x 10Ø Conc. Reduction(2)	SA312 TP304								
Thermal Sleeve	SA312 TP304(4)								

Notes:

1. The material properties applied in the analyses are taken from ASME Code, Section II, Part D 1998 Edition, with 2000 Addenda. This is consistent with information provided in the Design Input Record (page 13 of [6]). The use of a later code edition than that used for the original design code is acceptable, since later editions typically reflect more accurate material properties than was published in prior Code editions. Material Properties are evaluated at 300°F from the 1998 ASME Code, 2000 Addenda, Section II, Part D, except for density and Poisson's ratio, which are assumed typical values [3].
2. In the FEM, the 8Ø x 10Ø Conc. Reduction was modeled as a straight pipe with the material properties of the original design. Later this piping section was replaced by a new material (SA403 T316L). These two stainless steels have the same modulus of elasticity and thermal coefficient properties [3].
3. Calculated as $[k/(\rho d)]/12^3$.
4. Per Reference [9].

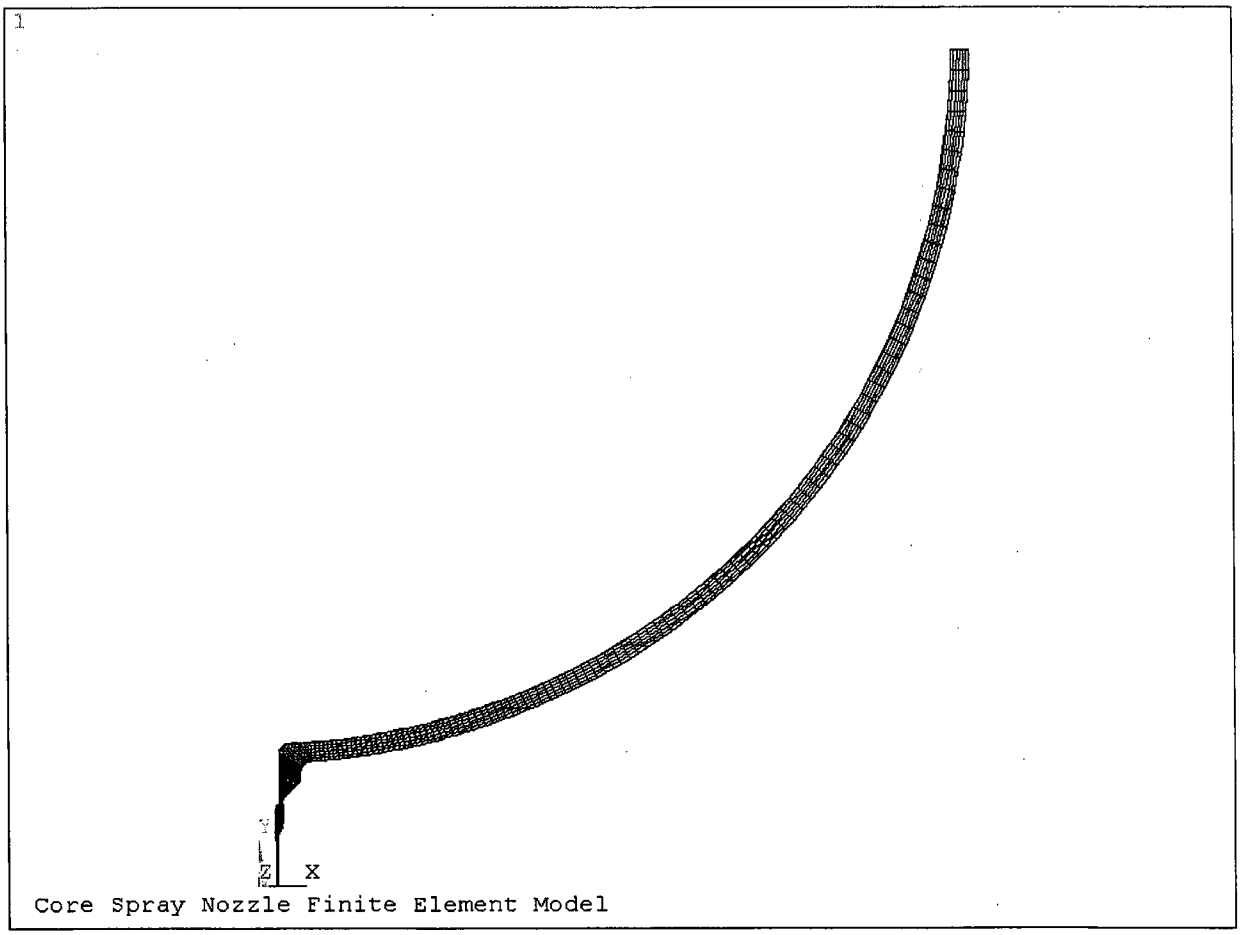

Figure 1: ANSYS Finite Element Model

3.0 APPLIED LOADS

Both pressure and thermal loads were applied to the finite element model.

3.1 Pressure Load

A uniform pressure of 1000 psi was applied along the inside surface of the core spray nozzle and the reactor vessel wall (Figure 2). A pressure load of 1000 psi was used because it is easily scaled up or down to account for different pressures that occur during transients. In addition, a cap load was applied to the piping at the end of the nozzle. This cap load was calculated as follows:

$$P_{CAP} = \frac{P \cdot D_i^2}{D_o^2 - D_i^2}$$

where:

P = Pressure = 1,000 psi
D_i = Inside Diameter = 9.834 in
D_o = Outside Diameter = 10.815 in

Therefore, the cap load is 4,774 psi. The calculated value was given a negative sign in order for it to exert tension on the end of the model. The nodes on the end of the safe end are coupled in the axial direction (UY, Figure 3) to ensure mutual displacement of the end of the nozzle due to attached piping. The boundary conditions at the end of the modeled portion of the reactor pressure vessel wall constructed to be "symmetric" (Figure 4).

The ANSYS input file VY_16Q_P.inp generates the core spray nozzle geometry from VY_CSN_Geom.inp [1] and performs the internal pressure load case just described. Figure 2, 3, and 4 show the internal pressure distribution, cap load, and symmetry conditions applied to the vessel end of the model, respectively.

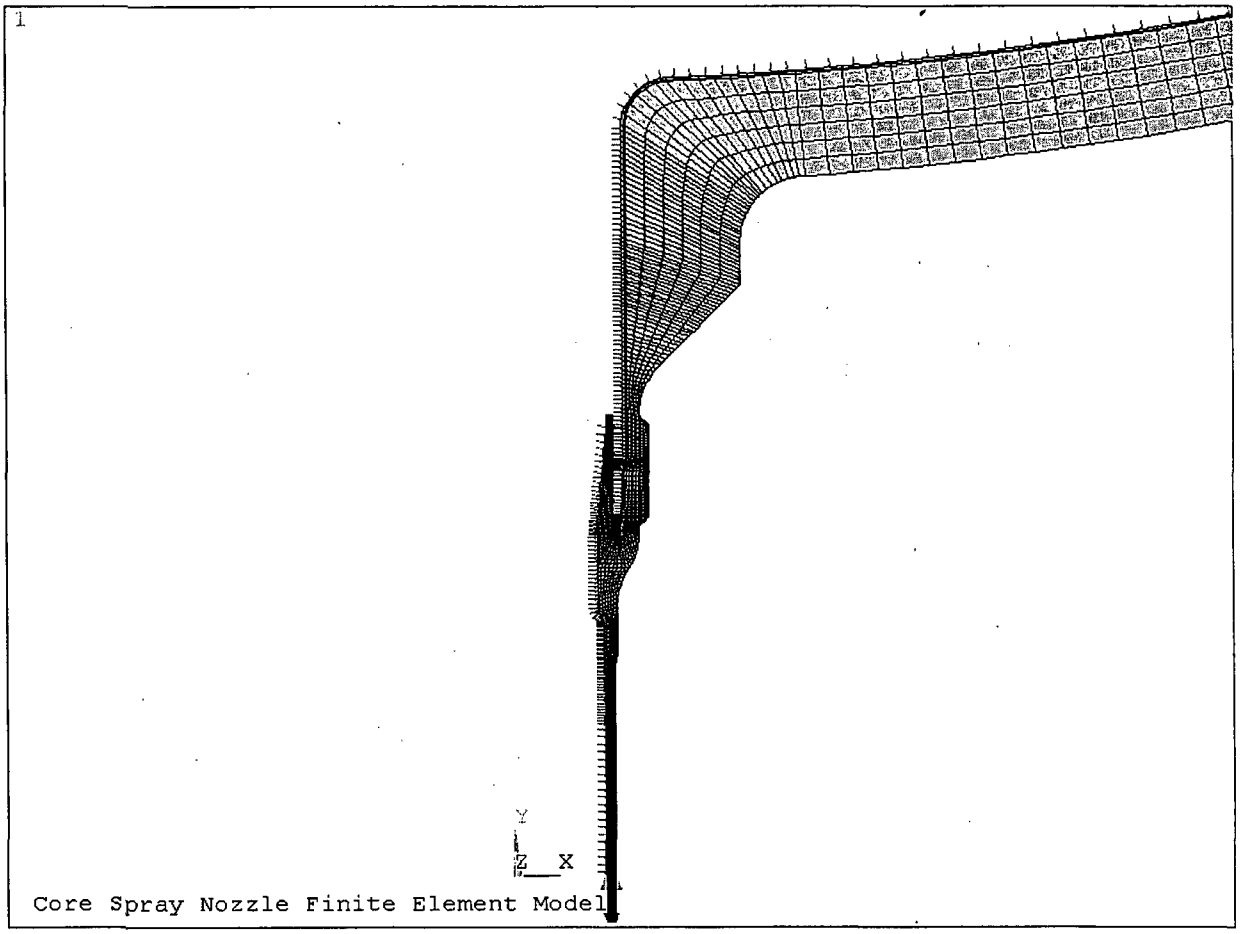

Figure 2: Core Spray Nozzle Internal Pressure Distribution

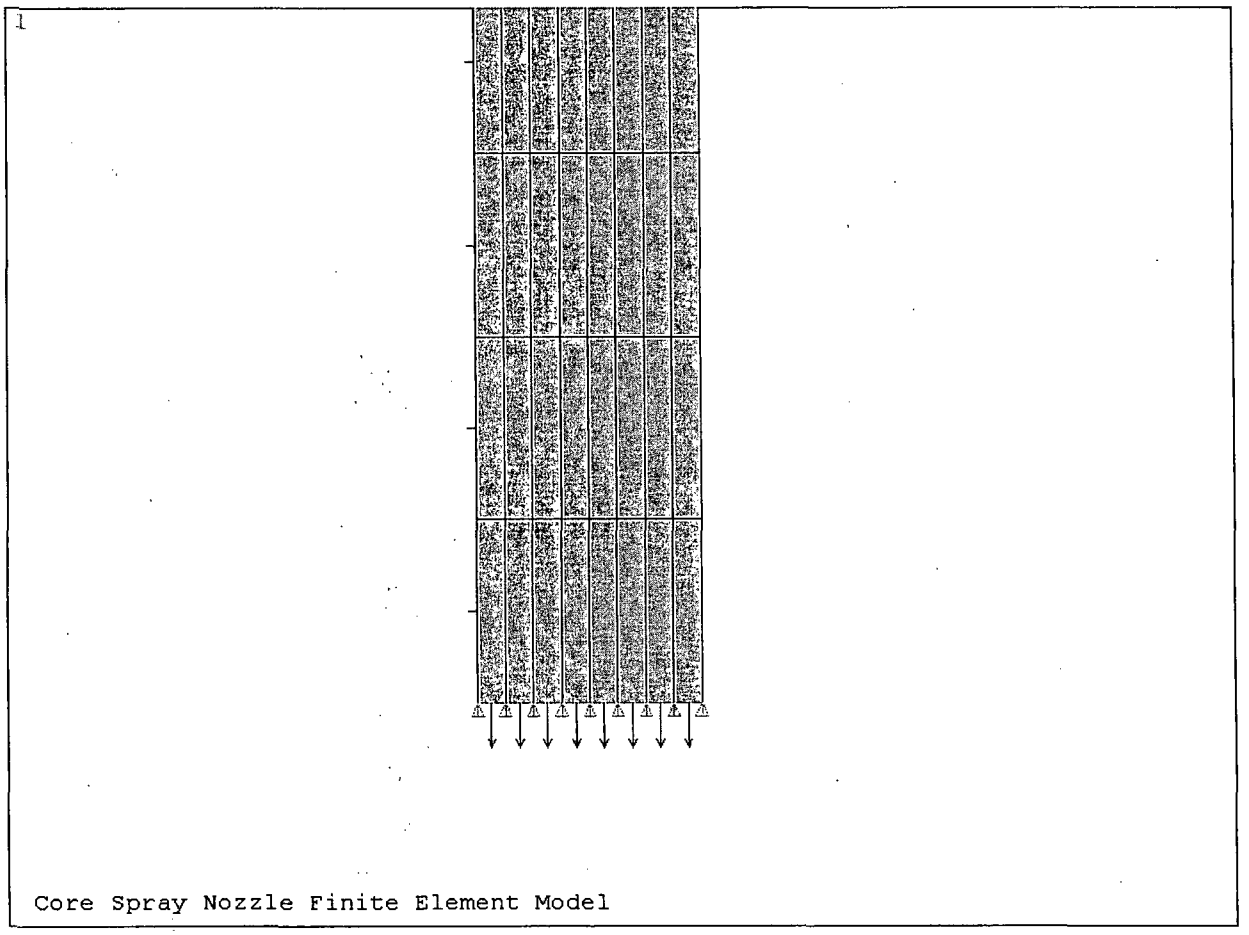

Figure 3: Core Spray Nozzle Pressure Cap Load

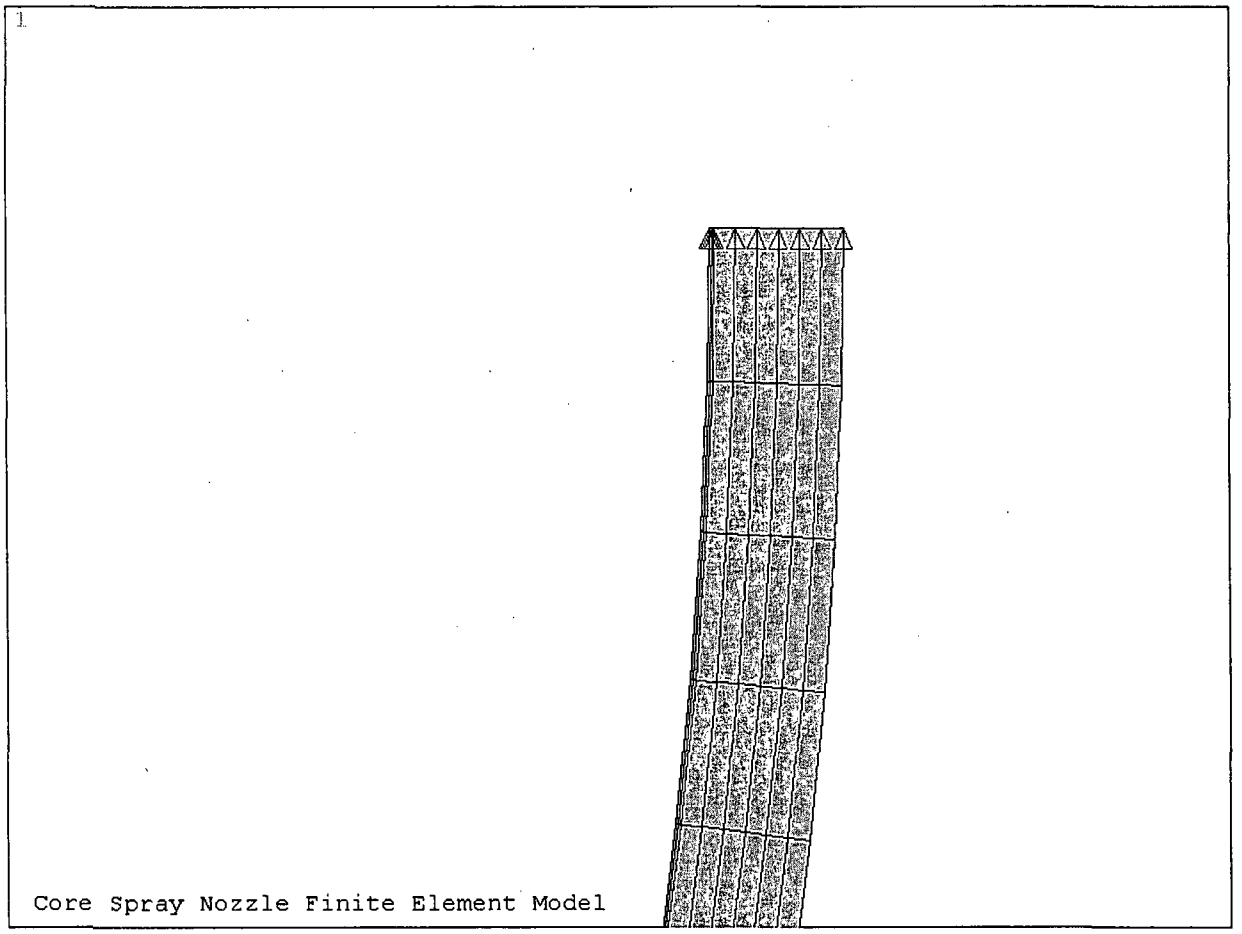

Figure 4: Core Spray Nozzle Vessel Wall Boundary Conditions

3.2 Thermal Load

Thermal loads are applied to the core spray nozzle model. The heat transfer coefficients (HTC) were determined using the methodology in the Excel spreadsheet "Heat Transfer Coefficients.xls", which is included in the project files. The HTCs were determined for various regions of the core spray FEM, (see Figure 5) for two different flow cases. The flow cases are for 100% (3200 gpm [6]) and 0% core spray flow through the nozzle.

The 0% flow case simulates a stagnant condition of the core spray nozzle when not in operation (i.e., the entire core spray nozzle is at the same temperature as the reactor pressure vessel due to reflooding). The HTCs for the no flow case are for free convection (stagnant) at the temperature of the reactor pressure vessel 500°F. The applied boundary fluid temperature is changed to simulate a thermal shock from 500°F to 100°F to develop the stress response on the core spray nozzle in the stagnant condition.

The 100% flow case simulates operational condition of the core spray nozzle (i.e., the entire core spray nozzle experiences 100°F water due to injection). The HTCs for the high flow case are for forced and free convection depending on the region of the FEM. The applied boundary fluid temperature is changed to simulate a thermal shock from 500°F to 100°F to develop the stress response on the core spray nozzle due to injection.

For both Green's Functions, a 500°F – 100°F thermal shock was run to determine the stress response. For the 0% flow case, the entire inside surface of the FEM was shocked. For the 100% flow case, only the nozzle flow path was shocked.

3.2.1 Boundary Fluid Temperatures

For the Green's Functions, a 500°F – 100°F thermal shock was run to determine the stress response to a degree change in temperature. The temperature on the exterior of the reactor, nozzle, safe end and the pipe is assumed to be 120 °F (ambient).

3.2.2 Heat Transfer Coefficients

Figure 5 shows where the heat transfer coefficients were applied to the FEM for the 0% (steady-state) and 100% core spray flow injection load case. For all the regions, the applied heat transfer coefficients and the initial temperatures are summarized in Table 2. The heat transfer coefficient for outside the reactor vessel wall is 0.2 BTU/hr-ft^2-°F and the heat transfer coefficient for inside the reactor vessel wall is 500 BTU/Hr-ft^2-°F, from page I-T7-5 of Reference [8].

Table 3 through Table 12 show the excel spreadsheets to calculate the HTC for regions 1, 3, 5, 7, and 9 respectively. These tables calculate the HTC for a certain part of the nozzle using the geometry of the bounding piping, the flow rate, and other physical fluid parameters. These tables calculate the Reynolds, Grashof and Rayleigh numbers in order to determine the HTC for inside surface/annulus forced and natural convection [4]. For several regions, the resultant HTCs had to be calculated from the partial heat transfer coefficients. These resultant HTCs are summarized in Table 13. In regions 2, 4, 6, 8, and 10 the HTCs are interpolated because of the complexity of the material profile.

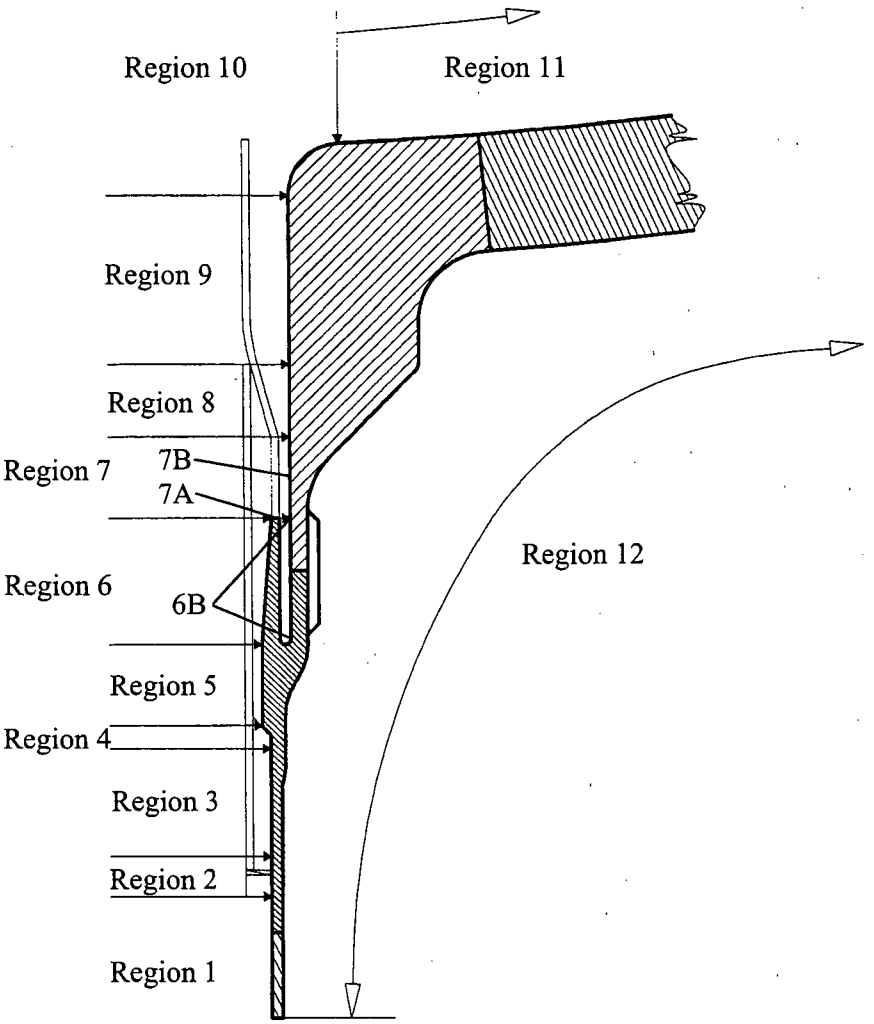

Figure 5: Nozzle and Vessel Wall Thermal and Heat Transfer Boundaries (not to scale)

Table 2: Heat Transfer Coefficients

Regions	0% Flow		100% Flow	
	Initial Temperature °F	HTC Btu/hr-ft^2-°F	Initial Temperature °F	HTC Btu/hr-ft^2-°F
R1	500	143	500	2693
R2	500	Interpolated	500	Interpolated
R3 (1)	500	49	500	71
R4	500	Interpolated	500	Interpolated
R5 (1)	500	61	500	101
R6	500	Interpolated	500	Interpolated
R6B	500	97	500	97
R7A (1)	500	47	500	68
R7B (1)	500	29	500	36
R8	500	Interpolated	500	Interpolated
R9 (1)	500	39	500	52
R10	500	Interpolated	500	Interpolated
R11	500	500	500	500
R12	120	0.20	120	0.2

(1) See Table 13

Table 3: Heat Transfer Coefficients for Region 1

Pipe Inside Diameter, D =	9.834	inches =	0.820	ft		100% rated flow =	3,200	gpm
		=	0.250	m		@ T =	549	°F
Flow, % of rated =	100%					Density, ρ =	48.087	lbm/ft³
Fluid Velocity, V =	13.517	ft/sec =	3,200.0	gpm =	1.234236214	Mlb/hr		
Characteristic Length, L = D =	0.820	ft =	0.250	m				

T_{fluid} - $T_{surface}$, ΔT = assumed to be 12% of fluid temperature =	8.40	12.00	24.00	36.00	48.00	60.00	72.00	°F
=	4.67	6.67	13.33	20.00	26.67	33.33	40.00	°C

Note: The above assumption is based on experience with past RPV heat transfer analyses.

		Value at Fluid Temperature, T [7]							Units
Water Property	**Conversion Factor [4]**	**70**	**100**	**200**	**300**	**400**	**500**	**600**	**°F**
		21.11	**37.78**	**93.33**	**148.89**	**204.44**	**260.00**	**315.56**	**°C**
k	1.7307	0.5997	0.6300	0.6784	0.6836	0.6611	0.6040	0.5071	W/m-°C
(Thermal Conductivity)		0.3465	0.3640	0.3920	0.3950	0.3820	0.3490	0.2930	Btu/hr-ft-°F
c_p	4.1869	4.185	4.179	4.229	4.313	4.522	4.982	6.322	kJ/kg-°C
(Specific Heat)		1.000	0.998	1.010	1.030	1.080	1.190	1.510	Btu/lbm-°F
ρ	16.018	997.1	994.7	962.7	917.8	858.6	784.9	679.2	kg/m³
(Density)		62.3	62.1	60.1	57.3	53.6	49.0	42.4	lbm/ft³
β	1.8	1.89E-04	3.24E-04	6.66E-04	1.01E-03	1.40E-03	1.98E-03	3.15E-03	m³/m³-°C
(Volumetric Rate of Expansion)		1.05E-04	1.80E-04	3.70E-04	5.60E-04	7.80E-04	1.10E-03	1.75E-03	ft³/ft³-°F
g	0.3048	9.806	9.806	9.806	9.806	9.806	9.806	9.806	m/s²
(Gravitational Constant)		32.17	32.17	32.17	32.17	32.17	32.17	32.17	ft/s²
μ	1.4881	9.96E-04	6.82E-04	3.07E-04	1.93E-04	1.38E-04	1.04E-04	8.62E-05	kg/m-s
(Dynamic Viscosity)		6.69E-04	4.58E-04	2.06E-04	1.30E-04	9.30E-05	7.00E-05	5.79E-05	lbm/ft-s
Pr		6.980	4.510	1.910	1.220	0.950	0.859	1.070	—
(Prandtl Number)									
Calculated Parameter	**Formula**	**70**	**100**	**200**	**300**	**400**	**500**	**600**	**°F**
Reynold's Number, Re	$\rho VD/\mu$	1.0307E+06	1.5019E+06	3.2317E+06	4.8825E+06	6.3843E+06	7.7540E+06	8.1118E+06	---
Grashof Number, Gr	$g\beta\Delta TL^3/(\mu/\rho)^2$	1.3522E+08	7.0314E+08	1.3383E+10	6.9351E+10	2.2021E+11	5.7264E+11	1.1964E+12	---
Rayleigh Number, Ra	GrPr	9.4382E+08	3.1712E+09	2.5562E+10	8.4608E+10	2.0920E+11	4.9189E+11	1.2802E+12	---
From [4]:									
Inside Surface Forced Convection Heat Transfer Coefficient:									
H_{forced} =	$0.023Re^{0.8}Pr^{0.4}k/D$	7,765.07	9,257.25	13,050.72	15,291.12	16,581.64	16,999.27	16,154.74	W/m²-°C
		1,367.53	**1,630.33**	**2,298.41**	92.0%	**2,920.25**	**2,993.80**	**2,845.07**	Btu/hr-ft²-°F
		2.638E-03	**3.145E-03**	**4.434E-03**	**5.195E-03**	**5.633E-03**	**5.775E-03**	**5.488E-03**	Btu/sec-in²-°F
From [4]:									
Inside Surface Natural Convection Heat Transfer Coefficient:									
Case:	Enclosed cylinder		C =	0.56	n =	0.25	(see page 256 of [4])		
H_{free} =	$C(GrPr)^n k/L$	231.44	329.18	597.32	811.84	984.52	1,113.82	1,187.70	W/m²-°C
		40.76	**57.97**	**105.20**	92.0%	**173.39**	**196.16**	**209.17**	Btu/hr-ft²-°F
		7.863E-05	**1.118E-04**	**2.029E-04**	**2.758E-04**	**3.345E-04**	**3.784E-04**	**4.035E-04**	Btu/sec-in²-°F

Table 4: First Partial Heat Transfer Coefficients for Region 3

Pipe Inside Diameter, D =	7.981	inches =	0.665	ft	100% rated flow =	3,200	gpm
		=	0.203	m	@ T =	549	°F
Flow, % of rated =	100%				Density, ρ =	48.087	lbm/ft³
Fluid Velocity, V =	20.522	ft/sec =	3,200.0	gpm =	1.234236214	Mlb/hr	
Characteristic Length, L = D =	0.665	ft =	0.203	m			

$T_{fluid} - T_{surface}$, ΔT = assumed to be 12% of fluid temperature =	8.40	12.00	24.00	36.00	48.00	60.00	72.00	°F
=	4.67	6.67	13.33	20.00	26.67	33.33	40.00	°C

Note: The above assumption is based on experience with past RPV heat transfer analyses.

		Value at Fluid Temperature, T [7]							Units
Water Property	**Conversion Factor [4]**	**70**	**100**	**200**	**300**	**400**	**500**	**600**	**°F**
		21.11	**37.78**	**93.33**	**148.89**	**204.44**	**260.00**	**315.56**	**°C**
k	1.7307	0.5997	0.6300	0.6784	0.6836	0.6611	0.6040	0.5071	W/m-°C
(Thermal Conductivity)		0.3465	0.3640	0.3920	0.3950	0.3820	0.3490	0.2930	Btu/hr-ft-°F
c_p	4.1869	4.185	4.179	4.229	4.313	4.522	4.982	6.322	kJ/kg-°C
(Specific Heat)		1.000	0.998	1.010	1.030	1.080	1.190	1.510	Btu/lbm-°F
ρ	16.018	997.1	994.7	962.7	917.8	858.6	784.9	679.2	kg/m³
(Density)		62.3	62.1	60.1	57.3	53.6	49.0	42.4	lbm/ft³
β	1.8	1.89E-04	3.24E-04	6.66E-04	1.01E-03	1.40E-03	1.98E-03	3.15E-03	m³/m³-°C
(Volumetric Rate of Expansion)		1.05E-04	1.80E-04	3.70E-04	5.60E-04	7.80E-04	1.10E-03	1.75E-03	ft³/ft³-°F
g	0.3048	9.806	9.806	9.806	9.806	9.806	9.806	9.806	m/s²
(Gravitational Constant)		32.17	32.17	32.17	32.17	32.17	32.17	32.17	ft/s²
μ	1.4881	9.96E-04	6.82E-04	3.07E-04	1.93E-04	1.38E-04	1.04E-04	8.62E-05	kg/m-s
(Dynamic Viscosity)		6.69E-04	4.58E-04	2.06E-04	1.30E-04	9.30E-05	7.00E-05	5.79E-05	lbm/ft-s
Pr		6.980	4.510	1.910	1.220	0.950	0.859	1.070	---
(Prandtl Number)									
Calculated Parameter	**Formula**	**70**	**100**	**200**	**300**	**400**	**500**	**600**	**°F**
Reynold's Number, Re	ρVD/μ	1.2700E+06	1.8507E+06	3.9821E+06	6.0161E+06	7.8665E+06	9.5543E+06	9.9952E+06	---
Grashof Number, Gr	$g\beta\Delta TL^3/(\mu/\rho)^2$	7.2279E+07	3.7586E+08	7.1540E+09	3.7071E+10	1.1771E+11	3.0610E+11	6.3954E+11	---
Rayleigh Number, Ra	GrPr	5.0451E+08	1.6951E+09	1.3664E+10	4.5226E+10	1.1183E+11	2.6294E+11	6.8430E+11	---
From [4]:									
Inside Surface Forced Convection Heat Transfer Coefficient:									
H_{forced} =	$0.023Re^{0.8}Pr^{0.4}k/D$	11,307.23	13,480.10	19,004.02	22,266.42	24,145.63	24,753.78	23,524.01	W/m²-°C
		1,991.36	2,374.03	3,346.87	[redacted]	4,252.38	4,359.49	4,142.90	Btu/hr-ft²-°F
		3.841E-03	4.580E-03	6.456E-03	7.564E-03	8.203E-03	8.409E-03	7.992E-03	Btu/sec-in²-°F
From [4]:									
Inside Surface Natural Convection Heat Transfer Coefficient:									
Case:	Enclosed cylinder		C =	0.55	n =	0.25	(See page 289 of [4])		
H_{free} =	$C(GrPr)^n k/L$	243.85	346.81	629.32	855.34	1,037.27	1,173.50	1,251.33	W/m²-°C
		42.94	61.08	110.83	[redacted]	182.68	206.67	220.38	Btu/hr-ft²-°F
		8.284E-05	1.178E-04	2.138E-04	2.906E-04	3.524E-04	3.987E-04	4.251E-04	Btu/sec-in²-°F

Table 5: Second Partial Heat Transfer Coefficients for Region 3

Pipe Inside Diameter, D =	9.834	inches =	0.820	ft	
		=	0.250	m	
Outer Pipe, Inside radius, r_o =	4.917	inches =	0.410	ft	
			0.125	m	
Inner Pipe Outside Diameter, D =	8.625	inches =	0.719	ft	
		=	0.219	m	
Inner Pipe, Outside radius, r_i =	4.3125	inches =	0.359	ft	
			0.110	m	
Fluid Velocity, V =	13.517	ft/sec =	3200.000	gpm	
Characteristic Length, L = D =	0.820	ft =	0.250	m	

(Outside) T_{fluid} - $T_{surface}$, ΔT =	8.40	12.00	24.00	36.00	48.00	60.00	72.00	°F
=	4.67	6.67	13.33	20.00	26.67	33.33	40.00	°C

		Value at Fluid Temperature, T [7]							Units
Water Property	**Conversion Factor [4]**	**70**	**100**	**200**	**300**	**400**	**500**	**600**	**°F**
		21.11	**37.78**	**93.33**	**148.89**	**204.44**	**260.00**	**315.56**	**°C**
k	1.7307	0.5997	0.6300	0.6784	0.6836	0.6611	0.6040	0.5071	W/m-°C
(Thermal Conductivity)		0.3465	0.3640	0.3920	0.3950	0.3820	0.3490	0.2930	Btu/hr-ft-°F
c_p	4.1869	4.185	4.179	4.229	4.313	4.522	4.982	6.322	kJ/kg-°C
(Specific Heat)		1.000	0.998	1.010	1.030	1.080	1.190	1.510	Btu/lbm-°F
ρ	16.018	997.1	994.7	962.7	917.8	858.6	784.9	679.2	kg/m^3
(Density)		62.3	62.1	60.1	57.3	53.6	49.0	42.4	lbm/ft^3
β	1.8	1.89E-04	3.24E-04	6.66E-04	1.01E-03	1.40E-03	1.98E-03	3.15E-03	m^3/m^3-°C
(Volumetric Rate of Expansion)		1.05E-04	1.80E-04	3.70E-04	5.60E-04	7.80E-04	1.10E-03	1.75E-03	ft^3/ft^3-°F
g	0.3048	9.806	9.806	9.806	9.806	9.806	9.806	9.806	m/s^2
(Gravitational Constant)		32.17	32.17	32.17	32.17	32.17	32.17	32.17	ft/s^2
μ	1.4881	9.96E-04	6.82E-04	3.07E-04	1.93E-04	1.38E-04	1.04E-04	8.62E-05	kg/m-s
(Dynamic Viscosity)		6.69E-04	4.58E-04	2.06E-04	1.30E-04	9.30E-05	7.00E-05	5.79E-05	lbm/ft-s
Pr		6.980	4.510	1.910	1.220	0.950	0.859	1.070	---
(Prandtl Number)									
Calculated Parameter	**Formula**	**70**	**100**	**200**	**300**	**400**	**500**	**600**	**°F**
Reynold's Number, Re	ρVD/μ	1030724	1501950	3231741	4882481	6384268	7754027	8111787	---
Grashof Number, Gr	$g\beta\Delta TL^3/(\mu/\rho)^2$	135217684.2	703144247.6	13383382850	69350803914	2.2021E+11	5.72636E+11	1.19642E+12	---
Grashof Number, Gr_δ	$g\beta\Delta T(r_o-r_i)^3/(\mu/\rho)^3$	3.14E+04	1.63E+05	3.11E+06	1.61E+07	5.11E+07	1.33E+08	2.78E+08	---
Rayleigh Number, Ra	GrPr	943819435.9	3171180557	25562261244	84607980776	2.092E+11	4.91894E+11	1.28017E+12	---
Rayleigh Number, Ra	$Gr_\delta Pr$	2.19E+05	7.37E+05	5.94E+06	1.97E+07	4.86E+07	1.14E+08	2.97E+08	---

From [4]:

Annulus Natural Convection Heat Transfer Coefficient:

Case:	Enclosed cylinder		C =	0.40	n =	0.20	(see page 291 of [5])		
H_{free}	$C(Gr_\delta Pr)^n k/(r_o-r_i)$	182.78	244.68	400.00	512.07	593.51	643.36	653.99	W/m^2-°C
		32.19	43.09	70.45	[illegible]	104.53	113.30	115.18	$Btu/hr-ft^2$-°F

Table 6: First Partial Heat Transfer Coefficients for Region 5

Pipe Inside Diameter, D =	7.981	inches =	0.665	ft		100% rated flow =	3,200	gpm
		=	0.203	m		@ T =	549	°F
Flow, % of rated =	100%					Density, ρ =	48.087	lbm/ft³
Fluid Velocity, V =	20.522	ft/sec =	3,200.0	gpm =	1.234236214	Mlb/hr		
Characteristic Length, L = D =	0.665	ft =	0.203	m				

$T_{fluid} - T_{surface}$, ΔT = assumed to be 12% of fluid temperature =	8.40	12.00	24.00	36.00	48.00	60.00	72.00	°F
=	4.67	6.67	13.33	20.00	26.67	33.33	40.00	°C

Note: The above assumption is based on experience with past RPV heat transfer analyses.

		Value at Fluid Temperature, T [7]							Units
Water Property	**Conversion Factor [4]**	**70**	**100**	**200**	**300**	**400**	**500**	**600**	°F
		21.11	**37.78**	**93.33**	**148.89**	**204.44**	**260.00**	**315.56**	°C
k	1.7307	0.5997	0.6300	0.6784	0.6836	0.6611	0.6040	0.5071	W/m-°C
(Thermal Conductivity)		0.3465	0.3640	0.3920	0.3950	0.3820	0.3490	0.2930	Btu/hr-ft-°F
c_p	4.1869	4.185	4.179	4.229	4.313	4.522	4.982	6.322	kJ/kg-°C
(Specific Heat)		1.000	0.998	1.010	1.030	1.080	1.190	1.510	Btu/lbm-°F
ρ	16.018	997.1	994.7	962.7	917.8	858.6	784.9	679.2	kg/m³
(Density)		62.3	62.1	60.1	57.3	53.6	49.0	42.4	lbm/ft³
β	1.8	1.89E-04	3.24E-04	6.66E-04	1.01E-03	1.40E-03	1.98E-03	3.15E-03	m³/m³-°C
(Volumetric Rate of Expansion)		1.05E-04	1.80E-04	3.70E-04	5.60E-04	7.80E-04	1.10E-03	1.75E-03	ft³/ft³-°F
g	0.3048	9.806	9.806	9.806	9.806	9.806	9.806	9.806	m/s²
(Gravitational Constant)		32.17	32.17	32.17	32.17	32.17	32.17	32.17	ft/s²
μ	1.4881	9.96E-04	6.82E-04	3.07E-04	1.93E-04	1.38E-04	1.04E-04	8.62E-05	kg/m-s
(Dynamic Viscosity)		6.69E-04	4.58E-04	2.06E-04	1.30E-04	9.30E-05	7.00E-05	5.79E-05	lbm/ft-s
Pr		6.980	4.510	1.910	1.220	0.950	0.859	1.070	---
(Prandtl Number)									
Calculated Parameter	**Formula**	**70**	**100**	**200**	**300**	**400**	**500**	**600**	°F
Reynold's Number, Re	ρVD/μ	1.2700E+06	1.8507E+06	3.9821E+06	6.0161E+06	7.8665E+06	9.5543E+06	9.9952E+06	---
Grashof Number, Gr	$g\beta\Delta TL^3/(\mu/\rho)^2$	7.2279E+07	3.7586E+08	7.1540E+09	3.7071E+10	1.1771E+11	3.0610E+11	6.3954E+11	---
Rayleigh Number, Ra	GrPr	5.0451E+08	1.6951E+09	1.3664E+10	4.5226E+10	1.1183E+11	2.6294E+11	6.8430E+11	---
From [4]:									
Inside Surface Forced Convection Heat Transfer Coefficient:									
H_{forced} =	$0.023Re^{0.8}Pr^{0.4}k/D$	11,307.23	13,480.10	19,004.02	22,266.42	24,145.63	24,753.78	23,524.01	W/m²-°C
		1,991.36	**2,374.03**	**3,346.87**	[redacted]	**4,252.38**	**4,359.48**	**4,142.90**	Btu/hr-ft²-°F
		3.841E-03	**4.580E-03**	**6.456E-03**	**7.564E-03**	**8.203E-03**	**8.409E-03**	**7.992E-03**	Btu/sec-in²-°F
From [4]:									
Inside Surface Natural Convection Heat Transfer Coefficient:									
Case:	Enclosed cylinder		C =	0.55	n =	0.25	(see page 289 of [4])		
H_{free} =	$C(GrPr)^n k/L$	243.85	346.81	629.32	855.34	1,037.27	1,173.50	1,251.33	W/m²-°C
		42.94	**61.08**	**110.83**	[redacted]	**182.68**	**206.67**	**220.38**	Btu/hr-ft²-°F
		8.284E-05	**1.178E-04**	**2.138E-04**	**2.906E-04**	**3.524E-04**	**3.987E-04**	**4.251E-04**	Btu/sec-in²-°F

Table 7: Second Partial Heat Transfer Coefficients for Region 5

Title = No Flow Region between nozzle and thermal sleeve

Pipe Inside Diameter, D =	9.000	inches =	0.750	ft	
		=	0.229	m	
Outer Pipe, Inside radius, r_o =	4.5	inches =	0.375	ft	
			0.114	m	
Inner Pipe Outside Diameter, D =	8.625	inches =	0.719	ft	
		=	0.219	m	
Inner Pipe, Outside radius, r_i =	4.3125	inches =	0.359	ft	
			0.110	m	
Fluid Velocity, V =	16.138	ft/sec =	3200.000	gpm	
Characteristic Length, L = D =	0.750	ft =	0.229	m	

(Outside) T_{fluid} - $T_{surface}$, ΔT =	8.40	12.00	24.00	36.00	48.00	60.00	72.00	°F
=	4.67	6.67	13.33	20.00	26.67	33.33	40.00	°C

		Value at Fluid Temperature, T [7]							Units
	Conversion	70	100	200	300	400	500	600	°F
Water Property	Factor [4]	21.11	37.78	93.33	148.89	204.44	260.00	315.56	°C
k	1.7307	0.5997	0.6300	0.6784	0.6836	0.6611	0.6040	0.5071	W/m-°C
(Thermal Conductivity)		0.3465	0.3640	0.3920	0.3950	0.3820	0.3490	0.2930	Btu/hr-ft-°F
c_p	4.1869	4.185	4.179	4.229	4.313	4.522	4.982	6.322	kJ/kg-°C
(Specific Heat)		1.000	0.998	1.010	1.030	1.080	1.190	1.510	Btu/lbm-°F
ρ	16.018	997.1	994.7	962.7	917.8	858.6	784.9	679.2	kg/m^3
(Density)		62.3	62.1	60.1	57.3	53.6	49.0	42.4	lbm/ft^3
β	1.8	1.89E-04	3.24E-04	6.66E-04	1.01E-03	1.40E-03	1.98E-03	3.15E-03	m^3/m^3-°C
(Volumetric Rate of Expansion)		1.05E-04	1.80E-04	3.70E-04	5.60E-04	7.80E-04	1.10E-03	1.75E-03	ft^3/ft^3-°F
g	0.3048	9.806	9.806	9.806	9.806	9.806	9.806	9.806	m/s^2
(Gravitational Constant)		32.17	32.17	32.17	32.17	32.17	32.17	32.17	ft/s^2
μ	1.4881	9.96E-04	6.82E-04	3.07E-04	1.93E-04	1.38E-04	1.04E-04	8.62E-05	kg/m-s
(Dynamic Viscosity)		6.69E-04	4.58E-04	2.06E-04	1.30E-04	9.30E-05	7.00E-05	5.79E-05	lbm/ft-s
Pr		6.980	4.510	1.910	1.220	0.950	0.859	1.070	---
(Prandtl Number)									
Calculated Parameter	**Formula**	**70**	**100**	**200**	**300**	**400**	**500**	**600**	**°F**
Reynold's Number, Re	$\rho VD/\mu$	1126238	1641130	3531215	5334924	6975877	8472567	8863480	---
Grashof Number, Gr	$g\beta\Delta TL^3/(\mu/\rho)^2$	103650263.4	538990790.5	10258947757	53160421562	1.68801E+11	4.3895E+11	9.17108E+11	---
Grashof Number, Gr_δ	$g\beta\Delta T(r_o-r_i)^3/(\mu/\rho)^3$	9.37E+02	4.87E+03	9.28E+04	4.81E+05	1.53E+06	3.97E+06	8.29E+06	---
Rayleigh Number, Ra	GrPr	723478838.9	2430848465	19594590215	64855714305	1.60361E+11	3.77058E+11	9.81306E+11	---
Rayleigh Number, Ra	$Gr_\delta Pr$	6.54E+03	2.20E+04	1.77E+05	5.86E+05	1.45E+06	3.41E+06	8.87E+06	---

From [4]:

Annulus Natural Convection Heat Transfer Coefficient:

Case:	Enclosed cylinder		C =	0.40	n =	0.20	(see page 29 of 5)		
H_{free}	$C(Gr_\delta Pr)^n k/(r_o-r_i)$	291.94	390.80	638.87	817.88	947.95	1,027.56	1,044.55	W/m^2-°C
		51.41	68.83	112.51	[illegible]	166.95	180.97	183.96	$Btu/hr-ft^2$-°F

Table 8: First Partial Heat Transfer Coefficients for Region 7

Pipe Inside Diameter, D =	7.981	inches =	0.665	ft	100% rated flow =	3,200	gpm
		=	0.203	m	@ T =	549	°F
Flow, % of rated =	100%				Density, ρ =	48.087	lbm/ft³
Fluid Velocity, V =	20.522	ft/sec =	3,200.0	gpm =	1.234236214	Mlb/hr	
Characteristic Length, L = D =	0.665	ft =	0.203	m			

$T_{fluid} - T_{surface}$, ΔT = assumed to be 12% of fluid temperature =	8.40	12.00	24.00	36.00	48.00	60.00	72.00	°F
=	4.67	6.67	13.33	20.00	26.67	33.33	40.00	°C

Note: The above assumption is based on experience with past RPV heat transfer analyses.

		Value at Fluid Temperature, T [7]							Units
Water Property	**Conversion Factor [4]**	**70**	**100**	**200**	**300**	**400**	**500**	**600**	**°F**
		21.11	**37.78**	**93.33**	**148.89**	**204.44**	**260.00**	**315.56**	**°C**
k (Thermal Conductivity)	1.7307	0.5997	0.6300	0.6784	0.6836	0.6611	0.6040	0.5071	W/m-°C
		0.3465	0.3640	0.3920	0.3950	0.3820	0.3490	0.2930	Btu/hr-ft-°F
c_p (Specific Heat)	4.1869	4.185	4.179	4.229	4.313	4.522	4.982	6.322	kJ/kg-°C
		1.000	0.998	1.010	1.030	1.080	1.190	1.510	Btu/lbm-°F
ρ (Density)	16.018	997.1	994.7	962.7	917.8	858.6	784.9	679.2	kg/m³
		62.3	62.1	60.1	57.3	53.6	49.0	42.4	lbm/ft³
β (Volumetric Rate of Expansion)	1.8	1.89E-04	3.24E-04	6.66E-04	1.01E-03	1.40E-03	1.98E-03	3.15E-03	m³/m³-°C
		1.05E-04	1.80E-04	3.70E-04	5.60E-04	7.80E-04	1.10E-03	1.75E-03	ft³/ft³-°F
g (Gravitational Constant)	0.3048	9.806	9.806	9.806	9.806	9.806	9.806	9.806	m/s²
		32.17	32.17	32.17	32.17	32.17	32.17	32.17	ft/s²
μ (Dynamic Viscosity)	1.4881	9.96E-04	6.82E-04	3.07E-04	1.93E-04	1.38E-04	1.04E-04	8.62E-05	kg/m-s
		6.69E-04	4.58E-04	2.06E-04	1.30E-04	9.30E-05	7.00E-05	5.79E-05	lbm/ft-s
Pr (Prandtl Number)		6.980	4.510	1.910	1.220	0.950	0.859	1.070	---
Calculated Parameter	**Formula**	**70**	**100**	**200**	**300**	**400**	**500**	**600**	**°F**
Reynold's Number, Re	ρVD/μ	1.2700E+06	1.8507E+06	3.9821E+06	6.0161E+06	7.8665E+06	9.5543E+06	9.9952E+06	---
Grashof Number, Gr	$g\beta\Delta TL^3/(\mu/\rho)^2$	7.2279E+07	3.7586E+08	7.1540E+09	3.7071E+10	1.1771E+11	3.0610E+11	6.3954E+11	---
Rayleigh Number, Ra	GrPr	5.0451E+08	1.6951E+09	1.3664E+10	4.5226E+10	1.1183E+11	2.6294E+11	6.8430E+11	---
From [4]:									
Inside Surface Forced Convection Heat Transfer Coefficient:									
H_{forced} =	$0.023Re^{0.8}Pr^{0.4}k/D$	11,307.23	13,480.10	19,004.02	22,266.42	24,145.63	24,753.78	23,524.01	W/m²-°C
		1,991.36	2,374.03	3,346.87		4,252.38	4,359.48	4,142.90	Btu/hr-ft²-°F
		3.841E-03	4.580E-03	6.456E-03	7.564E-03	8.203E-03	8.409E-03	7.992E-03	Btu/sec-in²-°F
From [4]:									
Inside Surface Natural Convection Heat Transfer Coefficient:									
Case:	Enclosed cylinder		C =	0.55	n =	0.25	(see page 289 of [4])		
H_{free} =	$C(GrPr)^nk/L$	243.85	346.81	629.32	855.34	1,037.27	1,173.50	1,251.33	W/m²-°C
		42.94	61.08	110.83		182.68	206.67	220.38	Btu/hr-ft²-°F
		8.284E-05	1.178E-04	2.138E-04	2.906E-04	3.524E-04	3.987E-04	4.251E-04	Btu/sec-in²-°F

Table 9: Second Partial Heat Transfer Coefficients for Region 7

Pipe Inside Diameter, D =	10.020	inches =	0.835	ft	
		=	0.255	m	
Outer Pipe, Inside radius, r_o =	5.01	inches =	0.418	ft	
			0.127	m	
Inner Pipe Outside Diameter, D =	8.625	inches =	0.719	ft	
		=	0.219	m	
Inner Pipe, Outside radius, r_i =	4.3125	inches =	0.359	ft	
			0.110	m	
Fluid Velocity, V =	13.020	ft/sec =	3200.000	gpm	
Characteristic Length, L = D =	0.835	ft =	0.255	m	

(Outside) $T_{fluid} - T_{surface}$, ΔT =	8.40	12.00	24.00	36.00	48.00	60.00	72.00	°F
=	4.67	6.67	13.33	20.00	26.67	33.33	40.00	°C

		Value at Fluid Temperature, T [7]							Units
Water Property	**Conversion Factor [4]**	**70**	**100**	**200**	**300**	**400**	**500**	**600**	**°F**
		21.11	**37.78**	**93.33**	**148.89**	**204.44**	**260.00**	**315.56**	**°C**
k	1.7307	0.5997	0.6300	0.6784	0.6836	0.6611	0.6040	0.5071	W/m-°C
(Thermal Conductivity)		0.3465	0.3640	0.3920	0.3950	0.3820	0.3490	0.2930	Btu/hr-ft-°F
c_p	4.1869	4.185	4.179	4.229	4.313	4.522	4.982	6.322	kJ/kg-°C
(Specific Heat)		1.000	0.998	1.010	1.030	1.080	1.190	1.510	Btu/lbm-°F
ρ	16.018	997.1	994.7	962.7	917.8	858.6	784.9	679.2	kg/m^3
(Density)		62.3	62.1	60.1	57.3	53.6	49.0	42.4	lbm/ft^3
β	1.8	1.89E-04	3.24E-04	6.66E-04	1.01E-03	1.40E-03	1.98E-03	3.15E-03	m^3/m^3-°C
(Volumetric Rate of Expansion)		1.05E-04	1.80E-04	3.70E-04	5.60E-04	7.80E-04	1.10E-03	1.75E-03	ft^3/ft^3-°F
g	0.3048	9.806	9.806	9.806	9.806	9.806	9.806	9.806	m/s^2
(Gravitational Constant)		32.17	32.17	32.17	32.17	32.17	32.17	32.17	ft/s^2
μ	1.4881	9.96E-04	6.82E-04	3.07E-04	1.93E-04	1.38E-04	1.04E-04	8.62E-05	kg/m-s
(Dynamic Viscosity)		6.69E-04	4.58E-04	2.06E-04	1.30E-04	9.30E-05	7.00E-05	5.79E-05	lbm/ft-s
Pr		6.980	4.510	1.910	1.220	0.950	0.859	1.070	---
(Prandtl Number)									
Calculated Parameter	**Formula**	**70**	**100**	**200**	**300**	**400**	**500**	**600**	**°F**
Reynold's Number, Re	ρVD/μ	1011591	1474069	3171750	4791848	6265758	7610090	7961209	---
Grashof Number, Gr	$g\beta\Delta TL^3/(\mu/\rho)^2$	143036227.2	743801381.9	14157235436	73360798959	2.32943E+11	6.05747E+11	1.2656E+12	---
Grashof Number, Gr_δ	$g\beta\Delta T(r_o-r_i)^3/(\mu/\rho)^3$	4.82E+04	2.51E+05	4.78E+06	2.47E+07	7.86E+07	2.04E+08	4.27E+08	---
Rayleigh Number, Ra	GrPr	998392866.2	3354544233	27040319682	89500174730	2.21296E+11	5.20336E+11	1.35419E+12	---
Rayleigh Number, Ra	$Gr_\delta Pr$	3.37E+05	1.13E+06	9.12E+06	3.02E+07	7.46E+07	1.76E+08	4.57E+08	---

From [4]:

Annulus Natural Convection Heat Transfer Coefficient:

Case:	Enclosed cylinder		C =	0.40	n =	0.20	(see page 291 of 51)		
H_{free}	$C(Gr_\delta Pr)^n k/(r_o-r_i)$	172.61	231.07	377.74	483.58	560.49	607.56	617.61	W/m^2-°C
		30.40	40.69	66.53		98.71	107.00	108.77	$Btu/hr\text{-}ft^2$-°F

Table 10: Third Partial Heat Transfer Coefficients for Region 7

Pipe Inside Diameter, D =	11.750	inches =	0.979	ft	
		=	0.298	m	
Outer Pipe, Inside radius, r_o =	5.875	inches =	0.490	ft	
			0.149	m	
Inner Pipe Outside Diameter, D =	10.750	inches =	0.896	ft	
		=	0.273	m	
Inner Pipe, Outside radius, r_i =	5.375	inches =	0.448	ft	
			0.137	m	
Fluid Velocity, V =	9.468	ft/sec =	3200.000	gpm	
Characteristic Length, L = D =	0.979	ft =	0.298	m	

(Outside) T_{fluid} - $T_{surface}$, ΔT =	8.40	12.00	24.00	36.00	48.00	60.00	72.00	°F
=	4.67	6.67	13.33	20.00	26.67	33.33	40.00	°C

		Value at Fluid Temperature, T [7]							Units
Water Property	**Conversion Factor [4]**	**70**	**100**	**200**	**300**	**400**	**500**	**600**	°F
		21.11	**37.78**	**93.33**	**148.89**	**204.44**	**260.00**	**315.56**	°C
k	1.7307	0.5997	0.6300	0.6784	0.6836	0.6611	0.6040	0.5071	W/m-°C
(Thermal Conductivity)		0.3465	0.3640	0.3920	0.3950	0.3820	0.3490	0.2930	Btu/hr-ft-°F
c_p	4.1869	4.185	4.179	4.229	4.313	4.522	4.982	6.322	kJ/kg-°C
(Specific Heat)		1.000	0.998	1.010	1.030	1.080	1.190	1.510	Btu/lbm-°F
ρ	16.018	997.1	994.7	962.7	917.8	858.6	784.9	679.2	kg/m^3
(Density)		62.3	62.1	60.1	57.3	53.6	49.0	42.4	lbm/ft^3
β	1.8	1.89E-04	3.24E-04	6.66E-04	1.01E-03	1.40E-03	1.98E-03	3.15E-03	m^3/m^3-°C
(Volumetric Rate of Expansion)		1.05E-04	1.80E-04	3.70E-04	5.60E-04	7.80E-04	1.10E-03	1.75E-03	ft^3/ft^3-°F
g	0.3048	9.806	9.806	9.806	9.806	9.806	9.806	9.806	m/s^2
(Gravitational Constant)		32.17	32.17	32.17	32.17	32.17	32.17	32.17	ft/s^2
μ	1.4881	9.96E-04	6.82E-04	3.07E-04	1.93E-04	1.38E-04	1.04E-04	8.62E-05	kg/m-s
(Dynamic Viscosity)		6.69E-04	4.58E-04	2.06E-04	1.30E-04	9.30E-05	7.00E-05	5.79E-05	lbm/ft-s
Pr		6.980	4.510	1.910	1.220	0.950	0.859	1.070	---
(Prandtl Number)									
Calculated Parameter	**Formula**	**70**	**100**	**200**	**300**	**400**	**500**	**600**	°F
Reynold's Number, Re	$\rho VD/\mu$	862650	1257036	2704761	4086325	5343225	6489626	6789048	---
Grashof Number, Gr	$g\beta\Delta TL^3/(\mu/\rho)^2$	230651605.4	1199409312	22829105215	1.18297E+11	3.75631E+11	9.76791E+11	2.04083E+12	---
Grashof Number, Gr_δ	$g\beta\Delta T(r_o-r_i)^3/(\mu/\rho)^3$	1.78E+04	9.24E+04	1.76E+06	9.12E+06	2.89E+07	7.53E+07	1.57E+08	---
Rayleigh Number, Ra	GrPr	1609948206	5409335995	43603590961	1.44323E+11	3.56849E+11	8.39063E+11	2.18369E+12	---
Rayleigh Number, Ra	$Gr_\delta Pr$	1.24E+05	4.17E+05	3.36E+06	1.11E+07	2.75E+07	6.47E+07	1.68E+08	---

From [4]:

Annulus Natural Convection Heat Transfer Coefficient:

Case:	Enclosed cylinder		C =	0.40	n =	0.20	(see page 291 of [5])		
H_{free}	$C(Gr_\delta Pr)^n k/(r_o-r_i)$	197.20	263.98	431.55	552.46	640.32	694.10	705.57	W/m^2-°C
		34.73	46.49	76.00	[illegible]	112.77	122.24	124.26	Btu/hr-ft^2-°F

Table 11: First Partial Heat Transfer Coefficients for Region 9

Pipe Inside Diameter, D =	[redacted]	inches =	0.665	ft	100% rated flow =	3,200	gpm
		=	0.203	m	@ T =	549	°F
Flow, % of rated =	[redacted]				Density, ρ =	48.087	lbm/ft³
Fluid Velocity, V =	20.522	ft/sec =	3,200.0	gpm =	1.234236214	Mlb/hr	
Characteristic Length, L = D =	0.665	ft =	0.203	m			

$T_{fluid} - T_{surface}$, ΔT = assumed to be 12% of fluid temperature =	8.40	12.00	24.00	36.00	48.00	60.00	72.00	°F
=	4.67	6.67	13.33	20.00	26.67	33.33	40.00	°C

Note: The above assumption is based on experience with past RPV heat transfer analyses.

		Value at Fluid Temperature, T [7]							Units
Water Property	**Conversion Factor [4]**	**70**	**100**	**200**	**300**	**400**	**500**	**600**	**°F**
		21.11	**37.78**	**93.33**	**148.89**	**204.44**	**260.00**	**315.56**	**°C**
k	1.7307	0.5997	0.6300	0.6784	0.6836	0.6611	0.6040	0.5071	W/m-°C
(Thermal Conductivity)		0.3465	0.3640	0.3920	0.3950	0.3820	0.3490	0.2930	Btu/hr-ft-°F
c_p	4.1869	4.185	4.179	4.229	4.313	4.522	4.982	6.322	kJ/kg-°C
(Specific Heat)		1.000	0.998	1.010	1.030	1.080	1.190	1.510	Btu/lbm-°F
ρ	16.018	997.1	994.7	962.7	917.8	858.6	784.9	679.2	kg/m³
(Density)		62.3	62.1	60.1	57.3	53.6	49.0	42.4	lbm/ft³
β	1.8	1.89E-04	3.24E-04	6.66E-04	1.01E-03	1.40E-03	1.98E-03	3.15E-03	m³/m³-°C
(Volumetric Rate of Expansion)		1.05E-04	1.80E-04	3.70E-04	5.60E-04	7.80E-04	1.10E-03	1.75E-03	ft³/ft³-°F
g	0.3048	9.806	9.806	9.806	9.806	9.806	9.806	9.806	m/s²
(Gravitational Constant)		32.17	32.17	32.17	32.17	32.17	32.17	32.17	ft/s²
μ	1.4881	9.96E-04	6.82E-04	3.07E-04	1.93E-04	1.38E-04	1.04E-04	8.62E-05	kg/m-s
(Dynamic Viscosity)		6.69E-04	4.58E-04	2.06E-04	1.30E-04	9.30E-05	7.00E-05	5.79E-05	lbm/ft-s
Pr		6.980	4.510	1.910	1.220	0.950	0.859	1.070	---
(Prandtl Number)									
Calculated Parameter	**Formula**	**70**	**100**	**200**	**300**	**400**	**500**	**600**	**°F**
Reynold's Number, Re	ρVD/μ	1.2700E+06	1.8507E+06	3.9821E+06	6.0161E+06	7.8665E+06	9.5543E+06	9.9952E+06	---
Grashof Number, Gr	$g\beta\Delta TL^3/(\mu/\rho)^2$	7.2279E+07	3.7586E+08	7.1540E+09	3.7071E+10	1.1771E+11	3.0610E+11	6.3954E+11	---
Rayleigh Number, Ra	GrPr	5.0451E+08	1.6951E+09	1.3664E+10	4.5226E+10	1.1183E+11	2.6294E+11	6.8430E+11	---
From [4]:									
Inside Surface Forced Convection Heat Transfer Coefficient:									
H_{forced} =	$0.023Re^{0.8}Pr^{0.4}k/D$	11,307.23	13,480.10	19,004.02	22,266.42	24,145.63	24,753.78	23,524.01	W/m²-°C
		1,991.36	**2,374.03**	**3,346.87**	[redacted]	**4,252.38**	**4,359.48**	**4,142.90**	Btu/hr-ft²-°F
		3.841E-03	**4.580E-03**	**6.456E-03**	**7.564E-03**	**8.203E-03**	**8.409E-03**	**7.992E-03**	Btu/sec-in²-°F
From [4]:									
Inside Surface Natural Convection Heat Transfer Coefficient:									
Case:	Enclosed cylinder		C =	[redacted]	n =	[redacted]			
H_{free} =	$C(GrPr)^n k/L$	243.85	346.81	629.32	855.34	1,037.27	1,173.50	1,251.33	W/m²-°C
		42.94	**61.08**	**110.83**	[redacted]	**182.68**	**206.67**	**220.38**	Btu/hr-ft²-°F
		8.284E-05	**1.178E-04**	**2.138E-04**	**2.906E-04**	**3.524E-04**	**3.987E-04**	**4.251E-04**	Btu/sec-in²-°F

Table 12: Second Partial Heat Transfer Coefficients for Region 9

Pipe Inside Diameter, D =	[redacted]	inches =	0.979	ft	
		=	0.298	m	
Outer Pipe, Inside radius, r_o =	5.875	inches =	0.490	ft	
			0.149	m	
Inner Pipe Outside Diameter, D =	[redacted]	inches =	0.719	ft	
		=	0.219	m	
Inner Pipe, Outside radius, r_i =	4.3125	inches =	0.359	ft	
			0.110	m	
Fluid Velocity, V =	9.468	ft/sec =	[redacted]	gpm	
Characteristic Length, L = D =	0.979	ft =	0.298	m	

(Outside) T_{fluid} - $T_{surface}$, ΔT =	8.40	12.00	24.00	36.00	48.00	60.00	72.00	°F
=	4.67	6.67	13.33	20.00	26.67	33.33	40.00	°C

		Value at Fluid Temperature, T [7]							Units
Water Property	**Conversion Factor [4]**	**70**	**100**	**200**	**300**	**400**	**500**	**600**	°F
		21.11	**37.78**	**93.33**	**148.89**	**204.44**	**260.00**	**315.56**	°C
k	1.7307	0.5997	0.6300	0.6784	0.6836	0.6611	0.6040	0.5071	W/m-°C
(Thermal Conductivity)		0.3465	0.3640	0.3920	0.3950	0.3820	0.3490	0.2930	Btu/hr-ft-°F
c_p	4.1869	4.185	4.179	4.229	4.313	4.522	4.982	6.322	kJ/kg-°C
(Specific Heat)		1.000	0.998	1.010	1.030	1.080	1.190	1.510	Btu/lbm-°F
ρ	16.018	997.1	994.7	962.7	917.8	858.6	784.9	679.2	kg/m^3
(Density)		62.3	62.1	60.1	57.3	53.6	49.0	42.4	lbm/ft^3
β	1.8	1.89E-04	3.24E-04	6.66E-04	1.01E-03	1.40E-03	1.98E-03	3.15E-03	m^3/m^3-°C
(Volumetric Rate of Expansion)		1.05E-04	1.80E-04	3.70E-04	5.60E-04	7.80E-04	1.10E-03	1.75E-03	ft^3/ft^3-°F
g	0.3048	9.806	9.806	9.806	9.806	9.806	9.806	9.806	m/s^2
(Gravitational Constant)		32.17	32.17	32.17	32.17	32.17	32.17	32.17	ft/s^2
μ	1.4881	9.96E-04	6.82E-04	3.07E-04	1.93E-04	1.38E-04	1.04E-04	8.62E-05	kg/m-s
(Dynamic Viscosity)		6.69E-04	4.58E-04	2.06E-04	1.30E-04	9.30E-05	7.00E-05	5.79E-05	lbm/ft-s
Pr		6.980	4.510	1.910	1.220	0.950	0.859	1.070	---
(Prandtl Number)									
Calculated Parameter	**Formula**	**70**	**100**	**200**	**300**	**400**	**500**	**600**	°F
Reynold's Number, Re	$\rho VD/\mu$	862650	1257036	2704761	4086325	5343225	6489626	6789048	---
Grashof Number, Gr	$g\beta\Delta TL^3/(\mu/\rho)^2$	230651605.4	1199409312	22829105215	1.18297E+11	3.75631E+11	9.76791E+11	2.04083E+12	---
Grashof Number, Gr_δ	$g\beta\Delta T(r_o-r_i)^3/(\mu/\rho)^3$	5.42E+05	2.82E+06	5.37E+07	2.78E+08	8.83E+08	2.30E+09	4.80E+09	---
Rayleigh Number, Ra	GrPr	1609948206	5409335995	43603590961	1.44323E+11	3.56849E+11	8.39063E+11	2.18369E+12	---
Rayleigh Number, Ra	$Gr_\delta Pr$	3.79E+06	1.27E+07	1.03E+08	3.39E+08	8.39E+08	1.97E+09	5.13E+09	---

From [4]:

Annulus Natural Convection Heat Transfer Coefficient:

Case:	Enclosed cylinder		C =	[redacted]	n =	[redacted]			
H_{free}	$C(Gr_\delta Pr)^n k/(r_o-r_i)$	125.02	167.35	273.58	350.24	405.94	440.03	447.30	W/m^2-°C
[redacted]		22.02	29.47	48.18	[redacted]	71.49	77.50	78.78	$Btu/hr-ft^2$-°F

Although the thermal sleeve was excluded from the analysis, its effect had to be included in the finite element model. For several thermal regions, the resultant HTCs had to be calculated from the partial heat transfer coefficients (HTC_i in Table 13). These are generated by "Heat Transfer Coefficients.xls".

$$\frac{1}{HTC_{Res}} = \left(\frac{1}{HTC_I} + \frac{T_I}{TC_I}\right) + \left(\frac{1}{HTC_{II}} + \frac{T_{II}}{TC_{II}}\right) + \left(\frac{1}{HTC_{III}} + \frac{T_{III}}{TC_{III}}\right)$$

Where:

HTC_{Res}	=	Resultant HTC
HTC_i	=	HTC of ith material
T_i	=	Thickness of ith material
TC_i	=	Thermal Conductivity of ith material

The reference for this equation is [4].

Table 13: Resultant Heat Transfer Coefficients for the Regions

100% Flow

Regions	HTC I	Material		HTCII	Material		HTCIII	HTC resultant
		Thermal Conductivity, Btu/hr-ft-°F	Thickness [ft]		Thermal Conductivity, Btu/hr-ft-°F	Thickness [ft]		
	2,692.98							2693
R2								
	3,921.42	9.8	0.0268	90.18				71
R4								
	3,921.42	9.8	0.0268	144.04				101
R6								
R6b							97.30	97
	3,921.42	9.8	0.0268	85.17				68
	3,921.42	9.8	0.0268	85.17	9.8	0.0304	97.30	36
R8								
	3,921.42	9.8	0.0268	61.68				52
R10								
	500							500
R12	0.2							0.2

0% Flow

Regions	HTC I	Material		HTCII	Material		HTCIII	HTC resultant
		Thermal Conductivity, Btu/hr-ft-°F	Thickness [ft]		Thermal Conductivity, Btu/hr-ft-°F	Thickness [ft]		
	142.98							143
R2								
	150.64	9.8	0.0268	90.18				49
R4								
	150.64	9.8	0.0268	144.04				61
R6								
R6b							97.30	97
	150.64	9.8	0.0268	85.17				47
	150.64	9.8	0.0268	85.17	9.8	0.0304	97.30	29
R8								
	150.64	9.8	0.0268	61.68				39
R10								
	500							500
R12	0.2							0.2

Note: 1. Using the same value that is calculated from Table 10.

4.0 THERMAL AND PRESSURE LOAD RESULTS

The two flow dependent thermal load cases outlined in previous section were run on the core spray FEM. For ANSYS, the thermal transient input files "VY_16Q_T100.inp," "VY_16Q_T0.inp," for 100% and 0% flow, respectively. The stress input filenames are "VY_16Q_ST100.inp"and "VY_16Q_ST0.inp," respectively.

The limiting safe end location was chosen based on the highest thermal stress intensity at 100% flow. Node 3719 on the inside surface of the core spray nozzle was selected for the safe end analysis and shown in Figure 6.

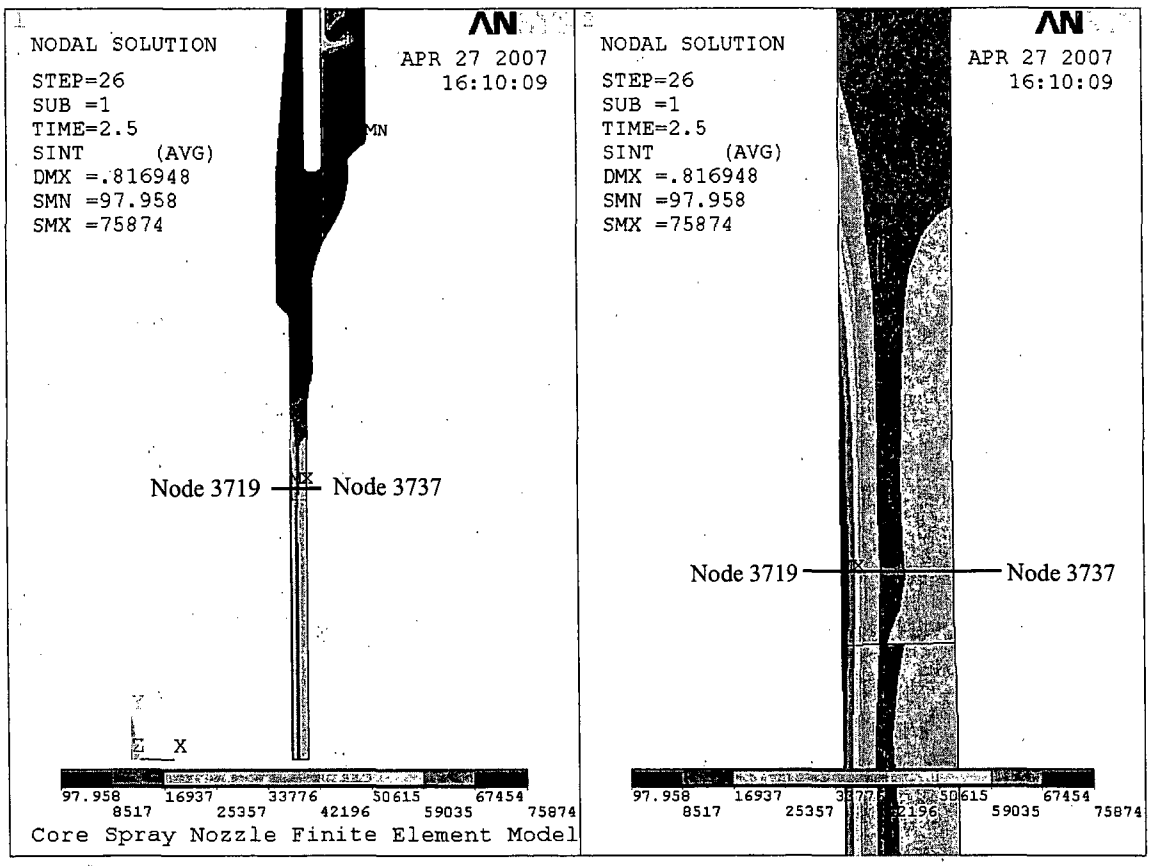

Figure 6: Safe End Critical Thermal Stress Location, Node 3719

The limiting blend radius location was chosen based upon the highest pressure stress intensity. Node 2166 on the inside surface of the blend radius was therefore selected for the nozzle forging analysis and shown in Figure 7. The highest thermal stress and pressure stress occur very close to the same location in the nozzle forging region. Therefore, this location is a reasonable choice for the limiting location.

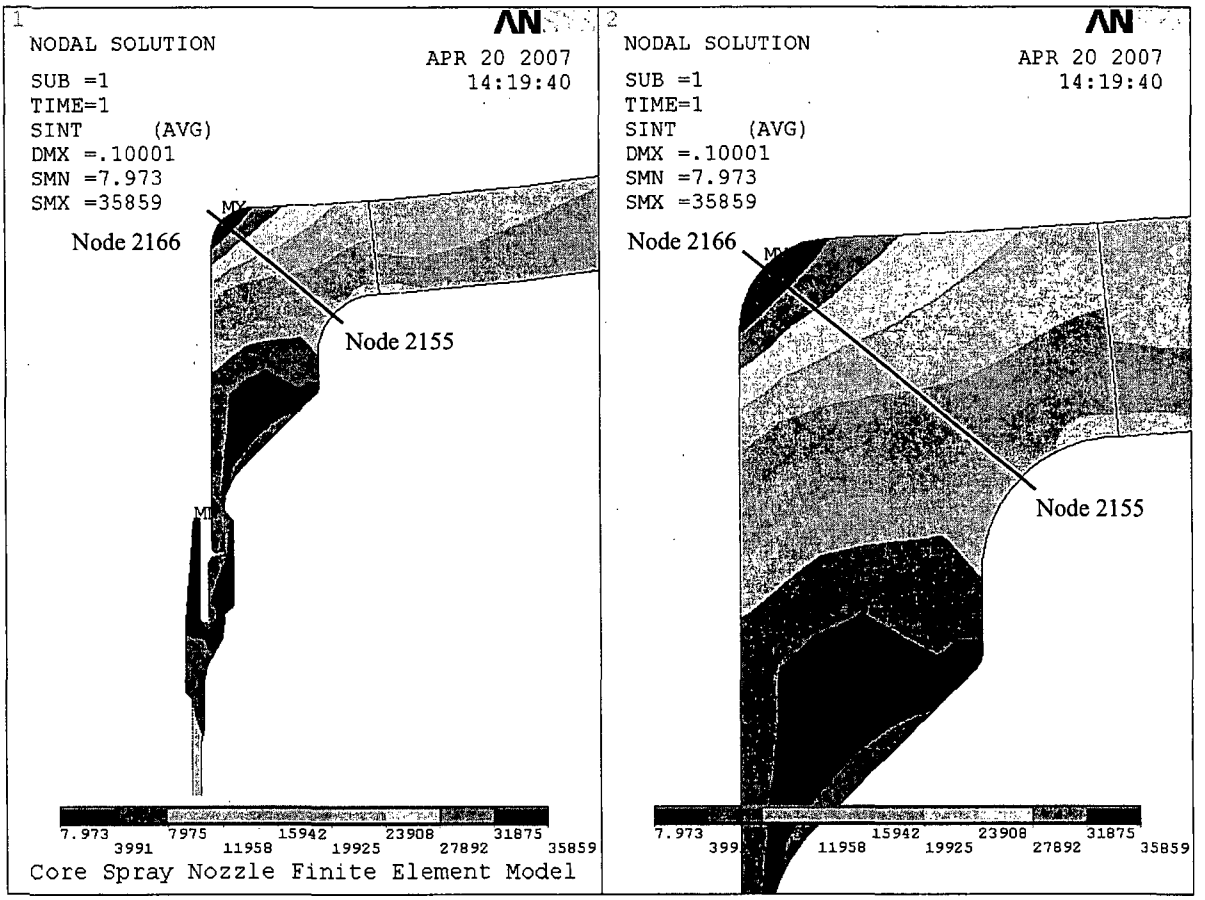

Figure 7: Blend Radius Limiting Pressure Stress Location, Node 2166

The stress intensity for use in the Green's functions are calculated from the component stresses (X, Y, and Z) and compared to the stress intensity reported by ANSYS. As seen in Figure 8, the Z-X calculated total stress intensity best matches the ANSYS reported stress intensity for 100% flow at the safe end. Therefore, the Z-X stress will be used for the total and membrane plus bending Green's functions for all flow rates for the safe end. As seen in Figure 9, the Z-X calculated total stress intensity best matches the ANSYS reported stress intensity for 100% flow at the blend radius in very beginning. Therefore, the Z-X stress will be used for the total and membrane plus bending Green's functions for all flow rates for the blend radius.

The stress intensity time history for the critical safe end and blend radius paths were extracted using the ANSYS post-processing file "extract100.inp" for 100% flow. This produced the two files, "SE_F100.out" and "BR_F100.out," which contain the thermal stress history. The membrane plus bending stresses and total stresses for the Green's Functions were extracted from these files to produce the four files "SE_F100.cln, BR_F100.cln" and "SE_F100_INSIDE.RED, BR_F100_ INSIDE.RED."

The stress intensity time history for the critical safe end and blend radius paths were extracted using the ANSYS post-processing file "extract0.inp" for 0% flow. This produced the two files, "SE_F0.out" and "BR_F0.out," which contain the thermal stress history. The membrane plus bending stresses and total stresses for the Green's Functions were extracted from these files to produce the four files "SE_F0.cln, BR_F0.cln" and "SE_F0_INSIDE.RED, BR_F0_ INSIDE.RED."

The governing stress histories for the core spray nozzle during 100% flow and 0% flow are shown in Figures 10 through 17. The stress history data is included in EXCEL spreadsheets *100-Green-SE.xls*, *100-Green-Blend.xls*, *0-Green-SE.xls* and *0-Green-Blend.xls*.

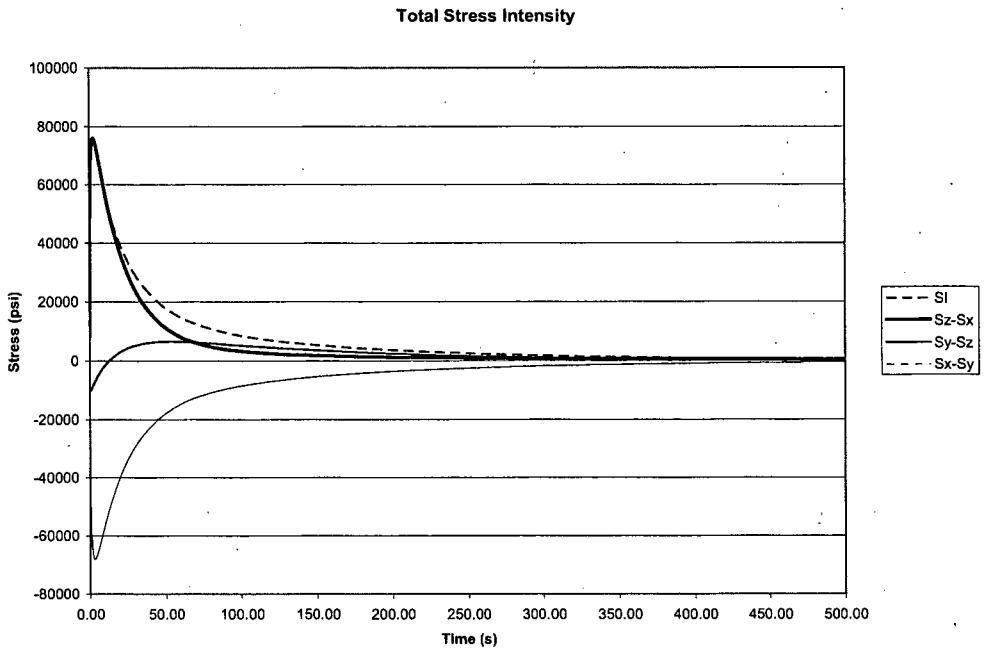

Figure 8: Safe End 100% Flow Total Stress Intensity

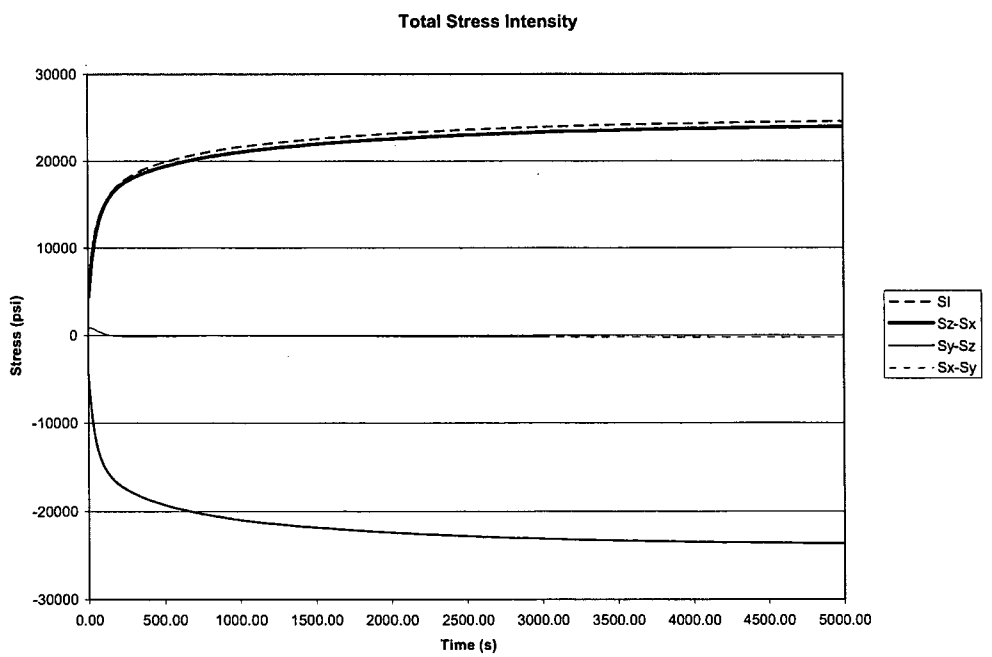

Figure 9: Blend Radius 100% Flow Total Stress Intensity

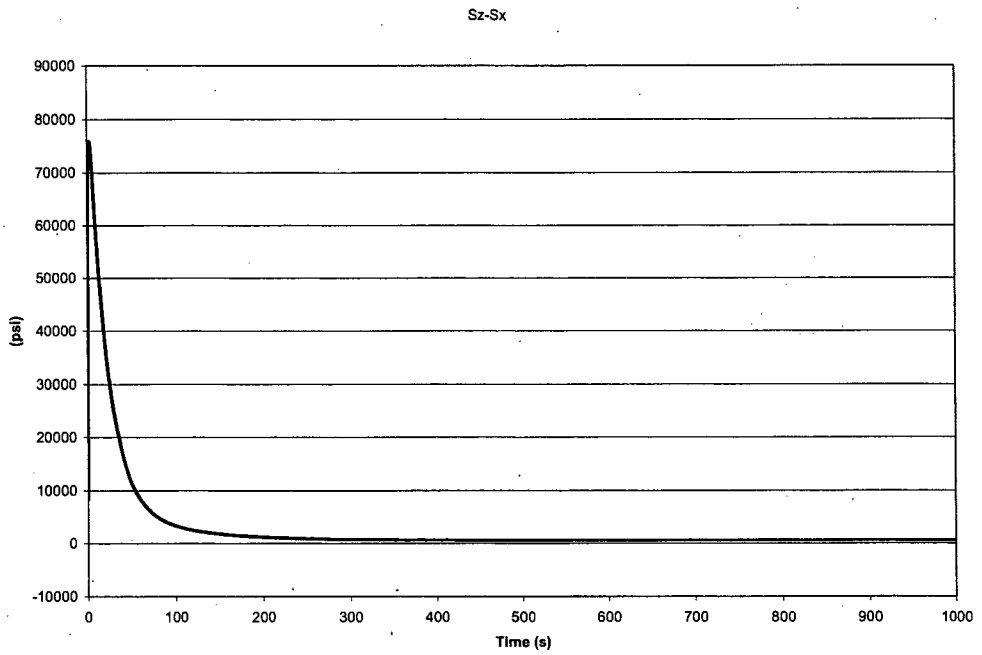

Figure 10: Safe End Total Stress History, 100% Flow, (Sz-Sx)

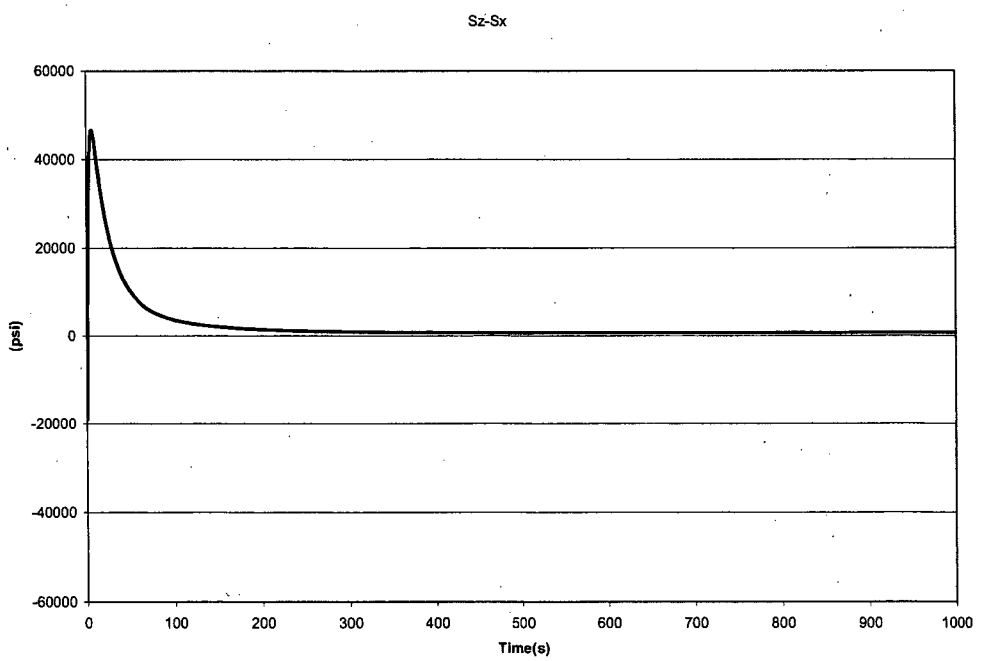

Figure 11: Safe End Membrane + Bending Stress History, 100% Flow, (Sz-Sx)

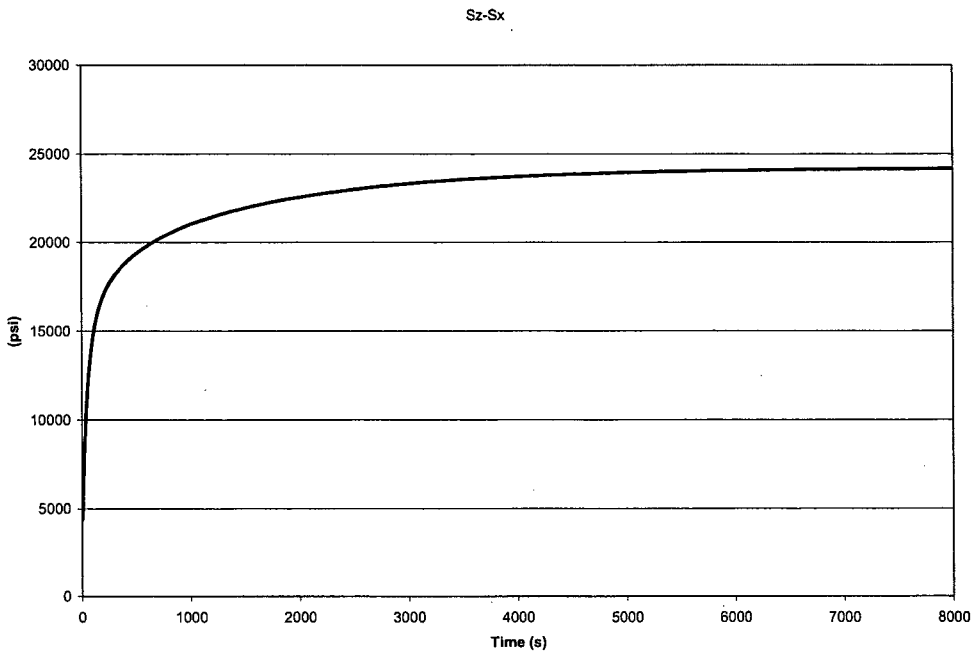

Figure 12: Blend Radius Total Stress History, 100% Flow, (Sz-Sx)

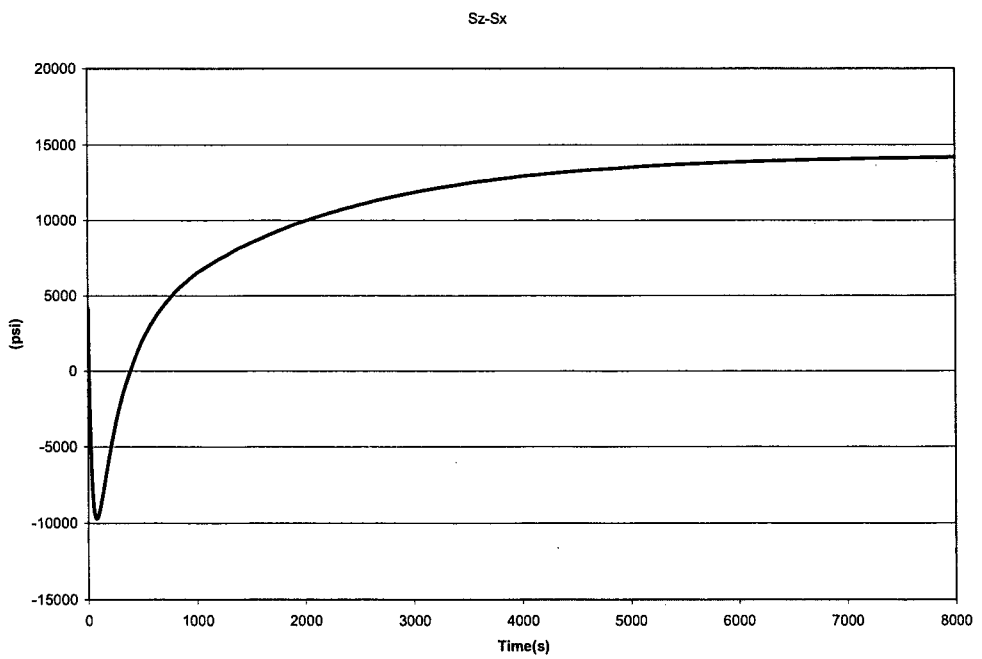

Figure 13: Blend Radius Membrane + Bending Stress History, 100% Flow, (Sz-Sx)

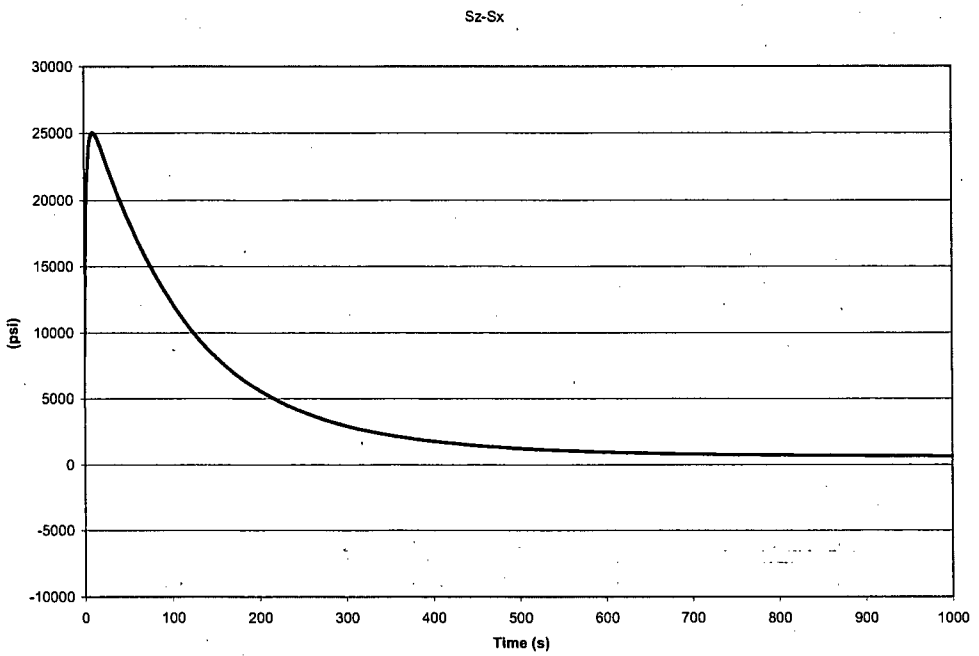

Figure 14: Safe End Total Stress History, 0% Flow, (Sz-Sx)

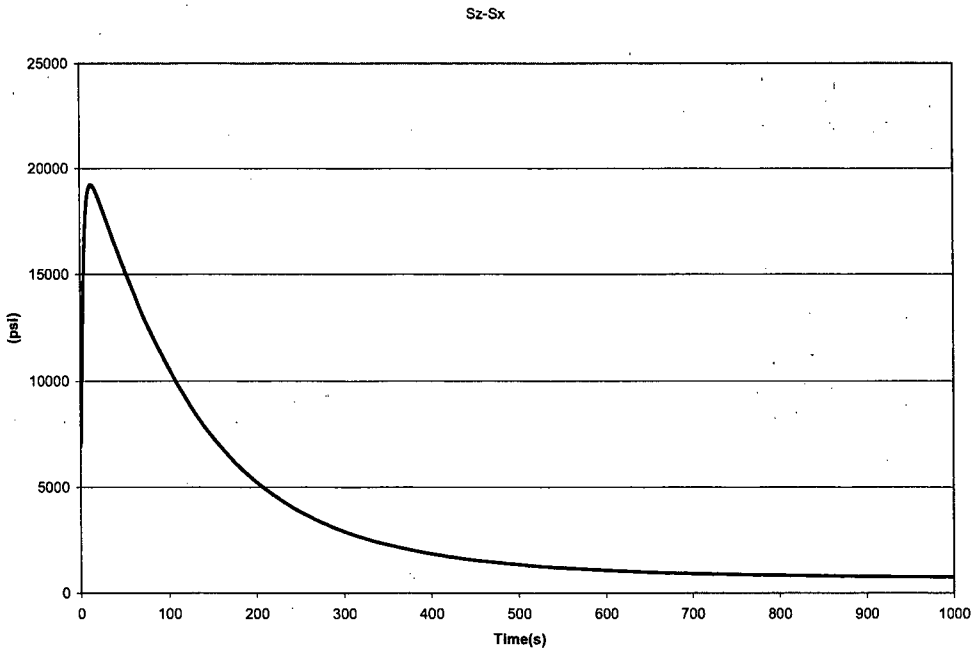

Figure 15: Safe End Membrane + Bending Stress History, 0% Flow, (Sz-Sx)

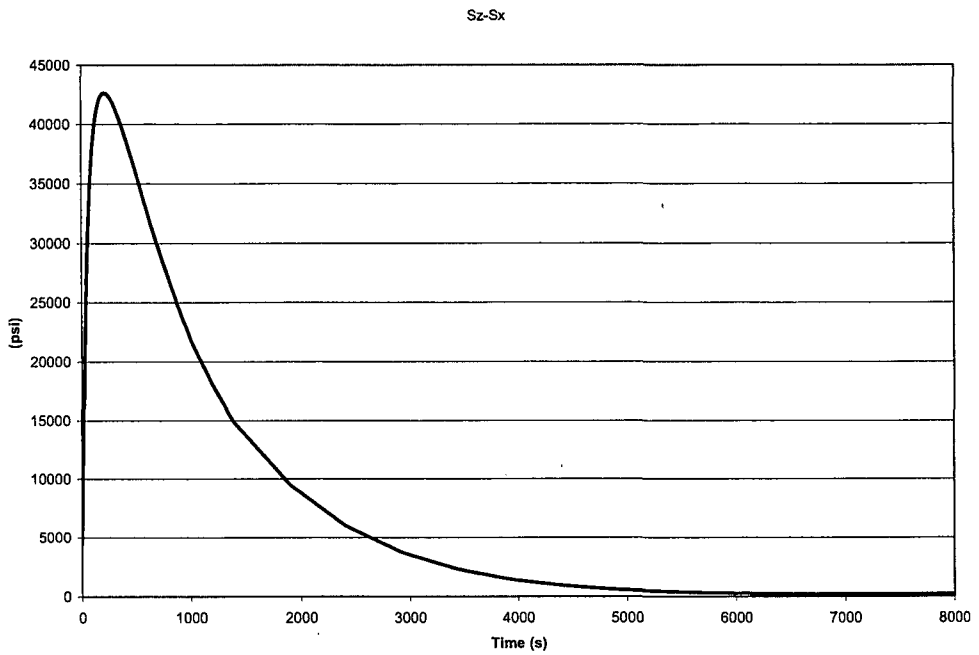

Figure 16: Blend Radius Total Stress History, 0% Flow, (Sz-Sx)

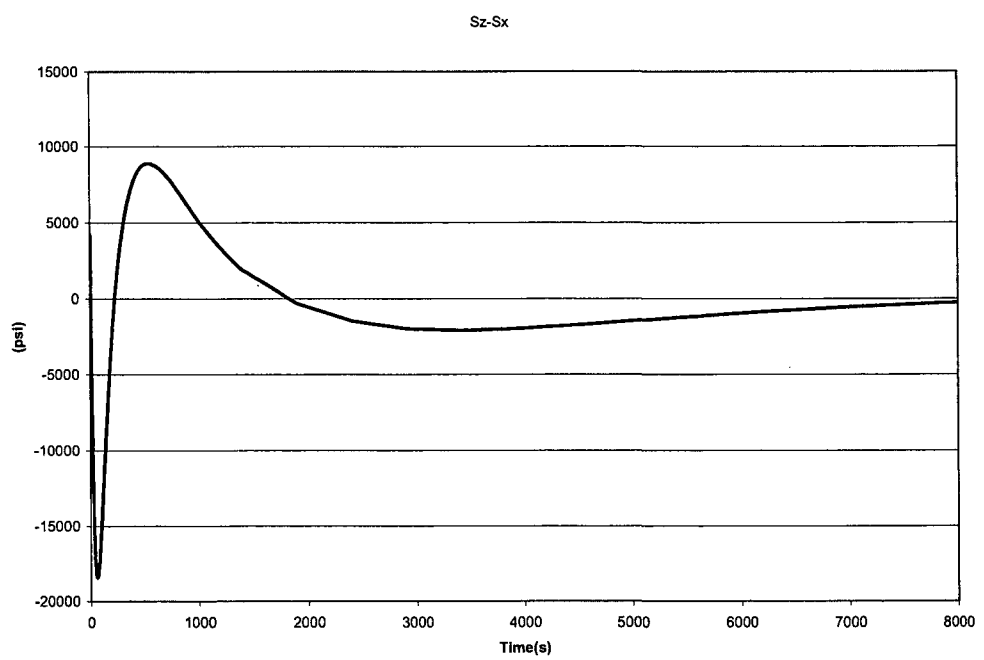

Figure 17: Blend Radius Membrane + Bending Stress History, 0% Flow, (Sz-Sx)

The pressure stress intensities for the safe end and blend radius paths were extracted using the ANSYS post-processing file "extractP.inp." This produced two files, SE_P.OUT for the safe end and BR_P.OUT for the blend radius.

Results of the internal pressure load case for Node 2166 (blend radius) is a total stress intensity of 35,860 psi and for Node 3719 (safe end), a total stress intensity of 12,030 psi. The membrane plus bending stress intensity at Node 2166 and Node 3719 are 34970 psi and 12,020 psi, respectively. Table 14 shows the final pressure results for the safe end and blend radius.

Table 14: Pressure Results (1,000 psi)

Location	Membrane plus Bending Stress Intensity (psi)	Total Stress Intensity (psi)
Safe End	12,020	12,030
Blend Radius	34,970	35,860

Results were also extracted from the vessel portion of the model to verify the accuracy of the results obtained from the ANSYS model, and to check the results due to the use of the 2.0 multiplier on the vessel radius. These results are contained in the file VESSEL_P.OUT. The radius of the finite element model (FEM) was multiplied by a factor of 2.0 [1] to account for the fact that the vessel portion of the 2D axisymmetric model is a sphere, but the true geometry is the intersection of two cylinders.

The equation for the membrane hoop stress in a sphere is:

$$\sigma = \left(\frac{(pressure) \times (radius)}{2 \times thickness} \right)$$

Considering a vessel base metal radius, R, of 105.906 inches increased by a factor of 2.0, a vessel base metal thickness, t, of 5.4375 inches, and an applied pressure, P, of 1,000 psi, the calculated stress for a sphere is PR/(2t) = 19,477 psi. This compares very well with the remote vessel wall membrane hoop stress from the ANSYS result file, VESSEL_P.OUT, of 18,530 psi. Thus, considering the peak total pressure stress of 35,860 psi reported above, the stress concentrating effect of the nozzle corner is 35,860/19,477 = 1.84. In other words, the peak nozzle corner stress is 1.84 times higher than nominal vessel wall stress for the 2D axisymmetric model.

The equation for the membrane hoop stress in a cylinder is:

$$\sigma = \left(\frac{(pressure) \times (radius)}{thickness} \right).$$

Based on the previous dimensions, the calculated stress for a cylinder without the 2.0 factor is 19,477 psi. Increasing this by a factor of 1.84 yields an expected peak nozzle corner stress of 35,838 psi, which would be expected from a cylindrical geometry that is representative of the nozzle configuration. Therefore, the result from the ANSYS file for the peak nozzle corner stress (35,860 psi) is close to the peak nozzle corner stress for a cylindrical geometry because of the use of the 2.0 multiplier. This is consistent with SI's experience where a factor of two increase in radius is typical for representing the three-dimensional (3D) effect in a 2D axisymmetric model.

5.0 REFERENCES

1. SI Calculation No. VY-16Q-308, Revision 0, "Core Spray Nozzle Finite Element Model".

2. ANSYS, Release 8.1A1 (w/Service Pack 1), ANSYS, Inc., June 2004.

3. American Society of Mechanical Engineers, Boiler and Pressure Vessel Code, Section II, Part D, 1998 Edition, 2000 Addenda.

4. J. P. Holman, "Heat Transfer," 4th Edition, McGraw-Hill, 1976.

5. J. P. Holman, "Heat Transfer," 5th Edition, 1981.

6. Entergy Design Input Record (DIR) EC No. 1773, Revision 0, "Environmental Fatigue Analysis for Vermont Yankee Nuclear Power Station," 7/26/07, SI File No. VY-16Q-209.

7. N. P. Cheremisinoff, "Heat Transfer Pocket Handbook," Gulf Publishing Co., 1984.

8. CB&I RPV Stress Report, Section T7, -"Thermal Analysis of Core Spray Nozzle, Vermont Yankee Reactor Vessel, CB&I Contract 9-6201, -SI File No. VY-16Q-206.

9. Entergy Nuclear Vermont Yankee Drawing No.,- 5920-624 Rev. 8, "Reactor 8 In. Dia. Nozzles Mk. N5A & B," SI File No. -VY-16Q-207.

APPENDIX A

FINITE ELEMENT ANALYSIS FILES

ANSYS Input Files

File Name	Description
vy_csn_geom.inp	ANSYS input file includes the geometry and material properties
Heat Transfer Coefficients.xls	Excel file to calculate Heat Transfer coefficients
VY_16Q_P.inp	ANSYS input file for the pressure stress analysis
VY_16Q_T100.inp	ANSYS input file for the thermal analysis, 100% flow rate
VY_16Q_T0.inp	ANSYS input file for the thermal analysis, 0% flow rate
VY_16Q_ST100.inp	ANSYS input file for the thermal stress analysis, 100% flow rate
VY_16Q_ST0.inp	ANSYS input file for the thermal stress analysis, 0% flow rate
extract100.inp	ANSYS input file to extract the limiting paths, 100% flow rate
extract0.inp	ANSYS input file to extract the limiting paths, 0% flow rate
extractP.inp	ANSYS input file to extract the limiting paths

ANSYS Output Files

File Name	Description
BR_F100.out	ANSYS output file, Results of running: extract100.inp, Blend Radius 100% Flow
SE_F100.out	ANSYS output file, Results of running: extract100.inp, Safe End 100% Flow
BR_F100.cln	Reduced ANSYS output file, contains the stress values in time, Blend Radius 100% Flow
SE_F100.cln	Reduced ANSYS output file, contains the stress values in time, Safe End 100% Flow
BR_F100_ INSIDE.RED	Reduced ANSYS output file, contains detailed stress values in time, Blend Radius 100% Flow
SE_F100_INSIDE.RED	Reduced ANSYS output file, contains detailed stress values in time, Safe End 100% Flow
BR_F0.out	ANSYS output file, Results of running: extract0.inp, Blend Radius 0% Flow
SE_F0.out	ANSYS output file, Results of running: extract0.inp, Safe End 0% Flow
BR_F0.cln	Reduced ANSYS output file, contains the stress values in time, Blend Radius 0% Flow
SE_F0.cln	Reduced ANSYS output file, contains the stress values in time, Safe End 0% Flow
BR_F0_ INSIDE.RED	Reduced ANSYS output file, contains detailed stress values in time, Blend Radius 0% Flow
SE_F0_INSIDE.RED	Reduced ANSYS output file, contains detailed stress values in time, Safe End 0% Flow
SE_P.OUT	Stress Output at Safe End with Pressure Load
BR_P.OUT	Stress Output at Blend Radius with Pressure Load
VESSEL_P.OUT	Stress Output at Vessel with Pressure Load

Structural Integrity Associates, Inc.	File No.: VY-16Q-310
CALCULATION PACKAGE	Project No.: VY-16Q

PROJECT NAME:

Environmental Fatigue Analysis of VYNPS

CONTRACT NO.:

10150394

CLIENT:	**PLANT:**
Entergy Nuclear Operations, Inc.	Vermont Yankee Nuclear Power Station

CALCULATION TITLE:

Fatigue Analysis of Core Spray Nozzle

Document Revision	Affected Pages	Revision Description	Project Manager Approval Signature & Date	Preparer(s) & Checker(s) Signatures & Date
0	1-27 Appendix: A1-A2	Initial issue	Terry J. Herrmann 07/26/2007	Roland Horvath/ Minghao Qin 07/26/2007 Carl Limpus 07/26/2007
1	1-27 Appendix: A1-A2	Revised fatigue results per Revision 1 of Reference 1 (CAR 07-25, NCR 07-11)	Terry J. Herrmann 12/10/2007	Minghao Qin 12/10/2007 Carl Limpus 12/10/2007

Table of Contents

1.0 OBJECTIVE 4
2.0 METHODOLOGY 4
3.0 ANALYSIS 6
3.1 Transient Definitions (for program STRESS.EXE) 7
3.2 Peak and Valley Points of the Stress History (for program P-V.EXE) 7
3.3 Pressure Load 7
3.4 Attached Piping Loads 8
3.5 Fatigue Analysis (for program FATIGUE.EXE) 11
4.0 Fatigue Usage Results 11
5.0 Environmental Fatigue Analysis 12
6.0 References 13
APPENDIX A INPUT AND OUTPUT FILES A1

List of Tables

Table 1: Blend Radius Transients 14
Table 2: Safe End Transients 15
Table 3: Maximum Piping Stress Intensity Calculations for Blend Radius 16
Table 4: Maximum Piping Stress Intensity Calculations for Safe End 17
Table 5: Blend Radius Stress Summary 18
Table 6: Safe End Stress Summary 19
Table 7: Fatigue Results for Blend Radius (60 Years) 20
Table 8: Fatigue Results for Safe End (60 Years) 21
Table 9: Fatigue Results for Stainless Steel Piping (60 Years) 22

List of Figures

Figure 1: Transient 03: Start Up 23
Figure 2: Transient 11: Loss of Feedwater Pumps, Isolation Valves Closed 23
Figure 3: Transient 14: Single Relief or Safety Valve Blow Down 24
Figure 4: Transient 21-23: Shut Down Vessel Flooding 24
Figure 5: Transient 30: Emergency Shut Down 100% Flow (Safe End) 25
Figure 6: Transient 30: Emergency Shut Down 100% Flow (Blend Radius) 25
Figure 7: External Forces and Moments on the Core Spray Nozzle 26
Figure 8: Typical Green's Functions for Thermal Transient Stress 26
Figure 9: Typical Stress Response Using Green's Functions 27

1.0 OBJECTIVE

The purpose of this calculation is to perform a revised fatigue analysis for the core spray nozzle. Two locations will be analyzed for fatigue acceptance: the blend radius (SA508 Class II) and the safe end (SB 166 N06600). Both locations are chosen based on the highest overall stress of the analysis performed in Reference [1]. A revised fatigue usage will be determined for both locations, the nozzle forging and safe end, respectively. In the end, the environmental fatigue usage factors will be determined for the limiting locations.

2.0 METHODOLOGY

In order to provide an overall approach and strategy for evaluating the core spray nozzle, the Green's Function methodology and associated ASME Code stress and fatigue analyses are described in this section.

Revised stress and fatigue analyses are being performed for the core spray nozzle using ASME Code, Section III methodology. These analyses are being performed to address license renewal requirements to evaluate environmental fatigue for this component in response to Generic Aging Lessons Learned (GALL), Report [12] requirements. The revised analysis is being performed to refine the fatigue usage so that an environmental fatigue factor can be determined for subsequent license renewal efforts.

Two sets of rules are available under ASME Code, Section III, Class 1 [8]. Subparagraph NB-3600 of Section III provides simplified rules for analysis of piping components, and NB-3200 allows for more detailed analysis of vessel components. The NB-3600 piping equations combine by absolute sum the stresses due to pressure, moments and through wall thermal gradient effects, regardless of where within the pipe cross-section the maximum value of the components of stress are located. By considering stress signs, affected surface (inside or outside) and azimuthal position, the stress ranges may be significantly reduced. In addition, NB-3600 assigns stress indices by which the stresses are multiplied to conservatively incorporate the effects of geometric discontinuities. In NB-3200, stress indices are not required, as the stresses are calculated by finite element analysis and consider applicable stress concentration factors. In addition, NB-3200 methodology accounts for the different locations within a component where stresses due to thermal, pressure or other mechanical loading are a maximum. This generally results in a net reduction of the stress ranges and consequently, in the calculated fatigue usage. Article 4 [14] methodology was originally used to evaluate the core spray nozzle. NB-3200 methodology, which is the modern day equivalent to Article 4, is used in this analysis to be consistent with the Section III design bases for this component, as well as to allow a more detailed analysis of this component. In addition, several of the conservatisms originally used in the original core spray nozzle evaluation (such as grouping of transients) are removed in the current evaluation so as to achieve a more refined CUF.

For the core spray nozzle evaluated as a part of this work, stress histories will be computed by a time integration of the product of a pre-determined Green's Function and the transient data. This Green's Function integration scheme is similar in concept to the well-known Duhamel theory used in structural dynamics. A detailed derivation of this approach and examples of its application to specific plant locations is contained in Reference [11]. A general outline is provided in this section.

The steps involved in the evaluation are as follows:

- Develop finite element model
- Develop heat transfer coefficients and boundary conditions for the finite element model
- Develop Green's Functions
- Develop thermal transient definitions
- Perform stress analysis to determine stresses for all thermal transients
- Perform fatigue analysis

A Green's Function is derived by using finite-element methods to determine the transient stress response of the component to a step change in loading (usually a thermal shock). The critical location in the component is identified based on the maximum stress, and the thermal stress response over time is extracted for this location. This response to the input thermal step is the "Green's Function." Figure 8 shows a typical set of two Green's Functions, each for a different set of heat transfer coefficients (representing different flow rate conditions).

To compute the thermal stress response for an arbitrary transient, the loading parameter (usually local fluid temperature) is deconstructed into a series of step-loadings. By using the Green's Function, the response to each step can be quickly determined. By the principle of superposition, these can be added (algebraically) to determine the response to the original load history. The result is demonstrated in Figure 9. The input transient temperature history contains five step-changes of varying size, as shown in the upper plot in Figure 9. These five step changes produce the five successive stress responses in the lower plot shown in Figure 9. By adding all five response curves, the real-time stress response for the input thermal transient is computed.

The Green's Function methodology produces identical results compared to running the input transient through the finite element model. The advantage of using Green's Functions is that many individual transients can be run with a significant reduction of effort compared to running all transients through the finite element model. The trade-off in this process is that the Green's Functions are based on constant material properties and heat transfer coefficients. Therefore, these parameters are chosen to bound all transients that constitute the majority of fatigue usage, i.e., the heat transfer coefficients at 300°F bound the cold water injection transient. In addition, the instantaneous value for the coefficient of thermal expansion is used instead of the mean value for the coefficient of thermal expansion. This conservatism is more than offset by the benefit of not having to analyze every transient, which was done in the VY core spray nozzle evaluation.

Once the stress history is obtained for all transients using the Green's Function approach, the remainder of the fatigue analysis is carried out using traditional methodologies in accordance with ASME Code, Section III requirements.

Fatigue calculations are performed in accordance with ASME Code, Section III, Subsection NB-3200 methodology. Fatigue analysis is performed for the two limiting locations (one in the safe end and one in the nozzle forging, representing the two materials of the nozzle assembly) using the Green's Functions developed for these two locations and 60-year projected cycle counts.

Three Structural Integrity utility programs will be used to perform the fatigue analysis. The first two calculate stresses in response to transients. The transients analyzed are those described in the

thermal cycle diagrams [2] for the core spray nozzle. These transients are shown in Figure 1– Figure 6. The temperatures and pressures for these transients have been modified to account for power uprate [3]. The power uprate pressures and temperatures were used for this analysis. The last program calculates fatigue based on the stress output. The three programs are STRESS.EXE, P-V.EXE, and FATIGUE.EXE. The first program, STRESS.EXE, calculates a stress history in response to a thermal transient using a Green's Function. The second program, P-V.EXE, reduces the stress history to peaks and valleys, as required by ASME Code fatigue evaluation methods. The third program, FATIGUE.EXE, calculates fatigue from the reduced peak and valley history using ASME Code, Section III range-pair methodology. All three programs are explained in detail and have been independently verified for generic use in the Reference [4] calculation.

In order to perform the fatigue analysis, Green's Functions are developed using the finite element model. Then, input files with the necessary data are prepared and the three utility computer programs are run. The first program (STRESS.EXE) requires the following three input files:

- Input file "GREEN.DAT": This file contains the Green's Function for the location being evaluated. For each flow condition, two Green's Functions are determined: a membrane plus bending stress intensity Green's Function and a total stress intensity Green's Function. This allows computation of total stress, as well as membrane plus bending stress, which is necessary to compute K_e per ASME Code, Section III requirements.
- Input file "GREEN.CFG": This file is a configuration file containing parameters that define the Green's Function (i.e., number of points, temperature drop analyzed, etc.).
- Input file "TRANSNT.INP": This file contains the input transient definition for all thermal transients to be analyzed for the location being evaluated.

Pressure and piping stress intensities are also included for each transient case, based on pressure stress results from finite element analysis and attached piping load calculations.

The second program (P-V.EXE) simply extracts only the maxima and minima stress (i.e., the peaks and valleys) from the stress histories generated by program STRESS.EXE.

The third program (FATIGUE.EXE) performs the ASME Code peak event-pairing required to calculate a fatigue usage value. The input data consists of the output peak and valley history from program P-V.EXE, and a configuration input file that provides ASME Code configuration data relevant to the fatigue analysis (i.e., K_e parameters, S_m, Young's modulus, etc.). The output is the final fatigue calculation for the location being evaluated.

The Green's Function methodology described above uses standard industry stress and fatigue analysis practices, and is the same as the methodology used in typical stress reports. Special approval for the use of this methodology is therefore not required.

3.0 ANALYSIS

The transients analyzed for the core spray nozzle were developed based on the definitions in the original RPV Design Specification [10], as modified for EPU [3], as well as more recent definitions based on BWR operating experience [2] for BWR. The final transients evaluated in the stress and fatigue analyses are shown in Figure 1 thru Figure 6.

The fatigue analysis involves the preparing of input files for, and running of three programs [4]. The programs STRESS.EXE and P-V.EXE are run together through the use of a batch file. The program FATIGUE.EXE is run after processing the output from P_V.EXE.

The steps associated with this process are described in the following sub-sections.

3.1 Transient Definitions (for program STRESS.EXE)

The program STRESS.EXE requires the following three input files for analyzing an individual transient:

- Green.dat. There are 8 stress history functions obtained from References [1]. They represent the membrane plus bending and total stress intensities at the blend radius and safe end locations. Both of the blend radius and the safe end have two stress history functions for flow condition of 0% and 100%. Per [1], Sz-Sx stress intensities are used for the total and membrane plus bending Green's Functions for all flow rates of both locations.
- Green.cfg is configured as described in Reference [4].
- Transnt.inp. These files are created to represent the selected transients obtained from the thermal cycle diagrams [2] and redefined by power uprate [3]. Table 1 and Table 2 contain the loading defined for each transient. Based upon the thermal cycle diagram for the RPV and the core spray nozzle, the transients are split into the following groups based upon flow rate:
    - Transients 02, 03, 11, 14, 21-23 and 24 are run at 0% flow.
    - Transient 30 runs at 100% flow rate per [3]. The transient of emergency shutdown is numbered as 30.

The remaining transients are not included in this analysis, as temperature changes from them are considered negligible to have impact on the results.

3.2 Peak and Valley Points of the Stress History (for program P-V.EXE)

The program P-V.exe is then run to extract the peaks and valleys from the STRESS.OUT file produced by the STRESS.EXE program. The only input required for this program is STRESS.OUT and it outputs all the peaks and valleys to P-V.OUT. Columns 2 through 5 of Table 5 (for the blend radius) and Table 6 (for the safe end) show the final peak and valley output. The pressure for column six is then filled in using the thermal cycle diagrams. Pressure and piping loads have to be added to the peak and valley points to calculate the final stress values used for fatigue analysis.

3.3 Pressure Load

The pressure stress associated with a 1000 psi internal pressure was determined in Reference [1]. These values are as follows:

Location	Membrane plus Bending Stress Intensity (psi)	Total Stress Intensity (psi)
Safe End	12,020	12,030
Blend Radius	34,970	35,860

These pressure stress values for each location were linearly scaled according to the pressure of the transient. The actual pressure for column 6 of Table 5 and Table 6 is obtained from Reference [2] and shown in Tables 1 and 2. The scaled pressure stress values are shown in columns 7 and 8 of Table 5 (for the blend radius) and Table 6 (for the safe end).

The pressure stress is combined with the peak and valley points to calculate the final stress values used for fatigue analysis.

3.4 Attached Piping Loads

Additionally, the piping stress intensity (stress caused by the attached piping) was determined. These piping forces and moments are determined as shown in Figure 7.

The following formulas are used to determine the maximum stress intensity in the nozzle at the two locations of interest. From engineering statics, the piping loads at the end of the model can be translated to the first cut (blend radius) and second cut (safe end) locations using the following equations:

For Cut I:

$$(M_x)_1 = M_x - F_y L_1$$
$$(M_y)_1 = M_y + F_x L_1$$

For Cut II:

$$(M_x)_2 = M_x - F_y L_2$$
$$(M_y)_2 = M_y + F_x L_2$$

The total bending moment and shear loads are obtained using the equations below:

For Cut I:

$$M_{xy} = \sqrt{(M_x)_1^{\,2} + (M_y)_1^{\,2}}$$
$$F_{xy} = \sqrt{(F_x)_1^{\,2} + (F_y)_1^{\,2}}$$

For Cut II:

$$M_{xy} = \sqrt{(M_x)_2^{\,2} + (M_y)_2^{\,2}}$$
$$F_{xy} = \sqrt{(F_x)_2^{\,2} + (F_y)_2^{\,2}}$$

The distributed loads for a thin-walled cylinder are obtained using the equations below:

$$N_z = \frac{1}{\pi R_N}\left[\frac{1}{2}F_z + \frac{M_{xy}}{R_N}\right]$$
$$q_N = \frac{1}{\pi R_N}\left[F_{xy} - \frac{M_z}{2R_N}\right]$$

To determine the primary stresses, PM, due to internal pressure and piping loads, the following equations are used.

For Cut I, using thin-walled equations:

$$(P_M)_z = \frac{Pa_N}{2t_N} + \frac{Nz}{t_N}$$
$$(P_M)_\theta = \frac{Pa_N}{t_N}$$
$$(P_M)_R = -P$$
$$\tau_M = \frac{q_N}{t_N}$$
$$SI_{MAX} = 2\sqrt{\left(\frac{(P_M)_\theta - (P_M)_R}{2}\right)^2 + (\tau_M)_{z\theta}^{\,2}}$$

or

$$SI_{MAX} = 2\sqrt{\left(\frac{(P_M)_z - (P_M)_R}{2}\right)^2 + (\tau_M)_{z\theta}^{\,2}}$$

Where:

L_1 = The length from the end of the nozzle where the piping loads are applied to the location of interest in the blend radius.

L_2 = The length from the end of the nozzle where the piping loads are applied to the location of interest in the safe end.

M_{xy} = The maximum bending moment in the xy plane.
F_{yx} = The maximum shear force in the xy plane.
N_z = The normal force per inch of circumference applied to the end of the nozzle in the z direction.
q_N = The shear force per inch of circumference applied to the nozzle.
R_N = The mid-wall nozzle radius.

Because pressure was not considered in this analysis, the equations used for Cut I are valid for Cut II. In addition, the equations can be simplified as follows:

$$(P_M)_z = \frac{Nz}{t_N}$$
$$(P_M)_\theta = 0$$
$$(P_M)_R = 0$$
$$\tau_M = \frac{q_N}{t_N}$$
$$SI_{MAX} = 2(\tau_M)_{z\theta}$$
$$or$$
$$SI_{MAX} = 2\sqrt{\left(\frac{Nz}{2t_N}\right)^2 + (\tau_M)_{z\theta}{}^2}$$

Per Reference [5], the core spray nozzle piping loads are as follows:

F_x	=	2,500	lbs	M_x	=	22,000	ft-lb =	264,000	in-lb
F_y	=	4,600	lbs	M_y	=	7,100	ft-lb =	85,200	in-lb
F_z	=	1,700	lbs	M_z	=	8,800	ft-lb =	150,600	in-lb

The location of the nozzle piping loads is assumed to be at the end of the connection of the safe end and the attached pipe. Therefore, the L1 is equal to 30.817 inches and the L2 is equal to 0.303 inches. The calculations for the blend radius and safe end are shown in Table 3 and Table 4. The first cut location is the middle of Green's Function cross section for the blend radius (Node 2181) per [1], and the second cut is from Node 3719 (inside) to Node 3737 (outside). The maximum stress intensities, due to piping loads are 322.52 psi at the blend radius and 6949.94 psi at the safe end, respectively. The piping load sign is set as the same as the thermal stress sign.

These piping stress values are scaled assuming no stress occurs at an ambient temperature of 70°F and the full values are reached at reactor design temperature, 575°F [2]. The scaled piping stress values are shown in columns 9 and 10 of Table 5 and Table 6. Columns 11 and 12 of Table 5 and Table 6 show the summation of all stresses for each thermal peak and valley stress point.

3.5 Fatigue Analysis (for program FATIGUE.EXE)

The number of cycles projected for the 60-year operating life is used for each transient, as obtained from Reference [2]. Column 13 in Table 5 and Table 6 shows the number of cycles associated with each transient.

The program FATIGUE.EXE performs the "ASME Code style" peak event pairing required to calculate a fatigue usage value. The input data for FATIGUE.CFG is as follows:

	Blend Radius (SA508 Class II)	Safe End (N06600)	Piping (Stainless Steel)
Parameters *m* and *n* for Computing K_e	2.0 & 0.2 (low alloy steel) [8]	1.7 & 0.3 [8]	1.7 & 0.3 [8]
Design Stress Intensity Values, S_m	26,700 psi [6] @ 600°F	23,300 psi [6] @ 600°F	17,000 psi [6] @ 600°F
Elastic Modulus from Applicable Fatigue Curve	30.0×10^6 psi [8]	28.3×10^6 psi [8]	28.3×10^6 psi [8]
Elastic Modulus Used in Finite Element Model (300°F)	26.7×10^6 psi [1]	29.8×10^6 psi [1]	27.0×10^6 psi [1]
The Geometric Stress Concentration Factor K_t	1.0	4.0 See Note	1.8 [14]

Note: Conservative bounding value per ASME Code, Section NB-3600 to cover thread and weld regions.

The results of the fatigue analyses are presented in Table 7 through Table 9 for the blend radius, safe end and stainless steel piping for 60 years, respectively.

The Core Spray piping adjacent to the safe end was also analyzed because of its proximity to the maximum safe end thermal stress location. For this fatigue analysis, the stress results of the safe end were used with stainless steel material properties and a value of 1.8 was selected for K_t at the weld location, based on the maximum value given in ASME Code, Section III, table NB-3681(a)-1 [8].

The results described are contained in EXCEL files BRresults.xls and SEresults.xls, which are contained in the computer files.

4.0 FATIGUE USAGE RESULTS

The blend radius Cumulative Usage Factor (CUF) from system cycling is 0.0166 for 60 years. The safe end CUF is 0.0398 and the CUF of stainless steel piping is 0.0011 for 60 years.

5.0 ENVIRONMENTAL FATIGUE ANALYSIS

Per Reference [7], the dissolved Oxygen (DO) calculation shows the overall HWC availability is 47%. It means the pre-HWC is 53%.

The fatigue calculation will be re-performed for the nozzle base material, since cladding is structurally neglected in modern-day fatigue analyses, per ASME Code, Section III, NB-3122.3 [8]. This is also consistent with Sections 5.7.1 and 5.7.4 of NUREG/CR-6260 [9]. Therefore, the cladding will be neglected and EAF assessment of the nozzle base material is performed.

For the blend radius location, the environmental fatigue factors for pre-HWC and post-HWC are 11.14 and 8.82 from Table 4 of Reference [7]. It results in an EAF adjusted CUF of (11.14 x 53% + 8.82 x 47%) x 0.0166 = 0.16683 for 60 years, which is acceptable (i.e., less than the allowable value of 1.0). The overall environmental multiplier is 10.05.

For the safe end location, the environmental fatigue factors for post-HWC and pre-HWC are all 1.49 from Reference [13]. It results in an EAF adjusted CUF of 1.49 x 0.0398 = 0.05930 for 60 years, which is acceptable (i.e., less than the allowable value of 1.0). The overall environmental multiplier is 1.49.

For the stainless steel piping, the environmental fatigue factors for post-HWC and pre-HWC are all 8.36 from Table 4 of Reference [7]. It results in an EAF adjusted CUF of 8.36 x 0.0011 = 0.009196 for 60 years, which is acceptable (i.e., less than the allowable value of 1.0). The overall environmental multiplier is 8.36.

A Fatigue Environmental Multiplier of 1.49 for Ni-Cr-Fe was applied to the safe end fatigue usage and 8.36 for stainless steel to the piping. This results in the safe end being the limiting location for fatigue.

6.0 REFERENCES

1 SI Calculation No. VY-16Q-309, Revision 1, "Core Spray Nozzle Green's Functions."

2 "Reactor Thermal Cycles for 60 Years of Operation," Attachment 1 of Entergy Design Input Record (DIR), Revision 1, EC No. 1773, Revision 0, "Environmental Fatigue Analysis for Vermont Yankee Nuclear Power Station," 7/26/07, SI File No. VY-16Q-209.

3 GE Certified Design Specification No. 26A6019, Revision 1, "Reactor Vessel – Extended Power Uprate," August 29, 2003, SI File No. VY-05Q-236.

4 Structural Integrity Associates Calculation (Generic) No. SW-SPVF-01Q-301, Revision 0, "STRESS.EXE, P-V.EXE, and FATIGUE.EXE Software Verification."

5 VY Drawing 5920-0024, Revision 11, Sht. No. 7, "Reactor Vessel," (GE Drawing No. 919D294), SI File No. VY-05Q-241.

6 American Society of Mechanical Engineers, Boiler and Pressure Vessel Code, Section II, Part D, 1998 Edition, 2000 Addenda.

7 SI Calculation No. VY-16Q-303, Revision 0, "Environmental Fatigue Evaluation of Reactor Recirculation Inlet Nozzle and Vessel Shell Bottom Head."

8 American Society of Mechanical Engineers, Boiler and Pressure Vessel Code, Section III Subsection NB, 1998 Edition, 2000 Addenda.

9 NUREG/CR-6260 (INEL-95/0045), "Application of NUREG/CR-5999 Interim Fatigue Curves to Selected Nuclear Power Plant Components," March 1995.

10 GE Design Specification No. 21A1115, Revision 4, "Vermont Yankee Reactor Pressure Vessel," October 21, 1969, SI File No. VY-05Q-210.

11 Kuo, A. Y., Tang, S. S., and Riccardella, P. C., "An On-Line Fatigue Monitoring System for Power Plants, Part I - Direct Calculation of Transient Peak Stress Through Transfer Matrices and Green's Functions," ASME PVP Conference, Chicago, 1986.

12 NUREG-1801, Revision 1, "Generic Aging Lessons Learned (GALL) Report," U. S. Nuclear Regulatory Commission, September 2005.

13 EPRI Report No. TR-105759, "An Environmental Factor Approach to Account for Reactor Water Effects in Light Water Reactor Pressure Vessel and Piping Fatigue Evaluations," December 1995.

14 American Society of Mechanical Engineers, Boiler and Pressure Vessel Code, Section III, Subsection A, Article 4, 1965 Edition with Winter 1966 Addenda.

Table 1: Blend Radius Transients [1, 2, 3]

Transient Number	Time (s)	Temp (°F)	Time Step (s)	Pressure (psig)	Flow Rate (GPM)
2. Design HYD Test	---	100	---	0	
				1100	
120 Cycles				50	
3. Startup	0	100		0	0
300 Cycles	16164	549	16164	1010	(0%)
	24164	549	8000	1010	
11. Loss of Feedwater	0	526		1010	0
Pumps	3	526	3	1190	(0%)
10 Cycles	13	526	10	1135	
	233	300	220	1135	
	2213	500	1980	1135	
	2393	300	180	885	
	6893	500	4500	1135	
	7313	300	420	675	
	7613	300	300	675	
	11213	400	3600	240	
	16577	549	5364	1010	
	16637	549	60	1010	
	16638	542	1	1010	
	16698	542	60	1010	
	16699	526	1	1010	
	24699	526	8000	1010	
14. SRV Blowdown	0	526		1010	0
1 Cycle	600	375	600	400	(0%)
	11580	70	10980	50	
	19580	70	8000	50	
21-23. Shutdown	0	549		1010	0
300 Cycles	6264	375	6264	50	(0%)
	6864	330	600	50	
	16224	100	9360	50	
	24224	100	8000	50	
24. Hydrostatic Test	---	100	---	50	
1 Cycle				1563	
				50	
30. Emergency Shut Down	0	549		1010	3200
1 Cycle	10	406	10	250	(100%)
	11	70	1	250	
	8011	70	8000	0	

Note:

1. Instant temperature change is 1 sec.
2. This is due to the length of the Green's Function. The transients are plotted using an 8000 second steady state increment.
3. The number of cycles for 60 years is from Reference [2].

Table 2: Safe End Transients [1, 2, 3]

Transient Number	Time (s)	Temp (°F)	Time Step (s)	Pressure (psig)	Flow Rate (GPM)
2. Design HYD Test	---	100	---	0	
120 Cycles				1100	
				50	
3. Startup	0	100		0	0
300 Cycles	16164	549	16164	1010	(0%)
	17164	549	1000	1010	
11. Loss of Feedwater	0	526		1010	0
Pumps	3	526	3	1190	(0%)
10 Cycles	13	526	10	1135	
	233	300	220	1135	
	2213	500	1980	1135	
	2393	300	180	885	
	6893	500	4500	1135	
	7313	300	420	675	
	7613	300	300	675	
	11213	400	3600	240	
	16577	549	5364	1010	
	16637	549	60	1010	
	16638	542	1	1010	
	16698	542	60	1010	
	16699	526	1	1010	
	17699	526	1000	1010	
14. SRV Blowdown	0	526		1010	0
1 Cycle	600	375	600	400	(0%)
	11580	70	10980	50	
	12580	70	1000	50	
21-23. Shutdown	0	549		1010	0
300 Cycles	6264	375	6264	50	(0%)
	6864	330	600	50	
	16224	100	9360	50	
	17224	100	1000	50	
12. Hydrostatic Test	---	100	---	50	
1 cycle				1563	
				50	
30. Emergency Shut Down	0	549		1010	3200
1 Cycle	10	406	10	250	(100%)
	11	70	1	250	
	1011	70	1000	0	

Note:

1. Instant temperature change is 1 sec.
2. The transients are plotted using a 1000 second steady state increment. The difference is due to the length of the Green's Function for the safe end.
3. The number of cycles for 60 years is from Reference [2].

Table 3: Maximum Piping Stress Intensity Calculations for Blend Radius

Blend Radius External Piping Loads		
Parameters		
F_x =	2.50	kips
F_y =	4.60	kips
F_z =	1.70	kips
M_x =	264.00	in-kips
M_y =	85.20	in-kips
M_z =	105.60	in-kips
OD=	18.87	in
ID=	11.750	in
R_N =	7.65	in
L =	30.82	in
t_N =	3.56	in
$(M_x)_2$ =	122.24	in-kips
$(M_y)_2$ =	162.24	in-kips
M_{xy} =	203.14	in-kips
F_{xy} =	5.24	kips
N_z =	1.14	kips/in
q_N =	-0.07	kips/in
Primary Membrane Stress Intensity		
PM_z =	0.32	ksi
τ =	-0.02	ksi
SI_{max} =	0.32	ksi
SI_{max} =	322.52	psi

Note: The locations for Cut I and Cut II were defined in Reference [1] for safe end and blend radius paths, respectively.

Table 4: Maximum Piping Stress Intensity Calculations for Safe End

Safe End External Piping Loads		
Parameters		
F_x =	2.50	kips
F_y =	4.60	kips
F_Z =	1.70	kips
M_x =	264.00	in-kips
M_y =	85.20	in-kips
M_Z =	105.60	in-kips
OD=	10.82	in
ID=	9.834	in
R_N =	5.16	in
L =	0.30	in
t_N =	0.49	in
$(M_x)_1$ =	262.60	in-kips
$(M_y)_1$ =	85.96	in-kips
M_{xy} =	276.31	in-kips
F_{xy} =	5.24	kips
N_Z =	3.35	kips/in
q_N =	-0.31	kips/in
Primary Membrane Stress Intensity		
PM_Z =	6.84	ksi
τ =	-0.63	ksi
SI_{max} =	6.95	ksi
SI_{max} =	6949.94	psi

Note: The locations for Cut I and Cut II were defined in Reference [1] for safe end and blend radius paths, respectively.

Table 5: Blend Radius Stress Summary

1	2	3	4	5	6	7	8	9	10	11	12	13
Transient Number	Time (s)	Total Stress (psi)	M+B Stress (psi)	Temperature F	Pressure (psig)	Total Pressure Stress (psi)	M+B Pressure Stress (psi)	Total Piping Stress (psi)	M+B Piping Stress (psi)	Total Total Stress (psi)	Total M+B Stress (psi)	Number of Cycles (60 years)
2				100	0	0	0	19	19	19	19	120
				100	1100	39446	38467	19	19	39465	38486	120
				100	50	1793	1749	19	19	1812	1768	120
3	0	209	-265	100	0	0	0	19	-19	228	-284	300
	2812	-2517	5184	549	176	6311	6155	-306	306	3488	11645	300
	24164	4983	4795	549	1010	36219	35320	306	306	41508	40421	300
11	0	4734	4480	526	1010	36219	35320	291	291	41244	40091	10
	3	4734	4480	526	1190	42673	41614	291	291	47699	46386	10
	13	4734	-3711	526	1135	40701	39691	291	-291	45726	35689	10
	333	25225	7792	343	1135	40701	39691	174	174	66100	47657	10
	2217	-2805	-6398	496	1131	40558	39551	-272	-272	37481	32881	10
	2546	16808	4980	322	894	32059	31263	161	161	49028	36404	10
	6394	-1427	-523	478	1107	39697	38712	-260	-260	38010	37928	10
	7415	18450	6299	304	675	24206	23605	149	149	42805	30053	10
	11931	19	1976	420	343	12300	11995	223	223	12542	14194	10
	24699	4734	4480	526	1010	36219	35320	291	291	41244	40091	10
14	0	4734	2382	526	1010	36219	35320	291	291	41244	37993	1
	673	17490	5600	373	398	14272	13918	193	193	31956	19712	1
	19580	-114	-659	70	50	1793	1749	0	0	1679	1090	1
21-23	0	4978	4504	549	1010	36219	35320	306	306	41503	40130	300
	2794	7705	4663	518	582	20871	20353	286	286	28862	25302	300
	6273	6921	2273	374	50	1793	1749	194	194	8908	4216	300
	6915	9103	2756	329	50	1793	1749	165	165	11061	4670	300
	24224	205	-324	100	50	1793	1749	19	-19	2017	1405	300
24				100	50	1793	1749	19	19	1812	1768	1
				100	1563	56049	54658	19	19	56068	54677	1
				100	50	1793	1749	19	19	1812	1768	1
30	0	2036	2954	549	1010	36219	35320	306	306	38561	38580	1
	2	2035	-13651	515	858	30768	30004	284	-284	33087	16069	1
	8011	25660	14907	70	0	0	0	0	0	25660	14907	1

NOTES: Column 1: Transient number identification.
Column 2: Time during transient where a maxima or minima stress intensity occurs from P-V.OUT output file.
Column 3: Maxima or minima total stress intensity from P-V.OUT output file.
Column 4: Maxima or minima membrane plus bending stress intensity from P-V.OUT output file.
Column 5: Temperature per total stress intensity.
Column 6: Pressure per Table 1.
Column 7: Total pressure stress intensity from the quantity (Column 6 x 35,860)/1000 [1].
Column 8: Membrane plus bending pressure stress intensity from the quantity (Column 6 x 34,970)/1000 [1].
Column 9: Total external stress from calculation in Table 3, 322.52 x (Column 5 -70°F)/(575°F -70°F).
Column 10: Same as Column 9, but for M+B stress.
Column 11: Sum of total stresses (Columns 3, 7, and 9).
Column 12: Sum of membrane plus bending stresses (Columns 4, 8, and 10).
Column 13: Number of cycles for the transient (60 years).

Table 6: Safe End Stress Summary

1	2	3	4	5	6	7	8	9	10	11	12	13
Transient Number	Time (s)	Total Stress (psi)	M+B Stress (psi)	Temperature F	Pressure (psig)	Total Pressure Stress (psi)	M+B Pressure Stress (psi)	Total Piping Stress (psi)	M+B Piping Stress (psi)	Total Total Stress (psi)	Total M+B Stress (psi)	Number of Cycles (60 years)
2				100	0	0	0	413	413	413	413	120
				100	1100	13233	13222	413	413	13646	13635	120
				100	50	602	601	413	413	1014	1014	120
3	0	659	757	100	0	0	0	413	413	1072	1170	300
	153	582	720	104	10	120	120	471	471	1173	1311	300
	24164	9239	10745	549	1010	12150	12140	6592	6592	27981	29477	300
11	0	8803	10236	526	1010	12150	12140	6276	6276	27229	28652	10
	3	8803	10236	526	1190	14316	14304	6276	6276	29394	30815	10
	13	8803	10236	526	1135	13654	13643	6276	6276	28733	30154	10
	162	11647	11599	409	1135	13654	13643	4660	4660	29961	29901	10
	669	4807	5790	344	1135	13654	13643	3772	3772	22233	23204	10
	2374	11141	10842	362	911	10959	10950	4022	4022	26122	25814	10
	2955	4721	5576	325	916	11019	11010	3509	3509	19249	20095	10
	7056	9518	10162	440	956	11501	11491	5090	5090	26109	26743	10
	7931	4490	5274	309	637	7663	7657	3287	3287	15440	16217	10
	16709	9960	11116	526	1010	12150	12140	6276	6276	28386	29532	10
	24699	8803	10236	526	1010	12150	12140	6276	6276	27229	28652	10
14	0	8803	10236	526	1010	12150	12140	6276	6276	27229	28652	1
	154	9499	10570	497	853	10262	10253	5872	5872	25633	26695	1
	12580	89	92	70	50	602	601	0	0	691	693	1
21-23	0	9242	10748	549	1010	12150	12140	6592	6592	27984	29480	300
	164	9319	10785	546	985	11850	11840	6546	6546	27715	29171	300
	6265	6141	7065	375	50	602	601	4196	4196	10939	11862	300
	6368	6209	7079	370	50	602	601	4131	4131	10942	11811	300
	17224	662	760	100	50	602	601	413	413	1676	1774	300
24				100	50	602	601	413	413	1014	1014	1
				100	1563	18803	18787	413	413	19216	19200	1
				100	50	602	601	413	413	1014	1014	1
30	0	9280	9155	549	1010	12150	12140	6592	6592	28022	27887	1
	13	85620	52710	70	250	3008	3005	0	0	88628	55715	1
	1011	-12	-10	70	0	0	0	0	0	-12	-10	1

NOTES: Column 1: Transient number identification.
Column 2: Time during transient where a maxima or minima stress intensity occurs from P-V.OUT output file.
Column 3: Maxima or minima total stress intensity from P-V.OUT output file.
Column 4: Maxima or minima membrane plus bending stress intensity from P-V.OUT output file.
Column 5: Temperature per total stress intensity.
Column 6: Pressure per Table 2.
Column 7: Total pressure stress intensity from the quantity (Column 6 x 12,030)/1000.
Column 8: Membrane plus bending pressure stress intensity from the quantity (Column 6 x 12,020)/1000.
Column 9: Total external stress from calculation in Table 4, 6949.94 x (Column 5-70°F)/(575°F -70°F).
Column 10: Same as Column 9, but for M+B stress.
Column 11: Sum of total stresses (Columns 3, 7, and 9).
Column 12: Sum of membrane plus bending stresses (Columns 4, 8, and 10).
Column 13: Number of cycles for the transient (60 years).

Table 7: Fatigue Results for Blend Radius (60 Years)

LOCATION = LOCATION NO. 2 -- BLEND RADIUS
FATIGUE CURVE = 1 (1 = CARBON/LOW ALLOY, 2 = STAINLESS STEEL)
m = 2.0
n = .2
Sm = 26700. psi
Ecurve = 3.000E+07 psi
Eanalysis = 2.670E+07 psi
Kt = 1.00

MAX	MIN	RANGE	MEM+BEND	Ke	Salt	Napplied	Nallowed	U
66100.	19.	66081.	47638.	1.000	37124.	1.000E+01	1.083E+04	.0009
56068.	19.	56049.	54658.	1.000	31488.	1.000E+00	1.896E+04	.0001
49028.	19.	49009.	36385.	1.000	27533.	1.000E+01	2.878E+04	.0003
47699.	19.	47680.	46367.	1.000	26787.	1.000E+01	3.132E+04	.0003
45726.	19.	45707.	35670.	1.000	25678.	1.000E+01	3.566E+04	.0003
42805.	19.	42786.	30034.	1.000	24037.	1.000E+01	4.367E+04	.0002
41508.	19.	41489.	40402.	1.000	23308.	6.900E+01	4.800E+04	.0014
41508.	228.	41280.	40705.	1.000	23191.	2.310E+02	4.875E+04	.0047
41503.	228.	41275.	40414.	1.000	23188.	6.900E+01	4.876E+04	.0014
41503.	1679.	39824.	39040.	1.000	22373.	1.000E+00	5.735E+04	.0000
41503.	1812.	39691.	38362.	1.000	22298.	1.200E+02	5.830E+04	.0021
41503.	1812.	39691.	38362.	1.000	22298.	1.000E+00	5.830E+04	.0000
41503.	1812.	39691.	38362.	1.000	22298.	1.000E+00	5.830E+04	.0000
41503.	2017.	39486.	38725.	1.000	22183.	1.080E+02	5.982E+04	.0018
41244.	2017.	39227.	38686.	1.000	22038.	1.000E+01	6.181E+04	.0002
41244.	2017.	39227.	38686.	1.000	22038.	1.000E+01	6.181E+04	.0002
41244.	2017.	39227.	36588.	1.000	22038.	1.000E+00	6.181E+04	.0000
39465.	2017.	37448.	37081.	1.000	21038.	1.200E+02	7.780E+04	.0015
38561.	2017.	36544.	37175.	1.000	20530.	1.000E+00	8.783E+04	.0000
38010.	2017.	35993.	36523.	1.000	20221.	1.000E+01	9.470E+04	.0001
37481.	2017.	35464.	31476.	1.000	19924.	1.000E+01	1.014E+05	.0001
33087.	2017.	31070.	14664.	1.000	17455.	1.000E+00	1.633E+05	.0000
31956.	2017.	29939.	18307.	1.000	16820.	1.000E+00	1.866E+05	.0000
28862.	2017.	26845.	23897.	1.000	15081.	2.800E+01	3.015E+05	.0001
28862.	3488.	25374.	13657.	1.000	14255.	2.720E+02	3.900E+05	.0007
25660.	3488.	22172.	3262.	1.000	12456.	1.000E+00	1.043E+06	.0000
12542.	3488.	9054.	2549.	1.000	5087.	1.000E+01	1.000E+20	.0000
11061.	3488.	7573.	-6975.	1.000	4254.	1.700E+01	1.000E+20	.0000
11061.	8908.	2153.	454.	1.000	1210.	2.830E+02	1.000E+20	.0000
							TOTAL USAGE FACTOR =	.0166

Table 8: Fatigue Results for Safe End (60 Years)

LOCATION = LOCATION NO. 2 -- SAFE END
FATIGUE CURVE = 2 (1 = CARBON/LOW ALLOY, 2 = STAINLESS STEEL)
m = 1.7
n = .3
Sm = 23300. psi
Ecurve = 2.830E+07 psi
Eanalysis = 2.980E+07 psi
Kt = 4.00

MAX	MIN	RANGE	MEM+BEND	Ke	Salt	Napplied	Nallowed	U
88628.	-12.	88640.	55725.	1.000	121469.	1.000E+00	9.368E+02	.0011
88628.	413.	88215.	55302.	1.000	120665.	0.000E+00	9.568E+02	.0000
29961.	413.	29548.	29488.	1.000	56036.	1.000E+01	1.909E+04	.0005
29394.	413.	28981.	30402.	1.000	57069.	1.000E+01	1.746E+04	.0006
28733.	413.	28320.	29741.	1.000	55813.	1.000E+01	1.946E+04	.0005
28386.	413.	27973.	29119.	1.000	54762.	1.000E+01	2.140E+04	.0005
28022.	413.	27609.	27474.	1.000	52246.	1.000E+00	2.714E+04	.0000
27984.	413.	27571.	29067.	1.000	54497.	7.900E+01	2.193E+04	.0036
27984.	691.	27293.	28787.	1.000	53967.	1.000E+00	2.304E+04	.0000
27984.	1014.	26970.	28466.	1.000	53356.	1.200E+02	2.441E+04	.0049
27984.	1014.	26970.	28466.	1.000	53356.	1.000E+00	2.441E+04	.0000
27984.	1014.	26970.	28466.	1.000	53356.	1.000E+00	2.441E+04	.0000
27984.	1072.	26912.	28310.	1.000	53106.	9.800E+01	2.499E+04	.0039
27981.	1072.	26909.	28307.	1.000	53100.	2.020E+02	2.501E+04	.0081
27981.	1173.	26808.	28166.	1.000	52852.	9.800E+01	2.561E+04	.0038
27715.	1173.	26542.	27860.	1.000	52289.	2.020E+02	2.703E+04	.0075
27715.	1676.	26039.	27397.	1.000	51391.	9.800E+01	2.951E+04	.0033
27229.	1676.	25553.	26878.	1.000	50421.	1.000E+01	3.249E+04	.0003
27229.	1676.	25553.	26878.	1.000	50421.	1.000E+01	3.249E+04	.0003
27229.	1676.	25553.	26878.	1.000	50421.	1.000E+00	3.249E+04	.0000
26122.	1676.	24446.	24040.	1.000	45853.	1.000E+01	5.273E+04	.0002
26109.	1676.	24433.	24969.	1.000	47170.	1.000E+01	4.551E+04	.0002
25633.	1676.	23957.	24921.	1.000	46875.	1.000E+00	4.697E+04	.0000
22233.	1676.	20557.	21430.	1.000	40288.	1.000E+01	1.071E+05	.0001
19249.	1676.	17573.	18321.	1.000	34442.	1.000E+01	2.591E+05	.0000
19216.	1676.	17540.	17426.	1.000	33152.	1.000E+00	3.288E+05	.0000
15440.	1676.	13764.	14443.	1.000	27110.	1.000E+01	1.137E+06	.0000
13646.	1676.	11970.	11861.	1.000	22580.	1.200E+02	2.085E+06	.0001
10942.	1676.	9266.	10037.	1.000	18697.	9.000E+00	4.669E+06	.0000
10942.	10939.	3.	-51.	1.000	-71.	2.910E+02	4.669E+06	.0001
							TOTAL USAGE FACTOR =	.0398

Table 9: Fatigue Results for Stainless Steel Piping (60 Years)

```
       LOCATION = LOCATION NO. 2 -- SS Piping
  FATIGUE CURVE = 2 (1 = CARBON/LOW ALLOY, 2 = STAINLESS STEEL)
              m = 1.7
              n =  .3
             Sm = 17000. psi
         Ecurve = 2.830E+07 psi
      Eanalysis = 2.700E+07 psi
             Kt = 1.80
```

MAX	MIN	RANGE	MEM+BEND	Ke	Salt	Napplied	Nallowed	U
88628.	-12.	88640.	55725.	1.309	91378.	1.000E+00	2.503E+03	.0004
88628.	413.	88215.	55302.	1.281	88936.	0.000E+00	2.771E+03	.0000
29961.	413.	29548.	29488.	1.000	27848.	1.000E+01	1.042E+06	.0000
29394.	413.	28981.	30402.	1.000	27935.	1.000E+01	1.031E+06	.0000
28733.	413.	28320.	29741.	1.000	27311.	1.000E+01	1.110E+06	.0000
28386.	413.	27973.	29119.	1.000	26868.	1.000E+01	1.171E+06	.0000
28022.	413.	27609.	27474.	1.000	25988.	1.000E+00	1.305E+06	.0000
27984.	413.	27571.	29067.	1.000	26636.	7.900E+01	1.205E+06	.0001
27984.	691.	27293.	28787.	1.000	26373.	1.000E+00	1.244E+06	.0000
27984.	1014.	26970.	28466.	1.000	26069.	1.200E+02	1.292E+06	.0001
27984.	1014.	26970.	28466.	1.000	26069.	1.000E+00	1.292E+06	.0000
27984.	1014.	26970.	28466.	1.000	26069.	1.000E+00	1.292E+06	.0000
27984.	1072.	26912.	28310.	1.000	25973.	9.800E+01	1.308E+06	.0001
27981.	1072.	26909.	28307.	1.000	25970.	2.020E+02	1.308E+06	.0002
27981.	1173.	26808.	28166.	1.000	25858.	9.800E+01	1.327E+06	.0001
27715.	1173.	26542.	27860.	1.000	25591.	2.020E+02	1.372E+06	.0001
27715.	1676.	26039.	27397.	1.000	25133.	9.800E+01	1.456E+06	.0001
27229.	1676.	25553.	26878.	1.000	24661.	1.000E+01	1.549E+06	.0000
27229.	1676.	25553.	26878.	1.000	24661.	1.000E+01	1.549E+06	.0000
27229.	1676.	25553.	26878.	1.000	24661.	1.000E+00	1.549E+06	.0000
26122.	1676.	24446.	24040.	1.000	22891.	1.000E+01	1.974E+06	.0000
26109.	1676.	24433.	24969.	1.000	23273.	1.000E+01	1.870E+06	.0000
25633.	1676.	23957.	24921.	1.000	23004.	1.000E+00	1.943E+06	.0000
22233.	1676.	20557.	21430.	1.000	19758.	1.000E+01	3.688E+06	.0000
19249.	1676.	17573.	18321.	1.000	16891.	1.000E+01	8.373E+06	.0000
19216.	1676.	17540.	17426.	1.000	16498.	1.000E+00	9.647E+06	.0000
15440.	1676.	13764.	14443.	1.000	13269.	1.000E+01	1.000E+20	.0000
13646.	1676.	11970.	11861.	1.000	11246.	1.200E+02	1.000E+20	.0000
10942.	1676.	9266.	10037.	1.000	9064.	9.000E+00	1.000E+20	.0000
10942.	10939.	3.	-51.	1.000	-20.	2.910E+02	1.000E+20	.0000
							TOTAL USAGE FACTOR =	.0011

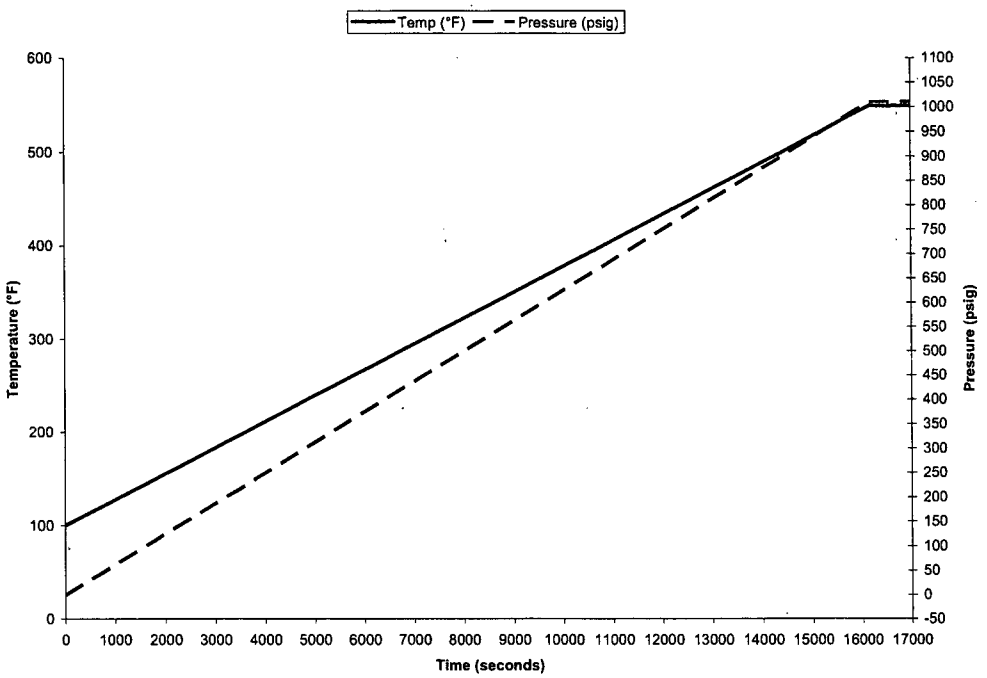

Figure 1: Transient 03: Start Up

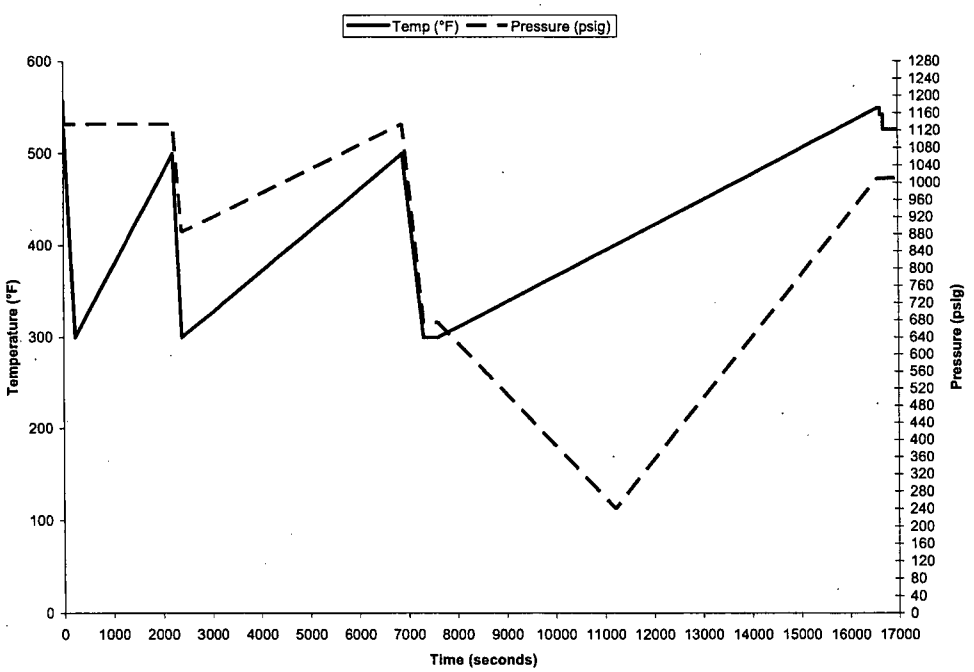

Figure 2: Transient 11: Loss of Feedwater Pumps, Isolation Valves Closed

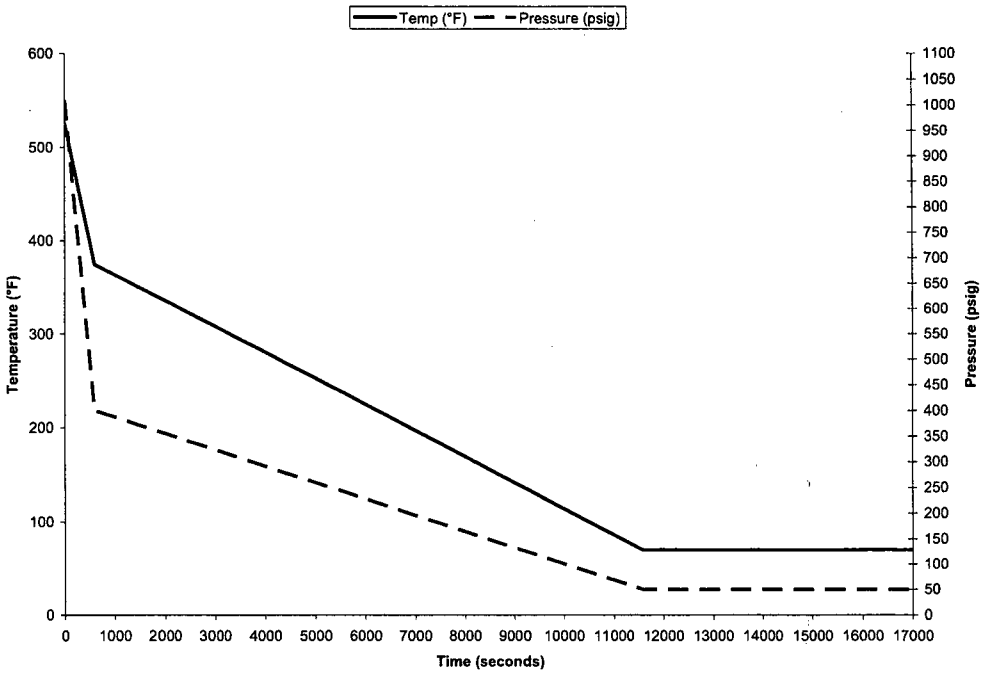

Figure 3: Transient 14: Single Relief or Safety Valve Blow Down

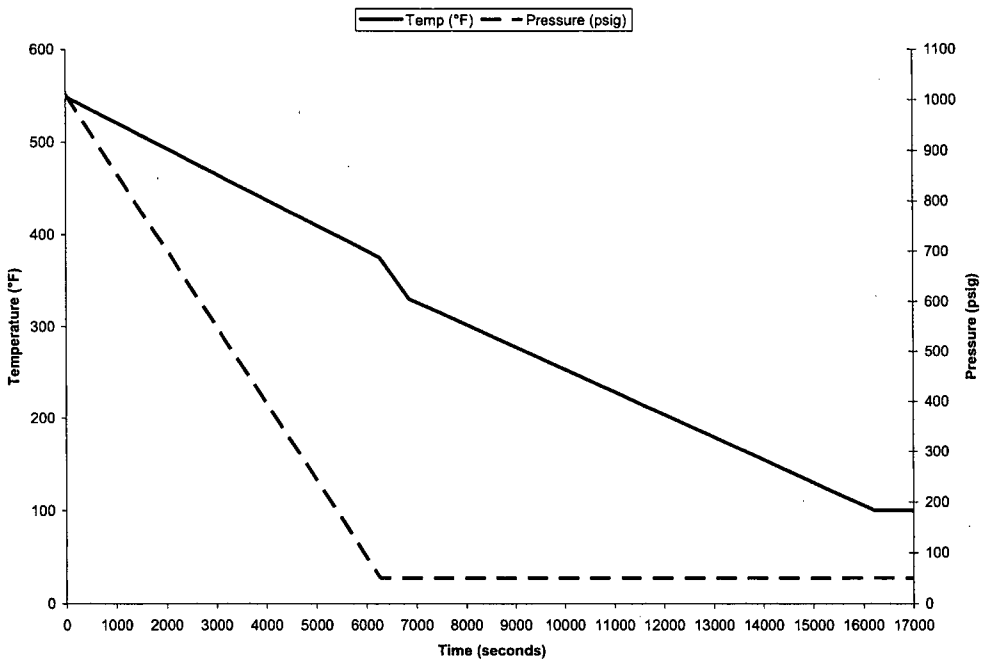

Figure 4: Transient 21-23: Shut Down Vessel Flooding

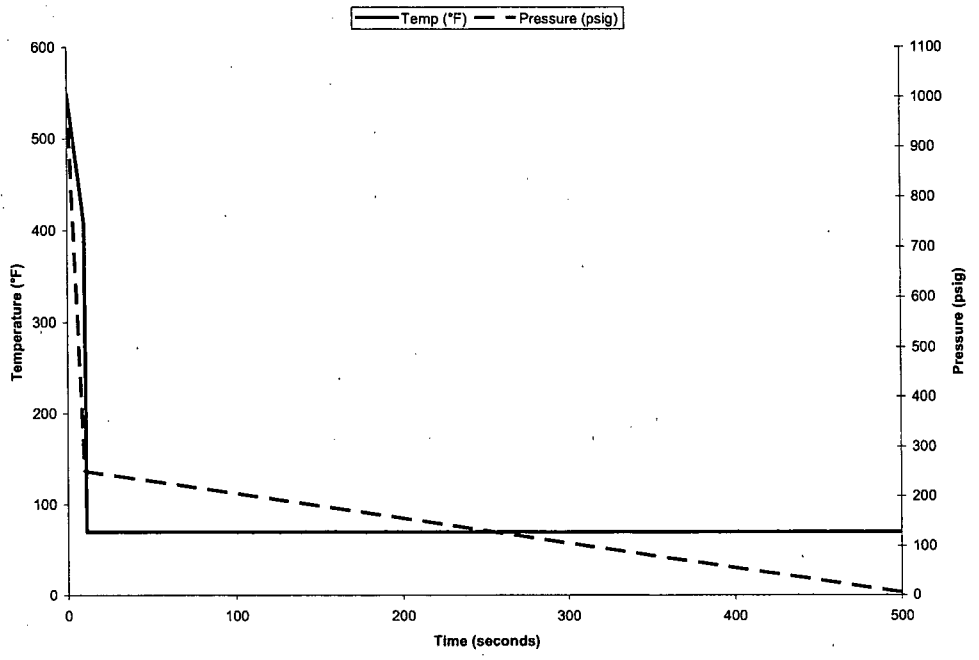

Figure 5: Transient 30: Emergency Shut Down 100% Flow (Safe End)

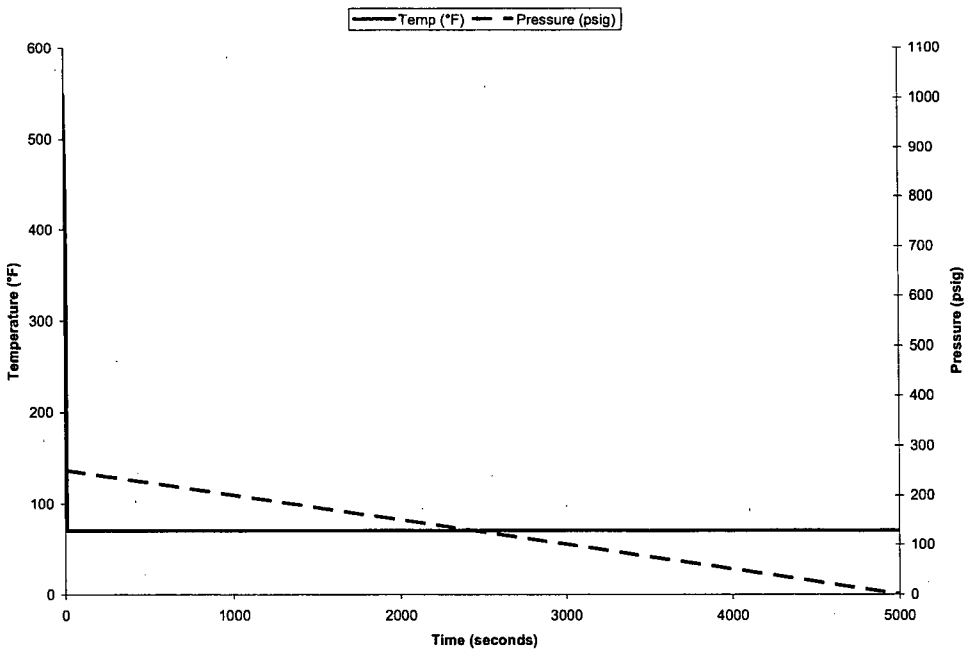

Figure 6: Transient 30: Emergency Shut Down 100% Flow (Blend Radius)

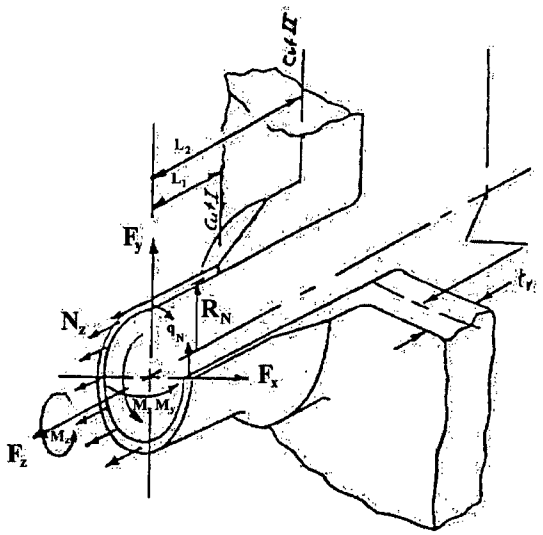

Figure 7: External Forces and Moments on the Core Spray Nozzle

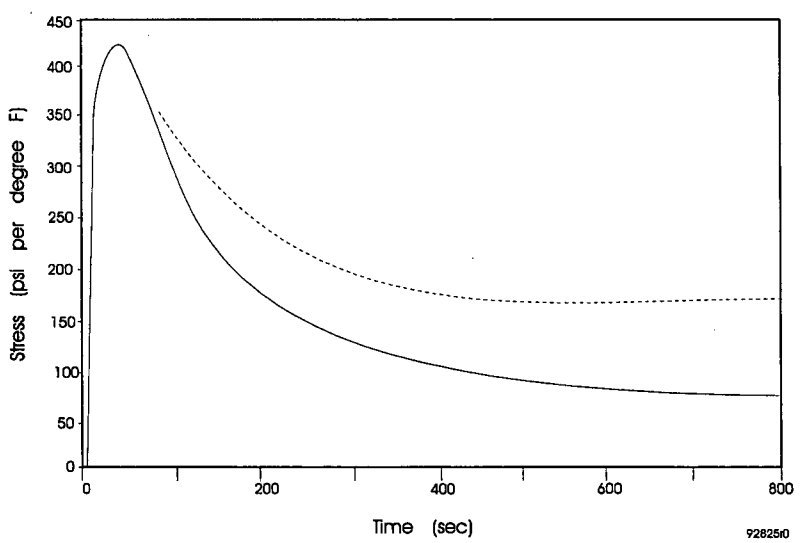

Figure 8: Typical Green's Functions for Thermal Transient Stress

Note: A typical set of two Green's Functions is shown, each for a different set of heat transfer coefficients (representing different flow rate conditions).

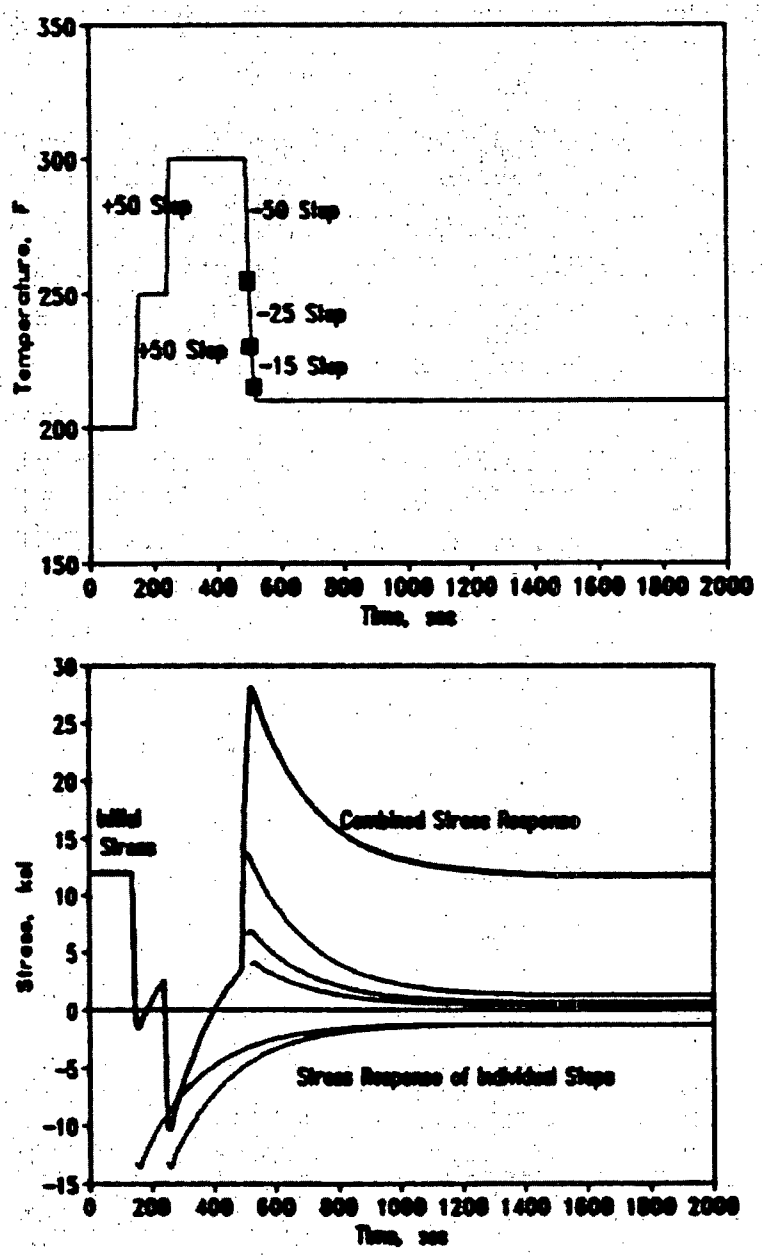

Figure 9: Typical Stress Response Using Green's Functions

APPENDIX A

INPUT AND OUTPUT FILES

Input Files

File Name	Description
TRANSNT_03.INP	Text file describing transient 03 for STRESS.EXE
TRANSNT_11.INP	Text file describing transient 11 for STRESS.EXE
TRANSNT_14.INP	Text file describing transient 14 for STRESS.EXE
TRANSNT_21_22_23.INP	Text file describing transients 21-23 for STRESS.EXE
TRANSNT_30.INP	Text file describing transient 30 for STRESS.EXE

Output Files

File Name	Description
P-V_03.OUT	Output text file of STRESS.EXE and P-V.EXE, Stress peaks and valleys of transient 03
P-V_11.OUT	Output text file of STRESS.EXE and P-V.EXE, Stress peaks and valleys of transient 11
P-V_14.OUT	Output text file of STRESS.EXE and P-V.EXE, Stress peaks and valleys of transient 14
P-V_21_22_23.OUT	Output text file of STRESS.EXE and P-V.EXE, Stress peaks and valleys of transients 21-23
P-V_30.OUT	Output text file of STRESS.EXE and P-V.EXE, Stress peaks and valleys of transient 30

Structural Integrity Associates, Inc.	File No.: VY-16Q-311
CALCULATION PACKAGE	**Project No.:** VY-16Q

PROJECT NAME:

Environmental Fatigue Analysis of VYNPS

CONTRACT NO.:

10150394

CLIENT:	**PLANT:**
Entergy Nuclear Operations, Inc.	Vermont Yankee Nuclear Power Station

CALCULATION TITLE:

Feedwater Class 1 Piping Fatigue Analysis

Document Revision	Affected Pages	Revision Description	Project Manager Approval Signature & Date	Preparer(s) & Checker(s) Signatures & Date
0	1-17, A1 – A38, B1 – B45 In Computer Files	Initial Issue	Terry J. Herrmann 7/20/2007	Keith R. Evon 7/16/2007 Ryan V. Perry 7/16/2007

Table of Contents

1.0 OBJECTIVE 3
2.0 METHODOLOGY 3
3.0 ASSUMPTIONS/DESIGN INPUT 11
4.0 ANALYSIS 14
5.0 RESULTS OF ANALYSIS 16
6.0 REFERENCES 17
APPENDIX A PIPESTRESS INPUT FILE ("FWHPCI.FRE") A1
APPENDIX B PIPESTRESS OUTPUT FILE ("FWHPCI.PRF") B1

List of Tables

Table 1: Thermal Cycle Definitions for Feedwater Line 4
Table 2: Material Properties for Feedwater System Class 1 Piping [2 App. E, 5] 12
Table 3: Feedwater/HPCI Piping Size Information [2] 13
Table 4: Thermal Cycle Load Cases 15

List of Figures

Figure 1: Feedwater/HPCI Piping from Anchor HD-36 to RPV Nozzles N-4A and N-4B 10

1.0 OBJECTIVE

The purpose of this calculation is to perform an ASME Section III, NB-3600 fatigue calculation (Including environmental fatigue) of the Vermont Yankee (VY) Class 1 feedwater piping located inside the drywell (originally analyzed to B31.1 requirements). This section of piping was originally identified in the Recommendation Report [6] for installing a fatigue monitoring system at VY.

The fatigue calculation performed herein is not a certified ASME Code NB-3600 stress and fatigue analysis. Rather, it is an evaluation for the purposes of establishing fatigue usage to accommodate fatigue monitoring of the subject B31.1 piping. Although the PIPESTRESS program implements all ASME Code NB-3600 equations, only the fatigue usage results are utilized. All stress limit checks, although calculated by the program, are ignored since satisfactory stress limit checks were performed as a part of the already existing governing B31.1 stress analyses for all piping systems.

2.0 METHODOLOGY

The Class 1 Loop A feedwater piping system line extending from anchor HD-36 to reactor pressure vessel (RPV) nozzles N-4A and N-4B was evaluated. This includes a portion of the HPCI line to support HPCI-HD35A [7], so that the appropriate stiffness affects of this line on the feedwater piping are included. This evaluation is also considered valid for the Loop B line extending from anchor HD-39 to RPV nozzles N-4C and N-4D for the following reasons:

1. The Class 1 sections of Loop A and Loop B are mirror images of each other. This evaluation includes piping beyond the Class 1 boundary check valve so that its influence on the Class 1 piping is taken into account. The final fatigue analysis will only consider points on the Class 1 portion of the piping.
2. A 14" HPCI line tees into Loop A and a 4" RCIC line tees into Loop B. The HPCI line is more than three times the size of the RCIC line and will therefore have a greater influence on the feedwater piping.
3. The transients defined in this calculation are the bounding set for the two loops.

The operating conditions for the Class 1 portion of the feedwater line were defined based on References [11 and 12]. The resulting piping transient definitions are specified in Table 1. For each thermal cycle, the operating temperatures for Regions I through V define the conditions to be applied to the model.

Region boundaries are defined at branches, transitions, or locations where temperature and flow conditions change. These boundary locations are also shown in Figure 1. A listing of the PIPESTRESS input file "FWHPCI.FRE" is given in Appendix A and is also included in the project computer files.

Table 1: Thermal Cycle Definitions for Feedwater Line

Transient Cycle	Description (1)	Piping Region (3)	Thermal Conditions (2)									Pressure Conditions		No. of Cycles (1)
			Oper. Temp. (°F)	T_{init} (°F)	T_{final} (°F)	Time (sec.)	Rate (°F/hr)	T_{avg} (°F)	Flow (%)	Ratio	(gpm)(4)	Pinit (psig)	Pfinal (psig)	
1	Design Hydrotest (Leak Test) (+)	I	100	70	100	1800	60	85	0	1	200.0	0.0	1100	120
		IIa	100	70	100	1800	60	85	0	1	150.0	0.0	1100	
		IIb	100	70	100	1800	60	85	0	1	150.0	0.0	1100	
		II	100	70	100	1800	60	85	0	1	150.0	0.0	50	
		III	100	70	100	1800	60	85	0	1	200.0	0.0	1100	
		IV	100	70	100	1800	60	85	0	1/2	100.0	0.0	1100	
		IVa	100	70	100	1800	60	85	0	1/2	100.0	0.0	1100	
		IVb	100	70	100	1800	60	85	0	1/2	100.0	0.0	1100	
		V	100	70	100	1800	60	85	0	1/2	100.0	0.0	1100	
2	Design Hydrotest (Leak Test) (-)	I	100	100	100	0	0	100	0	1	200.0	1100.0	50	120
		IIa	100	100	100	0	0	100	0	1	150.0	1100.0	50	
		IIb	100	100	100	0	0	100	0	1	150.0	1100.0	50	
		II	100	100	100	0	0	100	0	1	150.0	50.0	50	
		III	100	100	100	0	0	100	0	1	200.0	1100.0	50	
		IV	100	100	100	0	0	100	0	1/2	100.0	1100.0	50	
		IVa	100	100	100	0	0	100	0	1/2	100.0	1100.0	50	
		IVb	100	100	100	0	0	100	0	1/2	100.0	1100.0	50	
		V	100	100	100	0	0	100	0	1/2	100.0	1100.0	50	
3	Startup (+)	I	150	100	150	16164	11.1	125	0	1	200.0	50.0	1010	300
		IIa	150	100	150	16164	11.1	125	0	1	150.0	50.0	1010	
		IIb	125	100	125	16164	5.6	113	0	1	150.0	50.0	1010	
		II	100	100	100	16164	0.0	100	0	1	150.0	50.0	50	
		III	150	100	150	16164	11.1	125	0	1	200.0	50.0	1010	
		IV	150	100	150	16164	11.1	125	0	1/2	100.0	50.0	1010	
		IVa	283	100	283	16164	40.8	192	0	1/2	100.0	50.0	1010	
		IVb	416	100	416	16164	70.4	258	0	1/2	100.0	50.0	1010	
		V	549	100	549	16164	100	325	0	1/2	100.0	50.0	1010	
4	Turbine Roll & Increase to Rated Power 1 (-) (Includes 10 SCRAM, Loss of Feedwater Pumps and 300 Hot Standby - Feedwater Cycling)	I	100	150	100	0	STEP	125	15	1	1377.0	1010.0	1010	610
		IIa	100	150	100	0	STEP	125	0	1	150.0	1010.0	1010	
		IIb	100	125	100	0	STEP	113	0	1	150.0	1010.0	1010	
		II	100	100	100	0	STEP	100	0	1	150.0	50.0	50	
		III	100	150	100	0	STEP	125	15	1	1377.0	1010.0	1010	
		IV	100	150	100	0	STEP	125	15	1/2	688.5	1010.0	1010	
		IVa	100	283	100	0	STEP	192	15	1/2	688.5	1010.0	1010	
		IVb	100	416	100	0	STEP	258	15	1/2	688.5	1010.0	1010	
		V	100	549	100	0	STEP	325	15	1/2	688.5	1010.0	1010	
5	Turbine Roll & Increase to Rated Power 2 (+) (Includes 10 SCRAM, Loss of Feedwater Pumps, 1 Reactor Overpressure, 228 Other SCRAMS and 60 Turbine Generator Trip)	I	260	100	260	0	STEP	180	15	1	1377.0	1010.0	1010	599
		IIa	260	100	260	0	STEP	180	0	1	150.0	1010.0	1010	
		IIb	180	100	180	0	STEP	140	0	1	150.0	1010.0	1010	
		II	100	100	100	0	STEP	100	0	1	150.0	50.0	50	
		III	260	100	260	0	STEP	180	15	1	1377.0	1010.0	1010	
		IV	260	100	260	0	STEP	180	15	1/2	688.5	1010.0	1010	
		IVa	260	100	260	0	STEP	180	15	1/2	688.5	1010.0	1010	
		IVb	260	100	260	0	STEP	180	15	1/2	688.5	1010.0	1010	
		V	260	100	260	0	STEP	180	15	1/2	688.5	1010.0	1010	
6	Turbine Roll & Increase to Rated Power 3 (+) (Includes 10 SCRAM, Loss of Feedwater Pumps, 1 Reactor Overpressure, 228 Other SCRAMS and 60 Turbine Generator Trip)	I	392	260	392	1800	264	326	100	1	9180.0	1010.0	1010	599
		IIa	392	260	392	1800	264	326	0	1	150.0	1010.0	1010	
		IIb	246	180	246	1800	132	213	0	1	150.0	1010.0	1010	
		II	100	100	100	1800	0	100	0	1	150.0	50.0	50	
		III	392	260	392	1800	264	326	100	1	9180.0	1010.0	1010	
		IV	392	260	392	1800	264	326	100	1/2	4590.0	1010.0	1010	
		IVa	392	260	392	1800	264	326	100	1/2	4590.0	1010.0	1010	
		IVb	392	260	392	1800	264	326	100	1/2	4590.0	1010.0	1010	
		V	392	260	392	1800	264	326	100	1/2	4590.0	1010.0	1010	
7	Daily Reduction to 75% Power (-)	I	310	392	310	900	-328	351	75	1	6885.0	1010.0	1010	10000
		IIa	310	392	310	900	-328	351	0	1	150.0	1010.0	1010	
		IIb	205	246	205	900	-164	226	0	1	150.0	1010.0	1010	
		II	100	100	100	900	0	100	0	1	150.0	50.0	50	
		III	310	392	310	900	-328	351	75	1	6885.0	1010.0	1010	
		IV	310	392	310	900	-328	351	75	1/2	3442.5	1010.0	1010	
		IVa	310	392	310	900	-328	351	75	1/2	3442.5	1010.0	1010	
		IVb	310	392	310	900	-328	351	75	1/2	3442.5	1010.0	1010	
		V	310	392	310	900	-328	351	75	1/2	3442.5	1010.0	1010	
8	Daily Reduction to 75% Power (+)	I	392	310	392	900	328	351	75	1	6885.0	1010.0	1010	10000
		IIa	392	310	392	900	328	351	0	1	150.0	1010.0	1010	
		IIb	246	205	246	900	164	226	0	1	150.0	1010.0	1010	
		II	100	100	100	900	0	100	0	1	150.0	50.0	50	
		III	392	310	392	900	328	351	75	1	6885.0	1010.0	1010	
		IV	392	310	392	900	328	351	75	1/2	3442.5	1010.0	1010	
		IVa	392	310	392	900	328	351	75	1/2	3442.5	1010.0	1010	
		IVb	392	310	392	900	328	351	75	1/2	3442.5	1010.0	1010	
		V	392	310	392	900	328	351	75	1/2	3442.5	1010.0	1010	
9	Weekly Reduction to 50% Power (-)	I	280	392	280	1800	-224	336	50	1	4590.0	1010.0	1010	2000
		IIa	280	392	280	1800	-224	336	0	1	150.0	1010.0	1010	
		IIb	190	246	190	1800	-112	218	0	1	150.0	1010.0	1010	
		II	100	100	100	1800	0	100	0	1	150.0	50.0	50	
		III	280	392	280	1800	-224	336	50	1	4590.0	1010.0	1010	
		IV	280	392	280	1800	-224	336	50	1/2	2295.0	1010.0	1010	
		IVa	280	392	280	1800	-224	336	50	1/2	2295.0	1010.0	1010	
		IVb	280	392	280	1800	-224	336	50	1/2	2295.0	1010.0	1010	
		V	280	392	280	1800	-224	336	50	1/2	2295.0	1010.0	1010	

For notes, see last page of table.

Table 1: Thermal Cycle Definitions for Feedwater Line (continued)

Transient Cycle	Description (1)	Piping Region (3)	Thermal Conditions (2) Oper. Temp. (°F)	T_{init} (°F)	T_{final} (°F)	Time (sec.)	Rate (°F/hr)	T_{avg} (°F)	Flow (%)	Ratio	(gpm)(4)	Pressure Conditions Pinit (psig)	Pfinal (psig)	No. of Cycles (1)
10	Weekly Reduction to 50% Power (+)	I	392	280	392	1800	224	336	50	1	4590.0	1010.0	1010	2000
		IIa	392	280	392	1800	224	336	0	1	150.0	1010.0	1010	
		IIb	246	190	246	1800	112	218	0	1	150.0	1010.0	1010	
		II	100	100	100	1800	0	100	0	1	150.0	50.0	50	
		III	392	280	392	1800	224	336	50	1	4590.0	1010.0	1010	
		IV	392	280	392	1800	224	336	50	1/2	2295.0	1010.0	1010	
		IVa	392	280	392	1800	224	336	50	1/2	2295.0	1010.0	1010	
		IVb	392	280	392	1800	224	336	50	1/2	2295.0	1010.0	1010	
		V	392	280	392	1800	224	336	50	1/2	2295.0	1010.0	1010	
11	Loss of Feedwater Heater, Turbine Trip 1 (-) (Includes 10 Loss of Feedwater Heater Turbine Trip, and 300 Reduction to 0% Power)	I	265	392	265	1800	-254	329	50	1	4590.0	1010.0	1010	310
		IIa	265	392	265	1800	-254	329	0	1	150.0	1010.0	1010	
		IIb	182.5	246	182.5	1800	-127	214	0	1	150.0	1010.0	1010	
		II	100	100	100	1800	0	100	0	1	150.0	50.0	50	
		III	265	392	265	1800	-254	329	50	1	4590.0	1010.0	1010	
		IV	265	392	265	1800	-254	329	50	1/2	2295.0	1010.0	1010	
		IVa	265	392	265	1800	-254	329	50	1/2	2295.0	1010.0	1010	
		IVb	265	392	265	1800	-254	329	50	1/2	2295.0	1010.0	1010	
		V	265	392	265	1800	-254	329	50	1/2	2295.0	1010.0	1010	
12	Loss of Feedwater Heater, Turbine Trip 2 (-)	I	90	265	90	360	-1750	178	15	1	1377.0	1010.0	1010	10
		IIa	90	265	90	360	-1750	178	0	1	150.0	1010.0	1010	
		IIb	95	182.5	95	360	-875	139	0	1	150.0	1010.0	1010	
		II	100	100	100	360	0	100	0	1	150.0	50.0	50	
		III	90	265	90	360	-1750	178	15	1	1377.0	1010.0	1010	
		IV	90	265	90	360	-1750	178	15	1/2	688.5	1010.0	1010	
		IVa	90	265	90	360	-1750	178	15	1/2	688.5	1010.0	1010	
		IVb	90	265	90	360	-1750	178	15	1/2	688.5	1010.0	1010	
		V	90	265	90	360	-1750	178	15	1/2	688.5	1010.0	1010	
13	Loss of Feedwater Heater, Turbine Trip 3 (+)	I	265	90	265	900	700	178	15	1	1377.0	1010.0	1010	10
		IIa	265	90	265	900	700	178	0	1	150.0	1010.0	1010	
		IIb	182.5	95	182.5	900	350	139	0	1	150.0	1010.0	1010	
		II	100	100	100	900	0	100	0	1	150.0	50.0	50	
		III	265	90	265	900	700	178	15	1	1377.0	1010.0	1010	
		IV	265	90	265	900	700	178	15	1/2	688.5	1010.0	1010	
		IVa	265	90	265	900	700	178	15	1/2	688.5	1010.0	1010	
		IVb	265	90	265	900	700	178	15	1/2	688.5	1010.0	1010	
		V	265	90	265	900	700	178	15	1/2	688.5	1010.0	1010	
14	Loss of Feedwater Heater, Turbine Trip 4 (+)	I	392	265	392	1800	254	329	50	1	4590.0	1010.0	1010	10
		IIa	392	265	392	1800	254	329	0	1	150.0	1010.0	1010	
		IIb	246	182.5	246	1800	127	214	0	1	150.0	1010.0	1010	
		II	100	100	100	1800	0	100	0	1	150.0	50.0	50	
		III	392	265	392	1800	254	329	50	1	4590.0	1010.0	1010	
		IV	392	265	392	1800	254	329	50	1/2	2295.0	1010.0	1010	
		IVa	392	265	392	1800	254	329	50	1/2	2295.0	1010.0	1010	
		IVb	392	265	392	1800	254	329	50	1/2	2295.0	1010.0	1010	
		V	392	265	392	1800	254	329	50	1/2	2295.0	1010.0	1010	
15	Loss of Feedwater Heater, FW Heater Bypass (-)	I	265	392	265	90	-5080	329	100	1	9180.0	1010.0	1010	70
		IIa	265	392	265	90	-5080	329	0	1	150.0	1010.0	1010	
		IIb	182.5	246	182.5	90	-2540	214	0	1	150.0	1010.0	1010	
		II	100	100	100	90	0	100	0	1	150.0	50.0	50	
		III	265	392	265	90	-5080	329	100	1	9180.0	1010.0	1010	
		IV	265	392	265	90	-5080	329	100	1/2	4590.0	1010.0	1010	
		IVa	265	392	265	90	-5080	329	100	1/2	4590.0	1010.0	1010	
		IVb	265	392	265	90	-5080	329	100	1/2	4590.0	1010.0	1010	
		V	265	392	265	90	-5080	329	100	1/2	4590.0	1010.0	1010	
16	Loss of Feedwater Heater, FW Heater Bypass (+)	I	392	265	392	180	2540	329	100	1	9180.0	1010.0	1010	70
		IIa	392	265	392	180	2540	329	0	1	150.0	1010.0	1010	
		IIb	246	182.5	246	180	1270	214	0	1	150.0	1010.0	1010	
		II	100	100	100	180	0	100	0	1	150.0	50.0	50	
		III	392	265	392	180	2540	329	100	1	9180.0	1010.0	1010	
		IV	392	265	392	180	2540	329	100	1/2	4590.0	1010.0	1010	
		IVa	392	265	392	180	2540	329	100	1/2	4590.0	1010.0	1010	
		IVb	392	265	392	180	2540	329	100	1/2	4590.0	1010.0	1010	
		V	392	265	392	180	2540	329	100	1/2	4590.0	1010.0	1010	
17	SCRAM, T.G. Trip, Reactor Overpressure, and All Other Scrams 1 (-) (Includes 1 Reactor Overpressure, 228 Other SCRAMS and 60 Turbine Generator Trip)	I	275	392	275	60	-7020	334	110	1	10098.0	1010.0	1010	289
		IIa	275	392	275	60	-7020	334	0	1	150.0	1010.0	1010	
		IIb	187.5	246	187.5	60	-3510	217	0	1	150.0	1010.0	1010	
		II	100	100	100	60	0	100	0	1	150.0	50.0	50	
		III	275	392	275	60	-7020	334	110	1	10098.0	1010.0	1010	
		IV	275	392	275	60	-7020	334	110	1/2	5049.0	1010.0	1010	
		IVa	275	392	275	60	-7020	334	110	1/2	5049.0	1010.0	1010	
		IVb	275	392	275	60	-7020	334	110	1/2	5049.0	1010.0	1010	
		V	275	392	275	60	-7020	334	110	1/2	5049.0	1010.0	1010	
18	SCRAM, T.G. Trip, Reactor Overpressure, and All Other Scrams 2 (-) (Includes 1 Reactor Overpressure, 228 Other SCRAMS and 60 Turbine Generator Trip)	I	100	275	100	900	-700	188	3	1	275.4	1010.0	1010	289
		IIa	100	275	100	900	-700	188	0	1	150.0	1010.0	1010	
		IIb	100	187.5	100	900	-350	144	0	1	150.0	1010.0	1010	
		II	100	100	100	900	0	100	0	1	150.0	50.0	50	
		III	100	275	100	900	-700	188	3	1	275.4	1010.0	1010	
		IV	100	275	100	900	-700	188	3	1/2	137.7	1010.0	1010	
		IVa	100	275	100	900	-700	188	3	1/2	137.7	1010.0	1010	
		IVb	100	275	100	900	-700	188	3	1/2	137.7	1010.0	1010	
		V	100	275	100	900	-700	188	3	1/2	137.7	1010.0	1010	

For notes, see last page of table.

Table 1: Thermal Cycle Definitions for Feedwater Line (continued)

Transient Cycle	Description (1)	Piping Region (3)	Thermal Conditions (2) Oper. Temp. (°F)	T_{init} (°F)	T_{final} (°F)	Time (sec.)	Rate (°F/hr)	T_{avg} (°F)	Flow (%)	Ratio	(gpm)(4)	Pressure Conditions Pinit (psig)	Pfinal (psig)	No. of Cycles (1)
19	Hot Standby 1 (+)	I	265	265	265	0	STEP	265	0	1	200.0	1010.0	1010	300
		IIa	265	265	265	0	STEP	265	0	1	150.0	1010.0	1010	
		IIb	182.5	182.5	182.5	0	STEP	183	0	1	150.0	1010.0	1010	
		II	100	100	100	0	STEP	100	0	1	150.0	50.0	50	
		III	265	265	265	0	STEP	265	0	1	200.0	1010.0	1010	
		IV	265	265	265	0	STEP	265	0	1/2	100.0	1010.0	1010	
		IVa	323	265	323	0	STEP	294	0	1/2	100.0	1010.0	1010	
		IVb	382	265	382	0	STEP	324	0	1/2	100.0	1010.0	1010	
		V	440	265	440	0	STEP	353	0	1/2	100.0	1010.0	1010	
20	Hot Standby 2 (+)	I	265	265	265	0	0	265	0	1	200.0	1010.0	1010	300
		IIa	265	265	265	0	0	265	0	1	150.0	1010.0	1010	
		IIb	182.5	182.5	182.5	0	0	183	0	1	150.0	1010.0	1010	
		II	100	100	100	0	0	100	0	1	150.0	50.0	50	
		III	265	265	265	0	0	265	0	1	200.0	1010.0	1010	
		IV	265	265	265	0	0	265	0	1/2	100.0	1010.0	1010	
		IVa	360	323	360	3924	34	342	0	1/2	100.0	1010.0	1010	
		IVb	454	382	454	3924	66	418	0	1/2	100.0	1010.0	1010	
		V	549	440	549	3924	100	495	0	1/2	100.0	1010.0	1010	
21	Hot Standby 3 (-)	I	150	265	150	4140	-100	208	0	1	200.0	1010.0	1010	300
		IIa	150	265	150	4140	-100	208	0	1	150.0	1010.0	1010	
		IIb	125	182.5	125	4140	-50	154	0	1	150.0	1010.0	1010	
		II	100	100	100	0	0	100	0	1	150.0	50.0	50	
		III	150	265	150	4140	-100	208	0	1	200.0	1010.0	1010	
		IV	150	265	150	4140	-100	208	0	1/2	100.0	1010.0	1010	
		IVa	283	360	283	4140	-67	322	0	1/2	100.0	1010.0	1010	
		IVb	416	454	416	4140	-33	435	0	1/2	100.0	1010.0	1010	
		V	549	549	549	0	0	549	0	1/2	100.0	1010.0	1010	
22	Shutdown 1 (-)	I	150	150	150	0	0	150	0	1	200.0	1010.0	170	300
		IIa	150	150	150	0	0	150	0	1	150.0	1010.0	170	
		IIb	125	125	125	0	0	125	0	1	150.0	1010.0	170	
		II	100	100	100	0	0	100	0	1	150.0	50.0	50	
		III	150	150	150	0	0	150	0	1	200.0	1010.0	170	
		IV	150	150	150	0	0	150	0	1/2	100.0	1010.0	170	
		IVa	225	283	225	6264	-33	254	0	1/2	100.0	1010.0	170	
		IVb	300	416	300	6264	-67	358	0	1/2	100.0	1010.0	170	
		V	375	549	375	6264	-100	462	0	1/2	100.0	1010.0	170	
23	Shutdown 2 (-)	I	150	150	150	0	0	150	0	1	200.0	170.0	88	300
		IIa	150	150	150	0	0	150	0	1	150.0	170.0	88	
		IIb	125	125	125	0	0	125	0	1	150.0	170.0	88	
		II	100	100	100	0	0	100	0	1	150.0	50.0	50	
		III	150	150	150	0	0	150	0	1	200.0	170.0	88	
		IV	150	150	150	0	0	150	0	1/2	100.0	170.0	88	
		IVa	210	225	210	600	-90	218	0	1/2	100.0	170.0	88	
		IVb	270	300	270	600	-180	285	0	1/2	100.0	170.0	88	
		V	330	375	330	600	-270	353	0	1/2	100.0	170.0	88	
24	Shutdown 3 (-)	I	100	150	100	8280	-22	125	0	1	200.0	88.0	50	300
		IIa	100	150	100	8280	-22	125	0	1	150.0	88.0	50	
		IIb	100	125	100	8280	-11	113	0	1	150.0	88.0	50	
		II	100	100	100	8280	0	100	0	1	150.0	50.0	50	
		III	100	150	100	8280	-22	125	0	1	200.0	88.0	50	
		IV	100	150	100	8280	-22	125	0	1/2	100.0	88.0	50	
		IVa	100	210	100	8280	-48	155	0	1/2	100.0	88.0	50	
		IVb	100	270	100	8280	-74	185	0	1/2	100.0	88.0	50	
		V	100	330	100	8280	-100	215	0	1/2	100.0	88.0	50	
25	SCRAM, Loss of Feedwater Pumps 1 (+)	I	392	392	392	12	0	392	0	1	200.0	1010.0	1190	10
		IIa	392	392	392	12	0	392	0	1	150.0	1010.0	1190	
		IIb	246	246	246	12	0	246	0	1	150.0	1010.0	1190	
		II	100	100	100	12	0	100	0	1	150.0	50.0	50	
		III	392	392	392	12	0	392	0	1	200.0	1010.0	1190	
		IV	392	392	392	12	0	392	0	1/2	100.0	1010.0	1190	
		IVa	450	392	450	12	17400	421	0	1/2	100.0	1010.0	1190	
		IVb	507	392	507	12	34500	450	0	1/2	100.0	1010.0	1190	
		V	565	392	565	12	51900	479	0	1/2	100.0	1010.0	1190	
26	SCRAM, Loss of Feedwater Pumps 2 (-) (First HPCI)	I	50	392	50	0	STEP	221	40	1	3672.0	1190.0	1135	10
		IIa	50	392	50	0	STEP	221	40	1	3672.0	1190.0	1135	
		IIb	50	246	50	0	STEP	148	40	1	3672.0	1190.0	1135	
		II	50	100	50	0	STEP	75	40	1	3672.0	50.0	1135	
		III	50	392	50	0	STEP	221	40	1	3672.0	1190.0	1135	
		IV	50	392	50	0	STEP	221	40	1/2	1836.0	1190.0	1135	
		IVa	50	450	50	0	STEP	250	40	1/2	1836.0	1190.0	1135	
		IVb	50	507	50	0	STEP	279	40	1/2	1836.0	1190.0	1135	
		V	50	565	50	0	STEP	308	40	1/2	1836.0	1190.0	1135	
27	SCRAM, Loss of Feedwater Pumps 3 (+)	I	150	50	150	1380	261	100	0	1	200.0	1135.0	1135	10
		IIa	150	50	150	1380	261	100	0	1	150.0	1135.0	1135	
		IIb	125	50	125	1380	196	88	0	1	150.0	1135.0	1135	
		II	100	50	100	1380	130	75	0	1	150.0	1135.0	50	
		III	150	50	150	1380	261	100	0	1	200.0	1135.0	1135	
		IV	150	50	150	1380	261	100	0	1/2	100.0	1135.0	1135	
		IVa	247	50	247	1380	514	149	0	1/2	100.0	1135.0	1135	
		IVb	343	50	343	1380	764	197	0	1/2	100.0	1135.0	1135	
		V	440	50	440	1380	1017	245	0	1/2	100.0	1135.0	1135	

For notes, see last page of table.

Table 1: Thermal Cycle Definitions for Feedwater Line (continued)

Transient Cycle	Description (1)	Piping Region (3)	Thermal Conditions (2) Oper. Temp. (°F)	T_{init} (°F)	T_{final} (°F)	Time (sec.)	Rate (°F/hr)	T_{avg} (°F)	Flow (%)	Ratio	(gpm)(4)	Pressure Conditions Pinit (psig)	Pfinal (psig)	No. of Cycles (1)
28	SCRAM, Loss of Feedwater Pumps 4 (+)	I	150	150	150	0	STEP	150	0	1	200.0	1135.0	1135	10
		IIa	150	150	150	0	STEP	150	0	1	150.0	1135.0	1135	
		IIb	125	125	125	0	STEP	125	0	1	150.0	1135.0	1135	
		II	100	100	100	0	STEP	100	0	1	150.0	50.0	50	
		III	150	150	150	0	STEP	150	0	1	200.0	1135.0	1135	
		IV	150	150	150	0	STEP	150	0	1/2	100.0	1135.0	1135	
		IVa	288	247	288	0	STEP	268	0	1/2	100.0	1135.0	1135	
		IVb	427	343	427	0	STEP	385	0	1/2	100.0	1135.0	1135	
		V	565	440	565	0	STEP	503	0	1/2	100.0	1135.0	1135	
29	SCRAM, Loss of Feedwater Pumps 5 (-) (Second HPCI)	I	50	150	50	0	STEP	100	30	1	2754.0	1135.0	885	10
		IIa	50	150	50	0	STEP	100	30	1	2754.0	1135.0	885	
		IIb	50	125	50	0	STEP	88	30	1	2754.0	1135.0	885	
		II	50	100	50	0	STEP	75	30	1	2754.0	1135.0	885	
		III	50	150	50	0	STEP	100	30	1	2754.0	1135.0	885	
		IV	50	150	50	0	STEP	100	30	1/2	1377.0	1135.0	885	
		IVa	50	288	50	0	STEP	169	30	1/2	1377.0	1135.0	885	
		IVb	50	427	50	0	STEP	239	30	1/2	1377.0	1135.0	885	
		V	50	565	50	0	STEP	308	30	1/2	1377.0	1135.0	885	
30	SCRAM, Loss of Feedwater Pumps 6 (+)	I	150	50	150	3060	118	100	0	1	200.0	885.0	1060	10
		IIa	150	50	150	3060	118	100	0	1	150.0	885.0	1060	
		IIb	125	50	125	3060	88	88	0	1	150.0	885.0	1060	
		II	100	50	100	3060	59	75	0	1	150.0	885.0	50	
		III	150	50	150	3060	118	100	0	1	200.0	885.0	1060	
		IV	150	50	150	3060	118	100	0	1/2	100.0	885.0	1060	
		IVa	247	50	247	3060	232	149	0	1/2	100.0	885.0	1060	
		IVb	343	50	343	3060	345	197	0	1/2	100.0	885.0	1060	
		V	440	50	440	3060	459	245	0	1/2	100.0	885.0	1060	
31	SCRAM, Loss of Feedwater Pumps 7 (+)	I	150	150	150	0	STEP	150	0	1	200.0	1060.0	1135	10
		IIa	150	150	150	0	STEP	150	0	1	150.0	1060.0	1135	
		IIb	125	125	125	0	STEP	125	0	1	150.0	1060.0	1135	
		II	100	100	100	0	STEP	100	0	1	150.0	50.0	50	
		III	150	150	150	0	STEP	150	0	1	200.0	1060.0	1135	
		IV	150	150	150	0	STEP	150	0	1/2	100.0	1060.0	1135	
		IVa	283	247	283	0	STEP	265	0	1/2	100.0	1060.0	1135	
		IVb	416	343	416	0	STEP	380	0	1/2	100.0	1060.0	1135	
		V	549	440	549	0	STEP	495	0	1/2	100.0	1060.0	1135	
32	SCRAM, Loss of Feedwater Pumps 8 (-) (Third HPCI)	I	50	150	50	0	STEP	100	17	1	1560.6	1135.0	675	10
		IIa	50	150	50	0	STEP	100	17	1	1560.6	1135.0	675	
		IIb	50	125	50	0	STEP	88	17	1	1560.6	1135.0	675	
		II	50	100	50	0	STEP	75	17	1	1560.6	50.0	675	
		III	50	150	50	0	STEP	100	17	1	1560.6	1135.0	675	
		IV	50	150	50	0	STEP	100	17	1/2	780.3	1135.0	675	
		IVa	50	283	50	0	STEP	167	17	1/2	780.3	1135.0	675	
		IVb	50	416	50	0	STEP	233	17	1/2	780.3	1135.0	675	
		V	50	549	50	0	STEP	300	17	1/2	780.3	1135.0	675	
33	SCRAM, Loss of Feedwater Pumps 9 (+)	I	150	50	150	300	1200	100	0	1	200.0	675.0	675	10
		IIa	150	50	150	300	1200	100	0	1	150.0	675.0	675	
		IIb	125	50	125	300	900	88	0	1	150.0	675.0	675	
		II	100	50	100	300	600	75	0	1	150.0	675.0	50	
		III	150	50	150	300	1200	100	0	1	200.0	675.0	675	
		IV	150	50	150	300	1200	100	0	1/2	100.0	675.0	675	
		IVa	200	50	200	300	1800	125	0	1/2	100.0	675.0	675	
		IVb	250	50	250	300	2400	150	0	1/2	100.0	675.0	675	
		V	300	50	300	300	3000	175	0	1/2	100.0	675.0	675	
34	SCRAM, Loss of Feedwater Pumps 10 (+)	I	150	150	150	8964	0	150	0	1	200.0	240.0	1010	10
		IIa	150	150	150	8964	0	150	0	1	150.0	240.0	1010	
		IIb	125	125	125	8964	0	125	0	1	150.0	240.0	1010	
		II	100	100	100	8964	0	100	0	1	150.0	50.0	50	
		III	150	150	150	8964	0	150	0	1	200.0	240.0	1010	
		IV	150	150	150	8964	0	150	0	1/2	100.0	240.0	1010	
		IVa	283	200	283	8964	33	242	0	1/2	100.0	240.0	1010	
		IVb	416	250	416	8964	67	333	0	1/2	100.0	240.0	1010	
		V	549	300	549	8964	100	425	0	1/2	100.0	240.0	1010	
35	SCRAM, SRV Blowdown 1 (-)	I	275	392	275	60	-7020	334	110	1	10098.0	1010.0	885	1
		IIa	275	392	275	60	-7020	334	0	1	150.0	1010.0	885	
		IIb	187.5	246	187.5	60	-3510	217	0	1	150.0	1010.0	885	
		II	100	100	100	60	0	100	0	1	150.0	50.0	50	
		III	275	392	275	60	-7020	334	110	1	10098.0	1010.0	885	
		IV	275	392	275	60	-7020	334	110	1/2	5049.0	1010.0	885	
		IVa	275	392	275	60	-7020	334	110	1/2	5049.0	1010.0	885	
		IVb	275	392	275	60	-7020	334	110	1/2	5049.0	1010.0	885	
		V	275	392	275	60	-7020	334	110	1/2	5049.0	1010.0	885	
36	SCRAM, SRV Blowdown 2 (-)	I	100	275	100	900	-700	188	3	1	275.4	885.0	50	1
		IIa	100	275	100	900	-700	188	0	1	150.0	885.0	50	
		IIb	100	187.5	100	900	-350	144	0	1	150.0	885.0	50	
		II	100	100	100	900	0	100	0	1	150.0	50.0	50	
		III	100	275	100	900	-700	188	3	1	275.4	885.0	50	
		IV	100	275	100	900	-700	188	3	1/2	137.7	885.0	50	
		IVa	100	275	100	900	-700	188	3	1/2	137.7	885.0	50	
		IVb	100	275	100	900	-700	188	3	1/2	137.7	885.0	50	
		V	100	275	100	900	-700	188	3	1/2	137.7	885.0	50	

For notes, see last page of table.

Table 1: Thermal Cycle Definitions for Feedwater Line (continued)

Transient Cycle	Description (1)	Piping Region (3)	Thermal Conditions (2) Oper. Temp. (°F)	T_{init} (°F)	T_{final} (°F)	Time (sec.)	Rate (°F/hr)	T_{avg} (°F)	Flow (%)	Ratio	(gpm)(4)	Pressure Conditions Pinit (psig)	Pfinal (psig)	No. of Cycles (1)
37	Hydrostatic Test (+)	I	100	100	100	0	0	100	0	1	200.0	50.0	1563	1
		IIa	100	100	100	0	0	100	0	1	150.0	50.0	1563	
		IIb	100	100	100	0	0	100	0	1	150.0	50.0	1563	
		II	100	100	100	0	0	100	0	1	150.0	50.0	50	
		III	100	100	100	0	0	100	0	1	200.0	50.0	1563	
		IV	100	100	100	0	0	100	0	1/2	100.0	50.0	1563	
		IVa	100	100	100	0	0.0	100	0	1/2	100.0	50.0	1563	
		IVb	100	100	100	0	0.0	100	0	1/2	100.0	50.0	1563	
		V	100	100	100	0	0	100	0	1/2	100.0	50.0	1563	
38	Hydrostatic Test (-)	I	100	100	100	0	0	100	0	1	200.0	1563.0	50	1
		IIa	100	100	100	0	0	100	0	1	150.0	1563.0	50	
		IIb	100	100	100	0	0	100	0	1	150.0	1563.0	50	
		II	100	100	100	0	0	100	0	1	150.0	50.0	50	
		III	100	100	100	0	0	100	0	1	200.0	1563.0	50	
		IV	100	100	100	0	0	100	0	1/2	100.0	1563.0	50	
		IVa	100	100	100	0	0.0	100	0	1/2	100.0	1563.0	50	
		IVb	100	100	100	0	0.0	100	0	1/2	100.0	1563.0	50	
		V	100	100	100	0	0	100	0	1/2	100.0	1563.0	50	
39	SCRAM, T.G. Trip, Reactor Overpressure, and All Other Scrams 1 (-) (Includes 1 Reactor Overpressure, 228 Other SCRAMS and 60 Turbine Generator Trip)	I	392	392	392	60	0	392	110	1	10098.0	1010.0	1375	289
		IIa	392	392	392	60	0	392	0	1	150.0	1010.0	1375	
		IIb	246	246	246	60	0	246	0	1	150.0	1010.0	1375	
		II	100	100	100	60	0	100	0	1	150.0	50.0	50	
		III	392	392	392	60	0	392	110	1	10098.0	1010.0	1375	
		IV	392	392	392	60	0	392	110	1/2	5049.0	1010.0	1375	
		IVa	392	392	392	60	0	392	110	1/2	5049.0	1010.0	1375	
		IVb	392	392	392	60	0	392	110	1/2	5049.0	1010.0	1375	
		V	392	392	392	60	0	392	110	1/2	5049.0	1010.0	1375	
40	SCRAM, T.G. Trip, Reactor Overpressure, and All Other Scrams 2 (-) (Includes 1 Reactor Overpressure, 228 Other SCRAMS and 60 Turbine Generator Trip)	I	392	392	392	900	0	392	3	1	275.4	1375.0	940	289
		IIa	392	392	392	900	0	392	0	1	150.0	1375.0	940	
		IIb	246	246	246	900	0	246	0	1	150.0	1375.0	940	
		II	100	100	100	900	0	100	0	1	150.0	50.0	50	
		III	392	392	392	900	0	392	3	1	275.4	1375.0	940	
		IV	392	392	392	900	0	392	3	1/2	137.7	1375.0	940	
		IVa	392	392	392	900	0	392	3	1/2	137.7	1375.0	940	
		IVb	392	392	392	900	0	392	3	1/2	137.7	1375.0	940	
		V	392	392	392	900	0	392	3	1/2	137.7	1375.0	940	
41	SCRAM, T.G. Trip, Reactor Overpressure, and All Other Scrams 3 (-) (Includes 1 Reactor Overpressure, 228 Other SCRAMS and 60 Turbine Generator Trip)	I	392	392	392	900	0	392	3	1	275.4	940.0	1010	289
		IIa	392	392	392	900	0	392	0	1	150.0	940.0	1010	
		IIb	246	246	246	900	0	246	0	1	150.0	940.0	1010	
		II	100	100	100	900	0	100	0	1	150.0	50.0	50	
		III	392	392	392	900	0	392	3	1	275.4	940.0	1010	
		IV	392	392	392	900	0	392	3	1/2	137.7	940.0	1010	
		IVa	392	392	392	900	0	392	3	1/2	137.7	940.0	1010	
		IVb	392	392	392	900	0	392	3	1/2	137.7	940.0	1010	
		V	392	392	392	900	0	392	3	1/2	137.7	940.0	1010	
42	Hot Standby, Feedwater Cycling 1 (+)	I	125	100	125	60	1500	113	0	1	200.0	1010.0	1010	300
		IIa	125	100	125	60	1500	113	0	1	150.0	1010.0	1010	
		IIb	112.5	100	112.5	60	750	106	0	1	150.0	1010.0	1010	
		II	100	100	100	60	0	100	0	1	150.0	50.0	50	
		III	125	100	125	60	1500	113	0	1	200.0	1010.0	1010	
		IV	125	100	125	60	1500	113	0	1/2	100.0	1010.0	1010	
		IVa	180	100	180	60	4800	140	0	1/2	100.0	1010.0	1010	
		IVb	235	100	235	60	8100	168	0	1/2	100.0	1010.0	1010	
		V	290	100	290	60	11400	195	0	1/2	100.0	1010.0	1010	
43	Hot Standby, Feedwater Cycling 2 (+)	I	150	125	150	210	429	138	0	1	200.0	1010.0	1010	300
		IIa	150	125	150	210	429	138	0	1	150.0	1010.0	1010	
		IIb	125	112.5	125	210	214	119	0	1	150.0	1010.0	1010	
		II	100	100	100	210	0	100	0	1	150.0	50.0	50	
		III	150	125	150	210	429	138	0	1	200.0	1010.0	1010	
		IV	150	125	150	210	429	138	0	1/2	100.0	1010.0	1010	
		IVa	283	180	283	210	1766	232	0	1/2	100.0	1010.0	1010	
		IVb	416	235	416	210	3103	326	0	1/2	100.0	1010.0	1010	
		V	549	290	549	210	4440	420	0	1/2	100.0	1010.0	1010	

For notes, see next page.

Table 1: Thermal Cycle Definitions for Feedwater Line (concluded)

Notes:

1. From Reference [13].

2. Normal operating conditions are 1,010 psig, 549°F (steam dome), 392°F (feedwater), and 4590 gpm (feedwater nozzle) [14].

3. See Figure 1.

4. For the transients where flow is stopped, the natural convection heat transfer coefficient was used. The same approximate value was used within each region. These values are:

   - 200 gpm for Regions I and III.
   - 150 gpm for Regions II, IIa, and IIb.
   - 100 gpm for Regions IV and V.

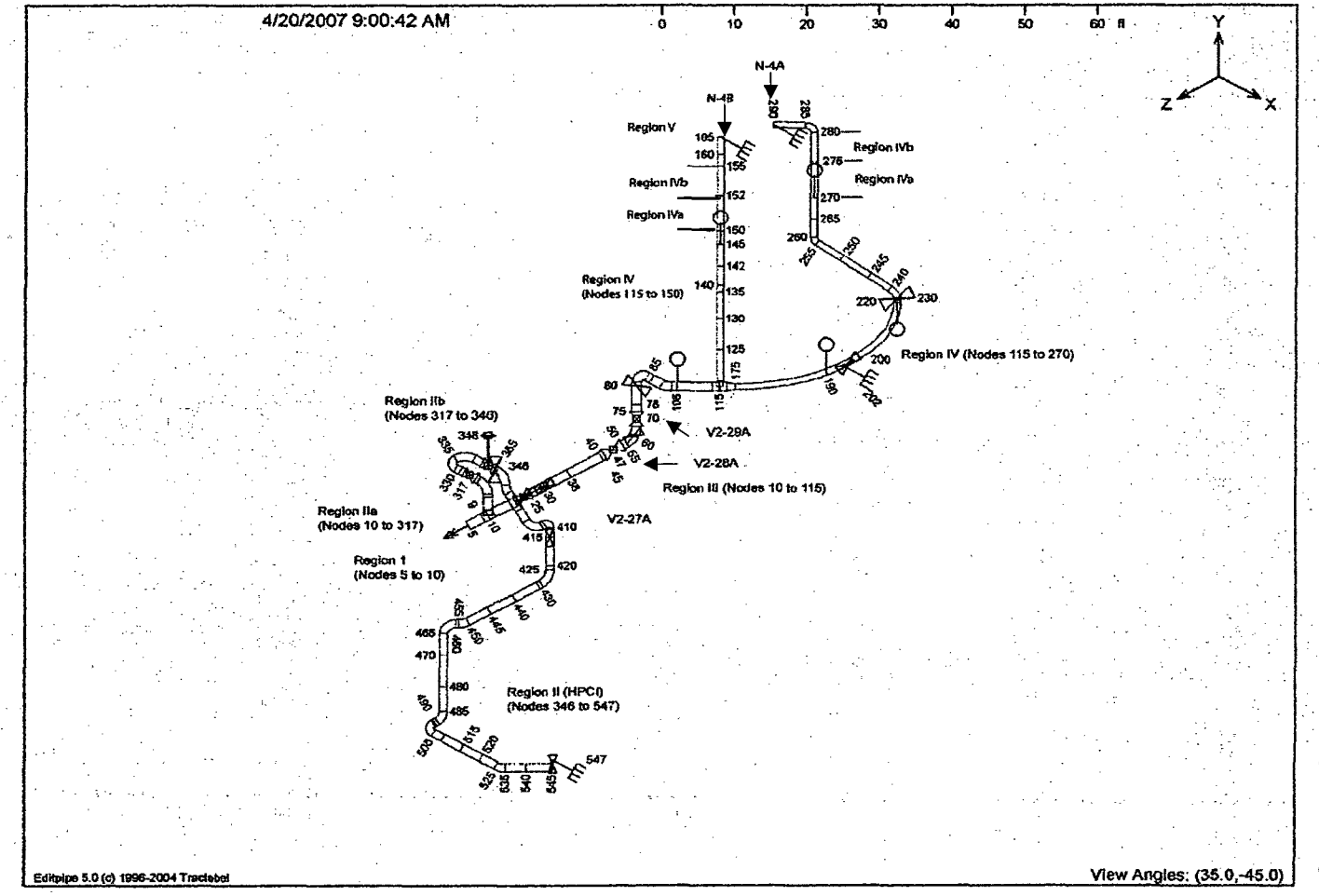

Figure 1: Feedwater/HPCI Piping from Anchor HD-36 to RPV Nozzles N-4A and N-4B

3.0 ASSUMPTIONS/DESIGN INPUT

In order to take advantage of improvements in the ASME Code that result in a lower calculated fatigue usage, this evaluation is done to the ASME Boiler and Pressure Vessel Code, Section III, 1998 Edition with 2000 Addenda [9]. The 1998 Edition of Section III (with 2000 Addenda) has been accepted by the US NRC for use in design analyses. Although there are a few restrictions on the application of this Edition, they involve the use of optional increased allowables that are not being used in this calculation.

A piping model was created using PIPESTRESS [1]. The calculation [2] that had previously analyzed the subject Class 1 feedwater piping contains the ADLPIPE input file used to create the PIPESTRESS input file for this evaluation. Valve dimensions and properties were also obtained from the ADLPIPE input file. The piping model is composed of one carbon steel grade (maximum carbon content of 0.30 %) [2]. Temperature dependent material properties were used with values obtained from Reference [5]. Table 2 summarizes these values. The resulting PIPESTRESS model (including boundary conditions) is shown in Figure 1. The drawings for both feedwater loops [3, 4] and the HPCI line [7] were also consulted to aid in building the PIPESTRESS model.

Assumptions:

1) The weight of insulation is included in the analysis and PIPESTRESS calculates the heat transfer effects of insulation.
2) Node 545 is the end of the as-modeled HPCI piping system. This is appropriate because of the distance from the HPCI/Feedwater tee, six pipe supports in the segment and multiple pipe direction changes.

The feedwater and HPCI line sizes are specified in the previous calculation [2] and are shown in Table 3.

Table 2: Material Properties for Feedwater System Class 1 Piping [2 App. E, 5]

SA 106 B and SA-234 WPB (Carbon Silicon Steel, C-Si)							
Temperature (°F)	Young's Modulus ($x10^6$ psi)	Coefficient of Linear Thermal Expansion (in/100 ft)	Mean Coefficient of Thermal Expansion(1) (10^{-6} /in/in/°F)	Thermal Conductivity(1) (btu/hr/ft/°F)	Thermal Diffusivity(1) (ft^2/hr)	Yield Stress S_y (ksi)	Design Stress Intensity S_m (ksi)
50	29.6	0(2)				35.0	20.0
70	29.5	0	6.4	27.5	0.529	35.0	20.0
100	29.3	0.2		27.6	0.512	35.0	20.0
150				27.6	0.496		
200	28.8	1.0		27.6	0.486	32.1	20.0
250				27.4	0.467		
300	28.3	1.9		27.2	0.453	31.0	20.0
350				27.0	0.440		
400	27.7	2.8		26.7	0.428	29.9	20.0
450				26.3	0.413		
500	27.3	3.7		25.9	0.398	28.5	18.9
550				25.5	0.387		
600	26.7	4.7		25.0	0.374	26.8	17.3

Notes:

1. These properties are used for the transient analysis only.
2. Assumed equivalent to the value at 70°F.

The material properties applied in the analyses are taken from ASME Section II Part D 1998 Edition with 2000 Addenda. This is consistent with information provided in the Design Input Record (page 13 of VY EC No. 1773, SI File No. VY-16Q-209). The use of a later code edition than that used for the original design code is acceptable since later editions typically reflect more accurate material properties than was published in prior Code editions.

Table 3: Feedwater/HPCI Piping Size Information [2]

	16" FW Downstream of V2-29A	16" FW Upstream of V2-29A	10" FW	14" HPCI
Pipe Schedule	80	120	120	120
Fittings Schedule	120	---	120	---
Piping O.D. (in.)	16.0	16.0	10.75	14.0
Piping Nom. Wall (in.)	0.843	1.218	0.843	1.093
Fitting Nom. Wall (in.)	1.218	---	0.843	---
Pipe Weight[1] (lb/ft)	136.46	192.3	89.20	150.7
Insulation Weight (lb/ft)	14.64	11.98	8.92	10.65[2]

Note:
1. Weight of contents automatically added by the PIPESTRESS Program.
2. Insulation weight assumed to be consistent with thickness (2 inches) and composition of insulation on the 16" FW upstream of V2-29A.

4.0 ANALYSIS

Through-wall thermal gradient terms were calculated by the PIPESTRESS program for all of the transients. Table 1 defines each thermal cycle definition (i.e., transient load case) and the region of the modeled piping those conditions are applicable.

The forces and moments due to differential thermal expansion need to be included in the fatigue evaluation. The differential thermal expansion cases as analyzed by the piping program, PIPESTRESS, correspond to the end temperature and pressure of the transient. Table 4 lists the thermal expansion cases.

The material properties were obtained from the ASME Code Section II, 1998 Edition, Part D, with 2000 Addenda [5]. E and α are taken at 70°F, and k, ρ, and c_p are taken at the average temperature over the range of the individual transients.

The internal heat transfer coefficient h for the transients with flow occurring in the pipe is calculated based on the following relation for forced convection [8]:

$$h = 0.023\ Re^{0.8}\ Pr^{0.4}\ k/D$$

Where Re = Reynolds number
Pr = Prandtl number

The heat transfer coefficients were calculated by PIPESTRESS using the above relation. The flow rates described for each transient in Table 1 were used. For the transients where flow is stopped, the natural convection heat transfer coefficient was used. The formula for h is [8]:

$$h = 0.55\ (Gr\ Pr)^{0.25} k/L$$

Where Gr = Grashof Number
L = pipe diameter

PIPESTRESS only has the forced convection heat transfer formula built in, so an equivalent flow rate was determined that would give the same heat transfer coefficient as the free convection coefficient.

As discussed in the next section, the PIPESTRESS input file "FWHPCI.FRE" will be run and analyzed to Section III, Subsection NB-3600 of ASME 1998 Edition [9] in order to evaluate acceptable fatigue usage values for the Class 1 feedwater loop A system. The code option available in PIPESTRESS is the 1998 edition without addenda. This is acceptable as the 1999 and 2000 addenda to the 1998 code did not change the fatigue analysis method which PIPESTRESS uses.

A Listing of the PIPESTRESS input is included as Appendix A.

Table 4: Thermal Cycle Load Cases

Load Set	Transients Represented	Region I Temp. (°F)	Region IIa Temp. (°F)	Region IIb Temp. (°F)	Region II Temp. (°F)	Region III Temp. (°F)	Region IV Temp. (°F)	Region IVa Temp. (°F)	Region IVb Temp. (°F)	Region V Temp. (°F)	Vessel Temp. (°F)	Region II Pressure (psig)	All other Regions Pressure (psig)
1	1	100	100	100	100	100	100	100	100	100	100	50	1100
2	2, 24, 36, 38	100	100	100	100	100	100	100	100	100	100	50	50
3	3, 21, 34, 43	150	150	125	100	150	150	283	416	549	549	50	1010
4	5	260	260	180	100	260	260	260	260	260	549	50	1010
5	6, 8, 10, 14, 16	392	392	246	100	392	392	392	392	392	549	50	1010
6	7	310	310	205	100	310	310	310	310	310	549	50	1010
7	9	280	280	190	100	280	280	280	280	280	549	50	1010
8	11, 13, 15	265	265	182.5	100	265	265	265	265	265	549	50	1010
9	12	90	90	95	100	90	90	90	90	90	549	50	1010
10	20	265	265	182.5	100	265	265	360	454	549	549	50	1010
11	22	150	150	125	100	150	150	225	300	375	375	50	170
12	23	150	150	125	100	150	150	210	270	330	330	50	88
13	25	392	392	246	100	392	392	450	507	565	565	50	1190
14	26	50	50	50	50	50	50	50	50	50	565	1135	1135
15	27	150	150	125	100	150	150	247	343	440	565	50	1135
16	28	150	150	125	100	150	150	288	427	565	565	50	1135
17	30	150	150	125	100	150	150	247	343	440	555	50	1060
18	31	150	150	125	100	150	150	283	416	549	565	50	1135
19	32	50	50	50	50	50	50	50	50	50	502	675	675
20	33	150	150	125	100	150	150	200	250	300	502	50	675
21	35	275	275	187.5	100	275	275	275	275	275	549	50	885
22	37	100	100	100	100	100	100	100	100	100	100	50	1563
23	39	392	392	246	100	392	392	392	392	392	600	50	1375
24	40	392	392	246	100	392	392	392	392	392	539	50	940
25	41	392	392	246	100	392	392	392	392	392	549	50	1010
26	17	275	275	187.5	100	275	275	275	275	275	539	50	1010
27	19	265	265	182.5	100	265	265	323	382	440	549	50	1010
28	4	100	100	100	100	100	100	100	100	100	549	50	1010
29	18	100	100	100	100	100	100	100	100	100	539	50	1010
30	42	125	125	112.5	100	125	125	180	235	290	549	50	1010
31	29	50	50	50	50	50	50	50	50	50	532	885	885

5.0 RESULTS OF ANALYSIS

Since the piping at VY was designed in accordance with USAS B31.1 methodology, fatigue analysis does not exist for the piping. Therefore, fatigue calculations are being developed for selected locations in the Class 1 piping systems at VY. This will result in detailed, Class 1 fatigue calculations for each selected location. Piping models and transient definitions have been developed for the Class 1 portion of the feedwater system, as documented in the previous sections of this calculation.

The limiting total fatigue usage for the analyzed feedwater/HPCI piping system occurs at Node 155 on the riser to the feedwater nozzle. The total usage at this location is U = 0.1661 (per the PIPESTRESS report FWHPCI.PRF) which passes Class 1 fatigue evaluation. The second highest total fatigue usage for the analyzed feedwater/HPCI piping system occurs at Node 175, the 16" to 10" reducer on the feedwater piping. The total usage at this location is U = 0.1114 (per the PIPESTRESS report FWHPCI.PRF) which passes Class 1 fatigue evaluation. The environmental fatigue multiplier to use from Reference [10] is 1.74. The total usage including environmental effects is therefore 0.289.

Appendix B contains the fatigue usage summary for node 155.

6.0 REFERENCES

1. PIPESTRESS, Version 3.5.1+0.26, DST Computer Services S.A., QA-1670-301, June, 2004.

2. HPCI/FW Piping Stress Information. ADLPIPE listing for FDW & HPCI piping from Calculation No. VYC-551, Rev. 2, Appendix A, SI File No. VY-05Q-229.

3. Vermont Yankee Nuclear Power Corp. Drawing No. VYI-FDW-Part 5, Rev. 1, "Piping Isometric Feedwater: Drywell-Main Steam Tunnel (FDW) Part 5," SI File No. VY-05Q-221.

4. Vermont Yankee Nuclear Power Corp. Drawing No. VYI-FDW-Part 5A, Rev. 1, "Piping Isometric Feedwater: Main Steam Tunnel and Drywell FDW-Part 5A," SI File No. VY-05Q-221.

5. American Society of Mechanical Engineers Boiler & Pressure Vessel Code, Section II, Materials, Part D, "Properties (Customary)," 1998 Edition including the 2000 Addenda.

6. Structural Integrity Associates Report No. SIR-01-130, Revision 0, "System Review and Recommendations for a Transient and Fatigue Monitoring System at the Vermont Yankee Nuclear Power Station," February 2002, SI File No. VY-05Q-401.

7. Vermont Yankee Nuclear Power Corp. Drawing No. VYI-HPCI-Part 5, Rev. 0, "Piping Isometric Drawing High Pressure Coolant Injection Main Steam Tunnel-Torus Area (HPCI) Part 5," SI File No. VY-05Q-223.

8. Holman, J.P., *Heat Transfer*, Fifth Edition, McGraw-Hill, 1981.

9. American Society of Mechanical Engineers Boiler & Pressure Vessel Code, Section III, Rules for Construction of Nuclear Facility Components, 1998 Edition including the 2000 Addenda.

10. Structural Integrity Associates Calculation No. VY-16Q-303, Revision 0, "Environmental Fatigue Evaluation of Reactor Recirculation Inlet Nozzle and Vessel Shell/Bottom Head."

11. "Reactor Thermal Cycles," Attachment 1, page 2, of Entergy Design Input Record (DIR) EC No. 1773, Revision 0, "Environmental Fatigue Analysis for Vermont Yankee Nuclear Power Station," 7/3/07, SI File No. VY-16Q-209.

12. "Nozzle Thermal Cycles (Feedwater)," Attachment 1, page 3, of Entergy Design Input Record (DIR) EC No. 1773, Revision 0, "Environmental Fatigue Analysis for Vermont Yankee Nuclear Power Station," 7/3/07, SI File No. VY-16Q-209.

13. "Reactor Thermal Cycles for 60 Years of Operation," Attachment 1 of Entergy Design Input Record (DIR) EC No. 1773, Revision 0, "Environmental Fatigue Analysis for Vermont Yankee Nuclear Power Station," 7/3/07, SI File No. VY-16Q-209.

14. GE Certified Design Specification No. 26A6019, Revision 1, "REACTOR VESSEL – EXTENDED POWER UPRATE," August 29, 2003, SI File No. VY-05Q-236.

APPENDIX A

PIPESTRESS INPUT FILE ("FWHPCI.FRE")

(Pages A1 – A38)

```
IDEN JB=2     *Job number (1 to 9999)
     CD=1     *1=ASME Section III
     VA=0     *0=Calculate            2=Verify
     GR=-Y    *Direction of gravity
     IU=1     *Input units            0=SIU        1=USA
     OU=1     *Output units           0=SIU        1=USA
     CH=$     *Delimiter character
     AB=T     *FREE errors =abort
     PL=$Vermont Yankee$
     EN=$KRE$
TITL BL=3     *Modeling option:
              *  3 =uniform mass for static analysis
              *      lumped mass for dynamic analysis
              *      rotational inertia ignored
     GL=1     *Report forces/moment         0=Global     1=Local     2=G et L
     SU=1     *Support summary              0=No         1=Yes
     CV=15    *Code version - See Manual
     HS=1     *Highest 20 stress ratios for each case
     MD=1     *Hot modulus
     TI=$Vermont Yankee Feedwater Piping$
        $SI Fatigue Analysis$
FREQ RF=1 RP=8 FR=33 MP=20 MX=70 TI=$SEISMIC$
*
*************************************
**** THERMAL CYCLE LOAD CASES****
*************************************
LCAS RF=0 CA=1 TY=0 TI=$LC-1$      *TC-1
LCAS RF=0 CA=2 TY=0 TI=$LC-2$      *TC-2,24,36,38
LCAS RF=0 CA=3 TY=0 TI=$LC-3$      *TC-3,21,34,43
LCAS RF=0 CA=4 TY=0 TI=$LC-4$      *TC-5
LCAS RF=0 CA=5 TY=0 TI=$LC-5$      *TC-6,8,10,14,16
LCAS RF=0 CA=6 TY=0 TI=$LC-6$      *TC-7
LCAS RF=0 CA=7 TY=0 TI=$LC-7$      *TC-9
LCAS RF=0 CA=8 TY=0 TI=$LC-8$      *TC-11,13,15
LCAS RF=0 CA=9 TY=0 TI=$LC-9$      *TC-12
LCAS RF=0 CA=10 TY=0 TI=$LC-10$    *TC-20
LCAS RF=0 CA=11 TY=0 TI=$LC-11$    *TC-22
LCAS RF=0 CA=12 TY=0 TI=$LC-12$    *TC-23
LCAS RF=0 CA=13 TY=0 TI=$LC-13$    *TC-25
LCAS RF=0 CA=14 TY=0 TI=$LC-14$    *TC-26, 29
LCAS RF=0 CA=15 TY=0 TI=$LC-15$    *TC-27
LCAS RF=0 CA=16 TY=0 TI=$LC-16$    *TC-28
LCAS RF=0 CA=17 TY=0 TI=$LC-17$    *TC-30
LCAS RF=0 CA=18 TY=0 TI=$LC-18$    *TC-31
LCAS RF=0 CA=19 TY=0 TI=$LC-19$    *TC-32
LCAS RF=0 CA=20 TY=0 TI=$LC-20$    *TC-33
LCAS RF=0 CA=21 TY=0 TI=$LC-21$    *TC-35
LCAS RF=0 CA=22 TY=0 TI=$LC-22$    *TC-37
LCAS RF=0 CA=23 TY=0 TI=$LC-23$    *TC-39
LCAS RF=0 CA=24 TY=0 TI=$LC-24$    *TC-40
LCAS RF=0 CA=25 TY=0 TI=$LC-25$    *TC-41
LCAS RF=0 CA=26 TY=0 TI=$LC-26$    *TC-17
LCAS RF=0 CA=27 TY=0 TI=$LC-27$    *TC-19
LCAS RF=0 CA=28 TY=0 TI=$LC-28$    *TC-4
LCAS RF=0 CA=29 TY=0 TI=$LC-29$    *TC-18
LCAS RF=0 CA=30 TY=0 TI=$LC-30$    *TC-42
```

```
LCAS RF=0 CA=31 TY=0 TI=$LC-31     *TC-29
LCAS RF=6 CA=32 TY=6 TI=$SAM$
*********************
**** WEIGHT CASES****
*********************
LCAS CA=101  RF=1  TY=3  TI=$OPERATING WEIGHT$
LCAS CA=102  RF=2  TY=4  TI=$HYDROTEST WEIGHT$
*
*******************************
**** THERMAL TRANSIENT CASES****
*******************************
TCAS CA=201 RP=1 TI=$Design Hydrotest +$
TCAS CA=202 RP=1 TI=$Design Hydrotest -$
TCAS CA=203 RP=1 TI=$Startup +$
TCAS CA=204 RP=1 TI=$TRoll & Inc. PWR1 -$
TCAS CA=205 RP=1 TI=$TRoll & Inc. PWR2 +$
TCAS CA=206 RP=1 TI=$TRoll & Inc. PWR3 +$
TCAS CA=207 RP=1 TI=$DlyReduction to 75% -$
TCAS CA=208 RP=1 TI=$DlyReduction to 75% +$
TCAS CA=209 RP=1 TI=$WklyReduct to 50% -$
TCAS CA=210 RP=1 TI=$WklyReduct to 50% +$
TCAS CA=211 RP=1 TI=$LOFWH+TT 1 -$
TCAS CA=212 RP=1 TI=$LOFWH+TT 2 -$
TCAS CA=213 RP=1 TI=$LOFWH+TT 3 +$
TCAS CA=214 RP=1 TI=$LOFWH+TT 4 +$
TCAS CA=215 RP=1 TI=$LOFWH+PFWHTR Byp -$
TCAS CA=216 RP=1 TI=$LOFWH+PFWHTR Byp +$
TCAS CA=217 RP=1 TI=$SCRAM+TT+AllOtrScm -$
TCAS CA=218 RP=1 TI=$SCRAM+TT+AllOtrScm -$
TCAS CA=219 RP=1 TI=$HotStandby 1 +$
TCAS CA=220 RP=1 TI=$HotStandby 2 +$
TCAS CA=221 RP=1 TI=$HotStandby 3 -$
TCAS CA=222 RP=1 TI=$Shutdown 1 -$
TCAS CA=223 RP=1 TI=$Shutdown 2 -$
TCAS CA=224 RP=1 TI=$Shutdown 3 -$
TCAS CA=225 RP=1 TI=$SCRAM+LOFWP1 +$
TCAS CA=226 RP=1 TI=$SCRAM+LOFWP2 -$
TCAS CA=227 RP=1 TI=$SCRAM+LOFWP3 +$
TCAS CA=228 RP=1 TI=$SCRAM+LOFWP4 +$
TCAS CA=229 RP=1 TI=$SCRAM+LOFWP5 -$
TCAS CA=230 RP=1 TI=$SCRAM+LOFWP6 +$
TCAS CA=231 RP=1 TI=$SCRAM+LOFWP7 +$
TCAS CA=232 RP=1 TI=$SCRAM+LOFWP8 -$
TCAS CA=233 RP=1 TI=$SCRAM+LOFWP9 +$
TCAS CA=234 RP=1 TI=$SCRAM+LOFWP10+$
TCAS CA=235 RP=1 TI=$SCRAM+SRVBLDN1-$
TCAS CA=236 RP=1 TI=$SCRAM+SRVBLDN2-$
TCAS CA=237 RP=1 TI=$Hydro Test +$
TCAS CA=238 RP=1 TI=$Hydro Test -$
TCAS CA=239 RP=1 TI=$SCRAM+TG+OPres1 -$
TCAS CA=240 RP=1 TI=$SCRAM+TG+OPres2 -$
TCAS CA=241 RP=1 TI=$SCRAM+TG+OPres3 -$
TCAS CA=242 RP=1 TI=$HotSby_FWcyc +$
TCAS CA=243 RP=1 TI=$HotSby_FWcyc +$
**********************
**** SEISMIC CASES****
```

```
**********************
RCAS CA=103 EQ=3 EV=1 TY=1 SU=1 LO=1 FX=1 FY=1 FZ=1 TI=$OBE INERTIA$
*
** *************************
**** LOAD COMBINATION CASES *
** *************************
CCAS RF=1 CA=104      ME=1 FL=1  C1=103 CY=10  TI=$OBE$
CCAS RF=1 CA=401 SS=1 ME=1 EQ=3  C1=102 C2=103 TI=$EQUATION 9 LEVEL B$
CCAS RF=1 CA=402 SS=1 ME=3 F1=1  C1=103 C2=6 C3=32 TI=$NORMAL+OBE$
CCAS RF=1 CA=403 SS=1 ME=3 F1=-1 C1=103 C2=6 C3=32 TI=$NORMAL-OBE$
*
******************
**** LOAD SETS****
******************
*RF field is the highest temperature and pressure of the transient
*PR and MO fields are the final temperature and pressure of the transient
LSET RF=1  RP=1 CY=120   PR=1  MO=1  TR=+201 TI=$Design Hydrotest +    LS-1$
LSET RF=2  RP=1 CY=120   PR=2  MO=2  TR=-202 TI=$Design Hydrotest -    LS-2$
LSET RF=3  RP=1 CY=300   PR=3  MO=3  TR=+203 TI=$Startup +             LS-3$
LSET RF=3  RP=1 CY=610   PR=28 MO=28 TR=-204 TI=$TRoll & Inc. PWR1 -   LS-4$
LSET RF=4  RP=1 CY=599   PR=4  MO=4  TR=+205 TI=$TRoll & Inc. PWR2 +   LS-5$
LSET RF=5  RP=1 CY=599   PR=5  MO=5  TR=+206 TI=$TRoll & Inc. PWR3 +   LS-6$
LSET RF=5  RP=1 CY=10000 PR=6  MO=6  TR=-207 TI=$DlyReduction to 75% - LS-7$
LSET RF=5  RP=1 CY=10000 PR=5  MO=5  TR=+208 TI=$DlyReduction to 75% + LS-8$
LSET RF=5  RP=1 CY=2000  PR=7  MO=7  TR=-209 TI=$WklyReduct to 50% -   LS-9$
LSET RF=5  RP=1 CY=2000  PR=5  MO=5  TR=+210 TI=$WklyReduct to 50% +   LS-10$
LSET RF=5  RP=1 CY=310   PR=8  MO=8  TR=-211 TI=$LOFWH+TT 1 -          LS-11$
LSET RF=8  RP=1 CY=10    PR=9  MO=9  TR=-212 TI=$LOFWH+TT 2 -          LS-12$
LSET RF=8  RP=1 CY=10    PR=8  MO=8  TR=+213 TI=$LOFWH+TT 3 +          LS-13$
LSET RF=5  RP=1 CY=10    PR=5  MO=5  TR=+214 TI=$LOFWH+TT 4 +          LS-14$
LSET RF=5  RP=1 CY=70    PR=8  MO=8  TR=-215 TI=$LOFWH+PFWHTR Byp -    LS-15$
LSET RF=5  RP=1 CY=70    PR=5  MO=5  TR=+216 TI=$LOFWH+PFWHTR Byp +    LS-16$
LSET RF=5  RP=1 CY=289   PR=26 MO=26 TR=-217 TI=$SCRAM+TT+AllOtrScm -  LS-17$
LSET RF=26 RP=1 CY=289   PR=29 MO=29 TR=-218 TI=$SCRAM+TT+AllOtrScm -  LS-18$
LSET RF=27 RP=1 CY=300   PR=27 MO=27 TR=+219 TI=$HotStandby 1 +        LS-19$
LSET RF=10 RP=1 CY=300   PR=10 MO=10 TR=+220 TI=$HotStandby 2 +        LS-20$
LSET RF=10 RP=1 CY=300   PR=3  MO=3  TR=-221 TI=$HotStandby 3 -        LS-21$
LSET RF=3  RP=1 CY=300   PR=11 MO=11 TR=-222 TI=$Shutdown 1 -          LS-22$
LSET RF=11 RP=1 CY=300   PR=12 MO=12 TR=-223 TI=$Shutdown 2 -          LS-23$
LSET RF=12 RP=1 CY=300   PR=2  MO=2  TR=-224 TI=$Shutdown 3 -          LS-24$
LSET RF=13 RP=1 CY=10    PR=13 MO=13 TR=+225 TI=$SCRAM+LOFWP1 +        LS-25$
LSET RF=13 RP=1 CY=10    PR=14 MO=14 TR=-226 TI=$SCRAM+LOFWP2 -        LS-26$
LSET RF=15 RP=1 CY=10    PR=15 MO=15 TR=+227 TI=$SCRAM+LOFWP3 +        LS-27$
LSET RF=16 RP=1 CY=10    PR=16 MO=16 TR=+228 TI=$SCRAM+LOFWP4 +        LS-28$
LSET RF=16 RP=1 CY=10    PR=31 MO=31 TR=-229 TI=$SCRAM+LOFWP5 -        LS-29$
LSET RF=17 RP=1 CY=10    PR=17 MO=17 TR=+230 TI=$SCRAM+LOFWP6 +        LS-30$
LSET RF=18 RP=1 CY=10    PR=18 MO=18 TR=+231 TI=$SCRAM+LOFWP7 +        LS-31$
LSET RF=18 RP=1 CY=10    PR=19 MO=19 TR=-232 TI=$SCRAM+LOFWP8 -        LS-32$
LSET RF=20 RP=1 CY=10    PR=20 MO=20 TR=+233 TI=$SCRAM+LOFWP9 +        LS-33$
LSET RF=3  RP=1 CY=10    PR=3  MO=3  TR=+234 TI=$SCRAM+LOFWP10+        LS-34$
LSET RF=5  RP=1 CY=1     PR=21 MO=21 TR=-235 TI=$SCRAM+SRVBLDN1-       LS-35$
LSET RF=21 RP=1 CY=1     PR=2  MO=2  TR=-236 TI=$SCRAM+SRVBLDN2-       LS-36$
LSET RF=22 RP=1 CY=1     PR=22 MO=22 TR=+237 TI=$Hydro Test +          LS-37$
LSET RF=2  RP=1 CY=1     PR=2  MO=2  TR=-238 TI=$Hydro Test -          LS-38$
LSET RF=23 RP=1 CY=289   PR=23 MO=23 TR=-239 TI=$SCRAM+TG+OPres1 -     LS-39$
LSET RF=24 RP=1 CY=289   PR=24 MO=24 TR=-240 TI=$SCRAM+TG+OPres2 -     LS-40$
```

```
LSET RF=25 RP=1 CY=289   PR=25 MO=25 TR=-241 TI=$SCRAM+TG+OPres3 -     LS-41$
LSET RF=30 RP=1 CY=300   PR=30 MO=30 TR=+242 TI=$HotSbyFWcyc + .       LS-42$
LSET RF=3  RP=1 CY=300   PR=3  MO=3  TR=+243 TI=$HotSbyFWcyc +         LS-43$
*
LSET RF=6 CY=5 FL=1 PR=6 MO=402 TI=$NORMAL+OBE  LS-132$
LSET RF=6 CY=5 FL=1 PR=6 MO=403 TI=$NORMAL-OBE  LS-133$

**************************
**** RESPONSE SPECTRA****
*************************
*SSE response spectra conservatively used
SPEC FS=OBE EV=1 ME=3 FP=1 TI=$RESPONSE$
      LV=1 DX=1 DY=1 DZ=1
       DI=X
         0.30/0.125  0.80/0.300  2.00/0.650  3.00/0.725  3.50/1.000  4.40/1.200
         5.00/1.900  5.75/2.850  6.00/3.375  8.25/3.375  9.00/3.000 10.00/2.400
        14.00/1.325 19.00/1.600 21.00/1.000 22.00/0.800 30.00/0.700 36.00/0.650
       DI=Y
         0.30/0.075  1.25/0.250  1.75/0.325  2.40/0.450  2.75/0.475  3.80/0.500
         4.40/0.500  4.80/0.600  7.25/0.600  7.50/0.700  8.50/0.700 10.00/0.925
        12.00/1.450 16.00/1.900 18.00/1.700 20.00/0.750 25.00/0.450 30.00/0.350
        36.00/0.325 36.10/0.325 36.20/0.325 36.30/0.325 36.40/0.325 36.50/0.325
       DI=Z
         0.30/0.150  1.00/0.350  2.00/0.625  4.00/1.000  4.50/1.400  5.00/2.000
         5.75/2.950  6.00/3.450  6.25/3.800  8.75/3.800 10.00/2.625  12.0/2.150
        15.00/1.300 17.50/1.450 20.00/0.875 30.00/0.650 36.00/0.650 36.10/0.650
*****************************
**** MATERIAL PROPERTIES ****
*****************************
* SA-106 Grade B and SA-234 WPB
MATH CD=106 EX=0 TY=1 *C-Si
*MATD TE=-100 EH=30.2 EX=0 SM=20 SY=35
MATD TE=50   EH=29.6 EX=0 SM=20 SY=35
MATD TE=70   EH=29.5 EX=0   SM=20   SY=35
MATD TE=100  EH=29.3 EX=0.2 SM=20.0 SY=35
MATD TE=200  EH=28.8 EX=1.0 SM=20.0 SY=32.1
MATD TE=300  EH=28.3 EX=1.9 SM=20.0 SY=31
MATD TE=400  EH=27.7 EX=2.8 SM=20.0 SY=29.9
MATD TE=500  EH=27.3 EX=3.7 SM=18.9 SY=28.5
MATD TE=600  EH=26.7 EX=4.7 SM=17.3 SY=26.8
*** Cross Sectional Properties
*REGION I- LINE 16 INCH FDW-16 SCH. 120 Run from 5 to 10
*Anchor HD36 to HPCI brnch
CROS CD=1 OD=16.0  WT=1.218 MA=204.28
          SO=1  ST=1  IN=0
*FEEDWATER Valves - V2-27A, V2-28A, V2-29A
CROS CD=2 OD=24.0  WT=2.436 MA=0.12
          SO=1  ST=1  IN=0  KL=1
*REGION III- LINE 16 INCH FDW-16 SCH. 80
*Piping Downstream of Valve V2-29A TO FW TEE
CROS CD=3 OD=16.0  WT=0.843 MA=151.1
          SO=1  ST=1  IN=0
*REGION III- LINE 16 INCH FDW-16 SCH. 120
*Fittings Downstream of Valve V2-29A TO FW TEE
CROS CD=4 OD=16.0  WT=1.218 MA=204.28
          SO=1  ST=1  IN=0
```

```
*REGION IV & V- LINES 10 INCH INCH FDW-21 AND 10 INCH FDW-19 SCH. 120
*Piping Downstream of FW TEE TO NOZZLES
CROS CD=5 OD=10.75 WT=0.843 MA=98.12
          SO=1  ST=1  IN=0
*REGION II- LINE 14 INCH HPCI-15A SCH. 120 FROM NODE 10 TO 547
CROS CD=6 OD=14.0  WT=1.093 MA=161.35
          SO=1  ST=1  IN=1
*REGION II- HPCI Valves
CROS CD=7 OD=21.0  WT=2.186 MA=0.12
          SO=1  ST=1  IN=1  KL=1
*
**********************
* STRUCTURE AND LOADS
*-------------------------------------------------------------------------------
DESN  TE=400.0  PR=1900.0 *FEEDWATER AND HPCI PIPING
*-------------------------------------------------------------------------------
*BEGIN REGION 1
*-----------
*Same for all regions except II
OPER CA=1  TE=100 PR=1100
OPER CA=22 TE=100 PR=1563
OPER CA=28 TE=100 PR=1010
OPER CA=29 TE=100 PR=1010

*Same for all regions
OPER CA=2  TE=100 PR=50
OPER CA=19 TE=50  PR=675
OPER CA=31 TE=50  PR=885

*Unique
OPER CA=3  TE=150 PR=1010
OPER CA=4  TE=260 PR=1010
OPER CA=5  TE=392 PR=1010
OPER CA=6  TE=310 PR=1010
OPER CA=7  TE=280 PR=1010
OPER CA=8  TE=265 PR=1010
OPER CA=9  TE=90  PR=1010
OPER CA=10 TE=265 PR=1010
OPER CA=11 TE=150 PR=170
OPER CA=12 TE=150 PR=88
OPER CA=13 TE=392 PR=1190
OPER CA=14 TE=50  PR=1135
OPER CA=15 TE=150 PR=1135
OPER CA=16 TE=150 PR=1135
OPER CA=17 TE=150 PR=1060
OPER CA=18 TE=150 PR=1135

OPER CA=20 TE=150 PR=675
OPER CA=21 TE=275 PR=885

OPER CA=23 TE=392 PR=1375
OPER CA=24 TE=392 PR=940
OPER CA=25 TE=392 PR=1010
OPER CA=26 TE=275 PR=1010
OPER CA=27 TE=265 PR=1010
```

```
OPER CA=30 TE=125 PR=1010

*
TRAN CA=201 IS=1 FS=1 IT=70 FT=100 TT=1800 FL=200 IP=15 FP=1115 TP=1800
TRAN CA=202 IS=1 FS=1 IT=100 FT=100 TT=0 FL=200 IP=1115 FP=65 TP=0
TRAN CA=203 IS=1 FS=1 IT=100 FT=150 TT=16164 FL=200 IP=65 FP=1025 TP=16164
TRAN CA=204 IS=1 FS=1 IT=150 FT=100 TT=0 FL=1377 IP=1025 FP=1025 TP=0
TRAN CA=205 IS=1 FS=1 IT=100 FT=260 TT=0 FL=1377 IP=1025 FP=1025 TP=0
TRAN CA=206 IS=1 FS=1 IT=260 FT=392 TT=1800 FL=9180 IP=1025 FP=1025 TP=1800
TRAN CA=207 IS=1 FS=1 IT=392 FT=310 TT=900 FL=6885 IP=1025 FP=1025 TP=900
TRAN CA=208 IS=1 FS=1 IT=310 FT=392 TT=900 FL=6885 IP=1025 FP=1025 TP=900
TRAN CA=209 IS=1 FS=1 IT=392 FT=280 TT=1800 FL=4590 IP=1025 FP=1025 TP=1800
TRAN CA=210 IS=1 FS=1 IT=280 FT=392 TT=1800 FL=4590 IP=1025 FP=1025 TP=1800
TRAN CA=211 IS=1 FS=1 IT=392 FT=265 TT=1800 FL=4590 IP=1025 FP=1025 TP=1800
TRAN CA=212 IS=1 FS=1 IT=265 FT=90 TT=360 FL=1377 IP=1025 FP=1025 TP=360
TRAN CA=213 IS=1 FS=1 IT=90 FT=265 TT=900 FL=1377 IP=1025 FP=1025 TP=900
TRAN CA=214 IS=1 FS=1 IT=265 FT=392 TT=1800 FL=4590 IP=1025 FP=1025 TP=1800
TRAN CA=215 IS=1 FS=1 IT=392 FT=265 TT=90 FL=9180 IP=1025 FP=1025 TP=90
TRAN CA=216 IS=1 FS=1 IT=265 FT=392 TT=180 FL=9180 IP=1025 FP=1025 TP=180
TRAN CA=217 IS=1 FS=1 IT=392 FT=275 TT=60 FL=10098 IP=1025 FP=1025 TP=60
TRAN CA=218 IS=1 FS=1 IT=275 FT=100 TT=900 FL=275.4 IP=1025 FP=1025 TP=900
TRAN CA=219 *IS=1 FS=1 IT=265 FT=265 TT=0 FL=200 IP=1025 FP=1025 TP=0
TRAN CA=220 *IS=1 FS=1 IT=265 FT=265 TT=0 FL=200 IP=1025 FP=1025 TP=0
TRAN CA=221 IS=1 FS=1 IT=265 FT=150 TT=4140 FL=200 IP=1025 FP=1025 TP=4140
TRAN CA=222 IS=1 FS=1 IT=150 FT=150 TT=0 FL=200 IP=1025 FP=185 TP=0
TRAN CA=223 IS=1 FS=1 IT=150 FT=150 TT=0 FL=200 IP=185 FP=103 TP=0
TRAN CA=224 IS=1 FS=1 IT=150 FT=100 TT=8280 FL=200 IP=103 FP=65 TP=8280
TRAN CA=225 IS=1 FS=1 IT=392 FT=392 TT=12 FL=200 IP=1025 FP=1205 TP=12
TRAN CA=226 IS=1 FS=1 IT=392 FT=50 TT=0 FL=3672 IP=1205 FP=1150 TP=0
TRAN CA=227 IS=1 FS=1 IT=50 FT=150 TT=1380 FL=200 IP=1150 FP=1150 TP=1380
TRAN CA=228 IS=1 FS=1 IT=150 FT=150 TT=0 FL=200 IP=1150 FP=1150 TP=0
TRAN CA=229 IS=1 FS=1 IT=150 FT=50 TT=0 FL=2754 IP=1150 FP=900 TP=0
TRAN CA=230 IS=1 FS=1 IT=50 FT=150 TT=3060 FL=200 IP=900 FP=1075 TP=3060
TRAN CA=231 IS=1 FS=1 IT=150 FT=150 TT=0 FL=200 IP=1075 FP=1150 TP=0
TRAN CA=232 IS=1 FS=1 IT=150 FT=50 TT=0 FL=1560.6 IP=1150 FP=690 TP=0
TRAN CA=233 IS=1 FS=1 IT=50 FT=150 TT=300 FL=200 IP=690 FP=690 TP=300
TRAN CA=234 IS=1 FS=1 IT=150 FT=150 TT=8964 FL=200 IP=255 FP=1025 TP=8964
TRAN CA=235 IS=1 FS=1 IT=392 FT=275 TT=60 FL=10098 IP=1025 FP=900 TP=60
TRAN CA=236 IS=1 FS=1 IT=275 FT=100 TT=900 FL=275.4 IP=900 FP=65 TP=900
TRAN CA=237 IS=1 FS=1 IT=100 FT=100 TT=0 FL=200 IP=65 FP=1578 TP=0
TRAN CA=238 IS=1 FS=1 IT=100 FT=100 TT=0 FL=200 IP=1578 FP=65 TP=0
TRAN CA=239 IS=1 FS=1 IT=392 FT=392 TT=60 FL=10098 IP=1025 FP=1390 TP=60
TRAN CA=240 IS=1 FS=1 IT=392 FT=392 TT=900 FL=275.4 IP=1390 FP=955 TP=900
TRAN CA=241 IS=1 FS=1 IT=392 FT=392 TT=900 FL=275.4 IP=955 FP=1025 TP=900
TRAN CA=242 IS=1 FS=1 IT=100 FT=125 TT=60 FL=200 IP=1025 FP=1025 TP=60
TRAN CA=243 IS=1 FS=1 IT=125 FT=150 TT=210 FL=200 IP=1025 FP=1025 TP=210

PAIR CA=201 CO=27.6 DI=0.521 EX=6.4 * Tavg=85
PAIR CA=202 CO=27.6 DI=0.512 EX=6.4 * Tavg=100
PAIR CA=203 CO=27.6 DI=0.504 EX=6.4 * Tavg=125
PAIR CA=204 CO=27.6 DI=0.504 EX=6.4 * Tavg=125
PAIR CA=205 CO=27.6 DI=0.490 EX=6.4 * Tavg=180
PAIR CA=206 CO=27.1 DI=0.446 EX=6.4 * Tavg=326
PAIR CA=207 CO=27.0 DI=0.440 EX=6.4 * Tavg=351
PAIR CA=208 CO=27.0 DI=0.440 EX=6.4 * Tavg=351
PAIR CA=209 CO=27.1 DI=0.444 EX=6.4 * Tavg=336
```

```
PAIR CA=210 CO=27.1 DI=0.444 EX=6.4 * Tavg=336
PAIR CA=211 CO=27.1 DI=0.445 EX=6.4 * Tavg=329
PAIR CA=212 CO=27.6 DI=0.490 EX=6.4 * Tavg=178
PAIR CA=213 CO=27.6 DI=0.490 EX=6.4 * Tavg=178
PAIR CA=214 CO=27.1 DI=0.445 EX=6.4 * Tavg=329
PAIR CA=215 CO=27.1 DI=0.445 EX=6.4 * Tavg=329
PAIR CA=216 CO=27.1 DI=0.445 EX=6.4 * Tavg=329
PAIR CA=217 CO=27.1 DI=0.444 EX=6.4 * Tavg=334
PAIR CA=218 CO=27.6 DI=0.488 EX=6.4 * Tavg=188
PAIR CA=219 CO=27.3 DI=0.463 EX=6.4 * Tavg=265
PAIR CA=220 CO=27.3 DI=0.463 EX=6.4 * Tavg=265
PAIR CA=221 CO=27.6 DI=0.483 EX=6.4 * Tavg=208
PAIR CA=222 CO=27.6 DI=0.496 EX=6.4 * Tavg=150
PAIR CA=223 CO=27.6 DI=0.496 EX=6.4 * Tavg=150
PAIR CA=224 CO=27.6 DI=0.504 EX=6.4 * Tavg=125
PAIR CA=225 CO=26.7 DI=0.430 EX=6.4 * Tavg=392
PAIR CA=226 CO=27.5 DI=0.478 EX=6.4 * Tavg=221
PAIR CA=227 CO=27.6 DI=0.512 EX=6.4 * Tavg=100
PAIR CA=228 CO=27.6 DI=0.496 EX=6.4 * Tavg=150
PAIR CA=229 CO=27.6 DI=0.512 EX=6.4 * Tavg=100
PAIR CA=230 CO=27.6 DI=0.512 EX=6.4 * Tavg=100
PAIR CA=231 CO=27.6 DI=0.496 EX=6.4 * Tavg=150
PAIR CA=232 CO=27.6 DI=0.512 EX=6.4 * Tavg=100
PAIR CA=233 CO=27.6 DI=0.512 EX=6.4 * Tavg=100
PAIR CA=234 CO=27.6 DI=0.496 EX=6.4 * Tavg=150
PAIR CA=235 CO=27.1 DI=0.444 EX=6.4 * Tavg=334
PAIR CA=236 CO=27.6 DI=0.488 EX=6.4 * Tavg=188
PAIR CA=237 CO=27.6 DI=0.512 EX=6.4 * Tavg=100
PAIR CA=238 CO=27.6 DI=0.512 EX=6.4 * Tavg=100
PAIR CA=239 CO=26.7 DI=0.430 EX=6.4 * Tavg=392
PAIR CA=240 CO=26.7 DI=0.430 EX=6.4 * Tavg=392
PAIR CA=241 CO=26.7 DI=0.430 EX=6.4 * Tavg=392
PAIR CA=242 CO=27.6 DI=0.508 EX=6.4 * Tavg=113
PAIR CA=243 CO=27.6 DI=0.500 EX=6.4 * Tavg=138
*
*REGION I GEOMETRY
* RUN 1 FROM ANCHOR HD36 TO HPCI brnCH- FDW-16 LINE A
MATL CD=106
CROS CD=1
COOR PT=5   AX=0 AY=0 AZ=0 *ANCHOR HD36
JUNC PT=5
TANG PT=9   DZ=-2.75  EW=1
TANG PT=10  DZ=-1 *WELDING TEE PER ANSI B16.9
*-----------------------------------------------------------------------------
*END REGION I
*-----------------------------------------------------------------------------
*BEGIN REGION 3
*---------------
*OPER cards same as those for region I
*
TRAN CA=201 IS=1 FS=1 IT=70 FT=100 TT=1800 FL=200 IP=15 FP=1115 TP=1800
TRAN CA=202 IS=1 FS=1 IT=100 FT=100 TT=0 FL=200 IP=1115 FP=65 TP=0
TRAN CA=203 IS=1 FS=1 IT=100 FT=150 TT=16164 FL=200 IP=65 FP=1025 TP=16164
TRAN CA=204 IS=1 FS=1 IT=150 FT=100 TT=0 FL=1377 IP=1025 FP=1025 TP=0
TRAN CA=205 IS=1 FS=1 IT=100 FT=260 TT=0 FL=1377 IP=1025 FP=1025 TP=0
TRAN CA=206 IS=1 FS=1 IT=260 FT=392 TT=1800 FL=9180 IP=1025 FP=1025 TP=1800
```

```
TRAN CA=207 IS=1 FS=1 IT=392 FT=310 TT=900 FL=6885 IP=1025 FP=1025 TP=900
TRAN CA=208 IS=1 FS=1 IT=310 FT=392 TT=900 FL=6885 IP=1025 FP=1025 TP=900
TRAN CA=209 IS=1 FS=1 IT=392 FT=280 TT=1800 FL=4590 IP=1025 FP=1025 TP=1800
TRAN CA=210 IS=1 FS=1 IT=280 FT=392 TT=1800 FL=4590 IP=1025 FP=1025 TP=1800
TRAN CA=211 IS=1 FS=1 IT=392 FT=265 TT=1800 FL=4590 IP=1025 FP=1025 TP=1800
TRAN CA=212 IS=1 FS=1 IT=265 FT=90 TT=360 FL=1377 IP=1025 FP=1025 TP=360
TRAN CA=213 IS=1 FS=1 IT=90 FT=265 TT=900 FL=1377 IP=1025 FP=1025 TP=900
TRAN CA=214 IS=1 FS=1 IT=265 FT=392 TT=1800 FL=4590 IP=1025 FP=1025 TP=1800
TRAN CA=215 IS=1 FS=1 IT=392 FT=265 TT=90 FL=9180 IP=1025 FP=1025 TP=90
TRAN CA=216 IS=1 FS=1 IT=265 FT=392 TT=180 FL=9180 IP=1025 FP=1025 TP=180
TRAN CA=217 IS=1 FS=1 IT=392 FT=275 TT=60 FL=10098 IP=1025 FP=1025 TP=60
TRAN CA=218 IS=1 FS=1 IT=275 FT=100 TT=900 FL=275.4 IP=1025 FP=1025 TP=900
TRAN CA=219 *IS=1 FS=1 IT=265 FT=265 TT=0 FL=200 IP=1025 FP=1025 TP=0
TRAN CA=220 *IS=1 FS=1 IT=265 FT=265 TT=0 FL=200 IP=1025 FP=1025 TP=0
TRAN CA=221 IS=1 FS=1 IT=265 FT=150 TT=4140 FL=200 IP=1025 FP=1025 TP=4140
TRAN CA=222 IS=1 FS=1 IT=150 FT=150 TT=0 FL=200 IP=1025 FP=185 TP=0
TRAN CA=223 IS=1 FS=1 IT=150 FT=150 TT=0 FL=200 IP=185 FP=103 TP=0
TRAN CA=224 IS=1 FS=1 IT=150 FT=100 TT=8280 FL=200 IP=103 FP=65 TP=8280
TRAN CA=225 IS=1 FS=1 IT=392 FT=392 TT=12 FL=200 IP=1025 FP=1205 TP=12
TRAN CA=226 IS=1 FS=1 IT=392 FT=50 TT=0 FL=3672 IP=1205 FP=1150 TP=0
TRAN CA=227 IS=1 FS=1 IT=50 FT=150 TT=1380 FL=200 IP=1150 FP=1150 TP=1380
TRAN CA=228 *IS=1 FS=1 IT=150 FT=150 TT=0 FL=200 IP=1150 FP=1150 TP=0
TRAN CA=229 IS=1 FS=1 IT=150 FT=50 TT=0 FL=2754 IP=1150 FP=900 TP=0
TRAN CA=230 IS=1 FS=1 IT=50 FT=150 TT=3060 FL=200 IP=900 FP=1075 TP=3060
TRAN CA=231 IS=1 FS=1 IT=150 FT=150 TT=0 FL=200 IP=1075 FP=1150 TP=0
TRAN CA=232 IS=1 FS=1 IT=150 FT=50 TT=0 FL=1560.6 IP=1150 FP=690 TP=0
TRAN CA=233 IS=1 FS=1 IT=50 FT=150 TT=300 FL=200 IP=690 FP=690 TP=300
TRAN CA=234 IS=1 FS=1 IT=150 FT=150 TT=8964 FL=200 IP=255 FP=1025 TP=8964
TRAN CA=235 IS=1 FS=1 IT=392 FT=275 TT=60 FL=10098 IP=1025 FP=900 TP=60
TRAN CA=236 IS=1 FS=1 IT=275 FT=100 TT=900 FL=275.4 IP=900 FP=65 TP=900
TRAN CA=237 IS=1 FS=1 IT=100 FT=100 TT=0 FL=200 IP=65 FP=1578 TP=0
TRAN CA=238 IS=1 FS=1 IT=100 FT=100 TT=0 FL=200 IP=1578 FP=65 TP=0
TRAN CA=239 IS=1 FS=1 IT=392 FT=392 TT=60 FL=10098 IP=1025 FP=1390 TP=60
TRAN CA=240 IS=1 FS=1 IT=392 FT=392 TT=900 FL=275.4 IP=1390 FP=955 TP=900
TRAN CA=241 IS=1 FS=1 IT=392 FT=392 TT=900 FL=275.4 IP=955 FP=1025 TP=900
TRAN CA=242 IS=1 FS=1 IT=100 FT=125 TT=60 FL=200 IP=1025 FP=1025 TP=60
TRAN CA=243 IS=1 FS=1 IT=125 FT=150 TT=210 FL=200 IP=1025 FP=1025 TP=210

*
PAIR CA=201 CO=27.6 DI=0.521 EX=6.4 * Tavg=85
PAIR CA=202 CO=27.6 DI=0.512 EX=6.4 * Tavg=100
PAIR CA=203 CO=27.6 DI=0.504 EX=6.4 * Tavg=125
PAIR CA=204 CO=27.6 DI=0.504 EX=6.4 * Tavg=125
PAIR CA=205 CO=27.6 DI=0.490 EX=6.4 * Tavg=180
PAIR CA=206 CO=27.1 DI=0.446 EX=6.4 * Tavg=326
PAIR CA=207 CO=27.0 DI=0.440 EX=6.4 * Tavg=351
PAIR CA=208 CO=27.0 DI=0.440 EX=6.4 * Tavg=351
PAIR CA=209 CO=27.1 DI=0.444 EX=6.4 * Tavg=336
PAIR CA=210 CO=27.1 DI=0.444 EX=6.4 * Tavg=336
PAIR CA=211 CO=27.1 DI=0.445 EX=6.4 * Tavg=329
PAIR CA=212 CO=27.6 DI=0.490 EX=6.4 * Tavg=178
PAIR CA=213 CO=27.6 DI=0.490 EX=6.4 * Tavg=178
PAIR CA=214 CO=27.1 DI=0.445 EX=6.4 * Tavg=329
PAIR CA=215 CO=27.1 DI=0.445 EX=6.4 * Tavg=329
PAIR CA=216 CO=27.1 DI=0.445 EX=6.4 * Tavg=329
PAIR CA=217 CO=27.1 DI=0.444 EX=6.4 * Tavg=334
```

```
PAIR CA=218 CO=27.6 DI=0.488 EX=6.4 * Tavg=188
PAIR CA=219 CO=27.3 DI=0.463 EX=6.4 * Tavg=265
PAIR CA=220 CO=27.3 DI=0.463 EX=6.4 * Tavg=265
PAIR CA=221 CO=27.6 DI=0.483 EX=6.4 * Tavg=208
PAIR CA=222 CO=27.6 DI=0.496 EX=6.4 * Tavg=150
PAIR CA=223 CO=27.6 DI=0.496 EX=6.4 * Tavg=150
PAIR CA=224 CO=27.6 DI=0.504 EX=6.4 * Tavg=125
PAIR CA=225 CO=26.7 DI=0.430 EX=6.4 * Tavg=392
PAIR CA=226 CO=27.5 DI=0.478 EX=6.4 * Tavg=221
PAIR CA=227 CO=27.6 DI=0.512 EX=6.4 * Tavg=100
PAIR CA=228 CO=27.6 DI=0.496 EX=6.4 * Tavg=150
PAIR CA=229 CO=27.6 DI=0.512 EX=6.4 * Tavg=100
PAIR CA=230 CO=27.6 DI=0.512 EX=6.4 * Tavg=100
PAIR CA=231 CO=27.6 DI=0.496 EX=6.4 * Tavg=150
PAIR CA=232 CO=27.6 DI=0.512 EX=6.4 * Tavg=100
PAIR CA=233 CO=27.6 DI=0.512 EX=6.4 * Tavg=100
PAIR CA=234 CO=27.6 DI=0.496 EX=6.4 * Tavg=150
PAIR CA=235 CO=27.1 DI=0.444 EX=6.4 * Tavg=334
PAIR CA=236 CO=27.6 DI=0.488 EX=6.4 * Tavg=188
PAIR CA=237 CO=27.6 DI=0.512 EX=6.4 * Tavg=100
PAIR CA=238 CO=27.6 DI=0.512 EX=6.4 * Tavg=100
PAIR CA=239 CO=26.7 DI=0.430 EX=6.4 * Tavg=392
PAIR CA=240 CO=26.7 DI=0.430 EX=6.4 * Tavg=392
PAIR CA=241 CO=26.7 DI=0.430 EX=6.4 * Tavg=392
PAIR CA=242 CO=27.6 DI=0.508 EX=6.4 * Tavg=113
PAIR CA=243 CO=27.6 DI=0.500 EX=6.4 * Tavg=138

*
*REGION III GEOMETRY
CROS CD=1
*JUNC PT=10
TANG PT=11  DZ=-1  EW=1
TANG PT=15  DZ=-4.17
TANG PT=20  DZ=-0.333  EW=1  *TA=1
CROS CD=2
VALV PT=22  DZ=-1.333 PL=1 MA=2.7  *VALVE V2-27A
VALV PT=25  DZ=-1.333 PL=2  EW=1  *TA=1
CROS CD=1
TANG PT=30  DZ=-2.792
LUMP PT=30  MA=1.285
TANG PT=38  DZ=-4.6
TANG PT=40  DZ=-6.317
TANG PT=45  DZ=-0.625  EW=1  *TA=1
CROS CD=2
VALV PT=47  DZ=-1.792 PL=1 MA=2.7  *VALVE V2-28A
VALV PT=50  DZ=-1.792 PL=2  EW=1  *TA=1
CROS CD=1
*TANG PT=55  DZ=-2.791  EW=1
TANG PT=55  DZ=-.791 EW=1
*BRAD PT=65  RA=2  SD=2  EW=1 Used this to determine midpoint viw .prd output
BEND PT=60 X1=0 Y1=0 Z1=-.828 X2=0 Y2=.586 Z2=-.586
BEND PT=65 X1=0 Y1=.586 Z1=-.586 X2=0 Y2=.828 Z2=0
*TANG PT=67  DY=2.084  EW=1  *TA=1
TANG PT=67  DY=.084
CROS CD=2
VALV PT=70  DY=1.333 PL=1 MA=3.25  *VALVE V2-29A
```

```
VALV PT=75  DY=1.333 PL=2  EW=1  *TA=1
CROS CD=3
TANG PT=78  DY=1.25
TANG PT=80  DY=3.5
TANG PT=82  DY=2.667  EW=1
CROS CD=4
BRAD PT=85  RA=2  EW=1
CROS CD=3
TANG PT=90  DX=2.875
TANG PT=95  DX=2.875  EW=1
CROS CD=4
BRAD PT=100 RA=2  EW=1
CROS CD=3
TANG PT=105 DX=1.12  DZ=-1.12
TANG PT=110 DX=3.477 DZ=-3.477  EW=1
CROS CD=4
TANG PT=115 DX=0.7071 DZ=-0.7071 EW=1
*
*-----------------------------------------------------------------------------
*END REGION III
*-----------------------------------------------------------------------------
*BEGIN REGION IV
*---------------
*OPER cards same as those for regions I and III
*
TRAN CA=201 IS=1 FS=1 IT=70 FT=100 TT=1800 FL=100 IP=15 FP=1115 TP=1800
TRAN CA=202 IS=1 FS=1 IT=100 FT=100 TT=0 FL=100 IP=1115 FP=65 TP=0
TRAN CA=203 IS=1 FS=1 IT=100 FT=150 TT=16164 FL=100 IP=65 FP=1025 TP=16164
TRAN CA=204 IS=1 FS=1 IT=150 FT=100 TT=0 FL=688.5 IP=1025 FP=1025 TP=0
TRAN CA=205 IS=1 FS=1 IT=100 FT=260 TT=0 FL=688.5 IP=1025 FP=1025 TP=0
TRAN CA=206 IS=1 FS=1 IT=260 FT=392 TT=1800 FL=4590 IP=1025 FP=1025 TP=1800
TRAN CA=207 IS=1 FS=1 IT=392 FT=310 TT=900 FL=3442.5 IP=1025 FP=1025 TP=900
TRAN CA=208 IS=1 FS=1 IT=310 FT=392 TT=900 FL=3442.5 IP=1025 FP=1025 TP=900
TRAN CA=209 IS=1 FS=1 IT=392 FT=280 TT=1800 FL=2295 IP=1025 FP=1025 TP=1800
TRAN CA=210 IS=1 FS=1 IT=280 FT=392 TT=1800 FL=2295 IP=1025 FP=1025 TP=1800
TRAN CA=211 IS=1 FS=1 IT=392 FT=265 TT=1800 FL=2295 IP=1025 FP=1025 TP=1800
TRAN CA=212 IS=1 FS=1 IT=265 FT=90 TT=360 FL=688.5 IP=1025 FP=1025 TP=360
TRAN CA=213 IS=1 FS=1 IT=90 FT=265 TT=900 FL=688.5 IP=1025 FP=1025 TP=900
TRAN CA=214 IS=1 FS=1 IT=265 FT=392 TT=1800 FL=2295 IP=1025 FP=1025 TP=1800
TRAN CA=215 IS=1 FS=1 IT=392 FT=265 TT=90 FL=4590 IP=1025 FP=1025 TP=90
TRAN CA=216 IS=1 FS=1 IT=265 FT=392 TT=180 FL=4590 IP=1025 FP=1025 TP=180
TRAN CA=217 IS=1 FS=1 IT=392 FT=275 TT=60 FL=5049 IP=1025 FP=1025 TP=60
TRAN CA=218 IS=1 FS=1 IT=275 FT=100 TT=900 FL=137.7 IP=1025 FP=1025 TP=900
TRAN CA=219 *IS=1 FS=1 IT=265 FT=265 TT=0 FL=100 IP=1025 FP=1025 TP=0
TRAN CA=220 *IS=1 FS=1 IT=265 FT=265 TT=0 FL=100 IP=1025 FP=1025 TP=0
TRAN CA=221 IS=1 FS=1 IT=265 FT=150 TT=4140 FL=100 IP=1025 FP=1025 TP=4140
TRAN CA=222 IS=1 FS=1 IT=150 FT=150 TT=0 FL=100 IP=1025 FP=185 TP=0
TRAN CA=223 IS=1 FS=1 IT=150 FT=150 TT=0 FL=100 IP=185 FP=103 TP=0
TRAN CA=224 IS=1 FS=1 IT=150 FT=100 TT=8280 FL=100 IP=103 FP=65 TP=8280
TRAN CA=225 IS=1 FS=1 IT=392 FT=392 TT=12 FL=100 IP=1025 FP=1205 TP=12
TRAN CA=226 IS=1 FS=1 IT=392 FT=50 TT=0 FL=1836 IP=1205 FP=1150 TP=0
TRAN CA=227 IS=1 FS=1 IT=50 FT=150 TT=1380 FL=100 IP=1150 FP=1150 TP=1380
TRAN CA=228 *IS=1 FS=1 IT=150 FT=150 TT=0 FL=100 IP=1150 FP=1150 TP=0
TRAN CA=229 IS=1 FS=1 IT=150 FT=50 TT=0 FL=1377 IP=1150 FP=900 TP=0
TRAN CA=230 IS=1 FS=1 IT=50 FT=150 TT=3060 FL=100 IP=900 FP=1075 TP=3060
TRAN CA=231 IS=1 FS=1 IT=150 FT=150 TT=0 FL=100 IP=1075 FP=1150 TP=0
```

```
TRAN CA=232 IS=1 FS=1 IT=150 FT=50 TT=0 FL=780.3 IP=1150 FP=690 TP=0
TRAN CA=233 IS=1 FS=1 IT=50 FT=150 TT=300 FL=100 IP=690 FP=690 TP=300
TRAN CA=234 IS=1 FS=1 IT=150 FT=150 TT=8964 FL=100 IP=255 FP=1025 TP=8964
TRAN CA=235 IS=1 FS=1 IT=392 FT=275 TT=60 FL=5049 IP=1025 FP=900 TP=60
TRAN CA=236 IS=1 FS=1 IT=275 FT=100 TT=900 FL=137.7 IP=900 FP=65 TP=900
TRAN CA=237 IS=1 FS=1 IT=100 FT=100 TT=0 FL=100 IP=65 FP=1578 TP=0
TRAN CA=238 IS=1 FS=1 IT=100 FT=100 TT=0 FL=100 IP=1578 FP=65 TP=0
TRAN CA=239 IS=1 FS=1 IT=392 FT=392 TT=60 FL=5049 IP=1025 FP=1390 TP=60
TRAN CA=240 IS=1 FS=1 IT=392 FT=392 TT=900 FL=137.7 IP=1390 FP=955 TP=900
TRAN CA=241 IS=1 FS=1 IT=392 FT=392 TT=900 FL=137.7 IP=955 FP=1025 TP=900
TRAN CA=242 IS=1 FS=1 IT=100 FT=125 TT=60 FL=100 IP=1025 FP=1025 TP=60
TRAN CA=243 IS=1 FS=1 IT=125 FT=150 TT=210 FL=100 IP=1025 FP=1025 TP=210

*
PAIR CA=201 CO=27.6 DI=0.521 EX=6.4 * Tavg=85
PAIR CA=202 CO=27.6 DI=0.512 EX=6.4 * Tavg=100
PAIR CA=203 CO=27.6 DI=0.504 EX=6.4 * Tavg=125
PAIR CA=204 CO=27.6 DI=0.504 EX=6.4 * Tavg=125
PAIR CA=205 CO=27.6 DI=0.490 EX=6.4 * Tavg=180
PAIR CA=206 CO=27.1 DI=0.446 EX=6.4 * Tavg=326
PAIR CA=207 CO=27.0 DI=0.440 EX=6.4 * Tavg=351
PAIR CA=208 CO=27.0 DI=0.440 EX=6.4 * Tavg=351
PAIR CA=209 CO=27.1 DI=0.444 EX=6.4 * Tavg=336
PAIR CA=210 CO=27.1 DI=0.444 EX=6.4 * Tavg=336
PAIR CA=211 CO=27.1 DI=0.445 EX=6.4 * Tavg=329
PAIR CA=212 CO=27.6 DI=0.490 EX=6.4 * Tavg=178
PAIR CA=213 CO=27.6 DI=0.490 EX=6.4 * Tavg=178
PAIR CA=214 CO=27.1 DI=0.445 EX=6.4 * Tavg=329
PAIR CA=215 CO=27.1 DI=0.445 EX=6.4 * Tavg=329
PAIR CA=216 CO=27.1 DI=0.445 EX=6.4 * Tavg=329
PAIR CA=217 CO=27.1 DI=0.444 EX=6.4 * Tavg=334
PAIR CA=218 CO=27.6 DI=0.488 EX=6.4 * Tavg=188
PAIR CA=219 CO=27.3 DI=0.463 EX=6.4 * Tavg=265
PAIR CA=220 CO=27.3 DI=0.463 EX=6.4 * Tavg=265
PAIR CA=221 CO=27.6 DI=0.483 EX=6.4 * Tavg=208
PAIR CA=222 CO=27.6 DI=0.496 EX=6.4 * Tavg=150
PAIR CA=223 CO=27.6 DI=0.496 EX=6.4 * Tavg=150
PAIR CA=224 CO=27.6 DI=0.504 EX=6.4 * Tavg=125
PAIR CA=225 CO=26.7 DI=0.430 EX=6.4 * Tavg=392
PAIR CA=226 CO=27.5 DI=0.478 EX=6.4 * Tavg=221
PAIR CA=227 CO=27.6 DI=0.512 EX=6.4 * Tavg=100
PAIR CA=228 CO=27.6 DI=0.496 EX=6.4 * Tavg=150
PAIR CA=229 CO=27.6 DI=0.512 EX=6.4 * Tavg=100
PAIR CA=230 CO=27.6 DI=0.512 EX=6.4 * Tavg=100
PAIR CA=231 CO=27.6 DI=0.496 EX=6.4 * Tavg=150
PAIR CA=232 CO=27.6 DI=0.512 EX=6.4 * Tavg=100
PAIR CA=233 CO=27.6 DI=0.512 EX=6.4 * Tavg=100
PAIR CA=234 CO=27.6 DI=0.496 EX=6.4 * Tavg=150
PAIR CA=235 CO=27.1 DI=0.444 EX=6.4 * Tavg=334
PAIR CA=236 CO=27.6 DI=0.488 EX=6.4 * Tavg=188
PAIR CA=237 CO=27.6 DI=0.512 EX=6.4 * Tavg=100
PAIR CA=238 CO=27.6 DI=0.512 EX=6.4 * Tavg=100
PAIR CA=239 CO=26.7 DI=0.430 EX=6.4 * Tavg=392
PAIR CA=240 CO=26.7 DI=0.430 EX=6.4 * Tavg=392
PAIR CA=241 CO=26.7 DI=0.430 EX=6.4 * Tavg=392
PAIR CA=242 CO=27.6 DI=0.508 EX=6.4 * Tavg=113
```

```
PAIR CA=243 CO=27.6 DI=0.500 EX=6.4 * Tavg=138

*
*REGION IV GEOMETRY DOWNSTREAM OF FW brnCH TEE/REDUCER - 10 INCH PIPING
*RUN FROM FW TEE TO ELBOW BEFORE NOZZLE NBA, NODE 275
CROS CD=4
TANG PT=170  DX=0.7071  DZ=-0.7071  EW=1
ERED PT=175  DX=0.825 DZ=-0.825  AN=30
CROS CD=5
*RUN FROM FW TEE TO ELBOW BEFORE NOZZLE N4B, NODE 152
BEND PT=190  X1=4.813  Y1=0  Z1=-4.813  X2=1.283  Y2=0  Z2=-6.685
BEND PT=200  X1=0.449  Y1=0  Z1=-2.342  X2=-0.059  Y2=0  Z2=-2.384
STRU PT=201 DX=.198 DZ=.9802
STRU PT=202 DX=.198 DZ=.9802
ANCH PT=202
JUNC PT=200
BEND PT=220  X1=-0.2196  Y1=0  Z1=-8.859  X2=-6.266  Y2=0  Z2=-6.266
TANG PT=225  DX=-0.3388  DZ=-0.3388
TANG PT=230  DX=-0.3388  DZ=-0.3388
TANG PT=235  DX=-1.002  DZ=-1.002
BRAD PT=240  RA=1.25
TANG PT=245  DX=-2.693  DY=3.196  DZ=2.693
TANG PT=250  DX=-2.693  DY=3.196  DZ=2.693
TANG PT=255  DX=-2.693  DY=3.196  DZ=2.693
BRAD PT=260  RA=1.25
TANG PT=265  DY=3.958
TANG PT=270  DY=3.959
*-----------------------------------------------------------------------------
*END REGION IV
*-----------------------------------------------------------------------------
*BEGIN REGION IVa
*-----------------------------------------------------------------------------
OPER CA=3  TE=283 PR=1010
OPER CA=4  TE=260 PR=1010
OPER CA=5  TE=392 PR=1010
OPER CA=6  TE=310 PR=1010
OPER CA=7  TE=280 PR=1010
OPER CA=8  TE=265 PR=1010
OPER CA=9  TE=90  PR=1010
OPER CA=10 TE=360 PR=1010
OPER CA=11 TE=225 PR=170
OPER CA=12 TE=210 PR=88
OPER CA=13 TE=450 PR=1190
OPER CA=14 TE=50  PR=1135
OPER CA=15 TE=247 PR=1135
OPER CA=16 TE=288 PR=1135
OPER CA=17 TE=247 PR=1060
OPER CA=18 TE=283 PR=1135

OPER CA=20 TE=200 PR=675
OPER CA=21 TE=275 PR=885

OPER CA=23 TE=392 PR=1375
OPER CA=24 TE=392 PR=940
OPER CA=25 TE=392 PR=1010
OPER CA=26 TE=275 PR=1010
```

```
OPER CA=27 TE=323 PR=1010
OPER CA=30 TE=180 PR=1010
*
TRAN CA=201 IS=1 FS=1 IT=70 FT=100 TT=1800 FL=100 IP=15 FP=1115 TP=1800
TRAN CA=202 IS=1 FS=1 IT=100 FT=100 TT=0 FL=100 IP=1115 FP=65 TP=0
TRAN CA=203 IS=1 FS=1 IT=100 FT=283 TT=16164 FL=100 IP=65 FP=1025 TP=16164
TRAN CA=204 IS=1 FS=1 IT=283 FT=100 TT=0 FL=688.5 IP=1025 FP=1025 TP=0
TRAN CA=205 IS=1 FS=1 IT=100 FT=260 TT=0 FL=688.5 IP=1025 FP=1025 TP=0
TRAN CA=206 IS=1 FS=1 IT=260 FT=392 TT=1800 FL=4590 IP=1025 FP=1025 TP=1800
TRAN CA=207 IS=1 FS=1 IT=392 FT=310 TT=900 FL=3442.5 IP=1025 FP=1025 TP=900
TRAN CA=208 IS=1 FS=1 IT=310 FT=392 TT=900 FL=3442.5 IP=1025 FP=1025 TP=900
TRAN CA=209 IS=1 FS=1 IT=392 FT=280 TT=1800 FL=2295 IP=1025 FP=1025 TP=1800
TRAN CA=210 IS=1 FS=1 IT=280 FT=392 TT=1800 FL=2295 IP=1025 FP=1025 TP=1800
TRAN CA=211 IS=1 FS=1 IT=392 FT=265 TT=1800 FL=2295 IP=1025 FP=1025 TP=1800
TRAN CA=212 IS=1 FS=1 IT=265 FT=90 TT=360 FL=688.5 IP=1025 FP=1025 TP=360
TRAN CA=213 IS=1 FS=1 IT=90 FT=265 TT=900 FL=688.5 IP=1025 FP=1025 TP=900
TRAN CA=214 IS=1 FS=1 IT=265 FT=392 TT=1800 FL=2295 IP=1025 FP=1025 TP=1800
TRAN CA=215 IS=1 FS=1 IT=392 FT=265 TT=90 FL=4590 IP=1025 FP=1025 TP=90
TRAN CA=216 IS=1 FS=1 IT=265 FT=392 TT=180 FL=4590 IP=1025 FP=1025 TP=180
TRAN CA=217 IS=1 FS=1 IT=392 FT=275 TT=60 FL=5049 IP=1025 FP=1025 TP=60
TRAN CA=218 IS=1 FS=1 IT=275 FT=100 TT=900 FL=137.7 IP=1025 FP=1025 TP=900
TRAN CA=219 IS=1 FS=1 IT=265 FT=323 TT=0 FL=100 IP=1025 FP=1025 TP=0
TRAN CA=220 IS=1 FS=1 IT=323 FT=360 TT=3924 FL=100 IP=1025 FP=1025 TP=3924
TRAN CA=221 IS=1 FS=1 IT=360 FT=283 TT=4140 FL=100 IP=1025 FP=1025 TP=4140
TRAN CA=222 IS=1 FS=1 IT=283 FT=225 TT=6264 FL=100 IP=1025 FP=185 TP=6264
TRAN CA=223 IS=1 FS=1 IT=225 FT=210 TT=600 FL=100 IP=185 FP=103 TP=600
TRAN CA=224 IS=1 FS=1 IT=210 FT=100 TT=8280 FL=100 IP=103 FP=65 TP=8280
TRAN CA=225 IS=1 FS=1 IT=392 FT=450 TT=12 FL=100 IP=1025 FP=1205 TP=12
TRAN CA=226 IS=1 FS=1 IT=450 FT=50 TT=0 FL=1836 IP=1205 FP=1150 TP=0
TRAN CA=227 IS=1 FS=1 IT=50 FT=247 TT=1380 FL=100 IP=1150 FP=1150 TP=1380
TRAN CA=228 IS=1 FS=1 IT=247 FT=288 TT=0 FL=100 IP=1150 FP=1150 TP=0
TRAN CA=229 IS=1 FS=1 IT=288 FT=50 TT=0 FL=1377 IP=1150 FP=900 TP=0
TRAN CA=230 IS=1 FS=1 IT=50 FT=247 TT=3060 FL=100 IP=900 FP=1075 TP=3060
TRAN CA=231 IS=1 FS=1 IT=247 FT=283 TT=0 FL=100 IP=1075 FP=1150 TP=0
TRAN CA=232 IS=1 FS=1 IT=283 FT=50 TT=0 FL=780.3 IP=1150 FP=690 TP=0
TRAN CA=233 IS=1 FS=1 IT=50 FT=200 TT=300 FL=100 IP=690 FP=690 TP=300
TRAN CA=234 IS=1 FS=1 IT=200 FT=283 TT=8964 FL=100 IP=255 FP=1025 TP=8964
TRAN CA=235 IS=1 FS=1 IT=392 FT=275 TT=60 FL=5049 IP=1025 FP=900 TP=60
TRAN CA=236 IS=1 FS=1 IT=275 FT=100 TT=900 FL=137.7 IP=900 FP=65 TP=900
TRAN CA=237 IS=1 FS=1 IT=100 FT=100 TT=0 FL=100 IP=65 FP=1578 TP=0
TRAN CA=238 IS=1 FS=1 IT=100 FT=100 TT=0 FL=100 IP=1578 FP=65 TP=0
TRAN CA=239 IS=1 FS=1 IT=392 FT=392 TT=60 FL=5049 IP=1025 FP=1390 TP=60
TRAN CA=240 IS=1 FS=1 IT=392 FT=392 TT=900 FL=137.7 IP=1390 FP=955 TP=900
TRAN CA=241 IS=1 FS=1 IT=392 FT=392 TT=900 FL=137.7 IP=955 FP=1025 TP=900
TRAN CA=242 IS=1 FS=1 IT=100 FT=180 TT=60 FL=100 IP=1025 FP=1025 TP=60
TRAN CA=243 IS=1 FS=1 IT=180 FT=283 TT=210 FL=100 IP=1025 FP=1025 TP=210


PAIR CA=201 CO=27.6 DI=0.521 EX=6.4 * Tavg=85
PAIR CA=202 CO=27.6 DI=0.512 EX=6.4 * Tavg=100
PAIR CA=203 CO=27.6 DI=0.488 EX=6.4 * Tavg=192
PAIR CA=204 CO=27.6 DI=0.488 EX=6.4 * Tavg=192
PAIR CA=205 CO=27.6 DI=0.490 EX=6.4 * Tavg=180
PAIR CA=206 CO=27.1 DI=0.446 EX=6.4 * Tavg=326
PAIR CA=207 CO=27.0 DI=0.440 EX=6.4 * Tavg=351
PAIR CA=208 CO=27.0 DI=0.440 EX=6.4 * Tavg=351
```

```
PAIR CA=209 CO=27.1 DI=0.444 EX=6.4 * Tavg=336
PAIR CA=210 CO=27.1 DI=0.444 EX=6.4 * Tavg=336
PAIR CA=211 CO=27.1 DI=0.445 EX=6.4 * Tavg=329
PAIR CA=212 CO=27.6 DI=0.490 EX=6.4 * Tavg=178
PAIR CA=213 CO=27.6 DI=0.490 EX=6.4 * Tavg=178
PAIR CA=214 CO=27.1 DI=0.445 EX=6.4 * Tavg=329
PAIR CA=215 CO=27.1 DI=0.445 EX=6.4 * Tavg=329
PAIR CA=216 CO=27.1 DI=0.445 EX=6.4 * Tavg=329
PAIR CA=217 CO=27.1 DI=0.444 EX=6.4 * Tavg=334
PAIR CA=218 CO=27.6 DI=0.488 EX=6.4 * Tavg=188
PAIR CA=219 CO=27.2 DI=0.455 EX=6.4 * Tavg=294
PAIR CA=220 CO=27.0 DI=0.442 EX=6.4 * Tavg=342
PAIR CA=221 CO=27.1 DI=0.447 EX=6.4 * Tavg=322
PAIR CA=222 CO=27.4 DI=0.466 EX=6.4 * Tavg=254
PAIR CA=223 CO=27.5 DI=0.479 EX=6.4 * Tavg=218
PAIR CA=224 CO=27.6 DI=0.495 EX=6.4 * Tavg=155
PAIR CA=225 CO=26.5 DI=0.422 EX=6.4 * Tavg=421
PAIR CA=226 CO=27.4 DI=0.467 EX=6.4 * Tavg=250
PAIR CA=227 CO=27.6 DI=0.496 EX=6.4 * Tavg=149
PAIR CA=228 CO=27.3 DI=0.462 EX=6.4 * Tavg=268
PAIR CA=229 CO=27.6 DI=0.492 EX=6.4 * Tavg=169
PAIR CA=230 CO=27.6 DI=0.496 EX=6.4 * Tavg=149
PAIR CA=231 CO=27.3 DI=0.463 EX=6.4 * Tavg=265
PAIR CA=232 CO=27.6 DI=0.493 EX=6.4 * Tavg=167
PAIR CA=233 CO=27.6 DI=0.504 EX=6.4 * Tavg=125
PAIR CA=234 CO=27.4 DI=0.470 EX=6.4 * Tavg=242
PAIR CA=235 CO=27.1 DI=0.444 EX=6.4 * Tavg=334
PAIR CA=236 CO=27.6 DI=0.488 EX=6.4 * Tavg=188
PAIR CA=237 CO=27.6 DI=0.512 EX=6.4 * Tavg=100
PAIR CA=238 CO=27.6 DI=0.512 EX=6.4 * Tavg=100
PAIR CA=239 CO=26.7 DI=0.430 EX=6.4 * Tavg=392
PAIR CA=240 CO=26.7 DI=0.430 EX=6.4 * Tavg=392
PAIR CA=241 CO=26.7 DI=0.430 EX=6.4 * Tavg=392
PAIR CA=242 CO=27.6 DI=0.499 EX=6.4 * Tavg=140
PAIR CA=243 CO=27.5 DI=0.474 EX=6.4 * Tavg=232


TANG PT=275  DY=6.583  EW=0
*
*-----------------------------------------------------------------------------
*END REGION IVa
*-----------------------------------------------------------------------------
*BEGIN REGION IVb
*-----------------------------------------------------------------------------
OPER CA=3  TE=416 PR=1010
OPER CA=4  TE=260 PR=1010
OPER CA=5  TE=392 PR=1010
OPER CA=6  TE=310 PR=1010
OPER CA=7  TE=280 PR=1010
OPER CA=8  TE=265 PR=1010
OPER CA=9  TE=90  PR=1010
OPER CA=10 TE=454 PR=1010
OPER CA=11 TE=300 PR=170
OPER CA=12 TE=270 PR=88
OPER CA=13 TE=507 PR=1190
OPER CA=14 TE=50  PR=1135
```

```
OPER CA=15 TE=343 PR=1135
OPER CA=16 TE=427 PR=1135
OPER CA=17 TE=343 PR=1060
OPER CA=18 TE=416 PR=1135

OPER CA=20 TE=250 PR=675
OPER CA=21 TE=275 PR=885

OPER CA=23 TE=392 PR=1375
OPER CA=24 TE=392 PR=940
OPER CA=25 TE=392 PR=1010
OPER CA=26 TE=275 PR=1010
OPER CA=27 TE=382 PR=1010
OPER CA=30 TE=235 PR=1010
TRAN CA=201 IS=1 FS=1 IT=70 FT=100 TT=1800 FL=100 IP=15 FP=1115 TP=1800
TRAN CA=202 IS=1 FS=1 IT=100 FT=100 TT=0 FL=100 IP=1115 FP=65 TP=0
TRAN CA=203 IS=1 FS=1 IT=100 FT=416 TT=16164 FL=100 IP=65 FP=1025 TP=16164
TRAN CA=204 IS=1 FS=1 IT=416 FT=100 TT=0 FL=688.5 IP=1025 FP=1025 TP=0
TRAN CA=205 IS=1 FS=1 IT=100 FT=260 TT=0 FL=688.5 IP=1025 FP=1025 TP=0
TRAN CA=206 IS=1 FS=1 IT=260 FT=392 TT=1800 FL=4590 IP=1025 FP=1025 TP=1800
TRAN CA=207 IS=1 FS=1 IT=392 FT=310 TT=900 FL=3442.5 IP=1025 FP=1025 TP=900
TRAN CA=208 IS=1 FS=1 IT=310 FT=392 TT=900 FL=3442.5 IP=1025 FP=1025 TP=900
TRAN CA=209 IS=1 FS=1 IT=392 FT=280 TT=1800 FL=2295 IP=1025 FP=1025 TP=1800
TRAN CA=210 IS=1 FS=1 IT=280 FT=392 TT=1800 FL=2295 IP=1025 FP=1025 TP=1800
TRAN CA=211 IS=1 FS=1 IT=392 FT=265 TT=1800 FL=2295 IP=1025 FP=1025 TP=1800
TRAN CA=212 IS=1 FS=1 IT=265 FT=90 TT=360 FL=688.5 IP=1025 FP=1025 TP=360
TRAN CA=213 IS=1 FS=1 IT=90 FT=265 TT=900 FL=688.5 IP=1025 FP=1025 TP=900
TRAN CA=214 IS=1 FS=1 IT=265 FT=392 TT=1800 FL=2295 IP=1025 FP=1025 TP=1800
TRAN CA=215 IS=1 FS=1 IT=392 FT=265 TT=90 FL=4590 IP=1025 FP=1025 TP=90
TRAN CA=216 IS=1 FS=1 IT=265 FT=392 TT=180 FL=4590 IP=1025 FP=1025 TP=180
TRAN CA=217 IS=1 FS=1 IT=392 FT=275 TT=60 FL=5049 IP=1025 FP=1025 TP=60
TRAN CA=218 IS=1 FS=1 IT=275 FT=100 TT=900 FL=137.7 IP=1025 FP=1025 TP=900
TRAN CA=219 IS=1 FS=1 IT=265 FT=382 TT=0 FL=100 IP=1025 FP=1025 TP=0
TRAN CA=220 IS=1 FS=1 IT=382 FT=454 TT=3924 FL=100 IP=1025 FP=1025 TP=3924
TRAN CA=221 IS=1 FS=1 IT=454 FT=416 TT=4140 FL=100 IP=1025 FP=1025 TP=4140
TRAN CA=222 IS=1 FS=1 IT=416 FT=300 TT=6264 FL=100 IP=1025 FP=185 TP=6264
TRAN CA=223 IS=1 FS=1 IT=300 FT=270 TT=600 FL=100 IP=185 FP=103 TP=600
TRAN CA=224 IS=1 FS=1 IT=270 FT=100 TT=8280 FL=100 IP=103 FP=65 TP=8280
TRAN CA=225 IS=1 FS=1 IT=392 FT=507 TT=12 FL=100 IP=1025 FP=1205 TP=12
TRAN CA=226 IS=1 FS=1 IT=507 FT=50 TT=0 FL=1836 IP=1205 FP=1150 TP=0
TRAN CA=227 IS=1 FS=1 IT=50 FT=343 TT=1380 FL=100 IP=1150 FP=1150 TP=1380
TRAN CA=228 IS=1 FS=1 IT=343 FT=427 TT=0 FL=100 IP=1150 FP=1150 TP=0
TRAN CA=229 IS=1 FS=1 IT=427 FT=50 TT=0 FL=1377 IP=1150 FP=900 TP=0
TRAN CA=230 IS=1 FS=1 IT=50 FT=343 TT=3060 FL=100 IP=900 FP=1075 TP=3060
TRAN CA=231 IS=1 FS=1 IT=343 FT=416 TT=0 FL=100 IP=1075 FP=1150 TP=0
TRAN CA=232 IS=1 FS=1 IT=416 FT=50 TT=0 FL=780.3 IP=1150 FP=690 TP=0
TRAN CA=233 IS=1 FS=1 IT=50 FT=250 TT=300 FL=100 IP=690 FP=690 TP=300
TRAN CA=234 IS=1 FS=1 IT=250 FT=416 TT=8964 FL=100 IP=255 FP=1025 TP=8964
TRAN CA=235 IS=1 FS=1 IT=392 FT=275 TT=60 FL=5049 IP=1025 FP=900 TP=60
TRAN CA=236 IS=1 FS=1 IT=275 FT=100 TT=900 FL=137.7 IP=900 FP=65 TP=900
TRAN CA=237 IS=1 FS=1 IT=100 FT=100 TT=0 FL=100 IP=65 FP=1578 TP=0
TRAN CA=238 IS=1 FS=1 IT=100 FT=100 TT=0 FL=100 IP=1578 FP=65 TP=0
TRAN CA=239 IS=1 FS=1 IT=392 FT=392 TT=60 FL=5049 IP=1025 FP=1390 TP=60
TRAN CA=240 IS=1 FS=1 IT=392 FT=392 TT=900 FL=137.7 IP=1390 FP=955 TP=900
TRAN CA=241 IS=1 FS=1 IT=392 FT=392 TT=900 FL=137.7 IP=955 FP=1025 TP=900
TRAN CA=242 IS=1 FS=1 IT=100 FT=235 TT=60 FL=100 IP=1025 FP=1025 TP=60
```

```
TRAN CA=243 IS=1 FS=1 IT=235 FT=416 TT=210 FL=100 IP=1025 FP=1025 TP=210


PAIR CA=201 CO=27.6 DI=0.521 EX=6.4 * Tavg=85
PAIR CA=202 CO=27.6 DI=0.512 EX=6.4 * Tavg=100
PAIR CA=203 CO=27.4 DI=0.465 EX=6.4 * Tavg=258
PAIR CA=204 CO=27.4 DI=0.465 EX=6.4 * Tavg=258
PAIR CA=205 CO=27.6 DI=0.490 EX=6.4 * Tavg=180
PAIR CA=206 CO=27.1 DI=0.446 EX=6.4 * Tavg=326
PAIR CA=207 CO=27.0 DI=0.440 EX=6.4 * Tavg=351
PAIR CA=208 CO=27.0 DI=0.440 EX=6.4 * Tavg=351
PAIR CA=209 CO=27.1 DI=0.444 EX=6.4 * Tavg=336
PAIR CA=210 CO=27.1 DI=0.444 EX=6.4 * Tavg=336
PAIR CA=211 CO=27.1 DI=0.445 EX=6.4 * Tavg=329
PAIR CA=212 CO=27.6 DI=0.490 EX=6.4 * Tavg=178
PAIR CA=213 CO=27.6 DI=0.490 EX=6.4 * Tavg=178
PAIR CA=214 CO=27.1 DI=0.445 EX=6.4 * Tavg=329
PAIR CA=215 CO=27.1 DI=0.445 EX=6.4 * Tavg=329
PAIR CA=216 CO=27.1 DI=0.445 EX=6.4 * Tavg=329
PAIR CA=217 CO=27.1 DI=0.444 EX=6.4 * Tavg=334
PAIR CA=218 CO=27.6 DI=0.488 EX=6.4 * Tavg=188
PAIR CA=219 CO=27.1 DI=0.447 EX=6.4 * Tavg=324
PAIR CA=220 CO=26.6 DI=0.423 EX=6.4 * Tavg=418
PAIR CA=221 CO=26.4 DI=0.418 EX=6.4 * Tavg=435
PAIR CA=222 CO=27.0 DI=0.438 EX=6.4 * Tavg=358
PAIR CA=223 CO=27.3 DI=0.457 EX=6.4 * Tavg=285
PAIR CA=224 CO=27.6 DI=0.489 EX=6.4 * Tavg=185
PAIR CA=225 CO=26.3 DI=0.413 EX=6.4 * Tavg=450
PAIR CA=226 CO=27.3 DI=0.459 EX=6.4 * Tavg=279
PAIR CA=227 CO=27.6 DI=0.487 EX=6.4 * Tavg=197
PAIR CA=228 CO=26.8 DI=0.432 EX=6.4 * Tavg=385
PAIR CA=229 CO=27.4 DI=0.471 EX=6.4 * Tavg=239
PAIR CA=230 CO=27.6 DI=0.487 EX=6.4 * Tavg=197
PAIR CA=231 CO=26.8 DI=0.433 EX=6.4 * Tavg=380
PAIR CA=232 CO=27.5 DI=0.473 EX=6.4 * Tavg=233
PAIR CA=233 CO=27.6 DI=0.496 EX=6.4 * Tavg=150
PAIR CA=234 CO=27.1 DI=0.444 EX=6.4 * Tavg=333
PAIR CA=235 CO=27.1 DI=0.444 EX=6.4 * Tavg=334
PAIR CA=236 CO=27.6 DI=0.488 EX=6.4 * Tavg=188
PAIR CA=237 CO=27.6 DI=0.512 EX=6.4 * Tavg=100
PAIR CA=238 CO=27.6 DI=0.512 EX=6.4 * Tavg=100
PAIR CA=239 CO=26.7 DI=0.430 EX=6.4 * Tavg=392
PAIR CA=240 CO=26.7 DI=0.430 EX=6.4 * Tavg=392
PAIR CA=241 CO=26.7 DI=0.430 EX=6.4 * Tavg=392
PAIR CA=242 CO=27.6 DI=0.492 EX=6.4 * Tavg=168
PAIR CA=243 CO=27.1 DI=0.446 EX=6.4 * Tavg=326
*
TANG PT=280  DY=6.583
*-----------------------------------------------------------------------------
*END REGION IVb
*-----------------------------------------------------------------------------
*BEGIN REGION V TO NOZZLE N4A, NODE 290
*-----------------------------------------------------------------------------

OPER CA=3  TE=549 PR=1010
OPER CA=4  TE=260 PR=1010
```

```
OPER CA=5  TE=392 PR=1010
OPER CA=6  TE=310 PR=1010
OPER CA=7  TE=280 PR=1010
OPER CA=8  TE=265 PR=1010
OPER CA=9  TE=90  PR=1010
OPER CA=10 TE=549 PR=1010
OPER CA=11 TE=375 PR=170
OPER CA=12 TE=330 PR=88
OPER CA=13 TE=565 PR=1190
OPER CA=14 TE=50  PR=1135
OPER CA=15 TE=440 PR=1135
OPER CA=16 TE=565 PR=1135
OPER CA=17 TE=440 PR=1060
OPER CA=18 TE=549 PR=1135

OPER CA=20 TE=300 PR=675
OPER CA=21 TE=275 PR=885

OPER CA=23 TE=392 PR=1375
OPER CA=24 TE=392 PR=940
OPER CA=25 TE=392 PR=1010
OPER CA=26 TE=275 PR=1010
OPER CA=27 TE=440 PR=1010
OPER CA=30 TE=290 PR=1010
TRAN CA=201 IS=1 FS=1 IT=70 FT=100 TT=1800 FL=100 IP=15 FP=1115 TP=1800
TRAN CA=202 IS=1 FS=1 IT=100 FT=100 TT=0 FL=100 IP=1115 FP=65 TP=0
TRAN CA=203 IS=1 FS=1 IT=100 FT=549 TT=16164 FL=100 IP=65 FP=1025 TP=16164
TRAN CA=204 IS=1 FS=1 IT=549 FT=100 TT=0 FL=688.5 IP=1025 FP=1025 TP=0
TRAN CA=205 IS=1 FS=1 IT=100 FT=260 TT=0 FL=688.5 IP=1025 FP=1025 TP=0
TRAN CA=206 IS=1 FS=1 IT=260 FT=392 TT=1800 FL=4590 IP=1025 FP=1025 TP=1800
TRAN CA=207 IS=1 FS=1 IT=392 FT=310 TT=900 FL=3442.5 IP=1025 FP=1025 TP=900
TRAN CA=208 IS=1 FS=1 IT=310 FT=392 TT=900 FL=3442.5 IP=1025 FP=1025 TP=900
TRAN CA=209 IS=1 FS=1 IT=392 FT=280 TT=1800 FL=2295 IP=1025 FP=1025 TP=1800
TRAN CA=210 IS=1 FS=1 IT=280 FT=392 TT=1800 FL=2295 IP=1025 FP=1025 TP=1800
TRAN CA=211 IS=1 FS=1 IT=392 FT=265 TT=1800 FL=2295 IP=1025 FP=1025 TP=1800
TRAN CA=212 IS=1 FS=1 IT=265 FT=90 TT=360 FL=688.5 IP=1025 FP=1025 TP=360
TRAN CA=213 IS=1 FS=1 IT=90 FT=265 TT=900 FL=688.5 IP=1025 FP=1025 TP=900
TRAN CA=214 IS=1 FS=1 IT=265 FT=392 TT=1800 FL=2295 IP=1025 FP=1025 TP=1800
TRAN CA=215 IS=1 FS=1 IT=392 FT=265 TT=90 FL=4590 IP=1025 FP=1025 TP=90
TRAN CA=216 IS=1 FS=1 IT=265 FT=392 TT=180 FL=4590 IP=1025 FP=1025 TP=180
TRAN CA=217 IS=1 FS=1 IT=392 FT=275 TT=60 FL=5049 IP=1025 FP=1025 TP=60
TRAN CA=218 IS=1 FS=1 IT=275 FT=100 TT=900 FL=137.7 IP=1025 FP=1025 TP=900
TRAN CA=219 IS=1 FS=1 IT=265 FT=440 TT=0 FL=100 IP=1025 FP=1025 TP=0
TRAN CA=220 IS=1 FS=1 IT=440 FT=549 TT=3924 FL=100 IP=1025 FP=1025 TP=3924
TRAN CA=221 *IS=1 FS=1 IT=549 FT=549 TT=0 FL=100 IP=1025 FP=1025 TP=0
TRAN CA=222 IS=1 FS=1 IT=549 FT=375 TT=6264 FL=100 IP=1025 FP=185 TP=6264
TRAN CA=223 IS=1 FS=1 IT=375 FT=330 TT=600 FL=100 IP=185 FP=103 TP=600
TRAN CA=224 IS=1 FS=1 IT=330 FT=100 TT=8280 FL=100 IP=103 FP=65 TP=8280
TRAN CA=225 IS=1 FS=1 IT=392 FT=565 TT=12 FL=100 IP=1025 FP=1205 TP=12
TRAN CA=226 IS=1 FS=1 IT=565 FT=50 TT=0 FL=1836 IP=1205 FP=1150 TP=0
TRAN CA=227 IS=1 FS=1 IT=50 FT=440 TT=1380 FL=100 IP=1150 FP=1150 TP=1380
TRAN CA=228 IS=1 FS=1 IT=440 FT=565 TT=0 FL=100 IP=1150 FP=1150 TP=0
TRAN CA=229 IS=1 FS=1 IT=565 FT=50 TT=0 FL=1377 IP=1150 FP=900 TP=0
TRAN CA=230 IS=1 FS=1 IT=50 FT=440 TT=3060 FL=100 IP=900 FP=1075 TP=3060
TRAN CA=231 IS=1 FS=1 IT=440 FT=549 TT=0 FL=100 IP=1075 FP=1150 TP=0
TRAN CA=232 IS=1 FS=1 IT=549 FT=50 TT=0 FL=780.3 IP=1150 FP=690 TP=0
```

```
TRAN CA=233 IS=1 FS=1 IT=50 FT=300 TT=300 FL=100 IP=690 FP=690 TP=300
TRAN CA=234 IS=1 FS=1 IT=300 FT=549 TT=8964 FL=100 IP=255 FP=1025 TP=8964
TRAN CA=235 IS=1 FS=1 IT=392 FT=275 TT=60 FL=5049 IP=1025 FP=900 TP=60
TRAN CA=236 IS=1 FS=1 IT=275 FT=100 TT=900 FL=137.7 IP=900 FP=65 TP=900
TRAN CA=237 IS=1 FS=1 IT=100 FT=100 TT=0 FL=100 IP=65 FP=1578 TP=0
TRAN CA=238 IS=1 FS=1 IT=100 FT=100 TT=0 FL=100 IP=1578 FP=65 TP=0
TRAN CA=239 IS=1 FS=1 IT=392 FT=392 TT=60 FL=5049 IP=1025 FP=1390 TP=60
TRAN CA=240 IS=1 FS=1 IT=392 FT=392 TT=900 FL=137.7 IP=1390 FP=955 TP=900
TRAN CA=241 IS=1 FS=1 IT=392 FT=392 TT=900 FL=137.7 IP=955 FP=1025 TP=900
TRAN CA=242 IS=1 FS=1 IT=100 FT=290 TT=60 FL=100 IP=1025 FP=1025 TP=60
TRAN CA=243 IS=1 FS=1 IT=290 FT=549 TT=210 FL=100 IP=1025 FP=1025 TP=210

PAIR CA=201 CO=27.6 DI=0.521 EX=6.4 * Tavg=85
PAIR CA=202 CO=27.6 DI=0.512 EX=6.4 * Tavg=100
PAIR CA=203 CO=27.1 DI=0.447 EX=6.4 * Tavg=325
PAIR CA=204 CO=27.1 DI=0.447 EX=6.4 * Tavg=325
PAIR CA=205 CO=27.6 DI=0.490 EX=6.4 * Tavg=180
PAIR CA=206 CO=27.1 DI=0.446 EX=6.4 * Tavg=326
PAIR CA=207 CO=27.0 DI=0.440 EX=6.4 * Tavg=351
PAIR CA=208 CO=27.0 DI=0.440 EX=6.4 * Tavg=351
PAIR CA=209 CO=27.1 DI=0.444 EX=6.4 * Tavg=336
PAIR CA=210 CO=27.1 DI=0.444 EX=6.4 * Tavg=336
PAIR CA=211 CO=27.1 DI=0.445 EX=6.4 * Tavg=329
PAIR CA=212 CO=27.6 DI=0.490 EX=6.4 * Tavg=178
PAIR CA=213 CO=27.6 DI=0.490 EX=6.4 * Tavg=178
PAIR CA=214 CO=27.1 DI=0.445 EX=6.4 * Tavg=329
PAIR CA=215 CO=27.1 DI=0.445 EX=6.4 * Tavg=329
PAIR CA=216 CO=27.1 DI=0.445 EX=6.4 * Tavg=329
PAIR CA=217 CO=27.1 DI=0.444 EX=6.4 * Tavg=334
PAIR CA=218 CO=27.6 DI=0.488 EX=6.4 * Tavg=188
PAIR CA=219 CO=27.0 DI=0.439 EX=6.4 * Tavg=353
PAIR CA=220 CO=25.9 DI=0.400 EX=6.4 * Tavg=495
PAIR CA=221 CO=25.5 DI=0.387 EX=6.4 * Tavg=549
PAIR CA=222 CO=26.2 DI=0.409 EX=6.4 * Tavg=462
PAIR CA=223 CO=27.0 DI=0.439 EX=6.4 * Tavg=353
PAIR CA=224 CO=27.5 DI=0.480 EX=6.4 * Tavg=215
PAIR CA=225 CO=26.1 DI=0.404 EX=6.4 * Tavg=479
PAIR CA=226 CO=27.2 DI=0.451 EX=6.4 * Tavg=308
PAIR CA=227 CO=27.4 DI=0.469 EX=6.4 * Tavg=245
PAIR CA=228 CO=25.9 DI=0.397 EX=6.4 * Tavg=503
PAIR CA=229 CO=27.2 DI=0.451 EX=6.4 * Tavg=308
PAIR CA=230 CO=27.4 DI=0.469 EX=6.4 * Tavg=245
PAIR CA=231 CO=25.9 DI=0.400 EX=6.4 * Tavg=495
PAIR CA=232 CO=27.2 DI=0.453 EX=6.4 * Tavg=300
PAIR CA=233 CO=27.6 DI=0.491 EX=6.4 * Tavg=175
PAIR CA=234 CO=26.5 DI=0.421 EX=6.4 * Tavg=425
PAIR CA=235 CO=27.1 DI=0.444 EX=6.4 * Tavg=334
PAIR CA=236 CO=27.6 DI=0.488 EX=6.4 * Tavg=188
PAIR CA=237 CO=27.6 DI=0.512 EX=6.4 * Tavg=100
PAIR CA=238 CO=27.6 DI=0.512 EX=6.4 * Tavg=100
PAIR CA=239 CO=26.7 DI=0.430 EX=6.4 * Tavg=392
PAIR CA=240 CO=26.7 DI=0.430 EX=6.4 * Tavg=392
PAIR CA=241 CO=26.7 DI=0.430 EX=6.4 * Tavg=392
PAIR CA=242 CO=27.6 DI=0.487 EX=6.4 * Tavg=195
PAIR CA=243 CO=26.5 DI=0.422 EX=6.4 * Tavg=420
```

```
BRAD PT=285  RA=1.25
TANG PT=290  DX=-4.007  DZ=4.007  EW=1
NOZZ PT=290   *NOZZLE N4A
AMVT  CA=1 PT=290 DX=0.0196 DY=0.1069 DZ=-0.0196
AMVT  CA=2 PT=290 DX=0.0196 DY=0.1069 DZ=-0.0196
AMVT  CA=3 PT=290 DX=0.3130 DY=1.7067 DZ=-0.3130
AMVT  CA=4 PT=290 DX=0.3130 DY=1.7067 DZ=-0.3130
AMVT  CA=5 PT=290 DX=0.3130 DY=1.7067 DZ=-0.3130
AMVT  CA=6 PT=290 DX=0.3130 DY=1.7067 DZ=-0.3130
AMVT  CA=7 PT=290 DX=0.3130 DY=1.7067 DZ=-0.3130
AMVT  CA=8 PT=290 DX=0.3130 DY=1.7067 DZ=-0.3130
AMVT  CA=9 PT=290 DX=0.3130 DY=1.7067 DZ=-0.3130
AMVT CA=10 PT=290 DX=0.3130 DY=1.7067 DZ=-0.3130
AMVT CA=11 PT=290 DX=0.1993 DY=1.0867 DZ=-0.1993
AMVT CA=12 PT=290 DX=0.1699 DY=0.9264 DZ=-0.1699
AMVT CA=13 PT=290 DX=0.3234 DY=1.7637 DZ=-0.3234
AMVT CA=14 PT=290 DX=0.3234 DY=1.7637 DZ=-0.3234
AMVT CA=15 PT=290 DX=0.3234 DY=1.7637 DZ=-0.3234
AMVT CA=16 PT=290 DX=0.3234 DY=1.7637 DZ=-0.3234
AMVT CA=17 PT=290 DX=0.3169 DY=1.7281 DZ=-0.3169
AMVT CA=18 PT=290 DX=0.3234 DY=1.7637 DZ=-0.3234
AMVT CA=19 PT=290 DX=0.2823 DY=1.5392 DZ=-0.2823
AMVT CA=20 PT=290 DX=0.2823 DY=1.5392 DZ=-0.2823
AMVT CA=21 PT=290 DX=0.3130 DY=1.7067 DZ=-0.3130
AMVT CA=22 PT=290 DX=0.0196 DY=0.1069 DZ=-0.0196
AMVT CA=23 PT=290 DX=0.3463 DY=1.8884 DZ=-0.3463
AMVT CA=24 PT=290 DX=0.3064 DY=1.6711 DZ=-0.3064
AMVT CA=25 PT=290 DX=0.3130 DY=1.7067 DZ=-0.3130
AMVT CA=26 PT=290 DX=0.3064 DY=1.6711 DZ=-0.3064
AMVT CA=27 PT=290 DX=0.3130 DY=1.7067 DZ=-0.3130
AMVT CA=28 PT=290 DX=0.3130 DY=1.7067 DZ=-0.3130
AMVT CA=29 PT=290 DX=0.3064 DY=1.6711 DZ=-0.3064
AMVT CA=30 PT=290 DX=0.3130 DY=1.7067 DZ=-0.3130
AMVT CA=31 PT=290 DX=0.3019 DY=1.6461 DZ=-0.3019

AMVT CA=32 PT=290 DX=-.09   DY=.015   DZ=-.093
*-----------------------------------------------------------------------------
*END REGION V
*--------------
*BEGIN REGION IV
*--------------
OPER CA=3  TE=150 PR=1010
OPER CA=4  TE=260 PR=1010
OPER CA=5  TE=392 PR=1010
OPER CA=6  TE=310 PR=1010
OPER CA=7  TE=280 PR=1010
OPER CA=8  TE=265 PR=1010
OPER CA=9  TE=90  PR=1010
OPER CA=10 TE=265 PR=1010
OPER CA=11 TE=150 PR=170
OPER CA=12 TE=150 PR=88
OPER CA=13 TE=392 PR=1190
OPER CA=14 TE=50  PR=1135
OPER CA=15 TE=150 PR=1135
OPER CA=16 TE=150 PR=1135
OPER CA=17 TE=150 PR=1060
```

```
OPER CA=18 TE=150 PR=1135

OPER CA=20 TE=150 PR=675
OPER CA=21 TE=275 PR=885

OPER CA=23 TE=392 PR=1375
OPER CA=24 TE=392 PR=940
OPER CA=25 TE=392 PR=1010
OPER CA=26 TE=275 PR=1010
OPER CA=27 TE=265 PR=1010

OPER CA=30 TE=125 PR=1010
*
TRAN CA=201 IS=1 FS=1 IT=70 FT=100 TT=1800 FL=100 IP=15 FP=1115 TP=1800
TRAN CA=202 IS=1 FS=1 IT=100 FT=100 TT=0 FL=100 IP=1115 FP=65 TP=0
TRAN CA=203 IS=1 FS=1 IT=100 FT=150 TT=16164 FL=100 IP=65 FP=1025 TP=16164
TRAN CA=204 IS=1 FS=1 IT=150 FT=100 TT=0 FL=688.5 IP=1025 FP=1025 TP=0
TRAN CA=205 IS=1 FS=1 IT=100 FT=260 TT=0 FL=688.5 IP=1025 FP=1025 TP=0
TRAN CA=206 IS=1 FS=1 IT=260 FT=392 TT=1800 FL=4590 IP=1025 FP=1025 TP=1800
TRAN CA=207 IS=1 FS=1 IT=392 FT=310 TT=900 FL=3442.5 IP=1025 FP=1025 TP=900
TRAN CA=208 IS=1 FS=1 IT=310 FT=392 TT=900 FL=3442.5 IP=1025 FP=1025 TP=900
TRAN CA=209 IS=1 FS=1 IT=392 FT=280 TT=1800 FL=2295 IP=1025 FP=1025 TP=1800
TRAN CA=210 IS=1 FS=1 IT=280 FT=392 TT=1800 FL=2295 IP=1025 FP=1025 TP=1800
TRAN CA=211 IS=1 FS=1 IT=392 FT=265 TT=1800 FL=2295 IP=1025 FP=1025 TP=1800
TRAN CA=212 IS=1 FS=1 IT=265 FT=90 TT=360 FL=688.5 IP=1025 FP=1025 TP=360
TRAN CA=213 IS=1 FS=1 IT=90 FT=265 TT=900 FL=688.5 IP=1025 FP=1025 TP=900
TRAN CA=214 IS=1 FS=1 IT=265 FT=392 TT=1800 FL=2295 IP=1025 FP=1025 TP=1800
TRAN CA=215 IS=1 FS=1 IT=392 FT=265 TT=90 FL=4590 IP=1025 FP=1025 TP=90
TRAN CA=216 IS=1 FS=1 IT=265 FT=392 TT=180 FL=4590 IP=1025 FP=1025 TP=180
TRAN CA=217 IS=1 FS=1 IT=392 FT=275 TT=60 FL=5049 IP=1025 FP=1025 TP=60
TRAN CA=218 IS=1 FS=1 IT=275 FT=100 TT=900 FL=137.7 IP=1025 FP=1025 TP=900
TRAN CA=219 *IS=1 FS=1 IT=265 FT=265 TT=0 FL=100 IP=1025 FP=1025 TP=0
TRAN CA=220 *IS=1 FS=1 IT=265 FT=265 TT=0 FL=100 IP=1025 FP=1025 TP=0
TRAN CA=221 IS=1 FS=1 IT=265 FT=150 TT=4140 FL=100 IP=1025 FP=1025 TP=4140
TRAN CA=222 IS=1 FS=1 IT=150 FT=150 TT=0 FL=100 IP=1025 FP=185 TP=0
TRAN CA=223 IS=1 FS=1 IT=150 FT=150 TT=0 FL=100 IP=185 FP=103 TP=0
TRAN CA=224 IS=1 FS=1 IT=150 FT=100 TT=8280 FL=100 IP=103 FP=65 TP=8280
TRAN CA=225 IS=1 FS=1 IT=392 FT=392 TT=12 FL=100 IP=1025 FP=1205 TP=12
TRAN CA=226 IS=1 FS=1 IT=392 FT=50 TT=0 FL=1836 IP=1205 FP=1150 TP=0
TRAN CA=227 IS=1 FS=1 IT=50 FT=150 TT=1380 FL=100 IP=1150 FP=1150 TP=1380
TRAN CA=228 IS=1 FS=1 IT=150 FT=150 TT=0 FL=100 IP=1150 FP=1150 TP=0
TRAN CA=229 IS=1 FS=1 IT=150 FT=50 TT=0 FL=1377 IP=1150 FP=900 TP=0
TRAN CA=230 IS=1 FS=1 IT=50 FT=150 TT=3060 FL=100 IP=900 FP=1075 TP=3060
TRAN CA=231 IS=1 FS=1 IT=150 FT=150 TT=0 FL=100 IP=1075 FP=1150 TP=0
TRAN CA=232 IS=1 FS=1 IT=150 FT=50 TT=0 FL=780.3 IP=1150 FP=690 TP=0
TRAN CA=233 IS=1 FS=1 IT=50 FT=150 TT=300 FL=100 IP=690 FP=690 TP=300
TRAN CA=234 IS=1 FS=1 IT=150 FT=150 TT=8964 FL=100 IP=255 FP=1025 TP=8964
TRAN CA=235 IS=1 FS=1 IT=392 FT=275 TT=60 FL=5049 IP=1025 FP=900 TP=60
TRAN CA=236 IS=1 FS=1 IT=275 FT=100 TT=900 FL=137.7 IP=900 FP=65 TP=900
TRAN CA=237 IS=1 FS=1 IT=100 FT=100 TT=0 FL=100 IP=65 FP=1578 TP=0
TRAN CA=238 IS=1 FS=1 IT=100 FT=100 TT=0 FL=100 IP=1578 FP=65 TP=0
TRAN CA=239 IS=1 FS=1 IT=392 FT=392 TT=60 FL=5049 IP=1025 FP=1390 TP=60
TRAN CA=240 IS=1 FS=1 IT=392 FT=392 TT=900 FL=137.7 IP=1390 FP=955 TP=900
TRAN CA=241 IS=1 FS=1 IT=392 FT=392 TT=900 FL=137.7 IP=955 FP=1025 TP=900
TRAN CA=242 IS=1 FS=1 IT=100 FT=125 TT=60 FL=100 IP=1025 FP=1025 TP=60
TRAN CA=243 IS=1 FS=1 IT=125 FT=150 TT=210 FL=100 IP=1025 FP=1025 TP=210
```

```
*
PAIR CA=201 CO=27.6 DI=0.521 EX=6.4 * Tavg=85
PAIR CA=202 CO=27.6 DI=0.512 EX=6.4 * Tavg=100
PAIR CA=203 CO=27.6 DI=0.504 EX=6.4 * Tavg=125
PAIR CA=204 CO=27.6 DI=0.504 EX=6.4 * Tavg=125
PAIR CA=205 CO=27.6 DI=0.490 EX=6.4 * Tavg=180
PAIR CA=206 CO=27.1 DI=0.446 EX=6.4 * Tavg=326
PAIR CA=207 CO=27.0 DI=0.440 EX=6.4 * Tavg=351
PAIR CA=208 CO=27.0 DI=0.440 EX=6.4 * Tavg=351
PAIR CA=209 CO=27.1 DI=0.444 EX=6.4 * Tavg=336
PAIR CA=210 CO=27.1 DI=0.444 EX=6.4 * Tavg=336
PAIR CA=211 CO=27.1 DI=0.445 EX=6.4 * Tavg=329
PAIR CA=212 CO=27.6 DI=0.490 EX=6.4 * Tavg=178
PAIR CA=213 CO=27.6 DI=0.490 EX=6.4 * Tavg=178
PAIR CA=214 CO=27.1 DI=0.445 EX=6.4 * Tavg=329
PAIR CA=215 CO=27.1 DI=0.445 EX=6.4 * Tavg=329
PAIR CA=216 CO=27.1 DI=0.445 EX=6.4 * Tavg=329
PAIR CA=217 CO=27.1 DI=0.444 EX=6.4 * Tavg=334
PAIR CA=218 CO=27.6 DI=0.488 EX=6.4 * Tavg=188
PAIR CA=219 CO=27.3 DI=0.463 EX=6.4 * Tavg=265
PAIR CA=220 CO=27.3 DI=0.463 EX=6.4 * Tavg=265
PAIR CA=221 CO=27.6 DI=0.483 EX=6.4 * Tavg=208
PAIR CA=222 CO=27.6 DI=0.496 EX=6.4 * Tavg=150
PAIR CA=223 CO=27.6 DI=0.496 EX=6.4 * Tavg=150
PAIR CA=224 CO=27.6 DI=0.504 EX=6.4 * Tavg=125
PAIR CA=225 CO=26.7 DI=0.430 EX=6.4 * Tavg=392
PAIR CA=226 CO=27.5 DI=0.478 EX=6.4 * Tavg=221
PAIR CA=227 CO=27.6 DI=0.512 EX=6.4 * Tavg=100
PAIR CA=228 CO=27.6 DI=0.496 EX=6.4 * Tavg=150
PAIR CA=229 CO=27.6 DI=0.512 EX=6.4 * Tavg=100
PAIR CA=230 CO=27.6 DI=0.512 EX=6.4 * Tavg=100
PAIR CA=231 CO=27.6 DI=0.496 EX=6.4 * Tavg=150
PAIR CA=232 CO=27.6 DI=0.512 EX=6.4 * Tavg=100
PAIR CA=233 CO=27.6 DI=0.512 EX=6.4 * Tavg=100
PAIR CA=234 CO=27.6 DI=0.496 EX=6.4 * Tavg=150
PAIR CA=235 CO=27.1 DI=0.444 EX=6.4 * Tavg=334
PAIR CA=236 CO=27.6 DI=0.488 EX=6.4 * Tavg=188
PAIR CA=237 CO=27.6 DI=0.512 EX=6.4 * Tavg=100
PAIR CA=238 CO=27.6 DI=0.512 EX=6.4 * Tavg=100
PAIR CA=239 CO=26.7 DI=0.430 EX=6.4 * Tavg=392
PAIR CA=240 CO=26.7 DI=0.430 EX=6.4 * Tavg=392
PAIR CA=241 CO=26.7 DI=0.430 EX=6.4 * Tavg=392
PAIR CA=242 CO=27.6 DI=0.508 EX=6.4 * Tavg=113
PAIR CA=243 CO=27.6 DI=0.500 EX=6.4 * Tavg=138

*
*REGION IV GEOMETRY DOWNSTREAM OF FW brnCH TEE/REDUCER - 10 INCH PIPING
*RUN FROM FW TEE TO ELBOW BEFORE NOZZLE N4A, NODE 155
JUNC PT=115
CROS CD=5
BRAN PT=120  DX=-0.5022  DY=0.596   DZ=-0.5022  TE=1 EW=1
TANG PT=125  DX=-2.594  DY=3.078  DZ=-2.594
TANG PT=130  DX=-2.594  DY=3.078  DZ=-2.594
TANG PT=135  DX=-2.594  DY=3.078  DZ=-2.594  EW=0
```

```
BRAD PT=140  RA=1.25  EW=0
TANG PT=142  DY=4
TANG PT=145  DY=4
TANG PT=150  DY=2.53
*-----------------------------------------------------------------------------
*END REGION IV
*-----------------------------------------------------------------------------
*BEGIN REGION IVa
*-----------------------------------------------------------------------------
OPER CA=3  TE=283 PR=1010
OPER CA=4  TE=260 PR=1010
OPER CA=5  TE=392 PR=1010
OPER CA=6  TE=310 PR=1010
OPER CA=7  TE=280 PR=1010
OPER CA=8  TE=265 PR=1010
OPER CA=9  TE=90  PR=1010
OPER CA=10 TE=360 PR=1010
OPER CA=11 TE=225 PR=170
OPER CA=12 TE=210 PR=88
OPER CA=13 TE=450 PR=1190
OPER CA=14 TE=50  PR=1135
OPER CA=15 TE=247 PR=1135
OPER CA=16 TE=288 PR=1135
OPER CA=17 TE=247 PR=1060
OPER CA=18 TE=283 PR=1135

OPER CA=20 TE=200 PR=675
OPER CA=21 TE=275 PR=885

OPER CA=23 TE=392 PR=1375
OPER CA=24 TE=392 PR=940
OPER CA=25 TE=392 PR=1010
OPER CA=26 TE=275 PR=1010
OPER CA=27 TE=323 PR=1010
OPER CA=30 TE=180 PR=1010
*
TRAN CA=201 IS=1 FS=1 IT=70 FT=100 TT=1800 FL=100 IP=15 FP=1115 TP=1800
TRAN CA=202 IS=1 FS=1 IT=100 FT=100 TT=0 FL=100 IP=1115 FP=65 TP=0
TRAN CA=203 IS=1 FS=1 IT=100 FT=283 TT=16164 FL=100 IP=65 FP=1025 TP=16164
TRAN CA=204 IS=1 FS=1 IT=283 FT=100 TT=0 FL=688.5 IP=1025 FP=1025 TP=0
TRAN CA=205 IS=1 FS=1 IT=100 FT=260 TT=0 FL=688.5 IP=1025 FP=1025 TP=0
TRAN CA=206 IS=1 FS=1 IT=260 FT=392 TT=1800 FL=4590 IP=1025 FP=1025 TP=1800
TRAN CA=207 IS=1 FS=1 IT=392 FT=310 TT=900 FL=3442.5 IP=1025 FP=1025 TP=900
TRAN CA=208 IS=1 FS=1 IT=310 FT=392 TT=900 FL=3442.5 IP=1025 FP=1025 TP=900
TRAN CA=209 IS=1 FS=1 IT=392 FT=280 TT=1800 FL=2295 IP=1025 FP=1025 TP=1800
TRAN CA=210 IS=1 FS=1 IT=280 FT=392 TT=1800 FL=2295 IP=1025 FP=1025 TP=1800
TRAN CA=211 IS=1 FS=1 IT=392 FT=265 TT=1800 FL=2295 IP=1025 FP=1025 TP=1800
TRAN CA=212 IS=1 FS=1 IT=265 FT=90 TT=360 FL=688.5 IP=1025 FP=1025 TP=360
TRAN CA=213 IS=1 FS=1 IT=90 FT=265 TT=900 FL=688.5 IP=1025 FP=1025 TP=900
TRAN CA=214 IS=1 FS=1 IT=265 FT=392 TT=1800 FL=2295 IP=1025 FP=1025 TP=1800
TRAN CA=215 IS=1 FS=1 IT=392 FT=265 TT=90 FL=4590 IP=1025 FP=1025 TP=90
TRAN CA=216 IS=1 FS=1 IT=265 FT=392 TT=180 FL=4590 IP=1025 FP=1025 TP=180
TRAN CA=217 IS=1 FS=1 IT=392 FT=275 TT=60 FL=5049 IP=1025 FP=1025 TP=60
TRAN CA=218 IS=1 FS=1 IT=275 FT=100 TT=900 FL=137.7 IP=1025 FP=1025 TP=900
TRAN CA=219 IS=1 FS=1 IT=265 FT=323 TT=0 FL=100 IP=1025 FP=1025 TP=0
TRAN CA=220 IS=1 FS=1 IT=323 FT=360 TT=3924 FL=100 IP=1025 FP=1025 TP=3924
```

```
TRAN CA=221 IS=1 FS=1 IT=360 FT=283 TT=4140 FL=100 IP=1025 FP=1025 TP=4140
TRAN CA=222 IS=1 FS=1 IT=283 FT=225 TT=6264 FL=100 IP=1025 FP=185 TP=6264
TRAN CA=223 IS=1 FS=1 IT=225 FT=210 TT=600 FL=100 IP=185 FP=103 TP=600
TRAN CA=224 IS=1 FS=1 IT=210 FT=100 TT=8280 FL=100 IP=103 FP=65 TP=8280
TRAN CA=225 IS=1 FS=1 IT=392 FT=450 TT=12 FL=100 IP=1025 FP=1205 TP=12
TRAN CA=226 IS=1 FS=1 IT=450 FT=50 TT=0 FL=1836 IP=1205 FP=1150 TP=0
TRAN CA=227 IS=1 FS=1 IT=50 FT=247 TT=1380 FL=100 IP=1150 FP=1150 TP=1380
TRAN CA=228 IS=1 FS=1 IT=247 FT=288 TT=0 FL=100 IP=1150 FP=1150 TP=0
TRAN CA=229 IS=1 FS=1 IT=288 FT=50 TT=0 FL=1377 IP=1150 FP=900 TP=0
TRAN CA=230 IS=1 FS=1 IT=50 FT=247 TT=3060 FL=100 IP=900 FP=1075 TP=3060
TRAN CA=231 IS=1 FS=1 IT=247 FT=283 TT=0 FL=100 IP=1075 FP=1150 TP=0
TRAN CA=232 IS=1 FS=1 IT=283 FT=50 TT=0 FL=780.3 IP=1150 FP=690 TP=0
TRAN CA=233 IS=1 FS=1 IT=50 FT=200 TT=300 FL=100 IP=690 FP=690 TP=300
TRAN CA=234 IS=1 FS=1 IT=200 FT=283 TT=8964 FL=100 IP=255 FP=1025 TP=8964
TRAN CA=235 IS=1 FS=1 IT=392 FT=275 TT=60 FL=5049 IP=1025 FP=900 TP=60
TRAN CA=236 IS=1 FS=1 IT=275 FT=100 TT=900 FL=137.7 IP=900 FP=65 TP=900
TRAN CA=237 IS=1 FS=1 IT=100 FT=100 TT=0 FL=100 IP=65 FP=1578 TP=0
TRAN CA=238 IS=1 FS=1 IT=100 FT=100 TT=0 FL=100 IP=1578 FP=65 TP=0
TRAN CA=239 IS=1 FS=1 IT=392 FT=392 TT=60 FL=5049 IP=1025 FP=1390 TP=60
TRAN CA=240 IS=1 FS=1 IT=392 FT=392 TT=900 FL=137.7 IP=1390 FP=955 TP=900
TRAN CA=241 IS=1 FS=1 IT=392 FT=392 TT=900 FL=137.7 IP=955 FP=1025 TP=900
TRAN CA=242 IS=1 FS=1 IT=100 FT=180 TT=60 FL=100 IP=1025 FP=1025 TP=60
TRAN CA=243 IS=1 FS=1 IT=180 FT=283 TT=210 FL=100 IP=1025 FP=1025 TP=210


PAIR CA=201 CO=27.6 DI=0.521 EX=6.4 * Tavg=85
PAIR CA=202 CO=27.6 DI=0.512 EX=6.4 * Tavg=100
PAIR CA=203 CO=27.6 DI=0.488 EX=6.4 * Tavg=192
PAIR CA=204 CO=27.6 DI=0.488 EX=6.4 * Tavg=192
PAIR CA=205 CO=27.6 DI=0.490 EX=6.4 * Tavg=180
PAIR CA=206 CO=27.1 DI=0.446 EX=6.4 * Tavg=326
PAIR CA=207 CO=27.0 DI=0.440 EX=6.4 * Tavg=351
PAIR CA=208 CO=27.0 DI=0.440 EX=6.4 * Tavg=351
PAIR CA=209 CO=27.1 DI=0.444 EX=6.4 * Tavg=336
PAIR CA=210 CO=27.1 DI=0.444 EX=6.4 * Tavg=336
PAIR CA=211 CO=27.1 DI=0.445 EX=6.4 * Tavg=329
PAIR CA=212 CO=27.6 DI=0.490 EX=6.4 * Tavg=178
PAIR CA=213 CO=27.6 DI=0.490 EX=6.4 * Tavg=178
PAIR CA=214 CO=27.1 DI=0.445 EX=6.4 * Tavg=329
PAIR CA=215 CO=27.1 DI=0.445 EX=6.4 * Tavg=329
PAIR CA=216 CO=27.1 DI=0.445 EX=6.4 * Tavg=329
PAIR CA=217 CO=27.1 DI=0.444 EX=6.4 * Tavg=334
PAIR CA=218 CO=27.6 DI=0.488 EX=6.4 * Tavg=188
PAIR CA=219 CO=27.2 DI=0.455 EX=6.4 * Tavg=294
PAIR CA=220 CO=27.0 DI=0.442 EX=6.4 * Tavg=342
PAIR CA=221 CO=27.1 DI=0.447 EX=6.4 * Tavg=322
PAIR CA=222 CO=27.4 DI=0.466 EX=6.4 * Tavg=254
PAIR CA=223 CO=27.5 DI=0.479 EX=6.4 * Tavg=218
PAIR CA=224 CO=27.6 DI=0.495 EX=6.4 * Tavg=155
PAIR CA=225 CO=26.5 DI=0.422 EX=6.4 * Tavg=421
PAIR CA=226 CO=27.4 DI=0.467 EX=6.4 * Tavg=250
PAIR CA=227 CO=27.6 DI=0.496 EX=6.4 * Tavg=149
PAIR CA=228 CO=27.3 DI=0.462 EX=6.4 * Tavg=268
PAIR CA=229 CO=27.6 DI=0.492 EX=6.4 * Tavg=169
PAIR CA=230 CO=27.6 DI=0.496 EX=6.4 * Tavg=149
PAIR CA=231 CO=27.3 DI=0.463 EX=6.4 * Tavg=265
```

```
PAIR CA=232 CO=27.6 DI=0.493 EX=6.4 * Tavg=167
PAIR CA=233 CO=27.6 DI=0.504 EX=6.4 * Tavg=125
PAIR CA=234 CO=27.4 DI=0.470 EX=6.4 * Tavg=242
PAIR CA=235 CO=27.1 DI=0.444 EX=6.4 * Tavg=334
PAIR CA=236 CO=27.6 DI=0.488 EX=6.4 * Tavg=188
PAIR CA=237 CO=27.6 DI=0.512 EX=6.4 * Tavg=100
PAIR CA=238 CO=27.6 DI=0.512 EX=6.4 * Tavg=100
PAIR CA=239 CO=26.7 DI=0.430 EX=6.4 * Tavg=392
PAIR CA=240 CO=26.7 DI=0.430 EX=6.4 * Tavg=392
PAIR CA=241 CO=26.7 DI=0.430 EX=6.4 * Tavg=392
PAIR CA=242 CO=27.6 DI=0.499 EX=6.4 * Tavg=140
PAIR CA=243 CO=27.5 DI=0.474 EX=6.4 * Tavg=232

*
TANG PT=152  DY=6.53  EW=0
*
*-----------------------------------------------------------------------------
*END REGION IVa
*-----------------------------------------------------------------------------
*BEGIN REGION IVb
*-----------------------------------------------------------------------------
OPER CA=3  TE=416 PR=1010
OPER CA=4  TE=260 PR=1010
OPER CA=5  TE=392 PR=1010
OPER CA=6  TE=310 PR=1010
OPER CA=7  TE=280 PR=1010
OPER CA=8  TE=265 PR=1010
OPER CA=9  TE=90  PR=1010
OPER CA=10 TE=454 PR=1010
OPER CA=11 TE=300 PR=170
OPER CA=12 TE=270 PR=88
OPER CA=13 TE=507 PR=1190
OPER CA=14 TE=50  PR=1135
OPER CA=15 TE=343 PR=1135
OPER CA=16 TE=427 PR=1135
OPER CA=17 TE=343 PR=1060
OPER CA=18 TE=416 PR=1135

OPER CA=20 TE=250 PR=675
OPER CA=21 TE=275 PR=885

OPER CA=23 TE=392 PR=1375
OPER CA=24 TE=392 PR=940
OPER CA=25 TE=392 PR=1010
OPER CA=26 TE=275 PR=1010
OPER CA=27 TE=382 PR=1010
OPER CA=30 TE=235 PR=1010
TRAN CA=201 IS=1 FS=1 IT=70 FT=100 TT=1800 FL=100 IP=15 FP=1115 TP=1800
TRAN CA=202 IS=1 FS=1 IT=100 FT=100 TT=0 FL=100 IP=1115 FP=65 TP=0
TRAN CA=203 IS=1 FS=1 IT=100 FT=416 TT=16164 FL=100 IP=65 FP=1025 TP=16164
TRAN CA=204 IS=1 FS=1 IT=416 FT=100 TT=0 FL=688.5 IP=1025 FP=1025 TP=0
TRAN CA=205 IS=1 FS=1 IT=100 FT=260 TT=0 FL=688.5 IP=1025 FP=1025 TP=0
TRAN CA=206 IS=1 FS=1 IT=260 FT=392 TT=1800 FL=4590 IP=1025 FP=1025 TP=1800
TRAN CA=207 IS=1 FS=1 IT=392 FT=310 TT=900 FL=3442.5 IP=1025 FP=1025 TP=900
TRAN CA=208 IS=1 FS=1 IT=310 FT=392 TT=900 FL=3442.5 IP=1025 FP=1025 TP=900
TRAN CA=209 IS=1 FS=1 IT=392 FT=280 TT=1800 FL=2295 IP=1025 FP=1025 TP=1800
```

```
TRAN CA=210 IS=1 FS=1 IT=280 FT=392 TT=1800 FL=2295 IP=1025 FP=1025 TP=1800
TRAN CA=211 IS=1 FS=1 IT=392 FT=265 TT=1800 FL=2295 IP=1025 FP=1025 TP=1800
TRAN CA=212 IS=1 FS=1 IT=265 FT=90 TT=360 FL=688.5 IP=1025 FP=1025 TP=360
TRAN CA=213 IS=1 FS=1 IT=90 FT=265 TT=900 FL=688.5 IP=1025 FP=1025 TP=900
TRAN CA=214 IS=1 FS=1 IT=265 FT=392 TT=1800 FL=2295 IP=1025 FP=1025 TP=1800
TRAN CA=215 IS=1 FS=1 IT=392 FT=265 TT=90 FL=4590 IP=1025 FP=1025 TP=90
TRAN CA=216 IS=1 FS=1 IT=265 FT=392 TT=180 FL=4590 IP=1025 FP=1025 TP=180
TRAN CA=217 IS=1 FS=1 IT=392 FT=275 TT=60 FL=5049 IP=1025 FP=1025 TP=60
TRAN CA=218 IS=1 FS=1 IT=275 FT=100 TT=900 FL=137.7 IP=1025 FP=1025 TP=900
TRAN CA=219 IS=1 FS=1 IT=265 FT=382 TT=0 FL=100 IP=1025 FP=1025 TP=0
TRAN CA=220 IS=1 FS=1 IT=382 FT=454 TT=3924 FL=100 IP=1025 FP=1025 TP=3924
TRAN CA=221 IS=1 FS=1 IT=454 FT=416 TT=4140 FL=100 IP=1025 FP=1025 TP=4140
TRAN CA=222 IS=1 FS=1 IT=416 FT=300 TT=6264 FL=100 IP=1025 FP=185 TP=6264
TRAN CA=223 IS=1 FS=1 IT=300 FT=270 TT=600 FL=100 IP=185 FP=103 TP=600
TRAN CA=224 IS=1 FS=1 IT=270 FT=100 TT=8280 FL=100 IP=103 FP=65 TP=8280
TRAN CA=225 IS=1 FS=1 IT=392 FT=507 TT=12 FL=100 IP=1025 FP=1205 TP=12
TRAN CA=226 IS=1 FS=1 IT=507 FT=50 TT=0 FL=1836 IP=1205 FP=1150 TP=0
TRAN CA=227 IS=1 FS=1 IT=50 FT=343 TT=1380 FL=100 IP=1150 FP=1150 TP=1380
TRAN CA=228 IS=1 FS=1 IT=343 FT=427 TT=0 FL=100 IP=1150 FP=1150 TP=0
TRAN CA=229 IS=1 FS=1 IT=427 FT=50 TT=0 FL=1377 IP=1150 FP=900 TP=0
TRAN CA=230 IS=1 FS=1 IT=50 FT=343 TT=3060 FL=100 IP=900 FP=1075 TP=3060
TRAN CA=231 IS=1 FS=1 IT=343 FT=416 TT=0 FL=100 IP=1075 FP=1150 TP=0
TRAN CA=232 IS=1 FS=1 IT=416 FT=50 TT=0 FL=780.3 IP=1150 FP=690 TP=0
TRAN CA=233 IS=1 FS=1 IT=50 FT=250 TT=300 FL=100 IP=690 FP=690 TP=300
TRAN CA=234 IS=1 FS=1 IT=250 FT=416 TT=8964 FL=100 IP=255 FP=1025 TP=8964
TRAN CA=235 IS=1 FS=1 IT=392 FT=275 TT=60 FL=5049 IP=1025 FP=900 TP=60
TRAN CA=236 IS=1 FS=1 IT=275 FT=100 TT=900 FL=137.7 IP=900 FP=65 TP=900
TRAN CA=237 IS=1 FS=1 IT=100 FT=100 TT=0 FL=100 IP=65 FP=1578 TP=0
TRAN CA=238 IS=1 FS=1 IT=100 FT=100 TT=0 FL=100 IP=1578 FP=65 TP=0
TRAN CA=239 IS=1 FS=1 IT=392 FT=392 TT=60 FL=5049 IP=1025 FP=1390 TP=60
TRAN CA=240 IS=1 FS=1 IT=392 FT=392 TT=900 FL=137.7 IP=1390 FP=955 TP=900
TRAN CA=241 IS=1 FS=1 IT=392 FT=392 TT=900 FL=137.7 IP=955 FP=1025 TP=900
TRAN CA=242 IS=1 FS=1 IT=100 FT=235 TT=60 FL=100 IP=1025 FP=1025 TP=60
TRAN CA=243 IS=1 FS=1 IT=235 FT=416 TT=210 FL=100 IP=1025 FP=1025 TP=210

PAIR CA=201 CO=27.6 DI=0.521 EX=6.4 * Tavg=85
PAIR CA=202 CO=27.6 DI=0.512 EX=6.4 * Tavg=100
PAIR CA=203 CO=27.4 DI=0.465 EX=6.4 * Tavg=258
PAIR CA=204 CO=27.4 DI=0.465 EX=6.4 * Tavg=258
PAIR CA=205 CO=27.6 DI=0.490 EX=6.4 * Tavg=180
PAIR CA=206 CO=27.1 DI=0.446 EX=6.4 * Tavg=326
PAIR CA=207 CO=27.0 DI=0.440 EX=6.4 * Tavg=351
PAIR CA=208 CO=27.0 DI=0.440 EX=6.4 * Tavg=351
PAIR CA=209 CO=27.1 DI=0.444 EX=6.4 * Tavg=336
PAIR CA=210 CO=27.1 DI=0.444 EX=6.4 * Tavg=336
PAIR CA=211 CO=27.1 DI=0.445 EX=6.4 * Tavg=329
PAIR CA=212 CO=27.6 DI=0.490 EX=6.4 * Tavg=178
PAIR CA=213 CO=27.6 DI=0.490 EX=6.4 * Tavg=178
PAIR CA=214 CO=27.1 DI=0.445 EX=6.4 * Tavg=329
PAIR CA=215 CO=27.1 DI=0.445 EX=6.4 * Tavg=329
PAIR CA=216 CO=27.1 DI=0.445 EX=6.4 * Tavg=329
PAIR CA=217 CO=27.1 DI=0.444 EX=6.4 * Tavg=334
PAIR CA=218 CO=27.6 DI=0.488 EX=6.4 * Tavg=188
PAIR CA=219 CO=27.1 DI=0.447 EX=6.4 * Tavg=324
PAIR CA=220 CO=26.6 DI=0.423 EX=6.4 * Tavg=418
PAIR CA=221 CO=26.4 DI=0.418 EX=6.4 * Tavg=435
```

```
PAIR CA=222 CO=27.0 DI=0.438 EX=6.4 * Tavg=358
PAIR CA=223 CO=27.3 DI=0.457 EX=6.4 * Tavg=285
PAIR CA=224 CO=27.6 DI=0.489 EX=6.4 * Tavg=185
PAIR CA=225 CO=26.3 DI=0.413 EX=6.4 * Tavg=450
PAIR CA=226 CO=27.3 DI=0.459 EX=6.4 * Tavg=279
PAIR CA=227 CO=27.6 DI=0.487 EX=6.4 * Tavg=197
PAIR CA=228 CO=26.8 DI=0.432 EX=6.4 * Tavg=385
PAIR CA=229 CO=27.4 DI=0.471 EX=6.4 * Tavg=239
PAIR CA=230 CO=27.6 DI=0.487 EX=6.4 * Tavg=197
PAIR CA=231 CO=26.8 DI=0.433 EX=6.4 * Tavg=380
PAIR CA=232 CO=27.5 DI=0.473 EX=6.4 * Tavg=233
PAIR CA=233 CO=27.6 DI=0.496 EX=6.4 * Tavg=150
PAIR CA=234 CO=27.1 DI=0.444 EX=6.4 * Tavg=333
PAIR CA=235 CO=27.1 DI=0.444 EX=6.4 * Tavg=334
PAIR CA=236 CO=27.6 DI=0.488 EX=6.4 * Tavg=188
PAIR CA=237 CO=27.6 DI=0.512 EX=6.4 * Tavg=100
PAIR CA=238 CO=27.6 DI=0.512 EX=6.4 * Tavg=100
PAIR CA=239 CO=26.7 DI=0.430 EX=6.4 * Tavg=392
PAIR CA=240 CO=26.7 DI=0.430 EX=6.4 * Tavg=392
PAIR CA=241 CO=26.7 DI=0.430 EX=6.4 * Tavg=392
PAIR CA=242 CO=27.6 DI=0.492 EX=6.4 * Tavg=168
PAIR CA=243 CO=27.1 DI=0.446 EX=6.4 * Tavg=326
*
TANG PT=155  DY=6.523
*--------------
*END REGION IVb
*-----------------------------------------------
*BEGIN REGION V GEOMETRY TO NOZZLE N4B, NODE 165
*-----------------------------------------------
OPER CA=3  TE=549 PR=1010
OPER CA=4  TE=260 PR=1010
OPER CA=5  TE=392 PR=1010
OPER CA=6  TE=310 PR=1010
OPER CA=7  TE=280 PR=1010
OPER CA=8  TE=265 PR=1010
OPER CA=9  TE=90  PR=1010
OPER CA=10 TE=549 PR=1010
OPER CA=11 TE=375 PR=170
OPER CA=12 TE=330 PR=88
OPER CA=13 TE=565 PR=1190
OPER CA=14 TE=50  PR=1135
OPER CA=15 TE=440 PR=1135
OPER CA=16 TE=565 PR=1135
OPER CA=17 TE=440 PR=1060
OPER CA=18 TE=549 PR=1135

OPER CA=20 TE=300 PR=675
OPER CA=21 TE=275 PR=885

OPER CA=23 TE=392 PR=1375
OPER CA=24 TE=392 PR=940
OPER CA=25 TE=392 PR=1010
OPER CA=26 TE=275 PR=1010
OPER CA=27 TE=440 PR=1010
OPER CA=30 TE=290 PR=1010
```

```
TRAN CA=201 IS=1 FS=1 IT=70 FT=100 TT=1800 FL=100 IP=15 FP=1115 TP=1800
TRAN CA=202 IS=1 FS=1 IT=100 FT=100 TT=0 FL=100 IP=1115 FP=65 TP=0
TRAN CA=203 IS=1 FS=1 IT=100 FT=549 TT=16164 FL=100 IP=65 FP=1025 TP=16164
TRAN CA=204 IS=1 FS=1 IT=549 FT=100 TT=0 FL=688.5 IP=1025 FP=1025 TP=0
TRAN CA=205 IS=1 FS=1 IT=100 FT=260 TT=0 FL=688.5 IP=1025 FP=1025 TP=0
TRAN CA=206 IS=1 FS=1 IT=260 FT=392 TT=1800 FL=4590 IP=1025 FP=1025 TP=1800
TRAN CA=207 IS=1 FS=1 IT=392 FT=310 TT=900 FL=3442.5 IP=1025 FP=1025 TP=900
TRAN CA=208 IS=1 FS=1 IT=310 FT=392 TT=900 FL=3442.5 IP=1025 FP=1025 TP=900
TRAN CA=209 IS=1 FS=1 IT=392 FT=280 TT=1800 FL=2295 IP=1025 FP=1025 TP=1800
TRAN CA=210 IS=1 FS=1 IT=280 FT=392 TT=1800 FL=2295 IP=1025 FP=1025 TP=1800
TRAN CA=211 IS=1 FS=1 IT=392 FT=265 TT=1800 FL=2295 IP=1025 FP=1025 TP=1800
TRAN CA=212 IS=1 FS=1 IT=265 FT=90 TT=360 FL=688.5 IP=1025 FP=1025 TP=360
TRAN CA=213 IS=1 FS=1 IT=90 FT=265 TT=900 FL=688.5 IP=1025 FP=1025 TP=900
TRAN CA=214 IS=1 FS=1 IT=265 FT=392 TT=1800 FL=2295 IP=1025 FP=1025 TP=1800
TRAN CA=215 IS=1 FS=1 IT=392 FT=265 TT=90 FL=4590 IP=1025 FP=1025 TP=90
TRAN CA=216 IS=1 FS=1 IT=265 FT=392 TT=180 FL=4590 IP=1025 FP=1025 TP=180
TRAN CA=217 IS=1 FS=1 IT=392 FT=275 TT=60 FL=5049 IP=1025 FP=1025 TP=60
TRAN CA=218 IS=1 FS=1 IT=275 FT=100 TT=900 FL=137.7 IP=1025 FP=1025 TP=900
TRAN CA=219 IS=1 FS=1 IT=265 FT=440 TT=0 FL=100 IP=1025 FP=1025 TP=0
TRAN CA=220 IS=1 FS=1 IT=440 FT=549 TT=3924 FL=100 IP=1025 FP=1025 TP=3924
TRAN CA=221 *IS=1 FS=1 IT=549 FT=549 TT=0 FL=100 IP=1025 FP=1025 TP=0
TRAN CA=222 IS=1 FS=1 IT=549 FT=375 TT=6264 FL=100 IP=1025 FP=185 TP=6264
TRAN CA=223 IS=1 FS=1 IT=375 FT=330 TT=600 FL=100 IP=185 FP=103 TP=600
TRAN CA=224 IS=1 FS=1 IT=330 FT=100 TT=8280 FL=100 IP=103 FP=65 TP=8280
TRAN CA=225 IS=1 FS=1 IT=392 FT=565 TT=12 FL=100 IP=1025 FP=1205 TP=12
TRAN CA=226 IS=1 FS=1 IT=565 FT=50 TT=0 FL=1836 IP=1205 FP=1150 TP=0
TRAN CA=227 IS=1 FS=1 IT=50 FT=440 TT=1380 FL=100 IP=1150 FP=1150 TP=1380
TRAN CA=228 IS=1 FS=1 IT=440 FT=565 TT=0 FL=100 IP=1150 FP=1150 TP=0
TRAN CA=229 IS=1 FS=1 IT=565 FT=50 TT=0 FL=1377 IP=1150 FP=900 TP=0
TRAN CA=230 IS=1 FS=1 IT=50 FT=440 TT=3060 FL=100 IP=900 FP=1075 TP=3060
TRAN CA=231 IS=1 FS=1 IT=440 FT=549 TT=0 FL=100 IP=1075 FP=1150 TP=0
TRAN CA=232 IS=1 FS=1 IT=549 FT=50 TT=0 FL=780.3 IP=1150 FP=690 TP=0
TRAN CA=233 IS=1 FS=1 IT=50 FT=300 TT=300 FL=100 IP=690 FP=690 TP=300
TRAN CA=234 IS=1 FS=1 IT=300 FT=549 TT=8964 FL=100 IP=255 FP=1025 TP=8964
TRAN CA=235 IS=1 FS=1 IT=392 FT=275 TT=60 FL=5049 IP=1025 FP=900 TP=60
TRAN CA=236 IS=1 FS=1 IT=275 FT=100 TT=900 FL=137.7 IP=900 FP=65 TP=900
TRAN CA=237 IS=1 FS=1 IT=100 FT=100 TT=0 FL=100 IP=65 FP=1578 TP=0
TRAN CA=238 IS=1 FS=1 IT=100 FT=100 TT=0 FL=100 IP=1578 FP=65 TP=0
TRAN CA=239 IS=1 FS=1 IT=392 FT=392 TT=60 FL=5049 IP=1025 FP=1390 TP=60
TRAN CA=240 IS=1 FS=1 IT=392 FT=392 TT=900 FL=137.7 IP=1390 FP=955 TP=900
TRAN CA=241 IS=1 FS=1 IT=392 FT=392 TT=900 FL=137.7 IP=955 FP=1025 TP=900
TRAN CA=242 IS=1 FS=1 IT=100 FT=290 TT=60 FL=100 IP=1025 FP=1025 TP=60
TRAN CA=243 IS=1 FS=1 IT=290 FT=549 TT=210 FL=100 IP=1025 FP=1025 TP=210

PAIR CA=201 CO=27.6 DI=0.521 EX=6.4 * Tavg=85
PAIR CA=202 CO=27.6 DI=0.512 EX=6.4 * Tavg=100
PAIR CA=203 CO=27.1 DI=0.447 EX=6.4 * Tavg=325
PAIR CA=204 CO=27.1 DI=0.447 EX=6.4 * Tavg=325
PAIR CA=205 CO=27.6 DI=0.490 EX=6.4 * Tavg=180
PAIR CA=206 CO=27.1 DI=0.446 EX=6.4 * Tavg=326
PAIR CA=207 CO=27.0 DI=0.440 EX=6.4 * Tavg=351
PAIR CA=208 CO=27.0 DI=0.440 EX=6.4 * Tavg=351
PAIR CA=209 CO=27.1 DI=0.444 EX=6.4 * Tavg=336
PAIR CA=210 CO=27.1 DI=0.444 EX=6.4 * Tavg=336
PAIR CA=211 CO=27.1 DI=0.445 EX=6.4 * Tavg=329
PAIR CA=212 CO=27.6 DI=0.490 EX=6.4 * Tavg=178
```

```
PAIR CA=213 CO=27.6 DI=0.490 EX=6.4 * Tavg=178
PAIR CA=214 CO=27.1 DI=0.445 EX=6.4 * Tavg=329
PAIR CA=215 CO=27.1 DI=0.445 EX=6.4 * Tavg=329
PAIR CA=216 CO=27.1 DI=0.445 EX=6.4 * Tavg=329
PAIR CA=217 CO=27.1 DI=0.444 EX=6.4 * Tavg=334
PAIR CA=218 CO=27.6 DI=0.488 EX=6.4 * Tavg=188
PAIR CA=219 CO=27.0 DI=0.439 EX=6.4 * Tavg=353
PAIR CA=220 CO=25.9 DI=0.400 EX=6.4 * Tavg=495
PAIR CA=221 CO=25.5 DI=0.387 EX=6.4 * Tavg=549
PAIR CA=222 CO=26.2 DI=0.409 EX=6.4 * Tavg=462
PAIR CA=223 CO=27.0 DI=0.439 EX=6.4 * Tavg=353
PAIR CA=224 CO=27.5 DI=0.480 EX=6.4 * Tavg=215
PAIR CA=225 CO=26.1 DI=0.404 EX=6.4 * Tavg=479
PAIR CA=226 CO=27.2 DI=0.451 EX=6.4 * Tavg=308
PAIR CA=227 CO=27.4 DI=0.469 EX=6.4 * Tavg=245
PAIR CA=228 CO=25.9 DI=0.397 EX=6.4 * Tavg=503
PAIR CA=229 CO=27.2 DI=0.451 EX=6.4 * Tavg=308
PAIR CA=230 CO=27.4 DI=0.469 EX=6.4 * Tavg=245
PAIR CA=231 CO=25.9 DI=0.400 EX=6.4 * Tavg=495
PAIR CA=232 CO=27.2 DI=0.453 EX=6.4 * Tavg=300
PAIR CA=233 CO=27.6 DI=0.491 EX=6.4 * Tavg=175
PAIR CA=234 CO=26.5 DI=0.421 EX=6.4 * Tavg=425
PAIR CA=235 CO=27.1 DI=0.444 EX=6.4 * Tavg=334
PAIR CA=236 CO=27.6 DI=0.488 EX=6.4 * Tavg=188
PAIR CA=237 CO=27.6 DI=0.512 EX=6.4 * Tavg=100
PAIR CA=238 CO=27.6 DI=0.512 EX=6.4 * Tavg=100
PAIR CA=239 CO=26.7 DI=0.430 EX=6.4 * Tavg=392
PAIR CA=240 CO=26.7 DI=0.430 EX=6.4 * Tavg=392
PAIR CA=241 CO=26.7 DI=0.430 EX=6.4 * Tavg=392
PAIR CA=242 CO=27.6 DI=0.487 EX=6.4 * Tavg=195
PAIR CA=243 CO=26.5 DI=0.422 EX=6.4 * Tavg=420
BRAD PT=160  RA=1.25
TANG PT=165  DX=-4.007  DZ=-4.007  EW=1
NOZZ PT=165   *NOZZLE N4B
AMVT CA=1  PT=165 DX=0.0196 DY=0.1069 DZ=0.0196
AMVT CA=2  PT=165 DX=0.0196 DY=0.1069 DZ=0.0196
AMVT CA=3  PT=165 DX=0.3130 DY=1.7067 DZ=0.3130
AMVT CA=4  PT=165 DX=0.3130 DY=1.7067 DZ=0.3130
AMVT CA=5  PT=165 DX=0.3130 DY=1.7067 DZ=0.3130
AMVT CA=6  PT=165 DX=0.3130 DY=1.7067 DZ=0.3130
AMVT CA=7  PT=165 DX=0.3130 DY=1.7067 DZ=0.3130
AMVT CA=8  PT=165 DX=0.3130 DY=1.7067 DZ=0.3130
AMVT CA=9  PT=165 DX=0.3130 DY=1.7067 DZ=0.3130
AMVT CA=10 PT=165 DX=0.3130 DY=1.7067 DZ=0.3130
AMVT CA=11 PT=165 DX=0.1993 DY=1.0867 DZ=0.1993
AMVT CA=12 PT=165 DX=0.1699 DY=0.9264 DZ=0.1699
AMVT CA=13 PT=165 DX=0.3234 DY=1.7637 DZ=0.3234
AMVT CA=14 PT=165 DX=0.3234 DY=1.7637 DZ=0.3234
AMVT CA=15 PT=165 DX=0.3234 DY=1.7637 DZ=0.3234
AMVT CA=16 PT=165 DX=0.3234 DY=1.7637 DZ=0.3234
AMVT CA=17 PT=165 DX=0.3169 DY=1.7281 DZ=0.3169
AMVT CA=18 PT=165 DX=0.3234 DY=1.7637 DZ=0.3234
AMVT CA=19 PT=165 DX=0.2823 DY=1.5392 DZ=0.2823
AMVT CA=20 PT=165 DX=0.2823 DY=1.5392 DZ=0.2823
AMVT CA=21 PT=165 DX=0.3130 DY=1.7067 DZ=0.3130
AMVT CA=22 PT=165 DX=0.0196 DY=0.1069 DZ=0.0196
```

```
AMVT CA=23 PT=165 DX=0.3463 DY=1.8884 DZ=0.3463
AMVT CA=24 PT=165 DX=0.3064 DY=1.6711 DZ=0.3064
AMVT CA=25 PT=165 DX=0.3130 DY=1.7067 DZ=0.3130
AMVT CA=26 PT=165 DX=0.3064 DY=1.6711 DZ=0.3064
AMVT CA=27 PT=165 DX=0.3130 DY=1.7067 DZ=0.3130
AMVT CA=28 PT=165 DX=0.3130 DY=1.7067 DZ=0.3130
AMVT CA=29 PT=165 DX=0.3064 DY=1.6711 DZ=0.3064
AMVT CA=30 PT=165 DX=0.3130 DY=1.7067 DZ=0.3130
AMVT CA=31 PT=165 DX=0.3019 DY=1.6461 DZ=0.3019
AMVT CA=32 PT=165 DX=-.09   DY=.015   DZ=-.093
*-----------------------------------------------------------------------------
*END REGION V
*-----------------------------------------------------------------------------
*REGION II GEOMETRY - HPCI Line brnch
CROS CD=6
JUNC PT=10
*-----------------------------------------------------------------------------
*BEGIN REGION IIa
*-----------------------------------------------------------------------------
OPER CA=3  TE=150 PR=1010
OPER CA=4  TE=260 PR=1010
OPER CA=5  TE=392 PR=1010
OPER CA=6  TE=310 PR=1010
OPER CA=7  TE=280 PR=1010
OPER CA=8  TE=265 PR=1010
OPER CA=9  TE=90  PR=1010
OPER CA=10 TE=265 PR=1010
OPER CA=11 TE=150 PR=170
OPER CA=12 TE=150 PR=88
OPER CA=13 TE=392 PR=1190
OPER CA=14 TE=50  PR=1135
OPER CA=15 TE=150 PR=1135
OPER CA=16 TE=150 PR=1135
OPER CA=17 TE=150 PR=1060
OPER CA=18 TE=150 PR=1135

OPER CA=20 TE=150 PR=675
OPER CA=21 TE=275 PR=885

OPER CA=23 TE=392 PR=1375
OPER CA=24 TE=392 PR=940
OPER CA=25 TE=392 PR=1010
OPER CA=26 TE=275 PR=1010
OPER CA=27 TE=265 PR=1010

OPER CA=30 TE=125 PR=1010

TRAN CA=201 IS=1 FS=1 IT=70 FT=100 TT=1800 FL=150 IP=15 FP=1115 TP=1800
TRAN CA=202 IS=1 FS=1 IT=100 FT=100 TT=0 FL=150 IP=1115 FP=65 TP=0
TRAN CA=203 IS=1 FS=1 IT=100 FT=150 TT=16164 FL=150 IP=65 FP=1025 TP=16164
TRAN CA=204 IS=1 FS=1 IT=150 FT=100 TT=0 FL=150 IP=1025 FP=1025 TP=0
TRAN CA=205 IS=1 FS=1 IT=100 FT=260 TT=0 FL=150 IP=1025 FP=1025 TP=0
TRAN CA=206 IS=1 FS=1 IT=260 FT=392 TT=1800 FL=150 IP=1025 FP=1025 TP=1800
TRAN CA=207 IS=1 FS=1 IT=392 FT=310 TT=900 FL=150 IP=1025 FP=1025 TP=900
TRAN CA=208 IS=1 FS=1 IT=310 FT=392 TT=900 FL=150 IP=1025 FP=1025 TP=900
TRAN CA=209 IS=1 FS=1 IT=392 FT=280 TT=1800 FL=150 IP=1025 FP=1025 TP=1800
```

```
TRAN CA=210 IS=1 FS=1 IT=280 FT=392 TT=1800 FL=150 IP=1025 FP=1025 TP=1800
TRAN CA=211 IS=1 FS=1 IT=392 FT=265 TT=1800 FL=150 IP=1025 FP=1025 TP=1800
TRAN CA=212 IS=1 FS=1 IT=265 FT=90 TT=360 FL=150 IP=1025 FP=1025 TP=360
TRAN CA=213 IS=1 FS=1 IT=90 FT=265 TT=900 FL=150 IP=1025 FP=1025 TP=900
TRAN CA=214 IS=1 FS=1 IT=265 FT=392 TT=1800 FL=150 IP=1025 FP=1025 TP=1800
TRAN CA=215 IS=1 FS=1 IT=392 FT=265 TT=90 FL=150 IP=1025 FP=1025 TP=90
TRAN CA=216 IS=1 FS=1 IT=265 FT=392 TT=180 FL=150 IP=1025 FP=1025 TP=180
TRAN CA=217 IS=1 FS=1 IT=392 FT=275 TT=60 FL=150 IP=1025 FP=1025 TP=60
TRAN CA=218 IS=1 FS=1 IT=275 FT=100 TT=900 FL=150 IP=1025 FP=1025 TP=900
TRAN CA=219 *IS=1 FS=1 IT=265 FT=265 TT=0 FL=150 IP=1025 FP=1025 TP=0
TRAN CA=220 *IS=1 FS=1 IT=265 FT=265 TT=0 FL=150 IP=1025 FP=1025 TP=0
TRAN CA=221 IS=1 FS=1 IT=265 FT=150 TT=4140 FL=150 IP=1025 FP=1025 TP=4140
TRAN CA=222 IS=1 FS=1 IT=150 FT=150 TT=0 FL=150 IP=1025 FP=185 TP=0
TRAN CA=223 IS=1 FS=1 IT=150 FT=150 TT=0 FL=150 IP=185 FP=103 TP=0
TRAN CA=224 IS=1 FS=1 IT=150 FT=100 TT=8280 FL=150 IP=103 FP=65 TP=8280
TRAN CA=225 IS=1 FS=1 IT=392 FT=392 TT=12 FL=150 IP=1025 FP=1205 TP=12
TRAN CA=226 IS=1 FS=1 IT=392 FT=50 TT=0 FL=3672 IP=1205 FP=1150 TP=0
TRAN CA=227 IS=1 FS=1 IT=50 FT=150 TT=1380 FL=150 IP=1150 FP=1150 TP=1380
TRAN CA=228 IS=1 FS=1 IT=150 FT=150 TT=0 FL=150 IP=1150 FP=1150 TP=0
TRAN CA=229 IS=1 FS=1 IT=150 FT=50 TT=0 FL=2754 IP=1150 FP=900 TP=0
TRAN CA=230 IS=1 FS=1 IT=50 FT=150 TT=3060 FL=150 IP=900 FP=1075 TP=3060
TRAN CA=231 IS=1 FS=1 IT=150 FT=150 TT=0 FL=150 IP=1075 FP=1150 TP=0
TRAN CA=232 IS=1 FS=1 IT=150 FT=50 TT=0 FL=1560.6 IP=1150 FP=690 TP=0
TRAN CA=233 IS=1 FS=1 IT=50 FT=150 TT=300 FL=150 IP=690 FP=690 TP=300
TRAN CA=234 IS=1 FS=1 IT=150 FT=150 TT=8964 FL=150 IP=255 FP=1025 TP=8964
TRAN CA=235 IS=1 FS=1 IT=392 FT=275 TT=60 FL=150 IP=1025 FP=900 TP=60
TRAN CA=236 IS=1 FS=1 IT=275 FT=100 TT=900 FL=150 IP=900 FP=65 TP=900
TRAN CA=237 IS=1 FS=1 IT=100 FT=100 TT=0 FL=150 IP=65 FP=1578 TP=0
TRAN CA=238 IS=1 FS=1 IT=100 FT=100 TT=0 FL=150 IP=1578 FP=65 TP=0
TRAN CA=239 IS=1 FS=1 IT=392 FT=392 TT=60 FL=150 IP=1025 FP=1390 TP=60
TRAN CA=240 IS=1 FS=1 IT=392 FT=392 TT=900 FL=150 IP=1390 FP=955 TP=900
TRAN CA=241 IS=1 FS=1 IT=392 FT=392 TT=900 FL=150 IP=955 FP=1025 TP=900
TRAN CA=242 IS=1 FS=1 IT=100 FT=125 TT=60 FL=150 IP=1025 FP=1025 TP=60
TRAN CA=243 IS=1 FS=1 IT=125 FT=150 TT=210 FL=150 IP=1025 FP=1025 TP=210

PAIR CA=201 CO=27.6 DI=0.521 EX=6.4 * Tavg=85
PAIR CA=202 CO=27.6 DI=0.512 EX=6.4 * Tavg=100
PAIR CA=203 CO=27.6 DI=0.504 EX=6.4 * Tavg=125
PAIR CA=204 CO=27.6 DI=0.504 EX=6.4 * Tavg=125
PAIR CA=205 CO=27.6 DI=0.490 EX=6.4 * Tavg=180
PAIR CA=206 CO=27.1 DI=0.446 EX=6.4 * Tavg=326
PAIR CA=207 CO=27.0 DI=0.440 EX=6.4 * Tavg=351
PAIR CA=208 CO=27.0 DI=0.440 EX=6.4 * Tavg=351
PAIR CA=209 CO=27.1 DI=0.444 EX=6.4 * Tavg=336
PAIR CA=210 CO=27.1 DI=0.444 EX=6.4 * Tavg=336
PAIR CA=211 CO=27.1 DI=0.445 EX=6.4 * Tavg=329
PAIR CA=212 CO=27.6 DI=0.490 EX=6.4 * Tavg=178
PAIR CA=213 CO=27.6 DI=0.490 EX=6.4 * Tavg=178
PAIR CA=214 CO=27.1 DI=0.445 EX=6.4 * Tavg=329
PAIR CA=215 CO=27.1 DI=0.445 EX=6.4 * Tavg=329
PAIR CA=216 CO=27.1 DI=0.445 EX=6.4 * Tavg=329
PAIR CA=217 CO=27.1 DI=0.444 EX=6.4 * Tavg=334
PAIR CA=218 CO=27.6 DI=0.488 EX=6.4 * Tavg=188
PAIR CA=219 CO=27.3 DI=0.463 EX=6.4 * Tavg=265
PAIR CA=220 CO=27.3 DI=0.463 EX=6.4 * Tavg=265
PAIR CA=221 CO=27.6 DI=0.483 EX=6.4 * Tavg=208
```

```
PAIR CA=222 CO=27.6 DI=0.496 EX=6.4 * Tavg=150
PAIR CA=223 CO=27.6 DI=0.496 EX=6.4 * Tavg=150
PAIR CA=224 CO=27.6 DI=0.504 EX=6.4 * Tavg=125
PAIR CA=225 CO=26.7 DI=0.430 EX=6.4 * Tavg=392
PAIR CA=226 CO=27.5 DI=0.478 EX=6.4 * Tavg=221
PAIR CA=227 CO=27.6 DI=0.512 EX=6.4 * Tavg=100
PAIR CA=228 CO=27.6 DI=0.496 EX=6.4 * Tavg=150
PAIR CA=229 CO=27.6 DI=0.512 EX=6.4 * Tavg=100
PAIR CA=230 CO=27.6 DI=0.512 EX=6.4 * Tavg=100
PAIR CA=231 CO=27.6 DI=0.496 EX=6.4 * Tavg=150
PAIR CA=232 CO=27.6 DI=0.512 EX=6.4 * Tavg=100
PAIR CA=233 CO=27.6 DI=0.512 EX=6.4 * Tavg=100
PAIR CA=234 CO=27.6 DI=0.496 EX=6.4 * Tavg=150
PAIR CA=235 CO=27.1 DI=0.444 EX=6.4 * Tavg=334
PAIR CA=236 CO=27.6 DI=0.488 EX=6.4 * Tavg=188
PAIR CA=237 CO=27.6 DI=0.512 EX=6.4 * Tavg=100
PAIR CA=238 CO=27.6 DI=0.512 EX=6.4 * Tavg=100
PAIR CA=239 CO=26.7 DI=0.430 EX=6.4 * Tavg=392
PAIR CA=240 CO=26.7 DI=0.430 EX=6.4 * Tavg=392
PAIR CA=241 CO=26.7 DI=0.430 EX=6.4 * Tavg=392
PAIR CA=242 CO=27.6 DI=0.508 EX=6.4 * Tavg=113
PAIR CA=243 CO=27.6 DI=0.500 EX=6.4 * Tavg=138

*
BRAN PT=301  DY=1  TE=1 EW=1
TANG PT=302  DY=2.333
TANG PT=305  DY=2.333  EW=1
BRAD PT=310  RA=1.75  EW=1
TANG PT=315  DX=-2.333  EW=1
CROS CD=7
VALV PT=317  DX=-1.167 PL=1 MA=2.05
*-----------------------------------------------------------------------------
*BEGIN REGION IIb
*-----------------------------------------------------------------------------

OPER CA=3  TE=125   PR=1010
OPER CA=4  TE=180   PR=1010
OPER CA=5  TE=246   PR=1010
OPER CA=6  TE=205   PR=1010
OPER CA=7  TE=190   PR=1010
OPER CA=8  TE=182.5 PR=1010
OPER CA=9  TE=95    PR=1010
OPER CA=10 TE=182.5 PR=1010
OPER CA=11 TE=125   PR=170
OPER CA=12 TE=125   PR=88
OPER CA=13 TE=246   PR=1190
OPER CA=14 TE=50    PR=1135
OPER CA=15 TE=125   PR=1135
OPER CA=16 TE=125   PR=1135
OPER CA=17 TE=125   PR=1060
OPER CA=18 TE=125   PR=1135

OPER CA=20 TE=125   PR=675
OPER CA=21 TE=187.5 PR=885

OPER CA=23 TE=246   PR=1375
```

```
OPER CA=24 TE=246   PR=940
OPER CA=25 TE=246   PR=1010
OPER CA=26 TE=187.5 PR=1010
OPER CA=27 TE=182.5 PR=1010

OPER CA=30 TE=112.5 PR=1010

TRAN CA=201 IS=1 FS=1 IT=70 FT=100 TT=1800 FL=150 IP=15 FP=1115 TP=1800
TRAN CA=202 IS=1 FS=1 IT=100 FT=100 TT=0 FL=150 IP=1115 FP=65 TP=0
TRAN CA=203 IS=1 FS=1 IT=100 FT=125 TT=16164 FL=150 IP=65 FP=1025 TP=16164
TRAN CA=204 IS=1 FS=1 IT=125 FT=100 TT=0 FL=150 IP=1025 FP=1025 TP=0
TRAN CA=205 IS=1 FS=1 IT=100 FT=180 TT=0 FL=150 IP=1025 FP=1025 TP=0
TRAN CA=206 IS=1 FS=1 IT=180 FT=246 TT=1800 FL=150 IP=1025 FP=1025 TP=1800
TRAN CA=207 IS=1 FS=1 IT=246 FT=205 TT=900 FL=150 IP=1025 FP=1025 TP=900
TRAN CA=208 IS=1 FS=1 IT=205 FT=246 TT=900 FL=150 IP=1025 FP=1025 TP=900
TRAN CA=209 IS=1 FS=1 IT=246 FT=190 TT=1800 FL=150 IP=1025 FP=1025 TP=1800
TRAN CA=210 IS=1 FS=1 IT=190 FT=246 TT=1800 FL=150 IP=1025 FP=1025 TP=1800
TRAN CA=211 IS=1 FS=1 IT=246 FT=182.5 TT=1800 FL=150 IP=1025 FP=1025 TP=1800
TRAN CA=212 IS=1 FS=1 IT=182.5 FT=95 TT=360 FL=150 IP=1025 FP=1025 TP=360
TRAN CA=213 IS=1 FS=1 IT=95 FT=182.5 TT=900 FL=150 IP=1025 FP=1025 TP=900
TRAN CA=214 IS=1 FS=1 IT=182.5 FT=246 TT=1800 FL=150 IP=1025 FP=1025 TP=1800
TRAN CA=215 IS=1 FS=1 IT=246 FT=182.5 TT=90 FL=150 IP=1025 FP=1025 TP=90
TRAN CA=216 IS=1 FS=1 IT=182.5 FT=246 TT=180 FL=150 IP=1025 FP=1025 TP=180
TRAN CA=217 IS=1 FS=1 IT=246 FT=187.5 TT=60 FL=150 IP=1025 FP=1025 TP=60
TRAN CA=218 IS=1 FS=1 IT=187.5 FT=100 TT=900 FL=150 IP=1025 FP=1025 TP=900
TRAN CA=219 *IS=1 FS=1 IT=182.5 FT=182.5 TT=0 FL=150 IP=1025 FP=1025 TP=0
TRAN CA=220 *IS=1 FS=1 IT=182.5 FT=182.5 TT=0 FL=150 IP=1025 FP=1025 TP=0
TRAN CA=221 IS=1 FS=1 IT=182.5 FT=125 TT=4140 FL=150 IP=1025 FP=1025 TP=4140
TRAN CA=222 IS=1 FS=1 IT=125 FT=125 TT=0 FL=150 IP=1025 FP=185 TP=0
TRAN CA=223 IS=1 FS=1 IT=125 FT=125 TT=0 FL=150 IP=185 FP=103 TP=0
TRAN CA=224 IS=1 FS=1 IT=125 FT=100 TT=8280 FL=150 IP=103 FP=65 TP=8280
TRAN CA=225 *IS=1 FS=1 IT=246 FT=246 TT=12 FL=150 IP=1025 FP=1205 TP=12
TRAN CA=226 IS=1 FS=1 IT=246 FT=50 TT=0 FL=3672 IP=1205 FP=1150 TP=0
TRAN CA=227 IS=1 FS=1 IT=50 FT=125 TT=1380 FL=150 IP=1150 FP=1150 TP=1380
TRAN CA=228 *IS=1 FS=1 IT=125 FT=125 TT=0 FL=150 IP=1150 FP=1150 TP=0
TRAN CA=229 IS=1 FS=1 IT=125 FT=50 TT=0 FL=2754 IP=1150 FP=900 TP=0
TRAN CA=230 IS=1 FS=1 IT=50 FT=125 TT=3060 FL=150 IP=900 FP=1075 TP=3060
TRAN CA=231 IS=1 FS=1 IT=125 FT=125 TT=0 FL=150 IP=1075 FP=1150 TP=0
TRAN CA=232 IS=1 FS=1 IT=125 FT=50 TT=0 FL=1560.6 IP=1150 FP=690 TP=0
TRAN CA=233 IS=1 FS=1 IT=50 FT=125 TT=300 FL=150 IP=690 FP=690 TP=300
TRAN CA=234 IS=1 FS=1 IT=125 FT=125 TT=8964 FL=150 IP=255 FP=1025 TP=8964
TRAN CA=235 IS=1 FS=1 IT=246 FT=187.5 TT=60 FL=150 IP=1025 FP=900 TP=60
TRAN CA=236 IS=1 FS=1 IT=187.5 FT=100 TT=900 FL=150 IP=900 FP=65 TP=900
TRAN CA=237 IS=1 FS=1 IT=100 FT=100 TT=0 FL=150 IP=65 FP=1578 TP=0
TRAN CA=238 IS=1 FS=1 IT=100 FT=100 TT=0 FL=150 IP=1578 FP=65 TP=0
TRAN CA=239 IS=1 FS=1 IT=246 FT=246 TT=60 FL=150 IP=1025 FP=1390 TP=60
TRAN CA=240 IS=1 FS=1 IT=246 FT=246 TT=900 FL=150 IP=1390 FP=955 TP=900
TRAN CA=241 IS=1 FS=1 IT=246 FT=246 TT=900 FL=150 IP=955 FP=1025 TP=900
TRAN CA=242 IS=1 FS=1 IT=100 FT=112.5 TT=60 FL=150 IP=1025 FP=1025 TP=60
TRAN CA=243 IS=1 FS=1 IT=112.5 FT=125 TT=210 FL=150 IP=1025 FP=1025 TP=210

PAIR CA=201 CO=27.6 DI=0.521 EX=6.4 * Tavg=85
PAIR CA=202 CO=27.6 DI=0.512 EX=6.4 * Tavg=100
PAIR CA=203 CO=27.6 DI=0.508 EX=6.4 * Tavg=113
PAIR CA=204 CO=27.6 DI=0.508 EX=6.4 * Tavg=113
PAIR CA=205 CO=27.6 DI=0.499 EX=6.4 * Tavg=140
```

```
PAIR CA=206 CO=27.5 DI=0.481 EX=6.4 * Tavg=213
PAIR CA=207 CO=27.5 DI=0.476 EX=6.4 * Tavg=226
PAIR CA=208 CO=27.5 DI=0.476 EX=6.4 * Tavg=226
PAIR CA=209 CO=27.5 DI=0.479 EX=6.4 * Tavg=218
PAIR CA=210 CO=27.5 DI=0.479 EX=6.4 * Tavg=218
PAIR CA=211 CO=27.5 DI=0.481 EX=6.4 * Tavg=214
PAIR CA=212 CO=27.6 DI=0.500 EX=6.4 * Tavg=139
PAIR CA=213 CO=27.6 DI=0.500 EX=6.4 * Tavg=139
PAIR CA=214 CO=27.5 DI=0.481 EX=6.4 * Tavg=214
PAIR CA=215 CO=27.5 DI=0.481 EX=6.4 * Tavg=214
PAIR CA=216 CO=27.5 DI=0.481 EX=6.4 * Tavg=214
PAIR CA=217 CO=27.5 DI=0.480 EX=6.4 * Tavg=217
PAIR CA=218 CO=27.6 DI=0.498 EX=6.4 * Tavg=144
PAIR CA=219 CO=27.6 DI=0.489 EX=6.4 * Tavg=183
PAIR CA=220 CO=27.6 DI=0.489 EX=6.4 * Tavg=183
PAIR CA=221 CO=27.6 DI=0.495 EX=6.4 * Tavg=154
PAIR CA=222 CO=27.6 DI=0.504 EX=6.4 * Tavg=125
PAIR CA=223 CO=27.6 DI=0.504 EX=6.4 * Tavg=125
PAIR CA=224 CO=27.6 DI=0.508 EX=6.4 * Tavg=113
PAIR CA=225 CO=27.4 DI=0.469 EX=6.4 * Tavg=246
PAIR CA=226 CO=27.6 DI=0.497 EX=6.4 * Tavg=148
PAIR CA=227 CO=27.6 DI=0.519 EX=6.4 * Tavg=88
PAIR CA=228 CO=27.6 DI=0.504 EX=6.4 * Tavg=125
PAIR CA=229 CO=27.6 DI=0.519 EX=6.4 * Tavg=88
PAIR CA=230 CO=27.6 DI=0.519 EX=6.4 * Tavg=88
PAIR CA=231 CO=27.6 DI=0.504 EX=6.4 * Tavg=125
PAIR CA=232 CO=27.6 DI=0.519 EX=6.4 * Tavg=88
PAIR CA=233 CO=27.6 DI=0.519 EX=6.4 * Tavg=88
PAIR CA=234 CO=27.6 DI=0.504 EX=6.4 * Tavg=125
PAIR CA=235 CO=27.5 DI=0.480 EX=6.4 * Tavg=217
PAIR CA=236 CO=27.6 DI=0.498 EX=6.4 * Tavg=144
PAIR CA=237 CO=27.6 DI=0.512 EX=6.4 * Tavg=100
PAIR CA=238 CO=27.6 DI=0.512 EX=6.4 * Tavg=100
PAIR CA=239 CO=27.4 DI=0.469 EX=6.4 * Tavg=246
PAIR CA=240 CO=27.4 DI=0.469 EX=6.4 * Tavg=246
PAIR CA=241 CO=27.4 DI=0.469 EX=6.4 * Tavg=246
PAIR CA=242 CO=27.6 DI=0.510 EX=6.4 * Tavg=106
PAIR CA=243 CO=27.6 DI=0.506 EX=6.4 * Tavg=119
VALV PT=320  DX=-1.167 PL=2  EW=1
CROS CD=6
TANG PT=325  DX=-0.666
TANG PT=330  DX=-2.667  EW=1
BRAD PT=335  RA=1.75  EW=1
TANP         DZ=-3.5
BRAD PT=340  RA=1.75  EW=1
TANG PT=345  DX=3.333  EW=1
CROS CD=7
VALV PT=346  DX=1.167 PL=1 MA=1.725
*-----------------------------------------------------------------------------
*END REGION IIb
*-----------------------------------------------------------------------------
*BEGIN REGION II
*-----------------------------------------------------------------
OPER CA=1  TE=100 PR=50

OPER CA=3  TE=100 PR=50
```

```
OPER CA=4  TE=100 PR=50
OPER CA=5  TE=100 PR=50
OPER CA=6  TE=100 PR=50
OPER CA=7  TE=100 PR=50
OPER CA=8  TE=100 PR=50
OPER CA=9  TE=100 PR=50
OPER CA=10 TE=100 PR=50
OPER CA=11 TE=100 PR=50
OPER CA=12 TE=100 PR=50
OPER CA=13 TE=100 PR=50
OPER CA=14 TE=50  PR=1135
OPER CA=15 TE=100 PR=50
OPER CA=16 TE=100 PR=50
OPER CA=17 TE=100 PR=50
OPER CA=18 TE=100 PR=50

OPER CA=20 TE=100 PR=50
OPER CA=21 TE=100 PR=50
OPER CA=22 TE=100 PR=50
OPER CA=23 TE=100 PR=50
OPER CA=24 TE=100 PR=50
OPER CA=25 TE=100 PR=50
OPER CA=26 TE=100 PR=50
OPER CA=27 TE=100 PR=50
OPER CA=28 TE=100 PR=50
OPER CA=29 TE=100 PR=50
OPER CA=30 TE=100 PR=50

TRAN CA=201 IS=1 FS=1 IT=70 FT=100 TT=1800 FL=150 IP=15 FP=65 TP=1800
TRAN CA=202 *IS=1 FS=1 IT=100 FT=100 TT=0 FL=150 IP=65 FP=65 TP=0
TRAN CA=203 *IS=1 FS=1 IT=100 FT=100 TT=16164 FL=150 IP=65 FP=65 TP=16164
TRAN CA=204 *IS=1 FS=1 IT=100 FT=100 TT=0 FL=150 IP=65 FP=65 TP=0
TRAN CA=205 *IS=1 FS=1 IT=100 FT=100 TT=0 FL=150 IP=65 FP=65 TP=0
TRAN CA=206 *IS=1 FS=1 IT=100 FT=100 TT=1800 FL=150 IP=65 FP=65 TP=1800
TRAN CA=207 *IS=1 FS=1 IT=100 FT=100 TT=900 FL=150 IP=65 FP=65 TP=900
TRAN CA=208 *IS=1 FS=1 IT=100 FT=100 TT=900 FL=150 IP=65 FP=65 TP=900
TRAN CA=209 *IS=1 FS=1 IT=100 FT=100 TT=1800 FL=150 IP=65 FP=65 TP=1800
TRAN CA=210 *IS=1 FS=1 IT=100 FT=100 TT=1800 FL=150 IP=65 FP=65 TP=1800
TRAN CA=211 *IS=1 FS=1 IT=100 FT=100 TT=1800 FL=150 IP=65 FP=65 TP=1800
TRAN CA=212 *IS=1 FS=1 IT=100 FT=100 TT=360 FL=150 IP=65 FP=65 TP=360
TRAN CA=213 *IS=1 FS=1 IT=100 FT=100 TT=900 FL=150 IP=65 FP=65 TP=900
TRAN CA=214 *IS=1 FS=1 IT=100 FT=100 TT=1800 FL=150 IP=65 FP=65 TP=1800
TRAN CA=215 *IS=1 FS=1 IT=100 FT=100 TT=90 FL=150 IP=65 FP=65 TP=90
TRAN CA=216 *IS=1 FS=1 IT=100 FT=100 TT=180 FL=150 IP=65 FP=65 TP=180
TRAN CA=217 *IS=1 FS=1 IT=100 FT=100 TT=60 FL=150 IP=65 FP=65 TP=60
TRAN CA=218 *IS=1 FS=1 IT=100 FT=100 TT=900 FL=150 IP=65 FP=65 TP=900
TRAN CA=219 *IS=1 FS=1 IT=100 FT=100 TT=0 FL=150 IP=65 FP=65 TP=0
TRAN CA=220 *IS=1 FS=1 IT=100 FT=100 TT=0 FL=150 IP=65 FP=65 TP=0
TRAN CA=221 *IS=1 FS=1 IT=100 FT=100 TT=0 FL=150 IP=65 FP=65 TP=0
TRAN CA=222 *IS=1 FS=1 IT=100 FT=100 TT=0 FL=150 IP=65 FP=65 TP=0
TRAN CA=223 *IS=1 FS=1 IT=100 FT=100 TT=0 FL=150 IP=65 FP=65 TP=0
TRAN CA=224 *IS=1 FS=1 IT=100 FT=100 TT=8280 FL=150 IP=65 FP=65 TP=8280
TRAN CA=225 *IS=1 FS=1 IT=100 FT=100 TT=12 FL=150 IP=65 FP=65 TP=12
TRAN CA=226 IS=1 FS=1 IT=100 FT=50 TT=0 FL=3672 IP=65 FP=1150 TP=0
TRAN CA=227 IS=1 FS=1 IT=50 FT=100 TT=1380 FL=150 IP=1150 FP=65 TP=1380
TRAN CA=228 *IS=1 FS=1 IT=100 FT=100 TT=0 FL=150 IP=65 FP=65 TP=0
```

```
TRAN CA=229 IS=1 FS=1 IT=100 FT=50 TT=0 FL=2754 IP=1150 FP=900 TP=0
TRAN CA=230 IS=1 FS=1 IT=50 FT=100 TT=3060 FL=150 IP=900 FP=65 TP=3060
TRAN CA=231 *IS=1 FS=1 IT=100 FT=100 TT=0 FL=150 IP=65 FP=65 TP=0
TRAN CA=232 IS=1 FS=1 IT=100 FT=50 TT=0 FL=1560.6 IP=65 FP=690 TP=0
TRAN CA=233 IS=1 FS=1 IT=50 FT=100 TT=300 FL=150 IP=690 FP=65 TP=300
TRAN CA=234 *IS=1 FS=1 IT=100 FT=100 TT=8964 FL=150 IP=65 FP=65 TP=8964
TRAN CA=235 *IS=1 FS=1 IT=100 FT=100 TT=60 FL=150 IP=65 FP=65 TP=60
TRAN CA=236 *IS=1 FS=1 IT=100 FT=100 TT=900 FL=150 IP=65 FP=65 TP=900
TRAN CA=237 *IS=1 FS=1 IT=100 FT=100 TT=0 FL=150 IP=65 FP=65 TP=0
TRAN CA=238 *IS=1 FS=1 IT=100 FT=100 TT=0 FL=150 IP=65 FP=65 TP=0
TRAN CA=239 *IS=1 FS=1 IT=100 FT=100 TT=60 FL=150 IP=65 FP=65 TP=60
TRAN CA=240 *IS=1 FS=1 IT=100 FT=100 TT=900 FL=150 IP=65 FP=65 TP=900
TRAN CA=241 *IS=1 FS=1 IT=100 FT=100 TT=900 FL=150 IP=65 FP=65 TP=900
TRAN CA=242 *IS=1 FS=1 IT=100 FT=100 TT=60 FL=150 IP=65 FP=65 TP=60
TRAN CA=243 *IS=1 FS=1 IT=100 FT=100 TT=210 FL=150 IP=65 FP=65 TP=210

PAIR CA=201 CO=27.6 DI=0.521 EX=6.4 * Tavg=85
PAIR CA=202 CO=27.6 DI=0.512 EX=6.4 * Tavg=100
PAIR CA=203 CO=27.6 DI=0.512 EX=6.4 * Tavg=100
PAIR CA=204 CO=27.6 DI=0.512 EX=6.4 * Tavg=100
PAIR CA=205 CO=27.6 DI=0.512 EX=6.4 * Tavg=100
PAIR CA=206 CO=27.6 DI=0.512 EX=6.4 * Tavg=100
PAIR CA=207 CO=27.6 DI=0.512 EX=6.4 * Tavg=100
PAIR CA=208 CO=27.6 DI=0.512 EX=6.4 * Tavg=100
PAIR CA=209 CO=27.6 DI=0.512 EX=6.4 * Tavg=100
PAIR CA=210 CO=27.6 DI=0.512 EX=6.4 * Tavg=100
PAIR CA=211 CO=27.6 DI=0.512 EX=6.4 * Tavg=100
PAIR CA=212 CO=27.6 DI=0.512 EX=6.4 * Tavg=100
PAIR CA=213 CO=27.6 DI=0.512 EX=6.4 * Tavg=100
PAIR CA=214 CO=27.6 DI=0.512 EX=6.4 * Tavg=100
PAIR CA=215 CO=27.6 DI=0.512 EX=6.4 * Tavg=100
PAIR CA=216 CO=27.6 DI=0.512 EX=6.4 * Tavg=100
PAIR CA=217 CO=27.6 DI=0.512 EX=6.4 * Tavg=100
PAIR CA=218 CO=27.6 DI=0.512 EX=6.4 * Tavg=100
PAIR CA=219 CO=27.6 DI=0.512 EX=6.4 * Tavg=100
PAIR CA=220 CO=27.6 DI=0.512 EX=6.4 * Tavg=100
PAIR CA=221 CO=27.6 DI=0.512 EX=6.4 * Tavg=100
PAIR CA=222 CO=27.6 DI=0.512 EX=6.4 * Tavg=100
PAIR CA=223 CO=27.6 DI=0.512 EX=6.4 * Tavg=100
PAIR CA=224 CO=27.6 DI=0.512 EX=6.4 * Tavg=100
PAIR CA=225 CO=27.6 DI=0.512 EX=6.4 * Tavg=100
PAIR CA=226 CO=27.5 DI=0.526 EX=6.4 * Tavg=75
PAIR CA=227 CO=27.5 DI=0.526 EX=6.4 * Tavg=75
PAIR CA=228 CO=27.6 DI=0.512 EX=6.4 * Tavg=100
PAIR CA=229 CO=27.5 DI=0.526 EX=6.4 * Tavg=75
PAIR CA=230 CO=27.5 DI=0.526 EX=6.4 * Tavg=75
PAIR CA=231 CO=27.6 DI=0.512 EX=6.4 * Tavg=100
PAIR CA=232 CO=27.5 DI=0.526 EX=6.4 * Tavg=75
PAIR CA=233 CO=27.5 DI=0.526 EX=6.4 * Tavg=75
PAIR CA=234 CO=27.6 DI=0.512 EX=6.4 * Tavg=100
PAIR CA=235 CO=27.6 DI=0.512 EX=6.4 * Tavg=100
PAIR CA=236 CO=27.6 DI=0.512 EX=6.4 * Tavg=100
PAIR CA=237 CO=27.6 DI=0.512 EX=6.4 * Tavg=100
PAIR CA=238 CO=27.6 DI=0.512 EX=6.4 * Tavg=100
PAIR CA=239 CO=27.6 DI=0.512 EX=6.4 * Tavg=100
PAIR CA=240 CO=27.6 DI=0.512 EX=6.4 * Tavg=100
```

```
PAIR CA=241 CO=27.6 DI=0.512 EX=6.4 * Tavg=100
PAIR CA=242 CO=27.6 DI=0.512 EX=6.4 * Tavg=100
PAIR CA=243 CO=27.6 DI=0.512 EX=6.4 * Tavg=100

VALV PT=350  DX=1.167 PL=2  EW=1
CROS CD=6
TANG PT=355  DX=0.167
TANG PT=360  DX=2.083  EW=1
BRAD PT=380  RA=1.75  EW=1
TANP         DY=-2.479
BRAD PT=390  RA=1.75  EW=1
TANG PT=392  DX=2.585 DY=-2.585
TANG PT=395  DX=2.585 DY=-2.585  EW=1
BRAD PT=400  RA=1.75  EW=1
TANG PT=405  DZ=-3.417
BRAD PT=410  RA=1.17  EW=1
TANG PT=415  DY=-3
TANG PT=420  DY=-5.25
TANG PT=425  DY=-2.417
BRAD PT=430  RA=1.75  EW=1
TANG PT=435  DZ=2.333
TANG PT=440  DZ=4.757
TANG PT=445  DZ=4.757
TANG PT=450  DZ=4.757
BRAD PT=455  RA=1.75  EW=1
TANG PT=460  DX=-1.989  DZ=1.989
BRAD PT=465  RA=1.75  EW=1
TANG PT=470  DY=-5.722
TANG PT=480  DY=-5.722
TANG PT=485  DY=-5.722
BRAD PT=490  RA=1.17  EW=1
TANG PT=495  DZ=1.667
TANG PT=500  DZ=2.0833
BRAD PT=505  RA=1.75  EW=1
TANG PT=510  DX=3.682
TANG PT=515  DX=3.682
TANG PT=520  DX=3.682
TANG PT=525  DX=3.682
BRAD PT=535  RA=1.75
TANG PT=540  DX=2.556  DZ=-2.556
TANG PT=545  DX=2.555  DZ=-2.555
STRU PT=546  DX=-.7071 DZ=-.7071
STRU PT=547  DX=-.7071 DZ=-.7071
ANCH PT=547
*-----------------------------------------------------------------------------
*END REGION II
*-----------------------------------------------------------------------------
*
*** VALVE OPERATOR ***
CROS CD=7
JUNC PT=346
VALV PT=348 DY=5.567 PL=3 MA=2.52
*** SUPPORTS AND ANCHORS ***
CSUP PT=105 DY=1  KP=5000  PI=0 *FW-9
CSUP PT=190 DY=1  KP=1000  PI=0 *FW-6
CSUP PT=220 DY=-1 KP=1000  PI=0 *FW-4
```

```
CSUP PT=270 DY=1  KP=1000  PI=0 *FW-2
CSUP PT=145 DY=1  KP=1000  PI=0 *FW-7
*
RSTN PT=230 DX=-0.6123  DY=-0.5  DZ=0.6123  SP=370  *FW-3
*
RSTN PT=80   DX=1.0                          SP=200  *FDW-H10

RSTN PT=201  DX=0.198 DZ=0.9802    SP=1000  *FDW-H23
RSTN PT=546  DX=-0.7071  DZ=-0.7071            SP=1000 *BELLOWS
RSTN PT=355   DY=1.0                                   *HPCI-H31
RSTN PT=415   DX=1.0  DZ=1.0                           *HPCI-H32
RSTN PT=30    DX=1.0  DY=1.0                           *FDW-HD37 FLUED HEAD
ROTR PT=30    RZ=1                                     *FDW_HD37 FLUED HEAD
RSTN PT=60  DX=1.0 DY=1.0                      SP=200  *FDW-H24
RSTN PT=5 DX=1 DY=1 DZ=1
ROTR PT=5 RZ=1
ENDP
```

APPENDIX B

PIPESTRESS OUTPUT FILE ("FWHPCI.PRF")

CALCULATION NUMBER 2 CODE SECTION III CLASS 1 ASME-1998 KRE 2007/07/11 11:35:07 [1242]
Vermont Yankee Feedwater PipingSI Fatigue Analysis

DELTA T1 IN DEGREES F
PRESSURES IN PSI
STRESSES IN PSI

SUMMARY OF LOAD SETS AT POINT 155 LR ELBOW 155 TO 160 GLOBAL MOMENTS IN FT-LB

LOAD SET NO.	LOAD SET DESCRIPTION		CYCLES	DYNAM. CYCLES	PRESSURE	MOMENT X	MOMENT Y	MOMENT Z	TRANSIENT STRESSES EQ. 10	EQ. 11	EQ. 13	DELTA T1
1	Design Hydrotest +	LS-1	120		1100.	55.	22.	54.	0.	50.	0.	0.3
2	Design Hydrotest -	LS-2	120		50.	56.	21.	54.	0.	0.	0.	0.0
3	Startup +	LS-3	300		1010.	14505.	-695.	-12403.	25110.	25114.	12555.	0.5
4	TRoll & Inc. PWR1 -	LS-4	610		1010.	24012.	-983.	-21319.	-25109.	-54064.	-12555.	-169.9
5	TRoll & Inc. PWR2 +	LS-5	599		1010.	13760.	-442.	-11409.	0.	15049.	0.	78.5
6	TRoll & Inc. PWR3 +	LS-6	599		1010.	4661.	45.	-2630.	0.	252.	0.	1.4
7	DlyReduction to 75% -	LS-7	10000		1010.	10313.	-259.	-8082.	0.	-317.	0.	-1.7
8	DlyReduction to 75% +	LS-8	10000		1010.	4661.	45.	-2630.	0.	317.	0.	1.7
9	WklyReduct to 50% -	LS-9	2000		1010.	12381.	-369.	-10078.	0.	-215.	0.	-1.2
10	WklyReduct to 50% +	LS-10	2000		1010.	4661.	45.	-2630.	0.	215.	0.	1.2
11	LOFWH+TT 1 -	LS-11	310		1010.	13415.	-424.	-11077.	0.	-243.	0.	-1.3
12	LOFWH+TT 2 -	LS-12	10		1010.	24520.	-1009.	-21810.	0.	-1480.	0.	-7.9
13	LOFWH+TT 3 +	LS-13	10		1010.	13415.	-424.	-11077.	0.	619.	0.	3.3
14	LOFWH+TT 4 +	LS-14	10		1010.	4661.	45.	-2630.	0.	243.	0.	1.3
15	LOFWH+PFWHTR Byp -	LS-15	70		1010.	13415.	-424.	-11077.	0.	-4784.	0.	-25.7
16	LOFWH+PFWHTR Byp +	LS-16	70		1010.	4661.	45.	-2630.	0.	2433.	0.	13.1
17	SCRAM+TT+AllOtrScm -	LS-17	289		1010.	12192.	-365.	-9935.	0.	-6434.	0.	-34.4
18	SCRAM+TT+AllOtrScm -	LS-18	289		1010.	23480.	-960.	-20844.	0.	-593.	0.	-3.2
19	HotStandby 1 +	LS-19	300		1010.	10450.	-359.	-8332.	10951.	10969.	5476.	39.7
20	HotStandby 2 +	LS-20	300		1010.	8500.	-316.	-6524.	17948.	17967.	8974.	0.6
21	HotStandby 3 -	LS-21	300		1010.	14505.	-695.	-12403.	0.	0.	0.	0.0
22	Shutdown 1 -	LS-22	300		170.	7904.	-355.	-6594.	-25111.	-25113.	-12555.	-0.6
23	Shutdown 2 -	LS-23	300		88.	6239.	-269.	-5132.	-14160.	-14241.	-7080.	-1.4
24	Shutdown 3 -	LS-24	300		50.	56.	21.	54.	-11328.	-11330.	-5664.	-0.5
25	SCRAM+LOFWP1 +	LS-25	10		1190.	2347.	86.	-451.	10950.	10965.	5475.	42.2
26	SCRAM+LOFWP2 -	LS-26	10		1135.	26504.	-1110.	-23646.	-10950.	-57147.	-5475.	-251.2
27	SCRAM+LOFWP3 +	LS-27	10		1135.	17301.	-771.	-14962.	18318.	18515.	9159.	5.3
28	SCRAM+LOFWP4 +	LS-28	10		1135.	15136.	-727.	-12959.	26076.	26097.	13038.	31.3
29	SCRAM+LOFWP5 -	LS-29	10		885.	24686.	-1036.	-22025.	-26053.	-64906.	-13027.	-223.8
30	SCRAM+LOFWP6 +	LS-30	10		1060.	16738.	-747.	-14459.	18317.	18413.	9159.	2.4
31	SCRAM+LOFWP7 +	LS-31	10		1135.	15415.	-733.	-13217.	25130.	25158.	12565.	27.2

CALCULATION NUMBER 2 CODE SECTION III CLASS 1 ASME-1998 KRE 2007/07/11 11:35:07 [1243]
Vermont Yankee Feedwater PipingSI Fatigue Analysis

DELTA T1 IN DEGREES F
PRESSURES IN PSI
STRESSES IN PSI

SUMMARY OF LOAD SETS AT POINT 155 LR ELBOW 155 TO 160 GLOBAL MOMENTS IN FT-LB

LOAD SET NO.	LOAD SET DESCRIPTION		CYCLES	DYNAM. CYCLES	PRESSURE	MOMENT X	MOMENT Y	MOMENT Z	TRANSIENT STRESSES EQ. 10	EQ. 11	EQ. 13	DELTA T1
32	SCRAM+LOFWP8 -	LS-32	10		675.	23044.	-968.	-20560.	-25110.	-53661.	-12555.	-167.0
33	SCRAM+LOFWP9 +	LS-33	10		675.	16095.	-672.	-13953.	9507.	10417.	4754.	15.0
34	SCRAM+LOFWP10+	LS-34	10		1010.	14505.	-695.	-12403.	25119.	25126.	12559.	0.5
35	SCRAM+SRVBLDN1-	LS-35	1		885.	12714.	-388.	-10400.	0.	-6434.	0.	-34.4
36	SCRAM+SRVBLDN2-	LS-36	1		50.	56.	21.	54.	0.	-593.	0.	-3.2
37	Hydro Test +	LS-37	1		1563.	54.	22.	54.	0.	0.	0.	0.0
38	Hydro Test -	LS-38	1		50.	56.	21.	54.	0.	0.	0.	0.0
39	SCRAM+TG+OPres1 -	LS-39	289		1375.	7411.	-66.	-5088.	0.	0.	0.	0.0
40	SCRAM+TG+OPres2 -	LS-40	289		940.	4126.	66.	-2152.	0.	0.	0.	0.0
41	SCRAM+TG+OPres3 -	LS-41	289		1010.	4661.	45.	-2630.	0.	0.	0.	0.0
42	HotSbyFWcyc +	LS-42	300		1010.	20056.	-857.	-17600.	10427.	10652.	5214.	29.2
43	HotSbyFWcyc +	LS-43	300		1010.	14505.	-695.	-12403.	25130.	25446.	12565.	23.6
44	NORMAL+OBE LS-132		5	10(1)	1010.	14078.	-2008.	-11434.	0.	0.	0.	0.0
45	NORMAL-OBE LS-133		5	10(1)	1010.	10494.	1458.	-8380.	0.	0.	0.	0.0
101	WEIGHT					10013.	720.	-7200.				
104	DYNAMIC FLAG= 1					1792.	1733.	1527.				

B1	C1	K1	B2	C2	K2	C3	K3	C3PRIM	C4	Z	DIAM/TH	MATERIAL	E
0.106	1.247	1.000	2.022	3.034	1.000	1.000	1.000	0.500	1.100	0.60321E+02	12.752	CARBON STEEL	0.2950E+08

THIS ANALYSIS IS FOR THE BODY OF THE FITTING.

CALCULATION NUMBER 2 CODE SECTION III CLASS 1 ASME-1998 KRE 2007/07/11 11:35:07 [1244]
Vermont Yankee Feedwater PipingSI Fatigue Analysis

FATIGUE ANALYSIS AT POINT 155, LR ELBOW 155 TO 160

****
INDIVIDUAL STRESS RANGE CHECK
****

DELTA T1 IN DEGREES F
STRESSES IN PSI

LOAD SET PAIR		SN EQN.10	SE EQN.12	DELTA T1 RANGE	EQN.13	SP EQN.11	KE	SALT EQN.14	ALLOW CYCLES	3*SM	ALLOWABLE FOR DELTA T1 RANGE
28	29	62066.b	7949.	255.1	35508.	100939.	1.317	66456.	1808.	53580.	759.3
29	31	60890.b	7720.	251.0	35035.	99771.	1.273	63498.	2050.	53580.	763.1
29	43	60634.b	8457.	247.4	34041.	99802.	1.263	63040.	2098.	53580.	763.1
29	34	60622.b	8457.	224.3	34035.	99482.	1.263	62816.	2122.	53580.	763.1
3	29	60614.b	8457.	224.3	34031.	99470.	1.263	62793.	2125.	53580.	763.1
28	32	61463.b	6621.	198.3	36705.	90035.	1.294	58265.	2697.	53580.	763.1
20	29	58527.b	13533.	224.4	30450.	97400.	1.185	57693.	2783.	53580.	763.1
25	29	58182.b	18755.	266.0	28382.	97049.	1.172	56861.	2915.	53580.	759.3
31	32	60288.b	6392.	194.2	36232.	88867.	1.219	54146.	3406.	54348.	766.8
4	28	59539.b	7360.	201.2	34042.	88515.	1.222	54103.	3415.	53580.	763.1
32	43	60031.b	7129.	190.6	35238.	88898.	1.209	53745.	3488.	54348.	766.8
32	34	60020.b	7129.	167.6	35233.	88578.	1.209	53533.	3532.	54348.	766.8
3	32	60011.b	7129.	167.6	35228.	88566.	1.208	53512.	3536.	54348.	766.8
4	31	58364.b	7131.	197.0	33569.	87347.	1.148	50128.	4354.	54348.	766.8
4	43	58108.b	7868.	193.5	32576.	87378.	1.138	49733.	4465.	54348.	766.8
4	34	58096.b	7868.	170.4	32570.	87058.	1.138	49533.	4523.	54348.	766.8
3	4	58088.b	7868.	170.4	32566.	87046.	1.138	49512.	4529.	54348.	766.8
25	32	57580.b	17427.	209.2	29579.	86146.	1.149	49505.	4531.	53580.	763.1
20	32	57925.b	12205.	167.6	31647.	86496.	1.132	48941.	4700.	54348.	766.8
26	43	47001.g	9927.	274.8	26489.	93513.	1.000	46757.	5404.	53580.	763.1
26	34	46989.g	9927.	251.8	26484.	93193.	1.000	46597.	5460.	53580.	763.1
3	26	46980.g	9927.	251.7	26479.	93181.	1.000	46591.	5462.	53580.	763.1
26	28	46445.g	9419.	282.5	25969.	92663.	1.000	46332.	5553.	53580.	759.3
27	29	52528.g	6169.	229.1	31629.	91578.	1.000	45789.	5750.	53580.	788.7
2	29	52662.g	19973.	223.8	27119.	91515.	1.000	45758.	5762.	53580.	849.3
24	29	52662.g	19973.	223.3	27119.	91515.	1.000	45758.	5762.	53580.	810.3

Notes b,d,e,k: Fails
g: Weld ISI
h,i: Rupture Location
L: Information

CALCULATION NUMBER 2 CODE SECTION III CLASS 1 ASME-1998 KRE 2007/07/11 11:35:07 [1245]
Vermont Yankee Feedwater PipingSI Fatigue Analysis

FATIGUE ANALYSIS AT POINT 155, LR ELBOW 155 TO 160

****
INDIVIDUAL STRESS RANGE CHECK
****

DELTA T1 IN DEGREES F
STRESSES IN PSI

LOAD SET PAIR		SN EQN.10	SE EQN.12	DELTA T1 RANGE	EQN.13	SP EQN.11	KE	SALT EQN.14	ALLOW CYCLES	3*SM	ALLOWABLE FOR DELTA T1 RANGE
29	36	52662.g	19973.	220.6	27119.	91515.	1.000	45758.	5762.	53580.	821.0
29	38	52662.g	19973.	223.8	27119.	91515.	1.000	45758.	5762.	53580.	849.3
22	28	64676.b	5819.	31.9	40719.	64699.	1.414	45748.	5766.	53580.	763.1
26	31	45270.g	9190.	278.4	25496.	91495.	1.000	45747.	5766.	53580.	763.1
29	30	52386.g	6625.	226.2	31032.	91335.	1.000	45668.	5796.	53580.	788.7
4	25	55656.b	18165.	212.0	26916.	84625.	1.077	45590.	5825.	53580.	763.1
20	26	44893.g	15003.	251.8	22898.	91110.	1.000	45555.	5838.	53580.	763.1
29	37	51415.g	19974.	223.8	25871.	90268.	1.000	45134.	6002.	53580.	784.2
5	29	36248.		302.3		90149.	1.000	45075.	6025.	53580.	823.9
4	20	56000.b	12943.	170.5	28984.	84975.	1.061	45071.	6026.	54348.	766.8
19	29	49926.g	11928.	263.5	26952.	88796.	1.000	44398.	6302.	53580.	788.7
25	26	42561.		293.4		88773.	1.000	44386.	6307.	53580.	759.3
2	26	41017.		251.2		87213.	1.000	43607.	6647.	53580.	849.3
24	26	41395.		250.8		87213.	1.000	43607.	6647.	53580.	810.3
26	36	41017.		248.0		87213.	1.000	43607.	6647.	53580.	821.0
26	38	41017.		251.2		87213.	1.000	43607.	6647.	53580.	849.3
1	29	47735.g	19973.	224.1	22191.	86638.	1.000	43319.	6779.	53580.	849.3
22	31	63959.b	6048.	27.7	40246.	63989.	1.354	43310.	6783.	54348.	766.8
23	29	47490.g	15103.	222.4	26817.	86343.	1.000	43172.	6848.	53580.	801.6
16	29	43884.g	16837.	236.9	21476.	85169.	1.000	42585.	7132.	53580.	798.3
22	29	45501.g	13765.	223.2	26165.	84354.	1.000	42177.	7338.	53580.	763.1
26	30	37958.		253.6		84251.	1.000	42125.	7365.	53580.	788.7
29	33	44347.g	7118.	238.8	26905.	84109.	1.000	42055.	7402.	53580.	816.1
5	26	22614.		329.7		83859.	1.000	41930.	7467.	53580.	823.9
29	39	44560.g	14613.	223.8	24377.	83413.	1.000	41706.	7587.	53580.	787.5
26	27	36908.		256.6		83301.	1.000	41651.	7617.	53580.	788.7

Notes b,d,e,k: Fails
g: Weld ISI
h,i: Rupture Location
L: Information

CALCULATION NUMBER 2 CODE SECTION III CLASS 1 ASME-1998 KRE 2007/07/11 11:35:07 [1246]
Vermont Yankee Feedwater PipingSI Fatigue Analysis

FATIGUE ANALYSIS AT POINT 155, LR ELBOW 155 TO 160

****
INDIVIDUAL STRESS RANGE CHECK
****

DELTA T1 IN DEGREES F
STRESSES IN PSI

LOAD SET PAIR		SN EQN.10	SE EQN.12	DELTA T1 RANGE	EQN.13	SP EQN.11	KE	SALT EQN.14	ALLOW CYCLES	3*SM	ALLOWABLE FOR DELTA T1 RANGE
8	29	43884.g	16837.	225.5	21476.	83053.	1.000	41527.	7684.	53580.	798.3
6	29	43884.g	16837.	225.2	21476.	82988.	1.000	41494.	7702.	53580.	798.3
14	29	43884.g	16837.	225.1	21476.	82979.	1.000	41490.	7705.	53580.	798.3
10	29	43884.g	16837.	225.0	21476.	82951.	1.000	41475.	7713.	53580.	798.3
29	41	43884.g	16837.	223.8	21476.	82736.	1.000	41368.	7772.	53580.	798.3
29	40	43760.g	17270.	223.8	20920.	82613.	1.000	41307.	7807.	53580.	798.3
19	26	36292.		290.9		82507.	1.000	41253.	7836.	53580.	788.7
23	26	39055.		249.8		82041.	1.000	41021.	7969.	53580.	801.6
26	37	35796.		251.2		81993.	1.000	40996.	7983.	53580.	784.2
2	4	52124.g	19385.	169.9	27641.	81079.	1.000	40539.	8253.	54348.	851.7
4	24	52124.g	19385.	169.4	27641.	81079.	1.000	40539.	8253.	54348.	813.4
4	36	52124.g	19385.	166.7	27641.	81079.	1.000	40539.	8253.	54348.	824.1
4	38	52124.g	19385.	169.9	27641.	81079.	1.000	40539.	8253.	54348.	851.7
22	43	62228.b	5311.	24.1	39253.	62546.	1.290	40342.	8374.	54348.	766.8
27	32	51926.g	4842.	172.4	32826.	80674.	1.000	40337.	8377.	54348.	792.1
30	32	51784.g	5297.	169.4	32229.	80431.	1.000	40216.	8452.	54348.	792.1
29	42	41341.		253.0		80418.	1.000	40209.	8456.	53580.	818.0
22	34	62217.b	5311.	1.1	39247.	62226.	1.290	40123.	8510.	54348.	766.8
3	22	62208.b	5311.	1.1	39243.	62214.	1.289	40105.	8521.	54348.	766.8
22	26	48016.g	15236.	250.7	27681.	80052.	1.000	40026.	8571.	53580.	763.1
26	33	32701.		266.2		79807.	1.000	39904.	8649.	53580.	816.1
32	37	50812.g	18645.	167.0	27068.	79364.	1.000	39682.	8794.	54348.	788.7
5	32	35646.		245.5		79246.	1.000	39623.	8832.	54348.	827.0
4	27	50002.g	5580.	175.2	30163.	79153.	1.000	39577.	8863.	54348.	792.1
1	26	32672.		251.5		78918.	1.000	39459.	8942.	53580.	849.3
4	30	49860.g	6036.	172.2	29566.	78911.	1.000	39455.	8944.	54348.	792.1

Notes b,d,e,k: Fails
g: Weld ISI
h,i: Rupture Location
L: Information

CALCULATION NUMBER 2 CODE SECTION III CLASS 1 ASME-1998 KRE 2007/07/11 11:35:07 [1247]
Vermont Yankee Feedwater PipingSI Fatigue Analysis

FATIGUE ANALYSIS AT POINT 155, LR ELBOW 155 TO 160

****
INDIVIDUAL STRESS RANGE CHECK
****

DELTA T1 IN DEGREES F
STRESSES IN PSI

LOAD SET PAIR		SN EQN.10	SE EQN.12	DELTA T1 RANGE	EQN.13	SP EQN.11	KE	SALT EQN.14	ALLOW CYCLES	3*SM	ALLOWABLE FOR DELTA T1 RANGE
16	26	30250.		264.3		78880.	1.000	39440.	8955.	53580.	798.3
7	29	39141.		222.1		77994.	1.000	38997.	9260.	53580.	798.3
19	32	49324.g	10600.	206.7	28149.	77893.	1.000	38946.	9296.	54348.	792.1
29	45	39023.		223.8		77876.	1.000	38938.	9302.	53580.	814.2
4	37	48890.g	19386.	169.9	24406.	77845.	1.000	38922.	9313.	54348.	788.7
4	5	33721.		248.4		77724.	1.000	38862.	9356.	54348.	827.0
26	40	31239.		251.2		77436.	1.000	38718.	9459.	53580.	798.3
2	32	48721.g	18644.	167.0	24978.	77272.	1.000	38636.	9519.	54348.	851.7
24	32	48721.g	18644.	166.6	24978.	77272.	1.000	38636.	9519.	54348.	813.4
32	36	48721.g	18644.	163.9	24978.	77272.	1.000	38636.	9519.	54348.	824.1
32	38	48721.g	18644.	167.0	24978.	77272.	1.000	38636.	9519.	54348.	851.7
8	26	30250.		252.9		76764.	1.000	38382.	9707.	53580.	798.3
6	26	30250.		252.6		76698.	1.000	38349.	9732.	53580.	798.3
14	26	30250.		252.5		76689.	1.000	38345.	9735.	53580.	798.3
10	26	30250.		252.4		76661.	1.000	38331.	9746.	53580.	798.3
26	41	30250.		251.2		76447.	1.000	38223.	9827.	53580.	798.3
17	29	37547.		189.4		76400.	1.000	38200.	9845.	53580.	798.3
4	19	47399.g	11338.	209.6	25486.	76372.	1.000	38186.	9856.	54348.	792.1
9	29	37405.		222.7		76258.	1.000	38129.	9899.	53580.	798.3
13	29	36537.		227.1		76009.	1.000	38004.	9996.	53580.	822.9
4	23	46952.g	14514.	168.5	27338.	75906.	1.000	37953.	10042.	54348.	804.7
1	32	47132.g	18645.	167.3	23388.	75733.	1.000	37867.	10120.	54348.	851.7
11	29	36537.		222.5		75390.	1.000	37695.	10278.	53580.	798.3
15	29	36537.		198.1		75390.	1.000	37695.	10278.	53580.	798.3
26	39	28939.		251.2		75136.	1.000	37568.	10397.	53580.	787.5
29	35	36132.		189.4		74985.	1.000	37492.	10468.	53580.	798.3

Notes b,d,e,k: Fails
g: Weld ISI
h,i: Rupture Location
L: Information

CALCULATION NUMBER 2 CODE SECTION III CLASS 1 ASME-1998 KRE 2007/07/11 11:35:07 [1248]
Vermont Yankee Feedwater PipingSI Fatigue Analysis

FATIGUE ANALYSIS AT POINT 155, LR ELBOW 155 TO 160

****
INDIVIDUAL STRESS RANGE CHECK
****

DELTA T1 IN DEGREES F
STRESSES IN PSI

LOAD SET PAIR		SN EQN.10	SE EQN.12	DELTA T1 RANGE	EQN.13	SP EQN.11	KE	SALT EQN.14	ALLOW CYCLES	3*SM	ALLOWABLE FOR DELTA T1 RANGE
29	44	36112.		223.8		74965.	1.000	37482.	10477.	53580.	814.2
21	29	35503.		223.8		74356.	1.000	37178.	10772.	53580.	763.1
16	32	43282.		180.1		74266.	1.000	37133.	10817.	54348.	801.4
1	4	45210.g	19385.	170.1	20726.	74214.	1.000	37107.	10843.	54348.	851.7
26	42	27708.		280.4		74129.	1.000	37064.	10885.	53580.	818.0
4	22	44964.g	13177.	169.3	26687.	73917.	1.000	36959.	10992.	54348.	766.8
4	33	43808.g	6529.	184.9	27427.	73672.	1.000	36836.	11117.	54348.	819.2
4	16	41357.		182.9		72745.	1.000	36372.	11607.	54348.	801.4
32	39	43959.g	13286.	167.0	25574.	72510.	1.000	36255.	11735.	54348.	793.6
8	32	43282.		168.7		72150.	1.000	36075.	11936.	54348.	801.4
23	32	43549.g	13774.	165.6	24676.	72100.	1.000	36050.	11964.	54348.	804.7
6	32	43282.		168.4		72085.	1.000	36042.	11972.	54348.	801.4
14	32	43282.		168.3		72076.	1.000	36038.	11978.	54348.	801.4
10	32	43282.		168.2		72048.	1.000	36024.	11993.	54348.	801.4
32	41	43282.		167.0		71833.	1.000	35917.	12116.	54348.	801.4
32	40	43158.		167.0		71710.	1.000	35855.	12187.	54348.	801.4
7	26	25507.		249.5		71704.	1.000	35852.	12190.	53580.	798.3
26	45	25383.		251.2		71580.	1.000	35790.	12262.	53580.	814.2
4	40	42346.		169.9		71301.	1.000	35651.	12426.	54348.	801.4
4	39	42033.		169.9		70988.	1.000	35494.	12614.	54348.	793.6
26	35	24485.		216.8		70682.	1.000	35341.	12801.	53580.	798.3
4	8	41357.		171.6		70629.	1.000	35314.	12834.	54348.	801.4
4	6	41357.		171.2		70563.	1.000	35282.	12874.	54348.	801.4
4	14	41357.		171.2		70554.	1.000	35277.	12880.	54348.	801.4
4	10	41357.		171.0		70526.	1.000	35263.	12897.	54348.	801.4
4	41	41357.		169.9		70312.	1.000	35156.	13032.	54348.	801.4

Notes b,d,e,k: Fails
g: Weld ISI
h,i: Rupture Location
L: Information

CALCULATION NUMBER 2 CODE SECTION III CLASS 1 ASME-1998 KRE 2007/07/11 11:35:07 [1249]
Vermont Yankee Feedwater PipingSI Fatigue Analysis

FATIGUE ANALYSIS AT POINT 155, LR ELBOW 155 TO 160

****
INDIVIDUAL STRESS RANGE CHECK
****

DELTA T1 IN DEGREES F
STRESSES IN PSI

LOAD SET PAIR		SN EQN.10	SE EQN.12	DELTA T1 RANGE	EQN.13	SP EQN.11	KE	SALT EQN.14	ALLOW CYCLES	3*SM	ALLOWABLE FOR DELTA T1 RANGE
22	32	41561.		166.5		70111.	1.000	35056.	13159.	54348.	766.8
17	26	23913.		216.8		70110.	1.000	35055.	13160.	53580.	798.3
9	26	23771.		250.1		69968.	1.000	34984.	13251.	53580.	798.3
32	33	40406.		182.1		69867.	1.000	34934.	13316.	54348.	819.2
13	26	22903.		254.6		69719.	1.000	34860.	13413.	53580.	822.9
32	42	40739.		196.2		69515.	1.000	34757.	13548.	54348.	821.2
11	26	22903.		249.9		69100.	1.000	34550.	13826.	53580.	798.3
15	26	22903.		225.6		69100.	1.000	34550.	13826.	53580.	798.3
26	44	22472.		251.2		68669.	1.000	34334.	14124.	53580.	814.2
26	29	29511.		27.4		68364.	1.000	34182.	14340.	53580.	759.3
22	27	58697.b	7598.	5.9	36840.	58896.	1.160	34161.	14370.	54348.	792.1
21	26	21870.		251.2		68067.	1.000	34034.	14554.	53580.	763.1
4	42	38815.		199.0		67994.	1.000	33997.	14607.	54348.	821.2
29	32	29051.		56.8		67904.	1.000	33952.	14674.	53580.	763.1
24	28	58057.b	12029.	31.8	34782.	58080.	1.167	33893.	14760.	53580.	810.3
7	32	38539.		165.3		67091.	1.000	33545.	15288.	54348.	801.4
32	45	38428.		167.0		66979.	1.000	33489.	15375.	54348.	817.3
18	29	28066.		220.6		66919.	1.000	33459.	15422.	53580.	821.0
4	29	27637.		53.9		66490.	1.000	33245.	15763.	53580.	763.1
12	29	27212.		215.9		66064.	1.000	33032.	16111.	53580.	822.9
4	7	36614.		168.2		65569.	1.000	32785.	16530.	54348.	801.4
17	32	36945.		132.6		65496.	1.000	32748.	16592.	54348.	801.4
4	45	36498.		169.9		65453.	1.000	32726.	16630.	54348.	817.3
9	32	36804.		165.9		65355.	1.000	32677.	16715.	54348.	801.4
13	32	35935.		170.4		65106.	1.000	32553.	16934.	54348.	826.0
22	30	57644.b	7142.	2.9	36243.	57742.	1.121	32373.	17257.	54348.	792.1

Notes b,d,e,k: Fails
g: Weld ISI
h,i: Rupture Location
L: Information

CALCULATION NUMBER 2 CODE SECTION III CLASS 1 ASME-1998 KRE 2007/07/11 11:35:07 [1250]
Vermont Yankee Feedwater PipingSI Fatigue Analysis

FATIGUE ANALYSIS AT POINT 155, LR ELBOW 155 TO 160

****
INDIVIDUAL STRESS RANGE CHECK
****

DELTA T1 IN DEGREES F
STRESSES IN PSI

LOAD SET PAIR		SN EQN.10	SE EQN.12	DELTA T1 RANGE	EQN.13	SP EQN.11	KE	SALT EQN.14	ALLOW CYCLES	3*SM	ALLOWABLE FOR DELTA T1 RANGE
4	35	35592.		135.4		64547.	1.000	32273.	17438.	54348.	801.4
11	32	35935.		165.7		64487.	1.000	32243.	17493.	54348.	801.4
15	32	35935.		141.4		64487.	1.000	32243.	17493.	54348.	801.4
32	35	35530.		132.6		64082.	1.000	32041.	17873.	54348.	801.4
32	44	35518.		167.0		64070.	1.000	32035.	17884.	54348.	817.3
4	17	35020.		135.4		63975.	1.000	31987.	17974.	54348.	801.4
4	9	34878.		168.7		63833.	1.000	31917.	18111.	54348.	801.4
24	31	57340.b	12259.	27.6	34309.	57370.	1.110	31844.	18252.	54348.	813.4
26	32	31565.		84.2		63602.	1.000	31801.	18336.	53580.	763.1
4	13	34010.		173.2		63584.	1.000	31792.	18353.	54348.	826.0
21	32	34901.		167.0		63452.	1.000	31726.	18484.	54348.	766.8
4	11	34010.		168.6		62965.	1.000	31483.	18975.	54348.	801.4
4	15	34010.		144.2		62965.	1.000	31483.	18975.	54348.	801.4
4	44	33589.		169.9		62544.	1.000	31272.	19413.	54348.	817.3
4	21	32977.		169.9		61932.	1.000	30966.	20067.	54348.	766.8
18	26	14433.		248.0		60630.	1.000	30315.	21420.	53580.	821.0
23	28	55715.b	7157.	32.7	35896.	55816.	1.080	30132.	21821.	53580.	801.6
4	26	28162.		81.3		60199.	1.000	30100.	21893.	53580.	763.1
12	26	13576.		243.3		59773.	1.000	29886.	22376.	53580.	822.9
24	43	55610.b	11521.	24.0	33315.	55927.	1.046	29262.	23875.	54348.	813.4
24	34	55598.b	11521.	1.0	33309.	55607.	1.046	29083.	24329.	54348.	813.4
3	24	55590.b	11521.	1.0	33305.	55595.	1.046	29068.	24367.	54348.	813.4
12	32	28939.		159.1		57491.	1.000	28745.	25217.	54348.	826.0
4	32	28514.		2.8		57469.	1.000	28735.	25246.	54348.	766.8
18	32	28086.		163.9		56638.	1.000	28319.	26401.	54348.	824.1
23	31	54998.b	7386.	28.5	35423.	55107.	1.024	28212.	26708.	54348.	804.7

Notes b,d,e,k: Fails
g: Weld ISI
h,i: Rupture Location
L: Information

CALCULATION NUMBER 2 CODE SECTION III CLASS 1 ASME-1998 KRE 2007/07/11 11:35:07 [1251]
Vermont Yankee Feedwater PipingSI Fatigue Analysis

FATIGUE ANALYSIS AT POINT 155, LR ELBOW 155 TO 160

****
INDIVIDUAL STRESS RANGE CHECK
****

DELTA T1 IN DEGREES F
STRESSES IN PSI

LOAD SET PAIR		SN EQN.10	SE EQN.12	DELTA T1 RANGE	EQN.13	SP EQN.11	KE	SALT EQN.14	ALLOW CYCLES	3*SM	ALLOWABLE FOR DELTA T1 RANGE
4	18	25540.		166.7		54495.	1.000	27247.	29720.	54348.	824.1
4	12	25536.		161.9		54491.	1.000	27245.	29726.	54348.	826.0
23	43	53267.g	6649.	25.0	34429.	53664.	1.000	26832.	31155.	54348.	804.7
23	34	53256.g	6649.	1.9	34423.	53344.	1.000	26672.	31732.	54348.	804.7
3	23	53247.g	6649.	1.9	34419.	53332.	1.000	26666.	31754.	54348.	804.7
22	42	52114.g	9899.	29.7	31901.	52341.	1.000	26170.	33637.	54348.	821.2
24	27	52078.g	13808.	5.8	30903.	52277.	1.000	26138.	33763.	58680.	833.3
5	22	36363.		79.1		51414.	1.000	25707.	35533.	54348.	827.0
24	30	51025.g	13352.	2.8	30306.	51123.	1.000	25561.	36158.	58680.	833.3
20	22	50097.g	363.	1.1	35661.	50120.	1.000	25060.	38425.	54348.	766.8
23	27	49736.g	8936.	6.7	32017.	50014.	1.000	25007.	38676.	58680.	825.8
22	25	49174.g	5006.	42.7	33593.	49190.	1.000	24595.	40698.	53580.	763.1
23	30	48683.g	8480.	3.8	31420.	48860.	1.000	24430.	41549.	58680.	825.8
28	36	46729.g	12029.	34.5	29118.	47343.	1.000	23672.	45771.	53580.	821.0
2	28	46729.g	12029.	31.3	29118.	46750.	1.000	23375.	47577.	53580.	849.3
28	38	46729.g	12029.	31.3	29118.	46750.	1.000	23375.	47577.	53580.	849.3
31	36	46012.g	12259.	30.3	28644.	46633.	1.000	23317.	47944.	54348.	824.1
22	33	45280.g	6649.	15.6	28778.	46192.	1.000	23096.	49364.	54348.	819.2
2	31	46012.g	12259.	27.2	28644.	46040.	1.000	23020.	49865.	54348.	851.7
31	38	46012.g	12259.	27.2	28644.	46040.	1.000	23020.	49865.	54348.	851.7
24	42	45494.		29.6		45720.	1.000	22860.	51538.	60000.	856.2
12	22	45390.g	13603.	7.4	26687.	45392.	1.000	22696.	53409.	54348.	826.0
36	43	44282.g	11521.	26.8	27651.	45190.	1.000	22595.	54602.	54348.	824.1
34	36	44270.g	11521.	3.7	27645.	44871.	1.000	22435.	56559.	54348.	824.1
3	36	44262.g	11521.	3.7	27641.	44859.	1.000	22429.	56635.	54348.	824.1
5	24	29744.		79.0		44794.	1.000	22397.	57040.	60000.	860.7

Notes b,d,e,k: Fails
g: Weld ISI
h,i: Rupture Location
L: Information

CALCULATION NUMBER 2 CODE SECTION III CLASS 1 ASME-1998 KRE 2007/07/11 11:35:07 [1252]
Vermont Yankee Feedwater PipingSI Fatigue Analysis

FATIGUE ANALYSIS AT POINT 155, LR ELBOW 155 TO 160

****
INDIVIDUAL STRESS RANGE CHECK
****

DELTA T1 IN DEGREES F
STRESSES IN PSI

LOAD SET PAIR		SN EQN.10	SE EQN.12	DELTA T1 RANGE	EQN.13	SP EQN.11	KE	SALT EQN.14	ALLOW CYCLES	3*SM	ALLOWABLE FOR DELTA T1 RANGE
19	22	44599.g	1861.	40.2	32163.	44619.	1.000	22310.	58159.	54348.	792.1
2	43	44282.g	11521.	23.6	27651.	44597.	1.000	22299.	58299.	54348.	851.7
38	43	44282.g	11521.	23.6	27651.	44597.	1.000	22299.	58299.	54348.	851.7
18	22	44533.g	12746.	2.6	26687.	44536.	1.000	22268.	58701.	54348.	824.1
2	34	44270.g	11521.	0.5	27645.	44278.	1.000	22139.	60417.	54348.	851.7
34	38	44270.g	11521.	0.5	27645.	44278.	1.000	22139.	60417.	54348.	851.7
2	3	44262.g	11521.	0.5	27641.	44266.	1.000	22133.	60499.	54348.	851.7
3	38	44262.g	11521.	0.5	27641.	44266.	1.000	22133.	60499.	54348.	851.7
23	42	43153.		30.5		43458.	1.000	21729.	66286.	60000.	849.3
20	24	43368.		1.0		43390.	1.000	21695.	66803.	54348.	813.4
5	23	27401.		79.9		42530.	1.000	21265.	73771.	60000.	853.9
22	37	42394.		0.6		42396.	1.000	21198.	74933.	54348.	788.7
27	36	40750.		8.5		41540.	1.000	20770.	82915.	58680.	841.7
28	37	41509.		31.3		41529.	1.000	20765.	83019.	53580.	784.2
37	43	41048.		23.6		41364.	1.000	20682.	84683.	54348.	788.7
20	23	41038.		2.0		41138.	1.000	20569.	87007.	54348.	804.7
34	37	41036.		0.5		41044.	1.000	20522.	88005.	54348.	788.7
3	37	41028.		0.5		41032.	1.000	20516.	88134.	54348.	788.7
2	27	40750.		5.3		40947.	1.000	20473.	89044.	58680.	868.4
27	38	40750.		5.3		40947.	1.000	20473.	89044.	58680.	868.4
31	37	40792.		27.2		40820.	1.000	20410.	90429.	54348.	788.7
30	36	39697.		5.6		40386.	1.000	20193.	95348.	58680.	841.7
2	30	39697.		2.4		39793.	1.000	19897.	101886.	58680.	868.4
30	38	39697.		2.4		39793.	1.000	19897.	101886.	58680.	868.4
24	33	38661.		15.5		39572.	1.000	19786.	103950.	60000.	854.6
12	24	38769.		7.5		38770.	1.000	19385.	111907.	60000.	860.0

Notes b,d,e,k: Fails
g: Weld ISI
h,i: Rupture Location
L: Information

CALCULATION NUMBER 2 CODE SECTION III CLASS 1 ASME-1998 KRE 2007/07/11 11:35:07 [1253]
Vermont Yankee Feedwater PipingSI Fatigue Analysis

FATIGUE ANALYSIS AT POINT 155, LR ELBOW 155 TO 160

****
INDIVIDUAL STRESS RANGE CHECK
****

DELTA T1 IN DEGREES F
STRESSES IN PSI

LOAD SET PAIR		SN EQN.10	SE EQN.12	DELTA T1 RANGE	EQN.13	SP EQN.11	KE	SALT EQN.14	ALLOW CYCLES	3*SM	ALLOWABLE FOR DELTA T1 RANGE
1	22	38714.		0.8		38766.	1.000	19383.	111954.	54348.	851.7
1	28	38385.		31.1		38406.	1.000	19203.	115784.	53580.	849.3
19	24	37973.		40.1		37992.	1.000	18996.	120392.	58680.	833.3
18	24	37912.		2.7		37914.	1.000	18957.	121286.	60000.	858.4
1	31	37668.		26.9		37696.	1.000	18848.	123834.	54348.	851.7
1	43	37368.		23.3		37683.	1.000	18842.	123981.	54348.	851.7
23	25	37549.		43.5		37644.	1.000	18822.	124447.	53580.	801.6
1	34	37356.		0.3		37364.	1.000	18682.	127846.	54348.	851.7
1	3	37348.		0.3		37352.	1.000	18676.	127996.	54348.	851.7
25	28	37321.		10.8		37342.	1.000	18671.	128119.	53580.	759.3
16	22	34887.		13.6		37322.	1.000	18661.	128359.	54348.	801.4
23	33	36319.		16.4		37309.	1.000	18655.	128517.	60000.	847.8
25	43	36861.		18.6		37176.	1.000	18588.	130181.	53580.	763.1
21	22	37098.		0.6		37100.	1.000	18550.	131149.	54348.	766.8
28	40	36950.		31.3		36971.	1.000	18485.	132812.	53580.	798.3
25	34	36849.		41.6		36857.	1.000	18428.	134297.	53580.	763.1
3	25	36841.		41.6		36845.	1.000	18422.	134456.	53580.	763.1
13	22	36074.		3.9		36696.	1.000	18348.	136430.	54348.	826.0
28	35	30200.		65.8		36655.	1.000	18328.	136979.	53580.	798.3
25	31	36604.		15.0		36632.	1.000	18316.	137291.	53580.	763.1
22	44	36626.		0.6		36628.	1.000	18314.	137342.	54348.	817.3
12	23	36429.		6.5		36509.	1.000	18255.	138959.	60000.	853.1
12	28	34857.		39.3		36357.	1.000	18179.	141064.	53580.	822.9
31	40	36233.		27.2		36261.	1.000	18130.	142421.	54348.	801.4
17	28	29626.		65.8		36082.	1.000	18041.	144986.	53580.	798.3
11	22	36074.		0.7		36077.	1.000	18038.	145056.	54348.	801.4

Notes b,d,e,k: Fails
g: Weld ISI
h,i: Rupture Location
L: Information

CALCULATION NUMBER 2 CODE SECTION III CLASS 1 ASME-1998 KRE 2007/07/11 11:35:07 [1254]
Vermont Yankee Feedwater PipingSI Fatigue Analysis

FATIGUE ANALYSIS AT POINT 155, LR ELBOW 155 TO 160

****
INDIVIDUAL STRESS RANGE CHECK
****

DELTA T1 IN DEGREES F
STRESSES IN PSI

LOAD SET PAIR		SN EQN.10	SE EQN.12	DELTA T1 RANGE	EQN.13	SP EQN.11	KE	SALT EQN.14	ALLOW CYCLES	3*SM	ALLOWABLE FOR DELTA T1 RANGE
15	22	36074.		25.1		36077.	1.000	18038.	145056.	54348.	801.4
28	41	35960.		31.3		35981.	1.000	17991.	146447.	53580.	798.3
6	28	35960.		30.0		35981.	1.000	17991.	146449.	53580.	798.3
8	28	35960.		29.6		35981.	1.000	17991.	146449.	53580.	798.3
10	28	35960.		30.2		35981.	1.000	17991.	146449.	53580.	798.3
14	28	35960.		30.0		35981.	1.000	17991.	146449.	53580.	798.3
16	28	35960.		18.3		35981.	1.000	17991.	146449.	53580.	798.3
31	35	29482.		61.6		35944.	1.000	17972.	146991.	54348.	801.4
30	37	35668.		2.4		35764.	1.000	17882.	149673.	58680.	819.8
19	23	35632.		41.1		35730.	1.000	17865.	150191.	58680.	825.8
27	37	35529.		5.3		35726.	1.000	17863.	150253.	58680.	819.8
22	39	35660.		0.6		35662.	1.000	17831.	151224.	54348.	793.6
18	23	35572.		1.8		35653.	1.000	17826.	151370.	60000.	851.6
17	31	28909.		61.6		35371.	1.000	17686.	155755.	54348.	801.4
31	41	35243.		27.2		35272.	1.000	17636.	157347.	54348.	801.4
6	31	35243.		25.8		35271.	1.000	17636.	157350.	54348.	801.4
8	31	35243.		25.5		35271.	1.000	17636.	157350.	54348.	801.4
10	31	35243.		26.0		35271.	1.000	17636.	157350.	54348.	801.4
14	31	35243.		25.9		35271.	1.000	17636.	157350.	54348.	801.4
16	31	35243.		14.1		35271.	1.000	17636.	157350.	54348.	801.4
12	43	33425.		31.5		35220.	1.000	17610.	158176.	54348.	826.0
9	22	35211.		0.6		35213.	1.000	17606.	158293.	54348.	801.4
8	22	34887.		2.3		35206.	1.000	17603.	158403.	54348.	801.4
12	31	33681.		35.1		35189.	1.000	17595.	158680.	54348.	826.0
6	22	34887.		1.9		35141.	1.000	17570.	159466.	54348.	801.4
14	22	34887.		1.9		35132.	1.000	17566.	159612.	54348.	801.4

Notes b,d,e,k: Fails
g: Weld ISI
h,i: Rupture Location
L: Information

CALCULATION NUMBER 2 CODE SECTION III CLASS 1 ASME-1998 KRE 2007/07/11 11:35:07 [1255]
Vermont Yankee Feedwater PipingSI Fatigue Analysis

FATIGUE ANALYSIS AT POINT 155, LR ELBOW 155 TO 160

****
INDIVIDUAL STRESS RANGE CHECK
****

DELTA T1 IN DEGREES F
STRESSES IN PSI

LOAD SET PAIR		SN EQN.10	SE EQN.12	DELTA T1 RANGE	EQN.13	SP EQN.11	KE	SALT EQN.14	ALLOW CYCLES	3*SM	ALLOWABLE FOR DELTA T1 RANGE
10	22	34887.		1.7		35104.	1.000	17552.	160075.	54348.	801.4
17	22	35068.		33.9		35070.	1.000	17535.	160627.	54348.	801.4
36	42	34166.		32.3		34983.	1.000	17492.	162071.	60000.	864.5
12	34	33413.		8.5		34900.	1.000	17450.	163460.	54348.	826.0
22	41	34887.		0.6		34889.	1.000	17445.	163651.	54348.	801.4
3	12	33405.		8.5		34888.	1.000	17444.	163664.	54348.	826.0
40	43	34503.		23.6		34819.	1.000	17409.	164848.	54348.	801.4
22	40	34759.		0.6		34761.	1.000	17381.	165831.	54348.	801.4
28	39	34652.		31.3		34673.	1.000	17337.	167354.	53580.	787.5
18	28	34000.		34.5		34614.	1.000	17307.	168392.	53580.	821.0
39	43	34193.		23.6		34509.	1.000	17254.	170242.	54348.	793.6
35	43	27756.		58.0		34506.	1.000	17253.	170292.	54348.	801.4
34	40	34491.		0.5		34499.	1.000	17249.	170419.	54348.	801.4
22	35	34495.		33.9		34498.	1.000	17249.	170442.	54348.	801.4
3	40	34483.		0.5		34487.	1.000	17243.	170635.	54348.	801.4
2	42	34166.		29.2		34390.	1.000	17195.	172368.	60000.	893.7
38	42	34166.		29.2		34390.	1.000	17195.	172368.	60000.	893.7
34	39	34181.		0.5		34189.	1.000	17095.	176049.	54348.	793.6
34	35	27745.		35.0		34186.	1.000	17093.	176101.	54348.	801.4
3	39	34173.		0.5		34177.	1.000	17089.	176274.	54348.	793.6
3	35	27736.		35.0		34174.	1.000	17087.	176326.	54348.	801.4
5	36	18416.		81.7		34057.	1.000	17029.	178513.	60000.	869.1
22	45	33979.		0.6		33981.	1.000	16990.	179967.	54348.	817.3
31	39	33935.		27.2		33963.	1.000	16982.	180307.	54348.	793.6
17	43	27181.		58.0		33931.	1.000	16966.	180916.	54348.	801.4
41	43	33514.		23.6		33829.	1.000	16915.	182887.	54348.	801.4

Notes b,d,e,k: Fails
g: Weld ISI
h,i: Rupture Location
L: Information

CALCULATION NUMBER 2 CODE SECTION III CLASS 1 ASME-1998 KRE 2007/07/11 11:35:07 [1256]
Vermont Yankee Feedwater PipingSI Fatigue Analysis

FATIGUE ANALYSIS AT POINT 155, LR ELBOW 155 TO 160

****
INDIVIDUAL STRESS RANGE CHECK
****

DELTA T1 IN DEGREES F
STRESSES IN PSI

LOAD SET PAIR		SN EQN.10	SE EQN.12	DELTA T1 RANGE	EQN.13	SP EQN.11	KE	SALT EQN.14	ALLOW CYCLES	3*SM	ALLOWABLE FOR DELTA T1 RANGE
6	43	33514.		22.2		33829.	1.000	16915.	182890.	54348.	801.4
8	43	33514.		21.9		33829.	1.000	16915.	182890.	54348.	801.4
10	43	33514.		22.4		33829.	1.000	16915.	182890.	54348.	801.4
14	43	33514.		22.3		33829.	1.000	16915.	182890.	54348.	801.4
16	43	33514.		10.5		33829.	1.000	16915.	182890.	54348.	801.4
17	34	27170.		35.0		33612.	1.000	16806.	187194.	54348.	801.4
3	17	27161.		35.0		33599.	1.000	16800.	187437.	54348.	801.4
34	41	33502.		0.5		33510.	1.000	16755.	189252.	54348.	801.4
6	34	33502.		0.8		33510.	1.000	16755.	189256.	54348.	801.4
8	34	33502.		1.2		33510.	1.000	16755.	189256.	54348.	801.4
10	34	33502.		0.6		33510.	1.000	16755.	189256.	54348.	801.4
14	34	33502.		0.8		33510.	1.000	16755.	189256.	54348.	801.4
16	34	33502.		12.5		33510.	1.000	16755.	189256.	54348.	801.4
7	22	33497.		1.1		33499.	1.000	16750.	189470.	54348.	801.4
3	41	33494.		0.5		33498.	1.000	16749.	189499.	54348.	801.4
3	6	33494.		0.8		33497.	1.000	16749.	189503.	54348.	801.4
3	8	33494.		1.2		33497.	1.000	16749.	189503.	54348.	801.4
3	10	33494.		0.6		33497.	1.000	16749.	189503.	54348.	801.4
3	14	33494.		0.8		33497.	1.000	16749.	189503.	54348.	801.4
3	16	33494.		12.5		33497.	1.000	16749.	189503.	54348.	801.4
18	43	32568.		26.8		33477.	1.000	16738.	189930.	54348.	824.1
2	5	18416.		78.5		33465.	1.000	16732.	190176.	60000.	905.8
5	38	18416.		78.5		33465.	1.000	16732.	190176.	60000.	905.8
18	31	32824.		30.3		33445.	1.000	16723.	190566.	54348.	824.1
15	28	28620.		57.0		33425.	1.000	16713.	190984.	53580.	798.3
18	34	32556.		3.7		33157.	1.000	16578.	196612.	54348.	824.1

Notes b,d,e,k: Fails
g: Weld ISI
h,i: Rupture Location
L: Information

CALCULATION NUMBER 2 CODE SECTION III CLASS 1 ASME-1998 KRE 2007/07/11 11:35:07 [1257]
Vermont Yankee Feedwater PipingSI Fatigue Analysis

FATIGUE ANALYSIS AT POINT 155, LR ELBOW 155 TO 160

****
INDIVIDUAL STRESS RANGE CHECK
****

DELTA T1 IN DEGREES F
STRESSES IN PSI

LOAD SET PAIR		SN EQN.10	SE EQN.12	DELTA T1 RANGE	EQN.13	SP EQN.11	KE	SALT EQN.14	ALLOW CYCLES	3*SM	ALLOWABLE FOR DELTA T1 RANGE
3	18	32548.		3.7		33145.	1.000	16572.	196871.	54348.	824.1
12	20	31318.		8.5		32817.	1.000	16409.	205131.	54348.	826.0
24	25	32755.		42.6		32771.	1.000	16386.	206456.	53580.	810.3
15	31	27902.		52.8		32714.	1.000	16357.	208114.	54348.	801.4
20	28	32655.		30.7		32675.	1.000	16338.	209234.	53580.	763.1
20	36	32040.		3.8		32653.	1.000	16327.	209888.	54348.	824.1
1	27	32405.		5.1		32602.	1.000	16301.	211385.	58680.	868.4
12	25	30973.		50.1		32467.	1.000	16233.	215442.	53580.	822.9
2	22	32275.		0.6		32278.	1.000	16139.	221264.	54348.	851.7
22	24	32275.		0.1		32278.	1.000	16139.	221264.	54348.	813.4
22	36	32275.		2.6		32278.	1.000	16139.	221264.	54348.	824.1
22	38	32275.		0.6		32278.	1.000	16139.	221264.	54348.	851.7
1	30	31988.		2.1		32084.	1.000	16042.	227424.	58680.	868.4
2	20	32040.		0.6		32060.	1.000	16030.	228208.	54348.	851.7
20	38	32040.		0.6		32060.	1.000	16030.	228208.	54348.	851.7
20	31	31938.		26.6		31966.	1.000	15983.	231302.	54348.	766.8
25	30	31481.		39.8		31577.	1.000	15789.	244590.	53580.	788.7
7	28	31219.		33.0		31557.	1.000	15779.	245285.	53580.	798.3
25	27	31341.		36.8		31538.	1.000	15769.	245964.	53580.	788.7
15	43	26180.		49.2		31279.	1.000	15640.	255410.	54348.	801.4
28	45	31220.		31.3		31241.	1.000	15620.	256841.	53580.	814.2
28	42	31152.		2.2		31173.	1.000	15587.	259394.	53580.	818.0
27	40	30970.		5.3		31167.	1.000	15583.	259631.	58680.	822.5
37	42	30932.		29.2		31156.	1.000	15578.	260037.	60000.	868.4
18	20	30461.		3.8		31074.	1.000	15537.	263206.	54348.	824.1
19	28	31051.		8.4		31071.	1.000	15536.	263297.	53580.	788.7

Notes b,d,e,k: Fails
g: Weld ISI
h,i: Rupture Location
L: Information

CALCULATION NUMBER 2 CODE SECTION III CLASS 1 ASME-1998 KRE 2007/07/11 11:35:07 [1258]
Vermont Yankee Feedwater PipingSI Fatigue Analysis

FATIGUE ANALYSIS AT POINT 155, LR ELBOW 155 TO 160

****
INDIVIDUAL STRESS RANGE CHECK
****

DELTA T1 IN DEGREES F
STRESSES IN PSI

LOAD SET PAIR		SN EQN.10	SE EQN.12	DELTA T1 RANGE	EQN.13	SP EQN.11	KE	SALT EQN.14	ALLOW CYCLES	3*SM	ALLOWABLE FOR DELTA T1 RANGE
15	34	26168.		26.2		30959.	1.000	15480.	267678.	54348.	801.4
3	15	26159.		26.2		30947.	1.000	15474.	268157.	54348.	801.4
27	35	24217.		39.8		30848.	1.000	15424.	272130.	58680.	822.5
7	31	30502.		28.9		30847.	1.000	15424.	272146.	54348.	801.4
23	37	30758.		1.4		30838.	1.000	15419.	272503.	60000.	838.6
18	25	30116.		45.3		30723.	1.000	15362.	277200.	53580.	821.0
28	33	30567.		16.3		30588.	1.000	15294.	282853.	53580.	816.1
20	43	30208.		23.0		30523.	1.000	15262.	285593.	54348.	766.8
31	45	30493.		27.2		30521.	1.000	15260.	285693.	54348.	817.3
21	24	30480.		0.5		30481.	1.000	15241.	287400.	54348.	813.4
19	31	30333.		12.5		30362.	1.000	15181.	292600.	54348.	792.1
33	37	29424.		15.0		30334.	1.000	15167.	293826.	60000.	860.6
17	27	23644.		39.8		30276.	1.000	15138.	296416.	58680.	822.5
5	37	15182.		78.5		30231.	1.000	15115.	298432.	60000.	892.0
20	34	30196.		0.0		30203.	1.000	15102.	299660.	54348.	766.8
3	20	30188.		0.1		30191.	1.000	15096.	300210.	54348.	766.8
27	41	29980.		5.3		30178.	1.000	15089.	300835.	58680.	822.5
6	27	29980.		4.0		30177.	1.000	15089.	300844.	58680.	822.5
8	27	29980.		3.6		30177.	1.000	15089.	300844.	58680.	822.5
10	27	29980.		4.2		30177.	1.000	15089.	300844.	58680.	822.5
14	27	29980.		4.0		30177.	1.000	15089.	300844.	58680.	822.5
16	27	29980.		7.7		30177.	1.000	15089.	300844.	58680.	822.5
13	24	29455.		3.8		30076.	1.000	15038.	305510.	60000.	860.0
42	43	29721.		5.6		30036.	1.000	15018.	307361.	54348.	821.2
30	40	29917.		2.4		30014.	1.000	15007.	308417.	58680.	822.5
31	42	29977.		2.0		30005.	1.000	15003.	308818.	54348.	821.2

Notes b,d,e,k: Fails
g: Weld ISI
h,i: Rupture Location
L: Information

CALCULATION NUMBER 2 CODE SECTION III CLASS 1 ASME-1998 KRE 2007/07/11 11:35:07 (1259)
Vermont Yankee Feedwater PipingSI Fatigue Analysis

FATIGUE ANALYSIS AT POINT 155, LR ELBOW 155 TO 160

****
INDIVIDUAL STRESS RANGE CHECK
****

DELTA T1 IN DEGREES F
STRESSES IN PSI

LOAD SET PAIR		SN EQN.10	SE EQN.12	DELTA T1 RANGE	EQN.13	SP EQN.11	KE	SALT EQN.14	ALLOW CYCLES	3*SM	ALLOWABLE FOR DELTA T1 RANGE
24	44	29966.		0.5		29968.	1.000	14984.	310575.	60000.	853.1
9	28	29486.		32.5		29721.	1.000	14861.	322516.	53580.	798.3
34	42	29709.		28.6		29716.	1.000	14858.	322754.	54348.	821.2
3	42	29701.		28.6		29704.	1.000	14852.	323355.	54348.	821.2
30	35	23164.		36.8		29695.	1.000	14847.	323829.	58680.	822.5
11	24	29455.		0.8		29457.	1.000	14728.	335946.	60000.	840.6
15	24	29455.		25.2		29457.	1.000	14728.	335946.	60000.	840.6
33	43	29133.		8.6		29449.	1.000	14724.	336356.	54348.	819.2
31	33	29392.		12.1		29420.	1.000	14710.	337846.	54348.	819.2
7	43	28774.		25.3		29406.	1.000	14703.	338595.	54348.	801.4
33	34	29122.		14.5		29129.	1.000	14565.	353547.	54348.	819.2
17	30	22592.		36.8		29122.	1.000	14561.	353924.	58680.	822.5
3	33	29113.		14.5		29117.	1.000	14559.	354220.	54348.	819.2
43	45	28797.		23.6		29112.	1.000	14556.	354495.	54348.	817.3
7	34	28762.		2.2		29086.	1.000	14543.	355926.	54348.	801.4
3	7	28753.		2.2		29074.	1.000	14537.	356604.	54348.	801.4
30	41	28928.		2.4		29024.	1.000	14512.	359424.	58680.	822.5
6	30	28928.		1.0		29024.	1.000	14512.	359435.	58680.	822.5
8	30	28928.		0.7		29024.	1.000	14512.	359435.	58680.	822.5
10	30	28928.		1.2		29024.	1.000	14512.	359435.	58680.	822.5
14	30	28928.		1.1		29024.	1.000	14512.	359435.	58680.	822.5
16	30	28928.		10.7		29024.	1.000	14512.	359435.	58680.	822.5
9	31	28768.		28.3		29011.	1.000	14505.	360192.	54348.	801.4
2	12	27441.		7.9		28921.	1.000	14460.	365335.	60000.	903.8
12	36	27441.		4.8		28921.	1.000	14460.	365335.	60000.	868.4
12	38	27441.		7.9		28921.	1.000	14460.	365335.	60000.	903.8

Notes b,d,e,k: Fails
g: Weld ISI
h,i: Rupture Location
L: Information

CALCULATION NUMBER 2 CODE SECTION III CLASS 1 ASME-1998 KRE 2007/07/11 11:35:07 [1260]
Vermont Yankee Feedwater PipingSI Fatigue Analysis

FATIGUE ANALYSIS AT POINT 155, LR ELBOW 155 TO 160

****
INDIVIDUAL STRESS RANGE CHECK
****

DELTA T1 IN DEGREES F
STRESSES IN PSI

LOAD SET PAIR		SN EQN.10	SE EQN.12	DELTA T1 RANGE	EQN.13	SP EQN.11	KE	SALT EQN.14	ALLOW CYCLES	3*SM	ALLOWABLE FOR DELTA T1 RANGE
19	43	28604.		16.1		28920.	1.000	14460.	365397.	54348.	792.1
30	39	28811.		2.4		28907.	1.000	14454.	366116.	58680.	822.5
11	28	28620.		32.6		28884.	1.000	14442.	367461.	53580.	798.3
27	39	28671.		5.3		28868.	1.000	14434.	368386.	58680.	822.5
20	35	22397.		35.0		28851.	1.000	14425.	369387.	54348.	801.4
33	36	27333.		18.2		28836.	1.000	14418.	370288.	60000.	863.0
20	37	28806.		0.6		28826.	1.000	14413.	370834.	54348.	788.7
34	45	28785.		0.5		28792.	1.000	14396.	372829.	54348.	817.3
3	45	28777.		0.5		28780.	1.000	14390.	373546.	54348.	817.3
27	43	28412.		18.2		28727.	1.000	14364.	376708.	54348.	792.1
13	28	28620.		28.0		28641.	1.000	14321.	381903.	53580.	822.9
19	34	28592.		39.1		28600.	1.000	14300.	384425.	54348.	792.1
9	24	28590.		0.7		28591.	1.000	14296.	384960.	60000.	840.6
3	19	28584.		39.2		28588.	1.000	14294.	385169.	54348.	792.1
25	35	22050.		76.6		28499.	1.000	14249.	390691.	53580.	798.3
28	44	28431.		31.3		28451.	1.000	14226.	393669.	53580.	814.2
17	24	28447.		34.0		28449.	1.000	14224.	393854.	60000.	840.6
27	34	28400.		4.8		28407.	1.000	14204.	396461.	54348.	792.1
3	27	28392.		4.8		28395.	1.000	14198.	397234.	54348.	792.1
5	28	28333.		47.2		28354.	1.000	14177.	399912.	53580.	823.9
2	33	27333.		15.0		28243.	1.000	14121.	407140.	60000.	889.7
33	38	27333.		15.0		28243.	1.000	14121.	407140.	60000.	889.7
21	23	28137.		1.4		28218.	1.000	14109.	408793.	54348.	804.7
11	31	27902.		28.5		28173.	1.000	14086.	411773.	54348.	801.4
28	30	27997.		28.9		28018.	1.000	14009.	422270.	53580.	788.7
13	31	27902.		23.8		27930.	1.000	13965.	428376.	54348.	826.0

Notes b,d,e,k: Fails
g: Weld ISI
h,i: Rupture Location
L: Information

CALCULATION NUMBER 2 CODE SECTION III CLASS 1 ASME-1998 KRE 2007/07/11 11:35:07 [1261]
Vermont Yankee Feedwater PipingSI Fatigue Analysis

FATIGUE ANALYSIS AT POINT 155, LR ELBOW 155 TO 160

****
INDIVIDUAL STRESS RANGE CHECK
****

DELTA T1 IN DEGREES F
STRESSES IN PSI

LOAD SET PAIR		SN EQN.10	SE EQN.12	DELTA T1 RANGE	EQN.13	SP EQN.11	KE	SALT EQN.14	ALLOW CYCLES	3*SM	ALLOWABLE FOR DELTA T1 RANGE
27	28	27856.		26.0		27877.	1.000	13939.	432081.	53580.	788.7
24	35	27875.		34.0		27877.	1.000	13938.	432125.	60000.	840.6
13	23	27112.		4.7		27812.	1.000	13906.	436721.	60000.	853.1
23	44	27648.		1.4		27729.	1.000	13864.	442732.	60000.	846.3
31	44	27673.		27.2		27701.	1.000	13851.	444748.	54348.	817.3
30	43	27360.		21.2		27675.	1.000	13838.	446650.	54348.	792.1
5	31	27614.		51.4		27642.	1.000	13821.	449150.	54348.	827.0
20	42	27614.		28.6		27634.	1.000	13817.	449757.	54348.	821.2
15	27	22635.		31.0		27616.	1.000	13808.	451074.	58680.	822.5
3	28	27578.		30.8		27599.	1.000	13799.	452344.	53580.	763.1
21	28	27578.		31.3		27599.	1.000	13799.	452344.	53580.	763.1
28	34	27578.		30.8		27599.	1.000	13799.	452344.	53580.	763.1
28	43	27578.		7.7		27599.	1.000	13799.	452344.	53580.	763.1
9	43	27041.		24.7		27572.	1.000	13786.	454392.	54348.	801.4
1	42	27252.		28.9		27476.	1.000	13738.	461639.	60000.	893.7
17	20	20982.		35.0		27436.	1.000	13718.	464734.	54348.	801.4
30	34	27348.		1.8		27356.	1.000	13678.	470989.	54348.	792.1
3	30	27340.		1.9		27344.	1.000	13672.	471943.	54348.	792.1
25	42	27269.		13.0		27283.	1.000	13642.	476732.	53580.	818.0
24	39	27275.		0.5		27276.	1.000	13638.	477271.	60000.	840.6
19	36	26645.		42.9		27255.	1.000	13628.	478974.	58680.	841.7
9	34	27030.		1.7		27252.	1.000	13626.	479249.	54348.	801.4
3	9	27021.		1.7		27240.	1.000	13620.	480224.	54348.	801.4
1	23	27078.		1.7		27208.	1.000	13604.	482793.	60000.	878.3
11	23	27112.		0.1		27193.	1.000	13597.	483997.	60000.	833.8
15	23	27112.		24.3		27193.	1.000	13597.	483997.	60000.	833.8

Notes b,d,e,k: Fails
g: Weld ISI
h,i: Rupture Location
L: Information

CALCULATION NUMBER 2 CODE SECTION III CLASS 1 ASME-1998 KRE 2007/07/11 11:35:07 [1262]
Vermont Yankee Feedwater PipingSI Fatigue Analysis

FATIGUE ANALYSIS AT POINT 155, LR ELBOW 155 TO 160

****
INDIVIDUAL STRESS RANGE CHECK
****

DELTA T1 IN DEGREES F
STRESSES IN PSI

LOAD SET PAIR		SN EQN.10	SE EQN.12	DELTA T1 RANGE	EQN.13	SP EQN.11	KE	SALT EQN.14	ALLOW CYCLES	3*SM	ALLOWABLE FOR DELTA T1 RANGE
18	36	26584.		0.0		27177.	1.000	13589.	485280.	60000.	866.8
2	18	26584.		3.2		27177.	1.000	13589.	485286.	60000.	899.7
18	38	26584.		3.2		27177.	1.000	13589.	485286.	60000.	899.7
31	43	26861.		3.6		27177.	1.000	13588.	485321.	54348.	766.8
24	45	27103.		0.5		27105.	1.000	13552.	491227.	60000.	853.1
22	23	27100.		0.8		27103.	1.000	13551.	491420.	54348.	804.7
17	25	20635.		76.6		27084.	1.000	13542.	492958.	53580.	798.3
20	33	27026.		14.4		27046.	1.000	13523.	496131.	54348.	819.2
12	27	25319.		13.3		26996.	1.000	13498.	500727.	58680.	843.2
3	31	26861.		26.6		26889.	1.000	13445.	518868.	54348.	766.8
21	31	26861.		27.2		26889.	1.000	13445.	518868.	54348.	766.8
31	34	26861.		26.6		26889.	1.000	13445.	518868.	54348.	766.8
20	27	26676.		4.8		26872.	1.000	13436.	521787.	54348.	792.1
7	24	26861.		1.2		26862.	1.000	13431.	523582.	60000.	840.6
30	31	26821.		24.8		26850.	1.000	13425.	525802.	54348.	792.1
15	20	21992.		26.2		26795.	1.000	13398.	535458.	54348.	801.4
12	30	25177.		10.3		26753.	1.000	13376.	543158.	58680.	843.2
11	43	26180.		24.9		26738.	1.000	13369.	545912.	54348.	801.4
27	31	26681.		21.8		26709.	1.000	13355.	551258.	54348.	792.1
25	33	26682.		27.1		26696.	1.000	13348.	553668.	53580.	816.1
2	19	26645.		39.7		26662.	1.000	13331.	560023.	58680.	868.4
19	38	26645.		39.7		26662.	1.000	13331.	560023.	58680.	868.4
1	33	25744.		14.8		26654.	1.000	13327.	561655.	60000.	889.7
1	5	11502.		78.2		26550.	1.000	13275.	581619.	60000.	905.8
13	43	26180.		20.3		26495.	1.000	13248.	592663.	54348.	826.0
43	44	26148.		23.6		26464.	1.000	13232.	599029.	54348.	817.3

Notes b,d,e,k: Fails
g: Weld ISI
h,i: Rupture Location
L: Information

CALCULATION NUMBER 2 CODE SECTION III CLASS 1 ASME-1998 KRE 2007/07/11 11:35:07 {1263}
Vermont Yankee Feedwater PipingSI Fatigue Analysis

FATIGUE ANALYSIS AT POINT 155, LR ELBOW 155 TO 160

****
INDIVIDUAL STRESS RANGE CHECK
****

DELTA T1 IN DEGREES F
STRESSES IN PSI

LOAD SET PAIR		SN EQN.10	SE EQN.12	DELTA T1 RANGE	EQN.13	SP EQN.11	KE	SALT EQN.14	ALLOW CYCLES	3*SM	ALLOWABLE FOR DELTA T1 RANGE
15	30	21583.		28.0		26463.	1.000	13232.	599165.	58680.	822.5
15	25	21645.		67.8		26444.	1.000	13222.	603148.	53580.	798.3
11	34	26168.		1.8		26418.	1.000	13209.	608383.	54348.	801.4
3	11	26159.		1.8		26406.	1.000	13203.	610902.	54348.	801.4
9	23	26247.		0.2		26328.	1.000	13164.	627410.	60000.	833.8
28	31	26306.		4.2		26327.	1.000	13163.	627701.	53580.	763.1
5	43	25895.		54.9		26211.	1.000	13106.	653074.	54348.	827.0
17	23	26105.		33.1		26185.	1.000	13093.	658887.	60000.	833.8
13	34	26168.		2.8		26175.	1.000	13088.	661145.	54348.	826.0
3	13	26159.		2.8		26163.	1.000	13082.	663907.	54348.	826.0
34	44	26137.		0.5		26144.	1.000	13072.	668334.	54348.	817.3
3	44	26128.		0.5		26132.	1.000	13066.	671130.	54348.	817.3
5	25	21935.		36.4		26033.	1.000	13017.	694402.	53580.	823.9
5	34	25884.		78.0		25891.	1.000	12946.	729405.	54348.	827.0
3	5	25875.		78.0		25879.	1.000	12940.	732486.	54348.	827.0
16	23	23283.		14.4		25797.	1.000	12899.	753773.	60000.	833.8
7	27	25238.		7.0		25752.	1.000	12876.	765629.	58680.	822.5
20	30	25623.		1.8		25719.	1.000	12859.	774672.	54348.	792.1
12	37	24207.		7.9		25687.	1.000	12843.	783405.	60000.	888.0
23	35	25532.		33.1		25613.	1.000	12807.	803942.	60000.	833.8
5	12	9038.		86.5		25567.	1.000	12783.	817215.	60000.	870.6
3	43	25130.		23.1		25446.	1.000	12723.	852773.	54348.	766.8
21	43	25130.		23.6		25446.	1.000	12723.	852773.	54348.	766.8
34	43	25130.		23.0		25446.	1.000	12723.	852773.	54348.	766.8
27	45	25182.		5.3		25379.	1.000	12690.	873244.	58680.	836.3
19	27	25071.		34.3		25268.	1.000	12634.	908503.	58680.	813.2

Notes b,d,e,k: Fails
g: Weld ISI
h,i: Rupture Location
L: Information

CALCULATION NUMBER 2 CODE SECTION III CLASS 1 ASME-1998 KRE 2007/07/11 11:35:07 [1264]
Vermont Yankee Feedwater PipingSI Fatigue Analysis

FATIGUE ANALYSIS AT POINT 155, LR ELBOW 155 TO 160

****
INDIVIDUAL STRESS RANGE CHECK
****

DELTA T1 IN DEGREES F
STRESSES IN PSI

LOAD SET PAIR		SN EQN.10	SE EQN.12	DELTA T1 RANGE	EQN.13	SP EQN.11	KE	SALT EQN.14	ALLOW CYCLES	3*SM	ALLOWABLE FOR DELTA T1 RANGE
18	27	24462.		8.5		25252.	1.000	12626.	913613.	58680.	841.7
23	39	25107.		1.4		25188.	1.000	12594.	934874.	60000.	833.8
1	20	25126.		0.3		25146.	1.000	12573.	948882.	54348.	851.7
3	34	25119.		0.0		25126.	1.000	12563.	955635.	54348.	766.8
21	34	25119.		0.5		25126.	1.000	12563.	955635.	54348.	766.8
3	21	25110.		0.5		25114.	1.000	12557.	959796.	54348.	766.8
18	30	24320.		5.5		25009.	1.000	12505.	996650.	58680.	841.7
23	45	24883.		1.4		24963.	1.000	12482.	>1000000.	60000.	846.3
20	25	24601.		41.6		24621.	1.000	12310.	>1000000.	53580.	763.1
40	42	24388.		29.2		24612.	1.000	12306.	>1000000.	60000.	846.7
16	24	22175.		13.5		24609.	1.000	12305.	>1000000.	60000.	840.6
7	23	24523.		0.3		24604.	1.000	12302.	>1000000.	60000.	833.8
7	30	24186.		4.1		24599.	1.000	12300.	>1000000.	58680.	822.5
39	42	24075.		29.2		24300.	1.000	12150.	>1000000.	60000.	846.7
35	42	17634.		63.6		24292.	1.000	12146.	>1000000.	60000.	846.7
30	45	24139.		2.4		24235.	1.000	12118.	>1000000.	58680.	836.3
12	19	22716.		47.6		24214.	1.000	12107.	>1000000.	58680.	843.2
19	30	24018.		37.3		24114.	1.000	12057.	>1000000.	58680.	813.2
18	37	23350.		3.2		23943.	1.000	11972.	>1000000.	60000.	880.1
9	27	23503.		6.5		23914.	1.000	11957.	>1000000.	58680.	822.5
5	18	8182.		81.7		23823.	1.000	11912.	>1000000.	60000.	869.1
17	42	17061.		63.6		23720.	1.000	11860.	>1000000.	60000.	846.7
8	23	23283.		3.1		23681.	1.000	11841.	>1000000.	60000.	833.8
5	40	8626.		78.5		23674.	1.000	11837.	>1000000.	60000.	851.3
41	42	23398.		29.2		23623.	1.000	11811.	>1000000.	60000.	846.7
6	42	23398.		27.8		23622.	1.000	11811.	>1000000.	60000.	846.7

Notes b,d,e,k: Fails
g: Weld ISI
h,i: Rupture Location
L: Information

CALCULATION NUMBER 2 CODE SECTION III CLASS 1 ASME-1998 KRE 2007/07/11 11:35:07 [1265]
Vermont Yankee Feedwater PipingSI Fatigue Analysis

FATIGUE ANALYSIS AT POINT 155, LR ELBOW 155 TO 160

****
INDIVIDUAL STRESS RANGE CHECK
****

DELTA T1 IN DEGREES F
STRESSES IN PSI

LOAD SET PAIR		SN EQN.10	SE EQN.12	DELTA T1 RANGE	EQN.13	SP EQN.11	KE	SALT EQN.14	ALLOW CYCLES	3*SM	ALLOWABLE FOR DELTA T1 RANGE
8	42	23398.		27.5		23622.	1.000	11811.	>1000000.	60000.	846.7
10	42	23398.		28.0		23622.	1.000	11811.	>1000000.	60000.	846.7
14	42	23398.		27.8		23622.	1.000	11811.	>1000000.	60000.	846.7
16	42	23398.		16.1		23622.	1.000	11811.	>1000000.	60000.	846.7
6	23	23283.		2.7		23616.	1.000	11808.	>1000000.	60000.	833.8
14	23	23283.		2.7		23607.	1.000	11803.	>1000000.	60000.	833.8
10	23	23283.		2.5		23579.	1.000	11789.	>1000000.	60000.	833.8
2	17	17119.		34.4		23553.	1.000	11777.	>1000000.	60000.	875.7
17	36	17119.		31.3		23553.	1.000	11777.	>1000000.	60000.	849.0
17	38	17119.		34.4		23553.	1.000	11777.	>1000000.	60000.	875.7
33	39	22569.		15.0		23479.	1.000	11740.	>1000000.	60000.	845.2
19	37	23411.		39.7		23428.	1.000	11714.	>1000000.	58680.	819.8
23	41	23283.		1.4		23364.	1.000	11682.	>1000000.	60000.	833.8
5	39	8313.		78.5		23362.	1.000	11681.	>1000000.	60000.	851.3
24	37	23355.		0.5		23356.	1.000	11678.	>1000000.	60000.	851.8
5	35	1871.		113.0		23354.	1.000	11677.	>1000000.	60000.	851.3
23	40	23146.		1.4		23227.	1.000	11613.	>1000000.	60000.	833.8
27	33	22925.		9.7		23122.	1.000	11561.	>1000000.	58680.	837.9
11	27	22635.		6.6		23075.	1.000	11537.	>1000000.	58680.	822.5
20	21	23025.		0.6		23045.	1.000	11522.	>1000000.	54348.	766.8
2	35	16547.		34.4		22981.	1.000	11491.	>1000000.	60000.	875.7
35	36	16547.		31.3		22981.	1.000	11491.	>1000000.	60000.	849.0
35	38	16547.		34.4		22981.	1.000	11491.	>1000000.	60000.	875.7
2	15	18127.		25.7		22911.	1.000	11456.	>1000000.	60000.	875.7
15	36	18127.		22.5		22911.	1.000	11456.	>1000000.	60000.	849.0
15	38	18127.		25.7		22911.	1.000	11456.	>1000000.	60000.	875.7

Notes b,d,e,k: Fails
g: Weld ISI
h,i: Rupture Location
L: Information

CALCULATION NUMBER 2 CODE SECTION III CLASS 1 ASME-1998 KRE 2007/07/11 11:35:07 [1266]
Vermont Yankee Feedwater PipingSI Fatigue Analysis

FATIGUE ANALYSIS AT POINT 155, LR ELBOW 155 TO 160

****
INDIVIDUAL STRESS RANGE CHECK
****

DELTA T1 IN DEGREES F
STRESSES IN PSI

LOAD SET PAIR		SN EQN.10	SE EQN.12	DELTA T1 RANGE	EQN.13	SP EQN.11	KE	SALT EQN.14	ALLOW CYCLES	3*SM	ALLOWABLE FOR DELTA T1 RANGE
17	33	15555.		49.5		22900.	1.000	11450.	>1000000.	60000.	845.2
13	27	22635.		2.0		22832.	1.000	11416.	>1000000.	58680.	843.2
33	41	21891.		15.0		22801.	1.000	11400.	>1000000.	60000.	845.2
6	33	21891.		13.7		22801.	1.000	11400.	>1000000.	60000.	845.2
8	33	21891.		13.3		22801.	1.000	11400.	>1000000.	60000.	845.2
10	33	21891.		13.9		22801.	1.000	11400.	>1000000.	60000.	845.2
14	33	21891.		13.7		22801.	1.000	11400.	>1000000.	60000.	845.2
16	33	21891.		2.0		22801.	1.000	11400.	>1000000.	60000.	845.2
5	17	1299.		113.0		22783.	1.000	11391.	>1000000.	60000.	851.3
9	30	22450.		3.5		22761.	1.000	11381.	>1000000.	58680.	822.5
21	25	22681.		42.2		22695.	1.000	11348.	>1000000.	53580.	763.1
5	41	7636.		78.5		22685.	1.000	11342.	>1000000.	60000.	851.3
5	6	7636.		77.2		22685.	1.000	11342.	>1000000.	60000.	851.3
5	8	7636.		76.8		22685.	1.000	11342.	>1000000.	60000.	851.3
5	10	7636.		77.4		22685.	1.000	11342.	>1000000.	60000.	851.3
5	14	7636.		77.2		22685.	1.000	11342.	>1000000.	60000.	851.3
5	16	7636.		65.5		22685.	1.000	11342.	>1000000.	60000.	851.3
33	40	21767.		15.0		22677.	1.000	11339.	>1000000.	60000.	845.2
20	44	22548.		0.6		22567.	1.000	11284.	>1000000.	54348.	817.3
5	27	22346.		73.2		22543.	1.000	11271.	>1000000.	58680.	844.0
8	24	22175.		2.2		22493.	1.000	11247.	>1000000.	60000.	840.6
27	44	22291.		5.3		22488.	1.000	11244.	>1000000.	58680.	836.3
18	19	21860.		42.9		22470.	1.000	11235.	>1000000.	58680.	841.7
6	24	22175.		1.8		22428.	1.000	11214.	>1000000.	60000.	840.6
14	24	22175.		1.8		22419.	1.000	11210.	>1000000.	60000.	840.6
10	24	22175.		1.6		22391.	1.000	11195.	>1000000.	60000.	840.6

Notes b,d,e,k: Fails
g: Weld ISI
h,i: Rupture Location
L: Information

++ DST/PIPESTRESS ++ Vermont Yankee Version 3.5.1+026 PC-EXE Release: Jun 2004

CALCULATION NUMBER 2 CODE SECTION III CLASS 1 ASME-1998 KRE 2007/07/11 11:35:07 [1267]
Vermont Yankee Feedwater PipingSI Fatigue Analysis

FATIGUE ANALYSIS AT POINT 155, LR ELBOW 155 TO 160

****
INDIVIDUAL STRESS RANGE CHECK
****

DELTA T1 IN DEGREES F
STRESSES IN PSI

LOAD SET PAIR		SN EQN.10	SE EQN.12	DELTA T1 RANGE	EQN.13	SP EQN.11	KE	SALT EQN.14	ALLOW CYCLES	3*SM	ALLOWABLE FOR DELTA T1 RANGE
5	20	22281.		77.9		22301.	1.000	11150.	>1000000.	54348.	827.0
20	40	22243.		0.6		22263.	1.000	11132.	>1000000.	54348.	801.4
11	20	21992.		1.9		22254.	1.000	11127.	>1000000.	54348.	801.4
24	41	22175.		0.5		22176.	1.000	11088.	>1000000.	60000.	840.6
25	44	22161.		42.2		22175.	1.000	11088.	>1000000.	53580.	814.2
1	12	20527.		8.2		22056.	1.000	11028.	>1000000.	60000.	903.8
25	36	21427.		45.3		22035.	1.000	11017.	>1000000.	53580.	821.0
13	20	21992.		2.8		22011.	1.000	11006.	>1000000.	54348.	826.0
30	33	21873.		12.6		21969.	1.000	10984.	>1000000.	58680.	837.9
20	39	21947.		0.6		21967.	1.000	10983.	>1000000.	54348.	793.6
11	30	21583.		3.7		21922.	1.000	10961.	>1000000.	58680.	822.5
11	25	21645.		43.5		21902.	1.000	10951.	>1000000.	53580.	798.3
27	42	21615.		23.8		21812.	1.000	10906.	>1000000.	58680.	839.4
21	27	21600.		5.3		21797.	1.000	10898.	>1000000.	54348.	792.1
35	37	15300.		34.4		21734.	1.000	10867.	>1000000.	60000.	833.7
13	30	21583.		1.0		21679.	1.000	10840.	>1000000.	58680.	843.2
13	25	21645.		38.8		21660.	1.000	10830.	>1000000.	53580.	822.9
30	42	21473.		26.8		21569.	1.000	10784.	>1000000.	58680.	839.4
12	33	19125.		23.0		21514.	1.000	10757.	>1000000.	60000.	864.5
33	35	14141.		49.5		21486.	1.000	10743.	>1000000.	60000.	845.2
2	25	21427.		42.2		21442.	1.000	10721.	>1000000.	53580.	849.3
25	38	21427.		42.2		21442.	1.000	10721.	>1000000.	53580.	849.3
5	30	21294.		76.1		21390.	1.000	10695.	>1000000.	58680.	844.0
9	20	21124.		1.7		21358.	1.000	10679.	>1000000.	54348.	801.4
30	44	21261.		2.4		21358.	1.000	10679.	>1000000.	58680.	836.3
20	41	21254.		0.6		21274.	1.000	10637.	>1000000.	54348.	801.4

Notes b,d,e,k: Fails
g: Weld ISI
h,i: Rupture Location
L: Information

CALCULATION NUMBER 2 CODE SECTION III CLASS 1 ASME-1998 KRE 2007/07/11 11:35:07 [1268]
Vermont Yankee Feedwater PipingSI Fatigue Analysis

FATIGUE ANALYSIS AT POINT 155, LR ELBOW 155 TO 160

****
INDIVIDUAL STRESS RANGE CHECK
****

DELTA T1 IN DEGREES F
STRESSES IN PSI

LOAD SET PAIR		SN EQN.10	SE EQN.12	DELTA T1 RANGE	EQN.13	SP EQN.11	KE	SALT EQN.14	ALLOW CYCLES	3*SM	ALLOWABLE FOR DELTA T1 RANGE
6	20	21254.		0.8		21274.	1.000	10637.	>1000000.	54348.	801.4
8	20	21254.		1.1		21274.	1.000	10637.	>1000000.	54348.	801.4
10	20	21254.		0.6		21274.	1.000	10637.	>1000000.	54348.	801.4
14	20	21254.		0.7		21274.	1.000	10637.	>1000000.	54348.	801.4
16	20	21254.		12.5		21274.	1.000	10637.	>1000000.	54348.	801.4
24	40	21195.		0.5		21197.	1.000	10598.	>1000000.	60000.	840.6
15	42	16052.		54.8		21060.	1.000	10530.	>1000000.	60000.	846.7
9	25	20777.		43.3		21006.	1.000	10503.	>1000000.	53580.	798.3
21	30	20547.		2.4		20643.	1.000	10321.	>1000000.	54348.	792.1
12	16	16674.		21.0		20587.	1.000	10294.	>1000000.	60000.	850.5
5	42	15762.		49.4		20384.	1.000	10192.	>1000000.	60000.	866.8
17	37	13885.		34.4		20319.	1.000	10160.	>1000000.	60000.	833.7
1	18	19670.		3.4		20313.	1.000	10156.	>1000000.	60000.	899.7
19	35	13795.		74.1		20247.	1.000	10124.	>1000000.	58680.	822.5
15	33	14547.		40.7		20241.	1.000	10121.	>1000000.	60000.	845.2
5	15	289.		104.2		20122.	1.000	10061.	>1000000.	60000.	851.3
20	45	19910.		0.6		19930.	1.000	9965.	>1000000.	54348.	817.3
5	33	14258.		63.5		19800.	1.000	9900.	>1000000.	60000.	865.3
18	33	18268.		18.2		19771.	1.000	9885.	>1000000.	60000.	863.0
1	19	19731.		39.4		19748.	1.000	9874.	>1000000.	58680.	868.4
21	36	19151.		3.2		19744.	1.000	9872.	>1000000.	54348.	824.1
7	20	19391.		2.3		19728.	1.000	9864.	>1000000.	54348.	801.4
1	24	19674.		0.7		19726.	1.000	9863.	>1000000.	60000.	885.1
15	37	14893.		25.7		19677.	1.000	9839.	>1000000.	60000.	833.7
19	20	19553.		39.1		19573.	1.000	9786.	>1000000.	54348.	792.1
27	30	19370.		3.0		19567.	1.000	9784.	>1000000.	58680.	813.2

Notes b,d,e,k: Fails
g: Weld ISI
h,i: Rupture Location
L: Information

CALCULATION NUMBER 2 CODE SECTION III CLASS 1 ASME-1998 KRE 2007/07/11 11:35:07 (1269)
Vermont Yankee Feedwater PipingSI Fatigue Analysis

FATIGUE ANALYSIS AT POINT 155, LR ELBOW 155 TO 160

****
INDIVIDUAL STRESS RANGE CHECK
****

DELTA T1 IN DEGREES F
STRESSES IN PSI

LOAD SET PAIR		SN EQN.10	SE EQN.12	DELTA T1 RANGE	EQN.13	SP EQN.11	KE	SALT EQN.14	ALLOW CYCLES	3*SM	ALLOWABLE FOR DELTA T1 RANGE
2	23	19336.		1.4		19416.	1.000	9708.	>1000000.	60000.	878.3
23	24	19336.		0.9		19416.	1.000	9708.	>1000000.	60000.	843.2
23	36	19336.		1.8		19416.	1.000	9708.	>1000000.	60000.	851.6
23	38	19336.		1.4		19416.	1.000	9708.	>1000000.	60000.	878.3
7	25	19041.		43.9		19373.	1.000	9686.	>1000000.	53580.	798.3
13	36	18127.		6.5		19339.	1.000	9670.	>1000000.	60000.	868.4
25	45	19292.		42.2		19306.	1.000	9653.	>1000000.	53580.	814.2
36	44	18638.		3.2		19231.	1.000	9616.	>1000000.	60000.	861.5
19	25	19209.		2.5		19227.	1.000	9613.	>1000000.	53580.	788.7
7	42	18656.		30.9		19197.	1.000	9599.	>1000000.	60000.	846.7
2	21	19151.		0.0		19151.	1.000	9576.	>1000000.	54348.	851.7
21	38	19151.		0.0		19151.	1.000	9576.	>1000000.	54348.	851.7
12	40	17663.		7.9		19143.	1.000	9572.	>1000000.	60000.	850.5
19	42	19013.		10.5		19030.	1.000	9515.	>1000000.	58680.	839.4
16	18	15818.		16.2		18843.	1.000	9422.	>1000000.	60000.	849.0
17	19	12380.		74.1		18832.	1.000	9416.	>1000000.	58680.	822.5
12	39	17350.		7.9		18830.	1.000	9415.	>1000000.	60000.	850.5
42	45	18564.		29.2		18789.	1.000	9394.	>1000000.	60000.	859.2
2	13	18127.		3.3		18746.	1.000	9373.	>1000000.	60000.	903.8
13	38	18127.		3.3		18746.	1.000	9373.	>1000000.	60000.	903.8
11	36	18127.		1.9		18720.	1.000	9360.	>1000000.	60000.	849.0
2	44	18638.		0.0		18638.	1.000	9319.	>1000000.	60000.	888.2
38	44	18638.		0.0		18638.	1.000	9319.	>1000000.	60000.	888.2
8	12	16674.		9.6		18471.	1.000	9235.	>1000000.	60000.	850.5
19	33	18426.		24.7		18443.	1.000	9222.	>1000000.	58680.	837.9
6	12	16674.		9.3		18406.	1.000	9203.	>1000000.	60000.	850.5

Notes b,d,e,k: Fails
g: Weld ISI
h,i: Rupture Location
L: Information

++ DST/PIPESTRESS ++ Vermont Yankee Version 3.5.1+026 PC-EXE Release: Jun 2004

CALCULATION NUMBER 2 CODE SECTION III CLASS 1 ASME-1998 KRE 2007/07/11 11:35:07 [1270]
Vermont Yankee Feedwater PipingSI Fatigue Analysis

FATIGUE ANALYSIS AT POINT 155, LR ELBOW 155 TO 160

****
INDIVIDUAL STRESS RANGE CHECK
****

DELTA T1 IN DEGREES F
STRESSES IN PSI

LOAD SET PAIR		SN EQN.10	SE EQN.12	DELTA T1 RANGE	EQN.13	SP EQN.11	KE	SALT EQN.14	ALLOW CYCLES	3*SM	ALLOWABLE FOR DELTA T1 RANGE
12	14	16674.		9.2		18397.	1.000	9198.	>1000000.	60000.	850.5
7	33	17149.		16.7		18376.	1.000	9188.	>1000000.	60000.	845.2
2	11	18127.		1.3		18370.	1.000	9185.	>1000000.	60000.	875.7
11	38	18127.		1.3		18370.	1.000	9185.	>1000000.	60000.	875.7
10	12	16674.		9.1		18368.	1.000	9184.	>1000000.	60000.	850.5
5	7	2894.		80.2		18259.	1.000	9130.	>1000000.	60000.	851.3
15	19	13390.		65.3		18192.	1.000	9096.	>1000000.	58680.	822.5
12	41	16674.		7.9		18154.	1.000	9077.	>1000000.	60000.	850.5
1	35	11620.		34.7		18104.	1.000	9052.	>1000000.	60000.	875.7
33	45	17108.		15.0		18018.	1.000	9009.	>1000000.	60000.	857.7
5	45	2922.		78.5		17971.	1.000	8985.	>1000000.	60000.	863.8
9	36	17262.		2.0		17855.	1.000	8927.	>1000000.	60000.	849.0
5	19	13679.		38.8		17777.	1.000	8888.	>1000000.	58680.	844.0
2	9	17262.		1.2		17476.	1.000	8738.	>1000000.	60000.	875.7
9	38	17262.		1.2		17476.	1.000	8738.	>1000000.	60000.	875.7
18	40	16807.		3.2		17400.	1.000	8700.	>1000000.	60000.	849.0
9	42	16920.		30.3		17359.	1.000	8679.	>1000000.	60000.	846.7
12	35	10909.		26.5		17343.	1.000	8672.	>1000000.	60000.	850.5
18	39	16494.		3.2		17087.	1.000	8543.	>1000000.	60000.	849.0
19	40	16851.		39.7		16868.	1.000	8434.	>1000000.	58680.	822.5
12	17	10337.		26.5		16772.	1.000	8386.	>1000000.	60000.	850.5
8	18	15818.		4.9		16727.	1.000	8364.	>1000000.	60000.	849.0
1	17	10205.		34.7		16689.	1.000	8344.	>1000000.	60000.	875.7
6	18	15818.		4.5		16662.	1.000	8331.	>1000000.	60000.	849.0
14	18	15818.		4.5		16653.	1.000	8327.	>1000000.	60000.	849.0
10	18	15818.		4.3		16625.	1.000	8312.	>1000000.	60000.	849.0

Notes b,d,e,k: Fails
g: Weld ISI
h,i: Rupture Location
L: Information

CALCULATION NUMBER 2 CODE SECTION III CLASS 1 ASME-1998 KRE 2007/07/11 11:35:07 [1271]
Vermont Yankee Feedwater PipingSI Fatigue Analysis

FATIGUE ANALYSIS AT POINT 155, LR ELBOW 155 TO 160

****
INDIVIDUAL STRESS RANGE CHECK
****

DELTA T1 IN DEGREES F
STRESSES IN PSI

LOAD SET PAIR		SN EQN.10	SE EQN.12	DELTA T1 RANGE	EQN.13	SP EQN.11	KE	SALT EQN.14	ALLOW CYCLES	3*SM	ALLOWABLE FOR DELTA T1 RANGE
16	35	7752.		47.5		16619.	1.000	8309.	>1000000.	60000.	831.2
25	39	16565.		42.2		16580.	1.000	8290.	>1000000.	53580.	787.5
33	42	16341.		14.1		16565.	1.000	8283.	>1000000.	60000.	860.7
19	39	16541.		39.7		16559.	1.000	8280.	>1000000.	58680.	822.5
36	39	15947.		3.2		16540.	1.000	8270.	>1000000.	60000.	849.0
9	33	15414.		16.2		16539.	1.000	8269.	>1000000.	60000.	845.2
11	42	16052.		30.5		16519.	1.000	8259.	>1000000.	60000.	846.7
18	35	10053.		31.3		16487.	1.000	8244.	>1000000.	60000.	849.0
5	9	1158.		79.7		16421.	1.000	8210.	>1000000.	60000.	851.3
18	41	15818.		3.2		16410.	1.000	8205.	>1000000.	60000.	849.0
36	45	15775.		3.2		16368.	1.000	8184.	>1000000.	60000.	861.5
13	42	16052.		25.8		16276.	1.000	8138.	>1000000.	60000.	866.1
7	36	15533.		1.5		16126.	1.000	8063.	>1000000.	60000.	849.0
1	15	11213.		25.9		16047.	1.000	8023.	>1000000.	60000.	875.7
5	44	964.		78.5		16013.	1.000	8007.	>1000000.	60000.	863.8
2	39	15947.		0.0		15947.	1.000	7974.	>1000000.	60000.	875.7
38	39	15947.		0.0		15947.	1.000	7974.	>1000000.	60000.	875.7
21	37	15918.		0.0		15918.	1.000	7959.	>1000000.	54348.	788.7
17	18	9481.		31.3		15915.	1.000	7958.	>1000000.	60000.	849.0
42	44	15657.		29.2		15881.	1.000	7940.	>1000000.	60000.	859.2
19	41	15861.		39.7		15879.	1.000	7940.	>1000000.	58680.	822.5
6	19	15861.		38.3		15879.	1.000	7939.	>1000000.	58680.	822.5
8	19	15861.		38.0		15879.	1.000	7939.	>1000000.	58680.	822.5
10	19	15861.		38.5		15879.	1.000	7939.	>1000000.	58680.	822.5
14	19	15861.		38.4		15879.	1.000	7939.	>1000000.	58680.	822.5
16	19	15861.		26.6		15879.	1.000	7939.	>1000000.	58680.	822.5

Notes b,d,e,k: Fails
g: Weld ISI
h,i: Rupture Location
L: Information

CALCULATION NUMBER 2 CODE SECTION III CLASS 1 ASME-1998 KRE 2007/07/11 11:35:07 [1272]
Vermont Yankee Feedwater PipingSI Fatigue Analysis

FATIGUE ANALYSIS AT POINT 155, LR ELBOW 155 TO 160

****
INDIVIDUAL STRESS RANGE CHECK
****

DELTA T1 IN DEGREES F
STRESSES IN PSI

LOAD SET PAIR		SN EQN.10	SE EQN.12	DELTA T1 RANGE	EQN.13	SP EQN.11	KE	SALT EQN.14	ALLOW CYCLES	3*SM	ALLOWABLE FOR DELTA T1 RANGE
2	7	15533.		1.7		15850.	1.000	7925.	>1000000.	60000.	875.7
7	38	15533.		1.7		15850.	1.000	7925.	>1000000.	60000.	875.7
12	42	14132.		37.1		15836.	1.000	7918.	>1000000.	60000.	866.1
5	21	765.		78.5		15814.	1.000	7907.	>1000000.	54348.	827.0
2	45	15775.		0.0		15775.	1.000	7888.	>1000000.	60000.	888.2
38	45	15775.		0.0		15775.	1.000	7888.	>1000000.	60000.	888.2
11	33	14547.		16.3		15700.	1.000	7850.	>1000000.	60000.	845.2
5	11	289.		79.8		15581.	1.000	7790.	>1000000.	60000.	851.3
13	37	14893.		3.3		15512.	1.000	7756.	>1000000.	60000.	888.0
13	33	14547.		11.7		15457.	1.000	7729.	>1000000.	60000.	864.5
37	44	15404.		0.0		15404.	1.000	7702.	>1000000.	60000.	857.6
25	37	15333.		42.2		15347.	1.000	7673.	>1000000.	53580.	784.2
5	13	289.		75.2		15338.	1.000	7669.	>1000000.	60000.	870.6
21	42	15018.		29.2		15242.	1.000	7621.	>1000000.	54348.	821.2
16	17	6337.		47.5		15204.	1.000	7602.	>1000000.	60000.	831.2
33	44	14277.		15.0		15187.	1.000	7594.	>1000000.	60000.	857.7
11	37	14893.		1.3		15136.	1.000	7568.	>1000000.	60000.	833.7
35	39	8429.		34.4		14863.	1.000	7431.	>1000000.	60000.	831.2
15	16	7347.		38.7		14564.	1.000	7282.	>1000000.	60000.	831.2
8	35	7752.		36.1		14503.	1.000	7251.	>1000000.	60000.	831.2
19	21	14425.		39.7		14443.	1.000	7221.	>1000000.	54348.	792.1
6	35	7752.		35.8		14438.	1.000	7219.	>1000000.	60000.	831.2
25	40	14423.		42.2		14437.	1.000	7218.	>1000000.	53580.	798.3
14	35	7752.		35.8		14429.	1.000	7214.	>1000000.	60000.	831.2
21	33	13510.		15.0		14420.	1.000	7210.	>1000000.	54348.	819.2
10	35	7752.		35.6		14400.	1.000	7200.	>1000000.	60000.	831.2

Notes b,d,e,k: Fails
g: Weld ISI
h,i: Rupture Location
L: Information

++ DST/PIPESTRESS ++ Vermont Yankee Version 3.5.1+026 PC-EXE Release: Jun 2004

CALCULATION NUMBER 2 CODE SECTION III CLASS 1 ASME-1998 KRE 2007/07/11 11:35:07 [1273]
Vermont Yankee Feedwater PipingSI Fatigue Analysis

FATIGUE ANALYSIS AT POINT 155, LR ELBOW 155 TO 160

****
INDIVIDUAL STRESS RANGE CHECK
****

DELTA T1 IN DEGREES F
STRESSES IN PSI

LOAD SET PAIR		SN EQN.10	SE EQN.12	DELTA T1 RANGE	EQN.13	SP EQN.11	KE	SALT EQN.14	ALLOW CYCLES	3*SM	ALLOWABLE FOR DELTA T1 RANGE
25	41	14299.		42.2		14314.	1.000	7157.	>1000000.	53580.	798.3
6	25	14299.		40.8		14314.	1.000	7157.	>1000000.	53580.	798.3
8	25	14299.		40.5		14314.	1.000	7157.	>1000000.	53580.	798.3
10	25	14299.		41.0		14314.	1.000	7157.	>1000000.	53580.	798.3
14	25	14299.		40.8		14314.	1.000	7157.	>1000000.	53580.	798.3
16	25	14299.		29.1		14314.	1.000	7157.	>1000000.	53580.	798.3
9	37	14028.		1.2		14242.	1.000	7121.	>1000000.	60000.	833.7
35	41	7752.		34.4		14186.	1.000	7093.	>1000000.	60000.	831.2
12	15	9327.		17.7		14111.	1.000	7056.	>1000000.	60000.	850.5
18	42	13275.		32.3		14092.	1.000	7046.	>1000000.	60000.	864.5
35	40	7628.		34.4		14063.	1.000	7031.	>1000000.	60000.	831.2
19	44	13999.		39.7		14017.	1.000	7008.	>1000000.	58680.	836.3
16	36	10847.		16.2		13873.	1.000	6936.	>1000000.	60000.	849.0
17	40	7326.		34.4		13761.	1.000	6880.	>1000000.	60000.	831.2
11	19	13390.		41.0		13651.	1.000	6825.	>1000000.	58680.	822.5
17	39	7014.		34.4		13448.	1.000	6724.	>1000000.	60000.	831.2
7	12	11932.		6.2		13411.	1.000	6706.	>1000000.	60000.	850.5
13	19	13390.		36.3		13408.	1.000	6704.	>1000000.	58680.	843.2
12	45	11813.		7.9		13293.	1.000	6647.	>1000000.	60000.	863.0
2	16	10847.		13.1		13280.	1.000	6640.	>1000000.	60000.	875.7
16	38	10847.		13.1		13280.	1.000	6640.	>1000000.	60000.	875.7
15	18	8471.		22.5		13255.	1.000	6627.	>1000000.	60000.	849.0
15	40	8336.		25.7		13120.	1.000	6560.	>1000000.	60000.	831.2
1	25	13083.		41.9		13097.	1.000	6549.	>1000000.	53580.	849.3
8	17	6337.		36.2		13088.	1.000	6544.	>1000000.	60000.	831.2
6	17	6337.		35.8		13023.	1.000	6511.	>1000000.	60000.	831.2

Notes b,d,e,k: Fails
g: Weld ISI
h,i: Rupture Location
L: Information

CALCULATION NUMBER 2 CODE SECTION III CLASS 1 ASME-1998 KRE 2007/07/11 11:35:07 [1274]
Vermont Yankee Feedwater PipingSI Fatigue Analysis

FATIGUE ANALYSIS AT POINT 155, LR ELBOW 155 TO 160

****
INDIVIDUAL STRESS RANGE CHECK
****

DELTA T1 IN DEGREES F
STRESSES IN PSI

LOAD SET PAIR		SN EQN.10	SE EQN.12	DELTA T1 RANGE	EQN.13	SP EQN.11	KE	SALT EQN.14	ALLOW CYCLES	3*SM	ALLOWABLE FOR DELTA T1 RANGE
14	17	6337.		35.8		13014.	1.000	6507.	>1000000.	60000.	831.2
10	17	6337.		35.6		12986.	1.000	6493.	>1000000.	60000.	831.2
15	39	8023.		25.7		12807.	1.000	6404.	>1000000.	60000.	831.2
17	41	6337.		34.4		12771.	1.000	6386.	>1000000.	60000.	831.2
9	19	12522.		40.8		12755.	1.000	6377.	>1000000.	58680.	822.5
36	37	12027.		3.2		12620.	1.000	6310.	>1000000.	60000.	880.1
7	37	12299.		1.7		12616.	1.000	6308.	>1000000.	60000.	833.7
37	45	12541.		0.0		12541.	1.000	6271.	>1000000.	60000.	857.6
8	15	7347.		27.4		12448.	1.000	6224.	>1000000.	60000.	831.2
6	15	7347.		27.0		12382.	1.000	6191.	>1000000.	60000.	831.2
14	15	7347.		27.0		12373.	1.000	6187.	>1000000.	60000.	831.2
10	15	7347.		26.8		12345.	1.000	6173.	>1000000.	60000.	831.2
1	21	12237.		0.3		12287.	1.000	6144.	>1000000.	54348.	851.7
15	41	7347.		25.7		12131.	1.000	6065.	>1000000.	60000.	831.2
19	45	12049.		39.7		12066.	1.000	6033.	>1000000.	58680.	836.3
2	37	12027.		0.0		12027.	1.000	6013.	>1000000.	60000.	970.1
37	38	12027.		0.0		12027.	1.000	6013.	>1000000.	60000.	970.1
1	13	11213.		3.1		11832.	1.000	5916.	>1000000.	60000.	903.8
1	44	11724.		0.3		11774.	1.000	5887.	>1000000.	60000.	888.2
8	36	10847.		4.9		11757.	1.000	5878.	>1000000.	60000.	849.0
6	36	10847.		4.5		11691.	1.000	5846.	>1000000.	60000.	849.0
14	36	10847.		4.5		11682.	1.000	5841.	>1000000.	60000.	849.0
9	12	10196.		6.8		11676.	1.000	5838.	>1000000.	60000.	850.5
7	18	11075.		1.5		11668.	1.000	5834.	>1000000.	60000.	849.0
10	36	10847.		4.3		11654.	1.000	5827.	>1000000.	60000.	849.0
18	45	10961.		3.2		11553.	1.000	5777.	>1000000.	60000.	861.5

Notes b,d,e,k: Fails
g: Weld ISI
h,i: Rupture Location
L: Information

++ DST/PIPESTRESS ++ Vermont Yankee Version 3.5.1+026 PC-EXE Release: Jun 2004

CALCULATION NUMBER 2 CODE SECTION III CLASS 1 ASME-1998 KRE 2007/07/11 11:35:07 [1275]
Vermont Yankee Feedwater PipingSI Fatigue Analysis

FATIGUE ANALYSIS AT POINT 155, LR ELBOW 155 TO 160

****
INDIVIDUAL STRESS RANGE CHECK
****

DELTA T1 IN DEGREES F
STRESSES IN PSI

LOAD SET PAIR		SN EQN.10	SE EQN.12	DELTA T1 RANGE	EQN.13	SP EQN.11	KE	SALT EQN.14	ALLOW CYCLES	3*SM	ALLOWABLE FOR DELTA T1 RANGE
1	11	11213.		1.6		11506.	1.000	5753.	>1000000.	60000.	875.7
7	19	11134.		41.4		11469.	1.000	5734.	>1000000.	58680.	822.5
36	41	10847.		3.2		11440.	1.000	5720.	>1000000.	60000.	849.0
12	13	9327.		11.3		11426.	1.000	5713.	>1000000.	60000.	869.9
2	24	11328.		0.5		11330.	1.000	5665.	>1000000.	60000.	885.1
24	36	11328.		2.7		11330.	1.000	5665.	>1000000.	60000.	858.4
24	38	11328.		0.5		11330.	1.000	5665.	>1000000.	60000.	885.1
2	8	10847.		1.7		11164.	1.000	5582.	>1000000.	60000.	875.7
8	38	10847.		1.7		11164.	1.000	5582.	>1000000.	60000.	875.7
2	6	10847.		1.4		11098.	1.000	5549.	>1000000.	60000.	875.7
6	38	10847.		1.4		11098.	1.000	5549.	>1000000.	60000.	875.7
2	14	10847.		1.3		11090.	1.000	5545.	>1000000.	60000.	875.7
14	38	10847.		1.3		11090.	1.000	5545.	>1000000.	60000.	875.7
2	10	10847.		1.2		11061.	1.000	5531.	>1000000.	60000.	875.7
10	38	10847.		1.2		11061.	1.000	5531.	>1000000.	60000.	875.7
2	41	10847.		0.0		10847.	1.000	5423.	>1000000.	60000.	875.7
38	41	10847.		0.0		10847.	1.000	5423.	>1000000.	60000.	875.7
16	21	8383.		13.1		10816.	1.000	5408.	>1000000.	54348.	801.4
11	12	9327.		6.6		10807.	1.000	5404.	>1000000.	60000.	850.5
1	9	10348.		1.4		10612.	1.000	5306.	>1000000.	60000.	875.7
36	40	9867.		3.2		10460.	1.000	5230.	>1000000.	60000.	849.0
12	44	8904.		7.9		10384.	1.000	5192.	>1000000.	60000.	863.0
16	44	7878.		13.1		10311.	1.000	5156.	>1000000.	60000.	843.7
16	37	7613.		13.1		10046.	1.000	5023.	>1000000.	60000.	833.7
11	16	7347.		14.4		10023.	1.000	5011.	>1000000.	60000.	831.2
9	18	9339.		2.0		9932.	1.000	4966.	>1000000.	60000.	849.0

Notes b,d,e,k: Fails
g: Weld ISI
h,i: Rupture Location
L: Information

CALCULATION NUMBER 2 CODE SECTION III CLASS 1 ASME-1998 KRE 2007/07/11 11:35:07 [1276]
Vermont Yankee Feedwater PipingSI Fatigue Analysis

FATIGUE ANALYSIS AT POINT 155, LR ELBOW 155 TO 160

****
INDIVIDUAL STRESS RANGE CHECK
****

DELTA T1 IN DEGREES F
STRESSES IN PSI

LOAD SET PAIR		SN EQN.10	SE EQN.12	DELTA T1 RANGE	EQN.13	SP EQN.11	KE	SALT EQN.14	ALLOW CYCLES	3*SM	ALLOWABLE FOR DELTA T1 RANGE
2	40	9867.		0.0		9867.	1.000	4934.	>1000000.	60000.	875.7
38	40	9867.		0.0		9867.	1.000	4934.	>1000000.	60000.	875.7
13	16	7347.		9.7		9780.	1.000	4890.	>1000000.	60000.	850.5
12	21	8294.		7.9		9774.	1.000	4887.	>1000000.	54348.	826.0
13	18	8471.		6.5		9683.	1.000	4841.	>1000000.	60000.	868.4
35	45	3119.		34.4		9554.	1.000	4777.	>1000000.	60000.	843.7
7	35	3009.		32.7		9443.	1.000	4722.	>1000000.	60000.	831.2
21	40	9372.		0.0		9373.	1.000	4686.	>1000000.	54348.	801.4
9	16	6478.		14.2		9126.	1.000	4563.	>1000000.	60000.	831.2
11	18	8471.		1.9		9064.	1.000	4532.	>1000000.	60000.	849.0
21	39	9063.		0.0		9063.	1.000	4531.	>1000000.	54348.	793.6
21	35	2626.		34.4		9060.	1.000	4530.	>1000000.	54348.	801.4
1	36	8346.		3.4		8989.	1.000	4494.	>1000000.	60000.	899.7
1	7	8619.		2.0		8985.	1.000	4493.	>1000000.	60000.	875.7
13	40	8336.		3.3		8955.	1.000	4478.	>1000000.	60000.	850.5
1	45	8861.		0.3		8911.	1.000	4455.	>1000000.	60000.	888.2
40	44	8864.		0.0		8865.	1.000	4432.	>1000000.	60000.	843.7
35	44	2416.		34.4		8850.	1.000	4425.	>1000000.	60000.	843.7
8	21	8383.		1.7		8700.	1.000	4350.	>1000000.	54348.	801.4
18	44	8053.		3.2		8646.	1.000	4323.	>1000000.	60000.	861.5
13	39	8023.		3.3		8643.	1.000	4321.	>1000000.	60000.	850.5
13	35	1582.		37.8		8635.	1.000	4318.	>1000000.	60000.	850.5
6	21	8383.		1.4		8635.	1.000	4317.	>1000000.	54348.	801.4
14	21	8383.		1.3		8626.	1.000	4313.	>1000000.	54348.	801.4
10	21	8383.		1.2		8598.	1.000	4299.	>1000000.	54348.	801.4
11	40	8336.		1.3		8579.	1.000	4289.	>1000000.	60000.	831.2

Notes b,d,e,k: Fails
g: Weld ISI
h,i: Rupture Location
L: Information

CALCULATION NUMBER 2 CODE SECTION III CLASS 1 ASME-1998 KRE 2007/07/11 11:35:07 [1277]
Vermont Yankee Feedwater PipingSI Fatigue Analysis

FATIGUE ANALYSIS AT POINT 155, LR ELBOW 155 TO 160

****
INDIVIDUAL STRESS RANGE CHECK
****

DELTA T1 IN DEGREES F
STRESSES IN PSI

LOAD SET PAIR		SN EQN.10	SE EQN.12	DELTA T1 RANGE	EQN.13	SP EQN.11	KE	SALT EQN.14	ALLOW CYCLES	3*SM	ALLOWABLE FOR DELTA T1 RANGE
39	44	8578.		0.0		8579.	1.000	4289.	>1000000.	60000.	843.7
17	21	2051.		34.4		8485.	1.000	4243.	>1000000.	54348.	801.4
1	2	8346.		0.3		8396.	1.000	4198.	>1000000.	60000.	970.1
1	38	8346.		0.3		8396.	1.000	4198.	>1000000.	60000.	970.1
21	41	8383.		0.0		8383.	1.000	4192.	>1000000.	54348.	801.4
11	39	8023.		1.3		8266.	1.000	4133.	>1000000.	60000.	831.2
17	45	1772.		34.4		8206.	1.000	4103.	>1000000.	60000.	843.7
8	44	7878.		1.7		8195.	1.000	4098.	>1000000.	60000.	843.7
17	44	1760.		34.4		8194.	1.000	4097.	>1000000.	60000.	843.7
6	44	7878.		1.4		8130.	1.000	4065.	>1000000.	60000.	843.7
14	44	7878.		1.3		8121.	1.000	4060.	>1000000.	60000.	843.7
10	44	7878.		1.2		8093.	1.000	4046.	>1000000.	60000.	843.7
13	17	1010.		37.8		8064.	1.000	4032.	>1000000.	60000.	850.5
18	21	7438.		3.2		8031.	1.000	4015.	>1000000.	54348.	824.1
7	17	1594.		32.7		8029.	1.000	4014.	>1000000.	60000.	831.2
11	35	1582.		33.1		8016.	1.000	4008.	>1000000.	60000.	831.2
15	35	1582.		8.8		8016.	1.000	4008.	>1000000.	60000.	831.2
13	41	7347.		3.3		7966.	1.000	3983.	>1000000.	60000.	850.5
6	13	7347.		2.0		7966.	1.000	3983.	>1000000.	60000.	850.5
8	13	7347.		1.6		7966.	1.000	3983.	>1000000.	60000.	850.5
10	13	7347.		2.2		7966.	1.000	3983.	>1000000.	60000.	850.5
13	14	7347.		2.0		7966.	1.000	3983.	>1000000.	60000.	850.5
8	37	7613.		1.7		7930.	1.000	3965.	>1000000.	60000.	833.7
8	11	7347.		3.0		7906.	1.000	3953.	>1000000.	60000.	831.2
41	44	7878.		0.0		7878.	1.000	3939.	>1000000.	60000.	843.7
6	37	7613.		1.4		7865.	1.000	3932.	>1000000.	60000.	833.7

Notes b,d,e,k: Fails
g: Weld ISI
h,i: Rupture Location
L: Information

CALCULATION NUMBER 2 CODE SECTION III CLASS 1 ASME-1998 KRE 2007/07/11 11:35:07 [1278]
Vermont Yankee Feedwater PipingSI Fatigue Analysis

FATIGUE ANALYSIS AT POINT 155, LR ELBOW 155 TO 160

****
INDIVIDUAL STRESS RANGE CHECK
****

DELTA T1 IN DEGREES F
STRESSES IN PSI

LOAD SET PAIR		SN EQN.10	SE EQN.12	DELTA T1 RANGE	EQN.13	SP EQN.11	KE	SALT EQN.14	ALLOW CYCLES	3*SM	ALLOWABLE FOR DELTA T1 RANGE
14	37	7613.		1.3		7856.	1.000	3928.	>1000000.	60000.	833.7
17	35	1415.		0.0		7850.	1.000	3925.	>1000000.	60000.	831.2
6	11	7347.		2.7		7841.	1.000	3921.	>1000000.	60000.	831.2
11	14	7347.		2.6		7832.	1.000	3916.	>1000000.	60000.	831.2
10	37	7613.		1.2		7828.	1.000	3914.	>1000000.	60000.	833.7
10	11	7347.		2.5		7804.	1.000	3902.	>1000000.	60000.	831.2
37	40	7746.		0.0		7746.	1.000	3873.	>1000000.	60000.	833.7
9	35	1273.		33.3		7707.	1.000	3854.	>1000000.	60000.	831.2
9	40	7468.		1.2		7683.	1.000	3841.	>1000000.	60000.	831.2
1	39	7602.		0.3		7652.	1.000	3826.	>1000000.	60000.	875.7
37	41	7613.		0.0		7613.	1.000	3807.	>1000000.	60000.	833.7
11	41	7347.		1.3		7589.	1.000	3795.	>1000000.	60000.	831.2
16	39	5128.		13.1		7561.	1.000	3780.	>1000000.	60000.	831.2
7	16	4742.		14.8		7493.	1.000	3746.	>1000000.	60000.	831.2
16	45	5016.		13.1		7449.	1.000	3725.	>1000000.	60000.	843.7
11	17	1010.		33.1		7444.	1.000	3722.	>1000000.	60000.	831.2
15	17	1010.		8.8		7444.	1.000	3722.	>1000000.	60000.	831.2
15	45	2654.		25.7		7438.	1.000	3719.	>1000000.	60000.	843.7
7	15	2604.		24.0		7388.	1.000	3694.	>1000000.	60000.	831.2
9	39	7155.		1.2		7370.	1.000	3685.	>1000000.	60000.	831.2
8	9	6478.		2.9		7010.	1.000	3505.	>1000000.	60000.	831.2
6	9	6478.		2.5		6945.	1.000	3472.	>1000000.	60000.	831.2
9	14	6478.		2.5		6936.	1.000	3468.	>1000000.	60000.	831.2
37	39	6911.		0.0		6911.	1.000	3456.	>1000000.	60000.	833.7
9	10	6478.		2.3		6908.	1.000	3454.	>1000000.	60000.	831.2
9	41	6478.		1.2		6693.	1.000	3347.	>1000000.	60000.	831.2

Notes b,d,e,k: Fails
g: Weld ISI
h,i: Rupture Location
L: Information

CALCULATION NUMBER 2 CODE SECTION III CLASS 1 ASME-1998 KRE 2007/07/11 11:35:07 [1279]
Vermont Yankee Feedwater PipingSI Fatigue Analysis

FATIGUE ANALYSIS AT POINT 155, LR ELBOW 155 TO 160

****
INDIVIDUAL STRESS RANGE CHECK
****

DELTA T1 IN DEGREES F
STRESSES IN PSI

LOAD SET PAIR		SN EQN.10	SE EQN.12	DELTA T1 RANGE	EQN.13	SP EQN.11	KE	SALT EQN.14	ALLOW CYCLES	3*SM	ALLOWABLE FOR DELTA T1 RANGE
9	17	143.		33.3		6577.	1.000	3289.	>1000000.	60000.	831.2
1	16	3933.		12.8		6366.	1.000	3183.	>1000000.	60000.	875.7
39	40	6117.		0.0		6118.	1.000	3059.	>1000000.	60000.	831.2
7	40	5732.		1.7		6049.	1.000	3025.	>1000000.	60000.	831.2
40	45	5998.		0.0		5998.	1.000	2999.	>1000000.	60000.	843.7
15	44	1059.		25.7		5843.	1.000	2921.	>1000000.	60000.	843.7
15	21	1049.		25.7		5833.	1.000	2917.	>1000000.	54348.	801.4
39	45	5775.		0.0		5775.	1.000	2887.	>1000000.	60000.	843.7
7	39	5420.		1.7		5737.	1.000	2869.	>1000000.	60000.	831.2
9	15	868.		24.5		5652.	1.000	2826.	>1000000.	60000.	831.2
8	39	5128.		1.7		5445.	1.000	2722.	>1000000.	60000.	831.2
13	15	0.		29.0		5403.	1.000	2702.	>1000000.	60000.	850.5
6	39	5128.		1.4		5380.	1.000	2690.	>1000000.	60000.	831.2
7	8	4742.		3.4		5377.	1.000	2688.	>1000000.	60000.	831.2
14	39	5128.		1.3		5371.	1.000	2685.	>1000000.	60000.	831.2
10	39	5128.		1.2		5342.	1.000	2671.	>1000000.	60000.	831.2
8	45	5016.		1.7		5333.	1.000	2667.	>1000000.	60000.	843.7
6	7	4742.		3.1		5311.	1.000	2656.	>1000000.	60000.	831.2
7	14	4742.		3.0		5302.	1.000	2651.	>1000000.	60000.	831.2
7	10	4742.		2.9		5274.	1.000	2637.	>1000000.	60000.	831.2
6	45	5016.		1.4		5268.	1.000	2634.	>1000000.	60000.	843.7
14	45	5016.		1.3		5259.	1.000	2630.	>1000000.	60000.	843.7
10	45	5016.		1.2		5231.	1.000	2615.	>1000000.	60000.	843.7
39	41	5128.		0.0		5128.	1.000	2564.	>1000000.	60000.	831.2
7	41	4742.		1.7		5060.	1.000	2530.	>1000000.	60000.	831.2
41	45	5016.		0.0		5016.	1.000	2508.	>1000000.	60000.	843.7

Notes b,d,e,k: Fails
g: Weld ISI
h,i: Rupture Location
L: Information

CALCULATION NUMBER 2 CODE SECTION III CLASS 1 ASME-1998 KRE 2007/07/11 11:35:07 [1280]
Vermont Yankee Feedwater PipingSI Fatigue Analysis

FATIGUE ANALYSIS AT POINT 155, LR ELBOW 155 TO 160

****
INDIVIDUAL STRESS RANGE CHECK
****

DELTA T1 IN DEGREES F
STRESSES IN PSI

LOAD SET PAIR		SN EQN.10	SE EQN.12	DELTA T1 RANGE	EQN.13	SP EQN.11	KE	SALT EQN.14	ALLOW CYCLES	3*SM	ALLOWABLE FOR DELTA T1 RANGE
11	15	0.		24.4		4784.	1.000	2392.	>1000000.	60000.	831.2
1	8	3933.		1.4		4250.	1.000	2125.	>1000000.	60000.	875.7
1	6	3933.		1.1		4184.	1.000	2092.	>1000000.	60000.	875.7
1	14	3933.		1.0		4176.	1.000	2088.	>1000000.	60000.	875.7
1	10	3933.		0.9		4147.	1.000	2074.	>1000000.	60000.	875.7
1	40	4066.		0.3		4116.	1.000	2058.	>1000000.	60000.	875.7
1	41	3933.		0.3		3983.	1.000	1991.	>1000000.	60000.	875.7
7	21	3643.		1.7		3960.	1.000	1980.	>1000000.	54348.	801.4
1	37	3680.		0.3		3730.	1.000	1865.	>1000000.	60000.	970.1
21	45	3666.		0.0		3666.	1.000	1833.	>1000000.	54348.	0.0
7	13	2604.		5.0		3540.	1.000	1770.	>1000000.	60000.	850.5
7	44	3221.		1.7		3538.	1.000	1769.	>1000000.	60000.	843.7
44	45	3528.		0.0		3528.	1.000	1764.	>1000000.	60000.	0.0
16	40	990.		13.1		3423.	1.000	1712.	>1000000.	60000.	831.2
13	45	2654.		3.3		3273.	1.000	1636.	>1000000.	60000.	863.0
7	11	2604.		0.4		2921.	1.000	1461.	>1000000.	60000.	831.2
11	45	2654.		1.3		2897.	1.000	1448.	>1000000.	60000.	843.7
16	41	0.		13.1		2433.	1.000	1217.	>1000000.	60000.	831.2
6	16	0.		11.7		2433.	1.000	1217.	>1000000.	60000.	831.2
8	16	0.		11.4		2433.	1.000	1217.	>1000000.	60000.	831.2
10	16	0.		11.9		2433.	1.000	1217.	>1000000.	60000.	831.2
14	16	0.		11.8		2433.	1.000	1217.	>1000000.	60000.	831.2
12	18	857.		4.8		2337.	1.000	1168.	>1000000.	60000.	868.4
9	21	1911.		1.2		2126.	1.000	1063.	>1000000.	54348.	801.4
9	45	1887.		1.2		2102.	1.000	1051.	>1000000.	60000.	843.7
7	9	1736.		0.5		2053.	1.000	1027.	>1000000.	60000.	831.2

Notes b,d,e,k: Fails
g: Weld ISI
h,i: Rupture Location
L: Information

CALCULATION NUMBER 2 CODE SECTION III CLASS 1 ASME-1998 KRE 2007/07/11 11:35:07 [1281]
Vermont Yankee Feedwater PipingSI Fatigue Analysis

FATIGUE ANALYSIS AT POINT 155, LR ELBOW 155 TO 160

****
INDIVIDUAL STRESS RANGE CHECK
****

DELTA T1 IN DEGREES F
STRESSES IN PSI

LOAD SET PAIR		SN EQN.10	SE EQN.12	DELTA T1 RANGE	EQN.13	SP EQN.11	KE	SALT EQN.14	ALLOW CYCLES	3*SM	ALLOWABLE FOR DELTA T1 RANGE
9	44	1642.		1.2		1857.	1.000	929.	>1000000.	60000.	843.7
9	13	868.		4.5		1702.	1.000	851.	>1000000.	60000.	850.5
13	44	1059.		3.3		1678.	1.000	839.	>1000000.	60000.	863.0
13	21	1049.		3.3		1668.	1.000	834.	>1000000.	54348.	826.0
7	45	1057.		1.7		1374.	1.000	687.	>1000000.	60000.	843.7
8	40	990.		1.7		1307.	1.000	654.	>1000000.	60000.	831.2
11	44	1059.		1.3		1301.	1.000	651.	>1000000.	60000.	843.7
11	21	1049.		1.3		1292.	1.000	646.	>1000000.	54348.	801.4
6	40	990.		1.4		1242.	1.000	621.	>1000000.	60000.	831.2
14	40	990.		1.3		1233.	1.000	616.	>1000000.	60000.	831.2
10	40	990.		1.2		1205.	1.000	602.	>1000000.	60000.	831.2
9	11	868.		0.2		1111.	1.000	556.	>1000000.	60000.	831.2
21	44	1018.		0.0		1018.	1.000	509.	>1000000.	54348.	0.0
40	41	990.		0.0		990.	1.000	495.	>1000000.	60000.	831.2
11	13	0.		4.6		862.	1.000	431.	>1000000.	60000.	850.5
2	36	0.		3.2		593.	1.000	296.	>1000000.	60000.	899.7
36	38	0.		3.2		593.	1.000	296.	>1000000.	60000.	899.7
8	41	0.		1.7		317.	1.000	159.	>1000000.	60000.	831.2
6	8	0.		0.4		317.	1.000	159.	>1000000.	60000.	831.2
8	10	0.		0.5		317.	1.000	159.	>1000000.	60000.	831.2
8	14	0.		0.4		317.	1.000	159.	>1000000.	60000.	831.2
6	41	0.		1.4		252.	1.000	126.	>1000000.	60000.	831.2
6	10	0.		0.2		252.	1.000	126.	>1000000.	60000.	831.2
6	14	0.		0.0		252.	1.000	126.	>1000000.	60000.	831.2
14	41	0.		1.3		243.	1.000	121.	>1000000.	60000.	831.2
10	14	0.		0.2		243.	1.000	121.	>1000000.	60000.	831.2

Notes b,d,e,k: Fails
g: Weld ISI
h,i: Rupture Location
L: Information

```
D S T   C O M P U T E R   S E R V I C E S   S. A.                                   F-4.1                PAGE NO.  1013

++ DST/PIPESTRESS ++                  Vermont Yankee                          Version 3.5.1+026  PC-EXE      Release: Jun 2004

   CALCULATION NUMBER    2        CODE SECTION III CLASS 1  ASME-1998         KRE                 2007/07/11  11:35:07  [1282]
   Vermont Yankee Feedwater PipingSI Fatigue Analysis

                     FATIGUE ANALYSIS AT POINT  155, LR ELBOW       155 TO   160

                       ****************************                                          DELTA T1 IN DEGREES F
                       INDIVIDUAL STRESS RANGE CHECK                                        STRESSES IN PSI
                       ****************************

LOAD SET     SN       SE   DELTA T1              SP              SALT          ALLOW          ALLOWABLE FOR
 PAIR      EQN.10   EQN.12   RANGE    EQN.13   EQN.11     KE    EQN.14         CYCLES   3*SM  DELTA T1 RANGE

 10  41       0.              1.2               215.    1.000     107.      >1000000.  60000.      831.2
  2  38       0.              0.0                 0.    1.000       0.      >1000000.  60000.        0.0

                                                                                   Notes  b,d,e,k: Fails
                                                                                          g:       Weld ISI
                                                                                          h,i:     Rupture Location
                                                                                          L:       Information
```

CALCULATION NUMBER 2 CODE SECTION III CLASS 1 ASME-1998 KRE 2007/07/11 11:35:07 [1283]
Vermont Yankee Feedwater PipingSI Fatigue Analysis

FATIGUE ANALYSIS AT POINT 155, LR ELBOW 155 TO 160

****
INDIVIDUAL STRESS RANGE CHECK
****

DELTA T1 IN DEGREES F
STRESSES IN PSI

LOAD SET PAIR I	J	SALT EQN.14	------ OCCURENCES ------ NI	NJ	NUMBER USED	SETS ELIMINATED DYNAM.	NO. CYCLES TO FAILURE	USAGE FACTOR	REMARKS
28	29	66456.	10	10	10	28,29	1808.	0.0055	
			0	0					
31	32	54146.	10	10	10	31,32	3406.	0.0029	
			0	0					
4	43	49733.	610	300	300	43	4465.	0.0672	
			310	0					
4	34	49533.	310	10	10	34	4523.	0.0022	
			300	0					
3	4	49512.	300	300	300	3, 4	4529.	0.0662	
			0	0					
20	26	45555.	300	10	10	26	5838.	0.0017	
			290	0					
22	27	34161.	300	10	10	27	14370.	0.0007	
			290	0					
22	30	32373.	290	10	10	30	17257.	0.0006	
			280	0					
22	42	26170.	280	300	280	22	33637.	0.0083	
			0	20					
24	42	22860.	300	20	20	42	51538.	0.0004	
			280	0					
5	24	22397.	599	280	280	24	57040.	0.0049	
			319	0					
5	23	21265.	319	300	300	23	73771.	0.0041	
			19	0					
5	36	17029.	19	1	1	36	178513.	0.0000	
			18	0					
2	5	16732.	120	18	18	5	190176.	0.0001	
			102	0					
12	20	16409.	10	290	10	12	205131.	0.0000	
			0	280					

CALCULATION NUMBER 2 CODE SECTION III CLASS 1 ASME-1998 KRE 2007/07/11 11:35:07 [1284]
Vermont Yankee Feedwater PipingSI Fatigue Analysis

FATIGUE ANALYSIS AT POINT 155, LR ELBOW 155 TO 160

****
INDIVIDUAL STRESS RANGE CHECK
****

DELTA T1 IN DEGREES F
STRESSES IN PSI

LOAD SET I	PAIR J	SALT EQN.14	OCCURENCES NI	OCCURENCES NJ	NUMBER USED	SETS ELIMINATED DYNAM.	NO. CYCLES TO FAILURE	USAGE FACTOR	REMARKS
2	20	16030.	102	280	102	2	228208.	0.0004	
			0	178					
20	38	16030.	178	1	1	38	228208.	0.0000	
			177	0					
18	20	15537.	289	177	177	20	263206.	0.0007	
			112	0					
18	25	15362.	112	10	10	25	277200.	0.0000	
			102	0					
33	37	15167.	10	1	1	37	293826.	0.0000	
			9	0					
1	33	13327.	120	9	9	33	561655.	0.0000	
			111	0					
18	19	11235.	102	300	102	18	>1000000.	0.0000	
			0	198					
19	35	10124.	198	1	1	35	>1000000.	0.0000	
			197	0					
1	19	9874.	111	197	111	1	>1000000.	0.0000	
			0	86					
17	19	9416.	289	86	86	19	>1000000.	0.0000	
			203	0					
16	17	7602.	70	203	70	16	>1000000.	0.0000	
			0	133					
17	40	6880.	133	289	133	17	>1000000.	0.0000	
			0	156					
15	40	6560.	70	156	70	15	>1000000.	0.0000	
			0	86					
21	40	4686.	300	86	86	40	>1000000.	0.0000	
			214	0					
21	39	4531.	214	289	214	21	>1000000.	0.0000	
			0	75					

CALCULATION NUMBER 2 CODE SECTION III CLASS 1 ASME-1998 KRE 2007/07/11 11:35:07 [1285]
Vermont Yankee Feedwater PipingSI Fatigue Analysis

FATIGUE ANALYSIS AT POINT 155, LR ELBOW 155 TO 160

****
INDIVIDUAL STRESS RANGE CHECK
****

DELTA T1 IN DEGREES F
STRESSES IN PSI

LOAD SET PAIR I	J	SALT EQN.14	OCCURENCES NI	NJ	NUMBER USED	SETS ELIMINATED DYNAM.	NO. CYCLES TO FAILURE	USAGE FACTOR	REMARKS
13	39	4321.	10	75	10	13	>1000000.	0.0000	
			0	65					
39	44	4289.	65	5	5	44	>1000000.	0.0000	
			60	0 45					
11	39	4133.	310	60	60	39	>1000000.	0.0000	
			250	0					
8	11	3953.	10000	250	250	11	>1000000.	0.0000	
			9750	0					
8	9	3505.	9750	2000	2000	9	>1000000.	0.0000	
			7750	0					
7	8	2688.	10000	7750	7750	8	>1000000.	0.0000	
			2250	0					
6	7	2656.	599	2250	599	6	>1000000.	0.0000	
			0	1651					
7	14	2651.	1651	10	10	14	>1000000.	0.0000	
			1641	0					
7	10	2637.	1641	2000	1641	7	>1000000.	0.0000	
			0	359					
10	45	2615.	359	5	5	45	>1000000.	0.0000	
			354	0 45					
44	45	1764.	45	45	45	,45 44	>1000000.	0.0000	DYN. RANGE OF EVENT NO. 1
			0	0					
10	41	107.	354	289	289	41	>1000000.	0.0000	
			65	0					

TOTAL USAGE FACTOR = 0.1661j